NUREG/CP-0155

Proceedings of the U.S. Nuclear Regulatory Commission

Proceedings of the Seminar on Leak Before Break in Reactor Piping and Vessels

Held in
Lyon, France
October 9-11, 1995

U.S. Nuclear Regulatory Commission

Edited by
C. Faidy, EDF
Ph. Gilles, Framatome

Sponsored by
EDF (Electricit'e de France)
Framatome
CEA (Commissariat a l'Energie Atomique)
EC-WGCS (European Community, DGXI-WGCS)
Nuclear Electric
IAEA (International Atomic Energy Agency)
OECD-NEA-(OECD-Nuclear Energy Agency)
USNRC (United States Nuclear Regulatory Commission)
SFEN (French Nuclear Energy Society)

Proceedings Prepared by
EDF-Septen and Battelle

AVAILABILITY NOTICE

Availability of Reference Materials Cited in NRC Publications

Most documents cited in NRC publications will be available from one of the following sources:

1. The NRC Public Document Room, 2120 L Street, NW., Lower Level, Washington, DC 20555-0001

2. The Superintendent of Documents, U.S. Government Printing Office, P. O. Box 37082, Washington, DC 20402-9328

3. The National Technical Information Service, Springfield, VA 22161-0002

Although the listing that follows represents the majority of documents cited in NRC publications, it is not intended to be exhaustive.

Referenced documents available for inspection and copying for a fee from the NRC Public Document Room include NRC correspondence and internal NRC memoranda; NRC bulletins, circulars, information notices, inspection and investigation notices; licensee event reports; vendor reports and correspondence; Commission papers; and applicant and licensee documents and correspondence.

The following documents in the NUREG series are available for purchase from the Government Printing Office: formal NRC staff and contractor reports, NRC-sponsored conference proceedings, international agreement reports, grantee reports, and NRC booklets and brochures. Also available are regulatory guides, NRC regulations in the *Code of Federal Regulations*, and *Nuclear Regulatory Commission Issuances*.

Documents available from the National Technical Information Service include NUREG-series reports and technical reports prepared by other Federal agencies and reports prepared by the Atomic Energy Commission, forerunner agency to the Nuclear Regulatory Commission.

Documents available from public and special technical libraries include all open literature items, such as books, journal articles, and transactions. *Federal Register* notices, Federal and State legislation, and congressional reports can usually be obtained from these libraries.

Documents such as theses, dissertations, foreign reports and translations, and non-NRC conference proceedings are available for purchase from the organization sponsoring the publication cited.

Single copies of NRC draft reports are available free, to the extent of supply, upon written request to the Office of Administration, Distribution and Mail Services Section, U.S. Nuclear Regulatory Commission, Washington, DC 20555-0001.

Copies of industry codes and standards used in a substantive manner in the NRC regulatory process are maintained at the NRC Library, Two White Flint North, 11545 Rockville Pike, Rockville, MD 20852-2738, for use by the public. Codes and standards are usually copyrighted and may be purchased from the originating organization or, if they are American National Standards, from the American National Standards Institute, 1430 Broadway, New York, NY 10018-3308.

DISCLAIMER NOTICE

Where the papers in these proceedings have been authored by contractors of the United States Government, neither the United States Government nor any agency thereof, nor any of their employees, makes any warranty, expressed or implied, or assumes any legal liability or responsibility for any third party's use, or the results of such use, of any information, apparatus, product, or process disclosed in these proceedings, or represents that its use by such third party would not infringe privately owned rights. The views expressed in these proceedings are not necessarily those of the U.S. Nuclear Regulatory Commission.

DISCLAIMER

NUREG/CP-0155

Proceedings of the U.S. Nuclear Regulatory Commission

Proceedings of the Seminar on Leak Before Break in Reactor Piping and Vessels

Held in
Lyon, France
October 9-11, 1995

Manuscript Completed: February 1997
Date Published: April 1997

Edited by
C. Faidy, EDF
Ph. Gilles, Framatome

Sponsored by

EDF (Electricit'e de France)
Framatome
CEA (Commissariat a l'Energie Atomique)
EC-WGCS (European Community, DGXI-WGCS)
Nuclear Electric

IAEA (International Atomic Energy Agency)
OECD-NEA-(OECD-Nuclear Energy Agency)
USNRC (United States Nuclear Regulatory Commission)
SFEN (French Nuclear Energy Society)

Proceedings Prepared by
EDF-Septen
12 Av/ Dutrivoz
69628 Villeurbanne
France

Battelle
505 King Avenue
Columbus, OH 43201

M. Mayfield, NRC Project Manager

Prepared for
Division of Engineering Technology
Office of Nuclear Regulatory Research
U.S. Nuclear Regulatory Commission
Washington, DC 20555-0001
NRC Job Code D2060

ABSTRACT

The sixth in a series of international Leak-Before-Break (LBB) Seminars was held at Hotel Sofitel in Lyon, France on October 9 through 11, 1995. The seminar updated international policies and supporting research on LBB. The more than 210 attendees that joined the meeting included representatives from regulatory agencies, electric utility representatives, fabricators of nuclear power plants, research organizations, and academic institutions.

The objective of the seminar was to present the current state of the art in LBB methodology development, validation, and application in an international forum. With particular emphasis on industrial applications and regulatory policies, the seminar provided an opportunity to compare approaches, experiences, and codifications developed by different countries.

The seminar was organized into four topic areas:

- Status of LBB Applications
- Technical Issues in LBB Methodology
- Complementary Requirements (Leak Detection and Inspection)
- LBB Assessment and Margins.

In addition to the formal sessions where papers were presented by participants from France, Germany, Japan, Korea, Belgium, the United Kingdom, the Czech Republic, Finland, Russia, Sweden, Canada, the Netherlands, and the United States, informal LBB poster sessions were available outside the presentation hall. A keynote address (see Appendix B) by Mr. J. Branchu, Head of the Primary Nuclear Components Division of Framatome, was delivered at the LBB 95 Banquet and summarized the goals and objectives of the seminar.

As a result of this seminar, an improved understanding of LBB gained through sharing of different viewpoints from different countries, permits consideration of:

- Simplified pipe support design and possible elimination of loss-of-coolant-accident (LOCA) mechanical consequences for specific cases
- Defense-in-Depth type of applications without support modifications
- Support of safety cases for plants designed without the LOCA hypothesis.

In support of these activities, better estimates of the limits to the LBB approach should follow, as well as an improvement in codifying methodologies.

TABLE OF CONTENTS

TABLE OF CONTENTS (Continued)

TABLE OF CONTENTS (Continued)

TABLE OF CONTENTS (Continued)

TABLE OF CONTENTS (Continued)

TABLE OF CONTENTS (Continued)

TABLE OF CONTENTS (Continued)

ACKNOWLEDGEMENTS

The major efforts in organizing and supporting this seminar were made by EDF (Electricité de France), Framatome and CEA (Commissariant à l'Energie Atomique). Mr. Claude Faidy of EDF and Mr. Phillipe Gilles of Framatome were primarily responsible for the seminar. We owe a great deal of thanks to them and the other sponsors for their organizational efforts.

These conference proceedings were assembled and organized by Mr. Claude Faidy, Mr. Phillipe Gilles, and Dr. Gery Wilkowski of Battelle. We thank those who have contributed their presentations to these proceedings. Finally, a special thanks must go to Ms. Verna Kreachbaum of Battelle for her efforts in compiling this document, and the U.S. NRC for agreeing to publish it.

Gery Wilkowski
Battelle

Phillipe Gilles
Framatome

Claude Faidy
EDF

PREVIOUS DOCUMENTS IN THE SERIES

CSNI Specialist Meeting on Leak-Before-Break in Nuclear Reactor Piping. Proceedings of a CSNI seminar held at Monterey, California on September 1-2, 1983, NUREG/CP-0051, published in August 1984.

Leak Before Break: International Policies and Supporting Research. Proceedings of a seminar held at Columbus, Ohio on October 28-30, 1985, NUREG/CP-0077, published in June 1986.

Leak-Before-Break: Progress in Regulatory Policies and Supporting Research. Proceedings of a seminar held at Tokyo, Japan on May 14-15, 1987, NUREG/CP-0092, published in March 1987.

Leak-Before-Break: Further Developments in Regulatory Policies and Supporting Research. Proceedings of a seminar held at Taipei, Taiwan on May 11-12, 1989, NUREG/CP-0109, published February 1990.

Leak-Before-Break in Water Reactor Piping and Vessels. Proceedings of a seminar held at Toronto, Canada, on October 24-27, 1989, reprinted in The International Journal of Pressure Vessels and Piping, Vol. 43, Nos. 1-3, 1990.

SESSION 1: STATUS OF LBB APPLICATIONS

LBB APPLICATION IN THE U.S. OPERATING AND ADVANCED REACTORS

K. Wichman, J. Tsao, M. Mayfield
U.S. Nuclear Regulatory Commission

The primary pressure boundary piping in U.S. nuclear power plants is designed and constructed to stringent standards, and the materials and fabrication processes assure a high degree of ductility. In addition, the U.S. Nuclear Regulatory Commission (USNRC) regulations require postulation of instantaneous double-ended guillotine breaks (DEGB) in the large pipes for the purposes of designing other safety systems, such as the ECCS system, and for setting other design criteria, such as the environmental qualification requirements for electrical and mechanical equipment.

Beyond these design considerations, evaluation of the potential effects associated with the DEGB of the large piping led to concerns about asymmetric blowdown loads on the reactor internals and the pressure vessel supports. If the DEGB was treated as a realistic possibility, it was difficult to demonstrate that the integrity of the internals and vessel support system would not be challenged.

However, the DEGB was not generally believed to be a realistic event for the large diameter pipe because of the ductile materials and the relatively low loads even under postulated accident loads. Rather, it was expected that any cracks that might develop during service would produce detectable leaks that would permit the plant operators to safely shut down the plant rather than resulting in the catastrophic rupture of the pipe; that is, the piping would leak before it would break. The challenge was to quantitatively demonstrate this leak-before-break behavior.

In addition to requiring postulation of the DEGB for the large diameter pipe, the USNRC staff has required the postulation of breaks in other piping systems in evaluating a variety of design considerations. Similar to the situation with the DEGB of the large diameter pipe, consideration of these non-mechanistic breaks in other systems led to the imposition of requirements for pipe whip restraints and jet impingement barriers for many piping systems, even for systems where leak-before-break conditions were anticipated. Again, the challenge was to quantitatively demonstrate leak-before-break.

The USNRC staff and the nuclear industry performed extensive analyses and, as necessary, developed technical approaches to demonstrate leak-before-break for the primary system piping. On February 1, 1984, the USNRC issued Generic Letter 84-04 accepting that the double-ended guillotine break of the PWRs primary loop piping was unlikely to occur, provided it could be demonstrated by deterministic fracture mechanics

analyses that postulated small through-wall flaws in plant-specific piping would be detected by the plant's leakage monitoring systems long before the flaws could grow to unstable sizes.

The staff continued its evaluation of leak-before-break and in November 1984, the limitations and acceptance criteria for the LBB analysis was published in the USNRC document, NUREG-1061, Volume 3. Publication of these limitations and acceptance criteria eventually led the Commission to modify General Design Criterion (GDC) 4 of Appendix A to Part 50 of Title 10 of the Code of Federal Regulations (CFR) to eliminate the requirement to postulate DEGB for piping that met rigorous acceptance criteria. Additionally, the staff has published a draft of Standard Review Plan Section 3.6.3, "Leak Before Break Evaluation."

Since the mid-1980's, the NRC has reviewed and approved LBB analyses submitted by individual licensee or owners groups. The LBB technology has provided the USNRC not only a challenge to the regulatory process but also impetus to the development of advanced fracture mechanics analysis of degraded piping, which was sponsored by the NRC with the cooperation of the nuclear industry.

The balance of this paper describes the regulatory application of LBB in the U.S. and the developments in the technology that have supported this application.

LBB APPLICATIONS FOR OPERATING REACTORS

The NRC has approved 76 PWRs for the application of LBB in the primary coolant loop to eliminate pipe whip restraints and jet impingement barriers (see the attached table). LBB was applied to the hot legs, cold legs, and crossover legs with an average nominal diameter of 88.9 cm (35 inch). They were fabricated from austenitic stainless steel SA 376 Type 316; wrought stainless steel SA 376 Type 304N; cast stainless steel fittings SA351 C8M or CF8A; or ferritic steel SA 516 Grade 70 and SA 106 Grade C.

Some of the LBB applications for the above primary loop piping were based on NRC approved topical reports submitted by owners groups. For those licensees who were covered by the topical report and applied for LBB, the USNRC requires that their plant specific leak detection system satisfies USNRC Regulatory Guide 1.45, "Reactor Coolant Pressure Boundary Leakage Detection Systems."

Initially, LBB application was primarily for the primary loop piping; however, as operating experience has accumulated, licensees have applied LBB to other high energy lines to improve operational safety and performance. For example, licensees have found that pressurizer surge lines have developed thermal stratification which caused the pipe to move more than the design value in the original stress analysis. This thermal stratification posed a challenge to the LBB analysis for the surge line. The loads caused by the thermal stratification are in addition to the normal and faulted loads. Certain pipe restraints had to be removed to allow free movement and the fatigue usage factor had to meet the ASME Code limit. Some surge lines barely satisfied the USNRC

required margin of 2 on crack size. The USNRC was able to approve, however, LBB for 12 pressurizer surge lines.

Other piping that has been approved for LBB included 12 accumulator lines and one injection line of the Safety Injection (SI) System. The accumulator line is typically 30.5 cm (12 inch) nominal diameter with 0.927 cm (0.365 inch) thickness and is fabricated from austenitic stainless steel SA 312 TP 403. The accumulator line provides emergency core cooling injection to each of the cold legs at a pressure of about 4.8 MPa (700 psia). The safety injection line is typically 15.2 cm (6 inch) nominal diameter with a thickness of 1.82 cm (0.718 inch) and is fabricated from austenitic stainless steel SA 376 TP 316. The SI line provides core cooling at a pressure of 10.3 MPa (1500 psia).

There were six residual heat removal (RHR) system lines approved for LBB. LBB was applied to the high pressure portion of the RHR piping that connects to the hot legs, which provides suction water to the RHR pumps during shutdown cooling. The piping is typically 32.4 cm (12.75 inch) outside diameter with a thickness of 2.86 cm (1.125 inch) and is fabricated from austenitic stainless steel SA 376 TP 316.

Five reactor coolant (RC) loop bypass piping systems were approved for LBB. The RC bypass line connects the hot and cold legs of each primary loop and provides a recirculation path to a loop isolated from the reactor. The bypass line is typically 21.9 cm (8.625 inch) outside diameter with a thickness of 2.30 cm (0.906 inch). The piping is fabricated from austenitic stainless steel SA 312 or SA 376 TP 304.

In addition, the installation of permanent neutron shield/pool seals over the reactor vessel annulus was based on LBB application. The existing shield/pool seal needed to be removed during every refueling, which incurs personnel radiation exposure. A removable seal was originally installed because a permanent seal would not sustain the pressure loads from an LOCA event. With LBB approved, the postulated LOCA loads would not be considered for the pool seal, and thus a permanent seal could be installed.

Not all applications for LBB has been approved by the USNRC staff. For example, the USNRC has not approved any applications for BWR plants because the proposed LBB analyses have not satisfactorily addressed the susceptibility of the piping to intergranular stress corrosion cracking (IGSCC). The USNRC has also denied an application where a licensee proposed LBB on a 3.2 cm (1.25 inch) outside diameter line of the reactor coolant pump seal cooler.

LBB APPLICATIONS FOR ADVANCED REACTORS

In SECY-93-087, the USNRC staff recommended to the Commission that the LBB approach be approved for both evolutionary and passive advanced light water reactors (ALWRs) seeking design certification under 10 CFR Part 52, in lieu of postulating pipe breaks as required by GDC 4. This approval was limited to instances in which appropriate bounding limits are established using preliminary analysis results during the design certification phase and verified during the combined operating license (COL)

phase by implementing appropriate inspections, tests, analyses, and acceptance criteria (ITAAC). The Commission approved the staff's recommendation in its memorandum dated July 21, 1993. The staff also noted in SECY-93-087 the need to develop specific details as the process is implemented.

In CESSAR-DC for the System 80+ design, ABB-CE stated that the Class 1 piping with a diameter of 25.4 cm (10 inch) or greater and the main steam line (MSL) piping meet all the criteria for the application of LBB. The USNRC, however, must review the LBB analyses for specific piping design before ABB-CE can exclude the dynamic effects from the design basis. Applicants seeking design certification for ALWRs under 10 CFR Part 52 should establish preliminary stress analysis results, provided bounding limits (both upper and lower bound) are determined, in order to establish assurance that adequate margins are available for leakage, loads, and flaw sizes.

For through-wall flaw sizes, a lower bound, normal-operational stress limit must be established for dead weight, pressure, and thermal loadings. The mean or best-estimate stress-strain curve should be used. For flaw stability, an upper-bound stress limit should be established for normal loadings plus safe shutdown earthquake (SSE). A lower-bound stress-strain curve for base metal should be used regardless of whether the weld or base metal is limiting. In addition, a lower-bound toughness (weld metal or base metal) should be used.

These bounding values and preliminary analyses should be verified when as-built and as-procured information become available during the COL phase. Verification of the preliminary LBB analysis should be completed at the COL stage based on actual material properties and final, as-built piping analyses as part of ITAAC associated with 10 CFR Part 52 before fuel loading. The staff position on LBB application is stated in SECY-93-087 and the Commission approved it on July 21, 1993.

ABB-CE stated that it will perform bounding LBB evaluations based on preliminary pipe design analyses for piping evaluated for LBB using the guidelines of NUREG-1061, Volume 3. For each piping system evaluated for LBB, potential degradation mechanisms, steam hammer and water hammer, and thermal stratification were to be considered, as applicable. In addition, dynamic strain aging of carbon steel, environmental effects on fatigue, and thermal aging of cast stainless steel piping were to be considered in each LBB evaluation as appropriate. Each LBB piping system was to be evaluated from anchor point to anchor point. Leakage detection outside the containment would be considered for the MSL if the anchor-to-anchor portion of the piping evaluated includes piping that can leak outside the containment. A leak detection capability of 3.79 L/min (1.0 gpm) was to be used with a factor of 10 for calculating the length of a leakage crack. ABB-CE also submitted a reference for benchmarking its LBB calculations.

ABB-CE proposed to use the LBB acceptance limits given in NUREG-1061, Volume 3, to derive corresponding acceptable stress limits for the LBB piping. ABB-CE stated that the acceptable stress limits would form a "window" in stresses and the COL applicant would have to verify that the piping is within this window during the COL stage to justify the application of LBB. This window concept is a new approach in meeting the

staff's established LBB criteria. The staff noted that ABB-CE should perform the bounding LBB analyses based on the actual pipe routing.

Subsequently, the staff found that preliminary pipe routings were used in the bounding LBB analyses, and that stresses in LBB candidate piping systems were within the acceptance limits (or window) based on NUREG-1061, Volume 3. The preliminary routings were of conventional design. The stresses met the ASME Code and the LBB acceptance limits with ample margins. Consequently, the earlier USNRC concern was alleviated because it is extremely unlikely that the actual routings of the LBB candidate piping systems in the COL stage will not be able to meet the acceptance window limits. The USNRC staff also found that the related subcompartments are designed to withstand the pressures resulting from pipe breaks not eliminated by LBB, leakage cracks in piping for which LBB is approved, and postulated high-energy leakages from other sources. Thus the USNRC concluded that this ABB-CE approach was acceptable and asked ABB-CE to submit its bounding LBB analyses for USNRC review and approval for design certification.

CESSAR-DC indicated that LBB analyses are to be performed for the following piping systems:

* main coolant loop point, hot and cold legs
* surge line
* direct vessel injection line (main run inside the containment)
* shutdown cooling line (main run inside the containment)
* Main steam line (main run inside the containment)

Westinghouse proposes to use LBB extensively for its AP600 passive ALWR design. There are many controversial aspects to Westinghouse's planned LBB application which the USNRC staff is currently reviewing. These include: 1) application to main feedwater piping (inside containment); 2) application to piping as small as 10.2 cm (4 inch) nominal diameter; 3) use of 1.89 L/min (0.5 gpm) as the technical specification value for unidentified leakage and use of this leakage limit in the LBB analysis of piping inside containment.

LBB TECHNOLOGY DEVELOPMENT

Clearly, LBB has been applied widely in the U.S. since 1984. However, the technology that was used to resolve the asymmetric blowdown load concerns was not adequate to support the numerous applications of LBB described in the preceding section. Rather, the technology has evolved and been refined to support the applications.

The USNRC has maintained an active research program addressing pipe cracking, fracture analysis methods, material property evaluations, and other supporting analysis methods, such as leak rate estimation methods.

At the time the asymmetric blowdown load issue was being evaluated for PWRs, IGSCC was a major concern for BWRs. Thus, in the early 1980's the USNRC initiated

the Degraded Piping Program (1981-1989), and subsequently the Short Cracks in Piping and Piping Welds program (1990-1994). This research was to perform piping integrity research emphasizing fracture of stainless steel pipe and welds containing defects representative of IGSCC. However, the work was quickly expanded to address a wide variety of materials and material conditions, including carbon steels and welds, Inconel, and thermally aged cast stainless steels.

The research included the development of fracture analysis methods, material property measurements to provide typical properties for use in the analyses, and pipe fracture experiments to validate the analysis methods. Additionally, early work was underway to develop and validate leak rate estimation methods as a key consideration in applying leak-before-break.

The initial piping integrity research used slow loading rates, primarily because of the testing difficulties associated with more rapid loading rates. Additionally, it was generally believed that the loading rates associated with seismic events would not be sufficiently high to affect the fracture toughness of the piping materials. Another major factor was the high cost of performing realistic pipe fracture experiments under seismic loading conditions.

However, by the mid-1980's, interest in performing pipe fracture experiments under realistic pressure and temperature conditions and at representative seismic loading rates had grown. The International Piping Integrity Research Group (IPIRG), an international consortium of government and industrial organizations, was formed to conduct such experiments. Over the last 10 years, this group has supported a multi-million dollar research program that has advanced the state-of-the-art in pipe fracture analysis to the point that the fracture behavior of cracked pipe can be confidently predicted.

The research supported solely by the USNRC, combined with the IPIRG research, has produced approximately 150 pipe fracture experiments with diameters ranging from 10.2 cm (4 inch) to 106.7 cm (42 inch) nominal pipe size, with wall thickness ranging from approximately 0.635 cm (0.25 inch) to over 8.9 cm (3.5 inch). Additionally, material properties have been measured for over 75 different base metals and welds. These data provide an extremely strong validation of and technical basis for implementing LBB analysis methods.

Summary

The leak-before-break concept has been accepted in the U.S. for a variety of piping systems that can meet rigorous acceptance criteria. The early implementation resolved a significant issue for PWRs. Subsequent applications have permitted removal of pipe whip restraints and jet impingement barriers for a number of systems. Additionally, the LBB concept has been applied in the design of an advanced reactor system. While the application of the technology has been relatively rapid, it has been fully supported by an aggressive research program that has provided the technical bases for advancing the technology and the experimental validation of the key analysis methods.

Leak-before-break has evolved into a key regulatory position in the U.S. It has provided the double benefit of improved safety at reduced cost for present reactors, and its application is an important consideration in new designs. From a highly focussed beginning, LBB has evolved into a vital consideration in the design and operation of nuclear reactor piping systems, both in the U.S. and many other countries.

USNRC APPROVED PIPING SYSTEMS FOR LBB IN OPERATING REACTORS

AS OF AUGUST 1995

Piping systems for LBB Application	Number of plants approved
Reactor Coolant System--Primary Loop Piping	76
Pressurizer Surge Lines	12
Safety Injection Accumulator Lines	10
Residual Heat Removal Lines	6
Safety Injection Lines	1
Reactor Coolant Loop Bypass Lines	5

ADDITIONAL REQUIREMENTS FOR LEAK-BEFORE-BREAK APPLICATION TO PRIMARY COOLANT PIPING IN BELGIUM

G. Roussel
AIB Vinçotte Nuclear, Brussels, Belgium

ABSTRACT

Leak-Before-Break (LBB) technology has not been applied in the first design of the seven Pressurized Water Reactors the Belgian utility is currently operating. The design basis of these plants required to consider the dynamic effects associated with the ruptures to be postulated in the high energy piping. The application of the LBB technology to the existing plants has been recently approved by the Belgian Safety Authorities but with a limitation to the primary coolant loop.

LBB analysis has been initiated for the Doel 3 and Tihange 2 plants to allow the withdrawal of some of the reactor coolant pump snubbers at both plants and not reinstall some of the restraints after steam generator replacement at Doel 3. LBB analysis was also found beneficial to demonstrate the acceptability of the primary components and piping to the new conditions resulting from power uprating and stretch-out operation. LBB analysis has been subsequently performed on the primary coolant loop of the Tihange 1 plant and is currently being performed for the Doel 4 plant.

Application of the LBB to the primary coolant loop is based in Belgium on the U.S. Nuclear Regulatory Commission requirements. However the Belgian Safety Authorities required some additional analyses and put some restrictions on the benefits of the LBB analysis to maintain the global safety of the plant at a sufficient level.

This paper develops the main steps of the safety evaluation performed by the Belgian Safety Authorities for accepting the application of the LBB technology to existing plants and summarises the requirements asked for in addition to the U.S. Nuclear Regulatory Commission rules.

INTRODUCTION

Under the amendment to GDC-4 (Ref.[1]), the U.S. Nuclear Regulatory Commission (NRC) allows the use of an LBB analysis to exclude from the design basis the "dynamic effects" associated with postulated pipe ruptures of primary coolant loop piping in Pressurized Water Reactors.

Before authorizing the Belgian utility to apply the LBB technology to existing plants, the Belgian Safety Authorities reviewed the benefits of the LBB analysis as set forth by the U.S. NRC rules. Their review was made with reference to the defence-in-depth principles and led to define the conditions and limitations under which the LBB technology was allowed to be used for the reactor coolant circuit of existing plants.

POSTULATION OF THE LOCA

LOCA as a Design Basis Accident

The third level in the defence-in-depth concept is achieved by providing the plant with additional systems (Engineered Safety Features -ESF - systems) - as well as with the part of the Reactor Protection System necessary to initiate these systems - in order to limit the consequences of extremely unlikely accidents to an acceptable level for the public. In addition to the ESF systems, the reactor core and internals in conjunction with the reactor coolant system will be designed to ensure sufficient core reactivity control and core cooling during these events.

The postulation of the Loss-Of-Coolant-Accident (LOCA) originates so from the technical safety objective which requires to consider in the design of the plant those accidents of low probability. A design basis accident is then defined for each range of relating possible initiating events which could challenge the safety of the plant. The design basis accidents include the Loss-Of-Coolant-Accident. A deterministic analysis is performed to predict the course of the event and all its reallistically conceivable consequences. The analysis shall define the design parameters of the ESF sytems which are necessary to halt the progress of the LOCA and, when necessary, to mitigate its consequences.

Safety Design Principle

Most aspects of safety design are connected with the three functions that protect against the release and dispersal of radioactive material :(i) controlling core power /core shutdown, (ii) core cooling, and (iii) confinement of released radioactive fission products.
For the purpose of designing a nuclear power plant to cope with the postulated design basis accidents, design requirements are set forth to ensure that these functions are not impaired by the LOCA.

Core shutdown

In order that the boron delivered by the Emergency Core Cooling System (ECCS) together with the control rods provide sufficient negative reactivity for safe shutdown after LOCA, the reactor core and internals shall be designed so that their geometry is maintained after LOCA to allow the control rods to fall in the reactor core and the borated water to be delivered to the core.

Core cooling

- The ECCS shall be designed to ensure adequate core cooling in the event of a LOCA.
- The reactor vessel internals shall be designed to ensure the capability of the core to be cooled after the occurrence of a LOCA.
- The primary loop supports shall be designed to prevent large distorsion of the piping during a LOCA in order to ensure that water from the ECCS enters the reactor vessel.
- The containment structures and containment systems shall be designed to absorbe the energy released in the containment after a LOCA.

Confinement of released radioactive fission products

- Containment shall be designed to contain radioactive material leakage or releases from equipment located within the containment after the occurrence of a LOCA.
- The steam generator tube bundle shall be designed to ensure its integrity after the LOCA and so to avoid containment bypass and escape of radioactive fission products directly to the environment.

Two specific principles are also included for safety reasons, (i) equipment qualification and (ii) non-increase of the severity of the accident.

Equipment qualification

Mechanical and electrical equipment that are essential to emergency reactor shutdown, containment isolation, reactor core cooling, and containment and reactor heat removal shall be qualified to the environmental conditions that would prevail if they were required to function after a LOCA.

Non-increase of the severity of the accident

Design provisions shall be made at the design stage to maintain the LOCA accident within the design basis. Design provisions shall therefore be taken in order that :

- a Reactor Coolant System (RCS) pipe break is limited to the leg in which the break started
- an RCS pipe break does not cause a steam or feedwater line break
- propagation of a "small" break to a "large" break is prevented
- an RCS pipe break does not cause a steam generator tube rupture.

MECHANICAL ANALYSIS TO LOCA (PRIOR TO RULE CHANGE)

According to the Appendix A to 10 CFR Part 50, "Loss of coolant accidents mean those postulated accidents that result from the loss of reactor coolant at a rate in excess of the capability of the reactor coolant makeup system from breaks in the reactor coolant pressure boundary up to and

including a break equivalent in size to the double-ended rupture of the largest of the pipe of the reactor coolant system".

The containment design, ECCS performances and qualification of mechanical and electrical equipment are based on a complete spectrum of breaks type and size.

From the 1970s, the analysis of the reactor coolant circuit (piping, components and supports) and the reactor vessel internals is based on the postulation of specific pipe breaks in the primary circuit. In a generic analysis performed by Westinghouse (Ref.[2]), the postulated locations and types of pipe breaks are derived from the results of a stress and fatigue analysis. Eleven pipe breaks are postulated in each loop, ten of which are double-ended guillotine breaks and one of which is a longitudinal break. The loads resulting from a LOCA depend on the size of the break area and on the opening time of the break. The full cross sectional flow area of a circumferential break is not considered in the analysis if the presence of restraints limits the displacement of piping and components and so allows to justify a lower value of the break area. In the conventional break assumptions based on conservative estimates of equipment/piping displacements, the circumferential breaks on the primary piping -with the exception of the break postulated at the reactor coolant pump (RCP) outlet nozzle - have an opening area of less than 144 square inches. At the RCP outlet nozzle, a guillotine break of a double-ended pipe cross sectional flow area (2×4.125 square feet) is assumed. The circumferential breaks postulated at the connections of the auxiliary lines (Pressurizer Surge line, Safety Injection line, Residual Heat Removal line) with the primary piping have double-ended pipe cross sectional flow area. The opening area of the longitudinal break postulated on the intrados in the elbow of the steam generator inlet is equal to one time the flow area (5.241 square feet). The conventional opening time of the pipe breaks is assumed to be 1 msec.

RULE CHANGE TO GDC-4

The final "limited" scope rule published on 11April 1986 (Ref.[1]) amends GDC-4 by permitting the use of LBB analyses to eliminate from the design basis the dynamic effects associated to postulated pipe ruptures of primary coolant piping of PWRs. On 27 October 1987, a final "broad scope" rule (Ref.[3]) amends GDC-4 to permit the use of LBB analyses in all high energy piping.
Limiting the LBB analysis to the primary coolant piping leads to postulate breaks only at the branch connection of the auxiliary lines (Pressurizer Surge line, Safety Injection and Residual Heat Removal) with the reactor coolant loops.
Analysis of the U.S. NRC documents (GDC-4, Statement of Consideration, SRP 3.6.3 in Ref.[4]) and examination of the available documents (i.e., Safety Analysis Reports of U.S. plants and U.S. NRC Safety Evaluation Reports) lead to the plausible interpretation that the application of LBB allows to not consider :
(i) the loading of the primary component supports due to the pipe break reactions
(ii) the subcooled blowdown loading of the reactor vessel internals
(iii) the subcooled blowdown loading of the steam generator internals (divider plate and tube bundle)

(iv) the asymmetric pressurization of the reactor cavity
(v) the effects resulting from pipe whipping, jet impingement and missiles.

The U.S. NRC rules clearly exclude the containment design, the ECCS performances and the qualification of the mechanical and electrical equipment from the benefits of the LBB analysis.
The consequences of the LBB analysis on the protection of the unbroken loops against the effects from the broken leg (by the physical separation with concrete structures and by the decoupling of the mechanical effects at the reactor vessel) are not clearly stated in the U.S. NRC documents.

CONSEQUENCES OF THE MODIFIED GDC-4

Inconsistency in the Mitigation Measures

Before the GDC-4 was amended, the design bases for the reactor coolant circuit (piping, heavy components and their internals, supports), the containment systems, and the ECCS and the requirements for qualification of the mechanical and electrical equipment were coherent.
The modified GDC-4 introduces an inconsistency in the mitigation measures to face a LOCA. Firstly, it does not seem logical not to consider a double-ended guillotine break for designing the reactor internals and core whereas this break is assumed in the design basis of the ECCS. Secondly, the question can be raised why the ECCS should be designed for a double-ended guillotine break if the mechanical effects impair the core assembly geometry to such an extent that control rods cannot be dropped and the core cannot be adequately cooled or cause such large distorsion of the primary piping that the ECCS water cannot enter the reactor vessel.
The U.S. NRC acknowledged this inconsistency and clarified its position by introducing the distinction between the local and the global effects (Ref.[5]). However this clarification does not address the consequences on core reactivity control and core cooling of the large distorsions of the reactor core and internals or primary piping.

Non Increase of the Accident Severity

The safety requirement for non increasing the severity of the accident does not seem to have been considered.

Protection Against Non-Identified Events

For each plant condition a limited number of events is defined. These were analyzed to ensure that they enveloppe other (non identified) related possible initiating events belonging to the same plant condition. By eliminating from the design basis the dynamic effects associated with the postulated LOCA, the protection against some effects of the related possible initiating events could have been lost.

The consequences of the elimination of the protection against the dynamic effects of the LOCA on the protection against the related possible initiating events do not seem therefore to have been taken into account.

BELGIAN SAFETY AUTHORITIES POSITION

Applying Modified GDC-4 vs Retaining Safety Margins

The concept of defence-in-depth relies first on preventing the event and then mitigating the consequences. There is so far no reason to change this concept.

The consequences of the amendment to the GDC-4 on the measures mitigating the design basis LOCA should be analyzed. The modified GDC-4 does not change the design bases for the containment systems and the ECCS nor the requirements for qualification of the mechanical and electrical equipment. The elimination of the dynamic effects from the design basis of the reactor coolant circuit have potential consequences which cannot be accepted as such. The elimination of the mechanical effects associated to the postulated primary pipe breaks could result in unacceptable consequences in terms of core shutdown, core cooling and non-increase of the accident severity. Indeed, the modified GDC-4 results in decreasing the structural capacity of the

- primary component supports
- reactor cavity
- reactor core and internals
- steam generator tube bundle

and it furthermore does not consider the pipe whip nor jet impingement effects.

In a situation where an LBB analysis is only performed on the main primary piping but not on the auxiliary lines, the design basis circuit includes pipe breaks up to about 100 square inches. If the application of the LBB is extended to all auxiliary lines, as permitted by the modified "broad scope" GDC-4, the consideration of the dynamic effects of any pipe break shall be excluded from the design basis of the reactor coolant circuit. This would lead to an unacceptable safety loss in terms of core shutdown, core cooling and non-increase of the accident severity.

(Limited) Reevaluation of the Present Situation

Nevertheless a reevaluation of the conventional situation, i.e. before the amendment to the GDC-4, is deemed necessary and this leads to some suggestions for adjusting the mitigating measures. The key points of this reevaluation are :

(i) The protection against the pipe whip and impingement effects is somewhat theoritical. Pipe breaks occurring at locations different from the postulated locations cannot be excluded. Moreover experiments have shown that severance schemes different from the schemes postulated (circumferential or longitudinal break) can also be expected. The actual restraints are not demonstrated to ensure protection against breaks different from the postulated breaks with respect to location or severance scheme.

(ii) The assumed conventional opening time of 1 msec is very penalizing for the calculation of the blowdown loads and is also believed to be unnecessarily conservative. The use of more realistic opening times should lead to lower loads.

Acceptable Modifications to the Design Bases

The suggestions for adjusting the mitigating measures are based on :
(i) the acknowledgment that by removing the restraints and some of the snubbers, some of the construction features installed to ensure the non-increase of the severity of the event and the core cooling are eliminated,
(ii) the requirement that all the remaining features to mitigate the consequences of the LOCA shall be maintained because LOCA sources other than the primary pipe breaks and the related possible initiating events envelopped by the design basis LOCA are still to be considered.

The suggestions for adjusting the mitigating measures are :
(i) The LBB analysis can be considered as an acceptable method for removing the restraints. However some precaution against pipe whip and jet impingement effects resulting from primary pipe breaks remains required.
(ii) The LBB analysis can be considered as an acceptable method for not designing the heavy component supports (steel and concrete structure) to the postulated LOCA reaction loads. This may result in elimination or decrease in load rating of existing snubbers. However the ability of the component supports to avoid excessive distorsion of the reactor coolant piping under the dynamic loadings of the LOCA related possible events shall be maintained.
For plants initially designed for conventional LOCA breaks, the reactor cavity concrete structures and the steel supports of the heavy components are believed to have sufficient margin to accomodate any dynamic loadings during LOCA related possible initiating events.
(iii) The design basis of the reactor core and internals and of the steam generator tube bundle shall include the rapid rupture (opening time of 1 msec) of the steam generator manway covers (hot leg and cold leg) and a slow break (opening time of 3 sec) of one time the flow area anywhere in the primary coolant piping.
These breaks are postulated because they are physically acceptable and coherent with the design bases of the other ESF systems. They are also believed to induce hydrodynamic loads which cover the loads resulting from the full spectrum of the conceivable and realistic sources of LOCA in the reactor coolant pressure boundary other than the double-ended pipe rupture and to enveloppe the dynamic loads resulting from the LOCA related possible initiating events. They shall therefore be considered as design basis breaks for the reactor core and internals and the steam generator tube bundle.
(iv) The existing physical separation shall be maintained.

CONCLUSION : KEEPING THE GLOBAL SAFETY OF THE PLANT

The global safety of the plant should not be decreased. It is not believed that the removal of the restraints and of some of the snubbers after the LBB analysis of the primary piping reduces significantly the global safety of the plant. Some safety decrease at the third level of the defence-in-depth could be expected in the protection against the non-increase of the severity of the event or in the core cooling capability. However, as mentioned hereabove, the protection against the pipe whip and jet impingement effects by means of the actual restraints is somewhat theoretical and the structural capacity of the concrete and steel supports of the heavy components is not affected as long as their original design basis is maintained. A potential safety increase of the defence-in-depth can be expected from the removal of some of the snubbers and also to a certain extent (and with caution) by the LBB analysis itself.

Potential safety increase of the safety at the first level might be achieved by reinforcing the in-service inspection of the primary piping and at the second level by installing an improved system to detect or locate leaks from the primary circuit. Such requirements were however not imposed to the Belgian utility.

REFERENCES

[1] Modification of General Design Criterion 4 Requirements for Protection Against Dynamic Effects of Postulated Pipe Ruptures. *Federal Register*, Vol.51, No 70, published by the Office of the Federal Register, Washington, DC, 11 April 1986, pp.12502-5.
[2] WCAP-8082-P-A Pipe Breaks for the LOCA Analysis of the Westinghouse Primary Coolant Loop, January 1975.
[3] Modification of General Design Criterion 4 Requirements for Protection Against Dynamic Effects of Postulated Pipe Ruptures. *Federal Register*, Vol.52, No 207, published by the Office of the Federal Register, Washington, DC, 27 October 1987, pp.41288-95.
[4] Standard Review Plan ; Public Comment Solicited. *Federal Register*, Vol.52, No167 published by the Office of the Federal Register, Washington, DC, 28 August 1987, pp.33626-33.
[5] Leak-Before-Break Technology : Solicitation of Public Comment on Additional Applications *Federal Register*, Vol.53, No66, published by the Office of the Federal Register, Washington, DC, 6 April 1988, pp.11311-2.

INTEGRITY OF THE REACTOR COOLANT BOUNDARY OF THE EUROPEAN PRESSURIZED WATER REACTOR (EPR)

Requirements for the application of the break precluding concept for the main coolant lines

D. Goetsch (IPSN[1]) / K. Bieniussa (GRS[2]) / H. Schulz (GRS) / J. Jalouneix (IPSN)

1) INTRODUCTION

This paper is an abstract of the work performed in the frame of the development of the IPSN/GRS approach in view of the EPR conceptual safety features. EPR is a pressurized water reactor which will be based on the experience gained by utilities and designers in France and in Germany.

The reactor coolant boundary of a PWR includes the reactor pressure vessel (RPV), those parts of the steam generators (SGs) which contain primary coolant, the pressurizer (PSR), the reactor coolant pumps (RCPs), the main coolant lines (MCLs) with their branches as well as the other connecting pipes and all branching pipes including the second isolation valves.

The present work covering the integrity of the reactor coolant boundary is mainly restricted to the integrity of the main coolant lines (MCLs) and reflects the design requirements for the main components of the reactor coolant boundary. In the following the conceptual aspects, i.e. design, manufacture, construction and operation, will be assessed. A main aspect is the definition of break postulates regarding overall safety implications.

[1] Institut de Protection et de Sûreté Nucléaire, FRANCE

[2] Gesellschaft für Anlagen und Reaktorsicherheit, GERMANY

2) EPR PROPOSAL

2.1) Introduction

The EPR project proposes a concept which precludes any break for the main coolant lines (MCLs) of the primary circuit. This concept, sometimes referred to as "break preclusion", is expressed by EPR in the three following statements :

(a) a catastrophic failure of a main coolant line (MCL) is deterministically ruled out as a design event for the structures and components. Strictly speaking this is.the break precluding concept,

(b) additional engineering measures are implemented to harden some safety systems and some structures ; the fulfillment of the mitigation provisions necessary to ensure the main safety objectives (reactor shut down capability, decay heat removal and safe confinement of the radioactive materials) leads to defined design loading conditions using specific break postulates (see Table 1),

(c) breaks in branching lines for which the break precluding concept is not applied, are considered for the design of the systems, components and structures.

2.2) Basis and consistency of break precluding

For the designer, there are essentially two arguments which can support the option of precluding large breaks as stated above in (a) :

(1) any serious damage to the main coolant lines (MCLs) can be prevented with high confidence by design, high quality in manufacture, operation and surveillance measures,

(2) due to the design and construction measures of the main coolant lines (MCLs) which are of the same quality as for the main primary components including the reactor pressure vessel (RPV), a break can be ruled out.

The EPR designer would not consider postulated breaks of the main coolant lines (MCLs), only the mechanical consequences of pipe breaks in smaller lines, e.g. surge line and auxiliary lines, would be investigated. This approach is largely in compliance with current German practice but differs from current French practice.

2.3) Basis and consistency of break mitigation

In the EPR proposal, mitigation of the structural effects is based on the postulated guillotine break of anyone of the branching pipes. The safety objectives are to demonstrate :

- subcriticality by scram system (drop of a sufficient number of control rods),
- long term safe shutdown conditions,
- core coolability,
- non aggravation of the accident.

From the engineering point of view, the pressure drop forces resulting from the break of anvone of the branching lines will be applied to the mechanical components in a dynamic scheme to demonstrate that :

- the initiating break would not induce a failure of a main coolant line (MCL) or a break of another large branching line,
- the geometry of the internals of the reactor pressure vessel (RPV) would maintain the function with respect to the core coolability requirements,
- the geometry of the guide tubes would permit the control rods to be inserted,
- the reactor coolant pumps (RCPs) and the steam generators (SGs) as well as their internals and supports would remain intact (no consecutive rupture of the RCP shaft and no failure of the SG tubes).

2.4) Consistency of the additional measures

The designer proposes additional measures, implemented to "harden" the safety systems, the containment, the components and the civil engineering structures and respectively to stay with simple requirements for the designer (see Table 1) :

- the containment would withstand the pressure resulting from a 2 A-break (A as internal cross-sectional area of the main coolant line - MCL -),
- the Safety Injection System (SIS) would be functionally designed for breaks up to 2 A (e.g. flow capacity),
- the safety system components would be qualified for the ambient conditions resulting from a 2 A-break,
- the heavy components, their supports and the civil engineering structures surrounding the loops would be reinforced to limit the mechanical damage of a large pipe break within the loop compartment.

The first three conditions listed above are unchanged from the past practice. The engineering measures derived from the fourth one are expressed as follows :

- no mechanical damage would be transmitted to the intact loops ; the reactor pressure vessel (RPV) would be a fixed point and it would rest a strong support which "filters" the loads ; each primary loop would be surrounded by thick reinforced concrete walls which would prevent a missile to damage an intact loop or the containment,
- the stability of the steam generators (SG) would be such us to keep the displacements at the top small enough to prevent a failure of a main live steam line or a main feedwater line,
- the supports of the components and the civil engineering structures to which they are connected would be designed to absorb the loads resulting from an active static load P equal to $P = 2\,p\,A$ (p as reactor coolant system operating pressure and A as internal cross-sectional area of the main coolant line - MCL -). This $2\,p\,A$ load would be applied at every nozzle of the heavy components, colinearly with their centerline (one at a time and the pipe connected to the loaded nozzle is assumed to be failing).

3) ASSESSMENT OF THE EPR PROPOSAL

3.1) Architecture

The arrangement of the heavy main components and the architecture of the four loops would be based on the French N4 design which is similar to the German design.

3.2) Material selection

The material selection for the main coolant lines (MCLs) shows two options :

- forged low carbon unstabilized stainless steel (Z2 CN 19.10) with controlled nitrogen content, similar to the present French practice,
- forged ferritic steel (20MnMoNi55 = 16MND5) cladded with one layer of low carbon stabilized stainless steel, similar to the present German practice.

The material choice for the main coolant pumps shows two options : either forged ferritic steel (German practice) or cast stainless steel (French practice).

It must be noted that both options comprise dissimilar welds which require special attention with respect to fabrication and Non Destructive Examinations (NDEs) :

- in the present French plants, dissimilar welds are located at the connections of the main coolant lines (MCLs) (in stainless steel) with the main components (in ferritic steel). When using cast stainless steel for the main coolant pumps, there are - as part of the reactor coolant boundary - 16 locations of this type with a nominal diameter DN 750. A stainless steel ring called "safe end", is shop welded to each ferritic nozzle. The homogeneous weld between the main coolant line (MCL) and the safe end is made on site,
- in the present German plants, dissimilar welds are located at the branching of the main coolant lines (MCLs) (in ferritic steel) to the smaller auxiliary lines (in stainless steel). Altogether there are also 16 locations of this weld type : 1 for the surge line (less than DN 350 in the nozzle region), 8 for the safety injection system (DN 250), 2 for the spray system (DN 80) and 5 for the volume control system (four times DN 50 for the inlet and once DN 100 for the outlet). Precluding break for these smaller pipes is not included in the EPR proposal,

- the dissimilar welds would be made of Alloy 82 or Alloy 52. For both alloys, no case of in service degradation due to Primary Water Stress Corrosion Cracking (PWSCC) in nominal service and fluid chemistry conditions has been observed. However, experience with Alloy 52 is, so far, much more limited in service time[3].

3.3) Design and manufacturing

If the ferritic steel option is selected, the design and manufacturing aspects would retain minimization of welds and use of induction bent elbows with straight end parts and integrally forged large nozzles, according to the German practice. However, cladding would require suitable manufacturing lengths.

If the stainless steel option is used, the latest technology according to the present French practice would be retained. For example, hot and cold legs would be each manufactured as one part with integrated nozzles and integral bends. The cross over leg would consist of three parts. The qualification of such a prototypical forged stainless steel cold leg also with minimization of welds, use of induction bent elbows and integrally forged large nozzles, has been completed and accepted to be implemented for the Civaux 1 plant.

For both options, the mentioned design and manufacturing aspects intended for the main coolant lines (MCLs) are consistent with the latest state of the art in both countries and would result in an optimized piping design. Experience with the intended production technology is provided by the French and German practices.

3.4) Monitoring and surveillance systems

EPR intends to implement the following monitoring and surveillance systems to control components degradation and leakage :

- a transient bookkeeping system would be implemented for demonstrating the adequacy of design assumptions concerning the presupposed load histogram with respect to material damage due to stresses and fatigue. The current practice in France and Germany would be adopted :
  . monitoring of all thermal and pressure transients,

[3] It should however be noted that PWSCC has been observed in severe PWSCC laboratory testing on Alloy 82 as opposed to Alloy 52.

. identification and comparison of each actual transient to the reference design transients list,
. checking that transients occurred less than specified,

- a leak detection system would be installed in the compartments, in the sumps and on the heating, ventilating and air conditioning (HVAC) system using a combination of different sensors, detectors and measurements. A manual shutdown of the plant would be required if the leak cannot be localized nor isolated. The following requirements would be observed :
  . reliable detection of a leak before its size becomes critical,
  . use of two diverse and independent subsystems,
  . installation of alarms in the control room,

- the main parameters of the primary water chemistry (pH, boron content and hydrogen content) would be periodically monitored during normal operation and shutdown periods. The other parameters (e.g. lithium, chlorides and fluorides) would be periodically checked by chemical analysis. The chemical parameters to be analyzed, their operational limits and analysis frequencies, have not been yet fully defined,

- it would be favored that further monitoring systems will all be applied in the EPR design, e.g. loop displacement control, vibrations control of pump shafts and temperature - pressure of the volume between the first and the second isolation valves.

3.5) In Service Inspection (ISI)

Typical areas for inspection are

welds and piping parts with the highest fatigue usage factors.

The detailed program for In Service Inspection (ISI), i.e. where, how and when are the main coolant lines (MCLs) to be inspected, is not yet available. However the following principles are adopted by the designer :

- design and manufacture allowing inspectability of all parts as a principle with ALARA personnel exposure,
- implementation of inspection at locations with high stress level.

For volumetric examination, the following methods are foreseen by the designer :

- ferritic lines would be examined using ultrasonic methods and if necessary, radiography (welds at the reactor coolant pumps (RCPs) if using cast stainless steel),
- stainless steel lines including the dissimilar welds would be examined using ultrasonic methods and if necessary, also radiography for the dissimilar welds.

A focused In Service Inspection (ISI) program is an essential requirement for the acceptance of the break precluding concept.

The proved inspectability of ferritic steels by Ultrasonic examination Techniques (UT) allowing for defects detection and sizing constitutes one major feature for this class of material. UT examination of stainless steels is more difficult. Therefore, concerning UT examination of stainless steels, it would be mandatory to perform as early as the welding qualification process, a Non Destructive Examination (NDE) qualification, which should particularly take into account the metallurgical structure.

For cladded ferritic steel, the large cladded area with one layer of stainless steel might be a preferential zone for underclad defects and at least an adequate inspection at manufacturing (outer and/or inner inspection) is necessary. However, taking into account the validated material and manufacturing technology and results of the Non Destructive Examinations (NDEs), to date no problem appears in German nuclear plants.

For both materials, the stainless steel and the ferritic steel, as well as for the dissimilar welds, it appears necessary to use optimize UT performances by taking into account geometric factors, i.e. small dissimilar welds located at the branching of the main coolant lines, small diameter component, mismatch, thermal sleeves, fillet, surface condition and counterbore.

In Service Inspection (ISI) would cover visual, surface and volumetric examination. As a rule for ALARA personnel exposure and reproductibility of test results, visual and volumetric examinations should be performed using adequate handling techniques. The In Service Inspection (ISI) program would integrate feedback (e.g. In Service Inspection (ISI) results and feedback from similar plants), load/stress level (e.g. stresses and usage factors, geometrical discontinuities) and manufacturing (e.g. dissimilar welds). However, the influences due to the real loads and operating conditions would have to be covered for example by additional instrumentation. Influences coming from uncertainties in manufacturing, e.g. new materials and new welding techniques, would have to be eliminated by approved manufacturing techniques.

Due to the present limitations of some techniques to suitably and reliably detect cracklike defects (specially in stainless steels), it would be required to implement an additional detection method sensitive to surface defects.

3.6) Fracture mechanics methodology

3.6.1) EPR PROPOSAL

According to the EPR proposal, the demonstration of the controlled failure behavior of a structure, here of a selected part of the main coolant line (MCL), can be done either based on results of experiments with original pipe elements, or by using a verified fracture mechanics methodology.

The methodology based on fracture mechanics considers the crack growth of different crack configurations, and finally deduces the corresponding leak rates which have to be detected, taking into account a considerable margin before reaching critical crack sizes.

3.6.1.1) CONSIDERATION OF SURFACE DEFECTS

For selected surface reference defects, it has to be demonstrated that they do not grow significantly during the plant life. After crack growth, the final crack must be stable under the most severe transient load combination.

Reference defects are only considered in welds. Internal, elliptical surface defects, oriented in circumferential direction, are postulated having the depth "a" and the total length along the surface "2c". Two reference defects are investigated :

- the "envelope defect" resulting from a lack of fusion of layers which corresponds to the detection limit of the applied non destructive testing method,
- the "conventional defect" is twice as long as the envelope defect and mainly used for sensitivity studies.

The reference data must be identified on the bases of manufacturing processes and performances of inspection methods, e.g. reflecting local limitations of the Non Destructive Examinations (NDEs), as well as taking into account the operating feedback, e.g. corrosion of dissimilar welds and underclad defects of the main coolant lines (MCLs).

Fatigue crack growth computation of the surface defect is performed using the Paris formula and considering the transients under normal, upset and faulted operations.

The acceptance criteria taken into account for the end of life crack size are as follows :

- the "envelope defect" crack growth is small. Final size is less than twice the initial defect or less than 1/4 of the wall thickness of the considered pipe,
- the "conventional defect" crack growth is be such that it does not become through-wall before the end of plant life.

3.6.1.2) COMPARISON WITH THROUGH-WALL CRITICAL CRACKS

For the component geometry with the reference defects, the through-wall critical crack length is calculated using the worst loading case. Furthermore, the designer proposes to demonstrate that, if a reference defect is submitted to specified loadings, as much as necessary to grow through the wall, this defect leads to a smaller than the critical through-wall crack. This crack is called the "leakage crack".

The acceptance criterion taken into account by the designer requires a factor of 2 on the length of the "leakage crack" size when comparing with the length of the through-wall critical crack size. No safety margin is judged necessary between the "leakage crack" leak rate and the leak detection system proven capability.

3.6.2) ASSESSMENT BY IPSN/GRS

IPSN and GRS consider that the following topics are important and should be implemented in the design :

- the sensitivity of the leak detection system must be such that it is possible to detect with high confidence a guaranteed leak rate, here called "detection leak rate",

- the "leakage crack" as defined by the designer would not lead to a leak rate because this "leakage crack" is only the reference crack which has just grown through the wall ; the length of such a "leakage crack" can be zero on the opposite wall ; a clear definition, possibly conventional, must be given for this "leakage crack" precising the length which must be achieved after growing to the opposite wall, a significant safety factor must be introduced between this new defined "leakage crack" leak rate and the "detection leak rate",

- the crack opening displacement and area as well as the leak rate must be calculated with qualified models which are or will be verified or calibrated with experiments,

- a set of conservative assumptions must be selected to yield a lower bound of the leak rate,

- the crack growth analysis through the wall has to be performed by applying loadings whose stress fields contribute preferably to the lateral extension of the defects,

- transient loading conditions have to be included,

- margins in terms of loadings must also be considered, first on the "leakage crack", then on the critical through-wall crack. These two margins work in an opposite way and must be defined carefully especially concerning the "leakage crack" and the corresponding leak rate.

The assessment will be complemented after the designer will have provided a complete and detailed file describing the concrete application of this methodology to the EPR primary coolant boundary, including these topics.

4) POSITION TAKEN BY THE GERMAN AND FRENCH SAFETY AUTHORITIES

The justification elements in support of the break precluding concept for the main coolant lines (MCLs) as presented by the EPR project have been assessed by GRS/IPSN and reviewed commonly by the two advisory groups of experts - GPR (Groupe Permanent charge des Réacteurs nucléaires) for France and RSK (Reaktor Sicherheitskommission) for Germany. The common conclusions of the two groups are the following :

"Considering the state of technology, it appears feasible to design and to operate future PWR plants so as to "*exclude*" the complete guillotine break of a main coolant line (MCL) ; but it is stressed that the applicant has to precise the provisions he will implement for these lines at an early stage of the design, notably concerning the monitoring of the primary leaks and the In Service Inspection (ISI) of the lines (the accessibility and the inspectability of each point of these lines are of course prerequisites).

The loads to be considered for the design of the internal structures of the reactor vessel and for the design of the structures in the containment building can be limited to those resulting from a break equivalent to the complete guillotine rupture of the largest pipe connected to the main coolant line (MCL) (surge line).

It is however recalled that the mass flow equivalent to a double area opening of the main coolant line (MCL) has to be assumed for the design of the emergency core cooling function and of the containment pressure boundary, so as to implement safety margins concerning the cooling of the core to prevent core melt and concerning the containment function ; the double area opening is also to be assumed for the supports of the components and for the qualification of equipment.

These recommendations have been agreed on November 2, 1994, by the common structure set up by the German and French safety authorities, called DFD (Deutsch Französischen Direktionsausschuss).

TABLE 1 : Postulated Pipe Breaks and Associated Effects for Main Coolant Lines

Effects		Postulated pipe break size
on	**of**	
GLOBAL DESIGN :		
• performance of safeguard systems, e.g. : - safety injection system, - residual heat removal system.	Loss of coolant.	≤ 2 A (MCL)
• design of containment.	Pressure build-up, temperature.	2 A (MCL)
• environmental qualification of equipment, e.g. : - instrumentation, - electrical components.	Pressure, temperature, flooding / humidity, radiation.	2 A (MCL)
LOCAL DESIGN :		
• design of containment, internal structures, e.g. : - reactor cavity, - missile shield, - compartments.	Flooding, differential pressure, temperature, supports loads.	2 A [4] (MCL)
• stability of supports of main components, e.g. : - reactor pressure vessel, - main coolant pump, - steam generator, - pressurizer.	Fluid discharge forces : P = 2 p A.	A (considered line), p (operating pressure).
• design of internals of primary components and MCLs, e.g. : - reactor pressure vessel, - pump flywheel, - steam generator, - piping and valves.	Dynamic effect of pressure drop.	The larger value of 0.1 A (MCL) and A (connected line).
• withstanding thrust and reaction, forces for : - surrounding walls, - target components, - piping supports.	Jet impingement, fluid discharge forces.	The larger value of 0.1 A (MCL) and A (connected line).
DEFENSE IN DEPTH :		
• postulates for studies within the frame work of severe accidents, e.g. the consideration of a failure of the reactor coolant boundary, will be discussed in other working groups.		

[4] consideration of guard pipes or restraints for pressure build-up in reactor cavity

Session 1: Status of LBB Applications

Paper 04:

The Evolution of the Break Preclusion Concept for Nuclear Power Plants in Germany

Helmut Schulz
Gesellschaft für Anlagen- und Reaktorsicherheit (GRS) mbH,
Schwertnergasse 1, 50667 Köln, Germany

Summary

In the updating of the Guidelines for PWR's of the "Reaktor-Sicherheitskommission" (RSK) in 1981 the requirements on the design have been changed with respect to the postulated leaks and breaks in the primary pressure boundary. The major change was a revision in the requirements for pipe whip protection. As a logical consequence of the "concept of basic safety" a guillotine type break or any other break type resulting in a large opening is not postulated any longer for the calculation of reaction and jet forces.

As an upper limit for a leak an area of 0,1 A (A = open cross section of the pipe) is postulated. This decision was based on a general assessment of the present PWR system design in Germany.

Since then a number of piping systems have been requalified in the older nuclear power plants to comply with the break preclusion concept. Also a number of extensions of the concept have been developed to cover also leak-assumptions for branch pipes. Furthermore due considerations have been given to other aspects which could contribute to a leak development in the primary circuit, like vessel penetrations, manhole covers, flanges, etc.

Now the break preclusion concept originally applied to the main piping has been developed into an integrated concept for the whole pressure boundary within the containment and will be applied also in the periodic safety review of present nuclear power plants.

1 Reflections on the Historical Background

The concept of the so-called "design basis accidents" was developed in the 60ies when the design of commercial nuclear power plants started. So we are looking back only 30 years in time, but this has been a span of tremendous technological developments being triggered by the first decisions to develop large light water reactor nuclear power plants. At the moment the nuclear community has to find its way to enter the next decade with nuclear power plants which fulfil both main requirements: enhanced safety and increased competitiveness. So it is the right time to review decisions and developments to be prepared for the future.

When the designers in the 60ies were confronted with the question, what should be the largest leak to be covered by the design of the safety system in a nuclear power plant, we all know they decided to select a large break of a pipe as a postulated event. But they also decided at the same time that the available technology to build large vessels is sound enough to rule out an uncontrolled fracture of such vessels. At that time this was a rather courageous decision regarding the vessels. As we have seen the uncertainties connected to this decision have led to a number of long-going research programs on pressure vessel integrity to support this. The results of these research activities gave a lot of valuable input into the questions of piping integrity.

In the 60ies and 70ies the design of nuclear power plants was largely effected by the postulated piping failure of the main primary pipe. Historically the postulated piping failure was first the design basis to set the maximum pressure and temperature loads for the containment. In a second step the emergency core cooling systems were designed according to this postulate. This development was followed by a steadily increasing effort to analyse the system behaviour in case of a pipe rupture with respect to the reaction forces and mechanical damage due to pipe whip as well as the differential pressures between the compartments of the containment internal structures. This resulted in an enforcement of internal structures of the containment as well as internal structures of the primary pressure boundary for example the internals of the reactor pressure vessel and steam generators. To avoid mechanical damage caused by a whipping pipe restraints were designed and applied at several locations of the primary piping. These engineered safeguards were extended to all high energy piping wherever safety related items had to be protected.

At the same time we have also experienced that the different disciplines performing the design and review work in the organisations have developed requirements and criteria in the area of their responsibilities which may be judged today as not being coherent in all aspects. So specialists working in the mechanical branch found themselves in a situation that an increasing amount of engineered safeguards against the postulated double ended pipe rupture were required by the specialists of the accident analysis branch at a time where they themselves gained a better understanding and an increasing knowledge of the influencing factors to produce a high quality product and to analyse the overall system behaviour to an extent that a gross failure of a pipe could be ruled out.

Beside all the important knowledge we have gained in design work, fabrication and laboratory tests we have to admit that the operating experience is the most valuable source in the review of technical progress. The careful analysis of operating experience shows us that a number of damage mechanisms occured which we have not thought of, but it also demonstrates how the technical problems can be controlled or avoided by different solutions.

2 Basic Elements of Integrity Assessment

The basic elements in the assessment of the integrity of components are sufficient knowledge

- of the materials and component structures regarding material composition, mechanical properties as well as geometries,
- of the load conditions including environmental influences,
- of defects at the surfaces or contained in the volume of the structure.

At present we are performing integrity assessment mostly in the course of periodic safety reviews. So the following paragraphes include these aspects.

In the characterization of the **material condition** influences resulting from the manufacturing process as well as the operational aspects have to be considered. It has become popular to use the term "aging" for time-, temperature- or environment-related

degradation of material- or component conditions. With respect to the material properties it has to be discussed for each individual material if in the range of the service condition precipitation or diffusion related phenomena can cause changes in properties. Such changes have to be expected in areas of high neutron flux as it is known generally. Degradation in material toughness due to temperature effects only have been experienced for castings being manufactured out of non-stabilized austenitic steel. Investigations being performed on materials used for the pressure boundary components in German LWRs in general have not shown any significant change in material properties for more than 100.000 hours. The measured values have been almost within the scatterband of the technical acceptance test during manufacturing. Beside the already mentioned influence of the neutron exposure it is important to note that a plant specific review sometimes identifies one or two components or parts of components where a specific alloy has been applied where temperature effects over a long exposure time may need to be considered. Specific difficulties may also arise due to a lack of detailed information in the documentation regarding heat treatment conditions, trace elements in the chemical composition or on microstructure.

For the characterization of the **component structure** the most important aspects are the as built conditions regarding weld geometries, misalignment, thickness of cladding, etc. Specifically in some older units it may be difficult to find all necessary details in the documentation, so additional measurements are sometimes necessary.

In the design of systems and components for nuclear power plants a great effort is directed to the **analysis of loads** for all operational and emergency conditions. Even extreme load conditions are included in these analyses. The detailed evaluation of the operating experience demonstrate very clearly that significant phenomena like thermal stratification have been greatly underestimated in the design stage with respect to the local loads. Also dynamic effects due to variation in valve closure times or system conditions which led to condensation phenomena leading to acceleration of fluids and dynamic pulse loads have been identified as important aspects. In the estimation of real safety margins it is necessary to characterize limiting loading conditions.

Regarding the **environmental conditions** (temperature, water chemistry, neutron exposure, etc.) most emphasis has to be placed to characterize the water chemistry conditions with sufficient accuracy. It is usually not the bulk chemistry at normal operation which is the cause for corrosive attack, in most cases specific conditions (accumula-

tion of impurities, intermediate temperatures) related to certain operational modes or system malfunctions may create locally unfavourable conditions which together with specific local stress condition initiate corrosion assisted cracking. Experience shows that enhanced monitoring methods are a valuable tool to adjust operational procedures to decrease at least the frequency of occurance or better avoid unfavourable conditions.

Regarding the **detection and sizing of defects** in the structure it is difficult to characterize the reliability of NDE in general terms. First of all we have to realize that the accessibility for inspection may be locally restricted in the plants. In the German codes, standards and guidelines considerable attention has been given to these aspects to force the designer of the component as well as of the plant layout in the direction to allow full accessibility for the application of non-destructive methods. Further important items are the acoustic properties of the material itself as well as the arrangement of the welds. Limitations still exist in the application of ultrasonic methods to welds in austenitic materials. The experience with inservice inspections demonstrate that in these cases acceptable results are achieved by the complementary application of ultrasonic and radiographic methods.

It is present practice in the integrity assessment of components to supplement the regular stress analyses in specific cases with a **fracture mechanics analysis.** In principle any analysis is always connected to defined damage mechanisms like plastic collapse, fatigue, cleavage fracture, stress corrosion cracking, erosion, etc. So the identification of the failure mechanisms for which the analyses have to prove that protection is given and of the related boundary conditions is the difficult task in the assessment procedure.

3 Evaluation of Operating Experience with Respect to Damage and Leaks

An important part in integrity assessment is the review that all the damage mechanisms which may act in the different systems are clearly identified.

A general evaluation of the operating experience with pressure boundary components in German LWR systems demonstrates that the number of crack-like defects or leak-

ages is generally very small /1/. A basis for this review are the incident reports which identify all abnormal occurrences as well as unexpected indications in the inservice inspections or in the course of maintenance and repair work. The following paragraphs are more or less limited to defects and leaks being detected in the non-isolable area of the pressure boundary of PWR plants. The figures themselves are showing the distribution of the different issues investigated for the nuclear steam supply system.

Fig. 1 shows the distribution of failures/defects according to the different failure categories. The failure categories are defined as:

- through-wall cracks with leakage,
- break with leakage,
- leakage at gaskets,
- defects which gave reportable signals above registration limits during ISI, but are not penetrating the wall.

It is clearly seen that the fraction of "breaks" is very small and, which is more important, all these incidents are connected to pipes of less than 30 mm diameter. The small fraction of the category "defects" needs further comments. Present practice for inservice inspection requires mainly non-destructive testing of pipe welds with diameters above 200 mm. There might be an unknown population of defects contained in smaller piping which could lead to a different distribution. But additional information available from destructive test of replaced small bore piping does support the present view that the number of defects is very small.

For BWR piping the picture is quite different. Due to the very high percentage of defects caused by intergranular stress corrosion cracking the fraction of this category is very large. But none of these cracks has penetrated the pipe wall. All of the BWR piping being affected are replaced, using low carbon stabilized austenitic steel and special welding techniques. So a distribution being established for the past experience can not be used to establish relationships for the present situation.

Fig. 2 shows the distribution according to the causes of failures. The fraction attributed to the individual cause contains a certain degree of expert judgement. The reason for this is that in many cases different causes are participating to a failure. It also has to

be mentioned that certainly in the small bore piping area very detailed investigations are often not performed because of the limited safety implications.

Fig. 3 shows the distribution of the location of damage. It is clearly seen that the majority of the damages is related to welds. The fraction of damage related to base metal is mainly connected to stress corrosion cracking in small bore piping where accumulation of condensate at areas without insulation takes place. The fraction related to gaskets is probably a too low proportion, because not all the gasket leaks are within the limits of reportable events.

Looking again at the distribution of damages related to the size of the pipes as it is shown in the figures it clearly demonstrates that within the German operating experience for PWR's leaks have occurred only in small bore piping. If we look at cracks as being precursors of leaks we also see that the number of cracks is very limited. Including the information from the destructive testing of replaced piping one can state that leaks and cracks in the non-isolable portion of PWR's are very rare events. The results of such evaluations can be used to optimize requirements regarding

- quality assurance,
- inservice inspections,
- monitoring and surveillance methods including leak detection,
- operational procedures.

Furthermore such results are used in the integral assessment of piping reliability and estimation of frequency of leaks.

4 Results of Relevant R&D-Programs.

Within the German reactor safety research program continued effort was given over the last 20 years to develop and verify methods to describe the limit load behaviour of components as well as the resistance of the component to various types of fractures /2, 3/. Within the program a large number of small and large scale tests hase been performed including system tests for extreme load conditions as caused by external and internal events. Similar, R&D-efforts have been performed within the USNRC "De-

graded Piping Program", the NUPEC program in Japan, the ENEA program in Italy and last but not least the IPIRG program. Together this gives a huge amount of available experimental data. A large portion of this is summarized in figs. 4 to 8. These figures clearly indicate that a variation of crack dimensions and locations as well as through-wall-cracks have been investigated. Regarding the crack direction longitudinal as well as circumferential cracks are contained. Also complex geometries like bends and branches are included in the investigations. It is not the objective of this paper to review all the available research data, but it is important to note that for the verification of the LBB procedure a large experimental basis is given. Experiments being available from other technical areas like gas-pipeline industries are additional sources.

The results of the R&D program can be generalized in my view as follows:

- A large load carrying capacity has been demonstrated for pipes showing severe partly through or through-wall cracks.
- The fracture toughness of the material being used for piping where the LBB approach is applied is sufficiently high to exclude cleavage fracture at low stress condition and shows in most cases a fracture mode started by stable crack growth or plastic instability.
- The analysis methods being applied to calculate limit load conditions are verified on a large number of experiments, although the results are not consistent in every case.

5 Break Preclusion Concept and its Application

The break preclusion concept was developed in the late 70ies and finalized in the updating of the guidelines of PWR's of the Reaktor-Sicherheitskommission (RSK) in 1981 /4/. The underlined technical thinking and basis was published many times /5, 6, 7, 8/. Regarding the postulated leaks and breaks in the primary pressure boundary to be used in the accident analysis the major change was the revision in the requirement for pipe whip protection. For practical reasons an upper limit for a leak area of 0.1 A (A = open cross section of the pipe) was chosen. This decision was based on a general assessment of the present PWR system design in Germany. The major principles applied in this concept are summarized in Fig. 9 It reflects the present position of GRS

as it is applied in safety reviews and does include the experience gained in the course of requalification of piping systems in older units. Without going into technical details which are taken up by other papers in this conference I would like to summarize the 15 years of experience in the application of the break preclusion concept for PWR plants as follows:

- The break preclusion concept is applied generally to the large diameter primary piping and the branch connections down to a size of 200 mm diameter. In specific cases the concept was extended to pipes down to a size of about 100 mm diameter requiring additional analyses, load monitoring, and leak detection.

- The concept has been successfully applied in the requalification of primary piping in older units. The requalification is performed on a plant specific basis. Difficulties experienced in the requalification are: unfavourable weld misalignments caused by larger tolerances on diameter, ovality and wall thickness together with short bends being used; missing information in the documentation regarding certain material properties; reevaluation of load tables used in the design with special emphasis on past experience regarding thermal stratification and water hammer loads.

- Shortcomings identified in the plant specific reviews regarding base-line information or local stress conditions could be balanced in most cases by additional surveillance and inspection requirements. In specific cases replacement of pipe sections have been performed.

- For boiling water reactors a large portion of piping had to be replaced due to the specific problem of intergranular stress corrosion cracking which took unexpectedly place even in stabilized austenitic piping. The sensitization was restricted to the heat-affected zone and there only in local areas.

6 Further Steps towards an Integrative Approach to Assess the Reliability of the Primary Pressure Boundary

The basic idea behind the postulated leaks and breaks in the primary piping was the definition of design basis accidents for the whole pressure boundary. If the break preclusion or the leak-before-break concept is applied to limit the leak size in the primary piping we have to analyse the whole pressure boundary again in view of the

"Defence-in-Depth" principle and the safety goals. In this respect we have to demonstrate that the results of the deterministic approach and probabilistic analysis are consistent. This means if we claim that a sound basis is given to limit the leak size by the application of the LBB-approach we have to proof also by the best methods available that a very small probability for example less than 10^{-7} is justified on a probabilistic basis /9, 10/..

It is a common understanding that ample safety margins are available regarding the integrity of the large vessels, housings and castings in the pressure boundary. Limited leaks within these components have been covered implicitly by the postulated guillotine type rupture of the primary piping. It has to be realised that in the definition of leak sizes nozzles and penetrations at vessels have to be included in the evaluation.

For the sake of consistency we also have to demonstrate that the integrity of the primary pressure boundary is not jeopardized by other events which may initiate failures at higher frequencies. This means for example that a pipe failure due to load drop events or due to earthquake is a negligible quantity in the same sense as identified before. It also has to be demonstrated that damage mechanisms which could lead to a large failure of bolted connections (man-hole covers, flanges etc.) can be ruled out or being identified early enough. Furthermore pipe failures between the first and second isolation valve have to be negligible quantities too in connection with the reliability of the valve itself. It is important to note that low power and shutdown modes of operation have to be included in all investigations of the integrity of the pressure boundary. If accident management procedures are developed any negative impact on the pressure boundary integrity has to be limited.

Most of the aspects mentioned before are covered by certain requirements either in the codes and standards for the components, system requirements or being addressed in the surveillance or inservice inspection and plant monitoring in general. To achieve a consistent and balanced approach it is proposed to classify leaks according to their origin or causes. Fig. 10 shows an example of leak categories as it is applied presently by GRS. This integrative approach does combine component related analysis with system related effects. The leak sizes being derived by this approach do reflect the plant specific conditions, operating experience as well as experience from safety reevaluations.

7 References

/1/ Bieniussa K., H. Reck
Evaluation of Piping Damages in German Nuclear Power Plants
to be published in NED

/2/ Statusreport on Reactor Pressure Vessels
Volume 2, December 1976
Institut für Reaktorsicherheit (GRS)

/3/ MPA-Seminars, Safety of the Pressure Boundary of
Light Water Reactors
Seminar 1-8 1974-1982
Staatliche Materialprüfungsanstalt
Universität Stuttgart

/4/ RSK-Guidelines for Pressurized Water Reactors,
3rd Edition, Oct. 14. 1981,
Gesellschaft für Reaktorsicherheit (GRS) mbH

/5/ Kussmaul K., Blind D.:
"Basic Safety - A Challenge to Nuclear Technology"
IAEA Specialist Meeting, Madrid, 5-8 March 1979

/6/ Kussmaul K. et.al.:
Exclusion of Fracture in Piping of Pressure Boundary
Part 1: Experimental Investigations and Their Interpretation
International Symposion on Reliability of Reactor Pressure
Components, IAEA - SM - 269/7
Stuttgart, 21-25 March 1983

/7/ G. Bartholome´et.al.:
Exclusion of Fracture in Piping of Pressure Boundary
Part 2: Application to the Primary Coolant Piping
International Symposion on Reliability of Reactor Pressure
Components, IAEA - SM - 269/7
Stuttgart, 21-25 March 1983

/8/ H. Schulz:
Current Position and Actual Licensing
Decisions on Leack-Before-Break in the Federal Republic
of Germany, Monterey, 1-2 September 1983 CSNI Report
No 82, NUREG/CP-0051

/9/ H. Schulz:
Latest Development of LBB Policy and Future Subjects
in West Germany
Leak-Before-Break Seminar, May 14-15, 1987, Tokyo

/10/ S. Beliczey, H. Schulz:
Comments on Probabilities of Leaks and Breaks of
Safety-Related Piping in PWR Plants
Int. J. Pressure Vessels & Piping 43 (1990) 219-227

Fig. 1: Evaluation of Piping Incidents of Nuclear Heat Generation- Systems in PWRs Plants, Form of Damage

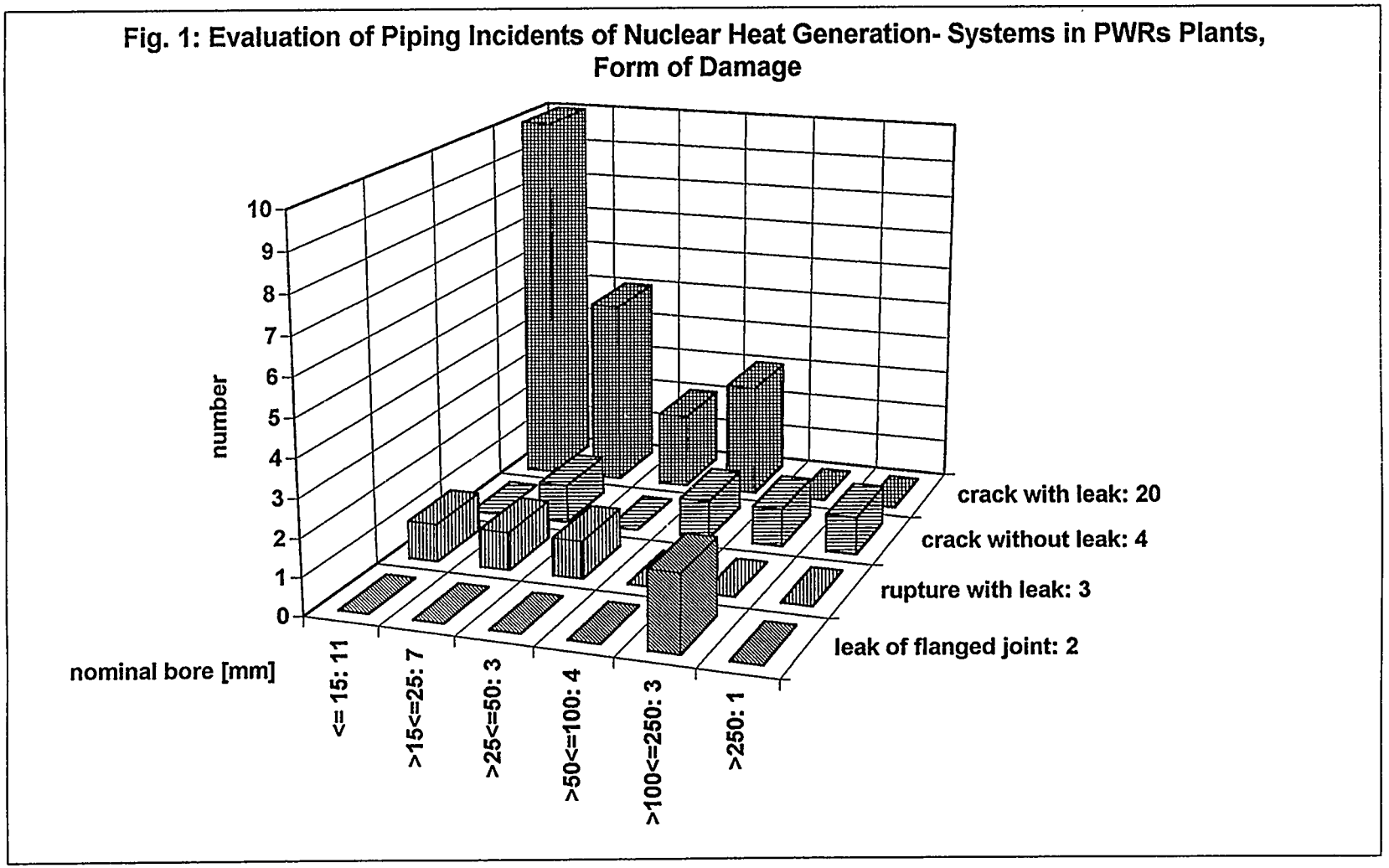

Fig. 2: Evaluation of Piping Incidents of Nuclear Heat Generation- Systems in PWRs Plants, Cause of Damage

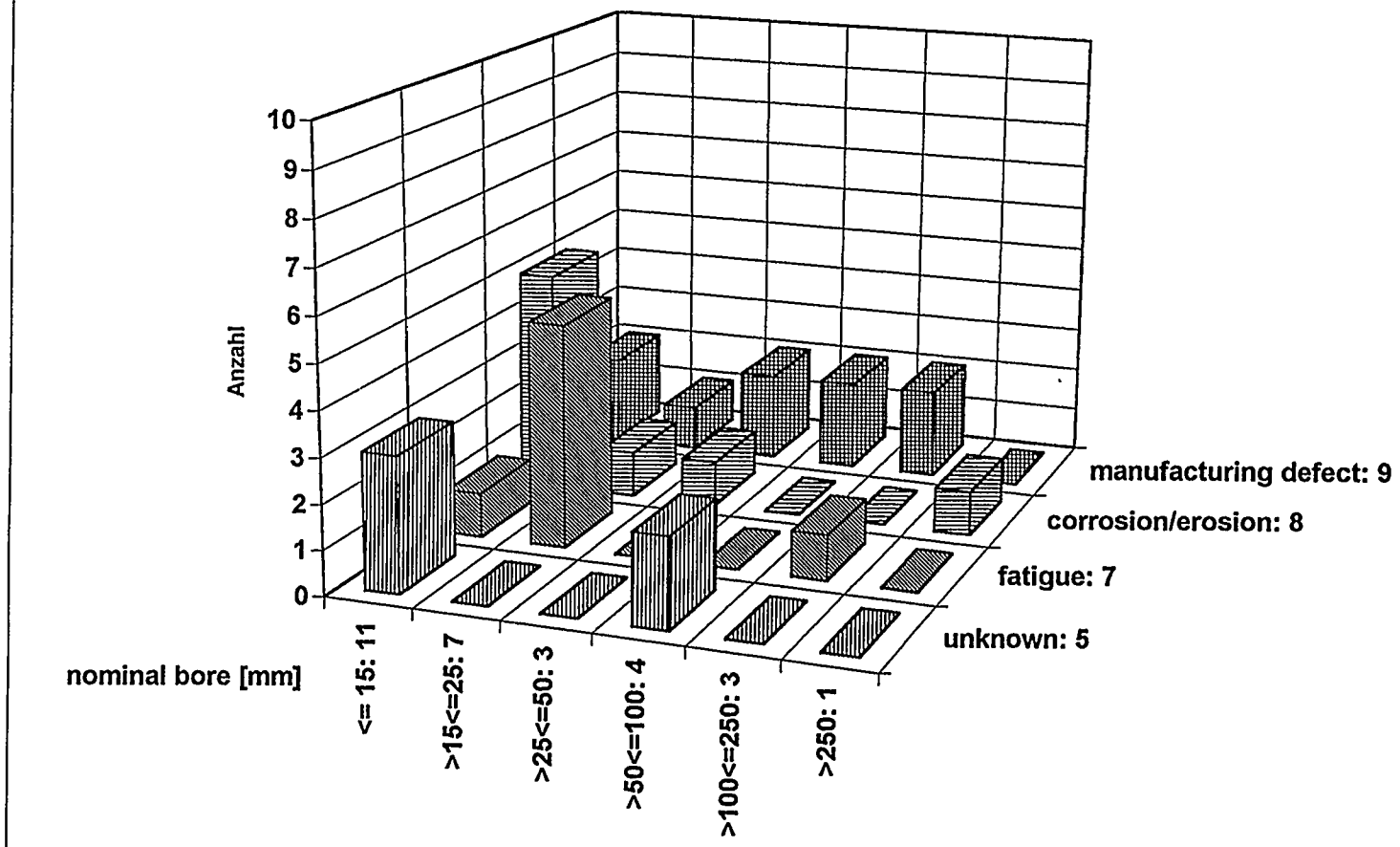

Fig. 3: Evaluation of Piping Incidents of Nuclear Heat Generation- Systems in PWRs Plants, Location of Damage

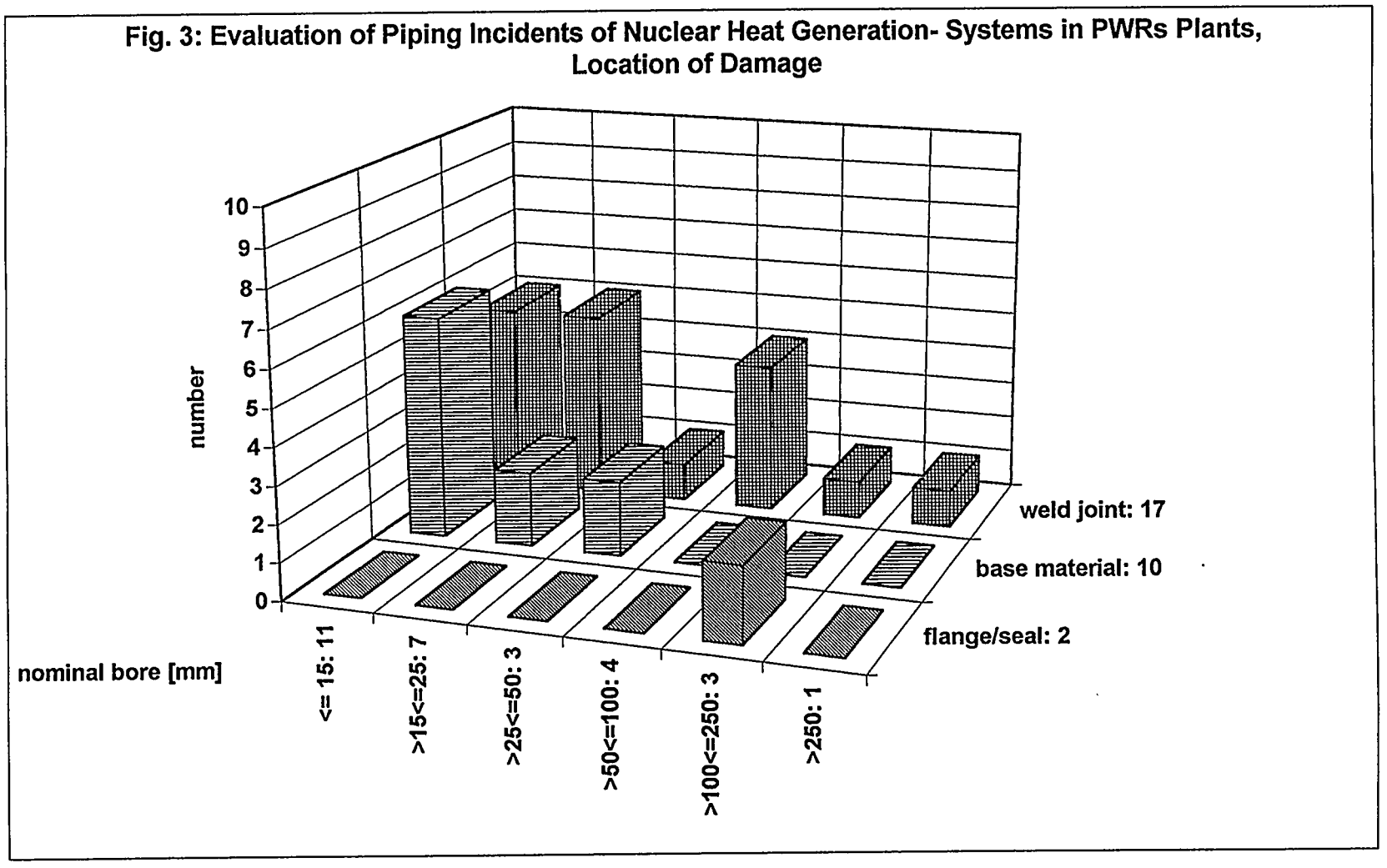

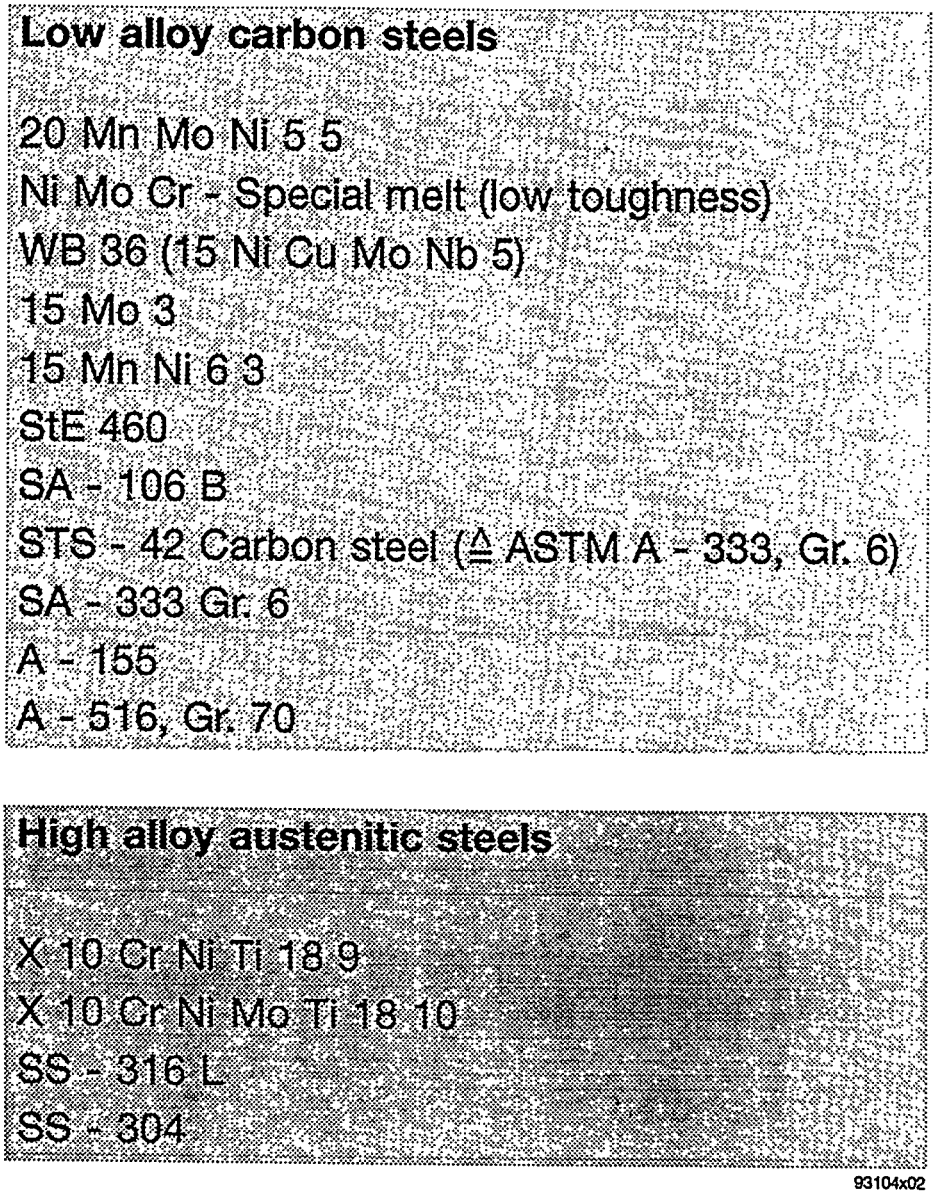

Fig. 4: Selection of Available Fracture Mechanics Experiments: Material Used

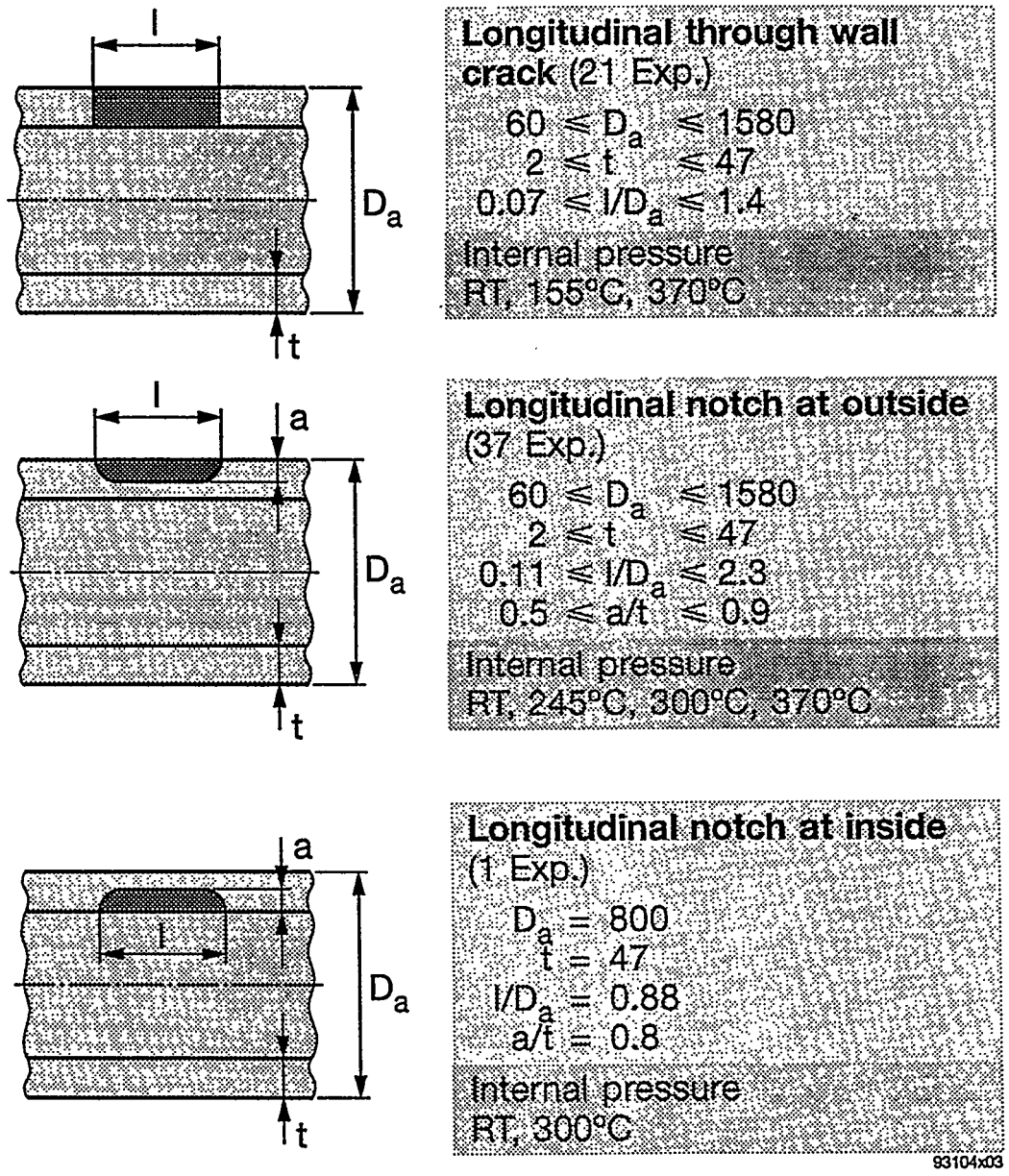

(MPA, Siemens, BAM, TÜV Essen)

Fig. 5: Selection of Available Fracture Mechanics Experiments: Longitudinal Cracks in Straight Pipes

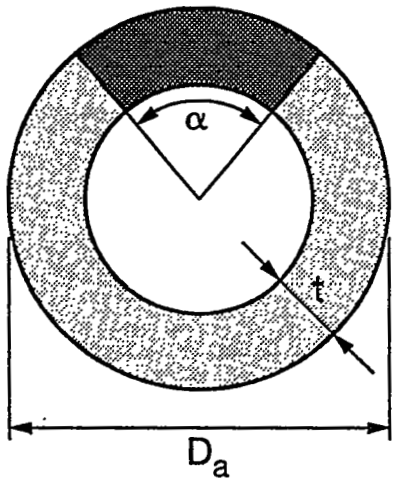

Circumferential through wall cracks (110 Experiments)

$34 \leq D_a \leq 1066$

$2 \leq t \leq 47$

$20° \leq \alpha \leq 190°$

Internal pressure, bending, cyclic load, dynamic load

RT, 130°C, 280°C, 300°C, 370°C

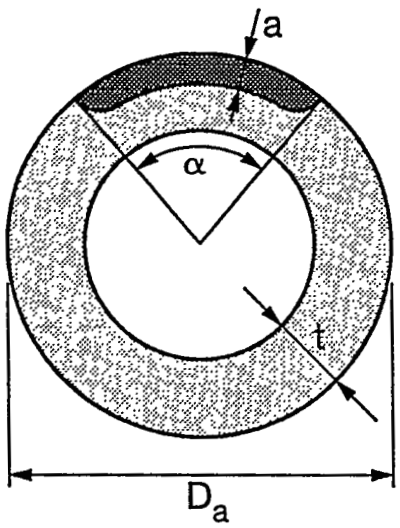

Circumferential notch at outside (59 Experiments)

$60 \leq D_a \leq 880$

$2 \leq t \leq 47$

$20° \leq \alpha \leq 360°$

$0.1 \leq a/t \leq 0.9$

Internal pressure, bending, cyclic load, dynamic load

RT, 80°C, ~ 300°C, 370°C

93104x04

(MPA, Siemens, BAM, PHDR, ENEA, Battelle, Japanese Exp.)

Fig. 6 : Selection of Available Fracture Mechanics Experiments: Circumferential Cracks in Straight Pipes (Part 1)

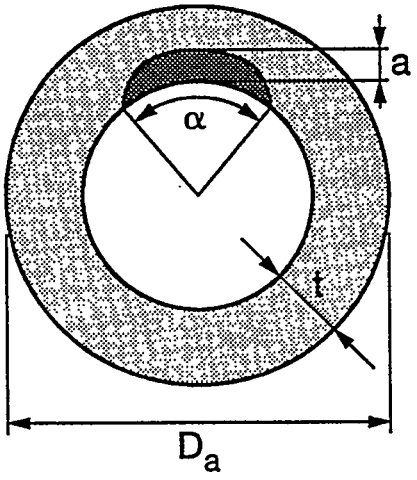

Circumferential notch at inside (62 Experiments)

$76 \leqslant D_a \leqslant 800$

$7 \leqslant t \leqslant 47$

$30° \leqslant \alpha \leqslant 360°$

$0{,}25 \leqslant a/t \leqslant 0{,}9$

Internal pressure, bending, cyclic load, dynamic load

RT, ~ 300°C

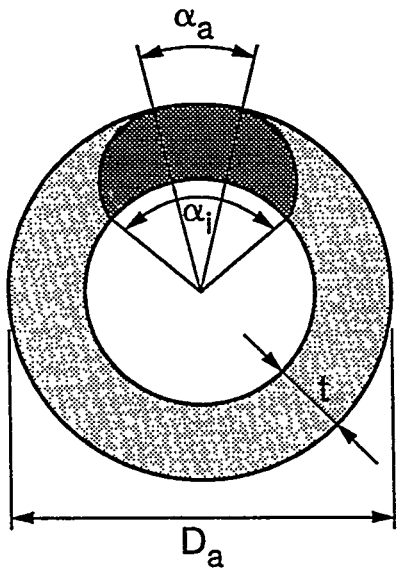

Complex crack shape (17 Experiments)

$89 \leqslant D_a \leqslant 457$

$5 \leqslant t \leqslant 26$

$90° \leqslant \alpha_i \leqslant 360°$

$28° \leqslant \alpha_a \leqslant 93°$

Internal pressure, bending

RT, ~ 300°C

93104x05

(MPA, Siemens, BAM, PHDR, ENEA, Battelle, Japanese Exp.)

Fig. 7: Selection of Available Fracture Mechanics Experiments: Circumferential Cracks in Straight Pipes (Part 2)

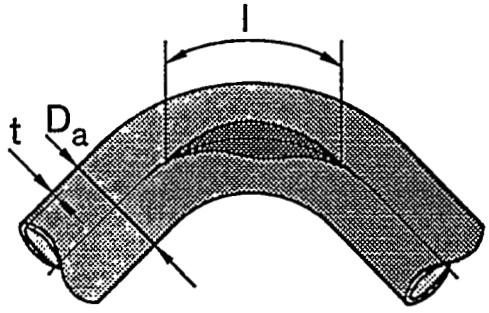

Bends with longitudinal or circumferential cracks
(12 Experiments)

$89 \leqslant D_a \leqslant 850$

$5 \leqslant t \leqslant 50$

$0.5 \leqslant l/D_a \leqslant 1.4$

$0.25 \leqslant a/t \leqslant 1$

Internal pressure, bending
cyclic, dynamic
RT, 240°C, 300°C

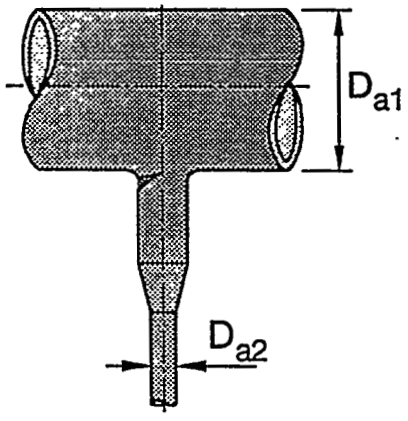

Branches with nozzle corner crack or welding crack
(7 Experiments)

$114 \leqslant D_{a1} \leqslant 863$

$33 \leqslant D_{a2} \leqslant 380$

Internal pressure, bending
RT, 300°C

93104x06

(MPA, Siemens, PHDR, Japanese Experiments)

Fig. 8 : Selection of Available Fracture Mechanics Experiments: Complex Components

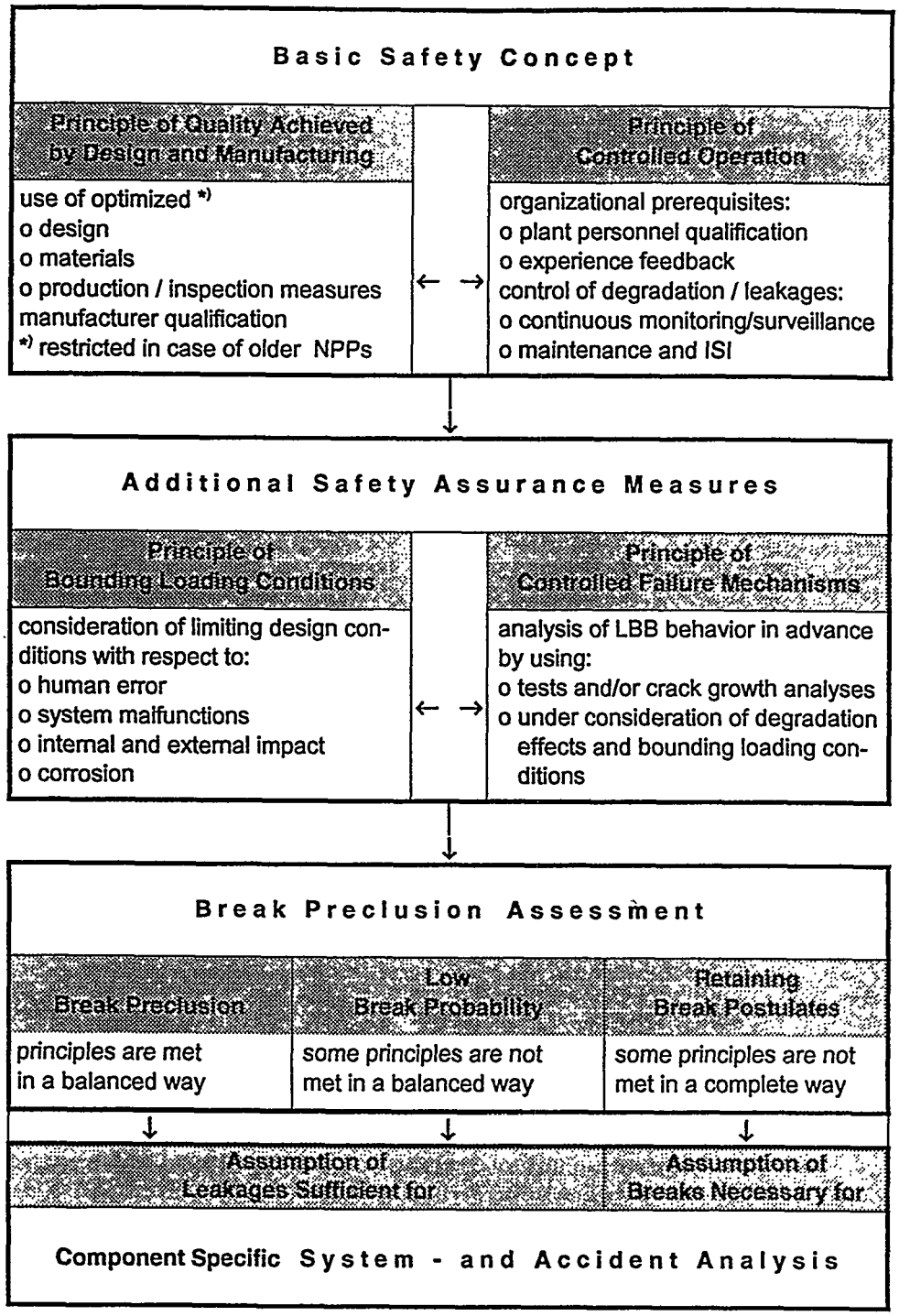

Fig. 9: General Concept of Break Preclusion for Pressure Retaining Structures of Nuclear Power Plants with Nominal Diameters of DN >= 150 mm

Fig. 10: Integrative Approach to Derive Leak Sizes for Safety Analysis

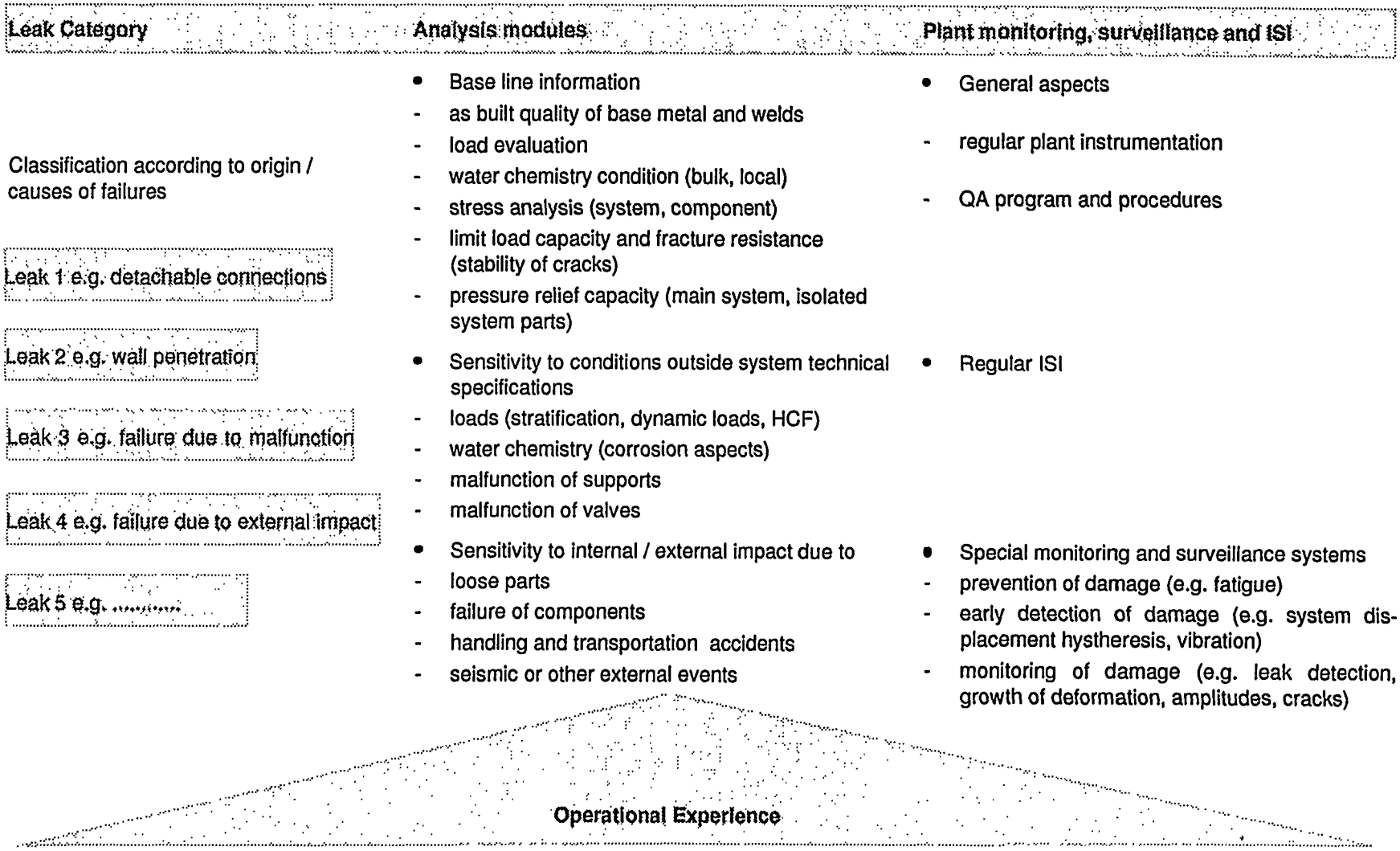

LBB EVALUATION FOR A TYPICAL JAPANESE PWR PRIMARY LOOP BY USING THE U.S. NRC APPROVED METHODS

S. A. Swamy, D. C. Bhowmick, D. E. Prager Westinghouse Nuclear Technology Division, Pittsburgh, PA U.S.A
T. Tanaka, Kansai Electric Power Company, Osaka, Japan
Y. Ogata, H. Yokota, Mitsubishi Heavy Industries, Ltd., Japan

Abstract

The regulatory requirements for postulated pipe ruptures have changed significantly since the first nuclear plants were designed. The Leak-Before-Break (LBB) methodology is now accepted as a technically justifiable approach for eliminating postulation of double-ended guillotine breaks (DEGB) in high energy piping systems. The previous pipe rupture design requirements for nuclear power plant applications are responsible for all the numerous and massive pipe whip restraints and jet shields installed for each plant. This results in significant plant congestion, increased labor costs and radiation dosage for normal maintenance and inspection. Also the restraints increase the probability of interference between the piping and supporting structures during plant heatup, thereby potentially impacting overall plant reliability. The LBB approach to eliminate postulating ruptures in high energy piping systems is a significant improvement to former regulatory methodologies, and therefore, the LBB approach to design is gaining worldwide acceptance. However, the methods and criteria for LBB evaluation depend upon the policy of individual country and significant effort continues towards accomplishing uniformity on a global basis.

In this paper the historical development of the U.S. LBB criteria will be traced and the results of an LBB evaluation for a typical Japanese PWR primary loop applying U.S. NRC approved methods will be presented.

In addition, another approach using the Japanese LBB criteria will be shown and compared with the U.S. criteria. The comparison will be highlighted in this paper with detailed discussion.

1.0 INTRODUCTION

The U.S. Regulatory requirements for postulated pipe ruptures have changed significantly since the first nuclear power plants were designed. Early plants were not designed for dynamic loads associated with postulated pipe ruptures. Designing for LOCA effects was generally limited to the containment sizing. Later, pipe breaks were postulated at locations with the worst dynamic effects, known as "break everywhere" approach. From the mid 1970's pipe breaks were postulated at high stress, high usage factor and a minimum of two arbitrary intermediate locations in addition to the terminal ends [1]. Thus, the original purpose and intent of the postulated double-ended guillotine (DEGB) break, which were to provide a clearly limiting basis for sizing the reactor containment system, were extended to postulation of breaks in all the high energy piping system design resulting in the construction of massive pipe whip restraints and jet impingement shields, simply because an alternate acceptable design basis was not available. The DEGB postulation was further extended to the design of Environmental Qualification (EQ) and even in the sizing of the Emergency Core Cooling Systems (ECCS). For many years the commercial nuclear industry has recognized that a DEGB is highly unlikely, even under severe accident loads, and that a design basis LOCA based on DEGB is an unnecessary and undesirable design restriction.

In the past several years the commercial nuclear industry has worked with the U.S. Nuclear Regulatory Commission (NRC) to eliminate the DEGB as the design basis LOCA based on the concept of Leak-Before-Break (LBB). The LBB concept is summarized in Appendix I. Simply stated, if a flaw in the piping should grow during service, it will tend to grow through the wall of the pipe so that it will leak and be detected well before the crack length approaches instability. The quantitative basis or criteria have been provided in a report by the NRC piping review committee namely NUREG-1061 Volume 3 [2]. The results of the research work by the commercial nuclear industry and the NRC culminated in a revision to 10CFR Part 50, Appendix A, General Design Criteria 4 [3] permitting elimination of postulated breaks from the structural design basis. The NRC guidelines for LBB demonstration are provided in Reference [4].

Use of LBB technology saved hundreds of millions of dollars in backfit costs to many operating Westinghouse plants. Application of this technology to plants under construction resulted in tens of millions of dollars cost savings due to elimination of whip restraints and jet shields. Added cost savings result due to reduced man rem exposure during inservice inspection and maintenance. The US NRC lead on this subject was followed by the regulatory authorities in various countries around the world. Today the LBB technology finds ever increasing applications worldwide. While the underlying LBB concept is identical in all the countries the specific criteria and the quantitative methods of evaluating defining and demonstrating safety margins somewhat vary in different countries. In this paper, historical development of the LBB criteria in the U.S. are traced followed by an example application to a typical Japanese PWR primary loop. The analytical evaluations are performed using the U.S. NRC approved methods. An alternate approach using the Japanese LBB criteria is compared with the U.S. approach.

2.0 HISTORICAL DEVELOPMENT OF THE LBB CRITERIA

In the late seventies, circumferential through wall flaws of length equal to three times the pipe wall thickness (3T flaws) were postulated. These flaws were subjected to normal plus Safe Shutdown Earthquake (SSE) loads to assess flaw stability. The leakages from these flaws were calculated using internal pressure in the piping system. The magnitude of the leakage was shown to be significantly greater than the plant leak detection capability, thereby assuring leak detection. In the early eighties, the Systematic Evaluation of Plants (SEP) procedural guidelines were provided by the U.S. NRC to enable piping integrity assessment. Accordingly, through wall flaws of lengths equal to two times the wall thickness were postulated and the calculated leakage resulting from normal operating loadings (including deadweight, thermal expansion and internal pressure) was compared with the plant leak detection capability (typically 1 gpm). In addition, through-wall circumferential flaws of length equal to four times the pipe wall thickness were shown stable when subjected to the normal operating plus the Safe Shutdown Earthquake (SSE) loads. In the latter part of the eighties the criteria currently in use became available [2,3,4]. These criteria and the resulting steps of the evaluation procedure can be briefly summarized as follow:

1) Calculate the applied loads. Identify the location at which the highest stress occurs.

2) Identify the materials and the associated material properties.

3) Postulate an inside surface flaw at the governing location. Determine fatigue crack growth. Show that a through-wall crack will not result.

4) Postulate a through-wall flaw at the governing location. The size of the flaw should be large enough so that the leakage is assured of detection with margin using the installed leak detection equipment when the pipe is subjected to normal operating loads. Demonstrate a margin of 10 between the calculated leak rate and the leak detection capability.

5) Using faulted loads (such as normal plus SSE), demonstrate that there is a margin of at least 2 between the leakage size flaw and the critical size flaw.

6) Review the operating history to ascertain that operating experience has indicated no particular susceptibility to failure from the effects of corrosion, water hammer or low and high cycle fatigue.

7) Provide the material properties including toughness and tensile test data. Justify that the properties used in the evaluation are representative of the plant specific material. Evaluate long term effects such as thermal aging where applicable.

The last statement is of crucial importance. The U.S. NRC piping review committee stated [2] "If the flawed structure is fabricated from a material that has a high fracture toughness and therefore is not sensitive to the presence of a crack, the load carrying capacity of the cracked structure may still be governed by material strength. If the structure of interest is fabricated from a material that has a low fracture toughness and is therefore sensitive to the presence of a flaw, other analytical techniques must be used." Thermal aging causes reduction of toughness in cast austenitic stainless steels - a material extensively used in PWR primary loop pipings and fittings. In order to demonstrate integrity of cast stainless steel piping systems subjected to thermal aging degradation, an analytical model was developed. This model was verified by experimental data correlation. This model was applied to demonstrate primary loop piping integrity of a typical Japanese PWR nuclear power plant.

3.0 LBB EVALUATION AND APPLICATION OF LBB CRITERIA

3.1 Operation and Stability of Reactor Coolant System

A typical PWR primary loop piping layout in a Japanese plant is shown in Figure 1. As a first step, extremely low susceptibility to cracking from the effects of corrosion e.g. intergranular stress corrosion cracking, IGSCC is demonstrated for the Westinghouse design primary loops. It is also noted that overall, there is almost no potential for water hammer in the Westinghouse type PWR RCS since it is designed and operated to preclude the voiding condition in normally filled lines and the operating transients of the RCS primary piping are such that no significant water hammer can occur. Low cycle fatigue considerations are accounted for in the design of the piping system through the fatigue usage factor evaluation to show compliance with the rules of Section III of the ASME Code. High cycle fatigue loads in the system would result primarily from pump vibrations. These are minimized by restrictions placed on shaft vibrations during hot functional testing and operation.

Based on the above the candidacy of the PWR primary loop piping, for an LBB application, is confirmed.

3.2 Loads

The next step of the evaluation is to establish geometric properties and applicable loads. A segment of the primary loop hot leg pipe is shown in Figure 2. In order to calculate the leak rates, lower bound normal operating loads are obtained by algebraically combining deadweight, thermal expansion and internal pressure loading components. The upper bound faulted loads for crack stability analysis are obtained by combining the loading components (Deadweight, Thermal expansion, pressure and SSE loads including SSE anchor motion) by the absolute summation method. The junction of primary loop hot leg and the reactor vessel outlet nozzle is typically the highest stress location. Therefore, the leak-before-break calculations are performed at this location which is designated as location 1 in Figure 3. The total normal operating stress and the upperbound faulted stress at this location are 20.86 ksi (143.86 MPa) and 23.85 ksi (164.48 MPa), respectively.

3.3 Material Characterization including the Effects of Thermal Aging

In order to accomplish a realistic yet conservative analysis, the leak-before-break evaluations were performed using plant specific material properties σ_y = 21.05 ksi (145.17 MPa) and σ_u = 61.17 ksi (421.86 MPa).

The primary loop piping material is SA351 Grade CF8M - a cast stainless steel product form. The material is known to be particularly susceptible to thermal aging degradation. The cast stainless steel exhibits very high toughness in the as-built condition; however, the fracture toughness may be significantly reduced with time at plant operating temperature. The toughness degradation in cast austenitic stainless steel has been attributed mainly to the successive precipitation of chromium in the ferrite phase due to the large miscibility gap in the Fe-Cr binary system. During aging at temperature, the ferrite phase gradually develops a cleavage transition behavior somewhat similar to that of ferrite stainless steel.

The thermal aging toughness degradation has only within the last fifteen years been recognized as occurring in cast stainless steels at operating temperatures of nuclear reactors. Useful material test data and acceptance criteria became available only recently. The thermal aging issue has been technically addressed by Westinghouse and the procedure currently used to address thermal aging has been approved by the United States Nuclear Regulatory Commission (US NRC).

The material certifications for the primary loop hot leg piping were examined. The chemistry of the material was used to determine the ferrite content and hence fracture toughness. The ferrite content was found to be about 10%. The lower bound allowable fracture toughness properties were conservatively established to be J_{IC} = 750 in-lb/in^2 (131.35 KJ/m^2), Tmat = 60 and J_{max} = 2200 in-lb/in^2 (385.29 KJ/m^2). This lower bound material test data was obtained from a similar cast stainless steel material with higher ferrite content. The toughness data was generated using small specimens with a maximum crack extension of 4.3 mm.

4.0 RESULTS

Leak-before-break evaluations were performed on the hot leg and reactor vessel nozzle junction. Specifically, two phase flow calculations were performed to determine the flaw size giving a 10 gpm leak rate - "leakage size flaw." The leakage size flaw was found to be 3.25 inches (82.55 mm) long. J-T analysis was performed by postulating a through-wall flaw 6.5 inches (165.10 mm) in length (i.e. two times the leakage size flaw). This flaw was subjected to the faulted condition loads. Calculated $J_{applied}$ value was 1429 in-lb/in^2 (250.26 KJ/m^2) and $T_{applied}$ value was 8.6. These values were lower than the lower bound material toughness, thus, flaw stability was demonstrated. If the limit load approach was used as the basis for "critical flaw" size calculation, the limiting size of the postulated through-wall flaw would exceed 32 inches (812.80 mm).

4.1 Comparison of the Evaluation Results

In the LBB evaluations for the primary loop piping, there are some differences between the U.S. and the Japanese approach. These differences are summarized in Table 1.

Table 1

U.S. Approach	Japanese Approach
a) Postulated through-wall crack Leakage Crack Size Factor of 10 margin with respect to leak detection capability. Leakage crack size is determined using plant normal operating loads. Leakage Crack Angle: 11.70 deg.	a) Postulated through-wall crack Leakage Crack Size Factor of 5 margin with respect to leak detection capability. Leakage crack size is determined using 0.5 Sm stress conservatively. Leakage Crack Angle: 25.6 deg. Also postulated through-wall crack size of 5T. Crack Angle: 56.6 deg. Leakage crack size is the larger of the two. For the primary loop the latter criterion governs.
b) Crack Stability Evaluation Demonstrate a margin of a factor of 2 between the leakage crack size and the critical crack size using J-T approach and the limit load approach. J-T Approach Incorporating the effects of thermal aging, calculate J-T applied value for 23.40 deg. through-wall crack as shown in section 4.0 and show them to be lower than the material toughness allowables. Limit Load Approach "Critical Crack Size" is 115.97 deg. A factor of 2 between the leakage crack size and the critical crack size is demonstrated by both the approaches.	b) Crack Stability Evaluation The postulated crack 56.6 deg. in angle is shown stable by comparing the allowable bending stress of 29.61 ksi (204.2 MPa) with the applied bending stress of 17.57 ksi (121.2 MPa). The limit load approach is used to demonstrate the crack stability.
Conclusion: LBB is demonstrated using the US approach and criteria	Conclusion: LBB is demonstrated using the Japanese approach and criteria

5.0 CONCLUSION

LBB evaluations have been performed for typical Japanese PWR primary loop piping, using NRC approved methods and criteria.

There are minor differences in the limit load results obtained in the U.S. and Japan. These differences stem from the input data for applied axial loads and the material strength property, namely the flow stress. Noteworthy is the difference in the magnitude of leakage size cracks and the stability crack size used in the U.S. and in Japan. The difference in the magnitude of leakage size cracks is attributed to the two-tier criteria used in Japan, and the difference in applied loads - normal plant operating loads vs. postulated 0.5 Sm load. From the flaw stability stand point, in the U.S. the stability of a flaw is established using a two-tier criteria based on the J-T approach and the limit load approach, whereas in Japan the stability is demonstrated by using the limit load approach.

Despite the observed differences in the methodology, the calculated leakage size cracks and the stability calculations, both the U.S. and Japanese approaches predicted LBB for the specific Japanese PWR primary loop considered in this study.

6.0 REFERENCES

1. S. A. Swamy, S. S. Palusamy, D. C. Adamonis, "Requirements for Leak-Before-Break Applications to Carbon Steel Piping." PVP-Vol. 238, Codes and Standards and Applications for High Pressure Equipment, ASME 1992.

2. Report of the U.S. Nuclear Regulatory Commission Piping Review Committee - Evaluation of Potential for Pipe Breaks, NUREG, 1061 Volume 3, November 1984.

3. Nuclear Regulatory Commission, Modification of General Design Criterion 4 Requirements for Protection Against Dynamic Effects of Postulated Pipe Ruptures, Federal Register/Vol. 52, No. 207/Tuesday, October 27, 1987/ pp. 41288 - 41293.

4. Standard Review Plan: Public Comments Solicited; 3.6.3 Leak-Before-Break Evaluation Procedures; Federal Register/Vol. 52, No. 167/Friday, August 28, 1987/Notices, pp. 32626-32633.

APPENDIX I
LEAK-BEFORE-BREAK-CONCEPT

The process of demonstrating that a pipe break will not occur in a piping system has been termed the "leak-before-break" concept. This concept is based on the following points:

1. The piping system is not susceptible to stress corrosion, thermal fatigue, or water hammer. Thus, the only failure mechanism is potential ductile failure resulting from a large load.

2. The fracture resistant material properties of piping systems make a rupture of the piping highly unlikely.

3. The service, pre-service, and in-service inspections will detect any piping flaws. If the flaw goes undetected its growth over plant life is insignificant (i.e., no mechanism exists to develop a through-wall crack).

4. If a through-wall crack is postulated in the piping system, the crack will not grow or become unstable under the worst case loading conditions.

5. A stable through-wall crack in a pipe will leak at a rate such that the leak can be identified by leak detection equipment, the plant shutdown, and the appropriate repairs completed.

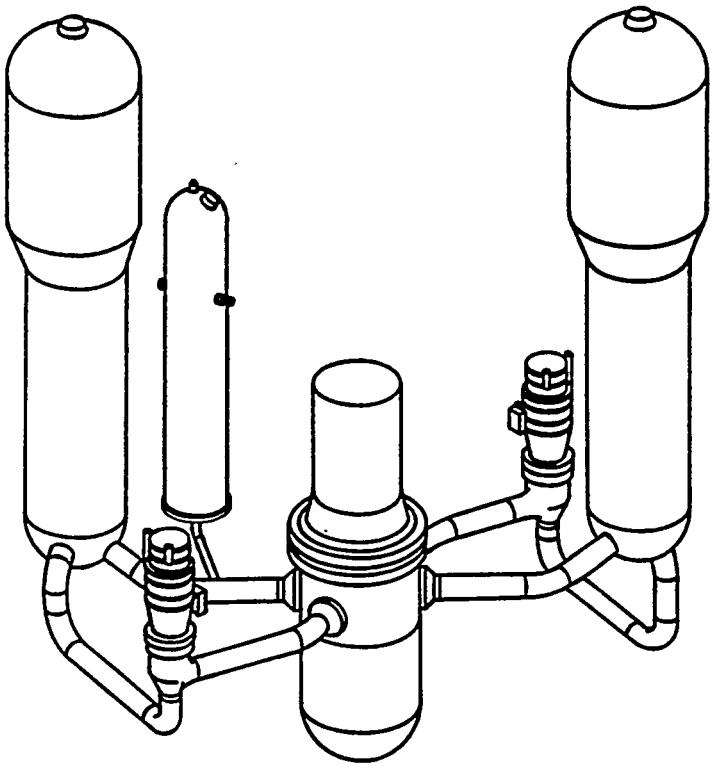

Figure 1 - Typical Primary Loop Piping Layout

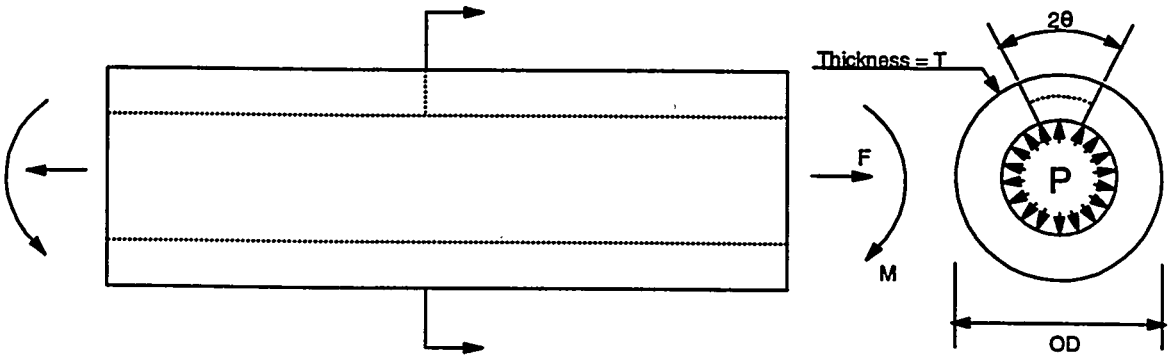

Figure 2 - Hot Leg Piping Segment

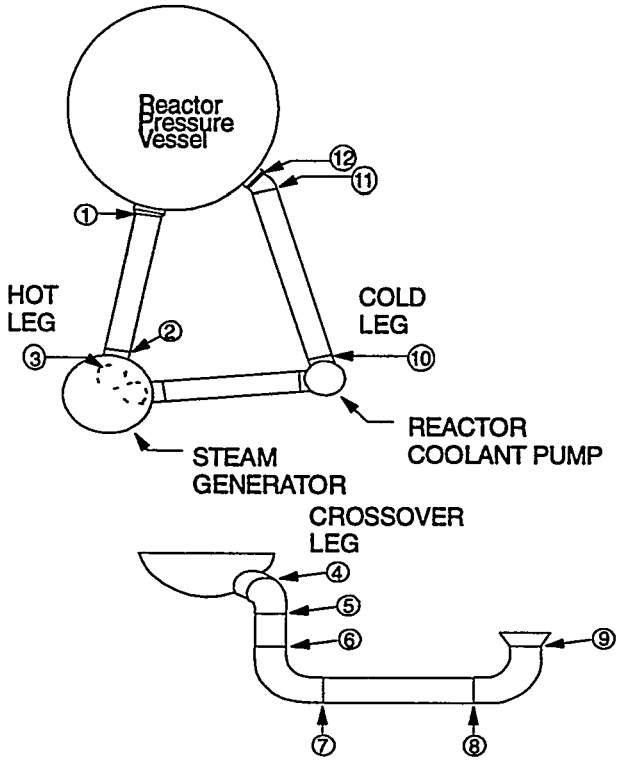

Figure 3 - Schematic Diagram of a RCS Primary Loop Showing Weld Locations

FRACTURE MECHANICS EVALUATION FOR A TYPICAL PWR PRIMARY COOLANT PIPE

T. Tanaka(*), S. Shimizu(**) and Y. Ogata(**)

(*) The Kansai Electric Power Company,Osaka,Japan.
(**) Mitsubishi Heavy Industries, Ltd. Kobe,Japan.

Abstract

For the primary coolant piping of PWRs in Japan, cast duplex stainless steel which is excellent in terms of strength, corrosion resistance, and weldability has conventionally been used. The cast duplex stainless steel contains the ferrite phase in the austenite matrix and thermal aging after long term service is known to change its material characteristics.

It is considered appropriate to apply the methodology of elastic plastic fracture mechanics for an evaluation of the integrity of the primary coolant piping after thermal aging. Therefore,we evaluated the integrity of the primary coolant piping for an initial PWR plant in Japan by means of elastic plastic fracture mechanics.

The evaluation results show that the crack will not grow into an unstable fracture and the integrity of the piping will be secured, even when such through wall crack length is assumed to equal the fatigue crack growth length for a service period of up to 60 years.

1. INTRODUCTION

For the primary coolant piping of PWRs in Japan, cast duplex stainless steel (ASME SA351 Gr. CF8M or equivalent) has been applied. This cast duplex stainless steel contains a ferrite phase of about 5 to 25% in the austenite matrix in order to improve its characteristics of corrosion resistance, strength, weldability, etc.

In the cast duplex stainless steel, the ferrite phase is gradually separated within the operating period at the PWR operation temperature (at about 300°C), and that causes changes in its material characteristics.

An aging of the material tends to increase its tensile strength but reduces its fracture toughness. The degree of the toughness reduction becomes more significant with increasing ferrite content and the rate of toughness reduction increases with rising temperature. Both of these tendencies are mitigated with the aging progress.

The present paper summarizes evaluation results on integrity of the primary coolant piping after thermal aging for initial PWR plant in Japan.

2. CRACK STABILITY ANALYSIS

2.1 Evaluation Method

Fracture toughness of the primary coolant piping decreases due to thermal aging under long-term plant operation, but this fracture type is considered to be a ductile fracture because ductile crack growth is recognized in the material test data after thermal aging. Therefore, it is appropriate to apply elastic plastic fracture mechanics for an evaluation of the stability of the assumed crack.
The evaluation flow is shown in Fig. 1.

2.2 Selection of Evaluating Location

Material toughness, which represents fracture resistance, will be reduced with increasing ferrite content and also with increasing operating temperature. In addition, a high temperature causes a large fracture force due to thermal bending moment. Therefore, the hot leg piping at the reactor vessel outlet nozzle was selected as the location to be evaluated since both temperature and imposed load are severer and ferrite content is relatively high in the evaluating plant.

2.3 Evaluation of Crack Growth

The size of the fatigue crack is calculated under the condition that the assumed initial defect on the piping inside surface grows due to the stress cycles applied by the plant operation.

(1) Evaluation Conditions

(a) Size of Initial Defect
The size of the initial defect was conservatively assumed, with a sufficient margin, to be about twice the size of the detectable single defect. Namely, the initial defect was assumed to be a semi-elliptical, circumferential defect on the piping inside surface and its size to be 0.2t (depth) $\times$ 1.0t (surface length), where "t" is the wall thickness.

(b) Stress Cycle Used in Crack Growth Analysis
The stress cycle was produced on the basis of the transient conditions with consideration of the actual operating status of the plant.

(c) Fatigue Crack Growth Law
The fatigue crack growth law is represented by the following equations provided on the basis of the test data under the PWR primary coolant environment[1]:

$$da/dN = C(\Delta Keff)^m \quad \cdots (1)$$

$$\Delta Keff = \Delta Kmax\,(1 - R)^{0.5} \quad \cdots (2)$$

$$R = Kmin/Kmax \quad \cdots (3)$$

where,

da /dN	: Fatigue crack growth rate [mm/cycle]
C	: Constant = 7.0×10^{-10}
m	: Constant = 4.0
Keff	: Effective stress intensity factor range [MPa$\sqrt{}$m]
Kmax, Kmin	: Maximum, minimum stress intensity factors [MPa$\sqrt{}$m]
R	: Stress ratio

(2) Evaluation Results

The results of the fatigue crack growth analysis are shown below. It reveals that the fatigue crack growth rate is low and the crack does not penetrate the pipe wall (67.4 mm thick) even after long-term plant operation.

1) Assumed initial crack size

Depth : 13.5 mm
Length : 67.4 mm

2) Crack size after plant operation of 60 years

Depth : 26.5 mm
Length : 108.8 mm

2.4 Crack Stability Evaluation

(1) Evaluation Method

Fracture toughness of the primary coolant pipe decreases after thermal aging, but this fracture type can be considered to be a ductile fracture because a ductile crack growth is recognized in its material tests. Therefore, elastic plastic fracture mechanics are to be applied for an evaluation of the stability of the assumed crack. Concretely, the crack stability is evaluated with the J integral value (Japp), which shows a fracture force in comparison to the fracture toughness value (Jmat), which shows the fracture resistance of the material after thermal aging.

(2) J Integral Value (Japp)

J integral value is calculated with the stress analysis by using the finite element method on the basis of the design load and the crack length for evaluation.

(a) Design Load

Loads imposed on the piping are those initiated under the normal operating condition and also those caused by S1 earthquake (maximum design earthquake).

(b) Analysis Model

For the analysis, the finite element model is applied to the elbow on the outlet side (high temperature side) of the reactor vessel with a circumferential crack on the inside surface.

Fig. 2 shows the finite element model used for the analysis.

The crack growth analysis was conducted with the assumption of an initial crack on the basis of the number of transients during the operating period of 60 years. Then, the calculated surface crack length was conservatively converted into the through wall crack which length is conservatively assumed 2t as shown in Fig. 1 for the

crack stability evaluation.

(c) Analysis Results

Fig. 3 shows the analysis results for the Japp value at the evaluating location.

(3) The Fracture Toughness Value (Jmat)

The ferrite content of the evaluating location was calculated by the method described in ASTM A800 with the chemical compositions on the material certificate. The Jmat value was determined by the lower bound curve of toughness (-2σ lower bound curve) obtained with the toughness prediction model (H3T Model: Hyperbolic-Time Temperature Toughness)[2] on the basis of the ferrite content at the evaluating location.

Fig. 4 shows the Jmat value (-2σ lower bound value) obtained by the chemical compositions at the evaluating location .

(4) Crack Stability Evaluation Results

The circumferential surface crack obtained on the basis of the fatigue crack growth analysis after the service period of 60 years was conservatively converted to the circumferential through wall crack of the same length. In order to estimate the stability of this assumed crack, the Japp and Jmat values obtained in Items (2) and (3) above were compared in Fig. 5.

Fig. 5 shows that $J_{IC} >$ Japp even after the service period of 60 years.

Therefore, even when fatigue crack growth is assumed after the service period of 60 years, the evaluation shows that any ductile crack will not be initiated under the design load conditions, and the integrity of the primary coolant piping is confirmed to be secured with sufficient margin.

3. CONCLUSION

Integrity evaluation was conducted by means of the elastic plastic fracture mechanics for the primary coolant piping after thermal aging in an initial PWR plant.

The results show that, even when fatigue crack growth is assumed after a service period of 60 years, the crack is estimated to be stable and the integrity of the piping is confirmed to be maintained in consideration of the thermal aging of cast duplex stainless steel after long-term plant operation.

ACKNOWLEDGEMENTS

This work was supported by Japanese PWR Utilities. The authors are grateful to Japanese PWR Utilities.

REFERENCES

1) Kanasaki, H, et.al, "Fracture toughness and fatigue crack growth of PWR materials in Japan ICONE-1.
2) Tanaka, T, et.al, "The effect of thermal aging on the mechanical properties of cast duplex stainless steels and weld metal" IIW DOC, IX-1973-94, June, 1995.

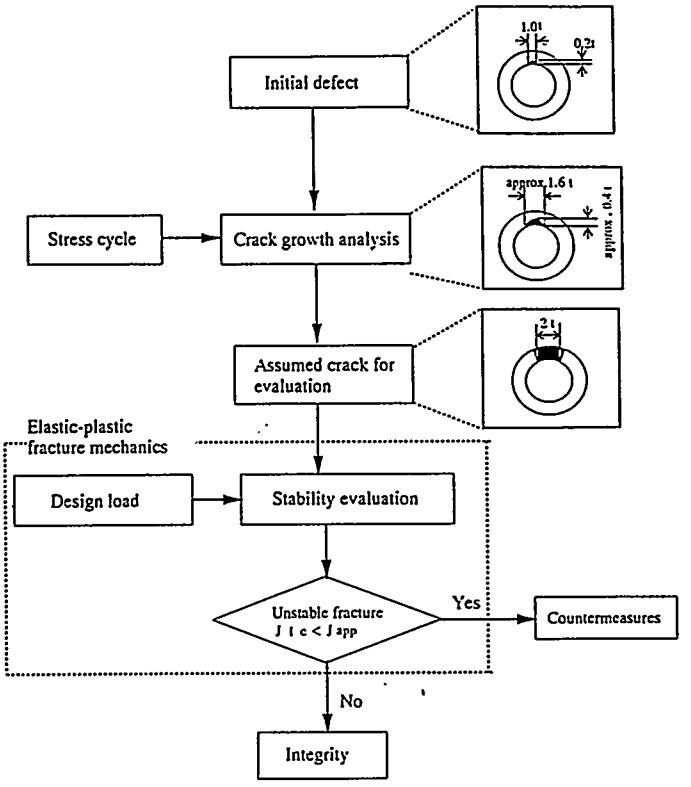

Fig.1 Evaluation Flow for Thermal Aging

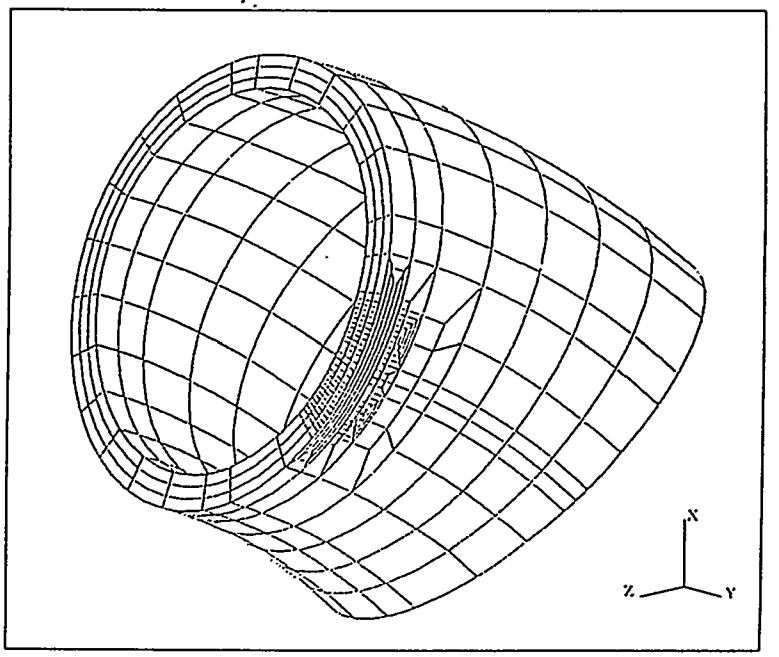

Fig.2 Elemental Division Diagram
(Crack length: 2c=2t)

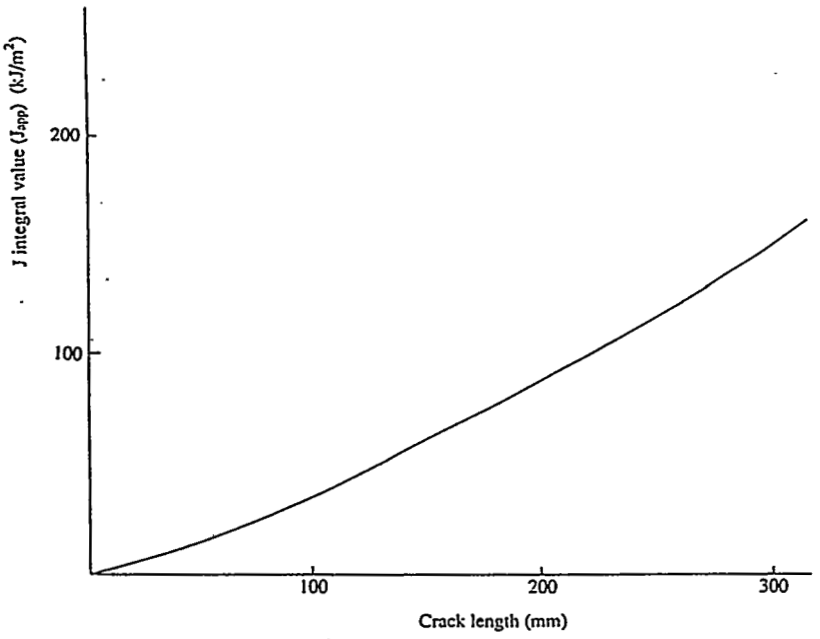

Fig. 3 J Integral Value at Evaluation Position

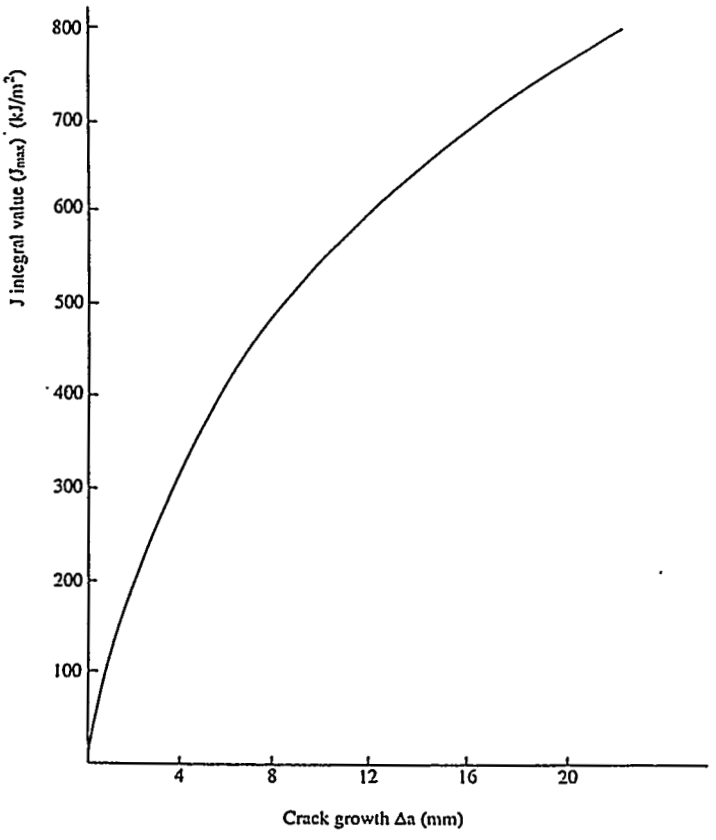

Fig. 4 J–Δa Curve (Hot Leg Pipe Material)

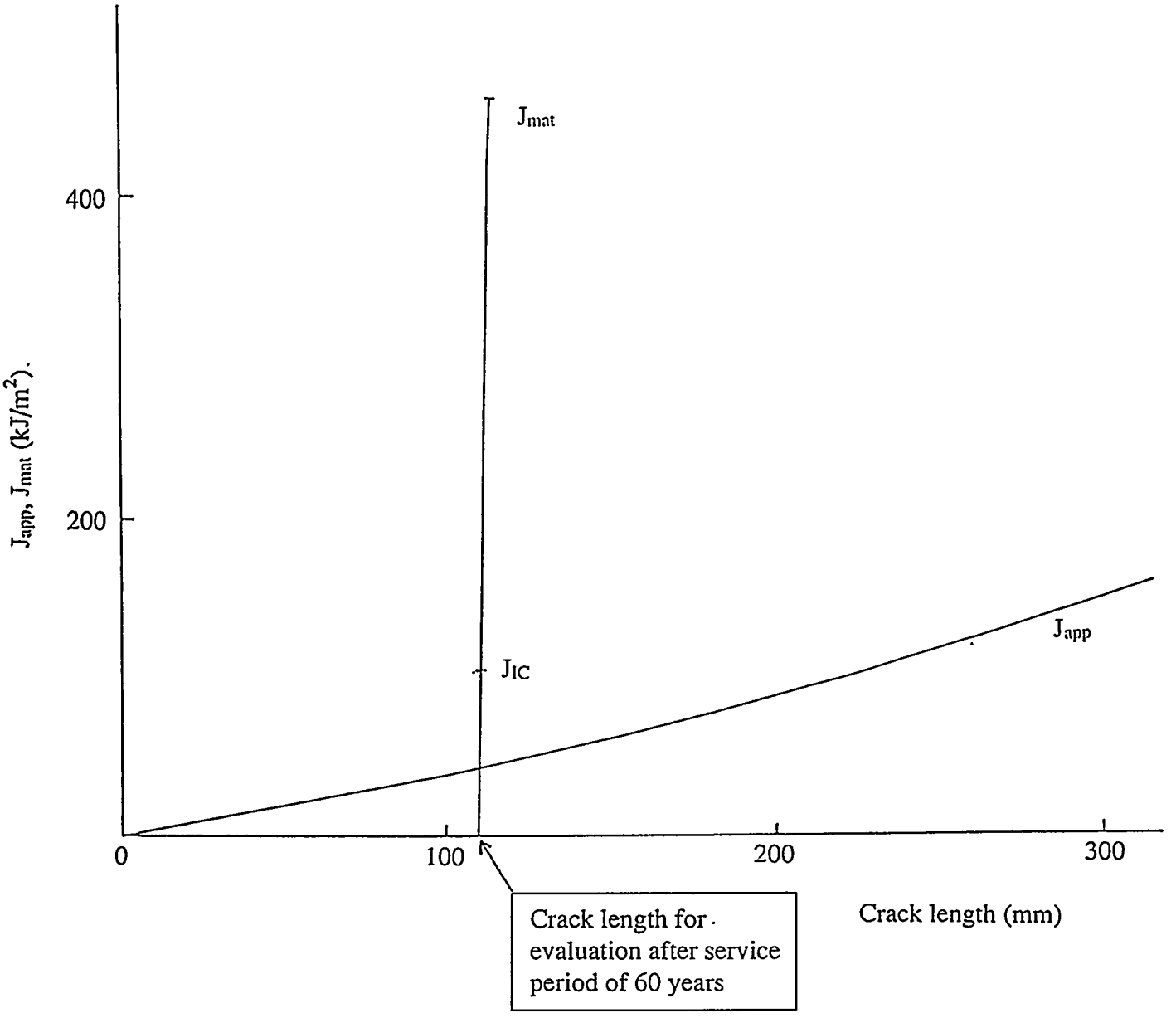

Fig. 5 Crack Stability Evaluation Diagram

CRACK STABILITY ANALYSIS OF LOW ALLOY STEEL PRIMARY COOLANT PIPE

T. Tanaka(*), M. Kameyama(*), Y. Urabe(**), K. Hojo(**) and Y. Ogata(***)

(*) The Kansai Electric Power Company,Osaka,Japan
(**) Mitsubishi Heavy Industries, Ltd. Takasago,Japan
(***) Mitsubishi Heavy Industries, Ltd. Kobe,Japan

Abstract

At present, cast duplex stainless steel has been used for the primary coolant piping of PWRs in Japan and joints of dissimilar material have been applied for welding to reactor vessels and steam generators.

For the primary coolant piping of the next APWR plants, application of low alloy steel ,that results in designing main loops with the same material is being studied. It means that there is no need to weld low alloy steel with stainless steel and that makes it possible to reduce the welding length. Attenuation of Ultra Sonic Wave Intensity is lower for low alloy steel than for stainless steel and they have advantageous inspection characteristics. In addition to that, the thermal expansion rate is smaller for low alloy steel than for stainless steel. In consideration of the above features of low alloy steel, the overall reliability of primary coolant piping is expected to be improved.

Therefore, for the evaluation of crack stability of low alloy steel piping to be applied for primary loops, elastic-plastic fracture mechanics analysis was performed by means of a three-dimensioned FEM.

The evaluation results for the low alloy steel pipings show that cracks will not grow into unstable fractures under maximum design load conditions, even when such a circumferential crack is assumed to be 6 times the size of the wall thickness.

1. INTRODUCTION

For austenite stainless and carbon steel pipings, the LBB concept is being employed as a rational technique for piping failure protection design and realization of the LBB is being studied[1),2),3)] by conducting various pipe tests in Japan and abroad. In Japan, LBB standardization for austenite stainless steel has already been established, while that for carbon steel is now being studied.

This paper summarizes evaluation results of crack stability on the basis of the elastic-plastic fracture mechanics

analysis as a link of LBB realization evaluation for low alloy steel (SFVQ1A, equivalent to ASME SA508, Cl. 3) which is being studied for use as the primary coolant piping of PWRs in Japan, in consideration of its future LBB standardization.

2. CRACK STABILITY ANALYSIS

2.1 Evaluation Method

Since ductile crack growth is recognized in material testing of low alloy steel, similar to that of austenite stainless steel and carbon steel, its fracture type can be considered to be a ductile fracture. Therefore, it is appropriate to apply the elastic-plastic fracture mechanics for an evaluation of the stability of an assumed crack.

The evaluation flow for the crack stability is shown in Fig. 1.

2.2 Selection of Evaluating Location

The reactor vessel outlet nozzle was selected as the location to be evaluated since the design load becomes the maximum at this point.

2.3 Evaluation of Assumed Throughwall Crack

(1) Evaluation Conditions

The assumed throughwall crack size is to be selected as the larger one of the following two circumferential throughwall cracks in the austenite stainless steel LBB standard that has already been established in Japan.Therefore, in the present paper, evaluation is to be carried out for the circumferential throughwall crack selected similarly.

1) A throughwall crack that generates a leakage of 5 gpm.

2) A throughwall crack of the same length as that of a piping inner surface crack when the crack penetrates the piping wall thickness in crack growth analysis performed without limiting the stress cycle frequency.

Since in such large pipings as the primary coolant pipes the throughwall crack of case 2) is larger than that of case 1) , we will analyze the throughwall crack size of case 2) as the evaluation conditions.

(a) Size of Initial Defect for Evaluation

The size of the initial defect was conservatively assumed to be about twice the size of the detectable

single defect with a sufficient margin to the defect detection limit in PSI.
Namely, the initial defect was assumed to be a semi-elliptical,circumferential defect on the piping inside surface and its size to be 0.1t (depth) × 0.5t (surface length), where "t" is the wall thickness.

(b) Stress Cycle Used in Assumed Crack Growth Analysis
The stress cycle was produced on the basis of design transient conditions.

(c) Fatigue Crack Growth Law
The fatigue crack growth law is represented by the following equations provided on the basis of the test data under the PWR primary coolant environment (Fig. 2).

$$da/dN = C \cdot \Delta K^m$$

where, da/dN : Fatigue crack growth rate [mm/cycle]
ΔK : Stress intensity factor range $[K_{max} - K_{min}]$ [kgf/mm$^{3/2}$]
C : Constant
m : Constant

Here, in the case of $\Delta K \leq 42.7$ kgf/mm$^{3/2}$, $C = 1.64 \times 10^{-13}$, $m = 5.95$
in the case of $\Delta K > 42.7$ kgf/mm$^{3/2}$, $C = 5.44 \times 10^{-7}$, $m = 1.95$

(2) Evaluation Results
As the results of the assumed throughwall crack analysis,the length of the circumferential inner surface crack becomes 5.5t at the time of crack penetration, and this value is rounded up to 6t.

2.4 Elastic-Plastic Fracture Mechanics Evaluation

(1) Evaluation Method
The crack stability evaluation is carried out with the J integral value (J_{app}) which is the parameter that shows a fracture force calculated from the load given to the structural system and with the fracture toughness value (J_{mat}) of the material.

(2) J Integral Value (J_{app})
J integral value is calculated with stress analysis by using the finite element method on the basis of the

load at the evaluating location and the assumed throughwall crack length.

(a) Design Load for Evaluation

Loads imposed on the piping are those initiated under the normal operating condition and also those caused by S1 earthquake. (maximum design earthquake)

Numerical values are as follows:

Internal pressure	:	157.0 kgf/cm^{2}G
Bending moment	:	369.7 ton f·m
Axial force	:	245.7 ton f

(b) Analysis Model

For the analysis, the finite element model is applied to the reactor vessel outlet nozzle with a circumferential throughwall crack. Fig.3 shows the FEM model used for the analysis. It also shows the load and boundary conditions for the analysis.

For the crack stability evaluation, the throughwall crack length was assumed to be 6 times the wall thickness "t" as described in item 2.3(2)above.

A FEM code 'MARC' was used for the analysis code and only 1/4 portion was analyzed due to the symmetry of the piping.

(c) Material Constant

Base metal has a lower yield stress and a lower work hardening rate than weld metal. Therefore, a stress-strain curve of the base metal was conservatively used for the J integral analysis.

1) Stress-Strain Curve

A stress-strain curve (Fig. 4) at a temperature of 325°C is used for the J integral analysis.

2) Young modules and Poisson's ratio

E = 19200 kgf/mm^2 and Poisson's ratio ν = 0.3 is used.

(3) The Fracture Toughness Value (J_{mat})

J_{Ic} and J–Δ a Curve at 325°C of the base metal and weld metal is used for fracture toughness (Fig. 5). An extrapolated J – Δa curve based on the equation shown in the figure is also used for evaluation of crack stability, as required.

(4) Crack Stability Evaluation Results

Fig. 6 shows the relation between the half crack length(3t) and J_{app}, J_{mat}. The fracture behavior can be evaluated from the values of J_{mat} and J_{app}. When the J_{mat} is greater than J_{app}, it indicates that the fracture toughness has a sufficient margin against the fracture force.

Table 1 shows the evaluation results of margins against the maximum design load and against the crack

length.

From Fig. 6 and Table 1, the safety margin of J_{Ic} against J_{app} is 2.6 times for base metal and 1.4 times for weld metal. This indicates that there was no initiation of ductile cracks under the maximum design load and that it will not lead to unstable fractures. Since J_{mat} is normally smaller for the weld metal than for the base metal according to Fig.5, the safety margins are always determined by the weld metal. The safety margin against the maximum design load is evaluated to be 2.2 times within the measured range of J_{mat} and 2.8 times against unstable fracture by the J-Tearing modulus evaluation method. Likewise, the safety margins against crack length are evaluated to be 1.7 times and 2.0 times respectively.

5. CONCLUSION

Crack stability evaluation was conducted by means of elastic-plastic fracture mechanics analysis.
As a result, it was found that no ductile fracture would be initiated under the design load conditions,even when a circumferential throughwall crack is assumed to have a size of 6 times the wall thickness.

Also, it can be evaluated that the safety margin against the maximum design load is 2.2 times within the measured range of J_{mat} and 2.8 times against unstable fracture by the J-Tearing modulus criteria. Likewise, the safety margins against crack length are evaluated to be 1.7 times and 2.0 times respectively.

From these results, the crack is estimated to be stable and the integrity of low alloy steel primary coolant pipings is to be maintained with sufficient margin.

ACKNOWLEDGEMENTS

This work was supported by Japanese PWR Utilities. The authors are grateful to Japanese PWR Utilities.

REFERENCES

1) Wilkowski, G.M et al., "Degraded piping program-phase I "Semiannual Report, October 1985-March 1986, NUREG/CR-4082 Vol. 3, 1986.
2) Wilkowski, G.M. et al., "Degraded piping program - phase II "Semiannual Report, April 1985-September 1985, NUREG/CR - 4082Vol. 4, 1986.
3) Shibata, K et al., "Results of reliability test program on light water reactor piping" Nucl. Eng. Des. 153 (1994) 71-86.

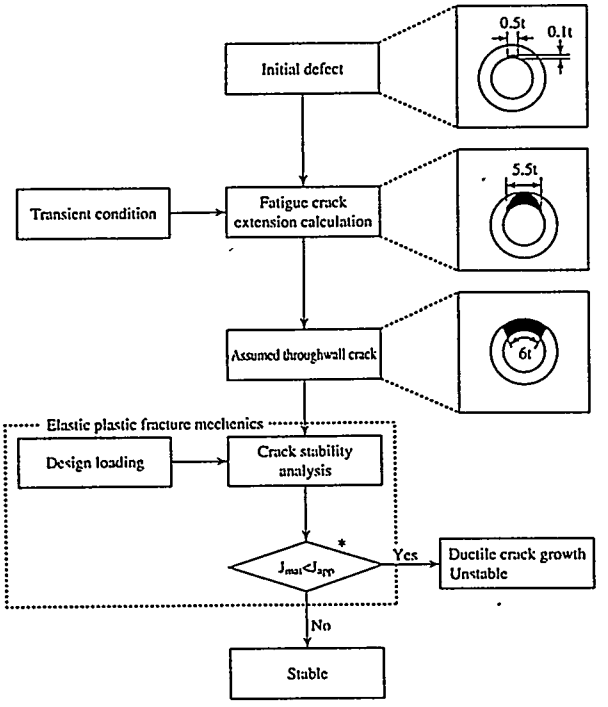

* J_{mat} : J_{IC}, measured J-R curve or J-T criteria as a stability criteria

Fig.1 Crack stability evaluation flow

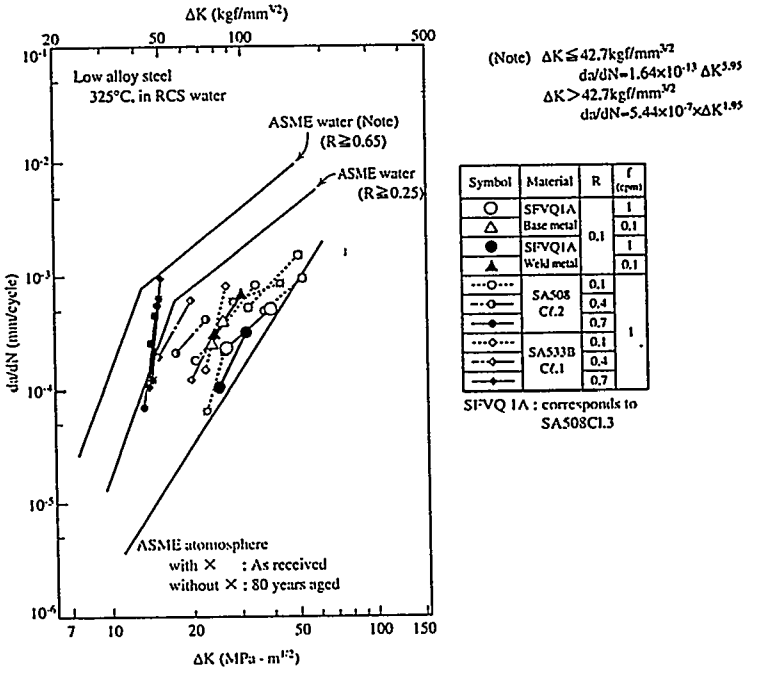

Fig.2 Fatigue crack growth rate of low alloy steel

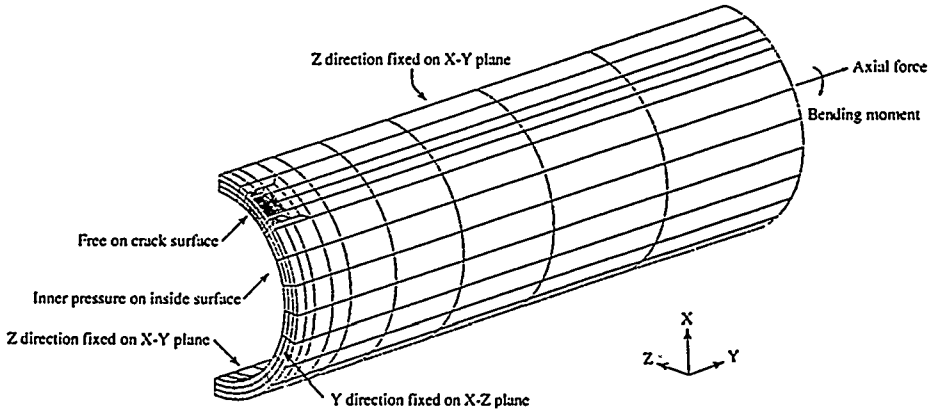

Fig.3 FEM model and boundary condition

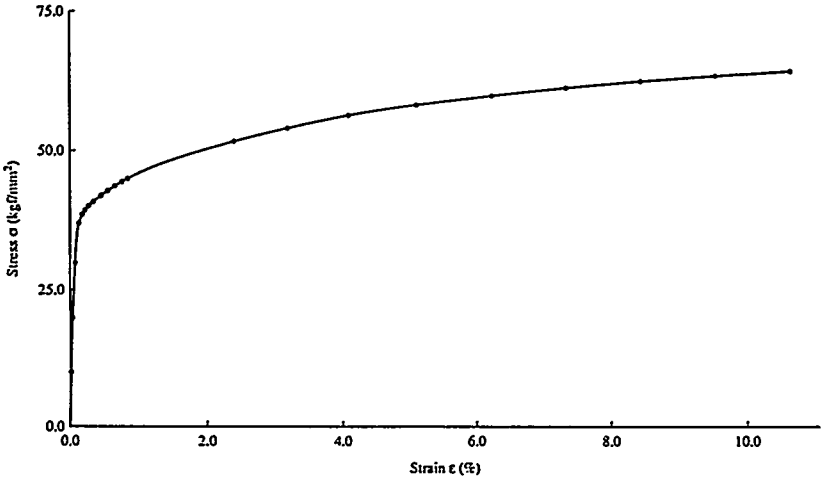

Fig.4 Stress-strain curve (Base metal, test temperature : 325°C)

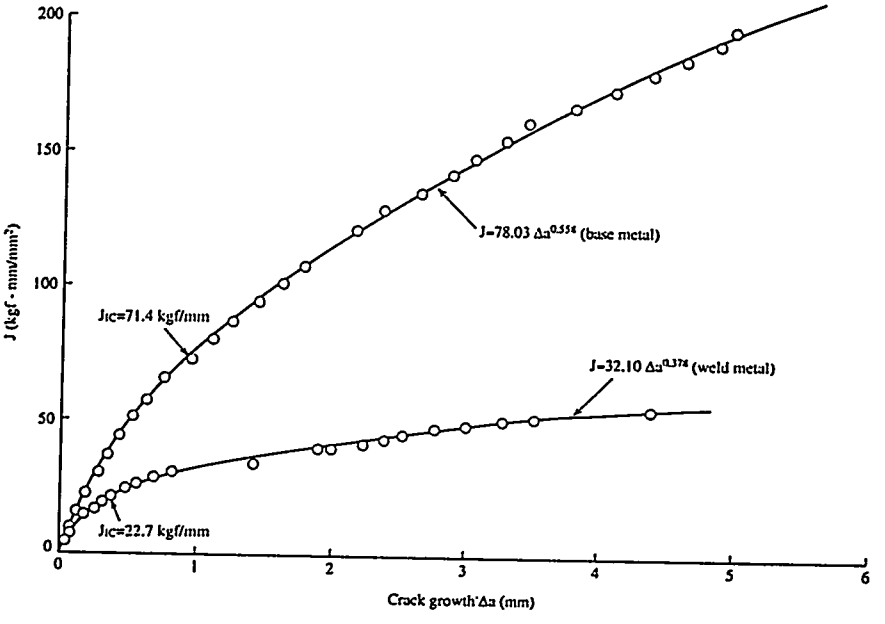

Fig.5 JIC and J-Δa curve (Test temperature : 325°C)

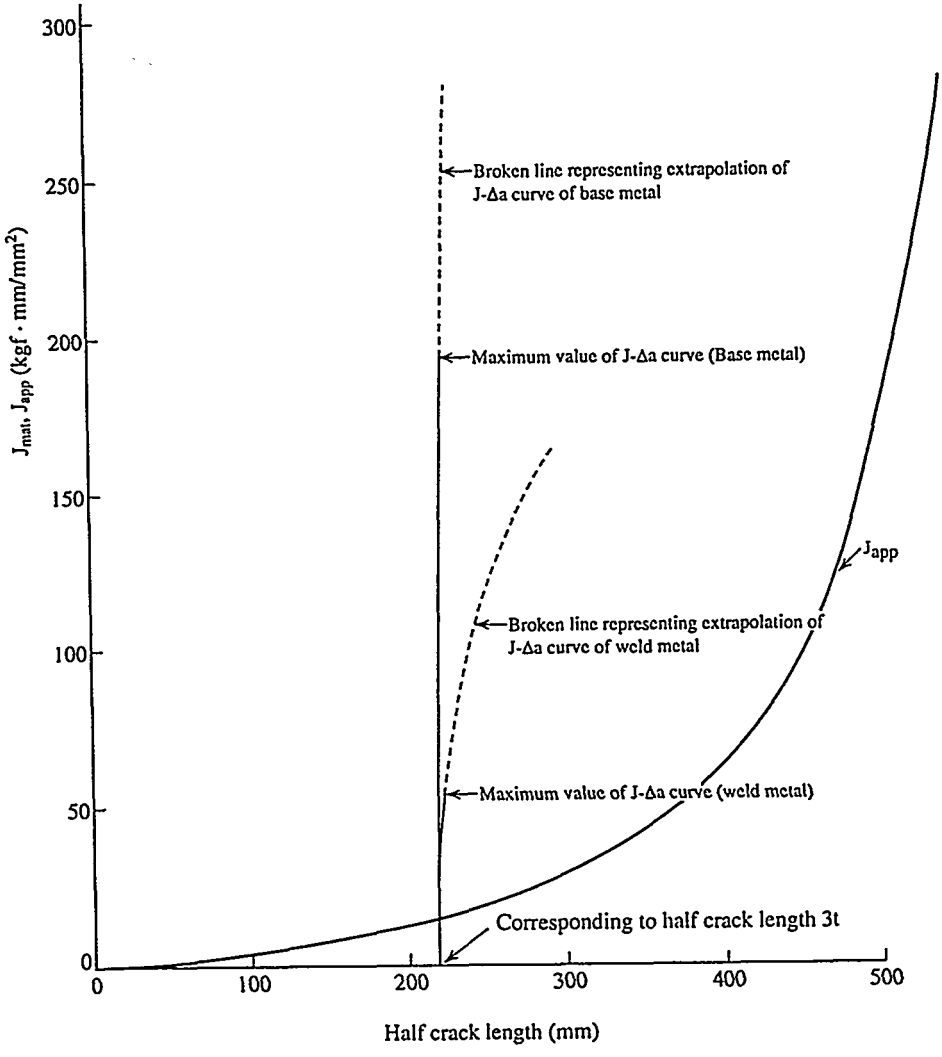

Fig.6 Crack stability Diagram

Table 1 Results of safety margin

Estimation Method			Safety margin of bending moment	Safety margin of initial crack length
FEM analysis Stress-strain curve: Base metal	J_{IC}	Base metal	2.6	1.9 (835)
		Weld metal	1.4	1.3 (558)
	Maximum value of measured J-Δa curve	Base metal	3.5	23 (1010)
		Weld metal	2.2	1.7 (758)
	J-T	Base metal	> 3.7	> 2.3 (> 1025)
		Weld metal	2.8	2.0 (872)

Note: The number within parenthesis means total crack length (mm)

APPLICATION OF LBB TO A NOZZLE-PIPE INTERFACE

Y.J. Yu[1], S.H. Park[1], G.H. Sohn[1],Y.J.Kim[2],William Urko[3]
1) Korea Atomic Energy Research Institute, 2) Sung Kyun Kwan University, 3) ABB Combustion Engineering

ABSTRACT

Typical LBB (Leak-Before-Break) analysis is performed for the highest stress location for each different type of material in the high energy pipe line. In most cases, the highest stress occurs at the nozzle and pipe interface location at the terminal end. The standard finite element analysis approach to calculate J-Integral values at the crack tip utilizes symmetry conditions when modeling near the nozzle as well as away from the nozzle region to minimize the model size and simplify the calculation of J-integral values at the crack tip. A factor of two is typically applied to the J-integral value to account for symmetric conditions. This simplified analysis can lead to conservative results especially for small diameter pipes where the asymmetry of the nozzle-pipe interface is ignored. The stiffness of the residual piping system and non-symmetries of geometry along with different material for the nozzle, safe end and pipe are usually omitted in current LBB methodology.

In this paper, the effects of non-symmetries due to geometry and material at the pipe-nozzle interface are presented. Various LBB analyses are performed for a small diameter piping system to evaluate the effect a nozzle has on the J-integral calculation, crack opening area and crack stability. In addition, material differences between the nozzle and pipe are evaluated. Comparison is made between a pipe model and a nozzle-pipe interface model, and a LBB PED (Piping Evaluation Diagram) (Ref. 1) curve is developed to summarize the results for use by piping designers.

INTRODUCTION

The fundamental premise of LBB is that the materials used in nuclear power plant piping are sufficiently tough that even a large through-wall crack, which could result in coolant leaking rates well in excess of those detectable by present leak detection systems, would remain stable and would not result in a double-ended guillotine break under maximum loading conditions. Therefore, using ductile fracture mechanics analysis to determine if a hypothesized crack is stable in a pipe when subjected to a given loading is a key element to the demonstration of LBB for a piping system.

Elastic-plastic fracture mechanics methods applied to finite element (FE) models have been used to develop evaluation procedures for flaws found or postulated to exist in piping. Application for these methods include the LBB evaluation for pipes with postulated through-wall flaws. They all strongly depend on the material tensile properties and its resistance to ductile crack extension. The LBB methodology used in this study is consistent with these methods and the guidance provided in NUREG 1061 Volume 3 (Ref. 2) and SRP 3.6.3 (Ref. 3) guidelines for ductile fracture analysis.

A parametric study is performed for three cases to investigate the effect a nozzle on the J-Integral calculation, crack opening area (COA) and crack stability. Both pipe and nozzle-pipe models are developed for this study. The two models have the same small diameter pipe dimensions (12 inch SCH160) for all cases. The only variables are the crack length, applied load, and material properties chosen to represent a typical small diameter high energy piping

system.

LBB EVALUATION PROCEDURE

The use of LBB criteria permits the elimination of the evaluation of dynamic effects of sudden circumferential pipe breaks in the structural analysis of piping systems. A piping system that satisfies the criteria leaks at a detectable rate from a postulated flaw prior to growth of the flaw to a size that would fail because of applied loads resulting from normal conditions, anticipated transient, and a postulated safe shutdown earthquake.

The LBB analysis in this study is a fracture mechanics based stability analysis. The analysis uses normal operating loads to determine a critical crack size for a postulated through-wall crack. The critical crack size is compared to the size of a leakage crack for which detection with appropriate margin is certain. When the critical crack size is sufficiently larger than the leakage crack size the LBB requirements are satisfied. This procedure is diagrammed in Figure 1.

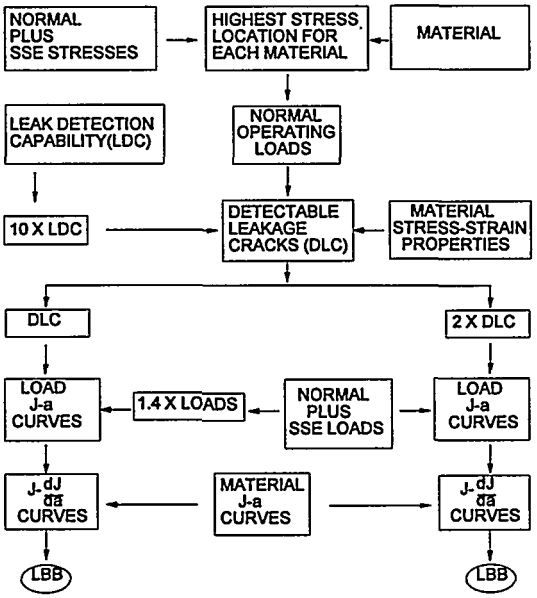

Figure 1. Overall Leak-Before-Break Process

The LBB procedure requires a margin on loading and crack length after a margin on detectable leak rate is applied. The margin on load (normal operating plus seismic) is a factor of 1.4 for an analysis of the detectable leakage size crack length which has a factor of 10 placed on the minimum detectable leakage rate. The margin on crack length is a factor of 2 in addition to the margin of 10 on detectable leak rate. The detectable leakage crack is a through-wall crack which leaks at 10 times the leak detection capability. For this study, the minimum detectable leakage rate of 1 gpm is used. The crack area and length is calculated using PICEP (Pipe Crack Evaluation Program) developed by EPRI (Ref. 4).

The J-Integral and its derivative with respect to crack extension, are calculated for load with a margin of 1.4 and given detectable leakage crack length; and twice the detectable leakage crack length and load. A J-Integral vs. dJ/da load curve (J-T diagram) is developed for each crack size and plotted against the material curve. The point of intersection of the load curve and material curve is the load that causes crack instability. The instability load is compared to the actual applied load at that point. If the applied load is less than the instability load, that point passes the LBB criteria. If the applied load is greater than the instability load then the point fails the LBB criteria. Figure 2 shows this

approach. For a detailed description of the LBB evaluation procedure refer to Ref. 5.

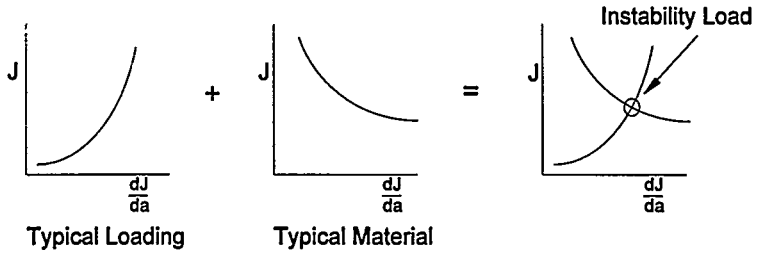

Figure 2. Stability Evaluation

ANALYSIS

The FE model is simply a means for applying loading to a section of pipe containing the hypothetical crack at some location in the piping system. It provides a way to characterize the local plastic deformation at the crack tip.

Two three dimensional, 20 node, isoparametric brick FE models are developed for this study using the CE MARC program (Ref. 6). One model is for a continuous straight pipe and the other model is for the nozzle-pipe interface. The FE model for the continuous pipe is shown in Figure 3(a). Since the crack is assumed to be aligned with the moment, two planes of symmetry (1st symmetry and 2nd symmetry) are used to minimize the size of the FE model. Therefore, the model represents one quarter of the pipe as shown in Figure 4. The model for the nozzle-pipe interface is also shown in Figure 3(b) which includes the pipe and nozzle. Here one plane of symmetry (2nd symmetry) is used to minimize the model size, meaning that one half of the nozzle-pipe interface is modeled. The length of the free end pipe is chosen to be at least five pipe diameters in order that the point of load application not be close to the crack location.

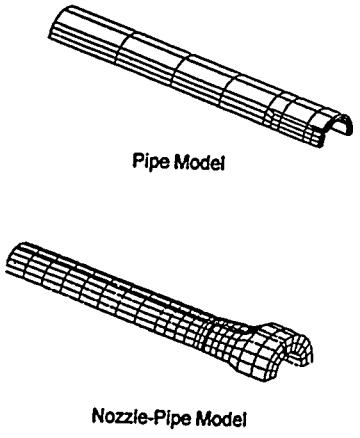

Figure 3. Finite Element Models

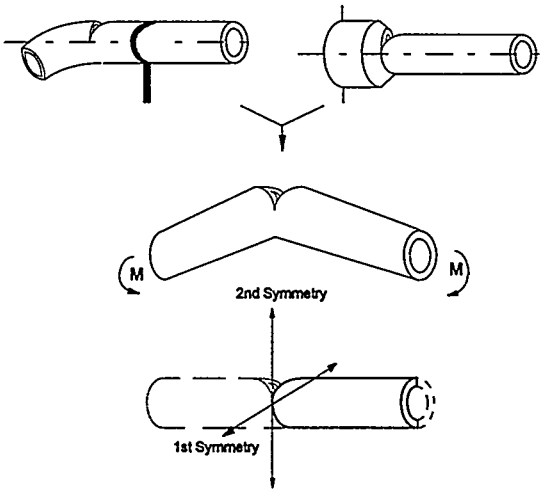

Figure 4. Typical Idealization of Nozzle-Pipe and Straight Pipe for LBB Analysis

The detailed analysis of through-wall cracks requires consideration of the material properties for the pipe and nozzle. The material toughness property (J-R curve) and the tensile strength (stress-strain curve) are essential to the LBB evaluation. The ductile fracture parameter, J-Integral, is used to characterize the propensity for crack extension and stability and is highly dependent on the stress-strain curve or load-displacement curve. To investigate the effect that

different material properties have on crack stability, two materials were chosen for this study - carbon steel and stainless steel. These materials are widely used for piping systems in the nuclear industry and have very different material properties. Stainless steel is more "plastic" than carbon steel. Also, stainless steel has much higher fracture toughness characteristics than those of carbon steel. Figure 5 presents the stress-strain curves used in the finite element analysis. Figure 6 shows the J-R curve for stainless steel weld material (SMAW). This material data represents the lower bound J-R curve for the stability analysis.

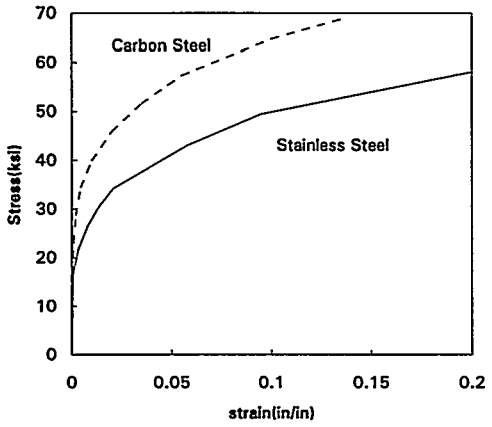

Figure 5. Stress-Starin Curve used in Analysis

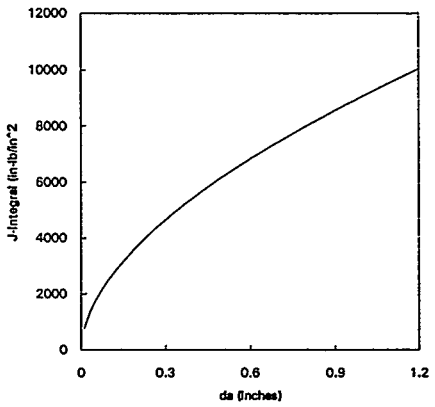

Figure 6. J-R curve for Stainless Steel Weld Material

For consistency, a transverse bending moment load is applied to each of the FE models at the far end of the pipe away from the crack. The moment is applied as a linear traction across the pipe cross section. Also, boundary conditions are imposed on each model based upon symmetry and crack location. The crack surface area is free from constraint.

For each of the FE models (1/4 and 1/2 symmetry) three different crack lengths are developed for the leakage crack and twice the leakage crack to consider the effect of crack extension. One set of models, having crack sizes of a-d, a, and a+d at normal operating loads is used to demonstrate safety margin on the load. "a" is the detectable leakage crack length, and "d" is a small increase or decrease in "a". Another set of models, having crack lengths 2a-d, 2a, and 2a+d, is used to demonstrate the margin on crack size. The J-Integral values are computed for each of the three different crack lengths per FE model. A polynomial curve fit of the J-Integral is made as a function of crack length and three constants. The curve is differentiated to provide loading J vs dJ/da curves for each of the stability evaluations. These evaluations are made by comparing the J vs dJ/da loading curve to the J vs dJ/da material curve.
Three cases are investigated in the parametric study to compare the effect of the stiffer nozzle-pipe model on the LBB stability results versus the conventional symmetric pipe model. Figure 7 shows the materials combinations used for the three cases studied. Both pipe and nozzle-pipe FE models are used in this study.

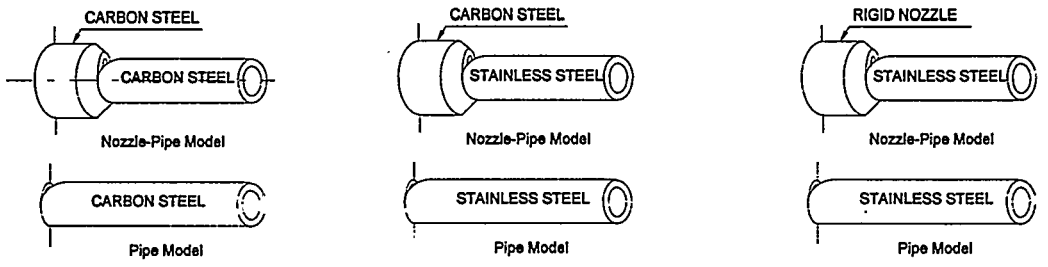

(CASE 1) (CASE 2) (CASE 3)

Figure 7. Material used for the Three Cases

The following comparison is made between the two models:

a) the calculated J-Integral
b) the crack opening area
c) the detectable leakage crack length
d) the stability calculation (J-T diagram)
e) the LBB PED curves

One LBB evaluation using the finite element method requires a minimum of six finite element analyses per model for the simple pipe model. In addition, for the nozzle-pipe model an iterative procedure of FE analyses and PICEP analyses is needed to find an appropriate crack length which leaks at 10 gpm. The stiffness of the nozzle being included in the stability analysis must also be included in determining the crack opening area to be used in the leakage calculation. This procedure is as follows:

Step 1: Assume a flaw length in FE model.
Step 2: Apply normal operating load to the FE model and calculate the crack opening area.
Step 3: Using PICEP with the same length flaw vary the applied moment until the area is the same area as calculated with the FE model.
Step 4: If the PICEP flow is greater than 10 gpm the crack length is decreased - go to step 1.
If the PICEP flow is less than 10 gpm the crack length is increased - go to step 1.
If PICEP flow is 10 gpm - STOP.

DISCUSSION OF RESULTS

A review of material and geometry characteristics provides a meaningful understanding of the results of this study. Typical piping stainless steel has higher fracture toughness properties, absorbs more plastic strain for a given load and is more ductile than typical piping carbon steel. For a given load, a stainless steel pipe can sustain a larger through-wall crack size before the crack becomes unstable. A stainless steel pipe with a fixed size through-wall crack will be able to absorb more load before the crack becomes unstable. Stainless steel has higher resistance to crack extension (requires more energy at the crack tip for the onset of crack extension) than carbon steel.

The size of pipe can also greatly influence the calculation of the J-Integral. Larger diameter pipes are stiffer than smaller diameter pipes. A large diameter pipe with the same crack size, load and material as a small diameter pipe will have less plastic deformation at the crack tip and a lower calculated J-Integral. Attaching a larger diameter nozzle to a smaller diameter pipe results in a stiffer piping system. A throughwall crack at the nozzle-pipe interface will have less plastic deformation at the crack tip than the same size pipe without the attached nozzle. The displacement contribution at the crack tip to the J-Integral calculation from the stiffer nozzle side is less than from the pipe side. Varying both material properties and geometry in the same model complicates the J-Integral calculation further.

In order to make comparison between the pipe model and nozzle-pipe model easier, the J-Integral calculations are presented as the ratio of nozzle to pipe versus the applied load where

Jpipe = calculated J from the pipe model
Jnozzle = calculated J from the nozzle-pipe model

The focus of this study is the relative results between the two models because of material property and geometry differences. The magnitude of the J-Integral for both models is of secondary importance. The results are plotted for Case 1, Case 2, Case 3 and different crack sizes - 30, 38, 64 and 72 degrees - in Figures 8 through 10.

The ductile fracture mechanics analysis using the FE models calculated the J-Integral values for incremental applied moments. These J-Integral results are tabulated and the ratio of nozzle-pipe model results to pipe model results are

shown in Figures 8 through 10. The nozzle is either carbon steel or rigid. The attached pipe is either stainless steel or carbon steel. The single pipe is also either stainless steel or carbon steel. Figures 8a and 8b show the ratio of the calculated Jnozzle to Jpipe results versus applied loads with a 30 degree and 64 degree crack size for the three material combinations cases. Figure 9 shows the same plots but for a carbon steel nozzle-stainless pipe interface and stainless single pipe with crack sizes of 30, 38, 64 and 72 degrees. Figure 10 has the same crack sizes and pipe material properties except the nozzle is rigid (having a very large modulus of elasticity) - the displacement contribution at the crack tip from the nozzle side is insignificant to the J-Integral calculation at the interface.

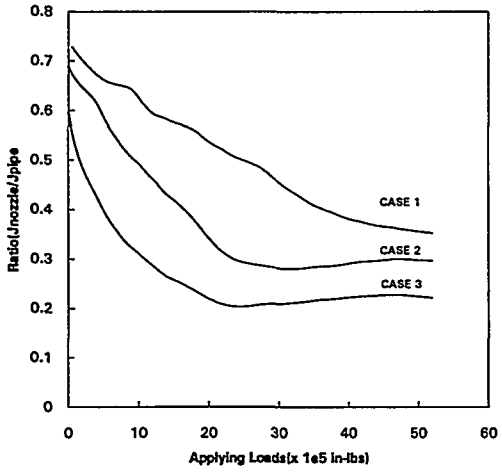

Figure 8a. J-Ratio for 30° Crack Angle

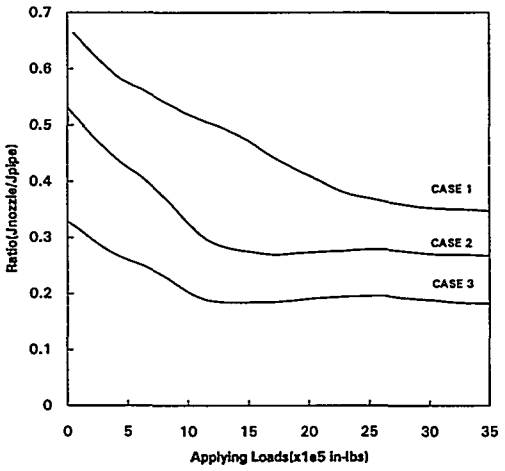

Figure 8b. J-Ratio for 64° Crack Angle

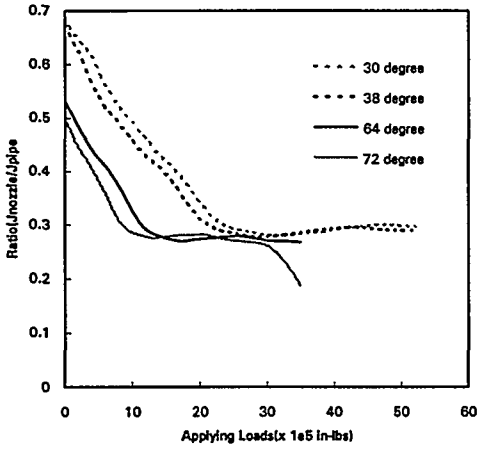

Figure 9. J-Ratio for Different Crack Angle (Case2)

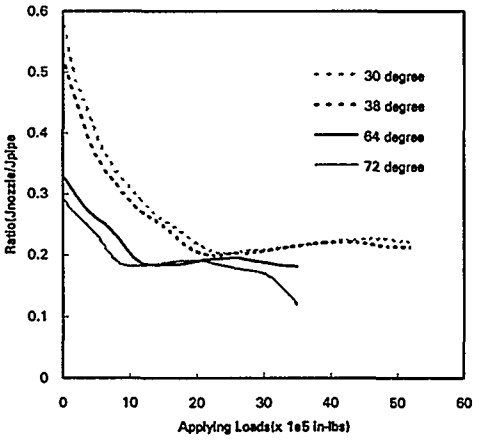

Figure 10. J-Ratio for Different Crack Angle (Case3)

Certain observations can be made regarding the J ratio and applied load. Looking at Figures 8 through 10, when the applied load is relatively low (highest J ratio), the difference in J ratio between the nozzle-pipe model and pipe model is smallest between case 1, case 2 and case 3 (reflecting material property) and largest between crack sizes. As the applied load increases, the differences in J ratio between the two models for case 1, case 2, case 3 and various crack sizes increase and converge to fixed values regardless of load increase. This indicates that with initial lower applied

loading the displacement at the crack tip is relatively small, having a large elastic component, is material and pipe size dependent, and is less influenced by the nozzle stiffness. As the applied load increases, the displacement at the crack tip accumulates very large local plastic strains caused by a large crack opening area. Also, at these large applied loads, the effect of material property and pipe size have less influence on the crack tip displacement, while the nozzle stiffness contributes significantly to the crack tip displacement.

Figure 11 compares the crack opening area (COA) between the pipe model and nozzle-pipe model. The nozzle is carbon steel while the pipe is assumed to be stainless steel - case 2. When the applied load is small the difference in COA between the two models is small even as the crack size is increased. Applying a large load results in a significant difference in the COA between the two models as the crack size is increased.

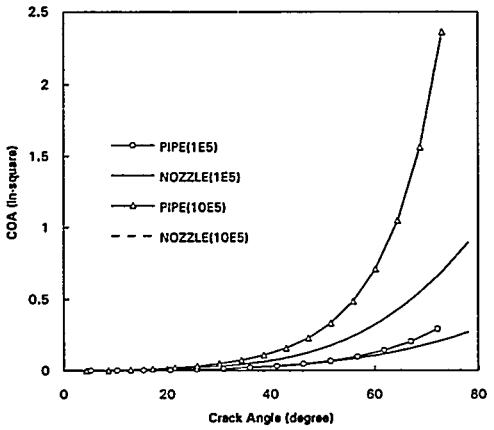

Figure 11. Crack Opening Areas for $1x10^5$ and $1x10^6$ Applied Load (Case 2)

A comparison is made between the two models (case 2) of the detectable leakage crack (DLC) length applying normal operating loads (NOP). Looking at Figure 12, for small NOP loads the difference between the nozzle-pipe model and pipe model is small. As the NOP load is increased, the detectable leakage crack length significantly varies. Figure 13 shows the same DLC results as a ratio of nozzle-pipe model to pipe model versus NOP loads.

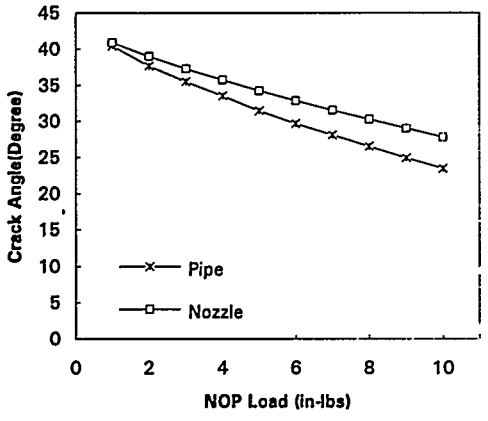

Figure 12. Comparison of Detectable Leakage Crack Angle (Case 2)

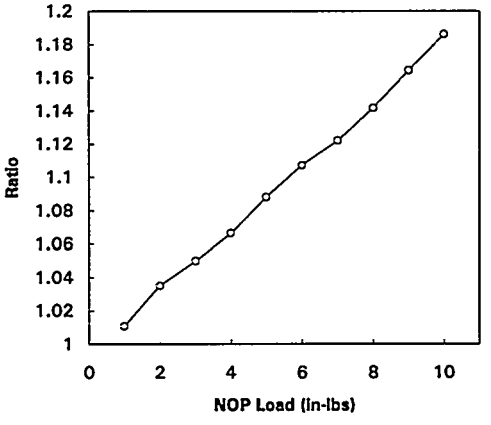

Figure 13. Ratio of Detectable Leakage Crack Size(Case 2)

Figure 14 presents a PED for the nozzle-pipe model and the pipe model (case 2) where "A" is the detectable leakage crack length. These results define the LBB requirements to the piping designer. Two complete LBB evaluations are

performed for each model to determine the maximum allowable stability load; one evaluation for a low normal operating load, and the other for a high operating load. These loads span the typical operating loads for the piping system. In developing the allowable loads, the appropriate LBB margins are included. The resulting LBB solutions are plotted as a set of allowable curves for the maximum design basis load, such as the seismic load versus the normal operating load. The stiffer nozzle-pipe model can absorb higher loads for a crack size that leaks at 10gpm than the same diameter size pipe model. Figure 15 takes the LBB results used to develop PED curves and shows the allowable loads as the ratio of nozzle-pipe model to pipe model versus normal operating loads.

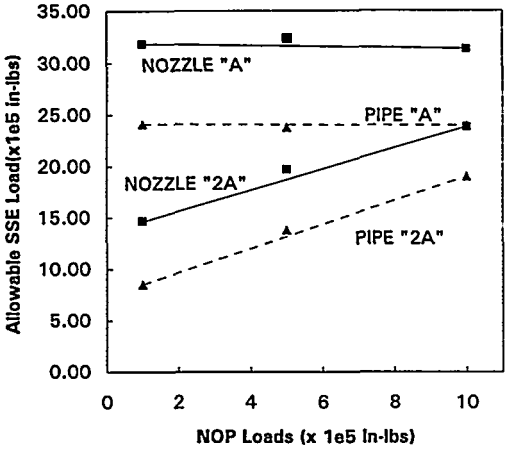

Figure 14. PED for Nozzle-Pipe Model and Pipe Model (Case 2)

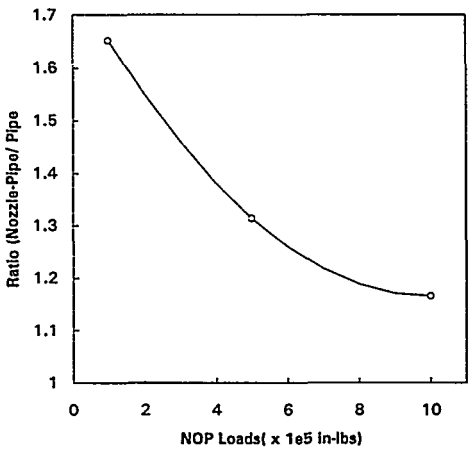

Figure 15. Ratio of Stability Load (Case2)

CONCLUSION

As part of an LBB evaluation, a series of elastic plastic fracture mechanics analysis results using the FE method has been presented for a nozzle-pipe model and a pipe model. The comparison between the two models are in the form of a ratio between the models. This provides a means of normalizing the results for easier comparison. Depending on the magnitude of applied load trying to open the crack area, the size of crack length and the materials used, the ratio of nozzle-pipe model to pipe model can be either small or very large for small diameter piping systems. This study concludes that using the traditional simplified FE pipe model to evaluate LBB for a small diameter pipe near the terminal end, where geometric and material properties usually vary, can lead to over conservatism by a factor of up to 5 compared to a FE nozzle and pipe model.

Since the nozzle-pipe analysis can be costly and time consuming, a parametric study, similar to that presented, could be extended to bound certain size piping systems and loads to obtain the corresponding ratios. These ratios or "correction factor," can then be applied to the simple pipe model analysis of future piping systems whose sizes fall inbetween the bounding cases. This would be cost effective and reduce conservatism inherent in the simple model approach.

REFERENCES

1. Fabi, R. J., and Peck, D. A.,"Leak Before Break Piping Evaluation Diagram", 1994 Pres. Ves. & Piping Vol. 283, pp 111-116.
2. NUREG-1061 Vol. 3, "Report of the US Nuclear Regulatory Commission Piping Review Committee, Evaluation of Potential Pipe Breaks", November 1984.
3. Standard Review Plan 3.6.3, Federal Register Volume 52, Number 167, August 28, 1987.
4. EPRI Report No. NP-3596-Sr, Revision 1, "PICEP Pipe Crack Evaluation Program (Revision 1)", special report,

December 1987.
5. Ayres, D. J., and Khant, L. H., "Benchmark Calculation for Leak Before Break Evaluation of Nuclear Plant Piping", 1991 Pres. Ves. & Piping Vol. 218, pp 13-17.
6. CE-MARC, Version Cycle 21, ABB CE, Windsor, CT. 1993.

APPLICATION OF THE LEAK-BEFORE-BREAK CONCEPT TO THE PRIMARY CIRCUIT PIPING OF THE LENINGRAD NPP

A.P. Eperin[1], Yu.O. Zakharzhevsky[1], A.I. Arzhaev[2]
V.A. Kiselyov[2], R.P. Keskinen[3], K. Ikonen[4] and H.J. Raiko[4]

[1] Leningrad Nuclear Power Plant, Russia
[2] ESC MAE RDIPE, Russia
[3] Finnish Centre for Radiation and Nuclear Safety (STUK), Finland
[4] VTT Energy, Finland

ABSTRACT

A two-year Finnish-Russian cooperation program has been initiated in 1995 to demonstrate the applicability of the leak-before-break concept (LBB) to the primary circuit piping of the Leningrad NPP. The program includes J-R curve testing of authentic pipe materials at full operating temperature, screening and computational LBB analyses complying with the USNRC Standard Review Plan 3.6.3, and exchange of LBB-related information with emphasis on NDE. Domestic computer codes are mainly used, and all tests and analyses are independently carried out by each party. The results are believed to apply generally to RBMK type plants of the first generation.

1 INTRODUCTION

Extensive measures have been in progress at the Leningrad nuclear power plant (LNPP) since the early 1990's to upgrade the integrity of the main pressure retaining components [1]. The Research and Development Institute of Power Engineering (RDIPE), representing the main designer has actively participated in development of automatic metal condition monitoring and leak detection systems. By proposal of RDIPE, a comprehensive and systematic program has been initiated to upgrade all RBMK plants by implementation of the LBB concept [2].

The Finnish-Russian cooperation for upgrading the LNPP stems from 1992. It has centered around operational safety, fire safety and integrity of pressure retaining components. The last item has involved numerous in-service inspections conducted by Finnish specialists. Quite recently, it was agreed between RDIPE, LNPP and the participating Finnish organizations STUK and VTT about extending the cooperation to LBB implementation. A two-year program was established in aim to demonstrate the applicability of the LBB concept to the primary circuit piping of the LNPP. The program includes a study of mechanical properties and static crack growth resistance characteristics of materials as well as detailed stress, fracture mechanics and leak rate calculation analyses. The results of these analyses will support the statement about LBB concept applicability to RBMK primary circuit piping and justify the requirements to in-service inspection and leak detection systems. This paper describes of the main tasks, the methodologies to be applied and the current status of the program.

2 THE LNPP PRIMARY CIRCUIT PIPING

2.1 Design and manufacture

The LNPP units 1 and 2 are located in Russia, 5 km south-west of the city of Sosnovy Bor, at a distance of ca. 100 km from the southern coast of Finland. The plants belong to the first generation of RBMK-1000 plants and were commissioned in 1974 and 1975, respectively. The second generation units 3 and 4 were commissioned 5 years later and their design fulfilled more stringent requirements. In 1989, the utility embarked on step-by-step upgrading of the units to meet the current Russian safety regulations.

As a pressure tube reactor plant, the LNPP involves a large amount of primary circuit piping of various sizes in close proximity to each other whose integrity is of vital importance to plant safety. The coolant circulates in 2 independent loops, each having 4 main circulating pumps (MCPs) for discharging the coolant to one half of the fuel channels via a system of headers. In each loop, the two-phase flow is fed from fuel channels to 2 drum-separators, from where the separated water flows towards the MCPs via 24 downcomers and a suction header. A section of one loop between the drum separator and the distribution groop header is shown in Figure 1. During normal operation, internal pressure is 8.6 MPa and the temperature of coolant is 270 ^{0}C.

The large diameter primary circuit piping on the suction and discharge sides of the MCPs is made from low-carbon 22K ferritic steel, which is gradually being replaced by ferritic 19MN5 steel during the upgrading program. The cross-sectional dimensions are given in Table 1. The radius of center-line curvature of elbows is 1100 mm. At either unit the piping is cladded with austenitic stainless steel of type 08Ch18H10T. Welds are made according to Rules [3 & 4] by austenitic arc welding with the use of wire Cv-08A and flux 348A or manual arc welding with the use of UONI 13/55 type electrode. The elbows of unit 1 contain axial welds. Dissimilar welds exist on the discharge side of each MCP owing to austenitic flow limiters appearing in Figure 1. The downcomers, 300 mm in diameter, are made from austenitic steel 08Ch18H10T.

Table 1. Cross-sectional dimensions of primary circuit piping of LNPP unit 2.

Item	Straight pipe	Elbow
Outer diameter [mm]	828	858
Wall thickness [mm] including 5 mm cladding (08Ch18H10T)	38	53

2.2 Leak and metal monitoring

The leak detection system of the first generation LNPP units is partially under development which aims at a sensitivity of 3.8 l/min and a localization accuracy of 1 m. The system is based on monitoring of humidity, radioactivity of air and acoustic signals.

In accordance with the current Russian Rules PNAE G-7-08-89 [5], a control of metal condition is foreseen in course of operation and an appropriate NDE instruction is developed. For all primary circuit piping welds a 100 percent ultrasonic control is carried out once during each period of four years. To assess control results, tables of allow-

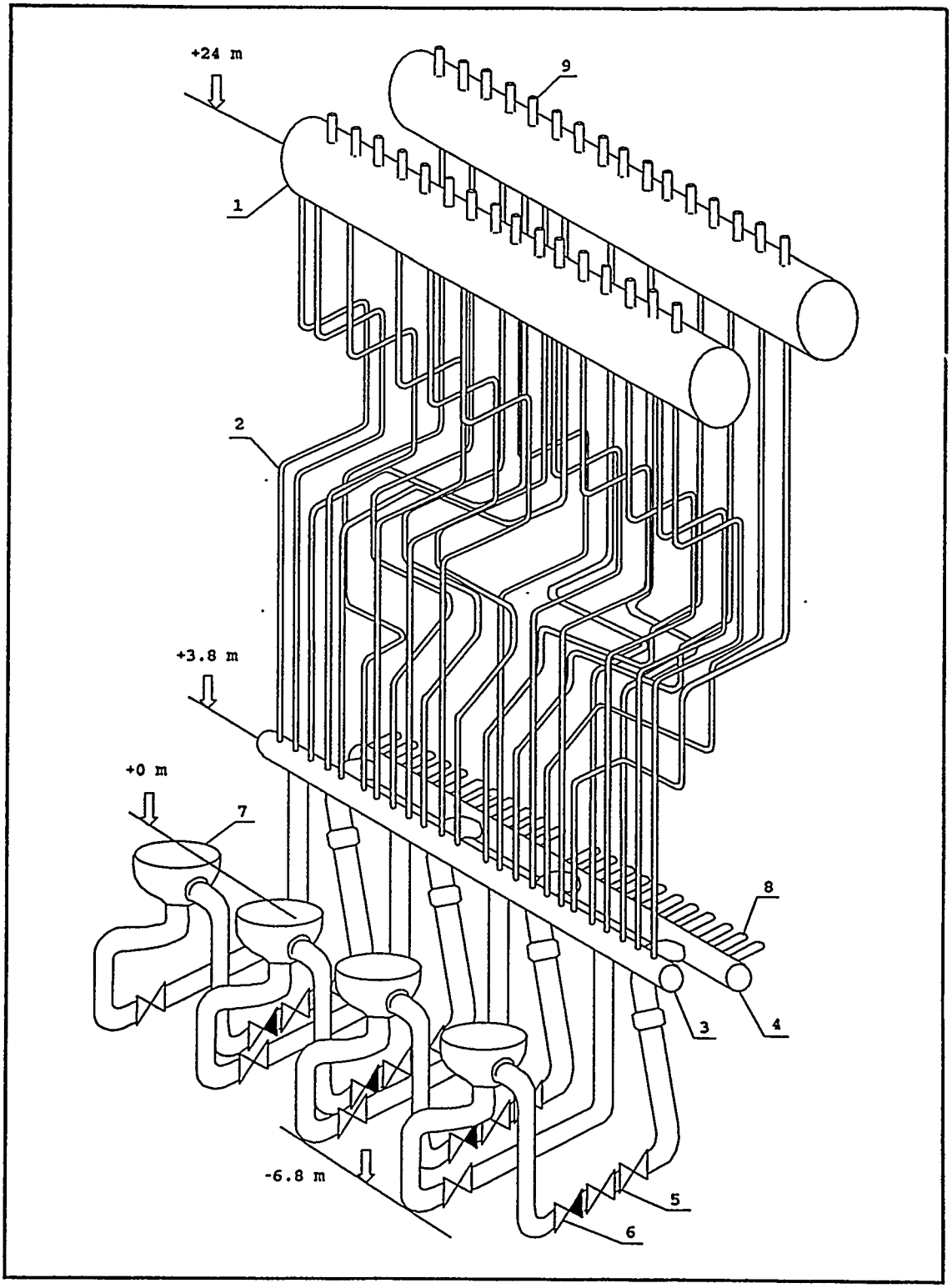

Figure 1. Layout of components in one circulation loop at the section from drum-separator to distribution group header [1]: drum-separator (1), downcomers (2), suction header (3), pressure header (4), valves (5), check valve (6), main circulation pump (7), distribution group header (8), stream branch (9)

able defects can be used. A feature specific to Russian Rules is cutting samples of the circuit for examination after every 100 000 hours of operation. A typical example of mechanical properties attained in such examination at full operating temperature is given in Table 2.

Table 2. Mechanical properties of piping materials of LNPP unit 2 at 300 ^{o}C after 100,000 hours of operation.

Material	E GPa	A %	Z %	R_m MPa	$R_{p0.2}$ MPa	*)K_{cJ} MPa$\sqrt{m}$
22K (base material)	180	25	52	430	196	140
UONI 13/55 (circumferential welds)	180	23	52	460	304	140
*)Cv-08A wire with flux 348A (axial welds)	180	26	45	500	248	-

*) Before operation

3 THE FINNISH-RUSSIAN UPGRADING PROGRAM

3.1 Main activities

Finnish-Russian cooperation for upgrading the safety of the LNPP has been under way since 1992. The program centers around three main areas which are operational safety, fire safety and integrity of pressure retaining components. Based on direct contacts between STUK and the LNPP, existing practices and technologies as well as ongoing upgrading efforts have been extensively reviewed within these areas via mutual discussions, walkdowns, in-service inspections and testing at Finnish laboratories. Comparative technical exchange visits to Finnish NPPs have also been organized for experts of the LNPP while representants of the Russian nuclear regulatory body Gosatomnadzor have been invited to attend. Whenever potential for further improving of safety has been found, the Finnish party has presented suggestions, supported the upgrading efforts and provided the plant with services and equipment based on Western technology.

3.2 LBB cooperation

As part of activities to improve the integrity of pressure retaining components, a two-year LBB cooperation program has been initiated in 1995. The Russian parties include the LNPP, the main designer RDIPE and its stress analysis centre ECS MAE RDIPE. The loading conditions are determined by the architect engineering company VNIPIET. In Finland, the nuclear regulatory body STUK coordinates analysis and testing tasks which are conducted by VTT Energy and VTT Manufacturing technology, respectively. The cooperation is funded in 1995 by the LNPP and the Finnish Ministry of Trade and Industry.

The cooperation program aims at demonstrating the LBB concept for the ferritic large diameter primary circuit piping and the austenitic downcomer piping. Special attention is given to discontinuities such as elbows and T-connections whereas the valves and the MCPs are not considered. The demonstration follows the principles of the USNRC Standard Review Plan 3.6.3 [6], also stated in the Russian standard M-LBB-01-93, [7]. The analysis and testing tasks are independently carried out by parties of each country whereupon the results are compared and final conclusions

are made.

A preliminary screening, conducted by the Russian parties, is available at the onset of the program. Based on quality assurance considerations regarding design and manufacture, the large diameter piping would qualify for LBB though potential for classical water hammer has not as yet been precluded. The water hammer issue, as well as stress corrosion cracking susceptibility of austenitic piping with possible cold formed bends will be subject of further screening during the bilateral program.

To check potential for thermal ageing and to yield the material stress-strain and J–R curves for fracture mechanics analyses, ferritic base and weld material samples, removed from service after over 100 000 h of operation since 1973, are tested at full operating temperature. A sample containing a ferritic to austenitic dissimilar weld is manufactured at the Izhora steel factory according to original procedure. The samples are identified and supplied with certificates of material and manufacture. VTT uses these samples to manufacture the specimens whose final size and type will be decided based on first observations on ductility. J–R curves are determined in accordance with the ASTM E1152–87 standard [8]. Crack plane orientations TL and LT (see Figure 2) are used, representing coplanar extension of axial and circumferential through-cracks. In case of the welds, radial extension of surface cracks is also considered via test for crack plane orientations TS and LS.

Non-linear finite element analyses are made for postulated cracks at axial and circumferential welds of straight pipes and elbows, and for axial crack at the crown of elbow. At most stressed locations, critical crack lengths are determined corresponding to normal operating and safe-shutdown earthquake (SSE) conditions. The internal forces and moments that constitute the loading at each location are taken from existing stress analyses where SSE intensity of 6^{o} MSK 64 was mandatory. The crack opening shapes and areas are evaluated for normal operating conditions; special-purpose thermal-hydraulic codes will be used for computing the respective leak rates. The finite element analysis results are compared with those obtained by means of estimation methods such as the R6, EPRI, Battelle, plastic limit load and moments methods.

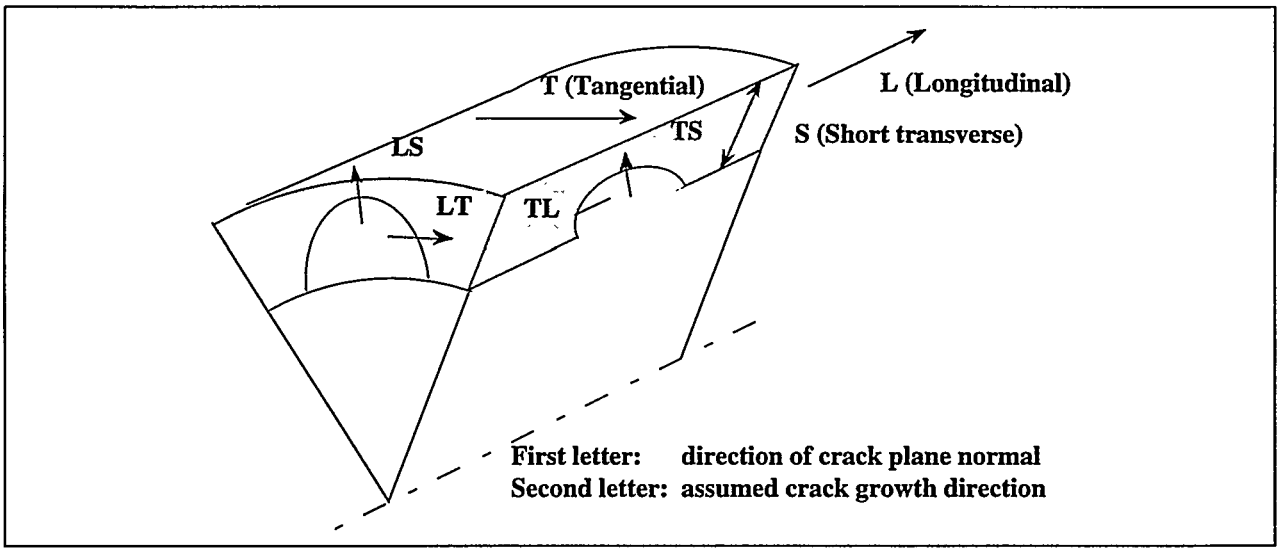

Figure 2. Crack plane orientations to be used in material toughness testing.

The program also involves exchanging LBB-related information in the areas of NDE, continuous monitoring techniques and experimental validation of analysis results. As to NDE, the Finnish party provides education seminars and guidelines regarding detection, characterization and acceptance of defects. Performance of Russian NDE equipment will be also reviewed.

3.3 Computational systems

Both parties will mainly use domestic computer codes for computational LBB analyses. In VNIPIET, the ASTRA code is used for stress analysis at normal operating and SSE conditions. For elastic-plastic 3D fracture mechanics analyses with isotropic strain hardening, ECS MAE RDIPE employs the TAKT code which has been developed at the Moscow Institute for Physics and Engineering (MIFI). The code uses 20-noded isoparametric solid elements with automatic mesh generator. Collapsed elements and shift of intermediate side nodes enable modelling the crack tip opening displacement (CTOD) and strain singularity at crack tip. J-integral is evaluated by means of the domain method. Various computer codes are also available for application of estimation methods. Homogeneous equilibrium two-phase models are used for leak rate analysis where the crack opening area is obtained from analytical solution of plasticity-corrected linear-elastic fracture mechanics.

The LBB computation system of VTT Energy has been mainly developed in course of a LBB project ordered by STUK [9]. An interactive code LBBCAL performs quick tentative fracture mechanics and leak rate analysis based on

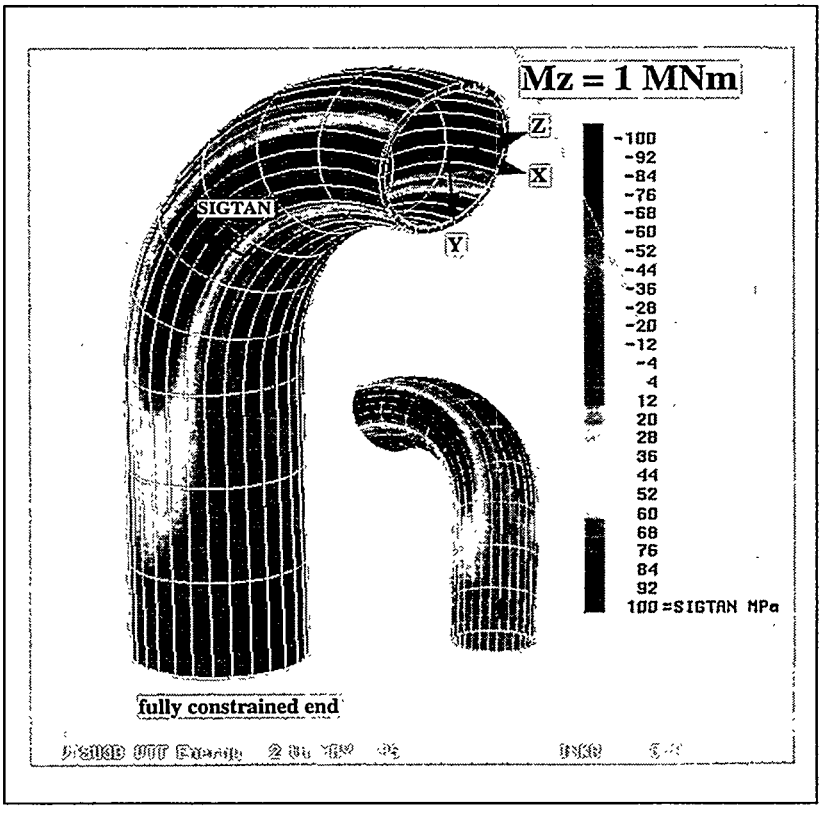

Figure 3. Tangential stresses of elbow under in-plane bending.

estimation methods. A finite element code EPFM3D is meant for complex situations and has a similar theoretical basis as TAKT. EPFM3D offers advanced colour graphics, mesh and distributed loading generators for various pipe component and crack geometry combinations, automatic crack area evaluation, J and CTOD evaluation along crack front and an option for analysis of entire piping system with cladding. Benchmarking of an in-house developed leak rate code CRAFLO, based on a homogeneous equilibrium two-phase flow model with phase slip, is under way; so far the well established SQUIRT2 code [10] has been used.

3.4 Preliminary results

In the initial phase, the TAKT and EPFM3D codes are compared by computing the stress fields at cantilevered uncracked elbow, subjected to unit forces and moments at the free end. A sample result given by EPFM3D for tangential stresses caused by in-plane bending is shown in Figure 3. The adjoining straight pipe section was added to enable easy modelling of the fixed end without constraining ovalization at elbow. Results of TAKT are expected after ongoing checks against the Russian stress analysis standard PNAE G-7-002-86 [11].

The first comparative fracture mechanics exercises include analyses for: a) straight pipe with axial through-crack of various lengths under internal pressure of 8.6 MPa; b) straight pipe with circumferential through-crack subtending an angle of 40^{o} and subjected to various bending moments. Figure 4 shows the finite element meshes used by VTT Energy. The crack front area was systematically modelled with well-shaped elements to prepare for abrupt stress and strain gradients. The stress-strain curve at temperature 270^{o}C was estimated using the PNAE G-7-002-86 standard. The respective leak rates, based on numerical crack opening area evaluation and SQUIRT2 analysis, are plotted in Figure 5. A progressive trend is visible in each case and may be attributed to dominance of skin friction at small crack opening displacements (CODs).

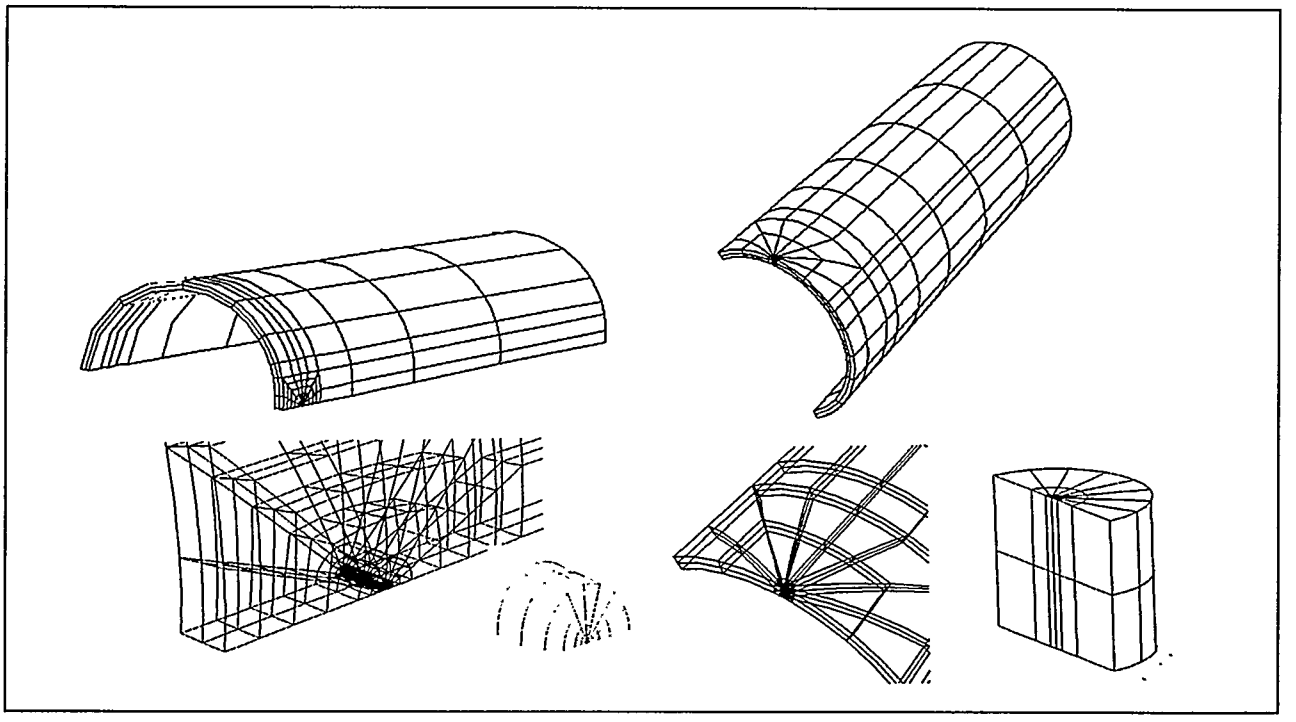

Figure 4. Element mesh for straight pipe with axial and circumferential through-cracks.

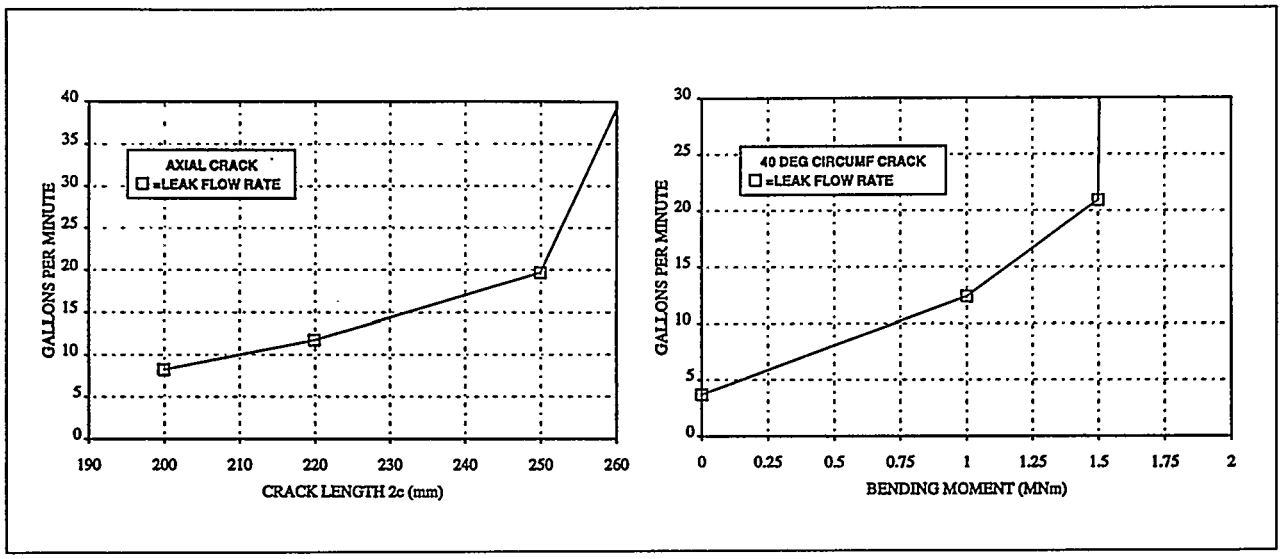

Figure 5 a,b. Leak rates from axially and circumferentially through-cracked straight pipes under internal pressure and bending moment, respectively.

Preliminary numerical analysis has also been carried out to assess the temperature used in material toughness testing. From leak rate tests conducted e.g. during the last phase of the HDR research program [12], it is known that vaporization lowers the temperature of a leakage flow which in turn causes cooling in the nearby pipe material. Thermal shrinking then results which may control the crack opening area and the state of stress ahead of the crack tip.

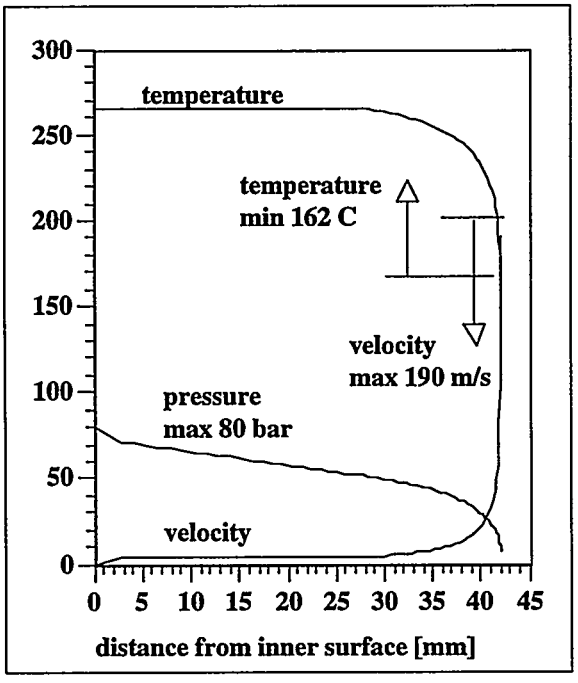

Figure 6. Temperature, pressure and velocity profiles indicating leakage-induced cooling at through-crack.

Reduction of the material toughness is also possible. The CRAFLO code was used to compute through-the-thickness temperature, pressure and flow velocity profiles for an illustrative application having wall thickness of 42mm and constant COD of 0.1 mm. The internal pressure and coolant temperature are 8 MPa and 263°C, respectively, and the leak discharges to atmospheric pressure. The liquid water is subcooled by 20°C. The resulting profiles are plotted in Figure 6, suggesting that for small CODs the effect is fairly local and occurs near the outlet only where the temperature drop is about 100°C. The affected area obviously increases with the COD; hence further studies of the overall impact on the LBB concept are being scheduled.

4 CONCLUSION

A two-year Finnish-Russian cooperation program has been initiated in 1995 to demonstrate the applicability of the LBB concept to the primary circuit piping of the Leningrad NPP. The results are believed to apply generally to RBMK type plants of the first generation. A preliminary screening, conducted by the Russian party based on quality aspects of design and manufacture, suggests that the large diameter ferritic piping would qualify for LBB. Further screening of potential for water hammer and stress corrosion susceptibility of austenitic piping will be undertaken. In material toughness testing, the test temperature will be assessed in view of a leakage-induced cooling of nearby pipe material. The comparative test and analysis schedules serve development of LBB methodology in both countries.

ACKNOWLEDGEMENTS

This work was supported by the Finnish Ministry of Trade and Industry. The authors want to thank Mr. Jaakko Miettinen for performing the thermal hydraulic computer runs.

REFERENCES

[1] Leningrad Nuclear Power Plant, a General Description, Ministry of Russian Federation for Atomic Energy, 1994, 86 p.

[2] Arzhaev, A.I., Bougaenko, S.E., Denisov, I.N., Kiselyov, V.A., Leak-Before-Break Criteria and Strength Monitoring Implementation Impact on In-service Inspection of RBMK Priamry Circuit Components, to be published in the Int. J. of Pressure Vessels & Piping.

[3] NPP Equipment and Pipes. Welded Joints and Cladding. Basic Rules (in Russian). PNAE G-7-009-89, Energoatizdat, Moscow, 1991, 320 p.

[4] NPP Equipment and Pipes. Welded Joints and Cladding. Examination Rules (in Russian). PNAE G-7-002-89, Energoatizdat, Moscow, 1991, 320 p.

[5] Rules and Manufacture and Safe Operation of NPP Equipment and Pipes (in Russian), PNAE G-7-08-89, Energoatomizdat, Moscow, 1990, 168 p.

[6] Wichman, K. & Lee, S. 1990. Development of USNRC Standard Review Plan 3.6.3 for Leak-Before-Break Applications to Nuclear Power Plants. Int. J. of Pressure Vessels & Piping Vol. 43, 1990, pp. 57-65.

[7] Piping Calculation Procedure for Nuclear Power Plants within The "Leak-Before-Break" Concept, M-LBB-01-93, ECS MAE RDIPE, Moscow, 1993, 21 p.

[8] ASTM Method E1152-87, Standard Test Method for Determining J-R Curves, Annual Book of ASTM Standards, Vol. 03.01, 1992, pp. 847-857.

[9] Ikonen, K. & Raiko, H., Leak-Before-Break Evaluation Procedures for Piping Components, Report STUK-YTO-TR 90, Finnish Centre for Radiation and Nuclear Safety, Helsinki, 1995, 58 p.

[10] SQUIRT User's Manual, Version 2.2, D. D. Paul, N. Ghadiali, S. Rahman, P. Krishnaswamy, and G. Wilkowski. Battelle, Columbus, OH, USA.

[11] Strength Analysis Standards for Equipment and Piping at Nuclear Power Plants, PNAE G-7-002-86, Energoatomizdat, Moscow, 1989 (translation: USNRC 2540).

[12] Talja, H., Koski, K., Rintamaa, R., Keskinen, R., A Review of the HDR Research Programme (in Finnish), Report STUK-YTO-TR 83, Finnish Centre for Radiation and Nuclear Safety, 1995, 95 p.

APPLICATION OF THE LBB CONCEPT TO NUCLEAR POWER PLANTS WITH WWER 440AND WWER 1000 REACTORS

J. Žďárek, L. Pečínka
Nuclear Research Institute Řež, Czech Republic

INTRODUCTION

For the WWER 440 Type 230 and 213 reactors and for the WWER 1000 Type 302, 320 and 338 reactors, there are two characteristic safety issues

- only very limited anti-pipe whip provisions have been applied
- there is a general lack of design information.

As a result of this situation the IAEA has decided to pay more attention to the LBB application issue in order to assist countries operating all this above mentioned reactors. A status report on the "Applicability of the Leak before Break Concept" was published IAEA /1/. More recently, "Guidance on the Application of the LBB Concept" was published in 1994 /2/.

The application of the LBB concept to the WWER NPPs in the former Czechoslovakia commenced in 1991. The final safety case for the NPP Jaslovské Bohunice, units 1 and 2 (WWER 440/230) was the first to be completed. This was submitted to the Office of Nuclear Supervision of Slovak Republic for approval. This safety case was based on the results of a plant specific LBB programme. By the end of 1994, the final safety cases for all the remaining WWER 440 type 213 NPPs in the Czech Republic (NPP Dukovany, units No 1 & 4) and Slovak Republic (NPP Jaslovské Bohunice, units No 3, 4 and NPP Mochovce, unit No 1, 2 (under construction)) had been completed. The have been submitted to the respective Regulatory Bodies for approval. In August 1995 the final safety case for the NPP Temelín (WWER 1000/320) was completed and submitted to the State Office of Nuclear Safety of Czech Republic for approval.

DEVELOPMENTS AND LEGISLATIVE MILESTONES FOR THE WWER REACTORS

Period before 1973

During this time the WWER 440 Type 230 were designed and put into operation. The standards (NTDs) for the design and construction of conventional power plants were used and only some nuclear NTDs had been introduced. These related to radiation protection, the nuclear chain reaction and irradiation effects of material. A design basis accident (DBA) was been postulated as the loss of integrity of the primary piping equivalent to a pipe break of 32 mm diameter. The safety concept also required that essential primary circuit equipment and its auxiliary systems should have high reliability during their lifetime. Furthermore, it was specified that protection against human errors be based, to a considerable extent, on organizational measures aimed primarily at the prevention of accident initiating events. These measures included in-service inspection (ISI) and control of the quality of the manufacturing and installation of primary circuit equipment. For these reasons pipe whip restraints and barriers against jet impingement forces were not introduced into design and construction.

Period from 1974 to July 1982

The WWER 440 Type 213, WWER 1000 Type 187 and WWER 1000 Type 302 were designed and a put into

operation during this time.

At the end of 1973, the basic nuclear document "General Provisions for Assuring Safety during Design, Construction and Operation of NPPs" OPB 73 was issued. The OPB - 73 was supplemented by a other NTDs. For design of pressure retaining components following NTDs are the most important relevant:

- Strength Calculation Standard for Components and Piping of NPPs, Experimental and Test Reactors
- General Provisions for Welded Joints and Components of NPPs, Experimental and Test Reactors (SP 1513 - 72)
- Regulations for Control of Welding Joints and Components of NPPs, Experimental and Test Reactors (PK 1514 - 72)

For all above mentioned reactors the double ended guillotine break (DEGB) has been postulated as a design basis accident. For the WWER 440/213 Type plant it was decided to introduce pipe whip restraints and jet impingement barriers for the primary piping, pressurizer surge lines, steam piping and feedwater lines inside containment. The pipe whip restraints have not yet been completed all the operating plants.

Period from July 1982 to June 1990
The WWER 1000/320 and WWER 1000/338 were designed and put into operation during this time. Also in July 1982 OPB - 73 was replaced by a new version, OPB - 82 and a new NTD system was established. The primary piping, steam piping and feedwater lines inside containment are designed without pipe whip restraints for the WWER 1000/320 & 1000/338 plant.

Period after July 1990
In July 1990, a new NTD document, OPB - 88, came into force replacing OPB - 82. This new version included many important changes. The NTD system related to OPB - 88 were used to design the new generation of WWER 1000 NPPs (Version 91 and 92).

LEGISLATIVE BASIS AND REQUIRED PROCEDURES FOR THE LBB CONCEPT IN CZECH REPUBLIC

The leak before break (LBB) concept adopted in the Czech Republic /3/ is based principally on US NRC NUREG - 1061 /4/ and the Standard Review Plan, Section 3.6.3 /5/. The guidelines in these documents require demonstration that a through thickness defect, from which the leak can be detected, will remain stable when subject to normal operation and seismic loadings.

The procedure is simple in principle and can be summarized as follows

i) identify those locations in the pipework at which the highest stresses occur in combination with the least favourable material properties
ii) demonstrate by fatigue crack growth analysis that a defect which would be permitted by the acceptance criteria of Section XI of the ASME Code at each of these locations will not grow significantly during service
iii) postulate through-wall cracks of sufficient size to ensure their detection by means of leak detection systems and demonstrate that these crack will be stable even when subjected to the loads imposed by a safe shutdown earthquake (SSE) occurring during normal operation
iv) show that the corrosion-erosion damage is negligible

To demonstrate that the requirements can be met , the following work is required:

- static and seismic analysis of main circulation loop and stress analysis of highly stressed components
- analysis of water hammer
- assessment of stability of heavy component supports
- determination of fracture mechanics properties.

The location of highest stress coincident with least favourable material properties is determined for base materials, weldments and safe ends and for the load combination associated with normal operation and the simultaneous occurrence of a SSE.

For each location where LBB is to be evaluated, a through wall crack of a length corresponding to a 3.8l/min leak multiplied by the safety factor 10 is postulated under normal operating condition. This crack length is called L_{leak}. If a critical through-wall circumferential crack length is introduced corresponding to the plastic collapse under normal operation conditions (NOC) and site specific SSE as $L_{crit,SSE}$ then the following condition must be fulfilled: $L_{crit,SSE}/L_{leak} > 2$. The safety factor for loads, defining the stability against brittle fracture must be higher than 1 or 1.4 according to the type summation (absolute or algebraic), see /2, 5/.

VALIDATION AND VERIFICATION OF PROCEDURES

The following validation and verification programmes have been performed

- experiments with through wall crack on full scale components including; the reactor pressure vessel safe-end, the pressuriser nozzle safe-end, and the steam generator elbow with circumferential and simulated longitudinal welds,
- leak rate and diagnostic tests on an experimental loop with coolant parameters 12.5 MPa (1785 psi) and t = 290°C (554°F) with a range of pipe sizes up to a max. pipe diameter 200 mm (7.9 in).

The experimental results have been compared with theoretical assessments (pre-test and post-test calculations). Note that the guidelines do not require all this programmes.

LESSONS LEARNED FROM THE LBB CONCEPT APPLICATION

For the WWER 440/230 type following lessons were learned

- the statistical evaluation of the leakage crack lengths L_{leak} in all weldments of the three loops of WWER 440 Type 230 shows that the median value is 199 mm. This is approximately 11.2% of the main circulating pipe outside diameter circumference. The corresponding L_{leak} value with 95% non-exceedance probability (median + twice of standard deviation) is then 290 mm, see Fig. 1,
- the statistical evaluation of calculated plastic collapse lengths $L_{crit,\ SSE}$ for Safe Shutdown Earthquake (SSE) with peak ground acceleration (PGA) of 0.25 g and gravel-sand type base, the median value is 718 mm (40.4% of the outside circumference). The corresponding 95% non-exceedance probability is then 915 mm, see Fig. 2,
- the statistical evaluation of safety margin $L_{crit,\ SSE}/L_{leak}$ give the median value 3.6, which is less twice the required value of 2, see Fig. 3,
- the comparison of the seismic upgrading criteria in terms of High Confidence of Low Probability of Failure values (HCLPF) and LBB safety coefficient $L_{crit,SSE}/L_{leak}$ shows that the LBB requirement $L_{crit,SSE}/L_{leak} > 2$ is much more restrictive than the seismic margin condition for HCLPF. It means that in some cases the additional installation of viscous dampers has been necessary /6/ for the fulfilment of $L_{crit,SSE}/L_{leak}$ criterion even though the HCLPF criterion has been fulfilled,
- the water hammer event is assumed to be caused by the sudden failure of the main circulating pump shaft with the consequent pressure wave propagation. The resulting stresses are shown to be negligible in comparison with seismic stresses,
- the fatigue crack growth of the initial cracks postulated in accordance with the IWB- 3500 article of the ASME Code, Section XI is not significant. The maximum value of the crack depth at the end of the design life (30 years) is 11.6% of the wall thickness,
- stability of heavy component support has been demonstrated. This addressees in part the indirect LOCA issue,

- three independent leak detection systems have been successfully installed, using acoustic emission, activity of nozzle gases and humidity or sump level measurements,
- the corrosion mechanisms, mainly stress corrosion cracking and combined corrosion fatigue damage are not significant based on experimental tests,
- the results of fracture mechanics tests on the base metal, HAZ and weld metal confirmed the high values of fracture toughness and adequate J-resistance curve data, see section "Validation and Verification Procedures".

For the WWER 440/213 type following lessons were learned

- the statistical evaluation of the leakage crack lengths L_{leak} in all the weldments of the six loops of a WWER 440 Type 213 shows that the median value is 142 mm. This is approximately 9% of the main circulating pipe outside diameter circumference. The corresponding L_{leak} value with 95% non-exceedance probability (median + twice of standard deviation) is then 238 mm, see Fig. 4,
- the statistical evaluation of calculated plastic collapse lengths $L_{crit, SSE}$ for Safe Shutdown Earthquake (SSE) with peak ground acceleration (PGA) of 0.25 g and for the two plants located on a good rock base but with different design response spectra shows that the median values are 710 mm and 700 mm (approximately 40% of the outside circumference). For the seismically upgraded primary loops with the Safe Shutdown Earthquake peak ground acceleration of 0.25 g and gravel-sand type base, the median value is 690 mm (38.8% of the outside circumference). The corresponding 95% non-exceedance probabilities are 840 mm, 825 mm and 816 mm respectively. These are show in figures Fig. 5, 6 and 7,
- the statistical evaluation of safety margin $L_{crit, SSE}/L_{leak}$ gives of 4.7, 4.45 and 4.3, which is approximately twice the required value of 2, as shown in 8, 9 and 10,
- the seismic upgrading criteria and LBB safety coefficient $L_{crit, SSE}/L_{leak}$ are in the same conflict as four WWER 440/230 type /7, 8, 9/
- the seismic upgrading criterion HCLPF and LBB safety coefficient $L_{crit, SSE}/L_{leak}$ are in the same conflict as for WWER 440/230 type /7, 8, 9/,
- the water hammer event, fatigue crack growth and corrosion mechanism are negligible as for WWER 440 Type 230,
- the used material is identical with WWER 440 Type 213 and therefore all previous conclusions are valid

For the WWER 1000/320 type the following lessons were learned

- the statistical evaluation of the leakage crack lengths L_{leak} in all the weldments of the four loops of the WWER 1000 Type 320 shows that the median value is 224 mm. This is approximately 7.2% of the main circulating pipe outside diameter circumference. The corresponding L_{leak} value with 95% non-exceedance probability (median + twice of standard deviation) is then 275 mm, see Fig. 11,
- the statistical evaluation of calculated values of plastic collapse crack length $L_{crit, SSE}$ for Safe Shutdown Earthquake with peak ground acceleration (PGA) of 0.1 g and for the plant located on a good rock base shows that the median value is 1195 mm (38.2% of the outside circumference). The corresponding 95% non-exceedance probability is 1585 mm (50.7% of the outside circumference), see Fig.12
- the statistical evaluation of safety margin $L_{crit, SSE}/L_{leak}$ gives the median value 5.6, which is approximately three times that the required value of 2, see Fig. 13,
- the seismic upgrading criterion HCLPF and the LBB safety coefficient $L_{crit, SSE}/L_{leak}$ are not in conflict. It means that the additional installation of viscous dampers has not been necessary for the fulfilment of $L_{crit, SSE}/L_{leak}$ criterion /10/,
- the water hammer event, fatigue crack growth and corrosion mechanisms are negligible as for WWER 440 Type 213 and 230,
- the results of fracture mechanics tests on the base metal, HAZ and weld metal confirmed the high values of fracture toughness and adequate J-Δa data for used ferritic steel 10GN2MFA.

CONCLUSIONS

In period 1991 to 1995 NRI, I & M Division have applied the LBB concept to four NPP's with three different types of WWER reactors. Experience shows that

- the main circulating pipework and pressurizer surge lines of WWER type reactor are able to meet the leak before break requirements of the ČSKAE which are based on NUREG 1061 & NUREG 0800, but the seismic measures are needed,
- the median values of L_{leak} are approximately 11% resp. 9% of the main circulating pipe outside diameter for WWER 440/230 resp. 440/213 types and 7.2% for WWER 1000/320 type reactors,
- the value of plastic collapse length $L_{crit, SSE}$ for SSE depend on the PGA value and type of soil. In general, the median value of $L_{crit, SSE}$ for all WWER reactors is approximately of 40% of outside diameter of the main circulating in loop piping,
- the median values of safety margin ratio $L_{crit, SSE}/L_{leak}$ are approximately 3.6 resp. 4.5 for WWER 440/230 resp. 440/213 types and 5.6 for WWER 1000/320 type,
- the standard deviations of L_{leak}, $L_{crit, SSE}$ and $L_{crit, SSE}/L_{leak}$ ratio are for WWER 440/230 and 440/213 higher than that for WWER 1000/320 type. This is as a result of the WWER 1000/320 type main circulating pipe being more rigid than that of the WWER 440/213 type,
- the findings confirm that although the WWER 440/230 and 440/213 plant can be shown to meet the necessary safety requirements, the WWER 1000/320 have larger safety margins on the basis of LBB assessment

REFERENCES

/1/ IAEA : Applicability of the leak-before-break concept.
IAEA-TECDOC 710, June 1993

/2/ IAEA : Guidance for the application of the leak-before-break concept
IAEA-TECDOC, 774, 1994

/3/ CSKAE : Requirements on Safety Report and their Additions. Procedure for LBB Status Determination.
Inst.for Nuclear Informations No 1, 1991

/4/ US NRC : Evaluation of Potential for Pipe Breaks.
Report of the US NRC Piping Review Committee, NUREG 1061, Vol. 3, 1984

/5/ US NRC : Leak before break procedures
Standard Review Plan 3.6.3, NUREG 0800, 1986

/6/ Žďárek J. et al : Conclusions from the LBB methodology application to the NPP Jaslovské Bohunice, units No 3, 4.
NRI Report, obtainable on application, Czech only

/7/ Žďárek J. et al : Conclusions from the LBB methodology application to the NPP Jaslovské Bohunice, unit 3, 4
NRI Report, obtainable on application, Czech only

/8/ Žďárek J. et al : Conlusions from the LBB methodology application to the NPP Dukovany
NRI Report, obtainable on application, Czech only

/9/ Žďárek J. et al : Conclusions from the LBB methodology application to the NPP Mochovce

NRI Report, obtainable on application, Czech only

/10/ Žďárek J. et al : Conclusions from the LBB methodology application to the NPP Temelín, units 1, 2
NRI Report, obtainable on application, Czech only

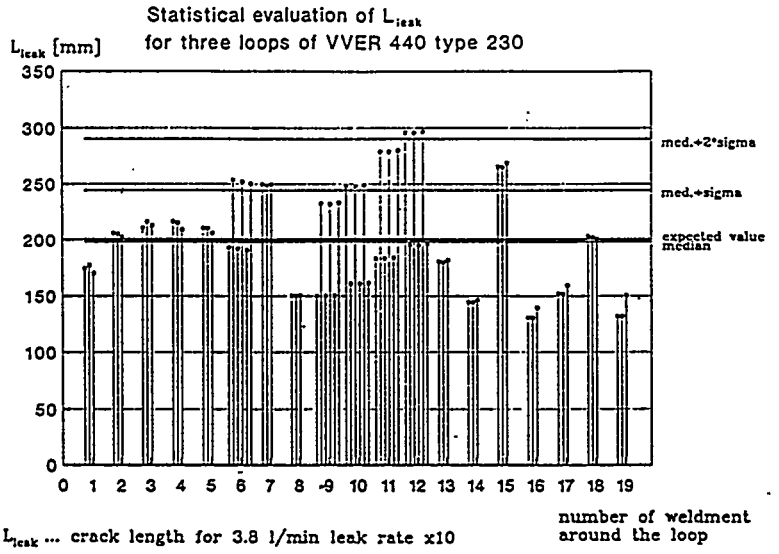

Fig. 1

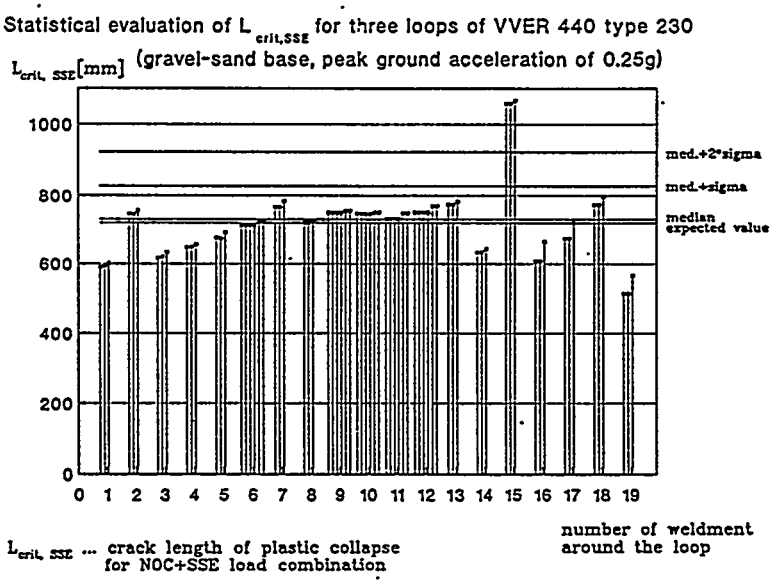

Fig. 2

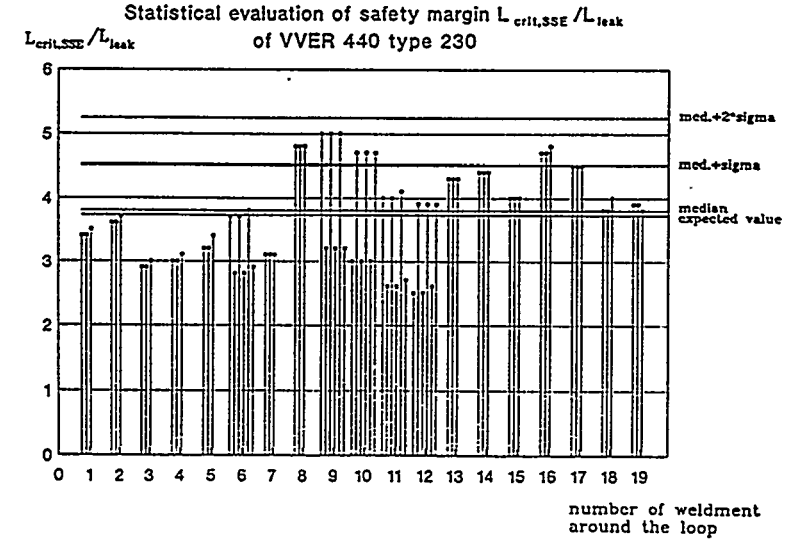

Fig. 3

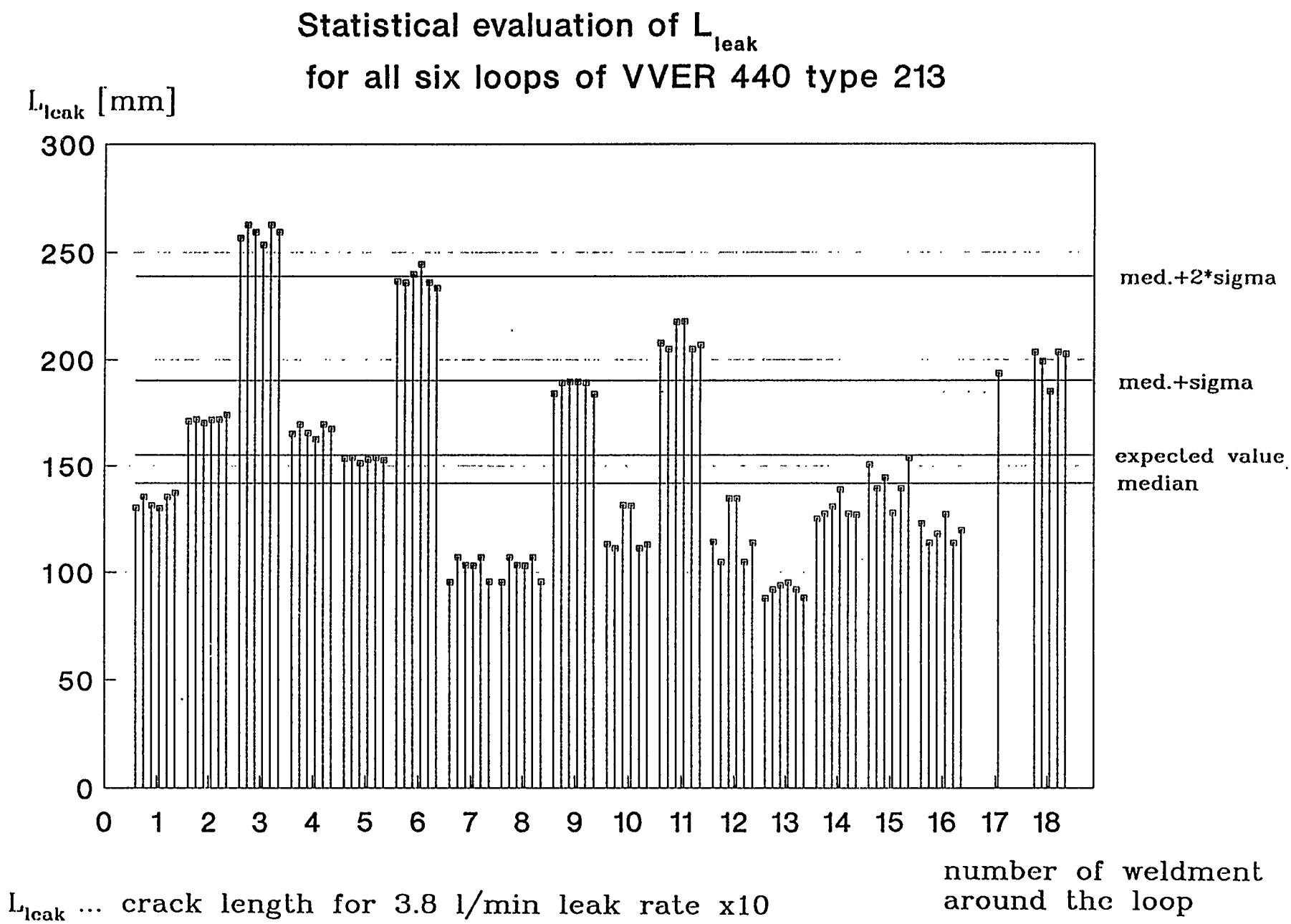
Statistical evaluation of L_{leak}
for all six loops of VVER 440 type 213
L_{leak} [mm]
300
250
200
150
100
50
0
0 1 2 3 4 5 6 7 8 9 10 11 12 13 14 15 16 17 18
med.+2*sigma
med.+sigma
expected value
median
number of weldment
around the loop
L_{leak} ... crack length for 3.8 l/min leak rate x10

Fig. 4

Statistical evaluation of $L_{crit,\ SSE}$ for all six loops of VVER 440 type 213
(good rock base, peak ground acceleration of 0.1g)

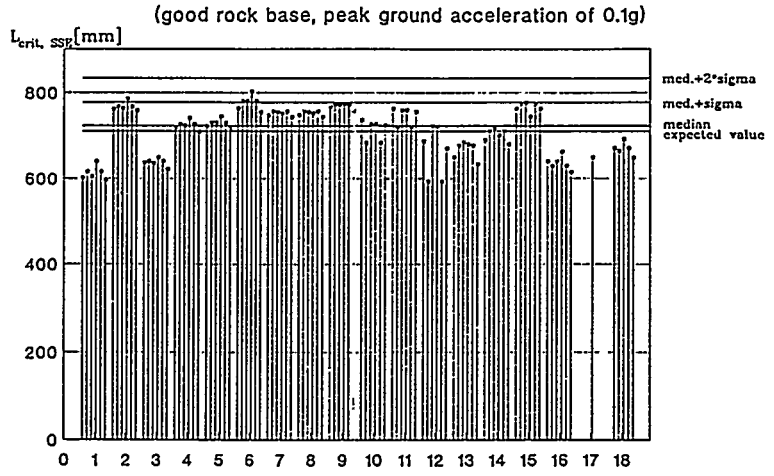

$L_{crit,\ SSE}$ ... crack length of plastic collapse for NOC+SSE load combination

Fig. 5

Statistical evaluation of $L_{crit,SSE}$ (peak ground acceleration of 0.1g, design response spectrum according RG 1.60)

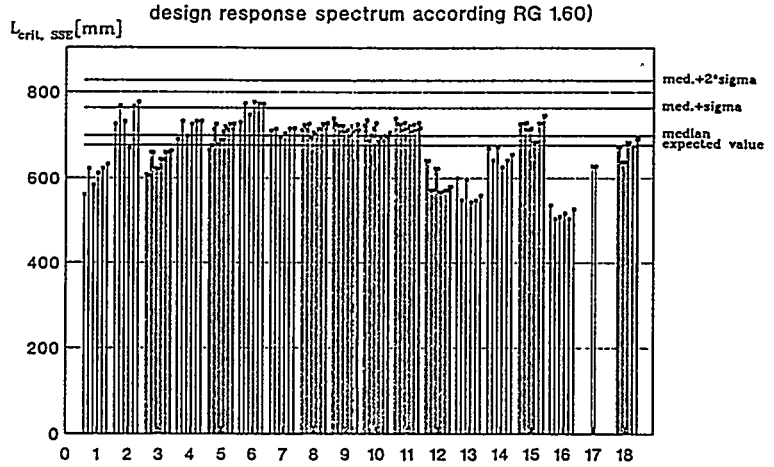

$L_{crit,\ SSE}$ ... crack length of plastic collapse for NOC+SSE load combination

Fig. 6

Statistical evaluation of $L_{crit,\ SSE}$ for all six loops of VVER 440 type 213
(gravel-sand base, peak ground acceleration of 0.25g)

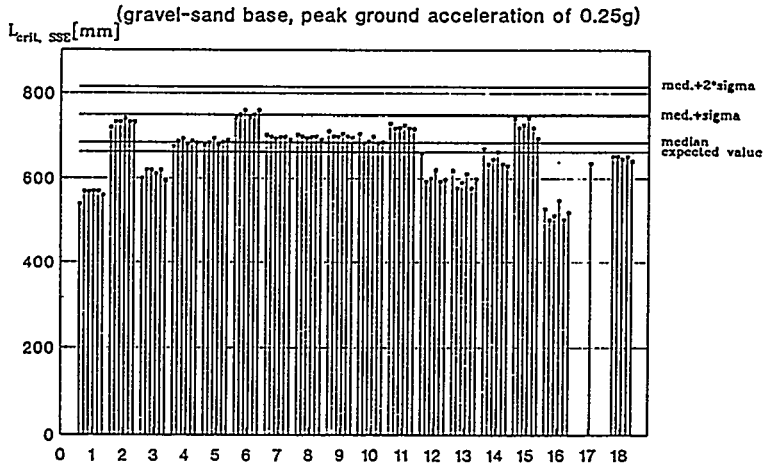

$L_{crit,\ SSE}$ ... crack length of plastic collapse for NOC+SSE load combination

Fig. 7

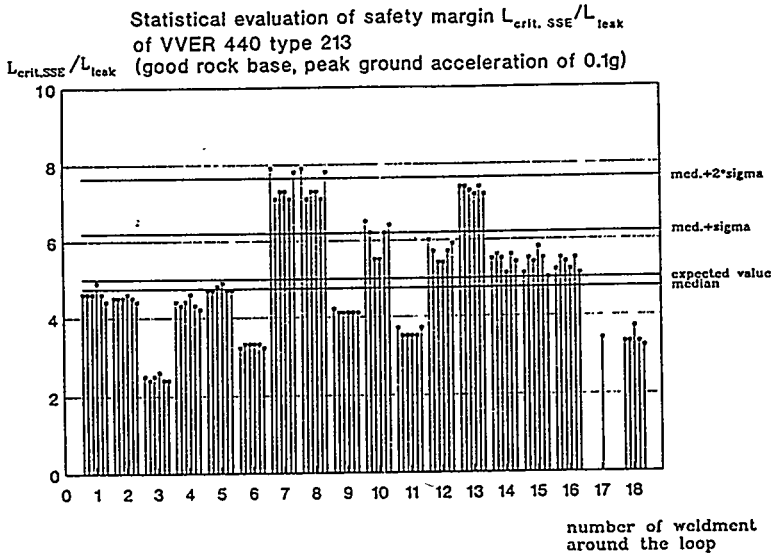

Fig. 8

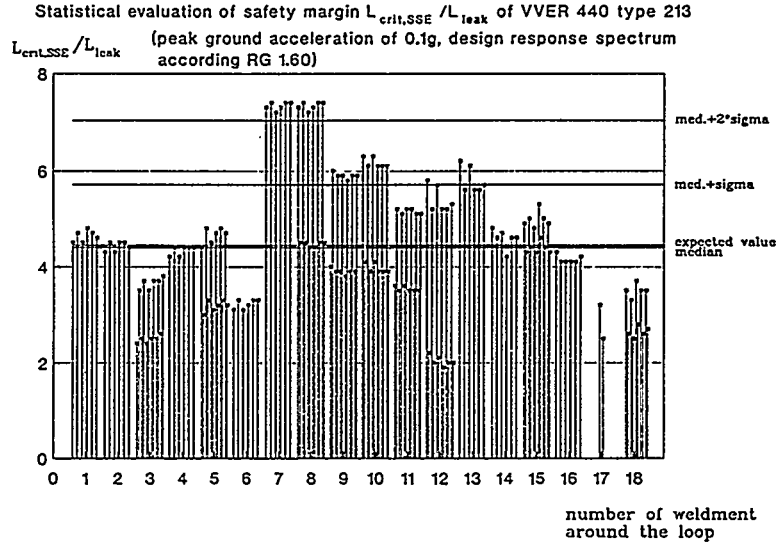

Fig. 9

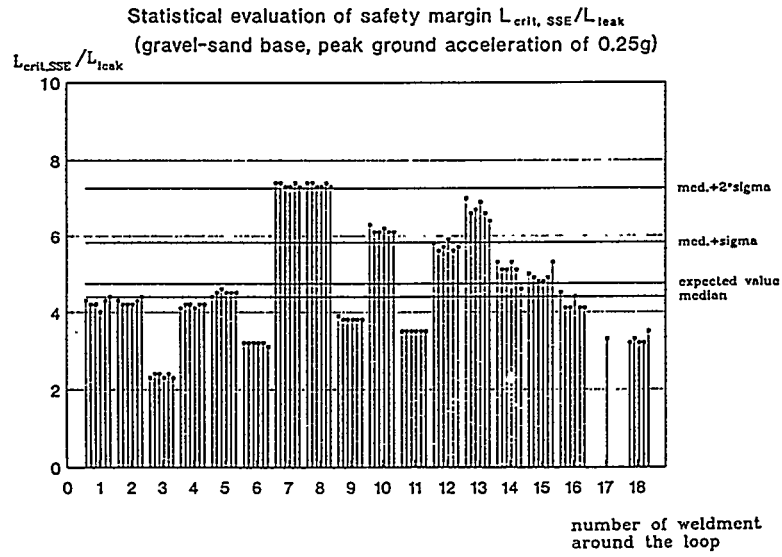

Fig. 10

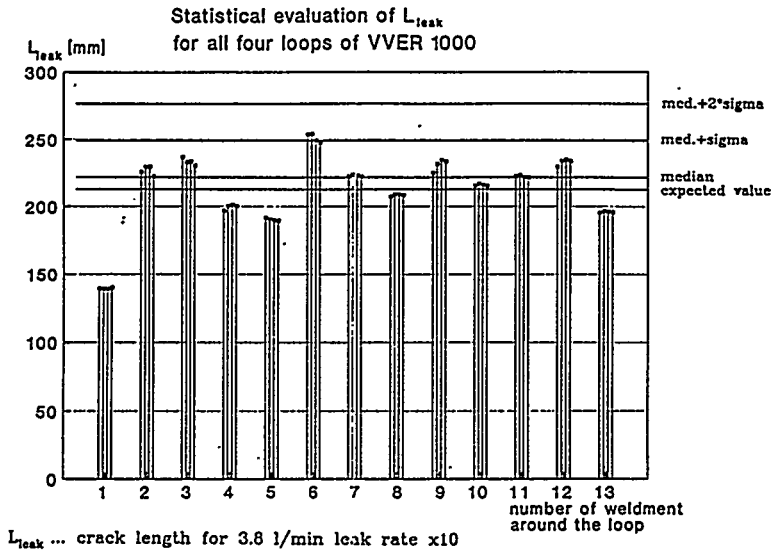

Fig. 11

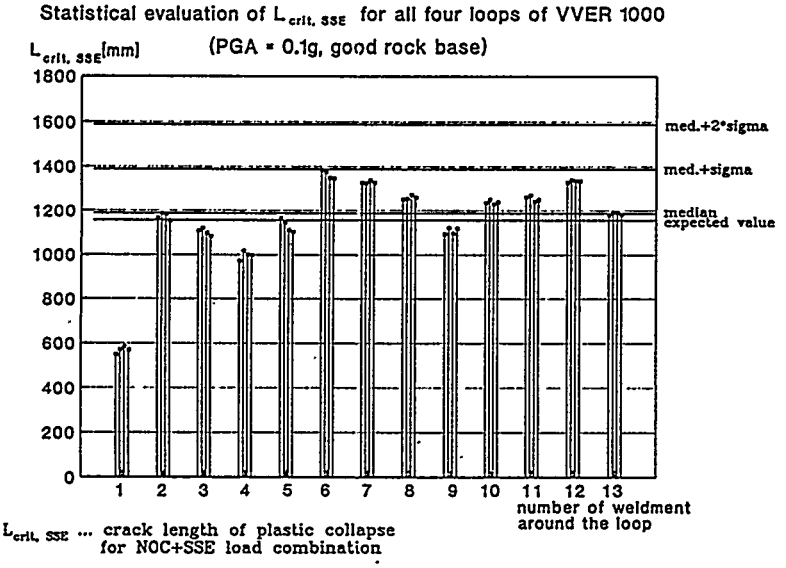

Fig. 12

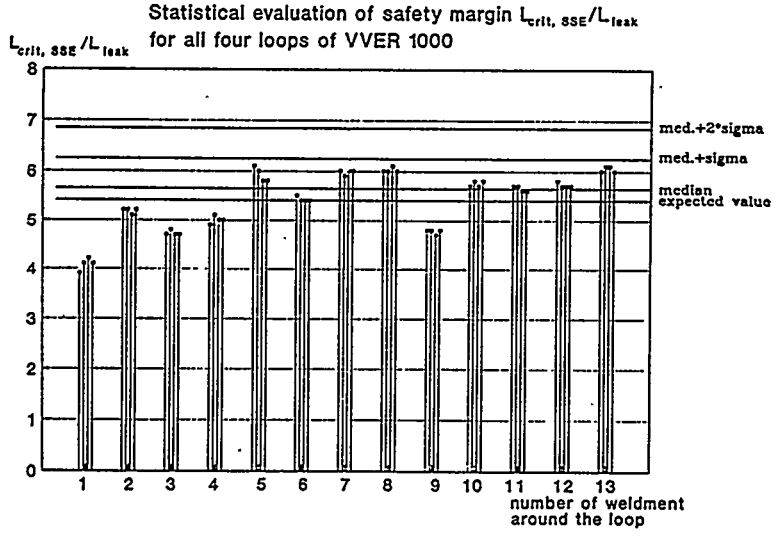

Fig. 13

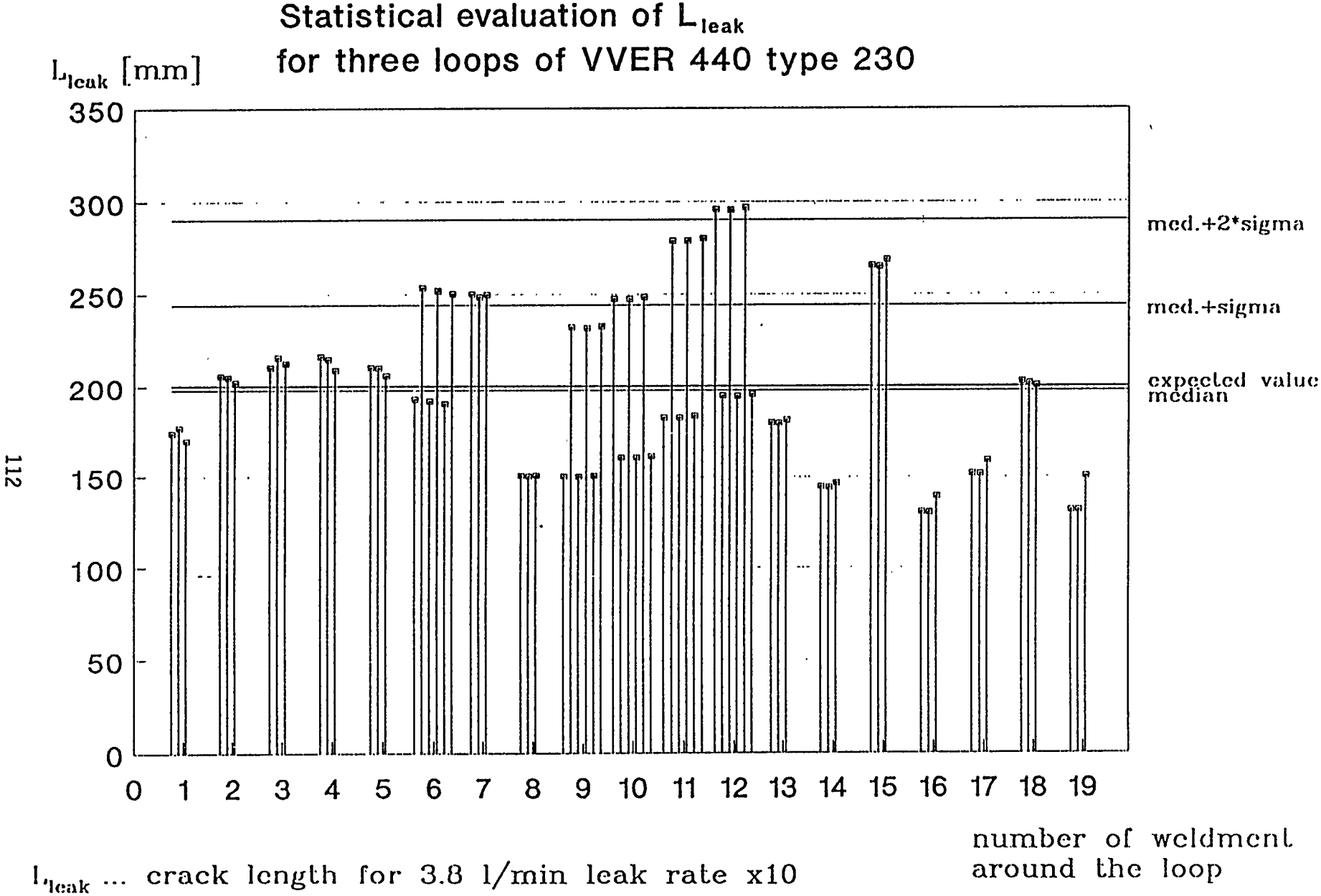
Statistical evaluation of L_{leak}
for three loops of VVER 440 type 230
L_{leak} [mm]
350
300
250
200
150
100
50
0
0 1 2 3 4 5 6 7 8 9 10 11 12 13 14 15 16 17 18 19
med.+2*sigma
med.+sigma
expected value
median
number of weldment
around the loop
L_{leak} ... crack length for 3.8 l/min leak rate x10

Fig. 1

Statistical evaluation of $L_{crit,SSE}$ for three loops of VVER 440 type 230 (gravel-sand base, peak ground acceleration of 0.25g)

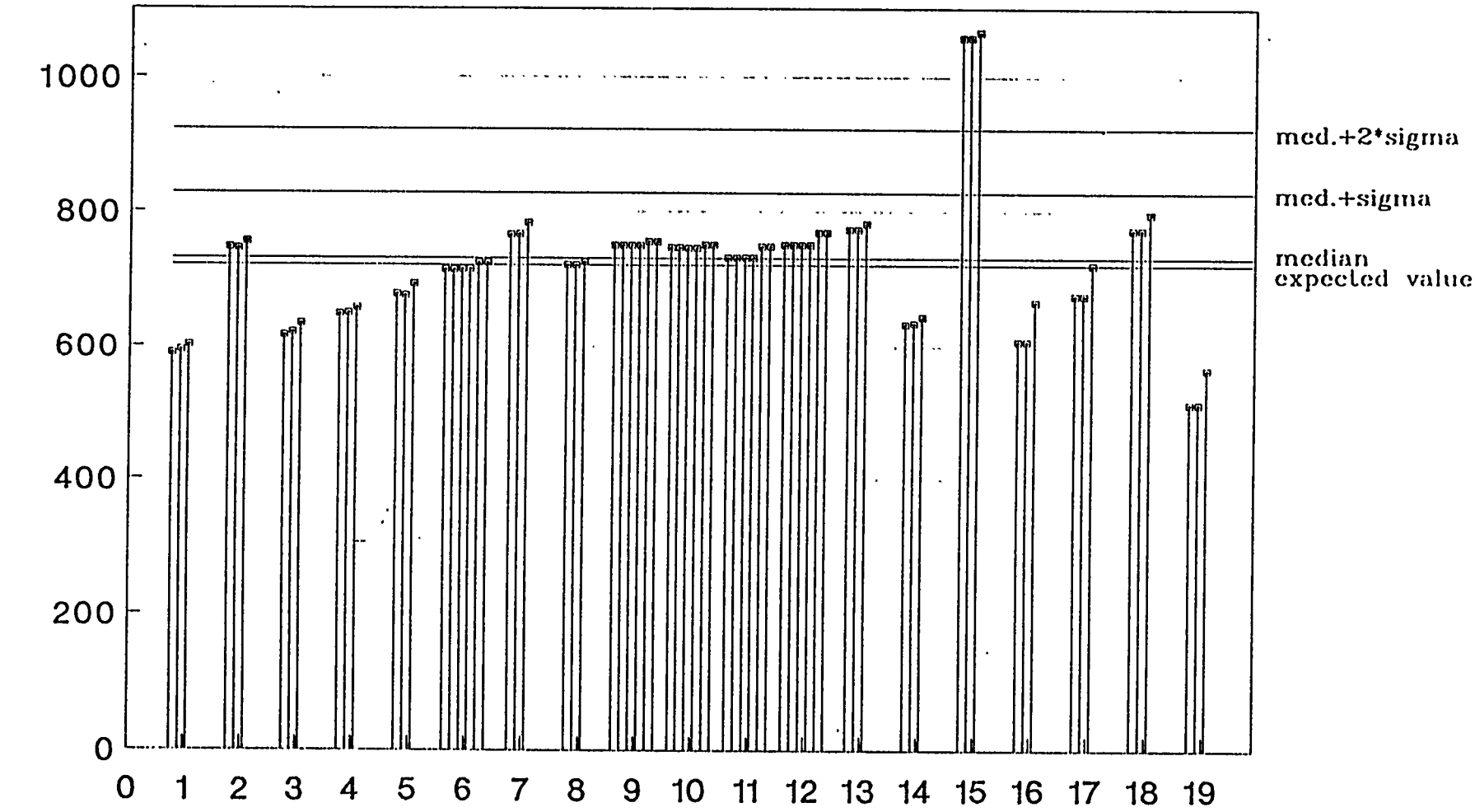

$L_{crit,\ SSE}$ ... crack length of plastic collapse for NOC+SSE load combination

Fig. 2

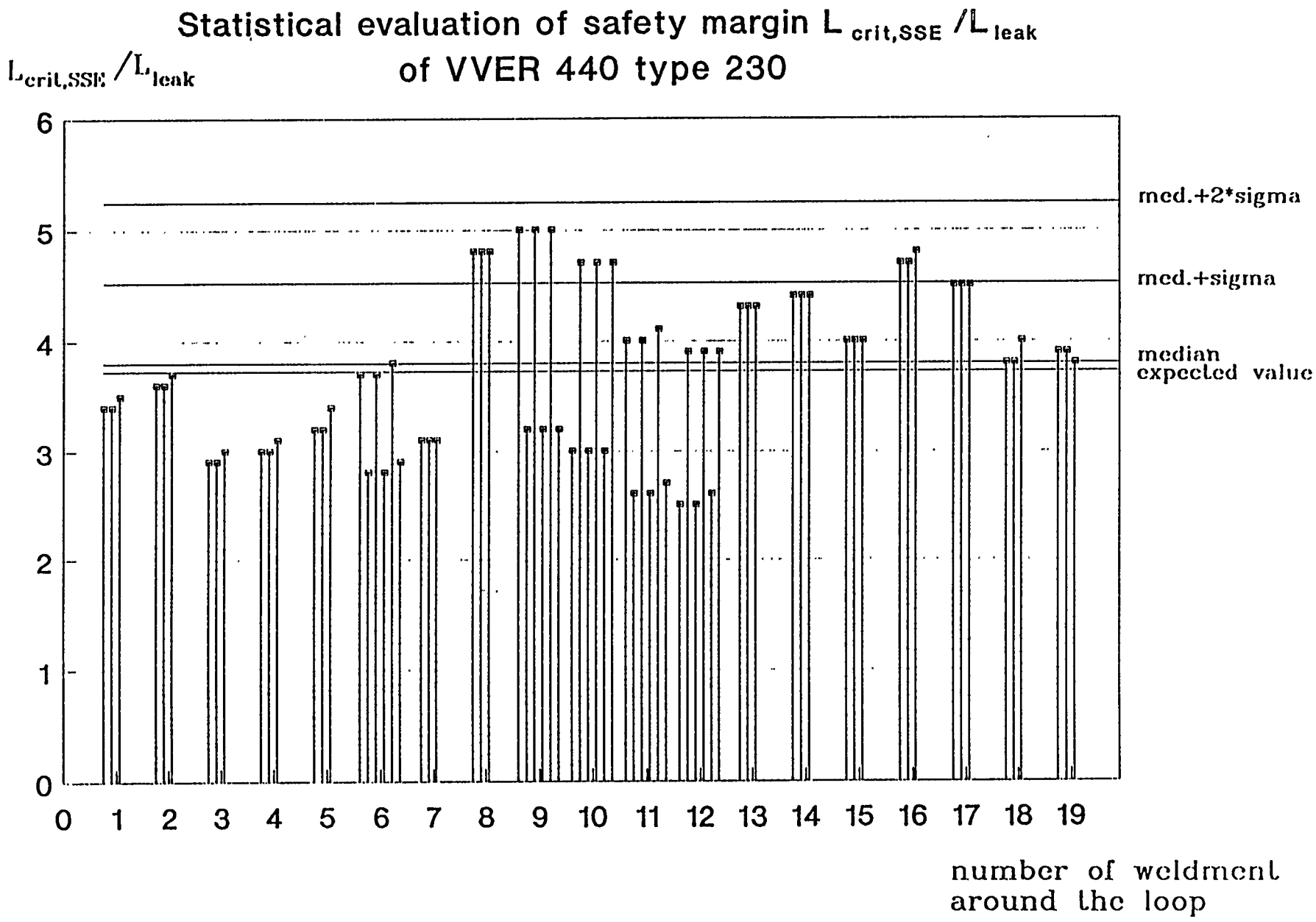
Statistical evaluation of safety margin $L_{crit,SSE}/L_{leak}$ of VVER 440 type 230
$L_{crit,SSE}/L_{leak}$
6
5
4
3
2
1
0
0 1 2 3 4 5 6 7 8 9 10 11 12 13 14 15 16 17 18 19
med.+2*sigma
med.+sigma
median expected value
number of weldment around the loop

Fig. 3

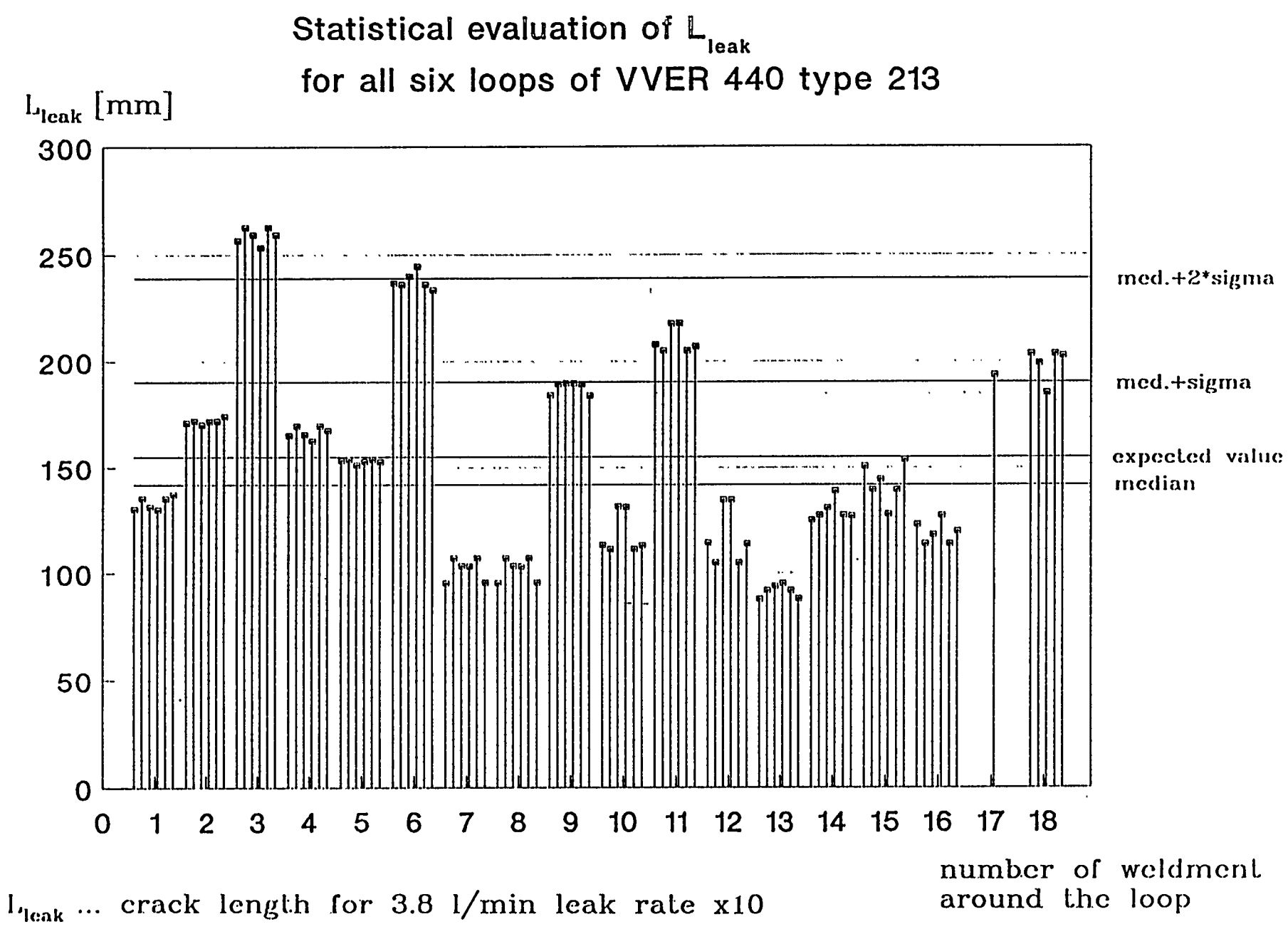
Statistical evaluation of L_{leak}
for all six loops of VVER 440 type 213
L_{leak} [mm]
300
250
200
150
100
50
0
0 1 2 3 4 5 6 7 8 9 10 11 12 13 14 15 16 17 18
med.+2*sigma
med.+sigma
expected value
median
number of weldment
around the loop
l_{leak} ... crack length for 3.8 l/min leak rate x10

Fig. 4

Statistical evaluation of $L_{crit,\ SSE}$ for all six loops of VVER 440 type 213

(good rock base, peak ground acceleration of 0.1g)

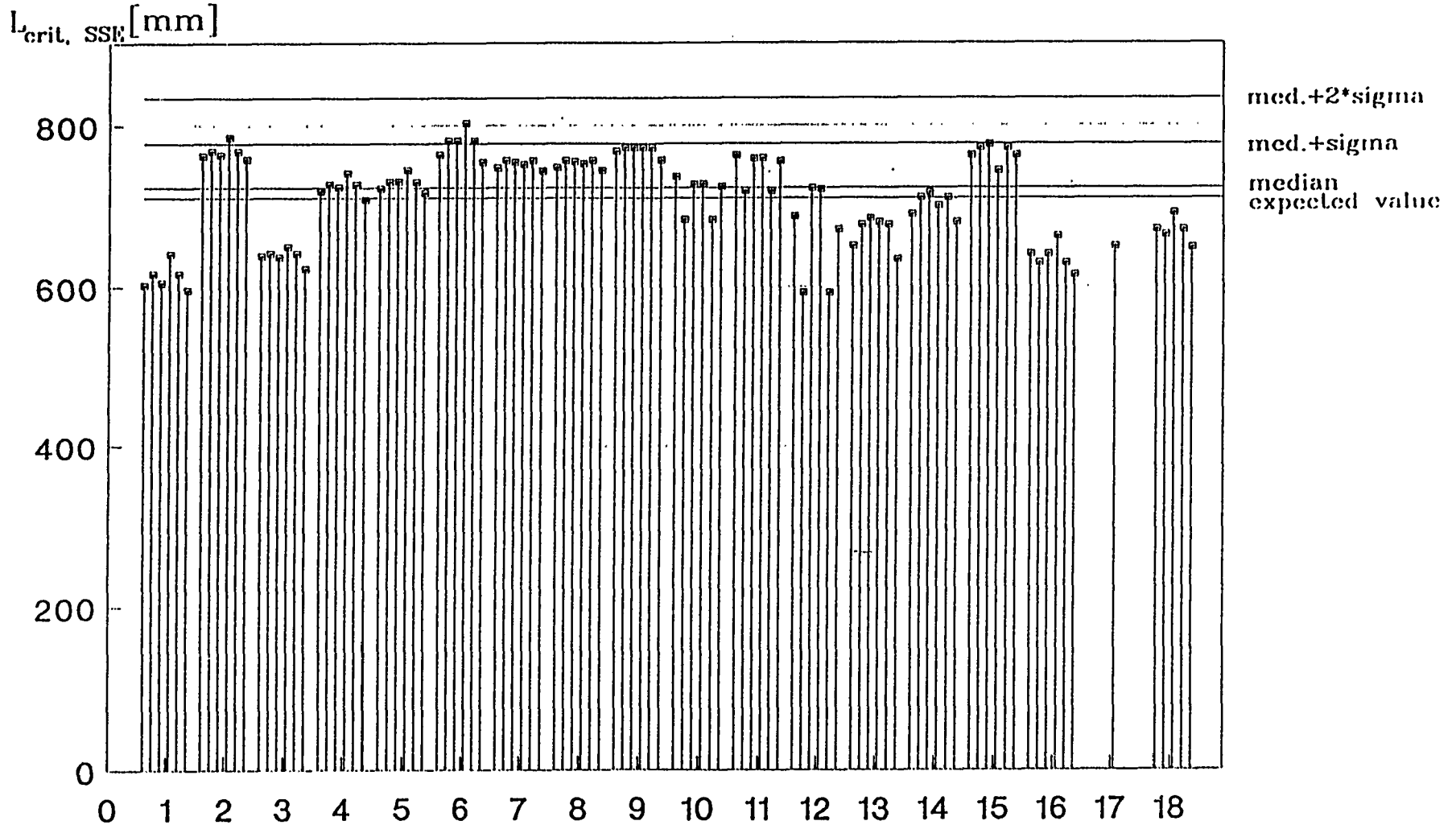

$L_{crit,\ SSE}$ ... crack length of plastic collapse for NOC+SSE load combination

Fig. 5

Statistical evaluation of $L_{crit,SSE}$ (peak ground acceleration of 0.1g, design response spectrum according RG 1.60)

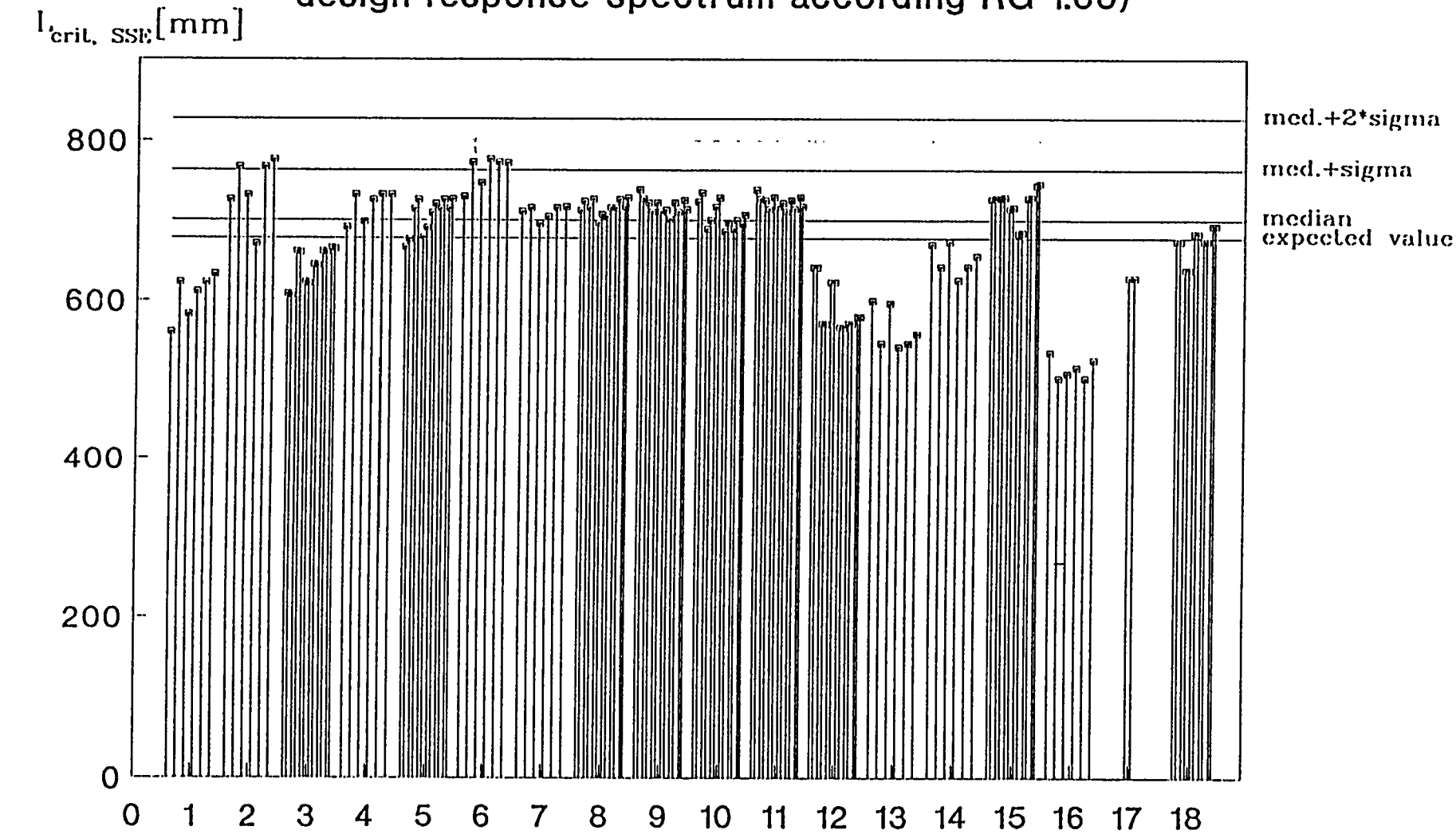

$L_{crit,\ SSE}$ ... crack length of plastic collapse for NOC+SSE load combination

Fig. 6

Statistical evaluation of $L_{crit,\ SSE}$ for all six loops of VVER 440 type 213

(gravel-sand base, peak ground acceleration of 0.25g)

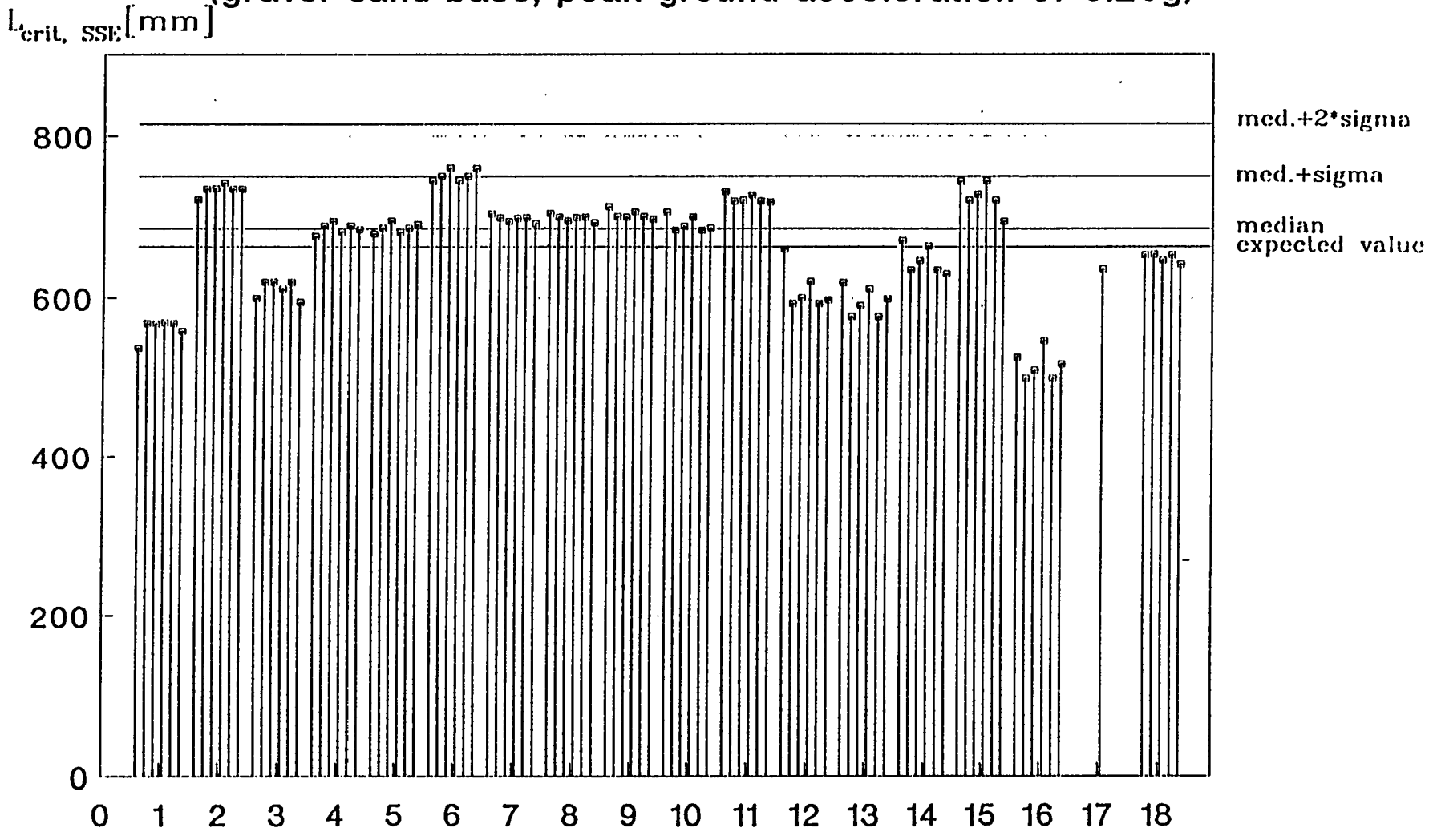

$L_{crit,\ SSE}$ ... crack length of plastic collapse for NOC+SSE load combination

Fig. 7

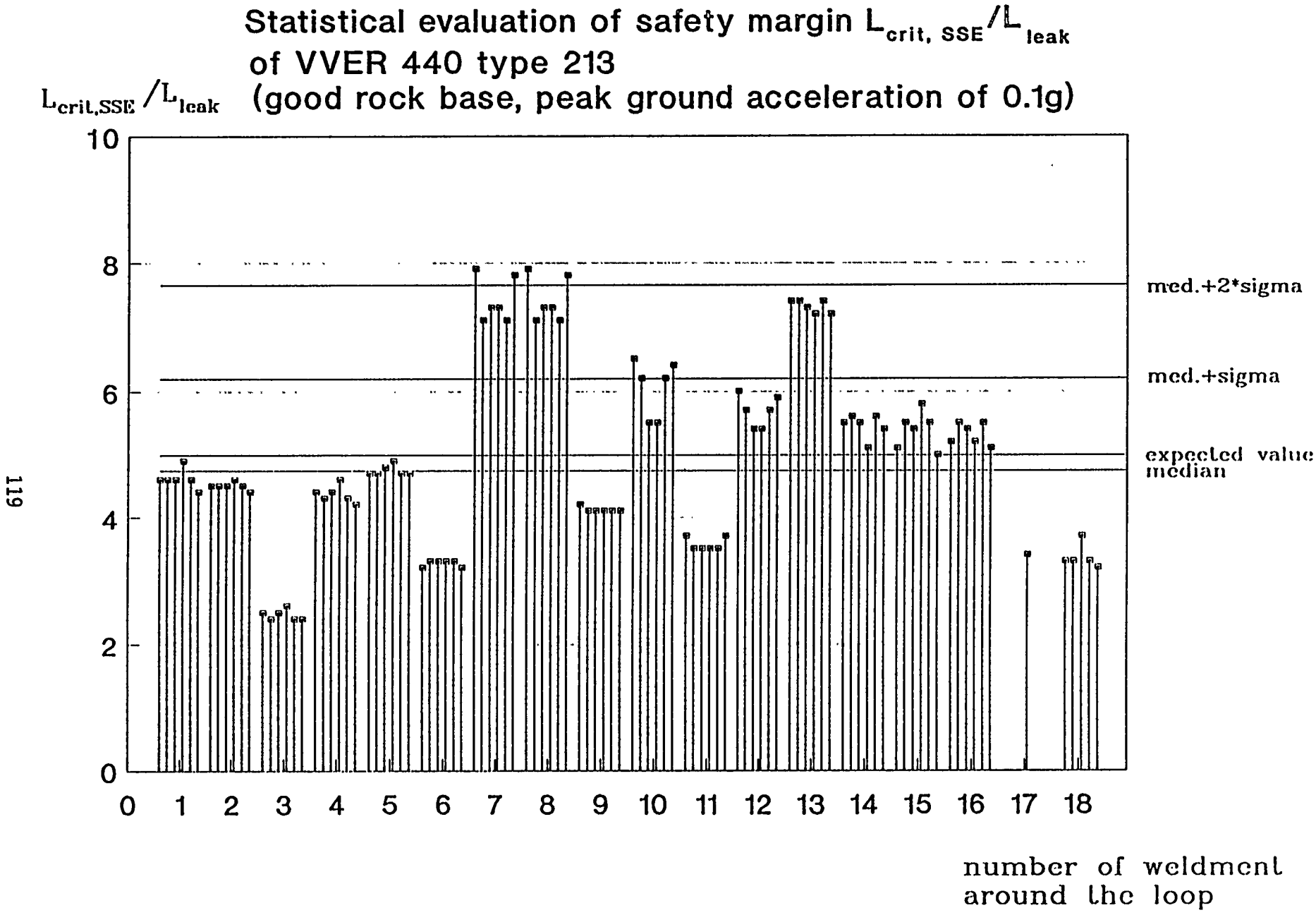
Statistical evaluation of safety margin $L_{crit, SSE}/L_{leak}$
of VVER 440 type 213
(good rock base, peak ground acceleration of 0.1g)
$L_{crit,SSE}/L_{leak}$
10
8
6
4
2
0
0 1 2 3 4 5 6 7 8 9 10 11 12 13 14 15 16 17 18
med.+2*sigma
med.+sigma
expected value
median
number of weldment
around the loop

Fig. 8

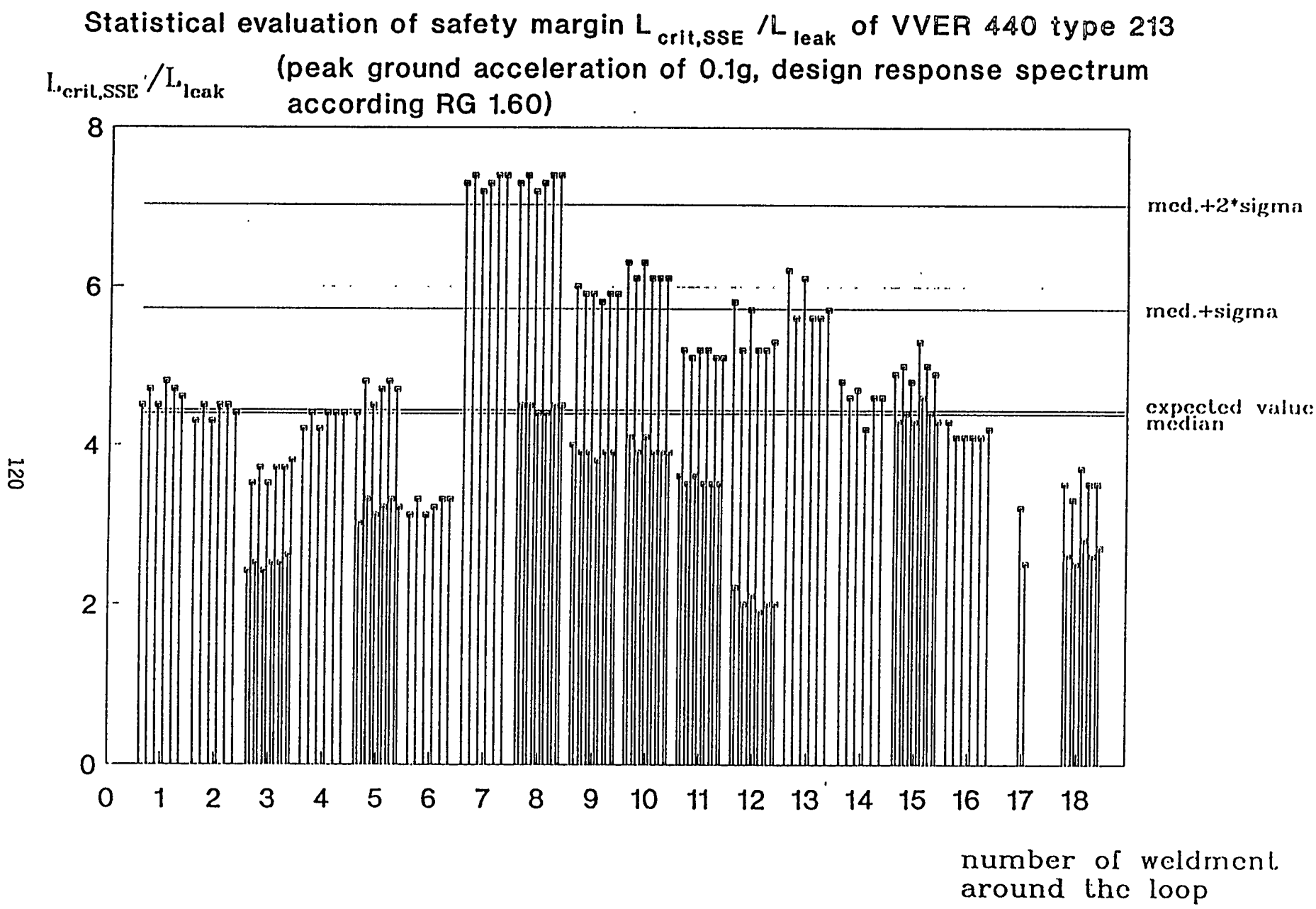
Statistical evaluation of safety margin $L_{crit,SSE}/L_{leak}$ of VVER 440 type 213
(peak ground acceleration of 0.1g, design response spectrum according RG 1.60)
$L_{crit,SSE}/L_{leak}$
8
6
4
2
0
0 1 2 3 4 5 6 7 8 9 10 11 12 13 14 15 16 17 18
med.+2*sigma
med.+sigma
expected value median
number of weldment around the loop

Fig. 9

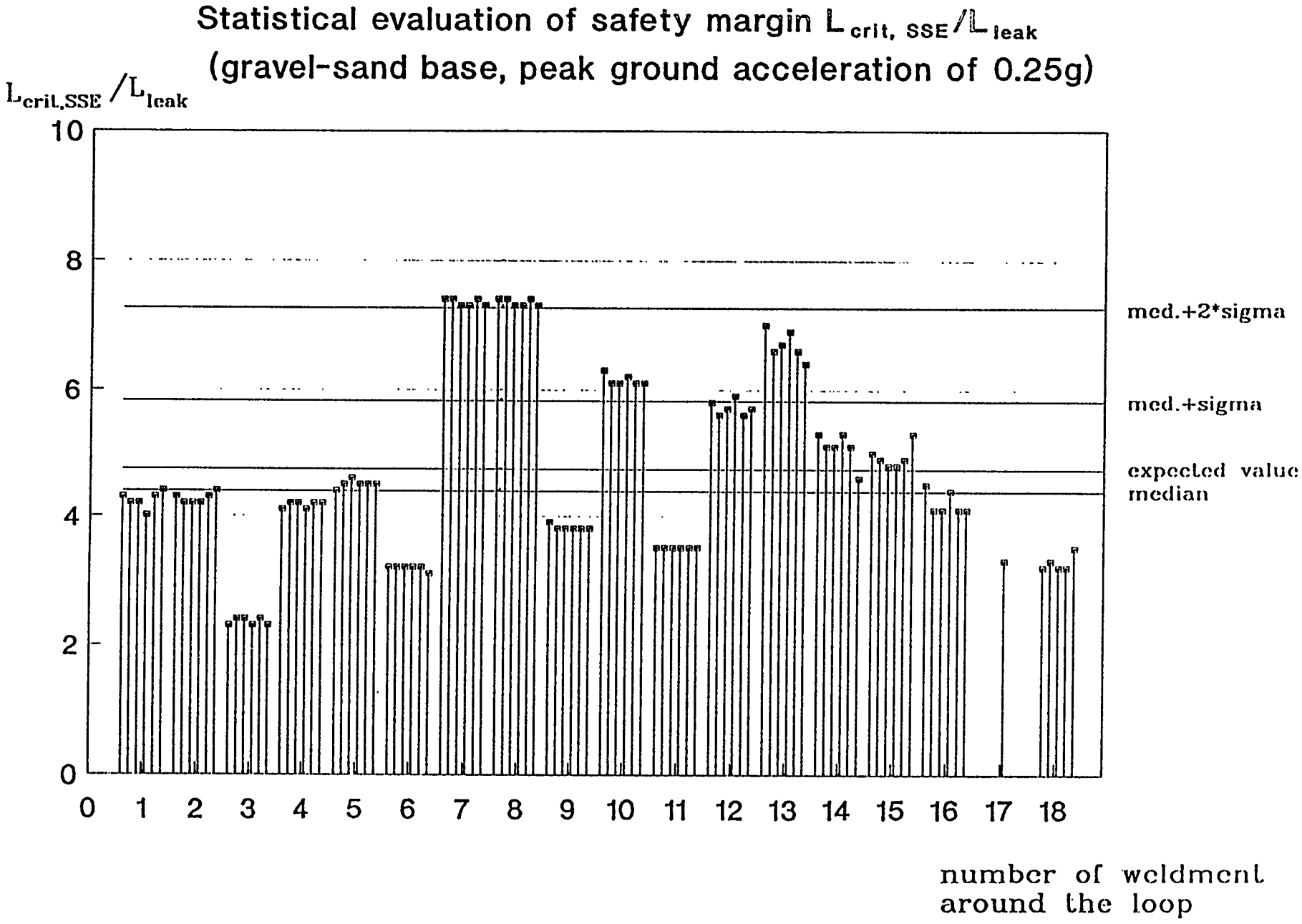
Statistical evaluation of safety margin $L_{crit, SSE}/L_{leak}$
(gravel-sand base, peak ground acceleration of 0.25g)
$L_{crit,SSE}/L_{leak}$
10
8
6
4
2
0
0 1 2 3 4 5 6 7 8 9 10 11 12 13 14 15 16 17 18
med.+2*sigma
med.+sigma
expected value
median
number of weldment
around the loop

Fig. 10

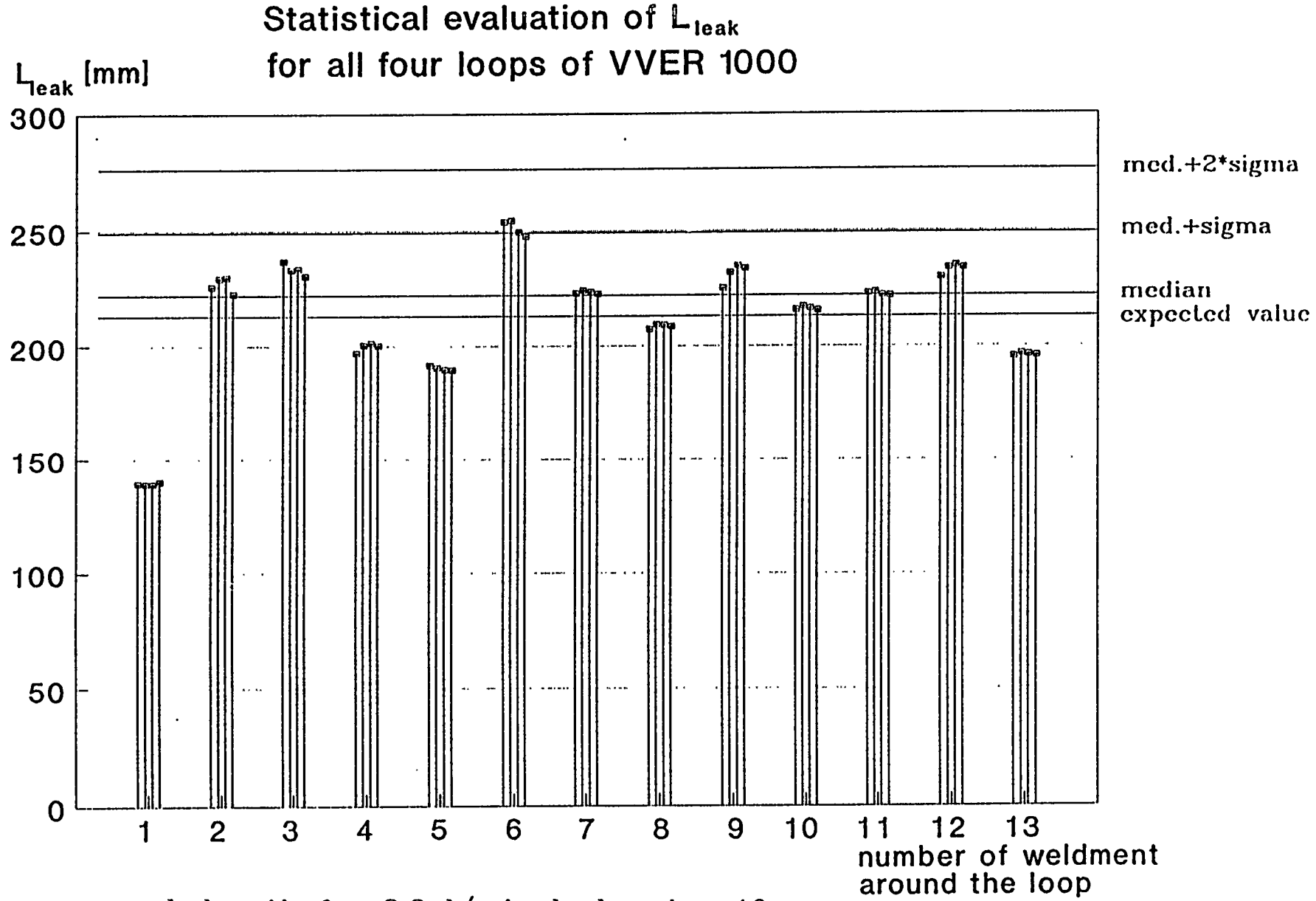

L_{leak} ... crack length for 3.8 l/min leak rate x10

Fig. 11

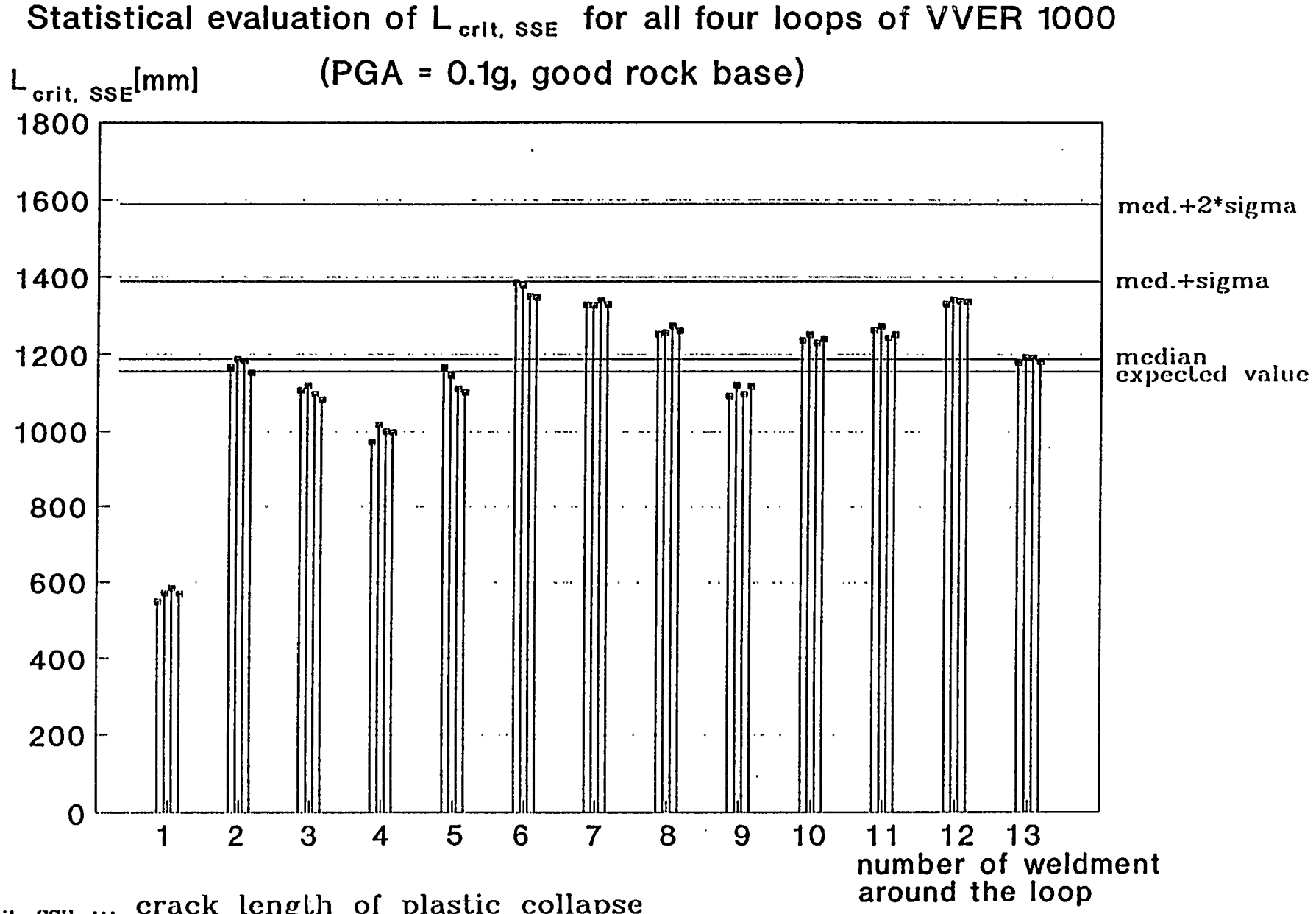

$L_{crit, SSE}$ ... crack length of plastic collapse for NOC+SSE load combination

Fig. 12

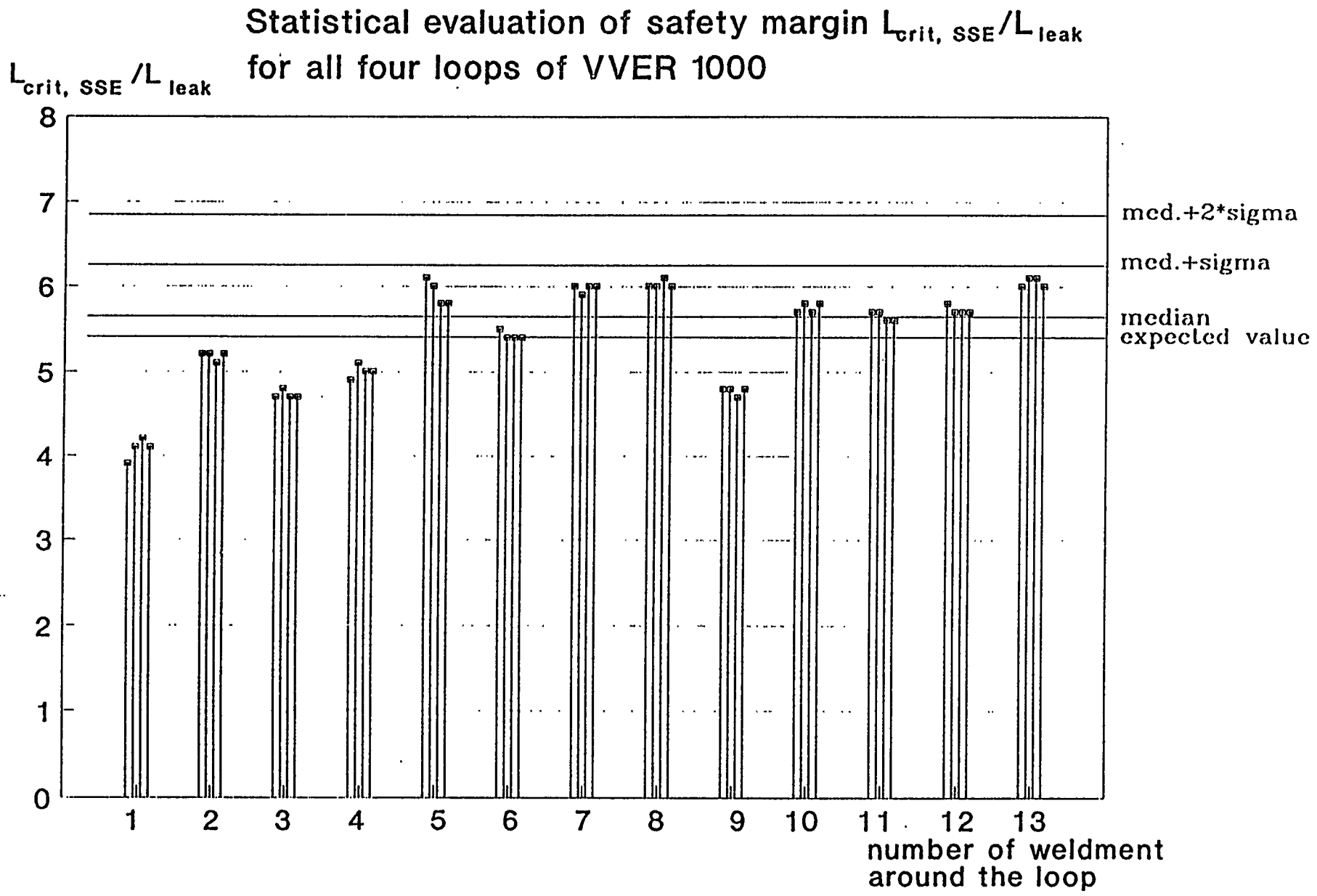
Statistical evaluation of safety margin $L_{crit, SSE}/L_{leak}$ for all four loops of VVER 1000
$L_{crit, SSE}/L_{leak}$
8
7
6
5
4
3
2
1
0
med.+2*sigma
med.+sigma
median expected value
1
2
3
4
5
6
7
8
9
10
11
12
13
number of weldment around the loop

Fig. 13

PRACTICAL APPLICATIONS OF THE R6 LEAK-BEFORE-BREAK PROCEDURE

P. J. BOUCHARD
NUCLEAR ELECTRIC PLC

ABSTRACT

A forthcoming revision to the R6 Leak-before-Break Assessment Procedure is briefly described. Practical application of the LbB concepts to safety-critical nuclear plant is illustrated by examples covering both low temperature and high temperature (>450°C) operating regimes. The examples highlight a number of issues which can make the development of a satisfactory LbB case problematic: for example, coping with highly loaded components, methodology assumptions and the definition of margins, the effect of crack closure owing to weld residual stresses, complex thermal stress fields or primary bending fields, the treatment of locally high stresses at crack intersections with free surfaces, the choice of local limit load solution when predicting ligament break-through, and the scope of calculations required to support even a simplified LbB case for high temperature steam pipe-work systems.

INTRODUCTION

Revision 3 of the R6 defect assessment procedure was first published in 1988 [1]. Since then R6 Revision 3 has been regularly reviewed and the document updated as knowledge and techniques in the field improve [2]. In November 1990 a new appendix to R6 was issued (Appendix 9) setting out a procedure for leak-before-break (LbB) assessment of pressurised components, with recommended methods for carrying out each of the steps involved. The main steps of this procedure are:

a) to characterise the development of postulated or actual part-penetrating defects,
b) to estimate the defect length after break-through,
c) to assess through-wall crack growth,
d) to determine leakage rates for idealised through-wall cracks,
e) to evaluate the largest through-wall crack size which can be tolerated under all plant operating conditions, and
f) to perform a sensitivity analysis supporting claimed LbB margins

For a satisfactory LbB case it must be shown that stable break-through of a part-penetrating defect occurs and that the resulting through-wall crack leaks at a sufficient rate to ensure detection before it can grow to the maximum tolerable size. However, the procedure does not preclude less rigorous LbB arguments based on postulated through-wall cracks such as the NUREG 1061 approach for light water reactor (LWR) pipe-work published by the US Nuclear Regulatory Commission [3]; that is a LbB case based on steps d) and e) listed above.

Knowledge and understanding of LbB issues have significantly advanced in the last five years; through practical applications of LbB concepts to operating plant world-wide, particularly in the nuclear industry; and via

experimental and theoretical work such as that carried out under the International Piping Integrity Research Group (IPIRG) Program and USNRC Short Cracks in Piping and Piping Welds Program.

These advances in understanding are reflected in a major revision to R6 Appendix 9, which is expected to be issued by the end of this year (1995). The underlying principles for LbB assessment remain unchanged in the new procedure. However, a best estimate approach is advocated for all steps of the assessment apart from limiting through-wall crack size evaluation. Updated guidance is provided to help users select appropriate locations for analysis and carry out detailed assessments of defect break-through, complex cracks, re-characterisation, the significance of residual weld stresses, crack opening area, leak rates and leak detection. Papers 23, 27 and 35 of this seminar [4], [5] and [6] describe some of the background to the advice on crack opening area, friction factors and leak detection systems.

A major addition to the new procedure is the application of LbB concepts to high temperature plant where creep mechanisms - continuum damage and creep crack growth - play an important role. Paper 36 of this seminar [7] specifically addresses these high temperature aspects LbB and describes their treatment within R6.

A further important change to Appendix 9 is to explicitly set out procedures allowing two levels of rigour: (1) a simplified procedure based on postulated through-wall cracks and 'detectable leakage' (analogous to a NUREG 1061 approach); (2) a full LbB procedure where flaw shape development is modelled as the crack grows through the wall until break-through (as in the 1990 Appendix 9 described above). For both levels of argument, acceptable margins have to be judged from sensitivity studies reflecting the level of confidence in the input data and simplifying assumptions adopted, and an appreciation of the application context.

The remainder of this paper describes the practical application of LbB concepts to safety-critical nuclear plant with examples covering both low temperature and high temperature (>450°C) operating regimes.

PRIMARY CIRCUIT APPLICATIONS

Main Coolant Loop Butt Welds

The first LbB example concerns the application of R6 Appendix 9 (1990) methods to demonstrate NUREG 1061 LbB margins for the main coolant loop pipe-work of a light water reactor. This example illustrates how the simplest of LbB assessments may not be straightforward.

NUREG 1061 requires that a through wall crack (TWC) should be postulated at locations where the highest stresses and poorest material properties coincide. Loading conditions to be considered are restricted to internal pressure and piping forces and moments (from dead-weight, thermal expansion and safe shut-down earthquake). The size of the postulated crack which gives a leak rate under normal operating conditions equal to 10 times the plant's installed detection capability is defined as the leakage crack size (LSC). It must be demonstrated that the postulated LSC is stable under normal plus safe shut-down earthquake (SSE) loads with a margin of at least 1.4 on total load. In addition, a crack size margin of at least 2 is required between the LSC and the limiting size of through-wall crack under normal plus SSE loads.

The scope of the LbB assessment was confined to the main pipe butt welds in the system. Six welds at piping terminal ends were chosen for detailed assessment as these were the most highly stressed, and the safe-end to nozzle transition welds had lower fracture toughness properties than welds elsewhere in the system. The installed plant leakage detection capability was taken to be 1.89 l/min.

A preliminary LbB assessment for each selected location was carried out following relevant R6 Appendix 9 guidelines. Limiting through-wall crack sizes were calculated using the main R6 procedure with ASME III tensile

properties and lower bound fracture toughness data for transition welds (for up to 2mm stable tearing). Crack opening areas were evaluated using the simple elastic formula quoted in R6 Appendix 9 (1990) and ASME properties. Leakage rates were calculated using SQUIRT [8] with the default friction factors for a fatigue crack supplied with the computer code. This preliminary study showed that the RPV inlet nozzle to safe end weld (see Figure 1) was the worst location, where a crack size margin of 2 could only just be met for a leakage rate margin of 5 (i.e. well short of the required NUREG margin of 10).

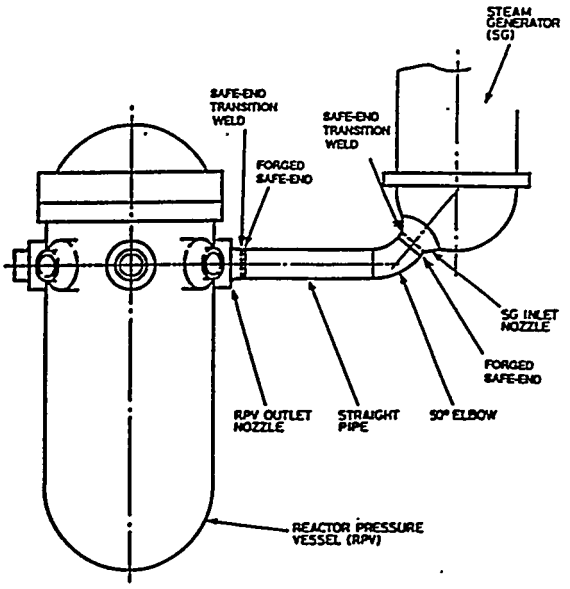

Figure 1: Hot Leg Piping

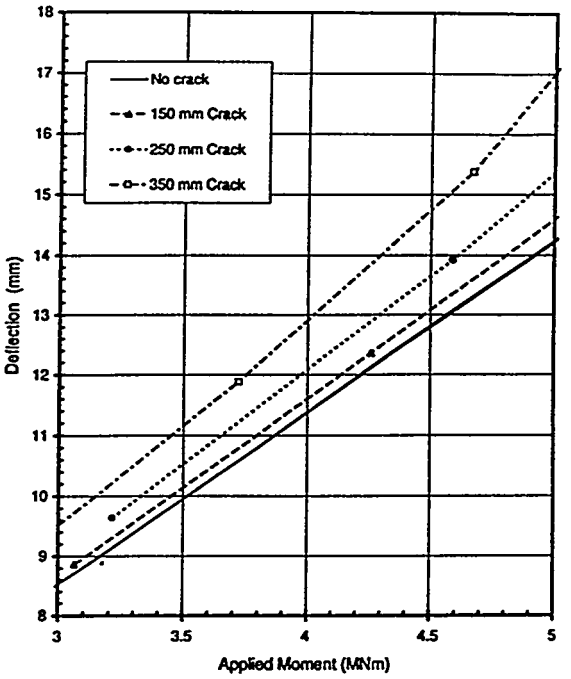

Figure 2: Thermal Expansion Moment Versus Hot Leg Deflection for Cracked Weld

A range of exploratory studies were carried out to investigate the sensitivity of the LbB assessment to the input data (pipe-work loadings, material properties) and assessment methods (for crack opening, leak rates and critical crack sizes). The studies showed that the LbB margins for the RPV outlet nozzle to safe end weld could be improved by:

a) reducing the assumed pipe-work global bending loads,
b) increasing the assumed material yield stress (for both COD and limiting crack size calculations),
c) invoking larger amounts of stable ductile tearing in the R6 category 3 analysis (as allowed by NUREG 1061),
d) using a less pessimistic crack opening area solution, and
e) using more realistic friction factors for the leak rate calculations [5].

In addition, a review of published LbB assessments for other similar plant revealed that the pipe-work loads used for the initial assessment were exceptionally high, and that sometimes the definition of load margin has been based on SSE loads alone rather than normal operation plus SSE loads (the latter being specified by NUREG 1061).

Given the outcome of these investigations, a more informed LbB analysis was carried out for the six selected locations. First, more realistic pipe-work loads were obtained, it being discovered that the original loads came from an over-constrained pipe-work analysis (the RPV nozzle terminal end had been rigidly fixed). The thermal expansion moment at the worst location was also reduced by about 9% (see Figure 2) through application of R6 Appendix 11 for displacement controlled loadings. Secondly, 25% higher yield stresses were justified from a data base of measured results for material manufactured to an identical specification (note mean yield stress data was used for the COD calculation and minimum yield for limiting defect size evaluation). Thirdly, conservative fracture

toughness data were obtained from full thickness test specimens, so that large amounts of tearing could be validly claimed in the R6 category 3 limiting crack size analysis. Finally, the crack opening area was evaluated using a reference stress elastic plastic solution [4], and more realistic but conservative friction factors used for the leak rate calculations [5].

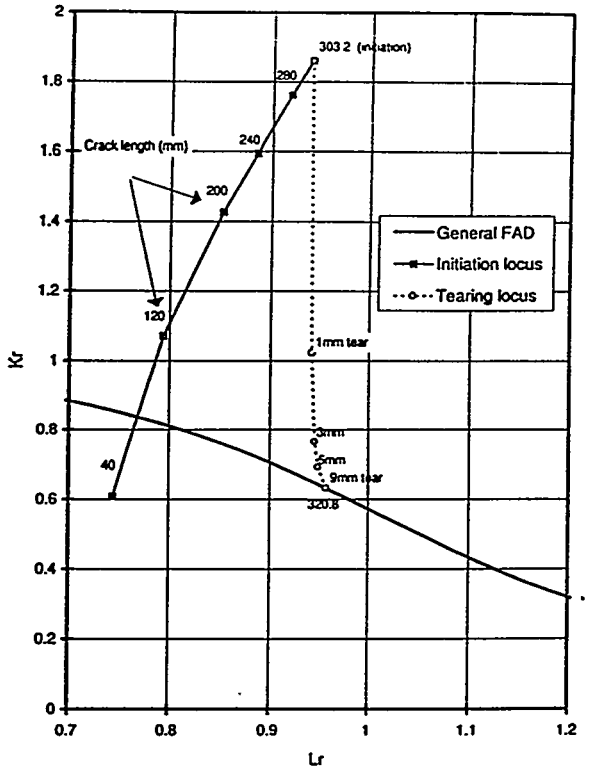

Figure 3: R6 Failure Assessment Diagram for a Typical Location

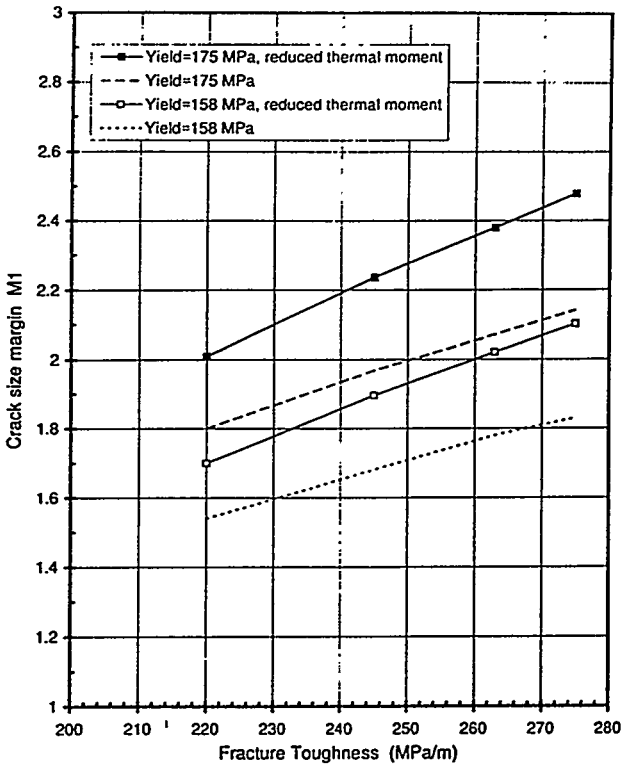

Figure 4: Sensitivity Study for Crack Size Margin

Application of these measures enabled a NUREG 1061 leak rate margin of 10 to be achieved for the worst location. Figure 4 presents results which illustrate the sensitivity of the crack size margin to fracture toughness, yield stress and reduction in thermal moment owing to displacement control.

This example of a very simple LbB application was far from straightforward. Even so, issues such as the effect of nozzle constraint and weld metal on the crack opening area, the circumferential location of postulated cracks with respect to the orientation of different applied loads, the through-wall variations in thermal and residual stress have not been addressed. A full LbB case would also require assessment of break-through from postulated part-penetrating cracks and consideration of all operating load conditions, not just normal operation and SSE.

An important underlying reason which made it difficult to demonstrate NUREG 1061 margins arose from the application of R6 based methods which may be more pessimistic than NUREG 1061 recommendations; for example NUREG 1061 permits extrapolation of J-R data well beyond the validity limits of normal CT specimens. R6 Appendix 9 avoids prescribing specific margins, placing the onus on users of the procedure to justify acceptable margins through sensitivity studies. The above example demonstrates how dependent the apparent LbB margins are on the analysis assumptions and methods, and thus emphasises the importance of the R6 margins philosophy.

Heat Exchanger Pressure Vessel

The key features of this LbB application involved the dominant role of residual weld stresses and complex thermal loadings in crack opening area and critical crack size calculations.

An angular sector of a circumferential butt weld in a heat exchanger pressure vessel had been operating at temperatures high enough to give a small theoretical risk of local creep damage. Although plant modifications were carried out to reduce local operating metal temperatures and thus avoid future creep damage, an assurance of detectable leak rates from sub-critical cracks was required to support the safety case for continued operation. The initial assessment for this component failed to provide a satisfactory LbB case because:

a) the limiting through-wall crack size was short (12% of circumference) being determined by high inner surface stress intensity factors from assumed weld residual stresses and bounding normal operation thermal stresses (note limiting crack sizes were determined by normal operating conditions and therefore stable tearing could not be invoked), and
b) cracks of near critical length were predicted to be completely closed under the combined effects of pressure loading and postulated through-wall bending weld residual stresses.

A detailed programme of 3D finite element analysis work was undertaken. First the residual weld stress distribution was modelled using a non-linear weld simulation analysis. Secondly, elastic stress intensity factors along the crack fronts were evaluated for the predicted residual stress distribution and complex three dimensional temperature loadings. The latter analysis had to model a large part of the vessel to properly represent large variations in axial and circumferential temperatures (see Figures 5 and 6). Thirdly, non-linear cracked body analysis was performed for combined loadings to predict crack opening areas.

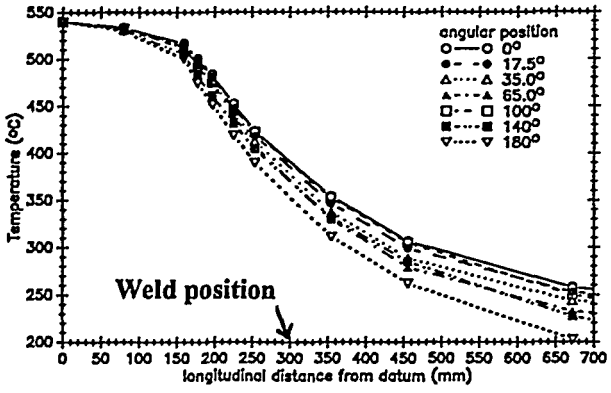

Figure 5: Temperature Distribution

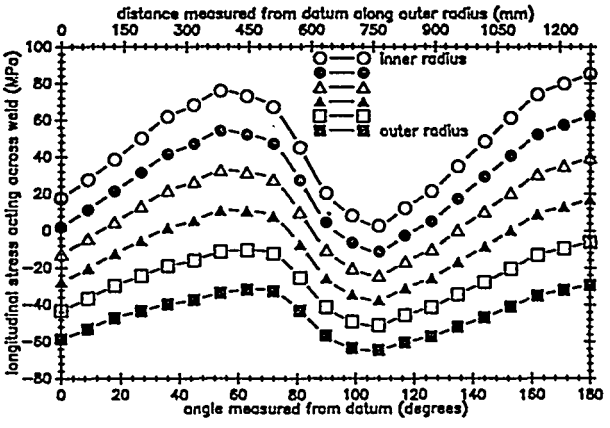

Figure 6 Thermal Stress Distribution at Weld

Residual stress studies demonstrated much lower through-wall bending axial residual weld stresses than originally assumed, and the substantial benefits of performing elastic plastic analysis for combined residual stress and plant loadings [9]. The three dimensional stress analyses for thermal loading gave surprising results in that they predicted negative stress intensity factors over the crack lengths of concern. Whilst this was beneficial to the critical crack side of the argument, the associated crack closure effects had to be included in the crack area and leak rate calculations.

A final LbB case was made for the heat exchanger weld on the basis of this analytical work and appropriate sensitivity studies. A significantly increased limiting crack size was demonstrated, which was over twice the length required to give leak rates an order of magnitude greater than the installed detection capability.

Coolant Pump

This example illustrates application of both the full R6 Appendix 9 procedure (i.e. including consideration of part-penetrating defects breaking through) and a simplified NUREG 1061 approach to a cast austenitic pump casing.

Some grades of cast duplex stainless steels are susceptible to thermal ageing embrittlement at LWR primary circuit operating temperatures. The degradation in fracture toughness properties with time for such steels can be estimated from the composition, delta ferrite content and Charpy impact energy of individual castings [10]. Given that significant variations in estimated fracture toughness were predicted with plant age and from casting to casting, the LbB analysis was performed parametrically with respect to fracture resistance.

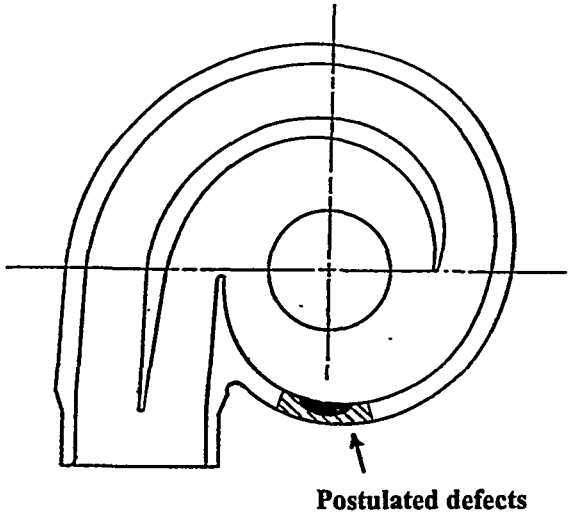

Figure 7: Postulated Defects in Pump Casing

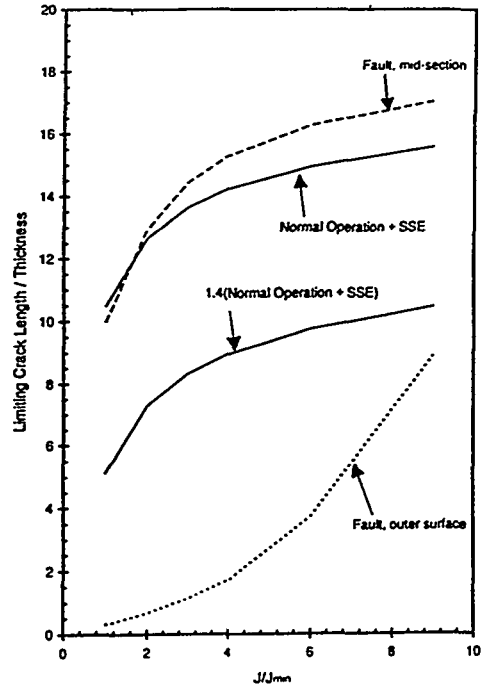

Figure 8: Limiting Through-wall Crack Sizes

Initially a NUREG 1061 type of analysis was performed for postulated cracks in the volute region of the casing as shown in Figure 7. Leakage size cracks were evaluated based on normal operation loads, an elastic crack opening area solution, best estimate friction factors [5] and an assumed leakage detection capability in the range 1.89 to 3.78 litre/min. Limiting crack sizes were calculated as a function of fracture resistance using R6. Figure 8 presents limiting crack size results, normalised with respect to section thickness, for different load cases as a function of J/J_{min}, where J_{min} is a notional lower bound material fracture resistance. NUREG 1061 margins of 1.4 on normal operation plus SSE loadings, 2 on crack size and 10 on the larger leak rate were successfully demonstrated for all values of initiation fracture toughness considered.

In describing the full R6 LbB analysis it is useful to refer to the LbB diagrams shown in Figure 9 and 10. First, R6 was used in a predictive manner to estimate the break-through boundary for postulated part-penetrating cracks. Best estimate loads and material properties were used to avoid under-predicting the break-through length. Break-through was found to be determined by pure plastic collapse and was therefore independent of fracture toughness. However, it is seen from Figure 9 that the break-through boundary is affected by the choice of local limit load solution. It is worth noting here that greater influences on the break-through boundary of the collapse solution have been observed in other studies carried out by the author, where fracture and tearing play a significant role.

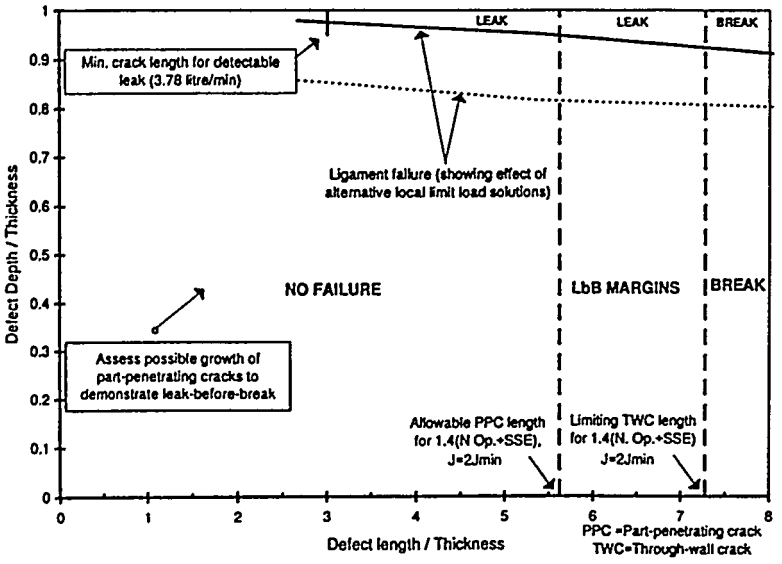

Figure 9: LbB Diagram for Normal Operation Plus SSE Loading

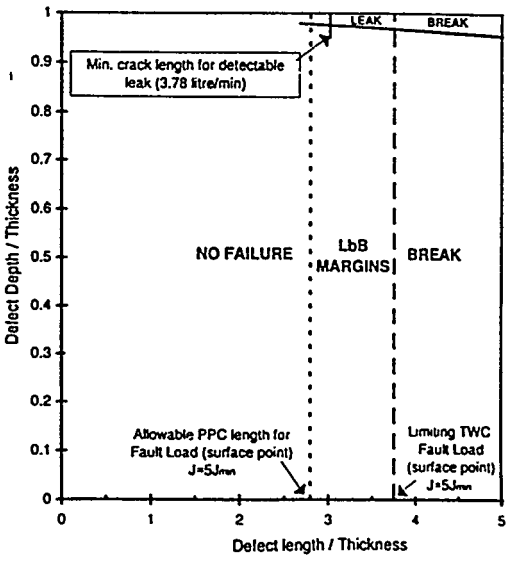

Figure 10: LbB Diagram for Worst Fault Condition

Figure 9 illustrates an LbB diagram for a fracture toughness level of $2J_{min}$, assuming that normal operation plus SSE is the most onerous extreme loading. The allowable part-penetrating crack (PPC) length assumes recharacterisation on break-through and a 25% margin for crack growth.

An important difference between the full R6 approach and NUREG 1061 is that the former requires assessment of all plant loading conditions, not just normal operation and SSE. The limiting load-case for the pump was found to be a pressurised thermal shock fault condition. This condition gave much smaller limiting through-wall crack sizes (see Figure 8), if the R6 analysis accounted for the large thermal stresses at the surface. The results from this analysis in Figure 10 can be compared with Figure 9 if it is conceded that the fracture resistance of $5J_{min}$ represents an enhancement owing to a few mm of stable ductile tear. Note that the Figure 9 assessment would bound the fault condition if the through-wall crack size was based on the mid-section point alone.

Three crucial LbB issues have been raised in this example: the problem of predicting part-penetrating crack break-through (choice of local limit load solution); the importance of considering all plant loading conditions in a full LbB assessment; and the treatment of high local stresses at surfaces.

SECONDARY CIRCUIT APPLICATIONS

This section describes applications of the new simplified R6 LbB procedure (as described earlier) to high temperature steam pipe-work systems and illustrates how creep degradation mechanisms can be accounted for in the assessments.

LbB cases were required for several steam pipe-work systems to provide an additional level of assurance against disruptive failure without forewarning, given that some examples of degradation had been found during historical operation. In addition, it had to be shown that the consequences of potential leakage (jet impingement, building

pressurisation, temperature rise etc.) were acceptable; that is upper bound leakage rates from postulated cracks were also required.

The first step in any LbB assessment is to select candidate locations for detailed analysis. This process may not be trivial for complex steam pipe-work systems which may contain a range of pipe sizes (e.g. 70mm OD to 413mm OD), various piping components (pipe bends and 'T' junctions), different materials (stainless steel, ½CrMoV, weld metals etc.), and varying operating conditions (temperature, pressure and system loads). Here, welds were considered to be more vulnerable to degradation than parent material. All the pipe butt welds were ranked first by the uncracked reference stress and then by pipe size. This approach recognised that it is generally more difficult to make a LbB case as the reference stress increases (particularly at high temperature) and as pipe size decreases. Fabricated 'Tee' junctions were regarded as important locations, owing to the high local stresses which can be induced by pressure and system loads, and isolated incidence of cracking in-service. The LbB assessment for these complex components had to be based on 3D finite element analysis. This analysis work is briefly discussed later.

Internal pressure, system loads and weld residual stresses were considered in the analysis for normal operation and maximum (Design or Fault loading) conditions. System loads were simplified by ignoring shear forces and lumping the 3 components of moment into an effective transverse bending moment. For most cases weld residual stresses could be discounted on the basis of applied post weld heat treatments and stress redistribution during historical operation. The operating history also had to be quantified for the creep calculations; that is effective temperatures, loadings and time.

Crack opening area was calculated using a best estimate reference stress approach [4]. Flow rates were derived using the approximate method of Ewing [11] assuming lower, mean and upper bound fluid friction parameters [5]. Note that the lower bound friction factor results provided maximum leak rates for the consequences assessment. Reference steam leak rates, corresponding to detectable levels from unlagged and lagged pipes using acoustic emission techniques [6], were chosen to establish leakage crack sizes. A leak detection time of 50 hours was initially assumed based on a proposed inspection regime.

The simplified LbB approach assumes that a through-wall crack instantly appears at a reference operating time. The leakage through this crack must be detectable before the crack can grow to a limiting crack size. Limiting lengths of postulated through-wall cracks were based on the smaller of:

a) the R6 fracture initiation size, or
b) the through-wall crack 50 hour creep rupture size under assumed future normal operating conditions, taking account of historical operation continuum damage,

assuming lower bound fracture or creep rupture materials data. Because materials degradation accumulates with time, both the R6 and creep rupture limiting crack sizes vary with plant age. Therefore a range of plant ages had to be considered. A further complication in the limiting crack size assessment is that the weakest constituent material at the welded joint has to be identified; for 2¼CrMo welds in ½CrMoV pipe-work at high temperature this was usually Type IV or heat affected zone material. For calculation b), prior operation damage was based on the reference stress for a postulated 50% part-penetrating crack of length equal to the rupture size, which was assumed to be present since start of life. Accumulated continuum damage was accounted for using a life fraction rule:

$$\sum \frac{t[\sigma_{ref}(P,a,L)]}{t_{rup}[\sigma_{ref}(P,a,L)]}$$

where t is time at reference stress $\sigma_{ref}(P,a,L)$, t_{rup} is the creep rupture time for $\sigma_{ref}(P,a,L)$, P is the applied load, a the part penetrating crack depth and L the crack length (here assumed to be the rupture length).

Table 1 shows some typical results for 2¼CrMo welds in ½CrMoV pipe-work assuming the limiting crack size is controlled by fracture. These can be compared with results based on rupture presented in Table 2. It is seen that for the first three examples, creep rupture determines the limiting crack size and that the LbB margins are operating time dependent. It is also evident that the LbB margins on crack size and leak rate are lower for the smaller pipes. Table 1 also gives maximum leakage rates (assuming low fluid friction) based on R6 crack sizes derived from mean materials data. It is seen that maximum leak rates are higher for the larger pipe sizes.

Pipe Details	LSC for 10 g/s	Limiting R6 Crack Size/Minimum Flow		Mean R6 Crack Size/Maximum Flow	
	(mm)	(mm)	g/s	(mm)	g/s
1) R_m=71mm, t=25.8mm, P=16.5MPa, T=543°C	93	178	229	204	2586
2) R_m=141mm, t=47.1mm, P=16.5MPa, T=543°C	167	429	1003	473	9350
3) R_m=154mm, t=16.4mm, P=3.9MPa, T=563°C	200	436	457	491	2424
4) R_m=270mm, t=31.7mm, P=3.9MPa, T=563°C	325	849	1124	939	6022

Table 1: Results Assuming Limiting Crack Size is Controlled by Fracture

Pipe Details	Plant Age Increment	50 hour Creep Rupture Crack Size/Minimum Flow Rate	
	(hours)	(mm)	g/s
1) R_m=71mm, t=25.8mm, P=16.5MPa, T=543°C	Time t_1	143	61
	Time t_2	111	19
2) R_m=141mm, t=47.1mm, P=16.5MPa, T=543°C	End of life	394	525
3) R_m=154mm, t=16.4mm, P=3.9MPa, T=563°C	Time t_1	379	191
	Time t_2	291	48
4) R_m=270mm, t=31.7mm, P=3.9MPa, T=563°C	<100000	R6 limited	-

Table 2: Results Where Limiting Crack Size is Controlled by Creep Rupture

A range of sensitivity studies were carried out to justify acceptable margins. For example, results from pressure loading alone and pressure plus bending were compared. Also creep and fatigue crack growths were calculated for selected cases and found to be small for the assumed inspection reaction time of 50 hours.

LbB assessments were also carried out for 'Tee' junctions judged to be most at risk (e.g. equal-equal junctions). Through-wall defects were postulated at the flank and margins assessed for combined internal pressure and out of plane bending moments using a similar overall approach to that outlined above for butt welds. However, simple cylinder-based analysis models were found to be inadequate for the complex 'Tee' geometries of concern. Crack opening areas, stress intensity factors (see Figure 12) and reference stresses had to be evaluated using finite element models for a series of crack lengths (e.g. Figure 11), and interpolation functions developed to enable a realistic LbB assessment to be confidently performed.

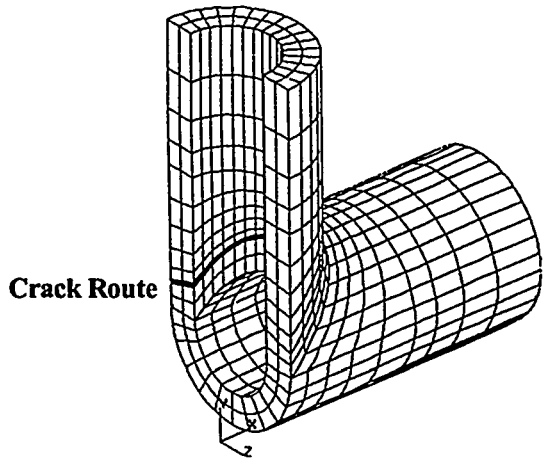

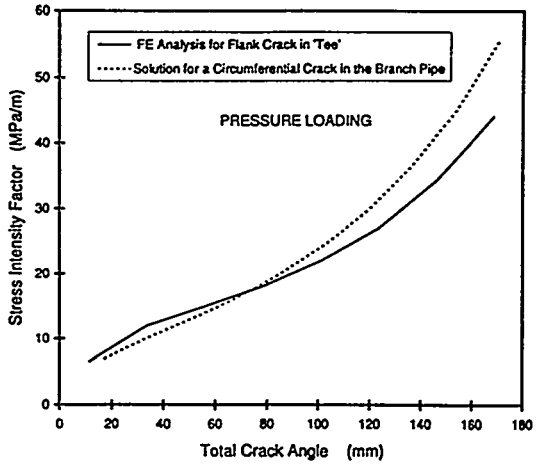

Figure 11: Cracked Body FE Model for a 'Tee' Junction **Figure 12: Stress Intensity Factor Results for 'Tee'**

CLOSURE

The forthcoming revision to the R6 LbB procedure has been briefly described and several practical applications discussed. The examples have highlighted a number of issues which can make the development of a satisfactory LbB case problematic. For example, coping with highly loaded components, methodology assumptions and the definition of margins, the effect of crack closure owing to weld residual stresses, complex thermal stress fields or primary bending fields, the treatment of locally high stresses at crack intersections with free surfaces, the choice of local limit load solution when predicting ligament break-through, and the scope of calculations required to support even a simplified LbB case for high temperature steam pipe-work systems.

ACKNOWLEDGEMENT

This paper is published with the permission of Nuclear Electric plc. The author wishes to acknowledge the contributions of Dr D C Connors and Mr. S. Booth to some of the examples quoted in this paper.

REFERENCES

1. Milne I, Ainsworth R A, Dowling A R and Stewart A T, 'Assessment of the Integrity of Structures Containing Defects', Int. J. Pres. Ves. & Piping, 32 (1988) 3-105.
2. R/H/R6 - Revision 3, 'Assessment of the Integrity of Structures Containing Defects', Nuclear Electric Maintained Document, April 1994.
3. NUREG 1061, 'Report of the US Nuclear Regulatory Commission Piping Review Committee, Volume 3, Evaluation of Potential for Pipe Breaks', US Nuclear Regulatory Commission, 1984.
4. Sharples J C and Bouchard P J, 'Assessment of Crack Opening Area for Leak Rates', this Seminar.
5. Chivers T C, 'Assesments of Fluid Friction Factors for Use in Leak Rate Calculations', this Seminar.
6. Chivers T C, 'Leak Detection', this Seminar.
7. Budden P J and Hooton D G, 'Margins in High Temperature Leak-Before-Break Assessments', this Seminar.
8. Paul D D, Ahmad J, Ghadiali N, and Wilkowski G M, SQUIRT, Seepage Quantification of Upsets in Reactor Tubes', User's Manual, Version 2.1, Battelle Columbus 1990.
9. Rahman S, Dong P, Wilkowski G, Moberg F and Brickstad B, 'Effects of Residual Stresses on Crack Opening Area Analysis of Pipes for LBB Applications', this Seminar.
10. Chopra O K, 'Long Term Embrittlement of Cast Duplex Stainless Steels in LWR Systems' Semi-annual Report, April-Sept 1992, NUREG/CR/CR-4744 Vol. 7, No.2, published July 1993.
11. Ewing D J F, 'Simple Methods for Predicting Gas Leakage Flows Through Cracks', 2nd Int. Conf. on Pipe-work Engineering and Operation, I Mech E, Paper C376/047, February 1989.

BELGIAN EXPERIENCE IN APPLYING THE "LEAK-BEFORE-BREAK" CONCEPT TO THE PRIMARY LOOP PIPING

R.Gérard, C.Malékian, O.Meessen
Tractebel Energy Engineering,
Avenue Ariane, 7
B-1200 Brussels, Belgium

ABSTRACT

The Leak Before Break (LBB) concept allows to eliminate from the design basis the double-ended guillotine break of the primary loop piping, provided it can be demonstrated by a fracture mechanics analysis that a through-wall flaw, of a size giving rise to a leakage still well detectable by the plant leak detection systems, remains stable even under accident conditions (including the Safe Shutdown Earthquake (SSE)).

This concept was successfully applied to the primary loop piping of several Belgian Pressurized Water Reactor (PWR) units, operated by the Utility Electrabel.

One of the main benefits is to permit justification of supports in the primary loop and justification of the integrity of the reactor pressure vessel and internals in case of a Loss Of Coolant Accident (LOCA) in stretch-out conditions. For two of the Belgian PWR units, the LBB approach also made it possible to reduce the number of large hydraulic snubbers installed on the primary coolant pumps. Last but not least, the LBB concept also facilitates the steam generator replacement operations, by eliminating the need for some pipe whip restraints located close to the steam generator. In addition to the U.S. regulatory requirements, the Belgian safety authorities impose additional requirements which are described in details in a separate paper.

An novel aspect of the studies performed in Belgium is the way in which residual loads in the primary loop are taken into account. Such loads may result from displacements imposed to close the primary loop in a steam generator replacement operation, especially when it is performed using the "two cuts" technique. The influence of such residual loads on the LBB margins is discussed in details and typical results are presented.

REGULATORY APPROACH

U.S.Rules

The US NRC issued Generic Letter 84-04 (ref.1) accepting that a double-ended guillotine break (DEGB) of the PWR primary loop piping was unlikely to occur, provided it could be demonstrated by a probabilistic fracture mechanics analysis that a postulated through-wall flaw yielding a leakage detectable with a large margin by the plant leak detection systems would remain stable even under accident conditions (SSE loading). Leakage exceeding the limit specified in the Plant Technical Specifications requires operator action to shut down the plant. This concept is known as "Leak-Before-Break".

The General Design Criterion-4 (GDC-4) (ref.6) was amended in April 1986 (limited scope rule) to permit to

eliminate from the design basis the dynamic effects of postulated pipe ruptures in primary coolant piping in PWRs. In October 1987, the GDC-4 was amended again to permit the use of leak-before-break in all qualified high-energy piping.

The detailed discussion of the limitations and acceptance criteria for LBB applications is provided in Nureg 1061 volume 3 (ref.2). A Standard Review Plan Section (3.6.3) entitled "Leak-before-break evaluation procedures" (ref.3) was published for comments in August 1987 and is not yet published in a final form at the present date.

The analyses performed for the Belgian units are based on these documents.

Additional requirements from the Belgian safety authorities

The only accident loading under which the through-wall flaw stability must be demonstrated according to the above mentioned documents is the SSE. For a low seismic region like Belgium, the loads resulting from this accident are far from being the most severe, and the steam line break (SLB), for example, may produce much higher loads in some specific locations of the primary coolant piping (see table 1). The Belgian safety authorities required to take this loading into account, which is more conservative than the usual U.S. procedure, and, to our knowledge, has never been considered in the LBB applications for U.S. or other foreign plants.

Rupture of the main auxiliary lines connected to the primary piping (pressurizer surge line, Emergency Core Cooling System (ECCS) line from the accumulators and shutdown cooling line) was considered as well.

Considering that some design basis events were not analyzed in details because they were enveloped by the postulated double-ended guillotine breaks of the primary loop piping, the Belgian safety authorities argued that the LBB application might reduce the protection against these other unspecified events. Therefore, they required to consider the following additional breaks in the design basis of the reactor core and internals, as well as for the steam generator tube bundle:

- rapid rupture (1 ms) of the steam generator manway cover (hot leg or cold leg);
- slow break (3 s) of one times the flow area, anywhere in the primary coolant piping.

More information on the regulatory aspects and the specific requirements of the Belgian safety authorities may be found in reference 5.

BENEFITS OF THE LBB APPLICATION

The first Belgian units to which the LBB methodology has been applied were Tihange 2 and Doel 3, which are three-loop 900 MW units, commissioned in 1983. In these units, three large capacity hydraulic snubbers were installed on each primary reactor coolant pump. These snubbers had to be replaced in both plants, due to maintenance problems. A preliminary evaluation showed that only one snubber was required on each pump for the SSE loading or other accident loadings (steam line break or auxiliary line breaks), and that a leak-before-break justification for these plants would allow to reduce the overall number of snubbers on the primary loops from 9 to 3 in each plant. This would represent a significant saving in terms of investment cost, but also on the integrated maintenance cost of this equipment for the remaining life of the plant, and would also allow to reduce the personnel radiation exposure. This was the main motivation for applying the leak-before-break methodology to these units.

An additional benefit was to facilitate the steam generator replacement operations that were carried out during the summer of 1993 in Doel 3, by allowing not to reinstall some pipe whip restraints that had to be dismantled for the replacement operation.

Another significant benefit of the LBB approach in conditions of stretch-out operations is to enable the justification of supports of the primary loop that already had a small margin with respect to the acceptable value at design conditions. It permits also the justification of the integrity of the reactor pressure vessel (RPV) and internals in these new stretch-out conditions. From the mechanical point of view, it is clear that in stretch-out conditions, LOCA analyses are more severe than in the original design conditions, due to the lower primary coolant temperature, which increases the amplitude of hydraulic force transients. The reactor pressure vessel, its supports and its internals were designed to withstand the loads arising from breaks at the inlet or outlet nozzles of the reactor pressure vessel. Under the loads corresponding to the original design conditions, the calculated response values (stresses, displacements..) are close to the acceptable values. Using the same methods as the original ones, the chances are high that the criteria would not be met under the loads corresponding to the stretch-out conditions. The LBB application, by eliminating the large LOCA, largely reduces this problem. It is not completely eliminated, however, because of the requirement by the Belgian safety authorities to consider the rupture of the steam generator manway cover, which still imposes significant hydraulic forces. Specific analyses remain necessary, but in this case the acceptance criteria can be met.

A last point for which the LBB approach is very beneficial is the primary coolant pump overspeed. In case of large LOCA at the pump outlet, with simultaneous loss of the connection to the grid, the overspeed of the pumps could reach values unacceptable for the flywheel. The same analysis performed with "LBB breaks" (auxiliary lines breaks and steam generator manway cover ejection) leads to an overspeed limited to a few percents of the nominal speed.

For the other Belgian units, for which the LBB was applied (Tihange 1, Doel 4) or shall be applied in the near future (Tihange 3), the benefits are essentially the same, except for the primary pump snubbers (these units have only one snubber per pump, combined with tie-rods). The reduction of the loads resulting from the elimination of the double-ended guillotine breaks is in itself sufficient to justify the application of the LBB methodology to these units.

MAIN STEPS OF THE ANALYSIS

"Classical" LBB

The LBB demonstration was performed in accordance with the requirement of the U.S. regulation, which are also applicable to the Belgian units (ref.1 and 3). These requirements form the basis of most LBB analyses performed to date, and have been described extensively in numerous publications. They do not need to be explained in details any more, and only the main steps of the analysis are summarized hereafter:

- demonstrate the absence of degradation mechanisms which could challenge the integrity of the piping (water hammer, stress-corrosion cracking, erosion/corrosion, fatigue..);
- demonstrate by a fatigue analysis that an existing flaw would not grow significantly under service transients;
- establish pipe material properties, taking into account service degradation (thermal ageing);
- calculate the service and accident loads at the different locations in the primary circuit (for the Belgian units, this information was either already available, or had to be recalculated anyway for other reasons like steam generator replacement or power uprating);
- calculate at different locations the size of the through-wall flaw yielding a leakage equal to ten times the detectable leakage under service loading which is called the "leakage crack size" a_q;
- demonstrate that a flaw two times longer remains stable under the accident loading, (for a combination of loads in absolute sum for the accident conditions). This is performed by calculating the critical crack size a_c under accident loading and verifying that $a_c/a_q>2$.

Leak detection systems

Defining the sensitivity of the leak detection systems is one of the first steps of any LBB analysis.

Several leak detection systems are used in the Belgian units:

- monitoring of the containment sump level (either by monitoring the frequency of the pumps startups, the volume between the low level and high level switch being known, or by means of a flow meter placed on the outlet line of the pump);
- monitoring of the condensate flow rate from the cooling batteries of the containment (in Doel 3 only);
- containment atmosphere particulate and gaseous radioactivity monitoring;
- primary circuit mass balance, on a period of three hours (in stabilized conditions), based on volumetric control tank level variations, corrected to take into account presurizer level variations, average temperature variations, pressurizer discharge tank and valve leakage collection tank level variations. This system makes it possible to detect small leaks (0.2 to 0.3 gallons per minute-GPM), but the balance is performed only once a day.

In each unit, there are at least three redundant systems allowing to detect a leakage of 1 GPM (226 liters/hour) in less than one hour, which fulfils the requirements of Regulatory Guide 1.45. Some systems are much more sensitive if a longer detection period is allowed, of the order of a few hours or one day. In this case, the detection capability could be as low as 0.2 to 0.3 GPM.

Conservatively, and in order not to penalize the operation of the plant, the limit of 0.5 GPM (113 liter/hour) was used to determine the leakage crack size a_q under service conditions.

Typical results ("classical" LBB)

The steam line break (SLB) case was analyzed assuming a double-ended guillotine break of the steam line at that location which results in the highest forces on the steam generator. If we assume that steam generator snubbers, located roughly at mid-height of the steam generator, practically constitute a fixed point, the loading due to a SLB results in a very high tensile force in the hot leg (additional with the tensile force due to the internal pressure) and a very high bending moment at the steam generator inlet elbow. This elbow being on the hot leg, and of a cast stainless steel material sensitive to the thermal ageing phenomenon, this clearly constitutes a critical combination.

Table 1 : Maxima of the axial force and of moments at the SG inlet in case of SLB compared to SSE results at various locations (Doel 3 unit)

Load case and Location	Axial force *kN*	Mx bending *kNm*	My bending *kNm*	Mz torsion *kNm*
SLB - SG inlet	4330	411	2690	798
SSE - SG inlet	289	473	198	437
SSE - SG outlet	303	191	715	285
SSE - Pump outlet	770	84	712	601

Typical results of the calculation for Doel 3 (comparable to Tihange 2 results) are given in Table 1, which compares the axial force and the three moments at the steam generator inlet in case of steam line break with the SSE results at a few locations in the primary loop. This table clearly shows the penalty resulting from considering the steam line break loading.

Influence of the steam generator replacement on the LBB analysis

In several instances, the LBB analysis was made on the occasion of steam generator replacements. In all cases, the replacement steam generators had slightly different characteristics from the existing ones, which modified the response of the primary loop piping. In addition to that, the replacement was generally coupled with power uprating or with a modification of the operating conditions (e.g. operation in stretch-out conditions). As a consequence, the primary loop piping had to be reanalyzed for the new characteristics or operating conditions, thereby providing the operating and accident loads needed for the LBB analysis.

The steam generator replacement may also have other impacts on the LBB analysis, depending on the technique used for the replacement operation and particularly for the welding in place of the new steam generators. In the case of a steam generator replacement in "two cuts", displacements may have to be imposed to the cold leg and hot leg, in order to close the loop. This clearly introduces residual moments that influence both the "leakage crack size" and the critical crack size, and must be taken into account in the LBB analysis. This is not required by the U.S. rules, and generally not considered in most LBB analyses, but was investigated systematically in the studies performed for the Belgian units where the steam generator replacement was planned in the "two cuts" option.

The moments induced in the loops by a displacement of a few milimeters necessary to close the gap become rapidly very large, and their effect on the LBB margins is far from negligible. The problem is in fact posed in slightly different terms, namely: what are the limits that must be imposed on the displacements applied to the primary loop piping by the steam generator replacement operations (permanent displacements after rewelding) in order to ensure that the resulting residual moments will not reduce the LBB margins below their required value?

Since this type of loads is not considered in the SRP 3.6.3, no rules are given for their combination with the other loads. It is clear that the combination must be algebraic for the definition of the resulting service moment to be used for the evaluation of the leakage crack size a_q. The criterion generally used in Belgium on the crack sizes is that there must exist a margin of 2.0 between the critical crack size a_c and the leakage crack size a_q, the load combination being made in absolute sum for a_c. In this case, the S.R.P.3.6.3 does not require to verify the margin of 1.4 on the loads. The reason for this choice is that it is felt that imposing a margin of 1.4 on loads like the pressure loads, which are very well known and furthermore limited by safety valves, may be very penalyzing and unrealistic.

The absolute sum combination, if applied blindly to all types of loads including the residual moments, does not make any sense since the residual moment has a direction and a value that are constant during the whole remaining life of the unit. The consequence would be that a residual moment reducing the service moment, which in itself is a beneficial effect reducing the probability to develop a crack, would appear as detrimental in the LBB analysis.

In order to overcome this difficulty, a slightly modified combination technique is used when residual moments have to be taken into account. First, the thermal and residual moments are combined algebraically, and, being both of secondary nature, are considered as an "equivalent secondary moment" (which by the way is treated conservatively as primary for the analysis). The rules of the SRP 3.6.3. are then followed rigorously, the only difference being that the thermal moments are replaced by this "equivalent secondary moment".

In order to determine the limits to be imposed on the displacements resulting from a steam generator replacement, an extensive parametric study must be performed.

In a first step, curves of the variation of a_q versus the resulting service moment, and a_c versus the resulting accident moment are established for the whole possible range of variation of these moments. (fig.1a and fig.1b)

A specific routine was developped to calculate automatically, for a given location in the primary loop, the resulting service moment and accident moments for a whole range of possible combinations of residual moments Mxr, Myr and Mzr. This is shown in Figure 2, which displays the variation of both bending moments Mxr and Myr for a given

value of the torsional moment Mzr. For each combination of these values, a_c and a_q are calculated. Then, it becomes possible to plot iso-curves of safety margins a_c/a_q for any combination of residual moments (fig.2).

In practice, the procedure is slightly more complicated, since we are not interested in limits on the residual moments, but rather in limits on the allowable displacements at the cut. This is done by calculating transfer matrices between displacements at the cut and moments in the different locations of the primary loop, taking into account the position of the hydraulic jacks that are used to impose these displacements, which for obvious reasons are located at some distance from the cuts. The complete procedure is the following :

- select a set of imposed displacements at the cuts;
- calculate the corresponding residual moments at the different locations of the primary loop;
- calculate the resulting service moment and accident moments for these locations, for different accident conditions;
- calculate the corresponding values of a_c, a_q and a_c/a_q at the different locations analyzed;
- go to the next set of imposed displacement.

By covering the whole range of horizontal and vertical displacements, for different given values of the axial displacements, limits on the displacement corresponding to $a_c/a_q = 2$ may be determined (fig.3). As long as the actual displacements imposed during the steam generator replacement remain within these limits, the LBB margins remain verified.

Typical results (taking into account residual loads induced by a steam generators replacement).

The procedure described hereabove has been followed at the principal locations in the primary loop.
Typical results of the margins at the RPV inlet nozzle are given hereafter for Tihange 1 unit.
The variation of critical size a_c with the resulting accident moment, and of the leakage crack size a_q with the resulting service moment are given on Figure 1a and 1b respectively.

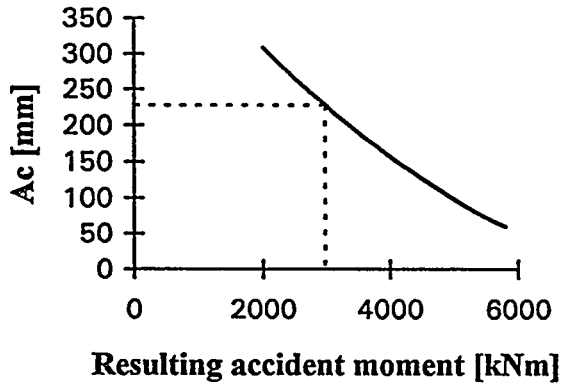

Figure 1a
Critical crack size vs.resulting accident moment.

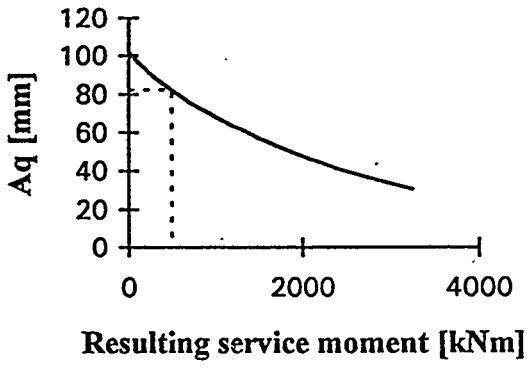

Figure 1b
Leakage crack size at 5 GPM vs.resulting service moment

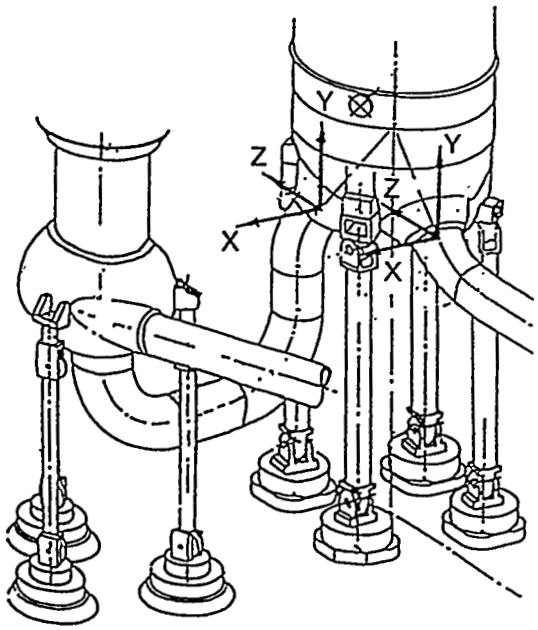

Figure 3 : Global axes at the cut
X : transverse horizontal axis
Y : vertical axis
Z: axis parallel to the hot leg

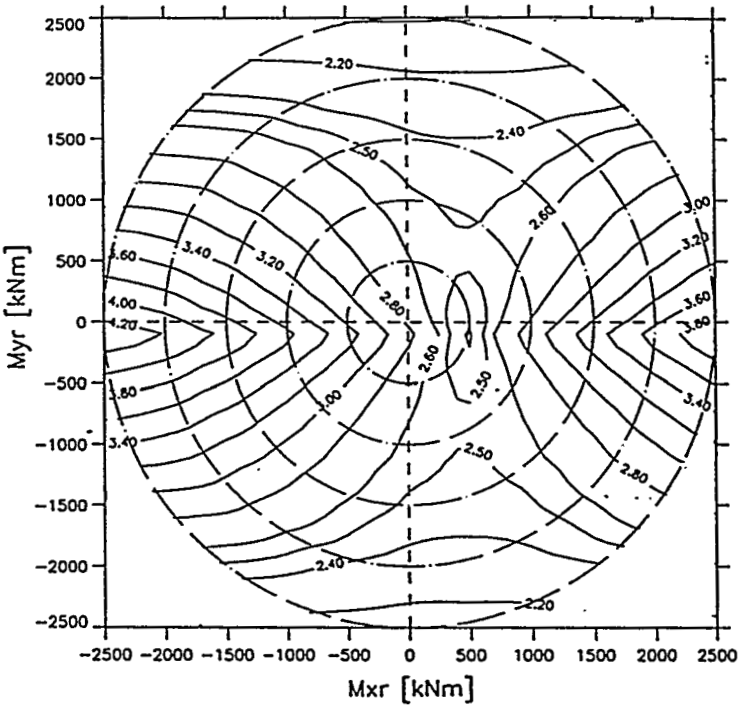

Figure 2 Influence of both residual bending moments Mxr and Myr on stability margins a_c/a_q (for Mzr=0).
(LBB Tihange 1 - RPV inlet nozzle)

Figure 4 shows the limits of displacements in the cross-over leg in the X-Y plane for different values of Z displacement (see definition of axes on figure 3). The limits presented here have a very simple form, but they can also take a more complicated form. These limits, once established for each location and put together on the same plot, yield the range of maximal allowable displacements at the cuts.

These limits must of course be combined with those resulting from tensiometric criteria.

These displacements are measured between the natural position of the hot-leg and cross-over leg end sections after cutting, and their position after re-welding.

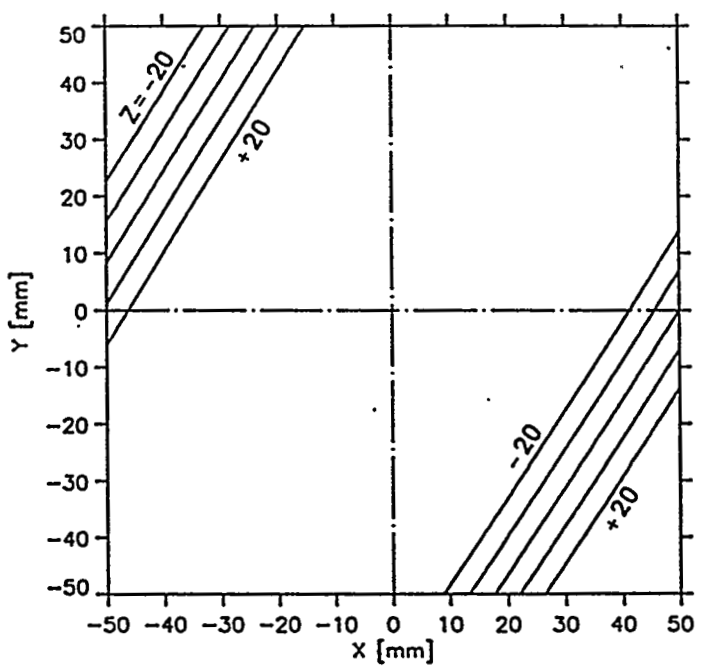

Figure 4 : Allowable displacements in the cross-over leg

CONCLUSIONS

The Leak Before Break concept has been successfully applied to the primary loop piping of several Belgian PWR units, operated by the Utility Electrabel.

Since it allows to eliminate from the design basis the double-ended guillotine break of the primary loop piping, it makes it possible to justify the integrity of the reactor pressure vessel and internals in case of LOCA in stretch-out conditions. For two of these units, the LBB also enables to reduce the number of large hydraulic snubbers installed on the primary coolant pumps. Last but not least, the LBB also facilitates the steam generator replacement operations, by eliminating some pipe whip restraints located close to the steam generators.

In addition to the U.S. regulatory requirements, the Belgian safety authorities impose additional requirements. They require to consider in the LBB analysis, in addition to the SSE, the rupture of the steam line and the main auxiliary lines. They also impose to study a "rapid" rupture of the steam generator manway covers and a "slow" break of one times the flow area, anywhere in the primary coolant piping.

A novel aspect of the studies performed in Belgium is the way in which residual loads in the primary loop are taken into account. Such loads may result from displacements imposed to close the primary loop in a steam generator replacement operation, especially when it is performed using the "two cuts" techniques. The influence of such residual moments has been evaluated in the principal locations of the primary circuit. Through the determination of transfer matrices between the displacements at the cut and these residual moments, limits of admissible displacements have been determined. Since they are given in a relatively simple form, they can be taken into account in the decision to make a "two cuts" or "three cuts" steam generator replacement.

REFERENCES

1) Generic Letter 84-04 *"Safety evaluation of Westinghouse topical reports dealing with elimination of postulated pipe breaks in primary main loops"*
US NRC, 1 February 1984

2) NUREG 1061 Vol.3 *"Evaluation of Potential for Pipe Breaks"*
November 1984

3) Standard Review Plan 3.6.3 *"Leak-Before-Break Evaluation Procedure"*
Federal register, Vol.52, N0 167, August 28, 1987

4) US Code of Federal regulations, Title 10, Part 50,
Appendix A, General Design Criterion 4 *"Environmental and dynamic effects design bases"*

5) *"Additional requirements for the application of the leak before break concept in Belgium"*
J.P.Lafaille , G.Roussel
Smirt-95, Porto Alegre , Brazil (to be published)

6) 10CFR50 (Code of [USA] Federal Regulations - Title 10 - Part 50)
Appendix A : *GDC4 (General Design Criterion 4)*. October 30, 1987

LEAK BEFORE BREAK APPLICATION

IN FRENCH PWR PLANTS UNDER OPERATION

C. Faidy - EDF SEPTEN

12-14 Avenue Dutrievoz

69 628 VILLEURBANNE CEDEX

FRANCE

ABSTRACT

Practical applications of the leak-before break concept are presently limited in French Pressurised Water Reactors (PWR) compared to Fast Breeder Reactors. Neithertheless, different fracture mechanic demonstrations have been done on different primary, auxiliary and secondary PWR piping systems based on similar requirements that the American NUREG 1061 specifications. The consequences of the success in different demonstrations are still in discussion to be included in the global safety assessment of the plants, such as the consequences on in-service inspections, leak detection systems, support optimisation,....

A large research and development program, realised in different co-operative agreements, completes the general approach.

INTRODUCTION

Presently in France, 54 Pressurised Water Reactors (PWR) are in operation, 4 are under construction and 2 Fast Breeder Reactors (FBR) are in operation. For these plants the Leak-Before-Break (LBB) was not used at the design level. Application in FBR's are presented in [1,2]. The specific application to PWR steam generator tubes is presented in [3].The LBB concept will be considered at design level for future plants[4]

All the high energy piping systems of the 58 French PWR's (54 in operation + 4 under construction) are designed with ASME [5] or RCCM [6] B 3600 Code and the

pipe rupture hypotheses of the initial American regulation (General Design Criteria [GDC] 4 of Appendice A to Part 50 of Title 10 of the Code of Federal Regulations [CFR] and Standard Review Plant [SRP] 3.6.3). In consequence, for the primary loop 11 instantaneous double-end-guillotine breaks have to be considered : 2 circumferential on cold leg, 2 circumferential on hot leg, 1 circumferential on cross-over leg, 3 circumferential on connected lines, 1 circumferential on Steam Line inside the containment and 1 instantaneous longitudinal break on a primary loop elbow . Different specific supports are needed to assess the level D Code criteria. But, all of the studies are done with limited area type of breaks; an example for a 4 loop PWR plant is presented on table 1 considering the effectiveness of the different supports :

Break	Type	Location	Size in cm^2
1	Circumferential	RPV inlet nozzle	500
2	Circumferential	RPV outlet nozzle	500
3	Circumferential	SG inlet nozzle	800
4	Circumferential	SG outlet nozzle	900
5	Circumferential	RCP inlet nozzle	800
6	Circumferential	RCP outlet nozzle	200
7	Longitudinal	SG inlet elbow	4860
8	Circumferential	Cross over leg	1000
9	Circumferential	RHR connection	580
10	Circumferential	SIS connection	410
11	Circumferential	Surge Line connection	830

Table 1

GENERAL LBB ASSESSMENT

Demonstration of LBB to large diameter pipes are usually carried out in 2 phases, similar to the USNRC requirements of NUREG 1061 [7] with some complementary requirements :

- a main phase, for each welds, to justify that a leak from a through-wall crack can be detected in normal operation for a crack length smaller than the normal operation and Safe Shutdown Earthquake (SSE) critical crack size,
- a complementary phase, for each welds, to justify that any initial reference defects can't grow through the thickness of the pipe wall up to the end of life of

the plant by fatigue or corrosion (corrosion is negligible for 316 stainless steel type of primary loop and connected lines).

Three steps have to be considered in the main phase, for each welds :

- examine the through wall crack stability under normal operation + SSE,
- evaluate the corresponding crack area under normal operation,
- compare the evaluated leak rate with the detectable one.

Three steps have to be considered in the complementary phase, for each welds :

- define a "reference" defect,
- determine the end of life defect corresponding to the design transient list, using the late available data to describe these transients,
- justify sufficient margins regarding the stability of the end of life defect for all the transients.

In FRANCE, we have proposed to consider defects in cast elbows, not only in the weld between elbow and straight pipe.

For all these different steps, we use the NUREG 1061 safety factors 10 on flow rate, 2 on crack length or 1.4 on load.

For the primary loop, no specific requirements for leak detection systems are directly connected to LBB application, we use the basic leak detection systems with same level of redundancy (mass balance, containment air activation, sink,...) and similar objective than initial design value : 1 Gpm; no specific increase of in-service inspection is directly connected with LBB considerations.

THROUGH WALL CRITICAL CRACK SIZE

To analyse the maximum crack size of the through wall crack defects under normal operation + safe shutdown earthquake, we use the generic seismic analysis of different series of plants (900 MWe, 1300 MWe, 1400 MWe) based on elastic modal analysis and the R6 [8] or EPRI [9] formula to determine the J value for different load levels and the dJ /da criteria for stability analysis (all the thermal expansion loads and seismic anchor motions are considered as primary loads for J evaluation. In a first step, we use limited crack growth propagation (few millimetres), if the J_{IC} is rather small, specific tests are necessary for justification of the J resistance curve used with larger crack growth.

For cracks in elbows, a specific experimental and analytical program is still under progress, in closed co-operation between FRAMATOME and EDF.

LEAK AREA EVALUATION

Different estimation schemes are available, but they give similar area for low load level, that is generally the case for French design under operation loads. We consider an elliptical crack shape with a crack mouth opening displacement evaluation based on a generalisation of TADA-PARIS method for an extended range of R/t (radius/thickness). The plasticity effects are evaluated using Dugdale model and reference stress concepts. The method is detailed in reference [10].

LEAK FLOW RATE EVALUATION

Again, different evaluation scheme are available, but in this case, the result scatter band can be larger. We use in FRANCE a di-phasic model derived from computation of different experiences run in a multi-party agreement between Westinghouse, CEA, FRAMATOME and EDF. The model is based on Fauske-Henry model with correction factor for surface roughness of the cracked surface. Presently, we are checking this model with the SQUIRT program develop by BATTELLE for NRC in different programs [11].

REFERENCE DEFECTS AND GEOMETRIES

The corresponding defect size is connected with the manufacturer experience, the fabrication process, the welding technique used, the different repaired process, the fabrication non destructive examinations and the in-service inspection results. For example, for stainless steel but weld in primary coolant loop we use a surface defect of 5mm depth and 20 mm long.

For each weld, we use the real on-plant design and local dimensions.

FATIGUE ANALYSIS AND STABILITY OF END OF LIFE SURFACE DEFECT

We use to do that classical fracture mechanic approaches similar to those presented in RCCM Appendice ZG [5] for fatigue analysis, and a French methodology similar to R6 procedure [12] for crack stability analysis.

EXAMPLE OF PRACTICAL ANALYSIS

The next table gives some rough ideas on the behaviour of a 4 loop plant regarding the LBB justification :

Weld Location	Unit	RCP outlet nozzle	RPV outlet nozzle safe end weld	RPV outlet nozzle dissimilar weld
critical crack length	2 a_{crit} in mm	586	500	582
critical crack angle	2 θ_{crit} en °	88	70	81
crack opening area	A en mm^2	510	505	659
leak flow rate	Q en kg/mn	1510	1030	1380
margin	Q / 3.8*	419	286	550
* 3.8 kg/mn = 1 Gpm		> 10	> 10	> 10

The criteria of NUREG 1061 are largely verified in this case. Similar work is in progress for different type of plants with the same type of conclusions.

RESEARCH AND DEVELOPMENT PROGRAM

After a minimum program realised in FRANCE [13], we have joined with FRAMATOME and CEA the IPIRG (International Piping Integrity Research Group) [14] in order to share the cost of large scale dynamic tests. The major topics are :

- finite element analysis of experimental results from cracked pipe tests [15,16],
- development of one-dimensional beam element for dynamic analysis[17,18],
- estimation scheme development and comparison with limit load analysis, comparison of different estimation schemes on different test results [19],
- leak area estimation scheme and validation [10],
- different round robin analysis at the international level.

The developed tools are reasonably validated, but some R&D works have to be completed to support some actual hypotheses :

- the large crack growth situation for low toughness welds,
- the change in direction of crack growth for some materials,
- the cyclic effects under negative load ratios for some materials,
- the multi-material situation in weld area (high mismatch, dissimilar-weld,...)
- the low crack area in weld and corresponding flow rate evaluation

CONCLUSIONS

The LBB concept has to be taken in the global safety evaluation of a plant. No French PWR's consider it at the design level. Neithertheless, different applications have been successfully applied using the USNRC recommendations (NUREG 1061), some detailed points require complementary works at the Research and Development level. The safety margin coefficients have to be connected with the conservativeness of the different hypotheses used in the analysis. The practical consequences has to be discussed and finalised with French Safety Authority. Presently, in French PWRs, the LBB concept is used for Steam Generator Tubes, or as complementary study to support high margins in front of large diameter piping system rupture.

REFERENCES

1. Faidy C., Maupré J-P, Martin Ph.,"Application of Leak Before Break Concept for Fast Breeder Reactor in France", Commission of European Communities, WGCS Contract RAP 085F, Brussels, 1989.
2. Turbat A., Deschanels H., Sperandio H., Faidy C.,"The LBB Concept in French Fast Reactors : Application to SPX plant", LBB95 specialist meeting on leak before break, Lyon, FRANCE, 1995.
3. Flesch B., Gâté R., Cochet B., "Recent developments in the field of leak before risk of break for steam generator tubes", SMIRT 11, paper D, Tokyo, JAPAN, 1991.
4. Cauquelin C., "LBB for European Pressurized Reactor - EPR", LBB95 specialist meeting on leak before break, Lyon, FRANCE, 1995.
5. ASME Boiler & PPressure Vessel Code-Section III-"Rules for Construction of Nuclear Power Plant Components", American Society of Mechanical Engineers, New-York, 1992.
6. RCCM, "Règles de Conception et de Construction des Matériels Mécaniques des Ilots Nucléaire REP", AFCEN, Paris, 1993.
7. The Pipe Break Task Group, " Evaluation of Potential for Ppe Breaks",NUREG 1061-Vol. 3, U.S. Nuclear Regulatory Commission, Washington D. C., 1994.
8. Milne I., Ainswoerth R.A., Dowling A.R., Stewart A.T., "Assessment of the integrity of structures containing defects", R/H/R6-Rev. 3, CEGB, 1986.
9. EPRI-GE Handbook, "Advances in Elastic-Plastic Fracture Analysis", EPRI Report NP 3607, Electric Power Institute, Palo-Alto, 1984.
10. S. Bhandari, C. Faidy, D. Acker, "Computation of leak areas of circumferential cracks in piping for application in demonstrating leak-before-break behaviour", Nuclear Engineering and Design 135, 141-149, 1992.
11. Paul D., Ahmad J., Scott P., Flanigan L., Wilkoski G.,"Evaluation and Refinement of Leak-Rate Estimation Models", NUREG/CR-5128, Rev. 1, U.S. Nuclear Regulatory Commission, Washington D. C., 1994.
12. Pellissier-Tanon A.,"Fracture Mechanics Procedure in France for PWR", Saclay International Seminar on Structural Integrity, Principles of Fracture Mechanics Application in Nuclear Power Plants, Gif-sur-Yvette, France, 1994.
13. Faidy C., Bhandari S., Jamet Ph.,"Leak-Before-Break in French Nuclear Power Plants", Int. J. Ves. & Piping, 43, 151-163, 1990.
14. Wilkoski G., Olson R., Scott P., Brust B., Ghadiali N., Kilinski T., Rudland D., Hopper A.,"The IPIRG Programs- Advances in Pipe Fracture Technology", LBB95 specialist meeting on leak before break, Lyon, FRANCE, 1995.
15. Moulin D., Le Delliou P.,"French Experimental Studies of circumferentially through-wall cracked austenitic pipes under static bending", Saclay International Seminar on Structural Integrity, Gif-sur-Yvette, France, 1991.
16. Brust F.W., Ahmad J., Brickstad B., Faidy C., Gilles Ph.,"Comparisons between Finite Element Analysis predictions and Pipe Fracture experiments", NUREG/CP 0037, U.S. Nuclear Regulatory Commission, Washington D. C., 1990.
17. Petit M., Jamet Ph., "Numerical evaluation of cracked pipes under dynamic loading using a special finite element", SMIRT 10, Division G, Anaheim, 1989.
18. Blay N, Gantenbein F.,"Interpretation of a seismic test of the IPIRG2 program", SMIRT13, Division K, Porto Alegre, Brasil, 1995.
19. Darlaston B.J., Bhandari S., Franco Ch.,"Predictions of failure for several of the international pipe tests using the R6 method", Proc. of the 7th Int. Conf. on Pressure Vessel Technology, FRG, 1992.

PL/S, Dr. Roos

Karlsruhe, July 6, 1995

Application of Break Preclusion Concept in German Nuclear Power Plants

Roos, E.[1]; Maier, V.[2]; Nagel, G.[3]; Otremba, F.[4]; Wolf, M.[5]

The break preclusion concept is based on "KTA rules", "RSK guidelines" and "Rahmenspezifikation Basissicherheit". These fundamental rules containing for example requirements on material, design, calculation, manufacturing and testing procedures are explained and the technical realisation is shown by means of examples.

The proof of the quality of these piping systems can be executed by means of fracture mechanics calculations by showing that in every case the leakage monitoring system already detect cracks which are clearly smaller than the critical cracks. Thus the leak before break behavior and the break preclusion concept is implicitly affirmed.

In order to further diminish conservativities in the fracture mechanics procedures, specific research projects are executed which are explained in this contribution.

[1] Energie-Versorgung Schwaben AG, Postfach 10 12 43, 70011 Stuttgart

[2] Bayernwerk AG, Postfach 20 03 40, 8003 München

[3] PreussenElektra AG, Postfach 48 49, 30048 Hannover

[4] Hamburgische Electricitäts-Werke AG, Überseering 12, 22297 Hamburg

[5] RWE-Energie AG, Kruppstraße 5, 45128 Essen

THE ANALYSIS OF NORMATIVE REQUIREMENTS TO MATERIALS OF VVER COMPONENTS, BASING ON LBB CONCEPTS

V. V. Anikovsky, G. P. Karzov, B. T. Timofeev
CRISM "Prometey", St.-Petersburg, Russia

Abstract

The paper demonstrates an insufficiency of some requirements native Norms (when comparing them with the foreign requirements) for the consideration of calculating situations:

- leak before break (LBB);
- short cracks;
- preliminary loading (warm prestressing).

In particular, the paper present:

- comparison of native and foreign normative requirements (PNAE G-7-002-86, Code ASME, BS 1515, KTA) on permissible stress levels and specifically on the estimation of crack initiation and propagation;
- comparison of RF and USA Norms of pressure vessel material acceptance and also data of pressure vessel hydrotests;
- comparison of Norms on the presence of defects (RF and USA) in NPP vessels, developments of defect schematization rules; foundation of a calculated defect (semi-axis correlation a/b) for pressure vessel and piping components;
- sequence of defect estimation (growth of initial defects and critical crack sizes) proceding from the concept LBB;
- analysis of crack initiation and propagation conditions according to the acting Norms (including crack jumps);
- necessity to correct estimation methods of ultimate states of brittle and ductile fracture and elastic-plastic region as applied to calculating situation : a) LBB and b) short cracks;
- necessity to correct estimation methods of ultimate states with the consideration of static and cyclic loading (warm prestressing effect) of pressure vessel; estimation of the effect stability;
- proposals on PNAE G-7-002-86 Norm corrections.

한국전력기술주식회사
KOREA POWER ENGINEERING COMPANY, INC.

P.O.BOX 631, YEONGDONG, SEOUL, KOREA
TELEX : KOPEN K 22562
FAX : 540-4184 TEL : 540-7701

Submitting to LBB 95 (Specialist meeting on LEAK BEFORE BREAK in Reactor Piping and Vessels), Lyon, FRANCE

Title : Leak Before Break Evaluation for Main Steam Piping System made of SA106 Gr.C

Authors : Kyoung Mo YANG, Kye Kwang JEE, Chang Ryul PYO and In Sik RA

Affiliation : Korea Power Engineering Company

Address : P.O.Box 631, Kang-Nam, Seoul, KOREA
Tel) +82-2-510-5117
Fax) +82-2-540-4184

ABSTRACT

The basis of the leak before break (LBB) concept is to demonstrate that piping will leak significantly before a double ended guillotine break (DEGB) occurs. This is demonstrated by quantifying and evaluating the leak process and prescribing safe shutdown of the plant on the basis of the monitored leak rate. The application of LBB for power plant design has reduced plant cost while improving plant integrity. Several evaluations employing LBB analysis on system piping based on DEGB design have been completed. However, the application of LBB on main steam (MS) piping, which is LBB applicable piping, has not yet been performed due to several uncertainties associated with occurrence of steam hammer and dynamic strain aging (DSA).

The objective of this paper is to demonstrate the applicability of the LBB design concept to main steam lines manufactured with SA106 Gr.C carbon steel. Based on the material properties, including fracture toughness and tensile properties obtained from the comprehensive material tests for base and weld metals, a parametric study was performed as described in this paper. The PICEP code was used to determine leak size crack (LSC) and the FLET code was used to perform the stability assessment of MS piping.

The effects of material properties obtained from tests were evaluated to determine the LBB applicability for the MS piping. It can be shown from this parametric study that the MS piping has a high possibility of design using LBB analysis.

Approach of Czech regulatory body to LBB.

Petr Tendera
State Office for Nuclear Safety (SONS), Prague

At present there are two NPPs equipped with PWR units in Czech Republic . The Dukovany NPP is about ten years in operation (four units 440 MW - WWER model 213) and Temelin NPP is under construction (two units 1000 MW - WWER model 320). Both NPPs were built to Soviet design and according to Soviet regulations and standards but most of equipment for primary circuits was supplied by home manufactureres.

The objective of the Czech LBB programme is to prove the LBB status of the primary piping systems of these NPPs and the LBB concept is a part of strategy to meet western style safety standards. The reason for the Czech LBB project is a lack of some standard safety facilities, too.

For both Dukovany and Temelin NPPs a full LBB analysis should be carried out. The application of LBB to the piping system should be also a cost effective means to avoid installations of pipe whip restraints and jet shields.

The Czech regulatory body issued non-mandatory requirement „ Leak Before Break" which is in compliance with national legal documents and which is based on the US NRC Regulatory Procedures and US standards (ASME CODE, ANSI). The requirement has been published in the document „Safety of Nuclear Facilities" No 1/1991 as „Requirements on the Content and Format of Safety Reports and their Supplements" and consist of two parts

- procedure for obtaining proof of evidence „Leak Before Break"
- leak detection systems for the pressurized reactor primary circuit .

At present some changes concerning both parts of the above document will be introduced. The reasons for this modifications will be presented.

APPLICATION OF THE CRACKED PIPE ELEMENT TO CREEP CRACK GROWTH PREDICTION

J. BROCHARD - T. CHARRAS
C.E.A. - C.E.-SACLAY DRN/DMT, GIF SUR YVETTE FRANCE
M. GHOUDI
C.E.A. - C.E.-SACLAY, INSTN, GIF SUR YVETTE FRANCE

Several years ago, a cracked pipe element was implemented is CASTEM2000 computer code for ductile fracture assessment of piping systems with postulated circumferential through-wall cracks under static or dynamic loading. We undertake a development to extend the capabilities of the element to the determination of fracture parameters under creep conditions (C*, $\dot{\Phi}c$ and $\dot{\Delta}c$).

In a first step, a time independant strain rate law ($\dot{\varepsilon} = A\sigma^n$) is considered, so that the ductile fracture formulae proposed by Zahoor can be used. Under combined tension and bending the C* expression is :

$$C^* = A\,R\,(\pi-\theta)\,(\theta/\pi)\,h_1\,\left(\frac{P}{P'_o}\right)$$

$$\text{with } P'_o = 0.5\left[-\lambda R P_o^2 / Mo + \left\{\left(\lambda R P_o^2 / Mo\right)^2 + 4P_0^2\right\}^{0,5}\right]$$

$\lambda = M/PR$
$Po = 2\,Rt\,[\pi-\theta-2\sin^{-1}(0,5\sin\theta)]$
$Mo = 4\,R^2\,t\,[\cos(\theta/2) - 0,5\sin\theta]$

Cinematic parameters $\dot{\phi}_c$ and $\dot{\Delta}_c$ are deduced from C* and loads values at each step of the calculation.

Under secondary creep conditions, this element is now available to carry out a complete simulation by performing successive resolutions increasing the defect size with the material rule : $\Delta a = B\,(C^*)^m$.

The main advantage of this element is that by modelling the complete piping system using classic pipe elements and this special element at the crack location, the secondarity of the loads such as thermal loads can correctly be evaluated. An application has been conducted on a FBR-type piping system, for which the crack growth predictions considering the thermal stresses as primary or secondary stresses are significantly different.

THE PRIMARY CIRCIUT MATERIALS PROPERTIES RESULTS ANALYSIS PERFORMED ON ARCHIVE MATERIAL USED IN NPP V-1 AND KOLA NPP UNITS 1 AND 2

KUPČA Ľudovít PhDr, BEŇO Peter, Nuclear Power Plants Research Institute Inc.
Okružná 5, 918 64 Trnava, SLOVAK REPUBLIC

SUMMARY

The primary circuit piping material properties analysis was close related to the LBB methodology applications on the both units of the NPP V-1.

The asessment was performed on the following piping materials:

a) primary piping archive material used in NPP V-1

b) primary piping material cut from NPP Kola Units 1 and 2 after 100000 hours of operation

c) final correlations between the Russian and our experimental results.

Main research program tasks were:

1) analysis of the piping material mechanical properties (static tension, charpy, fracture toughness, fatigue)

2) corrosion stability of the primary circuit material analysis (igscc)

3) microstructural properties analysis which involved:

   a) visual inspection of exposed internal surface

   b) chemical composition analysis

   c) hardness measurements

   d) stainless steel macro and microstructural properties evaluations

   e) delta-ferrite contents measurements

   f) thermal fatigue and operational influences evaluation

   g) substructure of both material evaluations using the TEM

   h) fractography of samples after mechanical tests.

LBB APPLICATION IN SWEDISH BWR DESIGN

Authors: H Kornfeldt, K-O Björk, P Ekström, ABB Atom, S-72163 Västerås, Sweden
Fax No. +46-21-14 48 57, E-mail atohako@qm.ato.abb.se

ABSTRACT

The protection against dynamic effects in connection with potential pipe breaks has been implemented in different ways in the development of BWR reactor designs. First-generation plant designs reflect code requirements in effect at that time which means that no piping restraint systems were designed and built into those plants. Modern designs have, in contrast, implemented full protection against damage in connection with postulated pipe breaks, as required in current codes and regulations.

Moderns standards and current regulatory demands can be met for the older plants by backfitting pipe whip restraint hardware. This could lead to several practical difficulties as these installations were not anticipated in the original plant design and layout. Meeting the new demands by analysis would in this situation have great advantages.

Application of leak-before-break criteria gives an alternative opportunity of meeting modern standards in reactor safety design. Analysis takes into account data specific to BWR primary system operation, actual pipe material properties, piping loads and leak detection capability. Special attention must be given to ensure that the data used reflects actual plant conditions.

WHY LBB IN SWEDISH BWRS?

The first generation ABB Atom BWR plants in Sweden were designed without pipe whip restraints. Pipe rupture was postulated only as design basis for containment and emergency cooling systems. In later generation plants restraints were introduced. Requirements have been developed in principle similar to U.S. regulations and current Swedish rules adhere to U.S. NRC Standard Review Plan 3.6.2.

The situation consequently is that the earlier plants lack protection against postulated pipe break dynamic effects. At the same time some of the later plants may have too many restraints installed leading to possible detrimental effects in other areas, such as serviceability, inspection and dose reduction.

As the plants now approach their mid-life several design reviews have been initiated. One of the purposes with this work is to modernize the plants bringing them up-to-date with current regulations and optimize their modes of operation.

The LBB concept is a promising way of meeting both objectives. In applying LBB special consideration should be taken of BWR technology and operating experience.

POTENTIAL FOR LBB APPLICATION.

The first 5 Swedish BWRs are equipped with external recirculation loops, schematically shown in figure 1. Their outside diameter is 670 mm with a wall thickness of 35 mm. The piping base material is carbon steel clad on the inside with stainless steel. Components are cast stainless steel and buttering and welds have been made of Alloy 182 to various extent. Other primary piping is made of stainless steel except the main steam lines that were made from carbon steel.

The relatively large number of high energy pipes in the containment together with the restricted space available for back-fitting restraints makes it a fundamentally important task to optimize the adherence to regulations in this area.

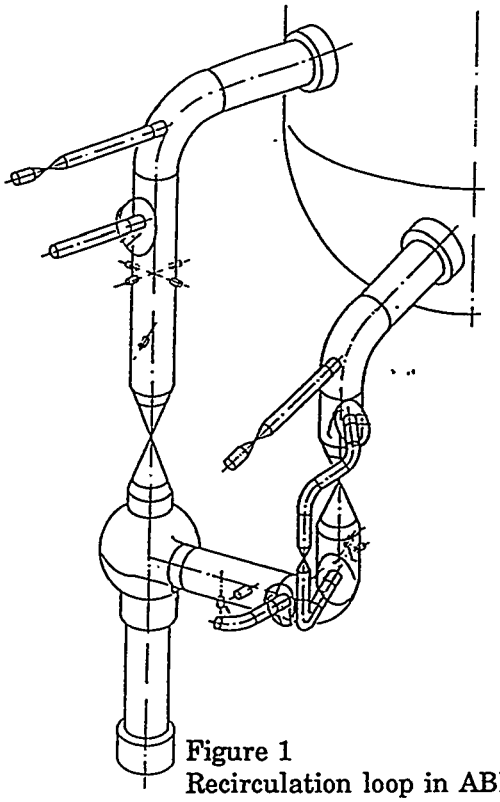

Figure 1
Recirculation loop in ABB Atom BWR

Later reactor designs are equipped with internal recirculation pumps which as a consequence has removed this large diameter piping from the plant. Other piping still needs consideration even though the regulatory aspect is being met with present installations.

APPLICATION OF LBB METHODOLOGY

Traditionally Swedish reactor design has looked at U.S. regulations and standards for references. The ASME Code has been used for design and fabrication and NRC regulations and guides have directed regulatory work. As a basis for evaluating the applicability of LBB to the ABB Atom BWRs the NRC Draft Standard Review Plan 3.6.3 is being used. There is, however, at this time no official Swedish regulation or guideline as to the application of the LBB concept.

Work is underway to evaluate the SRP 3.6.3 in a few specific application cases. The outcome of this work would form part of a basis for formulating rules fitting the Swedish design and regulatory environment.

One particular BWR aspect is the lower system pressure as compared with PWR primary pressure. This leads to a requirement to postulate larger cracks while at the same time the thinner wall thicknesses favour smaller crack postulates. The impact of these factors on LBB is determined according to SRP 3.6.3, taking into account plant-specific conditions.

Of particular interest are the special material conditions of BWR plants and observed cracking phenomena. The generic susceptibility of stainless steels to intergranular stress corrosion cracking (IGSCC) in BWR water environment has generally been considered prohibitive of LBB application to BWR piping in the U.S. ABB Atom plants have been designed and built taking these

material conditions into account. Low carbon contents have always been specified for stainless steels which have also been checked for sensitization susceptibility, and heat input during welding including the permitted number of repairs has been limited in welding procedure specifications. This has resulted in a very low probability for IGSCC which is supported by operational experience.

IGSCC growth rates in reactor design materials are well known from many multi-year tests. These include base materials as well as weld materials in different environments including hydrogenated water. All reported cracking in such tests indicate that crack growth is a controlled process which does not lead to sudden crack propagation and would not lead to a potential guillotine break in a pipe.

It is suggested here that the LBB assessment method as described in SRP 3.6.3 could be used also in BWR reactors. If the technical standards of ABB Atom have been implemented the probability of IGSCC is sufficiently low to permit the application of the LBB concept. A crack of the size postulated in the calculation, regardless of how it came to exist, could not grow uncontrollably by IGSCC. Other piping loads acting as possible crack drivers are included in the analysis methodology of SRP 3.6.3.

LBB IN OPERATING PLANTS

In applying LBB criteria to existing plants several aspects need to be addressed. First, of course is an assessment of the needs and the benefits that can be gained by the analysis. As indicated earlier it is a major undertaking to retro-fit large steel structures in already confined spaces.

Technical issues include such areas as the need for specific material data and an evaluation of the effectiveness of the leakage-detection system.

In order to perform the analysis in accordance with SRP 3.6.3 relevant material fracture data must be known. This is in many cases not a trivial task since more than 25 years may have passed since manufacture. In the analysis performed on selected piping it has been necessary to attempt to reconstitute basic data such as true stress-strain curves and fracture mechanics properties. In those cases base and welding material of the same standard specification is still being produced and when the original welding procedure is available new test samples can be fabricated and tested. Differences between heats and differences in the execution of the welding procedure can be taken into account by using data conservatively. If material of the original standard specification is not available it may be necessary to re-manufacture material for testing purposes.

An investigation of the J-R curves for steel used in recirculation piping has been done using refabricated material. Charpy testing has given impact data equivalent with actual pipe material data. Fracture mechanical testing has shown that the weld material has a toughness on the same level as the base material. A comparison with equivalent ASME materials indicates that this testing method can be justified.

If material data can not be certified there is the option of replacing part of the piping system, such as welds, or of course to replace the whole piping system. In that case LBB can be designed and manufactured into the system.

The plant leakage detection systems should also be subject to review and assessment. Normally these are based on the provisions of U.S. NRC Regulatory Guide 1.45. It may be a feasible option to upgrade these systems to get a higher detection sensitivity thereby getting the possibility of including more piping systems under the LBB criteria.

CONCLUSIONS

There is potentially a big need for LBB in Swedish BWR designs. This is particularly important for first-generation plants which lack protective devices against pipe break dynamic effects. The potential sensitivity to cracking of stainless steels in BWR environments need not be a deterrent as stress corrosion cracking is a slow process which does not act on the same scale as other crack propagation mechanisms relevant to the LBB analysis. The application of the LBB concept has been tentatively applied to selected primary systems in operating plants with good results.

A LEAK-BEFORE-BREAK STRATEGY FOR PRIMARY HEAT TRANSPORT PIPING OF 500 MWe INDIAN PHWR

J.Chattopadhyay, B.K.Dutta H.S.Kushwaha,S.C.Mahajan & A.Kakodkar
Reactor Design and Development Group
Bhabha Atomic Research Centre
Trombay, Bombay - 400085, India

ABSTRACT

The concept of Leak-Before-Break (LBB) is being used to design the primary heat transport piping system of 500 MWe Indian Pressurised Heavy Water Reactors (IPHWR). The work is categorised in three directions to demonstrate three levels of safety against sudden catastrophic break. Level 1 is inherent in the design procedure of piping system as per ASME Sec.III with a well defined factor of safety. Level 2 consists of fatigue crack growth study of a postulated part-through flaw at the inside surface of pipes. Level 3 consists of stability analysis of a postulated leakage size flaw under the maximum credible loading condition. Developmental work related to demonstration of level 2 and level 3 confidence is described in this paper. In a typical case study on fatigue crack growth on PHT straight pipes for level 2 of LBB, negligible amount of crack growth is predicted for the entire life period of the reactor. Regarding level 3 analysis of LBB, R6 method has been adopted. While the necessary inputs for the application of R6 method for straight pipes are easily available in literature, the same cannot be said for elbows and tees. A database to evaluate SIF of elbows with throughwall flaws under combined internal pressure and bending moment has been generated. This database will provide one of the inputs for R6 method. The methodology of safety assessment of elbow using R6 method has been demonstrated for a typical pump discharge elbow. In this analysis, limit load of the cracked elbow has been determined by carrying out elasto-plastic finite element analysis. The limit load results compared well with those given by Miller [14]. However, it requires further study to give a general form of limit load solution. On the experimental front, a set of small diameter pipe fracture experiments have been carried out at room temperature and 300°C.Two important observations of the experiments are - appreciable drop in maximum load at 300°C in case of SS pipes and out-of-plane crack growth in case of CS pipes. Experimental load deflection curves are finally compared with five J-estimation schemes predictions. A material database of PHT piping materials is also being generated for use in LBB analysis.

A LEAK-BEFORE-BREAK STRATEGY FOR PRIMARY HEAT TRANSPORT PIPING OF 500 MWe INDIAN PHWR

J.Chattopadhyay, B.K.Dutta H.S.Kushwaha,S.C.Mahajan & A.Kakodkar
Reactor Design and Development Group
Bhabha Atomic Research Centre
Trombay, Bombay - 400085, India

INTRODUCTION

The primary heat transport piping system of 500MWe Indian pressurised heavy water reactors (IPHWR) is made of ductile carbon steel of ASTM grade A333 Gr6 and is designed as per ASME Sec.III NB Boiler and Pressure Vessel code. It is installed and maintained as per stringent specifications due to economic and safety reasons.One of the design basis accidents considered during design of this piping system is double ended guillotine break (DEGB) of the largest heat transport pipe. Besides considering the pipe whip arising out of this postulated break,one has to also consider the secondary effects such as jet impingement and reaction forces in the design of piping and mechanical components. This has led in the past to the installation of a large number of pipe whip restraints and jet impingement barriers. However pipe whip restraints hamper access for in-service inspection and, if incorrectly installed, can lead to a significant increase in piping loads. Therefore, in the recent years, leak-before-break (LBB) approach is being applied for reactor PHT piping system as an alternative provision of pipe whip restraints.This application will lead to the elimination of pipe whip restraints and will ensure simplified layout, easy access for in-service inspection and no unaccounted stresses. The application of LBB is further supported by different leak monitoring systems, namely, D_2O tank level indication, vapour recovery system and beetles, in IPHWR.

LBB STRATEGY ADOPTED FOR IPHWR

The developmental work associated with the implementation of LBB to IPHWR PHT piping was started few years back [1]. The work is categorised in three directions to demonstrate three levels of safety against DEGB [2,3]. Level 1 is inherent in the design philosophy of PHT piping system, which is implemented using ASME Sec.III with a well defined factor of safety. However, this design procedure does not consider the presence of a reference flaw. The demonstration of level 2 confidence consists of postulating a part-through flaw on the inside surface at various locations of the piping system and to show its insignificant growth during the entire design life period under the fatigue loads associated with postulated service level A/B transients. Demonstration of level 3 confidence consists of postulating a throughwall flaw at highly stressed and welds locations of the piping system and prove its stability under the maximum credible loading condition. The size of the flaw is based on leak detection capability in the plants.

DEVELOPMENTAL WORK RELATED TO DEMONSTRATION OF LEVEL 2 CONFIDENCE

As described above, one has to deal with fatigue crack growth of part-through crack in different pipes in level 2 analysis. The following methodology is adopted for evaluation of part-through flaw [4] :

(1) Postulate a part-through flaw at weld/high stress locations of the piping system.
(2) Perform a sub-critical fatigue crack growth analysis to predict the increased flaw size, keeping the aspect ratio constant.
(3) Identify the appropriate failure mode for the material e.g. brittle fracture, ductile tearing or plastic collapse. Then depending on the failure mode, choose the appropriate analysis procedure among LEFM, EPFM and limit load theory.
(4) Find out allowable size with proper factor of safety using the appropriate analysis procedure and check acceptability of final flaw size.

This methodology has been applied to a number of straight pipes in PHT piping system [5]. In this analysis, both circumferential and axial flaw are considered. An initial flaw depth equal to 25% of pipe thickness and length equal to six times the depth has been postulated. This initial flaw size has been taken as stipulated in ASME Sec.III Appendix G [6] with a high degree of conservatism in the absence of detailed non-destructive test report. The crack is postulated at the inside surface of the PHT pipe.

The loads considered in the fatigue analysis are membrane load due to internal pressure and bending load due to thermal expansion, earthquake and non-linear temperature gradient across the pipe thickness. Table 1 shows the postulated transient events for 500 MWe IPHWR during the entire life period of the reactor.

Once the initial crack length and loads are known, fatigue crack growth calculations are done using the modified Paris power law equation as given in ASME Sec.XI [7]. In the fatigue crack growth calculation, flaw aspect ratio has been kept constant at 6:1. Subsequently the final flaw size has been found to be less than the allowable flaw size under the given loading condition. Allowable flaw size is determined by one of the three analysis methods, namely, LEFM, EPFM and limit load theory. The method is identified using a screening criterion [4] based on failure assessment diagram.Table 2 shows fatigue crack growth calculations of circumferential flaws on different pipe lines, namely, steam generator inlet (SGI) line, steam generator outlet (SGO) line, pump discharge line (PDL), reactor inlet header (RIH) and reactor outlet header (ROH). The same methodology is being adopted to calculate fatigue crack growth of postulated part-through flaws in elbows and tees. One of the difficulties in such analysis is the unavailability of analytical expression for Stress Intensity Factor (SIF) for various crack orientations and sizes. Due to this, it has been decided to perform finite element analysis of

Table 1 Postulated Transient Events

Serial No.	Transient Events	No. of Cycles
1	Operating Basis Erq.(OBE)	50
2	Heat up from Cold Shutdown (CSD) to Hot Stand-by (HSB)	1000
3	Start up from HSB to 100% Power	3500
4	Power Maneuvering at 100% Power	15000

Table 2 Fatigue Crack Growth of Circumferential Flaw at Different PHT Pipe Lines

PHT Pipe Line	Initial a/t (%)	Final a/t (%)	Allowable Flaw Depth [7]	
			Analysis Procedure	a/t (%)
SGI	25	27.26	EPFM	75
SGO	25	25.16	EPFM	75
PDL	25	25.37	EPFM	75
RIH	25	25.58	EPFM	75
ROH	25	25.61	EPFM	75

elbows and tees with part-through crack to evaluate SIF. However, preliminary calculations are based on Newman-Raju [8] SIF expression.

DEVELOPMENTAL WORK RELATED TO DEMONSTRATION OF LEVEL 3 CONFIDENCE

As mentioned earlier, level 3 analysis consists of stability analysis of a leakage size throughwall flaw under the maximum credible loading condition. To carry out such calculations, the first requirement is to develop a computer code which can correlate the leak rate with the flaw size under a given thermodynamic and mechanical condition. To accomplish this, a code **'LEAK'** has been developed [1] which adopts two phase critical flow based on Homogeneous Frozen Model (HFM) [3,9]. This is compatible with fluid and geometry conditions prevailing in leakage of sub-cooled liquid through cracks in PHT piping. The model assumes that average velocity of the two phase remain in thermodynamic equilibrium up to the end of crack but phase change is frozen at crack exit plane. The code also models the flow path friction. Originally, the flow path will be a zig zag crack across the thickness of the pipe. However, since it is very difficult to anticipate the crack path in advance, flow path has been assumed to be straight, with path length equal to the pipe thickness. Paris-Tada equation [10] with Irwin's plastic zone correction is

used to calculate crack opening area in straight pipes. The code has been verified for a circumferential cracked pipe under internal pressure and bending moment against the results quoted in [3]. Fig.1 shows the comparison. In case of other piping geometries e.g. elbows and tees, mass flux is being evaluated by the code 'LEAK' and crack opening area is being determined through finite element analysis.

Regarding stability analysis, 500 MWe PHT piping system comprises of straight pipes, elbows and tees. The most versatile method consists of calculation of applied J integral by elastoplastic finite element technique and comparing the same with the J-R curve of the material. However, this procedure requires expertise and large computation time. As an alternative, the stability analysis of throughwall cracked straight pipe can be easily performed using different J-estimation schemes such as GE/EPRI, LBB.NRC, Paris-Tada and LBB.BCL1 and LBB.BCL2 methods. A preliminary calculation has been done [11] for 610 mm suction line using these estimation schemes. The same approach is being followed for other PHT pipe lines. One of the limitations of these estimation schemes are their inability to consider crack face loadings. Figs.2,3 and 4 show the importance of crack face loading on SIF for straight pipes with different shell parameters, dominantly under internal pressure. It may also be noted here that similar estimation schemes are not available for elbows and tees.

To overcome these difficulties, the other simple and reliable alternative methodology ,which can be adopted for level 3 calculations, is the R6 method. The R6 method requires four inputs to evaluate the assessment points for a structure. These are SIF, material fracture toughness, applied load and the limit load of structure at plastic collapse. Out of these four inputs, fracture toughness is a material property and the applied load is known from the design analysis. However, the other two parameters, namely, SIF and limit load at plastic collapse are geometry dependent and vary with crack size. While the equations of SIF and limit load of straight pipe with different crack orientations under various types of loading conditions are well documented in open literature [12], the same is not true for elbows and tees. Finite element method is being used to calculate SIF and limit load for these geometries.

As a first step towards this purpose, a database has been generated by the authors to evaluate SIF of elbows with throughwall flaws under combined internal pressure and bending moment [13]. SIF is expressed as:

$$A_e = K_{mid} / \sigma_r \sqrt{(\pi a)}, \qquad \sigma_r = M/\pi r^2 t + pr/2t$$

where K_{mid} is the SIF at mid-surface, r is the mean radius of pipe, t is the thickness, M is the applied bending moment and p is the internal pressure.

Three parameters are chosen to characterise a cracked elbow, namely, the pipe factor ($h=tR/r^2$), r/t and the crack length. Another parameter (ρ) is selected to consider the relative magnitude of stress due to internal pressure and bending moment.

It is expressed as, $\rho = 2/\pi . (M/pr^3)$. A_e is expressed in terms of these parameters. Figs.5 and 6 show the elbow geometry and a sample database.

To determine other input for R6 method, namely, limit load, a study has also been performed on an elbow with a throughwall circumferential flaw at the extrados under bending moment [14] Fig.7 shows the moment rotation curve for circumferential crack angles, $2\psi_c = 90^\circ$, 140° and 180°. Limit moments are then evaluated by twice elastic slope method. The limit moment of a cracked elbow is then normalised with that of a healthy elbow. If an equation of the form $M_l/M_o = 1-C(\psi_c/\pi)$ is fitted to the above results, the average value of 'C' works out to be 1.52 which is very close to the value of C=1.5 suggested in [15]. Finally safety assessment of a pump discharge elbow of 500 MWe PHT piping system has been carried out using R6 option 2 method. A sensitivity study is also performed to study the effect of different parameters,namely, crack length, load and material fracture toughness on the safety of the component. Fig.8 shows the locus of assessment points. In another related study [16],collapse moment of pump discharge elbow with various longitudinal crack sizes at crown under combined internal pressure and bending moment has been evaluated. The future thrust of this work will be to develop a similar methodology for branch tees. As a first step, limit load of healthy ROH branch tee under internal pressure has been evaluated by FEM which compared well with reported experimental value.

EXPERIMENTAL PROGRAM IN SUPPORT OF LBB ANALYSIS

Parallel to the analytical work, an experimental program has also been undertaken to support and validate some of the analytical tools which are used in LBB analysis. Elasto-plastic Fracture Mechanics (EPFM) is one domain where a number of uncertainties prevail, which are to be addressed and understood through experiments. Since, LBB is applied to PHT piping of nuclear power plants, the relevant components are straight pipes, elbows and branch tees. Keeping these in view, a set of pipe fracture experiments have been carried out to understand the fracture characteristics of straight pipes with a circumferential crack under bending moment and also to compare the different analytical predictions of load vs. load-line deflection [17].

Experiments have been performed on small diameter (OD=60.5 mm) carbon steel (CS), SA106GrB and stainless steel (SS 316) pipes with various sizes of throughwall circumferential cracks under 4 point bending load on MTS m/c. Two sets of experiment- each set consisting of 4 CS pipes and 4 SS pipes, have been carried out. One set is done at room temperature and the other set at reactor operating temperature 300°C. Pipes are fatigue pre-cracked to have sharp crack tip. Subsequently, these are subjected to displacement controlled 4 point bending load on MTS m/c. Three parameters, namely, load, load-line displacement and crack mouth opening displacement (CMOD) have been continuously monitored during experiments. Figs.9 and 10 show typical load deflection curves of

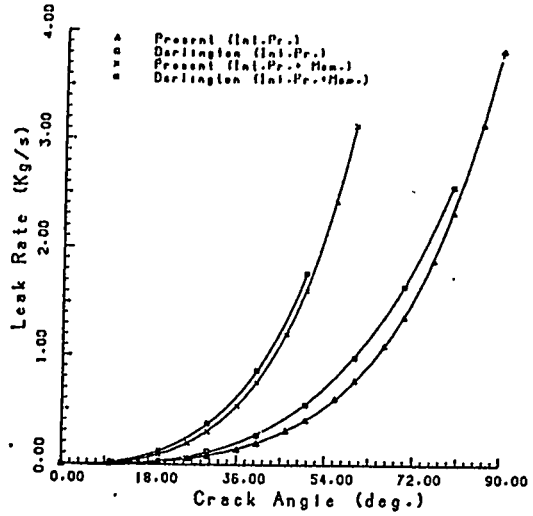

Fig.1 Leak rate variation with crack sizes, a comparison

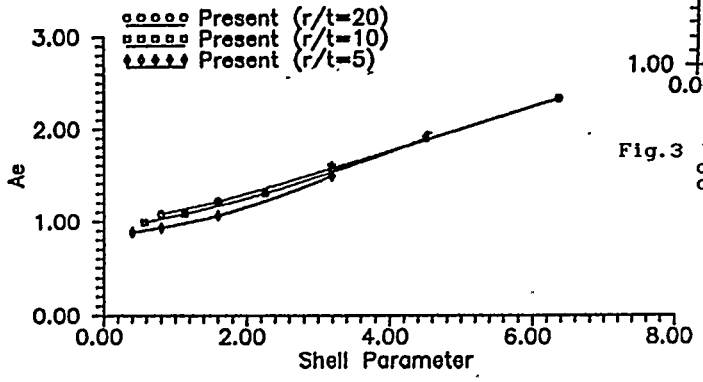

Fig.4 Variation of Ae with shell parameter for circumferentially cracked st.pipe (no crack face loading)

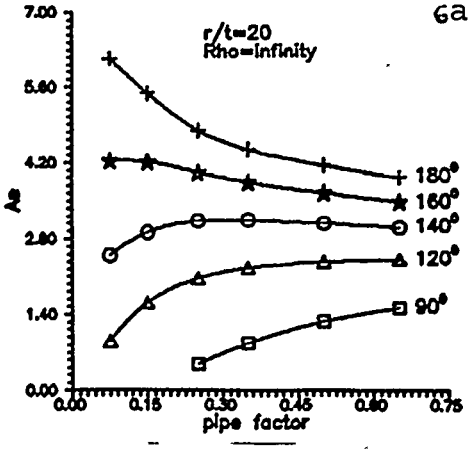

Fig.6 Sample database of SIF of elbow with a) circumferential b) longitudinal throughwall crack

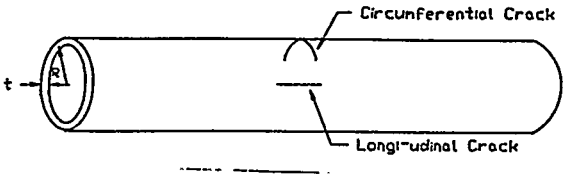

Fig.2 Locations of various postulated cracks on straight pipe

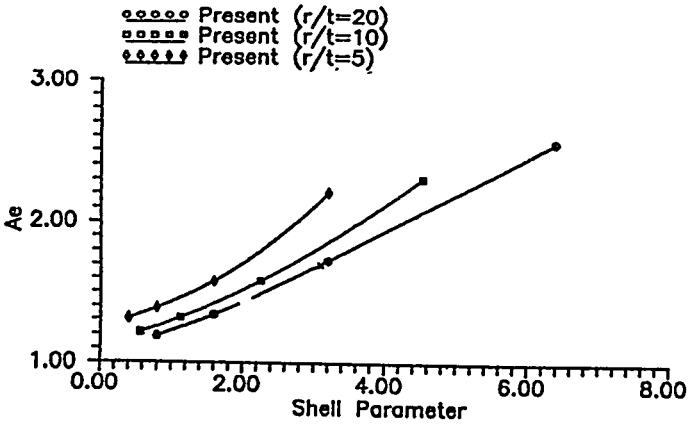

Fig.3 Variation of Ae with shell parameter for circumferentially cracked st.pipe (with crack face loading)

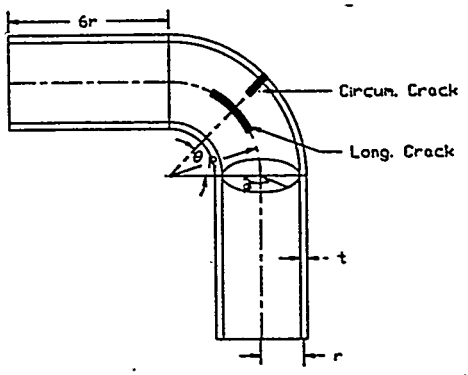

Fig.5 Locations of various postulated cracks on elbow

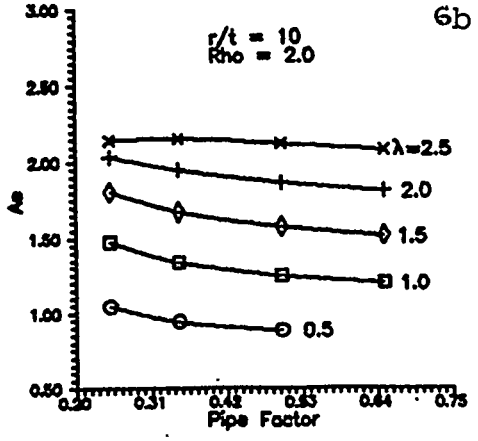

CS and SS pipe at room temperature and 300°C. Appreciable drop in maximum load may be observed in case of SS pipe. The experimental load deflection curve is compared with the analytical predictions by GE/EPRI, Paris-Tada, LBB.NRC, LBB.BCL1 and LBB.BCL2 methods. Fig.11 shows a typical comparison up to the maximum load. One interesting feature, observed during experiment is out-of-plane crack growth in case of CS pipes which has been reported in [18] also. Fig.12, 13 and 14 show the photographs of experimental set-up, out-of-plane and in-plane crack growth of CS and SS pipes respectively. A similar set of experiment is planned on large diameter pipes to study the effect of triaxiality on instability.

In another experiment [19], equal diameter (410 mm) PHT header tee junction was subjected to low cycle fatigue. The maximum crack depth of 30 mm was observed after 40000 cycles on the outer surface at the tee junction. Further studies are being planned to demonstrate LBB. Finally, a material database of PHT piping materials is also being generated for use in LBB analysis.

DISCUSSION AND CONCLUSIONS

Developmental work related to demonstration of level 2 and level 3 confidence is described in this paper. In a typical case study on PHT straight pipes for level 2 of LBB, negligible amount of fatigue crack growth is predicted for the entire life period of the reactor. The similar calculations will be done in future for other piping components e.g. elbows and tees. Regarding level 3 analysis of LBB, R6 method has been adopted. While the necessary inputs for the application of R6 method for straight pipes are easily available in literature, the same cannot be said for elbows and tees. A database to evaluate SIF of elbows with throughwall flaws under combined internal pressure and bending moment has been generated. This database will provide one of the inputs for R6 method. The methodology of safety assessment of elbow using R6 method has been demonstrated for a typical pump discharge elbow. In this analysis, limit load of the cracked elbow has been determined by carrying out elasto-plastic finite element analysis. The limit load results compared well with those given by Miller [15]. However, it requires further study to give a general form of limit load solution. Same approach will be adopted for branch tees also. Finally, a set of small diameter pipe fracture experiments have been carried out at room temperature and reactor operating temperature. Two important observations of the experiments are - appreciable drop in maximum load at 300°C in case of SS pipes and out-of-plane crack growth in case of CS pipes. Experimental load deflection curves are finally compared with five J-estimation schemes predictions.

ACKNOWLEDGEMENT

The authors express their thanks to Dr.S.Banerjee and Dr.J.K.Chakravarty, Metallurgy Divn.,BARC for continuous involvement to conduct the pipe fracture experiments in their laboratory.

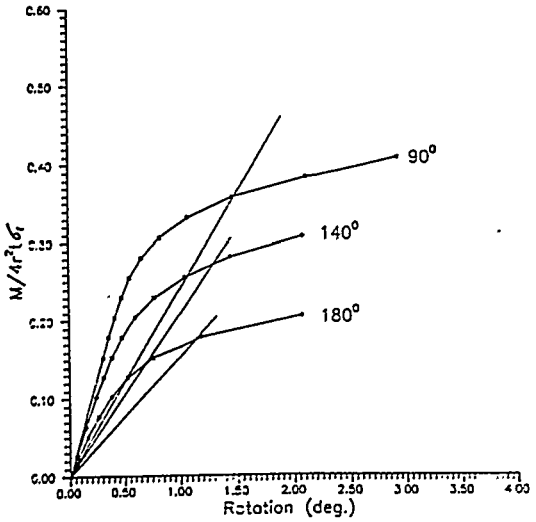

Fig.7 Moment rotation curves of pump discharge elbow with various cracks

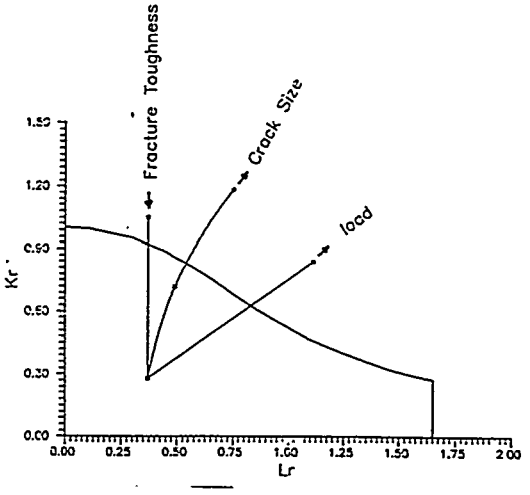

Fig.8 Assessment points on the failure assessment diagram for various parameters of pump discharge elbow

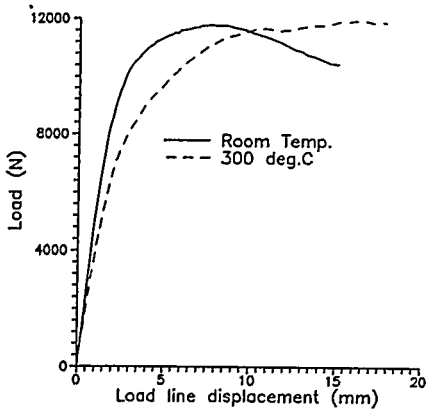

Fig.9 Typical comparison of load deflection curve of CS pipe at room temp. and 300 deg.C

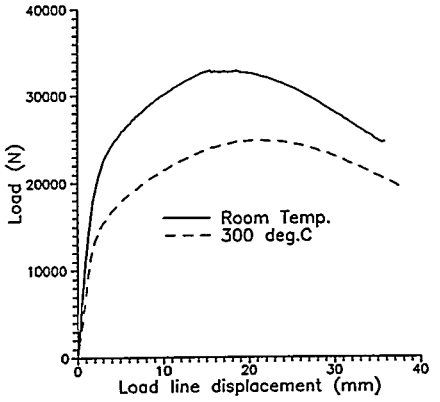

Fig.10 Typical comparison of load deflection curve of SS pipe at room temp. and 300 deg.C

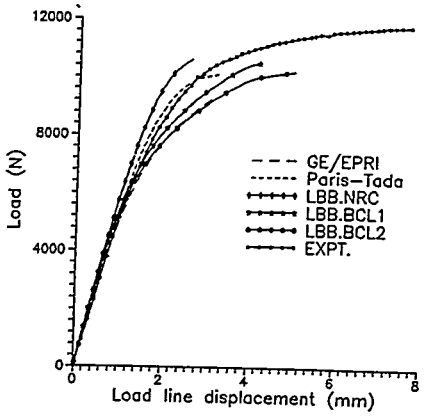

Fig.11 Typical comparison between experimental and predicted load deflection curves for CS pipe

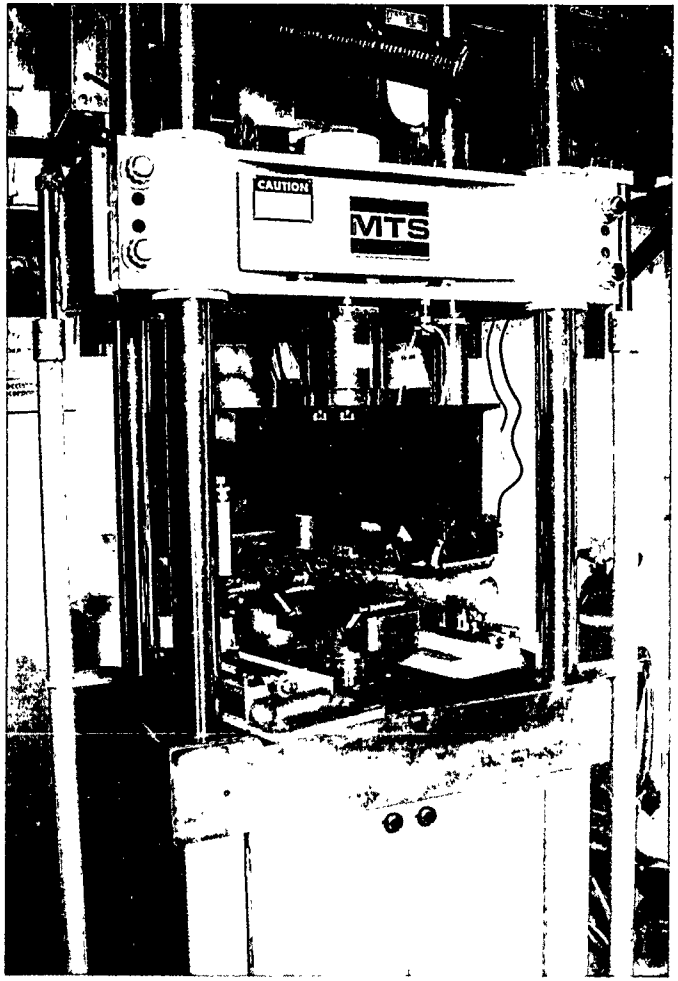

Fig.12 Photograph of the experimental set up

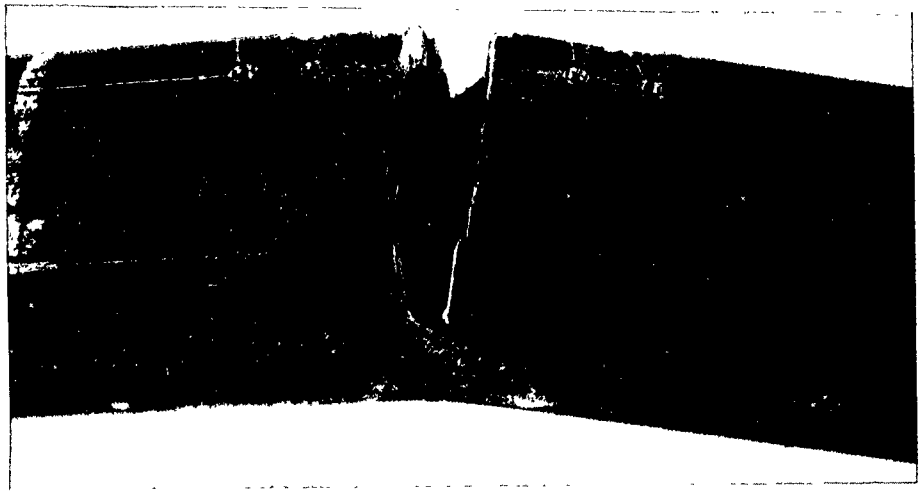

Fig.13 Out-of-plane crack growth in CS pipe

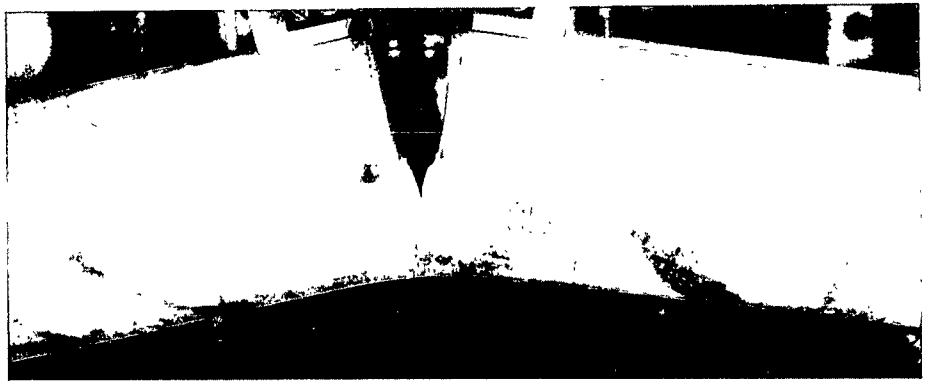

Fig.14 In-plane crack growth in SS pipe

REFERENCES

1) Chattopadhyay,J.,Dutta,B.K.& Kushwaha,H.S., Application of Leak-Before-Break Concept in the Design of High Temperature and High Pressure Primary Heat Transport Piping, *BARC External Report,* BARC/1992/E/033, 1992
2) Report of the U.S.Nuclear Regulatory Commission Piping Review Committee, *Evaluation of Potential for Pipe Breaks*, Prepared by the Pipe Break Task Group, NUREG-1061, Vol.3, 1984
3) Kee,B.L.& Nathwani,J.S.,Darlington NGS A Leak-Before-Break Approach for Large Diameter Heat Transport Piping,*Design and Development Report,*1985
4) *Evaluation of Flaws in Ferritic Piping*, EPRI-NP-6045, prepared by Novtech Corporation, 1988
5) Chattopadhyay,J., Dutta,B.K. & Kushwaha,H.S., Fatigue Crack Growth Studies on Primary Heat Transport Piping, *Workshop on Creep,Fatigue and Creep-Fatigue Interaction*, IGCAR,India,1995
6) ASME Sec.III,*Boiler and Pressure Vessel Code*, Appendix G,1992
7) ASME Sec.XI, *Boiler and Pressure Vessel Code,* 1992
8) Newman,J.C.,Jr.& Raju,I.S., *Engg. Fracture Mechanics,* **15**, 1981
9) Henry,R.E., The Two-Phase Critical Discharge of Initially Saturated or Subcooled Liquid,*Nuclear Science & Engg.*,**41**,1970
10) Paris,P.C. & Tada,H., NUREG/CR-3464,1983
11) Viswanathan,N., Mahanty,D.K. & Kushwaha,H.S., Stability Analysis of Throughwall Cracked PHT Pipe 500 MWe PHWR -Part I, *BARC External Report*, BARC/1994/E/011, 1994
12) Kumar,V., et al., EPRI-NP-3607, 1984
13) Chattopadhyay,J., Dutta,B.K., Kushwaha,H.S., Mahajan,S.C. & Kakodkar,A., A Database to Evaluate Stress Intensity Factors of Elbows with Throughwall Flaws Under Combined Internal Pressure and Bending Moment, *Int. J. Pres. Ves. & Piping*, **60**, 1994
14) Chattopadhyay,J., Dutta,B.K., Kushwaha,H.S., Mahajan,S.C. & Kakodkar,A.,Limit Load Analysis and Safety Assessment of an Elbow with a Circumferential Crack under Bending Moment, *Int. J. Pres. Ves. & Piping,* **62**, 1995
15) Miller,A.G., *Int. J. Pres. Ves. & Piping,* **32**, 1988
16) Bhattacharya,A., Kushwaha,H.S. & Mahajan,S.C., Collapse Characteristics of PHT Pump Discharge Elbow of an Indian PHWR, To be published in SMiRT 13, 1995
17) Chattopadhyay,J., Analytical and Experimental Studies on Leak-Before-Break, *Master of Technology Dissertation,* Indian Institute of Technology, Bombay, India, 1995
18) Wilkowski, G.M., et al., *Degraded Piping Program Phase II,* Battelle Columbus Laboratories, NUREG/CR-4082, Vol.3, 1986
19) Seetharaman,S., et al.,Fatigue and Crack Growth Studies on a Tee Junction, SERC, Madras, India, 1995

LBB IN CANDU PLANTS

M.J. Kozluk *and* D.K. Vijay
Nuclear Technology Services Division, Ontario Hydro Nuclear
Toronto, Ontario, Canada

Postulated catastrophic rupture of high-energy piping systems is the fundamental criterion used for the safety design basis of both light and heavy water nuclear generating stations. Historically, the criterion has been applied by assuming a *nonmechanistic* instantaneous double-ended guillotine rupture of the largest diameter pipes inside of containment. *Nonmechanistic*, meaning that the assumption of an instantaneous guillotine rupture has not been based on stresses in the pipe, failure mechanisms, toughness of the piping material, nor the dynamics of the ruptured pipe ends as they separate. This postulated instantaneous double-ended guillotine rupture of a pipe was a convenient simplifying assumption that resulted in a conservative accident scenario. This conservative accident scenario has now become entrenched as the design basis accident for: containment design, shutdown system design, emergency fuel cooling systems design, and to establish environmental qualification temperature and pressure conditions. The requirement to address *dynamic* effects associated with the postulated pipe rupture subsequently evolved. The *dynamic* effects include: potential missiles, pipe whipping, blowdown jets, and thermal-hydraulic transients.

Recent advances in fracture mechanics research have demonstrated that certain pipes under specific conditions cannot crack in ways that result in an instantaneous guillotine rupture. Canadian utilities are now using *mechanistic* fracture mechanics and leak-before-break assessments on a case-by-case basis, in limited applications, to support licensing cases which seek exemption from the need to consider the various *dynamic* effects associated with postulated instantaneous catastrophic rupture of high-energy piping systems inside and outside of containment.

WHAT IS LEAK-BEFORE-BREAK?

The term leak-before-break has been used in reference to a myriad of pressure retaining components. In this paper, the term is used in the context of nuclear power plant piping. In this context, the premise of leak-before-break is that the materials used are sufficiently tough (ductile) that small through-wall cracks resulting in coolant leak rates well in excess of those detectable

by installed leak detection systems would remain stable and not result in a double-ended guillotine break or equivalent rupture. The elements of leak-before-break are:

- exclusion of active failure mechanisms,
- adequate ductility in the piping material and welds,
- leakage detection capability,
- adequate time for safe shutdown,
- stability of large through-wall cracks.

A leak-before-break assessment is a mechanistic application of fracture mechanics which considers all of the potential failure mechanisms, the piping design loads (both normal and extreme loadings), installed leak detection capabilities, the geometry of the postulated crack, and the material properties of the piping. The objective of the assessment is to quantify the margins that are available between detectable through-wall cracks and idealized cracks that are at the point of instability. These margins are quantified with respect to: material properties, piping loads, crack size, and leak detection capabilities. If the margins are large enough, it can be concluded that the specific pipe rupture is incredible. It is then argued that it is not necessary to consider the *dynamic* effects associated with the postulated pipe ruptures. That is, it is justifiable to eliminate the need for devices (barriers/restraints) designed to deal with the dynamic effects of a full flow area rupture of the pipe. (Dynamic effects include: pipe whip, pipe break reaction forces, jet impingement forces, decompression waves within the ruptured pipe, and pressurization in cavities and compartments).

THE CANADIAN LICENSING ENVIRONMENT

Requirements for piping and pressure vessels in Canadian CANDU reactors are spelled out in a number of codes and standards, adherence to which is enforced by both provincial and federal authorities. Enforcement is done directly by inspection or indirectly by requesting evidence which would positively prove the adherence.

In the province of Ontario, the Boilers and Pressure Vessels Act and its attached Regulations is the statute applying to conventional boilers, pressure vessels, and plants. The Inspection Branch of the Ministry of Consumer and Commercial Relations (MCCR) is responsible for safety of boilers, pressure vessels, and plants. This Act, which outlines the basic rules and regulations only, stipulates that the MCCR Chief Inspector and Inspectors in carrying out their duties refer to Canadian Standards Association (CSA) and American Society of Mechanical Engineers (ASME) publications. Their duties under the Act are in reference to the approval of designs, the fabrication, installation, inspection, testing, operation, and use of boilers, pressure vessels, and plants. The principal codes and standards that are applicable to the nuclear piping systems are the Canadian Standards Association N-series of standards and the ASME Boiler and Pressure Vessel Code.

In Canada, the Atomic Energy Control Act and the Regulations made thereunder stipulate in very broad terms the powers of the Atomic Energy Control Board and the requirements to be fulfilled by licensees. The licensing approach taken in Canada is based on the principle that the primary responsibility for safety lies with the utility. The regulator determines whether this has been achieved to their satisfaction. In this licensing framework, the Atomic Energy Control Board issues only limited regulations. Reference [1] describes the general approach taken in Canada for analyzing and limiting the consequences of the postulated pipe rupture to containment, shutdown systems, and emergency core cooling systems.

ONTARIO HYDRO'S LEAK-BEFORE-BREAK APPROACH

In the mid-1980s, Ontario Hydro pursued the application of leak-before-break to the primary heat transport piping for a Canadian (CANDU) reactor. During the design and construction phase of Darlington NGS, Ontario Hydro realised that it was not possible to design and install pipe-whip restraints and impingement barriers that would guarantee protection from all of the postulated breaks of the heat transport piping. Ontario Hydro entered into discussions with the Atomic Energy Control Board of Canada on the potential use of a leak-before-break philosophy to preclude the installation of pipe-whip restraints for the postulated ruptures of the large diameter (21",22",24") heat transport piping inside containment. The outcome of these discussions was an agreement in principle for the limited use of leak-before-break. The principal caveats placed on the use of leak-before-break were it could only be used for those breaks:

- where the provision of pipe-whip restraints is impractical,
- which would not lead to a failure of the containment boundary or either of the two fast acting safety shutdown systems,
- which would not disrupt emergency coolant injection to both sides of the core.

The leak-before-break approach as applied to the Darlington nuclear generating station, is a conditional design alternative to the provision of pipe-whip restraints on large diameter primary heat transport system piping. Its application resulted in significant cost savings to Ontario Hydro. The remainder of this section briefly describes the salient features of this leak-before-break approach; for more specific details of the approach the reader is directed to References [2-8].

The Darlington Nuclear Generating Station: is the latest of Ontario Hydro's nuclear generating facilities. Darlington NGS is comprised of four identical CANDU units, each having a capacity of 881 MW(net). The station containment envelope comprises the four reactor vaults, the fuelling duct which runs the full length of the station and connects the fuel handling and service areas, the fuelling machine head removal area, the pressure relief duct, the pressure relief valve manifold, and the vacuum building. The lay out and design of the reactor building adopted for Darlington incorporates a number of features which result in reduced capital cost and

construction time, improved maintenance arrangements, and lower heavy water upgrading requirements. The reactor unit containment envelope encloses only those components and systems which cannot safely be located outside the containment boundary or which are so closely associated with the reactor and the coolant that they need to be located inside. The reactor containment vault has a rectangular shape and consists of reinforced-concrete floors supported by reinforced-concrete walls. The reactor vault structure is divided vertically into two areas: the fuelling duct and basement in the area below grade and the reactor vault which houses the reactor, primary piping in the heat transport system and the heat transport pump and the primary head of the steam generators.

The main heat transport circuit of each unit has a volume of 230m^3 (8,200 ft^3), is configured in two loops, and includes:

- 480 horizontal, reactor fuel channels with 960 feeder pipes.
- 4 vertical steam generators. Each has 4,663 U-tubes fabricated from 0.625" Inconel 600 tubing with a nominal wall thickness of 0.0445".
- 4 electric motor driven circulating pumps.
- 4 reactor inlet headers and 4 reactor outlet headers.
- interconnecting carbon steel piping. The smallest are the feeder (1½"-3½" schedule 80) pipes and the largest is the 24" schedule 100 pump suction pipe.

In addition to the main heat transport circuit described above, the heat transport system includes the following equipment and auxiliary systems outside containment: the steam generators, heat transport pump motors, purification circuit, pressure and inventory control, heat transport pump gland seal system, shutdown cooling system, and the autoclave circuit.

Systematic LBB Review: At the outset, Ontario Hydro undertook an extensive, systematic review to address all factors that could have an impact on the validity of leak-before-break as applied to the large diameter (21", 22", 24") primary heat transport piping of Darlington NGS. The objective of this evaluation was the formulation of a rational and comprehensive leak-before-break approach that would then be applied to the large diameter heat transport piping of Darlington NGS. The following are the key review activities that were initiated:

- A review of the leak-before-break approaches used in other jurisdictions.
- A critical review of potential for any failure mechanism known to affect piping systems and of the welding fabrication, installation, and pre-service/in-service inspection procedures used for the heat transport circuit.
- A critical review of the capability of installed leak detection systems.
- Development and validation of a leak rate model, appropriate for heavy water and the range of crack sizes being postulated in the leak-before-break assessments.

- Acquisition and validation of state-of-the-art elastic-plastic fracture mechanics stability assessments for cracks in all piping components used in the heat transport piping system.

- A critical review of all of the operating transients and accident scenarios for the heat transport circuit.

- A test program to characterize the material properties of all heats of piping steel and all welding procedures used in the large diameter heat transport piping. All heat transport piping is fabricated from seamless SA106 Grade B carbon steel piping and forged components are fabricated from SA105 carbon steel.

The results of these systematic reviews were used to arrive at the leak-before-break approach adopted by Ontario Hydro for Darlington NGS. The following provides a brief review of the key task group findings.

Other Licensing Approaches: At the time of the review, only two approaches had been established: Germany's *Basis Safety* approach and the approach recommended by the US-NRC Piping Review Committee. Elements from both approaches were considered in the approach adopted by Ontario Hydro.

Failure Mechanisms: It was concluded that all potential failure mechanisms of the primary heat transport piping are adequately addressed in the design requirements, commissioning program, operating procedures, and inspection programs. Fatigue mechanism identified as having a potential to be active in the large diameter heat transport piping. That is, there are no failure mechanisms that would challenge the implicit assumptions of leak-before-break. Modifications were made to the in-service inspection program in the area of erosion and corrosion to ensure the continued validity of this conclusion.

Inaugural Inspection: The primary heat transport system is designed and fabricated to meet the ASME Boiler and Pressure Vessel Code requirements for Class 1 piping. Volumetric examination, using radiography, is required for all welds in Class 1 piping systems. In addition, an inaugural inspection was performed of all heat transport piping welds in piping greater than 6" in size. The method of inspection was ultrasonics and this inspection was performed primarily to establish base line measurements for the in-service inspection program.

In-service Inspection: The role of the in-service inspection program, in the context of leak-before-break, is to ensure (verify) that the heat transport piping is not subject to degradation mechanism(s) which would challenge the assumptions used in the leak-before-break assessments.

Leak Detection: The Darlington generating station operating procedures require immediate shutdown of the reactor at confirmed leakage rates of 0.5 kg/second (8 Usgpm) from the heat transport system. Installed leak detection systems can reliably detect leak rates that are more than two orders of magnitude lower than this limit. This immediate shutdown action limit is self-imposed and is based on stringent emission limits for tritium and the economic penalties associated with lost or downgraded heavy water. No modifications to existing systems used to detect leakage from the heat transport system were required to support the application of leak-before-break. However, operating procedures and checks with respect to leak detection were formalized to support the application of leak-before-break.

Note, the time to detection does not enter into the leak-before-break assessment. Rather, the time from detection/confirmation of a specific leakage rate to shutdown is specified in plant operational procedures.

Leak Rate Model: The leak rate model employed for sizing the length of the through-wall (either axial or circumferential) crack that would leak at the immediate shutdown action limit is described in Reference [7]. The code uses a homogeneous frozen model applied at the choking plane or throat for estimating the critical mass flux. The thermal-hydraulic conditions at the throat are determined, by solving the one-dimensional mass and momentum equations, based on the homogeneous two-phase flow model. The flow-path is "nodalized" and a double-iterative solution technique applied until convergence is obtained on both the fluid exit pressure at each node, and the discharge mass flux at the crack exit plane. The leak rate model was validated against published and in-house experimental results.

Fracture Mechanics Evaluation: Ontario Hydro adopted the approach for demonstrating the structural integrity of piping system originally recommended by the US-NRC Piping Review Committee in Volume 3 of NUREG-1061. The fracture mechanics evaluation of piping involves five distinct steps:

(1) Demonstrate that the piping system meets all design requirements.

(2) Postulate the largest credible surface flaw in the piping component.

(3) Perform a fatigue analysis of the surface flaw specified in step (2). The purpose of the analysis is to demonstrate that the surface flaw will not grow through the pipe wall during the design service life of the piping system.

(4) Postulate a detectable through-wall (leaking) crack in the piping component. The size (length) of the through-wall crack should be such that the calculated leakage rate of fluids discharged from the crack under normal operating loads are equal to the immediate shutdown action limit.

(5) Perform an elastic-plastic fracture mechanics assessment to demonstrate that adequate margins exist against the onset of unstable crack extension. The minimum margins which must be meet are two on the size (length) of the through-wall crack and square root of two on the extreme piping loads.

For application to Darlington NGS large diameter heat transport piping, *circumferential* flaws/cracks are postulated at all girth-butt welds and *axial* flaws/cracks are postulated in the body of all in-line fittings (e.g., elbows and branch connections). The commercially available finite element program ABAQUS was used to perform the elastic-plastic fracture mechanics of these components. An extensive activity was undertaken to demonstrate and validate the elastic-plastic fracture mechanics capabilities of the ABAQUS program. Some details of the finite element modelling assumptions and findings are given in References [6,7].

Through-wall (leaking) cracks are sized using *only* the normal operating pressure, i.e., the normal operating piping section bending moment is *not* credited for increasing the crack-mouth opening area of the postulated circumferential crack. The length of the postulated cracks corresponds to a leakage rate equal to the immediate shutdown action limit of 0.5 kg/second (8 USgpm). This leads to conservative predictions on the size of leaking cracks used in the stability assessments.

Validation of Fracture Mechanics: In order to acquire the detailed database required to validate the elastic-plastic fracture mechanics models used in the leak-before-break assessments, and to better understand the response of degraded piping and components, Ontario Hydro joined the first and second International Piping Integrity Research Group (IPIRG) programs[9]. Ontario Hydro participated as a joint member together with the Atomic Energy Control Board. The results of the US-NRC funded Degraded Piping Program and the Short Cracks in Piping and Piping Welds Program were also made available to participants in the IPIRG programs. This provided Ontario Hydro with an extensive, high quality, pipe fracture database that is being used to validate the elastic-plastic fracture mechanics models that are used in performing leak-before-break assessments. Participation in these programs has also greatly improved our understanding of the response of degraded piping components and systems subjected to extreme loadings.

Piping Loads: To ensure that the largest credible loadings are used for the stability assessment of the postulated cracks, five leak-before-break reference transients were formulated. Existing design service transients and possible process failure scenarios were considered in developing these extreme transient scenarios. e.g., one transient scenario is a design basis earthquake together with seismically induced failures in non-qualified secondary systems. Another is a small break loss of coolant accident resulting in operation of the heat transport pumps under partially voided conditions, which can give rise to significant pressure pulsations in the heat transport piping. These leak-before-break reference transients are used only for the purposes of ensuring that the largest credible piping section loads, pressure, and thermal gradients are used in the leak-before-break assessments.

Material Characterization: All heat transport piping is fabricated from seamless SA106 Grade B carbon steel piping and forged components are fabricated from SA105 carbon steel. An extensive material testing program was undertaken to characterize all of the piping materials and welds that were used in the fabrication of the heat transport circuit. This material characterization was required to perform the elastic-plastic fracture mechanics analyses. The upper-shelf ductility of carbon steels, as measured by lateral contraction during tensile testing, shows a minimum value in the temperature range 200-300°C. Tensile tests were conducted in this temperature range and it was established that this material minimum was in the neighbourhood of 250°C for the heats of SA106B being used for fabrication of the Darlington heat transport piping systems. This temperature was conservatively selected for the material property testing that was performed to characterize the parent and weld properties for operating temperatures. The original test program involved 63 tensile tests and 91 J-resistance (compact tension) tests. The test matrix included: all heats of three different pipe sizes (12", 22", 24"), two SA105 vesselet forgings, all welding procedures, testing at 20°C and 250°, and testing in both the longitudinal (C-L) and circumferential (L-C) directions.

Reference [4] provides some details and results of this material testing program. The results from this material testing program have been included in the 1995 edition of the US-NRC's Piping Fracture Mechanics Data Base (PIFRAC Version 3.1).

Post-Weld Heat Treatment: Two out of three of the compact tension tests of one of the welding procedures tested at 20°C exhibited ~5mm crack jumps after ~2mm of ductile tearing. This particular welding procedure had been developed for piping less than 1½" in thickness and as such does not require a post-weld heat treatment. The welding procedure utilizes a gas tungsten arc root pass, a shielded metal arc second pass, and submerged arc for all remaining passes. The observation of the macro-cleavage (relatively large crack jumps) lead to an expansion of the material characterization program: literature review, Charpy impact tests, chemical analysis, metallography/fractography, and an additional 9 tensile and 12 compact tension tests. It was concluded that the reduction of as welded fracture toughness can be attributed to the phenomenon of *dynamic strain aging*, which in turn depends on the amount of carbon and soluble nitrogen. Post-weld heat treatment increased the J-resistance curve of welds; but it did not eliminate *dynamic strain aging* or the presence of micro-cleavage (very small crack jumps) completely. Based on these observations it was deemed prudent to apply post-weld heat treatment (beyond that required by the ASME B&PV Code) to all welds in piping systems to which leak-before-break was being applied.

LBB FOR OPERATING NUCLEAR GENERATING STATIONS

As in other jurisdictions, the application of leak-before-before introduces an inconsistency between the design basis for *dynamic* effects and the design basis used for the design of

shutdown system capability, fuel cooling, and containment for specifying and the environmental qualification conditions for safety related systems. With the potential for large cost savings in the area of environmental qualification (both within containment and in the balance of plant) and the integrity of steam generator divider plates, Canadian utilities are attempting to justify the use of *mechanistic* fracture mechanics and leak-before-break analyses techniques on a case-by-case basis to support licensing submissions. The overall goal is to ensure that an acceptable level of safety is achieved in a cost-effective manner through a better understanding of the response of degraded piping systems and more realistic predictions of postulated failures of high energy piping systems.

The elastic-plastic fracture mechanics models and material and test databases, available from the recent fracture mechanics developmental programs, are being used in fitness-for-service assessments of pressure retaining components containing in-service degradation. These fitness-for-service assessments are used to demonstrate compliance with the requirements of Section XI of the ASME B&PV Code. In the future these databases will be used to develop probabilistic models that can be used to better quantify the risk associated with the full spectrum of sizes of piping failures.

ACKNOWLEDGEMENTS

The development of the leak-before-break approach developed for Darlington NGS was only made possible by the significant contributions of more than 50 individuals. The authors wish to acknowledge the contribution of the individuals involved in developing the elastic-plastic fracture mechanics models and with the application of the leak-before-break approach to Darlington NGS: M.L. Aggarwal, S.G. Fabbri, K.L. Gilbert, B.L. Kee, T.C. Lin, B.W. Manning, A.S. Misra, B. Mukherjee, J.S. Nathwani, D.A. Scarth, and M.L. Vanderglas.

The authors would like to personally thank Brenda Kee for reviewing and commenting on this manuscript.

REFERENCES

[1] Jarman,B.L.
The Canadian Approach to Protection Against Postulated Primary Heat Transport Piping Failures
Proceedings of the Seminar on – Leak-Before-Break: International Policies and Supporting Research
NUREG/CP-0077, June 1986; pp.73-96
also available as Atomic Energy Control Board paper INFO-0170, October 1985

[2] Kee,B.L.
Leak-Before-Break Studies for Darlington NGS A
Proceedings of the Seminar on – Leak-Before-Break: International Policies and Supporting Research
NUREG/CP-0077, June 1986; pp.256-268

[3] Aggarwal,M.L., Kozluk,M.J., Lin,T.C., Manning,B.W., Vijay,D.K.
A Leak-Before-Break Strategy for CANDU Primary Piping Systems
International Journal of Pressure Vessel and Piping; Vol.25, 1986; pp.239-256

[4] Mukherjee,B., Carpenter,D., Kozluk,M.J.
Fracture resistance of SA106B Seamless Piping and Welds
SMiRT 9 Transactions; August 1987; paper G/F-11/5

[5] Kozluk,M.J., Vijay,D.K., Aggarwal,M.L., Lin,T.C., Manning,B.W., Misra,A.S.
Demonstrating Leak-Before-Break for CANDU Heat Transport Piping
International Journal of Pressure Vessel and Piping; Vol.34, 1988; pp.255-263

[6] Kozluk,M.J., Manning,B.W., Misra,A.S., Lin,T.C., Vijay,D.K.
Linear-Elastic solutions for Long radius Piping Elbows with Curvilinear Throughwall Cracks
ADVANCED TOPICS IN FINITE ELEMENT ANALYSIS; ASME PVP-Volume 143; June, 1988; pp.23-28

[7] Nathwani,J.S., Kee,B.L., Kim,C.S., Kozluk,M.J.
Ontario Hydro's Leak Before Break Approach: Application to the Darlington (CANDU) Nuclear Generating Station A
Nuclear Engineering and Design; Vol.111, 1989; pp.85-107

[8] Kozluk,M.J., Vijay,D.K.
Primary Systems Integrity of CANDU Nuclear Generating Stations
SMiRT 11 Transactions; Vol.SDO, August 1991; pp.413-418

[9] Schmidt,R.A., Wilkowski,G.M., Mayfield,M.
The International Piping Integrity Research Group (IPIRG) Program – An Overview
SMiRT 11 Transactions; August 1991, Paper G23/1

THE USE OF LBB CONCEPT IN FRENCH FAST REACTORS : APPLICATION TO SPX PLANT

A. TURBAT, H. DESCHANELS, M. SPERANDIO, FRAMATOME Dir. NOVATOME
C. FAIDY, EDF-FRANCE

SUMMARY

The leak before break (LBB) concept was not used at the design level for SUPERPHENIX (SPX), but different studies have been performed or are in progress concerning different components : Main Vessel (MV), pipings. These studies were undertaken to improve the defense in depth, an approach used in all French reactors.

In a first study, the LBB approach has been applied to the MV of SPX plant to verify the absence of risk as regards the core supporting function and to help in the definition of in-service inspection (ISI) program.

Defining a reference semi-elliptic defect located in the welds of the structure, it is verified that the crack growth is limited and that the end-of-life defect is smaller than the critical one.

Then it is shown that the hoop welds (those which are the most important for safety) located between the roof and the triple point verify the leak-before-break criteria.

However, generally speaking, the low level of membrane primary stresses which is favourable for the integrity of the vessel makes the application of the leak-before-break concept more difficult due to small crack opening areas.

Finally, the extension of the methodology to the secondary pipings of SPX incorporating recent European works of DCRC is briefly presented.

INTRODUCTION

The leak-before-break (LBB) approach applied to the Main Vessel (MV) of SPX plant is used first to verify the absence of risk as regards the core supporting function (safety consideration) and then to help in the definition of in-service inspection (ISI) program.

It determines if the leak detection is feasible during normal operation before a possible collapse in accidental conditions and it allows to specify and to bound the MV areas to be inspected.

A general study was led about the application of LBB approach to the MV of SPX plant. This paper presents the synthesis of this study and the extension of the methodology to the secondary loops where a similar study is today in progress.

LBB IN THE MV : GENERAL CONTEXT

The absence of risk as regards the core supporting function is verified as follows : an initial hypothetical defect is considered in a hoop weld. Its propagation during the plant life is assessed and one tries to show that in every circumstance a leak will be detected before a complete break occurs even though we first prove the impossibility to obtain a through-wall or critical defect.

Selection of the initial defect

The reference defect considered is an isolated 170 mm long and 5 mm deep semi-elliptical defect. It would correspond to an electrode deposit, which is very pessimistic when compared to ISI results.

Locations investigated

The defects are located in the weld planes or in the heat affected zones at the most critical points (where the critical length is low or the stress range is high). Figure 1 shows the welds of the MV.

The study was extended to the axial welds and to the welds of the vessel bottom under the triple point, although they do not concern the core supporting function.

THE LBB PROCEDURE FOR MV

The LBB procedure consists of two different parts : the verification of integrity and the detection of leak.

Verification of integrity

The aim is to show that the initial defect cannot become neither through-wall nor critical under the fatigue propagation due to normal operation transients. This part of the procedure is illustrated on the left side of figure 2.

The margins are assessed by two different ways : increasing the number of cycles and increasing the range of the cyclic loadings. The stability of the defect at the end-of-life is verified under the action of the Safe Shutdown Earthquake (SSE), the highest accidental loading case.

Verification of the leak detection before break

Although, at the previous step, we tried to show that the initial defect does not become through-wall (assessing the margins), we assume then that, for an unknown reason, it goes through the wall. Therefore, the aim is to show that the corresponding flow rate will be detectable before the complete failure of the structure (right side of figure 2). The flow rate before break is calculated in a pessimistic way considering the length of a fictitious through-wall defect (due to an hypothetical propagation) on the back side of the wall a_3 :

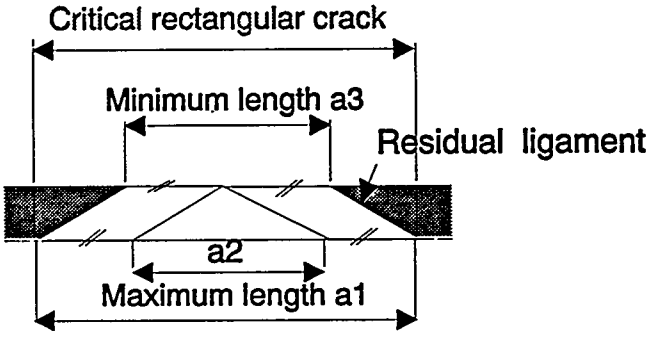

To evaluate the flow rate, we assume that the through-wall length a_3 on the back side is that existing when the maximum length is equal to that of the critical rectangular through-wall defect a_1 under the action of the SSE. The value of a_3 is given by $a_3 = a_1 - a_2$, where a_2 is the crack length at wall penetration.

The opening of the defect (leak area) and therefore the flow rate are calculated with the loading system corresponding to the normal operation.

We consider that the LBB concept is verified if this flow rate is greater than or equal to ten times the detectable leak.

Material properties

The constitutive material of the MV is the 316 SPH stainless steel. The minimum mechanical properties of base metal at 400 °C are :
Yield strength : σ_y = 121 MPa
Ultimate strength : R_m = 429 MPa.

For the fatigue propagation, the PARIS law is used :

$$\frac{da}{dN} = C\,(\Delta K)^n$$

$\frac{da}{dN}$: m/cycle

ΔK : MPa $\sqrt{m}$

The characteristics are taken at 550 °C (maximum temperature for nominal and incidental transients) :

$$C = 4.39 \times 10^{-11} \; ; \; n = 3.28$$

Creep effects are neglected due to normal operating temperature of 390 °C.

For the stability assessment, a tearing curve has been established from experimental results of reference 2 up to 200 mm. It was used for a tearing length lower than 10 mm. The main parameters are :

J_{IC} = 150 kJ/m^2

$\frac{dJ}{da}$ = 100 MPa (initial value).

Residual stresses

The residual stresses were taken into account differently for fatigue, stability and leak area :

* For the fatigue propagation and stability of surface defects, a stress equal to the yield stress (in mode 1) was considered.

* For the stability of through-wall defects and leak area calculations, it was shown (see the results below), that the effect of residual stresses is negligible ; so they were not taken into account.

Loadings

The fatigue propagation through the thickness was evaluated considering a cycle enveloping all normal and incidental transients with a number of occurrence equal to 1105 (number of start-ups and shutdowns in design data). This cycle leads also to the defect shape which is the most conservative for leak detection, due to a high bending stress level which results in a large residual ligament.

Fatigue propagation analysis

The method used is similar to that of appendix ZG of RCC-M based on PARIS law (Ref.3). The value of the stress intensity factor is corrected to take into account the plastic area and the mean stress (R ratio).

Stability analysis

The stability of the end-of-life and the hypothetical through-wall defects is investigated using the R6 rule based on the (K_R, L_R) diagram (Ref.4). In this study, a possible tearing of the rectangular through-wall defect ($<$ 10 mm) is taken into account and if the defect becomes stable again after a limited tearing, it is considered as acceptable.

Leak area calculation

The residual stresses are not taken into account as it was shown that their effect is negligible (see results). The general (simplified) method used for leak area evaluation is based on the application of the formula of reference 5 :

$$\delta = \frac{4c\sigma^*}{E} \quad (c = \text{semi-length})$$

with $\sigma^* = \sigma_m - 0.37\ \sigma_b$

Then the flow rate is calculated assuming an elliptic shape and a laminar or turbulent flow according to the value of the REYNOLDS number (Ref.6).

In the case of the hoop weld located in the gas area, the opening was directly computed with a finite element model of the cracked structure (Ref.7).

LEAK AREA VALIDATION

Specific calculation on a through-wall hoop defect located in the homogeneous weld of the gas area

This calculation (Ref.7) was performed because this weld submitted to a high bending is the most difficult to justify for leak detection. The results obtained are however rather general as regards residual stresses.

The opening and the stress intensity factor K were calculated for a through-wall defect submitted to the loadings acting during normal operating : weight (membrane), axial thermal gradient (bending), residual stresses. For the latter, a simplified distribution deduced from reference 8 and limited to a height equal to the thickness of the MV (25 mm) was considered .

The through-thickness distribution of axial stresses was taken as follows :

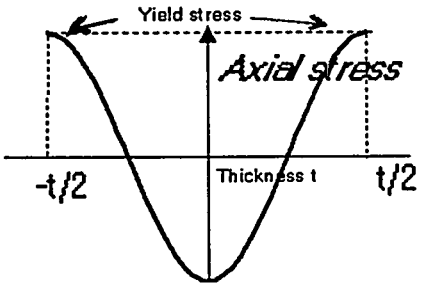

Circumferential stresses were considered as membrane stresses located in the vicinity of the weld.

An elastic calculation was led for 3 crack lengths (400 mm, 1 000 mm, 1 400 mm) using a finite element model consisting of 3 dimensional 20-noded brick elements (figure 3).

The main results can be summarized as following :

* The effect of residual stresses is negligible both for defect opening and stress intensity factor. As a matter of fact, the residual stresses act on a rather narrow area in the vicinity of the weld and the symmetrical shape of the groove gives a favourable stress distribution.

* The effect of a bending stress on the K factor is weaker than a membrane stress of the same value. Therefore, the simplified methods used to evaluate K under bending loading are verified for crack lengths greater than or equal to 1 000 mm. For a length of 400 mm, the finite element calculation gives a value 25 % higher than handbook results (Ref. 1).

* Concerning the effect of a bending stress on the crack opening (or closure), the equivalent membrane stress is equal to 0.37 σ_b (value of reference 5) for a crack length close to 700 mm. When the length is about 400 mm, the influence of the bending stress is more important ; but at 1 000 mm or more, the influence of the bending is weaker. For the lengths investigated, the divergence does not go beyond 14 %.

* Concerning the effect of a membrane stress on the crack opening, the formula $\delta = \frac{4c\sigma^*}{E}$ (c = semi-length of the crack) is verified with an accuracy of 15 %.

* Evaluation of the leak area : the calculation of the leak area A (δ) is performed assuming an elliptical shape of the crack, which is confirmed by the results of the finite element calculation.

Finally, this preliminary calculation allowed to modify the LBB methodology as following :

* The crack opening of the hoop weld located in the cover gas volume is directly given by this calculation (with the standard simplified methodology, the critical through-wall defect did not open).

* The residual stresses are neglected everywhere both for the opening calculation and for the stability analysis of through-wall defects (the residual stresses are taken into account only for the surface defects).

VERIFICATION OF INTEGRITY

* *Circumferential welds*

The integrity conditions are verified in all locations investigated. The results are given in figure 4.

For the circumferential welds of the MV, the margins to obtain a through-wall defect are more than 10 in terms of number of cycles and more than 1.9 in terms of loading intensity.

The end-of-life defect is stable without tearing under SSE.

It is found that the minimum critical length of a through-wall rectangular defect for a tearing length of 10 mm is much greater than the length of the end-of-life defect.

* *Meridional welds*

The integrity conditions are also verified in all locations investigated, even so the margins are a little less higher (but the meridional welds are less important with respect to the core supporting function).

The non critical character of the end-of-life defects is respected : the maximum value of tearing length under SSE is 1 mm.

VERIFICATION OF THE LEAK DETECTION BEFORE BREAK

For the hoop welds, which support the core, the minimum of opening is 0.03 mm in the gas area and the corresponding argon flow is 22 l/h. In the sodium area, the openings are larger and leak detection is easier.

Theoretical flow rates obtained for the hoop welds show that all of them respect the leak-before-break criteria. However, it must be noted that this result assumes there is no plugging, but the plugging risks are low for the weld located in the gas area and very low for those in the sodium area.

For the meridional welds, the crack opening is in the order of 0.1 mm. The leak detection is also possible even so refined analyses are needed for the welds located in the cylindrical part of the vessel, the sodium free level area and the torical area where hoop compression stresses exist.

EXTENSION OF THE METHODOLOGY TO SECONDARY LOOPS

The LBB methodology used for the MV of SPX has been extended to the secondary loops of this plant. The analyses are presently in progress.

The specific points of the LBB approach related to this type of structure (geometry, loading) are briefly listed below.

All the hypothetical initial defects are located in the weld planes where the probability to have a significant defect is maximum and where material characteristics such as toughness are weaker. Two types of weld joints are considered : hoop welds and meridional welds located at intrados and extrados of elbows.

On each loop, the most loaded welds according to the design data are selected following different criteria :

* $\Delta\sigma_{max}$ for fatigue propagation.
* σ_{max} during hold time for creep propagation.
* $\left(\frac{\Delta\sigma_b}{\Delta\sigma_m}\right)_{max}$ or $\left(\frac{\sigma_b}{\sigma_m}\right)_{max}$ for the length of the asymptotic through-wall defect.

The latter criterion is related to results of recent DCRC (Design and Construction Rules Committee) works. A master curve (figure 5) has been established for the evaluation of the length of the asymptotic crack shape at wall penetration as a function of bending stress/membrane stress ratio.

The dimensions of the initial surface defect (semi-elliptical) are 4 × 40 mm. They are the same as the dimensions of the reference defect considered by FRAMATOME for PWR piping and are justified by a compilation of ISI results.

As far as integrity analysis is considered, three points are to be noted. First, for the loops where creep is significant (for instance, the Intermediate Heat Exchanger - Steam Generator line), the defect propagation is calculated for each cycle as the sum of creep and fatigue propagations. Secondly, the creep propagation is evaluated in a simple manner using the so-called R5 rule of CEGB (Ref.9) which expresses the propagation rate as :

$$\frac{da}{dt} = K_f\,(C^*)^n,$$

where K_f and n are coefficients identified from creep rupture tests.

$$C^* = \sigma_{ref} \cdot \dot{\varepsilon}_{ref} \left(\frac{K_I}{\sigma_{ref}}\right)^2,$$

σ_{ref} being the reference stress in the remaining ligament.

Thirdly, in the case of the most loaded welds in fatigue, because of a too extended plastic zone around the defect tip, the method issued from RCC-M (Ref.3) has to be replaced by the ΔJ method (Réf. 10) for evaluating ΔK and fatigue propagation. ΔJ is therefore calculated from a simplified elastic-plastic analysis.

For stability analysis, the same method as for the MV is used (Ref.4) except that adequate formulations are applied to evaluate the main parameters (K_I, limit load) in function of the loading type and $\frac{R}{t}$ ratio.

As far as leak detection is considered, the master curve issued from DCRC works is used to assess the length C_s of the asymptotic through-wall defect. Besides, it is likely that for the meridional welds of elbows, where shell bending is important, crack opening area evaluated by the simplified formula of reference 5 $\left(\delta = \frac{4c}{E}\ \sigma^*\right)$ will have to be replaced by a more accurate calculation using a finite element model.

Finally, it will be said that a piping verifies the LBB concept if all the points selected along the line respect it.

CONCLUSION

This paper presents the LBB methodology applied to SPX plant (main vessel and secondary loops) and the results obtained in the case of the MV.

Starting from an initial reference defect, it is shown that the defect remains non-critical and non-through-wall during all the plant life in every point of the MV.

Besides, it is possible to prove that the hoop welds, important for the core supporting function,verify the leak before break criteria.

For the meridional welds, the proposed margins of the LBB procedure are not verified in the cylindrical part of the MV, the sodium free level area and the torical area if simplified methods are applied, due to compressive stresses in normal operating conditions. Hypothesis and method refinements are needed.

The extension of the LBB methodology to the secondary loops of SPX based on recent works of European R and D leads to specific problems related to creep-fatigue propagation of defects and to meridional welds in the elbows.

REFERENCES

(1) D.P. ROOKE, D. J. CARTWRIGHT
Compendium of Stress intensity factors,
London Her Majesty's stationery office 1974.

(2) S. BHANDARI , H. DESCHANELS, M. SPERANDIO, C. FAIDY, W. SETZ,
Tests on large scale LMFBR piping, Part II : Analysis of through-cracked straight pipes DN 700 tested under bending at RT and 550°C, SMIRT 12, Stuttgart (15-20. Aug. 1993) - Paper GF10/2

(3) RCC-M - Edition 1985 - Annexe ZG
Résistance à la rupture brutale

(4) I. MILNE, R.A. AINSWORTH, A.R. DOWLING, A.T. STEWART
CEGB Report R/H/R6 - Revision 3 - 1986
Assessment of the integrity of structures containing defects

(5) A. NAGAI, M. TOYOSADA
Penetrated fatigue crack opening displacement and growth rate under combined tensile and bending loading.
The Hitachi Zosen Technical Review - Vol. 39, n° 2 - June 1978

(6) IDELCIK
Mémento des pertes de charges
Editions Eyrolles - 1969

(7) H. DESCHANELS, A. TURBAT, M. SPERANDIO
Numerical simulations of crack opening areas for leak-before-break applications in LMR components
SMIRT 13 - Porto Alegre, Brasil - Paper E01/3 - August 1995

(8) R.H. LEGGATT
Welding Institute Report LD 22398/9 - December 1981
Assessment of residual stresses in butt welded joints in AISI 316 stainless steel plate

(9) R.A. AINSWORTH, P.J. BUDDEN
Assessment of defects at high temperatures : the R5 procedures in Behaviour of Defects at High Temperatures, ESIS 15 - Mechanical Engineering Publications - 1993

(10) B. DRUBAY, D. MOULIN, C. FAIDY, C. POETTE, S. BHANDARI
French methodology for defect assessment in Fast Breeder Reactor, ASME-PVP Conference, Denver (26-30 July 1993)

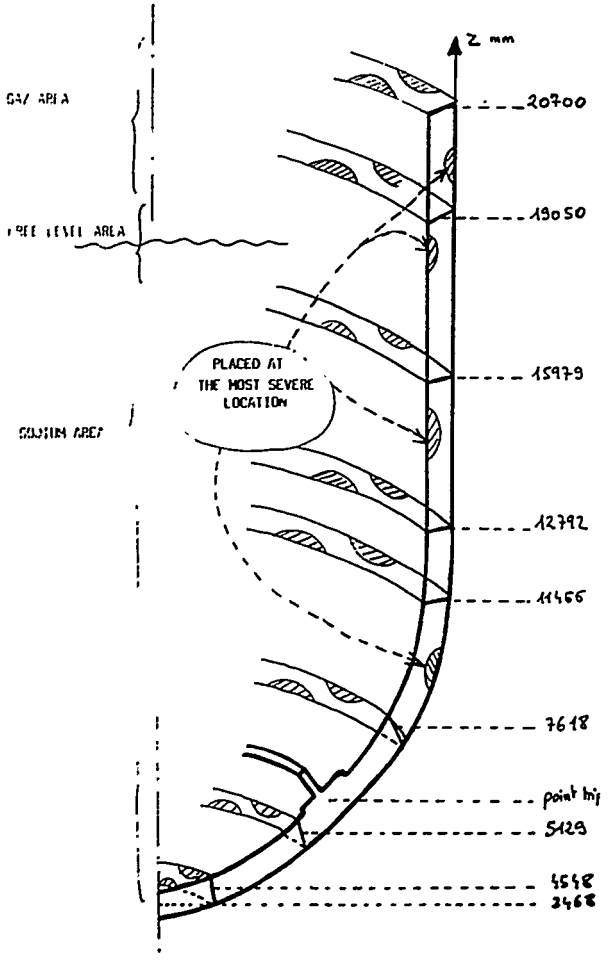

Fig. 1 - Defect locations considered in Main Vessel

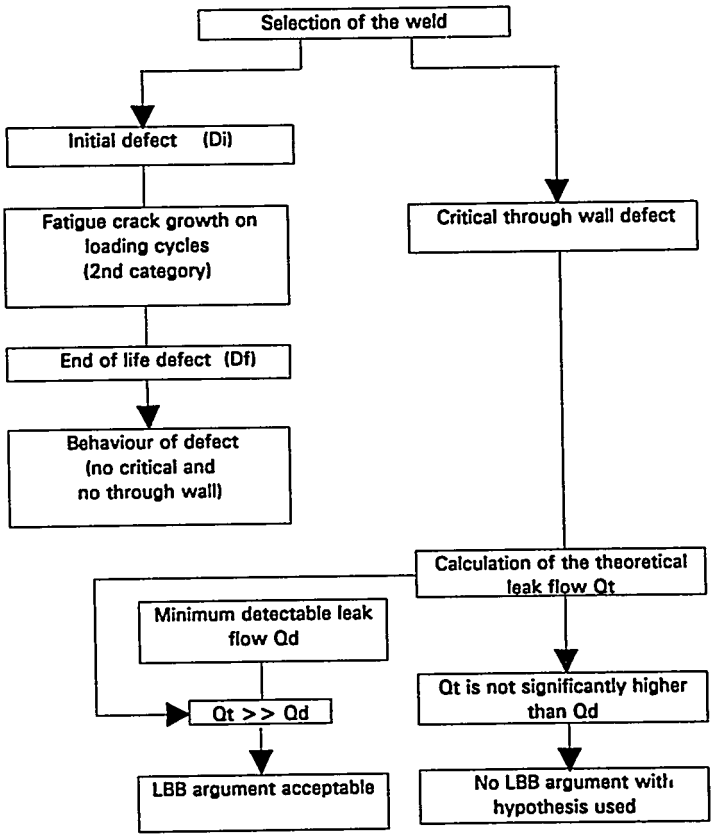

Fig. 2 - LMFBR leak-before-break procedure

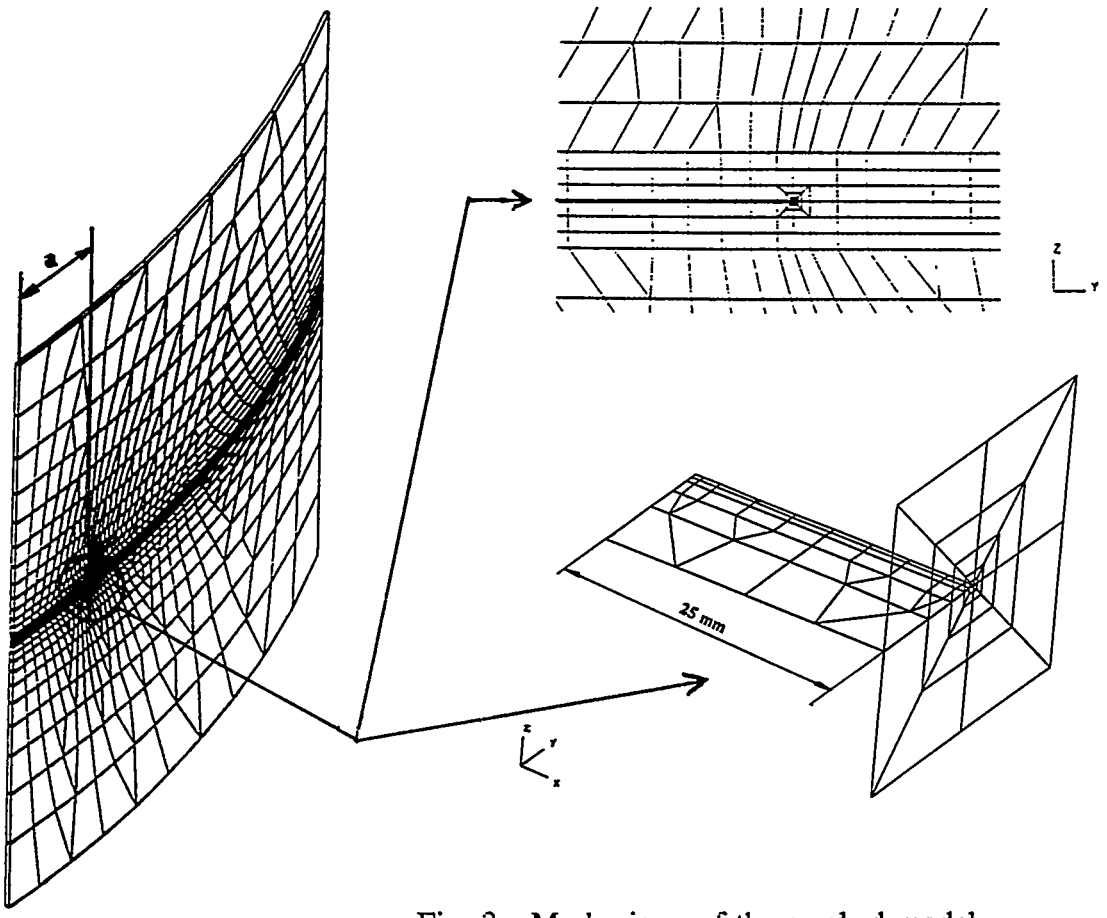

Fig. 3 - Mesh views of the cracked model

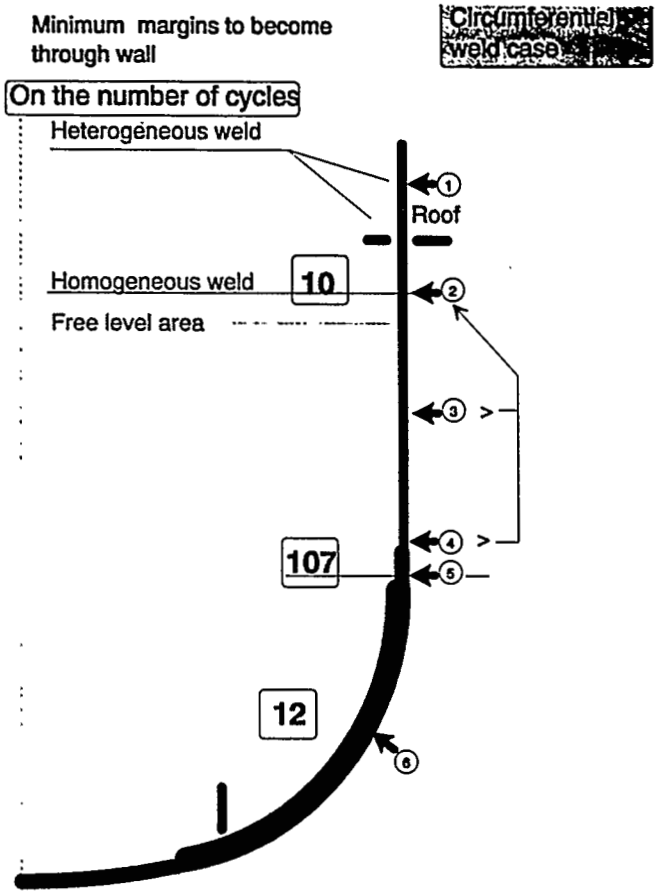

Fig. 4 - Margins for integrity (hoop welds)

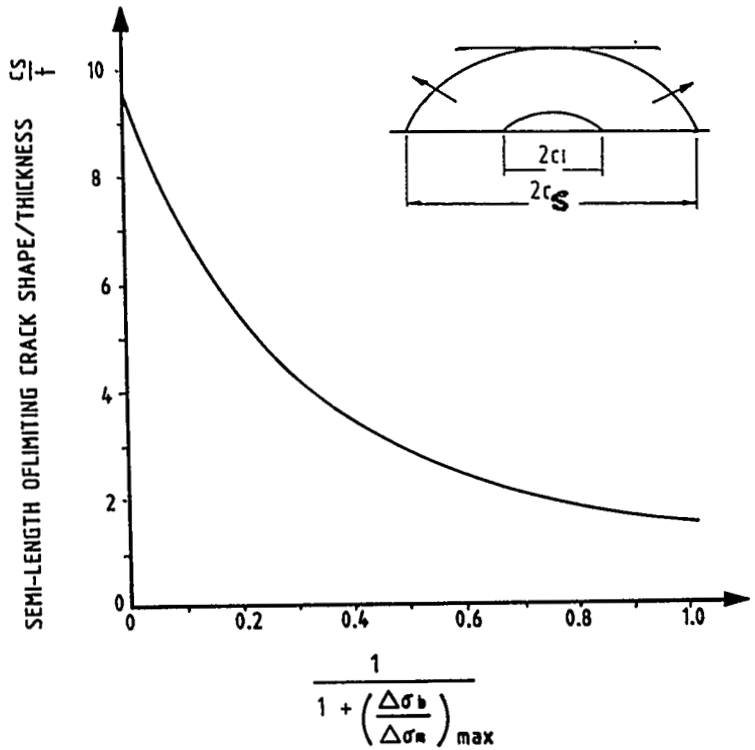

Fig. 5 -Semi-length of asymptotic defect as function of bending/membrane ratio

OVERVIEW OF LBB IMPLEMENTATION FOR THE EPR

C.Cauquelin
NPI

A few words on the EPR

The EPR is an *evolutionary* Nuclear Island of the 4 loop x 1500 Mwe class being presently designed by Framatome and Siemens , which, for that purpose, created Nuclear Power International, a joint company with its main offices in Paris. The Basic design phase shall be completed by mid-97 and is conducted in strong cooperation with EdF and a group of 9 German Utilities. As far as the NSSS mechanical components are concerned their technology is basically similar to those of the most recently erected plants in France and Germany, namely N4 and Konvoi. The main operating parameters i.e. pressure, temperatures in hot and cold leg, primary water chemistry are also quite close to those of existing plants at least as far as the mechanical components may be concerned.

Background on LBB in France and Germany (PWR)

The pre-EPR regulations and practices in France and Germany regarding the break assumptions considered for the purpose of designing the mechanical components, their supports and the surrounding civil structures are different [1].

LBB has never been implemented on French plants, the practice remains unchanged since the first PWR unit was built at Fessenheim in the mid-70's. Large breaks are postulated to occur on all high energy lines. Although there was some preliminary talks between the industry and the Safety Authorities in the mid-80's, they were not pursued to a successful end. On the Main Coolant Lines (MCL), guillotine breaks are assumed at the terminal ends. The resulting effects are fully considered for the design of the components, their supports and the Civil Works. To minimise the dynamic loads and the break flow area, antiwhipping structures are installed around the lines in the vicinity of the postulated breaks and small gaps are arranged around the components supports. In addition, because of the high loads, fairly large snubbers are required to support the steam generators and the reactor coolant pumps. Typically the French practice derives from the "defence-in-depth" principle. The large breaks are seen as one way to put margins into the structural design of the components and the surrounding structures.

In Germany, LBB was accepted by the licensing Authorities in 79 (see other papers from GRS and poster by Siemens for more details). Initially applied to the Main Coolant Lines (MCL) and the Main Steam and Feedwater lines it was later on extended to other high energy lines. Removing the antiwhipping structures and reducing the loads on the reactor internals were the main incentives to implement the LBB concept - part of a broader concept called Break Preclusion in Germany- to these lines. The primary components and their internals are designed for the loads resulting from a relatively smaller leak located anywhere on the main coolant lines (10% of MCL area = 0,1A). The

[1] The basis to design the containment, the safety systems and to qualify the safety equipment are the same and are not intended to be modified for the EPR. Breaks up to a double-ended guillotine are assumed to occur on the Main Coolant Lines.

German approach is typically based on a "mechanistic" rationale. Considering the stringent requirements applied to the design, manufacturing and operation of the MCL the large breaks are excluded.

The Break Preclusion concept as applied to the Main Coolant Lines of the EPR

We have today a conditional agreement from the Franco-German Safety Body to implement LBB on the Main Coolant Lines (MCL) as a part of the broader Break Preclusion concept, the philosophy of which is borrowed from the German practice. It includes all the measures contributing to minimizing the risk of failure of the MCL. It comprises the preventive measures implemented at the design and manufacturing stage and the surveillance measures implemented during operation of the plant (figure 1) . In this paper we limit ourselves to the main arguments which justify applicability of the concept to the MCL of the EPR and to some comments on the issues which are being discussed with our safety authorities.

Preventive measures

Because the EPR is an evolutionary PWR heavily based on operating plants, its operating conditions are pretty well known at the design stage. Quite clearly, the lines are not subject to severe or unpredictable loads like water hammer, stratification or erosion-corrosion phenomena. Field experience provides data on the vibratory level which remains very low and irrelevant in terms of stresses.
The best available manufacturing processes will be implemented. Two qualified options are offered for the material of the lines, one is ferritic cladded , the other austenitic (figure 3 shows a typical leg for each option). In both cases:

- all the main parts are forged
- the number of welds is minimised (total and site welds)
- all large nozzles are integrally forged

The two materials exhibit excellent ultrasonic permeability for shop and field testing. The mechanical properties, in particular the toughness, are stable with time. There will be no aging, for instance as it occurred with some castings in the past. The bimetallic welds are narrow-gap and Inconel 690 is used as a filler. This type of weld is proven to have good toughness properties.

LBB assessment

The LBB analytical assessment itself is rather classical in most aspects and rely on existing methods for crack propagation and stability. The only true specific point lays with the "multiple life crack growth" step, which is borrowed from the German approach. It must be demonstrated that a "reasonable cracklike defect", arbitrarily assumed at beginning of life at the worst location, tends to propagate through the wall rather than around if submitted to as many as necessary lifetime transients and that it remains significantly far from unstability when it gets through. Obviously the hard point remains to decide on the size of the "reasonable cracklike defect". On the basis of the non destructive test methods implemented our proposal to day is to take a 4x24 mm defect.

The main steps of the LBB assessment are summarised on figure 2a and 2b.

Leak detection system

As in operating plants, "global" sensors monitoring the containment atmosphere activity and the condensates in the air coolers will be installed. They are very efficient to detect leaks, specifically primary leaks.

"Local" sensors , located inside the loop compartment downstream the air flow, are also considered. They are of two types:

- humidity sensors (dew point)
- temperature sensors (thermocouples)

Both are very sensitive and reliable. Leaks as low as 30 g/s are detected in a very short time . Detection delay is expressed in minutes, depending on the size of the room and the air flow rate.

Surveillance in service

There is a general need to record the transients seen by all the primary components and this is already routine work on operating plants. In our opinion the LBB concept should not lead to additional requirements to those already implemented.

Regarding ISI it is honest to say that we have a difference in opinion with our Safety Authorities on this question. They argue that if large breaks are excluded, ISI must be more extensive. In our opinion ISI is a "sampling" process. Inspected areas are selected as "critical" or "typical" and the selection process is not LBB dependant. At any rate, layout measures are taken to give access to any part of the MCL for inspection either from outside or from inside if not both. As stated earlier the material is forged and well suited for UT and the large bimetallic welds may also be Xrayed (austenitic option).

Practical consequences on the design

Practically the large guillotine breaks, whether fully double-ended or limited in flow discharge area, will not be considered for the mechanical design of the primary components and their surrounding civil structures. Instead a complete break of any connected line is postulated. However, although it does not fit with the break exclusion principle, a "quasi- static load " equal to 2pA is applied to the components for the design of the supports.

Globally, and except for the "wandering" 0,1 A leak which disappears because it is covered by the connected line break, the whole procedure is very close to the German one.

It is definitely a change for the French who are used to the large breaks. If compared with the previous practice, the LOCA loads on some parts will be somewhat reduced. The loads resulting from a connected line break are smaller than those resulting from a double-ended guillotine break. However the reduction in loading will not be as large as it may look at first :

- the SSE free field acceleration is larger for the EPR than it was in the past
- the supports are still designed for a 2pA static load
- the design of the primary components is largely based on operating components.

There is one major safety benefit in implementing LBB to the MCL. As already stated , if large guillotine breaks are assumed , small gaps are necessary between the antiwhipping structures and the lines and around the components to minimize the displacements and the dynamic loads on the supports and the civil strutures. Because of the thermal expansion of the loops and the concrete and because the concrete properties vary with time it is necessary to shim these gaps in hot condition and to check periodically their magnitude to avoid hard interference. Should it occurit would prevent free expansion of the loop and induce unwanted stresses. With LBB there are no antiwhipping structures and the gaps around the components need not to be as small. The risk is eliminated.

From the doses point of view, having no antiwhipping structures around the lines will also improve access to the lines and the primary components for inspection and maintenance. On existing plants some of these structures have to be dismantled.

Conclusion

In our opinion, the LBB concept applies very well to the Main Coolant Lines of the EPR. The high reliability of these lines is guaranteed by :

- the stringency of the design rules (Class 1 ETC-M),
- predictability of the operating conditions (loads, chemitry...)
- quality and properties of the material (all forged parts)
- optimized welding process
- non desructive inspectability in shop and on site
- large margins against cracking and failure
- performances of the leak detection system

Implementing the concept improve access to the components for inspection and maintenance, and contribute to lessen the radiation doses. It also eliminates the risk of hard interference between the loops and the civil structures and therefore contributes to the reliability of the plant.

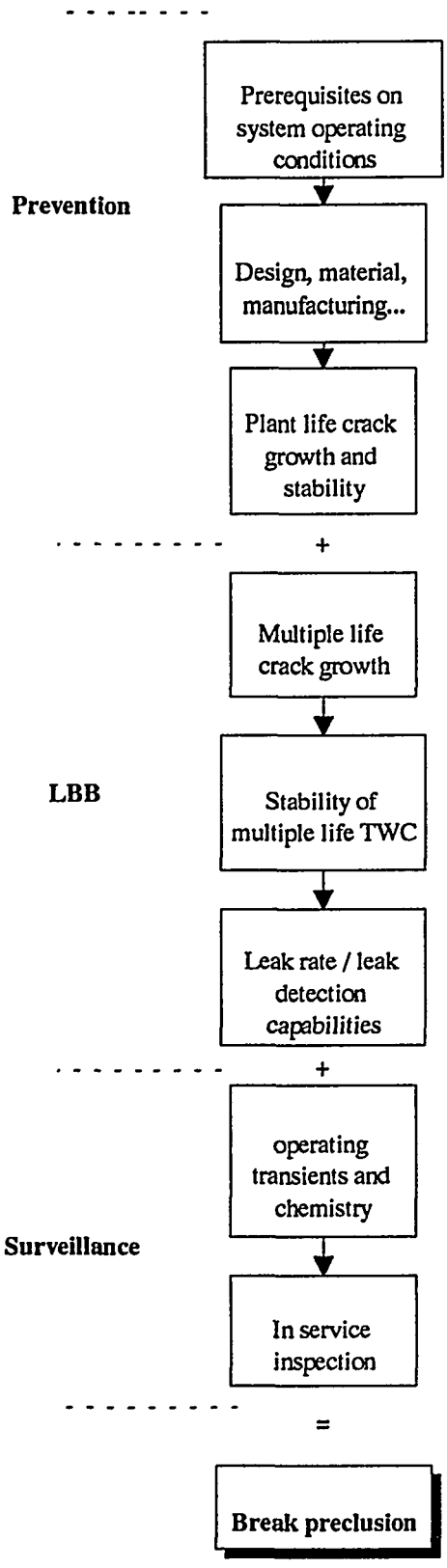

comments

operating modes, loads and potential damages well predicted at design stage

optimized design , material and manufacturing processes (class 1): forged parts, minimum number of welds extensive testing.

to prove margin against significant propagation during lifetime

to quantify margin against through wall cracking

margin against pipe failure

margin on leak detection

compliance of operating modes with design conditions

no additional requirement from LBB

figure 1

STEP	METHOD	LOADS	CRITERIA	MARGIN
Definition of reference defect	performance of NDT at manufacturing	-	a = 4 mm 2c = 24 mm	sensitivity analysis with larger defects
Plant life crack growth	Paris law over plant life	operating transients	small growth	on da/dN law and transients number and severity
Crack stability	austenitic: R6 or J-R	operating transients + SSE	J<J1C Tapplied<Tmat	on seismic loads and material properties
	ferritic: flow stress or plastic limit		stability of ligament	
Multiple life crack growth	Paris law	operating transients	stability	number of lives
leak rate	"open"	full power		margin on LDS proven capability

figure 2a

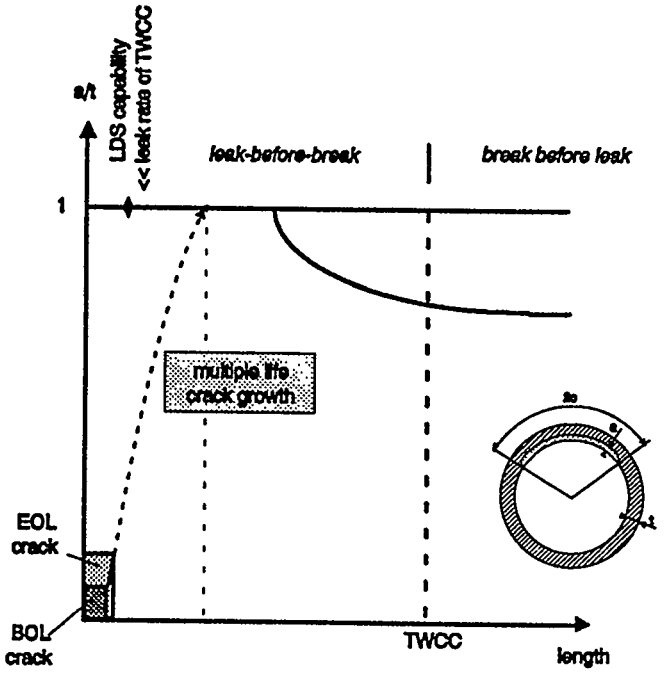

figure 2b

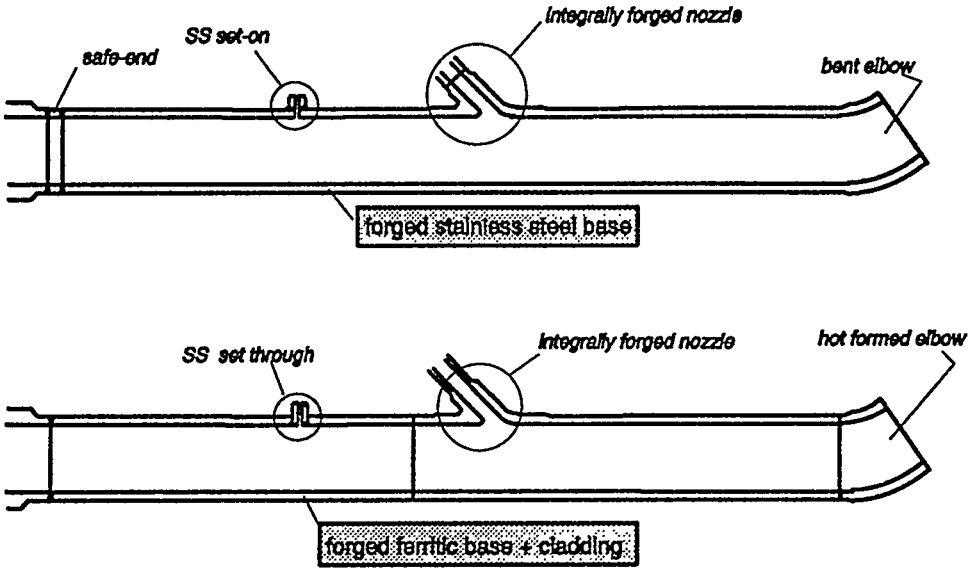
integrally forged nozzle
SS set-on
safe-end
bent elbow
forged stainless steel base
SS set through
integrally forged nozzle
hot formed elbow
forged ferritic base + cladding

figure 3

APPLICATION OF THE LBB REGULATORY APPROACH TO THE STEAMLINES OF ADVANCED WWER 1000 REACTOR

V.A.Kiselyov[a], L.M.Sokov[b]

[a] The Russian Minatom Engineering Center of Atomic Equipment Strength, Reliability & Lifetime

[b] EDO "Gidropress", Podolsk, Russian Federation

ABSTRACT

The LBB regulatory approach adopted in Russia in 1993 as an extra safety barrier is described for advanced WWER 1000 reactor steamline. The application of LBB concept requires the following additional protections. First, the steamline should be a highly qualified piping, performed in accordance with the applicable regulations and guidelines, carefully screened to verify that it is not subjected to any disqualifying failure mechanism. Second, a deterministic fracture mechanics analysis and leak rate evaluation have been performed to demonstrate that postulated through-wall crack that yields 95 l/min at normal operation conditions is stable even under seismic loads. Finally, it has been verified that the leak detection systems are sufficiently reliable, diverse and sensitive, and that adequate margins exist to detect a through wall crack smaller than the critical size. The obtained results are encouraging and show the possibility of the application of the LBB case to the steamline of advanced WWER 1000 reactor.

1. INTRODUCTION

The general methodology and criteria used for the LBB concept application to WWER 1000 primary circuit are presented in Ref. [1]. The calculational and experimental results obtained to date are very encouraging and demonstrate the possibility of the LBB concept application to primary circuit of advanced WWER 1000. Further researches have been directed to demonstrate the LBB case to the steamlines (SL) of secondary circuit.

The present Russian regulations do not require the application of LBB concept for SL. The guidelines and regulations [2,3,4,5] used for design, manufacturing, installation, operation, inspection and surveillance envisage high quality and reliability levels of these components. However, the possibility of the demonstration of the LBB concept for SL could be identified as an issue of major safety significance.

The LBB methodology provides early warning before a catastrophic failure in SL could evolve. Therefore, the LBB concept should be applied after the analysis of postulated deviation from design and manufacture aspects, materials and operating and in-service inspection, plant monitoring and leak detection systems (LDS). Then, potential SL should be carefully screened to verify that they are not subjected to any failure mechanism during operation. Next, it is necessary to demonstrate that the leak which might emanate from a through wall crack can indeed be detected by LDS and according to procedure [6,7] it should be demonstrated that the postulated cracks are stable at the maximum possible loading such as under a safe shutdown earthquake (SSE).

According to the procedure M-LBB-01-93 [7] which is now in effect in the Russian Federation an analysis of fatigue crack growth and surface crack stability is not required because the regulatory documents include standards

for calculation of allowable defects and assessment of control results during operation. Nowadays, this approach is used in the USA too, where Section XI of ASME Code gives the tables of allowable defects.

A through wall postulated crack stability analysis under maximum loads is performed using fracture mechanics methods, such as J-integral method [1], R6 procedure [9], Moments method and MPA method [10] in accordance with materials type, geometry, crack direction and applied load. In all cases the J-integral and R6 methods are applicable to many types of structure, crack shape and direction, loading and material.

2. OVERVIEW OF AVAILABLE STEAMLINE DATA

The SL has been designed in accordance with Regulations PN AE G7-002-86 [2] and Norms PN AE G-7-008-89 [5] and fully meet the requirements in main sizes, static and cyclic strength, resistance against brittle fracture, vibrations and seismic loading.

2.1. Design features, manufacturing and installation aspects

Four loops of the SL under consideration are different in layout and length, each is assembled at NPP from shopfabricated piping blocks, which reduces the number of installation welds. The principal layout is shown in Fig.1, where also the highly stressed cross-sections are given. The SL is each 630 mm outside diameter, the nominal wall thickness is 25 mm. The straight pipes and elbows are seamless. They are fabricated by hot stamping and are subject to normalization, quenching and tempering. Elbows include a straight ends of pipes. All circumferential welds are made in situ and after manufacturing they are subjected to heat treatment to remove weld residual stresses. The negative tolerance in wall thickness is 15%, the permissible out of roundness is 8%. There are no dissimilar and axial welds inside the containment.

2.2. Material

The material used is 16GS type steel. Circumferential welds are made in accordance with Rules [3,4] by automatic arc welding with the use of additional wire Sv-08GS and flux FZ16 or manual arc welding with the use of UONI 13/55 type electrode. The chemical composition and mechanical properties of base material and weld materials without heat treatment are given in **Table 1** and **Table 2**, respectively.

Table 1. Chemical Composition

Type of Materials	C	Si	Mu	P	S	Cr	Cu	N
16 GS	0.13-0.14	0.60-0.80	0.9-1.0	max 0.015	max 0.011	max 0.15	0.06-0.10	0.13-0.18
Sv-08 GS	0.092	0.65	1.5	0.017	0.008	-	-	-
UONI 13/55	0.095	0.26	1.17	0.010	0.019	-	-	-

The Charpy-V test data for circumferential welds and heat affected zone at temperature T, being equal to -10°C, 0°C and 20°C, are more than 40 J/cm^2, 60 J/cm^2 and 80 J/cm^2, respectively.

The upper shelf level of the fracture toughness K_{Ic} of base metal and welds is more than 160 MPa m$^{1/2}$ at 20°C, minimum fracture toughness K_{Jc} for all welds including heat affected zone at 300°C is 140 MPa m$^{1/2}$. The critical brittleness temperature T_c does not exceed +10°C.

Table 2. Mechanical Properties

Type of materials	Temperature T(°C)	Ultimate Strength R_m (MPa)	Yield Strength $R_{p0.2}$ (MPa)	Ductility A_5 (%)	Contraction Z (%)
16GS type steel	20	min 491	min 294	min 19	min 47
	350	min 412	min 226	min 15	min 40
Sv-08GS	20	526-538	325-332	14.7-16.4	64.8-70.1
	350	471-483	275-309	14.3-17.5	63.9-69.8
UONI 13/55	20	513-534	316-328	17.9-22.0	66.0-69.8
	350	474-482	285-316	15.0-17.6	64.0-71.3

2.3. Metal inspection

Prior to being used, chemical composition, mechanical properties and critical brittle temperature of welding materials are checked. After fabrication, all welds are subject to total (100°C) pre-service inspection (visual and measurement checks, liquid penetrant or magnetic-particle examinations, ultrasonic examinations).

In visual inspection, cracks, spilling, burnthrough, blowholes, rolls, shrink holes, notches, incomplete penetration, metal splashes, groups and non-single discontinuities are not allowed. The tolerance for permissible single inclusions, aggregations and non-uniformities for all type of examination is established by the corresponding requirements of Rules [3,4].

In service, total (100%) non-destructive inspection by ultrasonic testing is envisaged for all welded joints. The tables of allowable defects are calculated according to the procedure [8]. The checking of metal mechanical properties by destructive or non-destructive methods must be accomplished in every 100 000 operation hours.

The fulfillment of inspection requirements proves the high quality of the welds from the manufacturing to end of life.

2.4. Leak diagnostics

The LDS is designed for detection and location of leaks inside containment and the limit on unidentified coolant leakage for all SL is 9.5 l/min. The LDS is a complex of diagnostic systems based on monitoring of temperature, moisture and humidity in closed boxes, fluid level in the drain, condensate accumulation in the recirculation air coolers and ventilation filters, pump water or gully water levels, radioactivity of air and acoustic signals.
Basic parameters of the design LDS are:
- sensitivity detection, 3-9.5 l/min;
- accuracy of leak localization, 1-2 m;
- distance between sensors, 6-10 m;
- period of signal generation, 1 s;
- time of leakage indication, less than 120 s.

2.5. Fatigue

The SL under consideration must have no particular susceptibility to a failure from the effects of excessive low-and high-cycle fatigue. It is required to demonstrate that fatigue crack growth is not significant unless unique fatigue mechanisms, such as thermal stratification or mechanical vibration, are present. Therefore fatigue analysis was performed and results of calculation indicated that fatigue damage due to the design loading cycles is insignificant and fatigue growth of the maximum allowable surface cracks under normal operation conditions (NOC) and upset conditions made some decimal millimeter and hence it may be ignored. The pipe vibration level is so low that it is practically of no effect on the fatigue damage and crack growth assessment. To control the vibration level some

high frequency sensors must be installed directly on components of each steamline.

Temperature expansions of the SL are provided by displacement of steam generator on roller supports, and the pipe layout features high compensation capability. The SL operation conditions ensure prevention of thermal shocks. The heating and cooling rates are limited by values of 20°C and 30°C/hour, respectively. Therefore one should not expect random overloads due to wedging of individual SL elements, which is proved by operational experience.

2.6. Water hammer

Particular attention was paid to estimation of potential water hammer (WH), which results in excessive load. During NOC, where coolant parameters are within the design limit, there are no causes for the initiation of any WH conditions. The classical WH effect in the SL may be initiated by main steam isolation valve closure. Therefore, it was analyzed at the instantaneous and real time (5 sec) operation of the valve closure. Calculational value of WH is 0.68 MPa in the first case and 0.12 MPa in the second one. These magnitudes are small and may be ignored.

2.7. Corrosion damage analysis

Another screening criterion for the candidate LBB piping is that the corrosion and stress corrosion effects does not contribute significantly to the total damage of the system analyzed. The ferritic steel type 16GS and circumferential welds UONI 13/55 have no particular susceptibility to intergranular stress corrosion cracking and are highly resistant to erosion-corrosion, that leads to a wall thinning of the piping exposed to wet steam.
According to autoclave tests the kinetics of corrosion for secondary circuit environment (temperature 300°C, pressure 9 MPa, [CL'] in the medium 5 mg/kg) proceeds with a time-retard (see **Table 3**).

Table 3. Autoclave Corrosion Tests

Time, h	250		500		1000		2000		2500	
	Kinetics of uniform corrosion									
	g/m^2	mu/y	g/m^2	mu/y	g/m^2	mu/y	g/m^2	mu/y	g/m^2	mu/y
Base metal	10.6	47.0	17.0	38.0	28.0	31.0	45.0	24.0	52.5	23.0
Welds	11.5	50.0	21.0	47.0	26.0	29.0	45.5	25.0	56.0	25.0
	Depth of Pittings (mu)									
	min	max	min	max	min	max	min	max	min	max
Base metal	6	51	14	210	15	220	27	210	45	288
Welds	6	30	12	87	21	93	21	165	48	252

Steel welding through accepted technology practically does not increase any changes in the corrosion process. The screening of profilegrams by samples of welds does not detect a localization of the corrosion processes in fusion zone. Steel 16GS in the secondary circuit medium is susceptible to pitting corrosion (see **Table 3**). The maximum observed flaw size is less than 0.3 mm. The dependence of the environment on fatigue damage and crack growth was taken into account. The total damage is negligible (0.003). Corrosion fatigue is not a limiting LBB concern.

The SL operating experience data in real environment in acting units with WWER 1000 reactor does not show failures of carbon steel components due to erosion-corrosion effects. The current research program envisages further erosion-corrosion tests of steel 16GS and welded joints in saturated steam medium.

2.8. Indirect causes of failure

The indirect causes of degradation or failure of the SL such as fires, missiles, etc., failures of heavy components supports and systems and components in close proximity have been analyzed. Potential of damage from fires, missiles, etc. is ruled out because of the design features (layout and the existence of appropriate tight boxes). Potential for the failure of heavy component and equipment supports could not cause the rupture of the SL as well as systems in close proximity because the major equipment and equipment supports are seismically qualified. Other indirect causes, such as pipe hangers failure, failure of snubbers are remote. No indirect degradation or failure of the SL were observed in the operation of WWER 1000 reactors.

3. STATIC AND SEISMIC STRESS ANALYSIS

The purpose of the analysis was to evaluate tensile, bending and torsion loads (forces and moments), the reaction in hinges, supports and anchorages for all possible operating and loading conditions. In the static analysis, the internal pressure, deadweight, thermal expansion were taken into account, for seismic analysis the SSE 8° MSK 64 intensity was mandatory. Verified computer codes were used in static and seismic analysis.

The results of stress analysis under normal and seismic loads for layout shown in Fig.1 are presented in **Table 4.**

Critical locations in SL are chosen for the higher stressed sections, particularly the welds. As a result fracture mechanics analysis was performed for the "worst" 17 cross-sections.

4. LBB ANALYSIS

According to the U.S. approach [11,12] and procedure M-LBB-01-93 [7] the LBB analysis was conducted to demonstrate that leakage from a postulated through-wall crack will be detected and any preexisting leakage size crack (LSC) will remain stable even under (NOC+SSE) loads and not cause a rupture even if SSE occurs before leak detection. Base information for this analysis is given in **Table 5** and **Table 6.** Design stresses are given in terms membrane, bending, primary and secondary ones in the **Table 4.**

Table 4. Elastic Stress Analysis (MPa)

	Steamline Normal Load

-Section	σ_β(p)	σ_β(T)	σ_β(s) Seismic Load
1-1	7.3	74.5	43.8
1-2	1.7	80.5	28.0
1-3	0.6	101.0	18.2
1-4	2.9	90.6	16.4
2-1	9.0	21.1	45.1
2-2	2.3	61.1	13.5
2-3	2.3	69.4	14.4
2-4	5.7	43.0	35.0
3-1	7.7	44.1	52.1
3-2	1.4	56.5	13.7
3-3	1.0	36.3	49.2
3-4	0.8	60.9	14.8
4-1	7.1	76.4	74.7
4-2	6.8	85.7	14.9
4-3	3.8	78.6	17.8
4-4	5.9	81.8	13.4
4-5	15.2	4.5	48.3

σ_β (p) is primary global bending stress

σ_β (T) is secondary global bending thermal expansion stress

σ_β (s) is primary global bending seismic stress

σ_μ (p) = 43.6 MPa is primary axial tensile stress

σ_ρ (R) = 45 MPa is assumed secondary axial weld residual stress

Table 5. Steamlines Characteristics for LBB Analysis

Outer diameter,	630 mm
Wall thickness,	25 mm
Material,	16GS type low carbon steel

	UONI 13/55 weld metal
Design Pressure,	7.84 MPa
Temperature,	280°C
Crack type,	circumferential
Cross-section crack shape,	through-wall
Location,	inside containment
Loading condition,	NOC and NOC+SSE

4.1. Leak rate calculation

The scope of this calculation is to define the LSC, the leakage through which can be reliably detected by the design LDS. Because the steam lines under consideration are inside containment, the leakage detection capability is assumed

Table 6. Calculational Material Data

Properties	Leakage Calculation (Best Fit)	Crack Stability (Lower Bound)
Modulus of elasticity E, GPa	195	195
Yield strength $R_{p0.2}$, MPa	309	225
Ultimate strength R_m , MPa	483	392
Flow stress σ_f , MPa	396	308
Fracture toughness K_{Jc} , MPa $m^{1/2}$	-	140

to be less then 9.5 l/min, and a margin of 10 is applied to this leak rate. The crack size that results in a detectable leakage Q_p = 95 l/min under NOC is L_p and used in the subsequent stability calculation as the postulated crack [13]. For the leakage calculation (at 280°C), the appropriate best-fit tensile parameters for the base metal and welds are used. The weld residual stresses are ignored.

The leakage **Q** under NOC is calculated as follows

$$Q = GA \qquad (1)$$

where **G** is the leak rate, **A** is the crack opening area which is determined from the Paris/Tada solution [14].

The leak rate **G** can be estimated from Ref. [15] as follows

$$G = 2\mu \frac{k}{k-1} \frac{p_{in}}{\rho_{in}} \left[1-\left(\frac{p_{out}}{p_{in}}\right)^{\frac{k-1}{k}}\right] \qquad (2)$$

$$k = C_p/C_v$$

where μ = 0.65 is the parameter of the flow rate, k = 1.135 is the parameter of the steam capacity, C_p and C_v are the heat capacity of the steam at constant pressure and volume respectively, p_{in} = 7.05 MPa is the internal pressure, p_{out} is the outlet steam pressure, ρ_{tv} = 36.9 kg/m³ is the density of the steam in the piping.
The outlet pressure of the steam is determined from the critical condition p_{out}/p_{in}= 0.5.

Using conservative data the values of A_p and corresponding values of crack lengths L_p resulting in the postulated leakage Q_p were determined. The calculation results are given in **Table 7**.

4.2. Crack stability analysis

In accordance with the procedure M-LBB-01-93 for the first stability check, a crack size of $2L_p$ is subjected to normal

Table 7. LBB Analysis Results

						R6-Method	
						Moments Method	
Steam line-Section	Crack Length along midsurface L_p (mm)	L_{c1} (mm)	L_{c2} (mm)	Margins (N+SSE) loads	1.4(N+SSE) loads	L_{c1} (mm)	Margin (N+SSE) loads
1-1	63	169.9	104.0	2.7	1.6	338	5.4
1-2	63	190.2	122.6	3.0	2.0	384	6.1
1-3	58	177.5	113.2	3.0	2.0	354	6.1
1-4	60	190.5	123.7	3.2	2.1	384	6.4
2-1	84	244.6	164.1	2.9	2.0	496	5.9
2-2	80	242.8	168.9	3.0	2.1	579	7.2
2-3	81	226.8	154.5	3.4	2.3	460	5.7
2-4	75	230.6	155.1	3.1	2.1	467	6.2
3-1	74	197.3	123.5	2.7	1.7	403	5.4
3-2	72	253.0	178.1	3.5	2.5	508	7.0
3-3	81	225.2	148.5	2.8	1.8	458	5.6
3-4	70	243.8	169.6	3.5	2.4	401	5.7
4-1	63	133.3	71.4	2.1	1.1	247	3.9
4-2	60	194.0	126.4	3.2	2.1	392	6.5
4-3	63	204.4	135.1	3.2	2.1	415	6.6
4-4	61	203.0	134.0	3.3	2.2	410	6.7
4-5	90	256.8	171.2	2.8	1.9	521	5.8

(N) plus seismic loads, for the second stability check, a crack size of L_p is subjected to 1.4 (N+SSE) loads. Therefore it is necessary to calculate a critical crack size L_c for these two cases.

The stability of the postulated crack and design LBB criterion can be demonstrated if the two conditions are fulfilled simultaneously

$$L_p/L_{c1} \text{ and } L_p/L_{c2} \quad (3)$$

where L_{c1} and L_{c2} are the critical crack sizes for (N+SSE) loads and 1.4 (N+SSE) loads, respectively.

The UK two-parameter R6 procedure [9] and Moments Method [10] were used for calculation of the critical crack sizes. In the first case Option 1, Category 1 (conservative assessment) was used. Taking into account a dependence of elastic fracture parameter K_R on weld residual stresses σ_x, value σ_x is assumed as secondary axial stress being equal conservatively to 20% of yield stress $R_{p\,0.2}$.

Using Moments Method the analysis was made without reference secondary weld residual stresses because for a ductile material behavior it is postulated that the failure occurs when the effective primary stress at the relevant location produced by external loading (internal pressure, deadweight and SSE load) reached locally the flow stress of the material σ_f. Conservatively thermal expansion stresses were taken into account in this calculation. The analysis was performed with flow stress value as the average of the yield and ultimate strengths.

The calculation results are given in **Table 7**. The results made by the R6 procedure using Opt.1, Cat.1 are more conservative than Moments Method ones. Both methods indicate that the crack stability criteria (3) are met for all welds. Critical cross-section is the site of steam generator-pipe connection in line No 4. So, for the R6 procedure the minimum stability margin (L_{c1} / L_p) in this place for combined (N+SSE) load case is 2.1 and the margin for the 1.4 (N+SSE) load case (L_{c2} / L_p) is 1.1.

5. REQUIREMENTS FOR FURTHER WORK

Research work undertaken in Russia last years has shown that it is not necessary to assume a full guillotine break in steamlines if the LBB behavior can be demonstrated with a sufficient confidence and if sufficient engineering procedures are in place. For the development of LBB safety case, it is necessary to take into account the degree and frequency of in-service inspection and environmental effects. The LBB case can be demonstrated by a range of experiments and tests on full size pipes with cracks. The tests would validate data on corrosion and crack growth resistance, crack initiation toughness and J-R curves for base and weld materials. In addition to these studies it is necessary to validate fracture mechanics and leak rate calculations. Consideration should also be given to assessment of detectability, sensitivity and accuracy of the LDS. Capability of the LDS should be assessed and validated in place for each advanced nuclear power plant. These activities and further tests are included in the current research program.

REFERENCES

1. Kiselev V.A., Application of Leak-Before-Break Concept to Integrity and Safety of PWR Primary Piping with WWER 1000, Nucl.Eng.Des. 151 (1994) 409-424.
2. Rules and manufacture and safe operation of NPP equipment and pipes PN AE G-7-08-89, Moscow, Energoatomizdat, 1990, 168 pp. (In Russian).
3. NPP equipment and pipes. Welded joints and cladding. Basic rules. PN AE G-

7-009-89, Moscow, Energoatomizdat, 1991, 320 pp. (In Russian).
4. NPP equipment and pipes. Welded joints and cladding. Examination rules. PN AE G-7-010-89, Moscow, Energoatomizdat, 1991, 320 pp. (In Russian).
5. Norms for NPP equipment and pipe strength calculation. PN AE G-7-002-89, Moscow, Energoatomizdat, 1989, 525 pp. (In Russian).
6. Leak-Before-Break Evaluation Procedures. Standard Review Plan 3.6.3. The US Nuclear Regulatory Commission. Federal Register, v.52, No. 167, August 1987.
7. ECS MAE RDIPE, Piping Calculation Procedure for Nuclear Power Plants within the "Leak-Before-Break" Concept, M-LBB-01-93, Moscow, 1993.
8. VNIIAES, NIKIET, Method for Determination of Allowable Equipment and Pipe Metal Defects during NPP Operation, M-02-91, Moscow, 1991 (in Russian).
9. I.Milne, R.A.Ainsworth, A.R.Dowling, A.T.Stewart. Assessment of the Integrity of Structures Containing Defects. CEGB Report R/H/R6, Rev.3, UK, 1986.
10. Roos E., et. al. Assessment of Large Scale Pipe Tests by Fracture Mechanics Approximation Procedures with regard to Leak Before Break, Nucl.Eng.Des. 112 (1989) 183-195.
11. The Pipe Break Task Group. Evaluation of Potential for Pipe Breaks. Report of the US Nuclear Regulatory Commission Piping Review Committee. NUREG-1061, v. 3, 1984.
12. Beandoin B.F., et.al. Leak-Before-Break Application in Light-Water-Reactor Plant Piping, Nucl. Safety 30 (1989) 189-200.
13. Applicability of the leak Before Break Concept. IAEA-TECDOC-710, 1993.
14. P.C.Paris and H.Tada. The application of Fracture Proof Design Methods Using Tearing Instability Theory to Nuclear Piping Postulating Circumferential Through Wall Cracks. NUREG/CR-3640 (1983).
15. Troyanovsky B.N. Steam and Gas Turbines of NPP. Moscow, Energoatomizdat, 1985 (In Russian).

LBB CONSIDERATIONS FOR A NEW PLANT DESIGN

S. A. Swamy, P. R. Mandava, D. C. Bhowmick, D. E. Prager
Westinghouse Electric Corporation
Nuclear Technology Division
Pittsburgh, PA U.S.A.

Abstract

The leak-before-break (LBB) methodology is accepted as a technically justifiable approach for eliminating postulation of Double-Ended Guillotine Breaks (DEGB) in high energy piping systems. This is the result of extensive research, development, and rigorous evaluations by the NRC and the commercial nuclear power industry since the early 1970s. The DEGB postulation is responsible for the many hundreds of pipe whip restraints and jet shields found in commercial nuclear plants. These restraints and jet shields not only cost many millions of dollars, but also cause plant congestion leading to reduced reliability in inservice inspection and increased man-rem exposure. While use of leak-before-break technology saved hundreds of millions of dollars in backfit costs to many operating Westinghouse plants, value-impacts resulting from the application of this technology for future plants are greater on a per plant basis. These benefits will be highlighted in this paper. The LBB technology has been applied extensively to high energy piping systems in operating plants. However, there are differences between the application of LBB technology to an operating plant and to a new plant design.

In this paper an approach is proposed which is suitable for application of LBB to a new plant design such as the Westinghouse AP600. The approach is based on generating Bounding Analyses Curves (BAC) for the candidate piping systems. The general methodology and criteria used for developing the BACs are based on modified GDC-4 and Standard Review Plan (SRP) 3.6.3. The BAC allows advance evaluation of the piping system from the LBB standpoint thereby assuring LBB conformance for the piping system. The piping designer can use the results of the BACs to determine acceptability of design loads and make modifications (in terms of piping layout and support configurations) as necessary at the design stage to assure LBB for the piping systems under consideration.

1.0 INTRODUCTION

The U.S. Regulatory requirements for postulated pipe ruptures have changed significantly since the first nuclear power plants were designed. The pipe rupture design requirements on nuclear power plants are responsible for numerous pipe whip restraints and jet shields associated with each plant. These pipe whip restraints and jet impingement barriers cause significant plant congestion, increased labor costs (in design, fabrication, installation and maintenance) and increased radiation dosage for normal maintenance and inspection. The pipe rupture design requirements have also influenced the design of compartments and subcompartments.

Extensive research, development and rigorous evaluations by the NRC and the commercial nuclear power industry since the early 1970's resulted in the application of leak-before-break technology (LBB) which involves a demonstration by analysis that the detection of small flaws, either by inservice inspection or by leakage monitoring systems, is assured long before the flaws can grow to critical or unstable sizes. Consistent with the development of the LBB technology, the NRC formally revised General Design Criterion 4, "Environmental and Missile Design Basis," in October 1987 [1] to permit the exclusion of dynamic effects associated with postulated pipe ruptures form the design basis when analyses reviewed and approved by the NRC demonstrate that the probability of fluid system piping rupture is extremely low under conditions consistent with the design basis for the piping. The LBB approach has been extensively used to eliminate postulation of breaks from the structural design basis of PWRs because of the safety benefits and economic benefits.

2.0 ECONOMIC IMPACTS ASSOCIATED WITH THE SAFETY BENEFITS

The economic impacts associated with the safety benefits are highlighted in Reference 1 as follows:

"For existing PWRs, considering primary coolant loops only, cost savings of $186 million and reduction of 34,000 man-rem are estimated for a population of 85 PWRs. These figures do not include savings resulting from redesign of heavy component supports." The NRC further states, "Value-impacts resulting from this rule are greatest for future plants, where estimated costs can be reduced approximately $100 million per unit." The NRC determines the acceptability of the LBB applications and to assist licensees in implementation of the LBB approach, the NRC issued general acceptance criteria in the form of NUREG-1061 Volume 3 [2] and proposed Standard Review Plan [3]. As stated earlier the LBB technology has been applied extensively to high energy piping systems in operating plants. However, there are differences between the application of LBB technology to an operating plant and to a new plant design. On a simplistic basis, for an operating plant the material, loads and leak detection systems are pre-existing prior to initiating LBB analyses. On the contrary, for a new plant design these parameters can be selected to enhance success of LBB applications. For an operating plant the LBB calculations are performed for an existing piping configuration with associated loads whereas for a new plant a method needs to be developed which will provide an acceptability of a piping system configuration prior to the design stage. The margins recommended in Reference 3 must also be met.

3.0 APPROACH

In this paper an approach is proposed which is suitable for application of LBB to a new plant design. The approach is based on generating Bounding Analysis Curves (BAC) for the "candidate" piping systems. The candidacy of the piping system is established [3,4] by ensuring that the piping system is not particularly susceptible to degradation due to Intergranular Stress Corrosion Cracking (IGSCC), Erosion-corrosion, Water Hammer and Low and High cycle fatigue. The material selected for the piping and the associated welds must have adequate toughness consistent with the method used for flaw stability evaluation. This paper concentrates on the loading aspects of the design. High material toughness is assured by selecting appropriate materials for the base metal and welds.

The BAC allows for the evaluation of the piping system in advance of the final piping analysis, incorporating LBB considerations early into the piping design process. The LBB BAC is developed prior to the piping design and analysis and is used to evaluate critical points in the piping system. A minimum of two points are required to develop the BAC. Typically one point is selected to represent the low normal stress condition and the other point represents high normal stress condition. If any variation in pipe size, material, pressure and temperature occurs for a specific piping system, an additional BAC must be generated. The BACs are generated by incorporating the following margins:

- Margin of a factor of 10 on Leak Detection Capability
- Margin of a factor of 2 on flaw size
- Margin of a factor of $\sqrt{2}$ on loads. This margin is reduced to 1.0 if the maximum loads are obtained by using the absolute load combination method. The latter criterion is used in this study.

4.0 DEVELOPMENT OF BAC

The applicable material strength properties are compiled for the candidate piping system. Specific steps of the evaluation are described below:

- Using normal operating pressure, establish the applicable axial force F_p
- Assume a low magnitude of Bending Stress
- Calculate corresponding bending moment
- Calculate the leakage flaw size which yields leakage of 10 times the leak detection sensitivity. The leak detection sensitivity of Westinghouse new generation PWRs (AP600) is 0.5 gpm.
- Perform flaw stability analysis by keeping F_p constant and by varying the applied bending moment such that the critical flaw size is twice the leakage flaw size.

- Determine total normal stress and corresponding maximum stress and plot this information as point 1 on the BAC.

- The same steps are performed for point 2. The variation between points results from the increase in the assumed bending stress and corresponding higher bending moment.

- The BAC is the straight line between points 1 and 2. For a smooth curvefit between these points, these steps can be repeated for intermediate levels of bending stress.

Figure 1 shows a typical BAC.

5.0 LOADING COMBINATIONS FOR BAC

- Determine the highest maximum stress location which is identified as the critical location.

- Determine number of BACs needed for each analyzable piping system using the parameters of pipe size, pipe schedule, operating pressures and operating temperatures

- Determine load combinations for the maximum stress calculation by absolute summation method at the critical location

  |Pressure| + |Deadweight| + |Thermal (100% Power)| + |SSE|

- Determine corresponding normal stress at the critical location

  (1) Pressure + Deadweight + Thermal (100% Power) by algebraic summation method.

- Calculation of stresses

  The stresses due to axial loads and bending moments are calculated by the following equation:

  where:

$$\sigma = \frac{F}{A} + \frac{M}{Z}$$

σ	=	stress
F	=	axial load
M	=	bending moment
A	=	cross-sectional area
Z	=	section modulus

The bending moments for the desired loading combinations are calculated by the following equation:

$$M = \sqrt{M_Y^2 + M_Z^2}$$

where:

M	=	bending moment for required loading
M_Y	=	Y component of bending moment
M_z	=	Z component of bending moment

The axial load and bending moments for the normal case and maximum load case are computed by using the loading components and methods shown above.

6.0 TYPICAL RESULTS

Using the steps of the BAC evaluation procedure described above, a typical bounding analysis curve is constructed as shown in Figure 1. This curve is constructed for a 254 mm (10") diameter pipe subjected to 15.50 MPa (2250 psia) pressure and 316°C (600°F) temperature. The normal operating stress and the maximum stress at the critical location can be plotted on the BAC to determine the LBB qualification.

For example, in Figure 1, the stress level represented by point X qualifies the piping for LBB whereas the point Y does not meet the LBB criteria.

7.0 CONCLUSION

An approach is presented which is suitable for application of LBB to a new plant design. The approach is based on generating a bounding analysis curve for the candidate piping system. The BAC is developed independently from the actual piping design analysis. This feature is beneficial since the application of the BAC during the piping design layout phase permits optimization of design by eliminating unnecessary pipe whip restraints and jet impingement devices. The optimized design results in significant cost savings.

Another benefit is decreased analysis time to the final design of piping systems. The BAC will allow rapid turnaround in modification of system configuration while satisfying the LBB criteria. If a system configuration does not satisfy the BAC, it is immediately clear that the configuration of supports or line routing must be modified to satisfy the curve.

8.0 REFERENCES

1. Federal Register Notice, "Modification of General Design Criterion 4 Requirements for Protection Against Dynamic Effects of Postulated Pipe Rupture," Volume 52, No. 207 (41288-41295), U. S. Nuclear Regulatory Commission, October 27, 1987.

2. NUREG-1061, Volume 3, "Report of the U. S. Nuclear Regulatory Commission Piping Review Committee, Evaluation of Potential Pipe Breaks," U. S. Nuclear Regulatory Commission, November 1984.

3. Standard Review Plan 3.6.3, "Leak-Before-Break Evaluation Procedure," U. S. Nuclear Regulatory Commission, as published in the Federal Register, Volume 52, No. 167 (32626-32633) August 28, 1987.

4. Wichman, K., Lee, S., 1990, "Development of U.S. NRC Standard Review Plan 3.6.3 for Leak-Before-Break Applications to Nuclear Power Plants," Int. J. Press. Ves. & Piping, Vol. 43 pp. 57-65.

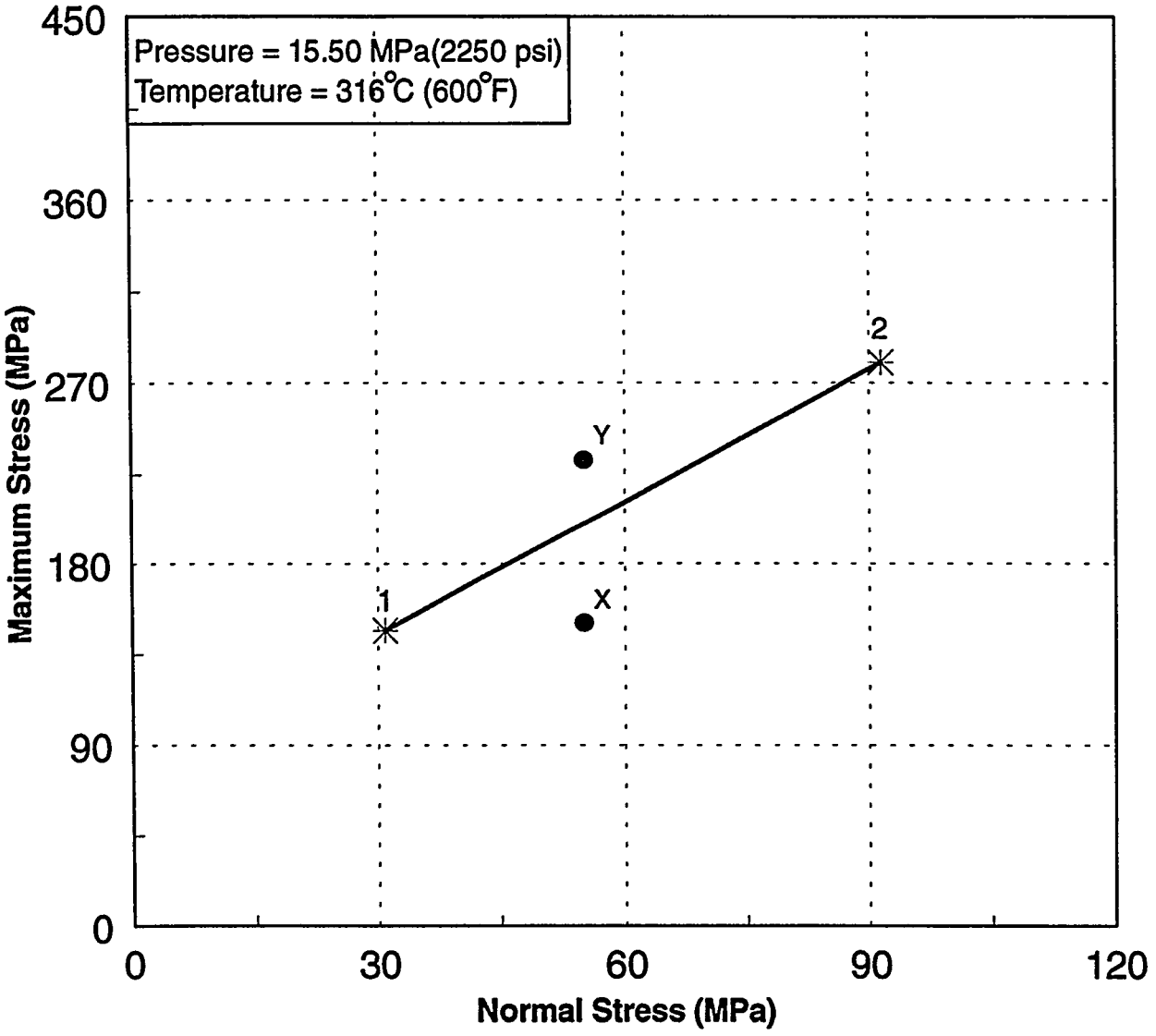

Figure 1 - Typical Boundary Analysis Curve (BAC) for 254 mm (10") Pipe

SESSION 2: TECHNIOCAL ISSUES IN LBB METHODOLOGY

DEFECT OCCURRENCE, DETECTION, LOCATION AND CHARACTERISATION; ESSENTIAL VARIABLES OF THE LBB CONCEPT APPLICATION TO PRIMARY PIPING

S. CRUTZEN, T.D. KOBLE, P. LEMAITRE, K. TÖRRÖNEN

1. INTRODUCTION

Applications of the Leak Before Break (LBB) concept involve the knowledge of flaw presence and characteristics (1) (2). In Service Inspection is given the responsibility of detecting flaws of a determined importance to locate them precisely and to classify them in broad families. Often LBB concepts application imply the knowledge of flaw characteristics such as through wall depth; length at the inner diameter (ID) or outer diameter (OD) surface; orientation or tilt and skew angles; branching; surface roughness; opening or width; crack tip aspect. Besides detection and characterisation LBB evaluations consider important the fact that a crack could be in the weld material or in the base material or in the heat affected zone. Cracks in tee junctions, in homogenous simple welds and in elbows are not considered in the same way (3) (4).

Figure 1 illustrates these essential variables of a flaw or defect and shows some examples of flaws found in primary piping as reported by plant operators or service vendors.

If such flaw variables are important in the applications of LBB concepts, essential is then the knowledge of the performance achievable by NDE techniques, during an ISI, in detecting such flaws, in locating them and in correctly evaluating their characteristics.

2. DETECTION OF FLAWS IN PIPING COMPONENTS

2.1. Parameters for NDE effectiveness presentation

Typical LBB concept applications consider or conclude that large cracks must be detected by means of routine NDE before growing to critical dimensions. Two parameters have to be considered to evaluate the detection capability of such flaws called large cracks:

a. the length or, often, the circumferential extent of the crack (2c or DY)
b. the depth of the cracks (a or DZ).

In general, values considered are such that DY is larger than 20 degrees in piping and even more than 500 mm in pump casings. DZ is larger than 10% wall thickness (T) in several cases but considered up to 70% T in several experiments or evaluations (5) (6) (7).

For NDE techniques based on ultrasonics, the circumferential extent of the crack looses its importance for detection when the crack length is of the order of the ultrasonic beam diameter. This happens with 20mm long cracks.

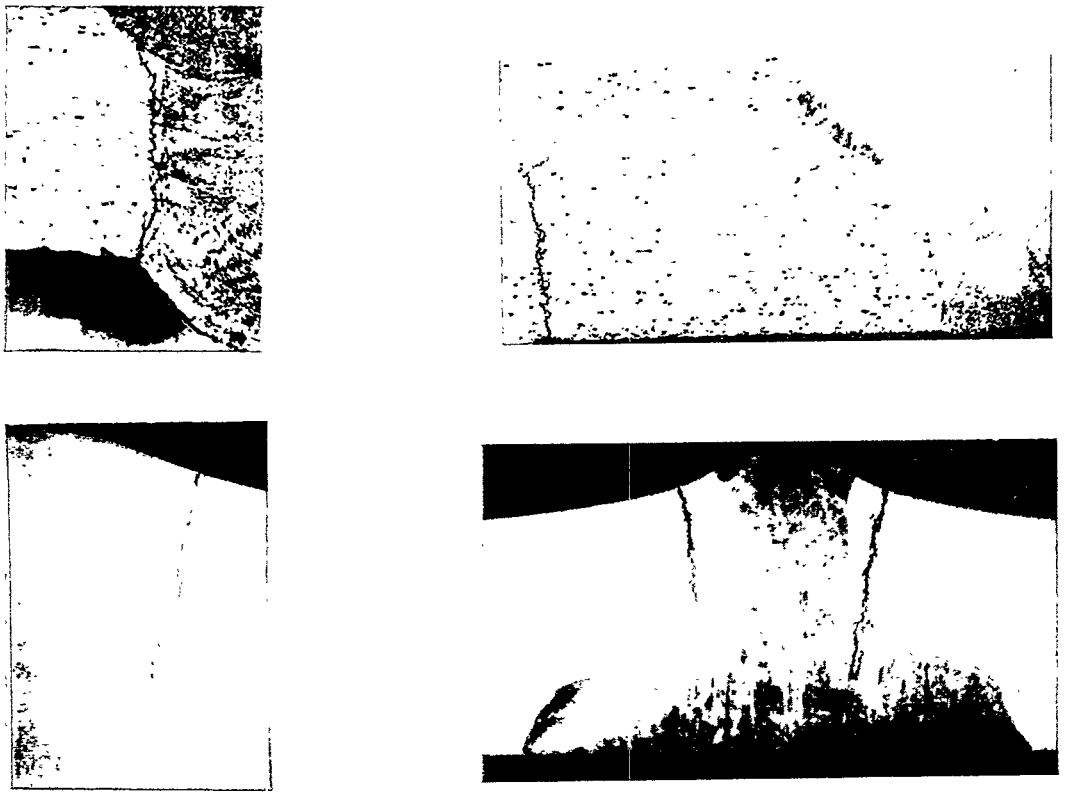

Typical IGSCCs found in a BWR primary piping weld

Mechanical fatigue crack
in a BWR primary piping

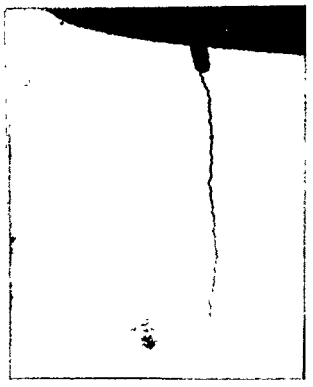

Thermal fatigue crack (with starter notch) in
a primary piping assembly

Figure 1. Real flaws in primary piping

Assemblies 31 - 36 made of wrought steel (BWR type)

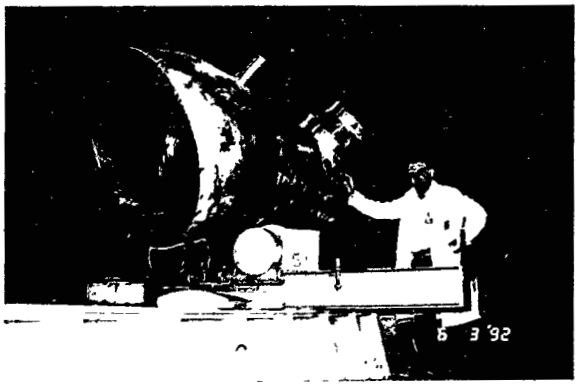

Assembly 51 combining wrought and cast steel (PWR type)

Assemblies 41,42,43 made of centrifugally cast steel (PWR type)

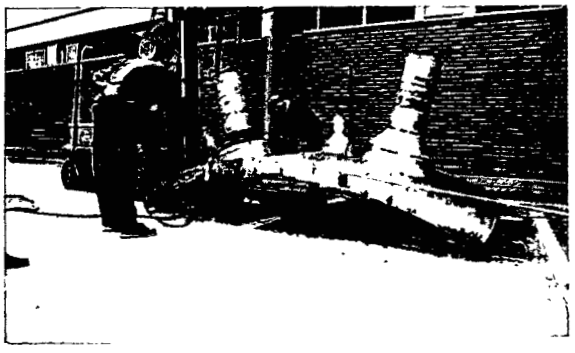

Assembly 20 containing two safe-end welds (BWR type)

Figure 2: PISC assemblies used for the primary piping and safe-end welds inspection procedures effectiveness assessment

The parameter to be used for presentation and discussion of NDE results is thus the flaw depth expressed as a percentage of the wall thickness

Obviously variables such as crack type or family, crack position, crack tilt, skew angles can also be considered as parameters.

During several NDT exercises, other parameters were used to quantify detection capabilities: the Flaw Detection Frequency, FDF, (for one procedure) or the Flaw Detection Probability, FDP (for one flaw considered by a large number of teams or techniques). Often Inspection Performance is used as well which means detection capability and acceptable evaluation according to the ASME XI criteria.

Besides safety of detection, economy aspects were considered as well: false calls leading to rejection are the basis for a parameter called False Call Rate in Rejection, FCRR.

To quantify sizing performance presentation pure sizing capabilities evaluations were often made which showed the measured sizes (in depth, DZ, and length, DY) compared to the reference.
Moreover, for the assessment of the sizing performance for the depth and the length of the flaws a linear regression analysis was performed. From this the following parameters are obtained:

- slope of the regression line between the real flaw length (depth) and the measured one
- intercept of the regression line with the Y-axis
- correlation coefficient, calculated for the regression line.

Also the RMS (Root-Mean-Square) error was used to assess the sizing performance.

2.2. PISC III detection results of the primary piping welds inspection

2.2.1 The exercise

Within the framework of Action 4 of the third phase of the Programme for the Inspection of Steel Components (PISC III) three capability studies on stainless steel welded assemblies (Figure 2) have been conducted (8) (9) (10). The first capability study used a series of 6 wrought-to-wrought stainless steel assemblies that contained a number of flaws such as intergranular stress corrosion cracks, mechanical and thermal fatigue cracks and PISC type A flaws. The second capability study used two wrought-to-cast austenitic steel assemblies that contained lack of fusion flaws and PISC type A flaws. The third capability study used three cast-to-cast austenitic steel assemblies that contained lack of fusion flaws, mechanical fatigue cracks and PISC type A flaws. In total more than 25 teams from 10 different countries participated. Much information was obtained on the performance of the inspection techniques used with respect to detection, false calls, depth and length sizing. Different flaw categories were considered to identify those difficult to detect. Furthermore, an analysis at the level of techniques was performed which identified some of the more effective techniques and procedures.

Several fabrication processes were used to introduce the flaws. Special attention has been devoted to the zones where different teams reported false calls.

2.2.2. Welds of Wrought Stainless Steel Pipe Sections

The six wrought-to-wrought assemblies (diameter 320 mm) are shown in Figure 2. These piping assemblies are typical of Boiling Water Reactor (BWR) primary piping.
The type of material used was wrought AISI 304. The wall thickness of the tubes varied between 10 and 25 mm. In total 26 flaws were introduced of which 12 are intergranular stress corrosion cracks (IGSCCs) amongst which 5 are of the complex type each comprising several branching cracks with separate openings to the surface, 4 fatigue cracks, 7 PISC type A flaws, 2 embedded notches and 1 lack-of-weld root penetration. Most of the flaws were close to either the weld root or the counterbore.

Figure 3 shows the detection performance versus the false call performance for the wrought-to-wrought assemblies. In this type of representation the optimum performance is located in the upper left corner (CRF $\geq$ 0.8, FCRR $\leq$ 0.2).

Half of the teams detected more than 75% of all the flaws present. Furthermore all flaws above 7 mm in depth were detected with an FDP equal or larger than 0.9. These results show that the detection performance in general was quite good (Figure 4).

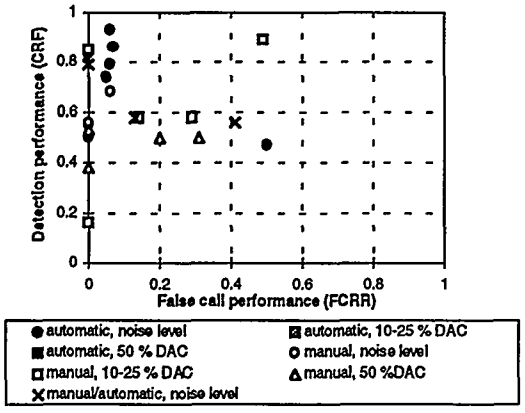

Figure 3: Inspection performance: Detection performance (safety aspects) versus false call performance (economical aspects)

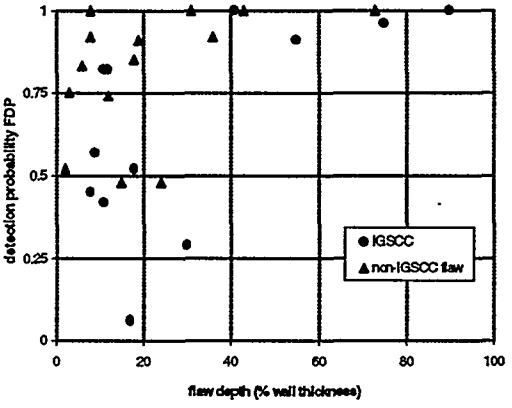

Figure 4: FDP as a function of flaw depth (considering all defects)

There was a large scatter in the data including the cases where teams used similar procedures. It was, however, confirmed that working at 50% DAC in general does not lead to good inspection results. Most of the teams that did well for detection, false calls and correct sentencing all used an automated procedure and worked at noise level, as shown in Figure 3.

The flaws difficult to detect were complex IGSCCs, axial IGSCCs and notches in the weld (Figure 4). There was no significant difference in performance for detection or false calls between the IGSCCs and the non-IGSCCs flaws. The evaluation at the level of individual techniques provided useful insights into how best to inspect these stainless steel components and welds (6).

2.2.3. Welds of Cast Stainless Steel Pipe Sections

The second capability study deals with cast-to-cast welded assemblies (Figure 2). These assemblies are typical of PWR primary piping.

They contained mechanical fatigue cracks, PISC type A flaws (EDM notch), lack of interrun fusion flaws and side drilled holes (SDH) filled with weld material simulating lacks of sidewall fusion.

These assemblies contained mainly two different grades of centrifugally cast stainless steels obtained from two different heats of the same manufacturer. Equiaxial and columnar structures were considered.

Figure 5 shows detection performance versus false call performance for the cast-to-cast assemblies. Note again that in this type of representation the optimum performance is located in the upper left corner. Good performance appears possible. The better teams all used mechanised scanning equipment and worked at noise level.

Detection of flaws as a function of the through wall extent is given in Figure 6.

Techniques have to be selected and combined to constitute an effective procedure as indicated by this PISC exercise (10).

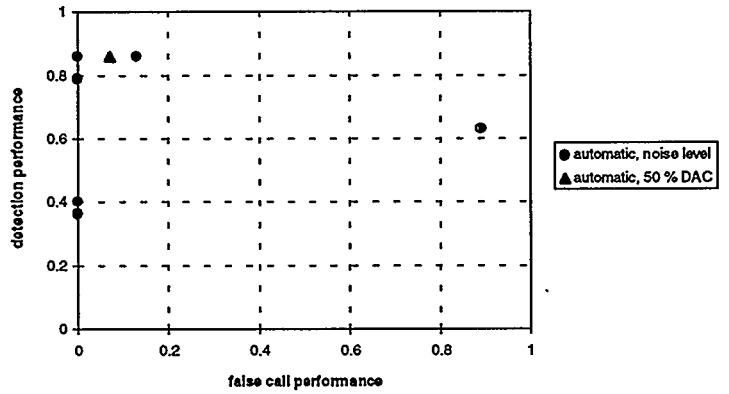

Figure 5: Inspection performance = Detection performance (safety aspects) versus false calls (economical aspects) on a team-by-team basis for the austenitic cast-to-cast assemblies

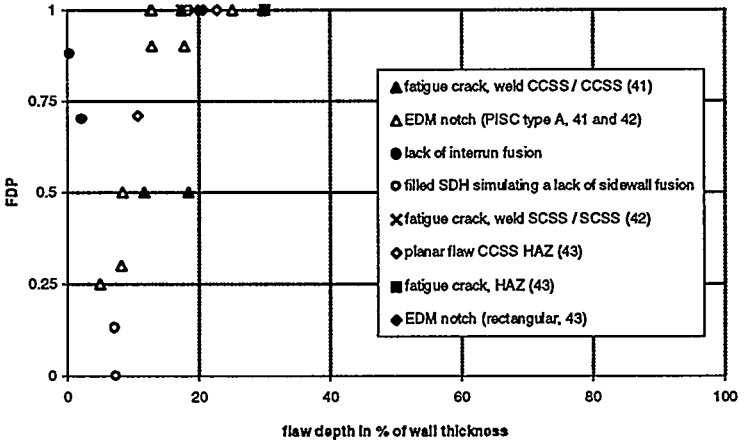

Figure 6: Flaw Detection Probability (FDP) as a function of the through wall extent of the flaws given in % of the wall thickness for the cast-to-cast assemblies

2.2.4 Welds of Cast and Wrought Stainless Steel Pipe Sections

The assembly shown in Figure 2 weighed 5750 kg which created some difficulty in handling. The assembly was nearly 3 meters long and 1 meter in diameter. The outer diameter of Assembly 51 was 937 mm. The wall thickness varied between 70 and 82 mm. Eight teams from 7 different countries participated in the Round Robin Test. The assembly contained 11 PISC type A flaws (EDM notches) and 4 internal lack of fusion flaws distributed over the two welds. Most of the flaws were located either in the weld material or in the heat affected zone (HAZ).

Figure 7 shows detection performance versus false call performance for the wrought-to-cast welds. Note again that the optimum performance is located in the upper left corner. The better teams worked at noise level and two of these 3 used mechanised scanning equipment.

The false call performance was very good. Most teams made only a few false calls. One team however, performed badly.

As shown in Figure 8, the detection performance for the rejectable flaws (through wall extent larger than 10% of the wall thickness) was very good. 70% of the teams detected them all.

The following flaws were difficult to detect

- lack of interrun fusion
- EDM notches (PISC type A) present in the HAZ of the statically cast stainless steel
- filled SDH's to simulate lack of sidewall fusion.

Again, several techniques are necessary to reach good detection of the different types of flaws located in different positions (9).

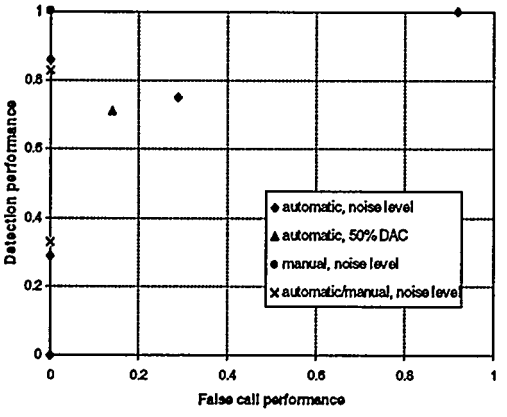

Figure 7: Inspection performance = Detection performance (safety aspects) versus false call performance (economical aspects) on a team-by team basis for the austenitic wrought-to-cast assemblies

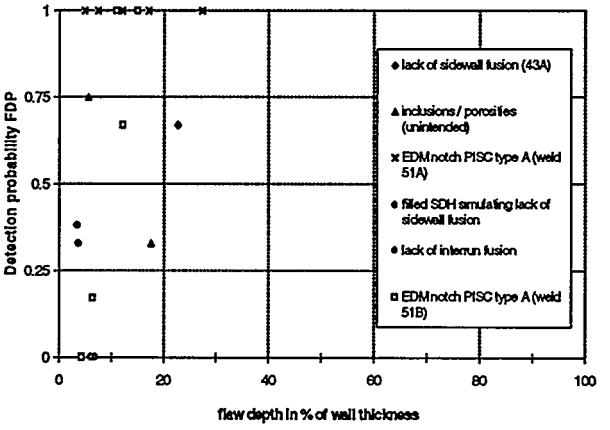

Figure 8: Flaw Detection Probability (FDP) as a function of the through wall extent of the flaws given in % of the wall thickness

2.3. PISC III Detection Results of Safe-Ends Areas Inspection

Three safe-end specimens were made available for the RRT. As a rule, drawings, materials and manufacturing procedures typical of the nuclear industry were used for the fabrication. All nozzle ends were stainless steel cladded and Inconel buttered, and all dissimilar metal welds were made from Inconel (11) (12) (13) (14) (Figure 2).

A total of 25 flaws had been intentionally introduced in the three assemblies (total of four safe-ends): 3 in the thermal sleeve area, 13 in the dissimilar metal welds and 9 in the homogenous welds. As the depth dimensions ranged from 10 to 50% of the wall thickness, only few of them were acceptable according to ASME XI article IWB-3514 (13). No flaw was intentionally introduced in the dissimilar weld nor in the homogenous weld of one safe-end.

Most flaws were planar reflectors, located close to the inside surface, and oriented perpendicular to it or parallel to the fusion lines, to simulate service-induced cracks. Also some sub-surface crack-like reflectors and some fabrication flaws, such as slag inclusions, were considered.

All flaws were fully certified to allow for a reliable assessment of the inspection capability. The certification process revealed additionally a number of unintended manufacturing flaws. A total of 47 reference flaws was recorded for the evaluation of the inspection data. Their characteristics and distribution make the specimens as a reasonable set for a performance demonstration test.

Figure 9 illustrates the average results obtained by all participating teams. Only a few of the teams reach a flaw detection frequency of 80%, whereas a significant number of false calls are reported.

Correlation between the inspection sensitivity and its capability is found in all cases.

During the round robin tests, access was allowed to the inner surface of the PWR-like safe-end. Four teams submitted data collected from this side only. Three of the four procedures applied from the inside were based on immersion focusing transducers; this procedure family demonstrated high inspection capability (Fig.9).

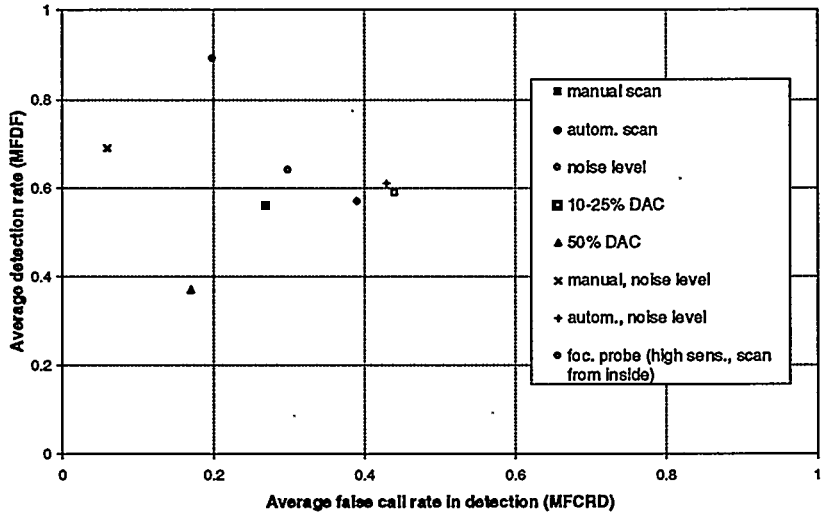

Figure 9: Average detection performance of different procedures

Taking all teams into consideration, Figure 10 shows the average probability of detection for each flaw, as a function of its depth dimension. Distributing flaws among categories, on the basis of their location and morphology, leads to the conclusion that the reflectors located in carbon steel or in wrought austenitic steel, far enough from welds, are much better characterised than those neighbouring or embedded in fused material.

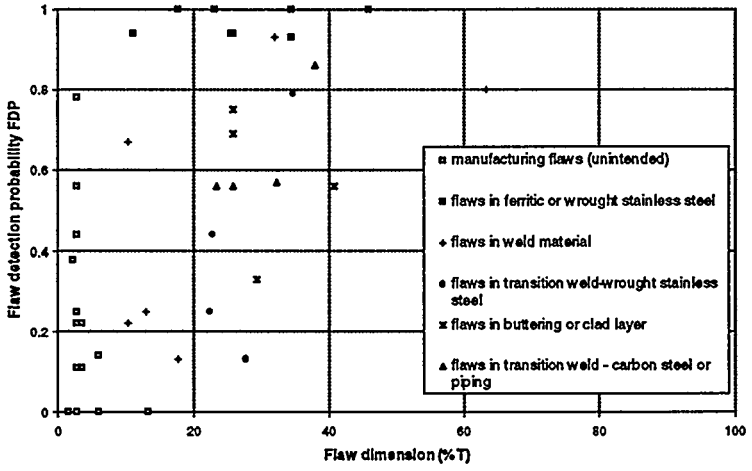

Figure 10: Flaw detection probability as a function of flaw depth in the PISC safe-end components.

Seemingly, flaws extending within the welds or along the safe-end fusion lines appear most difficult. Furthermore, it turns out that the detection of reflectors smaller than 2 mm (i.e. about 5% of the wall thickness) lies beyond the reach of today's common technology. This observation is confirmed by additional measurements done by some teams after the RRT.

2.4 PISC III results relative to flaw detection using Radiographic Techniques

For cast primary piping and cast-to-wrought steel welds, the detection performance of one team that used X-rays was very good (detection rate higher than 0.8). However, a relatively high number of false calls was made. The length sizing performance was also better than that of most of the teams which used ultrasonic techniques.

During the exercise on safe-ends, two teams provided radiographic inspection results, obviously with no depth sizing on a PWR type assembly. The flaw detection capability is similar to the average UT performance, but with a higher false call rate. In addition, it can be noted that the same flaws proved to be difficult for X-ray and ultrasonic testing.

It is to be noted that the Reference Laboratory of PISC inspected all assemblies of PISC in view of flaw certification and subsequent destructive examination. All flaws were detected except some acceptable ones (much less than 10% wall thickness). RL techniques, even if using industrial equipment, tend to reach maximum performance levels due to:

- preknowledge of defective areas characteristics
- parametrisation of the RT techniques
- set up of the most sensitive techniques for each particular case
- no time limitation for inspection and films examination.

3. SIZING OF FLAWS IN PIPING COMPONENTS

3.1. Sizing of Flaws in Primary Piping using Ultrasonics

3.1.1. Wrought Stainless Steel Piping Components

The assemblies and flaws described in 2.2. were used for the sizing exercise. Figure 11 shows the NDT measured flaw depth as a function of the real flaw depth for all flaws and teams. The large scatter between real size and NDT measured size shows clearly that the depth sizing performance was poor. In Figure 12 the slope of the regression line between NDT measured flaw depth and real flaw depth and the corresponding correlation coefficient are shown for all teams. A team can be considered to have a satisfactory depth sizing performance if the slope and the correlation coefficient is greater than 0.7. Figure 12 shows that only 4 teams were in this case. This confirms that the depth sizing performance in general was poor, though it should be stressed that some teams did well. These teams all had in common that they were able to detect crack tip diffraction.

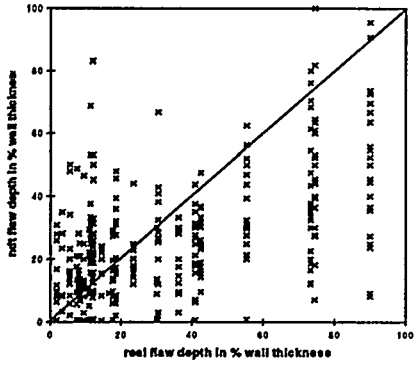

Figure 11: NDT measured flaw depth: Results for all teams and all flaws of the wrought-to-wrought capability study

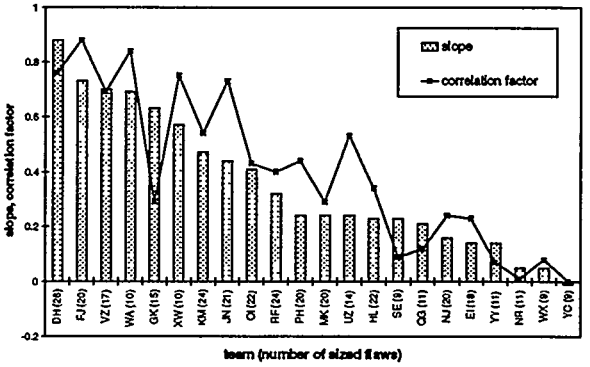

Figure 12: Regression analysis to quantify the depth sizing performance for the wrought-to-wrought assemblies: slope and correlation coefficient for the different teams. The number of flaws considered for each team is given in brackets.

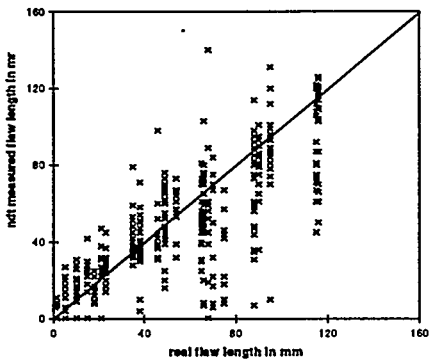

Figure 13: NDT measured flaw length. Results for all teams and all flaws of the wrought-to-wrought capability study

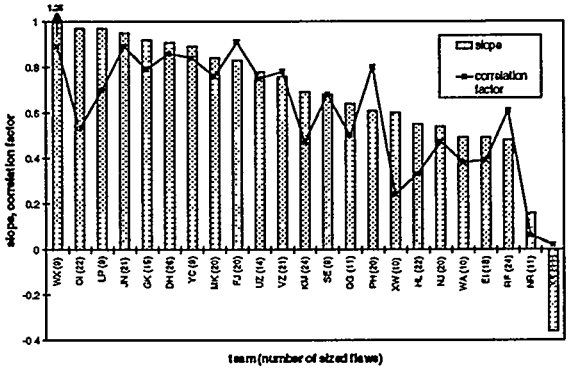

Figure 14: regression analysis to quantify the length sizing performance for the wrought-to-wrought assemblies: slope and correlation coefficient for the different teams. The number of flaws for each team is given in brackets.

Figure 13 shows the NDT measured flaw length as a function of the real flaw length for all flaws and all teams. The scatter is smaller than that for depth sizing showing that the performance for length sizing in general was better than that for depth sizing. The results of the regression analysis are shown in Figure 14.

3.1.2. Cast Stainless Steel Piping Components

Cast steel welded assemblies and cast and wrought steel welded assemblies were used to generate sizing performance evaluations as well. In general, performance in depth sizing is poor and correlation coefficients defined here above remain lower than 0.5 (0.3 is average). Length sizing was poor in cast steel assemblies where the correlation coefficient defined here above remained as low as 0.5 in the best cases. It is to be noted that one team performed well on the two welds of Assembly No. 51 using focusing probes.

3.1.3. Safe-Ends

Sizing capability in safe-ends is comparable to the one found in wrought stainless steel assemblies. Regarding the capability of flaw sizing in the through-wall direction, a slight tendency to oversize appears, on average, but the standard deviation is comparatively large. The overall dispersion of the sizing error is of the order of +/- 5 mm, as for the wrought steel piping.

Sizing in length was also better than depth sizing in the case of safe-end assemblies as was the case for the piping assemblies.

3.1.4 Sizing in Length with Radiographic Techniques

Length sizing with RT produced better results than the sizing of length with UT, but only 3 data sets are available.

3.1.5. Experts Declarations

A comparison was attempted between the actual flaw distribution and that reported by a virtual inspector matching the average performance of all teams (Figure 15). Disregarding the very small flaws, the total number of declared indications is roughly correct ; the actual peak in the range of 25 to 35% of the thickness is however flattened by the flaw sizing error.

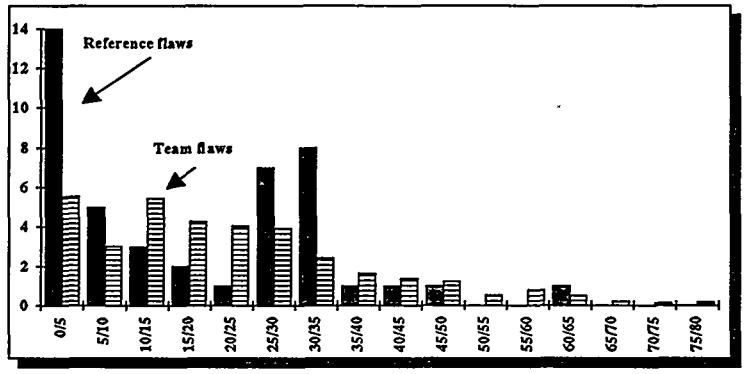

Figure 15: Comparison of depth size (size is given in % of wall thickness) distribution in all PISC Safe-end assemblies as obtained by (The diagram gives the number of flaws for a different depth intervals):
- destructive examination (Reference flaws)
- NDE and expert evaluation (Team flaw)
Critical size defects are apparently undersized.

4. ERROR OF LOCATION OF FLAWS.

Ultrasonic testing does not locate flaws in a perfect manner due to the principle of the techniques. Error of location of a circumferential flaw happens in the axial direction. If no clear geometrical indication is obtained as a reference from the weld root or from the counterbore extremities flaws can be mislocated of about +/- 5 mm as shown by the diagramme in Figure 16 for one of the most clean assembly made of wrought stainless steel and for a wall thickness less than 30 mm. In cast stainless steel, with wall thickness of more than 70 mm, this uncertainty reaches about +/- 10 mm, also in the axial direction (10).

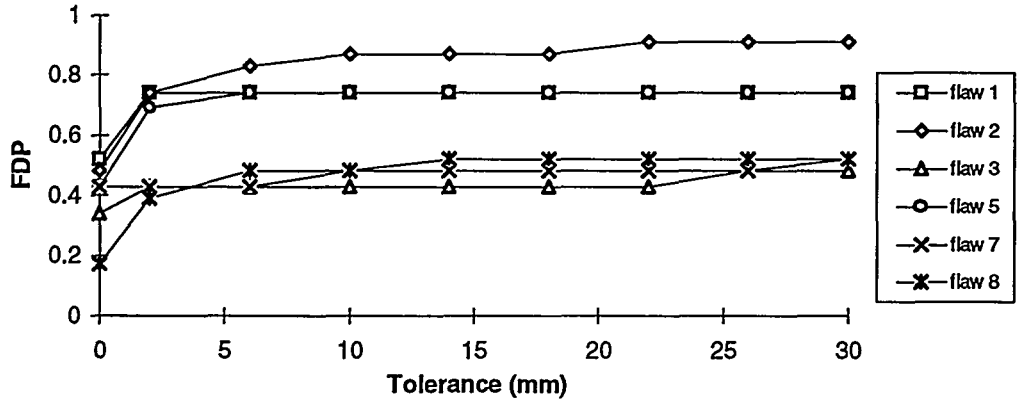

Figure 16: Flaw detection probability as a function of the tolerance on defect location

5. FLAWS CHARACTERISATION

NDE techniques are rarely effective for flaw characterisation. In PISC, inspection teams were asked to declare that a flaw was a crack or not. Generally, in the context of the exercise, declaring crack was often successful due to a conservative attitude. Procedures for flaw characterisation were however not found in the inspection process description.

6. OCCURRENCE OF FLAWS

Presence of flaws in primary piping was often revealed by plant operators and inspection companies. Reports were written about IGSCCs, fatigue cracks and erosion corrosion. Figure 1 illustrates some of these flaws.

However few full metallurgic expertises were made which describe the defects and relate them to the NDE results (15).

During the destructive expertise of components fabricated for NDE effectiveness evaluation exercises (Figure 2), flaws were found which were of planar type and reached up to 10% of the wall thickness. Such flaws were almost not detected by UT or by RT. The certainty that flaws are introduced by manufacturing and by service and the uncertain detection of them if the depth is less than 20-30% of the wall thickness implies that components could exist with defects of that range of depth.

7. CONCLUSIONS

In the context of flaw detection, sizing and characterisation for the LBB evaluation it seems reasonable to state the following:

- Procedures exist for effective detection of flaws in primary piping of nuclear reactors if such flaws are deeper than 30% of the wall thickness and have a length of 20 mm to 50 mm or more.

- Depth sizing of cracks is possible with well established procedures in wrought austenitic steel components. Uncertainty of +/- 3 mm is a good performance.

- Depth sizing of flaws in cast austenitic steel components is unsafe and rare good results appear to depend very much on the skill of a few experts.

- Length sizing of flaws is effective in all cases of material combinations, taking into account the tolerance accepted by an LBB evaluation.

- The difficult defects to detect remain the circumferential and axial IGSCC's and complex defects in the weld material.

- The large scatter in the data, in particular when one identical procedure is used by several teams, shows the potential danger of error and the necessity for a well managed and full quality controlled inspection.

- No substantial difference exists between detection and sizing of flaws in homogeneous welds and trimetallic welds (safe-ends).

- Classification of flaws in cracks and non cracks is often successful in wrought steel but no procedure, based on industrial techniques, was validated to date.

- Location errors that could displace defects from 10 mm away from their real location are frequent.

- Occurrence of defects is real but few cases were fully expertised. Fabrication of test assemblies revealed the unexpected presence of planar flaws at the limit of acceptance. Their uncertain detection reinforce their probability of presence in austenitic steel piping welds.

8. REFERENCES

(1) G. BARTOLOME, R. WELLEIN, G. SENSKI
LBB ANALYSIS; VERIFICATION OF FRACTURE MECHANICS APPROACHES BY COMPONENTS TESTING
SMiRT -12, Vol G, pp 393-398, Elsevier 1993

(2) J. ZSAEREK et al.
LARGE SCALE EXPERIMENTS TO SUPPORT THE APPLICATION OF THE LBB CONCEPT TO WWER 440 REACTOR PIPING
SMiRT - 12, Vol G, pp 387-392, Elsevier 1993

(3) G. YAGAWA and all
FRACTURE BEHAVIOUR OF CRACKED TYPE 304 STAINLESS STEEL PIPES UNDER TENSILE AND THERMAL LOADING.
Int. J. Pres. Ves. and Piping, Vol 19, pp 247-281

(4) B. BRICKSTAD AND M. BERGMAN
SOME ASPECTS OF PERFORMING LBB ANALYSIS OF FLAWS IN SWEDISH NUCLEAR POWER PLANT PIPING
Sissi 94, Saclay France, April 28-29, 1994

(5) G. BARTOLOME, W. KASTNER, E. KEIN AND G. SENSKI
LBB ANALYSIS: VERIFICATION OF LEAKAGE AREA AND LEAKAGE RATE EVALUATION BY TESTS
SMiRT -12, Vol G, pp 87-92, Elsevier 1993

(6) M.B. WRIGHT
MAGNOX REACTOR STEEL PRESSURE VESSELS: FRACTURE MECHANICS BASED ASSESSMENT PROCEDURE DEVELOPED IN THE U.K.
Saclay International Seminar on Structural Integrity, April 1994.

(7) I.MILNE, R.A.AINSWORTH, A.R. DOWLING AND A.T. STEWART
ASSESSMENT OF THE INTEGRITY OF STRUCTURES CONTAINING DEFECTS.
Int. J. Pres. Ves. Piping, 32, 1988 (latest version Rep R/H/R-Rev.3, Nuclear Electric plc, UK, 1995).

(8) P. LEMAITRE, T.D. KOBLE, S. DOCTOR
PISC III CAPABILITY STUDY ON WROUGHT-TO-WROUGHT AUSTENITIC STEEL WELDS: EVALUATION AT THE LEVEL OF PROCEDURES AND TECHNIQUES
Proceedings of the 1995 ASME Pressure Vessels and Piping Conference, PVP-Vol 317 NDE-Vol 14, pp 81-88, Honolulu, Hawaii (USA), July 23-27, 1995

(9) P. LEMAITRE, T.D. KOBLE, S. DOCTOR
MAIN RESULTS OF THE PISC III CAPABILITY STUDY ON WROUGH-TO-CAST AUSTENITIC STEEL WELDS
Proceedings of the 1995 ASME Pressure Vessels and Piping Conference, PVP-Vol 317 NDE-Vol 14, pp 39-52, Honolulu, Hawaii (USA), July 23-27, 1995

(10) P. LEMAITRE, T.D. KOBLE, S. DOCTOR.
MAIN RESULTS OF THE PISC III CAPABILITY STUDY ON CAST-TO-CAST AUSTENITIC STEEL WELDS
Proceedings of the 1995 ASME Pressure Vessels and Piping Conference, PVP Vol 317 NDE-Vol 14, pp 53-62, Honolulu, Hawaii (USA), July 23-27, 1995

(11) P. DOMBRET
PISC III RESULTS ON ACTION 3 "NOZZLE AND DISSIMILAR WELDS"
IAEA - OECD - CEC Specialist Meeting on NDE Effectiveness
JRC-IAM Petten, The Netherlands, March 1994, Kluwer

(12) PISC III Report No. 20 EVALUATION OF THE INSPECTION RESULTS OF THE PISC III SAFE-END ASSEMBLY NO. 20, EUR 15558EN, 1993

(13) PISC III Report No. 24. EVALUATION OF THE INSPECTION RESULTS OF THE SAFE-END AREAS OF THE PISC II ASSEMBLY NO. 24, EUR 15369EN, 1993

(14) PISC III Report No. 25. EVALUATION OF THE INSPECTION RESULTS OF THE PISC III SAFE-END ASSEMBLY NO. 25, EUR 15370EN, 1993

(15) M. CAMBINI, S. CRUTZEN, P. JEHENSON, X. EDELMAN
PISC III Report No. 15. INVESTIGATION ON FIELD REMOVED PIPE SECTIONS IN THE PISC HOT LABORATORIES, EUR 12922EN, 1990

CRACK SHAPE DEVELOPMENTS AND LEAK RATES FOR CIRCUMFERENTIAL COMPLEX-CRACKED PIPES

B. Brickstad, M. Bergman
SAQ Inspection Ltd, P O Box 49306 S-100 29 Stockholm, Sweden

ABSTRACT

A computerized procedure has been developed that predicts the growth of an initial circumferential surface crack through a pipe and further on to failure. The crack growth mechanism can either be fatigue or stress corrosion. Consideration is taken to complex crack shapes and for the through-wall cracks, crack opening areas and leak rates are also calculated. The procedure is based on a large number of three-dimensional finite element calculations of cracked pipes. The results from these calculations are stored in a database from which the PC-program, denoted LBBPIPE, reads all necessary information. In this paper, a sensitivity analysis is presented for cracked pipes subjected to both stress corrosion and vibration fatigue.

INTRODUCTION

The LBB-procedure described in this paper differs from the widely used concept expressed by USNRC in [1]. The starting point in [1] is to postulate a through wall crack of a simple shape and show that such a crack would lead to a detectable leak before failure. Thus the development of the crack before wall penetration is not considered. Usually a condition for using the procedure in [1] has been to exclude all degradation mechanisms such as stress corrosion or fatigue. In the procedure described in this paper the starting point is a surface crack (postulated or real) and a growth mechanism of fatigue or stress corrosion is considered. This procedure is more suitable when it is desired to investigate leak before break for real defects detected during inservice inspections in pipe systems.

LEAK BEFORE BREAK PROCEDURE

Here it is assumed that linear elastic fracture mechanics (LEFM) conditions prevail for the subcritical crack growth so that the stress intensity factor K_I can be used to describe the growth. This assumption implies that K_I can be calculated using the principle of superposition which states that the stress state due to two or more loads acting together is equal to the sum of the stresses due to each load acting separately. As a consequence of this, K_I can be calculated with respect to the elastic uncracked body stress state by applying the stress state as a pressure on the crack face. Note that the redistributions of stresses that occur due to the presence of a crack, growing or non-growing, does not imply that the principle of superposition for calculating K_I is invalid. This fact has been pointed out by Parker [2] for fatigue crack growth and demonstrated by Quinones and Reaugh [3] for stress corrosion crack growth.
At wall penetration of the surface crack and at final failure of the pipe plasticity are likely to be significant. Here it is assumed that criteria based on non-linear measures such as the J-integral and limit load are able to describe when these events occur.

Stage 1, growth of a surface crack

The surface crack is assumed to have a semi-elliptical shape as shown in Fig. 1. The crack front is described by a cylindrically transformed ellipse with the parameters a and $2c$ as the depth and length of the crack, respectively. Both experience and experiments, Nam *et al.* [6, 7] for fatigue cracks and Yagawa *et al.* [4] for stress corrosion cracks, indicate that the elliptical shape is reasonable for the crack growth mechanisms studied here. However, it is recognised that an initially semi-elliptical crack may during growth tend to deviate from its elliptical shape while the stress intensity factor solutions only are known for successive elliptical cracks. To overcome this problem a special

procedure by Nilsson [5] is used that fits the arisen crack shape to an assumed shape. The procedure is described in more detail in the paper by Bergman and Brickstad [8].

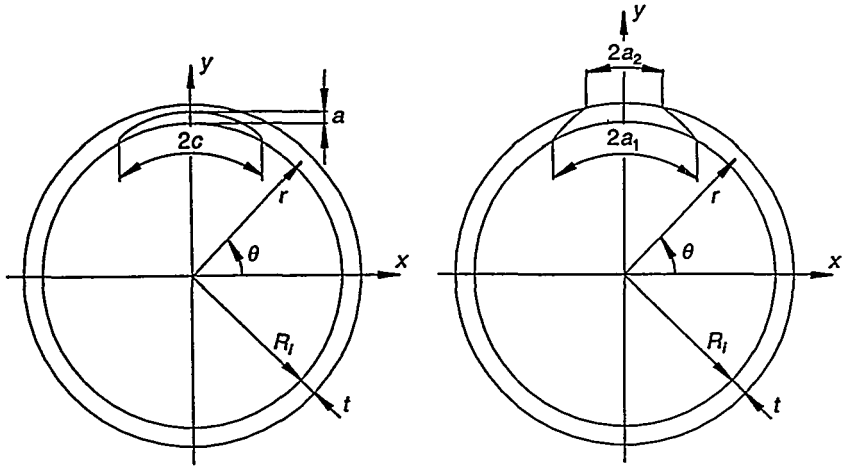

Fig. 1. Description of surface and leaking crack geometry.

Stage 2, wall penetration

After some time of growth the surface crack penetrates the pipe wall and leakage occurs. This is assumed to take place if either ductile crack growth or plastic failure of the ligament is predicted, i.e.

$$J \geq J_{Ic} \text{ or } P \geq P_L \tag{1}$$

Since materials used in nuclear piping usually show a high degree of ductility, the last relationship is believed to be the most limiting one. For simplicity reasons, J is estimated according to the option 1 type analysis of the R6-method [9].

$$J = \frac{(1-\nu^2)K_I^2}{E} \cdot \frac{1}{[f_{R6}(P/P_L)-\rho]^2} \tag{2}$$

where the second fraction on the right hand can be interpreted as a plasticity correction function based on the limit load P_L for the linear elastic value of J determined by K_I. Here P_L is a so-called local limit load solution by Sattari-Far [10] which predicts when a limited region of the ligament yields assuming an elastic-perfectly plastic material behaviour. Account is taken for materials that show a significant strain-hardening by defining the yield strength as the flow stress, here set to the mean value of the yield and ultimate tensile strength.

Since the validity of the stress intensity factor and limit load solutions are limited, wall penetration is also assumed to occur if

$$a \geq 0.9t \tag{3}$$

The surface crack is recharacterised to a through thickness crack with a shape as shown in Fig. 1 if either one of the conditions given in Eqs. (1) and (3) is fulfilled. The crack front of the leaking crack is described by a cylindrically transformed straight line with the parameters $2a_1$ and $2a_2$ as inner and outer crack length, respectively. The experiments reported in [4], [6] and [7] indicate that this shape is reasonable for leaking fatigue and stress corrosion cracks. Immediately after wall penetration, the crack is assumed to have the dimensions

$$2a_1^* = \text{surface crack length 2c just before wall penetration, } 2a_2^* = \min(2t, 2a_1/4) \tag{4}$$

The value of $2a_2^*$ is somewhat arbitrarily defined in order to ensure a sufficiently small outer crack length at wall penetration. If compared to the results by Nam *et. al* [7], the assumption seems reasonable (see Fig. 4).
Ductile crack growth may occur at the pointed ligament towards the outside of the pipe that arises for small values of the ratio a_2^*/a_1^*. If this is the case, the inner crack length is kept fixed and the outer crack length is gradually expanded while a quasi-static check is made if the crack becomes arrested, i.e. if J falls below J_{IC} for a crack with a larger outer crack length. The arrest crack size defines the initial size for the continuing subcritical crack growth of the leaking crack. As for the surface crack, J is estimated by the R6-method but here a so-called global limit load solution which predicts when the net section yields is used instead. The limit load solution is given in [8]. Here as well as in other parts of the procedure when initiation of ductile crack growth is analysed, it would be possible to take J controlled crack growth into account by use of an appropriate J_R-curve. But for simplicity reasons, this has not been utilised.

Stage 3, growth of a leaking crack to final failure
The initial geometry for this stage is given by the above criteria. The subcritical crack growth is continued until final failure of the pipe is predicted. This is judged to occur if either ductile crack growth is initiated and the crack growth is non-arresting, or if plastic failure of the net section is predicted.
At this stage also the crack opening areas (*COA*) at the in- and outside of the pipe are calculated. Together with information about the internal pressure, temperature, fluid and crack surface properties, *COA* is used to calculate the mass leak rate through the crack.
Situations may occur where the time between a detectable leakage and final failure is to short or the leakage to small to be detected before final failure. These two situations are identified by the procedure and although LBB occurs, it is not possible from a practical point of view to take credit of LBB. Small mass leak rates occur if the crack grows in such a fashion that the crack length on the outside becomes substantially smaller than on the inside, or if the distribution of the weld residual stresses leads to crack closure. Here, crack closure is assumed to occur if K_I becomes negative which is a reasonable assumption for stress corrosion cracks or for fatigue crack growth at high R-values as is the case for vibration fatigue ($R = K_I^{min}/K_I^{max}$). Aspects of fatigue induced crack closure due to plasticity are not considered.

NUMERICAL TECHNIQUE

In this section the numerical realisation of the procedure which resulted in a computer program denoted LBBPIPE will briefly be discussed. Further information can be found in [8]. A basic flow chart of the procedure is shown in Fig. 2.

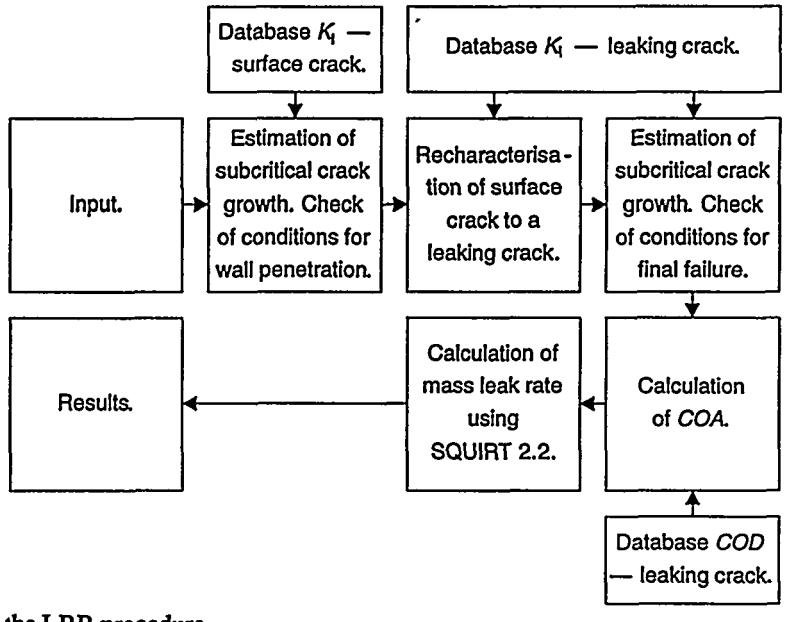

Fig. 2 Flow chart of the LBB procedure

Required input data are the dimensions of the pipe and the initial crack, material data as fracture toughness, elastic modulus, yield and ultimate tensile strength, loads expressed as the elastic stress state in an uncracked pipe divided into an axisymmetrical stress distribution through the thickness and global bending stresses, type of subcritical crack growth law and the value of its parameters and finally data needed for the mass leak rate calculations as fluid and crack surface properties, internal pressure and temperature.
As mentioned before the estimation of subcritical crack growth is done with a special procedure for approximate description of growth of cracks with complex shapes by Nilsson [5]. During this process, the conditions for wall penetration, recharacterisation and final failure as described before are checked for. Next for the obtained sizes of the leaking crack, *COA* at the in- and outside of the pipe are calculated by integrating the crack opening displacements (*COD*) and from that the mass leak rates are evaluated. The mass leak rate is calculated with a somewhat modified version of the program SQUIRT [11]. Results are presented in a tabular text and a special program can also be used to display how the crack size, crack opening area and mass leak rate vary as a function of time.
The database of K_I and *COD* was generated with the finite element method using the program ABAQUS [12]. A total number of 47 surface crack and 56 leaking crack geometry configurations were analysed. Three dimensional solids elements were used in the calculations and specific mesh generators were utilised that made the modelling more easy. In all cases, the pipe dimension ratio, R_i/t, was fixed to 8.6 corresponding to the dimension of the main circulation pipes in Swedish BWRs. The procedure may be used for moderately deviations from $R_i/t = 8.6$. Within the range of the database, interpolation is used to determine K_I and *COD* for an arbitrary geometry configuration.
Each geometry configuration was subjected to six different load cases ($i = 0, 1, \ldots, 5$) in form of elastic stress components, σ_i, in the axial direction of an uncracked pipe. The first four components describe a third degree axisymmetrical stress distribution through the thickness according to

$$\sigma = \sigma_0 + \sigma_1 \cdot \frac{r - R_i}{\zeta} + \sigma_2 \cdot \left(\frac{r - R_i}{\zeta}\right)^2 + \sigma_3 \cdot \left(\frac{r - R_i}{\zeta}\right)^3 \qquad (5)$$

where ζ is equal to a for a surface crack and to t for a leaking crack. The last two components describe global bending stresses with respect to the x and y axes (see Fig. 1) according to

$$\sigma = \sigma_4 \cdot \frac{y}{R_i + t} + \sigma_5 \cdot \frac{x}{R_i + t} \qquad (6)$$

The load cases considered make it possible to analyse complex weld residual stresses in IGSCC cases as well as bending arbitrarily oriented with respect to the location of the crack in vibration fatigue cases. According to the principle of superposition, the load cases were in the finite element models applied as pressures on the crack face. This was realised with the user subroutine DLOAD in ABAQUS which makes it possible to define arbitrary pressure distributions on element faces. Again, a more extensive presentation of the numerical technique as well as a comparison of the obtained K_I- and *COD*-solutions with other published solutions, are given in [8].

The experiments by Nam et. al. [6]-[7] can provide some verification of the crack growth predictions in LBBPIPE. Fig. 3 shows a comparison with a fatigue experiment on a large plate (width 200 mm, thickness 12 mm) subjected to cyclic tension loading. Fig. 3 shows the crack growth after wall penetration. The size of the initial half-elliptical crack was $a_0 = 6$ mm and $2c_0 = 60$ mm. $2a_1$ and $2a_2$ represent the front and back surface crack length, respectively. In this case the membrane loading promotes a uniform crack shape after breakthrough. Note that both the initial size of the breakthrough crack and the subsequent growth are fairly well predicted by LBBPIPE.

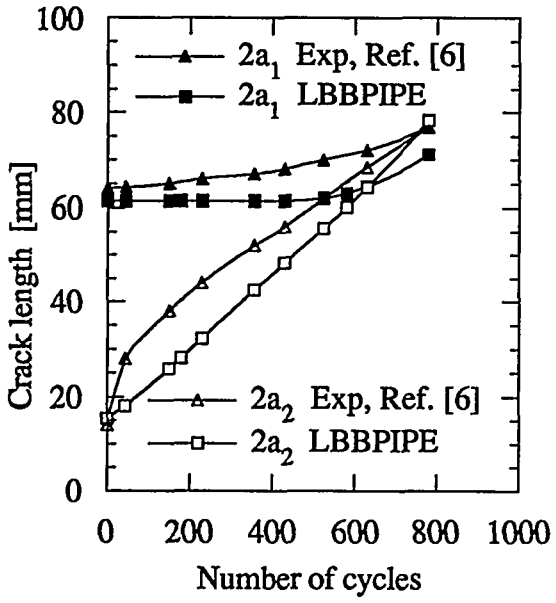

Fig. 3 Comparison of LBBPIPE with a fatigue crack growth experiment [6].

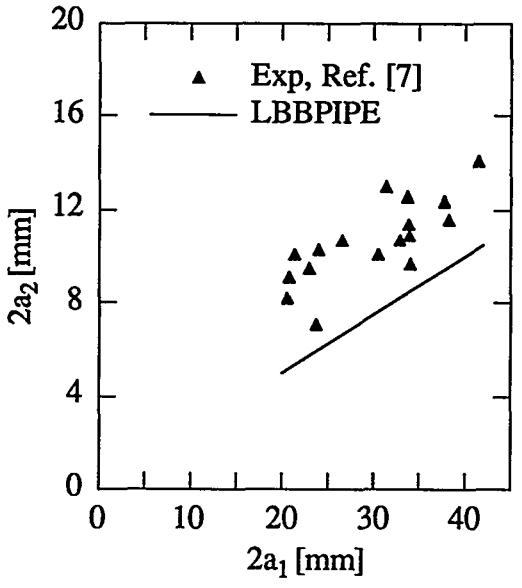

Fig. 4 Comparison of LBBPIPE with fatigue experiments in [7] at wall penetration.

Fig. 4 illustrates how well the wall penetration condition in LBBPIPE compares with fatigue experiments reported by Nam et al [7]. In [7] the front surface crack length $2a_1$ and back surface crack length $2a_2$ at wall penetration were recorded for a number of fatigue experiments on half-elliptical surface cracks in plates with different cyclic membrane and bending stresses. In light of these results the assumption in LBBPIPE from Eqn. (4) seems to be reasonable. However, further experimental verifications as well as analytical studies should be performed to establish the crack shape at wall penetration.

NUMERICAL EXAMPLES

Stress corrosion

In this section the LBBPIPE-program is applied to a pipe containing a circumferential stress corrosion crack with initial size (a_0, $2c_0$). The following data define the first example.

Geometry:
$a_0 = 7$ mm
$2c_0 = 70$ mm
$t = 35$ mm
$R_i = 300$ mm

Material:
SMAW in a TP-304 stainless steel pipe.
$R_{p0,2} = 133$ MPa, base material
$R_m = 438$ MPa
$S_m = 120$ MPa
$J_{Ic} = 0{,}168$ MJ/m^2 (weld)

Crack growth data:

$$\frac{da}{dt} = 2{,}07 \cdot 10^{-13} K_I^{2{,}161} \quad \text{m/s}$$

Loads:
Internal pressure 7 MPa at 285 °C
Global bending stress 30 MPa
Non-linear weld residual stress from Ref. [13] with 207 MPa (30 ksi) at inner pipe surface

The above pipe dimensions correspond to a main circulating pipe system in a Swedish BWR. Recommended values by Battelle [11] for stress corrosion cracks are used for fluid and crack surface properties in the mass leak rate

calculations. The resulting crack growth as predicted by LBBPIPE is shown in Fig. 5 for both the surface crack and the leaking through wall crack. Due to the high residual stresses along the inside of the pipe, the crack is growing faster in the length direction. Leakage is predicted after approximately 124 000 hours (14 years). The leaking crack in Fig. 5 is then growing circumferentially until failure is predicted after approximately 164 000 hours (19 years). The pointed form of the leaking crack raises K_I at the outside of the pipe which here means that after breakthrough the crack front will tend to a more uniform shape.

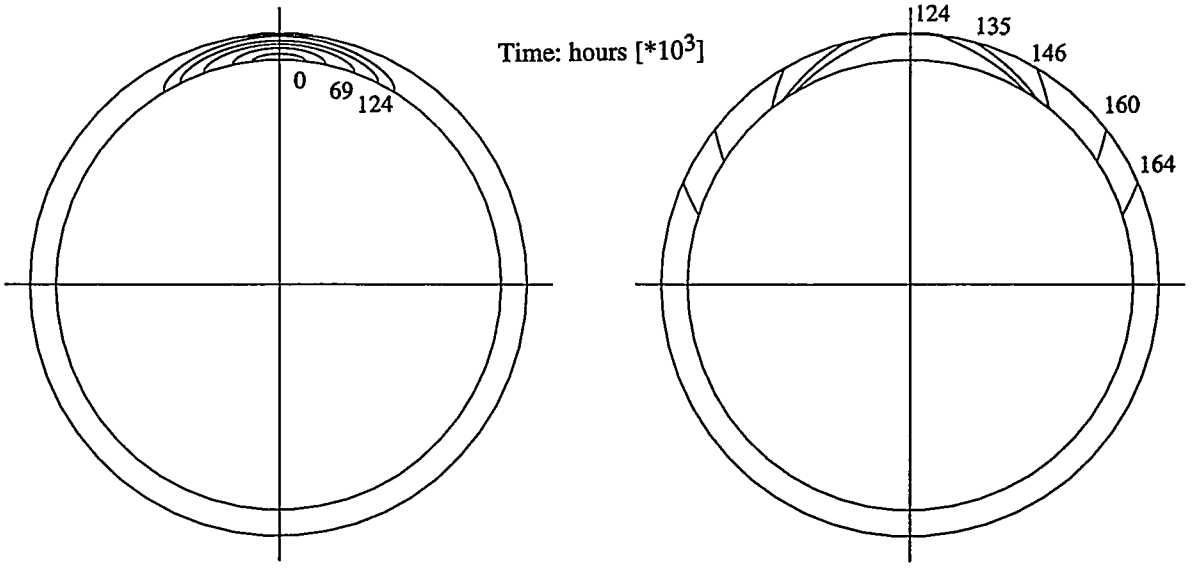

Fig. 5 Estimated successive crack shapes as function of time for a growing stress corrosion crack.

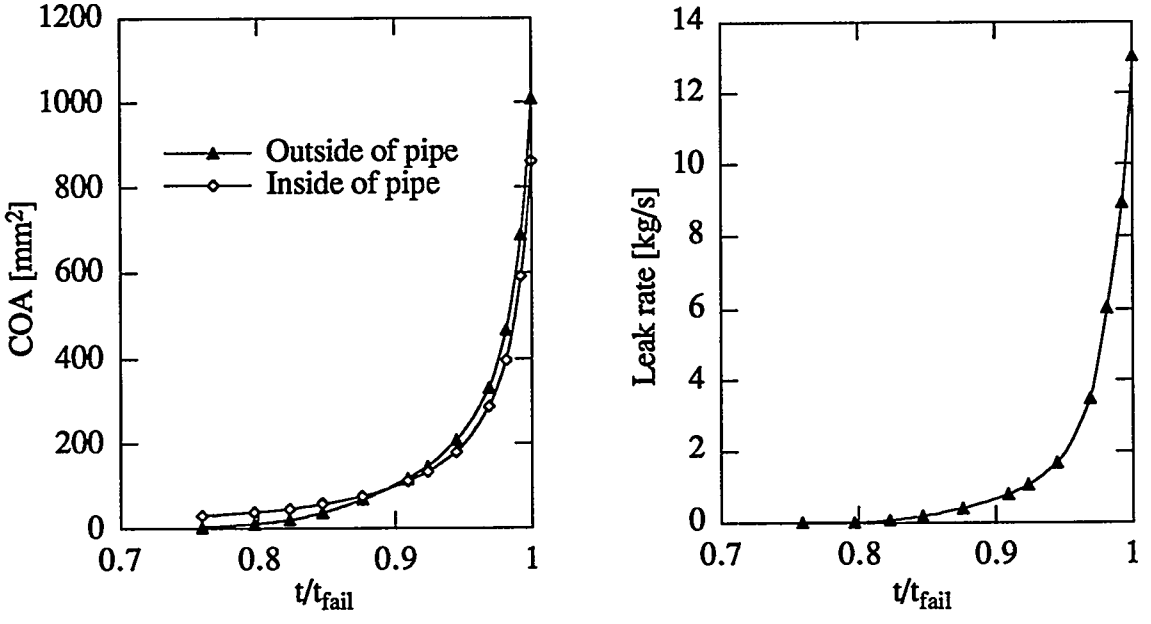

Fig. 6-7 COA and leak rate as function of normalised time for the IGSCC-case.

Fig. 6-7 show the crack opening area *COA* and the calculated leak rate, respectively, as function of time. The time is here normalised with respect to the predicted time to failure t_{fail}.
Due to the limited crack opening area at the outside of the pipe at breakthrough, the leak rate is very small at the beginning, only 0,012 kg/s at wall penetration which is difficult to detect. As the crack grows, the *COA* and the leak rate will increase. Just before fracture, the calculated leak rate is 13,0 kg/s. By considering the time between fracture and when the leak rate is judged to be detectable, an assessment of leak before break can be made. These kind of analyses are very instructive to obtain information of possible events when growing cracks are a concern in piping systems. For instance if the global bending stress is zero in the above example, the compressive weld residual stress in the center of the wall thickness will reduce the crack growth in the depth direction and instead the crack may grow along the entire circumference. Under such circumstances, leak before break cannot be ensured.
To further investigate the loading effects on LBB, a sensitivity analysis has been performed for different pipe dimensions. In Fig. 8 the Time between Detection and Break (TDB) is plotted versus load factor for different leak rate detection levels d. Fig. 8 considers the same pipe as in the above example (670 x 35 mm) with a non-linear weld residual stress distribution and in all cases starting with a surface crack of depth 7 mm (20 % of the thickness) and a crack length of 70 mm (10 times the crack depth). The load factor is defined as $(P_m+P_b+P_e)/S_m$, i e the sum of primary membrane and bending stress together with the thermal expansion stress, all normalized with S_m. P_m is due to the internal pressure only and P_b is here set to zero which means that the variation of the load factor is entirely due to the variation in P_e. A variation of P_b would not influence the times to leakage or failure much even if the leak rate at failure would be lower due to smaller crack geometry at failure for a higher portion of P_b.

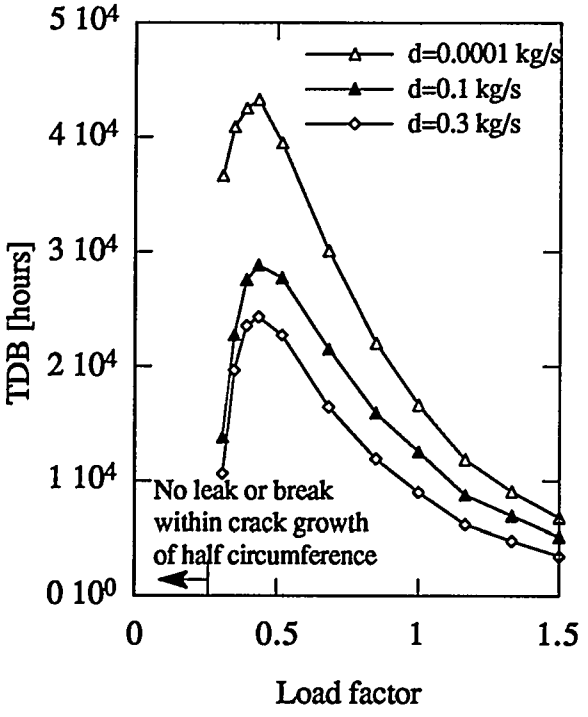

Fig. 8 TDB for a 670 x 35 mm pipe with $2c_0/a_0 = 10$.

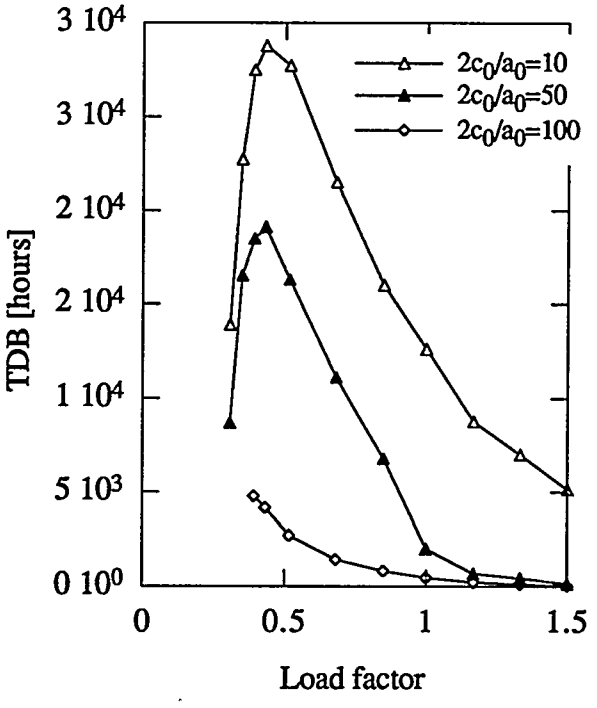

Fig. 9 TDB for a 670 x 35 mm pipe with d=0.1 kg/s.

From Fig. 8 it is observed that for larger loads the TDB is decreasing. It is true that large loads give a relatively fast leakage, but these large loads also give a fast propagation of the leaking crack which means that the TDB will also be small. On the other hand, small loads tend to promote crack growth in the circumferential direction (due to the large tensile residual stresses at the inside of the pipe). When such a crack eventually breaks through the thickness, the resulting leaking crack will be very large and thus the TDB will be small. However, the total time for such cracks to grow from a small surface crack to failure of a leaking crack will be very large, several decades with the assumed crack growth data. For even lower loads in Fig. 8 it is indicated that no leak or break occurs within crack growth of half the pipe circumference, which represents the limit of the database for K_I in LBBPIPE. It is also clearly seen the effect of the different detection limits d. Being able to detect a small leak rate will give a higher margin in time between detection and break. The smallest leak rate of 0,0001 kg/s is included to give an idea of the time between leak and break which would be the margin if even the smallest leak rate could be detected. In general the TDB is satisfactory large for the large diameter pipe in Fig. 8 provided that the initial crack length $2c_0$ is not extremely large in combination with very high load factors. This is illustrated in Fig. 9 where a variation of the initial crack length has been performed while keeping the initial crack depth constant at 7 mm. A long initial crack length will result in a large crack size at wall penetration, especially along the inside of the pipe, which reduces the TDB. This reduction is most significant for the combination long initial crack lengths and large load factors.

The same type of analysis has also been performed for other pipe dimensions. Fig. 10-11 show the TDB as function of load factor for a 324 x 17.5 mm pipe and a 88.9 x 6.3 mm pipe. These pipe dimensions correspond to a feedwater pipe system and a cooling system for a shut-down reactor in Swedish BWR:s, respectively. Both cases are starting with a surface crack of depth 20 % of the thickness and a crack length of 10 times the crack depth. The weld residual stresses, however, are different from the large diameter case. In Figs. 10-11 the weld residual stresses are assumed as a pure bending stress through the thickness of the pipe with magnitude +207 MPa at the inside and -207 MPa at the outside of the pipe. This is in accordance with the recommendations in [13] for thin-walled pipes.

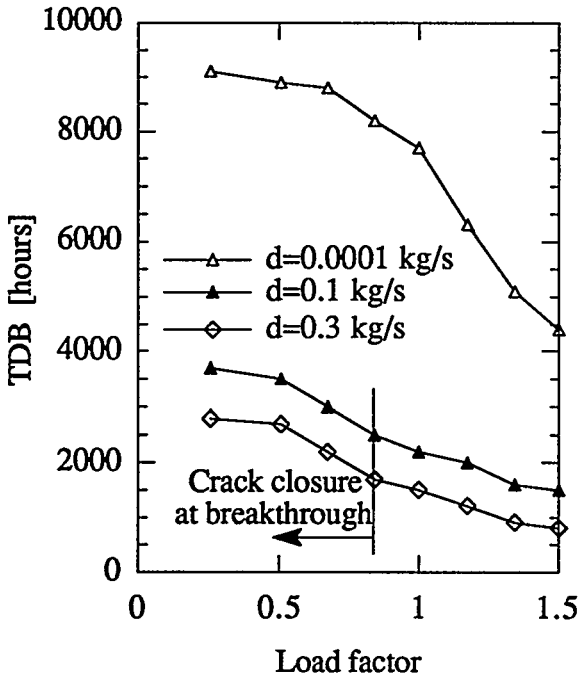

Fig. 10 TDB as function of load factor for a 324 x 17.5 mm stainless steel pipe.

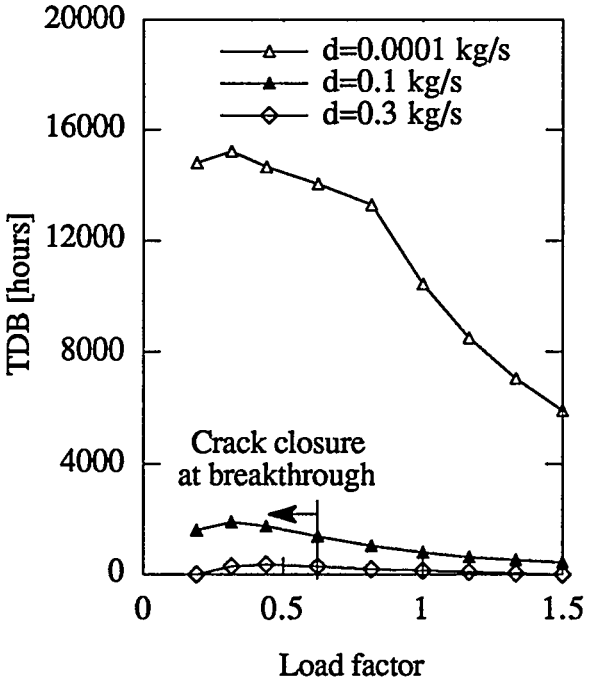

Fig. 11 TDB as function of load factor for a 88.9 x 6.3 mm stainless steel pipe.

For a small diameter pipe, all leak rates decrease drastically due to pure geometrical reasons. However, the time to leakage or failure does not change significantly provided the stress state is unchanged. Even if the stress intensity factor decreases for a shorter crack length, the crack will experience a shorter absolute length to grow compared to a corresponding crack in a large diameter pipe. The time between detection and failure (TDB) will however be smaller for a small diameter pipe, regardless of the weld residual stress distribution. Otherwise, a small diameter pipe usually implies a change towards a more linear residual stress distribution through the wall thickness, which tend to decrease all times to leakage and failure. Figs. 10-11 demonstrates how the TDB is smaller for successively smaller pipe dimensions for all realistic detection limits. Note also that for common values of the load factor in Figs. 10-11, crack closure will occur at wall penetration along the outer pipe surface. This is due to the compressive residual stresses at the outer pipe surface which implies that initially the through-wall crack will have zero or a very small leak rate. Eventually when the crack has grown to a sufficient length along the inside of the pipe, crack growth starts also along the outside and the pipe begins to leak. The leak rate and COA just before the predicted failure for the different pipe dimensions are shown as function of load factor in Figs. 12-13. Note the relatively small leak rates for the small diameter pipe in Fig. 12. This merely indicates that due to the small dimensions, the COA and leak rate will be small for a small diameter pipe even for a through-wall crack with length half the circumference.

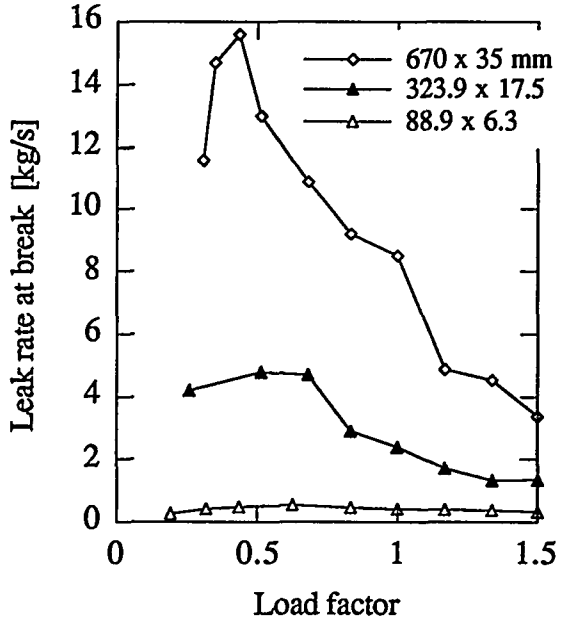

Fig. 12 Leak rate at break as function of load factor for different pipe dimensions.

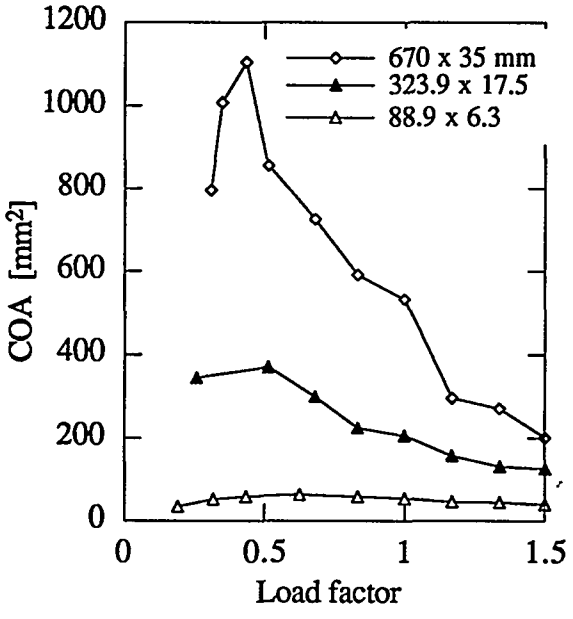

Fig. 13 COA (inner surface) at break as function of load factor for different pipe dimensions.

Vibration fatigue

We consider here the same large diameter pipe (670 x 35 mm) as in the first stress corrosion example. The pipe has the same material properties and initial crack size as before and is subjected to the same loading conditions except for an additional alternating global bending stress with a constant amplitude of 9 MPa at 20 Hz. The crack growth law is set to

$$\frac{da}{dN} = 3{,}66 \cdot 10^{-10} \Delta K_I^{3,3} \qquad \text{m/cycle} \qquad (7)$$

in conjunction with a threshold value, ΔK_{th}, of 2.5 MPa$\sqrt{m}$. Eqn. (7) is taken from the recommendations in Ref. [13] with an environmental factor of 4. Recommended values by Battelle [11] for fatigue cracks are used for fluid and crack surface properties in the mass leak rate calculations. The resulting crack growth as predicted by LBBPIPE is shown in Fig. 14 for both the surface crack and the leaking through wall crack.

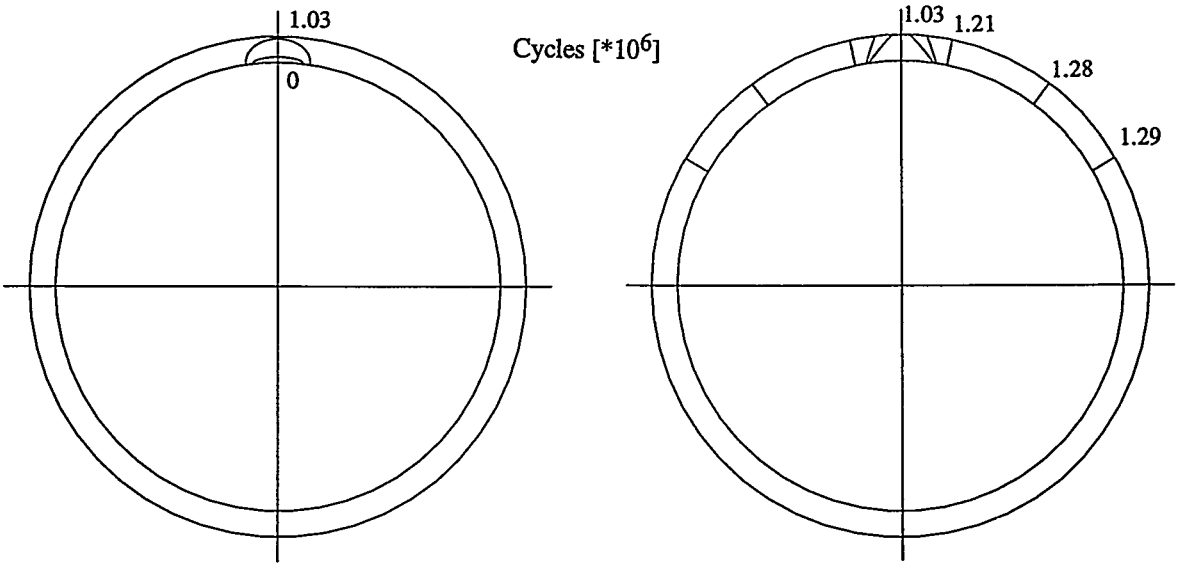

Fig. 14 Estimated successive crack shapes as function of number of cycles for a growing fatigue crack.

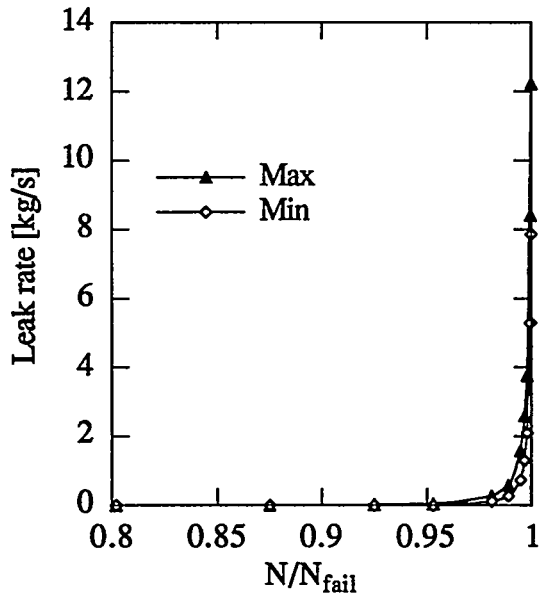

Leakage is predicted after $1.03 \cdot 10^6$ cycles corresponding to 14.3 hours. The surface crack only grows in the depth direction where the threshold value is exceeded. The leaking crack then grows extremely fast and failure is predicted after $1.29 \cdot 10^6$ cycles (17.9 hours). Fig. 15 shows the resulting leak rate (maximum and minimum) as function of number of cycles, here normalised with respect to the predicted number of cycles to failure N_{fail}. The leak rate immediately after wall penetration is very small and unable to detect. A detectable mass leak rate of 0.1 kg/s (1.6 gpm) gives a time interval of less than one hour between detection and failure. Under such circumstances LBB is not ensured. A lower detection level will not improve the situation much since the crack growth is so fast due to the high frequency loading once the threshold value is exceeded.

Fig. 15 Leak rate as function of normalised number of cycles.

High cycle fatigue due to vibrations is assumed to occur as long as ΔK_I exceeds the threshold value ΔK_{th}. In the above example the vibration stress amplitude is set so high that this condition is fulfilled at some part of the initial crack front. Sensitivity analyses have been performed for a pipe with an alternating global bending stress at 20 Hz and a crack growth law according to Eqn. (7). The analyses show that all the following conditions have to be fulfilled in order to grow the crack due to high frequency vibration fatigue:

i) High vibration stress amplitudes.
ii) Deep surface cracks.
iii) Low threshold values.

If one of the above conditions is not fulfilled, in general ΔK_I will be below the threshold value and crack growth will not take place. On the other hand, if the conditions for crack growth are fulfilled, the time to grow the crack until leak or break will be very short. The leak rates are generally small immediately after wall penetration. In all the studied cases, for which the breakthrough crack length along the outside of the pipe was less than 10 percent of the circumference, the initial leak rate was less than 0.01 kg/s which hardly is detectable. The time between a detectable leak and break will be extremely small, in most cases only a few hours with the assumed crack growth law. Fig. 16 shows for the 670 x 35 mm pipe, the limit at which $\Delta K_I > \Delta K_{th}$ for at least some part of the initial crack front for different combinations of stress range $\Delta\sigma$, threshold value ΔK_{th} and initial crack geometry (a_0, $2c_0$).

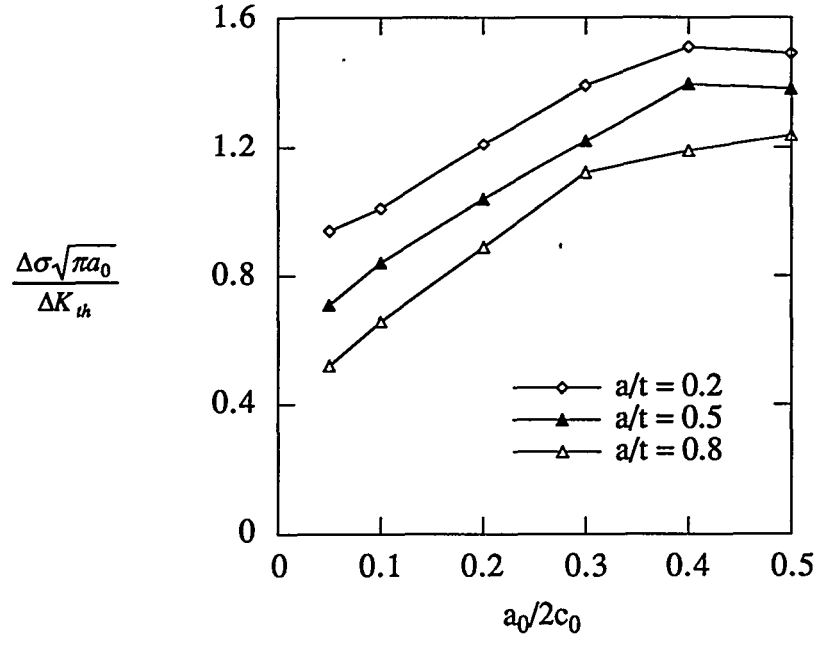

Fig. 16 Combinations of stress range, threshold value and initial crack size for which vibration fatigue occurs in a 670 x 35 mm pipe.

The weld residual stresses are here not as important for fatigue as for stress corrosion. Residual stresses do however influence the crack growth and the threshold value through the R-value. Also, compressive residual stresses may cause local crack closure even if ΔK_I is above the threshold value. In general this occurs for thin walled pipes with a linear weld residual stress distribution through the thickness. In these cases the breakthrough crack is in general closed along the outside of the pipe with zero leak rate. For points along the crack front near the inside of the pipe, crack growth still occurs which eventually may cause crack growth also to occur along the outside of the pipe until break is predicted.

CONCLUSIONS

1. The computerized procedure represents a significant step forward in order to be able to perform rapid analysis of growing cracks and leak rates when service induced flaws are detected in pipes in nuclear power plants. By performing sensitivity analyses, one can obtain a better understanding of the relative importance of the different input parameters and thus make a better judgement of the probability of a detectable leak instead of break.
2. For the IGSCC-cases studied, there should not be any problem to detect leak rates from large diameter pipes and the time between detection and break is in general large for these pipes provided that the initial crack length is not extremely large in combination with high loads. For very small diameter pipes, there may be problems to detect leak rates since COA and leak rates will be small due to pure geometrical reasons.
3. For normally loaded pipe systems in BWR-plants the conditions for vibration fatigue crack growth to occur are not likely to be fulfilled. However, if high cycle fatigue may take place, the rapid crack growth that follows makes it difficult to take any credit of LBB arguments.

REFERENCES

1. US Nuclear Regulatory Commission (1984) Evaluation of potential for pipe breaks. NUREG 1061, Vol. 3.
2. A. P. Parker (1981) Stress intensity factors, crack profiles and fatigue crack growth in residual stress fields. *ASTM STP 776*, ASTM, Philadelphia, U.S.A., 13-31.
3. D. F. Quinones and J. E. Reaugh (1983) Weld residual distribution near growing cracks. *EPRI Report NP-2964*, EPRI, Palo Alto, U.S.A.
4. G. Yagawa, Y. Takahashi, N. Kato, M. Saito, K. Hasegawa and T. Umemoto (1985) Fracture behaviour of cracked type 304 stainless steel pipes under tensile and thermal loading. *Int. J. Pres. Ves. & Piping* **19**, 247-281.
5. F. Nilsson (1992) A consistent few parameter crack growth description procedure. *Int. J. Fracture* **54**, 35-44.
6. K. W. Nam, K. Ando, S. Yuzuru and N. Ogura (1992) LBB conditions of plates and pipes under high fatigue stresses. *Fatigue Fract. Engng Mater. and Struct.*, **15(8)**, 808-824.
7. K. W. Nam, K. Ando, N. Ogura and K Matui (1994) Fatigue life and penetration behaviour of a surface cracked plate under combined tension and bending. *Fatigue Fract. Engng Mater. and Struct.*, **17(8)**, 873-882.
8. M. Bergman and B Brickstad (1995) A procedure for analysis of leak before break in pipes subjected to fatigue or IGSCC accounting for complex crack shapes. To appear in *Fatigue Fract. Engng Mater. and Struct.*
9. I. Milne, R. A. Ainsworth, A. R. Dowling and A. T. Stewart (1987) *Assessment of the integrity of structures containing defects*, R/H/R6-Revision 3, Nuclear Electric, Berkeley, U.K.
10. I. Sattari-Far (1994) Finite element analysis of limit loads for surface cracks in pipes. *Int. J. Pres. Ves. & Piping* **57**, 237-243.
11. D. D. Paul, N. Ghadiali, J. Ahmad and G. Wilkowski (1992) *Seepage quantification of upsets in reactor tubes.* SQUIRT User's manual version 2.2, Battelle, Columbus, Ohio, U.S.A.
12. ABAQUS (1993) *User's manual, version 5.2*, Hibbit, Karlsson and Sorenson Inc., Providence, R. I., U.S.A.
13. ASME XI Task group for piping flaw evaluation (1986) Evaluation of flaws in austenitic steel piping. *ASME J. Pres. Ves. Tech.* **108**, 352-366.

DEVELOPMENT OF CRACK SHAPE : LBB METHODOLOGY FOR CRACKED PIPES

D.MOULIN, S.CHAPULIOT, B.DRUBAY
Commissariat à l'Energie Atomique, RDMS
GIF sur YVETTE FRANCE

1. INTRODUCTION

For structures like vessels or pipes containing a fluid, the Leak-Before-Break (LBB) assessment requires to demonstrate that it is possible, during the lifetime of the component, to detect a rate of leakage due to a possible defect, the growth of which would result in a leak before-break of the component. This LBB assessment could be an important contribution to the overall structural integrity argument for many components.
The aim of this paper is to review some practices used for LBB assessment and to describe how some new R & D results have been used to provide a simplified approach of fracture mechanics analysis and especially the evaluation of crack shape and size during the lifetime of the component.

2. LBB METHODOLOGIES

It is considered here only two particular procedures available in the open literature in order to illustrate two different cases (large thin vessel and pipe) for which special requirements are proposed.

2.1. LBB methodology for SPX1 main vessel

The approach applied to the main vessel of Superphénix [1]contains three main steps :

- the first step is to assume the existence of an initial realistic defect located in a weld, and to check that the propagation of such a defect remains limited, i.e. the end-of-life-defect, as calculated by application of the 2nd category design situation loads, does not fully penetrate the section thickness (non-crossing defect), and is not a critical type (stable defect). The initial defect is assumed to be of the plane, semi-elliptic type.
- The crack propagation is further continued until a through-wall and detectable defect is reached either by increasing the number of occurences of the load sequence, or by increasing the load intensity. By doing this it is possible to have an evaluation of the margins on the number of cycles or on the load level. To assure conservatism in the calculation of the crack opening area, it is assumed that during the growth of a through-wall defect the crack front profile remains constant, corresponding to the one existing at the instant of penetration. This assumption also recognises, in the consideration of the development of the initial part-through defects to large through- thickness defects, that it is non conservative, for determination of crack opening area, that the crack is of equal length at the initiation and at the penetration surfaces.
- The third step is to check that this resulting through-wall crack, detectable under normal operating conditions, does not reach the size of the smallest critical defect obtained when considering maximum design load conditions.

2.2. LBB methodology for nuclear piping

The steps of the evaluation proposed in the NUREG 1061 Volume 3 for pipes [2] are summarized [3] below :

- Postulate a through-wall crack flaw in the pipe. The size of the flaw should be large enough so that leakage is assured of detection using the installated leak detection equipment, when the pipe is subjected to normal operating loads.

- Using the above crack size, perform an elastic-plastic fracture mechanics assessment to determine the maximum load (M_{max}) the pipe can carry.
- Determine the extreme load (M_{N+SSE}) from normal plus safe-shutdown earthquake stresses.

For satisfactory performance, demonstrate the following condition : $M_{max} > M_{N+SSE}$. Based on some engineering judgment the recommended margins for the leak-rate detection, leakage flaw size and for N+SSE stresses are respectively 10, 2 and $\sqrt{2}$.

2.3. Interest of simplified methods

According to the LBB methodologies, there is a need for :

- the analysis of the crack propagation under normal operating conditions to determine the through-wall and the detectable crack sizes starting from a postulated initial part-through wall defect,
- a model for hydraulic analysis for estimation of leak rates,
- a crack-opening area analysis for determination of crack geometry,
- an elastic-plastic fracture mechanics evaluation for the prediction of the maximum load-carrying capacity of the cracked structures.

For the crack propagation analysis and for the calculation of the maximum loading, handbooks for stress intensity factor KI and simplified methods for J are needed. Experimental results for example on cracked plates and cracked pipes are also usefull in order to validate such simplified methods.

3. NEW R&D RESULTS

3.1. Cracked plates under bending.

3.1.1. Experimental results on crack propagation

An experimental study concerning the propagation by fatigue bending at room temperature of semi-elliptical crack in large plates made of in 316L(N) stainless steel was performed at CEA. Different kinds of initial defects and loadings were chosen (Table 1) :

TABLE 1 CEA Plates experimental tests conditions

Test number	Maximum load (kN)	Minimum load (kN)	Frequency (Hz)	Initial crack depth (mm)	Initial crack width (mm)
1	22.5	3.1	0.1	2	80
2	20.3	-22.2	0.05	2	80
3	22.5	3.1	0.1	2	40
4	20.3	-22.2	0.033	2	40

The **figure 1** gives the dimensions of the plates that were tested on a conventionnal testing machine with an ad'hoc experimental test device illustrated in the **figure 2**. Such an experimental procedure allows to perform reversed bending. The **figure 3** shows the cracks profiles obtained at the end of the tests when penetration is achieved, by comparison to the profile of the initial crack obtained by machining. These tests show that, for a R-ratio (R = minimum bending stress / maximum bending stress on one skin) near 0.1, the deepest point of the crack reaches 85% of the thickness and then, rapidly, the penetration is obtained in a few cycles. For a R-ratio near -1, the conditions of penetration are somewhat different. Multiple fatigue cracks appear on the opposite skin of the initial notch. One of these fatigue crack quickly joints the initial propagated crack for a depth near to 65% of the thickness.The through-wall crack at penetration in this later case is a two-chevrons crack and the smallest ligament to be used for leak-rate evaluation is not on the outer skin but close to the middle of the thickness. In addition, due to the multiple cracking the crack after penetration is not contained in a perfect plane.

3.1.2. Calculation of crack propagation - Master Curves

The evaluation of the crack shapes during fatigue loading is very time consuming if it is necessary to take into account every initial crack dimensions, every Paris law for base material or welments and every loading conditions. In fact the main results concerning L.B.B. assessment is the crack profile at penetration. To do this a simplified procedure has been proposed for cracked plates and applied for instance for E.F.R main vessel [4]. This procedure relies on the calculation of master curves giving for different initial crack size ratios (a/c and a/t) and different loading ratios (membrane stress/ bending stress) the evolution of a/c versus a/t. These curves are independent of Paris law parameters and are calculated with K_I values established by Raju and Newman [5]. Good agreement of these curves was shown with experimental results of cracked plates made of homogeneous base material and tested under simple bending load controlled conditions. Most of the loading of tests considered were also restricted to global elastic behavior.

The **figure 4** gives the paths followed by the crack dimensions of the 4 specimens tested and the two paths calculated by the Master Curve Method. For positive R ratio the calculated curves are conservative : they overestimate the crack width at the penetration when a/t=1. One can see that the negative R ratio experimental results give wider crack than with positive R ratio for the same load range. However after junction of the two opposite cracks, for negative R ratio the width of the cracks are almost equal to the width of crack reached at the penetration for positive R ratio. The Master Curves are conservative because they give an over-estimation of the maximal overall width. The problem remaining is to estimate the smallest leaking ligament width.

3.1.3. J-estimation.

In order to evaluate the effect of plasticity during the experimental tests local J values were calculated considering only the first ¼ loading cycle. A numerical estimation of J with the CASTEM 2000 finite elements code and the G-THETA method was done for an intermediate measured crack front. The three dimensionnal mesh is shown **figure 5**. The **figure 6** gives the evolution of elastic and elatoplastic J versus loading normalised to the maximal loading. One can see that at the maximal loading the elastoplastic J is equal to 5 times the elastic value. This means that the duration of propagation are underestimated by elastic calculation even if the crack shape path is correctly evaluated.To be able to calculate the propagation phase, it is proposed to calculate a ΔJ parameter by a simplified method [6, 7]. This Js method is used to modify the elastic J_e value given by Raju and Newman formulae. In a few words, the method consists in modifying the elastic J_e value with a factor k_{A16} using a reference stresse σ_{ref} and the corresponding strain ε_{ref} taken on the tensile curve:

$$J = J_e \cdot k_{A16} = \frac{K_I^2}{E^*} \cdot \left[\frac{\sigma_{ref}^2}{2\left(\sigma_{ref}^2 + R_{0.002}^2\right)} + \frac{E\varepsilon_{ref}}{\sigma_{ref}} \right]$$

where $R_{0.002}$ is the yield stress and E is the elasticity modulus. E*is the equivalent 2D E value calculated with the relevant stress or strain distribution (plane stress or plane strain).

The evolution of J, calculated by the Js method, is shown in the **figure 6**. The curve is labelled simplified method A16. In this estimation, the reference stress is set equal to the bending reference stress of the crack-free plate. It is worth noting that the Js method gives a good estimation of the numerical elastoplastic local J at the deepest point.

3.2. Cracked pipes.

3.2.1. Experimental results.

It is interesting to try to develop also Master Curves for L.B.B. assessment of cracked pipes. An experimental study on fatigue propagation of axisymetrical internal defects in tubes subjected to 4 points reversed bending was performed at the CEA. The **figure 7** gives a drawing of the experimental configuration used. The initial defect was introduced by machining.

A stable fatigue propagation of the crack was obtained until 80% of the thickness and then unstable penetration of the defect is achieved. At penetration in almost one cycle the width on the outside skin reaches the width obtained at penetration on the inside skin as illustrated on the **figure 8**.

3.2.2. K_I handbooks for semi-elliptical defects.

More and more local K_I handbook are available, for an increasing number of structure and crack geometries and loadings configurations. Their most important interest is to define a data basis, in most cases coming from finite elements calculation, which are the first input for the construction of simplified methods : Master curves or simplified J estimations for example. In the cracked pipes domain a parametric study of different K_I handbook for tubes with internal circumferential cracks was performed. Shape factors are compared for a stress field expressed by :

$$\sigma = \sigma_0 + \sigma_1 \frac{r - Ri}{a} + \sigma_2 . \left(\frac{r - Ri}{a} \right)^2 + \sigma_3 . \left(\frac{r - Ri}{a} \right)^3 + \sigma_4 . \left(\frac{x_3}{Ri + t} \right),$$

where σ_0 is a constant stress field, σ_1 σ_2 and σ_3 are linear, quadratic and cubic axisymétrical in the thickness stress field and σ_4 is a global bending. The expression of K_I derived from the stress distributions is :

$$K_I = \left(\sum_{i=0}^{4} \sigma_i . f_i \right) . \sqrt{\pi a}$$

where f_i is the geometrical shape factor associated to σ_i stress component.
Some examples of the comparisons made by the authors considering the f_i results given by Bergman and Brickstad **[8]**, Poette and Albaladejo **[9]** and Héliot **[10]** are shown in the **figures 9 to 13** for a/t=0.5. The results are presented as a function of a/c. It shows a good agreement for membrane and global bending load, but more dispersed results for the axisymetric through thickness stress. The Bergman and Brickstad handbook, which is based on more recent 3D and very refined meshes gives an important panel of geometries and loadings.

3.2.3. Calculation of crack propagation - Master Curves.

Master curves, used in LBB methods to evaluate crack shape, are constructed from analytical K_I solutions. These are available now for cracked pipes configurations. It is possible to calculate the Master Curves of cracked pipes. With the Bergman and Brickstad results, the Master Curves for tubes with circumferential and internal defects were drawn and compared with the plates ones for the pipe geometry considered. The **figures 14 and 15** show the paths obtained by the plate and tube formulae for the membrane stress and the linear bending cases respectively. A good agreement is obtained between plates and tubes suggesting that plate formulae are sufficient for the configurations tested here. The circumferential curvature of the tube for a ratio t/Ri=0.12 has no effect on the flaw shape. However, the software allowes also to outline Master Curves for other special loadings like global bending or global bending combined with axisymetrical stresses.

3.2.4. Determination of the through wall defect

A finite elements interpretation with shell and linespring elements was made by the authors. The mesh used is presented in the **figure 16**. At this occasion a proposal to evaluate the width of through-wall defect for global bending was made :

- The crack propagation is estimated along the crack front, with a step by step scheme and with K_I handbook or finite elements calculations, with the Paris law of the material until the deepest point reaches 80% of the thickness. At this instant the crack profile is the one shown on the **figure 17** (front A).
- Assuming a constant velocity of the crack growth along the crack front, the crack is propagated to a depth equal to the thickness (front B in the **figure 17**).
- All the points of the crack above 0.8t are assumed to reach the surface (B→C) and the lateral crack fronts are assumed to be linear (AC).

This proposal gives, for the fatigue propagated flaw at penetration, a 53° external width compared to the 62° experimental results. This result is more accurate than the external width obtained by the formulae deduced from **[11]** :

External width = Mini (2t, 2xinternal width/4) = 9.6 °

4. CONCLUSIONS

This paper has presented some particular aspects of L.B.B. methodologies recently proposed for application to vessel and pipe components of nuclear reactor. Attention is here focused not on the instability of cracked components but on the evaluation of the shape and dimensions of the defect during the lifetime of the component.
Simplified methods are very interesting in this context and in particular the Master Curves giving the geometry of the defect at penetration.
The experimental results show some interesting features concerning the effect of negative R ratio leading to non plane two-chevrons through-wall crack, the effect of plasticity, the differences between plates and tubes and the characterization of penetration.
As far as simplified methods are concerned some K_I analytical solutions, now available, are compared and applied to draw automatically the paths of crack dimensions developments. The comparisons with experimental results are encouraging. Problems concerning the effects of different R ratio, of plasticity and of weldment were not presented in this paper.
K_I solutions were also used to apply the Js simplified method to evaluate the effect of local plasticity. The comparison with the numerical values is good with a simple reference stress.
A proposal to evaluate the width of the penetration crack in a pipe gives good results.

ACKNOWLEDGMENTS

The results presented in this paper were obtained during studies concerning R&D works for development of fast breeder and pressure vessel reactors. They were performed at the Commissariat à l'Energie Atomique at Saclay (France) in the framework of collaborative contracts with the utility Electricité de France and the design company Framatome .

REFERENCES :

[1] "Fracture mechanics applied to Superphénix reactor components" JB Ricard, M.Sperandio - International seminar on "Fracture in austenitic components" SISSI Saclay Conference on Structural Integrity , October 8th-9th 1991. To be issued in Int.J. of PVP

[2] "Report to the US Nuclear Regulatory Commission Piping Review Committee", prepared by the pipe Break task Group, NUREG/CR-1061, Vol.3, November 1984.

[3] "Pipe fracture evaluations for leak-rate detection : deterministic models" G.Wilkowski, S.Rahman, D.Paul and N.Ghadiali, PVP-Vol.266, Creep, Fatigue evaluation and Leak-Before-Break assessment ASME 1993, pp243-254

[4] "The development of Structural Integrity Criteria for Austenitic Components" D G Hooton, B Tomkins - International seminar on "Fracture in austenitic components SISSI Saclay Conference on Structural Integrity , October 8th-9th 1991.To be issued in Int.J. of PVP.

[5] "An empirical stress intensity factor equation for the surface crack", J.C.Newmann, I.S.Raju, Engineering Fracture Mechanics, Vol.15, N°1-2, pp 185-192, 1981.

[6] "Defect assessment procedure based on a simplified method to estimate J", D.Moulin, B.Drubay, European Conference on Fracture ECF10, Berlin, 20-23 September 1994. Editors K.H.Schwalbe, C.Berger.pp1359-1368.

[7] "Defect assessment procedure based on a simplified method to estimate J", D.Moulin, B.Drubay, European Conference on Fracture ECF10, Berlin, 20-23 September 1994. Editors K.H.Schwalbe, C.Berger.pp1359-1368.

[8] "A new computerized procedure to analyse LBB in pipes with complex crack shapes", M.Bergman and B.Brickstadt, 20. MPA Seminar, 6 and 7 October 1994, Vol.2, paper 45.

[9] "Stress intensity factors and influence functions for circumferential surface cracks in pipes", C.Poette and S.Albaladejo. Engineering Fracture Mechanics, Vol.39, N°4, pp 641-650, 1991.

[10] J. Héliot, private communication.

[11] "A procedure for analysis of leak before break in pipes subjected to fatigue or IGSCC accounting for complex crack shapes", M.Bergman and B.Brickstadt, SA/FoU-report 93/08.

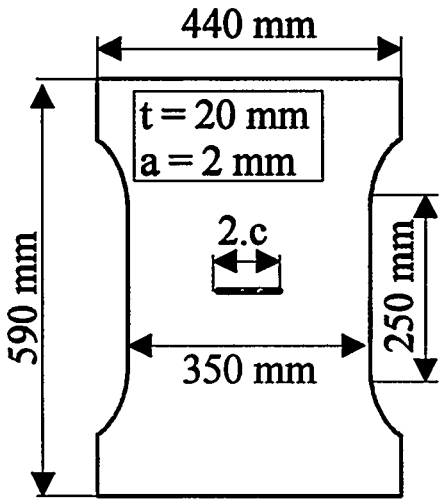

Fig. 1 : Plate geometry.

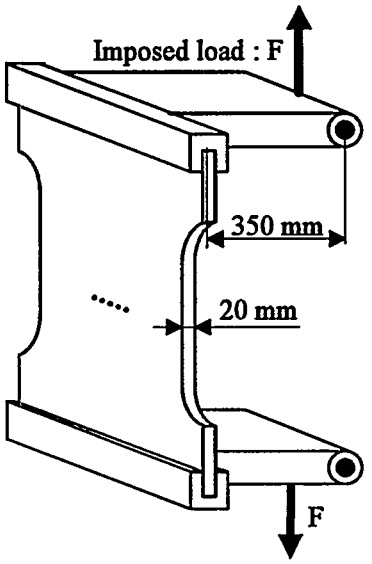

Fig. 2 : Bending load

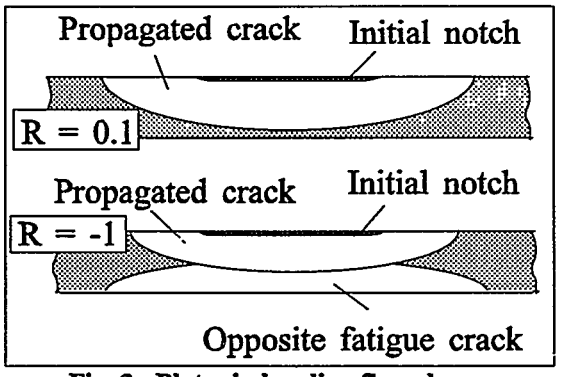

Fig. 3 : Plates in bending flaw shapes

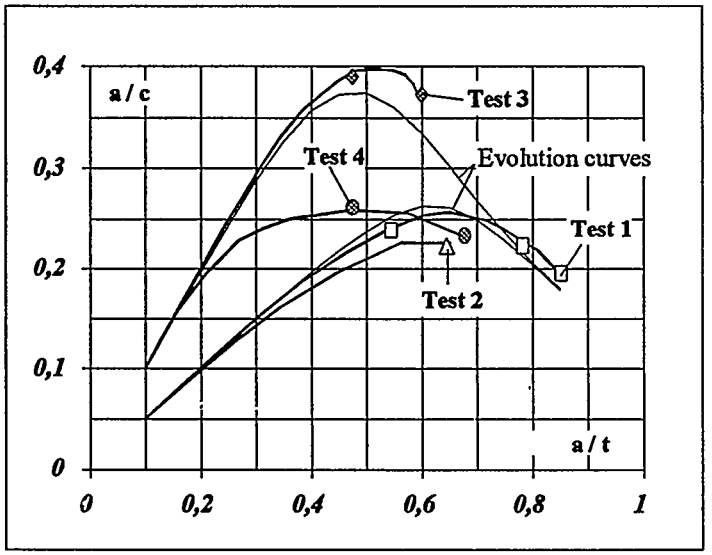

Fig. 4 : Evolution curves

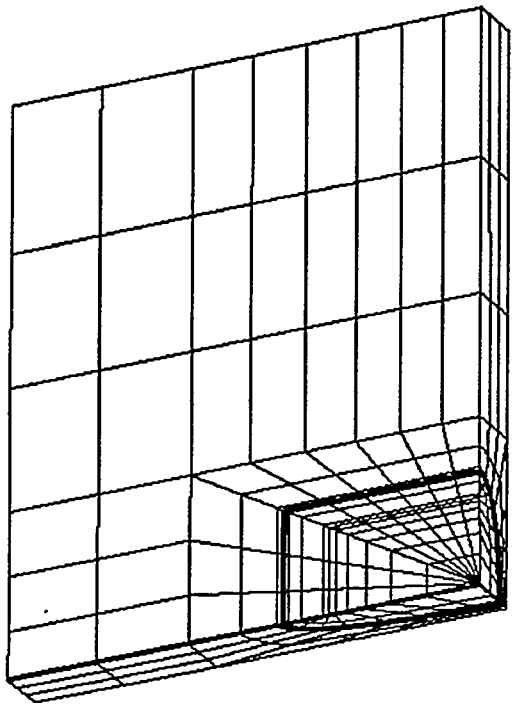

Fig. 5 : 3D plate mesh.

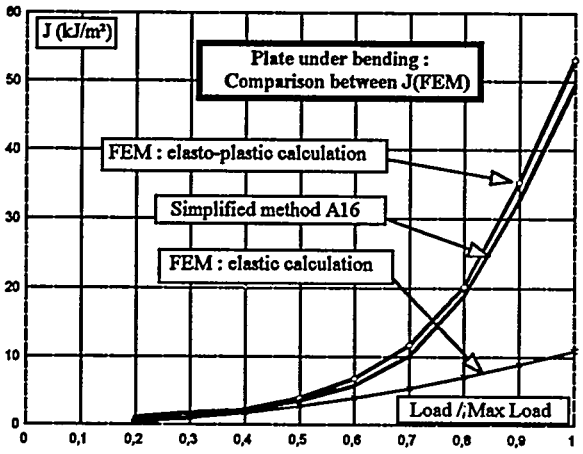

Fig. 6 : J integral at deepest point

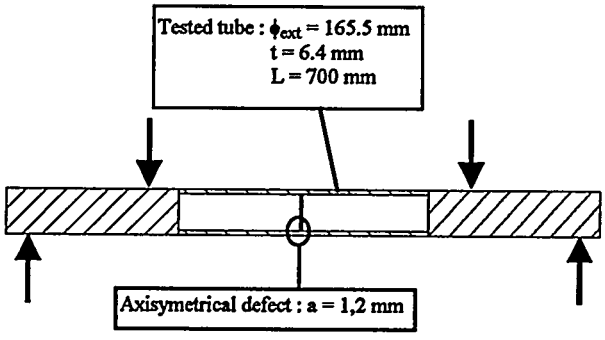

Fig. 7 : Tube geometry

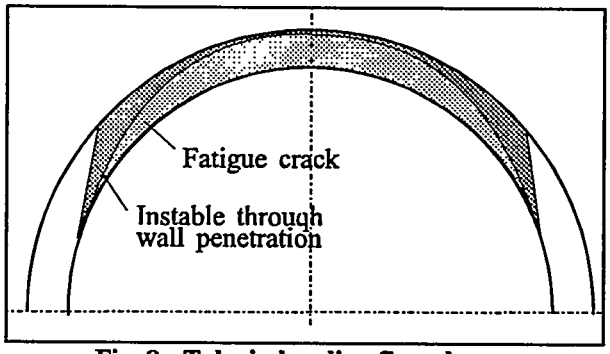

Fig. 8 : Tube in bending flaw shapes

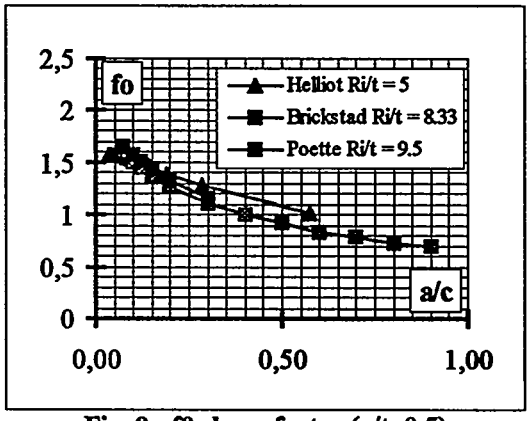

Fig. 9 : f0 shape factor (a/t=0.5)

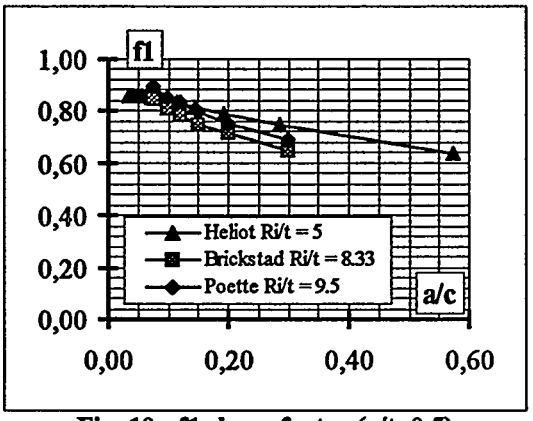

Fig. 10 : f1 shape factor (a/t=0.5)

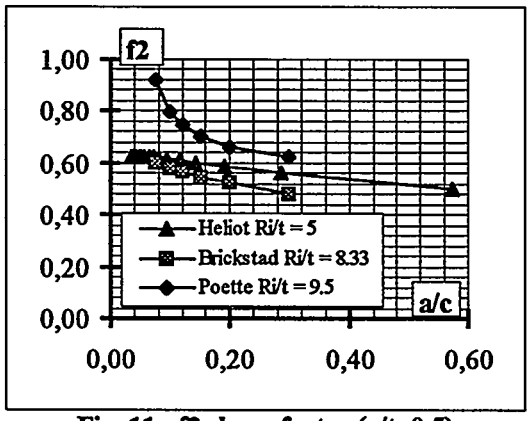

Fig. 11 : f2 shape factor (a/t=0.5)

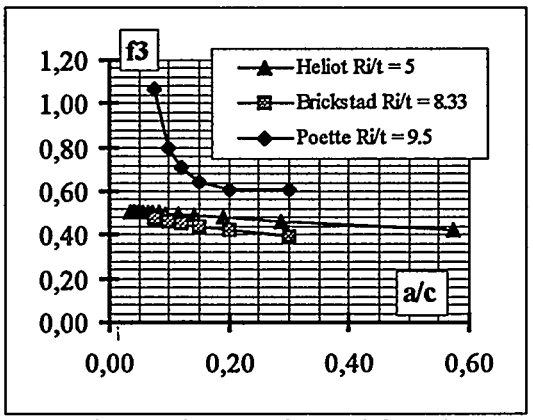

Fig. 12 : f3 shape factor (a/t=0.5)

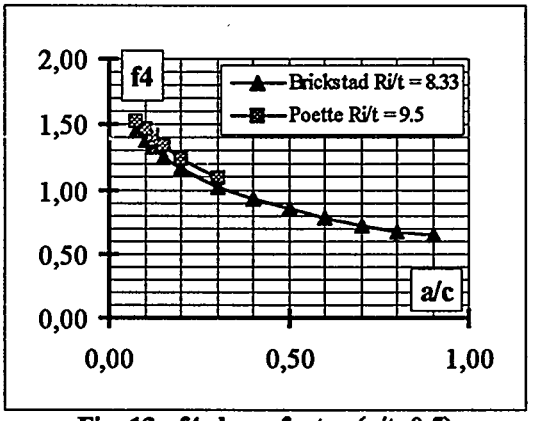

Fig. 13 : f4 shape factor (a/t=0.5)

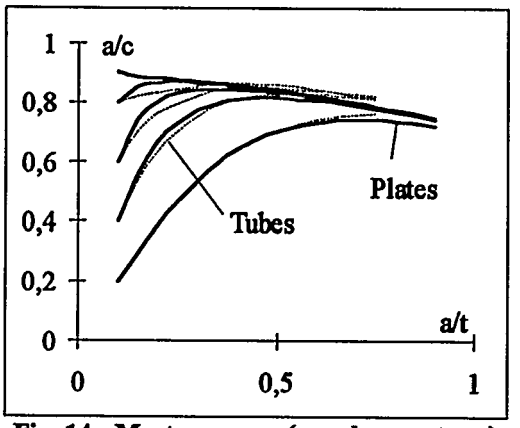

Fig. 14 : Master curves (membrane stress)

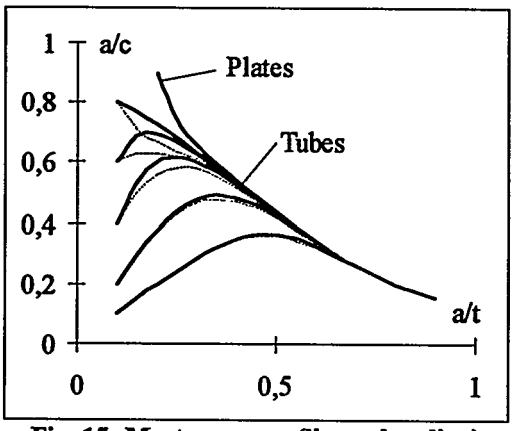

Fig. 15: Master curves (linear bending)

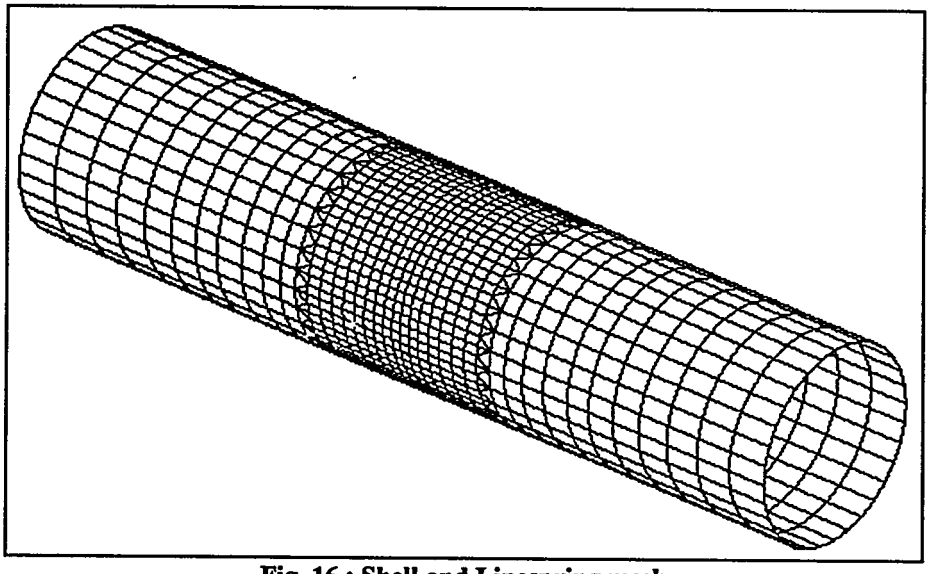

Fig. 16 : Shell and Linespring mesh

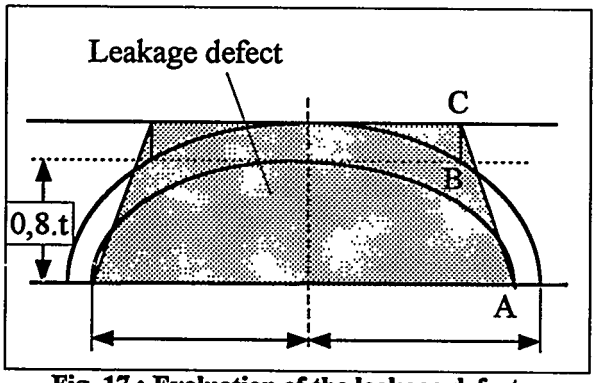

Fig. 17 : Evaluation of the leakage defect

FATIGUE FLAW GROWTH ASSESSMENT AND INCLUSION OF STRATIFICATION TO THE LBB ASSESSMENT

Pavel Samohyl

ABSTRACT

Fatigue flaw growth assessment

The application of the LBB requires also fatigue flaw growth assessment. This analysis was performed for PWR nuclear power plants types VVER 440/230, VVER 440/213č, VVER 1000/320. Respecting that these NPP's were designed according to Russian codes that differ from US codes it was needed to compare these approaches. Comparison with our experimental data was accomplished, too. Margins of applicability of the US methods and their modifications for the materials used for construction of Czech and Slovak NPP's are shown. Computer code accomplishing the analysis according to described method is presented.

Including stratification to the LBB assessment

Some measurement and calculations show that thermal stratifications in horizontal pipelines can lead to additive loads that are not negligible and can be dangerous. An attempt to include these loads induced by steady-state stratification was made.

FATIGUE FLAW GROWTH ASSESSMENT

Preface:

A flaw can occur in the primary piping for of several reasons. They may originate either from manufacture or they can occur by affecting several mechanisms as corrosion, erosion-corrosion or fatigue. The aim of this article is to investigate flaw fatigue propagation in the PWR environment. This investigation is necessary to prevent rupture of the primary piping due to fatigue. Computer code FATLBB was developed for this purpose. It performs analysis of the given flaw using selected method.

Initial flaw size

Initial flaw for the growth analysis can be taken either from the real measured values obtained during inspection or as maximal allowable crack size according to ASME, section XI, IWB-3500. The second way is default in FATLBB code because it is more conservative. Tables in IWB-3500 were fitted using proper polynomials and they were included into FATLBB.

Loading sequences

Real or design operating conditions can be used for design of loading sequences. It is necessary to create a complex model including main circulation piping, pressurizer piping, cool emergency system, steam line and surge

line for examined NPP. Stress analysis for each operation state and each section is performed using standardized computer code STATIC. Membrane and bending stresses for each investigated section are saved to the fatigue database. Loading sequences for each section are made up from the operational states and total axial stresses. Service history of the NPP is taken as base time unit for loading sequence creating. Each loading sequence can be applied several times to be more conservative. It is needed to distinguish between sections laying in separable part (in front of motor operated isolation valve) and unseparable part (behind motor operated isolation valve).

Flaw growth

Fatigue flaw growth is described by well-known Paris' law. It is done in a form

$$da/dN = C_0(\delta K)^n \qquad (1)$$

in ASME code, section XI, C-3210. da/dN is flaw increment per one cycle, δK is amplitude of stress intensity factor, C_0, n are material constants. For austenitic steel in air environment they are

$$C_0 = S \times 10^{-10.009 + 8.12\times10^{-4}T - 1.13\times10^{-6}T^2 + 1.02\times10^{-9}T^3}$$
$S = 1$ when $R \le 0$
$S = 1.0 + 1.8\,R$ when $0 < R < 0.79$
$S = -43.35 + 57.97\,R$ when $0.79 < R < 1.0$
$n = 3.3$

T is temperature in °F, $T \le 800$ °F, $R = K_{min}/K_{max}$ is loading factor. $[K]$ = ksi√in, $[a]$ = in.

Flaw growth in austenitic steel tested in PWR environment is not solved in ASME code. This case is solved in NUREG and EPRI [1], [2]. Because V1 NPP material was produced in Russia and other our plants are designed according to Russian standards and codes it is proper to use also Interatomenergo code [3] and compare the results. All listed methods are available in FATLBB computer code.

NUREG

Fatigue flaw rate consists of three contributions: mechanical fatigue in air, SCC and environment contribution.

$$\dot{a} = \dot{a}_{SCC} + \dot{a}_{env} + \dot{a}_{env} \qquad (2)$$

For oxygen reached water (8 ppm) corresponding to transients we could use the following equations:

$$\dot{a}_{scc} = 2.1\times10^{-13}K^{2.161} \qquad (3)$$

$$\dot{a}_{air} = \frac{a_{air}}{T_R} \qquad (4)$$

$$\dot{a}_{env} = A\dot{a}_{air}^{m} \qquad (5)$$

A, m are experimental constants, T_R is rising time in s.
$[K]$ = MPa√m, $[\dot{a}]$ = m/s.

Computer code FATLBB uses modified equation

$$\dot{a}=\dot{a}_{env}+\dot{a}_{air} \qquad (6)$$

assuming $\dot{a}_{scc}$ can be included to $\dot{a}_{env}$. This assumption is valid if dependence $\dot{a}_{env}$vs $\dot{a}_{air}$ is linear in the logarithmic scale. In Fig. 1 dependence $\dot{a}_{env}$vs $\dot{a}_{air}$ is plotted. Coefficients A, m are determined from this dependence. $\dot{a}_{air}$ is an ASME value calculated using (1) and (4), $\dot{a}_{env}$ is an experimental value minus $\dot{a}_{air}$.

EPRI

This method is described in [2]. It is very simple, but very conservative. Influence of environment is included into constants of Paris' law.

$$da = C.E.S.(\delta K)^n, \qquad (7)$$

where

$C = 2\text{x}10^{-19}$, $n = 3.3$, material constants,
$S = (1 - 0.5\ R^2)^{-4}$, R ratio correction factor
$E = 2$ for PWR (environmental factor)

Interatomenergo

This method is described in [3].

if $\delta K \geq \delta K_{lim}$then

$$da/dN = 2.135\text{x}10^{-6}(3.75R + 0.06).(\delta K)^{1.95}. \qquad (8)$$

if $\delta K < \delta K_{lim}$then

$$da/dN = 1.475\text{x}10^{-11}(26.9R\text{-}5.725).(\delta K)^{5.95}. \qquad (9)$$

$$\delta K_{\text{lim}}=19.492\sqrt[4]{\frac{3.75R+0.06}{26.9R-5.725}}$$

if $R < 0.25$ then $R = 0.25$, if $R > 0.65$ then $R = 0.65$, $[da]$ = mm/cycle, $[\delta K]$ = MPa$\sqrt{}$m.

This method gives an interesting dependence da/dN vs δK (see Fig. 2). It is less conservative then EPRI method and more conservative then NUREG method.

Experiment

The target of the experiment was to verify validity of EPRI and IAE methods and to obtain experimental constants for the NUREG method. Description of the experiment is in [5]. The experiment was performed on archive base and weld material in PWR oxygen saturated water (8 ppm). The saw-like waveform pulse was used with frequency $f = 0.085$ Hz, load ratio $R = 0.2$, water temperature $T = 300$°C. The most conservative cover curve was obtained. In the Figure 2 comparison ASME, EPRI, IAE and experiment are drawn. NUREG values are the same as experiment because coefficients A, m were obtained from the experiment.

Growth analysis

Rain flow method was applied to each block of total stress (sum of membrane and bending stresses) to decompose sequence of stresses to cycles and halfcycles. We determine amplitude of membrane and bending stresses $\delta\sigma_m$, $\delta\sigma_b$ and number of cycle occurrences N_{cycl}. If cycle is half-cycle then $N_{cycl} = N_{block} / 2$ else $N_{cycl} = N_{block}$. N_{block} is number of loading sequence occurrence.

Stress intensity factor amplitude is calculated according to ASME A-3300 for semi-elliptical surface flaw:

$$\delta K = \delta\sigma_m M_m \sqrt{(\pi a/Q)} + \delta\sigma_b M_b \sqrt{(\pi a/Q)} \qquad (10)$$

where M_m, M_b are correction factors for membrane and bending stresses, Q is flaw shape parameter, a is flaw depth. Factors M_m, M_b, Q from Fig. A-3300-1, A-3300-3, A-3300-5 [4] were fitted with using proper polynomials and were included into the computer code.

Choosing NUREG method the calculation proceeds in this way:

1) Determine δK according to (10)
2) Find the flaw increment for one cycle in air environment according to (1)
3) Evaluate flaw rate in air according to (4) and in environment according to (5)
4) Find result flaw rate according to (6)
5) Assess new flaw size and return to 1)

This procedure was repeated through number of block occurrences, all cycles, all sections.

Choosing IAE resp. EPRI method the procedure is rather easier:

1) Determine δK according to (8)
2) Find the flaw increment in one cycle according to (7) resp. (6)
3) Assess new flaw size and return to 1)

Program description

Flow chart of FATLBB code is in Fig. 3. Program is based on the communication with database file which is both input and output. Database file has a standard structure DBF making possible the following process and view conveniently. Each record contains one section. Tube thickness, name of the file with service history, membrane and bending stresses for each operating state. Program creates loading sequence, accomplishes decomposition using raining flaw method and performs calculation as described in the previous chapter. It writes results of the analysis down to the fatigue database. Results of analysis are: initial crack length and depth, final crack length and depth, relative final crack depth and maximal stress intensity factor amplitude.

Conclusions

The methodology for fatigue flaw growth assessment in corrosion environment of PWRs was worked out in the frame of LBB, being based on both experiments and theoretical analyses. Several methods were taken over and tested on our archive material. It has been concluded that it is not possible to take over a method without experimental checking. Coefficients A, m recommended for ASME steels were rather different from our ones. Comparison of NUREG values for ASME steels and our steels is in Fig. 4. It is seen that the fatigue flaw growth in the US steel has a different character.

We developed our computer code for fatigue flaw growth assessment. Using this program we assessed NPPs V1, V2, EDU and ETE.

References

[1] Environmentally Assisted Cracking in Light Water Reactors, NUREG/CR-4667, Vol. 12, ANL-91/24, R5
[2] Evaluation of Flaws in Austenitic Steel Piping, EPRI NP-4690-SR, Special Report, July 1986
[3] M.Brumovský, L.Horáček, K.Kálma, S.Vejvoda: Metodika hodnocení přípustnosti defektů v zařízeních primárního okruhu JE V-213, Plzeň, 1992, Ae 7944/Dok
[4] ASME Boiler and Pressure Vessel Code, Section XI, 1989, July 1, 1989
[5] Hodnocení odolnosti oceli 08CH18N12T ke koroznímu poškození při parametrech primárního okruhu, M.Ruščák, J.Burda, P.Chvátal, J.Kaplan, D.Kárník, J.Otruba, K.Šplíchal, ÚJV Řež, 1992, ÚJV 9708 M

INCLUSION OF STRATIFICATION TO THE LBB ASSESSMENT

Preface:

The contribution presented shows our suggestion how to include stratification into the LBB assessment. The first LBB analyses considering the effect of thermal stratification were performed for NPP's in the Slovak Republic.

The measuring of stratification and stress fields

The effect of the coolant thermal stratification can be observed in the horizontal parts of pipelines with limited coolant flow. Our attention was focused to pressurizer surge line. Three dangerous places were chosen to be analyzed, in each of them outer temperature in five points of pipe half circumference was measured. These analyzed places are marked in the fig. 5. The highest difference in measured temperature between upper and bottom part of the pipe was 70° C. This temperature difference was used as input for the stress analyzes using finite element method.

Loading calculation

Additional load due to stratification was calculated from the finite element calculation according to the following equations (assuming pipe axis lies in x-axis).

$$F_{x,strat.} = \int_f \sigma_x df$$

$$M_{x,strat.} = \int_f \tau_{yz} \sqrt{y^2+z^2} df$$

$$M_{y,strat.} = \int_f \sigma_x z df$$

$$M_{z,strat.} = \int_f \sigma_x y df$$

where F_x is axial force, $M = (M_x, M_y, M_z)$ is force moment, σ_x, τ_{yz} are components of stress tensor, f is area of intercircles affected by σ_x.

Inclusion of stratification to the LBB assessment

Force and moment were added to normal operating condition loadings in such a way that the expression $M_{noc} + kM_{strat.}$ takes its minimum value over $0 \leq k \leq 1$. This minimum value is used for evaluation of crack through which the minimum detectable coolant amount leaks. For the crack stability analysis we include stratification loads as additional thermal dilatations:

$$M_{i,SUP} = |M_{i,deadweight}| + |M_{i,dilat.} + M_{i,strat.}| + |M_{i,pressure}| + |M_{i,MDE}|$$

$$M_{SUP} = \sqrt{\sum_{i=1}^{3} M_{i,SUP}}$$

$$F_{SUP} = |F_{deadweight}| + |F_{dilat.} + F_{strat.}| + |F_{pressure}| + |F_{MDE}|$$

Evaluation of measured results is not ready yet, but we can say that stratification can lead to additive loads that are not negligible and can be dangerous.

Fig. 1
Fatigue flaw rate in air and environment

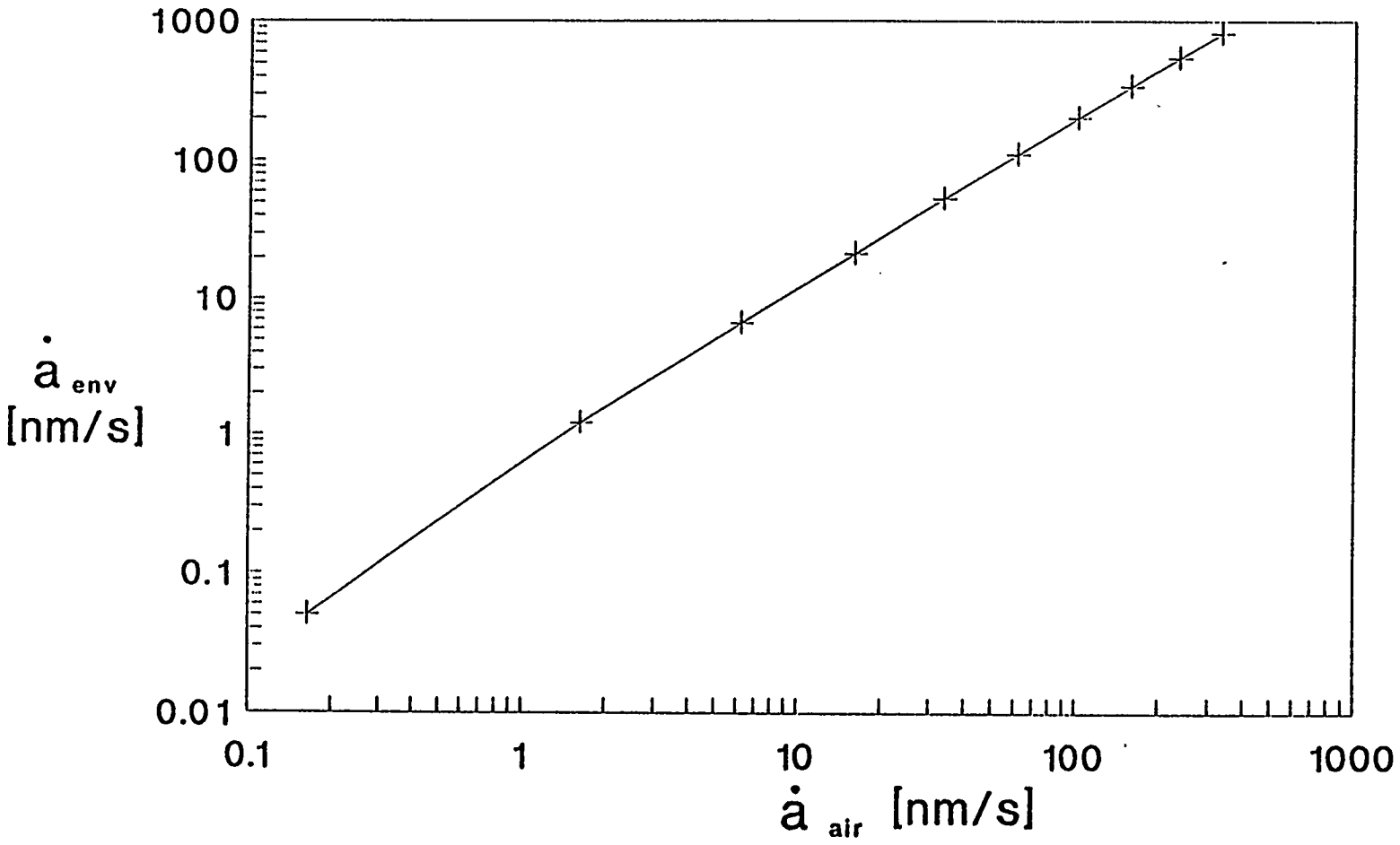

Fig. 2

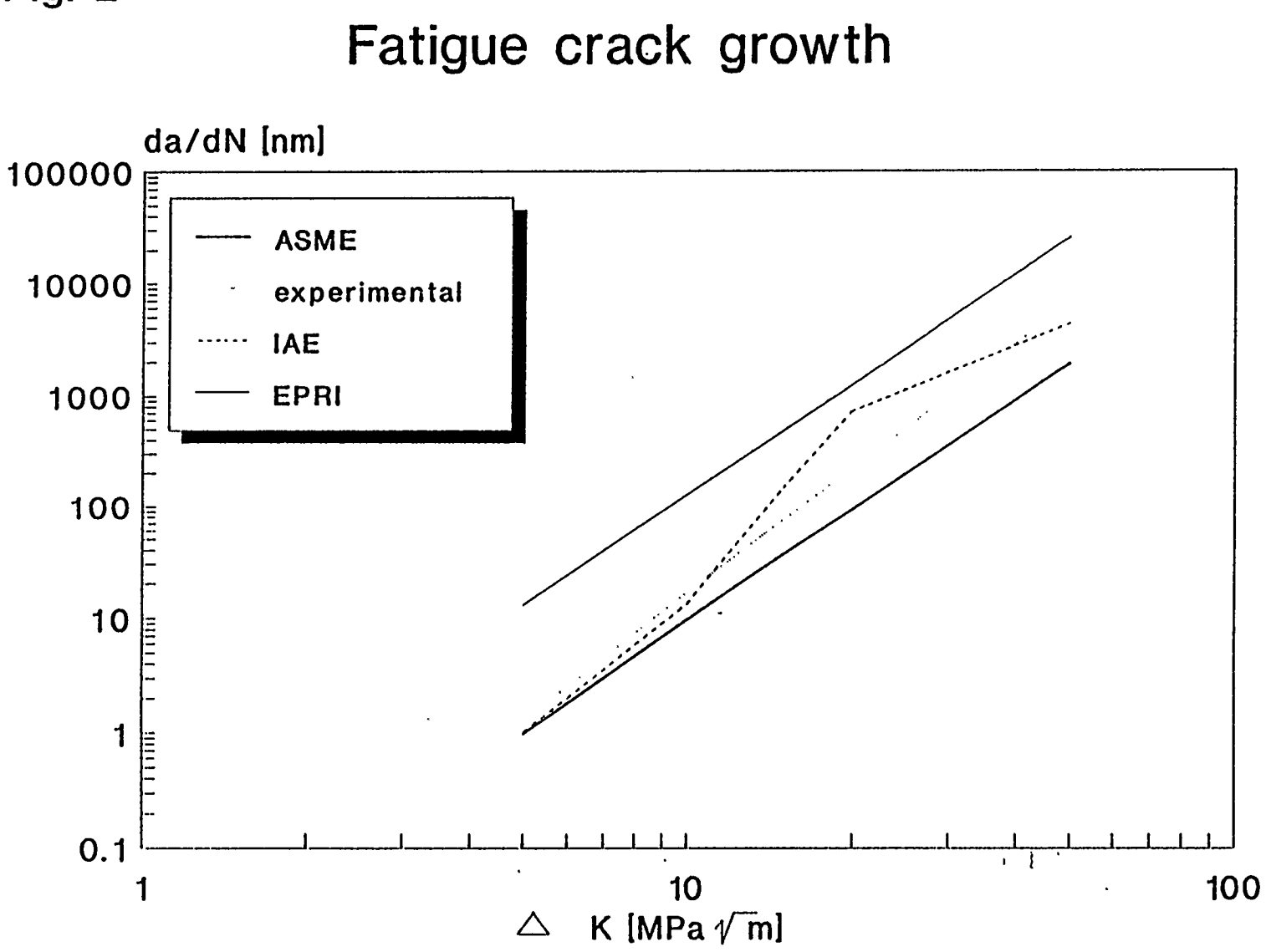
Fatigue crack growth
da/dN [nm]
100000
10000
1000
100
10
1
0.1
ASME
experimental
IAE
EPRI
1
10
100
△ K [MPa √m]

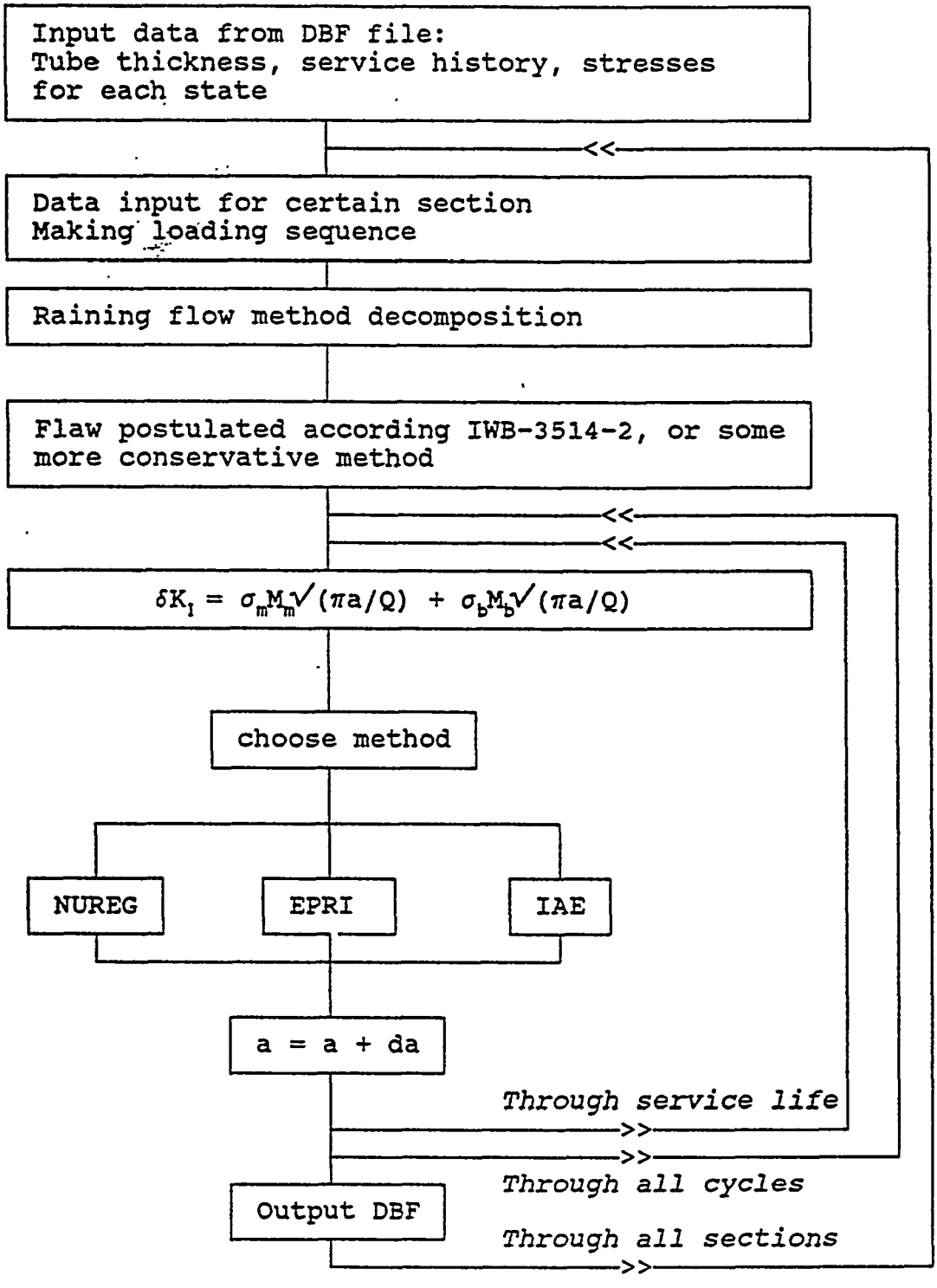

Fig. 3: Flow Chart for the Calculation of Flaw Growth due to Fatigue

Fig. 4

Fatigue flaw growth for ASME steels

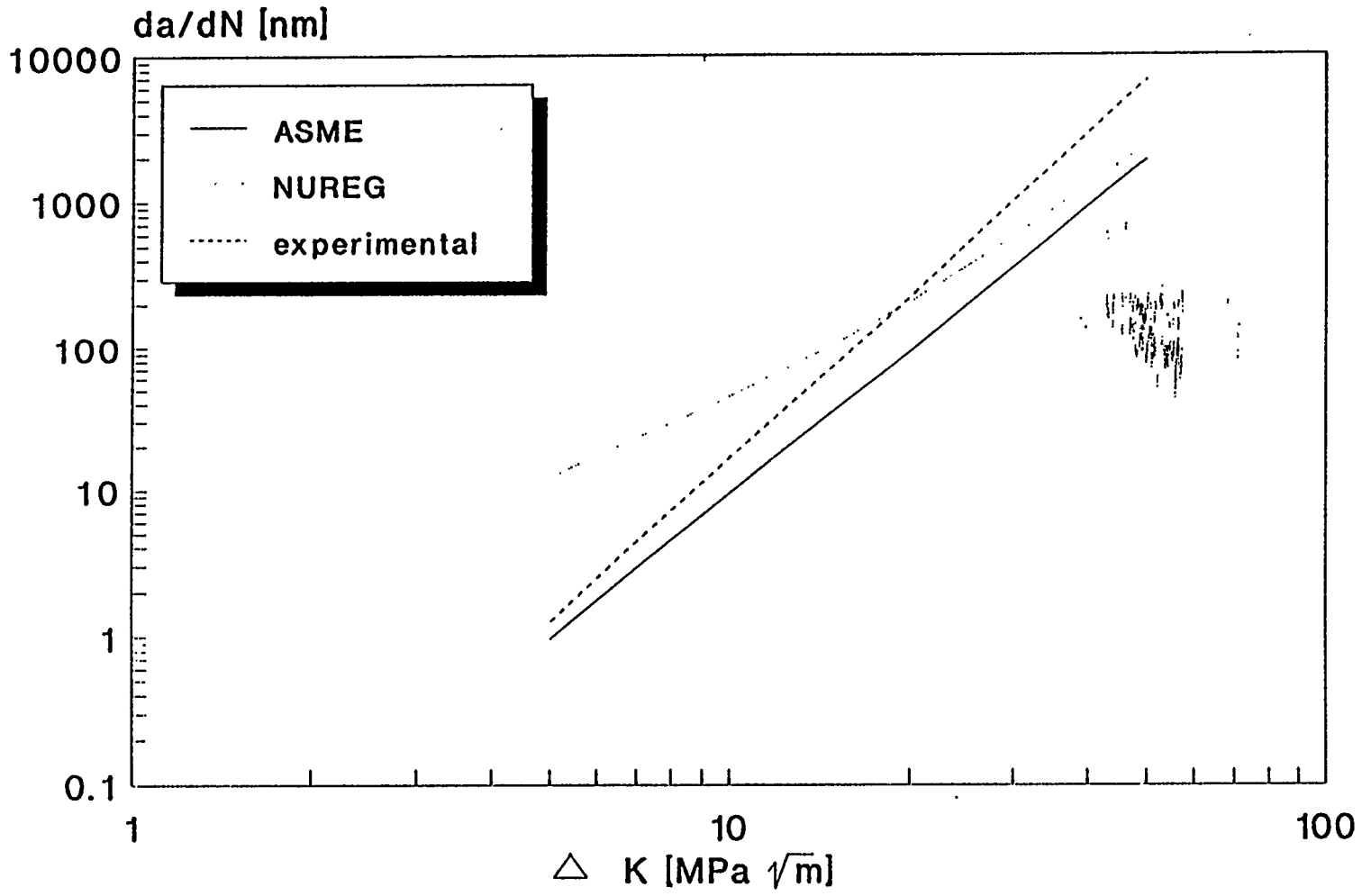

ASSESSMENT OF CRACK OPENING AREA FOR LEAK RATES

J K Sharples[+], P J Bouchard*
AEA Technology, UK[+], Nuclear Electric plc., UK*

ABSTRACT

This paper outlines the background to recommended crack opening area solutions given in a proposed revision to leak before break guidance for the R6 procedure. Comparisons with experimental and analytical results are given for some selected cases of circumferential cracks in cylinders. It is shown that elastic models can provide satisfactory estimations of crack opening displacement (and area) but they become increasingly conservative for values of L_r greater than approximately 0.4. The Dugdale small scale yielding model gives conservative estimates of crack opening displacement with increaing enhancement for L_r values greater than 0.4. Further validation of the elastic-plastic reference stress method for up to L_r values of about 1.0 is presented by experimental and analytical comparisons. Although a more detailed method, its application gives a best estimate of crack opening displacement which may be substantially greater than small scale plasticity models. It is also shown that the local boundary conditions in pipework need to to be carefully considered when evaluating crack opening area for through-wall bending stresses resulting from welding residual stresses or geometry discontinuities.

INTRODUCTION

Crack opening area is a key element in leak before break (LBB) assessment of pressurised plant. Estimates of crack opening area for postulated through-wall cracks can vary widely depending on how the crack is idealised, which crack opening model is used and what material properties are assumed. Estimation methods for crack opening area can be classified into three categories: linear elastic models; elastic models incorporating a small scale plasticity correction; and elastic-plastic models. A wide range of published solutions are available for idealised slot-like cracks in simple geometries subject to basic loadings (pressure, membrane and bending). Their accuracy varies with geometry (e.g. R/t ratio), crack size, type of load and magnitude of load.

A proposed revision to LBB guidance for the R6 procedure [1] (by way of Appendix 9 of the procedure) gives recommended crack opening area solutions for cracks in plates, spheres and cylinders. These solutions include those, which as part of the continuing R6 development programme, have recently been obtained by finite elements for cylinders loaded under internal pressure, global bending and local through-wall bending. Local through-wall bending is of particular relevance to weld residual stresses and geometry discontinuities.

This paper outlines the background to the recommended solutions and gives comparisons with experimental and analytical results for some selected cases of circumferential cracks in cylinders.

REVISED GUIDANCE GIVEN IN R6

The crack opening area solutions recommended in the proposed revision of Appendix 9 for R6 are given in Table 1 and they are for plates, spheres and cylinders ([2], [3] to [7] and [9]). The Appendix recommends the more accurate elastic-plastic model of Langston [7] for best estimate LBB calculations where stress levels are high enough

to induce significant plasticity (i.e. L_r greater than about 0.4). However, this method requires a description of the material stress-strain curve. For bounding conditions, the linear elastic finite element results presented in [5] and [9] are recommended. These results cover a wide range of cylinder geometries (R/t from 5 to 100) and crack lengths. It is also noted that where high accuracy elastic estimates are required, non-linear geometric deformation effects can be important in some circumstances. This statement arises from the findings of an additional study undertaken by Sharples and Kemp [8] to provide guidance as to when non-linear geometry effects can be significant in terms of load level and cylinder size.

Table 1: Crack Opening Area Solutions Recommended In New Appendix 9 For R6

Geometry	Loading	Elastic Or Small Scale Yielding		Elastic-Plastic
		Elastic Model	Plasticity Model	
Plates	Membrane	Westergaard [2]	Dugdale [4]	-
	TWB	Miller [3]	-	-
Spheres	Pressure	Wuthrich [4] $R/t \geq 10, \lambda \leq 5$	Dugdale [4]	-
	TWB	Miller [3]	-	-
Cylinders With Axial Cracks	Pressure	Knowles & Kemp [5] $5 \leq R/t \leq 100$	Dugdale [4]	-
	TWB	Knowles & Kemp [5] $5 \leq R/t \leq 100$	-	-
Cylinders With Circumferential Cracks	Membrane (Pressure)	Knowles & Kemp [5] $5 \leq R/t \leq 100$	Dugdale [4]	Langston [7] $5 \leq R/t \leq 20$
	Global Bending	France & Sharples [9] $5 \leq R/t \leq 100$	Dugdale [4]	Langston [7] $5 \leq R/t \leq 20$
	Membrane + Global Bending	Add elastic components	Dugdale [4]	Kumar [6] $5 \leq R/t \leq 20$
	TWB	Knowles & Kemp [5] $5 \leq R/t \leq 100$	-	-

TWB - Through-Wall Bending Stress

N.B. Where the estimated model gives centre-crack opening displacement rather than area, an elliptical crack opening shape should be assumed (i.e. Crack Opening Area = δ c π / 2, where δ is centre-crack opening displacement and c is semi-crack length)

BACKGROUND TO RECOMMENDED SOLUTIONS FOR CYLINDERS WITH CIRCUMFERENTIAL CRACKS

The background to the recommended solutions given in Table 1 are summarised as follows:

Elastic Model - Knowles and Kemp [5] and France and Sharples [9]

Analytical programmes of work were undertaken to evaluate crack opening areas for cracks in long cylinders or pipes. Analyses were carried out using a full 3-D finite element elastic model with 20 node quadratic interpolation,

reduced integration elements. Both longitudinal and part-circumferential through-wall cracks were considered with centres half way along the cylinder length.

The radius of the cylinder was fixed and thickness, t, was varied giving R/t values of 5, 10, 20, 50 and 100 where R is mean radius. A range of crack lengths were considered, characterised by the thin shell analysis parameter λ:

$$\lambda = [\, 12\,(\,1 - \nu^2\,)\,]^{0.25}\, a\,/\,(\,Rt\,)^{0.5} \qquad (1)$$

where a is the half crack length and ν is Poisson's ratio. λ values ranged from 1 to 12 for the longitudinal cracks and from 0.18 to 63 for the circumferential cracks. These values corresponded to crack lengths of between 2 mm to 120 mm and of between 5° and 180° around the circumference respectively.

Internal pressure and through-wall bending moment loading conditions were considered for both types of crack in [5]. The bending moment load was applied by specifying an appropriate pressure loading distribution to the crack face elements. The finite element calculations were extended to include the global bending case [9]. Considerations relating to the through-wall bending work are covered below in a later section.

Small Scale Yielding Model - Dugdale [4]

Wuthrich used the Dugdale model [4] in order to extend the range in which plasticity effects can be described and this results in crack opening area, A, for cylindrical geometries being given by:

$$A = \alpha\,(\lambda)\,\gamma\,(s)\,A_0 \qquad (2)$$

A_0 is the crack opening area for a plane sheet given by:

$$A_0 = 2\,\pi\,\sigma\,a^2\,/\,E' \qquad (3)$$

where σ is membrane stress, a is crack semi-length and E' is E for plane stress and $E\,/\,(\,1 - \nu^2\,)$ for plane strain, E being Young's modulus and ν, Poisson's ratio.

$\alpha\,(\lambda)$ is a bulging factor which according to Kastner et. al. [10], is approximately:

$$\alpha = (\,1 + 0.117\,\lambda^2\,)^{0.5} \qquad (4)$$

for circumferential cracks in pipes.

The plasticity factor developed by Wuthrich is given by:

$$\gamma = 1/s\,[\,(1-s\,)^2\,\sec^2(\pi s/2) + 4/\pi(1-s\,)\,\tan(\pi s/2) - 8/\pi^2\,\ln\cos(\pi s/2)\,]$$

$$+\,(1-1/s)\,[\,2/\pi\,\sqrt{}\,(\sec^2(\pi s/2) - 1) + (1-s)\sec^2(\pi s/2)\,] \qquad (5)$$

where $s = \sigma/\sigma_F$ and σ_F is flow stress.

Numerical values for this formula are given as follows:

s	0	0.1	0.2	0.3	0.4	0.5	0.6	0.7	0.8	0.9
γ	1.00	1.01	1.03	1.07	1.12	1.20	1.30	1.45	1.68	2.12

Elastic-Plastic Model - Kumar (GE/EPRI) [6]

For a material whose uniaxial stress-strain (σ-ε) curve is described by:

$$\varepsilon / \varepsilon_0 = \sigma / \sigma_0 + \alpha (\sigma / \sigma_0)^n \qquad (6)$$

the estimation scheme of [6] suggests that the crack opening displacement δ at the centre of a circumferential crack of half-length, a, in a cylinder of mean radius R and thickness t can be written as:

$$\delta = (4 \sigma a_e / E) V_1 (a_e / b, R/t) + \alpha \varepsilon_0 a h_2 (a/b, n, R/t) (P / P_0)^n \qquad (7)$$

In Eq. 6, ε_0, σ_0, α and n are constants with σ_0 usually taken to be the yield stress and ε_0 to be σ_0 / E.

In Eq. 7, the first term represents the elastic contribution to the crack opening displacement with σ the applied stress acting to open the crack and a_e an effective crack half-length defined as:

$$a_e = a + 1 / (\beta \pi) [(n - 1) / (n + 1)] [K_1(a) / \sigma_0]^2 [1 + (P / P_0)^2]^{-1} \qquad (8)$$

where $K_1(a)$ is the elastic stress intensity factor and β a constant with $\beta = 2$ for plane stress and $\beta = 6$ for plane strain. P is the applied load and P_0 is a normalising factor equal in this case to the limit load of the cracked structure.

The dimensionless function V_1 in Eq. 7 depends purely on geometry through the normalised crack length a/b, with $b = \pi R$ the half-circumference of the cylinder, and the ratio R/t.

The second term in Eq. 7 represents the fully-plastic contribution to the crack opening displacement and h_2 is a dimensionless function depending on geometry and the strain hardening exponent n. The dimensionless functions V_1 and h_2 were derived by fitting Eq. 7 to the results of finite element calculations and are tabulated in [6] for a range of normalised crack lengths, cylinder radius to thickness ratios and values of strain hardening exponent n.

Elastic-Plastic Reference Stress Method - Langston [7]

Langston developed, and validated by comparison with experiments, a reference stress based approximation for calculating the crack opening displacement of circumferential cracks in cylinders, derived from the GE/EPRI estimation scheme referred to above [6]. This development is based on Eq. 7. Defining the reference stress, σ_{ref} as:

$$\sigma_{ref} = (P / P_0) \sigma_0 \qquad (9)$$

and replacing a_e and h_2 (a/b, n, R/t) with functions which depend only on geometry and loading and are independent of any parametric fit to the stress-strain curve (according to Ainsworth [11]), the crack opening displacement becomes:

$$\delta = (4 \sigma a_e / E) V_1 (a_e / b, R/t) +$$

$$[4 \sigma a V_1 (a/b, R/t) / E] [h_2^* (a/b, R/t) / h_2 (1)] [E \varepsilon_{ref} / \sigma_{ref} - 1] \qquad (10)$$

Since with increasing n, the factor (n - 1) / (n + 1) rapidly approaches unity, and only varies between 0 and 1 for all $n \geq 1$, the dependence on n can be removed in Eq. 8 by setting (n - 1) / (n + 1) to its mid-range value of 1/2. The effective crack half-length defined by Eq. 8 then becomes:

$$a_e = a + 1/(2\beta\pi)\ [K_1(a)/\sigma_0]^2\ [1 + (P/P_0)^2]^{-1} \qquad (11)$$

Equation 10, together with the modified definition of a_e in Eq. 11, therefore form the reference stress approximation for crack opening displacement.

The normalised functions $h_2^*(a/b,\ R/t)/h_2(1)$ necessary to use the reference stress approximation are shown in graphical form in Fig. 1. Although the normalised functions depend markedly on crack length, they vary little with R/t or the type of loading. The dimensionless functions $V_1(a/b, R/t)$ are tabulated in [6].

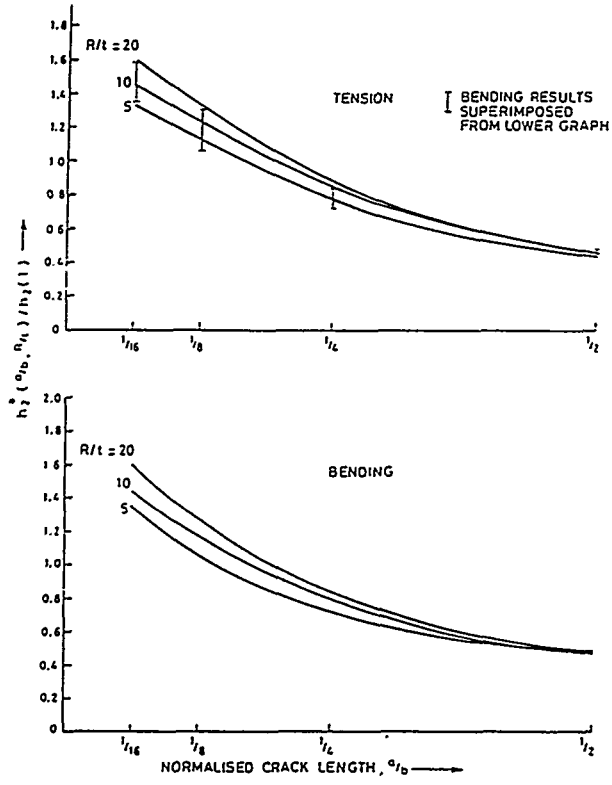

Figure 1 Variation of the Normalised Functions $h_2^*(a/b,\ R/t)/h_2(1)$ with a/b, R/t and Loading

IPIRG EXPERIMENTS AND ROUND ROBIN PROBLEMS

The results of two IPIRG pipe experiments [12] have been used in the comparison. These are Experiment 4111-2 for global bending and Experiment 1-8 for combined membrane (internal pressure) plus global bending. Details of the test specimens and material properties for these two experiments are given in Table 2.

UK finite element results of two IPIRG round-robin problems have been used in the comparison. The problems under consideration were A3.b and B1.b, the test specimen and material property details of which are also given in Table 2.

As can be seen, Problem A3.b is relevant to Experiment 4111-2 but with E being some 8% higher. Problem B1.b is relevant to Experiment 1-8 but with the yield properties being approximately 10% higher.

Lynch [13] performed linear elastic and non-linear elastic-plastic finite element calculations for Problem A3.b using the BERSAFE suite of programmes. May et. al. [14] performed finite element calculations for Problem B1.b using the ABAQUS programme.

Table 2: IPIRG Experiment And Round Robin Problem Details

	IPIRG Experiments		IPIRG Round Robin Problems	
	Expt. 4111-2	Expt. 1-8	Problem A3.b	Problem B1.b
Outer Diameter (mm)	711	399	711	402.6
Pipe Thickness (mm)	23.6	26.2	23.6	26.4
Pipe Material	A515 Gr. 60	A106 Gr. B		
Internal Pressure (MPa)	0	15.5	0	15.5
$2a/\pi D_m$[(a)]	0.37	0.12	0.37	0.12
Inner Span (m)	3.35	3.35	3.35	3.35
Outer Span (m)	11.58	11.58	11.58	11.58
Initiation Load (kN)	396	302		
Maximum Load (kN)	585	504		
Young's modulus, E (GPa)	179.3	193.1	193.06	193.06
Yield Stress, σ_y (MPa)	231	217	230.1	237.2
Ultimate Stress, σ_u (MPa)	544	508	544	610.2
Ramberg-Osgood Coeff, α[(b)]	1.10	174	1.107	2.157
Ramberg-Osgood Coeff, n[(b)]	5.50	4.66	5.55	4.042

(a) 2a = through-wall crack length at mean pipe diameter; D_m = mean pipe diameter

(b) Stress-strain curve is represented by: $\varepsilon/\varepsilon_0 = \sigma/\sigma_0 + \alpha(\sigma/\sigma_0)^n$, where $\sigma_0 = \sigma_y$, $\varepsilon_0 = \sigma_0/E$

COMPARISON OF RESULTS

A comparison of crack opening displacements evaluated from different solutions and relevant IPIRG data was made for the loading cases of (i) global bending, (ii) membrane (i.e. pressure), and, (iii) combined membrane and global bending. The results of the comparisons are given in Fig. 2 for different values of the R6 L_r parameter (i.e. reference stress/yield stress).

Global Bending

Figure 2 (a) contains the results for the global bending case which is based on the IPIRG 4111-2 experiment and associated round robin A3.b problem (see Table 3). The elastic finite element results of [5] (as recommended in the new Appendix 9 of R6, Table 1) are the same as those of [13] as expected. Plasticity corrections to these results based on the Dugdale small scale yielding model [4] show an increasing enhancement of crack opening displacement with increasing L_r. The non-linear elastic-plastic finite element results (shown for both the inner and outer surfaces) show even higher values of crack opening displacement as anticipated. The results based on the Langston reference stress method [7] are fairly consistent with the elastic-plastic finite element results, thus providing good validation for the method. The values of crack opening displacement measured in the IPIRG experiment are generally higher than the calculated values. However, for L_r values below approximately 0.4, the experimental results are shown to be lower than even the calculated elastic curve. This is probably a consequence of the sensitivity of the experimental measuring equipment which requires further investigation.

Membrane (Pressure)

Figure 2 (b) contains the results for the membrane (pressure) case which is based on the geometry of the round robin A3.b problem associated with the IPIRG 4111-2 experiment. As can be seen from this figure, the elastic finite element calculations of [5] show crack opening displacement values approximately 6% higher than those obtained

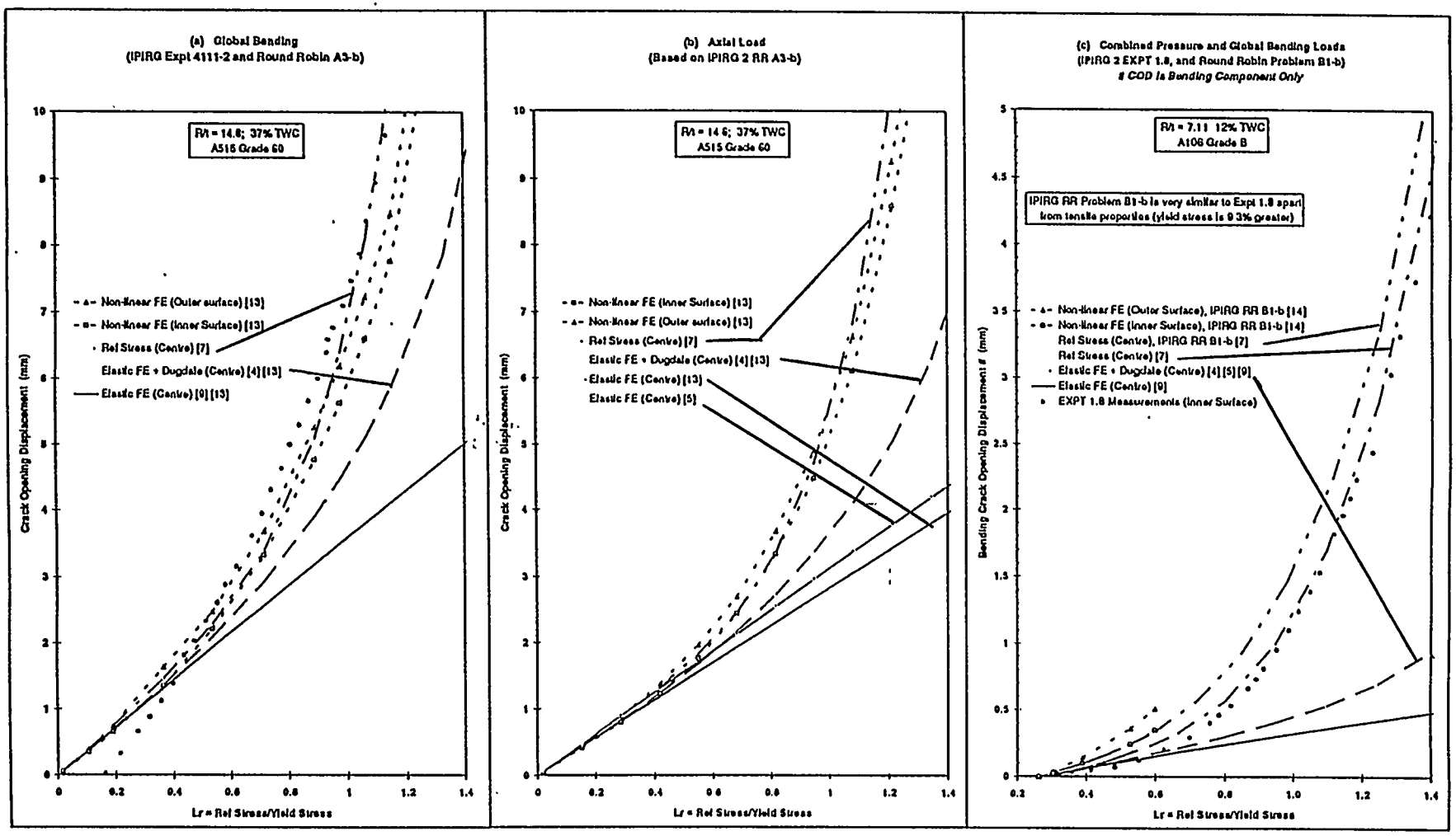

Figure 2 Crack Opening Displacement Versus Lr for Circumferentially Cracked Pipes

from the finite element calculations of [13]. This small difference is likely to be due to a combination of the different meshes generated in the two sets of analyses and the fact that the results from [5] for the specific geometry under consideration here were obtained by linear interpolation. The trend for the results based on the other methods is similar to that discussed above with reference to Fig. 2 (a).

Membrane + Global Bending

Figure 2 (c) contains the results for the combined pressure and global bending case which is based on the IPIRG 2 experiment 1.8 and associated round robin B1-b problem whereby the crack length is smaller than for the case considered in Fig. 1(a) and (b) (12% of the circumference compared with 37% of the circumference). The crack opening displacement values are for the global bending component only. Two sets of values for the reference stress method of [7] are presented to reflect the fact that there is a difference of approximately 9% between the yield stress of the pipe material used in the experiment and that specified in the round robin problem. It should be noted that although the reference stress method of [7] was used in this comparison, the method has not been fully validated for combined loadings and hence it is not currently recommended for such in the proposed revision to Appendix 9 of R6 (Table 1). As with Fig. 2 (a), it can be seen that the results for the Langston reference stress method [7] are fairly consistent with those of the elastic-plastic finite element results.The experimental points measured at the inner surface are shown to be slightly lower than the reference stress method results obtained for the centre of the crack. Experimental points for the centre would therefore be coincident with or slightly higher than the reference stress curve. The experimental and analytical comparisons therefore again provide good validation for the reference stress method.

CONSIDERATIONS FOR THROUGH-WALL BENDING IN RELATION TO RESIDUAL STRESSES

Local through-wall bending stresses can induce elastic crack face rotations which will reduce effective crack opening area. If complete crack closure occurs, no LBB case can be made. Significant local through-wall bending stresses may be present in thick-walled shells under internal pressure loading, or be associated with weld residual stresses or geometric discontinuities.

The models considered in the elastic finite element analysis of [5] for local through-wall bending, as previously referred to, were for long cylinders. However, it is likely that in many practical pipework configurations, e.g. at pipe nozzle welds, the local pipe boundary conditions may significantly influence the crack opening displacements. To investigate this effect, the cases of the two extreme values of cylinder R/t ratio of 5 and 100 and circumferential crack lengths of 5° and 180°, presented in [5], were re-analysed with a reduced length of cylinder (1 pipe diameter) and two end restraint conditions. The two end boundary conditions modelled were (i) totally un-restrained (as in the analysis of [5], and, (ii) restrained in all directions.

Crack opening displacement values calculated from the analysis are given in Table 3 at the inner, mid-wall and outer surfaces. The applied through-wall bending resulted in nominal tension on the inner wall and nominal compression on the outer wall. The displacements are assumed positive in the direction of crack opening and it should be noted that the computed negative values of crack opening are a consequence of the fact that contact elements, modelling crack closure effects, were not used in the finite element analyses. Computed negative values of crack opening therefore result in crack closure in practice. Even allowing for this, it can be seen that the modelled cylinder length and restraint conditions have a significant effect on the results for the 180° cracks but a minimal effect for the shorter crack (5°) considered.

It is very important therefore, for local boundary conditions to be carefully considered when evaluating crack opening area (and indeed critical crack length) in LBB assessments where through-wall bending stresses resulting from welding residual stresses or geometry discontinuities are present.

Table 3: Comparison Of Crack Opening Displacements For Short And Long Cylinder Models

Case	R/t	Crack Length (Deg.)	t (mm)	λ	Inner (μm)	Mid (μm)	Outer (μm)
Long - NR	5	5	4	0.177	1.147	-0.037	-1.354
Short - NR	5	5	4	0.177	1.232	-0.036	-1.432
Short - FR	5	5	4	0.177	1.232	-0.035	-1.430
Long - NR	5	180	4	6.385	-13.960	-19.240	-26.920
Short - NR	5	180	4	6.385	-35.070	-46.320	-57.400
Short - FR	5	180	4	6.385	4.660	-1.561	-7.635
Long - NR	100	5	0.2	0.793	0.646	-0.035	-0.715
Short -NR	100	5	0.2	0.793	0.604	-0.034	-0.670
Short - FR	100	5	0.2	0.793	0.604	-0.033	-0.669
Long - NR	100	180	0.2	28.55	-2.749	-4.096	-5.443
Short - NR	100	180	0.2	28.55	-21.800	-23.290	-24.780
Short -FR	100	180	0.2	28.55	1.306	-0.030	-1.346

NR - No end restraint conditions
FR - End nodes of model fixed in all directions

CONCLUSIONS

1. Elastic models can provide satisfactory estimations of crack opening displacement (and area) but they become increasingly conservative for values of L_r greater than approximately 0.4.

2. The Dugdale small scale yielding model gives conservative estimates of crack opening displacement with increaing enhancement for L_r values greater than 0.4.

3. Further validation of the elastic-plastic reference stress method for up to L_r values of about 1.0 has been presented by experimental and analytical comparisons. Although a more detailed method, its application gives a best estimate of crack opening displacement which may be substantially greater than small scale plasticity models.

4. The local boundary conditions in pipework need to to be carefully considered when evaluating crack opening area for through-wall bending stresses resulting from welding residual stresses or geometry discontinuities.

ACKNOWLEDGEMENTS

This paper was written under the R6 development programme which is sponsored by Nuclear Electric plc., AEA Technology, British Nuclear Fuels plc. and Scottish Nuclear plc. and the paper is published by permission of AEA Technology and Nuclear Electric plc.

The authors wish to specifically acknowledge Mrs C C France of AEA Technology for undertaking the finite element analyis of the short cylinder model referred to.

REFERENCES

1. Milne I, Ainsworth R A, Dowling A R and Stewart A T, Assessment Of The Integrity Of Structures Containing Defects, Int. J. Pres.Ves. & Piping, 32 (1988) 3-105.

2. Westergaard H M, Bearing Pressure And Cracks, J. Applied Mech. 60, June (1939).

3. Miller A G, Elastic Crack Opening Displacements And Rotatiions In Through Cracks In Spheres And Cylinders Under Membrane And Bending Loading, Eng. Fract. Mech. 23, 631-648, (1994).

4. Wuthrich C, Crack Opening Areas In Pressure Vessels And Pipes, Eng. Frac. Mechanics Vol. 18, No. 5, pp.1049-1057 (1983).

5. Knowles J A and Kemp S, Crack Opening Areas For Longitudinal And Part-Circumferential Through-Wall Cracks In Cylinders, AEA/RS/4498 (1994), AEA Technology Document.

6. Kumar V and German M D, Elastic-Plastic Analysis Of Through-Wall And Surface Flaws In Cylinders, EPRI Report NP-5596, January (1988).

7. Langston D B, A Reference Stress Approximation For Determining Crack Opening Displacements In Leak-Before-Break Calculations, TD/SID/REP/0112 (1991), Nuclear Electric Document.

8. Sharples J K and Kemp S, Effect Of Non-Linear Geometry On results Of Finite Element Calculated Crack Opening Displacements In Cylinders, AEA/RS/4463 (1994), AEA Technology Document.

9. France C C and Sharples J K, Stress Intensity Factor and Crack Opening Area Solutions For Through-Wall Circumferential Cracks In Cylinders Loaded Under Global Bending, AEA/TSD/0813, (1995), AEA Technology Document.

10. Kastner W, Rohrich E, Schmitt W and Steinbuch R, Int. J. Pres.Ves. & Piping, 9 (1981) 197-219.

11. Ainsworth R A, The Assessment Of Defects In Structures Of Strain-Hardening Material, Engineering Fracture Mechanics, Vol. 19, N0. 4 (1984).

12. Rahman et. al., Refinement And Evaluation Of Crack Opening Area Analyses For Circumferential Through-Wall Cracks In Pipes, NUREG/CR-6300, BM1-2184 (1995).

13. Lynch K M, Finite Element Fracture Analysis For A Cylinder Containing A Through-Wall Circumferential Crack Under Bending Load, TIGA/REP/0008/93 (1993), Nuclear Electric Document.

14. May K A, Sanderson D J and Wintle J B, Investigation Of The Effect Of Plasticity And Non-Centred Bending On Crack Opening Area For Leak-Before-Break Of Piping Systems, AEA/RS/4528 (1994), AEA Technology Document.

DETERMINATION OF LEAKAGE AREAS IN NUCLEAR PIPING

by

E. Keim
Siemens/KWU
Erlangen/Germany

INTRODUCTION

For the design and operation of nuclear power plants the Leak-Before-Break (LBB) behaviour of a piping component has to be shown. This means that the length of a crack resulting in a leak is smaller than the critical crack length and that the leak is safely detectable by a suitable monitoring system. The LBB-concept of Siemens/KWU [1] is based on computer codes for the evaluation of critical crack lengths, crack openings, leakage areas and leakage rates, developed by Siemens/KWU. In [2] the experience with the leak rate program is described while this paper deals with the computation of crack openings and leakage areas of longitudinal and circumferential cracks by means of fracture mechanics.

The leakage areas are determined by the integration of the crack openings along the crack front, considering plasticity and geometrical effects. They are evaluated with respect to minimum values for the design of leak detection systems, and maximum values for controlling jet and reaction forces. By means of fracture mechanics LBB for subcritical cracks has to be shown and the calculation of leakage areas is the basis for quantitatively determining the discharge rate of leaking subcritical through-wall cracks.

The analytical approach and its validation will be presented for two examples of complex structures. The first one is a pipe branch containing a circumferential crack and the second one is a pipe bend with a longitudinal crack.

MODELS FOR CRACK OPENING DISPLACEMENTS AND LEAKAGE AREAS

The analytical model is based on solutions of crack opening areas in plates containing through-wall cracks. Analogous to the assumptions in plates relations between crack area, through-wall crack length and loading are established for through-wall cracks in cylindrical structures (pipe lines, pressure vessels etc.).

In general, the method is founded on well known relationships between the displacement of the crack surface due to external load and by taking into account the plastic zones at the crack tip. The leakage area is the integral of the crack opening displacements V(x) along the crack front x, where $0 < x < c$:

$$A(2c) = 4 \int v(x)\, dx \qquad (1)$$

Applying a plastic zone size correction on the crack tip according to the Dugdale-model /3/ the crack opening displacements can be given in a general form:

$$v(x) = \frac{1+k}{8\pi G} \cdot \sigma_F \cdot (c+p) \cdot \left\{ \cos\varphi \cdot \ln\left[\frac{\sin^2(\theta-\varphi)}{\sin^2(\theta+\varphi)}\right] + \cos\theta \cdot \ln\left[\frac{(\sin\theta+\sin\varphi)^2}{(\sin\theta-\sin\varphi)^2}\right]\right\} \quad (2)$$

with $k = \frac{3-\nu}{1+\nu}$ for plane stress condition, (3)

$k = 3 - 4\nu$ for plane strain condition (4)

ν = Poisson's ratio; E = Young's modulus; $G = \frac{E}{2\cdot(1+\nu)}$ (5)

$$\Theta = \frac{\pi\sigma}{2\sigma_F}; \qquad p = \left(\frac{1}{\cos\Theta} - 1\right) \cdot c \quad (6),(7)$$

σ = applied stress; σ_F = flow stress; p = length of the plastic zone.

This generalised form is split up in more detail for the loaded and unloaded condition [5] and leads to methods for calculation of minimum (unloaded) and maximum (loaded) values.

The leakage areas in cylindrical components (pipes and vessels) are estimated using the bulging functions $\alpha(\lambda)$, which take into account the curvature of the cylinder and the crack orientation:

$$A(2c)cyl = \alpha(\lambda)\ A(2c) \quad (8)$$

with

$\alpha(\lambda) = \sqrt{1 + 0.117\lambda^2}$ for circumferential cracks (9)

$\alpha(\lambda) = 1 + 0.1\lambda + 0.16\lambda^2$ for axial cracks (10)

$\lambda^2 = \sqrt{12(1-\nu^2)} \cdot \frac{c^2}{r_m \cdot t}$, r_m = mean cylinder radius, t = wall thickness. (11)

For the calculation of the crack openings and leakage areas Siemens has developed an own code, called LECKV [4]. The verification of the theoretical model is performed by comparison with experiments and numerical calculations, where in [5,6] a comparison with the results of straight pipes is performed and in the next chapter special geometries are investigated.

VALIDATION OF THEORETICAL MODELS

The methods presented are compared to experimental and numerical results of complex structures. Two examples are analysed which confirm the applicability of the analytical models also for non straight pipes.

Example 1: Circumferential crack in a pipe branch (HDR experiment E22.12, [7])

This example demonstrates the application to a through-wall crack in a pipe branch which has a length of 180° along the circumference. The crack is located in the intersection of two stainless steel pipes. Applying the program LECKV leads to minimum and maximum values for the crack opening displacement in the centre of the crack (COD) and the leakage areas. The pipe branch was loaded by a constant internal pressure and external bending moment. In [7] the experimental results are given at three different bending moment steps.

A comparison of the analytical and experimental results of COD is given in Figure 1, where following input data are used:

- crack angle: 180°
- outer diameter: 50 mm
- wall thickness: 12.5 mm
- internal pressure: 105 bar
- temperature: 310 °C
- bending moment: up to 1.4 kNm
- material: stainless steel 1.4571
- flow stress: $\sigma_F = \frac{R_{p0,2} + R_m}{2} = 299.5$ MPa

The results show, that the experimental data are enveloped by the minimum and the maximum values of the analytical model, that means that a good approximation also for a complex geometry like the pipe branch could be performed.

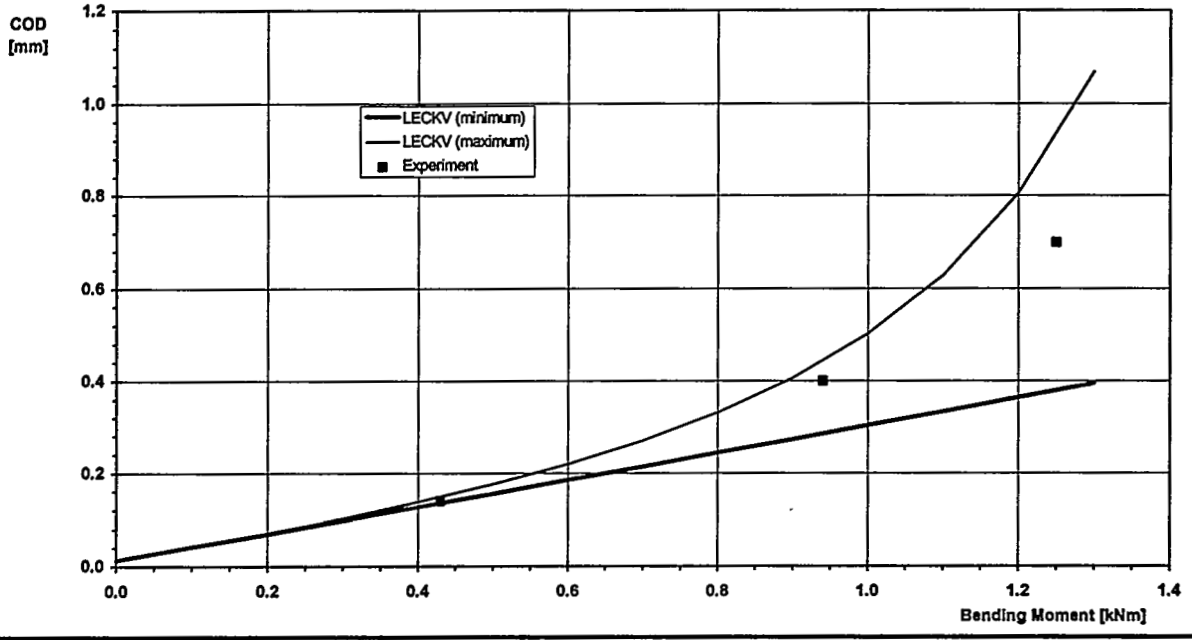

Fig. 1: Crack Opening Displacement for a Pipe Branch (Circumferential Crack, HDR Experiment E22.12)

Example 2: Longitudinal crack in a pipe bend (Siemens/KWU finite element calculations)

For a longitudinal crack in the crown of a main coolant pipe bend the leakage areas are determined. The crack opening area was assumed to be of a diamond shape for the minimum values and of trapezoidal shape for the maximum values.

Following input data are used:

- crack length: 900 mm
- outer diameter: 900 mm
- wall thickness: 45 mm
- internal pressure: 100 bar
- temperature: 310 °C
- material: ferritic steel 20 MnMoNi 5 5
- flow stress: $\sigma_F = \frac{R_{p0,2} + R_m}{2} = 540$ MPa.

The finite element calculations allows for the integration of the crack opening displacements along the crack front on the inner surface and on the outer surface. Those values are compared to the minimum and maximum solution of the analytical LECKV code, as shown in Figure 2. The agreement is very good.

SIEMENS

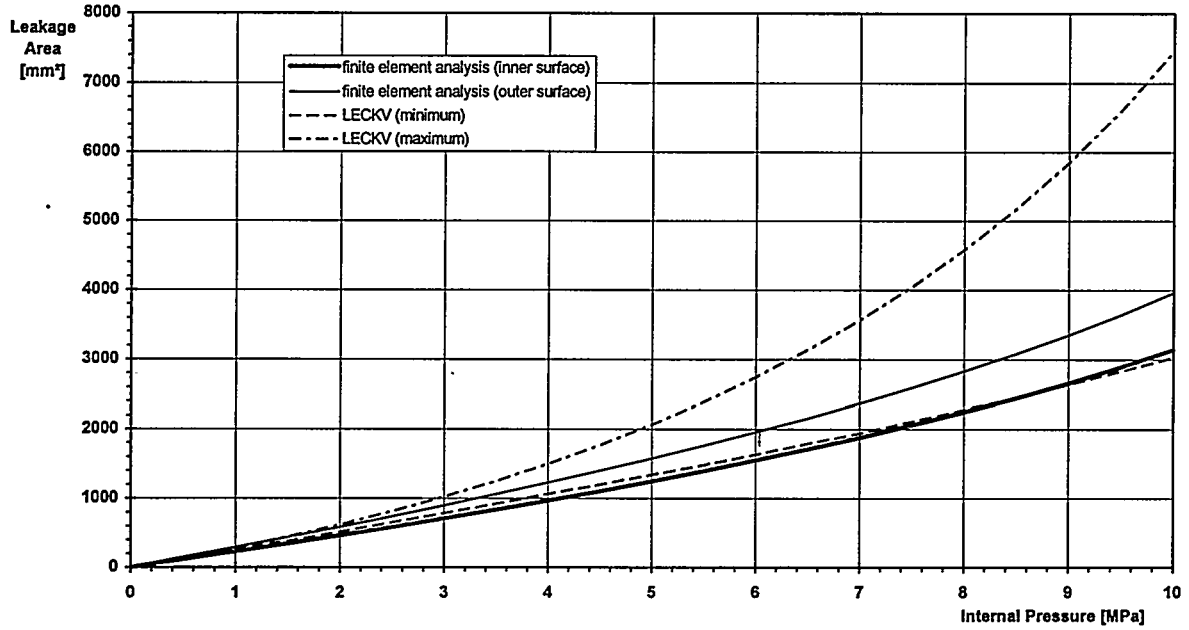

Fig. 2: Leakage Area of a Pipe Bend Under Internal Pressure (Longitudinal Crack, Main Coolant Pipe Bend)

SUMMARY

The calculation models for the determination of crack opening displacements and leakage areas are introduced in a general form. Besides the application of the models to through-wall cracks in straight pipes given in [5,6], examples for the evaluation of cracks in complex structures like pipe branch and pipe bend are demonstrated. A comparison with either experimental or numerical results leads to a very good agreement, so the LECKV program has turned out to be an effective tool in the assessment of cracks in piping applying the LBB-concept.

REFERENCES

/1/ G. Bartholomé, R. Wellein, G. Senski; 12th SMiRT, 1993, paper GF08/2, Stuttgart FRG

/2/ H. Grebner, W. Kastner, A. Höfler, G. Maussner; LBB '95, paper no. 26, Lyon, Oct. 9-11, 1995

/3/ D. S. Dugdale; J. Mech. Phys. Solids, 1960, Vol.8, 100 - 104

/4/ LECKV - Program for calculation of leckage areas and crack openings; Siemens/KWU

/5/ G. Bartholomé, W. Kastner, E. Keim; 11th SMiRT, 1991, paper G22/2, Tokyo, Japan

/6/ G. Bartholomé, W. Kastner, E. Keim; Nucl. Eng. and Design 142 , 1993, 1-13

/7/ H. Grebner, A. Höfler, H. Hunger; Technical Report PHDR 125-94, March 1994

EFFECTS OF WELD RESIDUAL STRESSES ON CRACK-OPENING AREA ANALYSIS OF PIPES FOR LBB APPLICATIONS

P. Dong, S. Rahman, and G. Wilkowski, Battelle, USA
B. Brickstad and M. Bergman, SAQ, Sweden

ABSTRACT

This paper summarizes four different studies undertaken to evaluate the effects of weld residual stresses on the crack-opening behavior of a circumferential through-wall crack in the center of a girth weld. The effect of weld residual stress on the crack-opening-area and leak-rate analyses of a pipe is not well understood. There are no simple analyses to account for these effects, and, therefore, they are frequently neglected. The four studies involved the following efforts:

(1) Full-field thermoplastic finite element residual stress analyses of a crack in the center of a girth weld

(2) A comparison of the crack-opening displacements from a full-field thermoplastic residual stress analysis with a crack-face pressure elastic stress analysis to determine the residual stress effects on the crack-opening displacement,

(3) The effects of hydrostatic testing on the residual stresses and the resulting crack-opening displacement, and

(4) The effect of residual stresses on crack-opening displacement with different normal operating stresses.

1. INTRODUCTION

Leak-before-break (LBB) analysis from a U.S. nuclear regulatory view point has typically involved evaluating a hypothetical crack where the piping system is not susceptible to mechanisms which form long surface cracks, the stresses are low, and the leakage size crack at normal operating conditions is detectable and stable at seismic loads with some safety factors applied. However, the above approach can be restrictive as there are benefits to be gained by applying LBB arguments to situations where surface cracking mechanisms may exist or arise. In this type of LBB analysis, the technical considerations need to be more rigorous than those in the U.S. NRC draft Standard Review Plan 3.6.3 for LBB.

An important consideration in a more detailed LBB analysis for circumferentially cracked pipes is accurate prediction of crack-opening area (COA). At present, the development of COA models have been based on idealized conditions for cracked pipes. A comprehensive report on this subject can be found in Reference 1. Among some of the important issues, effects of weld residual stresses on crack-opening behavior in LBB analysis are not well understood. Recently, linear-elastic finite element analyses based on a simplified model using equivalent crack-face pressure were performed to study the residual stress effects (Ref. 2). Along the same line, Sanderson et al. (Ref. 3) employed a simple residual stress estimation scheme by imposing a prescribed temperature field along the girth weld. Similar results were obtained with the two methods. In addition, the results have shown that the effects of residual stresses are most pronounced on the crack-opening variations through the wall thickness.

However, a more detailed assessment of the residual stress effects in COA predictions may be required in view of the following residual stress characteristics pertaining to girth-welded pipes:

- Hoop residual stresses of high magnitude are present in girth welds which may affect the crack-opening displacements.
- Axial residual stresses tend to exhibit periodic variations along the hoop direction, in particular, away from the weld centerline or near start/stop positions.
- Pre-deformation (thermoplastic) histories due to welding, which cannot be accounted for in linear elastic models, may have important effects on crack-opening area behavior.

In this paper several different evaluations of the effects of residual stresses on crack-opening displacement for leak-rate analyses were made. These studies included more rigorous residual stress analyses based on detailed thermoplastic modelling of pipe girth welding process for a representative pipe weld. Crack-opening analyses were then carried out by introducing a circumferential through-wall crack in the residual stress model. The results are compared with the results obtained using linear elastic finite element techniques with the residual stresses simulated as a crack-face pressure. Additional analyses involving the effects of hydrostatic testing on the residual stress field and resulting crack-opening displacements, and the effects of residual stresses on the crack-opening displacement at different normal operating stresses were conducted.

2.0 FULL-FIELD THERMOPLASTIC RESIDUAL STRESS FINITE ELEMENT ANALYSIS

2.1 Problem Definition

In this study, a through-wall-cracked pipe was used with an outer diameter of 812.8 mm (32 inch) and wall thickness of 15.9 mm (0.625 inch). The geometric details are shown in Figure 1. A six-pass girth weld was assumed in the residual stress model, where the welding start/stop positions were assumed at 0 degrees measured from the positive x-axis. A crack size of 250 mm (9.84 inches) in length was defined with the crack center located at approximately 90 degrees counter clockwise. An internal pressure of 3 MPa (430 psi) with equivalent end loading of 36.1 MPa (5.23 ksi) was used. The pipe material modelled was TP316 stainless steel. Temperature-dependent material properties were used in both thermal and mechanical analyses. The yield strengths for both base and weld materials were assumed to be the same, being 278 MPa (40.3 ksi) at room temperature.

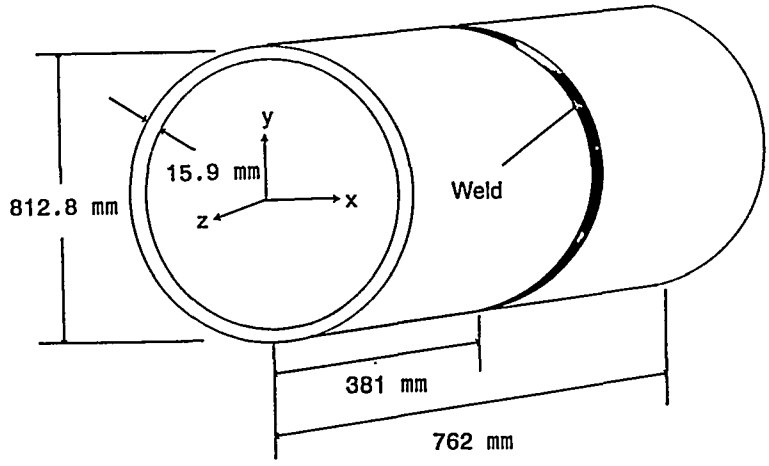

Figure 1. Geometry detail of girth-welded pipe

2.2 Finite Element Model

There have been numerous published and unpublished reports where extensive experimental measurements indicate that residual stresses in pipe girth welds may not be axisymmetric (Refs. 4-6). The deviation from axisymmetry is believed to be dependent on a number of parameters, such as welding conditions, and pipe geometry. Past experience has shown that 3-D shell element modelling can be a cost-effective way to capture some of the important non-axisymmetric features in pipe girth weld residual stress fields. Thus, the 3-D shell element model, shown in Figure 2, was used to simulate the full-field residual stress distribution and to model crack-opening behavior. The shell finite element model consisted of 1,200 four-noded thick-shell elements. Half symmetry was imposed along the weld center line. A moving arc effect was simulated and assumed to start/stop at an angle of zero degrees measured from the positive x-axis. The details may be found in Reference 7.

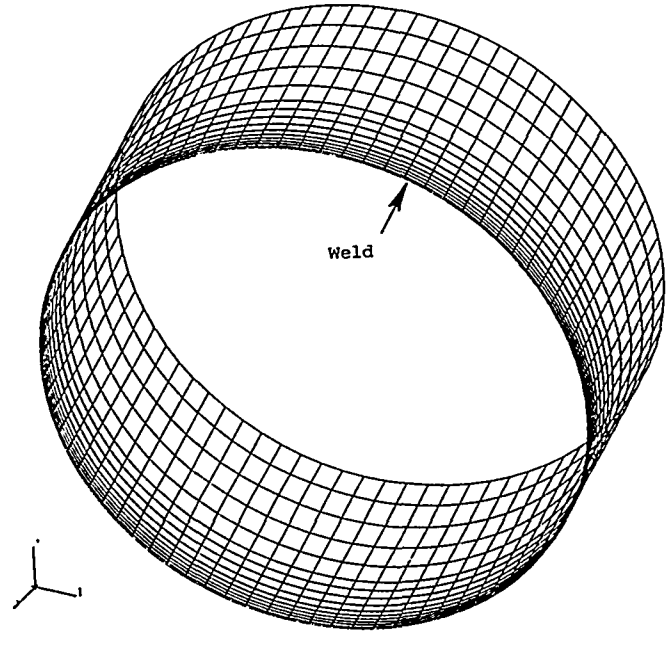

Figure 2. Shell Element Model

2.3 Finite Element Results

Figure 3 shows the distributions of the axial and hoop residual stresses on both inner and outer surfaces of the pipe, respectively. Note that the scale for stresses is in MPa. The following observations can be made:

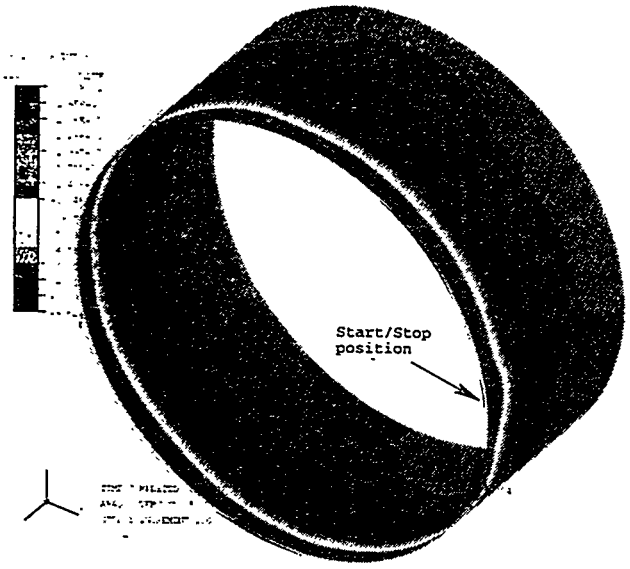

Figure 3a. Final Axial Residual Stress: Outer

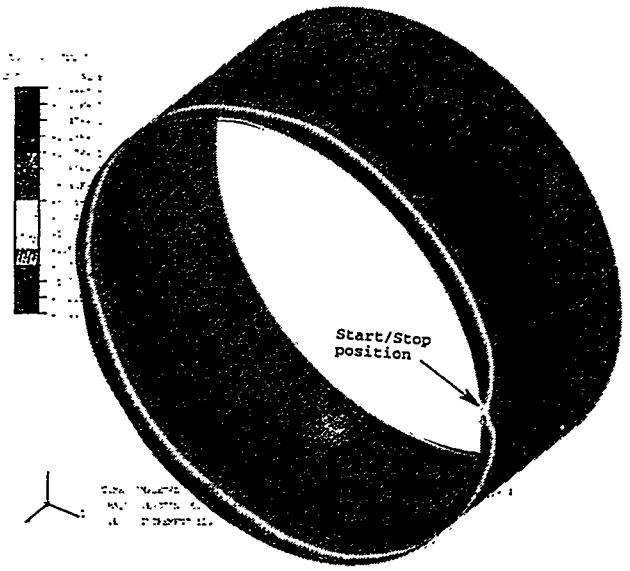

Figure 3b. Final Axial Residual Residual Stress: Inner

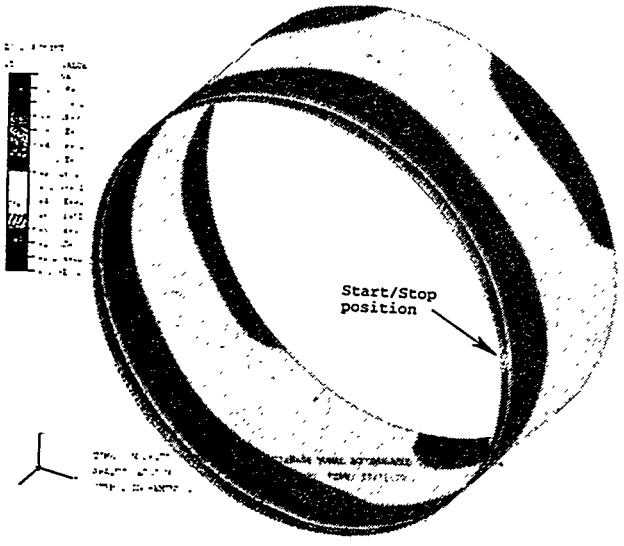

Figure 3c. Final Hoop Residual Stress: Inner Surface

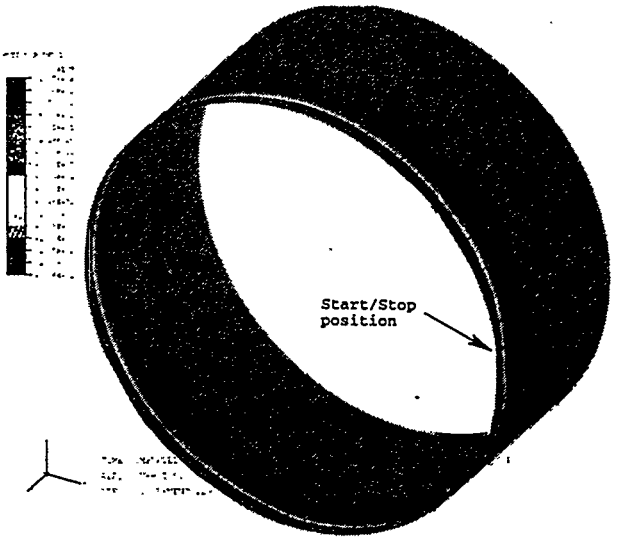

Figure 3d. Final Hoop Residual Stress: Outer Surface

- The axial residual stresses within the weld region were primarily in the form of bending across the wall thickness, with compression on the outer surface and tension on the inner surface. This feature was consistent with the results obtained with the axisymmetric model (Refs. 7 and 8).

- A relatively small periodic variation of the axial stress component along the circumferential weld was present. This variation was more pronounced on both the mid-section and remote from the weld center-line on the outer surface. The circumferential variation is characteristic of residual stress distributions in girth-welded pipes. Among the underlying mechanisms, it is believed that solidification history along the weld plays a major role.

- Hoop residual stresses were highest on the inner surface, which is consistent with the previous axisymmetric results (Reference 7). The hoop stresses were much more uniform than the axial residual stresses along the circumferential weld. This can be explained by the fact that the development of the hoop residual stresses are insensitive to the solidification history associated with the welding process. The restraint conditions along the weld, as far as hoop stresses are concerned, tend to be always high regardless of the arc position once quasi-steady-state conditions are established.

Some of the above general characteristics are consistent with observations independently reported by other researchers (see Refs. 4-6). The axial residual stress distributions are plotted both across the pipe wall thickness and away from the weld center line in Figure 4.

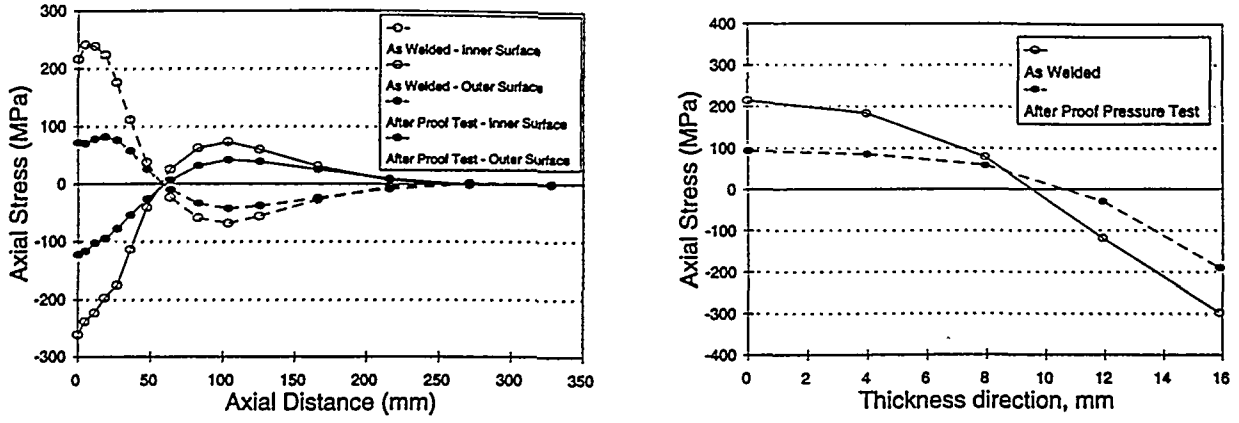

(a) Away from the weld center **(b) Through-thickness**

Figure 4. Axial residual stress distributions

3.0 FINITE ELEMENT COA ANALYSIS PROCEDURE

Two methods for accounting for weld residual stresses on the crack-opening displacement were used for comparison purposes in this investigation. The first method assumed that superposition principles for the residual stress effects were applicable in the crack-opening analysis (Ref. 2). It will be referred to as, crack-face pressure method in this paper. The second method involves extension of the detailed finite element thermoplastic modelling of the weld residual stresses described earlier by incorporating the crack into the shell element model.

3.1 Analysis Using Crack-Face Pressure

With this method, the as-welded residual stresses (Figure 4) estimated in Section 2.3 were applied as equivalent crack-face pressure, assuming that superposition principles were applicable in this situation (Ref. 2). Linear elastic finite element analysis was performed to compute the crack-opening area. Note that the prior deformation history due to welding was ignored here. The finite element model, consisting of 2,400 twenty-noded brick elements is shown in Figure 5. Again, half symmetry was assumed along the weld center line, and the circumferential crack is assumed to be in the centerline of the weld.

3.2 Analysis Using Full-Field Residual Stresses

In this part of the study, the COA analysis was carried out as a natural extension of the thermoplastic residual stress analysis (see Section 2.3). The introduction of the crack (250 mm [9.8 inches] in length) was accomplished by gradually releasing the nodes representing the entire length of the through-wall crack. All prior stress/strain histories were retained as initial conditions throughout the COA analysis.

3.3 Crack-Opening Displacement Analysis Results

Crack-opening results obtained from the two approaches are plotted in Figures 6-8 for three cases: linear elastic analysis with pressure loading only, residual stresses, and combined residual stresses and pressure loading. Battelle's solutions in both Figures 7 and 8 were obtained using detailed nonlinear thermoplastic solutions for residual stresses. Note that oscillation of the shell element results was due to the fact that the four-node shell elements with reduced integration in ABAQUS tend to introduce hour-glass deformation modes which could be reduced by either refining the model or specifying appropriate hour-glass control parameters. Given the exploratory nature of this effort, the results were believed to be adequate based on past experience. Data-smoothing techniques can be used to extract the crack-opening profiles.

It is as expected that the linear elastic COA results under pressure loading conditions (Fig. 6) agreed well between the shell and solid element models. The net crack-opening area was controlled by the inside diameter edge of the through-wall crack.

The COA results predicted due to only residual stresses showed that the net crack-opening area was controlled by outside diameter edge of the through-wall crack by both analysis techniques. The discrepancy between the shell element model and solid element model results (Fig. 7) was not significant. The shell element analysis took into account the thermoplastic history due to welding, while the linear solid element analysis only considered the equivalent crack pressure derived from Figure 4.

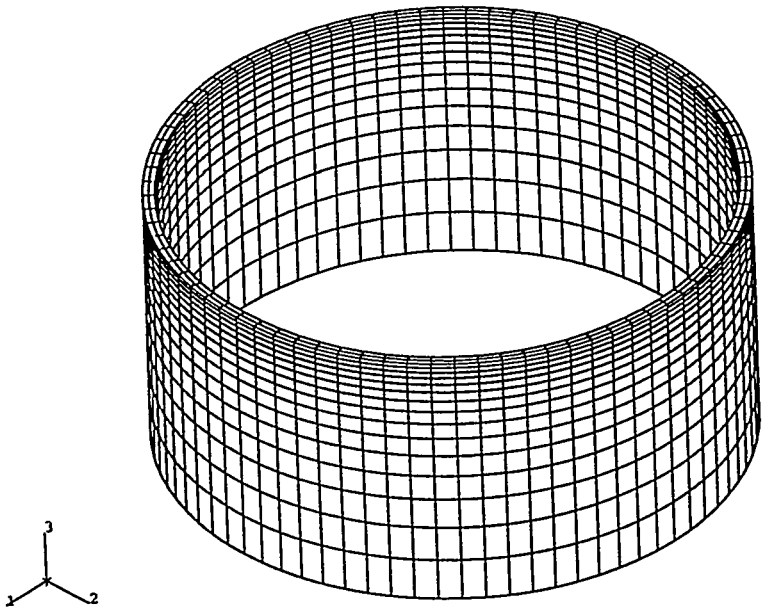

Figure 5. Solid element model

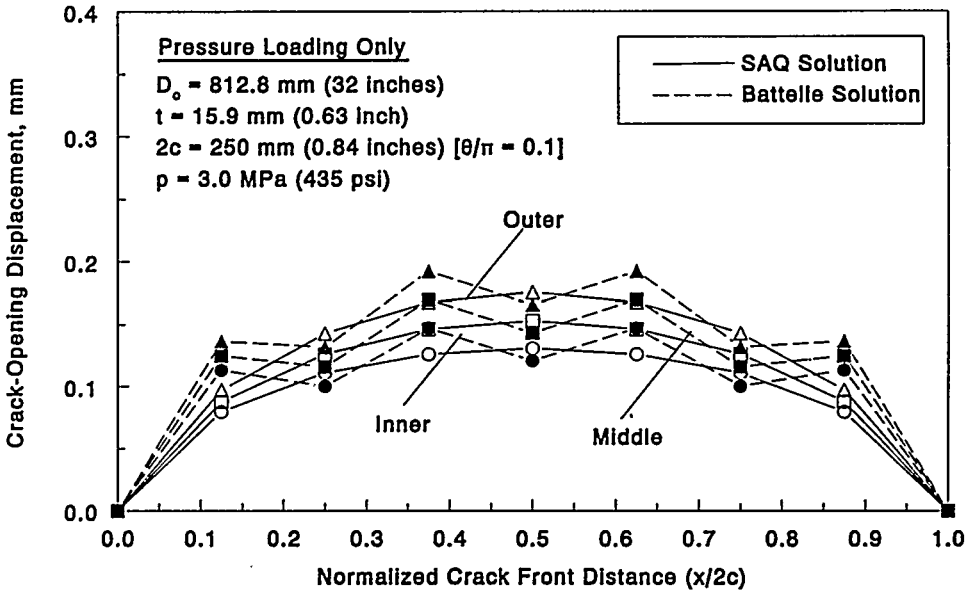

Figure 6. Total crack-opening displacement under pressure loading only (linear elastic solution)

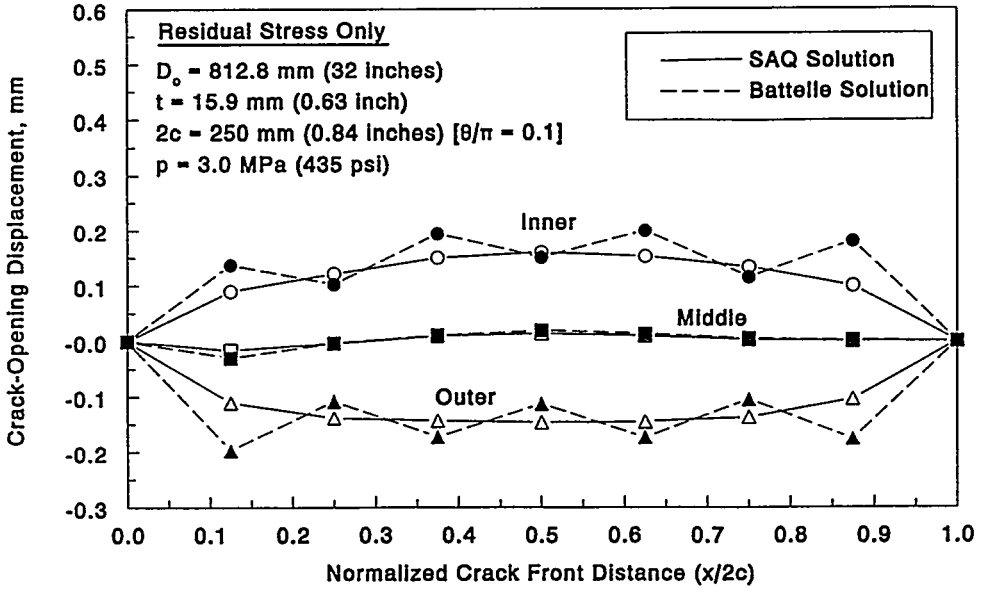

Figure 7. Total crack-opening displacements due to weld residual stresses

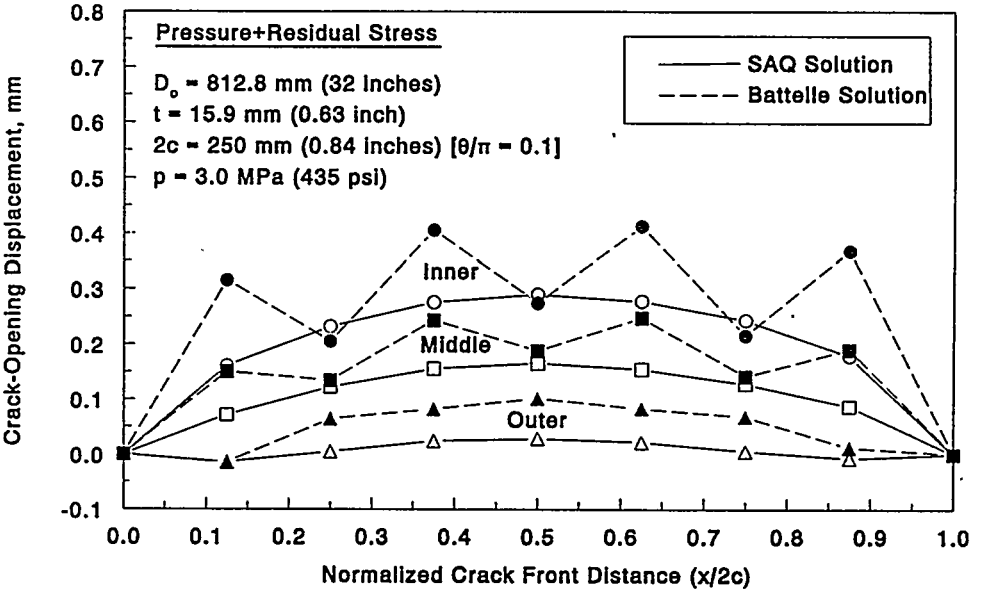

Figure 8. Total crack-opening displacement due to residual stresses and pressure

As pressure loading was applied, pure elastic loading or unloading was no longer present in the shell element model. The contributions to COA due to nonlinear crack-tip behavior became more dominant due to the presence of both high residual stresses (yield magnitude) and plastic straining histories in the weld area. As a result, the difference between the elastic (SAQ) solution and non-linear shell analysis become more pronounced, as shown in Figure 8. The presence of prior plastic straining rendered higher COA values under pressure loading conditions due to additional plastic deformation at the crack tips.

As a circumferential crack was introduced, the high tensile hoop residual stresses (along the crack plane) were also redistributed in the cracked area, as shown in Figure 9. As a result of this redistribution, the cracked-pipe wall tends to be bent in the radial direction towards the center of the pipe. This bending effect is believed to be more pronounced as the crack length increases.

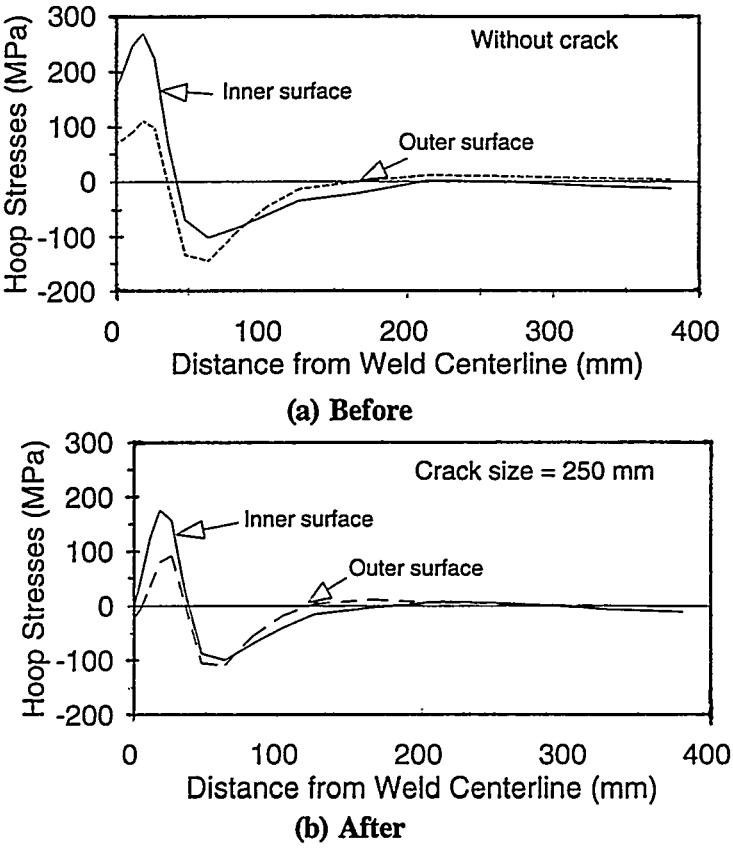

Figure 9. Hoop stress distributions before and after a crack was introduced

The above observations have demonstrated that to clearly understand the residual stress effects on crack-opening behavior requires detailed information on weld residual stresses and pre-deformation histories of the girth welds. For this purpose, full weld residual stress simulations using advanced finite element techniques can be performed on selected cases. The lack of detailed information about weld residual stresses was probably among the reasons why the analysis performed recently by Deschanels et al. (Ref. 9) showed insignificant contributions of the residual stresses to crack-opening behavior.

4.0 EFFECTS OF PROOF-PRESSURE TEST ON RESIDUAL STRESSES AND COD

It is generally accepted that proof pressure tests reduce weld residual stresses, depending on pressure level applied. An important issue is how the crack-opening behavior will be influenced by such proof-pressure tests. Within this context, the residual stress model shown in Figure 2 was used to assess the effects of proof-pressure tests. The full-field residual stress results obtained in Section 2.2 were used as initial conditions in this model. A proof-pressure test with a pressure loading of 7.7 MPa (1,117 psi) and consistent end loading in the axial direction was then simulated. The reduction of the residual stresses was illustrated in Figure 4. Figure 10 shows the crack-opening profiles for a crack of the same size as before. It is evident from comparisons with Figure 10, that the crack-face rotations (signified by the difference in COD between the inner and outer surfaces) was significantly reduced.

Figure 11 shows the crack-opening displacement results at room temperature after the operating pressure of 3 MPa (435 psi) was applied with consistent end-loading conditions. It is clearly indicated that the crack opening measured by the pipe outer surface was significantly increased as a result of the proof-pressure test. Figure 12 compares the outer crack-opening profiles with and without proof-pressure loading effects, as taken from Figures 8 and 11.

5.0 EFFECTS OF OPERATING STRESS LEVEL

Under typical operating conditions, the effects of residual stresses on crack-opening can be variable depending on the operating stress levels. To assess the effect of through-wall bending residual stresses on the COD as a function of normal operating load (bending moment only), the crack-face pressure analysis results from Reference 1 were used. Since the analyses performed in Reference 1 were linear-elastic, the effects of residual stresses for pipes with any other applied load levels could also be evaluated by linearly scaling the results for given residual stress distributions (Ref. 1).

Based on linear scaling, Figures 13 and 14 show the percent change in center COD due to the inclusion of residual stresses for both thicker-wall [i.e., greater than 25-mm (1-inch) thick] large-diameter and thinner-wall [less than 25-mm (1-inch) thick] small-diameter pipes, respectively. In both figures, the horizontal axis defines the applied moment that corresponds to an applied elastic stress as a percentage of ASME Service Level A stress limits. The vertical axis represents the difference of the calculated center COD with residual stresses (δ_{M+RS}) and without residual stresses (δ_M) normalized by the center COD without residual stresses. In general, the effects of residual stresses are significant when the normal operating stresses are lower. Relative comparisons of the crack-opening results in Figures 13 and 14 indicate that at any given applied load the residual stress effects are more severe for the thin-walled small-diameter pipe than for the thick-walled large-diameter pipe.

According to Figure 13, for the thick-walled large-diameter pipe, the calculated center CODs which account for residual stresses are larger than those estimated without residual stresses at both inner and outer surfaces of the pipe. The assumed residual stresses were in the form of tension-compression-tension from the inner surface, as given in Reference 1. However, the center COD at the mid-thickness location can be smaller when the residual stresses are considered. For the thin-walled small-diameter pipe, the results are shown in Figure 14. In this case, the residual stresses were assumed to be in the form of bending with outer surface being under compression. The calculated center COD with residual stresses are higher at the inner surface and lower at the outer or middle surfaces than those without residual stresses. Consequently, the crack-opening area and the subsequentleak-rate calculations can be affected

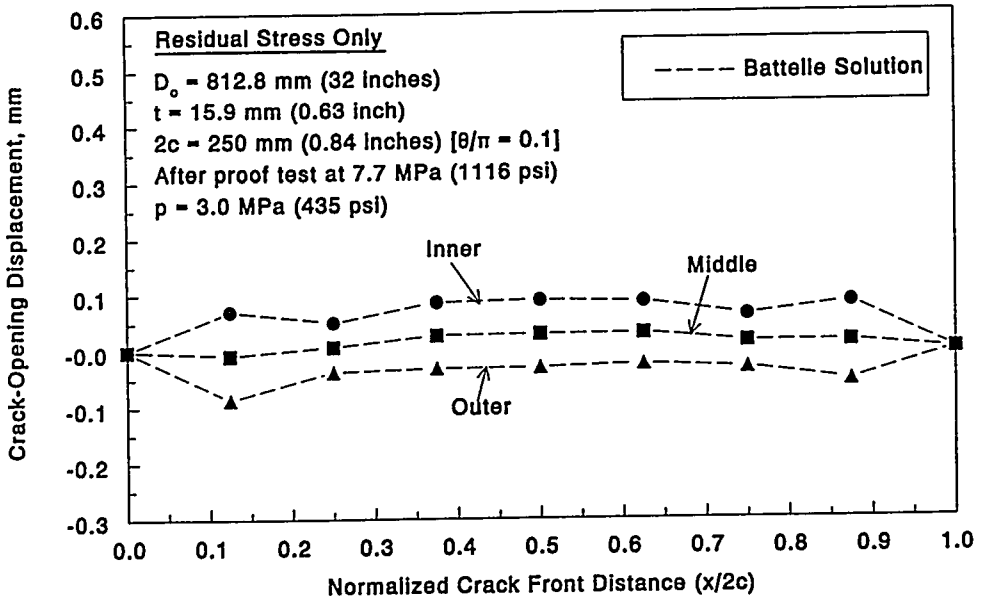

Figure 10. Total crack-opening displacements due to residual stresses: after proof-pressure test

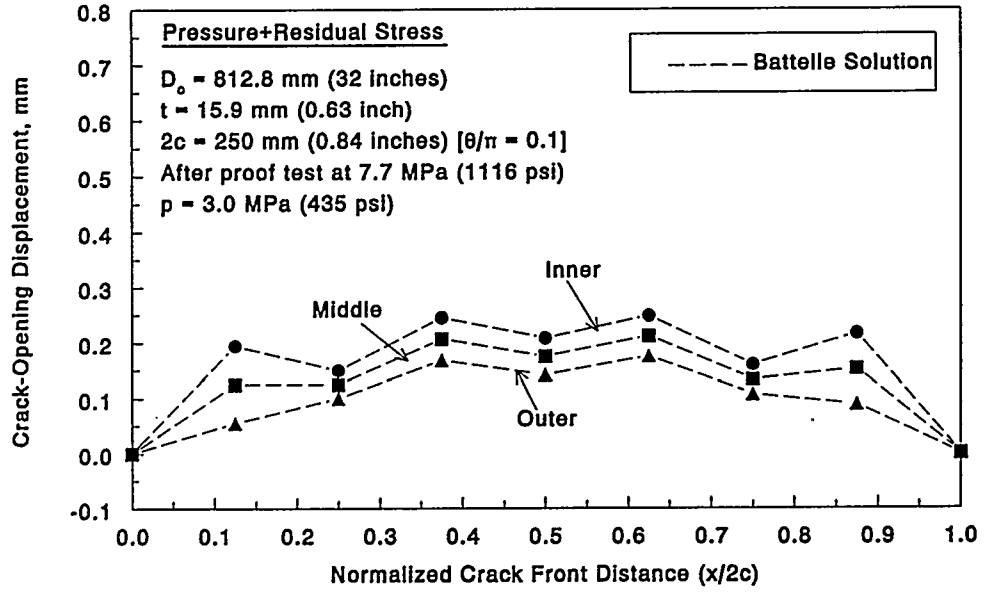

Figure 11. Total crack-opening displacements due to residual stresses: after proof-pressures test

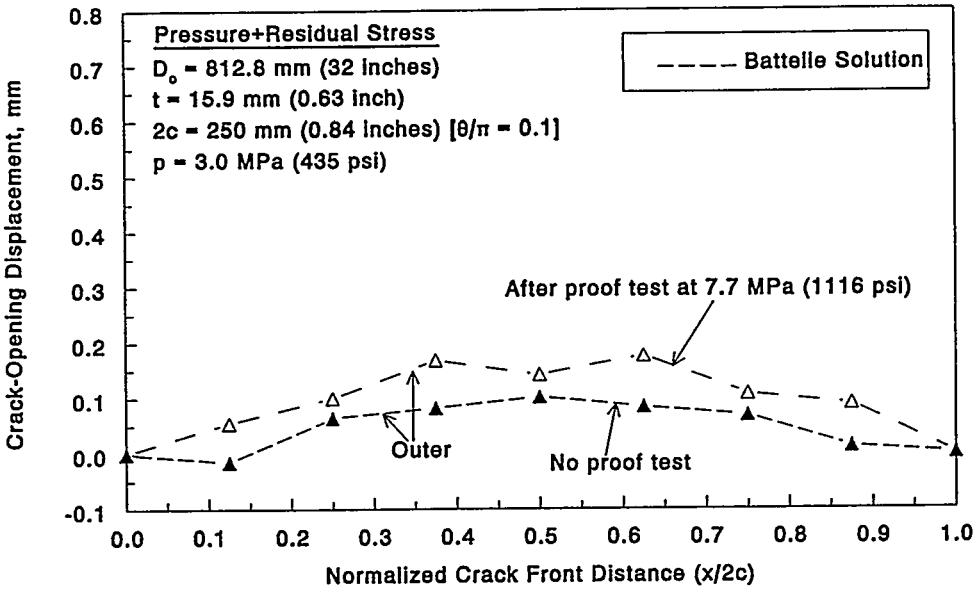

Figure 12. Comparison of CODs predicted with and without proof-pressure loading effect

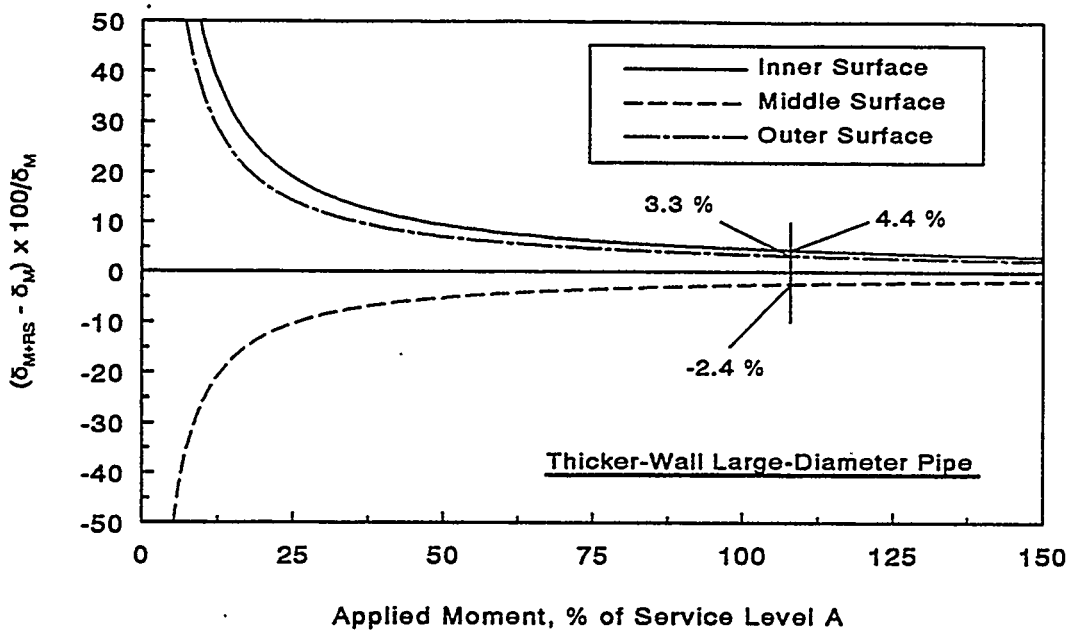

Figure 13. Percentage change in calculated COD due to residual stress as a function of applied moment for the thick-walled, large-diameter pipe

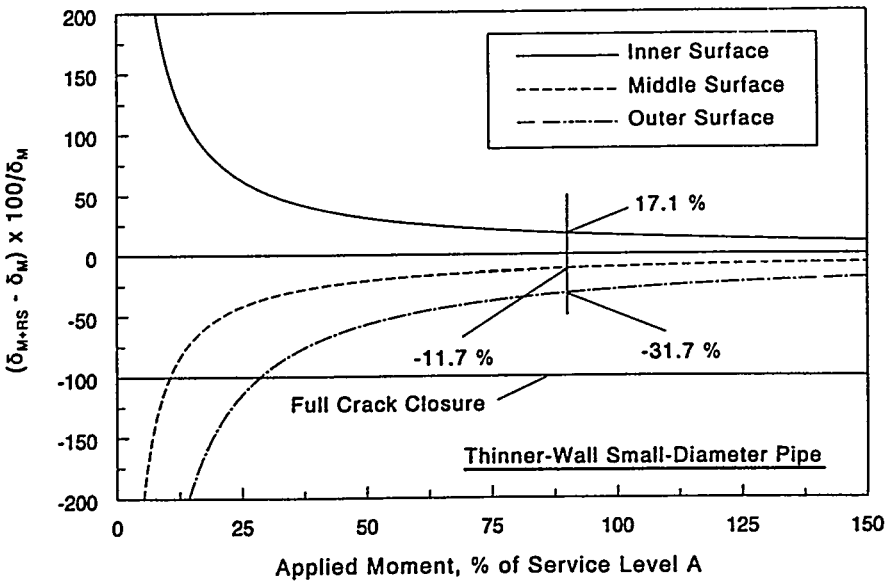

Figure 14. Percentage change in calculated COD due to residual stress as a function of applied moment for the thin-walled, small-diameter pipe

by the residual stresses in those pipes. In particular, when the values of δ_{M+RS} and δ_M are such that $(\delta_{M+RS} - \delta_M) \times 100/\delta_M$ (the variable in the vertical axis) reaches a value of -100, the calculated center COD with residual stresses becomes zero. Hence, there would be no leakage even for a pipe containing a through-wall crack, which clearly demonstrates how important the residual stresses are for the leak-rate calculations. This is especially true for the thin-walled small-diameter pipe in which case the results in Figure 14 predict that due to the residual stress, the outer surface of the pipe will close (thus preventing any leakage) when the applied load is equal to 28.6 percent of the ASME Service Level A stress limit. Similar calculations can also be made for the middle surface of both pipes, but the trend curves in Figures 13 and 14 suggest that for closure to occur, the applied stresses would have to be very small, i.e., 2.60 and 10.5 percent of the ASME Service Level A stress limit for the thicker-wall large-diameter and thinner-wall small-diameter pipes, respectively.

Finally, the above results of COD should be viewed as the preliminary estimates for the residual stress effects. In this case, no efforts were undertaken to determine the accuracy of this approximate finite element analysis using the linear elastic crack-face pressure method compared with more rigorous thermo-plastic finite element analysis, where the residual stress field is numerically simulated.

6.0 IMPLICATIONS of RESULTS FOR LBB APPLICATIONS

A consideration not evident in Figures 13 and 14 is that these results are only for the center crack-opening displacement, not area. There are four other consideration in determining the significance of these results. These are:

(1) Even if the center COD does not close all the way, there may be at some point along the crack closer to the crack tips where the crack faces do close. In fact this is evident in Figure 8 where the effective crack length with the residual stresses is about 70 percent of that without residual stresses. For a given leak rate, this effective crack length will

change with the magnitude of the applied residual stresses, where the higher the applied stresses the shorter the effective crack length becomes. If the center COD change with residual stresses is known, and it is assumed that the crack is elliptical in shape, then one can calculate the change in the effective crack length. This approach would have to be validated to see if the center COD from just the residual stresses changes much with crack length and if all these effects are additive. Crack closure effects need to be investigated as well.

(2) The effect of the crack-face rotation on the leak rate needs to be determined. For example, the results in Figures 10, 11, 13, and 14 show that the COD at the outer surface is smaller and the inner surface COD is much larger than normally calculated. The net effect of the pressure drops needs to calculated on the leak rate. Using the SQUIRT Code (Ref. 1), it was found that if the center COD was the same for parallel crack faces and rotated crack faces, the leak rate had a negligible change. If this is true, then the main effect of the residual stresses on COD may be in the change in the effective crack length described above.

(3) In Figure 8, it can be seen that the magnitude of the COD values from the elastic crack-face pressure (SAQ) analysis and the full-field residual stress analysis at the outside surface location were significantly different. Although more refined analysis may be required to eliminate the data oscillations for the Battelle results, it appears that the SAQ results are generally lower. Interestingly, in Figure 7, the crack-face pressure (SAQ) and full residual stress (Battelle) results for just residual stresses with no applied loads are very similar. Thus, the differences between these two methods with applied loads are likely to be due to inelastic deformation in the full-field residual stress model.

(4) The hydrostatic test analysis showed that pressure testing to higher levels than typically done in the ASME Code will help relieve the weld residual stresses and result in a larger crack opening, and hence leak rate at a given load. This helps to ensure LBB can be satisfied, although the differences in the leak rates for these crack openings still needs to be calculated.

7.0 CONCLUDING REMARKS

Preliminary analysis of crack-opening behavior considering residual stress effects has been performed by finite element methods using both crack-face pressure and full-field residual stress solutions. In the latter, the full-field residual stresses and pre-deformation history were obtained by detailed thermomechanical simulations of the girth welding process. The following observations can be made:

- Weld residual stresses can play a significant role in the crack-opening behavior of circumferential through-wall cracks. For the pipe configuration studied here, a strong bending feature of the axial residual stress component was present. As result, the crack-opening displacement showed a strong variation across the pipe wall thickness and a significant crack closure effect at the outer surface of the circumferential through-wall crack.

- The introduction of a circumferential through-wall crack resulted in redistribution of the axial residual stresses as well as the hoop residual stresses. The effects of hoop residual stress may be secondary, but could become important as the crack length increases.

- Non-linear COA analysis for operating loads combined with full-field weld residual stresses is likely to provide a less pessimistic estimate of COA than superimposed linear elastic solutions.

- The crack-face pressure method seems to underestimate the crack-opening area under operating load conditions. Using initial stress methods by specifying given axial and hoop residual stress distributions near the weld could improve the performance of linear elastic finite element predictions.

- Detailed information on full-field weld residual stresses is essential in understanding the crack-opening behavior for leak-before-break applications. The present shell element modelling technique proves to be cost-effective for this purpose.

ACKNOWLEDGEMENT

Part of this work was sponsored by Nuclear Electric, U.K. under contract with Battelle. The authors are grateful to Mr. J. Bouchard and Dr. T. Chivers for their encouragements and valuable comments during the preparation of this paper. We would also like to thank Mr. N. Ghadiali of Battelle for preparing some of the plots in this report.

REFERENCES

1. Rahman, S., et al., "Refinement and Evaluation of Crack-Opening Area Analyses for Circumferential Through-Wall Cracks in Pipes," NUREG/CR-6300, BMI-2184, U.S. Nuclear Regulatory Commission, Washington, D.C.

2. Bergman, M. and Brickstad, B., "A New Computerized Procedure to Analyze LBB in Pipes with Complex Crack Shapes," *Proceedings of the 20th MPA-Seminar*, Stuttgart, Germany, October 1994.

3. Sanderson, D., May, K.A.k, Green, D., and Wintle, J.B., "Solution to IPIRG Round-Robin Problem B.4b," Nuclear Electric Report SPD/D(95)/354.

4. Dong, P. and Hong, J.K., "Residual Stress Characteristics in Multi-Pass Girth Welds in Pipes," in Preparation for submittal to Welding Journal, 1995.

5. Karlsson, R.I. and Josefson, B.L., "Three-Dimensional Finite Element Analysis of Temperatures and Stresses in a Single-Pass Butt-Welded Pipe," *Journal of Pressure Vessel Technology*, Transactions of the ASME, 76/Vol. 112, Feb., 1990

6. Shack, W. J., Ellington, W. A., and Pahis, L. E., "Measurement of Residual Stresses in Type 304 Stainless Steel Butt Weldments," EPRI NP-1413, June 1980.

7. Dong, P., Ghadiali, N., and Brust, F., Battelle Report No. N001334 to Nuclear Electric, U.K., June, 1995.

8. Brust, F.W. and Kanninen, M.F., "Analysis of Residual Stresses in Girth Welded Type 304 Stainless Steel Pipes," *Journal of Materials for Energy Systems*, Vol. 3, pp. 56-62, December, 1981.

9. Deschanels, H., Turbat, A., Sperandio, M., "Numerical Simulations of Crack Opening Areas for Leak Before Break Applications in LMR Components," *Transactions of the 13th International Conference on Structural Mechanics in Reactor Technology* (SMiRT 13), Porto Alegre, Brazil, August 13-18, 1995, Volume 1, Division E, pp. 371-376.

Recent Evaluations of Crack-Opening-Area in Circumferentially Cracked Pipes

S. Rahman (University of Iowa),
F. Brust, N. Ghadiali, and G. Wilkowski (Battelle)
N. Miura (CRIEPI/Japan)

ABSTRACT

Leak-before-break (LBB) analyses for circumferentially cracked pipes are currently being conducted in the nuclear industry to justify elimination of pipe whip restraints and jet impingement shields which are present because of the expected dynamic effects from pipe rupture. The application of the LBB methodology frequently requires calculation of leak rates. The leak rates depend on the crack-opening area of the through-wall crack in the pipe. In addition to LBB analyses which assume a hypothetical flaw size, there is also interest in the integrity of actual leaking cracks corresponding to current leakage detection requirements in NRC Regulatory Guide 1.45, or for assessing temporary repair of Class 2 and 3 pipes that have leaks as are being evaluated in ASME Section XI. The objectives of this study were to review, evaluate, and refine current predictive models for performing crack-opening-area analyses of circumferentially cracked pipes. The results from twenty-five full-scale pipe fracture experiments, conducted in the Degraded Piping Program, the International Piping Integrity Research Group Program, and the Short Cracks in Piping and Piping Welds Program, were used to verify the analytical models. Standard statistical analyses were performed to assess quantitatively the accuracy of the predictive models. The evaluation also involved finite element analyses for determining the crack-opening profile often needed to perform leak-rate calculations.

1. Introduction

The application of the leak-before-break (LBB) methodology frequently requires determination of leak rates. In addition to LBB analyses which assume a hypothetical flaw size, there is also interest in the integrity of actual leaking cracks corresponding to current leakage detection requirements in NRC Regulatory Guide 1.45, or for assessing temporary repair of Class 2 and 3 pipes that have leaks as are being evaluated in ASME Section XI. Generally, the leak-rate calculations are performed for one of the following two purposes: (1) given a flaw size, pipe dimension, material properties, and loading, it is desired to know the crack-opening area (COA) and corresponding fluid flow rate through a crack to determine whether the given flaw size would result in a reliably detectable leak rate and (2) given a leak rate with known pipe dimension, material properties, and loading, it is also desired to know the COA and the corresponding flaw size which is subsequently used to evaluate its fracture stability. For either of the two purposes, accurate models are needed to predict COA for subsequent leak-rate evaluations. Besides the finite element method, there are a number of engineering (or estimation) methods which are available in the current literature to determine the crack-opening for a pipe with a circumferential crack. However, due to the lack of systematic studies involving combined experimental and analytical efforts, the accuracy of these methods for different pipe materials, crack geometries, and loading conditions have yet to be evaluated.

The objectives of the study reported in this paper were to review, evaluate, and refine current predictive models for performing crack-opening-area analyses of circumferentially cracked pipes. The results from twenty-five full-scale pipe fracture experiments, conducted in the Degraded Piping Program (Ref. 1), the International Piping Integrity Research Group Program (Ref. 2), and the Short Cracks in Piping and Piping Welds Program (Ref. 3), were used to verify the analytical models. Standard statistical analyses were performed to assess quantitatively the accuracy of the predictive models. The statistics involved calculation of the mean and coefficient of variation of the predictive crack-opening ratio, defined as the ratio between the experimental and predicted values of the center-crack-opening displacement, when the applied load is 40 percent of the experimental maximum load. (Note, the cracked pipe behavior at this load is primarily elastic.) The results are presented for various crack geometries (i.e., simple through-wall and complex cracks), crack size (i.e., long and short cracks), crack location (i.e., cracks in base and weld metals), and loading conditions (i.e., pure bending, pure tension, and combined bending and tension).

2. Elastic-Plastic Fracture Mechanics Models

Fracture-mechanics models are often required to evaluate the fracture response and crack-opening of a through-wall-cracked (TWC) pipe. In this paper, the elastic-plastic fracture mechanics models were used to determine the accuracy of crack-opening predictions. There are two types of elastic-plastic fracture mechanics methods: (1) finite element or numerical methods, and (2) engineering

approximation (estimation) methods. A finite element analysis can always be performed to determine accurate crack-opening displacement and precise crack-opening area for a given pipe geometry, crack size, and material. However, for most practical LBB applications, a full finite element computation is not always necessary. Also, such computations are too time-consuming and expensive to be used for routine LBB evaluations. On the other hand, simple mathematical models, often referred to as the estimation methods, can be applied to determine approximate crack-opening characteristics of a TWC pipe. However, these methods require various assumptions necessary to minimize the need for elaborate numerical analysis. Typically, such assumptions lead to simpler representations of the material's stress-strain behavior, flaw shape and orientation, loading, and boundary conditions. In this paper, both finite element and estimation methods were used for the crack-opening predictions.

2.1 Estimation Methods

Consider a simple TWC pipe with mean radius, R_m, wall thickness, t, and a crack angle, 2θ, located in the center of the bending plane. Several loading conditions can be considered. For example, the pipe may be under a pure bending moment, M; or pure tension (axial), P, due to internal pipe pressure, p; or combined bending (M) and tension (P). Figure 1 shows a schematic representation of a TWC pipe subjected to combined bending and tension. In a typical estimation scheme, it is generally assumed that the load-point rotation and axial displacement (or stretch) due to the presence of a crack, ϕ^c and Δ^c, the relevant crack-driving force, J, and center-crack-opening displacement, δ, allow additive decomposition into elastic and plastic components given by (Refs. 4 to 16)

$$\phi^c = \phi^c_e + \phi^c_p \tag{1}$$

$$\Delta^c = \Delta^c_e + \Delta^c_p \tag{2}$$

$$J = J_e + J_p \tag{3}$$

$$\delta = \delta_e + \delta_p \tag{4}$$

where the subscripts "e" and "p" refer to the elastic and plastic contributions, respectively. In the elastic range, ϕ^c_e and M, and Δ^c_e and P are uniquely related. In addition, if the deformation theory of plasticity holds, a unique relationship also exists between ϕ^c_p and M and Δ^c_p and P. These relationships provide important information in determining J or COD in a pipe (Refs. 5 to 16).

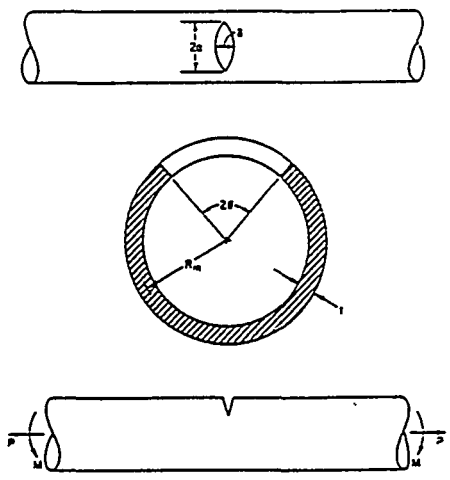

Figure 1. Schematic representation of pipe with a circumferential through-wall crack subjected to bending and tension

Five different estimation methods that are currently available in the literature were considered for predicting fracture response and crack-opening displacements of a circumferential TWC pipe under various loads. They are the:

(1) GE/EPRI method (Refs. 5 to 7),
(2) Paris/Tada method (Ref. 9),
(3) LBB.NRC method (Ref. 10),
(4) LBB.ENG2 method (Refs. 11 to 13), and
(5) LBB.ENG3 method (Refs. 14 to 16).

Earlier studies on fracture response and crack-opening in pipes were concerned for the most part with larger cracks (i.e., $\theta/\pi \geq 30$ percent) where the nominal failure stresses were below yield. The estimation methods developed to date, some of which are considered here, are well-suited for analyzing pipes with large cracks. The ability of these methods to predict crack-opening for small cracks ($\theta/\pi \leq 12$ percent) has not been established even though such small cracks are often the concern in practical LBB analyses. A short crack is typical of one for LBB analyses in large diameter pipes. Indeed, the finite element solutions compiled in the GE/EPRI handbook (Ref. 6) can become inadequate for small-size cracks. In this study, new finite-element results of GE/EPRI influence functions were developed by Battelle with particular emphasis given to short-cracked pipes. The explicit details of these finite element calculations are discussed in Reference 4.

3. Validation of Analytical Models

3.1 Finite Element Analyses of a Through-Wall-Cracked Pipe

As part of the Short Cracks in Piping and Piping Welds Program, a full three-dimensional finite element analysis was conducted to predict crack-opening displacement in a TWC pipe under pure bending loads. The data used to verify the finite element predictions were obtained from Experiment 1.1.1.21 and were also developed in the same program. This experiment was conducted on a 711.2-mm (28-inch) nominal diameter Schedule 60 A515 Grade 60 carbon steel unwelded pipe with a short circumferential through-wall crack which has length equal to 6.25-percent of the pipe circumference. Such crack lengths are typical in LBB applications for larger diameter pipes. Figure 2 shows the longitudinal dimensions of the pipe sections used to make up the specimen for Experiment 1.1.1.21. Figure 3 shows the cross-sectional geometry in the cracked section and instrumentation for collecting experimental data.

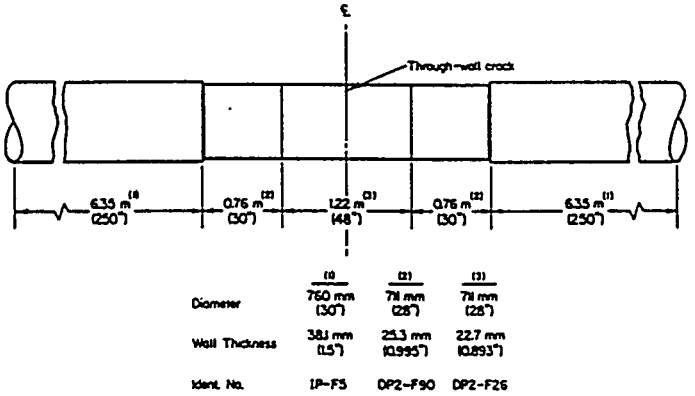

Figure 2. Schematic of pipe used in Experiment 1.1.1.21

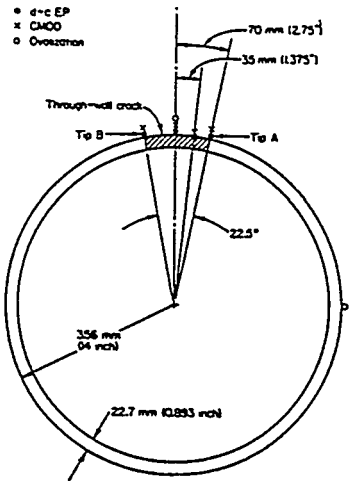

Figure 3. Schematic of crack geometry and instrumentation near the crack for Experiment 1.1.1.21

A three-dimensional elastic-plastic finite element model was developed to analyze this pipe experiment. The finite element model consisted of a 1/4 symmetric portion of the pipe with three different cross-sections. It consisted of 579 elements and 3,761 nodes. The number of elements through the thickness was one. The finite element analysis was performed under displacement control to a maximum load-line displacement of 160 mm (6.3 inches). Based on the experimental data, the crack initiated at a load-line displacement of 62.5 mm (2.46 inches). Crack growth calculations were performed using the ABAQUS (Version 5.3) code (Ref. 17) with several load steps. The first load step was up to crack initiation. Subsequent steps consisted of releasing appropriate crack front nodes while simultaneously increasing the load-line displacement. The crack-growth and applied displacement data were obtained from the experimental record. Hence, the finite element predictions of crack-opening displacement following crack initiation were based on crack growth data from the test. As an alternative, the crack growth criteria based on J-integral evaluations could have been used, but were not adopted in this particular analysis.

Figure 4 shows the plots of total load versus center-crack-opening displacement from the experiment and the three-dimensional finite element calculations. The analysis results compare very well with the experimental data. The results of predicted load versus load-line displacement and center-crack-opening displacement versus load-line displacement, available in Reference 4, also showed good comparisons with corresponding experimental data. See Reference 4 for further details.

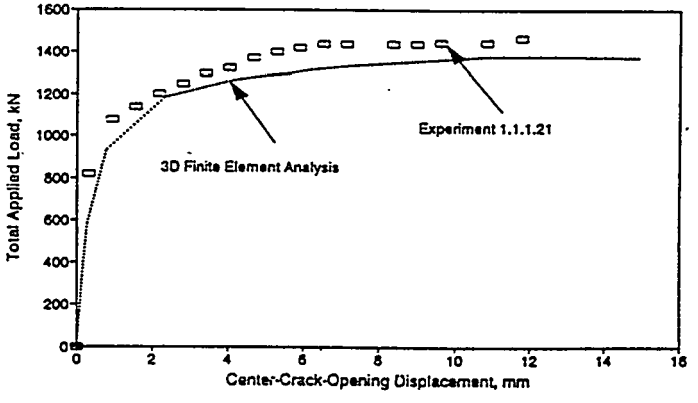

Figure 4. Comparison of predicted load versus center-crack-opening displacement for Experiment 1.1.1.21

3.2 Experimental Verification of Estimation Models

A total of twenty-five full-scale pipe fracture experiments were analyzed to determine the predictive capability of the COA estimation models considered in this study. In all of these experiments, the pipes had circumferential through-wall cracks. Two cases of crack geometry were considered. One was a simple through-wall crack which has the same crack length on the inside and outside pipe diameter in terms of percentage of pipe circumference. The other was a complex-crack which consists of a 360-degree internal surface crack that penetrates the pipe thickness for a shorter through-wall-crack length. See Figure 5 for the definitions of these two crack geometries and the associated crack-size parameters.

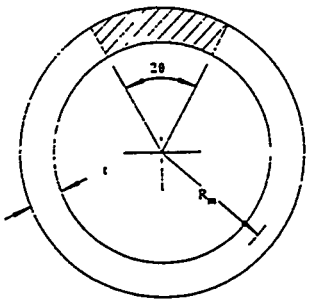

(a) Simple through-wall crack

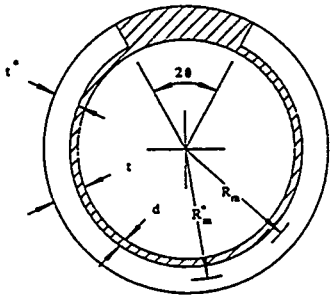

(b) Complex crack

Figure 5. Various through-wall-crack geometries and definitions of their parameters

The experiments involved both austenitic and ferritic steel piping with cracks located in the base metal, the weld metal, and the fusion line of a bimetallic weld. A wide range of pipe (outer) diameters from 114.3 mm (4.5 inches) to 1067 mm (42 inches) were considered. The initial through-wall crack lengths were both short and long and ranged between 6.25 and 38.6 percent of the pipe circumference. For the pipes with complex-crack geometry, the 360-degree internal surface cracks were both shallow and deep and the depths of these cracks varied from 32 to 64 percent of the pipe thickness. In all experiments, the cracks were placed in the center of the bending plane. For the welded pipe tests, the cracks were located in the center of the weld, except for the bimetallic weld pipe test in which case the crack was placed along the fusion line between the ferritic base metal and Inconel weld metal (see details in a forthcoming section). The test temperature varied from 7 C (45F) to 288 C (550 F) with one experiment at 7 C (45 F), one experiment at room temperature, and the rest of the experiments at 288 C (550 F). The loading conditions were pure bending, pure tension, and combined bending and tension. All loading rates were quasi-static. Table 1 shows the summary of pipe fracture experiments analyzed in this study.

3.2.1 The NRCPIPE Computer Program

The NRCPIPE computer code was developed to perform elastic-plastic fracture-mechanics analysis for establishing the fracture-failure conditions of a piping system in terms of sustainable load (or stress) or displacement (Refs. 1 and 3). For nuclear applications, engineering elastic-plastic fracture-mechanics techniques are based on the J-integral fracture parameter. To perform a fracture analysis, the user provides the input data describing the pipe and crack geometries, material stress-strain curve, and fracture resistance of the material (i.e., a J-R curve) as obtained from a laboratory test specimen. A wide variety of results for a pipe including crack-opening-area predictions can be obtained.

The NRCPIPE code was originally developed under the Degraded Piping Program (Ref. 1). A significant amount of development and numerous enhancements were made in the Short Cracks in Piping and Piping Welds Program (Ref. 3). Further details on these enhancements can be obtained from Reference 3.

The pipe fracture experiments listed in Table 1 were analyzed by the various estimation methods described earlier. All of these methods considered in this paper are available in the current version of the NRCPIPE code (Version 2.0). All crack-opening results for the analyses of these experiments were generated using this program. The details of input data consisting of material properties, pipe and crack geometries, and loads can be obtained from Reference 4. Only, the results are discussed in the forthcoming sections.

Table 1. A list of 25 quasi-static pipe experiments for crack-opening-area analysis

Pipe Test No.	Outer Diameter, mm	Schedule	Material	Temperature, C	Flaw Shape[a]	$2a/\pi D_m$[b]	d/t[c]	Loading Condition[d]	Reference
			(a) Pipe Experiments with Base-Metal Cracks (19 Experiments)						
1.1.1.21	711	60	A515 Gr. 60	288	TWC	0.0625	0	B	3
1.1.1.26	106	160	TP316L	21	TWC	0.244	0	B	3
4111-1	114	80	A333 Gr. 6	288	TWC	0.370	0	B	1
4111-2	711	60	A515 Gr. 60	288	TWC	0.370	0	B	1
4111-3	1067	NA[e]	TP304	7	TWC	0.370	0	B	1
4121-1	168	120	TP304	288	TWC	0.386	0	T	1
4131-1	166	120	TP304	288	TWC	0.370	0	B+T	1
4131-3	274	100	A333 Gr. 6	288	TWC	0.370	0	B+T	1
1-8	399	100	A106 Gr. B	288	TWC	0.120	0	B+T	-[f]
4113-1	168	120	TP304	288	CC	0.370	0.32	B	1
4113-2	168	120	TP304	288	CC	0.370	0.63	B	1
4113-3	168	80	Inconel 600	288	CC	0.370	0.34	B	1
4113-4	168	80	Inconel 600	288	CC	0.370	0.61	B	1
4113-5	168	120	A106 Gr. B	288	CC	0.370	0.31	B	1
4113-6	168	120	A106 Gr. B	288	CC	0.370	0.64	B	1
4114-1	165	120	A106 Gr. B	288	CC	0.370	0.47	B	1
4114-2	166	120	TP304	288	CC	0.370	0.32	B	1
4114-3	413	100	TP304	288	CC	0.373	0.34	B	1
4114-4	413	100	TP304	288	CC	0.373	0.34	B	1
			(b) Welded Pipe Experiments (5 Experiments)[g]						
1.1.1.23	711	80	TP316L SAW	288	TWC	0.0625	0	B	3
1.1.1.24	612	80	A333 Gr. 6 SAW	288	TWC	0.079	0	B	3
4141-1	168	120	TP304 SAW	288	TWC	0.371	0	B	1
4141-5	168	120	TP304 SA-SAW	288	TWC	0.383	0	B	1
4111-5	720	80	TP316 SMAW	288	TWC	0.370	0	B	1
			(c) Bimetallic Weld Pipe Experiment (1 Experiment)[g]						
1.1.1.28	930	160	A516 Gr. 70/F316/ Inconel 182 SMAW	288	TWC	0.359	0	B	3

(a) TWC = simple through-wall crack; CC = complex crack
(b) 2a = through-wall crack length at mean pipe diameter; D_m = mean pipe diameter
(c) d = depth of 360-degree internal surface crack in a complex-cracked pipe; t = pipe wall thickness
(d) B = pure bending; T = pure tension (pressure); B+T = combined bending and tension (pressure)
(e) Not applicable
(f) Data were developed in the IPIRG-2 Program at Battelle (See Reference 2 for information on the IPIRG Program)
(g) SAW = submerged-arc weld; SMAW = shielded-metal arc weld; SA-SAW = solution-annealed submerged-arc weld

3.2.2 Typical Results from Estimation Analyses

Figures 6 and 7 show the plots of total applied load (in four-point bending) versus center-crack-opening displacement for two simple TWC pipes with base-metal cracks from Experiment 1.1.1.21 and 1.1.1.26 involving pure bending load. The results suggest that for the pipe in Experiment 1.1.1.26 that involved a long crack ($2a/\pi D_m$ = 24.4 percent), the LBB.ENG2 method provided excellent predictions of experimental COD. In Experiment 1.1.1.21, the initial crack was very short ($2a/\pi D_m$ = 6.25 percent) for which case the GE/EPRI method using either the original or the Battelle-developed influence functions predicted COD with better accuracy than the other methods. For both of these experiments, the LBB.NRC and Paris/Tada methods underpredicted COD for applied loads that are less than the initiations loads, although the results from the LBB.NRC method were relatively closer to the experimental data.

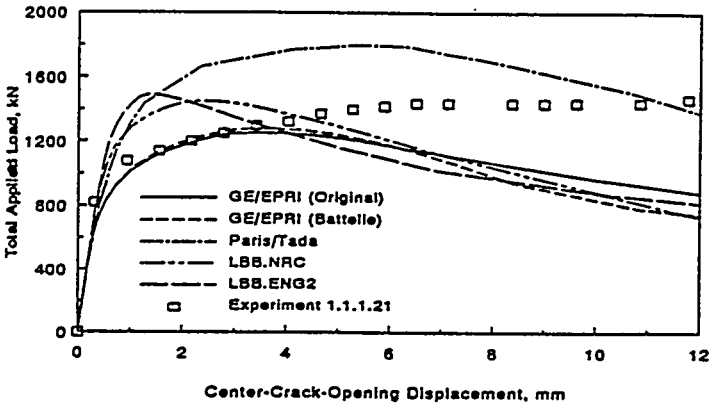

Figure 6. Load versus center-crack-opening displacement in Experiment 1.1.1.21

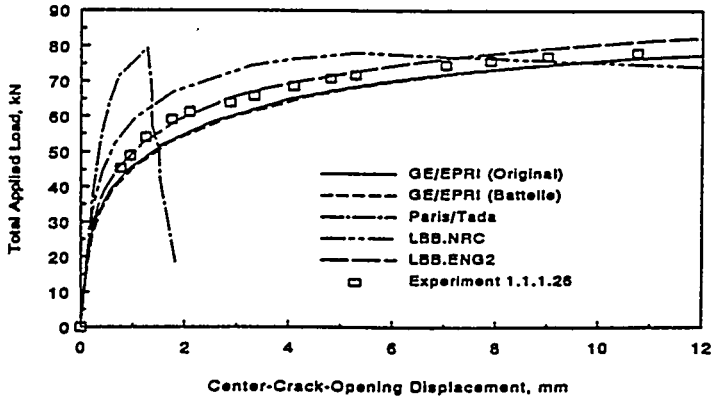

Figure 7. Load versus center-crack-opening displacement in Experiment 1.1.1.26

Figures 8 and 9 show the plots of total load versus center-crack-opening displacement for the two complex-cracked pipes with base-metal cracks from Experiments 4113-1 and 4113-2, both of which were performed under four-point bending without any internal pressure. These plots contain results from the analyses by the LBB.ENG2 method with and without constraint factor, C_F and the corresponding experimental data. The constraint factor, C_F denotes the ratio of J-R curves from the complex-cracked pipes and C(T) specimens and was obtained experimentally in Reference 18 as a function of the internal surface-crack depth-to-thickness (d/t) ratio. In performing analytical calculations, it was assumed that the simple TWC pipe estimation formulas from the LBB.ENG2 method can be applied to analyze complex-cracked pipes by adjusting pipe radius and wall thickness via $R_m^* = R_m + d/2$ and $t^* = t - d$, respectively. However, the results suggest that this adjusted estimation model (LBB.ENG2), with either case of J-R curves, overestimates the COD at all load levels. This can be explained by noting that the "equivalent" through-wall-cracked pipe assumed in the estimation model (with $t^* = t - d$) would have lower stiffness than the actual complex-cracked pipe. Hence, the predicted crack-opening displacements were larger than the experimental results.

Obviously, when the surface cracks become deeper (e.g., Experiment 4113-2), the magnitudes of these overestimates of the COD will also become larger and can be significantly different from the experimental results, as exhibited in Figure 9. This general loss of accuracy can be attributed to the over-simplification in the estimation formulas for through-wall-cracked pipes used for predicting the COD of complex-cracked pipes. Further studies are needed in this area.

Further details of the analysis procedures and experimental data are available in Reference 4. The analyses of other experiments listed in Table 1, the results of which are not explicitly presented and discussed here due to space limitations, can be obtained from Reference 4.

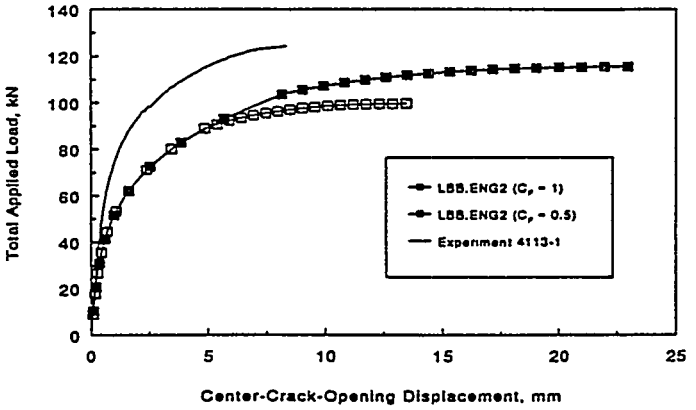

Figure 8. Load versus center-crack-opening displacement in Experiment 4113-1

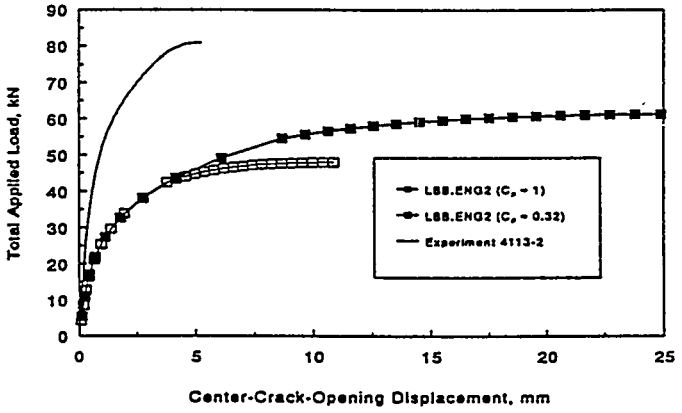

Figure 9. Load versus center-crack opening displacement in Experiment 4113-2

4. Performance Evaluation of Predictive Analyses

In general, for LBB applications, one is more interested in the accuracy of the models in the elastic load range than at crack initiation load, maximum load, or beyond maximum load. Since stresses in LBB or leak-rate analyses for piping under normal operating loads are generally thought to be in the elastic range, we have statistically qualified the accuracy of the various methods in this region. To simplify this evaluation, we defined the linear-elastic region to occur when the applied load was 40 percent of the maximum experimental load or less. According to the ASTM guidelines for J-R curve testing, 40 and 50 percent of the limit load using yield strength as the collapse stress are currently used for fatigue precracking of C(T) and bend specimens (Ref. 19). Hence, at 40 percent of the maximum experimental load, the cracked pipes should experience primarily linear-elastic behavior with very little plasticity.

Figure 10 shows a schematic of load versus center-crack-opening displacement for a TWC pipe. For LBB applications, it is generally desired that an analysis method would underpredict the maximum load slightly. It is also desirable to underpredict the COD in the elastic range. This is because, for a given leak rate, if the COD is underpredicted then the crack length for the crack stability analysis is overpredicted. Therefore, the final maximum load in the crack stability analysis will underpredict the actual maximum load. It should also be noted that in the comparisons of crack-opening displacements, the estimation methods predict the crack-opening at the mid-thickness, whereas the experimental data (except the IPIRG-2 Experiment 1-8) have the crack-opening measurements slightly above the outside diameter of the pipe. In Experiment 1-8 the crack-opening displacement was measured on the pipe inside surface. No corrections were made for this difference since that would involve considerable additional effort, however, it is safe to say that the outer surface experimental COD values are greater than the mid-thickness COD values (expect for Experiment 1-8). The available COD values are experimental outside diameter COD values.

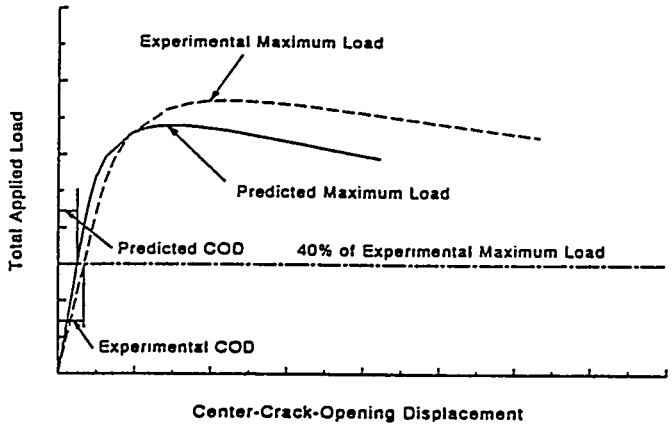

Figure 10. Schematic comparison of predicted and experimental load versus center-crack-opening displacement in a pipe (ideally COD and load are underpredicted for LBB analyses)

4.1 Statistics of Predicted Crack-Opening Ratio

Standard statistical analyses were performed to assess the accuracy of the predictive models in estimating the center-crack-opening displacements for pipes analyzed in this study. The statistics involved calculation of the mean and coefficient of variation (COV) [COV is equal to the ratio of standard deviation to the mean] of the ratio between the experimental and predicted values of the center-crack-opening displacement when the applied load is 40 percent of the experimental maximum load. This ratio is denoted as the predicted crack-opening ratio for further discussions in this paper. It is desired to have this ratio greater than one to ensure smaller values of predicted crack-opening displacement than the experimental results. It should also be noted that a margin of 10 on leak-rate is generally applied in LBB analyses to account for various uncertainties including inaccuracy in crack-opening predictions (Ref. 20)

4.1.1 Simple Through-Wall-Cracked (TWC) Pipes

Table 2 shows the mean and COV of the predicted crack-opening ratio for fifteen TWC pipes subjected to various loading conditions. From the results of this table, when all TWC pipe experiments are considered, all of the predictive models underpredicted the mean value of the COD. The GE/EPRI methods (with the original and newly developed influence functions from this study) predicted experimental COD with very good accuracy in terms of the mean value of the crack-opening ratio, but their predicted COVs were much higher. The differences between the statistics for the GE/EPRI method based on the original influence functions and the present study were not significant. The LBB.ENG2 and LBB.ENG3 methods slightly underpredicted the mean experimental COD with much lower COVs. The LBB.NRC method underpredicted the COD more than the LBB.ENG2 or LBB.ENG3 methods with higher values of COV. Among all methods, the Paris/Tada method underpredicted COD by the largest margin in terms of both mean and COV of the predicted crack-opening ratio.

Table 2 provides a further breakdown of statistics for three different loading conditions involving pure bending, pure tension, and combined bending and tension. For pipes under pure bending loads, the LBB.ENG2 and LBB.ENG3 methods slightly underpredicted the experimental COD when the mean values were compared. The LBB.NRC and Paris/Tada methods also underpredicted the COD with the Paris/Tada method underpredicting the most. It is interesting to note that the GE/EPRI methods overpredicted the mean COD for this loading condition.

For a pipe under pure tension from pressure loading, similar trends were exhibited by the GE/EPRI, LBB.ENG2, and LBB.ENG3 methods. The comparisons of the COD predictions by the LBB.ENG2 and LBB.ENG3 methods with the experimental data were excellent for this one experiment.

For pipes under combined bending and tension, all methods considered in this study underpredicted the experimental COD. The qualitative behavior is similar to that exhibited for the results of all pipe experiments discussed earlier. On a quantitative scale, however, the magnitudes of underprediction were much higher regardless of the methods used. Once again, the Paris/Tada method significantly underpredicted the COD. It should be noted, that for the combined load experiments, the COD during pressurizing was not recorded. This was because the specimens were pressurized at low temperatures, then heated for 1 to 2 days, and then the bending load was applied.

Table 3 shows the statistics of the predicted crack-opening ratio for pipes with short cracks ($\theta/\pi \leq 12$ percent) and pipes with cracks in the girth welds. The mean results indicate that for pipes with short cracks, the crack-opening would be underpredicted by the Paris/Tada, LBB.NRC, LBB.ENG2, and LBB.ENG3 methods and overpredicted by the GE/EPRI method. A similar trend was found for pipes under pure bending. The results for pipes with cracks in girth welds also reveal a similar qualitative behavior. For the girth weld cracks, the LBB.ENG2 and LBB.ENG3 methods predicted crack-opening displacement with reasonable accuracy with mean ratios close to one.

4.1.2 Complex-Cracked Pipes

Table 4 shows the mean and COV of the predicted crack-opening ratio of ten complex-cracked pipes under pure bending. These statistics were developed only for the LBB.ENG2 method. Note: since the loads of 40 percent of the maximum load were used, this eliminates the concern about the appropriate J-R curve to use since the crack has not initiated at this load level. The results in Table 4 show that the LBB.ENG2 method overpredicts (in terms of the mean value) crack-opening displacement for pipes with complex cracks. This is clearly opposite to the behavior exhibited by this method in analyzing simple TWC pipes. Further breakdown of the statistics for shallow cracks ($d/t \leq 0.5$) and deep cracks ($d/t \geq 0.5$), also shown in Table 4, reveals that the estimation method provides better predictions of the experimental COD if the depth of the 360-degree surface crack is smaller. Nevertheless, the LBB.ENG2 predictions for complex-cracked pipes were much larger than the experimental values of the COD. As mentioned before, this overprediction of the LBB.ENG2 method is due to the over-simplification in the estimation formulas for TWC pipes used for predicting COD of complex-cracked pipes. Hence, further developments are necessary to improve crack-opening models for complex-cracked pipes.

In analyzing pipes with a leaking crack that may potentially be a complex crack, it may not be always possible to estimate accurately the depth of the internal surface crack unless detailed nondestructive examination is performed. For such a crack, if the depth of the surface crack is overestimated, the current analysis methods would overpredict crack-opening. Hence, for a given leak rate, this will cause the crack length to be underestimated resulting overprediction of the pipe's maximum load-carrying capacity. On the other hand, if the depth of the surface crack is underestimated or ignored, the predictive methods would underestimate crack-opening, and hence, also underestimate the load-carrying capacity of the pipe.

Table 2. Mean and coefficient of variation of the ratio between experimental and predicted values of center-crack-opening displacement by various methods for simple through-wall-cracked pipes under various loading conditions

Fracture Analysis Methods	Ratio of Center-Crack-Opening Displacement[a]: All TWC Pipes (15 Tests) Mean	All TWC Pipes (15 Tests) Coefficient of Variation[b], percent	TWC Pipes Under Pure Bending (11 Tests) Mean	TWC Pipes Under Pure Bending (11 Tests) Coefficient of Variation[b], percent	TWC Pipes Under Pure Tension (1 Test) Mean	TWC Pipes Under Pure Tension (1 Test) Coefficient of Variation[b], percent	TWC Pipes Under Bending and Tension (3 Tests) Mean	TWC Pipes Under Bending and Tension (3 Tests) Coefficient of Variation[b], percent
GE/EPRI (Original)	1.01	72.8	0.84	51.7	0.75	-[c]	1.70	69.9
GE/EPRI (NRC/Battelle)	1.02	86.5	0.74	59.5	-[d]	-[c]	1.78	69.8
Paris/Tada	2.96	146	1.60	39.2	-[d]	-[c]	6.59	107
LBB.NRC	1.61	90.9	1.16	47.6	-[d]	-[c]	2.82	79.4
LBB.ENG2	1.16	47.0	1.07	45.5	1.0	-[c]	1.57	41.4
LBB.ENG3	1.18	45.7	1.10	44.1	1.0	-[c]	1.57	41.4

(a) Ratio of center-crack-opening displacement = experimental center COD/predicted center COD; the CODs were measured and calculated at 40 percent of experimental maximum load
(b) Coefficient of variation = (standard deviation/mean) × 100
(c) Not applicable
(d) Not determined

Table 3. Mean and coefficient of variation of the ratio between experimental and predicted values of center-crack-opening displacement by various methods for simple through-wall-cracked pipes with short cracks and cracks in girth welds

Fracture Analysis Methods	Ratio of Center-Crack-Opening Displacement[a]: TWC Pipes with Short Cracks ($\theta/\pi \leq 0.12$) (4 Tests) Mean	TWC Pipes with Short Cracks ($\theta/\pi \leq 0.12$) (4 Tests) Coefficient of Variation[b], percent	TWC Pipes with Cracks in Girth Welds (6 Tests) Mean	TWC Pipes with Cracks in Girth Welds (6 Tests) Coefficient of Variation[b], percent
GE/EPRI (Original)	0.74	31.0	0.67	70.4
GE/EPRI (NRC/Battelle)	0.76	36.0	0.62	67.0
Paris/Tada	1.42	37.2	1.61	33.5
LBB.NRC	1.30	21.4	1.04	45.1
LBB.ENG2	1.45	26.8	1.01	58.3
LBB.ENG3	1.47	27.3	1.06	55.3

(a) Ratio of center-crack-opening displacement = experimental center COD/predicted center COD; the CODs were measured and calculated at 40 percent of experimental maximum load
(b) Coefficient of variation = (standard deviation/mean) × 100

Table 4. Mean and coefficient of variation of the ratio between experimental and predicted values of center-crack-opening displacement by the LBB.ENG2 method for complex-cracked pipes with shallow and deep surface cracks

	Ratio of Center-Crack-Opening Displacement[a]					
	All CC Pipes (10 Tests)		CC Pipes with Shallow Cracks (d/t ≤ 0.5) (7 Tests)		CC Pipes with Deep Cracks (d/t ≥ 0.5) (3 Tests)	
Fracture Analysis Methods	Mean	Coefficient of Variation[b], percent	Mean	Coefficient of Variation[b], percent	Mean	Coefficient of Variation[b], percent
LBB.ENG2	0.63	41.5	0.77	24.7	0.33	36.5

(a) Ratio of center-crack-opening displacement = experimental center COD/predicted center COD; the CODs were measured and calculated at 40 percent of experimental maximum load
(b) Coefficient of variation = (standard deviation/mean) × 100

5. Finite Element Evaluations of Crack-Opening Shapes

During this study, several finite-element analyses were performed to evaluate the adequacy of the elliptical representation of a crack-opening profile. Two pipes, one with large diameter containing a short crack and the other with small diameter containing a long crack, were analyzed. The crack sizes are typical of leakage size flaws in LBB applications for nuclear piping systems. For the large-diameter pipe, there was one elastic analysis under pure bending. For the small-diameter pipe, there were two elastic-plastic analyses, one for pure bending and the other for combined bending and tension. They are explained below.

5.1 Large-Diameter Pipes with Short Cracks

In this analysis, the pipe had outer diameter, D_o = 406.4 mm (16 inches), wall thickness, t = 26.19 mm (1.031 inches), crack size, θ/π = 12 percent, and a single applied bending moment, M = 522.61 kN-m (4,626 inch-kip). The elastic modulus, E, was 193.06 GPa (28,000 ksi) and Poisson's ratio, ν, was 0.3. The loading was assumed to be linear-elastic with no plasticity or crack growth. Hence, the results of this analysis can be scaled for any other moments, if needed. The finite element analysis was performed by the ABAQUS code (Ref. 17) with twenty-noded three-dimensional solid elements. The total number of elements and nodal points were 1,260 and 9,030, respectively. Only one element through the thickness was used.

Figure 11 shows the results of finite element analysis in terms of COD plotted as a function of normalized crack-tip angle, $\xi/2\theta$, where ξ is an angle from a crack tip. In this figure, two plots are shown, one for the crack-opening profile at the outer surface and the other for the crack-opening profile at the inner surface of the pipe. For each case, the continuous line indicates the crack-opening shape assuming an elliptical representation with the center COD estimated by FEM analysis. The points indicate explicit calculations by FEM as a function of $\xi/2\theta$. It appears that both outer and inner crack-opening profiles can be accurately modeled by an elliptical shape.

5.2 Small-Diameter Pipes with Long Cracks

To understand the crack-opening characteristics for long cracks in small-diameter pipes, additional finite element computations were also conducted in this study. In this case, the pipe had mean diameter, D_m = 101.6 (4 inches), wall thickness, t = 8.56 mm (0.337 inch), and crack size, θ/π = 37 percent. Two loading cases were studied: (1) pure bending and (2) combined bending and tension (pressure induced) with 15.51 MPa (2,250 psi) internal pressure. For each loading case, the results due to several values of moment were investigated. The internal pressure in the pipe was simulated by applying the axial (tension) force only. No hoop stress or crack-face pressure were modeled.

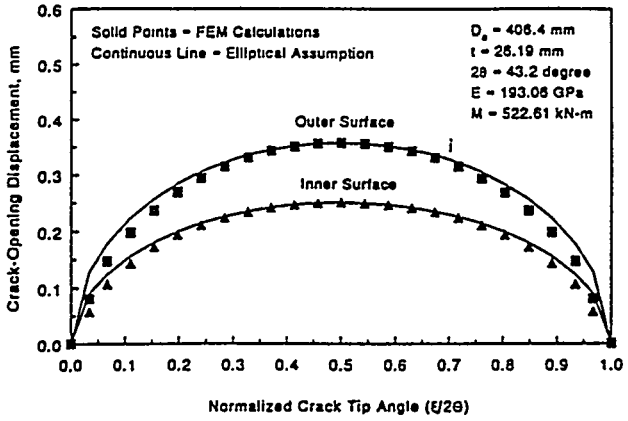

Figure 11. Crack-opening shape for a large-diameter pipe with a short crack under pure bending (elastic analysis)

The elastic modulus and Poisson's ratio were 193.06 GPa (28,000 ksi) and 0.29, respectively. The analyses were elastic-plastic and, therefore, a nonlinear stress-strain curve for the pipe material needs to be specified as well. In this regard, the Ramberg-Osgood model [$\epsilon/\epsilon_0 = \sigma/\sigma_0 + \alpha(\sigma/\sigma_0)^n$] was chosen to represent the tensile properties with the parameters: σ_0 = 210 MPa (30.5 ksi), $\epsilon_0 = \sigma_0/E$, $\alpha = 2.6$, and $n = 4.06$ (Ref. 4). No crack growth was assumed for any of the applied loads. The finite element analyses were performed by the ABAQUS code (Ref. 17) with twenty-noded three-dimensional solid elements. The total number of elements and nodal points were 949 and 4,984, respectively. There were four elements through the thickness. The size (length along the cracked plane) of the smallest element near the crack tip was 0.051 mm (0.002 inch).

The crack-opening displacements calculated by the FEM at the mid-thickness level of the pipe are given in Figures 12 and 13. Figure 12 shows several plots of crack-opening displacement as a function of the normalized crack angle from the crack tip ($\xi/2\theta$) for several bending moments without any internal pressure. Similar results are plotted in Figure 13 for the pipe under combined bending and tension with four different moments. For each loading case and applied moment, the crack-opening shapes based on elliptical representations with crack length as the major axis and the center

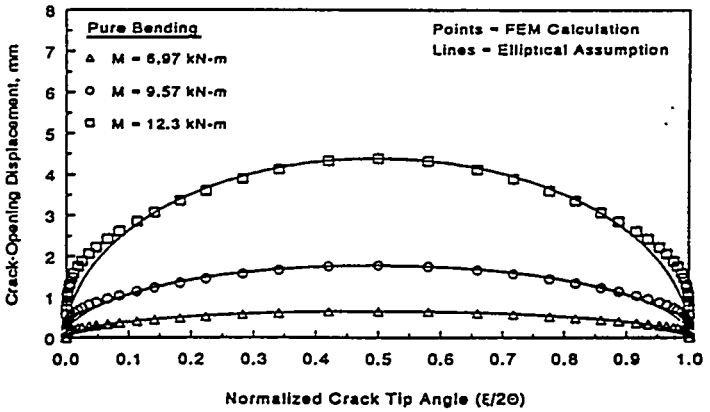

Figure 12. Crack-opening shape for a small-diameter pipe with a long crack under pure bending (elastic-plastic analysis

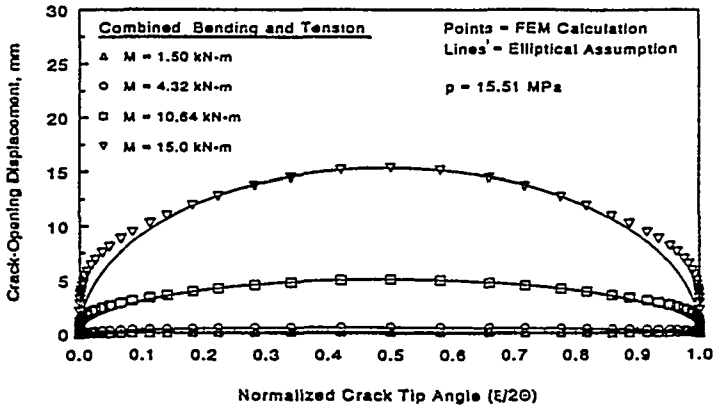

Figure 13. Crack-opening shape for a small-diameter pipe with a long crack under combined bending and tension (elastic-plastic analysis)

COD as the minor axis are also shown. The comparisons between finite element results (points) and the elliptical equation (lines) suggest that, indeed, the crack-opening profile can be modeled by an elliptical shape, regardless of load intensity and hence, the amount of plasticity in the cracked pipe.

For very large moments, the crack-driving force (applied J) was much higher than typical fracture initiation toughness (J_{Ic}) of austenitic or ferritic materials. This explains why there were slight crack-tip blunting in the finite element calculations in which no crack growth was allowed.

6. Summary and Conclusions

Twenty-five pipe experiments were analyzed to determine the accuracy of current estimation models for predicting center-crack-opening displacements for pipes with simple through-wall and complex cracks. Standard statistical analyses were performed to determine the statistics (mean and COV) of crack-opening ratio when the applied load is 40 percent of the experimental maximum load. (Note, the fracture behavior at this load is primarily elastic.) The results showed the following:

From Analyses of Simple Through-Wall-Cracked Pipes

- When all TWC pipe experiments were considered, all of the predictive models underpredicted the mean value of the COD (i.e., mean ratio greater than 1). The GE/EPRI methods (with the original and newly developed influence functions from this work) predicted experimental COD with very good accuracy in terms of the mean value of the crack-opening ratio, but their predicted COVs were much higher. The differences between the statistics for the GE/EPRI method based on the original influence functions and those from the present study were not significant. The LBB.ENG2 and LBB.ENG3 methods slightly underpredicted the mean experimental COD with much lower COVs. The LBB.NRC method underpredicted the COD more than the LBB.ENG2 or LBB.ENG3 methods with higher values of COV. Among all methods, the Paris/Tada method underpredicted COD by the largest margin in terms of both mean and COV of the predicted crack-opening ratio.

- The mean results for pipes with short cracks indicate that the crack-opening would be underpredicted by the Paris/Tada, LBB.NRC, LBB.ENG2, and LBB.ENG3 methods and overpredicted by the GE/EPRI method. A similar trend was found for pipes under pure bending. The results for pipes with cracks in girth welds also reveal a similar qualitative behavior. For the girth weld cracks, the LBB.ENG2 and LBB.ENG3 methods predicted crack-opening displacements with reasonable accuracy with mean ratios close to one.

From Analyses of Complex-Cracked Pipes

- Complex-cracked pipe experiments, i.e., a pipe with a 360-degree circumferential surface crack and a finite length through-wall crack, were also analyzed using only the LBB.ENG2 method. Regardless of whether a constraint factor was applied to the J-R curves, the LBB.ENG2 method overpredicted (in terms of the mean value) crack-opening displacement

for pipes with complex cracks. This is clearly opposite to the behavior exhibited by this method in analyzing simple through-wall-cracked pipes. Further breakdown of the statistics for shallow cracks ($d/t \leq 0.5$) and deep cracks ($d/t \geq 0.5$) reveals that this estimation method provides better predictions of the experimental COD if the depth of the 360-degree surface crack is smaller. For example, the mean values of the crack-opening ratio were 0.77 for shallow cracks and 0.33 for deep cracks. Nevertheless, the LBB.ENG2 predictions for complex-cracked pipes were much larger than the experimental COD values. This overprediction of the LBB.ENG2 method is due to the over-simplification in the estimation formulas for TWC pipes used for predicting the COD of complex-cracked pipes. Hence, further developments are necessary to improve crack-opening models for complex-cracked pipes.

The finite element predictions of the center-crack-opening displacement for Experiment 1.1.1.21 containing a short through-wall crack (θ/π = 6.25 percent) were in very good agreement with the experimental data from the pipe test.

The results from several finite element analyses showed that the crack-opening shape for a pipe would approximately follow an elliptical profile. Both large-diameter pipes with short cracks and small-diameter pipes with long cracks were analyzed under pure bending and combined bending plus tension to reach this conclusion.

Finally it should be noted that the experimental/COD values were at the outside surface, whereas the analyses were for mid-thickness COD values. Hence the experimental COD values at the mid-thickness should be slightly smaller, and the experimental-to-predicted COD ratio should be slightly less on the average for all the values in Tables 2, 3 and 4. Making the experimental mid-thickness COD corrections would involve considerable effort and was beyond the resources of this effort.

7. Acknowledgements

The authors would like to thank Mr. Michael Mayfield and the USNRC Office of Research, Electrical, Materials and Mechanical Engineering Branch for their encouragement and support of this effort as part of the USNRC's "Short Cracks in Piping and Piping Welds" program, Contract No. NRC-04-90-069. Their support and guidance are sincerely appreciated.

8. References

1. Wilkowski, G. M., Ahmad, J., Barnes, C. R., Brust, F., Ghadiali, N., Guerrieri, D., Jones, D., Kramer, G., Landow, M., Marschall, C. W., Olson, R., Papaspyropoulos, V., Pasupathi, V., Rosenfeld, M., Scott. P., and Vieth, P., "Degraded Piping Program - Phase II: Summary of Technical Results and Their Significance to Leak-Before-Break and In-Service Flaw Acceptance Criteria, March 1984 - January 1989," NUREG/CR-4082, Vol. 8, U.S. Nuclear Regulatory Commission, Washington, D.C., March 1989.

2. Schmidt, R. A., Wilkowski, G. M., and Mayfield, M. E., "The International Piping Integrity Research Group (IPIRG) Program: An Overview," *Transactions of the 11th International Conference on Structural Mechanics in Reactor Technology, Vol. G2: Fracture Mechanics and Non-Destructive Evaluation - 2*, Edited by H. Shibata, Tokyo, Japan, Paper No. G23/1, pp. 177-188, August 1991.

3. Wilkowski, G. M., and others, "Short Cracks in Piping and Piping Program," Semiannual reports by Battelle, NUREG/CR-4599, Vols. 1 to 3, Nos. 1 and 2, U.S. Nuclear Regulatory Commission, Washington, D.C., 1991-1994.

4. Rahman, S., Brust, F., Ghadiali, N., Choi, Y. H., Krishnaswamy, P., Moberg, F., Brickstad, B., and Wilkowski, G., "Refinement and Evaluation of Crack-Opening-Area Analyses for Circumferential Through-Wall Cracks in Pipes," NUREG/CR-6300, U.S. Nuclear Regulatory Commission, Washington, D.C., April 1995.

5. Kumar, V., German, M., and Shih, C., "An Engineering Approach for Elastic-Plastic Fracture Analysis," EPRI Report NP-1931, Electric Power Research Institute, Palo Alto, CA, July 1981.

6. Kumar, V., German, M., Wilkening, W., Andrews, W., deLorenzi, H., and Mowbray, D., "Advances in Elastic-Plastic Fracture Analysis," EPRI Final Report NP-3607, Electric Power Research Institute, Palo Alto, CA, August 1984.

7. Kishida, K. and Zahoor, A., "Crack-Opening Area Calculations for Circumferential Through-Wall Pipe Cracks," EPRI Special Report NP-5959-SR, Electric Power Research Institute, Palo Alto, CA, August 1988.

8. Wilkowski, G. M., and others, "Short Cracks in Piping and Piping Program," Semiannual reports by Battelle, NUREG/CR-4599, Vols. 1 to 3, Nos. 1 and 2, U.S. Nuclear Regulatory Commission, Washington, D.C., 1991-1994.

9. Paris, P. C. and Tada, H., "The Application of Fracture Proof Design Methods Using Tearing Instability Theory to Nuclear Piping Postulating Circumferential Through-Wall Cracks," NUREG/CR-3464, U.S. Nuclear Regulatory Commission, Washington, D.C., September 1983.

10. Klecker, R., Brust, F., and Wilkowski, G., "NRC Leak-Before-Break (LBB.NRC) Analysis Method for Circumferentially Through-Wall-Cracked Pipes Under Axial Plus Bending Loads," NUREG/CR-4572, U.S. Nuclear Regulatory Commission, Washington, D.C., May 1986.

11. Brust, F. W., "Approximate Methods for Fracture Analyses of Through-Wall Cracked Pipes," NUREG/CR-4853, U.S. Nuclear Regulatory Commission, Washington, D.C., February 1987.

12. Gilles, P., and Brust, F., "Approximate Fracture Methods for Pipes - Part I: Theory," *Nuclear Engineering and Design*, Vol. 127, pp. 1-27, 1991.

13. Gilles, P., Chao, K. S., and Brust, F., "Approximate Fracture Methods for Pipes - Part II: Applications," *Nuclear Engineering and Design*, Vol. 127, pp. 13-31, 1991.

14. Rahman, S., Brust, F., Nakagaki, M., and Gilles, P., "An Approximate Method for Estimating Energy Release Rates of Through-Wall Cracked Pipe Weldments," *Fatigue, Fracture, and Risk*, PVP-Vol. 215, San Diego, California, 1991.

15. Rahman, S. and Brust, F., "An Estimation Method for Evaluating Energy Release Rates of Circumferential Through-Wall Cracked Pipe Welds," *Engineering Fracture Mechanics*, Vol. 43, No. 3, pp. 417-430, 1992.

16. Rahman, S. and Brust, F., "Elastic-Plastic Fracture of Circumferential Through-Wall Cracked Pipe Welds Subject to Bending," *Journal of Pressure Vessel Technology*, Vol. 114, No. 4, pp. 410-416, November 1992.

17. ABAQUS, User's Guide and Theoretical Manual, Version 5.3, Hibbitt, Karlsson, & Sorensen, Inc., Pawtucket, RI, 1993.

18. Kramer, G. and Papaspyropoulos, V., "An Assessment of Circumferentially Complex-Cracked Pipe Subjected to Bending," NUREG/CR-4687, U.S. Nuclear Regulatory Commission, Washington, D.C., October 1986.

19. ASTM Standard E1152-87, "Standard Test Method for Determining J-R Curve," *Annual Book of ASTM Standards*, Volume 03.01, 1991.

20. "Report to the U.S. Nuclear Regulatory Commission Piping Review Committee," Prepared by the Pipe Break Task Group, NUREG/CR-1061, Vol. 3, U.S. Nuclear Regulatory Commission, Washington, D.C., November 1984.

CRACK OPENING AREA ESTIMATES IN PRESSURIZED THROUGH-WALL CRACKED ELBOWS UNDER BENDING

FRANCO Ch., GILLES Ph., FRAMATOME, FRANCE
PIGNOL M., FRAMASOFT+CSI, FRANCE

INTRODUCTION

One of the most important aspects in the leak-before-break approach is the estimation of the crack opening area corresponding to potential through-wall cracks at critical locations during plant operation. In order to provide a reasonable lower bound to the leak area under such loading conditions, numerous experimental and numerical programmes have been developed in USA, U.K. and FRG and widely discussed in literature [1, 2, 3].

This paper aims to extend these investigations on a class of pipe elbows characteristic of PWR main coolant piping. The paper is divided in three main parts. First, a new simplified estimation scheme for leakage area is described, based on the reference stress method. This approach mainly developed in U.K. [4] and more recently in France [5, 6] provides a convenient way to account for the non-linear behavior of the material. Second, the method is carried out for circumferential through-wall cracks located in PWR elbows subjected to internal pressure. Finite element crack area results are presented and comparisons are made with our predictions. Finally, in the third part, the discussion is extended to elbows under combined pressure and in plane bending moment.

ASSESSMENT OF CRACK OPENING AREAS

In linear elastic fracture mechanics, one can establish that, under uniform membrane stress σ_m, the crack opening area A may be derived from the strain energy release rate G through the relationship :

$$A = \frac{4}{\sigma_m} \int_0^a G(x)\, dx \qquad (1)$$

where a represents the half crack length.

In order to extend our investigations in Elastic Plastic Fracture Mechanics (EPFM)., we replace G in the previous expression by the crack driving force J as it has been suggested in reference [7]. This new expression, indicated hereafter, can be demonstrated as a reasonable lower bound of the elastic plastic crack opening area :

$$A = \frac{4}{\sigma_m} \int_0^a J(x)\, dx \qquad (2)$$

Equation 2 gives the opening area as soon as an expression for J is known. For example, let us consider a circumferential through-wall crack located in a section of a straight pipe. If the material stress-strain law is modelled by a Ramberg-Osgood law, finite element J solutions may be provided by the EPRI handbook [3]. Then, by integrating numerically equation 2, one can obtain the crack opening area and then check the conservatism of equation 2 using the Crack Opening Displacement EPRI solutions [3].

Even if such an approach is of great interest, some limitations are introduced (Ramberg-Osgood law - Geometry of straight pipe circumferential through-wall crack). In order to remove these difficulties, we propose to use in equation 2 a J estimate based on R6/3 option 2 K_R - L_R relationship. Developed by Ainsworth [4] and discussed recently in [5 - 6], this approach provides a convenient way to determine an approximate value of J in a non-linear material from the elastic value G. As shown hereafter, the K_R - L_R relationship depends only on the material stress-strain curve, therefore the determination of L_R gives the K_R value and then the J value. Consequently, equation 2 can be written as follows :

$$A = \frac{4}{\sigma_m} \int_0^a \frac{G(x)}{K_R^2(x)} dx \qquad (3)$$

with

$$K_R = \left[E \frac{\varepsilon_{ref}}{\sigma_{ref}} + 0.5 \frac{L_R^2}{1 + L_R^2} \right]^{\frac{1}{2}} \qquad (4)$$

and

$$L_R = \sigma_{ref}/\sigma_y = \frac{\text{Applied load}}{\text{Reference load}} \qquad (5)$$

The reference load may be considered as given by writing the yield condition in the ligament. Finally solving equation 3 requires only the knowledge of elastic G and the reference stress σ_{ref} as functions of the crack length. Detailed parametric studies of elbows with longitudinal and circumferential through-wall cracks have been performed by Chattopadhyay and al [8] or A. Zahoor [9], providing fitted solutions of Stress Intensity Factors for cracked elbows subjected to pressure or in plane bending moment. Thus, the problem is reduced to the derivation of an expression for the reference stress σ_{ref} relative to a through-wall cracked elbow under pressure or combined pressure and in plane bending.

The pure bending case is not examined in this study. On one hand, solving equation 3 requires the existence of prevailing membrane stresses in order to guarantee the consistency with the assumptions mentioned previously. On the other hand, such loading conditions are not representatives for the main cooling line of PWR at normal operating conditions.

REFERENCE STRESS SOLUTION FOR A CIRCUMFERENTIALLY CRACKED ELBOW UNDER PRESSURE

In a constant thickness elbow, an approximation of a statically and plastically admissible field for a Rigid Perfectly Plastic material having a yield strength of σ_0 , is given by the following expressions:

$$n_r = -\frac{P}{2\sigma_0}$$

$$n_\theta = C_1 \frac{P}{\sigma_0} \left(\frac{r_m}{t} - \frac{1}{2} \right) \qquad (6)$$

$$n_z = \frac{P}{\sigma_0} \frac{r_m}{2t}$$

where C_1 is the stress index which varies with the position along the circumference in the elbow cross section (see RCC-M code [10] appendix B3600). At the extrados, where the crack is located, the C_1 value is less than unity. In that

case we consider that the axial stress is about half the sum of the circumferential and the radial stress, therefore the yield condition is the same as in a straight pipe. This condition is expressed through the following set of equations:

$$\alpha = -\frac{\gamma}{2} \frac{\frac{n_\theta + n_r}{2} + \sqrt{1 - \frac{3}{4}(n_\theta - n_r)^2}}{\sqrt{1 - \frac{3}{4}(n_\theta - n_r)^2}} \qquad (7)$$

$$\left[\cos\alpha - \frac{1}{2}\sin\gamma\right]\sqrt{1 - \frac{3}{4}(n_\theta - n_r)^2} - \frac{n_\theta + n_r}{2} \cdot \frac{1}{2}\sin\gamma = 0$$

L_R is derived by solving these equations in which the stress components have been divided by L_R. Using equation (7) and conventional numerical integration techniques, equation (3) provides the crack opening area estimate (more details are given in the next paragraph).

COMPARISONS WITH FINITE ELEMENT RESULTS

In order to estimate the validity of such a method, now we compare our predictions to finite element crack area results. The selected finite element model is an elbow characteristic of PWR main coolant piping whose the main geometrical parameters are plotted in Table 1. Tensile properties are given in Figure 1.

R_c (mm)	r_m (mm)	t (mm)	λ	α (degrees)
1354	412	62.5	0.5	50

Table 1 : Geometry of F.E. model

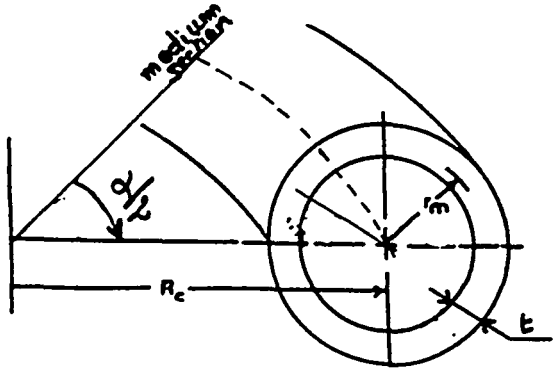

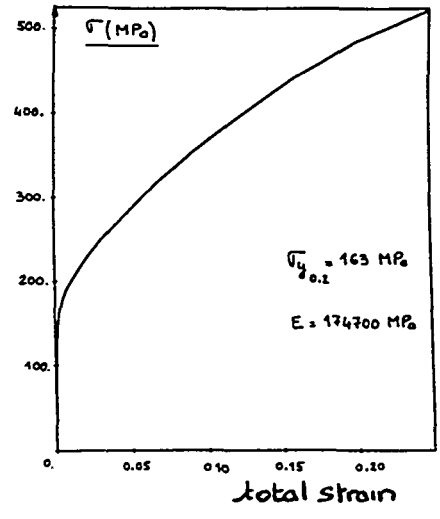

FIG. 1 : Tensile curve

In order to examine the influence of the crack position and the crack length, two configurations have been investigated. In the first one, the crack is located in the medium section of the elbow, at the extrados with an half crack angle γ of 16.7 degrees. In the second case, the crack is located in the same section, but 30° degrees away from the crown, in between the crown and the extrados. The crack length is larger than the first one, with an half angle value of 25° degrees.

The finite element models, plotted in Figures 2 and 3, contain respectively 486 and 1920 20 noded elements, 2827 and 10197 nodes. Pressure is increased up to normal operating pressure (P = 15.5 MPa). In each case a pressure of P/2 value is applied normally to the crack faces. The computations have been performed with SYSTUS F.E. code [11] using an incremental Von-Mises rule, taking into account an updated Lagrangian procedure.

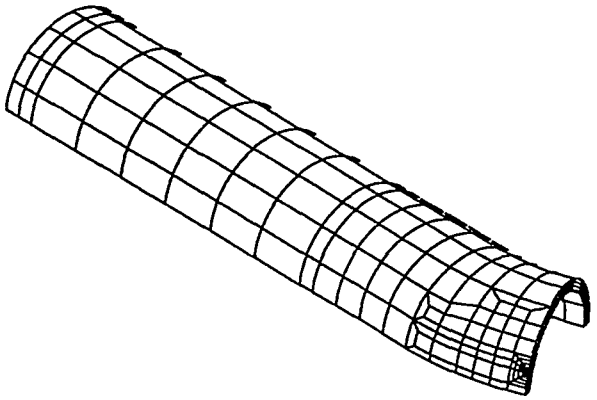

FIG. 2 : Finite Element model with the circumferential through-wall crack located at the extrados

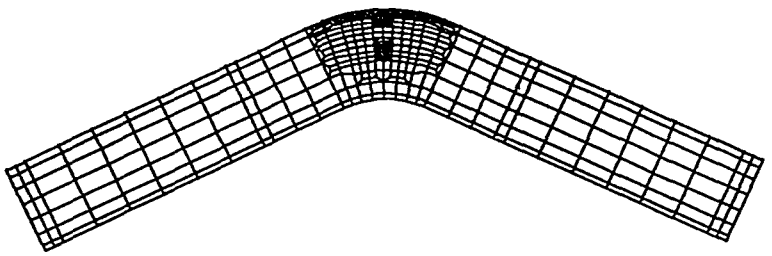

FIG. 3 : Finite element model with the crack located 30° degrees away from the crown

We have plotted in Figures 4 and 5 the finite element results in term of J values and crack opening areas versus applied pressure. J values are computed from G-θ method, presented in reference [12] and crack opening areas are obtained on external and internal sides from the crack opening displacement results.

The good agreement between J estimation based on K_R - L_R relationship and finite element solutions (see Figures 4-a or 5.a) ensures first the validity of elastic G solutions drawn from [8]. On the other-hand, even if plastic deformations are contained surrounding the crack, the spread of plasticity is large enough when p is greater than 12 MPa to conclude favourably on our choice of σ_{ref} in the range of pressure considered in this study.

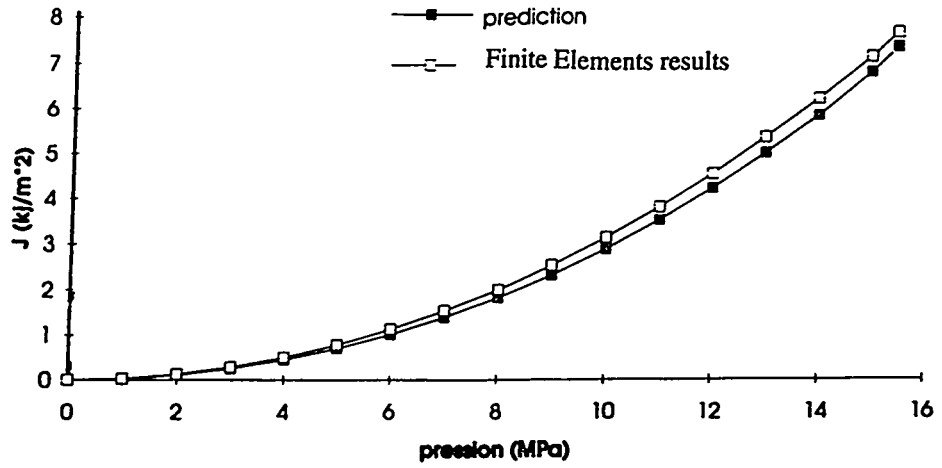

4-a : J predictions up to operating pressure

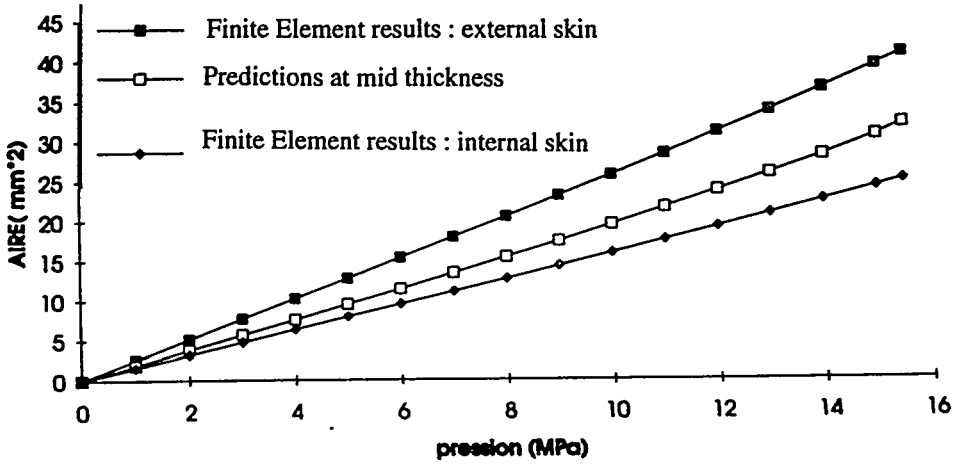

4-b : Crack area predictions up to operating pressure

FIG. 4 : Comparisons with Finite Element results
for the crack located at the extrados

Finally the crack opening area results are collected on Figures 4b and 5b. The comparisons with F.E. results indicate that solving equation 3 gives excellent predictions at mid thickness for the both configurations.

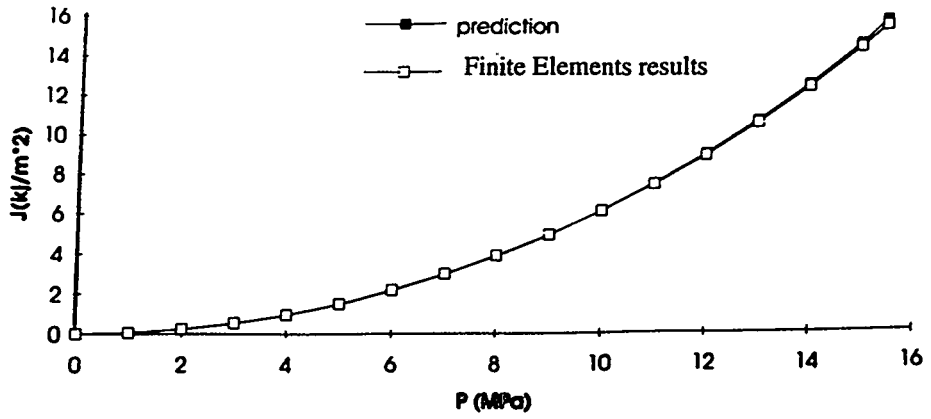

5-a : J predictions up to operating pressure

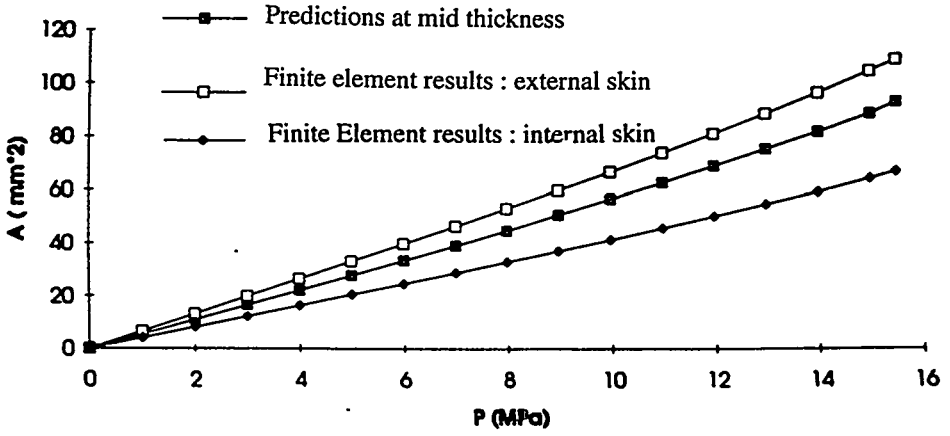

5-b : Crack area predictions up to operating pressure

FIG. 5 : Comparisons with Finite Element results when the crack is located 30° degrees away from the crown

EXTENSION FOR AN ELBOW UNDER COMBINED INTERNAL PRESSURE AND IN PLANE BENDING MOMENT

Recently, Ph. GILLES and al [6] have realised a very consequent work on the existence of reference stresses for surface cracked pipes. Their investigations provide a convenient way to identify reference stress solutions for combined loading conditions where the major ideas are recalled hereafter.

Under combined loading, the reference load has to be replaced by a loading surface which may be approximated by a local yield limit surface, just as the limit load is a good approximation of the reference load. The equation of this yield surface, which is expressed as a function of the external loads Q_i , is denoted by $\Phi\ (Q_i, A) = 0$, where A represents the geometrical parameters defining the crack. Then for a given loading point P in the space of the parameters of the yield function, L_R represents the ratio of the distance between the origin O and P to the distance OL, where l is the intersecting point of the OP line with the loading surface. L_R is obtained by simply solving the non-linear equation $\phi\ (Q_i / L_R, A) = 0$.

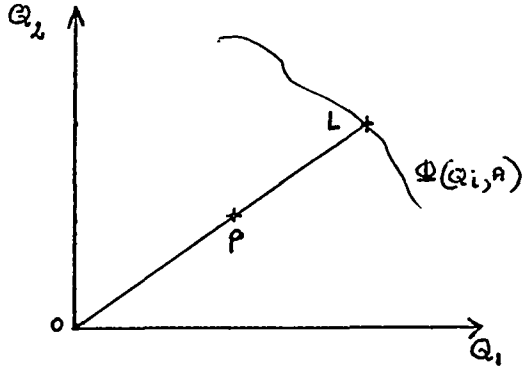

Let us consider the finite element models described previously. The computations have been completed by introducing an increasing bending closing moment as the normal operating pressure is reached. Using the K_R - L_R relationship and the finite element J solutions, one can derive for each step of loading the L_R value and consequently the computed yield surface $\Phi\ (Q_i, A)$.

Results relatives to the crack located at the extrados are plotted in Figure 6. Each co-ordinate indicates the ratio of the applied load to limit load under pure loading conditions : P_0 is given by equation 4 and M_0 is the limit in plane bending moment drawn from Griffiths experimental work [13]. Starting from Calladine's expression [14], our numerical investigations leaded us to write M_0 as:

$$M_0 = 0.935 \cdot \lambda^{2/3} \quad 4\ \sigma_y\ r_m^2\ t\ \ f(a/r_m) \cdot \beta \qquad (8)$$

$f(a/r_m)$ is a reducing factor due to the crack and β an amplification factor depending on the opening angle of elbow. By using this formalism, the finite element computed loading surfaces can be approximated, as it is shown on figure 6, by circles described by the following set of empirical equations :

$$\begin{aligned} \Phi &= \left(\frac{P}{P_0} - x_C\right)^2 + \left(\frac{M}{M_0} - x_C\right)^2 - r^2 \\ r^2 &= (1 - x_C)^2 + x_C \\ x_C &= 0.4 \end{aligned} \qquad (9)$$

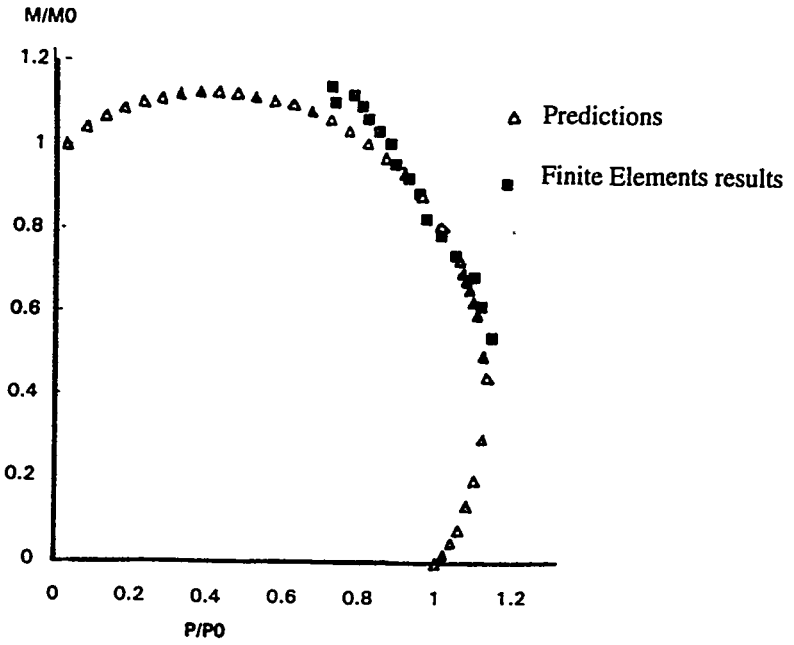

FIG. 6 : Loading surface results for an elbow subjected to combined loadings with a circumferential crack at the extrados

the relative value x_c depends mainly on the curvature parameter $\left(R_c t/r_m^2 \equiv 0.5\right)$, and accounts for the beneficial effect of internal pressure which minimises the ovalization.

Consequently, under combined loading (pressure + in plane bending moment) the reference stress is calculated using the yield surface equation (9) as explained at the beginning of this paragraph. Then, the L_R solution is replaced in equations (4) and solving equation (3) gives the crack opening area. The membrane stress σ_m is written as the sum of the membrane stress σ due to combined loading and approximated by the expressions given in appendix B3600 of the RCC-M code [10]. Mid thickness crack area predictions are plotted on Figures 7 and 8 for the two circumferential through-wall cracks discussed in this paper. The comparisons with finite element results are in a good agreement, even if plastic deformations are noticeably spreading ahead the crack front with the increase of bending moments. The simplified approach ensures a reasonable lower bound at normal operating conditions. Beyond these normal operating conditions, the effects of bending stress through the thickness become important and solving equation 3 could lead to unconservative predictions.

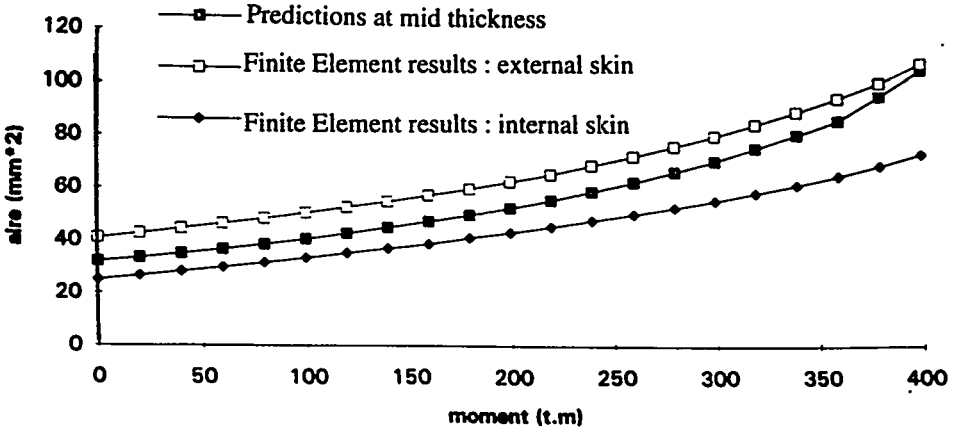

FIG. 7 : Crack areas predictions for crack located at the extrados

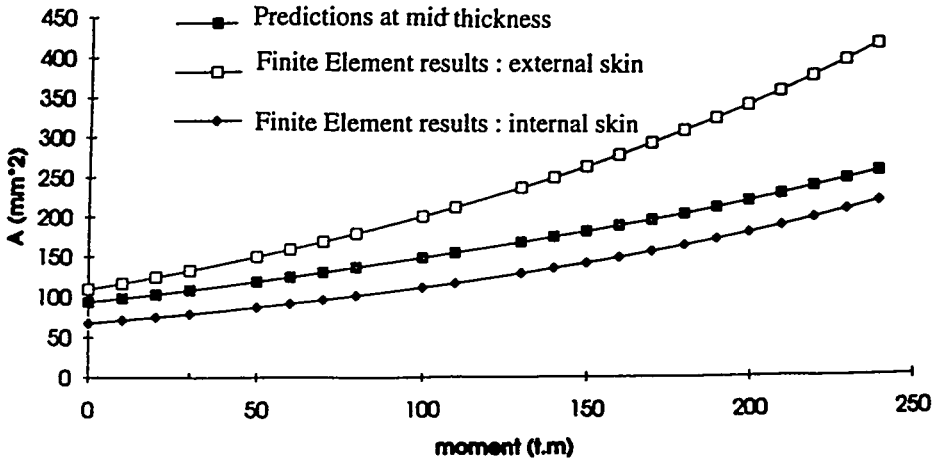

FIG. 8 : Crack areas predictions for crack 30° degrees away from the crown

CONCLUSION

This paper focuses on the crack opening area predictions of a class of pipe elbows characteristic of PWR main coolant piping. A new simplified estimation scheme for the crack opening area has been developed in Elastic Plastic Fracture Mechanics, using the reference stress method.
The predictions are compared to refined elastoplastic finite element calculations, covering a representative range of crack length. The loading involved are either internal pressure or a combination of pressure and in plane bending moment. For all the considered configurations, a good agreement is shown between computed and estimated crack opening areas.

ACKNOWLEDGEMENTS

The authors wish to acknowledge EDF for supporting this study.

REFERENCES

[1] G.M. WILKOWSKI and al.
"Short cracks in Piping and Piping Welds, task 6 : Crack opening area evaluation"
NUREG/CR.4599 BMI 2173, Vol. 3, n° 1 - Semi annual Report April 1992-September 1992.

[2] W. KASTNER, E. RÖTTRICH, W. SCHMITT and R. STEINBUCK
"Critical crack sizes in ductile piping"
Int. J. Pressure Vessel and Piping 9 (1981), pp. 197-219.

[3] V. KUMAR, M.D. GERMAN, W.W. WILKENING, W.R. ANDREWS, H.G. De LORENZI, D.F. MOWBRAY
"Advances in Elastic-Plastic Fracture Analysis"

N.P. 3607 Research Project 1237-1, August 1984.

[4] AINSWORTH, R.A.
"The assessment of defect in structures of strain hardening material"
Engineering Fracture Mechanics, 19, 1984, pp. 633-642.

[5] Ph. GILLES, A. PELLISSIER TANON, Ch. FRANCO, J. VAGNER,
"Validity of J Estimation in Piping Components based on R6/3 Option 2 K_R-L_R Relationship"
ECF 10 Conference Proceedings, Berlin, 1994.

[6] Ph. GILLES and C. BOIS
"Existence and Expressions of reference stresses in surface cracked pipes"
Proc. of the 2nd Griffiths Conference, Sheffield, September 1995.

[7] S. BHANDARI, C. FAIDY, D. ACKER
"Computation of Leak Areas of Circumferential Cracks in Piping for Application in demonstrating leak-before-break behaviour"
Int. Journal Pressure Vessel in Piping 42 (1990), pp. 287-302.

[8] J. CHATTOPADHYAY and al.
"A database to evaluate stress intensity factors of elbows with through-wall flaws under combined internal pressure and bending moment"
Int. Journal Pressure Vessel and Piping 60 (1994), pp. 71-83.

[9] A. ZAHOOR
"Ductile Fracture Handbook, Vol. 3"
Research Project 1757-69, January 1991.

[10] RCC-M, Règle de Conception et de Construction des Matériels Mécaniques des ilots PWR.
App. B3600 "Conception des Tuyauteries"
App. B3685 "Indices de Contraintes utilisables dans le cadre de l'analyse détaillée"
AFNOR, Edition Juin 1988.

[11] SYSTUS
Finite element Code. Version 1993. FRAMASOFT- CSI.

[12] DESTUYNDER, Ph., DJAOUA, M.
"Sur une interprétation mathématique de l'intégrale de Rice en théorie de la rupture fragile"
Mathematical Methods in Applied Sciences, 3, pp. 70-87, 1981.

[13] J.G. GRIFFITHS
"The effect of cracks on the limit load of pipe bends under in-plane bending experimental study"
Int. J. Mech. Sci., Vol. 21, pp. 119-130 (1979).

[14] CALLADINE C. R.
"Limit analysis of curved tubes", Jour. Mech. Eng. Science, Vol. 16 (1974), pp. 85-87.

Influence of wetting effect at the outer surface of the pipe on increase in leak rate - experimental results and discussion -

Toshikuni ISOZAKI and Katsuyuki SHIBATA
Division of Reactor Safety Research, Japan Atomic Energy Research Institute

1. Introduction

In the nuclear industry, leak through crack from the piping system is beneficial, since it allows the operator time for suitable actions at an early stage before failure. This is so called "Leak Before Break". JAERI conducted the leak rates tests using the circumferentially fatigue-cracked-piping under pressure and/or bending loads since the proper estimation of the leak rates was definitely one of the key issues in the LBB analysis[1,2]. Until now, there has been some problems that the experimental and computed leak rate did not agree[3]. The leak rate is given by the product of the critical flow rate through the crack and the COA(crack opening area). In the present paper we don't refer to the former, describe instead the dependency of temperature of the test pipe near the crack upon the increase in COA or COD(crack opening displacement) and leak rate, which is due to the thermal shrinkage at the locally wetted part of the piping.

2. Experiments

In the present paper, experimental and computed results are described for the two straight pipes, 12SS2(12inch outer diameter, made of stainless steel) and 12CF1(made of centrifugal steel) subjected both to internal pressure and thermal load but to no bending load. They are modelled after the recirculation line of the BWR and primary coolant line of the PWR, respectively. Table 1 shows the testing conditions and measured leak rates. Roughness at the crack surface was measured after the test.

Table 1 testing conditions and leak rates

test pipe ident.	outer dia. mm	thick-ness mm	rough-ness Rz (DIN) μm	outer surface crack length mm	test ident.	slitted/ complete heat insulator	leak rate kg/min	pressure in pipe MPa	water temp. ℃
12SS2	316	17.4	35	93 west 64 east 157 total	L3	slitted	20.6	7.00	272
					L4	complete	50.8	6.52	272
12CF1	316	33.3	87	50 west 52 east 104 total	L3	slitted	14.9	12.25	312
					L4	complete	17.9	12.15	307

Figure 1 shows the leak rate experiment using 12CF1 piping, from the top:
A, B; before the test: Both sides were already covered with fixed heat insulator. Only the central part(length= 1150mm) was left uncoverd for attaching the 1.6mm diameter theathed thermo-couples, high temperature strain gages and clip gage to measure the COD.

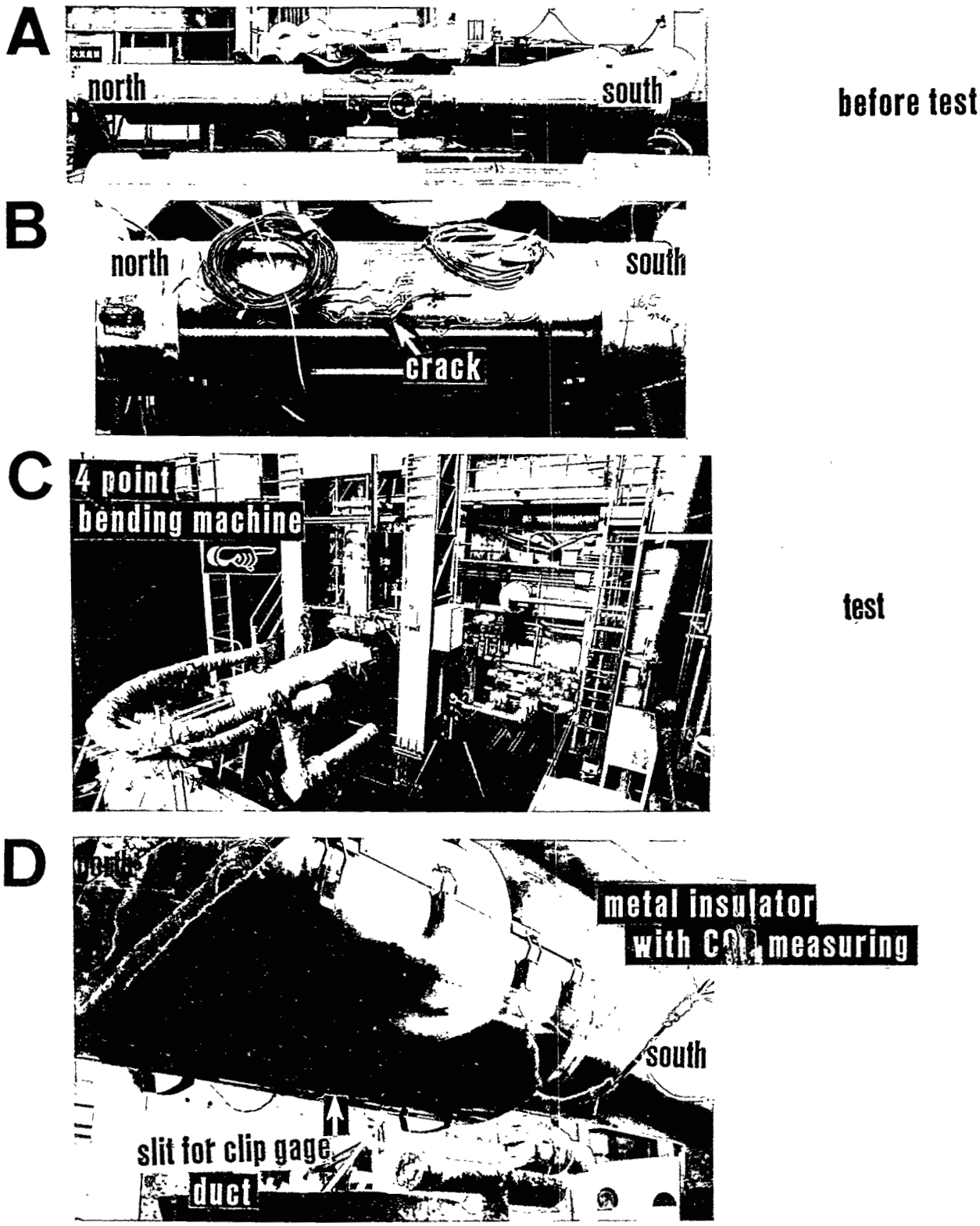

Figure1 sequence of leak rate experiment of 12CF1 piping

C; in the test: The jack was available to apply the bending load to the pipe supported with 4000 mm span.
D; in the test: The leak went downwards to the duct. Leak rate was measured with differential pressure transducer attached on the pressure vessel.
While conducting the tests, two types of metal insulator(length= 850mm) were used for the lower half of the insulator. One is complete, another is slitted(width=50mm, angle=70degree, see Figure 2) intentionally for the clip gage to be attached. This is shown in Figure 1 D. However, in the real piping system there is of course no such a slit in the heat insulator. It was easily anticipated that the leak rate would change under the different downstream conditions. To satisfy both the demands, that is,
(1) to obtain the COD
(2) to measure the leak rate under the same condition as real plants as far as possible,
we conducted the test by changing the complete(= without slit) heat insulator with slitted one alternatively and succesively. COD measurements were not successful, however, because clip gage caught both the real COD and thermal expansion or shrinkage of the pipe simultaneously.

3. Temperature distribution around crack and leak rate

Figure 2 shows the details of cross section at the crack surface of 12CF1 piping. TE stands for the thermocouple elements. TE7 and 72 were used for the fluid temperature measurement, while other TEs metal temperature. As is seen from the bottom and front view of Figure 2, TE10 to TE15 were located near the crack and TE8 and TEs 17, 19, 20 and 21 were used to obtain the surface temperature of the test pipe. Among them, TE11, 13 and 15 were embedded in the pipe wall to measure the midsurface temperature.
Figure 3 shows the temperature distribution measured by those thermocouples. Abscissa expresses the number of them. It is interesting that both L3 experiments are similar and also both L4s are and that there are clear differences between L3 and L4. In the L3 experiment slitted heat insulator was used to obtain the space for the clip gage, while in the L4 experiment the complete heat insulator was in use.
When we see the output of the bottom TEs in the test 12SS2-L4 and 12CF1-L4, the temperature is kept at 100 ℃. This explains that the water was stagnant within the bottom of annular region between the pipe and heat insulator around the crash. On the other hands, the output of the bottom TE21 in the test 12SS2-L3 is 200 ℃ and 235℃ in 12CF1-L3. This means that the leak went straight downwards outside the metal insulator through the slit without wetting the neighboring surface of the pipe, which kept the surface temperature of the test pipe enough high above 200℃. Leak rate increased from L3 to L4 for both 12SS2 and 12CF1 experiments, which was due to the larger COD caused by the temperature differences in the the two experiments.

4. Calculation by ADINA

ADINA[4] was used to follow these experimental phenomena. Loads applied to the model are
(1) internal pressure
(2) dead weight
(3) temperature.
(1) and (3) are given by the experimental data. Material data are shown in Table 2. Yield strength σy and strain hardening modulus Et were obtained from our tensile test results, while other constants were from[5].
Computed results consist of
(a) the deformation of the piping
(b) COD(= displacement in the axial direction at the crack) distribution along the crack
under
(i) the uniform nodal temperature equal to the hot water temperature
(ii) the interpolated nodal temperature based upon the output of thermocouples.
Condition (i) is important since normally no precise temperature distibution in the pipe is given to the analytical model and therefore there is no choice but to have the equal temperature input in the calculation. Condition (ii) is our original. We managed to interpolate the nodal temperature linearly with distance between two TEs by making full use of the results of temperature measurements in the test.

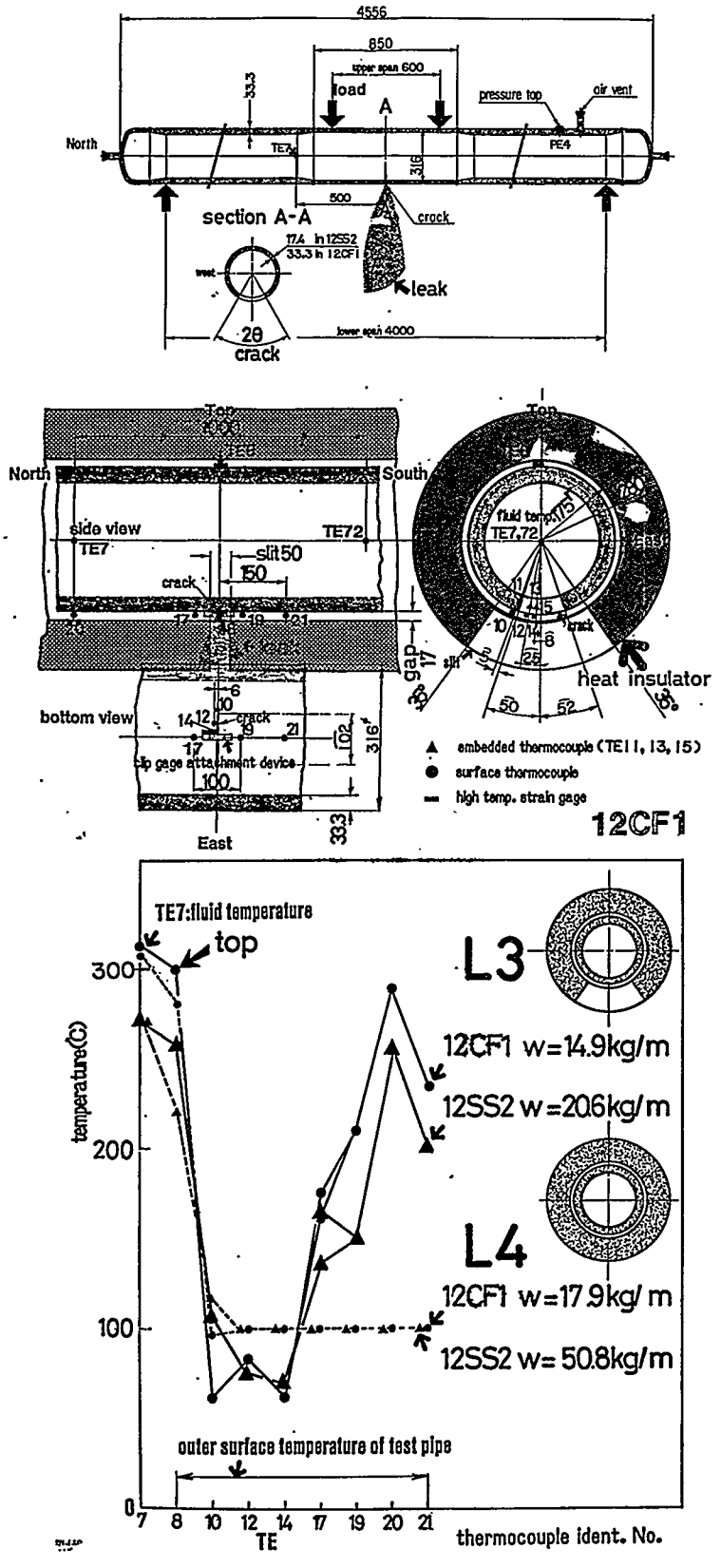

Figure2 geometry and location of thermocouples of 12CF1 piping

Figure3 temperature distribution during leak rate experiment of 12SS2 and 12CF1 piping

Isozaki

Table 2 Material data

$\nu = 0.3$

	yield strength (MPa)	Youngs modulus (MPa)	strain hardening modulus (MPa)	thermal coefficient (1/℃)
SUS304				
20℃	255	1.95×10^5	4018	16.4×10^{-6}
300℃	157	1.76×10^5	3038	18.7×10^{-6}
CF8M				
20℃	235	1.95×10^5	5390	16.4×10^{-6}
300℃	157	1.76×10^5	2940	18.7×10^{-6}

Figure 4 shows nodal temperature distribution in the longitudinal(left side) and circumferential (right side) direction of 12CF1-L3(upper half) and L4(lower half). From these figures, it is shown that the bottom surface temperature is over 200 ℃ in L3 while it is strictly 100℃ in L4.

5. Discussion

Figures 5 and 6 show the deformation near the crack about 12SS2 and 12CF1 piping. The four figures in the upper left shows the original configurations composed of bird(total model), front, side and bottom(partial models) view. Owing to the symmetry only one half model of the pipe is sufficient. Three dimensional solid element, shell element and beam elements were used where th e crack was at the front of the model. Only the solid elements including the crack surface useth ermo-plastic model, while others do the thermo-elastic model. All the deformation is magnifiedeq ually by a factor of 100.
Those in the upper right shows the deformation under uniform nodal temperature loading which plays an important role as a standard thermal condition. In the same manner, the lower left and lower right four figures show that under the L3 and L4 temperature load, respectively.
The uniform temperature for 12SS2 and 12CF1 are 272 ℃and 312 ℃ whose value were determined from the water temperature by TE7 or TE72 in the pipe at each experiments. The bottom views show us how the COA is dependent on the load temperature. The most remarkable COA deformation was observed at L4 conditions for both experiments. To see the influences of surface temperature on the COA, Figure 7 is convenient. The abscissa is the anticlockwise distance between the two nodes near the both crack edges and each one along the inner-, mid- and outer- surfaces of the pipe.

For 12SS2 piping,
(1) The uniform 272 ℃ temperature load generates the equal COD among three surfaces and the smallest COD compared with L3 and L4 load temperature.
(2) The L4 temperature brings about the most remarkable COD. The COD at the inner surface is the smallest in 272 ℃ temperature load, the largest in L3. However, the outer surface COA is the largest at L4. These are caused by the tensile thermal stress at the outer surface and compressive stress at the inner surface. This may explain the large increase in leak rate from L3's 20.6kg/min to L4's 50.8kg/min.

For 12CF1 piping,
(3) The COD of 12CF1 is smaller than that of 12SS2, which is due to the smaller crack length.
(4) The uniform 312 ℃ temperature load generates the equal COD among three surfaces just like 12SS2.
(5) The inner COD tend to close for both L3 and L4 tests. However, the outer COD is the largest at L4 test. This may explain that only the slight increase in leak rate was observed from L3's 14.9kg/min to L4's 17.9kg/min.

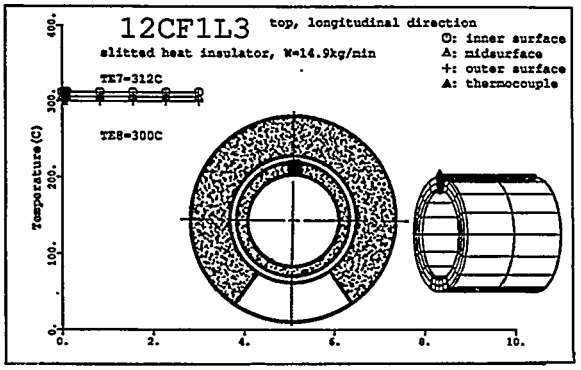

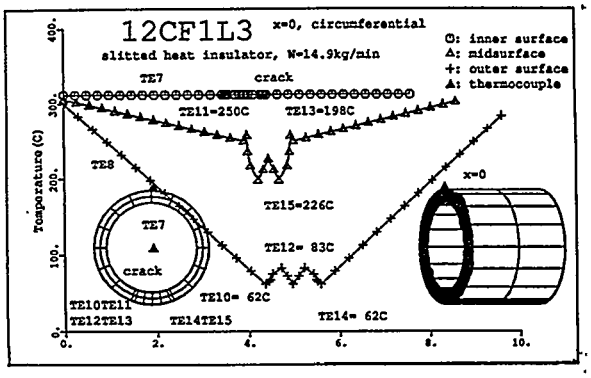

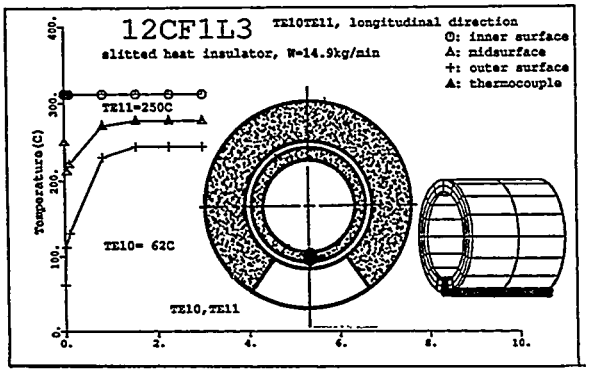

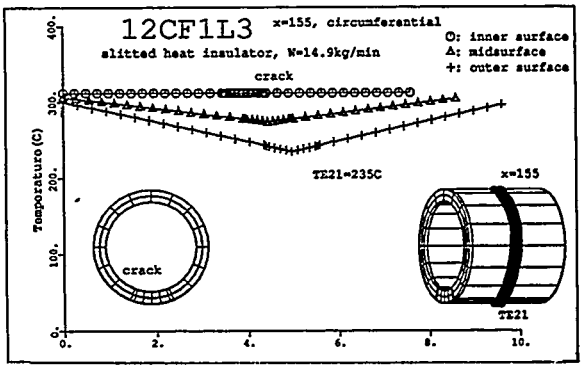

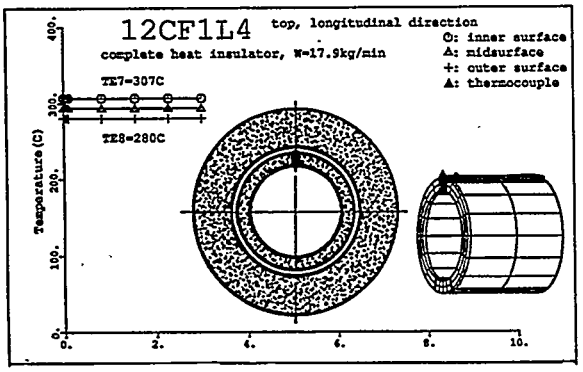

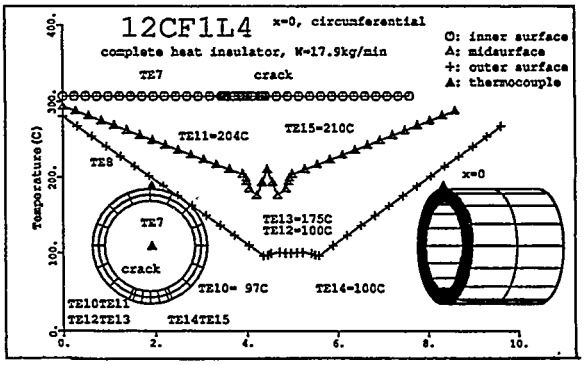

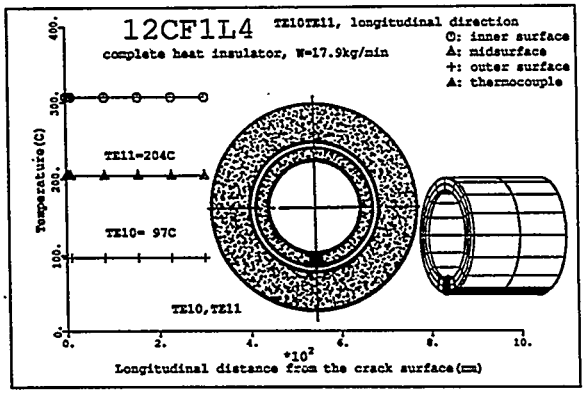

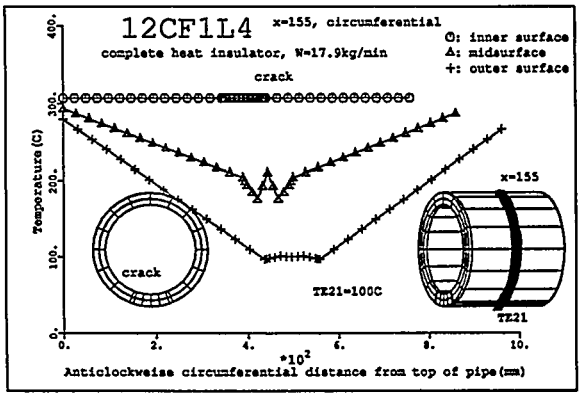

(a) longitudinal direction from crack surface (b) circumgferential direction from top

Figure4 input nodal temperature of 12CF1-L3 and 12CF1-L4

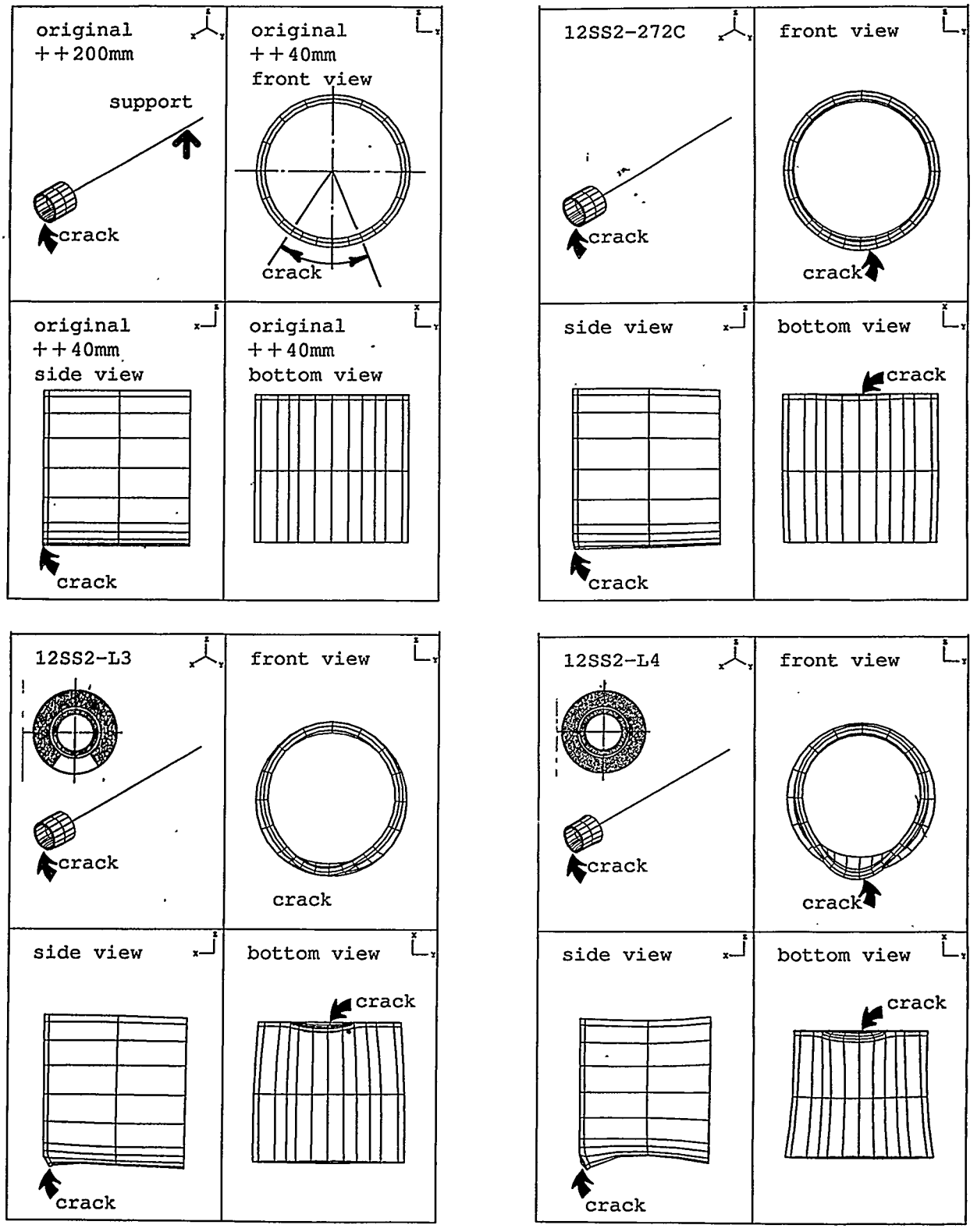

Figure5 deformation near crack of 12SS2 piping

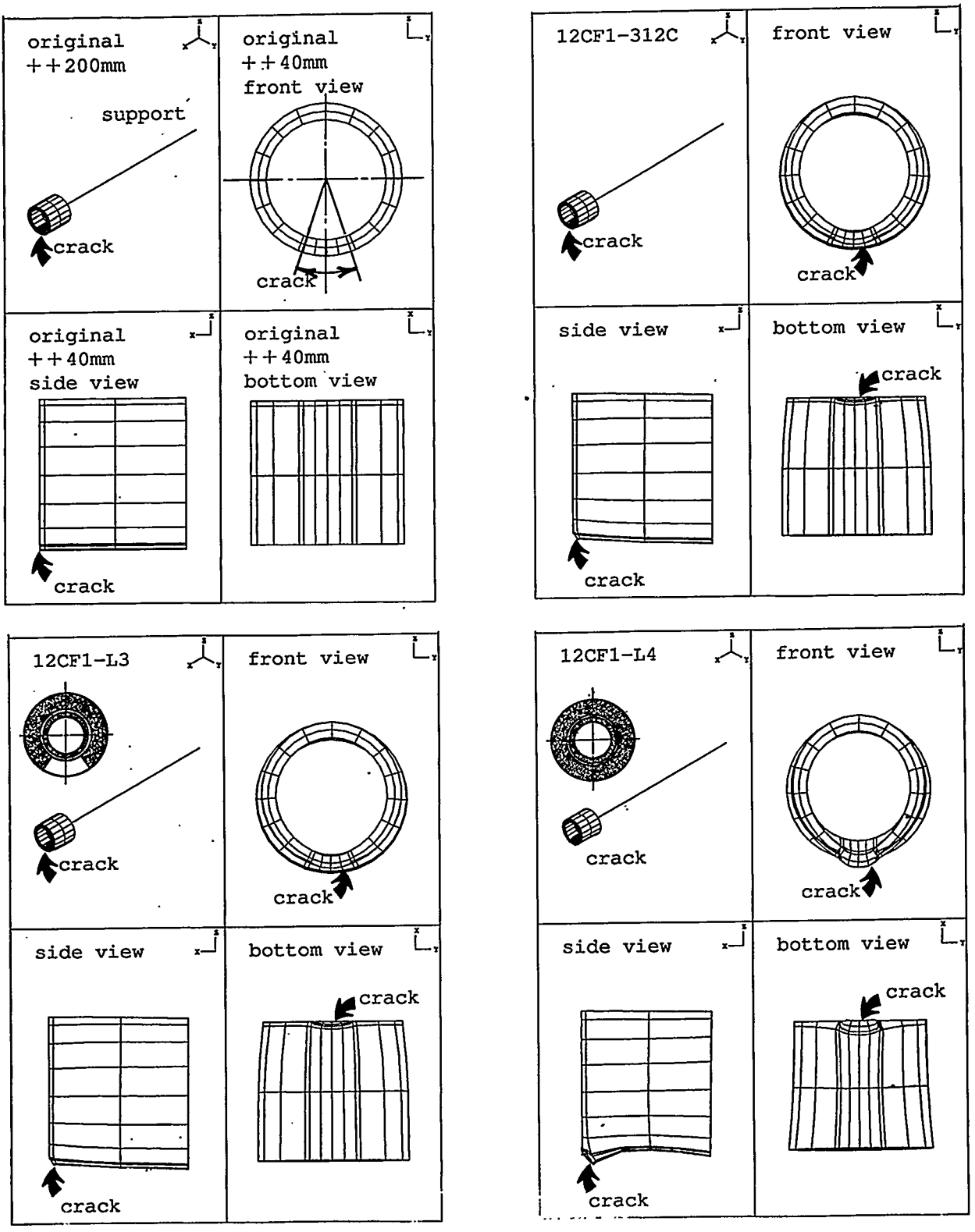

Figure6 deformation near crack of 12CF1 piping

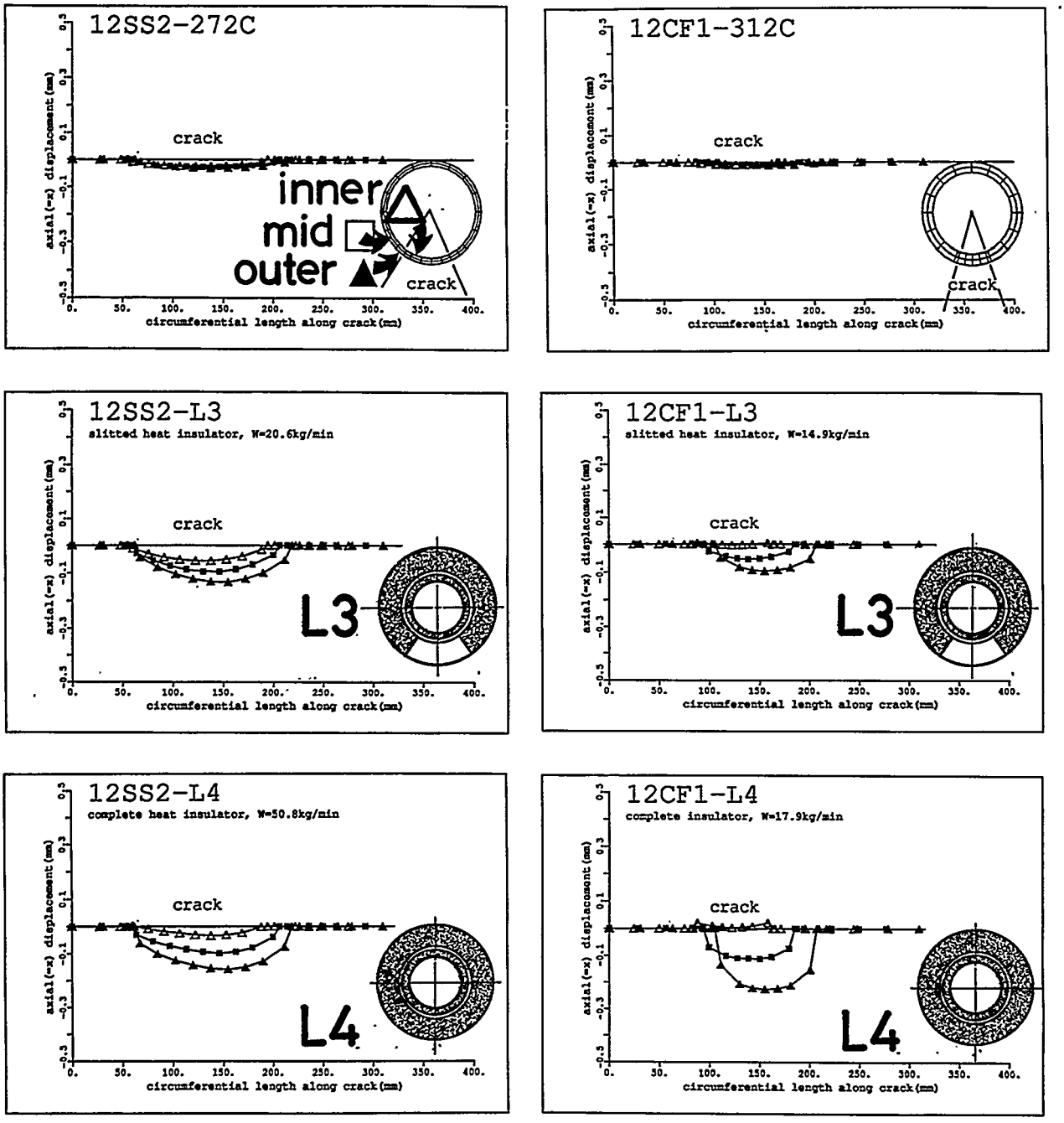

Figure7 COD distribution along inner-, mid- and outer-surface of crack

Table 3 shows the comparison of experimental(at 20℃!!) and computed COD for reference. They are relatively in good agreements and COD is the order of $10x10^{-3}$ mm while those by ADINA are $100x10^{-3}$ mm for the L3 and L4 experiments.

Table 3 Comparison of experimental and computed COD

water temperature was 20℃ in the experiment.

test pipe ident.	pressure (MPa)	jack load (kN)	COD(mm) experimental	computed
4SS1	6.9	0	$27x10^{-3}$	$10x10^{-3}$
6CS1	2.5	0	$7x10^{-3}$	$8x10^{-3}$
	0.1	9.8	$14x10^{-3}$	$14x10^{-3}$
12SS2	6.9	0	$53x10^{-3}$	$24x10^{-3}$
12CF1	15.8	0	$20x10^{-3}$	$12x10^{-3}$

6. Conclusion

It is pointed out that leak rate is very susceptible to the metal temperature of piping, since the COA or COD are sensitive to the temperature distribution of the piping. In the leak rate test, therefore, it is recommended that the distribution of metal temperature be measured precisely and widely. In the real piping system the leak will be larger than in the case where these thermal effect is neglected because leak rates are getting larger than those in the case of neglecting the influence of the thermal stress, which may be favorable from the standpoint of LBB of the real plants.
However, it remains still to be resolved that there may be a crack closure by the axial compressive stress(about 200MPa) at the bottom inner wall of the pipe, which may bring about the decrease in COD and leak rate and also that there may be some influence of the axial tensile stress(about 300MPa) at the outer surface of the pipe upon the crack opening, which may cause the fracture of the pipe.

References

[1] T. Isozaki, K. Shibata, H. Shinokawa, et al., Measurement of Leak-rate through fatigue-cracks in pipes under four-point bending and BWR conditions, Int. J. Pres. Ves. & Piping 43(1990)399-411.
[2] K. Shibata, T. Isozaki, S. Ueda, R. Kurihara, et al. , Results of reliability test program on light water reactor piping, Nucl. Eng. Des. 153(1994)71-86.
[3] H. Grebner, A. Höfler and H. Schulz, Report on Round Robin Activities on the Calculation of Crack Opening Behaviour and Leak Rates for small Bore Piping Componenst, GRS NEA/CSNI/R(95), March 1995.
[4] ADINA R&D, Inc., ARD 92- 4, ADINA-in for ADINA, Dec. (1992).
[5] Technical standards of the Nuclear Power Plants(in Japanese), Denryoku-sinpou-sya, 1989.

EXPERIENCES WITH LEAK RATE CALCULATION METHODS FOR LBB APPLICATION

H. Grebner, W. Kastner*, A. Höfler, G. Maussner*,
Gesellschaft für Anlagen- und Reaktorsicherheit (GRS) mbH, Köln
*Siemens/KWU, Erlangen

INTRODUCTION

For the application of LBB it must be safeguarded that a possible leak in the primary circuit or connected piping is detected early enough to prevent further or rapid crack growth. To find reliable requirements for the leak detection system installed an accurate calculation method of the leak rates of possible through wall cracks is necessary.

A benchmark test on crack opening and leak rate calculation recently performed [1,2] has shown a large scatter of the results, especially if the crack opening is also calculated. Furthermore, in real cases there is often only limited information on crack shape or crack surface topography. Thus further uncertainties are introduced in the evaluations.

In this paper three leak rate programs are described and compared by calculations of a HDR-experiment and two real crack cases.

METHODS OF LEAK RATE CALCULATION

Models for the estimation of the fluid flow through a crack have been investigated since about 30 years. Many programs used nowadays are based on the homogeneous model or on proposals by Moody [3] or Henry [4], published in the years 1965 and 1970, respectively. These models are developed especially for two-phase flow cases and are used also in the programs considered in this paper.

These programs are
- PIPELEAK, developed by GRS [5],
- FLORA, developed by Siemens/KWU [6]
  and
- PICEP, developed by EPRI [7].

The main features of the programs are summarized in Table 1.

Table 1: Features of the leak rate programs considered

Institution	Name	Basic Model	Range of Application
GRS	PIPELEAK	Pana [8]*	at present only initially subcooled fluid
		Henry*	initially subcooled or saturated fluid
Siemens/KWU	FLORA	Pana	all fluid states in NPP
EPRI	PICEP	Henry	initially subcooled or saturated fluid

*Model can be chosen by user.

The PIPELEAK-program consists of two main parts. One may be used for the evaluation of leakage areas by means of analytical solutions or on the basis of finite element calculations [5, 9, 10]. The second part performs the leak rate calculation. As table 1 indicates two different leak rate models according to proposals by Pana [8] or Henry [4] are available. The Pana model is described in combination with FLORA later on. Besides the differences in the theoretical derivations the Henry model as used in PIPELEAK and PICEP has the capability to include deviations of a straight crack path in the form of 90°- or 45°- kinks. This is modelled by an increase of the wall thickness to hydraulic diameter ratio t/d_h by the equation:

$$(t/d_h)_{mod} = (t/d_h) + 50\ N_1 + 26\ N_2 \qquad (1)$$

N_1 and N_2 are the numbers of 90°- and 45°- kinks, respectively. This feature is of special interest in the case of stress corrosion cracks.

The FLORA (Flow Rate)-program has no possibility to evaluate leakage areas. For this purpose separate programs are available at Siemens/KWU [11-13]. The main advantage of the Pana approach as completely used in the FLORA-program is that it connects correlations for three different fluid conditions, i.e. discharge of single-phase water, two-phase steam/water mixture and single-phase steam.

With respect to this
- for the discharge of cold water the Bernoulli equation
- for the discharge of subcooled water a modification of the Bernoulli equation
- for the discharge of saturated water and two-phase steam/water mixtures the homogeous equilibrium model, modified for a flow affected by friction or the model proposed by Moody [3] and
- for the discharge of saturated and superheated steam the gas theory, modified for a flow affected by friction

were selected and linked together. This method of calculation of flow discharge under steady-state condition has two noteworthy advantages over most of the other models to be found in the literature:
- the calculation procedure enables discharge rates to be determined over the entire thermodynamic range, i.e. for cold, hot and saturated water, water/steam mixtures, saturated and superheated steam
- it is easy-to-handle, i.e. as input parameters only stagnation conditions (pressure p, temperature T or steam quality x) and the hydraulic resistance coefficient ζ of the discharge opening geometry have to be known.

In most cases the fluid stagnation conditions are given. The hydraulic resistance coefficient can be determined using the equation:

$$\zeta = \zeta_{in} + \lambda \frac{t}{d_h} \qquad (2)$$

with

ζ_{in} = coefficient for sharp-edged entrance

t = length of the flow path, e.g. wall thickness of the cracked pipe

d_h = hydraulic diameter of the discharge opening ($d_h = 4\ A_L/P_L$ with A_L as leakage area and P_L as perimeter of the discharge opening. The determination of the leakage geometry is described in detail in [11 - 13]).

The friction factor λ can be calculated with a set of correlations which are based on extensive investigations of Siemens/KWU and KFK [14]:

$$\lambda = [2 \log (d_h/K) + 1.19]^{-2} \quad \text{for } 5\ \mu m \leq K \leq 50\ \mu m \qquad (3)$$

$$\lambda = [3.39 \log (d_h/K) - 0.866]^{-2} \quad \text{for } 50\ \mu m < K, \qquad (4)$$

where K is the surface roughness.

With these equations derived from an amount of ca. 600 experiments no further adaption of the leakage rate calculation procedure is necessary.

As PIPELEAK the PICEP-program again has capabilities for the evaluation of leakage areas. Details of the PICEP-program can be taken from [7].

TEST CASES

The models described before were applied to several test cases. As first one a straight pipe experiment from the leak rate tests performed in the HDR project [9] was chosen. The test under consideration (E22.05) was also part of the bench mark test mentioned before. The pipe with an outer diameter of 88.9 mm and 5.6 mm wall thickness had a circumferential crack with 130 degrees at the outside. The pipe was made of austenitic steel (1.4571) and loaded by internal pressure (10.5 MPa) and a stepwise changed bending moment (up to 3 kNm).

The other test cases are presented in Table 2. From the 5 real cracks shown in the table only the first two are used in the calculations. The other cases show the most common behaviour of very small leakages. From theory it is obvious that the models do not lead to accurate results in such cases.

GEOMETRIC CHARACTERISTICS OF REAL CRACKS

In order to verify the calculation model on the base of realistic data, the geometric characteristics of the leakage path were measured by metallographic and fractographic examinations for selected real leakage failures in nuclear power plants.

Evaluation of the geometric characteristics of real leakage paths

To obtain numerical data for the description of the geometrical characteristics of real leakage paths e.g. formed by cracking with different failure mechanisms, a quantitative analysis of metallographic or fractographic micrographs was performed with respect to the microscopic roughness and the length of the crack path through the wall, the macroscopic dimensions and shape of the crack contour, and the crack opening displacement under no-load conditions.

Table 2: Examples of failures in NPPs

Parameter	Symb.	Unit	Case				
Number	-	-	1	2	3	4	5
Line	-	-	volume control	seal water	sampling	feed water	minimum flow
Component	-	-	tee/bend	pipe	bend	pipe	45° bend
Outer diameter	D_a	mm	60,3	(33,7**) 37,7	21,4	626	88,9
Wall thickness	t	mm	6,3	(4**); 4,33	2,0	(18**); 20,33	(3,2**); 2,0
Material	-	-	1.4541	1.4550	1.4550	15 NiCuMoNb 5	St 35.8
Pressure	p	bar	155	159	159	70	13**
Temperature	T	°C	260 - 270	40 - 70	≤ 298	ca. 215	(200**); 30
Failure mechanism	-	-	fatigue cracking	fatigue cracking	chloride induced transgranular stress corrosion cracking	environmentally assisted cracking	environmentally assisted cracking
Rel. length (leak path)	l/t	-	1.174	1.004	1.080	1.011	1.060
Crack shape	-	-	semi-elliptical	circumferential with radial boundaries	semi-elliptical	maple leaf	semi-elliptical
Crack length, inside	$2c_i$	mm	46	40	2,0	9	40
Crack length, mean	$2c_m$	mm	40	36	7,5	16	10
Crack length, outside	$2c_a$	mm	20	34	8,2	2	4
Crack width, inside*	COD_i	mm	0,2 - 0,3	< 0,05***	- ≤ 0,01	0,015	1,04
Crack width, mean*	COD_m	mm	ca. 0,3	0,05***	0,01	0,020	0,06
Crack width, outside*	COD_a	mm	ca. 0,3	0,01	0,085	0,015	0,02
Roughness, mean	R_a	µm	10,3	2,3	5,1	9,5	21
Roughness, max.	R_t	µm	63,9	10,6	29,4	44,2	133
Roughness, average	R_z	µm	39,6	7,6	21,3	37,7	70
Vol. leakage rate	$\dot{V}$	l/h	3000 - 4000	478	ca. 0,05 (12 droplets per Min.)	0,05 - 0,10 (10-20 droplets per Min.)	ca. 0,008 (2 droplets per Min.)

* Without load ** Design values *** Estimated dimensions

As real cracks oftenly do not run perpendicular through the wall, a semiautomatic image analysis system was used to measure the length of the shortest leakage path through the wall in a metallographic section. The result is expressed in terms of l/t-ratio, where l corresponds to the length of the leakage path and t to the wall thickness.

For the evaluation of the microscopic roughness, the crack path was digitized in x/y coordinates with the x-direction corresponding to the direction of cracking and the y-direction perpendicular to x and the crack surface.

The macroscopic curvature of the crack, which is expressed by the l/t ratio, was linearized and omitted. Depending on the magnification of the photomicrograph, the method is sensitive in the roughness range from 10 to about 500 m. The numerical description of the roughness of the leakage path was performed by the use of the parameters R_a (mean roughness), R_t (maximal peak values), and R_z (floating average).

Considered cases of leakage failure

Due to safe design and intensive non-destructive testing activities, only few cases of through-wall cracking failures causing leakage in nuclear power plant systems have occured in the past. From the Siemens SDM-data base, which collects failure data of nuclear power systems, five cases which are characteristic for the most frequent occuring failure mechanisms were choosen, see Table 2. Two cases led to significant leakage rates, three cases resulted in the discharge of only droplets. The first two cases used for the calculations are described in brief as follows:

Case 1: High cycle fatigue in an austenitic tube (material: 1.4541). The crack originates in longitudinal direction at the inner surface, and is oriented slightly bowed in axial direction. Due to (unexpected) additional torsional stresses the crack propagation through the wall is considerably bowed, as can be seen from a cut through the wall just near the penetration, see Figure 1. Details of the crack surface topography are shown in Figs. 2 and 3.

Case 2: High cycle fatique crack in a small diameter austenitic tube weld (1.4550). The crack originates at the inner surface along the root notch of a circumferential weld to a flange, Figure 4. The crack propagation through the wall is very straight and the cracking is oriented in circumferential direction. Details of the topography of this crack surface can be seen from Figs. 5 and 6.

The other cases shortly described in table 2 are environmentally assisted cracks with very small leak rates. Although such cracks are the most frequent ones in real cases, they cannot be treated accurately with the leak rate models.

RESULTS OF THE CALCULATIONS

Calculations were made using the programs FLORA and PIPELEAK with both model options. The Henry based models in the PIPELEAK and the PICEP program are very similar. It is thus expected that PICEP would deliver similar results as PIPELEAK option 2.

Results to the HDR-experiment

In this case calculations with FLORA and with PIPELEAK option 2 were performed using a crack surface roughness of 10 μm in both evaluations. While in the Siemens/KWU analysis the COD-values were calculated, in the GRS case the experimental COD-values were used. Fig. 7 shows the results together with measured leak rates. A good agreement is found in this case among the calculations and also in comparison to the experiment.

FLORA calculation results for the real crack case

For the cases 1 and 2 of table 2, which led to significant leakage rates first pre-calculations were performed. This means, that only assumptions as input were taken into account, which were usually chosen by Siemens/KWU and were not based on detailed information after intensive crack investigation in a laboratory:

Case			1	2
Crack length, outside	$2c_a$	mm	20	34
Roughness	K	µm	30	30

The post-calculation for case 1 was performed for a complex crack type taking into account the results of the intensive crack investigation, see table 2. For case 2 the measured values of the roughness R_z as K-values were also considered, see table 2.

The results of pre-calculation, measurement and post-calculation of the volumetric leakage flow for the case 1 and 2 are shown in the Figure 8. For the circumferential crack of case 2 pre-calculation and measurement agree well. Surprisingly, the roughness of the crack surface was very small, so the post-calculation result deviated from the leakage measurement to a higher degree. For case 1 only the knowledge concerning the complexity of the loading (internal pressure and torsion) and the crack parameter (crack opening by internal pressure plus remaining COD of about 0.3 mm) led to a calculation result, which was in the range of the measured leakage rate.

PIPELEAK calculation results for the real crack case

As before pre- and post-calculations were performed. For the pre-calculations a crack surface roughness of 10 µm was assumed, according to experiences from other calculations. Furthermore, only the leakage area caused by internal pressure was considered. As Figure 9 shows this leads to a strong underestimation of the leak rate for case 1 and also a reasonable coincidence for case 2.

For the post-calculations the results of the crack investigation given in table 2 were also taken into account. For case 1 an additional leakage area due to the remaining COD of about 0.3 mm was superposed to the crack opening caused by internal pressure. For case 2 also the small roughness value R_z was considered.

The agreement with the measured values is significantly improved in the post-calculations for case 1. For case 2 the smaller roughness leads to a slight overestimation for the Pana model option. Generally the results with the Henry model are smaller than those gained by use of the Pana model.

In comparison with the FLORA results a satisfying agreement can be stated. The differences in the case 1 pre-calculation result clearly from the different leakage area assumptions.

SUMMARY

Different leak rate programs developed at GRS and Siemens/KWU have been used to evaluate leak rates for several test cases. While one case is a HDR leak rate experiment, the other test cases are real crack events. Two of these have relatively large leak rates, the others show the most common behaviour of very small leakages (only some droplets per minute). For such cases the leak rate models presently available are not applicable, because their lower limit assessed by experiments lies in the range of 0.01 kg/s or 30 l/h, respectively.

The real cracks were investigated in detail with respect to the geometric characteristics of the crack paths and the microscopic roughness. As the calculations showed a detailed information on the crack topography and also the load situation is necessary to gain realistic estimates of the leak rate.

While to the HDR-experiment only post-calculations were performed, the real crack cases were treated by pre- and post-calculations. Here pre-calculation means that only the commonly available information is used, whereas in the post-calculation also the results of the detailed investigation were applied.

Generally the different leak rate models give results which agree satisfactory. To get a reasonable agreement of measured and calculated leak rates, it is necessary to use also the information of the detailed crack investigations.

REFERENCES

[1] H. Grebner; SMIRT-12, Vol. F., 105-110, 1993

[2] H. Grebner; Int. J. Pres. Ves. & Piping 61 (1995) 35-39

[3] F.J. Moody; J. Heat Transfer 87 (1965) 134-142

[4] R.E. Henry; Nucl. Sci. & Engng. 41 (1970) 336-342

[5] PIPELEAK - A personal computer program for the evaluation of leakage areas and leak rates; GRS-report, 1995

[6] FLORA - Program for leak rate calculation; Siemens/KWU

[7] PICEP - Pipe crack evaluation program; EPRI NP - 3596 - SR, 1987

[8] P. Pana, M. Müller; Nucl. Engng. & Design 45 (1978) 117-125

[9] H. Grebner, A. Höfler, H. Hunger; Nucl. Engng. & Design 144 (1993) 101-109

[10] H. Grebner, A. Höfler, H. Hunger; 20. MPA-Seminar, Vol. 2, paper 47, 1994

[11] G. Bartholomé, W. Kastner, E. Keim, G. Senski; SMIRT-12, Vol. G, 87-92, 1993

[12] G. Bartholomé, W. Kastner, E. Keim; Nucl. Engng. & Design 142 (1993) 1-13

[13] E. Keim; LBB '95, paper no. 24, Lyon, Oct. 9-11, 1995

[14] V. Kefer, W. Kastner, F. Westphal, H. John, J. Reimann, L. Friedel; DECHEMA-Monographies, Vol. 111 (1988) 123-148

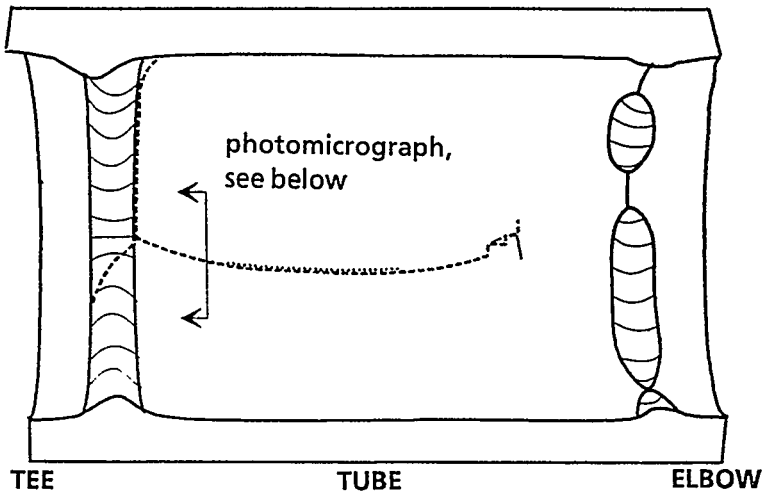

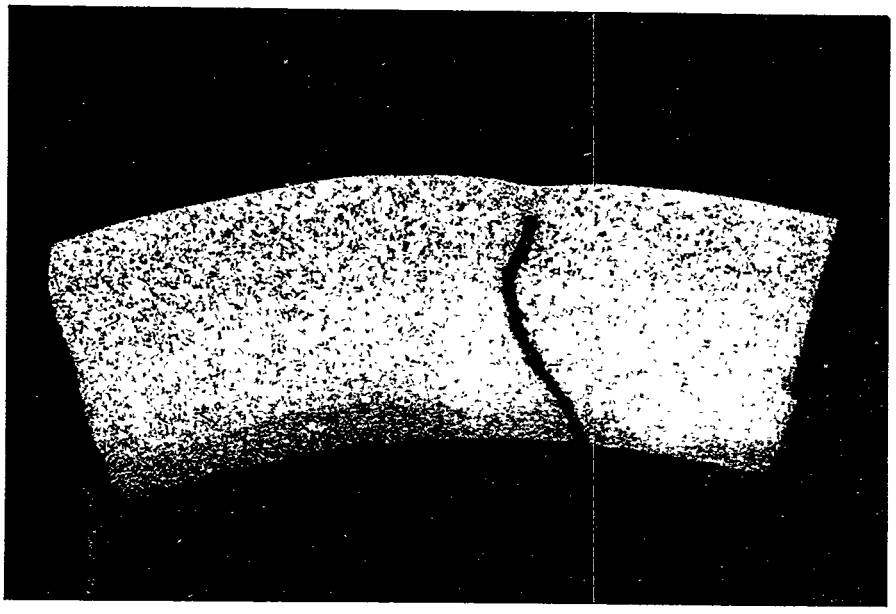

Fig. 1: Real crack case 1, fatigue crack in longitudinal direction, crack path

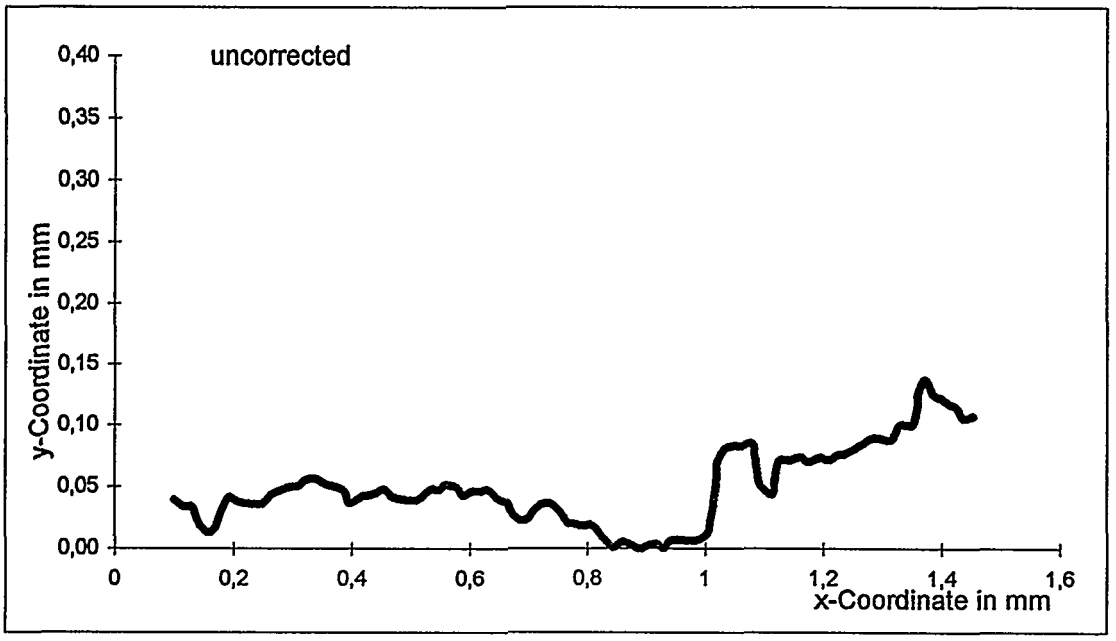

Fig. 2: Real crack case 1, crack surface profile of the leakage path, uncorrected

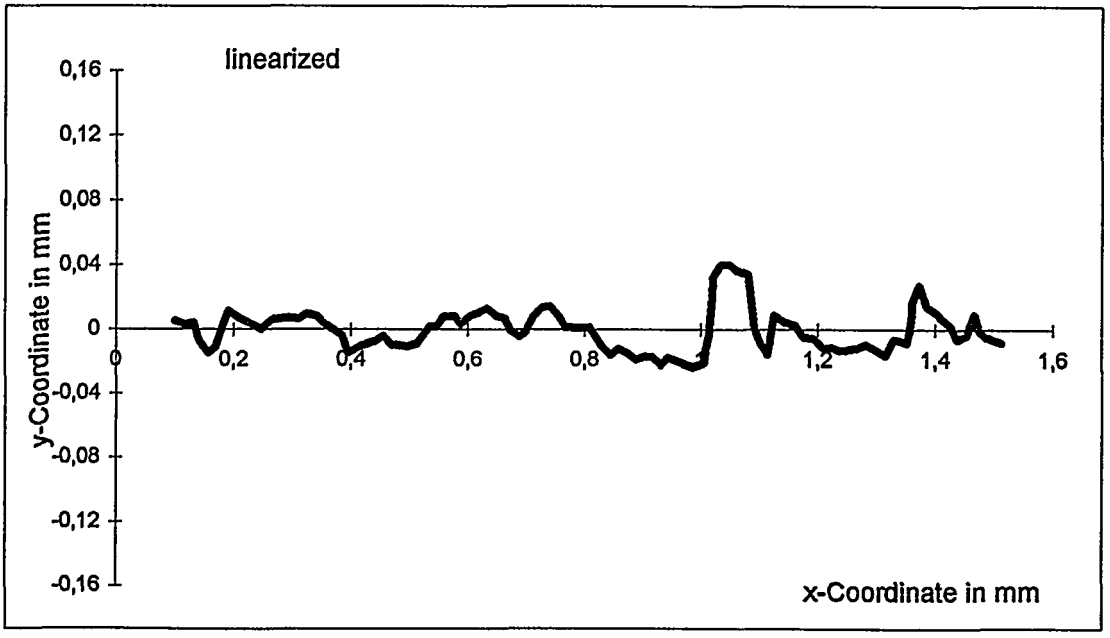

Fig. 3: Real crack case 1, crack surface profile of the leakage path, linearized

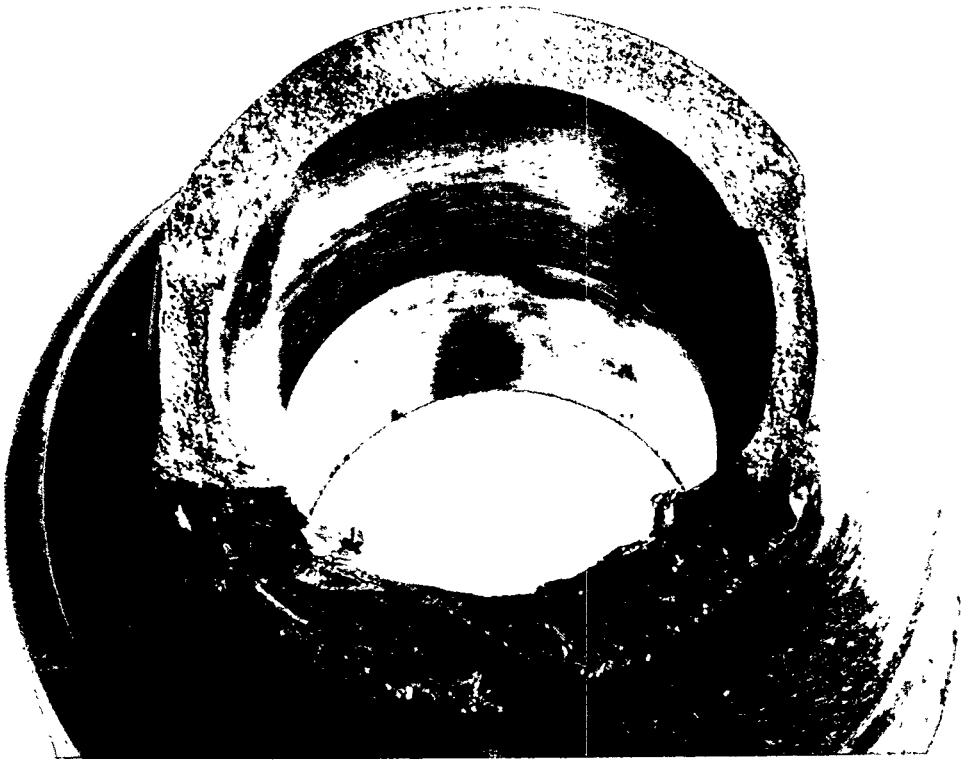

Fig. 4: Real crack case 2, fatigue crack in circumferential direction

ca. 5 mm 2,5:1

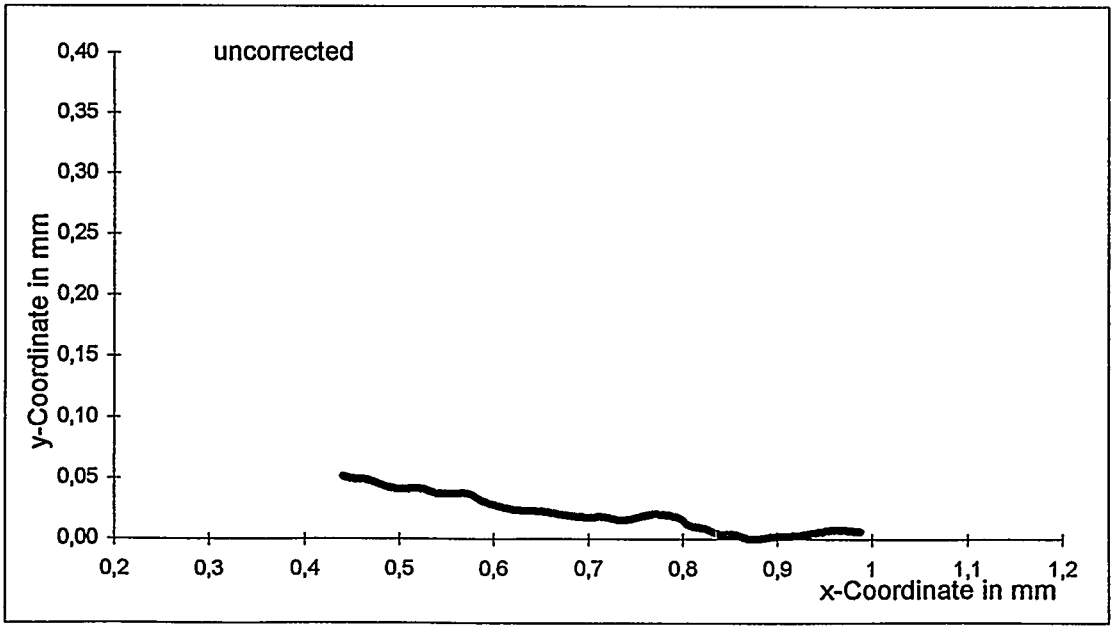

Fig. 5: Real crack case 2, crack surface profile of the leakage path, uncorrected

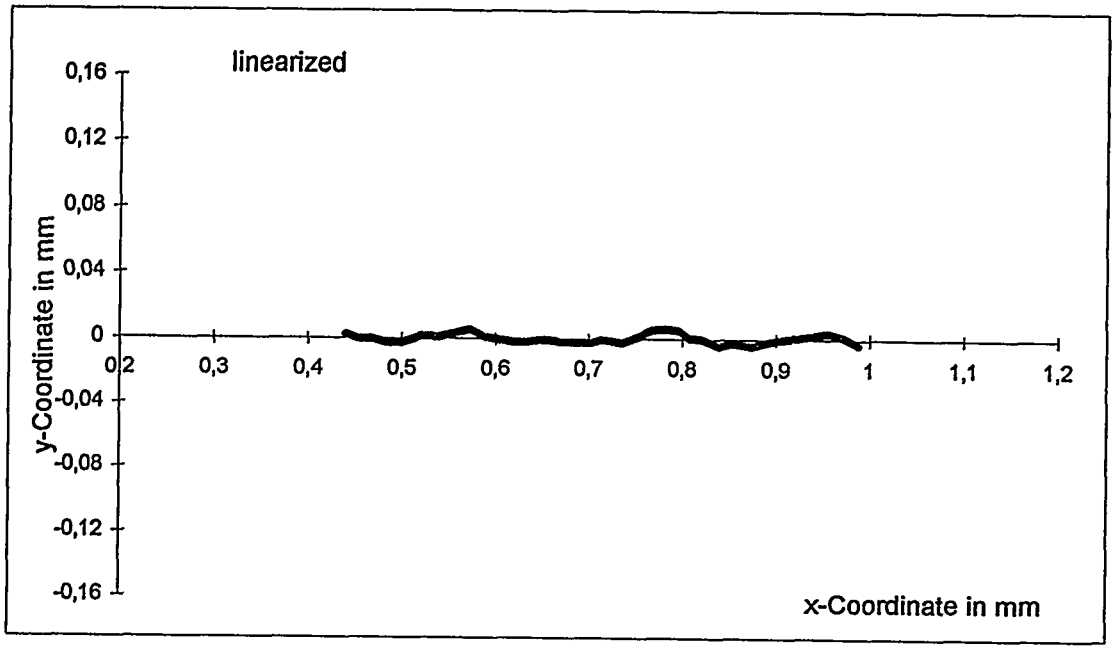

Fig. 6: Real crack case 2, crack surface profile of the leakage path, linearized

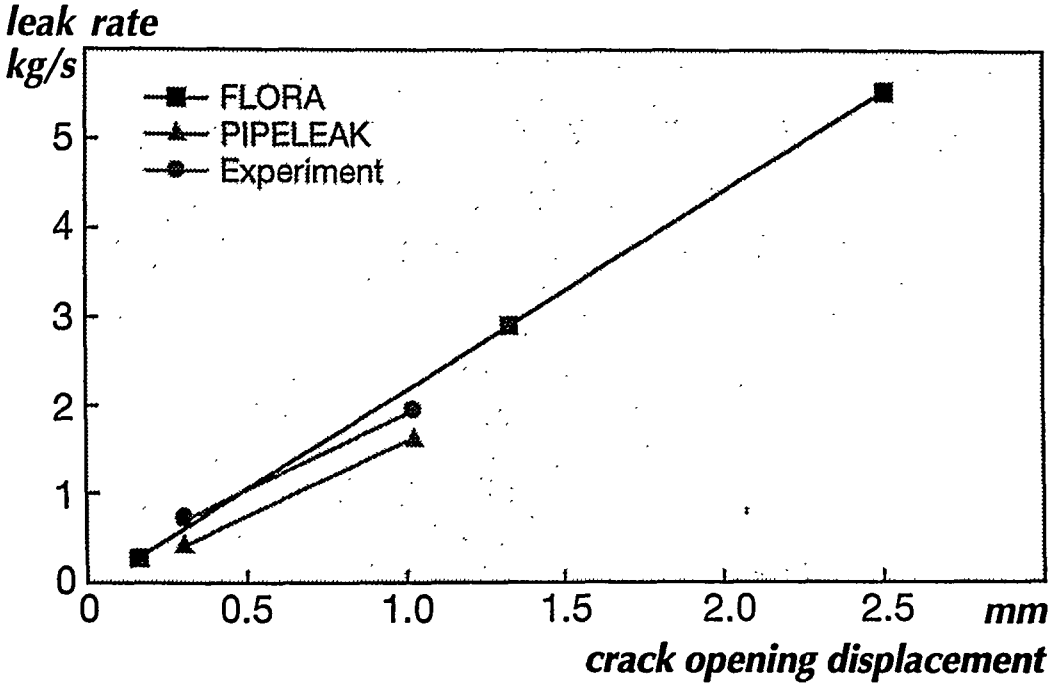

Fig. 7: HDR experiment E22.05, measured and calculated leak rate as function of COD

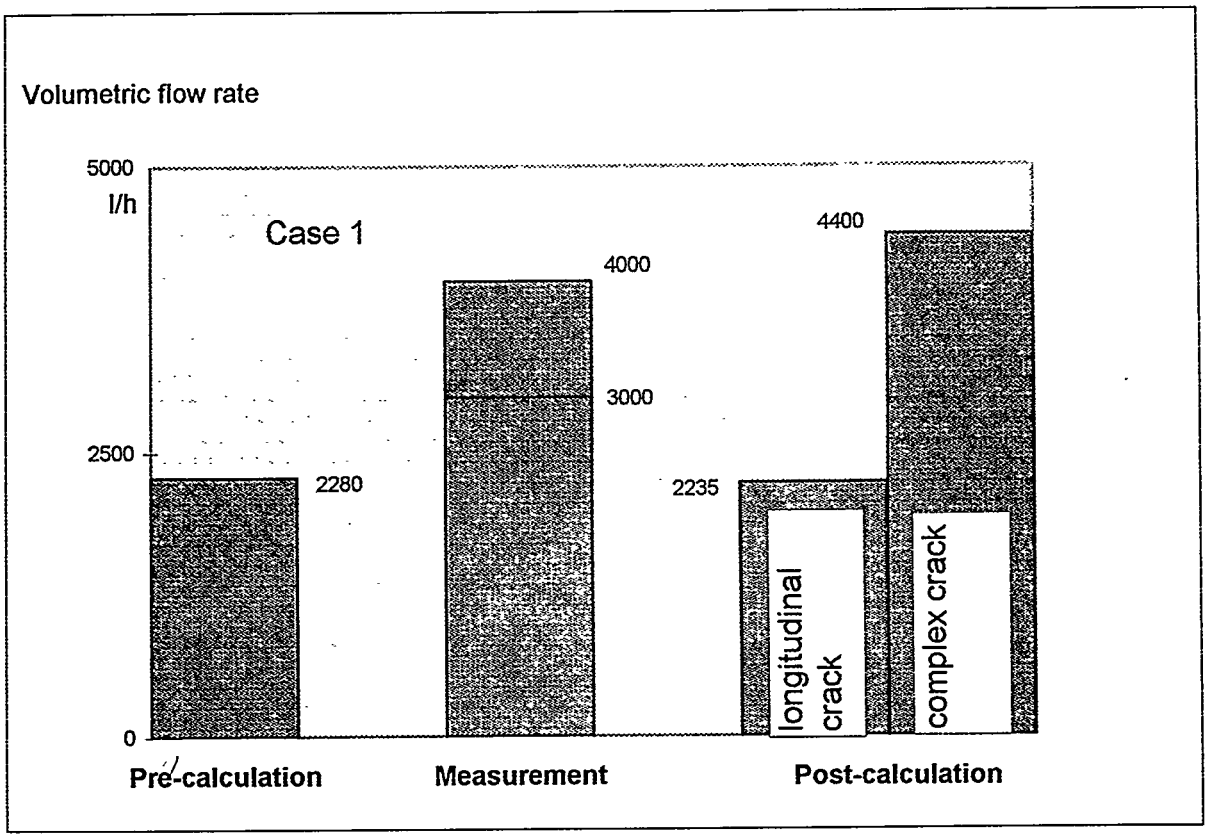

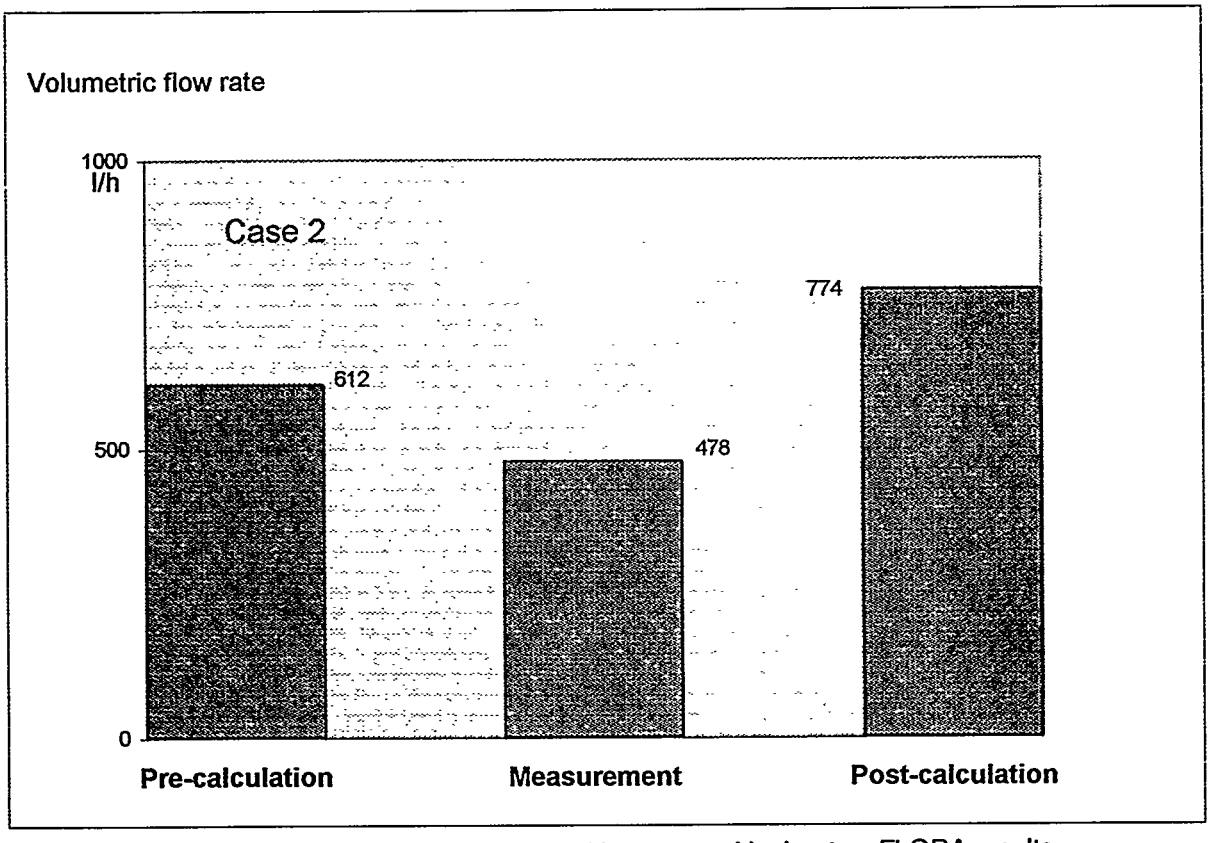

Fig. 8: Comparison of pre- and post-calculations with measured leak rates, FLORA results

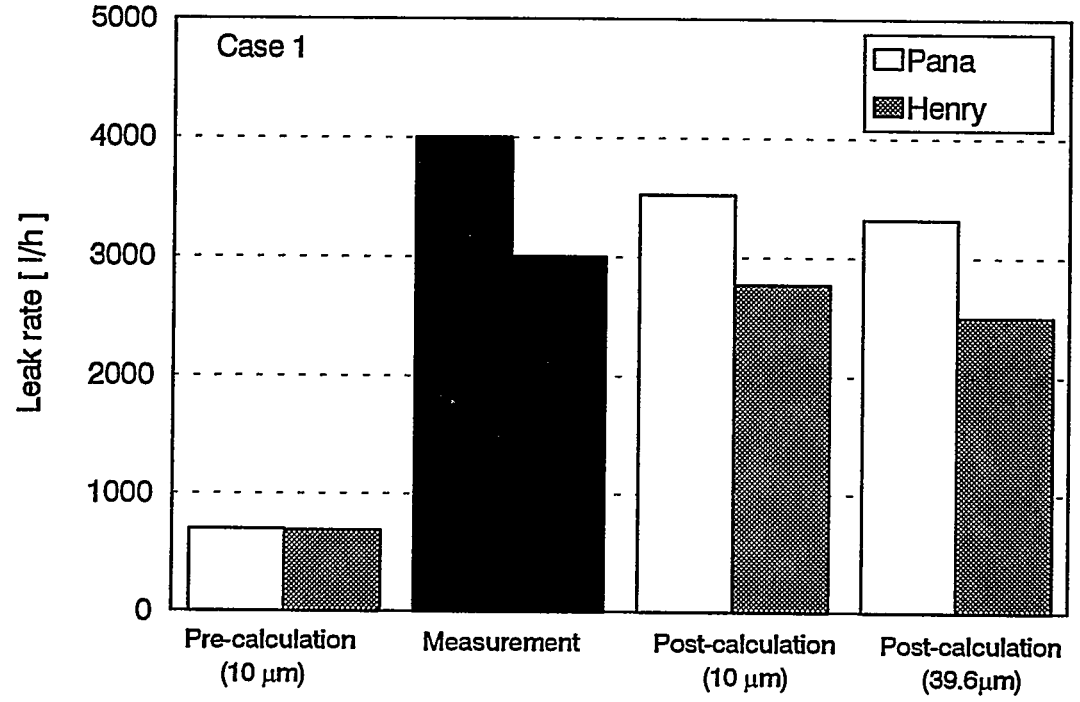

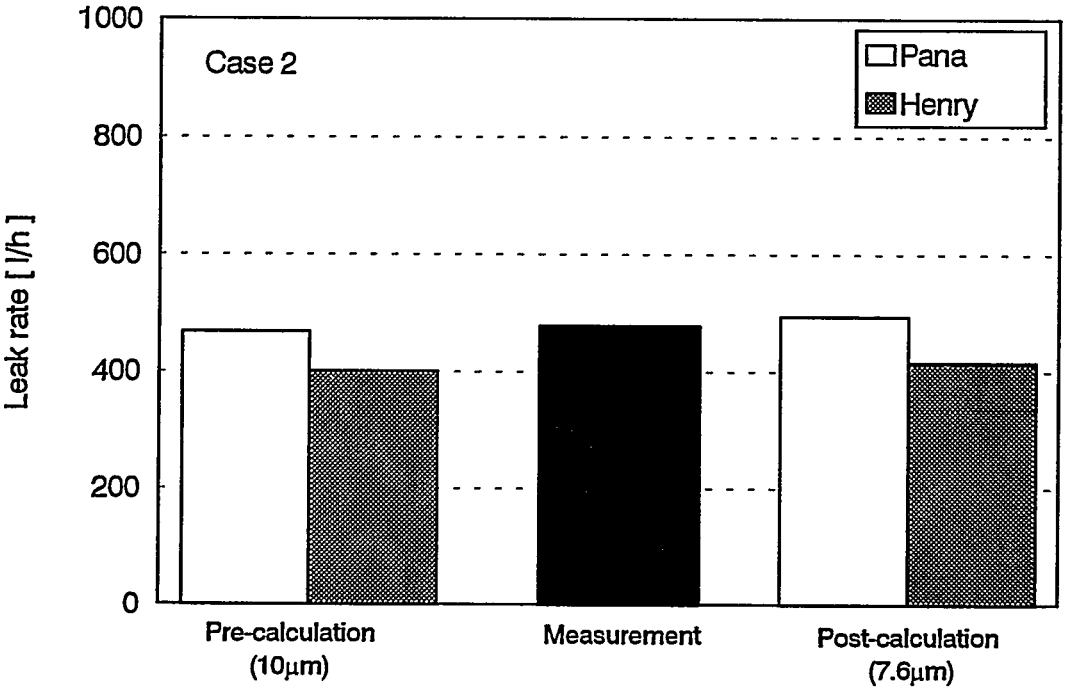

Fig. 9: Comparison of PIPELEAK results with measured leak rates

ASSESSMENTS OF FLUID FRICTION FACTORS FOR USE IN LEAK RATE CALCULATIONS

T C CHIVERS Nuclear Electric plc: Berkeley Technology Centre, Berkeley, Glos; UK

ABSTRACT. Leak before Break procedures require estimates of leakage, and these in turn need fluid friction to be assessed. In this paper available data on flow rates through idealized and real crack geometries are reviewed in terms of a single friction factor λ. It is shown that for $\lambda < 1$ flow rates can be bounded using correlations in terms of surface R_a values. For $\lambda > 1$ the database is less precise, but $\lambda \approx 4$ is an upper bound, hence in this region flow calculations can be assessed using $1 < \lambda < 4$.

1. INTRODUCTION

The production of a satisfactory Leak before Break (L-b-B) safety case involves a number of steps and calculations. These involve various aspects of structural assessment to derive through wall crack lengths and openings. The final stages involve estimates of likely flow rates and whether or not the leakage can be detected.

Leakage rate is governed by a number of parameters, and in simple terms can be expressed as:

$$Q_m = f(G,F_p,\Delta P,\lambda)$$

where Q_m is the mass flow rate; G represents the geometric description of the crack of width w, length L, and depth D (usually the through wall thickness, t); F_p represents fluid properties including the way that they vary with temperature and pressure, P; ΔP is the pressure drop across the flow path; and λ is a friction coefficient [Note that 'f' is normally used in the UK, and λ equals 4f]. Thus to calculate flow rates requires an estimate of the crack geometry, a relevant thermo-hydraulic model, and an assessment of fluid friction. This paper addresses issues related to the determination of λ for use in L-b-B calculations.

All fluid mechanics text books include a section on friction in pipe flows, and sometimes other geometries. The presentation is usually in terms of λ versus Reynolds Number (Re). At low Re flow is laminar, λ is relatively high and is assumed independent of roughness effects. As Re increases λ reduces until turbulence starts to develop when λ may increase to a maximum in a transition regime. As Re further increases λ reduces until it reaches a constant value independent of Re: this is the fully rough regime. The value of λ in this regime depends on the relative surface roughness. This classic behaviour is well established for pipe flows, and the concepts have been adopted in assessing flow through crack like defects. The behaviour of λ in this fully rough regime is discussed in this paper, but prior to this, aspects of surface roughness will be addressed.

2. THE ROLE OF R_a AS A SURFACE DESCRIPTOR

It is known that λ is influenced by the nature of the surface over which the fluid is flowing. One of the most commonly used descriptors of surface roughness is its R_a value, (a measure of the deviation of

the surface from its mean level) and it will be used frequently in the following discussion. However, R_a is not a unique surface descriptor; it is a measure of height distribution only, and only indirectly contains information on lateral variation. This latter arises as a consequence of waviness in the surface, thus R_a is a function of the length over which it is measured (usually R_a increases as traverse length increases), and also a function of any filtering in the measuring system. Thus surfaces with the same measured R_a value could have very different hydrodynamic characteristics, giving rise to different λ values.

In some of the work to be described R_a values were measured; in others different descriptions of the surfaces are given, and it is useful to consider approximate correlations. For a regular triangular array with peak to valley height, h, $R_a = h/4$. In the classic experiments of Nikuradse, (eg [1]) sand grains of "uniform" diameter, K_s, were adhered to the inside surface of pipes of radius R, If the effective surface is regarded as a close packed array of hemispheres then $R_a \approx K_s/8$. Crack surfaces will not conform to such simple models. However, if h is used to depict a maximum peak to valley height on a surface then, from [2]

$$4 \leq R_a/h \leq 9$$

Such relationships and observations will be used in the interpretation of data in the next section. However, it must be stressed that a single descriptor will never be adequate for characterizing a three dimensional surface, but given the uncertainties associated with the overall calculation of leakrate in a L-b-B context the use of R_a, alone, may be adequate for practical purposes.

3. HISTORICAL PERSPECTIVE

Historically the UK nuclear industries interest in estimating flow rates through defects has been concentrated on systems containing gases. In the early 1970's an isothermal model was derived using a single value treatment of fluid friction [3]. Isothermal assumptions were based on the premise that with small defects in relatively large structures, heat transfer rates would be high and temperature drops small: this was subsequently justified in experimental programmes ([4] and other unpublished work). However, it should be noted that calculated rates based on either isothermal or adiabatic assumptions are not significantly different in a L-b-B context. An artefact of the isothermal assumption is that Reynolds Number remains constant through the flow path permitting a simplified treatment of fluid friction.

A series of experiments was then conducted using rectangle slots and surfaces roughened by sand blasting. The data were analysed on the premise that the theory was correct, the geometry known, the only unknown being λ. In the full rough regime a simple correlation was found in terms of hydraulic radius (equal to w for a narrow crack) and surface roughness as measured by R_a; viz.

$$\lambda_D = \left[2.25 \log \frac{w}{R_a} - 0.573\right]^{-2} \qquad (1)$$

This equation is plotted in Figure 1, where it is compared with the classic work of Nikuradse (see e.g. [1]) represented as

$$\lambda_N = \left[2 \log \frac{R}{K_s} + 1.74\right]^{-2} \qquad (2)$$

A good correlation between the two sets of results arise if

$$\frac{K_s}{R_a} \sim 8 \text{ to } 10$$

and this accords very closely to the idealised relationship discussed in Section 2. The closeness between data from Nikuradse and that from crack geometry gives confidence in the use of equation 1 for assessing fluid friction. On the basis of this equation 1 was incorporated into the flowrate code DAFTCAT [5]. This programme requires an estimate of crack geometry, which comes from structural integrity assessments, knowledge of fluid properties and operating conditions and an estimate of surface roughness. Only roughness aspects will be considered further in this paper.

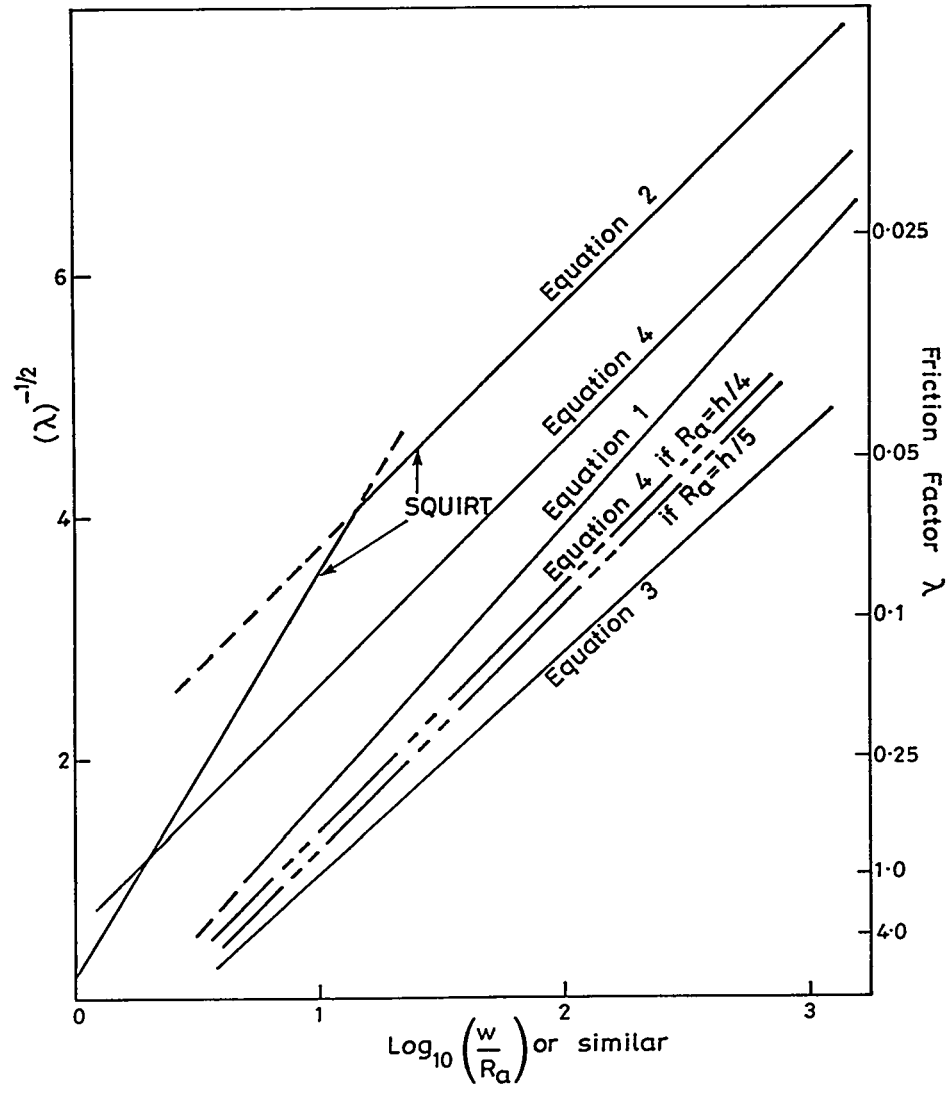

Figure 1. Variation of Friction Factor with (w/R_a), or similar, for various results.

4. SUBSEQUENT WORK WITH IDEALIZED CRACK GEOMETRIES

Other work has been conducted on idealized crack geometries since the work described above was published. A set of experiments using shot blasted surfaces of $R_a \approx 4\mu m$ was conducted using both rectangular and elliptic slot geometries [6]. A range of widths, w, was used and the friction factor correlation derived was

$$\lambda_A = \left[1.82 \log \frac{w}{R_a} - 0.77\right]^{-2} \qquad (3)$$

Reference [7] describes a set of experiments on some macroscopic artificial cracks. Here large scale roughness was used (~5mm) with crack face separation scaled to represent "typical" crack geometry. In these experiments conforming surfaces were used, ie the second face was a replica of the first, and the opposing surfaces could be closed completely together. Two surfaces were used, and face separation varied. Only in one case were fully rough conditions established and in these circumstances.

$$\lambda_G = \left[2.035 \log \frac{w}{h} + 0.568\right]^{-2} \qquad (4)$$

Equations (3) and (4) are also plotted in Figure 1. In addition equation (4) is replotted assuming (arbitrarily) that h ~ 4-5 R_a, as in the correlation between equations (1) and (2).

5. SUMMARY OF POSITION WITH IDEALIZED GEOMETRIES

Equations (1) to (4) give correlations between λ, the friction factor and the ratio of hydraulic radius to a roughness parameter. If it is assumed that h(or K_s)~4-5 R_a, then equations (1) and (2) become very close, and equation (4) plots between the lines from equations (2) and (3). See Figure 1.

6. VALIDITY LIMITS

No validity limits are indicated on the various lines in Figure 1, and a number of reasons exist for this. For example the data leading to equations (3) and (4) are based on single values of roughness. Experiments leading to equations (1) and (2) varied both Reynolds Number and roughness. However in the experiments leading to equation (1), λ did not exceed unity. The limits to extrapolation of these various curves will now be discussed.

6.1 LOWER BOUNDS

Extrapolation to low roughness, and/or large surface separation will lead to reduced fluid friction. However the experiments in ref [4], using smooth surfaces, shown that the classic lower bound curve derived by Blasius (See e.g. ref [1]) is not violated. Thus a lower bound can be given by:-

$$\lambda_B = 0.316\ Re^{-0.25} \qquad (5)$$

6.2 UPPER BOUNDS

The classic work of Nikuradse does not hint at the existence of an upper bound to λ, nor do the experiments reported in references [4] and [6]. However, in both sets of experiments reported in reference [7] using nesting macroscopic roughness (ie the surfaces could be closed completely together) it was shown that as separation reduced, λ did not continue to increase, as suggested by an extrapolation

of Figure 1, but reached a maximum as the roughness started to overlap. Two very different surfaces were used in these experiments. For one set of experiments $\lambda_{max} \approx 1$, and for the other approximately 4. The existence of a maximum, dependent upon geometry and Reynolds Number was supported by a simple theory. However, the correlation between the theory and the experimental results was not that good, but it was indicative that a maximum should exist.

7. DAFTCAT STRATEGY

DAFTCAT is a computer code for the calculation of flowrates through cracks. One of the required inputs is a value for R_a, which is then used, via equation (1), to calculate λ. R_a values can be determined from a pre-existing data base on surface roughness, and NE plc has such information for a range of crack types. Figure 1 can then be used to determine a range in R_a values that will cover the data spread between the curves for equations (1) and (3). The programme then proceeds to calculate an upper bound to flowrate based on λ_B, and a "best estimate" based on λ_D from equation (1). The former is used for assessing consequences (eg thermal or thrust effects); the latter for L-b-B purposes for determining detectability.

If $\lambda_D < \lambda_B$ then λ_D is set equal to λ_B and both calculated flow rates are the same.

If $\lambda_D > 1$ then the validation limits of the programme are exceeded and computation ceases and an alternative strategy has to be adopted by the user. This strategy is based on the choice, and input, of a specific value of λ. The choice of λ_{max} can be considered as a variable in a sensitivity analysis, but choice of too high a value can be a penalty. Currently it is advised that $\lambda_{max} \leq 4$.

To input effective values for $\lambda > 1$ requires the input parameters to be manipulated, but this is done in such a way as to permit a broad sensitivity study. The controlling parameter is:-

$$\frac{\lambda D}{W}$$

From equation (1), if λ=1 then R_a is w/5. This value for R_a is input together with a value for D which is scaled such that

$$D_{input} = D\lambda_r \qquad (6)$$

Where λ_r is the required value of λ(>1, <4).

8. DATA ON FLOW THROUGH REAL CRACKS

Information on flow through real cracks will now be reviewed against the modelling discussed above. It is, however, important to appreciate that for real cracks greater uncertainty will exist over geometric parameters than for idealized crack experiments. It is also evident that the reliable database on flow through real cracks is very limited as far as the ability to deduce friction factors is concerned. Good data on crack geometry is required, as also are accurate flow rate measurements. It is also important to ensure that the actual and assumed flow regimes coincide.

8.1 GAS FLOW THROUGH A CRACK IN A WELD

A through wall defect developed in a small bore (≈ 19mm diameter, 5mm wall thickness) steam pipe. The repair procedure was to cut out the leaking section, and to replace it. This meant that the damaged section could be examined.

The defective section was subjected to leakage tests [8] using a range of gasses and test pressures. In particular a number of repeat tests were conducted at a pressure of 4.2 MPa with helium as the test medium. The defect was examined non destructively, and then destructively. Crack face separation was assessed using a travelling microscopic. However, the defect was associated with a weld, and cap curvature confused measurements. Sectioning showed the crack length to be non uniform, as also was the flow path length (largely because of the welding process). The failure was at the weld parent-metal interface, and the opposing surfaces were conformal.

From the geometric measurements it was considered possible to bound the crack dimensions. The program DAFTCAT was then run using a range of dimensions and friction factors to calculate flow rates. These flowrates could then be compared with those measured. The resulting conclusion was that given the lack of precision in crack geometry, fluid friction could not be defined better than $2 < \lambda < 4$.

Surface roughness was measured as 16μm R_a, and the crack opening as some 100μm. Use of equations (1) and (3) would thus predict λ values of 0.8 and 2.0, somewhat lower than the inferred measurements. Using a mean measured value for λ of 3 would require a mean crack separation of 50 to 90μm. Thus the results would be compatible with a tapered crack geometry, but it was not possible to assess such a hypothesis. The result is also compatible with a conclusion that equations (1) and (3) underestimated fluid friction for this defect. However, it is entirely compatible with $1 < \lambda_{max} < 4$.

8.2 FATIGUE CRACKS IN WIDE PLATE TESTS

Reference [6] includes data on a fatigue crack grown in a large plate. [750mm wide; 69mm thick]. From a starter defect the crack was grown by fatigue cycling until penetration occurred. Leakage experiments were then conducted using air as the leaking fluid. A range of tests was conducted using different loading conditions and fluid pressures prior to additional fatigue cycling to promote crack growth and further leakage experiments. From the known geometry friction factors could be derived.

In many instances flow rates were very small, and flow laminar, and these results are ignored here for L-b-B assessment purposes. In other instances where the flow was turbulent, conditions where λ becomes independent of R_a were not achieved: those results, too, were ignored. This left very limited data where a plateau in the λ, Reynolds Number plot arose, and this at about the $\lambda \approx 1.2$ level. Based on a R_a value of some 20μm, reasonable agreement with equation 3 is obtained. It should be noted that R_a values are not quoted, but 20μm is not unreasonable for a fatigue crack. For the other data that were in the transitional regime, λ did not exceed 4.

In this instance the data conform both to a relationship close to equation (3) and to the premise, $\lambda_{max} < 4$.

Similar measurements were made in another wide plate test (unpublished). In this instance leakage was deduced as entirely within the transition regime and cannot be used to assess the friction factor relationships described above. However, although λ approached 4 in these tests, that value was not exceeded.

8.3 TWO PHASE FLOW THROUGH A FATIGUE CRACK

Reference [9] reports experimental data with a through wall crack in a pipe pressurized with hot water. On leaking there would be (generally) a phase change. Under these conditions Reynolds Number will not remain constant. However, if flow is in the fully rough regime then λ should remain essentially constant through the flow path, and analysis much as discussed previously can be followed. In this instance however, a thermo-hydraulic model that copes with two phase flow is required, and the code

SQUIRT [9] was used.

The Appendix to this paper discusses how SQUIRT can be used with specific values of λ, or to deduce values of λ to correspond to a measured flow rate.

SQUIRT calculations were performed assessing parallel cracks of width corresponding to the mean. The crack width was in fact tapered, with the largest width on the outside; but errors from this assumption will not be large.

Flowrates were calculated using the standard SQUIRT procedure with $R_a = 3\mu m$, and with $\lambda = 4$, and $\lambda = 1$. The results for $R_a = 3\mu m$ and $\lambda = 4$ are shown in Figure 2. This figure shows that the $R_a = 3\mu m$ data generally overestimates flowrate [$\lambda = 1$ results in larger flowrates than for $R_a = 3\mu m$], whereas $\lambda = 4$ gives a flowrate generally, lower than that measured: two points corresponded to λ values just in excess of 4. Thus these results show

$$1 < \lambda \leq 4$$

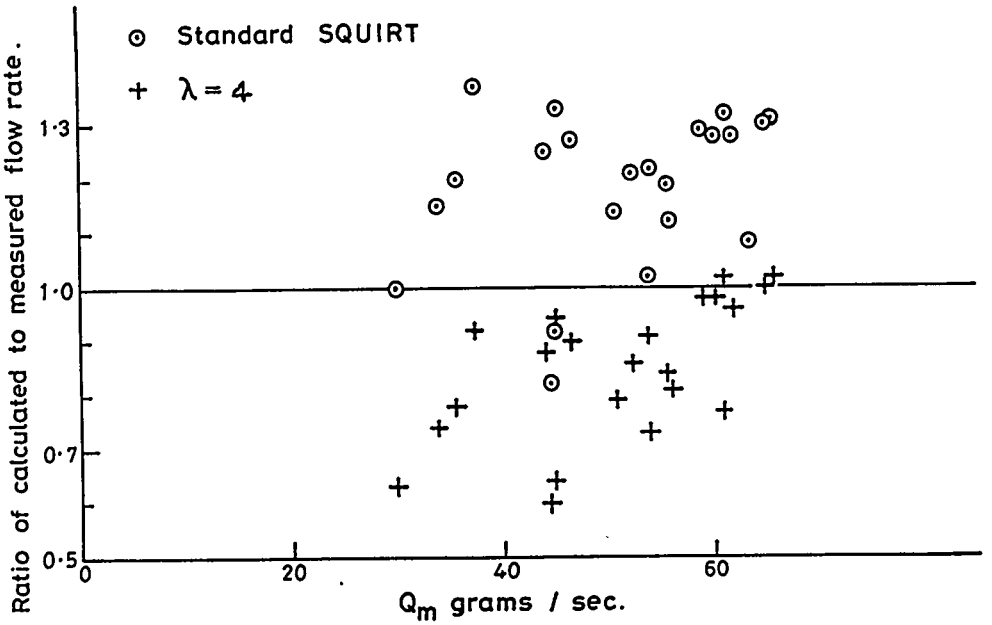

Figure 2. Flow ratio versus flow rate as determined from SQUIRT in standard format and with $\lambda = 4$.

Values of λ to fit the measured flowrates were also calculated. The simple wisdom would be to interrogate these values with Reynolds Number but these cannot be accurately determined since flow will not be at constant temperature or fluid phase. However, for constant geometry

$$R_e \propto \frac{Q_m}{\eta}$$

where η is the fluid viscosity. Thus a plot of λ versus Q_m will approximate to the form of a λ, Re plot, and this is shown in Figure 3. Clearly λ is not independent of Q_m (and hence Re). In terms of conventional wisdom it appears that the data might be in a transition regime as peaks, or apparent

peaks, are seen as Q_m increases. To obtain some feel for Re the data for the pressure extremes at the largest bending moments were assessed. This was done using the program DAFTCAT with the geometry as discussed above, and considering either water or steam as the leaking medium.

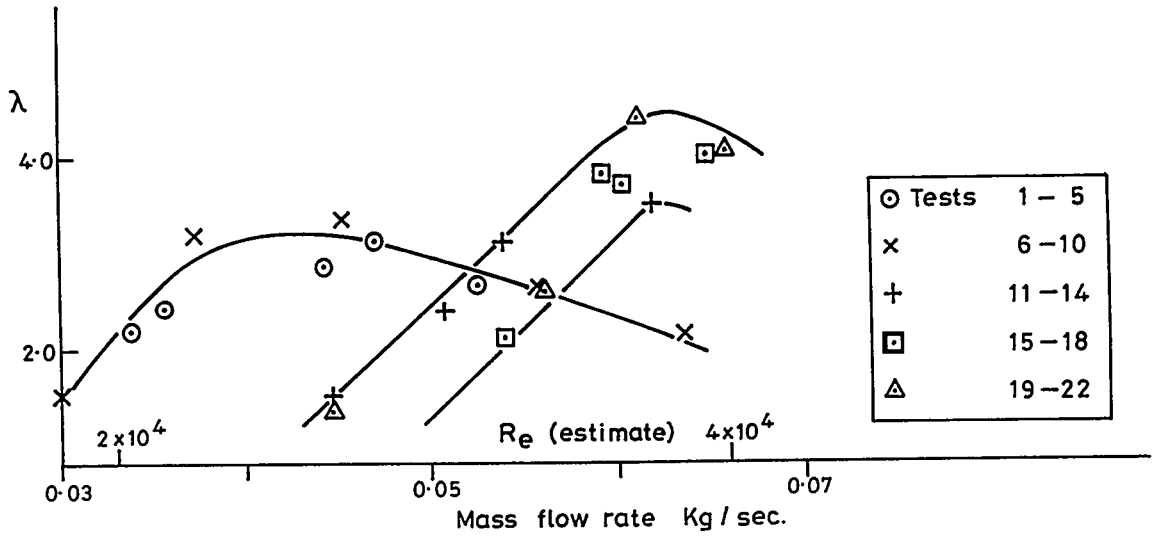

Figure 3. Variation of λ with flowrate (and approximate Reynolds Number) for two phase flow through a fatigue crack.

For water the relevant upstream pressures, density and viscosity were input and a mass flowrate and Reynolds Number calculated. The ratio between measured and calculated flowrates were then determined and Re scaled by the same ratio. For steam it was assumed that the appropriate upstream conditions would correspond to the saturation state, and the above process was repeated. For a specific example Re for water and steam were calculated as 4×10^4 and 2×10^5, respectively. If it is argued that transitional behaviour is likely to be controlled by the water phase, then the former number can be used to scale the Q_m axis in Figure 3, and this has been done. On this basis Figure 3 can be interpreted as showing the leakage data behaving in a transitional region, and out to high Re values. This is not incompatible with an extrapolation of the Nikuradse data, but is not compatible with that in [7]. However, the surfaces in [7] would be expected to precipitate early transitions.

Clearly accurate interpretation of these calculations and results is not possible. Never-the-less, they conform with the interpretation that

$$1.2 < \lambda \leq 4$$

Four is exceeded, marginally, but the value appears to be associated with a peak in the Re, λ plot.

9. DISCUSSION

The preceding sections have reviewed leakage data through idealized cracks, and through real cracks.

For the artificial defects correlations have been found between the ratio of hydraulic radius to R_a and friction factor λ. Making assumptions about the relationship between R_a values and other surface characterising features then the data appear to be bracketed by equations (1) and (3). Given that real

surfaces cannot be defined by a single parameter, but that correlations between R_a and λ can be deduced, then equations (1) and (3) could be used to assess likely frictional effects on flow rate. Appropriate ranges of R_a could be selected from an experience data base. A major constraint, however, in that in general, the correlations have not been validated beyond $\lambda \approx 1$.

If calculated λ values exceed unity then judgement must be exercised by the user. The data reviewed suggests that $\lambda \leq 4$ applies. This limit is based on experimental results in both transitional and fully rough regimes, where behaviour appears to conform to the expectations from such classic work as that of Nikuradse. A possible exception are those results for two phase flow that are analysed above. For these it appears that the peak in the λ: Re curve is not reached until $Re \approx 10^4$. This seems high, but such a characteristic is not incompatible with an extrapolation of the Nikuradse data (peak at $\lambda = 0.06$ for $Re = 2 \times 10^4$).

It is suggested that should λ, based on R_a assessments, exceed unity then λ equal to one and four should be used to assess uncertainties in flowrates. The variation in calculated flowrate will be dependent upon conditions, but, in the authors experience, is usually less than a factor of 3.

10. CONCLUSIONS

For calculated λ values less than unity equations (1) and (3) provide reasonable bounds for determining λ based on a R_a value appropriate to the likely cracking mechanism.

For $\lambda > 1$ the position is less well defined, but the evidence does support the general hypothesis that $\lambda_{max} \leq 4$.

11. ACKNOWLEDGEMENT

This paper is published with permission of Nuclear Electric plc.

12. REFERENCES

1) Schlichting, H, Boundary Layer Theory, 6th Ed, McGraw Hill, New York, 1968.
2) Peklenik, J, New Developments in Surface Characterization and Measurements by Means of Random Process Analysis, Proc I Mech E, Vol 182, Part 3K, Paper 24, 1968.
3) Chivers, T C, and Mitchell, L A, On the Limiting Velocity through Parallel Bore Tubes, J Phys D: Appl. Phys, Vol 4, 1971, pp. 1069-1076.
4) Button, B L, Grogan, A F, Chivers, T C, & Manning, P T. Gas flow through cracks. ASME Jnl of Fluids Engnrng Vol 100, pp 453-458. 1978
5) DAFTCAT User Manual, Nuclear Electric plc, Berkeley Technology Centre, Berkeley, Glos, UK. 1993
6) Wilkinson, J, Spence, G S M, and Chandler, R F, Leakage flow through small cracks -Report of second stage of experimental work, AEA Technology, Risley, UK. Report FMWG/P(91) 123D, 1991.
7) Gardiner, G C, & Tyrrell, R J, The flow resistance of experimental models of naturally occurring cracks. Proc Instn Mech Engnrs Vol 200 No C4. 1968
8) Unpublished NE plc memorandum.
9) Paul, D D, Ahmad, J, Scott, P M, Flanigan, L F, and Wilkowski, G M, Evaluation and refinement of leak-rate estimate models: Topical Report, NUREG/CR-5128, June 1994.

APPENDIX

The treatment of fluid friction within the SQUIRT code

SQUIRT calculates a friction factor based on the Nikuradse relationship (equation (2) in the main text), but modified as W/R_a reduces. The relationship is plotted in Figure 1. To this factor is added an additional head loss parameter.

$$\xi = \frac{\lambda D}{2w} \qquad (1a)$$

This relationship is identical in form to the controlling parameter in DAFTCAT leading to equation (6).

By inputting a very small (but non zero) value of surface roughness into SQUIRT, ξ can then be used to either input specific values for λ, or to deduce values to correlate with experimentally determined leakage rates.

DETERMINATION OF CRACK MORPHOLOGY PARAMETERS FROM SERVICE FAILURES FOR LEAK-RATE ANALYSES

G. Wilkowski*, S. Rahman**, N. Ghadiali*, and D. Paul*
* Battelle Memorial Institute, Columbus Ohio 43201
** The University of Iowa, Iowa City, Iowa 52245

ABSTRACT

In leak-rate analyses described in the literature, the crack morphology parameters are typically not well agreed upon by different investigators. This paper presents results on a review of crack morphology parameters determined from examination of service induced cracks. Service induced cracks were found to have a much more tortuous flow path than laboratory induced cracks due to crack branching associated with the service induced cracks. Several new parameters such as local and global surface roughnesses, as well as local and global number of turns were identified. The effect of each of these parameters are dependant on the crack-opening displacement. Additionally, the crack path is typically assumed to be straight through the pipe thickness, but the service data show that the flow path can be longer due to the crack following a fusion line, and/or the number of turns, where the number of turns in the past were included as a pressure drop term due to the turns, but not the longer flow path length. These parameters were statistically evaluated for fatigue cracks in air, corrosion-fatigue, IGSCC, and thermal fatigue cracks.

A refined version of the SQUIRT leak-rate code was developed to account for these variables. Sample calculations are provided in this paper that show how the crack size can vary for a given leak rate and the statistical variation of the crack morphology parameters.

INTRODUCTION

The key crack-morphology variables considered in past leak-rate analyses were surface roughness, number of turns in the leakage path, and entrance loss coefficients (Refs. 1 and 2). However, the examination of service cracks also shows that the cracks frequently do not grow radially through the pipe thickness. Hence, a fourth parameter, "actual crack path/thickness," representing deviation from straightness can also play an important role in the calculation of leak rates. Traditionally, this parameter has been ignored.

In addition, current leak-rate calculations do not explicitly account for the effects of crack-opening on the crack-morphology parameters. Examination of service cracks in pipes as well as theoretical considerations suggest that these variables should depend on the magnitude of crack-opening. But, currently, there are no engineering models that would allow for these crack-morphology variables to be functionally dependent on the crack-opening characteristics of a pipe (Ref. 3).

In this study, simple linear models were developed based on local and global definitions of the crack-morphology variables which can be measured from current service data. Standard statistical analyses of these data were conducted to determine the probabilistic characteristics (e.g., mean and standard deviation) of the crack-morphology parameters for several types of cracking mechanisms and pipe materials. Using these statistics, one can evaluate the effects of crack-morphology variability on the leak rate or leakage-size flaw for leak-before-break (LBB) or other applications.

IMPROVED DEFINITIONS OF CRACK-MORPHOLOGY PARAMETERS

Surface Roughness

This input parameter defines the peak-to-peak roughness of the crack-face surface to be used in the calculation of the friction factor and pressure loss due to friction for fluid flow through a crack in a pipe. In the past, the surface roughness was assumed to be invariant with respect to COD. For example, the constant numerical values, such as 0.0062 mm and 0.04 mm, were used to quantify surface roughness of intergranular stress-corrosion cracks and fatigue cracks, respectively (Ref. 1). However, a careful examination of Figure 1 suggests that the appropriate surface roughness could be

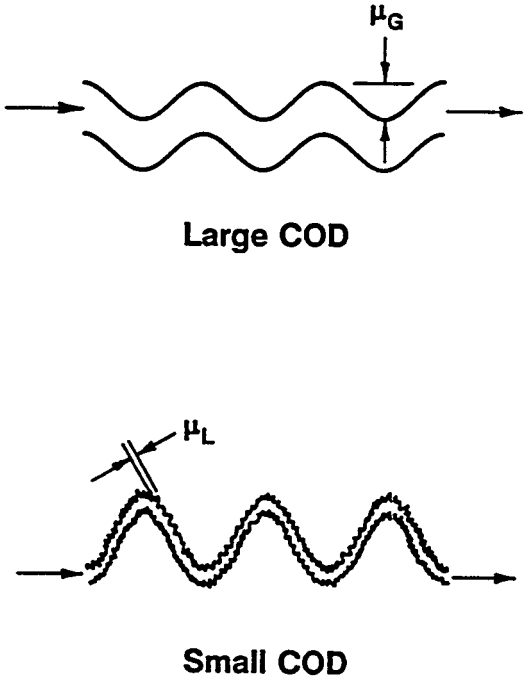

Figure 1 Local and global surface roughness and number of turns

large (global) or small (local) depending on whether the COD is large or small, respectively. In this study, the dependence of surface roughness, μ, was achieved by assuming a piecewise linear function given by

$$\mu = \begin{cases} \mu_L, & 0.0 \le \dfrac{\delta}{\mu_G} < 0.1 \\ \mu_L + \dfrac{\mu_G - \mu_L}{9.9}\left[\dfrac{\delta}{\mu_G} - 0.1\right], & 0.1 \le \dfrac{\delta}{\mu_G} \le 10 \\ \mu_G, & \dfrac{\delta}{\mu_G} > 10 \end{cases} \tag{1}$$

where μ_L is the local surface roughness, μ_G is the global surface roughness, and δ is the center-crack-opening-displacement. Figure 2 shows the schematic variation of μ with respect to δ.

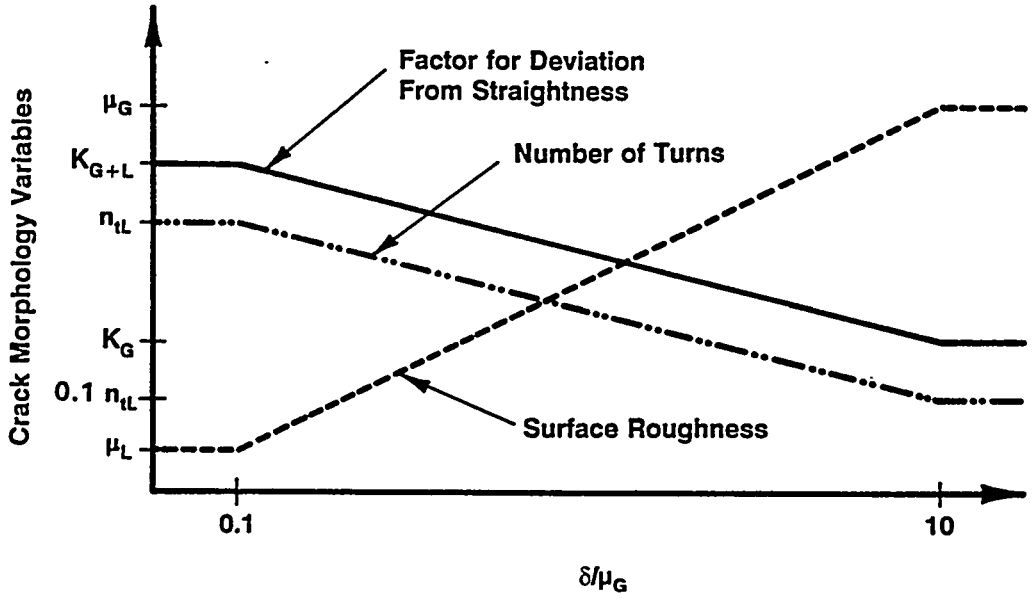

Figure 2 Crack-morphology variables versus normalized COD

Number of Turns

This input parameter defines the number of turns that the fluid must make when flowing through the crack. In fatigue and stress-corrosion cracks, the number and severity of the bends can in some circumstances account for upwards of one-half the total pressure loss of the fluid when flowing through the crack. Typically, a 45- or a 90-degree angle change in flow direction results in about a 0.4 and 1.0 velocity head loss, respectively. Norris et al. (Ref. 2) have shown this parameter to be of importance for stress-corrosion cracks. In the past, this parameter was thought to be of lesser importance for fatigue cracks because fatigue cracks generally break through in a fairly flat plane. However, the experimental results shown in Reference 1 indicate that the number of bends in the flow path can be significant even for fatigue cracks. This occurs when the variations in the contours of the relatively flat plane of a fatigue crack are large compared with the COD. Therefore, even though the fracture faces of a fatigue crack appear to be fairly flat to the naked eye, the fatigue cracks contain many flow path bends when the crack is tight.

Following similar considerations given above for the surface roughness, the appropriate number of turns, n_t, also depends on the COD. Once again, a piece-wise linear function was assumed, i.e.,

$$n_t = \begin{cases} n_{tL}, & 0.0 \le \dfrac{\delta}{\mu_G} < 0.1 \\ n_{tL} - \dfrac{n_{tL}}{11}\left[\dfrac{\delta}{\mu_G} - 0.1\right], & 0.1 \le \dfrac{\delta}{\mu_G} \le 10 \\ 0.1 n_{tL}, & \dfrac{\delta}{\mu_G} > 10 \end{cases} \qquad (2)$$

where n_{tL} is the local number of turns. A schematic plot of Equation 2 is also shown in Figure 2.

Discharge Coefficient

The discharge coefficient is the ratio of the flow areas associated with the *vena contracta* to the flow area at the crack entrance. For sharp-edged crack entrances, a typical discharge coefficient would be a value of 0.60. For round or smooth-edged crack entrances, a typical discharge coefficient would be close to 0.95.

Actual Crack Path/Thickness

This parameter represents the deviation of flow path from straightness. Depending on the COD (see Fig. 3), it can be defined as

$$\frac{L_a}{t} = \begin{cases} K_{G+L}, & 0.0 \le \dfrac{\delta}{\mu_G} < 0.1 \\ K_{G+L} - \dfrac{K_{G+L}-K_G}{9.9}\left[\dfrac{\delta}{\mu_G} - 0.1\right], & 0.1 \le \dfrac{\delta}{\mu_G} \le 10 \\ K_G, & \dfrac{\delta}{\mu_G} > 10 \end{cases} \quad (3)$$

where L_a is the actual length of the flow path, K_G is the correction factor for global path deviations for straightness (e.g., a crack following the fusion line of the weld), and K_{G+L} is the correction factor for global plus local path deviations for straightness (e.g., a crack following the grain boundaries for IGSCC). A schematic plot of Equation 3 is also shown in Figure 2.

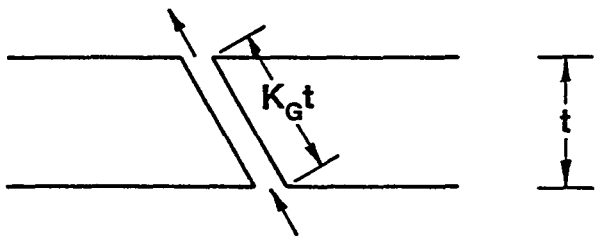

Large COD

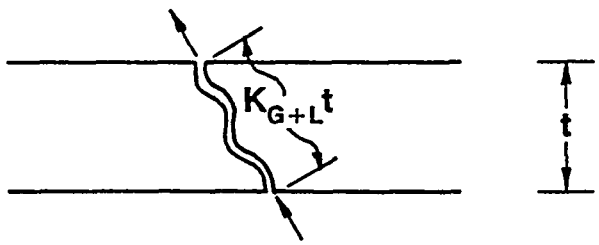

Small COD

Figure 3 Global-plus-local and global path deviations from straightness

Note that the piecewise linear variation of the above crack morphology variables is a first attempt to simulate their dependency on COD. The numerical constants in Equations 1 to 3 are based on a review of cracks found in service and expert opinion at Battelle. Additional studies are needed to evaluate these linear models.

Statistical Characterization of Crack Morphology Parameters

Surface Roughness

Some peak-to-peak roughness values for cracks found in pipes removed from service are summarized below. The statistics are listed in Tables 1 and 2 for stainless steel and carbon steel pipes, respectively, with various cracking mechanisms.

Table 1 Summary of surface roughness measurements in stainless steel pipes[a]

Mechanism	Source	Roughness, μm (μinch)	
		Local	Global
	(a) Stainless steel pipes - IGSCC		
IGSCC	NP-2472 Vol. 2 (see Figure I-1)	2.03 (80)	101 (3,990)
IGSCC	NP-2472 Vol. 2 (see Figure H-9)	--	107 (4,230)
IGSCC	NP-3684SR, Vol. 3 (Paper 4, Figure 11)	7.37 (290)	74.4 (2,930)
IGSCC	NP-3684SR, Vol. 3 (Paper 4, Figure 5)	10.5 (412)	41.9 (1,650)
IGSCC	NP-3684SR, Vol. 2 (Paper 5, Figure 21)	0.635 to 6.35 (25.0 to 250)	127 (5,000)
IGSCC	NP-3684SR, Vol. 2 (Paper 19, Figure 12)	1.40 (55)	27.9 (1,100)
Average		4.699 (185)	80.010 (3,150)
Standard Deviation		3.937 (155)	39.014 (1,536)
Range		0.635 to 10.5 (25 to 412)	27.94 to 127 (1,100 to 5,000)
Number of Samples		6	6
	(b) Stainless steel pipes - fatigue in air		
Fatigue (air)	Hitachi, (NED, Vol. 128, 1991, pp 24)	8.05 (317)	33.8 1,330

(a) Original measurements made in U.S. customary units and converted to SI units.

Table 2 Summary of surface roughness measurements in carbon steel pipes[a]

Mechanism	Source	Roughness, μm (μinch) Local	Global
	(a) Ferritic Steels - fatigue in air		
Fatigue (air)	NUREG/CR-5128 (girth weld)	3.02 (119)	--
Fatigue (air)	NUREG/CP-0051 Mayfield, pp 365 (A106B)	8.53 (336)	--
Fatigue (air)	Hitachi, NED, Vol. 128 1991, pp. 24 (STS 42)	8.05 (317)	33.8 (1,330)
Average		6.528 (257)	33.8 (1,300)
Standard Deviation		3.048 (120)	--
Range		3.02 to 8.53 (119 to 336)	--
Number of Samples		3	1
	(b) Ferritic Steels - corrosion fatigue in feedwater line		
Corrosion fatigue (Point Beach plant feedwater line)	NUREG/CR-1603, Figure 3.13	8.64 (340)	44.4 (1,750)
Corrosion fatigue (D.C. Cook plant feedwater line)	NUREG/CR-1603, Figure 3.17	3.05 (120)	20.1 (790)
Corrosion fatigue (Beaver Valley plant feedwater line)	NUREG/CR-1603, Figure 3.15	9.14 (360)	38.1 (1,500)
Corrosion fatigue (Palisades plant feedwater line)	NUREG/CR-1603, Figure 3.11	10.7 (420)	61.0 (2,400)
Corrosion fatigue (Ginna plant feedwater line)	NUREG/CR-1603, Figure 3.8	10.4 (410)	58.4 (2,300)
Corrosion fatigue (Salem plant feedwater line	NUREG/CR-1603, Figure 3.16	10.9 (430)	21.1 (830)
Average		8.814 (347)	40.513 (1,595)
Standard Deviation		2.972 (117)	17.653 (695)
Range		3.05 to 10.9 (120 to 430)	(20.1 to 61.0) (790 to 2,400)
Number of Samples		6	6

(a) Original measurements made in U.S. customary units and converted to SI units.

Stainless Steel - IGSCC

Surface roughness values for an IGSCC crack from the Battelle/EPRI Phase II pipe leak-rate experiments (Ref. 4) were measured to be 5.10 μm (200 microinches). (Note: The authors expressed doubt about the accuracy of this measurement in the paper.) Furthermore, the crack was thought to

grow at a 10 to 15 degree angle from the straight crack through the thickness, which would increase the global flow path by 1.5 to 3.5 percent.

From a typical stainless steel used in Ref. 5 (see Figure I-1 of Ref. 5), the global surface roughness that includes the peak-to-peak heights for intergranular crack growth was 101 μm (3,990 microinches). The roughness along the grain boundary was estimated to be 2.03 μm (80 microinches).

Using Figure H-9 in Reference 5, a global roughness for an IGSCC crack was estimated to be 107 μm (4,230 microinches).

From a paper by Christer Jansson on Swedish IGSCC studies (Ref. 6), Figure 11 of Reference 6 shows the typical global surface roughness for an IGSCC crack to be 74.5 μm (2,930 microinches), and Figure 5 of Reference 6 shows a global roughness of 41.9 μm (1,650 microinches). The roughness along a grain boundary could be up to 7.37 μm (290 microinches) in Figure 11 of Reference 6 and 10.5 μm (412 microinches) in Figure 5 of Reference 6.

From the paper by Olson et al. (Ref. 7) on large pipe IGSCC experiments at Battelle Pacific Northwest Laboratory (PNL), Figure 21 of Reference 7 shows that the typical global surface roughness of IGSCC cracks was 127.0 μm (5,000 microinches). The roughness along a grain boundary could be up to 6.4 μm (250 microinches) in some areas and perhaps a factor of 10 less in other areas (0.64 μm [25 microinches]).

From the paper by Kurtz (Ref. 8) on effects of sulfides on IGSCC at PNL, Figure 12 of Reference 8 shows the typical global surface roughness for an IGSCC crack to be 27.9 μm mm (1,100 microinches). The roughness along a grain boundary was 1.40 μm (55 microinches) in some relatively smooth areas.

Stainless Steel - Fatigue (Air)

Hitachi fatigue cracked pipe results showed a smaller or local surface roughness superimposed on a larger or global surface roughness (Ref. 9). The average value of the global roughness may correspond to the waviness of the fatigue crack, 33.8 μm (1,330 microinches). The average value of the local roughness was 8.05 μm (317 microinches). The results were very similar for their ferritic and stainless steel pipes.

Carbon Steel - Corrosion Fatigue

From an investigation on thermal fatigue cracks in a feedwater line from the Point Beach plant in the 1978 time period (Ref. 10), Figure 3.13 of Reference 10 showed a local surface roughness of 8.64 μm (340 microinches) and a global surface roughness of 44.4 μm (1,750 microinches).

From the same investigation (Ref. 10), a thermal fatigue crack in a feedwater line from the D.C. Cook plant in the 1978 time period, Figure 3.17 of Reference 10 showed a local surface roughness of 3.05 μm (120 microinches) and a global surface roughness of 20.1 μm (790 microinches).

From the same investigation (Ref. 10), a thermal fatigue crack in a feedwater line from the Beaver Valley plant in the 1978 time period, Figure 3.15 of Reference 10 showed a local surface roughness of 9.14 μm (360 microinches) and a global surface roughness of 38.1 μm (1,500 microinches).

From the same investigation (Ref. 10), a thermal fatigue crack in a feedwater line from the Palisades plant in the 1978 time period, Figure 3.11 of Reference 10 showed a local surface roughness of 10.7 μm (420 microinches) and a global surface roughness of 61.0 μm (2,400 microinches).

From the same investigation (Ref. 10), a thermal fatigue crack in a feedwater line from the Ginna plant in the 1978 time period, Figure 3.8 of Reference 10 showed a local surface roughness of 10.4 μm (410 microinches) and a global surface roughness of 58.4 μm (2,300 microinches).

Carbon Steel - Fatigue (Air)

In Reference 1, results on a carbon steel weld fatigue crack showed a roughness of 3.02 μm (119 microinches).

Measurements of a carbon steel base metal fatigue crack in air from the NRC Cold-Leg program showed a roughness of 8.53 μm (336 microinches). These are obtained from a technical paper authored by Mayfield and Collier (Ref. 11).

Hitachi fatigue cracked pipe results showed a local surface roughness superimposed on a global surface roughness (Ref. 9). The average value of the global roughness may correspond to the waviness of the fatigue crack, 33.8 μm (1,330 microinches). The average value of the local roughness was 8.05 μm (317 microinches). The results were very similar for their ferritic and stainless steel pipes.

Number of Turns per Unit Thickness

From the examinations of photomicrographs in References 8 to 12, Tables 3 and 4 show the number of 90-degree turns per inch of thickness for stainless steel and carbon steel pipes, respectively. For IGSCC cracks in stainless steels this can be a much larger number than for a corrosion fatigue crack, and can also vary significantly since the grain size may vary.

Entrance Loss Coefficient (C_D)

If entrance edges have a radius of 1/6 of the COD or larger, then they are considered to be rounded and $C_D = 0.62$. Consequently, for IGSCC with sharp edges (no pitting corrosion to smooth the edges), $C_D = 0.95$ for small COD values, i.e., COD < 0.006 inch. For Fatigue and corrosion fatigue typically at small pits with some surface corrosion to round the edges, $C_D = 0.62$ for all COD values of interest. These values were obtained from Reference 1.

Actual Crack Path/Thickness

Most leak-rate analyses assume that a crack grows straight through the thickness. This is not true for real cracks. In the first type of example, a crack could follow a weld. Here the length of the crack along a typical 37-degree weld bevel is 1/[cos (37 degrees)] or 1.25 times the thickness.

Table 3 Summary of measurements of the number of 90-degree turns in stainless steel pipes[a]

Mechanism	Source	Number of 90-degree Turns per Unit Distance, mm^{-1} ($inch^{-1}$)
	(a) Stainless steel pipes - IGSCC	
IGSCC	NP-2472, Vol. 2 (see Figure I-1)	57.1 (1,450)
IGSCC	NP-3684SR, Vol. 3 (Paper 4, Figure 11)	13.9 (352)
IGSCC	NP-3684SR, Vol. 3 (Paper 4, Figure 5)	34.4 (873)
IGSCC	NP-3684SR, Vol. 2 (Paper 5, Figure 21)	9.45 (240)
IGSCC	NP-3684SR, Vol. 2 (Paper 19, Figure 12)	26.4 (670)
Average		28.23 (717)
Standard Deviation		18.94 (481)
Range		9.45 to 57.1 (240 to 1,450)
Number of Samples		5
	(b) Stainless steel pipes - fatigue in air	
Fatigue (air)	Hitachi (NED, Vol. 128, 1991, pp. 24)	2.52 (64)

(a) Original measurements made in U.S. customary units and converted to SI units.

Table 4 Summary of measurements of the number of 90-degree turns in carbon steel pipes[a]

Mechanism	Source	Number of 90-degree Turns per Unit Distance, mm^{-1} ($inch^{-1}$)
	(a) Ferritic steels – fatigue in air	
Fatigue (air)	Hitachi, NED, Vol. 128 1991, pp. 24 (STS 42)	2.0 (51)
	(b) Ferritic steels - corrosion fatigue in feedwater lines	
Corrosion fatigue (Point Beach plant feedwater line)	NUREG/CR-1603, Figure 3.13	2.4 (61)
Corrosion fatigue (D.C. Cook plant feedwater line)	NUREG/CR-1603, Figure 3.17c	20.0 (507)
Corrosion fatigue (Beaver Valley plant feedwater line)	NUREG/CR-1603, Figure 3.15	2.3 (58)
Corrosion fatigue (Palisades plant feedwater line)	NUREG/CR-1603, Figure 3.11	13.7 (349)
Corrosion fatigue (Ginna plant feedwater line)	NUREG/CR-1603, Figure 3.8	1.42 (36.0)
Corrosion fatigue (Salem plant feedwater line)	NUREG/CR-1603, Figure 3.16	0.63 (16)
Average		6.73 (171)
Standard deviation		8.07 (205)
Range		1.42 to 20.0 (16 to 507)
Number of Samples		6

(a) Original measurements made in U.S. customary units and converted to SI units.

Reference 12 shows an example of such a service crack. Another example for angular crack growth of thermal fatigue cracks in feedwater piping, where from metallographic sections in Reference 10 showed that the flow path length was 1.05 times the thickness. These changes in the flow path length would effect the leak rate for small or large crack-opening displacements. We termed this effect the global flow path correction, K_G.

Additionally, many leak-rate analyses account for the pressure drop from a turn in the flow path, but do not account for the flow path being longer because of these turns. For instance, these small turns can occur along grain boundaries for an IGSCC. This local waviness is termed K_{G+L}, because of the way it was measured included the K_G effects. If the COD is small compared with the global roughness, then the local waviness will cause an increase in the flow path length. If the COD is small compared with the global roughness, then the local surface roughness should be used with this local plus global waviness flow-path multiplication factor, K_{G+L}, as well as the pressure drop from the number of turns.

Measured values of K_G and K_{G+L} from typical cracks for stainless steel and carbon steel, are presented in Tables 5 and 6. In general, these values are larger for IGSCC cracks in stainless steels than for corrosion fatigue cracks in carbon steels.

A separate evaluation was also made to assess the crack morphology parameters for a thermal fatigue crack in cast stainless steel. Photographs of fracture surfaces from Reference 13 were examined. Only a few cases were sufficiently documented for the level of detail needed in this work. Of these, the crack morphology parameters fell in the range of the carbon steel corrosion-fatigue cracks. Hence, the carbon steel crack morphology variables could be used for the cast stainless steel thermal fatigue-crack morphology. Further details on the statistical characterization of crack-morphology parameters are available in References 14 and 15.

Table 7 shows the summary of results in terms of statistics of the crack morphology variables. In general, it was found that the global surface roughness, local number of turns, and the path deviation factors for IGSCC in stainless steel are larger than those for corrosion fatigue in carbon steel. But, when the local surface roughness is considered, it was found to be larger for the corrosion fatigue type of cracking mechanism. However, note that the statistical properties presented in Table 7 were based on a small number of samples. Hence, these results should be viewed as preliminary estimates. Further studies are needed to verify these results.

Implications of Crack Morphology Variables

The statistical properties of crack-morphology variables developed in this work can be used to calculate the probabilistic characteristics of the leak rate and leakage flaw size for LBB applications. Calculations of this kind are routine in performing LBB evaluations. Based on the statistics, both deterministic and probabilistic evaluations can be made.

Battelle recently conducted a probabilistic study using these statistics to compute the probability distribution of crack size for given leak-rate detection capability, Ref. 16. In that study, a stainless steel pipe with a probable IGSCC cracking mechanism was analyzed. Assuming that the associated crack-morphology variables are lognormally distributed, 100 independent samples of these variable

Table 5 Crack flow-path-length to pipe thickness ratios for stainless steel pipes

Mechanism	Source	K_{G+L}	K_G
	(a) Stainless steel pipes - IGSCC		
IGSCC	NP-2472, Vol. 2 (See Figure G-14)	1.47	1.25
IGSCC	NP-3684SR, Vol. 3 (Paper 4, Figure 11, 75x)	1.35	1.02
IGSCC	NP-3684SR, Vol. 3 (Paper 4, Figure 5, 100x)	1.53	1.06
IGSCC	NP-3684SR, Vol. 2 (Paper 5, Figure 21)	1.15	1.02
IGSCC	NP-3684SR, Vol. 2 (Paper 19, Figure 12, 200x)	1.15	1.01
Average		1.33	1.07
Standard Deviation		0.17	0.10
Range		1.15 to 1.53	1.01 to 1.25
Number of Samples		5	5

Table 6 Crack flow-path-length to pipe thickness ratios for carbon steel pipes

Mechanism	Source	K_{G+L}	K_G
	(a) Ferritic Steels - Corrosion fatigue in feedwater lines		
Corrosion fatigue (Point Beach plant feedwater line)	NUREG/CR-1603, Figure 3.13	1.10	1.035
Corrosion fatigue (D.C. Cook plant feedwater line)	NUREG/CR-1603, Figure 3.17c	1.03	1.001
Corrosion fatigue (Beaver Valley plant feedwater line)	NUREG/CR-1603, Figure 3.15	1.08	1.03
Corrosion fatigue (Palisades plant feedwater line	NUREG/CR-1603, Figure 3.11	1.04	1.004
Corrosion fatigue (Ginna plant feedwater line)	NUREG/CR-1603, Figure 3.8	1.07	1.03
Corrosion fatigue (Salem plant feedwater line)	NUREG/CR-1603, Figure 3.16	1.02	1.001
Average		1.06	1.017
Standard Deviation		0.03	0.0163
Range		1.02 to 1.10	1.001 to 1.035
Number of Samples		6	6

Table 7 Mean and standard deviation of crack morphology parameters

Crack Morphology Variable	IGSCC		Corrosion Fatigue	
	Mean	Standard Deviation	Mean	Standard Deviation
μ_L, μm	4.70	3.94	8.81	2.97
μ_G, μm	80.0	39.0	40.5	17.7
n_L, mm^{-1}	28.2	18.9	6.73	8.07
K_G	1.07	0.10	1.02	0.016
K_{G+L}	1.33	0.17	1.06	0.03

were generated from the statistical properties in Table 7. An example calculation is shown here to see the effect of the crack morphology variables on calculating a flaw size for a given leak rate.

For each set of these crack morphology parameters, standard (deterministic) thermal-hydraulic and fracture-mechanics analyses were performed to compute the crack size for a leak rate of 3.785 l/min (1 gpm). This was done for a 711-mm (28-inch) diameter Schedule 80 stainless steel pipe assuming an IGSCC mechanism. The same deterministic analyses were repeated for each of the 100 sample sets of crack-morphology variables to generate the corresponding samples of the leakage flaw size. Following standard statistical analysis of these replicated samples, Figures 4 and 5 show the histogram and cumulative probability of leakage flaw size in this pipe. Comparisons with the theoretical distributions suggest that the flaw size can also be modeled as a lognormal variable.

Examples of this kind show how the uncertainties in the crack-morphology input can be accounted for in characterizing leakage flaw size for LBB evaluations. Further details on these calculations can be found in Reference 16. The report also contains subsequent probabilistic pipe fracture evaluations for a wide variety of nuclear piping systems in BWR and PWR plants.

CONCLUSIONS

The results of this study provided an initial data base for defining the surface roughness parameters for cracks that have been found in service. The crack morphology of these service cracks are typically more complicated than those typically used in laboratory leak-rate studies. Consequently the new local and global definitions to take into account the effect of how these parameters vary with COD were developed to improve the accuracy of leak-rate models. Further additions to the data base of crack morphology parameters is encouraged.

ACKNOWLEDGEMENTS

This work was supported by the U.S. Nuclear Regulatory Commission (NRC) through the Electrical, Materials and Mechanical Engineering Branch of the Office of Nuclear Regulatory Research under Contract No. NRC-04-90-069. Mr. A. Hiser was the NRC program manager during most of this work and Mr. M. Mayfield was the program manager at the end of the program.

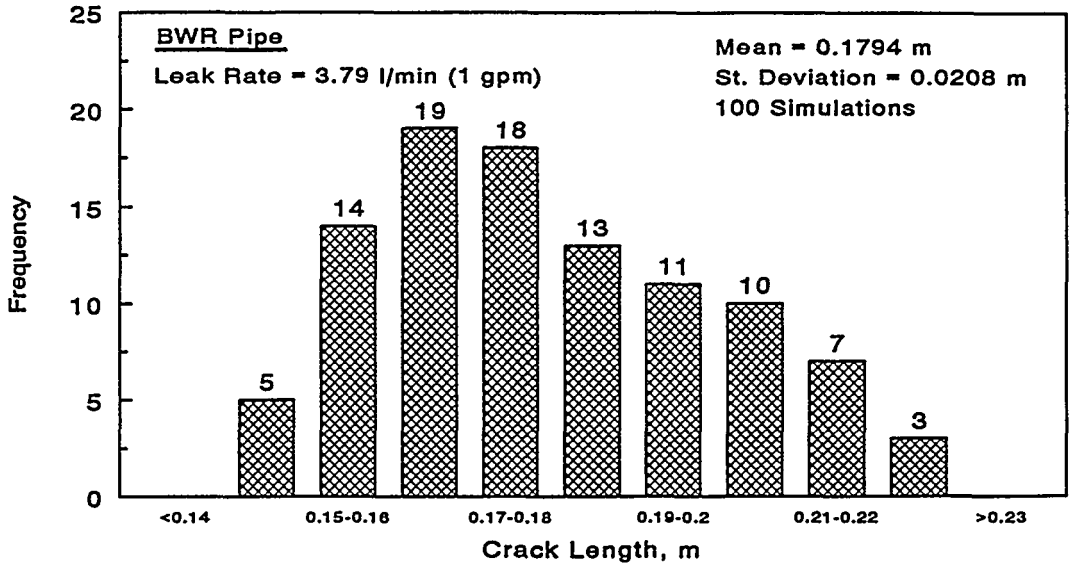

Figure 4 Histogram of leakage flaw size in a pipe for 3.785 l/min (1 gpm) leak rate and 50 percent of ASME Service Level A stress limit

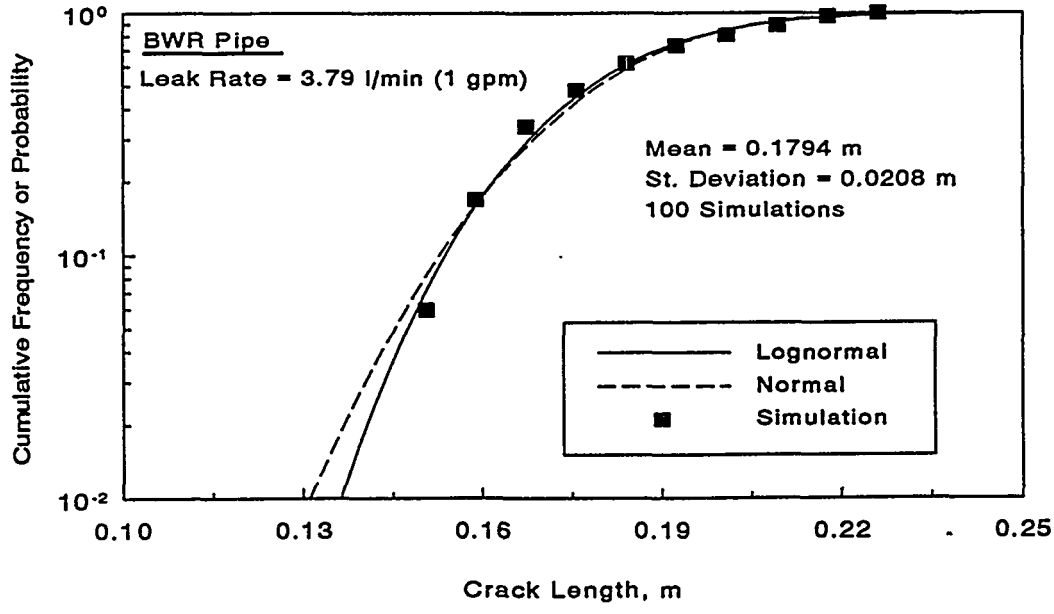

Figure 5 Probability distribution of leakage flaw size in a pipe for 3.785 l/min (1 gpm) leak rate and 50 percent of ASME Service Level A stress limit

REFERENCES

(1) Paul, D., Ahmad, J., Scott, P., Flanigan, L., and Wilkowski, G., "Evaluation and Refinement of Leak-Rate Estimation Models," NUREG/CR-5128, Rev. 1, U.S. Nuclear Regulatory Commission, Washington, D.C., June 1994.

(2) Norris, D. et al., "PICEP: Pipe Crack Evaluation Program," EPRI Report, NP-3596-SR, Electric Power Research Institute, Palo Alto, CA,1984.

(3) Wilkowski, G., Rahman, S., Paul. D., and Ghadiali, N., "Pipe Fracture Evaluations for Leak-Rate Detection: Deterministic Models," PVP-Vol. 266, *Creep, Fatigue Evaluation, and Leak-Before-Break Assessment*, Edited by Y. Garud, pp. 243-254, July 1993.

(4) Collier, R. P., Stulen, F. B., Mayfield, M. E., Pape, D. B., and Scott, P. M., "Two-Phase Flow Through Intergranular Stress Corrosion Cracks and Resulting Acoustic Emission," EPRI Report NP-3540-LD, Electric Power Research Institute, Palo Alto, CA, 1984.

(5) Hale, D. A., and others, "The Growth and Stability of Stress Corrosion Cracks in Large-Diameter BWR Piping," EPRI NP-2472, Vol. 2., Final Report, Electric Power Research Institute, Palo Alto, CA, July 1982.

(6) Jansson, C., and others, "BWR Pipe Repairs in Sweden," Paper 4 in *Proceedings: Second Seminar on Countermeasures for Piping Cracks in BWRs*, EPRI NP-3684-SR, Vol. 3, Special Report, Electric Power Research Institute, Palo Alto, CA, September 1984.

(7) Olson, N. H., and others, "Crack Growth Rates and Effectiveness of LPHSW Remedy in Large-Diameter Type 304 Stainless Steel BWR Pipe," Paper 5 in *Proceedings: Second Seminar on Countermeasures for Piping Cracks in BWRs*, EPRI NP-3684-SR, Vol. 2, Special Report, Electric Power Research Institute, Palo Alto, CA, September 1984.

(8) Kurtz, R. J., "Effect of Sulfate and Chloride Intrusions on Cracking of Stainless Steel at 288°C," Paper 19 in *Proceedings: Second Seminar on Countermeasures for Piping Cracks in BWRs*, EPRI NP-3684-SR, Vol. 2, Special Report, Electric Power Research Institute, Palo Alto, CA, September 1984.

(9) Matsumoto, K., Nakamura, S., Gotoh, N., Narabayashi, T., Tanaka, Y., and Horimizu, Y., "Study on Coolant Leak Rates Through Pipe Cracks," ASME PVP - Vol. 165, pp. 121-127, 1989.

(10) Goldberg, A., Streit, R. D., and Scott, R. G., "Evaluation of Cracking in Feedwater Piping Adjacent to the Steam Generators in Nine Pressurized Water Reactor Plants," NUREG/CR-1603, U.S. Nuclear Regulatory Commission, Washington, D.C., October 1980.

(11) Mayfield, M. E. and Collier, R. P., "Leak-Before-Break Due to Fatigue in the Cold Leg Piping System," *Proceedings of the CSNI Specialist Meeting on Leak-Before-Break in Nuclear Reactor Piping*, NUREG/CP-0051, U.S. Nuclear Regulatory Commission, Washington, D.C., September 1983.

(12) "Ultrasonic Sizing Capability of IGSCC and Its Relation to Flaw Evaluation Procedures," prepared by EPRI NDE Center and EPRI Staff, August 4, 1983.

(13) Bates, D. J., Doctor, S. R., Heasler, P. G., and Burck, E., "Stainless Steel Round Robin Test Centrifugally Cast Stainless Steel Screening Phase," NUREG/CR-4970, U.S. Nuclear Regulatory Commission, Washington, D.C., October 1987.

(14) Rahman, S., Wilkowski, G., and Ghadiali, N., "Pipe Fracture Evaluations for Leak-Rate Detection: Probabilistic Models," PVP-Vol. 266, *Creep, Fatigue Evaluation, and Leak-Before-Break Assessment*, Edited by Y. Garud, pp. 255-267, July 1993.

(15) Wilkowski. G. M., and others, "Short Cracks in Piping and Piping Welds," NUREG/CR-4599, U.S. Nuclear Regulatory Commission, Washington, D.C., Vol. 2., No. 2, May 1993.

(16) Rahman, S., Ghadiali, N., Paul, D., and Wilkowski, G., "Probabilistic Pipe Fracture Evaluations for Leak-Rate Detection Applications," NUREG/CR-6004, April 1995.

THE IPIRG PROGRAMS - ADVANCES IN PIPE FRACTURE TECHNOLOGY

G. Wilkowski, R. Olson, P. Scott, A. Hopper
Battelle, Columbus, Ohio USA

ABSTRACT

This paper presents an overview of the advances made in fracture control technology as a result of the research performed in the International Piping Integrity Research Group (IPIRG) program. The findings from numerous experiments and supporting analyses conducted to investigate the behavior of circumferentially flawed piping and pipe systems subjected to high-rate loading typical of seismic events are summarized.

Topics to be discussed include;

- Seismic loading effects on material properties,
- Piping system behavior under seismic loads,
- Advances in elbow fracture evaluations, and
- "Real" piping system response.

The presentation for each topic will be illustrated with data and analytical results. In each case, the state-of-the-art in fracture mechanics prior to the first IPIRG program will be contrasted with the state-of-the-art at the completion of the IPIRG-2 program.

OVERALL DESCRIPTION OF THE IPIRG PROGRAMS

Prior to summarizing the results of the IPIRG programs, the two programs are briefly described.

The IPIRG-1 Program

In the First International Piping Integrity Research Group (IPIRG-1) Program[1], Battelle conducted the first major research program to assess the fracture behavior of circumferentially cracked piping systems subjected to dynamic/cyclic loading. Virtually all prior programs involving pipe fracture evaluations considered straight pipe under quasi-static loading conditions. The IPIRG-1 Program evaluated the separate and combined effects of dynamic and single-frequency cyclic loading on circumferentially cracked pipe in four-point-bending experiments and in pipe system experiments. The results from both the load-history effects on fracture and the piping system evaluations gave

significant insight into the real behavior needed to assess the accuracy of leak-before-break (LBB) and in-service flaw evaluations.

The IPIRG-2 Program

Just as the IPIRG-1 Program built on the Degraded Piping Program[2], the Second International Piping Integrity Research Group (IPIRG-2) Program[3] built on what was learned during the IPIRG-1 program and the Short Cracks in Piping and Piping Welds program[4]. There were five tasks in the IPIRG-2 program, which are briefly defined as follows.

IPIRG-2 Task 1: The scope of Task 1 of the IPIRG-2 program was to conduct and evaluate pipe system experiments with flaws in straight pipe and welds, with specific attention to using a simulated seismic loading history in specific cases as opposed to the single-frequency loading used in the IPIRG-1 program. Nuclear piping fracture research in the international community over the past decade has focussed on relatively large cracks in straight pipe and welds joining straight pipe under simple monotonic loading. As a result, the technology for predicting the behavior of such cracks is relatively mature. In contrast, understanding; (1) the effects of complex load histories with variable amplitudes and multiple frequency content such as in a seismic event, (2) the effects of changes in geometry and local stiffness such as at the junction of a straight pipe and an elbow, and (3) the effects of shorter crack lengths more typical of in-service flaw evaluations or Leak-Before-Break (LBB) analyses, required further exploration and development. The Short Cracks in Piping and Piping Welds Program[4] conducted at Battelle for the USNRC has addressed the issue of shorter crack lengths, but the loading conditions for all of those experiments were quasi-static four-point bending. The experiments and analyses performed under Task 1 were intended to extend the database for validating pipe fracture analyses by building upon past and on-going research and providing additional experimental data in these relatively unexplored areas.

The eight pipe fracture experiments in Task 1 consisted of five pipe system experiments and three quasi-static monotonic loading experiments. The quasi-static companion experiments were conducted at quasi-static loading rates using the same flaw geometries and sizes, the same test conditions, and test specimens fabricated from the same heat of pipe as used in the pipe system experiments. These quasi-static pipe experiments were conducted for comparison purposes so that the effect of the dynamic, cyclic loading could be directly assessed.

An artist's conception of the IPIRG-2 experimental pipe system facility is shown in Figure 1. The pipe system is fabricated as an expansion loop with approximately 30.5 meters (100 feet) of straight pipe and five long-radius elbows. Special hardware, i.e., spherical bearings at the hanger locations and hydrostatic bearings at the vertical supports, were incorporated into the pipe system facility in order to create boundary conditions which could be easily modeled by finite element analyses.

IPIRG-2 Task 2: This task was a start at addressing the broad issue of fracture of flawed fittings, specifically elbows. The objective of this task was to develop engineering estimation methods to predict the fracture behavior of surface-cracked elbows and to validate these methods with large-diameter elbow fracture experiments. The vast majority of prior piping integrity research dealing with critical flaw assessment methodologies has addressed the problem of cracks in straight pipe only. Prior analytical and experimental work by Battelle and other research organizations has led to the development of elastic-plastic fracture mechanics and limit-load solutions applicable to straight pipe,

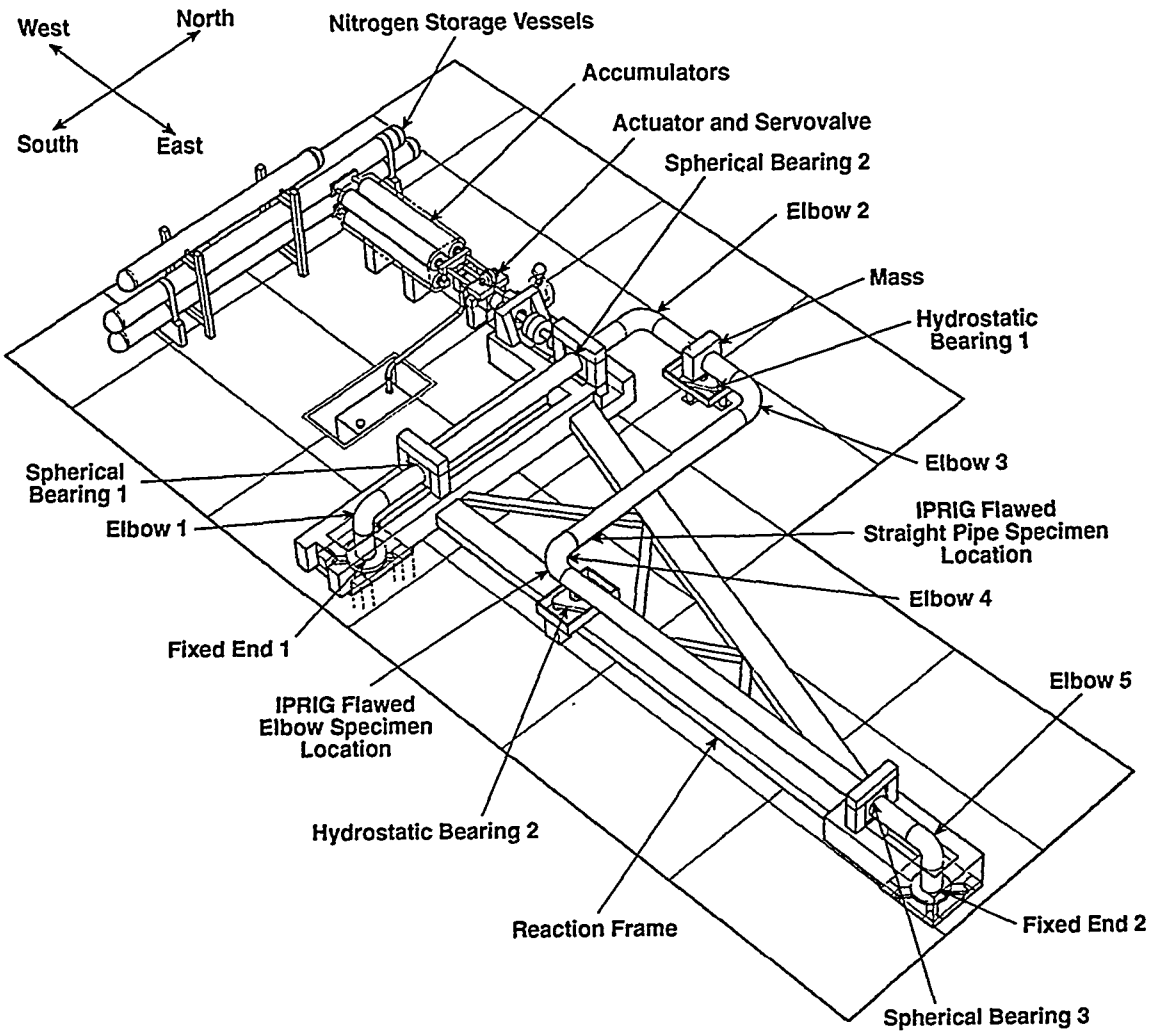

Figure 1. Artist's conception of the IPIRG pipe loop

which have been adopted by jurisdictional codes. However, the applicability of these methods to elbows or other fittings remains speculative.

Task 2 consisted of three subtasks directed toward improving the understanding of the fracture behavior of elbows under quasi-static and dynamic loading. The scope of Subtask 2.1 was to survey and assess existing flawed fitting data by; (1) reviewing and compiling the crack locations in elbows and other pipe fittings from actual service experience, (2) reviewing and compiling the existing experimental research data on flawed elbows, (3) comparing the data from existing flawed elbow

experiments with various existing flaw assessment methodologies developed for straight pipe, (4) reviewing fabrication methods to assess how material properties may be affected, and (5) describing the experimental difficulties which may be involved with testing elbows and other flawed fittings.

The purpose of Subtask 2.2 was to survey and assess existing $J_T$estimation methods applicable to elbows and to modify them as necessary. If these existing approaches proved inadequate, an optional activity was to develop valid J-estimation methods for those cases for which the existing analytical methods do not currently apply. In this effort, a J-estimation method was developed for circumferential surface cracks on the extrados of an elbow, and for an axial surface crack along the flank of the elbow. Both cases were for combined pressure (tension) and bending loads. The J-estimation scheme developed followed the GE/EPRI methodology where F, V, and h functions were developed from finite element analyses.

Subtask 2.3 was an experimental subtask in which full-scale elbow data were developed. There were a total of four experiments associated with this subtask. Two experiments involved an internal surface crack in the extrados of carbon steel elbows, and two involved an internal surface crack in the extrados of stainless steel elbows. For each set of experiments, there was a quasi-static four-point bend experiment and a companion dynamic pipe system experiment. The test conditions for each experiment were PWR conditions, i.e., 288 C and 15.5 MPa. The load history applied to the pipe system experiments was an increasing amplitude, constant frequency, sinusoidal excitation, similar to that used in the IPIRG-1 pipe system experiments.

IPIRG-2 Task 3: This task dealt with cyclic and dynamic load effects on fracture toughness. In the IPIRG-1 program, cyclic through-wall-cracked pipe experiments were conducted. These experiments showed that reversed cyclic loadings caused a significant decrease in the apparent toughness of the cracked pipe. In IPIRG-2, laboratory specimen data were developed to see if these experimental pipe results are predictable and to assess if the cyclic J-R curves determined from monotonic loading theory are reasonably valid for general application to structural predictions. To achieve the goals of this task, a comprehensive effort involving cyclic C(T) specimen fracture toughness tests, sensitivity analyses, finite element analyses, and full-scale pipe fracture experiments was undertaken.

IPIRG-2 Task 4: This task involved undertaking either unresolved issues that were discovered during the course of the program, or specific efforts for IPIRG members. Some efforts involved cyclic pipe tests on Japanese ferritic pipe, uncertainty analyses for LBB and in-service flaw evaluation criteria, and improvements to the SQUIRT leak-rate code.

IPIRG-2 Task 5: The objective of the final task in the IPIRG-2 program was to coordinate the program's seminars, workshops, and program management tasks. Part of the IPIRG tradition was to organize and conduct information exchange seminars and workshops focussed on pipe fracture technology and to provide the overall program management function for the program. On a regular basis, the members of the IPIRG Technical Advisory Group (TAG) met with researchers from Battelle. There were a total of seven TAG meetings scheduled during the course of the IPIRG-2 program. These TAG meetings provided a forum for the presentation of program progress and results which were scrutinized and reviewed by the members. Formal presentations by the TAG members, and informal exchange between members, provided a mechanism for the various members to share information. Associated with a number of these TAG meetings were round-robin workshops

and analyst's group meetings which further encouraged the free exchange of ideas through hands-on use of the analysis methodologies and presentations focused on particular technical issues.

SUMMARY OF RESULTS FROM THE IPIRG PROGRAMS

Although there are numerous results from these programs, only the major ones are summarized in this paper. These results are summarized in four categories: (1) seismic loading effects on material properties, (2) piping system seismic loads, and (3) advances in elbow fracture evaluations, and (4) "real" piping system response.

Seismic Loading Effects on Material Properties

In current leak-before-break (LBB) and in-service flaw evaluation criteria, the fracture evaluations typically use a quasi-static stress-strain curve and J-R curve data. Seismic loading, however, is both dynamic and cyclic in nature. Prior to the IPIRG programs, no efforts had been undertaken to determine if using quasi-static material properties was appropriate.

During the IPIRG-1 program, quasi-static and dynamic tensile tests were conducted. The dynamic tensile tests were conducted at rates of 1/s and 10/s. These rates were thought to bound the strain rates that may occur in a seismic event. In addition, quasi-static and dynamic monotonic loaded C(T) tests were conducted. These tensile and C(T) tests were conducted on a variety of ferritic and austenitic nuclear piping steels. All tests were conducted at 288 C (550 F) and are described in Reference 5.

Also during the IPIRG-1 program, a series of circumferential through-wall-cracked pipe fracture experiments were conducted with the intent of investigating the separate effects of dynamic and cyclic loading on the fracture toughness of typical ferritic and stainless steels. These experiments were conducted within IPIRG-1 Subtask 1.2, and are described in detail in References 6 and 7.

Subsequently in the IPIRG-2 program, additional data were developed to; (1) determine the effect of dynamic loading on a wider range of ferritic pipe steels, (2) to see if the effects found in the cyclic through-wall-cracked pipe test can be reproduced in C(T) tests, and (3) investigate the effects of R-ratios between 0 and -1 on the cyclic J-R curves. All data were determined at 288 C (550 F). At this point in time, some additional weld cyclic C(T) tests are being conducted, but the general trend of the rest of the data is as follows.

(1) The austenitic materials had a slight increase in their stress-strain curves at the higher strain rates. Hence, for pipe fracture analyses, the quasi-static stress-strain curves can be used.

(2) For the ferritic pipes evaluated, dynamic effects on the stress-strain curves were found to affect all 10 ferritic pipe materials evaluated. There was a 10 to 30 percent drop in the ultimate strength at strain-rates of 1/s to 10/s when compared to the quasi-static test at 10^{-5}/s. The important question to be addressed for ferritic materials is what is the effective strain rate for a cracked pipe under seismic loading. This is important since pipe fracture analyses typically use tensile test data from one loading rate, i.e., viscoplastic calculations are not done. If the crack is large, then the strain rates in the uncracked pipe are low and only the net-section and crack tip areas experience higher strain rates. If the crack is smaller, then the uncracked pipe may

experience higher strains and hence strain rates. Pipe tests to date with large cracks show that the quasi-static stress-strain curve is appropriate to use, but it is unsure if this will also be true for short-crack, dynamic, ferritic pipe experiments where the strain amplitudes and strain rates will be higher. The detrimental higher strain-rate effects may be occurring closer to the crack tip, and therefore may be captured in the dynamic J-R curve.

(3) For the austenitic weld, aged cast stainless steel, and the ferritic weld evaluated, the J-R curves increased about 30 percent at loading rates comparable to a seismic event, i.e., about 0.2 seconds to crack initiation. This effect seems to be related to the quasi-static yield-to-ultimate ratio at the same temperature, see Figure 2.

(4) For ferritic base metals at dynamic rates, the J-R curve was equal to or lower than the quasi-static J-R curve. The sensitivity of the material to dynamic strain aging (DSA) seemed to be the cause of this effect. This effect was initially investigated using the Short Cracks program DSA screening criteria[8], where the trends of the ratio of the quasi-static-to-dynamic J-R curves seemed to be related to the ratio of the Brinell hardness at high temperature to room temperature, see Figure 3. Interestingly, with the existing data there also seems to be a trend of the dynamic-to-quasi-static J-R curves as a function of the yield-to-ultimate strength of the material at the C(T) test temperature, see Figure 2. At this time, it is not certain if the trend in Figure 2 for the ferritic steels is an artifact of the available data, or indeed is universally correct. The implication of the trend in Figure 2 with yield-to-ultimate strength ratios is that for future plants, it is better to specify ferritic steels with higher yield-to-ultimate strength ratios. This trend should be validated for new material applications.

(5) The effect of cyclic loading was to decrease the J-R curve if the loading was fully reversed, i.e., R=-1. This was true for an A106 B and two TP304 stainless steel base metals investigated. Figure 4 shows that there seems to be a trend with yield-to-ultimate strength ratios, and the trend holds for both pipe and C(T) specimens. Separate stainless steel and ferritic steel weld cyclic C(T) tests are in progress. If the yield-to-ultimate strength ratio trend is correct, then the weld metal specimens should show lower damage to cyclic loading than the base metals.

(6) The effects of the R-ratio on the J-R curve appears to saturate to a minimum value at an R-ratio of -1. At R=0, there is negligible effect, i.e., equal to the monotonic J-R curve. The transition of the J-R curve from R= 0 to -1 appears to be sensitive to the material toughness. For instance, for the tough stainless steel, C(T) test results showed that the J-R curves started to drop from the monotonic J-R curve level at R=-0.8, whereas for a lower toughness A106 B carbon steel, the start of the drop in the cyclic J-R curve was at R=-0.6. Data on an even lower toughness material from a separate program at Battelle showed that this drop of the cyclic curve from the monotonic J-R curve occurred at an R-ratio between 0 and -0.3. Figure 5 shows the expected trends for the cyclic J-R curves at different R-ratios.

(7) Separate metallographic studies on cyclically loaded C(T) specimens showed that compressive loads flattened the voids ahead of the crack tip, which would be sharper and link together easier during subsequent tensile loading. Additionally, the compressive loads plastically deformed the crack-tip material. The void flattening and compressive crack-tip plastic strains vary as a gradient from the crack tip, hence there are two important parameters; (1) the

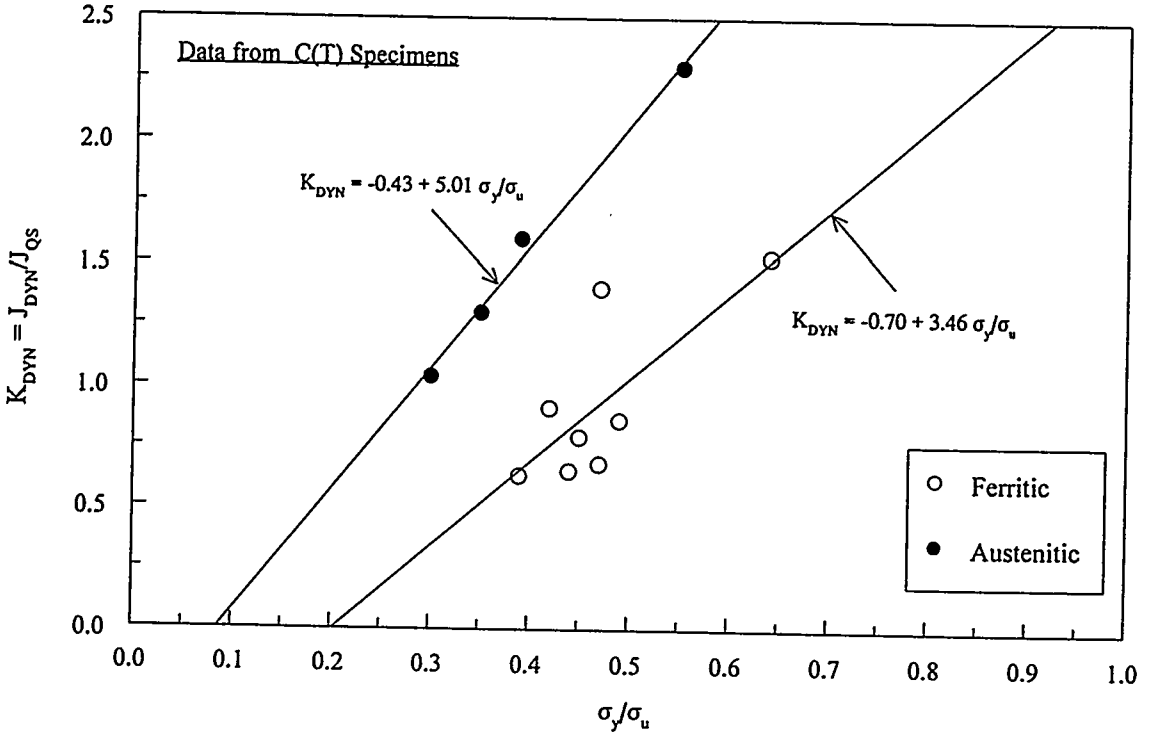

Figure 2 Ratio of dynamic to quasi-static J_{Ic} values versus quasi-static yield-to-ultimate strength (monotonic loading at 288 C for both C(T) and tensile specimens)

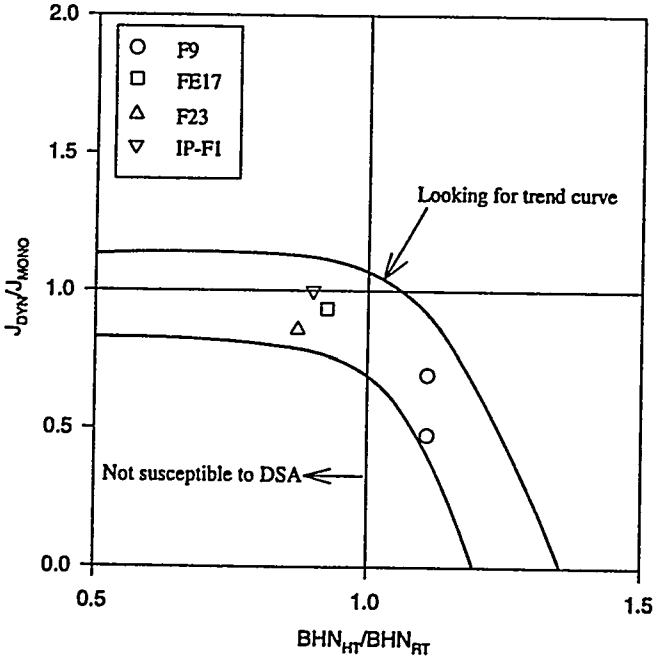

Figure 3 Ratio of ferritic pipe steel dynamic to quasi-static J_{Ic} values versus Brinell hardness ratio (monotonic loading at 288 C for C(T) specimens)

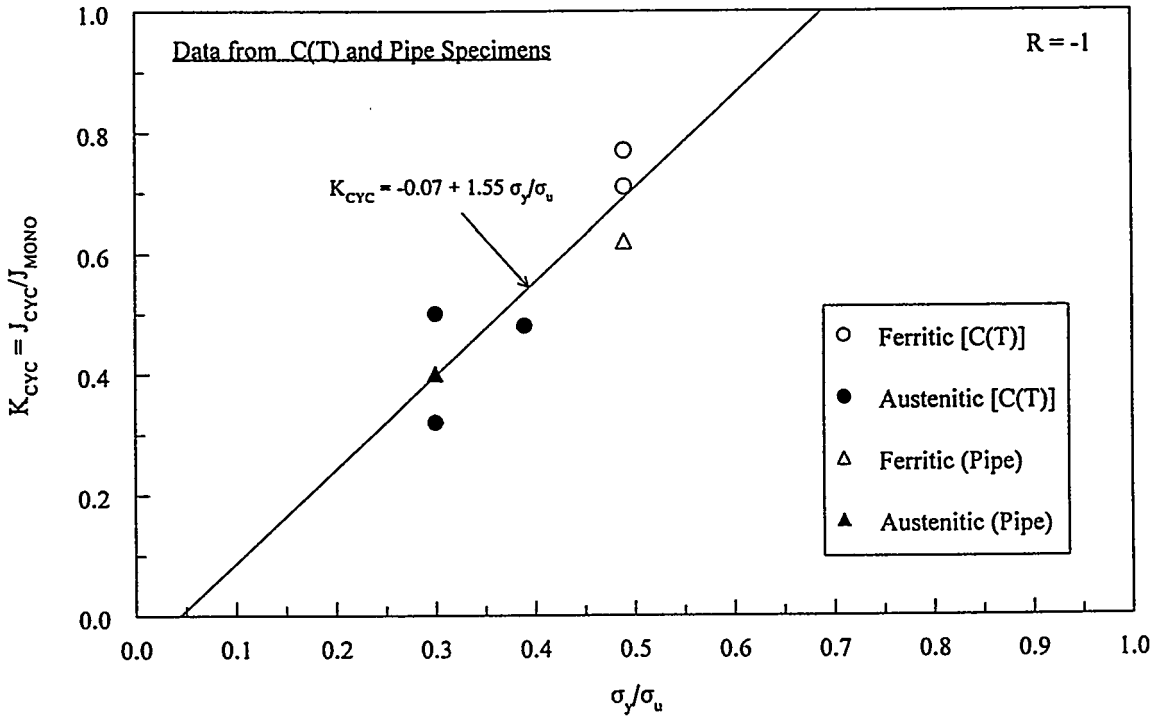

Figure 4 **Ratio of R=-1 J_{Ic} values to monotonic J_{Ic} values versus quasi-static yield-to-ultimate strength (All tests at 288 C)**

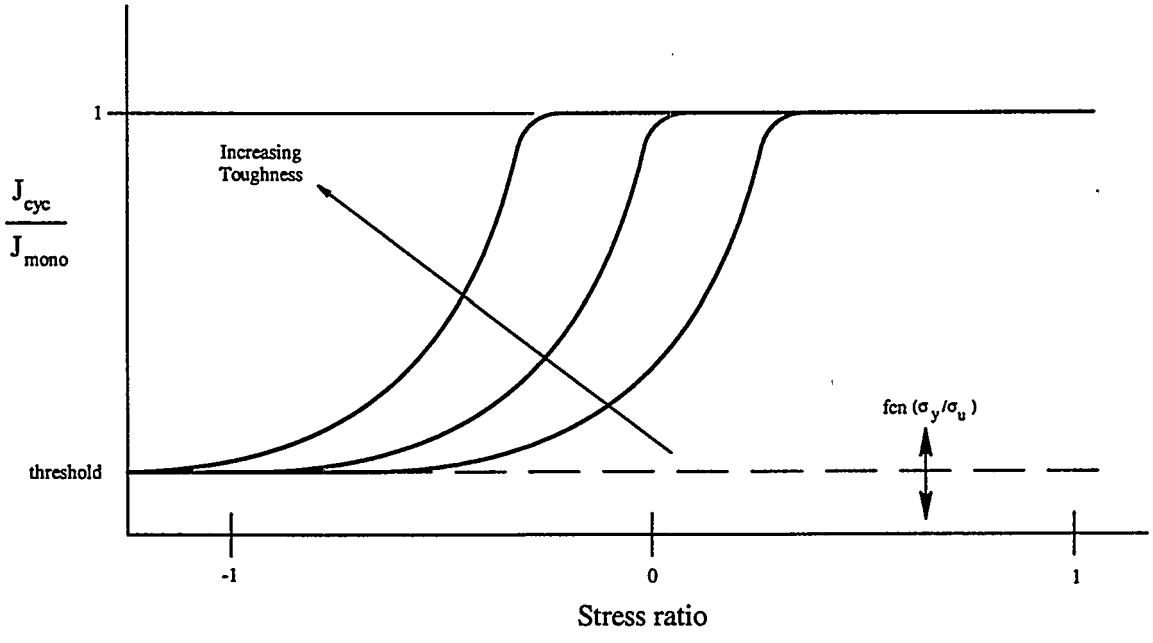

Figure 5 Schematic of the effect of R-ratio on the cyclic J-R curve

increment of crack growth between cyclic unloadings or cyclic plasticity prior to crack growth, and (2) the R-ratio.

Piping System Seismic Loads

During the IPIRG-1 program, the pipe system experiments were conducted with single-frequency loading where the excitation frequency was typically about 85 percent of the first natural frequency of the pipe system. In this way, there were pressure stresses, thermal expansion stresses, inertial stresses and seismic anchor motion stresses. The bending stresses were all in one plane, and there were negligible torsion and dead-weight stresses. Experiments were conducted with circumferential surface cracks in a straight-pipe high-bending stress region of the pipe loop, see Figure 1. Higher strength carbon steel piping materials were used everywhere in the pipe loop except within a short distance near the crack location. In this way, the only plasticity that occurred was at the cracked pipe section. This test procedure minimized the cost to reuse the pipe loop for subsequent tests. The IPIRG-1 pipe experiments were conduced with cracks in the base metals of A106 Grade B pipe (CSBM), TP304 stainless steel (SSBM), and an artificially aged cast stainless steel pipe (ACS). There were also pipe system experiments with cracks in the center of a ferritic submerged arc weld (CSW) and an austenitic submerged arc weld (SSW). For each pipe, there was a companion quasi-static pipe experiment conducted with a similar crack size.

A key aspect in the reduction of the IPIRG-1 pipe test data was the comparison of the maximum loads from the pipe system and the quasi-static pipe experiments. Figure 6 shows a bar graph of the maximum loads and differentiates these loads into the different components, i.e., pressure induced

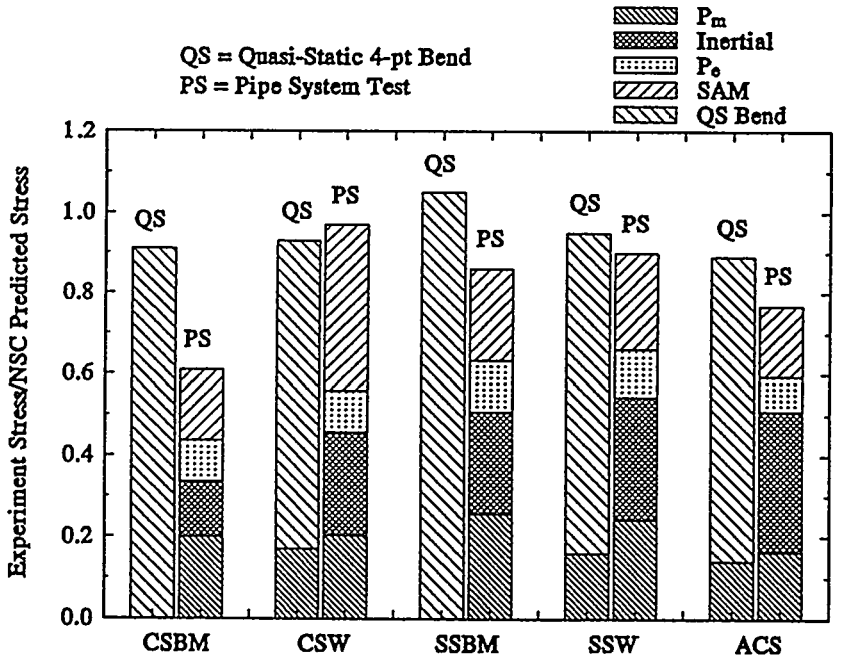

Figure 6 **Comparison of maximum loads for IPIRG-1 pipe system tests and companion quasi-static tests (CSBM=A106 B base metal, SSBM=TP304 base metal, ACS=aged CF8M, CSW=carbon steel SAW, SSW=stainless steel SAW)**

membrane loads (P_m), inertial, thermal expansion (P_e), seismic anchor motion (SAM), and the quasi-static bending loads (QS Bend). Note that in most cases, the pipe system maximum loads are lower than the quasi-static bend tests maximum loads. These data can be replotted by looking at a ratio of the maximum loads of the system experiments to the quasi-static experiments versus the quasi-static yield-to-ultimate strength ratio, see Figure 7. It can be seen in Figure 7 that there is generally a good

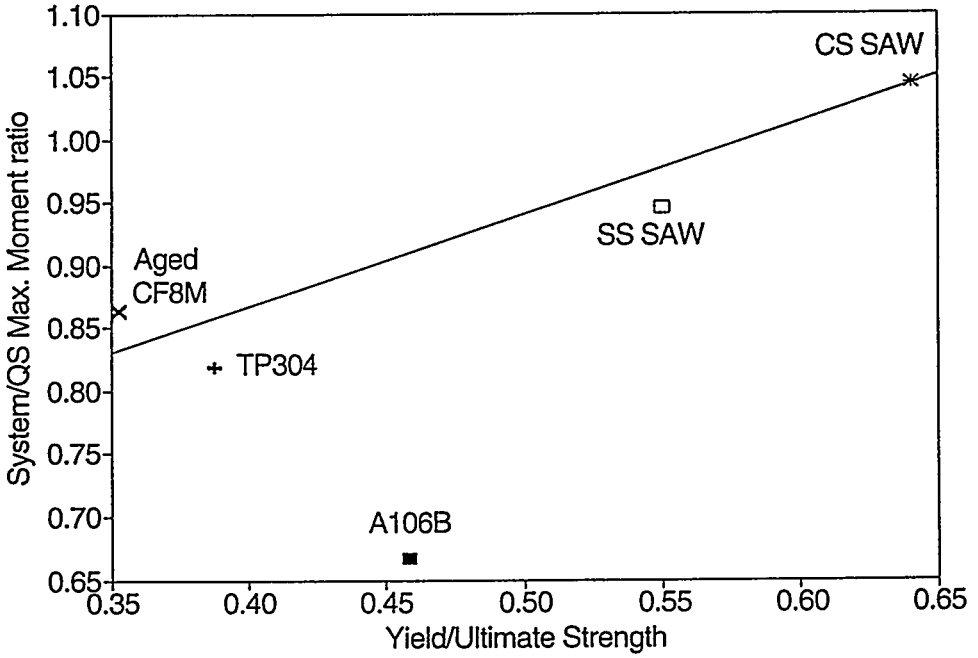

Figure 7 Ratio of IPIRG-1 pipe system maximum loads to the companion quasi-static pipe test maximum load versus quasi-static yield-to-ultimate strength (All data at 288 C)

correlation except for the ferritic base metal pipe experiment. For this material, the dynamic loading decreased the toughness, which was different behavior than the other pipe materials. Hence, these results coincide with the trends in the dynamic and cyclic J-R curve results as a function of yield-to-ultimate strength as shown earlier in Figures 2 and 4.

In the IPIRG-2 program, a seismic forcing function was used in several pipe system experiments. Great care was taken in designing the seismic forcing function. This design effort involved using a finite element model of a PWR and an artificial seismic ground motion acceleration time history with; (1) the USNRC Reg. Guide 1.60 horizontal and vertical spectra, (2) USNRC SRP 3.7.1 seismic design criteria for duration, spectra enveloping, frequency spacing, and minimum power spectral density, and (3) conformance with most of the requirements of nonmandatory ASME Section III Division 1 Appendix N. Assuming a pipe location in the plant, a corresponding moment-time history in uncracked pipe was determined. The basic time history was then scaled to get an SSE loading

(0.2g) and a loading that was predicted to cause surface-crack penetration (1.25g) using a nonlinear spring (cracked pipe) analysis (Ref. 9). Figures 8a, b, and c show the actuator displacement-time history, the uncracked pipe moment-time history at the proposed crack location, and the results of the cracked-pipe element in the dynamic analysis to scale the amplitude to get sufficient moment to initiate and grow the crack.

Seismic loading was applied in three IPIRG-2 pipe system experiments. Two of these were surface-cracked pipe experiments using the same A106 Grade B and TP304 pipe materials and flaw sizes used in the IPIRG-1 program. The third seismic pipe system experiment was a short through-wall-cracked pipe experiment in a different A106 B pipe. A quasi-static short through-wall-cracked pipe experiment was also conducted for comparison.

Figure 9a shows the cracked-section moment-time history from the IPIRG-2 stainless steel pipe system experiment. During the experiments, the local rotation of the pipe at the crack location was also recorded. The cracked-pipe-section moment versus the cracked-pipe-section rotation is shown in Figure 9b. Several interesting aspects can be noted in these figures. First, with this seismic time history, the crack initiated after the maximum load occurred. Increasing the amplitude of the seismic time history might have caused the two to be the same. In this case, the cyclic loading after the maximum load apparently caused the toughness to decrease and the crack to initiate and grow in low-cycle fatigue. From current LBB and in-service flaw evaluation criteria, the cyclic loading effects are not considered, so such analyses would expect that if the flaw survived the maximum load, then it would survive all subsequent cyclic loads. Secondly, it can be seen in the moment-rotation figure, that there were a few initial elastic cycles, followed by a large plastic cycle that caused the crack to blunt but not initiate. Hence, the crack effectively experienced monotonic dynamic loading with this seismic forcing function through the first large amplitude cycle.

Somewhat similar results occurred in the surface-cracked ferritic pipe seismic experiment. Figures 10a and 10b show the moment-time history and the cracked-pipe section moment-rotation curves. In this case, the ferritic pipe surface crack initiated and broke through the thickness during the first large amplitude cycle.

Comparing the seismic, single-frequency, and quasi-static pipe experiment results, the J-R curves were calculated directly from the pipe experiment moment-rotation data. For the case of the stainless steel base metal, for example, it was found that the single-frequency IPIRG-1 pipe experiment gave a much lower J_i value than the J_i values from the seismic pipe system or quasi-static pipe experiments. It is believed that the higher J_i value in the seismic pipe system experiment is apparently due to the seismic time history that was used. As shown in Figure 9b, the crack experienced some elastic loads, a large plastic load on one cycle, then subsequent cyclic loading. The first large plastic loading cycle effectively made the stainless steel behave as if it were monotonically loaded, hence there was not much cyclic damage.

It appears that the seismic time history used may have an effect on the cracked pipe behavior. As part of an IPIRG-2 round-robin effort, several members developed time-histories from the same

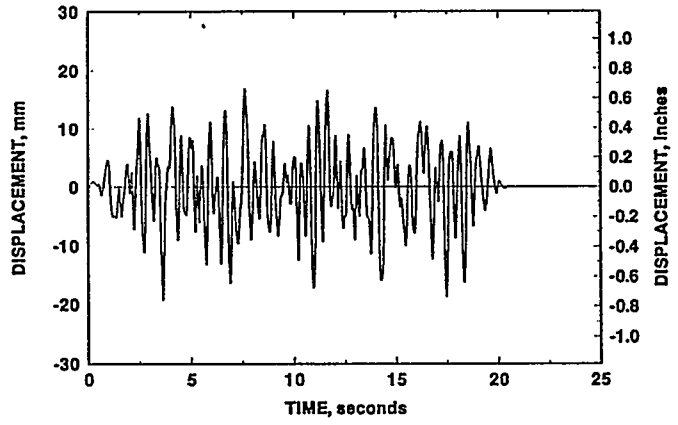

(a) IPIRG-2 actuator displacement-time history

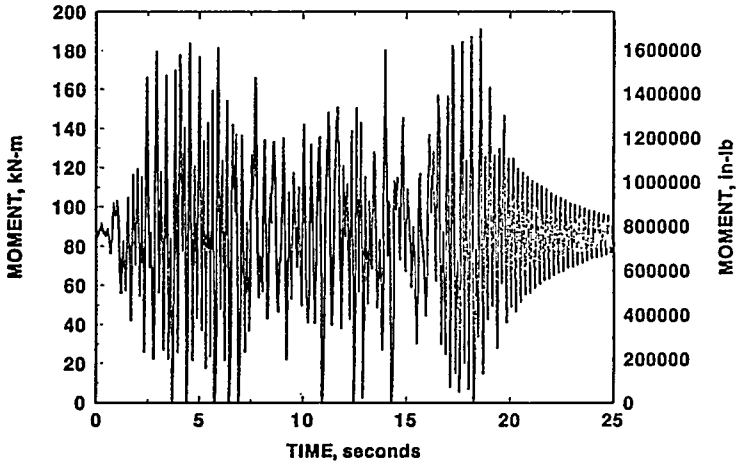

(b) Uncracked pipe moment-time history at the proposed crack location using 0.2 g base mat acceleration

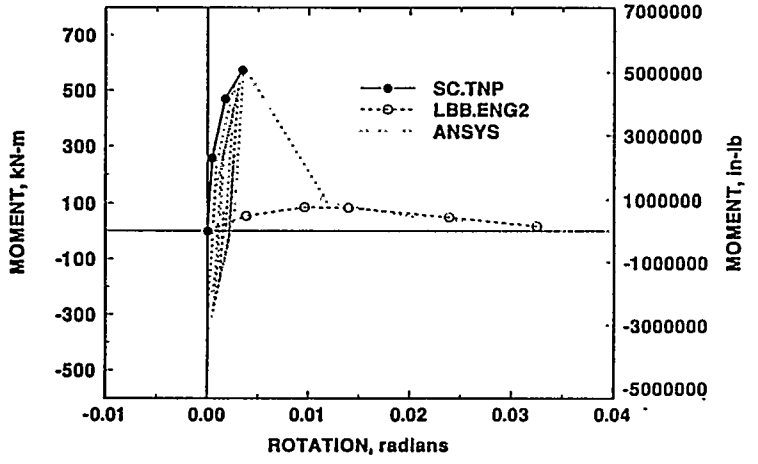

(c) Results of the cracked-pipe element analysis used to scale the actuator displacement-time amplitude to get the pipe to fail in the IPIRG-2 pipe loop

Figure 8 Steps used in determining the seismic forcing function used in the IPIRG-2 pipe system experiments

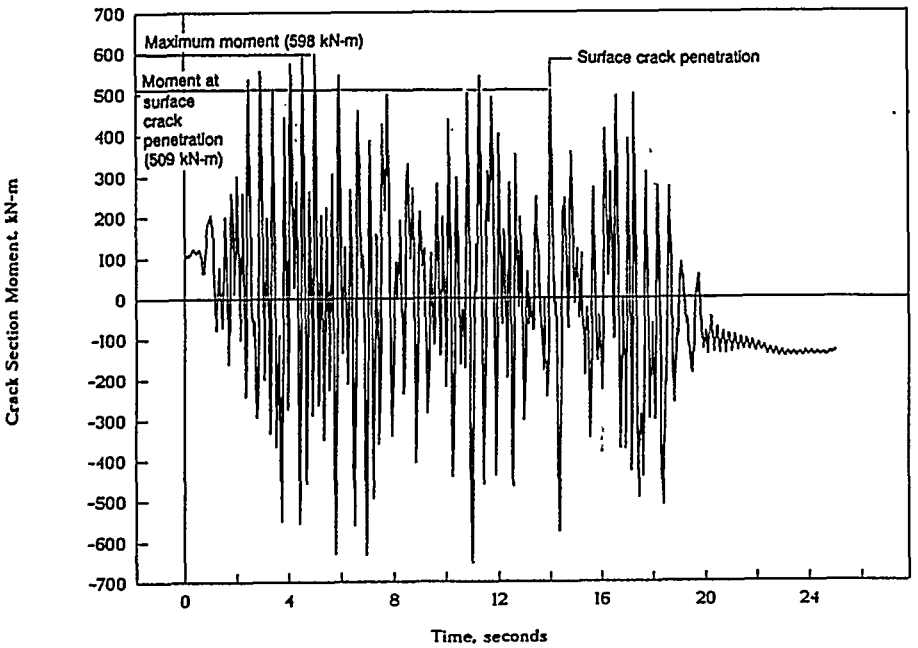

(a) Cracked-section moment-time history

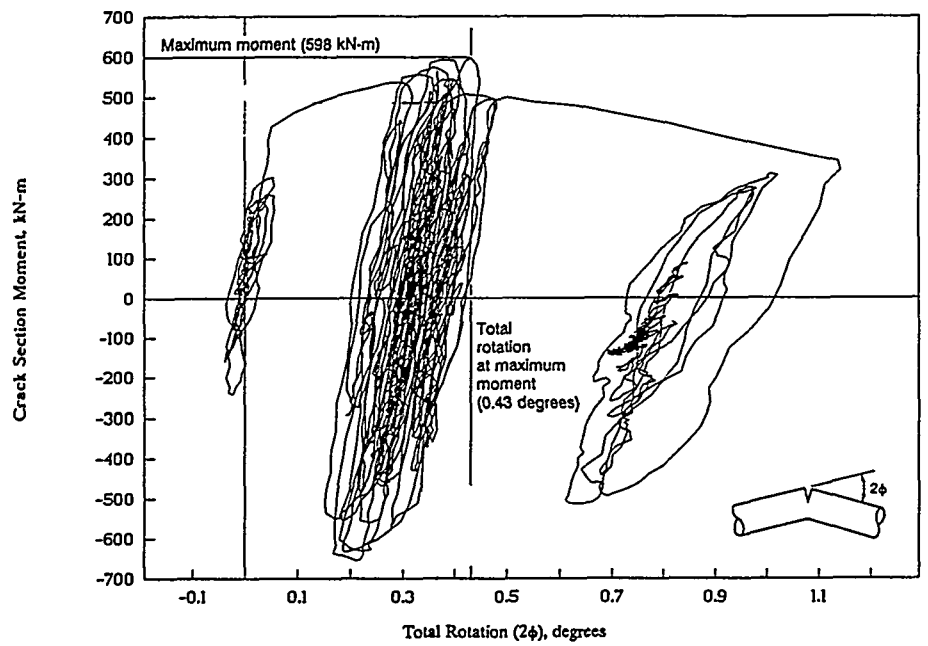

(b) Cracked-pipe-section moment versus the cracked-pipe-section rotation

Figure 9 **Results of IPIRG-2 Experiment 1-1 with seismic loading with an internal surface crack in TP304 stainless steel base metal**

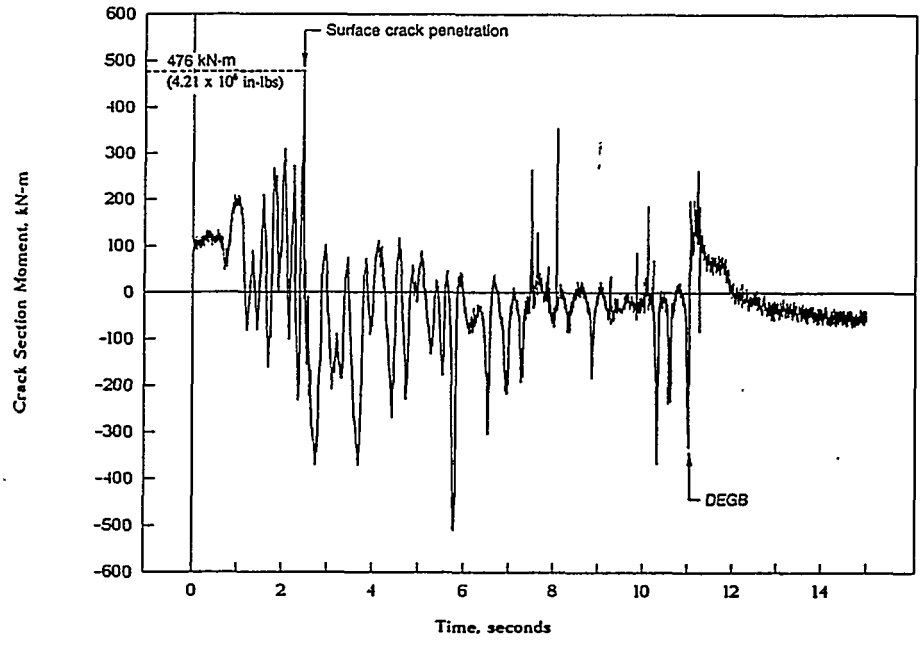

(a) cracked-section moment-time history

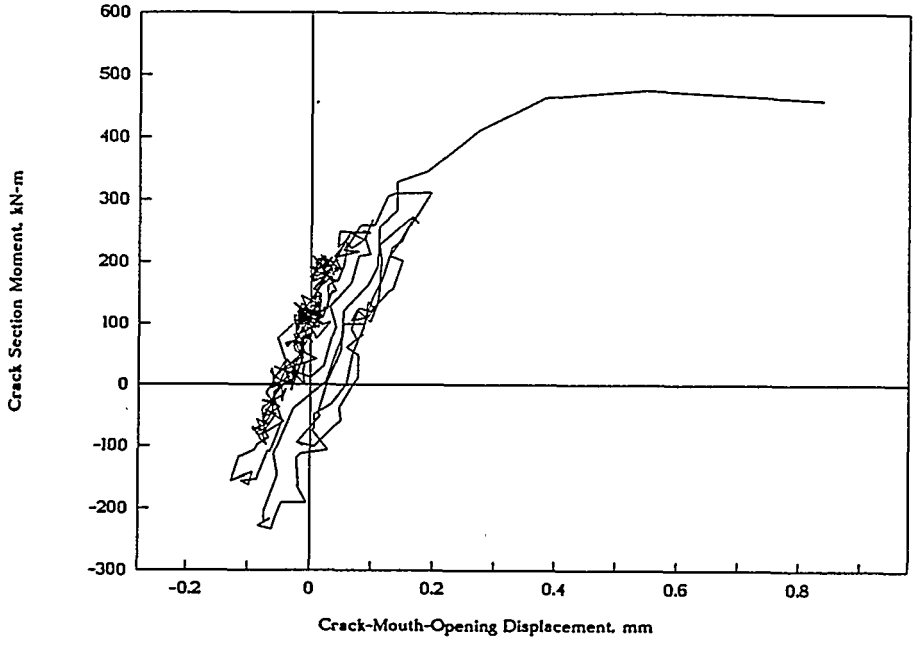

(b) cracked-pipe-section moment versus the center-crack-opening displacement

Figure 10 Results of IPIRG-2 Experiment 1-2 with seismic loading with an internal surface crack in A106 Grade B carbon steel base metal

response spectrum[10]. Figure 11 shows the results from several participants, where the displacement-time histories were all applied to Battelle's IPIRG pipe loop finite element model to determine the moment-time history at the crack location. Note that the time-history used in Figure 11c not only had a higher amplitude than the others, but there is a more gradual build up of the cyclic amplitudes to the first large amplitude cycle. Furthermore, the number of large amplitude cycles varies considerably in the different time histories. Therefore, we are not sure if the IPIRG-2 seismic time history represents a mean seismic behavior or not, but it certainly is not a lower bounding time history in terms of pipe fracture behavior.

Advances In Elbow Fracture Evaluations

The vast majority of prior piping integrity research dealing with critical flaw assessment methodologies has addressed the problem of cracks in straight pipe only. Although not as common as cracks in straight pipe, cracks have been found in elbows and other fittings within pipe systems. Current straight pipe elastic-plastic fracture mechanics and limit-load solutions have been used to analyze flawed fittings. However, their applicability for use on circumferentially and axially cracked elbows and other fittings has not been validated thoroughly. In this section, we describe efforts that are underway in the IPIRG-2 program, and as such represents a progress report.

As part of the IPIRG-2 program, the issues of fracture of elbows are being directly addressed through the development of engineering estimation methods for predicting crack growth and limit loads of surface-cracked elbows, and the validation of these methods with large-scale elbow fracture experiments. As an aid to understanding the problem, a database of existing elbow fracture experiments is being compiled. Also, comparisons are being made between existing straight pipe solutions, elbow limit-load solutions, and elbow fracture experiments, to critically assess the suitability of these existing analytical techniques for the prediction of fracture behavior of elbows.

Pipe Fitting Database Development

To properly document the existing fracture data for pipe elbows, a database is currently being compiled to help document the existing array of pipe test data that can be used to verify analytical approaches. To date, we have 33 documented experiments consisting of uncracked elbows and both circumferential and axial flaw orientations, in diameters ranging from nominal 6-inch to 16-inch. Additional data will be incorporated as they are acquired.

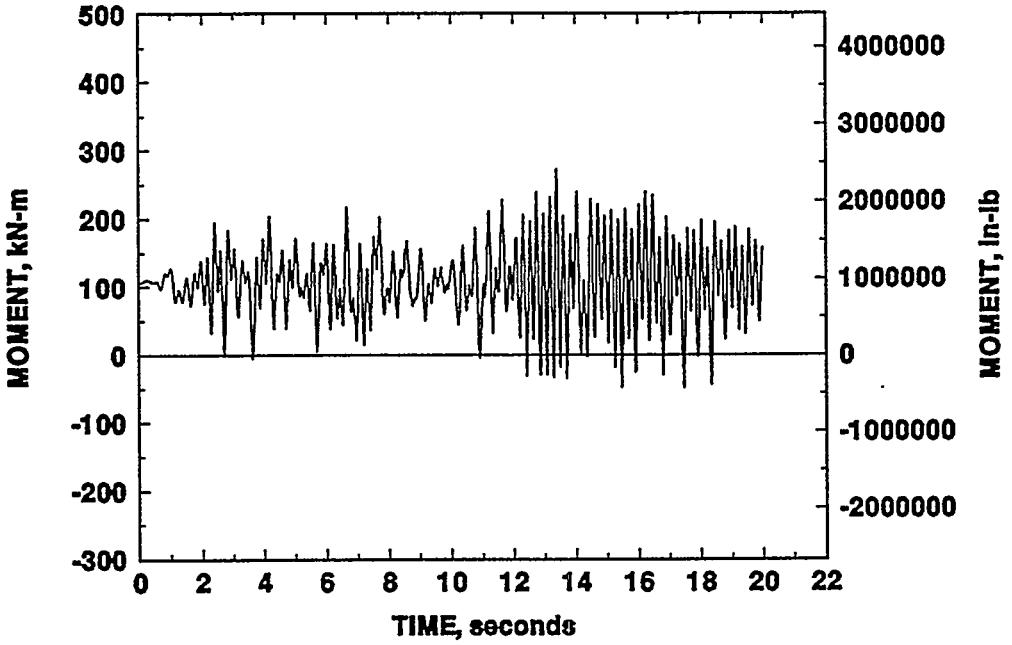

(a) IPIRG-2 moment-time history

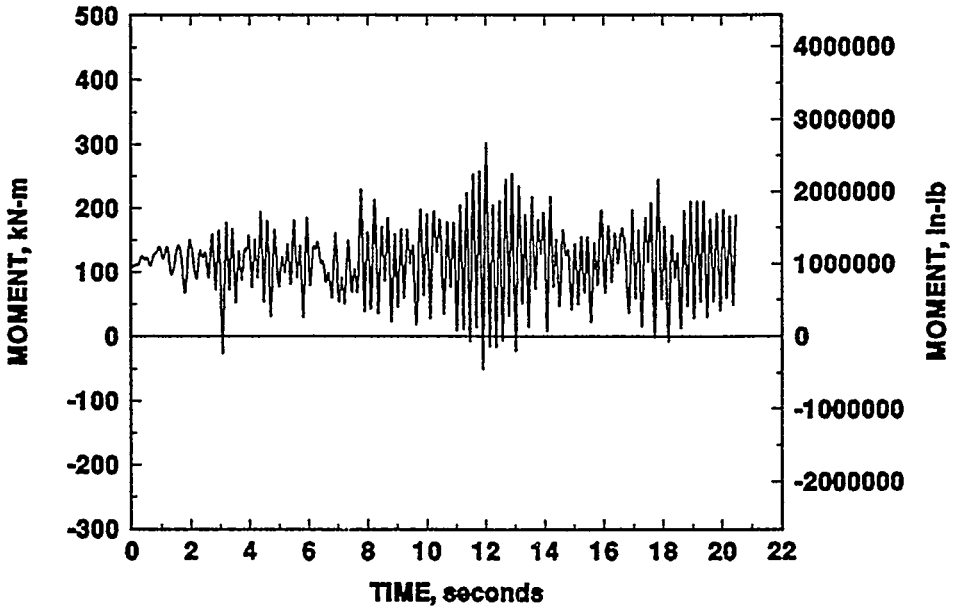

(b) Participant C solution

Figure 11 Comparison of moment-time histories developed from the same response-spectrum curve (0.5-percent damping and 0.2g)

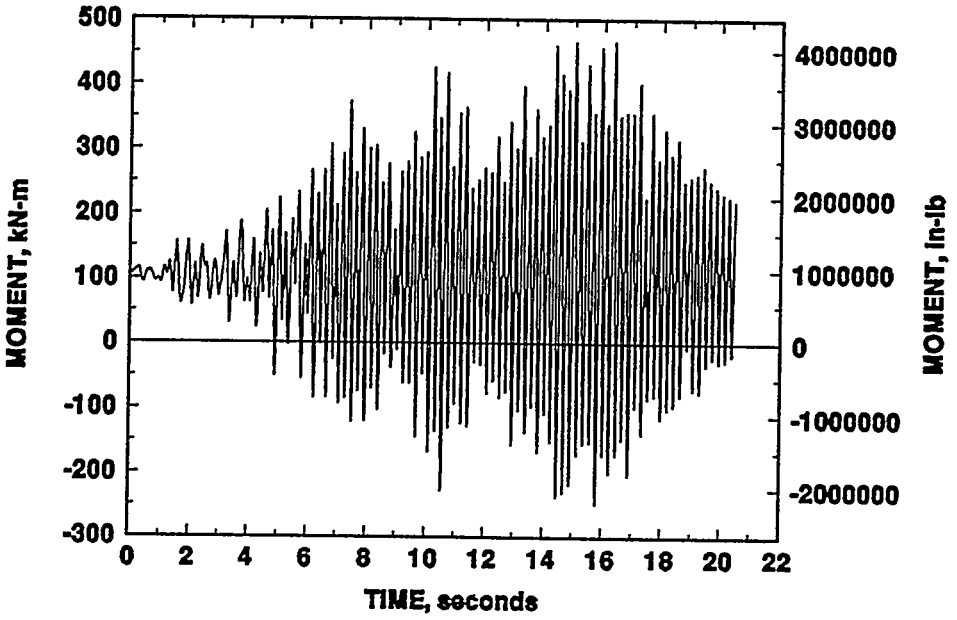

(c) Participant F-3 solution

Figure 11 Comparison of moment-time histories developed from the same response-spectrum curve (0.5-percent damping and 0.2g) (continued)

Comparison Of Existing Analysis Methods With Experimental Results

Limit-load solutions for flaws in straight pipe and elbows have been compared to experimental results to begin to assess the accuracy of these methods for predicting failure stresses for cracked elbows. Data for the case of a circumferential through-wall-cracked elbow are shown to demonstrate the range of accuracy for these solutions. Figure 12 shows data for such a crack loaded under in-plane bending with no internal pressure. For this case, the limit-load predictions give a fairly accurate prediction of the failure stresses for crack lengths larger than 20 percent of the circumference, i.e., $\theta/\pi=0.2$. Figure 13 shows data for a crack subjected to internal pressure with an additional applied moment. For this case, where the elbow has a short through-wall crack, the experimental failure stress was significantly lower than predicted by the straight pipe analysis.

J-Estimation Methods for Elbows

Following the spirit of the GE/EPRI estimation procedure of fracture parameters for circumferentially cracked straight pipes[13], estimation procedures were developed in the IPIRG-2 program for circumferentially and axially cracked elbows subjected to internal pressure and in-plane bending. The newly developed estimation procedures were restricted to 90-degree elbows. In the case of circumferentially cracked elbows, the crack was assumed to be an extrados, internal, constant depth surface crack with a total crack angle of 180 degrees. For axial cracks, the estimation procedure was developed for an internal, constant depth surface crack with a total crack angle of 30 degrees, located in the crown region of the elbow. These crack configurations were chosen to closely represent cracks

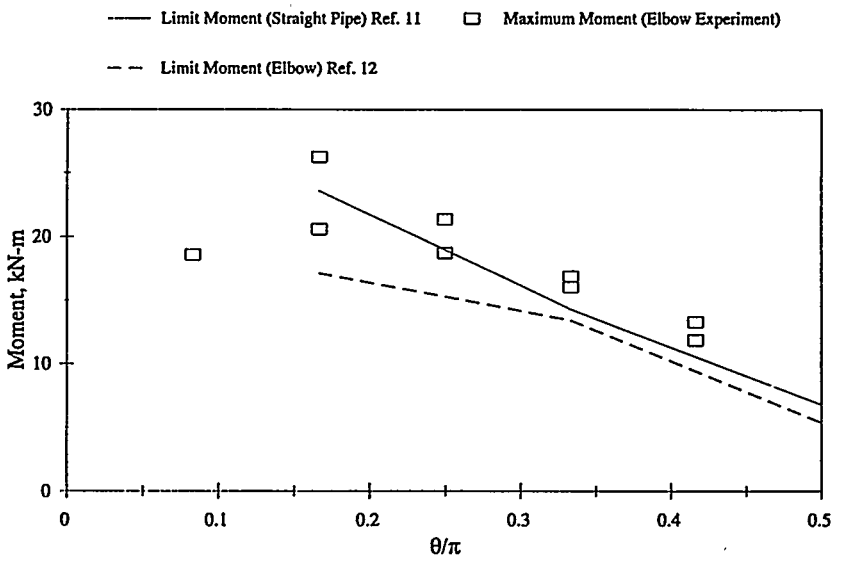

Circumferential Through-Wall-Cracked Elbow (90 degree, Extrados) under In-Plane Bending

(O.D=114.3mm, t=8.56mm, No Pressure)
(316L SS with YS=280MPa & UTS=410MPa)

Figure 12 Comparison of circumferential through-wall-cracked elbow bend tests available in the literature with limit-load solutions

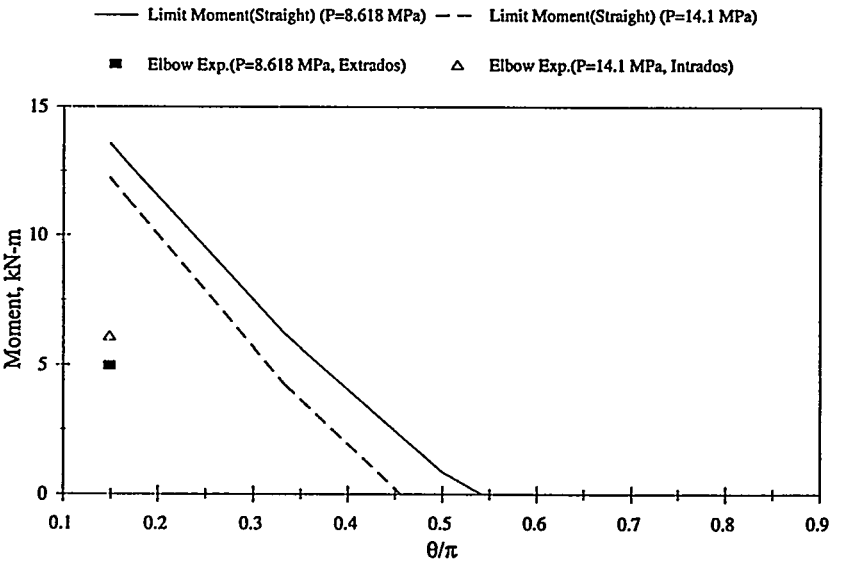

Circumferential Through-Wall-Cracked Elbow (Extrados) under Pressure - Burst Test

(O.D=114.3mm, t=3.81mm, Pressure)
(304LSS with YS=298MPa & UTS=564MPa)

Figure 13 Comparison of circumferential through-wall-cracked elbow pressure plus bend tests available in the literature with limit-load solutions

found in service. With these assumed configurations of cracks, "F" and "h" functions were developed for several R_m/t (mean radius to wall thickness) and several a/t (crack depth to wall thickness) ratios, as well as for several Ramberg-Osgood hardness coefficients, "n".

The analyses used a shell/line-spring finite element model, which has been proven to render quite accurate estimates of fracture parameters for cracked pipes in comparison with full three-dimensional finite element models. The applied internal pressure was obtained from allowable pressure values as given in Section III of the ASME Code, and by using an averaged S_m value for ferritic steels and austenitic stainless steels. Details of the developed estimation scheme will be presented in a future NUREG report.

Pipe Elbow Fracture Experiments

Four large-scale pipe fracture experiments using long-radius elbow test specimens are being conducted to generate data which will be used to provide validation and direction in the development of methods to predict critical crack growth and limit loads in pipe elbows. Two dynamic pipe system experiments and two companion monotonic experiments are being performed to investigate the complex interaction of loading conditions and system dynamics on pipe fracture behavior. The test elbows are 16-inch nominal diameter Schedule 100 long-radius elbows containing a circumferentially oriented internal surface crack centered on the extrados with a crack size approximately 66 percent deep and 50 percent of the elbow circumference in length. The elbows were manufactured from A106 Grade B and TP304 seamless straight pipe using typical hot-bending and heat-treatment processes. Material properties were also developed using specimens machined from elbows identical to the test elbows. All tests are performed at nominal pressurized water reactor conditions (PWR), i.e., 15.5 MPa (2,250 psi) pressure and 288 C (550 F).

The dynamic/cyclic experiments were conducted in the IPIRG pipe system. Specific details about the geometry, materials, boundary conditions, and finite element analysis of the pipe system can be found in other papers[9, 14]. The elbow test specimen was located at the Elbow 4 location, see Figure 1.

The dynamic pipe system experiments were loaded using a constant-frequency, increasing amplitude, displacement controlled sinusoidal waveform. The forcing function frequency used for the dynamic experiments, 3.95 Hz, is 90 percent of the first natural frequency of the pipe system. As a result of the loading history and PWR test conditions, the cracked section experiences a variety of stress components, i.e., thermal expansion, pressure induced membrane, and a mixture of displacement-controlled (seismic anchor motion) and inertial bending stresses.

Two companion monotonic experiments were performed to provide baseline data for the dynamic elbow experiments. The specimens were loaded using a displacement-controlled, increasing ramp waveform at a quasi-static rate of 5.08 mm/minute (0.2 inches/minute).

The data generated from these experiments will be used to improve the understanding of subcritical and critical crack growth behavior in pipe elbows. As example of the type of data collected from these experiments is shown in Figure 14. These data compare the applied moment versus crack-mouth-opening-displacement at the flaw centerline for the carbon steel dynamic and quasi-static experiments. The initial flaw depth was 80 percent of the pipe wall thickness for the quasi-static elbow and 84 percent for the dynamic elbow. However, a substantial difference can be seen in the

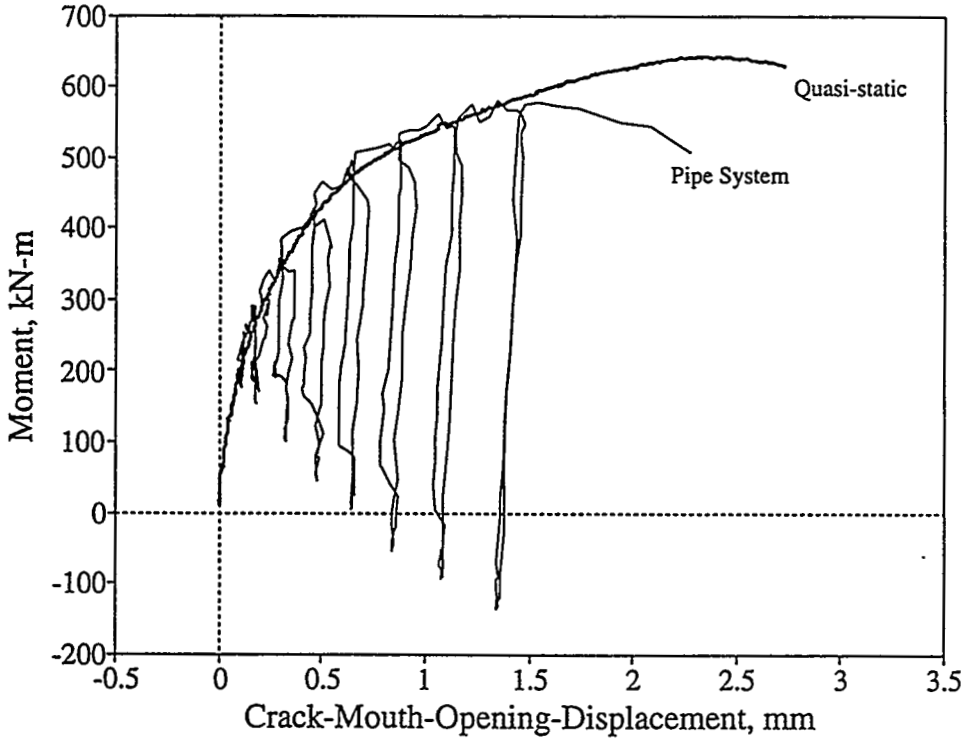

Figure 14 Comparison of IPIRG-1 carbon steel circumferential surface-cracked pressure plus bending elbow data

crack-mouth-opening displacement at surface crack penetration. This could be attributable to the difference in material toughness due to dynamic and cyclic loading effects. Direct comparison of experimental data can help determine the effects of dynamic loading on the fracture behavior of pipe fittings. These data can, in turn, be used to guide the development of improved estimation procedures.

"Real" Piping System Response

Several different factors concerning pipe system response are summarized next. These include understand:

- the basic behavior of cracked pipe under inertial loading,
- the significance of displacement-controlled stresses on pipe fracture,
- the possibility of an "instantaneous" DEGB, and
- the loading rate to be used for dynamic C(T) specimen testing.

Behavior of Cracked Pipe Under Inertial Loading

Prior to the IPIRG programs, little was understood about the dynamic fracture behavior of cracked pipe. As part of the IPIRG-1 program, separate-effect inertial pipe fracture experiments were conducted and analyzed[15]. These experiments were conducted on 6-inch nominal diameter stainless steel and A106 Grade B pipes. Through-wall and internal surface cracks were used. Tests had an internal pressure of 15.5 MPa (2,250 psi) and were at 288 C (550 F).

The results of the TP304 stainless steel surface-cracked pipe experiment are show in Figure 15. The moment-time and moment versus rotation of the cracked pipe section are shown in this figure. The moment-rotation data shows the surface-crack penetration and the subsequent through-wall crack growth. The significance of these test results are:

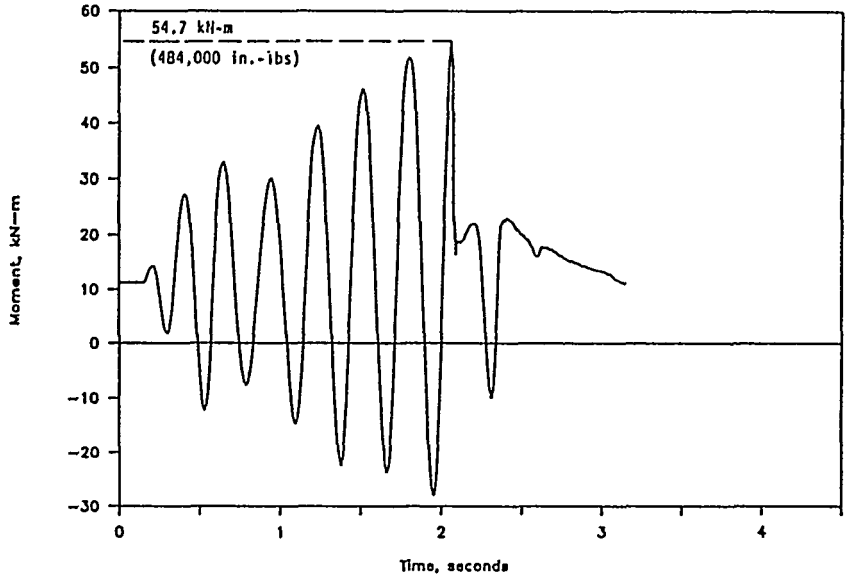

(a) moment-time data

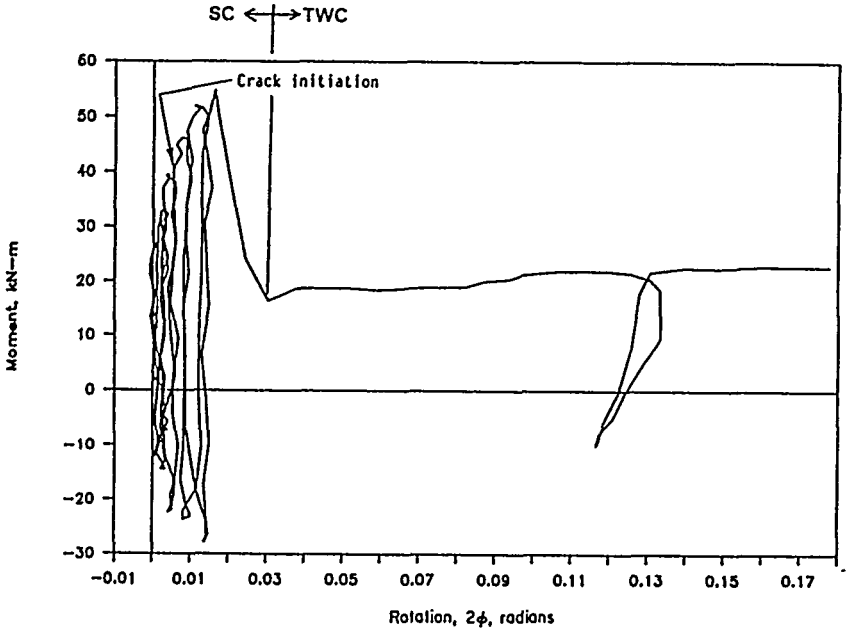

(b) moment-rotation data

Figure 15 IPIRG-1 inertially loaded TP304 surface-cracked pipe results

(1) Under inertial loading with dead-weight load and pressure loads, it was found that once maximum load was reached, then it only took a few cycles to get a DEGB. Hence, inertial loading here was closer to load-controlled conditions.

(2) The general shape of the moment-rotation curves were similar in both the inertially loaded and quasi-static pipe experiments. Hence, modelling of the crack could be done by a nonlinear spring that is calibrated by J-estimation scheme moment-rotation predictions. This was the basis of the modelling done for designing the IPIRG pipe system, and subsequently used in other programs to assess margins in full dynamic LBB analyses versus traditional LBB analyses[16].

Significance of Displacement-Controlled Stresses on Pipe Fracture

Displacement-controlled stresses, such as thermal expansion stresses and seismic anchor motion stresses, are frequently treated separately in fracture analyses than load-controlled (pressure, dead-weight, and inertial) stresses. For instance, in the R6 analyses thermal expansion and seismic anchor motion stresses are treated as load-controlled stresses; but in the ASME Section XI pipe flaw evaluation criteria, thermal expansion stresses are not included for stainless steel pipe and have a safety factor of 1.0 for ferritic pipe and stainless steel welds. Seismic anchor motion stresses are not specifically mentioned in the ASME Section XI pipe flaw evaluation criteria.

The reason the ASME pipe flaw evaluation criteria have different safety factors (or exclude P_e stresses altogether) is that at the time those criteria were made, it was assumed that the materials had sufficient toughness that these secondary stresses would be relieved by the crack deformation behavior. No pipe experiments existed at that time to validate that engineering judgement.

The IPIRG-1 pipe system experiments were the first to develop data to validate these engineering judgements. As shown in Figure 6, if you neglect the seismic anchor motion and thermal expansion stresses, the IPIRG-1 pipe system experiments have failure loads of 40 to 50 percent of the quasi-static pipe tests. Hence, these pipe system tests show that thermal expansion and seismic anchor motion stresses contributed equally to pipe fracture as did pressure and inertial stresses. The reasons why this occurred are; (1) the displacement at a **surface** crack is very small compared to the overall displacement of the pipe system, and (2) these were relatively large cracks where the entire pipe loop remained elastic, hence there was no opportunity for the uncracked pipe to yield and relieve the thermal expansion and seismic anchor motion stresses.

Consequently, for the case of surface cracks in pipe systems, the crack blunting behavior will not relieve the displacement-controlled stresses, and thermal expansion and seismic anchor motion stresses should be included as being equivalent to load-controlled stresses. If the stresses are above yield, then the uncracked pipe can reduce the elastically calculated stresses as noted in Reference 17. It should also be noted, that for a through-wall crack in the pipe system, there will be greater crack deformations, and the displacement-controlled stresses may be reduced by crack deformation. Also, if a surface crack is in a very short length of pipe, then there may be more relief of the secondary stresses by the crack opening, but calculations would have to be done to substantiate how short this pipe length needs to be. Reference 18 suggested that this is a very short pipe length.

Possibility of an "Instantaneous" DEGB

The assumption of an "instantaneous" double-ended guillotine break (DEGB) was made in early nuclear plant designs for the purpose of sizing emergency core cooling requirements. The DEGB criterion was subsequently applied to pipe support design, internal core support structures, etc.

The IPIRG pipe system experiments provided some insight to the duration of a fracture event under simulated seismic loading. The pipe system results showed the following:

(1) Typically, a crack would experience cyclic tearing, hence the decompression would take several seconds, not milliseconds.

(2) A DEGB could probably be produced in a single cycle if there was a deep surface crack more than 95-percent of the circumference. This conclusion is drawn from an IPIRG pipe system test, where the pipe was loaded until the crack was about 95 percent of the circumference at which point a DEGB occurred. The 95-percent crack length was determined to correspond to the saturation pressure induced failure load if the induced pipe bending is restrained in the Net-Section-Collapse analysis.

(3) Detailed nonlinear spring (cracked pipe) element analyses are capable of determining the crack velocities and time to produce a DEGB.

Loading Rate to be Used for Dynamic C(T) Specimen Testing

Since the ferritic steels can have fracture toughnesses that can be rate sensitive at LWR temperatures, the question of what rate to conduct C(T) testing at must be addressed. From the IPIRG program, the fastest time to reach crack initiation is that which would occur during a single large amplitude cycle as shown in Figure 10. Since the large amplitude cycles occur at close to the first natural frequency of the piping system containing the crack, the time to crack initiation corresponds to approximately one-quarter of the period of the first natural frequency. For the IPIRG pipe loop with the first natural frequency of 4.4 Hz, this time corresponds to 0.057 seconds.

CONCLUSIONS

The IPIRG programs advanced the state-of-the-art understanding of pipe fracture from a materials viewpoint, fracture mechanics analyses, and a basic understanding of the behavior of how real pipe systems behave. All of these factors will influence how LBB and pipe flaw evaluation will evolve in the future. The synergistic interactions of the IPIRG technical advisory group helped lead to these developments, and raised the overall understanding of all those involved.

ACKNOWLEDGMENTS

The IPIRG-2 Program is an international group program being coordinated by the U.S. Nuclear Regulatory Commission's Electrical, Materials and Mechanical Engineering Branch, Division of Engineering Technology of the Office of Nuclear Regulatory Research. We would like to express our appreciation to the IPIRG member organizations and their representatives for their interest and support throughout this program. We would also like to express our appreciation to the other

members of the Battelle IPIRG team who contributed to the work described in this paper. Finally, we would like to thank Mrs. V. Kreachbaum for her assistance in preparing this document.

REFERENCES

(1) R. A. Schmidt, G. M. Wilkowski, and M. Mayfield, "The International Piping Integrity Research Group (IPIRG) Program--An Overview", SMiRT-11 Proceedings, August 1991, Paper G23/1.

(2) Wilkowski, G. M., and others, "Degraded Piping Program - Phase II", Summary of Technical Results and Their Significance to Leak-Before-Break and In-Service Flaw Acceptance Criteria, March 1984-January 1989, by Battelle Columbus Division, NUREG/CR-4082, Vol. 8, March 1989.

(3) Hopper, A., Mayfield, M., Olson, R., Scott, P. and Wilkowski, G., "Overview of the IPIRG-2 Program - Seismic Loaded Cracked Pipe System Experiments," 13th SMiRT Conference, August 1995.

(4) Wilkowski, G. M. and others, "Short Cracks in Piping and Piping Welds," Seventh Semiannual Report, NUREG/CR-4599, Vol. 4, No. 1, April 1995.

(5) Marschall, C. W., Landow, M., and Wilkowski, G. M., "Loading Rate Effects on Strength and Fracture Toughness of Pipe Steels Used in Task 1 of the IPIRG Program", NUREG/CR-6098, October 1993.

(6) Scott, P., Kramer, G., Vieth, P., Francini, R., and Wilkowski, G., "The Effect of Dynamic and Cyclic Loading During Ductile Tearing on Circumferentially Cracked Pipe -- Experimental Results", ASME PVP Vol. 280, June 1994, pp 207-220.

(7) Wilkowski, G., Kramer, G., Vieth, P., Francini, R., and Scott, P., "The Effect of Cyclic Loading During Ductile Tearing on Circumferentially Cracked Pipe -- Analytical Results", ASME PVP Vol. 280, June 1994, pp 221-240.

(8) Marschall, C. W., Mohan, R., Krishnaswamy, P., and Wilkowski, G. M., "Effect of Dynamic Strain Aging on the Strength and Toughness of Nuclear Ferritic Piping at LWR Temperatures," NUREG/CR-6226, October 1994.

(9) Olson, R., Wolterman, R., Scott, P., Krishnaswamy, P., and Wilkowski, G., "The Next Generation Methodology for Cracked Pipe System Subjected to Dynamic Loads", ASME PVP Vol. 275-1, June 1994, pp 159-172.

(10) Rahman, S., Olson R., Rosenfield, A., and Wilkowski, G., "Summary of Results from the IPIRG-2 Round-Robin Analyses", NUREG/CR-6337, in press.

(11) Kanninen, M. F., Broek, D., Marschall, C. W., Rybicki, E. F., Sampath, S. G., Simonen, F. A., Wilkowski, G. M., "Mechanical Fracture Predictions for Sensitized Stainless Steel Piping with Circumferential Cracks", Final Report, EPRI NP-192, September 1976.

(12) Griffiths, J. E., "The Effect of Cracks on the Limit Load of Pipe Bends Under In-Plane Bending: Experimental Study", Intl. J. Mechanical Sciences, Vol. 21, 1979, pp 119-130.

(13) Kumar, V., and German, M., "Elastic-Plastic Fracture Analysis of Through-Wall and Surface Flaws in Cylinders", EPRI report NP-5596, January 1988.

(14) Scott, P., Olson, R., and Wilkowski, G., "The IPIRG-1 Pipe System Fracture Tests -- Analytical Results", ASME PVP Vol. 280, June 1994, pp 153-165.

(15) Scott, P. M., Wilson, M., Olson, R., Marschall, C., Schmidt, R., and Wilkowski, G., "Stability of Cracked Pipe Under Inertial Stresses - Subtask 1.1 Final Report", NUREG/CR-6233, Vol. 1, August 1994.

(16) Olson, R., Wolterman, R., and Wilkowski, G., "Margins for Dynamic FEM Analysis of Cracked Pipe Under Seismic Loading for the DOE New Production Reactor", ASME PVP Vol. 280, June 1994, pp 119-134.
(17) Krishnaswamy, P., Ghadiali, N., and Wilkowski, G., "An Assessment of Proposed Changes in ASME Section III Allowable Stresses on the Critical Flaw Size of Piping," 13th SMiRT Conference, August 1995.
(18) G. M. Wilkowski and G. Kramer, "An Energy Balance Approach to Estimate the Initiation and Arrest of Ductile Fracture Instability in Circumferentially Cracked Pipe", ASME Special Technical Publication, Vol. 167, July 1989, pp 103-114.

Specialist meeting on LEAK BEFORE BREAK in Reactor Piping and Vessels
LBB95
Lyon, France, 9 - 11 October 1995

Leak before Break Behaviour of Austenitic and Ferritic Pipes Containing Circumferential Defects

W. Stadtmüller and D. Sturm,
MPA Stuttgart
Germany

1 Summary

In recent years several research projects have been carried out at MPA Stuttgart to investigate the Leak-before-Break (LBB) behaviour of safety relevant pressure bearing components. In this work the test pipes have for the most part been made from ferritic material. Current investigations involve piping sections of austenitic materials. The results presented below relate to pipes containing circumferential defects subjected to internal pressure and external bending loading. As regards the ferritic components an overview of the experimentally determined results is presented. The predictive capability of engineering calculational methods are presented by way of example. The investigational programmes currently underway are presented together with the testing techniques and the initial results.

2 Introduction

The Leak-before-Break (LBB) criterion is frequently called upon in proving the safety margin against catastrophic failure in pressure bearing components. For components containing postulated or actual defects it shows the dependence of the (critical) loading limit on the defect size in the form of so-called LBB curves. These are determined experimentally and/or by calculation for the type of defect having the form of a through-wall slit and represent the boundary curve between leakage and' "massive fracture", **Fig. 1**. The respective failure curves for surface defects or partial-penetration cracks may also be related to them (family of curves for constant defect depths a/t). For surface defects and a given bending moment and internal pressure, by definition no fracture will occur so long as the length at leakage remains smaller than the critical defect length given by the LBB curve for through-wall defects.

3 Results from completed investigational programmes

MPA Stuttgart has carried out, inter alia, three major research projects in the field of Leak-before-Break of safety-relevant pressure bearing components:

- Phenomenological Vessel Burst Tests (BV) /1, 2/
- Safeguard Programme for the Proof of Integrity of Components (AIB) /3, 4/
- Superheated Steam Reactor Safety Programme (HDR) /5/

Some of the most important results for pipes containing circumferential defects are:

- The definition of the through-wall slit curve as the boundary between leakage and fracture could be verified experimentally, **Fig. 2.** In no case did a "massive fracture" occur beneath the LBB curve, that is in the leakage region.

- The path of the Leak-before-Break curve for pipes is dependent on the notch impact energy of the pipe material, **Fig. 3.** In pipes of high impact energy material a large critical through-wall slit length is attained.

- As regards the load bearing capacity of pipes with circumferential defects, the effect of the internal pressure is frequently regarded as negligible as compared with that of the external bending moment. Depending on the pres-

sure level however, it has an effect on the onset of plastification in the plane of the defect and thus on the Leak-before-Break behaviour. An elevation of the internal pressure leads to a displacement of the LBB curve towards smaller critical slit lengths, **Fig. 4.**

- Several engineering calculational methods are available for the analytical determination of the LBB curve /6-8 among others/. They differ through the assumptions and boundary conditions introduced into the formulations. These must be known for the choice of a suitable method and should as far as possible cover the conditions of the case of application in question. The results of the two most common methods
  - the plastic limit load (PLL) concept /8 among others/
  - the local flow stress (FSC) concept /6, 7/ also called the moment method,

are compared by way of example, with those from experiments in **Fig. 5.** In the cases of application shown here, the plastic limit load concept, in accordance with the wording, describes the component behaviour of the variety of piping of tough material very well. Here, the flow stress concept led to a significant undervaluation of the load bearing capability; however in the case of piping material of low notch impact energy (KV = 50 J) it produced a good agreement between calculation and experiment. As expected, the low toughness component was overvalued by the plastic limit load concept, and thus assessed non-conservatively.

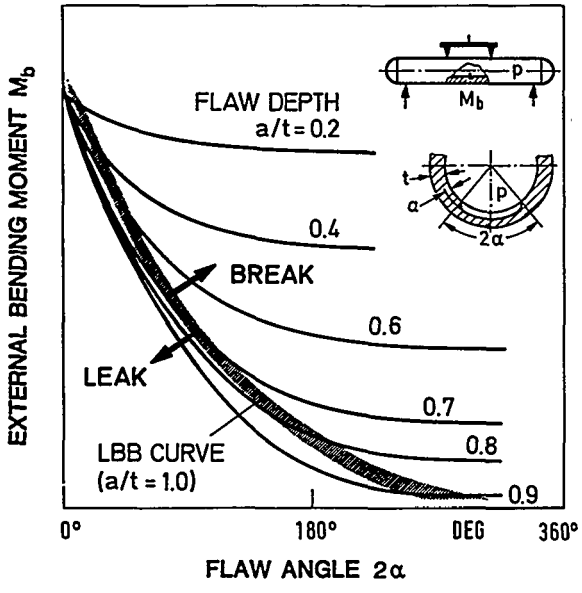

Fig. 1: Leak-before-Break diagramme

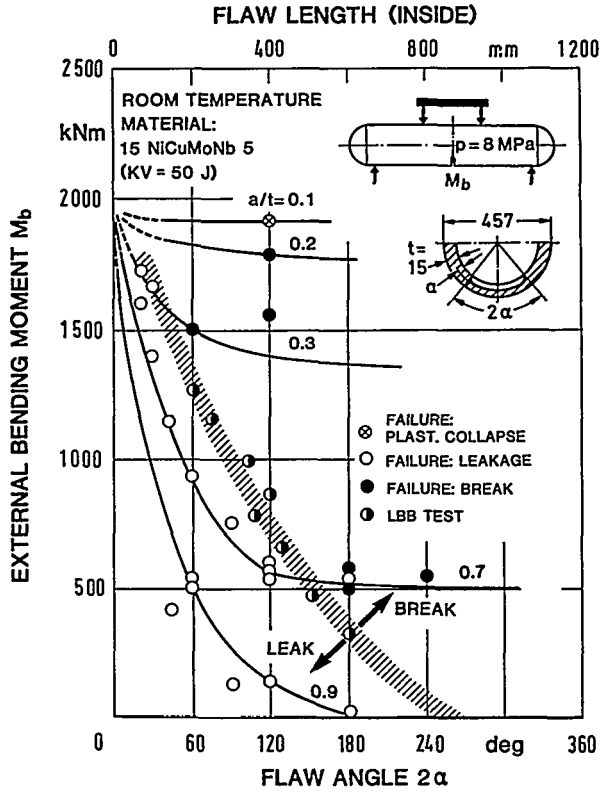

Fig.. 2: Load bearing capacity diagramme for feed water pipe (AIB-programme)

4 Current research projects

The majority of the research projects carried out thus far have dealt with pipes and components of ferritic materials. Generally, compared with piping of high toughness ferritic materials, the fracture mechanics behaviour of corresponding austenitic pipes is considered to be equal or superior. World-wide however, up to the present time only a few sys-

tematic programmes of investigation, in particular for the loading case with internal pressure, have been carried out for verification purposes. Further questions arise with regard to

- the effect of toughness gradients which can occur in the region of welded joints in welded components,
- the assessment of crack initiation with respect to the maximum load carrying capacity of austenitic components,
- the LBB behaviour with very large circumferential defects ($2\alpha \geq 180°$), particularly as the existing experiments and also analytical methods predominantly cover short defects ($2\alpha \leq 120°$).

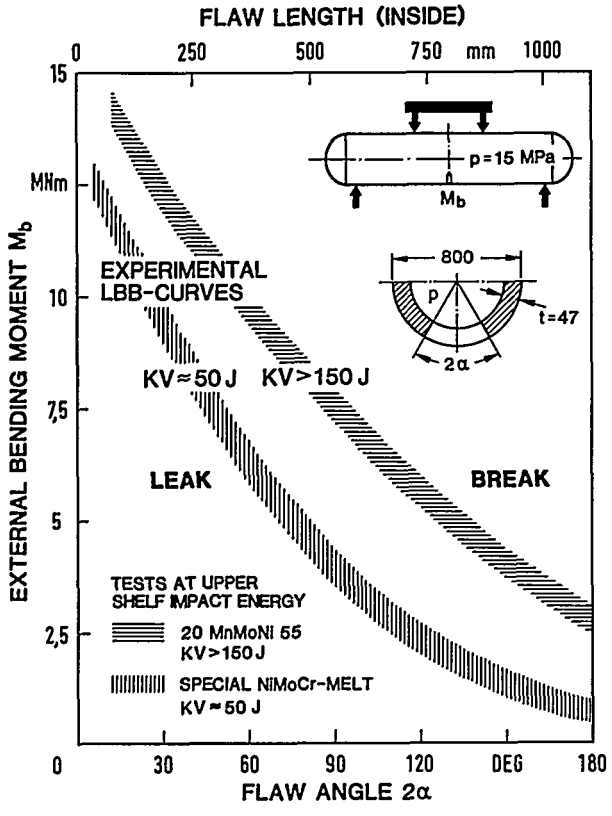

Fig. 3: Leak before Break curves as a function of the material toughness

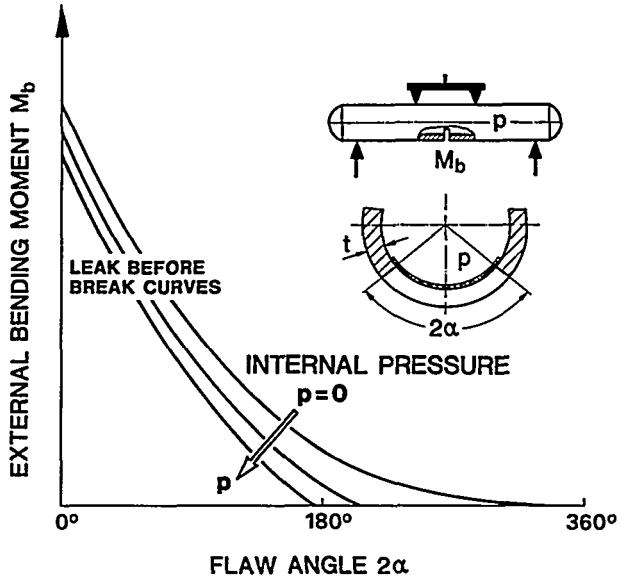

Fig. 4: Leak before Break curves as a function of internal pressure

In order to obtain answers to these questions two major research projects in this field are being conducted at MPA Stuttgart. One with the topic

„Contribution to the assurance of safety of piping of high toughness material using fracture mechanics"

is financed by the Federal Minister for Education, Science, Research and Technology (BMBF), Bonn , and the other with the topic

„Tests of austenitic components with analytical technology"

is being conducted under contract from the Association of Large Power Plant Operators (VGB).

4.1 Test programme

In total 25 tests using austenitic pipes are planned, **Fig. 6.** These are manufactured as thin-walled pipes of 219.1 mm outer diameter (O.D.) and 14.2 mm wall thickness (t) or thick-walled pipes of 331 mm diameter and 32 mm wall thick-

ness. The thinner-walled pipes are representative of Boiling Water Reactors and the thicker-walled ones of Pressurised Water Reactors.

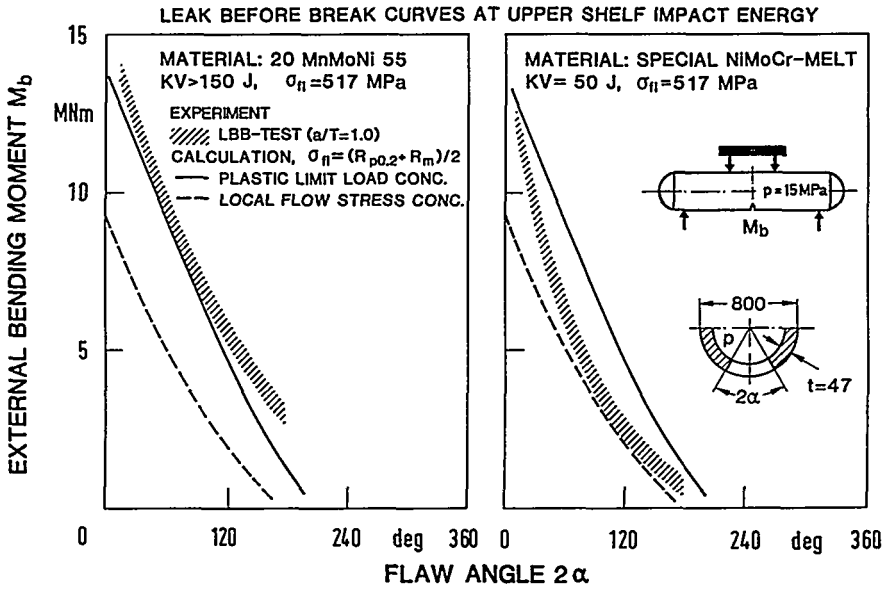

Fig. 5: Comparison between calculational determination and experiment (ferritic steel pipes)

The pipes are furnished with circumferential defects of various lengths up to a circumferential angle of $2\alpha = 270°$ and depths of up to through-wall slits. The defects are located in the base metal or in the case of the thinner-walled components, additionally in the weld metal of site-made circumferential welds. The defects were extended as fatigue cracks by cyclic loading.

RESEARCH PROJECTS

COMPONENT TESTS ON STAINLESS STEEL PIPES AND ANALYTICAL METHODS

COMPONENTS	CIRCUMFERENTIAL FLAWS		LOADING (ROOM TEMPERATURE)	GENERAL AIM
STRAIGHT PIPES X 10 CrNiTi 18 9 O.D. x t = 219.1 x 14.1 mm 20 TESTS	SURFACE FLAWS, THROUGH-WALL FLAWS $2\alpha \leq 270$ DEG FLAW WITH FATIGUE CRACK "AND" UNWEAKENED PIPES	BM WM (CIRCUMF. WELD)	AXIAL TENSION QUASISTATIC - DYNAMIC (STRAIN RATE ≤ 5/s) INTERNAL PRESSURE (7 MPa) + EXTERNAL BENDING MOMENT QUASISTATIC - CYCLIC	DEVELOPMENT OF AN ADVANCED PROOF OF INTEGRITY DETERMINATION OF - LOAD BEARING CAPACITY - DEFORMATION BEHAVIOUR - CRACK GROWTH - LEAK-BEFORE BREAK - CRACK OPENING - *TRANSFERABILITY* (SPECIMEN → COMPONENT)
STRAIGHT PIPES X 6 CrNiNb 18 10 O.D. x t = 331.2 x 32.1 mm 5 TESTS		BM	INTERNAL PRESSURE (16 MPa) + EXTERNAL BENDING MOMENT QUASISTATIC	

Fig. 6: MPA Stuttgart research projects in progress

Four thin-walled pipes are intended for tensile tests at different strain rates and the remainder for component tests under combined loading by internal pressure and superimposed external bending. The latter is applied quasi-statically and in two cases cyclically in the low cycle fatigue (LCF) range.

The tests with the thin-walled pipes make it possible to cover the whole range of the Leak-before-Break curve experimentally up to a defect length corresponding to $2\alpha = 180°$, **Fig. 7**. Parallel to this the failure curve is being established selectively for surface defects having depths of 0.5 and 0.7 x wall thickness (a/t = 0,5 or 0,7) with the defect located on the inner wall surface, for defects of length up to that corresponding to $2\alpha = 270°$.

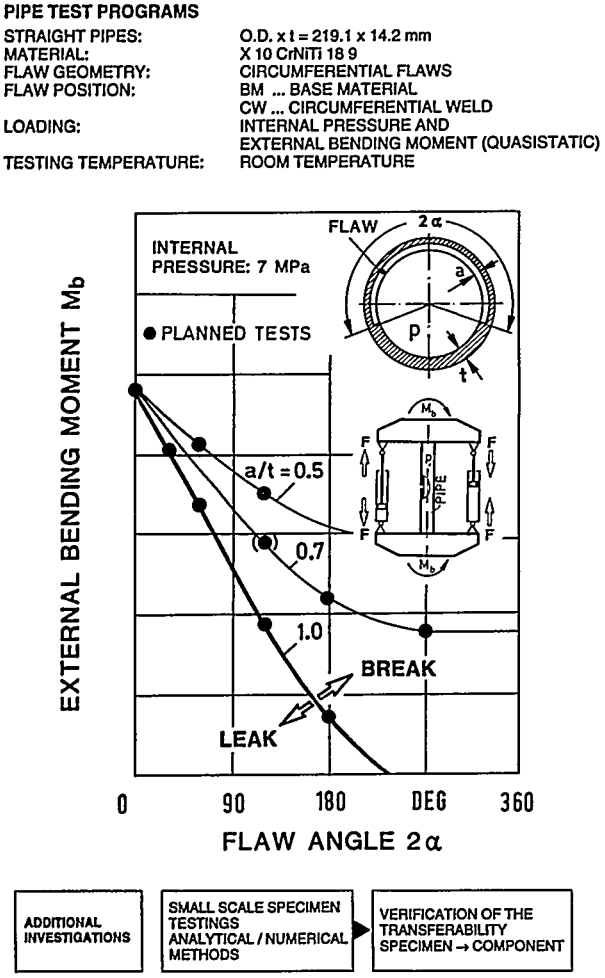

Fig. 7: Planned tests

SCHEME OF THE 2 MNm-BENDING DEVICE

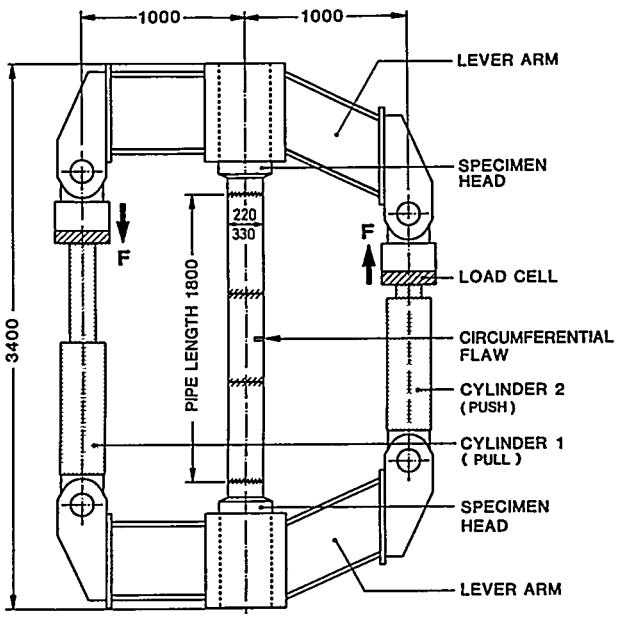

Fig. 8: 2 MNm-bending device

Parallel to the component tests, an exhaustive mechanical, and especially fracture mechanics, characterisation of the material is being carried out from the particular aspect of austenitic conditions. This serves as a basis for extensive analytical and numerical studies from which the transferability laws from small specimen to component can be checked and further developed to provide an advanced proof of integrity.

4.2 Testing equipment and test setup

For the performance of the pipe bend tests two similar bending devices which differed in their maximum bending moments of 200 kNm and 2 MNm respectively, were constructed, **Fig. 8**. The loading, which is virtually free of axial and

transverse forces, is generated by two double-acting hydraulic cylinders through two lever arms. The cylinders are connected to a servohydraulic unit which makes possible the application of the partial unloading procedure (compliance method) for the determination of stable crack growth during the test. As in the fracture mechanics test on small specimens the loading in the pipes is CMOD (crack mouth opening displacement) controlled. The relationship between pipe stiffness and defect-/crack size, on which the compliance technique rests, was determined in advance using finite element calculations.

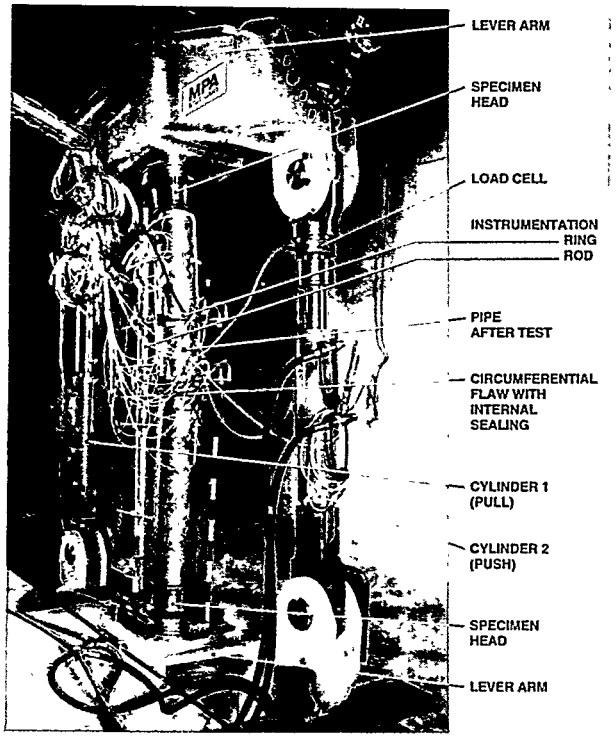

Fig. 9: 2MNm-bending device with pipe containing a through-wall defect after test

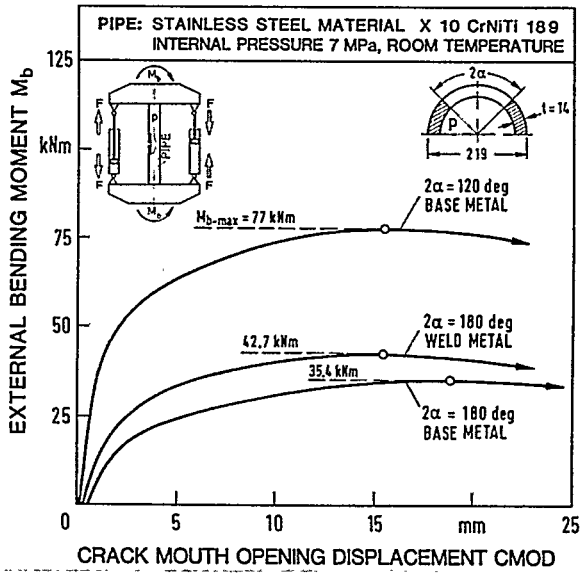

Fig. 10: External bending moment as a function of CMOD in case of stainless steel pipes containing through-wall defects

The instrumentation of a pipe with a 180° through-wall circumferential defect mounted in the 2 MNm-bending device is shown in **Fig. 9** following the test. For the internal pressure loading the defect was sealed on the pipe interior by a special technique before welding the pipe to the two specimen heads. The instrumentation of the pipes is carried out essentially each time for the determination of

- bending moment from the cylinder forces and also from pipe deformations in cross-sections remote from the influence of the defect
- bending deflection over the pipe length from the radial displacements and also from angular changes
- ovalisation in various cross-sections
- spread of plastic deformation in the pipe
- crack initiation and crack growth
- crack opening area.

5 Test results

From the example of the tested pipes having 120° or 180° circumferential through-wall defects it may be noted that the maximum bending moment was only attained after a large opening of the crack/defect. This holds both for pipes with defects in the base metal or in the weld metal, **Fig. 10**. The offset in the CMOD which can be observed is in reaction to the internal pressure loading which took place at the commencement of the test in the absence of external bending moment.

Fig. 11 shows the pipe with a 180 ° through-wall defect after the test. At maximum loading the pipe had yielded throughout in the region of the defect plane, as was also the case for the other pipes featured, whilst in cross-sections remote from the defect only elastic loading had occurred. The pipes kinked in the defect plane to a greater or lesser degree. Before the onset of crack initiation well developed blunting of the crack could be observed in all cases, **Fig. 12.** The fatigue crack was practically pulled into a U-shape and then tore with a wedge-like configuration.

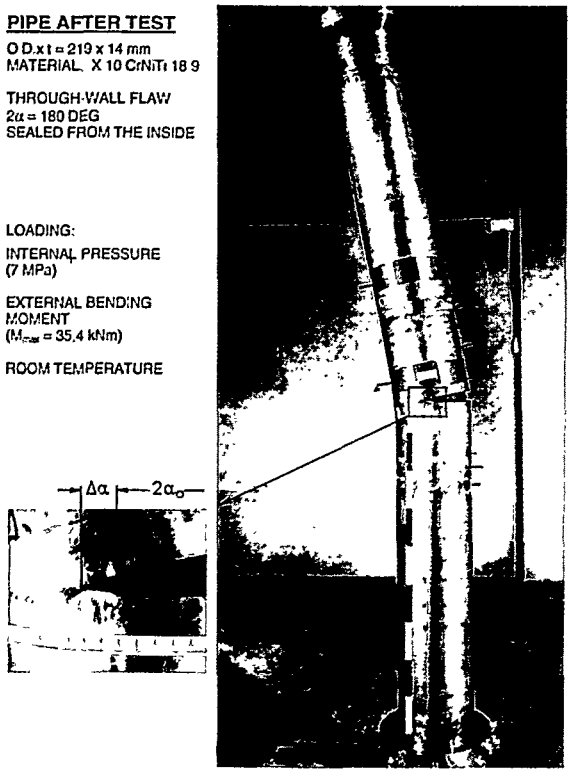

Fig. 11: Stainless steel pipe after test

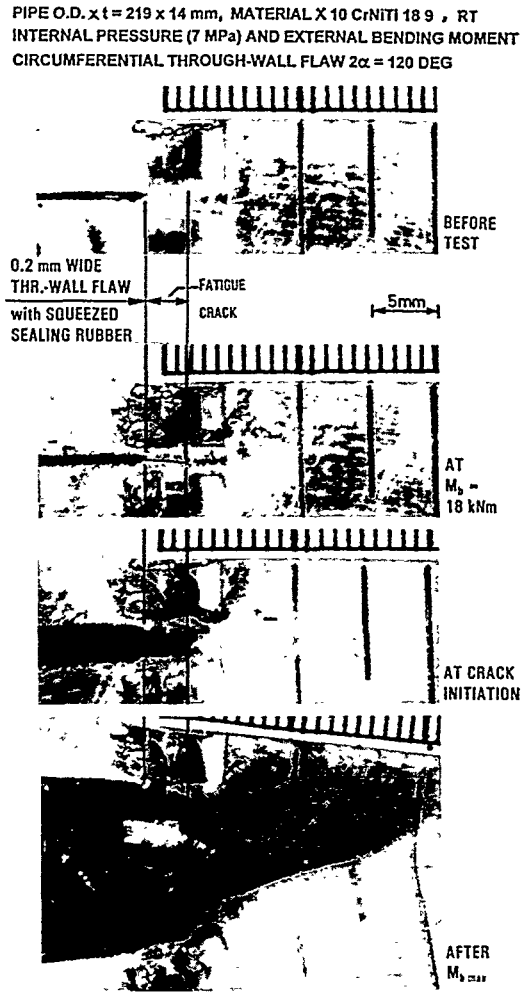

Fig. 12: Crack tip opening of a stainless steel pipe

A preliminary comparison between the Leak-before-Break curve determined analytically using the plastic limit load concept from /8/ and the experiments is shown in **Fig. 13.** The maximum bending moments of the pipes with the defect sited in the base metal lie on the calculated curve (through-wall defect $2\alpha = 180°$) or about 15% below it (through-wall

defect $2\alpha = 160°$ or $60°$). In the expressions used for the calculations the flow stress $\sigma_{fl} = (R_{p0,2} + R_m)/2$ was used as the material-specific failure criterion whilst in the case of the pipe with a circumferential joint the material properties of the weld metal formed the basis.

With the results obtained from the two current projects and an extensive literature search, inter alia, information should be obtained as to which of the material-specific failure criteria in the plastic limit load concept

$$\sigma_{fl} = (R_{p0,2} + R_m) / 2$$

or $$\sigma_{fl} = (R_{p0,2} + R_m) /2{,}4$$

better covers the experimental results, and whether the circumferential joint defect may be better described by the material properties of the weld metal or those of the base metal.

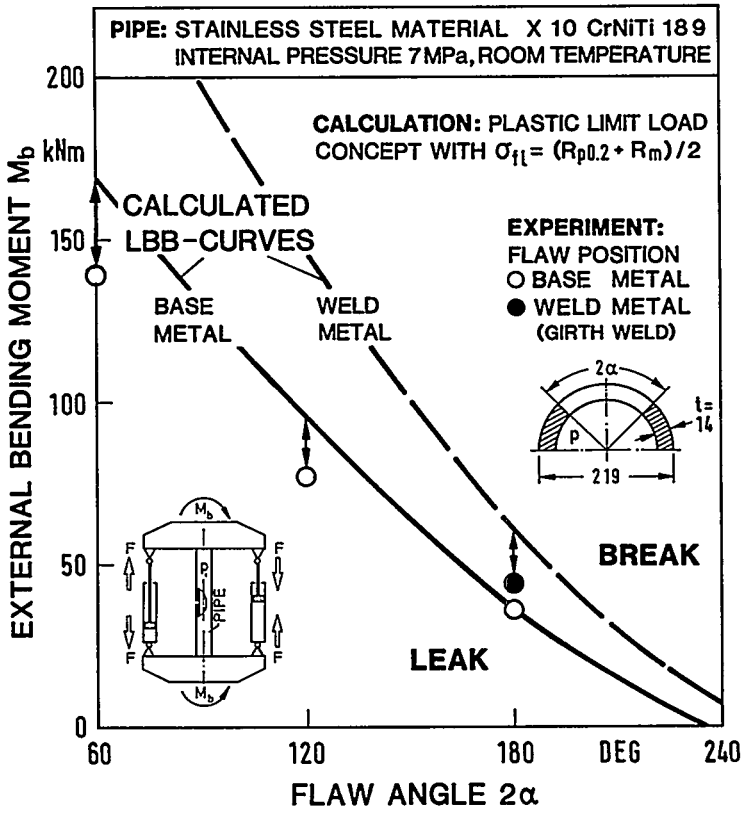

Fig. 13: Comparison between calculational determination and experiment (stainless steel pipes)

A further main focus will rest, inter alia, on the moment for crack initiation measured experimentally and that determined by analytical and numerical calculation, in which in comparison to ferritic material, data having a different basis, specific to austenitic material, has to be taken into consideration (see e.g. /9/). The basic prerequisites for a satisfactory conclusion are:

- determination of reliable fracture mechanics material data
- application of advanced, redundant measurement techniques to minimise the uncertainties in the experimental determination of crack initiation

- verification of the transferability of mechanical technology and fracture mechanics material characteristics to the component.

6 Acknowledgment

Sponsorship of the projects was provided by the Federal Minister for Education, Science, Research and Technology (BMBF), Bonn, but also by the Technische Vereinigung der Großkraftwerksbetreiber e.V. (VGB) - Kraftwerks technik GmbH, Essen. The Gesellschaft für Anlagen- und Reaktorsicherheit (GRS) mbH, Cologne, were responsible for the administration of the research work. Thanks are due at this juncture to all participants for their support of the research projects

7 References

/1/ Sturm, D. and W. Stoppler: Research Project 1500- 279, Phenomenological Vessel Burst Tests, Phase I. Final Report, MPA Stuttgart, July 1985 (in German)

/2/ Sturm, D. and W. Stoppler: Research Project 1500 279, Phenomenological Vessel Burst Tests, Phase II. Tests on the load-bearing- and fracture behaviour of pipes with circumferential defects. Research Report. MPA Stuttgart, December 1987 (in German)

/3/ Julisch, P. and M. Schick: Assurance programme for the proof of integrity of components, Single Project "Component Tests" Report 940 500 300. MPA Stuttgart, February 1989. (in German)

/4/ Julisch, P., D. Sturm and J. Wiedemann: Exclusion of rupture for welded piping of power stations by component tests and failure approaches. To be published in Nuclear Engineering and Design, North-Holland Amsterdam.

/5/ Katzenmeier, G., H.-U. Hahn and T. Cron: Investigations on reactor safety at HDR Karlstein. Final Report HDR Safety Programme, Phase III Technical Report No. 115/94. Publ. Kernforschungszentrum Karlsruhe GmbH March 1994 (in German)

/6/ Julisch, P., W. Stoppler and D. Sturm: Exclusion of rupture for safety relevant piping systems by component tests and a simple calculation. 8th. SMIRT Conference, Brussels, Belgium, Vol.G, paper G 3/8, Aug. 1985.

/7/ Circumferential cracks in cylinders under tensile and/or bending loading - Comparison of calculational methods for failure stresses. Tech. Report R214/84/347, Kraftwerk Union, Erlangen, 1984. (in German)

/8/ Kanninen, M. F. et al..: Instability predictions for circumferentially cracked type-304 stainless steel pipes under dynamic loading, EPRI NP-2347, Vol. 1 and 2, USA, April 1982.

/9/ Kußmaul, K. , H. K. D Diem, D. Blind, U. Eisele and W. Stadtmüller: Influence of material characteristics on crack initiation assessment of austenitic piping. SMIRT 13 Conference, Porto Alegre, Brazil, August 1995.

Specialist meeting on LEAK BEFORE BREAK in Reactor Piping and Vessels
LBB95
Lyon, France, 9 - 11 October 1995

German Experimental Programs and Results

Bartholomé, G., Bazant, E., Wellein, R., Siemens KWU
and Stadtmüller, W., Sturm, D., MPA Stuttgart
Germany

1 Introduction

Reactor pressure vessels and piping of the primary circuit form part of the safety research related components in nuclear power plant. The integrity of these components in the presence of defects of limited size has to be guaranteed under both operational and accident loading conditions.

In the period from 1973 to today, on the one hand, within the framework of reactor safety research, the Federal Minister for Education, Science, Research and Technology, Bonn, sponsored a series of research projects which, as seen in **Fig. 1**, are logically linked to each other /1 - 7/. On the other hand the utilities, manufacturers and vendors of nuclear power plants performed series of tests with pipes and components to solve their specific problems. Having regard to the results of the supporting projects the experimental verification of Leak-before-Break behavior was to be demonstrated, the postulation of fracture preclusion for piping (straight pipe, bends and branches) confirmed and thereby the safety margin against massive failure also quantified. **Fig 2** gives a general overview of the types of defects and loadings also the most important objectives.

As the following results reveal, they can be called upon for the safety assessment of ferritic and austenitic piping, in the primary and secondary circuits of nuclear power plant. Moreover, because of the great spread of the test parameters, they are also important for the design and assessment of piping in other technical plant.

On the strength of the test results it appears to be justified to rule out catastrophic fractures (2F-fractures) even on pipes of dimensions corresponding to those of a main coolant pipe of a pressurized water reactor plant on the basis of a mechanical deterministic safety analysis in correspondence with the Basis Safety Concept (Principle of Fracture Exclusion) /8/

2 General

2.1 Material and test pieces

For reasons of transferability of the results to actual components, mostly the Basis Safety material 20 MnMoNi 5 5 employed for piping and pressure vessels in LWR nuclear power plant was used. To cover specific problems also other ferritic materials on the basis of MnNi, MnMoV or austenitic steels as e.g. or X 10CrNiTi 18 9 were used. In the quality employed, these materials have a notch impact energy upper shelf value between 100 J and 200 J and thus lies above the minimum value of 100 J required in the RSK Guidelines /9/.

For the investigation of the effect of conditions which overstep the limiting values, especially with respect to a lower notch impact energy upper shelf value, special casts were used as further materials for the manufacture of the test pieces. For the simulation of the end-of-life (EOL) condition an upper shelf energy value of ≅ 50 J could be arrived.

The test pieces were straight pipes. They were closed by heads at each end. The dimensions of the test pieces lie in the range of those applicable to primary circuit components of pressurized water reactors. In preliminary tests other dimensions and materials were employed additionally so that the range shown in Fig. 3 could be investigated.

1. RESEARCH PROGRAMME TO PROVE A FRACTURE SAFETY DEVICE PROTECTION SYSTEM FOR REACTOR COMPONENTS
(RS 104, KWU) 1973 - 1976

2. INVESTIGATIONS ON INITIATION, PROPAGATION AND ARREST OF AXIAL CRACKS IN PIPES
(150 320, KWU) 1978 - 1982

3. PHENOMENOLOGICAL VESSEL BURST EXPERIMENTS (BV PHASE I + II) - PRIMARY PIPING OF PWR
(150 279, MPA) 1977 - 1987

4. FRACTURE RESISTANT DESIGN OF STEAM PIPES FOR THE THTR MATERIAL X 20 CrMoV 12 1
(BBC, RWTÜV) 1983 - 1984

5. PROOF OF INTEGRITY OF COMPONENTS - PRIMARY PIPING OF BWR
(VGB, KWU, MPA) 1985 - 1987

6. LOAD BEARING CAPACITY OF PIPES UNDER INTERNAL PRESSURE AND EXTERNAL BENDING MOMENT - FERRITIC AND AUSTENITIC MATERIALS
(UTILITIES, MPA) 1983 - 1988

7. HDR SAFETY PROGRAMME (PHASE I, PHASE II, PHASE III)
- BLOW DOWN; EARTHQUAKE AND IMPULSE LOAD ON PIPING SYSTEMS
- FAILURE BEHAVIOUR OF PIPING SYSTEMS
- THERMAL STRIATION
- FAILURE BEHAVIOUR UNDER CYCLIC LOADING
- TRANSIENT LOADING OF PREDAMAGED PIPING SYSTEMS (BLOW DOWN, EARTHQUAKE)
- LEAK RATE TEST OF DIFFERENT PIPING COMPONENTS
(150 123, PHDR KfK, MPA, INDUSTRIES) 1976 - 1994

8. ANALYSIS OF LEAK BEFORE BREAK BEHAVIOUR OF SNR 300 COMPONENTS
(INDUSTRY; RWTÜV) 1983 - 1984

9. ASSESSMENT OF CIRCUMFERENTIAL CRACKS IN HIGHLY LOADED WELDMENTS OF PIPING
(KWU) 1980 - 1982

10. INTERNAL PRESSURE TESTS WITH PIPE BENDS OF FERRITIC STEELS UNDER IN-PLANE BENDING AT TEMPERATURES IN THE CREEP REGIME
(150 726, 150 727, INTERATOM; MPA) 1986 - 1991

11. INELASTIC ANALYSIS OF PIPE BENDS, ANALYTICAL AND EXPERIMENTAL INVESTIGATIONS
(150 705, MPA, SDK) 1985 - 1989

12. LIMIT LOAD ANALYSIS OF FLAWED STREAM GENERATOR TUBES
(RS 624, GRS) 1983 - 1984

13. FLUID-STRUCTURE INTERACTION
(RS 478, GRS) 1983 - 1986

14. ANALYTICAL ACTIVITIES - RUPTURE PHENOMENA WITH VESSEL AND PIPES
(RS 477, GRS) 1980 - 1985

15. CENTRAL INVESTIGATION AND EVALUATION OF MANUFACTURE AND OPERATIONAL DEFECTS OF THE PRESSURIZED COMPONENTS IN NUCLEAR POWER PLANTS
(SR 10/1, MPA) 1983 - 1986

16. DEVELOPMENT OF FRACTURE MECHANICS METHODS FOR THE INTEGRITY DEMONSTRATION OF THE COOLANT BOUNDARY OF SNR-2
(INTERATOM, 29.926.06) 1984 - 1989

17. SNR-2 COMPONENT ASSESSMENT BY FRACTURE MECHANICS ANALYSES (INTERATOM, 22.926.17) 1984 - 1989

18. SNR-2 COMPONENT AND FRACTURE TESTS
(INTERATOM, 22.926/02) 1985 - 1989

19. STRAIN ESTIMATION METHODS FOR LOW CYCLE DYNAMIC LOADS
(INTERATOM, 22.927/02) 1985 - 1988

20. CREEP - FATIGUE EXPERIMENTS ON PIPE GEOMETRIES AND CALCULATIONS
(INTERATOM, V922/10) 1985 - 1989

21. ANALYSIS AND FURTHER DEVELOPMENT OF FRACTURE MECHANICS FAILURE CONCEPTS
(150 488, 150 489, 150 490, FhIWM, BAM, IEHK) 1986 - 1989

22. FRACTURE MECHANICS CHARACTERIZATION OF PIPE MATERIAL AT ELEVATED AND HIGH TEMPERATURES
(INDUSTRY; FhIWM) 1984 - 1987

23. THERMOMECHANICAL MEASURING PROCEDURE FOR FAST DUCTILE FRACTURE
(BMFT 03 S 289, FhIWM) 1982 - 1984

24. INTERNAL PRESSURE TEST ON PIPE BENDS MADE OF CREEP RESISTANT STEEL WITH ADDITIONAL BENDING MOMENTS APPLIED AT TEMPERATURES IN THE CREEP RANGE
(150 727, MPA) 1986 - 1994

25. HIGH RATE TENSILE TESTS WITH PIPE SPECIMENS
(150 749, MPA) 1987 - 1988

26. CRACK GROWTH AND FAILURE BEHAVIOUR OF CYLINDRICAL COMPONENTS WITH CIRCUMFERENTIAL FLAWS, LOADED BY INTERNAL PRESSURE AND CYCLIC OUTER BENDING MOMENT - BV PHASE III
(150 752, MPA) 1987 - 1991

27. TESTS ON THE MAIN COOLING PIPE TO FIND OUT ITS FAILURE DUE TO CREEP FRACTURE UNDER HIGH SYSTEM PRESSURE
(150 771, MPA) 1987

28. STRENGTH AND FRACTURE BEHAVIOUR OF ELBOWS AND T-BRANCHES UNDER INTERNAL PRESSURE AND SUPERIMPOSED OUTER BENDING MOMENT LOADING - BV PHASE IV.
(150 801, UTILITIES; MPA) 1988 - 1991

29. ANALYTICAL ACTIVITIES. COUPLED FLUID AND STRUCTURE DYNAMICS
(RS 478, GRS) 1983 - 1990

30. EXTENSION OF DUCTILE FRACTURE MECHANIC ANALYSES FOR EVALUATION OF THICK-WALLED PIPING LEAKAGE
(RS 697, GRS) 1986 - 1992

31. ANALYTICAL DESCRIPTION OF RUPTURE PHENOMENA IN PRESSURE VESSELS AND PIPES UNDER CYCLIC ELASTIC-PLASTIC LOADING
(RS 788, GRS) 1988 - 1992

32. NUMERICAL SIMULATION AND ASSESSMENT OF INELASTIC MATERIAL BEHAVIOUR USING COMPONENT TESTS IN THE TEMPERATURE RANGE BELOW 400 °C
(150 955, MPA) 1993 - 1996

33. EXPERIMENTAL AND ANALYTICAL INVESTIGATIONS ON AUSTENITIC PIPES
(UTILITIES, MPA) 1993 - 1995

34. CONTRIBUTION TO ENSURE THE FRACTURE MECHANICS INTEGRITY OF PIPING MADE OF HIGH TOUGH MATERIAL
(150 964, MPA) 1993 - 1996

Fig. 1: Piping research in the Federal Republic of Germany - experimental and analytical programs

2.2 Test conditions

As regard pressure and temperature the test conditions were orientated towards the operating conditions of a pressurized resp. boiling water reactor: internal pressure between 9 MPa and 17 MPa at temperatures from ambient temperature to 300 °C. Both water and air were chosen as pressurizing media. The failure of pipes with longitudinal resp. circumferential defects, was effected by raising the internal pressure, or when using an additional external bending moment, the bending moment was increased until failure occurred. In case of an alternating external bending moment was

used, the amplitude of which was chosen to correspond to the object of the test, a constant internal pressure of up to 15 MPa was superimposed on the pipe.

2.3 Introduction of defects

The longitudinal and circumferential defects were introduced mechanically using a milling device or by spark erosion. A number of the defects in the pipes were additionally fatigued.

3 Summary of experimental results

3.1 Strength and Leak-before-Break (LBB) behavior

3.1.1 Pipes with longitudinal defects under internal pressure loading

The Leak-before-Break curve which divides the leakage from the massive fracture is, assuming equal pipe dimensions, for corresponding stress values, essentially dependent on the toughness of the pipe material.

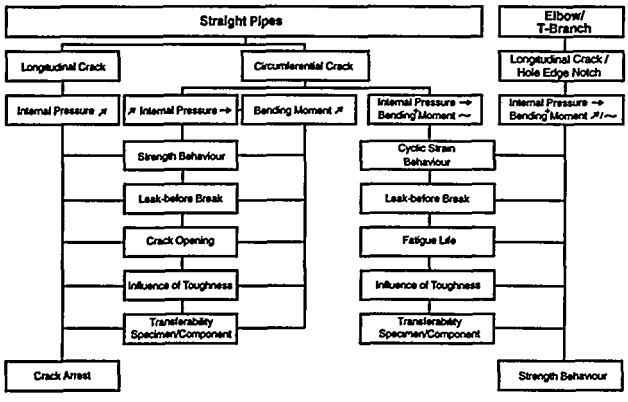

Fig. 2: Objectives of the research programmes

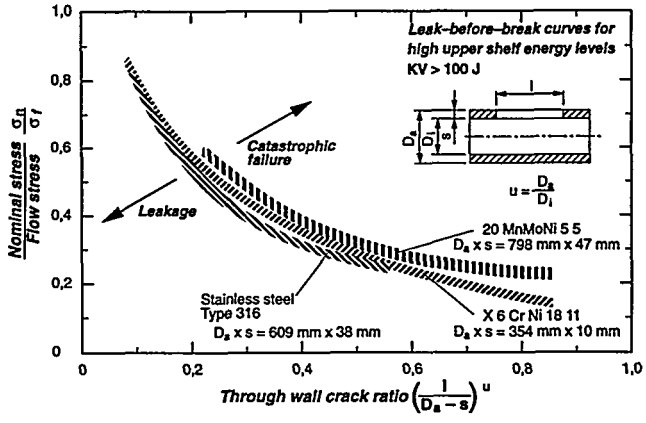

Fig. 3: Leak-before-Break curves for pipes of ferritic and austenitic materials

Fig. 3 illustrates that not only pipes of ferritic steels but also ones of austenitic steels may accommodated in this form of representation. In order to take account of the different material strengths, in this representation the circumferential stress at fracture σ_n was normalized with respect to the mean flow stress σ_f. The path of the Leak-before-Break curve appears to be independent of whether crack initiation occurs quasi-statically or dynamically.

If a pipe exhibits longitudinal through-wall defects which are shorter than the critical slit lengths derived from the Leak-before-Break curve then in the event of failure a leak or a limited fracture always develops. /10 - 15/

3.1.2 Pipes with circumferential defects under internal pressure and external bending moment loading

For the performance of the bending tests a 4 point bending rig was used. By changing the pressurizing medium (air instead of liquid) in the actuating cylinder of the rig the stiffness of the system could be varied over a wide range. In these pipe bend tests the stiffness of the bending rig exerted more influence on the fracture development than the compressibility of the pressurizing medium in the test pipe. If the stiffness of the bending rig is very large (hard system) then it is possible that after crack initiation, because of the rapidly changing deflection behavior of the test pipe the

bending moment can no longer be maintained. In this case an arrest of the initiated crack in the test pipe has to be reckoned with, i.e. this system favors the development of leakages.

On the contrary for a test rig having less stiffness, in the extreme case for having as infinitely soft system (e.g. creation of moments by dead weight loading) theoretically the bending moment on the test pipe is always present and indeed is independent of the magnitude of its deflection. A crack once initiated under these idealized conditions can more likely lead to a massive fracture, i.e. this system favors the development of a massive fracture.

If pipes with part-circumferential notches or defects are loaded by an external bending moment in addition to internal pressure then failure curves for different notch depth/wall thickness a/t ratios result. From this it holds that the deeper the notch for a given notch length or notch circumferential angle the smaller becomes the tolerable additional bending moment for a constant internal pressure.

As already established for pipes with longitudinal defects, a strong dependence of the failure curve on the toughness of the pipe material was also found for the pipes with circumferential defects, **Fig. 4**. Assuming a low toughness material condition (KV ≅ 50 J) and normal operational internal pressure loadir.g superimposed by a 5 MNm bending moment, then for the dimensions of the main coolant piping a safety margin of about x4 with respect to the critical slit length results if the maximum permissible defect sizes from the acceptance test, the repeated non-destructive testing and the leakage monitoring system (LMS) are taken as a basis. For toughness of KV > 100 J this safety margin rises to x8.

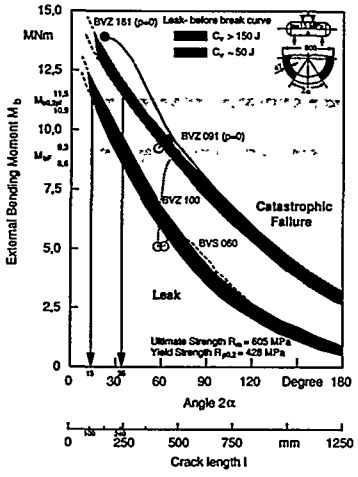

Fig. 4: Leak-before-Break curves for pipes with circumferential defects and different upper shelf notch impact energies

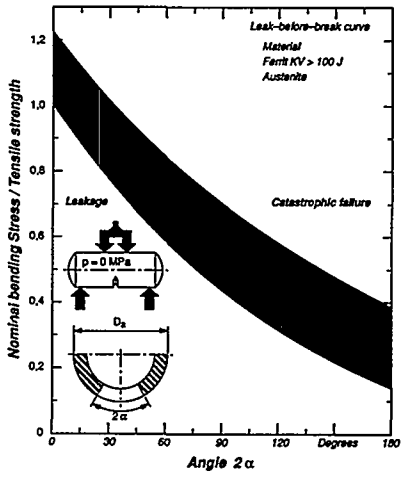

Fig. 5: Leak-before-Break curve for pipes of ferritic and austenitic materials

Fig. 5 illustrates again that not only pipes of ferritic steels but also ones of austenitic steels may accommodated in this form of representation. In order to take account of the different material strengths, in this representation the nominal bending stress at fracture was normalized with respect to the ultimate tensile strength. /16, 17/

3.1.2.1 Fracture opening behavior

The time-dependent development of fracture opening area for longitudinal and circumferential defects was investigated. From this the time required for the formation of a fracture opening of 0.1 F is between 2,5 and 5,4 ms for longitudinal defects and between 29 and 36 ms for circumferential ones.

3.1.3 Pipes with circumferential defects under internal pressure and cyclic external bending moment loading

The investigations served to provide further experimental confirmation of the fracture preclusion postulate for piping with (partial-) circumferential defects, especially under internal pressure loading and simultaneous loading by a cyclic external bending moment. The tests were conducted with the aim of providing data on the crack initiation, cyclic crack growth, the deformation and cyclic strain behavior and also the Leak-before-Break behavior.

For these tests a modified version of the bending rig was employed.

In **Fig. 6** are plotted both the number of cycles to crack formation (N_A) determined of smooth test bars as a function of the total strain amplitude in the form of a scatter band /18/ and also the number of cycles to through-cracking (N_B) determined in pipe bending fatigue tests as curves dependent on the particular defect size.

Test	Defect: Depth mm	Defect: Length mm	Defect: Position Spark Eroded	Test conditions: Temperature °C	Internal Pressure MPa	Bending Moment MNm Max.	Bending Moment MNm Min.	Equivalent Strain Range $\frac{mm}{m}$	Load cycles N_A	Remarks
BVZ 210 ◆	4.7 a/t = 0.1	292 (40 Deg.)	outer + inner surface	20	0	+9.5	−9.5	4.00	2200 2316	Outer Notch: Through Crack Inner Notch: Defect Depth = 35 mm
BVZ 220 ◆			outer surface		15			4.80	1000	Through Crack
BVZ 230 ◆							−0.5	1.80	7998	Test Discontinued Defect Depth: 9.8 mm
BVZ 231 ■	9.8 a/t = 0.2	294 (40 Deg.)				−11.5	−0.25	2.80	724	Test Discontinued Defect depth: 12.8 mm
BVZ 240 ●	23.6 a/t = 0.5	292 (40 Deg.)				+9.5	−9.5	4.80	30	Through crack
BVZ 250 ●				20		+6.5	−6.5	3.16	238	
BVZ 300 ●									320	
BVZ 260 ●						+11.9	−11.9	5.71	4	
BVS 200 ○				80		+6.0	−6.0	2.92	69	
BVS 240 ○									60	
BVS 210 △		140 (20 Deg.)							663	
BVS 220 △						+9.0	−9.0	4.60	41	
BVZ 270 ▲				20		+9.5	−9.5	4.80	274	
BVZ 280 ▲						+12.1	−12.1	5.96	13	
BVZ 290 ▼		838				+6.0	−6.0	3.25	84	
BVS 230 ▽		(120 Deg.)		80		+3.0	−3.0	1.45	606	

BVZ Material: 20 MnMoNi 5 5 BVS Material: MnMoNiV – Special Melt

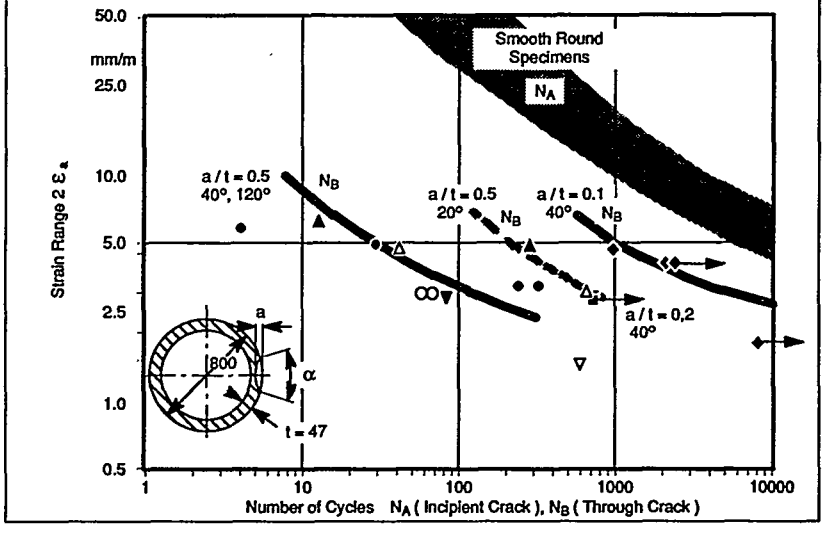

Fig. 6: Tabular and graphical representation of the number of cycles to through cracking as a function of the total strain amplitude

The number of cycles to through-cracking determined on pipes with circumferential defects lie, depending on defect depth and length, at a greater or lesser distance below the scatterband determined on smooth test bars, in which the test bars from the investigated pipe materials fit well.

The number of cycles to through-wall cracking of the pipes with circumferential defects having a starting defect depth of 10% of the wall thickness (defect depth/wall thickness = 0,1) and a circumferential angle of 42 degrees, lie about a half decade below the scatter band for smooth test bars.

For pipes with deeper starting defects (defect depth/wall thickness = 0,5, defect circumferential angle of 42 degrees) the cycles to through-wall cracking lie up to 2,5 decades lower than the scatter band for the onset of cracking in smooth test bars.

For deeper defects (defect depth/wall thickness = 0,5) with circumferential angle of ≅ 120 degrees only a small difference in the tolerable load cycles was found compared with shorter defects (≅ 40 degrees)

Pipes tested in the region of their natural frequency (4 Hz) lead to the same results as those having comparable defect dimensions when tested at a lower frequency (0,008 Hz).

No effect of pipe geometry (internal diameter of 10 mm to 706 mm) on the number of cycles to through-cracking could be found over the range investigated.

It can be concluded from the investigations that pipes of ferritic materials with crack-like circumferential defects can bear additional high external bending moments in the presence of simultaneously acting internal pressure even if the dimensions of the defects lie considerably above the defect size permitted in the non-destructive acceptance testing.

Furthermore it can be established that pipes with such circumferential defects can still tolerate a considerable number of bending cycles before through cracking of the ligament below the defect occurs. A prerequisite though in this regard is that the defect lengths are shorter than their associated through-wall critical lengths.

3.2 Analytical and numerical analyses

The Leak-before-Break (LBB) concept is an essential part of the Break Preclusion Concept /8,19,20,21/.

3.2.1 LBB Concept

The critical crack size for ductile material is determined using fracture mechanics. The growth of stable cracks is only conceivable due to cyclic loading (corrosion has to be precluded). The cyclic crack growth beyond design can lead to two situations, **Fig. 7**:

First situation: Crack growth smaller than critical through wall crack length (Leak-before-Break).

Second situation: Crack growth up to a crack length which is greater than the critical through-wall crack length (Break-before-Leak).

If LBB behaviour can be shown, break preclusion is proven with the necessary redundancies; if not, break preclusion can only be obtained by applying equivalent safety measures (e.g. Inservice Inspection, Load Monitoring, Fatigue Monitoring, Continuous Inspection).

3.2.2 Methods applied

LBB is demonstrated by means of fracture mechanics methodology, applying adequate criteria, **Fig. 8**. Siemens performed numerous analyses to preclude breaks based on simplified elasto-plastic fracture mechanics (Flow Stress Concept = FSC, Plastic Limit Load = PLL) for circumferential cracks, **Fig. 9**. The acceptability and applicability of these

concepts was discussed with and accepted by the authorities in Germany /20 - 22/. Analogous approaches are used for longitudinal cracks /23/. These approaches are also compared to the more sophisticated approach using J-Integral /27/.

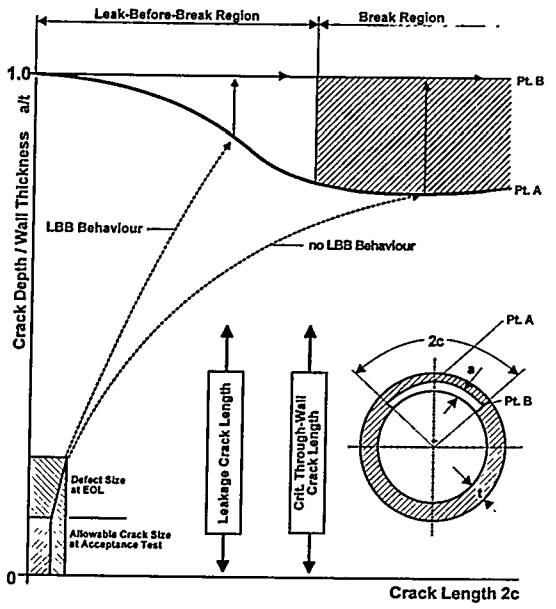

Fig. 7: Procedure of Leak-before-Break (schematic)

Description	Methodology	Loads	Results	Criteria
Definition of reference defects	Based on allowable defects + performance of inspection technologies		a_0 $2c_0$	allowable defects
Fatigue crack growth (F. C. G.)	Integration of crack growth law until end of life (EOL)	Normal and upset trans. for 1 specif. load collective	$a_f = a_0 + \Delta a$ $c_f = c_0 + \Delta c$	Small F. C. G. in 1 specif. load collective
Stability of EOL surface crack	qualified methods: Flow stress concept and / or Plastic limit load	all transients + SSE	a_c $2c_c$	Stability of ligament
T. W. C. stability analysis	Same as previous	all transients + SSE	$2c_c$ critical crack length	Stability of ligament
LBB Fatigue crack growth	Integration of crack growth law until break-through of ligament	Normal & upset transients for unlimited specif. load collectives	$2c_f$* leakage crack length	LBB is demonstrated, if $2c_f^* \approx 2c_c$ for unlimited specified load collectives if $2c_f^* > 2c_c$ equivalent safety measures
Opening area and Leak rate of T. W. C.	qualified methods	normal operation	A $\dot{m}$ $(2c_c)$	Detectability of leak rate

Fig. 8: Break Preclusion: Fracture Mechanics Methodology

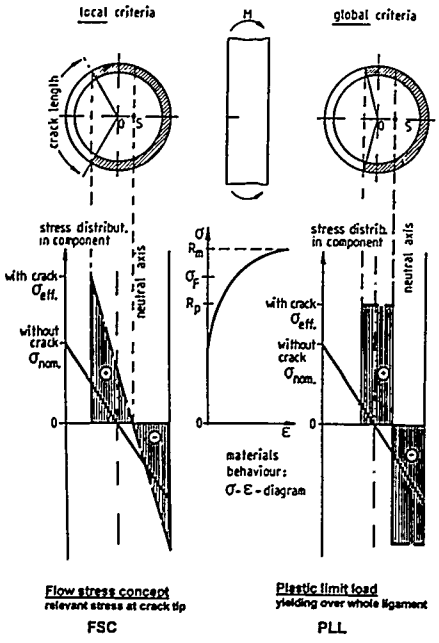

Fig. 9: Models for ductile failure (only bending moment)

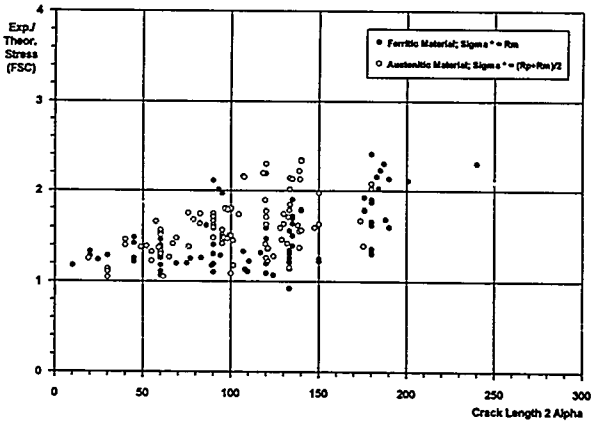

Fig. 10: Circumferential through-wall cracks: Flow Stress Concept (FSC) using experiments with KV> 45J and (WM=BM)

3.2.3 Experimental verification of the methods used for LBB

3.2.3.1 Simplified methods (FSC, PLL)

The calculation concepts used by Siemens are validated by numerous tests. As an example typical results for the conservatism of the simplified elasto-plastic fracture mechanics approaches are shown for circumferential through-wall cracks using FSC and PLL /22, 24, 26/,**Fig. 10 and 11.** The comparison of the theoretical prediction to the experimental results for longitudinal through-wall cracks /23/ using BMI and RUIZ shows the conservatism of the used approaches, **Fig. 12 and 13.**

3.2.3.2 J-Integral

The application of the J-Integral approach /27/ to the tests available at this time (Battelle, MPA, Siemens/Interatom) shows that, using J_i as the relevant material property, all tests can be predicted conservatively, see **Fig. 14.** The amount of conservatism using FSC and PLL for the same tests also can be seen.

4 Application of the Break Preclusion Concept

4.1 Break Preclusion Concept

In Germany the Break Preclusion Concept, often called Leak-before-Break, being applied since 1979 is based on the Basis Safety Concept /19, 25/. The Break Preclusion Concept for the main coolant line according to German practice is detailed in a logic chart (**Fig. 15**) for the different steps , Inservice Redundancies, Leak-before-Break (LBB), Break Preclusion (BP) and the Break Postulates, derived from the BP.

The two main prerequisites for the general procedure of BP /8/ are Basis Safety and Independent Redundancies.

The safety of the primary piping against break was proven by research programs performed at MPA, Siemens/KWU and Siemens/Interatom. These programs (Fig. 1) included tests on representative pipings under relevant loading conditions.

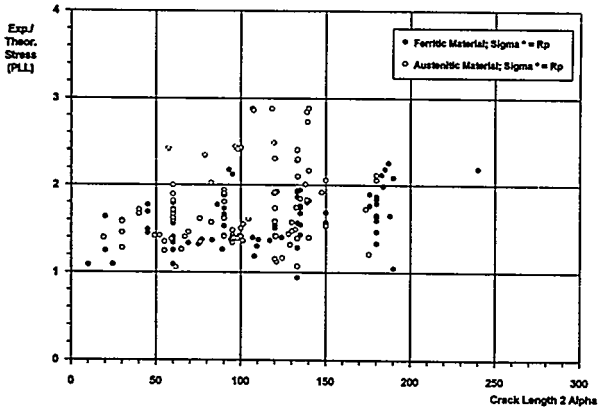

Fig. 11: Circumferential through-wall cracks: Plastic Limit Load (PLL) using experiments with KV> 45J and (WM=BM)

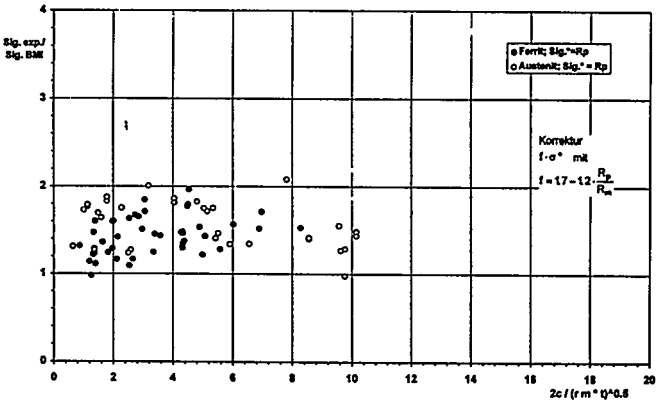

Fig. 12: Longitudinal cracks: All through-wall cracks calculated (KV> 45J) with BMI add. correction

4.2 Application of the Break Preclusion Concept to the main coolant piping

Siemens performed various analyses to preclude breaks based on simplified elasto-plastic fracture mechanics FSC /20/, PLL /22/. The results of the analysis of a typical PWR main coolant line to the Konvoi plant /20/ are given in **Fig. 16.** With these safety margins, resulting from Basis Safety (piping technology, operational loads and stresses, crack growth and crack stability) and from independent redundancies (field experience - no breaks, and leaks occurred, Break Preclusion was obtained for all plants, - leak detection requirements, transient monitoring and inservice inspection - the German Reactor Safety Commission (RSK) agreed on the application of preclusion of breaks. Restrictions were in the RSK and dealt essentially with corrosion and vibrations. These restrictions, if applicable, can be solved by recommendations for representative ISI-testing of relevant locations. In general the amount of ISI was reduced when following the requirements to succeed in Break Preclusion.

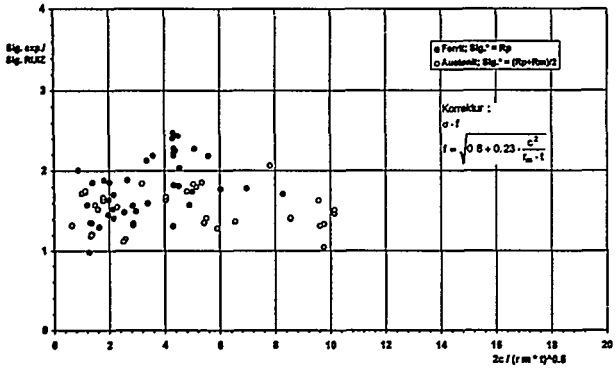

Fig. 13: Longitudinal cracks: All through-wall cracks calculated (KV> 45J) with RUIZ add. correction

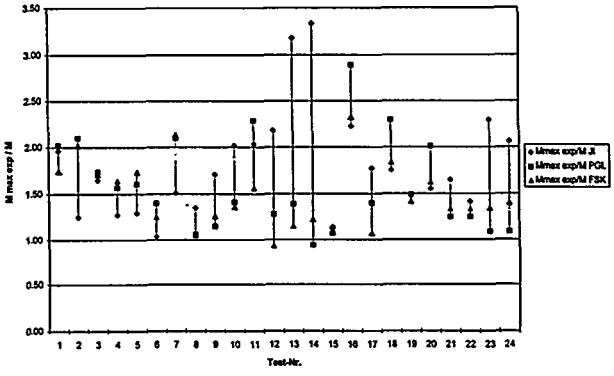

Fig. 14: Comparison of theoretical predictions J_i, FSC, PLL, with BMI-, MPA- and Siemens/Interatom-tests for base material

4.3 Break postulates

Applying the above criteria the RSK modified the RSK-Guidelines, the main content of which is given in **Fig. 17.** postulated leaks and breaks for primary and corresponding effects.

5 Summary

Extensive experimental and theoretical investigations on the fracture behaviour of pipes gave important results in the following areas:

- Experimental determination of the Leak-before-Break behavior under quasi-static and cyclic loading.
- Experimental determination of effect of toughness on the strength, Leak-before-Break and cyclic crack growth behavior.
- Experimental determination of the fatigue behavior of pipes under quasi-static internal pressure and cyclic external bending moment loading.
- Ascertaining the legitimacy of the transferability of data obtained from small specimens to components.
- Contribution to proving the performance capability of analytical and numerical calculational method
- Proof of the conservatism of the analytical fracture mechanics methods used in Germany for the evaluation of LBB of nuclear piping in respect to

- circumferential through-wall cracks, using flow stress criterion (FSC) and plastic limit load (PLL) and
- longitudinal through-wall cracks using (BMI) and (RUIZ) formulae
together with the adapted flow-stresses.

- Proof of the conservatism of the more sophisticated fracture mechanics method (J-Integral with J_i)

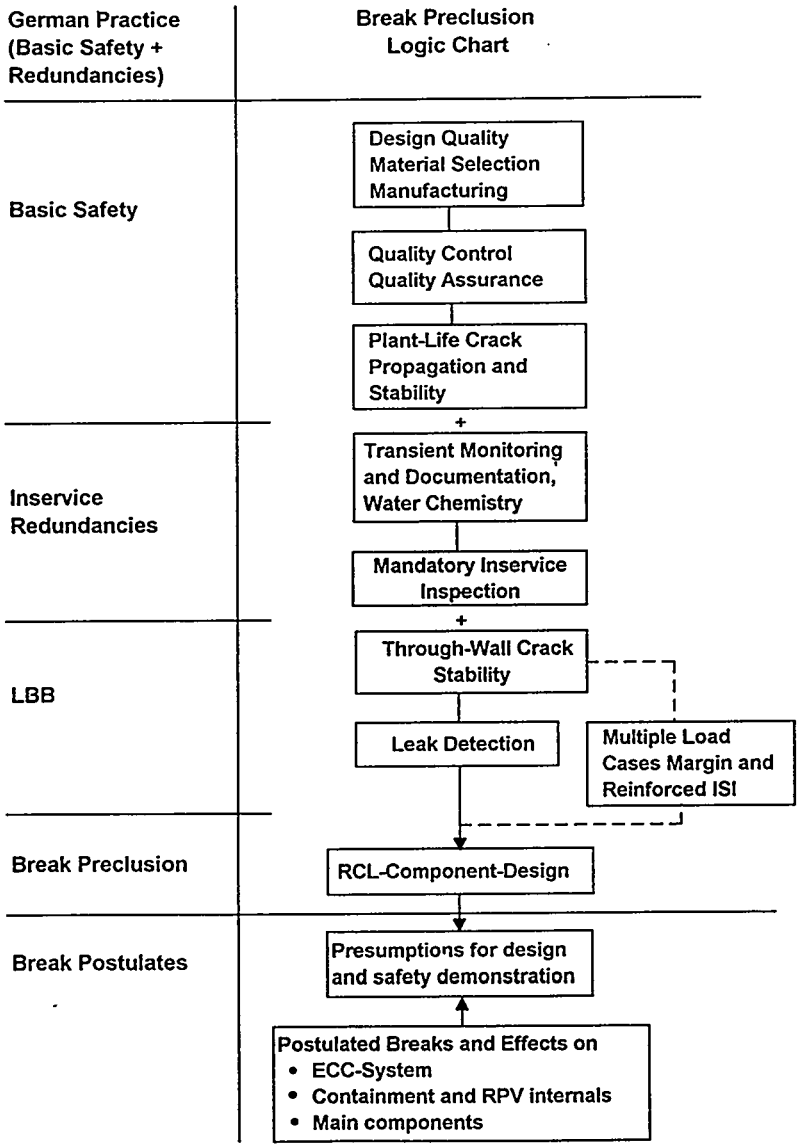

Fig. 15: Break Preclusion Concept according to German practice

Demonstrated by Means of:		Rule	Indication Depth a mm	Indication Length 2c mm	Safety Margin S_c $S_c = \frac{2c_c}{2c}$	Leak Cross Section A mm²	Safety Margin S_A $S_A = \frac{A_c}{A}$
Surface Crack Examination	$2c_0$	KTA 3201	0 1.5	0 6	- -	- -	- -
UT Examination: Acceptance		KTA 3201	6 4.2	10 30	50 17	- -	- -
UT Examination: In-Service Inspection		KTA 3201.4	3	20	25	-	-
	$2c_f'$			156	3.2		
Leakage Monitoring System: • Condensate, Moisture • Condensate, Moisture	$2c_0'$	min. max.	52 52	70 130	7 3.8	3 10	70 22
Crit. Through-Wall Crack Length $2c_c$, Cross-Section A_c	$2c_c$		52	500	1	220	1

Fig. 16: Typical analysis of main coolant line of Konvoi (D_i x t = 760 x 52 mm) circumferential crack (Flow Stress Concept, ferritic) and safety margin

Primary System (RSK Guidelines Chapter 21.1, version 3/1984)

	Leak and break postulates	effects
Reactor coolant lines	• 0.1 A, 15 ms, linear	• pressure waves (RPV internals)
	• 0.1 A, steady-state blowdown	• jet force (pipings, components, building) • reaction force (pipings, components, building)
	• < 2A	• LOCA analysis • containment • pressure differences (building) • qualification of I & C
Circumf. nozzle weld	• p·A·S, S = 2	• stability of the components (e. g. RPV, SG, RCP, PRZ)
RPV leak	• 20 cm²	• RPV supporting • RPV internals • LOCA analysis
Austenitic connection lines with DN > 200 (surgeline, ECCS up to the 1st isolation)	• 0.1 A	• jet force (pipings, components, building) • reaction force (pipings, components, building)

Fig. 17: Postulated leaks and breaks for piping systems

6 Acknowledgment

Sponsorship of most of the projects was provided by the Federal Minister for Education, Science, Research and Technology (BMBF), Bonn, but also by the Technische Vereinigung der Großkraftwerksbetreiber e.V. (VGB) - Kraftwerks technik GmbH, Essen. The Gesellschaft für Anlagen- und Reaktorsicherheit (GRS) mbH, Cologne, were responsible for the administration of the research work. Thanks are due at this juncture to all participants for their support of the research projects

7 References

/1/ HDR-Sicherheitsprogramm, Förderkennzeichen RS 1500 123, Kernforschungszentrum Karlsruhe, 1974 - 1994.

/2/ Sturm, D. und P. Julisch: 'Schnellzerreißversuche mit Rohrproben, 12 MN-Schnellzerreißmaschine (Phase III), Förderkennzeichen 1500 749, Forschungsbericht MPA-Auftrags-Nr. 8540 00 000, Staatliche Materialprüfungsanstalt (MPA) Universität Stuttgart, Dezember 1989.

/3/ Sturm, D. und W. Stoppler: Forschungsvorhaben 'Phänomenologische Behälterberstversuche' - Versuche zum Traglast- und Bruchverhalten von Rohren mit Längsfehlern -. Förderkennzeichen 1500 279, Phase I, Forschungsbericht MPA Stuttgart, Juli 1985.

/4/ Sturm, D und W. Stoppler: Forschungsvorhaben 'Phänomenologische Behälterberstversuche' - Versuche zum Traglast- und Bruchverhalten von Rohren mit Umfangsfehlern -. Förderkennzeichen 1500 279, Phase II, Forschungsbericht MPA Stuttgart, Dezember 1987.

/5/ Sturm, D. und W. Stoppler: Forschungsvorhaben 'Phänomenologische Behälterberstversuche' Versuche zum Traglast- und Bruchverhalten von Rohren mit Längs- und Umfangsfehlern -. Förderkennzeichen 1500 279, Phase II, Forschungsbericht MPA Stuttgart, November 1989.

/6/ Sturm, D. und W. Stoppler: Forschungsvorhaben 'Rißwachstum und Bruchverhalten von rohrförmigen Komponenten mit Umfangsfehlern bei Innendruckbelastung und überlagertem wechselnden äußeren Biegemoment'. Förderkennzeichen 1500 752, Forschungsbericht MPA Stuttgart, April 1993.

/7/ Herter, K.-H. und W. Stoppler: Forschungsvorhaben 'Festigkeits- und Bruchverhalten von Abzweigen und Rohrbogen bei Innendruckbelastung und überlagertem äußerem Biegemoment'. Förderkennzeichen 1500 801, Forschungsbericht MPA Stuttgart, März 1993.

/8/ Kussmaul, K.: German Concept Rules out Possibility of Catastrophic Failure. Nuclear Engineering International, No. 12, 1984, 41 - 46..

/9/ RSK-Leitlinien für Druckwasserreaktoren. 2. Ausgabe 24. Januar 1979.3. Ausgabe 14. Oktober 1981. Druck und Versand: GRS Köln.

/10/ Kußmaul, K., D. Sturm, P. Julisch, W. Stoppler and K. Hippelein: Crack Arrest Behaviour in Pressure Vessels. Transactions of 7th SMiRT Conference, vol. G-H, paper G/F 4/10, August 22-26., 1983, Chicago, USA.

/11/ Kußmaul, K., D. Sturm, W. Stoppler and D. Müller-Ecker: Experimental Investigation on the Crack Opening Behaviour of Cylindrical Vessels under Light Water Reactor Service Conditions. The Reliability and Safety of Pressure Components. The American Society of Mechanical Engineers, New York, N. Y., 1982, PVP-Vol. 62 pp. 97/134.

/12/ Sturm, D., W. Stoppler und K. Hippelein: Phänomenologische Behälterberstversuche - Bruchauslösung, Bruchöffnungsverhalten. Gemeinsames Seminar der MPA Stuttgart und RWTÜV 15.06.1982 in Essen, RWTÜV Schriftenreihe Heft 20.

/13/ Stoppler, W., D. Sturm, P. Scott und G. Wilkowski: Versagensanalyse von längsfehlerbehafteten Rohren und Behältern. 18. MPA-Seminar am 8. und 9.10.1992.

/14/ P. Scott, G. Wilkowski, D. Sturm and W. Stoppler: Development of a Database of Pipe Fracture Experiments. 18. MPA-Seminar am 8. und 9.10.1992, Stuttgart.

/15/ D. Sturm und W. Stoppler: Festigkeitsverhalten von Rohren mit Kerben unter Innendruck und äußerem Biegemoment - Vergleich zwischen Versuch und Rechnung-. 15. MPA-Seminar am 5. und 6.10.1989, Stuttgart.

/16/ Wilkowski, G. M. et al.: Degraded Piping Programm - Phase II. Summary of Technical Results and their Significance to Leak-before-Break and In-Service Flaw Acceptance Criteria. March 1984 - January 1989. NUREG/CR-4082, BMI-2120, Vol. 8, March 1989.

/17/ Takumi K., T. Marno et. al.: Proving Test on the Integrity of Carbon Steel Piping in LWR's. Nupec, 1989

/18/ Luft, G.: Zeitfestigkeitsverhalten von Stählen. Techn.-wiss. Bericht MPA Stuttgart, 1968.

/19/ Kußmaul, K.: Developments in nuclear pressure vessel and circuit technology in the Federal Republic of Germany. SMIRT-6, Post Conference Seminar No. 8, Session 1, Paper No. 1, Paris, Aug. 24, 1981

/20/ Bartholomé, G., R. Steinbuch, R. Wellein: Preclusion of Double-ended Circumferential Rupture of the Main Coolant Line. Nuclear Engineering and Design, 72 (1), 1982, p.97-105

/21/ Bartholomé, G., W. Kastner, E. Keim, R. Wellein: Ruling-out of Fractures in Pressure Boundary Piping. Part 2 "Application on Coolant Pipe of the Primary System" IAEA - Vienna 1983 "Reliability of Reactor Pressure Components" IAEA-SM-269/-7, p. 237-254

/22/ Roos, E., K.-H. Herter, P. Julisch, G. Bartholomé, G. Senski: Assessment of Large Scale Pipe Tests by Fracture Mechanics Approximation Procedures with Regard to Leak-before-Break. Nuclear Engineering and Design 112 (1989), p. 183-195

/23/ Bartholomé, G., R. Wellein: Bruchmechanische Auswertung von Bauteilversuchen (Rohrleitungen) mit Längsdurchrissen zur Absicherung des Leck-vor-Bruchverhaltens.(Fracture mechanics Evaluation of Components Tests (Pipings) with Longitudinal Through-Wall Cracks for Verification of LBB-Behaviour) DVM-Arbeitskreis "Bruchvorgänge", 26. Vortragsveranstaltung, 22./23.03.1994, Magdeburg, p. 407 - 421

/24/ Bartholomé, G., R. Wellein: Evaluation of Components Tests with Analytical Fracture Mechanics Methods (Circumferential Cracks). ECF 10, Berlin, 23.09.1994, p. 1317 - 1326

/25/ Bartholomé, G.: Break Preclusion Concept in Germany. SISSI 94 "Saclay International Seminar on Structural Integrity".April 28-19, 1994, INSTN, Saclay, France. Principles of fracture mechanics application in Nuclear Power Plants, p. 309 - 331

/26/ Bartholomé, G., E. Keim, W. Kastner, W. Knoblach and R. Wellein: Application of LBB in German NPP. LBB 95: Leak Before Break in Reactor Piping and Vessels, Lyon, 9/11 October 1995 (to be published)

/27/ Ricardella, P.: Computer Program pc-Crack. Version 2.1, 1991. Structural Integrity Associates Inc. San José, Ca, USA

EXAMPLES OF REFERENCE MATERIAL DATA NEEDED FOR LBB ANALYSIS DERIVED FROM WGCS-EC-DGXI STUDIES

P. PETREQUIN, CEA, B. HOUSSIN, Framatome, France
J. GUINOVART, EC-DG XI, Belgium

ABSTRACT

Mechanical data collected through the sponsorship of the Activity Group 3 «Materials» of the Working Group Codes and Standards of DG XI European Commission are pointed out to illustrate their potential use for Leak Before Break analyses. Most of the tensile, fatigue, creep and fracture toughness data have been generated for stainless steels, mainly on modified type 316 L (N), selected for the Super Phenix LMFBR.

Trends for ongoing programmes and future works on C-Mn and MnNiMo low alloy steels are provided.

EXAMPLES OF REFERENCE MATERIAL DATA NEEDED FOR LBB ANALYSIS DERIVED FROM WGCS - EC - DG XI STUDIES

P. PETREQUIN, CEA, B. HOUSSIN, Framatome, France
J. GUINOVART, EC - DG XI, Belgium

INTRODUCTION

Leak Before Break analyses require material data that must be validated for the various cases that are taken into account (material grade, temperature, strain rate, ...).

The AG 3 "materials" of the Working Group on Codes and Standards of the DG XI European Commission has sponsored different programmes to gather the mechanical properties of Fast Breeder Reactor materials (essentially on stainless steels) and is continuing its efforts on Light Water Reactor materials such as C-Mn and MnNiMo low alloy steels.

The paper presents some examples of results and technical benefits obtained in order to generate accurate design values for codification and the interest in the development of more restrictive specifications.

The illustrations are focussed on mechanical properties that are needed to evaluate the applicability of the Leak Before Break concept and to perform the mechanical analysis : tensile, fatigue, creep and fracture toughness. The stainless steels are considered first, followed by some results on C-Mn and low alloy steels.

MECHANICAL PROPERTIES OF TYPE 316L (N) STAINLESS STEEL

Tensile Properties

The tensile properties of type AISI 316L (N) steel for LMFBR were derived from experimental data determined on plates and from product forms like forgings or tubes.

The first phase of the study contract consisted in the collection and compilation of more than 2700 tensile test data concerning the yield strength, the ultimate tensile strength, uniform elongation, rupture elongation, and reduction of area available in the temperature range 20 to 800°C on type 316L (N) stainless steels.

The test materials selected were all in the as-received, solution-annealed condition. Solution heat treatment consisted of holding at a temperature between 1050°C and 1150°C followed by water cooling. The data bases of the participating organizations were tabulated and also stored on discs to enable a computer-assisted evaluation. The data of each tensile property have been statistically analysed by means of the method of least squares and a cubic equation of the form :

$$\text{Mechanical property} = A + BT + CT^2 + DT^3$$

where T is the test temperature and A, B, C, D are constants. Furthermore, lower 95 % confidence limits have been derived on the basis of the cubic equation employing two different methods.

The results of the evaluations [1] are presented in Fig. 1 for the yield strength and ultimate tensile strength included in these graphs are the plot of the data points over the temperature range considered as well as the average and the two lower confidence limit curves.

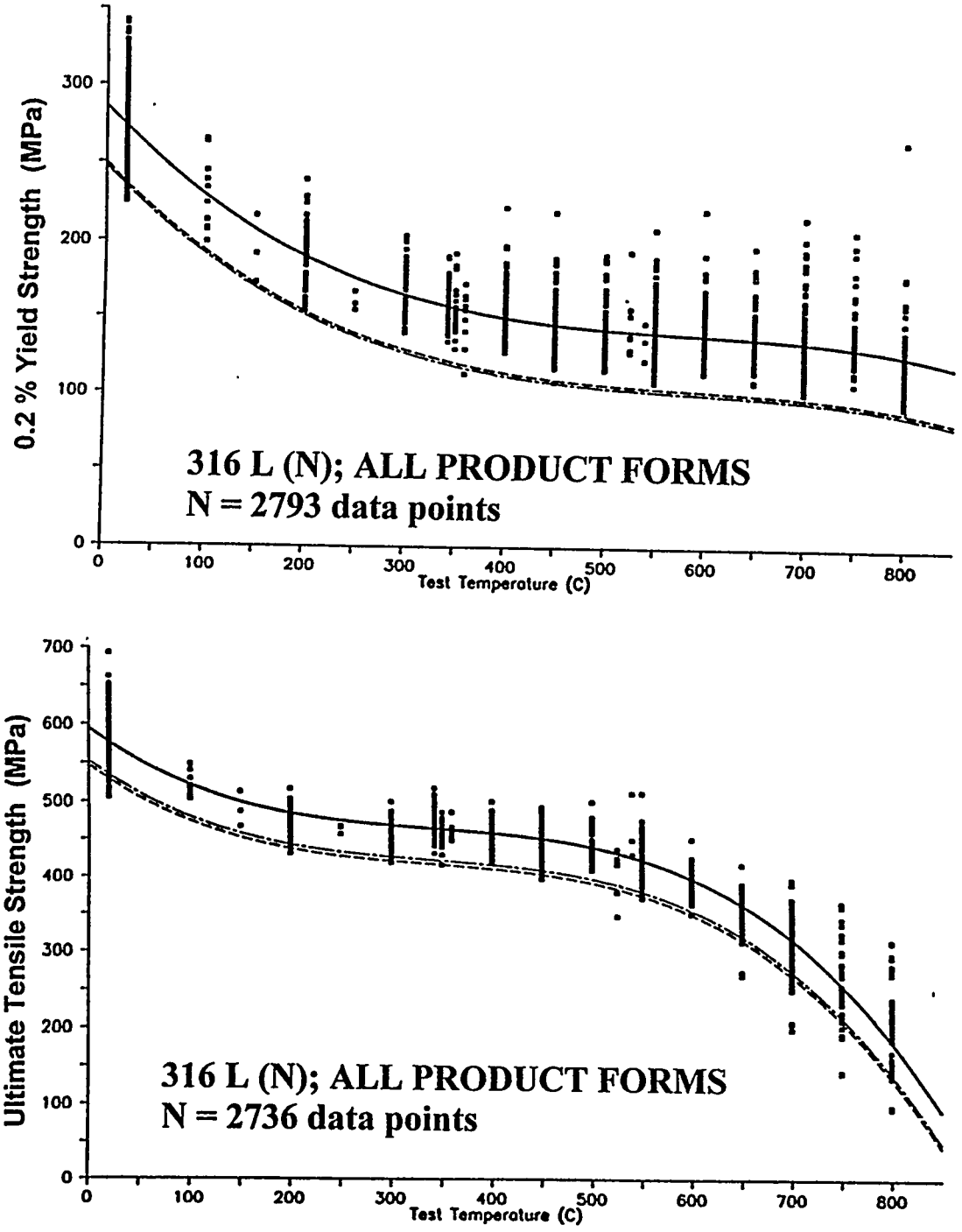

FIG. 1 : Derivation of tensile strength values for type 316L (N) steel for allowable design stresses [1]

The major conclusions and recommendations of the study were as follows :

In relation to the yield strength there are no reason to change the specified average and minimum values given in the RCC-MR. A slight improvement would be to reduce the minimum curve in a manner that, starting from the RT value of 220 MPa and turning the temperature curve downwards, the 550°C minimum value is lowered by 3 MPa to 110 MPa in order to correspond with the acceptance test requirement and thus to harmonize with the specification. This change might be the object of a later revision of the RCC-MR Code.

These data can be used as reference values of high statistical quality level for the normalisation of stress-strain curves.

The analysis of the UTS data has shown that the specified values according to RCC-MR do not satisfactorily describe the material behaviour at elevated temperatures. It was therefore recommended to replace the RCC-MR values for UTS by the results of the actual evaluation.

An other interesting feature was exhibited by the analysis of the results by specification type (FIG. 2). While there was little difference in the average yield strengths, almost for three of them, the so called new specification had lower confidence limit values significantly higher than the other steels. This was attributed to the smallest spread in data brought about by the narrow specification in manufacturing required by the new specification.

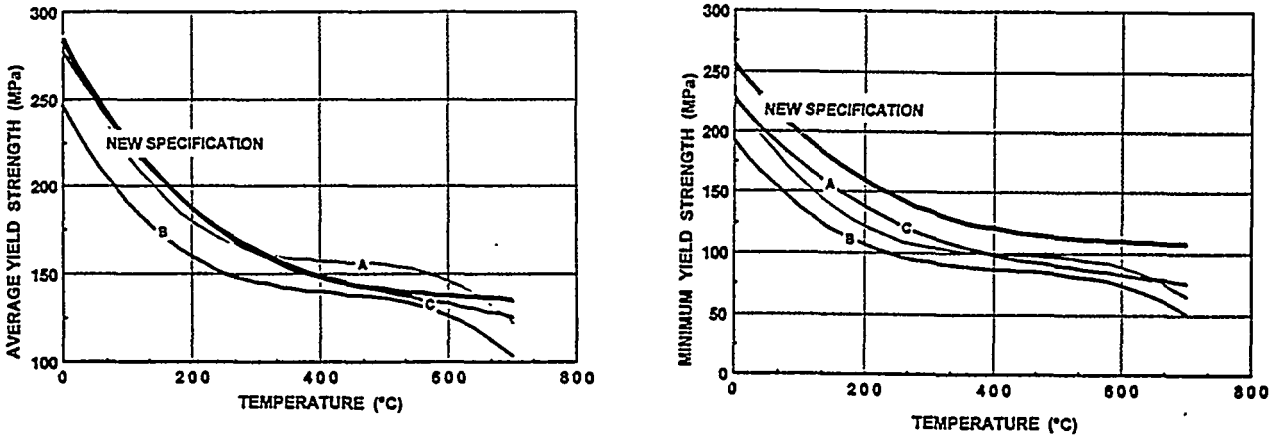

FIG. 2 : Variation of average and minimum yield strength as a function of temperature of 316L stainless steels of different types of European specification [2]

Generally, the fracture mechanics analyses for LBB applications require the knowledge of the stress-strain relationship of the different materials involved in the piping section.

As an example, results [3] of monotonic and cyclic behaviour obtained at 550°C on five heats of modified 316L (N) stainless steels are given in FIG. 3.

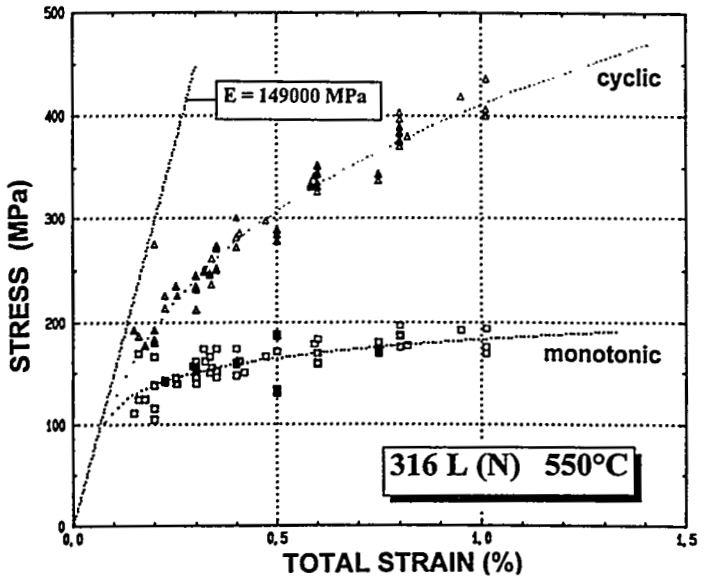

FIG. 3 : Monotonic and cyclic stress-strain curve of 316L (N) stainless steel at 550°C [3]

Tearing Resistance

The resistance against stable crack growth of the material is a parameter that is absolutely necessary to know to conduct a LBB analysis.

It is generally expressed by the J initiation value ($J_{0.2}$) and a J-Δa resistance curve as shows for example in FIG. 4 for a thermally aged 316L (N) tested at room temperature [4].

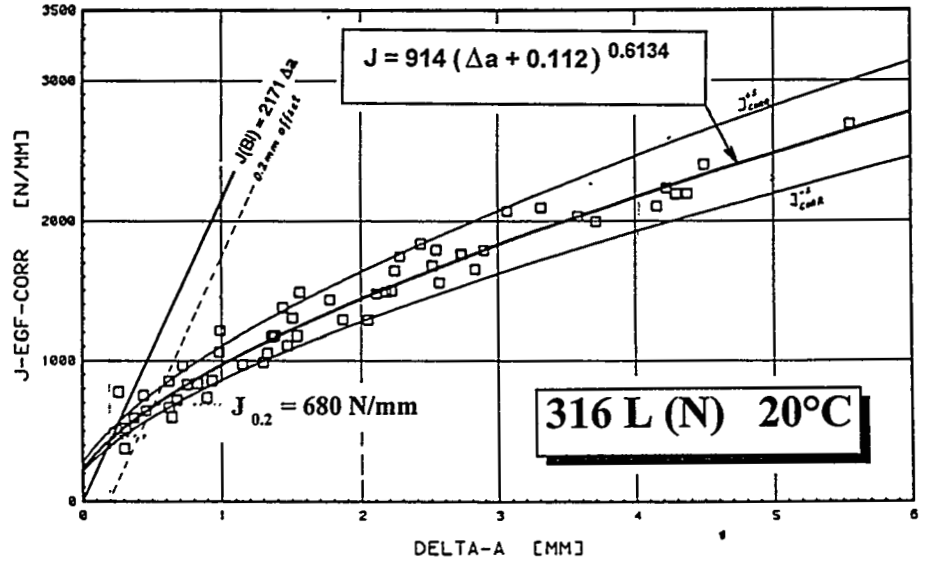

FIG. 4 : Regression curve with offset power law fit for J(CORR) versus Δa [4]

In most cases the analyses need to know the J resistance curve over large crack extensions. That is done by using CT specimens of large dimensions having an important ligament to characterize the decrease in the slope dJ/da of the J resistance curve at large extensions (FIG. 5).

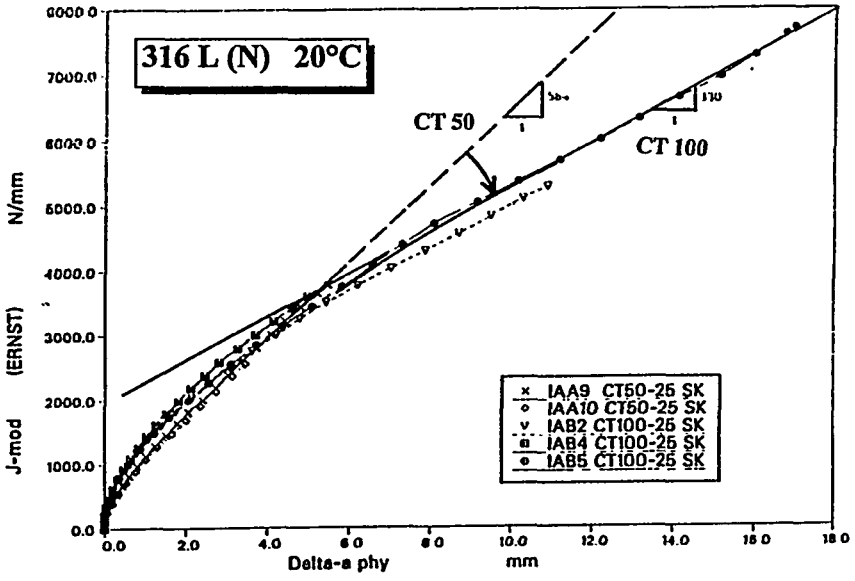

FIG. 5 : J_M-R curve comparison of CT 50 and CT 100 specimen type [4]

Fatigue and creep crack growth rate

The LBB evaluation procedures need the review of direct pipe failure mechanism over the entire life of the plant also of fatigue and creep damage.

In Figure 6 are presented data on creep fatigue crack growth behaviour of 316L (N) that have been developed through a E.C. study [5]. Creep crack growth rate data on 316L (N) stainless steel have been collected and analyzed [6].

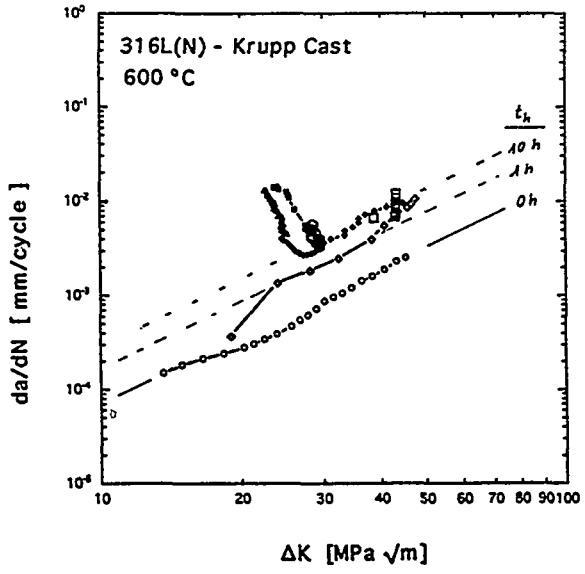

FIG. 6 : Crack growth rates versus ΔK with different holding times [5].

The result of the study was that the correlation of creep crack growth da/dt versus the non linear energy rate line integral C*, calculated from the experimentally determined load point displacement rate, has a lower scatter (Fig. 7) than other parameters such as K and σ_{net}. For practical purposes a reliable upper bound correlation between da/dt and C* can be defined [6].

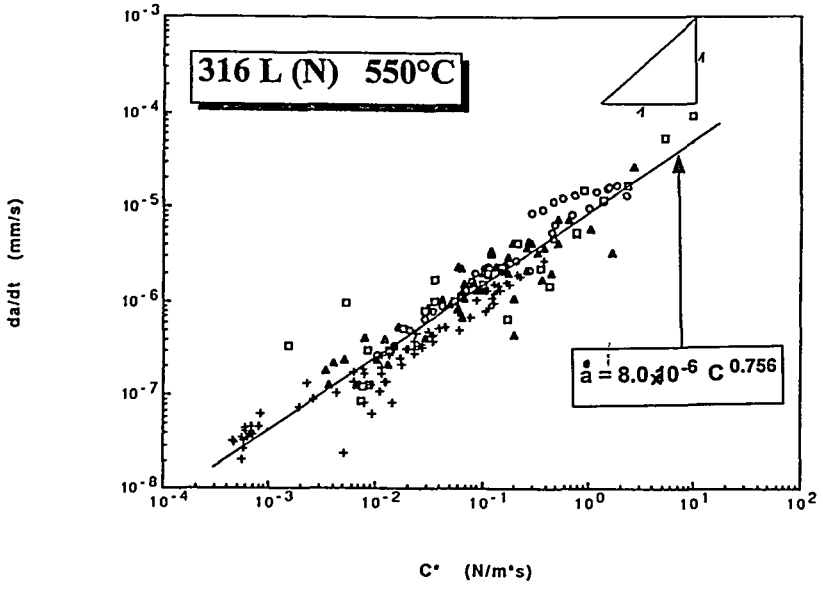

FIG. 7 : Creep Crack Growth rate versus C* integral [6]

MECHANICAL PROPERTIES OF C-Mn AND MnNiMo LOW ALLOY STEELS

Tensile Properties

The data collection was restricted to fully killed steel made preferably (but not solely) since 1975 with chemical compositions lying within the range given by the AFNOR standards for the A42 and A48 grades [7].

The products were generally in the normalized heat treatment condition. The tensile data are predominantly at ambient temperature (2447 out of 2724).

The 0.2 % yield strength and UTS are shown plotted against test temperature in Fig. 8 and 9 respectively.The 0.2 yield strength values for the total data bank have a spread of approximately ± 30 % of the mean value that falls off approximately linearly with test temperature.

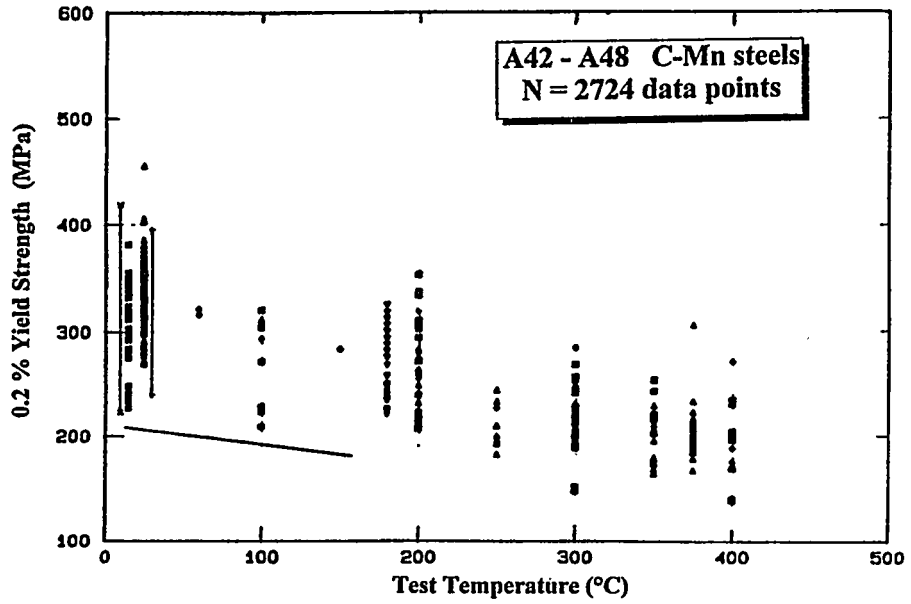

FIG. 8 : Variation of yield strength versus temperature of C-Mn steels [7]

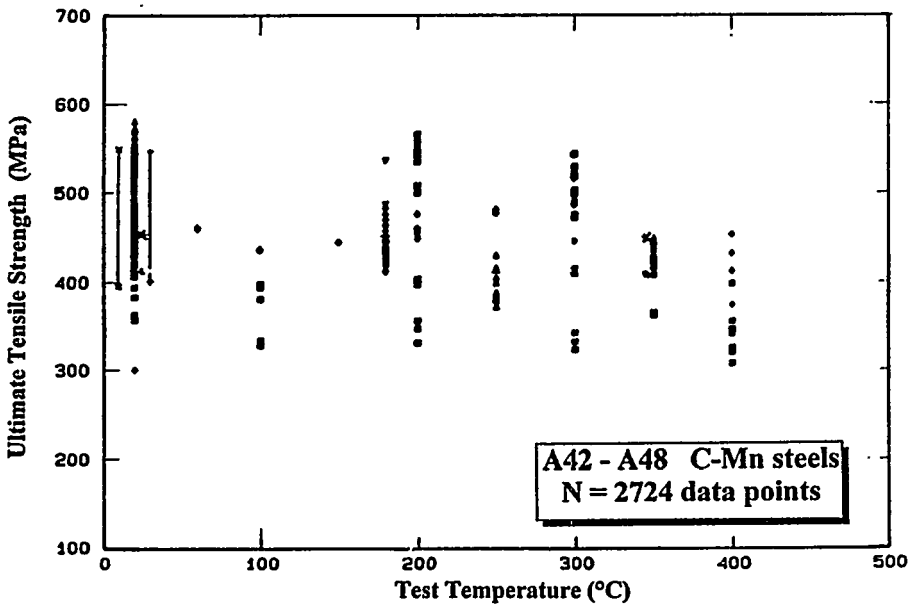

FIG. 9 : Variation of Ultimate Tensile Strength versus temperature of C-Mn steels [7]

The UTS values also fall with increasing test temperature, but the effect is less pronounced (FIG. 9). A significant effect of the thickness of the product has been found on both the yield strength an ultimate tensile strength at 20°C as shown on FIG. 10 for A42 and A48 C-Mn steels. The mechanical properties tend to fall shightly with section thickness.

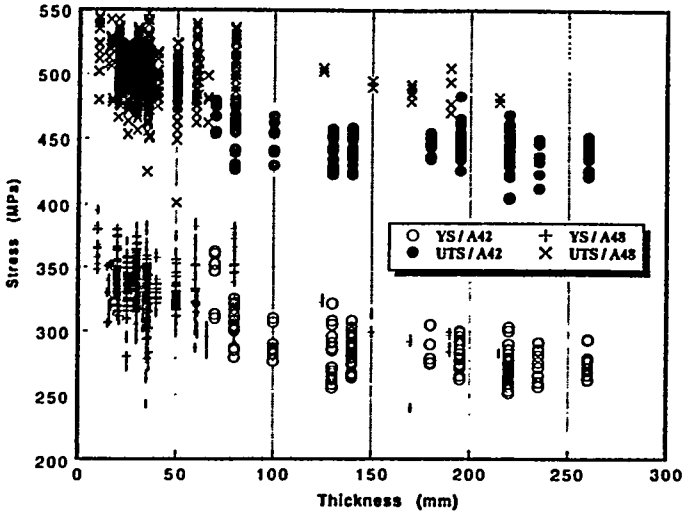

FIG. 10 : Influence of the product thickness on tensile stresses of C-Mn steels.

Tearing resistance

Tearing resistance data have been collected through a E.C. study contract [8]. The moderate influence of specimen dimensions on the J-Δa resistance curve at 100°C in transverse direction of a A48 C-Mn steel of 0.032 (weight %) in sulphur content is illustrated in FIG. 11.

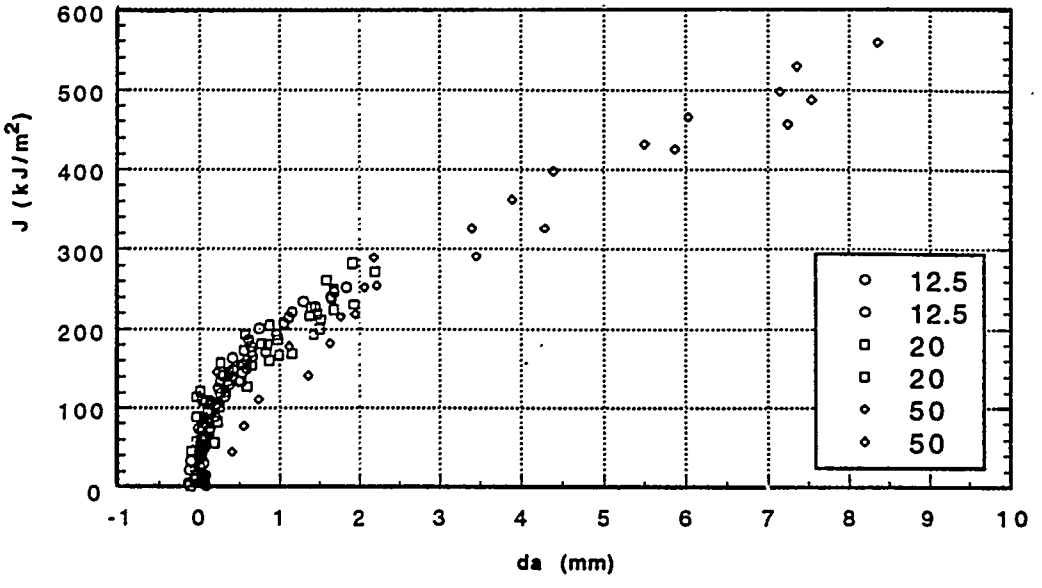

FIG.11 : J-Δa resistance curve at 100°C for A48 steel in TL orientation with specimen sizes varying from CT 12.5 to CT 50 [8].

Beyond the present scope of mechanical data needed for LBB, the E.C. has initiated study contracts on MnNiMo low alloy steel, for light Water Reactors. The first [9] was focussed on the reevaluation of the K_{IC} reference curve (FIG.12) used in fracture mechanics analysis to evaluate the resistance against fast fracture of the vessel. The AG3 "materials" has selected for its 1995 plan the work to be continued by a "Compendium of pressure vessel steel and weldment data required for structural analysis". That study will include data needed for LBB analysis (J-R curve ....)

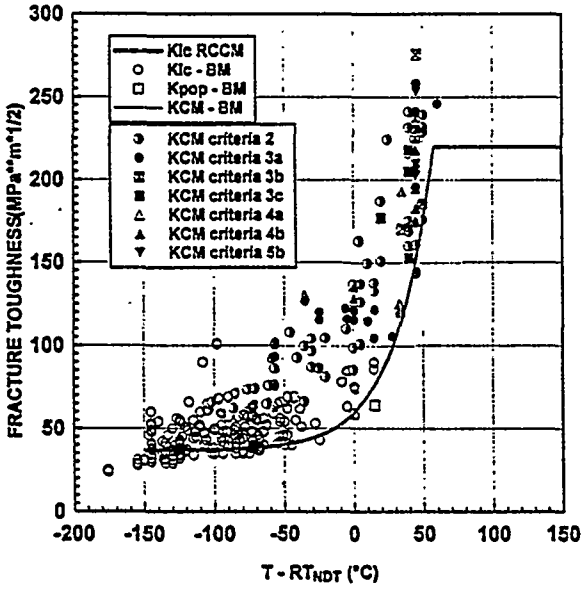

FIG. 12 : Comparison of K_{IC} data of recent European MnNiMo steels to the K_{IC} reference curve [9].

CONCLUSION

The various examples given in the present paper highlight that data of high valuable statistical significance for codification and definition of mechanical properties needed for LBB analysis have been generated by WGCS - DG XI Study Contracts of the E.C. Up to now, most of works were performed on the 316L (N) modified stainless steel for LMFBR application but recent activities are oriented for developing similar activities on C-Mn steels and low alloy steels for LWR.

REFERENCES

[1] E. te HEESEN, V.B. LIVESEY, M. AUBERT and D. LEHMANN, "Derivation of Strength values for type 316L (N) steel for allowable Design stresses", Technical Report Interatom N° 55.10.374.7, CEC Study Contract RA 1-0178D, (1991).

[2] D.S. WOOD, G. BRUNORI, E. te HEESEN and P. PETREQUIN, "Comparative study of the tensile properties of type 316L steel", Commission of the European Communities, Report EUR 7797 EN, (1982).

[3] E. STÄRK, V.B. LIVESEY, M. MOTTOT, A.A. TAVASOLI, M. REGER, "Cyclic hardening behavior of austenitic stainless steel", CEC Study Contract RA1-0140D, (1991).

[4] H. HUTHMANN, A. CORNEC, E. LUCON, S. RAGAZZONI, H.J.M. VAN RONGEN, G. WARDLE, "Fracture toughness round robin on type 316L mod. steel on a thermally aged condition", European Commission Report EUR 14998 EN, (1994).

[5] H. HUTHMANN, I. CURBISHLEY, R. PIQUES and D.J. SMITH, "Crack growth behaviour under creep fatigue conditions of 316L stainless steel", Final report Contract RA1-CT 92.0213, Report KWU NT 4/93/016, (1993).

[6] H. HUTHMANN, A. ALAMO, I. CURBISHLEY and D. ANGELO, 'Creep crack growth behaviour of type 316L steel - Round Robin and Post Test investigations", CEC Study Contracts RAP-071-D and RA1-0111-D, Interatom Report 55-10029-6, (1991).

[7] R. WARD, "The tensile and impact properties of Carbon steel", CEC Study Contract RA1-CT91-0198, NNC report FR/E/004502A, (1993).

[8] A.A. TAVASSOLI and D. LEHMANN, 'Properties of carbon steels - Part II Crack behaviour - Phase 1 Data collection - Phase 2 Data analysis", CEC Study Contract RA1-0212, Note Technique CEA-CEREM NT SRMA 93-2015, (1993).

[9] B. HOUSSIN, D. LIDBURY, P. SOULAT, C. RIEG and R. LANGER, "Reevaluation of K_{IC} reference curve of pressure vessel materials for fracture mechanics analysis", CEC Study Contract ETNU-CT-92.0057, Framatome Report to be published, (1995).

Specialists Seminar Leak Before Break in
Reactor Piping and Vessels, LBB 95, Lyon,
Hotel Sofitel, 9 - 11 October 1995

THE ANALYSIS OF NORMATIVE REQUIREMENTS TO MATERIALS OF PWR COMPONENTS, BASING ON LBB CONCEPTS

V. V. Anikovsky, G. P. Karzov, B. T. Timofeev
CRISM "Prometey", St. Petersburg, Russia

ABSTRACT

The paper discusses the advisability of the correction of Norms to solve in terms of material science the problem: how the normative requirements to materials must be changed in terms of the concept "leak before break" (LBB).

INTRODUCTION

The situation of leak appearance is considered in Section 5.87 of Norms (PNAE G-7-002-86) while selecting calculation defect sizes (the depth of "a" defect is stated to be equal to 1/4S thickness of the wall thickness S, and the safety margin on defect thickness $n_a = 4$), i.e. practically the defect, leading to leak under operation conditions, is allowable and the possibility of brittle fracture is out of the question. However, such approach does not permit to analyse the correlations of leak appearance conditions and to solve the problem of the optimization of properties in terms of LBB. It is known, that the conditions of fracture and leak appearance are determined by:

- material state (its characteristics by considering the factor of material degradation during operation);
- stress-strain state;
- defect sizes and growth and structure component geometry.

Fracture mechanics permits to establish material relation to fracture stresses and defect length. In this case various theoretical models can be used: δ_K-model, two-criteria approaches, the critical SIF, J_{Ic}-integral, J - R curves and T^*-criteria, dependences of PV stability loss (local and total). The field of the application of the stated approaches of ultimate state evaluation depends on structure element thickness and the type of applied material. Thus, pipings, made from austenitic materials, are characterized by a tough mechanism of fracture; for

thick-walled PV, made from pearlitic steels, a brittle fracture mechanism is possible. Norms (PNAE G-7-002-86; ASME; KTA; BS 1515) allow their operation in a brittle state, and the controlling calculation is based on the use of LFM parameters. The ultimate state of brittle, tough fractures and leak are described by the ultimate curves, permitting to analyse structure states (Norms for boilers).

MAIN RESULTS

The conditions of fracture and leak are determined by using the two criteria approach R6. The real safety margins and LBB realization conditions are determined by the fact, how far the calculated point, determining the real state of the given unit on load, crack shape and size is located, at the given moment of operation, from the ultimate curve, describing the unit material state, by the consideration the degradation of the material properties. By this, there variants are possible:

- a crack will not, practically, propagate under operation conditions (the evaluated crack groth of the size a = 0.1S under the action of cyclic loadings in VVER does not exceed 0.1 mm), i.e. safety margin is realized;
- while propagating a surface crack will reach the critical (for given material) size before going out to the other wall surface;
- by growing to the size S and breaking a ligament a crack becomes through, LBB is realized, and a through crack length will be smaller, than the critical one for a long time, sufficient to record leak.

In this connection, in the estimation of the possibility of leak, a practical methotology is as follows:

1. Giving of an initial defect on the base of NDE data (a_o, $2c_o$) by the consideration of a static distribution of technological defects and rules of their schematization.
2. Calculation of critical defect sizes by analysing the structure ultimate states (a_{cr}, $2c_{cr}$).
3. Evaluation of the geometry of initial cracks under conditions of cyclic and quasi-static loading, including ligament break loads ($a_K = a_o + \Delta a$, $2c_K = 2(c_o + \Delta c)$).
4. Calculation of a postulated through crack (on the cosumption of leak) and its comparison with the critical size.
5. Safety margin determination.

As a result of the performed analysis, it was necessary to establish:

- the fact of a stable existence of cracks of the size (a_K, $2c_K$) in PV and piping wall, which are calculated to the end of operation time with the relevant safety margins ($n_a = 2$) under maximum design loads in the normal, hydrotest and accident regimes for pressure vessels and normal and normal + earthquake regimes for pipings;
- stability of a postulated through crack, the sizes of which are

determined from the conditions of a reliable detection of leak. It is shown in (Erdogan 1974), that it is easy to detect leak with the consumption Q = 0.4 l/min. For VVER the consumption Q = 3.8 l/min is, practically, sufficient. However, for a conservative evaluation of a through crack in pipings the consumption Q = 38 l/min (n_Q = 10) is recommended (M-TMP-01-93), and the values of maximum design loads are recommended to increase by $n_\sigma=\sqrt{2}$ times.

For NPP operators the following criteria of LBB realization can be used $t > T/n_t$, where t is the calculated time for a crack increment evaluation from its length $2c_K$ at the moment of ligament break or the length equal to the critical size $2c_{cr}$; T is the real time for the realization of the leak detection system in piping in the normal regime; n_t is the safety margin. Hire $t = (2c_{cr} - 2c_K)/2V$ (V - an axial crack growth rate).

However, such approach does not take into account the history of a semi-elliptical crack growth and the analysis of stability loss of the ligament under crack, which is allowable only for a tough case, when brittle fracture is absent during a surface crack growth. For thick-walled pressure vessels it is necessary to exclude cases of brittle fracture (when a surface crack becomes a through one), and to determine stresses for ligament rupture and to establish the geometry of leak. In a pressure vessel wall, satisfying LBB conditions, a brittle unstable propagation of a through crack must occur under stresses greater, than those, which are necessary for its stable growth on thickness and length or for ligament ductile rupture under a surface crack. The range of LBB realization for a pressure vessel, containing a semi-elliptical crack, is determined as $\sigma^* / \sigma_c < 1$, i.e. by means of the comparison of nominal stresses in vessel wall, leading to the ligament rupture σ^*, with the critical stress σ_c for a through crack of the same length.
The FEM analysis (Broek 1980) shows, that in the absence of the anisotropy of K_{Ic} characteristics in the transversal K^a_{Ic} and axial K^b_{Ic} direction of the vessel 1:2 the LBB conditions are not realized. By using the simplified Irwin criterion (Irwin 1963) and the suggestion, that before the crack slipping through the wall the defect has the shape of a semicircle and the stresses in the wall are equal to the yield stress according to the calculated relation $K^2_{Ic}/(S \cdot YS^2) \geq \pi + 1/2$ it can be shown, that LBB is realized for thicknesses not more, than 30 mm. The ligament rupture conditions under a surface defect can be determined according to the Daffi empirical equation (Daffi 1977), having an empirical confirmation for tubes: $\sigma^* / \sigma_f = A_o \cdot A / [A_o - A(\sigma / \sigma_f)]$, where $A_o = 2c\delta$ is the area of a through defect of the same length as that of a surface defect; A - the surface defect area; σ_f - flow stresses [σ_f = (YS+ + UTS)/2].

For thick-walled vessels and pipings the conditions of plastic joint formation and plastic stability losses of the ligament under a surface defect is determined by the correlation (Norms of boilers) $\sigma^*/\sigma_f = (1 - a/S)/(1 - a/S \cdot 1/M_f)$, where M_f is the Follias correction on the vessel curvature for the through defect 2c: $M_f = [1 + 1.61\ c^2/(R \cdot S)]^{1/2}$. By using the FEM correlation the calculation results of the criterion $K_{Ic}/(\sigma_f \cdot \sqrt{S})$ were obtained for surface longitudinal semi-elliptical defects at a/c = 2/3 for various R/S ratios under nominal tangential stresses equal to 250 MPa. Fig. 1 gives the ultimate values of semi-elliptical defect sizes, for which the LBB condition is realized according to equation, mentioned above, without the correction on plasticity and by the consideraton of it. The LBB conditions are realized by the values of $K_{Ic}/(\sigma_f \cdot \sqrt{S})$ more, than 1.71; 1.76 and 1.81 at R/S = 5, 10; 15, respectively. These conditions are realized for all defect depths but only for pipings of the diameter less, than 36 mm and materials of 270 MPa$\sqrt{m}$ fracture toughness. By lower values of the nondimensional parameter the LBB conditions are realized only for cracks with a definite small or large relative depth, and there exists the range of depths, where brittle unstable fracture without a preliminary leak realization takes place. The loss of the plastic stability of ligament for a/S < 0.7 cracks occurs by nominal stresses, close to the yield stress. Therefore, a correct consideration of LBB conditions requires the application of elastic-plastic analysis metods.

Fig. 2 presents the calculated according to (Sturm 1985) graphical dependences of the ultimate load variation for vessels, containing surface cracks (c/a = 1.5; R/S = 5.0). This figure depicts three areas, calculated according to the methotology (M-01-88), which correspond to brittle fracture (I), developed plastic strains (II) and loss of the ligament plastic stability (III). The generalized toughness parameter $K_c/(\sigma_f \cdot \sqrt{S})$ is plotted on the axis of abscissae. Fig. 3 gives an example of PV calculation at c/a = 1.5 and R/S = 5 on the formulas for a surface and a through-wall defects. The LBB realization is determined by the intersection of the corresponding curves for both types of defects and the realization is possible at a/S > 0.55. A possible mechanism of PV fracture (see Fig. 2) is selected by the structure geometry, its operation conditions and first of all by the material resistance to defect and its strength properties. The LBB conditions can be sufficiently expressed by the introduction in the strength calculation the nondimensional parameter $K_{Ic}/\sigma_f \cdot \sqrt{S}$, controlling the LBB process. From the physical point of view the square of this value characterizes the relation of the crack (r_T) plastic zone size to the element (S) thickness. The loss of plastic stability takes place by r_T/S tending to unit.

In the process of design, production and operation (by the consideration of radiation influence) it is necessary to provide a high level of fracture toughness (K_c), a small resistance of

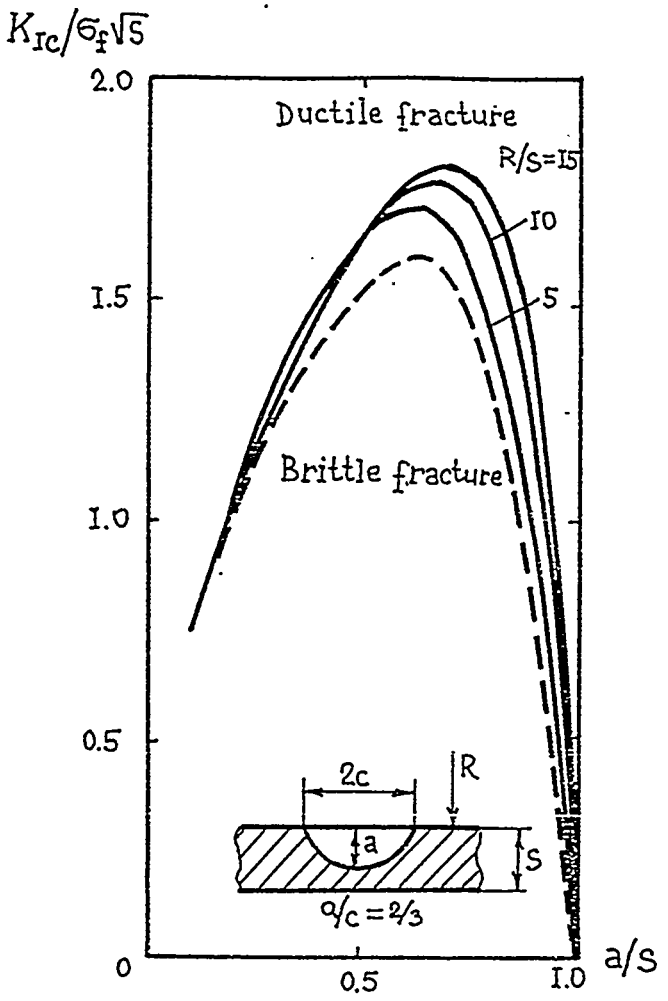

Fig.1. Evaluation of LBB conditions for longitudinal semi-elliptical defects with (—) and without (– – –) the correction on plasticity.

$$2a:\quad \sigma/\sigma_f = \frac{1}{M_F}\cdot\frac{2}{\pi}\arccos[\exp(-Z)]$$

$$Z=\left(\frac{K_c}{\sigma_f\sqrt{s}}\right)^2\cdot\frac{\pi}{8\beta(a/s)}\;;\; M_T=\frac{1-(a/s)/M_T}{1-a/s}$$

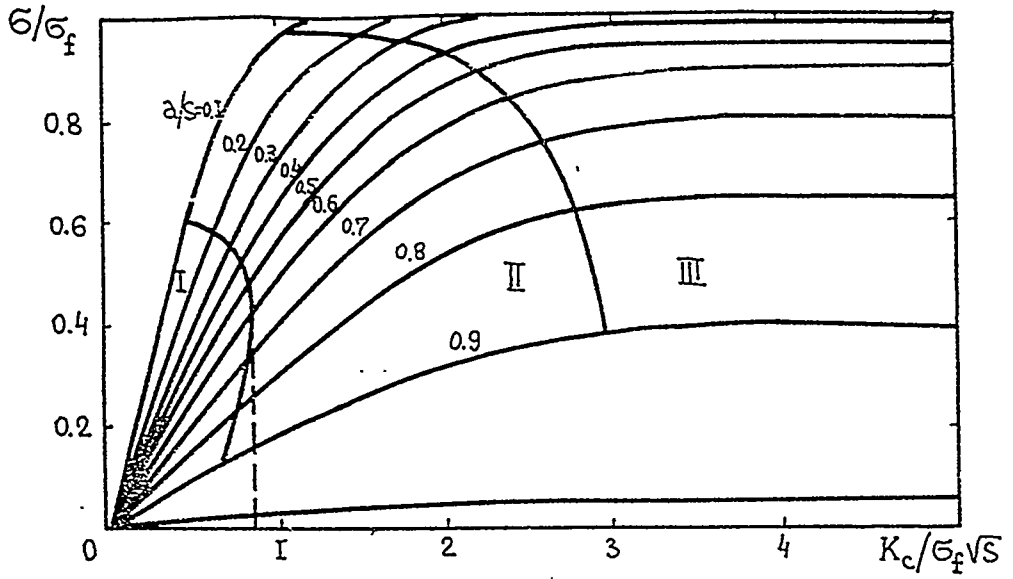

Fig.2.

$$4a:\quad \sigma/\sigma_f = \frac{2}{\pi}\arccos\left[\exp\left(\frac{-Z}{M_F^2}\right)\right]$$

$$M_F=\sqrt{1+1.61\frac{(\beta\cdot a/s)^2}{R/s}}$$

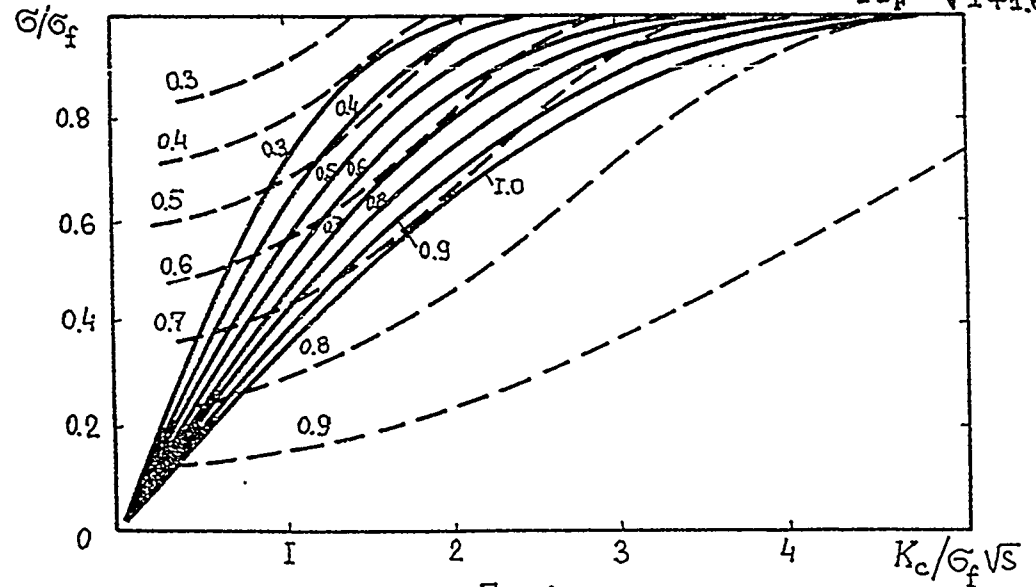

Fig.3.

Fig.2. Ultimate load for a vessel, containing a surface crack (calculation according to dependence 2a): I - area of brittle fracture, II - area of crack propagation by the developed plastic strains, III - area of plastic stability loss. c/a = 1.5, R/S = 5.0.

Fig.3. Ultimate load for a vessel, containing surface (--) and through (——) cracks (calculation according to dependence 4a). c/a = 1.5; R/S = 5.0.

material to plastic strain by considering its hardening (σ_f) and, if possible, not to overstate the wall thickness S. Besides, the geometrical character of structure R/S also has some influence on LBB achievement. It should be also taken into account, that a shape of initial technological defect, determining the crack critical size has a great importance from the point of LBB proceding. In this study for PV a calculated surface defect with the normative correlation of semiaxes a/c = 2/3 is taken, and for pipings (with a great contribution of bending stresses and in the presence of compensating stresses) a/c = 1/3. The simplest and most reliable way to realize LBB is the provision of a high level of material fracture toughness at the stages of design, production and operation. At the value of the parameter

$$Z = (K_c / \sigma_f \cdot \sqrt{S})^2 \cdot \pi / (8 \beta \cdot a/S) > 2.5$$

the conditions of PV fracture in the presence of through and surface defects are determined by the conditions of material Z value equipment materials can be devided in 3 groups:

- austenitic materials of pipings Z > 2.5;
- reactor pressure vessel materials (to the end of design service life) Z < 0.8;
- materials of the main equipment, materials of pressure vessels 0.8 < Z < 2.5.

When the parameter Z is less 0.8 PV materials are in the range of brittle fracture and the application of the LBB concept must be excluded. Within 0.8 < Z < 2.5 the ligament rupture is realized, but a stable crack growth is also possible. In this case, typical of PV materials for NPP equipment, LBB exists in the limitted range of operation time and crack lengths and the bounds of its realization can be established by the calculation.

The performed analysis permits to give recommendations on the correction of the normative documentation concerning the optimization of material properties in terms of LBB concepts:

- decrease of strength properties (i.e. material strength category) to the level of the guaranteed Norms (PNAE G-7-002-88) values;
- increase of the upper shelf of fracture toughness (J - R curves), controlled the acceptance criteria of impact strength and DBTT;
- the reduction of radiation embrittlement coefficient for pressure vessels owing to the application of pure on impurity elements materials.

Besides, the constructive measures are necessary to reduce radiation flow attack on PV wall.

From the positions of LBB realization the investigations are important on the groundation of the calculated defect shape (a/c) for pressure vessels and pipings, which should be supplemented with the statics accomodation on the leak geometry. In the concepts of LFM it is impossible to satisfy the condition $\sigma_c / \sigma^* > 1$ for cracks a = S even if one suggests that a crack start and its

stable increament is possible on the whole wall thickness. Therefore, the application of the LBB concept as a safety criterion should be prohibited in a brittle zone, because dynamic effects by the ligament rupture are difficult to consider. Due to a small power-intensity and a high speed of rupture process of ligament the critical crack length, in this case may decrease and will be determined by the value of stored energy in the system "pressure vessel - coolant" and its maintenance at a certain level.

CONCLUSION

Thus, there are preconditions for pipings and pressure vessels for the realization of the LBB concept. For this purpose it is necessary to select materials with low values of initial characteristics DBTT, σ_f and the coefficient of radiation resistance A_F (P < 0.010%, Cu < 0.1%) and to provide the given conditions of irradiation F < 1.2×10^{23} neutr/m^2. To ground the assumptions, taken in calculations, it is necessary to carry out investigations associated with the obtainment J - R curves and the correction of the upper shelf of K_c (J_c) curves by the consideration of the change of metal strength category by irradiation, by the groundation of the calculated defect geometry. It is also necessary to develop supplements to Norms on the consideration of the calculated LBB situation as well as for the case of shallow cracks and thermal prestressing.

REFERENCES

ASME Boiler and Pressure Vessel Code. Section XI. 1986.

Broek D. Bases of Fracture Mechanics. Moscow, 1980.

BS-1515. Fusion Welded Pressure Vessels. Part1. Carbon and Ferritic Alloy Steels. 1975; Part 2. Austenitic Stainless Steel. 1978.

Daffi A.P. Practical examples of brittle fracture resistance calculations of pressurized pipings. Fracture, vol.5, 1977, p.146-209.

Erdogan F., Ratwani M. Fracture Initiation and Propagation in a Cylindrical Shell Containing an Initial Surface Flaw. Nuclear Engineering and Design, 27, 1974, p.14-29.

Irwin G. Fracture of Pressure Vessels "Materials for Misriles and Spacecraft". 1963, p.204-229.

M-01-88. Procedure of Calculation of Permissible Defects Equipment and Pipes during NPP Operation. Moscow, 1988.

M-TMP-01-93. Calculation Procedure of Pipings with Using Criteria Leak Before Break. Moscow, Gosatomnadzor, 1993. Norms of Boilers. A special group on piping evaluation. Theoretical base of Engineering Calculations, nr.3, 1986, p.146-171.

PNAE G-7-002-86. Calculation Norms for Nuclear Power Plant Equipment and Pipings. Energoatomizdat, Moscow, 1989.

Sturm O., Stoppler W. Strength behaviour of flawed pipes under internal pressure and external bending moment: comparison between experiment and calculation. 17-th MPA Seminar, October, 1989.

THE NATURE THICKNESS PIPE ELEMENT TESTING METHOD TO VALIDATE THE APPLICATION OF LBB CONCEPTION

Vasilchenko G.S., Artemyev V.I., Merinov G.N., TSNIITMASH, Russia.

Rivkin E.Yu., NIKIET, Russia.

To validate the application of LBB conception to main pipe D850 VVER-1000 reactor the procedure for the test of a large-scale specimen on electrohydraulic machine PC 10.0C Schenck was developed.

For this aim from the pipe storage diameter 850x70 mm (steel 10ГН2МФА with circular weld and stainless cladding inside) was manufactured by PO ATOMMASH to a standard technology. The large-scale longitudinal specimens having 2000 mm length and 250x70 mm cross-section were cut out from this pipe storage. The remaining parts of the weld after cut out were used for determination standard tensile mechanical properties, critical temperature of brittlness and for manufacture of compact specimens.

The guaranteed [1] and experimental mechanical properties of weld are giving in the table.

Mechanical properties of weld metal of the steel 10ГН2МФА.

Temperature °C	Yield Stress $R_{p0.2}$, MPa	Ultimate Strength R_m, MPa	Elongation A, %	Area Reduction Z, %
		Guaranteed		
20	343	539	16	55
350	294	490	14	50
		Experimental		
20	427.3-548.8 (490.6)	559.6-666.4 (613.3)	19-28 (25.2)	41.6-73.3 (64.4)
320	367.5-454.7 (401.1)	506.7-579.5 (540.7)	19-20.3 (19.4)	64-71.6 (67.8)

Note: Middle values are showing in brackets.

The critical temperature of brittlness determined by standard method [2] was equal by minus 60 °C. The stress-strain diagrams were expressed

by dependence Ramberg-Osgood with parameters at 20 °C α=2.52, n=7.9 and at 320 °C - α=1.12, n=11.7.

The test of compact specimens. The compact specimens having been thickness 25 mm were used for test at temperatures 20 °C and 320 °C. The surfaces of stable growing up crack were checked by heat painting.

The values of J-integral were calculated with use of diagram load-displacement P-Δ according formula of Russia standard [3]:

$$J = \frac{\left(1-\mu^2\right)\cdot K_1^2}{E} + \frac{A_p}{(w-l)\cdot t}\left[2 + \frac{0.522\cdot(w-l)}{w}\right], \qquad (1)$$

were: μ - Poisson's ratio; E- elastic modules; w - specimen width; t- specimen thickness; A_p - plastic area under diagram P - Δ; l - crack length.

The calculations were showed that J_R-curve at 20 °C can be described by expression $J_R = 0.565\cdot\Delta l^{0.705}$ and at 320 °C - $J_R = 0.311\cdot\Delta l^{0.705}$ (Fig.1).

The value J_{1c} was determined [3] by intersection point of line blunting $J = \Delta l\cdot(R_{p0.2} + R_m)$ and straight line carried out across experimental points in reliable square. Next dates were received: at 20 °C J_{1c} = 0.28 MN/m, K_{1c} = 242.5 MPa·m$^{0.5}$, at 320 °C J_{1c} = 0.12MN/m, K_{1c} = 159 MPa·m$^{0.5}$.

The test of large-scale specimens with central through-wall crack by tension. The general kind of large-scale specimen mounted in machine PC 10.0C Schenck is showing on Fig.2. Three specimens having been 70x250 mm cross-section with initial length of through-wall crack $2l_0$ =67.3; 129.2 and 150.8 mm were tested at temperature 20 °C.

The static loading was carried out after growing up crack from the cut by cyclic loading. Stable growing up cracks were checked with use of intermediate cyclic loading. The stress-strain diagram with intermediate unloading written by the test of specimen 35 is showing on Fig.3.

The determination of values J were carried out at formula [4]:

$$J = J_e + \frac{1}{2\cdot t\cdot b}\cdot\left[2\cdot\int_0^{\Delta_{pl}} P\cdot d\Delta - P\cdot\Delta_{pl}\right], \qquad (2)$$

where

$$J_e = \frac{K_1^2\cdot(l_e)}{E}, \qquad b = \frac{w-2\cdot l}{2},$$

$$l_e = l + \frac{1}{2\pi}\cdot\left(\frac{n-1}{n+1}\right)\cdot\left(\frac{K_I}{R_{p0.2}}\right)^2\cdot\left(\frac{1}{1+P/P_0}\right),$$

$$P_0 = R_{p0.2}\cdot\left(1-\frac{2l}{w}\right)\cdot t\cdot w,$$

Δ_{pl} - plastic part of displacement.

J_R-curve for large-scale specimens with use of least square method and experimental points are showing on Fig.4.

The test of large-scale specimens with central surface semielliptical cracks by tension. Four specimens having been 70x250 mm cross-section with initial crack sizes (a_0-depth, c_0-semilength) a_0 = 34.8 mm, $2c_0$ = 182.4 mm; a_0 = 37.3 mm, $2c_0$ = 112.6 mm; a_0 = 36.3 mm, $2c_0$ = 140 mm; a_0 = 37.35 mm, $2c_0$ = 143.2 mm were tested at temperature 20 °C. Stable growing up cracks were checked also with use of intermediate cyclic loading. The general kind of break of specimen was showing on Fig.5.

The determination of values J were carried out at formula [5]:

$$J = \frac{P\cdot\Delta}{2\cdot t\cdot\left(w\cdot t/c-a\right)} + R_{p0.2}\cdot\Delta_{pl}/2. \qquad (3)$$

The calculating J_R -curve and experimental points are giving on Fig. 6.

Analysis of obtained results. J_R curves weld material constructed at test of difference specimens are giving on Fig.7. Least values at the some growing up of cracks were observed at the tests of compact specimens, most ones-at tests specimens with through-wall crack and intermediate ones-at tests specimens with surface crack. The results of tests specimens with through-wall central crack were showed that visible growing up of crack (0.5-1.0 mm) was observed at net stress near yield stress and loading before fracture was achieved at maximum stress equalled approximately $0.5(R_{p0.2}+R_m)$.

The investigation of cyclic crack resistance. The study of a crack kinetic of weld material at cyclic loading was carried out on an air at the temperature 20 °C with using specimens of small sizes at tensile and bend and the same one was carried out for large-scale specimens with through-wall and surface cracks. It was revealed that parameters of cyclic cracking resistance which had been measured on large-scale specimens and small standard specimens were identical. Summary dates of all tests are showing on Fig.8. The group of data was described by expression

$$\frac{da}{dN} = 2.1 \cdot 10^{-12} \cdot (\Delta K_I)^{3.1}. \qquad (4)$$

The reliable estimation with taking into consideration of data scatter was described by expression

$$\frac{da}{dN} = 4.75 \cdot 10^{-12} \cdot (\Delta K_I)^{3.1} \qquad (5)$$

where a in m and K in $MPa \cdot m^{0.5}$.

References

1. ПНА ЭГ–7–010–89. Оборудование и трубопроводы атомных энергетических установок. Сварные соединения и наплавки. Правила контроля. М. Энергоатомиздат, 1991, 319с.

2. ПНА ЭГ–7–002–86. Нормы расчета на прочность оборудования и трубопроводов атомных энергетических установок. М. Энергоатомиздат, 1989, 524 с.

3. ГОСТ 25.506–85. Методы механических испытаний металлов. Определение характеристик трещиностойкости (вязкость разрушения) при статическом нагружении. Госстандарт СССР. М. 1985, 61 с.

4. Rice J.R., Paris P.C., Mercl J.G. Some further results of J-integral analysis and estimates. ASTM STP 536.231 1973

5. Garwood S.J. A Method of Estimating the Value of J_R (the value of J for a propagating crack) from a Single Specimen. Int. J. Fracture, vol. 14,1978.

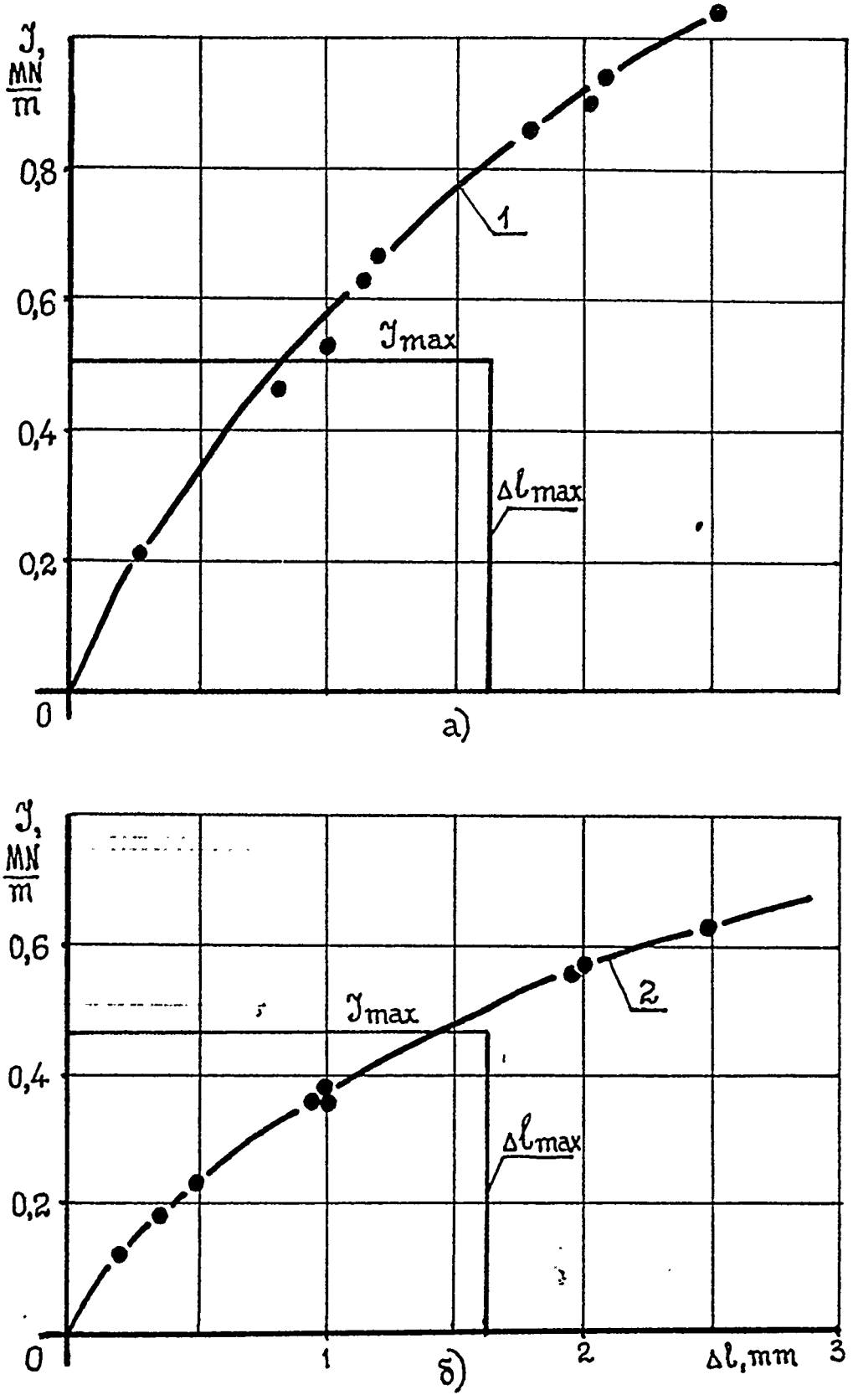

Fig.1. Diagrams of fracture resistance for pipe weld metal of steel 10ГН2МФА obtained by means of test of compact specimens at temperature 20 ^{0}C (a) and 320 ^{0}C (b).
1 - $J_R = 0.565 \cdot \Delta l^{0.705}$; 2 - $J_R = 0.311 \cdot \Delta l^{0.705}$.

Fig.2. General view of a large-scale specimen mounted in a test machine PC-10.0C Shenck.

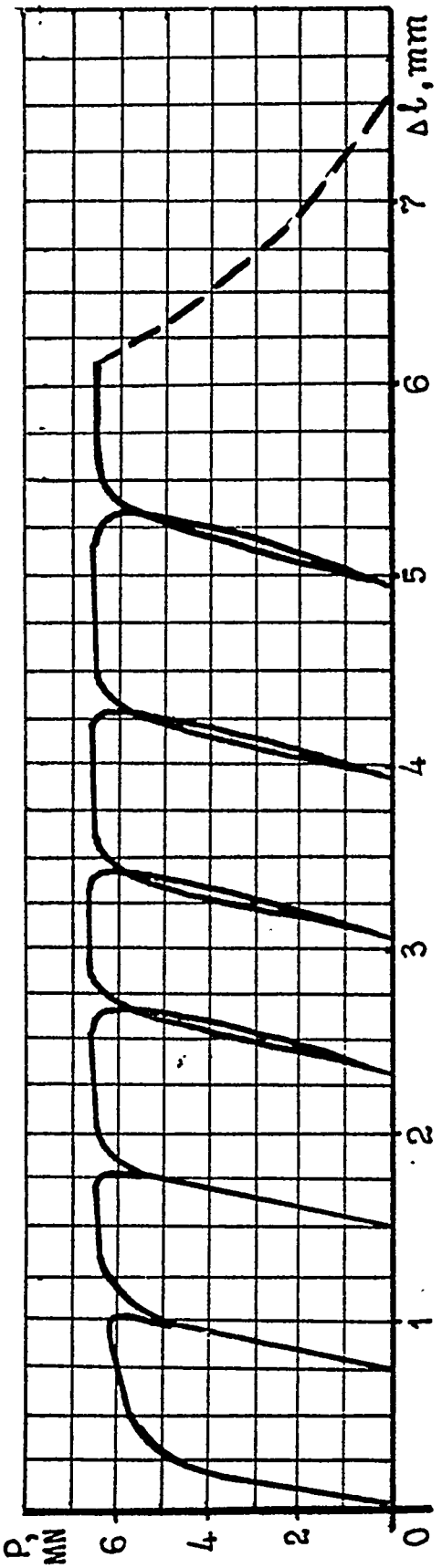

Fig.3. Diagram of load-strain for large-scale specimen 35 with through-wall crack.

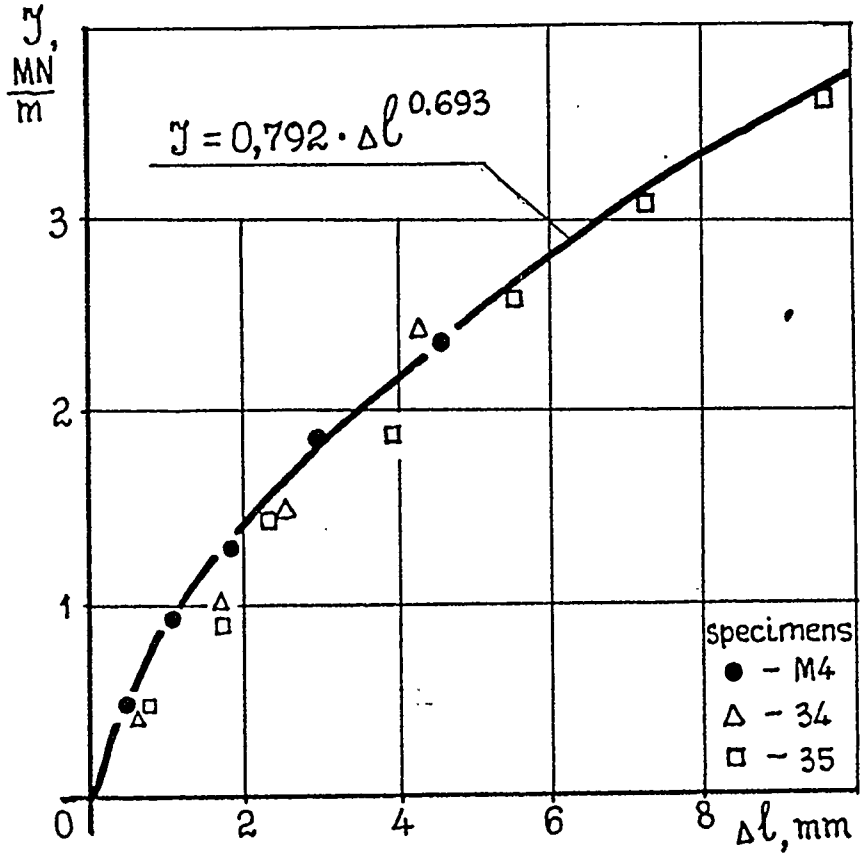

Fig.4. Diagram fracture resistance for pipe weld metal of steel 10ГН2МФА obtained by means of tensile test the large-scale specimens M4, 34, 35 with central through-wall crack.

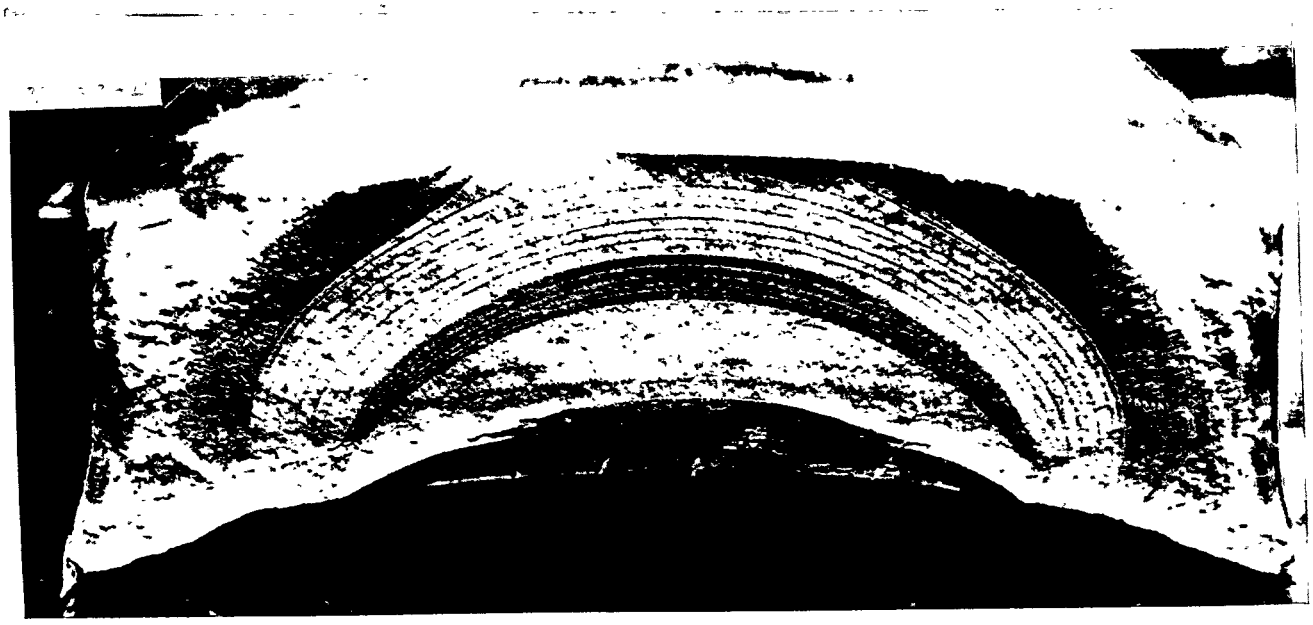

Fig.5. Fractured surface of the large-scale specimen 33 with surface crack.

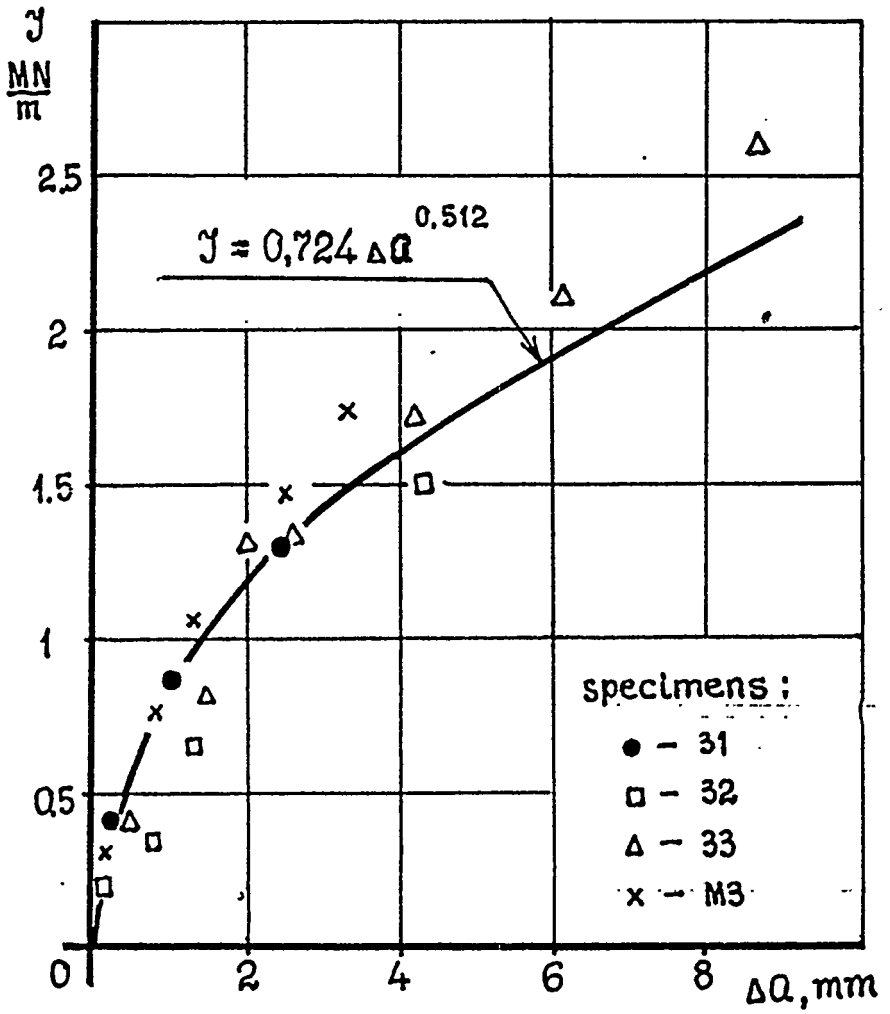

Fig.6. Diagram fracture resistance for pipe weld metal of steel 10ГН2МФА obtained by means of tensile test the large-scale specimens with surface crack.

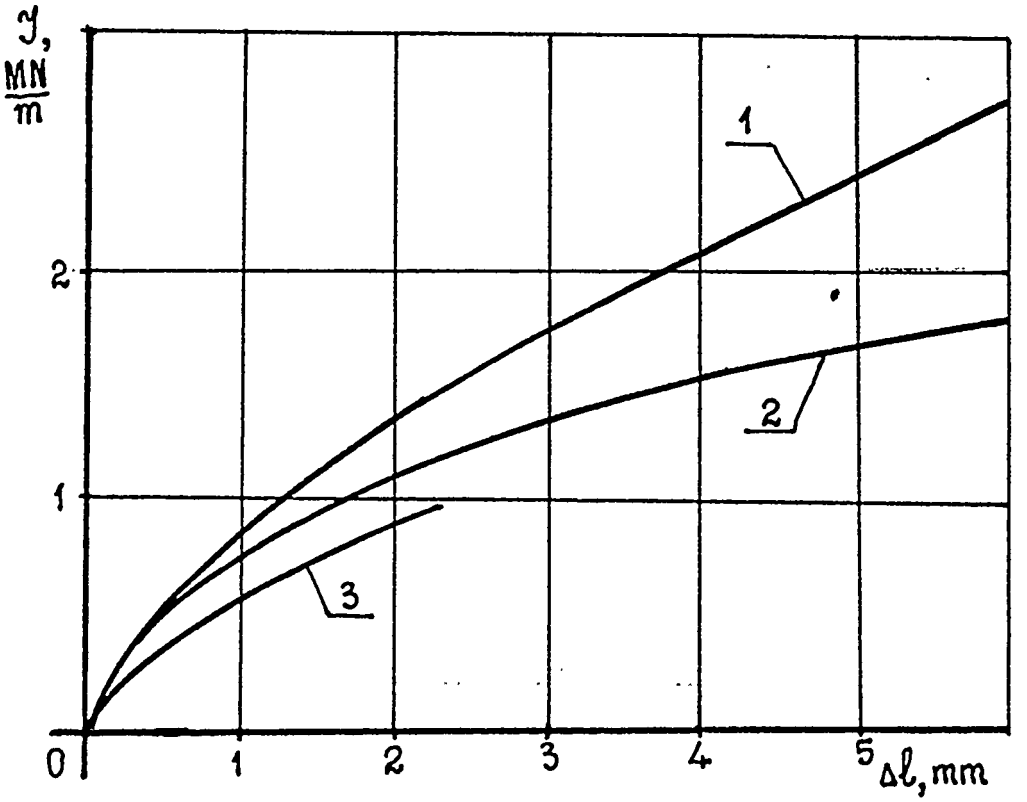

Fig.7. Calculating curves by results of different specimens.
1 - central through-wall crack;
2 - surface crack;
3 - compact specimen.

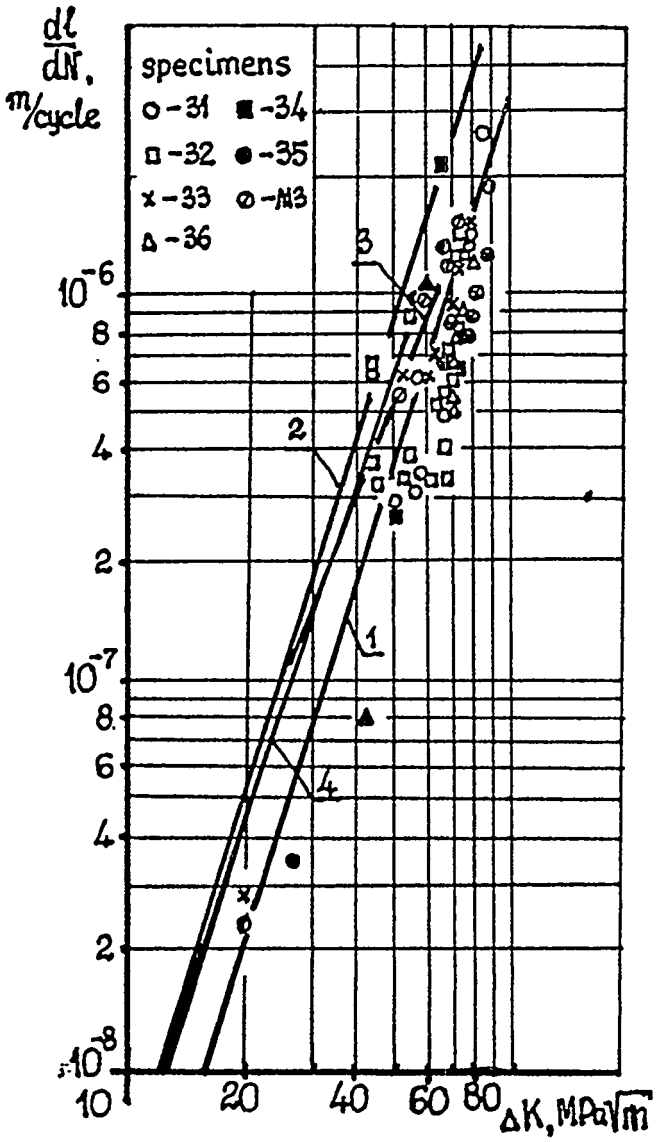

Fig.8. Cyclic curves crack grow up.

1 - bend specimens 18x12x160 mm, f=15 Hz;

2 - bend specimens 18x12x160 mm, f=1 Hz;

3 - compact specimens CT-1, f= 10 Hz;

4 - tensile specimens 10x60x300 mm, f= 20 Hz;

the large-scale specimens 31 - 36, M3 of cross-section 70x250 mm with surface and through-wall cracks.

Effect of Dynamic Monotonic and Cyclic Loading on Fracture Behavior for Japanese Carbon Steel Pipe STS410

BY

Kanji Kinoshita
Tokyo Electric Power Co.., Inc.
Kouichi Murayama
Hitachi, Ltd.
Hiroshi Yokota
Mitsubishi Heavy Industries,Ltd.
Keisuke Kitsukawa
Toshiba Corporation
Hiroyuki Ogata
Ishikawajima-Harima Heavy Industries Co., Ltd.
and
Koichi Kashima
Central Research Institute of Electric Power Industry

ABSTRACT

The fracture behavior for Japanese carbon steel pipe STS410 was examined under dynamic monotonic and cyclic loading through a reserch program of International Piping Integrity Research Group (IPIRG-2), in order to evaluate the strength of pipe during the seismic event. The tensile test and the fracture toughness test were conducted for base metal and TIG weld metal. Three base metal pipe specimens, 1,500mm in length and 6-inch diameter sch.120, were employed for a quasi-static monotonic, a dynamic monotonic and a dynamic cyclic loading pipe fracture tests. One weld joint pipe specimen was also employed for a dynamic cyclic loading test. In the dynamic cyclic loading test, the displacement was controlled as applying the fully reversed load (R=-1). The pipe specimens with a circumferential through-wall crack were subjected four point bending load at 300C in air.

Japanese STS410 carbon steel pipe material was found to have high toughness under dynamic loading condition through the CT fracture toughness test. As the results of pipe fracture tests, the maximum moment to pipe fracture under dynamic monotonic and cyclic loading condition, could be estimated by plastic collapse criterion, and the effect of dynamic monotonic loading and cyclic loading was a little on the maximum moment to pipe fracture of the STS410 carbon steel pipe. The STS410 carbon steel pipe seemed to be less sensitive to dynamic and cyclic loading effects than the A106Gr.B carbon steel pipe evaluated in IPIRG-1 program.

1. INTRODUCTION

Remarkable decrease of the tensile strength and toughness under dynamic loading and remarkable decrease of the maximum moment under dynamic cyclic loading for carbon steel pipe A106Gr.B pipe of ASTM standard had been found out through a reserch program of International Piping Integrity Research Group (IPIRG-1). [1] These results may influence the evaluation of the strength of cracked pipe during the seismic event, in other words LBB(Leak Before Break) evaluation.

In Japan, the dynamic cyclic tests have been conducted for small-diameter Japanese carbon steel pipes (STS410) [2][3] and showed little dynamic effect on pipe fracture. However, the dynamic-cyclic effect for larger diameter pipe must be evaluated in comparison with A106G.B pipe. Therfore, the fracture behavior for Japanese carbon steel pipe STS410 was examined under dynamic monotonic and cyclic loading to evaluate the sensitivity of STS410 to dynamic and cyclic effects as A106Gr.B.

These tests were performed by Battelle, using the specimens supplied by the Japanese joint research members through a reserch program of International Piping Integrity Reserch Group (IPIRG-2), Task 3 and Task 4.

2. MATERIAL CHARACTERIZATION TESTS

2.1 Test Material

STS410 pipe, used as a typical carbon steel pipe of RCPB(Reactor Coolant Pressure Boundary) in Japanese BWR plants, was selected for test material. All base metal specimens were fabricated from 6-inch diameter Sch.120, STS410 carbon steel pipe. All weld specimens were machined from tungsten-inert-gas(TIG) weld of 6-inch diameter Sch.120, STS410 carbon steel pipe. The pipe sections used in the fabrication of the base metal tensile and C(T) specimens, and the pipe sections used for weld metal specimens, were all from the same heat of pipe as the pipes used in the pipe fracture experiments. The welding for the pipe experiments and material tests were all made at the same time using the same procedures.

2.2 Test Conditions

Tensile tests and fracture toughness tests were conducted at 300C(572F). All tensile specimens were manufactured with the tensile axis parallel with the pipe axis. All C(T) specimens were manufactured without flattening and were fabricated in the L-C orientation, simulating the growth of circumferential through-wall crack in a pipe. Fracture toughness tests were conducted on both the base and weld metal per ASTM E1152/E813.

Both quasi-static and dynamic loading rates (nominally 1, 10sec $^{-1}$) were used in the tensile tests and the fracture toughness tests. All of these tests were conducted using monotonic increasing displacement-control, i.e., there was no cyclic loading in these material characterization tests.

Table2.1 shows the material characterization test matrix.

2.3 Results of Tensile and Fracure Toughness Test

Table2.2 shows the tensile test results for both the STS410 base metal and the TIG weld. As the strain rate is increased from quasi-static to dynamic rates, the tensile strength is decreased in both base and weld metal. The weld metal has high tensile strength than base metal at all cases of the loading rates. The serrations were

slightly observed in stress-strain curves at the dynamic loading, indicating that the material is not highly sensitive to dynamic strain aging.

Table2.3 shows the toughness test results for both the STS410 base metal and the TIG weld. Fig2.1 shows the J-R curves for base metal and Fig2.2 shows the J-R curves for weld. The effect of loading rate on the fracture toughness is minimal for base metal and weld though J at crack initiation is decreased for the weld metal when the strain rate is increased.

3. PIPE FRACTURE EXPERIMENTS

3.1 Test Procedures

Table3.1 shows the test matrix for four pipe experiments conducted in four-point bending. Three base metal pipe specimens which were 1,500mm in length, 6-inch diameter Sch.120, were employed for a quasi-static, a dynamic-monotonic, and a dynamic cyclic loading pipe fracture tests. One weld joint pipe specimen was also employed for a dynamic-cyclic loading test. In the dynamic-cyclic loading tests, the displacement was controlled as applying the fully reversed load (R=-1). The pipe specimens with a circumferential 60 degrees through-wall crack were subjected four point bending load at 300C in air.

Fig3.1 shows the schematic of test apparatus. This is Battelle's 580KN Material Testing Systems (Supplier of servo-hydraulic equipment) for displacement-controlled cyclic pipe experiment. Prior to the actual test loading, the circumferential through-wall flaws in these pipe experiments were introduced at the mid-length position of the pipe using Electric-Discharge-Machining.

3. 2 Results of Pipe Fracture Tests

The summary of the results from the pipe fracture tests is shown in Table 3.2. Figure 3.2a shows the moment-rotation curves measured in the quasi-static monotonic loading test (Experiment 3.3-1) and the dynamic monotonic loading test (Experiment 4.2-1). The curves measured in the dynamic-cyclic loading tests(Experiment4.2-2, 4.2-3) are shown in Figure 3.2b and 3.2c. The rotation data shown in these figures are the half rotation angle (ϕ), i.e., the average rotation of the pipe to its initial horizontal position.

The ratios of experimental maximum moment to predicted maximum moment based on plastic collapse criterion are listed in Table 3.3. The predicted maximum moment was calculated by the following equations.

$$M_{max} = 2\,\sigma_f\,R^2\,t\,(2\sin\beta - a/t\sin\theta) \qquad (1)$$

$$\beta = 1/2\,(\pi - a/t\,\theta) \qquad (2)$$

Here R and t are the nominal radius and thickness of pipe, a and θ are the the depth and half angle of crack, and σ_f is the flaw stress defined as the average of yield and tensile strength obtained in the material test under quasi-static loading.

Figure 3.3 shows the comparison of the maximum-moment ratios between the STS410 and A106Gr.B. The data of the A106Gr.B shown in this figure are based on the results from IPIRG-1 program. [4) 5)]

Based on these tests, The effects of dynamic monotonic and cyclic loading on the fracture behavior was evaluated for STS410 carbon steel pipe.

3.2.1 The Effect of Dynamic Loading

The comparison of the moment-rotation curve between the quasi-static monotonic loading test and the dynamic monotonic loading test is shown in Figure 3.2a. The maximum moment under the dynamic loading decreased slightly against that under quasi-static loading. However, the maximum moment under the dynamicloading could be also estimated by the plastic collapse criterion because the maximum-moment ratio was nearly equal to 1, as shown in Table 3.3.

According to the comparison of the ratios between the STS410 and the A106Gr.B, the ratios were decreased in both the STS410 and A106Gr.B with increasing loading rate. However, the extent of the reduction of the STS410 was slightly less than that of the A106Gr.B, as shown in Figure 3.3. In addition, the STS410 didn't show the behavior although the A106Gr.B under the dynamic loading showed the behavior of some crack instabilities, i.e., crack jumps,. Thus, the STS410 pipe seems to be less sensitive to dynamic loading effect than the A106Gr.B pipe. This suggestion is supported by the results of the tensile tests and fracture toughness tests. The STS410 pipe material seems to be less sensitive to dynamic strain aging than the A106Gr.B pipe material.

3.2.2 The Effect of Cyclic Loading

Figure 3.4 shows the comparison of the moment-rotation curve between the dynamic monotonic loading test and the dynamic cyclic loading tests. In this figure, only the envelope of the moment-rotation curves are presented.

The maximum moment under the cyclic loading was slightly decreased in base metal against that under the dynamic loading. However, the maximum moment under the cyclic loading could be also estimated by the plastic collapse criterion because the muximum-moment ratio was nearly equal to 1, as shown in Table 3.3. According to the comparison of the ratios between the STS410 base metal and the A106Gr.B base metal, the extent of the reduction of the STS410 base metal to the dynamic loading was less than that of the A106Gr.B, as shown in Figure 3.3. The STS410 pipe seems to be less sensitive to cyclic loading than the A106Gr.B pipe.

4. CONCLUSIONS

The fracture strength of the STS410 carbon steel pipe with circumfrencial through-wall crack has been examined under quasi-static monotonic, dynamic monotonic and dynamic cyclic loading conditions, in order to evaluate the dynamic monotonic and cyclic loading effects. The conclusions are summerised as follows :

(1) The STS410 carbon steel pipe material and the associated TIG weld may be slightly suspectible to dynamic strain aging effects. However, the extent of their suspectibility is probably slight.

(2) The STS410 carbon steel pipe seems to be less sensitive to dynamic monotonic and cyclic loading effects than the A106Gr.B carbon steel pipe evaluated in IPIRG-1 program.

5. ACKNOWLEDGMENTS

This study was conducted at BCL as one of the tasks in IPIRG-2 using the Japanese pipe specimen provided by the Japanese joint research group. The authors would like to express their gratitude to BCL staff for their effort and to Technical Advisory Group members for IPIRG-2 program for their valuable comments.

In Japan, this study was done as the joint study by the following Japanese IPIRG members.

Tokyo Electric Power Co., Inc. / Hokkaido Electric Power Co., Inc. / Tohoku Electric Power Co., Inc. / Chubu Electric Power Co., Inc. / Hokuriku Electric Power Co., Inc. / Kansai Electric Power Co., Inc. / Chugoku Electric Power Co., Inc. / Shikoku Electric Power Co., Inc. / Kyusyu Electric Power Co., Inc. / Japan Atomic Power Co., Inc / Toshiba Corporation / Hitachi, Ltd . / Mitsubishi Heavy Industries, Ltd. / Ishikawajima-Heavy Industries Co., Ltd. / Babcock-Hitachi K.K.

6. REFERENCES

1) Schmidt, R. A., Wilkowski, G. M., and Mayfield, M., "The International Piping Integrity Research Group (IPIRG) Program--An Overxiew", SMiRT-11 Proceedings, August 1991, Paper G23/1.

2) S. Kanno, H.Kimoto, M.Hayashi, M.Ishiwata, N.Gotoh, N.Miura, T.Fujioka, K.Kashima, " Low Cyclic Fatigue Crack Growth and Ductile Fracture under Dynamic / Cyclic Loadings for Japanese Carbon Steel Piping Part Ⅰ : Experimental Study ", PVP-Vol.266, 1993.

3) N.Miura, T.Fujioka, K.Kashima, S. Kanno, H.Kimoto, M.Hayashi, M.Ishiwata, N.Gotoh, " Low Cyclic Fatigue Crack Growth and Ductile Fracture under Dynamic / Cyclic Loadings for Japanese Carbon Steel Piping Part Ⅱ : Analytical Study ", PVP-Vol.266, 1993.

4) Wilkowski, G. M., Vieth, P., Kramer, G., Marschall, C., and Landow, M., "Results of separete-Efects Pipe Fracture Experiments", Post-SMiRT-11 Conference, August 1991, Paper 4.2.

5) Marschall, C. W., Landow, M., and Wilkowski, G. M., "Loading Rate Effects on Strength and Fracure Toughness of Pipe Steels Used in Task 1 of the IPIRG Program", NUREG/CR-6098, October 1993.

Table 2.1 Material characterization test matrix

Test Type		Longitudinal Tensile Tests		C(T) Specimen Tests (L-C Orientation)	
		Quasi-Static	Dynamic	Quasi-Static	Dynamic
Material	152-mm (6-inch) diameter STS 410 carbon steel	×	×	×	×
Crack Location	Base Metal Weld Metal	× ×	× ×	× ×	× ×
Test Temperature	300 C (572 F)	×	×	×	×
Strain Rate	1/second 10/second		× ×		
Time to Achieve Crack Initiation	600 seconds 0.2 second 10 seconds			×	 × ×
Duplicate Tests		×	×	×	×
Total Number of Tests		4	8	4	8

Table 2.2 Tensile test summary for Japanese carbon steel pipe (STS410) and associated TIG weld

	Specimen Identification Number	Actual Strain Rate, sec^{-1}	0.2 Percent Offset Yield Strength MPa	Ultimate Tensile Strength MPa	% Elongation
Base Metal	IPF13-T1	4×10^{-4}	215.8	492.6	28.5
	IPF13-T2	4×10^{-4}	217.2	493.7	28.3
	IPF13-T4	1.0	180.0	413.0	48.5
	IPF13-T6	9.9	224.1	423.5	42.6
	IPF13-T7	12.0	225.8	417.8	41.6
	IPF13-T8	1.4	260.6	430.9	48.0
Weld	IPF16-T2w	4×10^{-4}	479.9	671.6	36.3
	IPF14-T1w	4×10^{-4}	551.6	715.0	36.6
	IPF16-T3w	12	420.0	526.1	33.3
	IPF16-T4w	1.4	402.0	587.5	33.2
	IPF14-T2w	1.6	448.9	621.2	34.2

Table 2.3 Summary of toughness results for Japanese base and weld metals

	Specimen Identification	Approximate Time to Initiation, sec	J_i kN/m	dJ_M/da MN/m^2
Base Metal	IPF13-1	600	389.5	222.5
	IPF13-2	600	367.9	201.4
	IPF13-4	10	385.1	172.7
	IPF13-5	0.2	507.4	177.0
	IPF13-6	0.2	445.7	200.2
	IPF13-7	10	395.3	165.6
Weld	IPF16-1w	600	832.6	181.1
	IPF16-2w	600	689.3	240.9
	IPF16-3w	10	410.8	359.4
	IPF16-4w	10	458.7	353.9
	IPF16-5w	0.2	637.8	321.6
	IPF16-6w	0.2	434.8	354.6

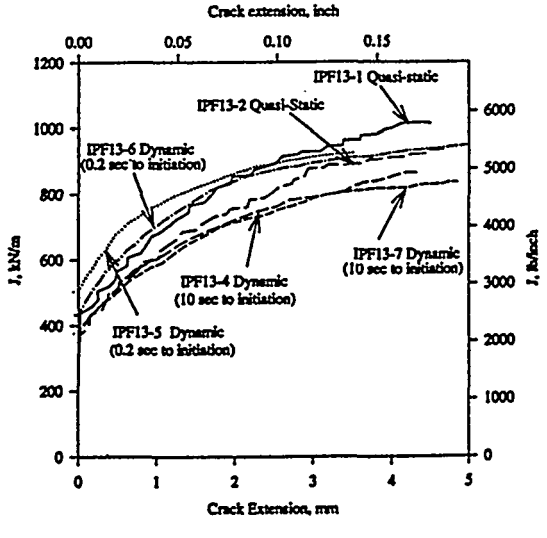

Figure 2.1 J-R curves for STS410 base metal C(T) specimens

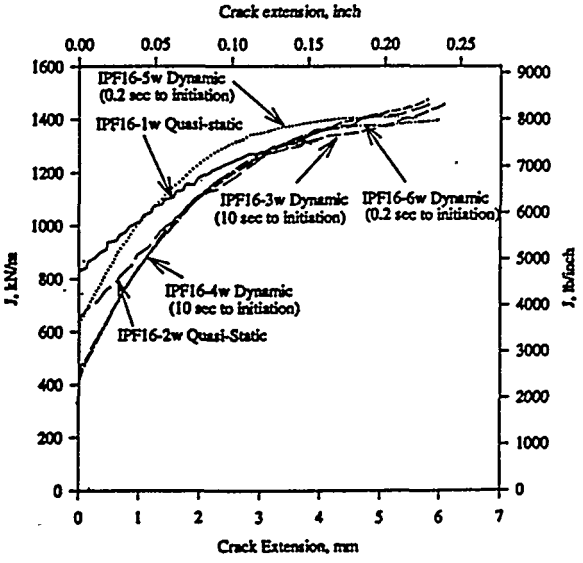

Figure 2.2 J-R curves for TIG weld C(T) specimens

Table 3.1 Test conditions for The STS410 carbon steel pipe test

	Quasi-static Monotonic Loading Test	Dynamic Monotonic Loading Test	Dynamic Cyclic Loading Test	Dynamic Cyclic Loading Test
Experiment Number	3.3-1	4.2-1	4.2-2	4.2-3
Specimen Number	IP-F13	IP-F10	IP-F11	IP-F12
Actual Pipe Diameter	166.0 mm	168.3 mm	165.6 mm	166.2 mm
Actual Pipe Wall Thickness	14.4 mm	14.5 mm	14.5 mm	14.4 mm
Crack Location	Base Metal	Base Metal	Base Metal	Weld Metal
Through-Wall Crack Length	60 degrees	60 degrees	60 degrees	60 degrees
Test Temperature	300 ℃	300 ℃	300 ℃	300 ℃
Load History	Quasi-Static Monotonic Four Point Bending	Dynamic Monotonic Four Point Bending	Dynamic Cyclic (R= -1) Four Point Bending	Dynamic Cyclic (R= -1) Four Point Bending
Target Loading Rate	——	25 mm/second (1 inch/second)	25 mm/second (1 inch/second)	25 mm/second (1 inch/second)
Outer Loading Span	1.524 m	1.524 m	1.524 m	1.524 m
Inner Loading Span	0.610 m	0.610 m	0.610 m	0.610 m

Table 3.2 Summary of the results from the pipe fracture tests

Experiment Number	3.3-1	4.2-1	4.2-2	4.2-3
Load History	Quasi-Static Monotonic	Dynamic Monotonic	Dynamic Cyclic :R=-1	Dynamic Cyclic :R=-1
Crack Location	Base Metal	Base Metal	Base Metal	Weld Metal
Moment at Crack Initiation	71.3 kN-m	68.7 kN-m	63.5 kN-m	83.2 kN-m
Maximum Moment	92.8 kN-m	84.1 kN-m	78.4 kN-m	88.0 kN-m
Number of Cycles to Crack Initiation	N/A	N/A	8	13
Number of Cycles to Maximum Moment	N/A	N/A	14	13

Table 3.3 Ratios of experimental maximum moment to predicted maximum moment

Experiment Number	Loading Condition	Material	Experimental maximum moment /NSC Predicted maximum moment
3.3-1	QS,Mono	STS410	1.103
4.2-1	Dyn,Mono	STS410	0.966
4.2-2	Dyn,Cyc(R=-1)	STS410	0.932
4.2-3	Dyn,Cyc(R=-1)	STS410 *1	1.043

*1 Crack in a TIG Weld.

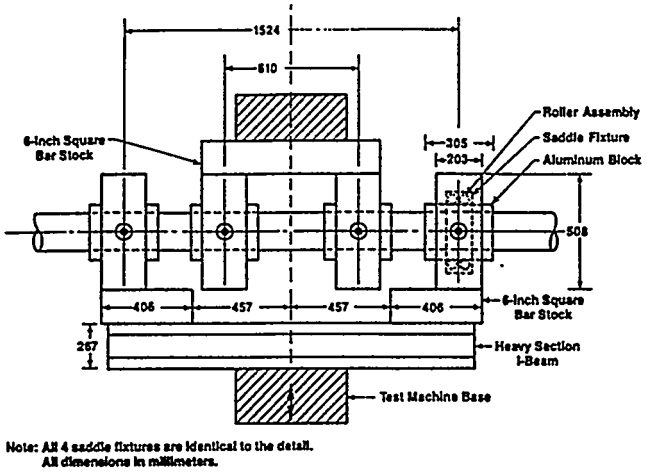

Figure 3.1 Schematic of test appratus

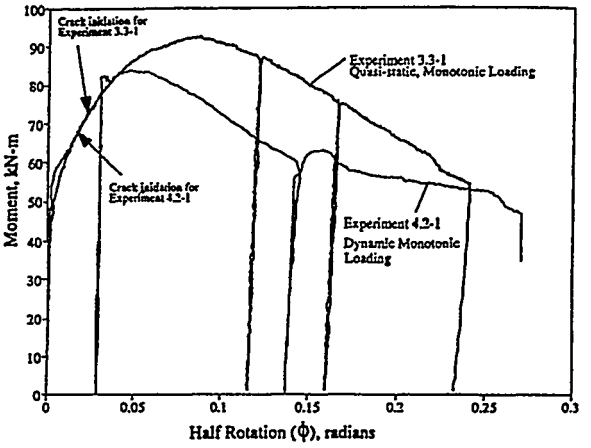

Figure 3.2a Moment versus half rotation for Experiment 4.2-1 and 3.3-1

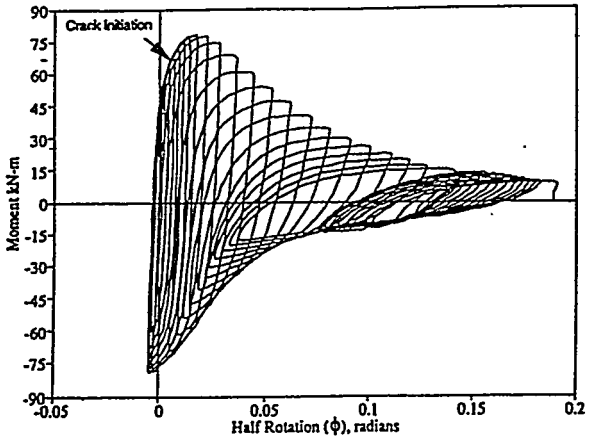

Figure 3.2b Moment versus half rotation for Experiment 4.2-2

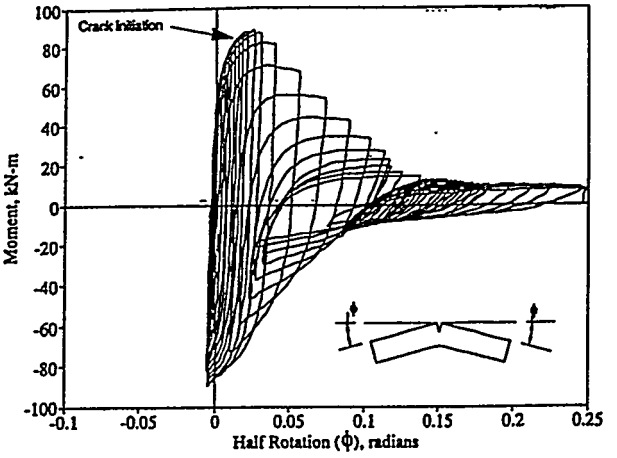

Figure 3.2c Moment versus half rotation for Experiment 4.2-3

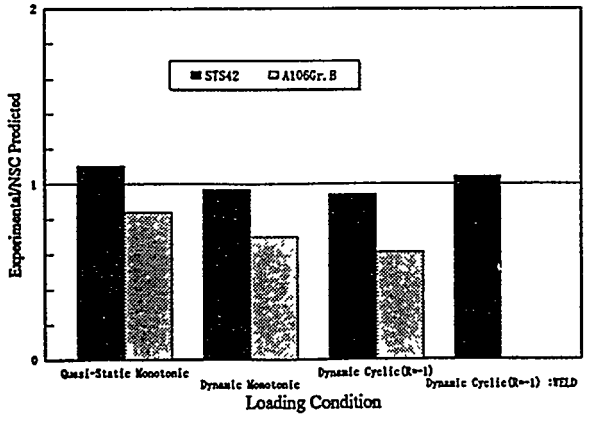

Figure 3.3 Comparison of the ratios of experimental maximum moment to predicted maximum moment between the STS410 pipe and the A106Gr.B pipe tested in IPIRG-1 program

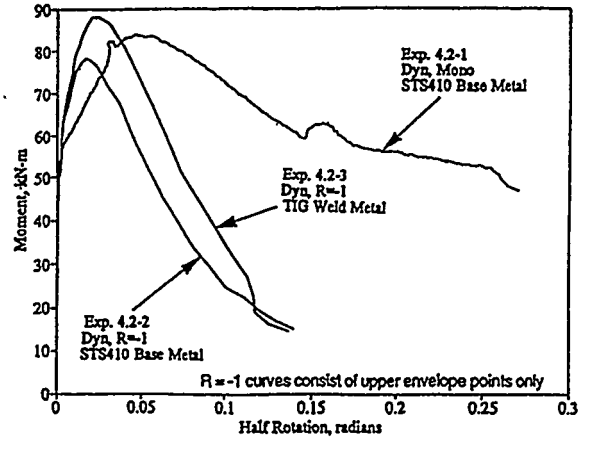

Figure 3.4 Comparison of the moment versus half rotation between monotonic loading test and cyclic loading test

APPLICATION OF CYCLIC J-INTEGRAL TO LOW CYCLE FATIGUE CRACK GROWTH OF JAPANESE CARBON STEEL PIPE

Miura N., Fujioka T., Kashima K. (CRIEPI, Japan)
Miyazaki K., Kanno S., Ishiwata M., and Gotoh N. (Hitachi, Japan)

INTRODUCTION

Piping for LWR power plants is required to satisfy the LBB concept for postulated (not actual) defects. With this in mind, research has so far been conducted on the fatigue crack growth under cyclic loading, and on the ductile crack growth under excessive loading. It is important, however, for the evaluation of the piping structural integrity under seismic loading condition, to understand the fracture behavior under dynamic and cyclic loading conditions, that accompanies large-scale yielding. CRIEPI together with Hitachi have started a collaborative research program on dynamic and/or cyclic fracture of Japanese carbon steel (STS410) pipes in 1991 [1 and 2]. Fundamental tensile property tests were conducted to examine the effect of strain rate on tensile properties. Cracked pipe fracture tests under some loading conditions were also performed to investigate the effect of dynamic and/or cyclic loading on fracture behavior. Based on the analytical considerations for the above tests, the method to evaluate the failure life for a cracked pipe under cyclic loading was developed and verified. Cyclic J-integral was introduced to predict cyclic crack growth up to failure.

This report presents the results of tensile property tests, cracked pipe fracture tests, and failure life analysis. The proposed method was applied to the cracked pipe fracture tests. The effect of dynamic and/or cyclic loading on pipe fracture was also investigated.

HIGH-RATE TENSILE PROPERTY TESTS

Tested materials are STS410 carbon steel base metal and submerged-arc weld metal. Table 1 shows the chemical compositions of the tested materials. Round-bar specimens of 5 mm diameter and 25 mm gauge length taken from the 4B × Sch. 80 pipe in the axial direction were used. Tensile tests were conducted at room temperature and high temperature (288 or 300 °C) under quasi-static and several high strain rates of 10^{-4} to 10^{1} /sec.

Figures 1(a) and (b) show the results of the tensile tests. Two specimens were used for each testing condition. Both 0.2 % proof stress and ultimate strength increase with increasing strain rate at room temperature. 0.2 % proof stress also increase with increasing strain rate at high temperature. Although ultimate strength goes down as increasing strain rate at high temperature, it is almost saturated at high strain rate over 10^{0} /sec. Supposing that the failure load of a cracked structure can be predicted by the net-section collapse criterion based on the flow stress, which is defined as the average of 0.2 % proof stress and ultimate strength, it can not be notably influenced by strain rate at high temperature.

Table 1 Chemical Compositions of Tested Materials

(wt%)

			C	Si	Mn	P	S
STS410 Carbon Steel	Base	*Specified*	*< 0.30*	*0.10 - 0.35*	*0.30 - 1.40*	*< 0.035*	*< 0.035*
		Measured	0.14	0.30	1.20	0.009	0.001
	Weld	*Specified*	*< 0.19*	*0.30 - 0.60*	*1.30 - 1.60*	*< 0.020*	*< 0.020*
		Measured	0.06	0.49	1.40	0.008	0.004

Engineering stress-strain relations were approximated to the Ramberg-Osgood curves,

$$\varepsilon / \varepsilon_0 = \sigma / \sigma_0 + \alpha (\sigma / \sigma_0)^n , \quad \varepsilon_0 = \sigma_0 / E \tag{1}$$

where σ_0 and ε_0 are reference stress and strain, respectively, α is a material constant, n is a strain hardening constant, and E is the Young's modulus. The stress-strain relation was definitely dependent on strain rate. Figure 2 shows typical stress-strain relations of base metal at room temperature. For pipe fracture analysis, a specific stress-strain relation as a function of an equivalent strain rate can be provided by the proposed method in [3].

DYNAMIC / CYCLIC PIPE FRACTURE TESTS

The pipe fracture test specimens are circumferentially through-wall or surface cracked pipes (4B × Sch. 80) subjected to four-point bending. Dimensions of the test specimen are 1200 mm in length, 114.3 mm outer diameter with 8.6 mm thickness. For welded joint, throat thickness was reduced to 7.65 mm by DC processing. Flaw with the angle of 30° or 60° was introduced by electric discharge machining.

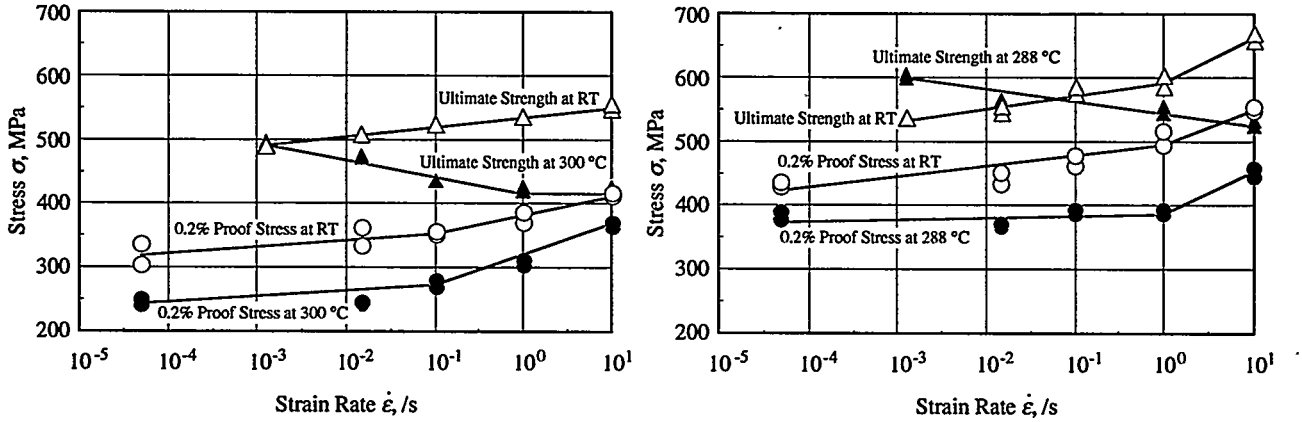

(a) Base Metal (b) Weld Metal

Figure 1 Results of High-Rate Tensile Property Tests

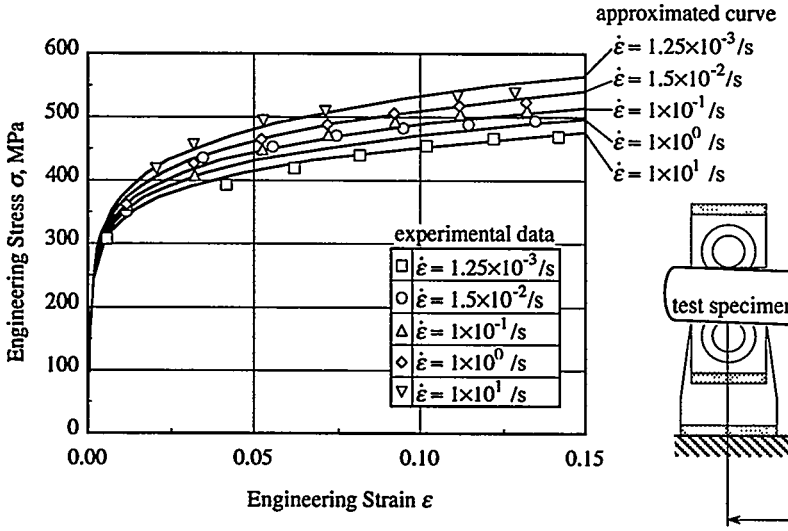

Figure 2 Engineering Stress-Strain Relations under Several Strain Rates for STS410 Carbon Steel Base Metal at RT

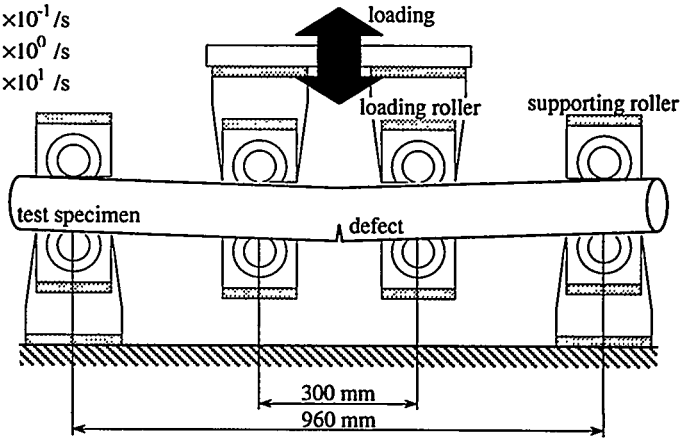

Figure 3 Test Apparatus for Pipe Fracture Test

The test apparatus is shown in Figure 3. They have a pair of outer supporting rollers with the span of 960 mm and a pair of inner loading rollers with the span of 300 mm to provide four-point bending loading. The test specimens are gripped between the rollers. Each pair of the rollers is set on a rotating device to follow the deformation of the test specimen. Pipe fracture tests were conducted at room temperature and high temperature. In high temperature tests, the test specimens were heated up at 265 to 285 °C by forced circulation of hot air. Tests were performed under monotonic loading and constant cyclic loading.

Monotonic Loading Tests

For monotonic loading tests, constant load-line displacement rate was controlled with 0.05 mm/sec (quasi-static) and higher rates than 5 mm/sec (dynamic). Results of the monotonic loading tests are summarized in Table 2. Each experimental maximum load, P_{max}, was compared with and normalized by the net-section collapse load, P_L, which is evaluated by the following equation [4]:

$$P_L = 4\, M_L / (L_{out} - L_{in}) \tag{2}$$

$$M_L = 2\, \sigma_f R^2 t \left(2 \sin \beta - \frac{a}{t} \sin \theta\right) \tag{3}$$

$$\beta = \frac{\pi}{2} - \frac{a}{t}\frac{\theta}{2} \tag{4}$$

where M_L is the net-section collapse moment, L_{out} and L_{in} are the outer and inner span, R is the mean pipe radius, t is the pipe thickness, a is the defect depth, and θ is half defect angle. σ_f is flow stress defined as the average of experimental 0.2 % proof stress and ultimate strength of the material of interest under quasi-static strain rate condition. It is found that the net-section collapse load gives conservative prediction of the maximum load except for weld joint at high temperature. Figure 4 shows the relation between the normalized P_{max} and load-line displacement rate. The ratio of P_{max}/P_L slightly increases as increasing strain rate, as shown in Figure 1. This result corresponds to the fact that the tensile strengths generally increase with increasing strain rate. The ratio of P_{max}/P_L for surface defect is larger than that for through-wall defect. The ratio at high temperature is smaller than that at room temperature. The ratio for weld joint is smaller than that for base metal. This aspect seems to be related with the effect of constraint of base metal surrounding weld joint.

Table 2 Results of Monotonic Loading Tests

Test No.	Material	Temperature	Total Defect Angle (Defect Depth/Thickness)	Displacement Rate (mm/s)	Maximum Load P_{max} (kN)	Net-Section Collapse Load P_L (kN)	P_{max}/P_L
M-1	STS410 Base Metal	RT	30° (1.0)	0.05	212	199	1.07
M-2			60° (1.0)	0.05	176	166	1.06
M-3				5	185		1.11
M-4				44	182		1.10
M-5			60° (0.5)	0.05	221	200	1.11
M-6				5	224		1.12
M-7				33	235		1.18
HM-1		265 °C	60° (1.0)	5	158	149	1.06
HM-2				37	160		1.07
HM-3			60° (0.5)	31	201	179	1.12
JM-1	STS410 Weld Joint	RT	60° (1.0)	0.05	180	179	1.01
JM-2				5	177		0.99
JM-3				35	190		1.06
HJM-1		285 °C	60° (1.0)	0.05	155	182	0.85
HJM-2				5	165		0.90
HJM-3				17	157		0.86

Constant Cyclic Loading Tests

For constant cyclic tests, constant load amplitude was controlled with about 50 to 90 % of the net-section collapse load. Alternating triangle wave loading (stress ratio = -1) was applied with the frequency of 0.1 Hz. Results of the constant cyclic loading tests are summarized in Table 3. Each experimental load amplitude, P_a, was compared and normalized by the net-section collapse load, P_L, which was evaluated by Equations (2) through (4). Number of cycles to failure listed in Table 3 is defined by the point where particular load amplitude could not be applied to the test specimen. Figure 5 shows the relation between the normalized P_a and the number of cycles to failure, N_b. It seems that the experimental ratio of P_a/P_L shows linear correlation with the logarithm of N_b for each condition regardless of type or size of defect. The ratio of P_a/P_L for 265 °C is smaller than that for room temperature as well as the case of the monotonic loading tests. Also the ratio of P_a/P_L for weld joint is smaller than that for base metal as well as the case of the monotonic loading tests.

Table 3 Results of Constant Cyclic Loading Tests

Test No.	Material	Temperature	Total Defect Angle (Defect Depth/Thickness)	Load Amplitude P_a (kN)	Net-Section Collapse Load P_L (kN)	P_a / P_L	No. of Cycles to Filure (cycles)
C-1	STS410 Base Metal	RT	30° (1.0)	±180	199	0.90	29
C-2				±161		0.81	67
C-3				±162	216*	0.75	202
C-4			60° (1.0)	±158	166	0.95	19
C-5				±142		0.86	47
C-6				±127		0.77	97
C-7				±122		0.73	108
C-8				±103		0.62	328
C-9			60° (0.5)	±182	200	0.91	42
C-10				±167		0.84	43
C-11				±142		0.71	310
C-12				±127		0.64	510
HC-1		265 °C	60° (1.0)	±135	149	0.91	16
HC-2				±113		0.76	57
JC-1	STS410 Weld Joint	RT	60° (1.0)	±166	179	0.92	11
JC-2				±143		0.78	33
JC-3				±125		0.70	82
JC-4				±108		0.57	241
HJC-1		285 °C	60° (1.0)	±143	182	0.78	11
HJC-2				±131		0.72	29
HJC-3				±119		0.65	57
HJC-4				±93		0.51	344

*: conducted with outer supporting span of 910 mm

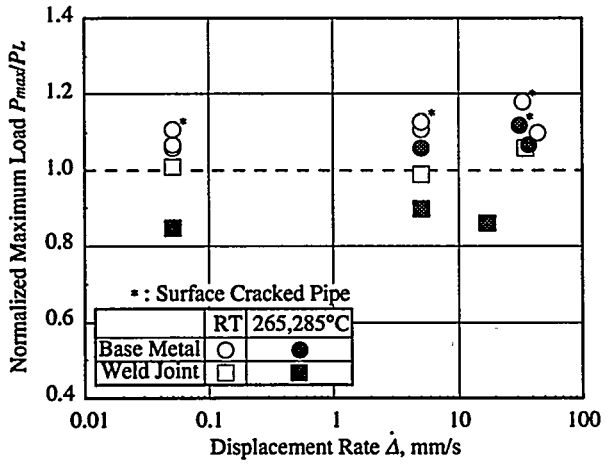

Figure 4 Normalized Maximum Load for Monotonic Loading Tests

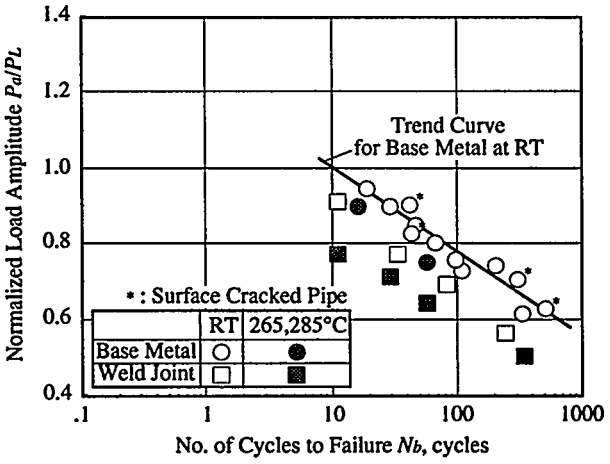

Figure 5 Normalized Load Amplitude for Constant Cyclic Loading Tests

PREDICTION OF FAILURE LIFE UNDER CONSTANT CYCLIC LOADING

Evaluation Procedure

An evaluation method to predict the crack growth behavior and the failure life for circumferentially through-wall cracked pipe subjected to constant cyclic bending was developed [2]. In this method, cyclic J-integral range, ΔJ, is considered to be a dominant parameter which provides the low cycle fatigue crack growth under elastic-plastic regime.

Cyclic maximum J-integral, J_{max}, is defined as the J-integral corresponding to peak load points under cyclic loading condition. The J_{max} for a circumferentially through-wall cracked pipe subjected to cyclic bending is experimentally evaluated by use of the η factor approach [5] as is the case with the monotonic J-integral. J estimation schemes such as the GE/EPRI estimation scheme [6] or the reference stress method [7] can be alternatively applied to calculate the J_{max}. Cyclic J-integral range, ΔJ, is effective to describe the fatigue crack growth in a large-scale yielding region [8 and 9]. The ΔJ for a circumferentially through-wall cracked pipe subjected to cyclic bending can be evaluated by the extended η factor approach developed in [2]. Otherwise, supposing that a cracked pipe is subjected to an alternating loading with stress ratio = -1, and a crack closure is negligible, ΔJ can be simply approximated by the following equation:

$$\Delta J \approx 4 J_{max} \tag{5}$$

More precise relation can be derived by particularly taking account for the crack growth during a cycle [2]:

$$\Delta J \approx \frac{2 a / a_0}{a / a_0 - 1/2} J_{max} \tag{6}$$

where a_0 is initial crack length. Figure 6 shows the relations between ΔJ evaluated by the extended η factor approach and the crack extension, Δa, together with the monotonic J-R curves obtained from monotonic loading pipe fracture tests. Comparing with the monotonic J-R curves, ΔJ nearly reach the monotonic J-R curves at the time of failure. This suggests that the failure criterion under high-level cyclic load is described as,

$$\Delta J\,(\sigma, a) \geq J_R\,(\Delta a) \tag{7}$$

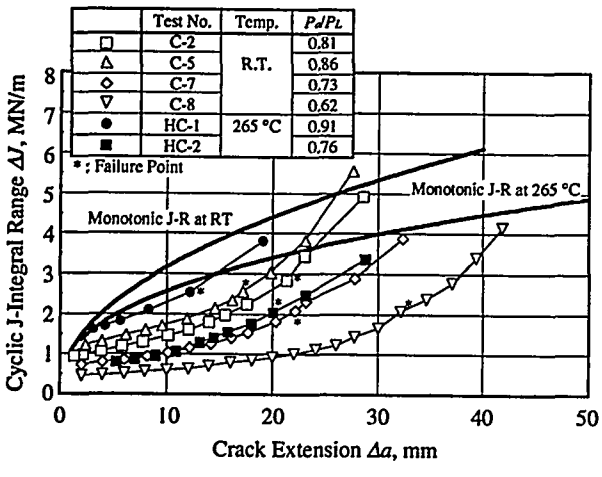

Figure 6 Experimantal ΔJ-Δa Curves under Constant Cyclic Loading with Monotonic J-R Curves for Base Metal

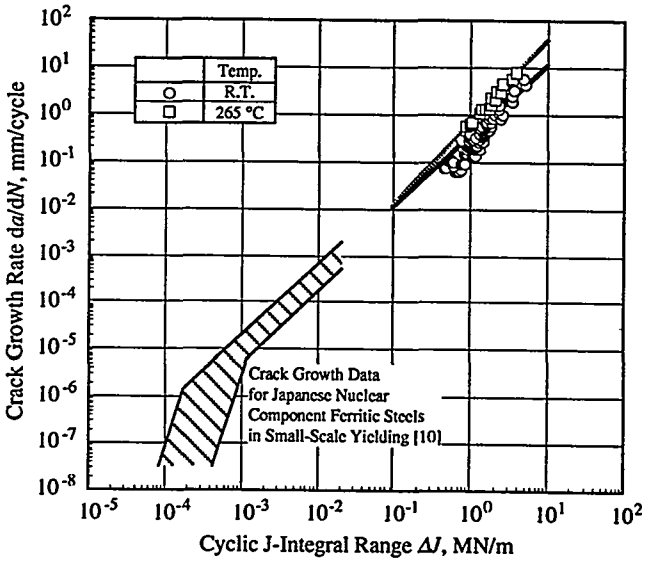

Figure 7 Low Cycle Crack Growth Law Based on ΔJ for Base Metal and Comparison with Crack Growth for Small-Scale Yielding

Another possible failure criterion is the net-section collapse criterion, since the maximum load under monotonic loading can be well predicted by the limit load based on the net-section collapse criterion. It seems that the failure of cracked pipe may occur when the applied moment, M, exceeds the net-section collapse moment, M_L,

$$M(\sigma, a) \geq M_L(\sigma_f, a) \tag{8}$$

It is ascertained that the difference of the failure criterion does not affect the predicted failure life [3]. The crack growth rate da/dN under the cyclic load accompanying large-scale yielding can be expressed by the power law with respect to ΔJ [7].

$$\frac{da}{dN} = C\,\Delta J^m \tag{9}$$

The constants of C and m in Equation (9) can be determined by the experimental relation between da/dN and ΔJ. Figure 7 shows the relation between da/dN and ΔJ evaluated by the extended η factor approach. The crack growth law of base metal is given by a unique relation for each temperature,

$$\begin{aligned} &\frac{da}{dN} = 0.339\,(\Delta J)^{1.51},\ \frac{da}{dN}:[\text{mm/cycle}],\ \Delta J:[\text{MN/m}], \quad \text{for Base Metal at R.T.} \\ &\frac{da}{dN} = 0.649\,(\Delta J)^{1.74},\ \frac{da}{dN}:[\text{mm/cycle}],\ \Delta J:[\text{MN/m}], \quad \text{for Base Metal at 265 °C} \end{aligned} \tag{10}$$

It is also found that the test results are in an extended regions of the relations between da/dN and ΔK obtained from the database for small-scale yielding on Japanese nuclear component ferritic steels [10].

Based on the preceding discussion, evaluation procedure of the crack growth and failure life for a circumferentially through-wall cracked pipe subjected to constant cyclic bending is shown in Figure 8. The method used in this study can be summarized as follows:

(a) Calculate J_{max} in the first cycle by GE/EPRI J estimation scheme.
(b) Calculate ΔJ in the first cycle by using Equation (5) or (6).
(c) Calculate da/dN in the first cycle by using Equation (10).
(d) Add da/dN to the initial crack length a_0 to update the crack length a.
(e) Determine the possibility of failure by using Equation (7).

Repeat the above steps in the next cycle, if no failure will result.

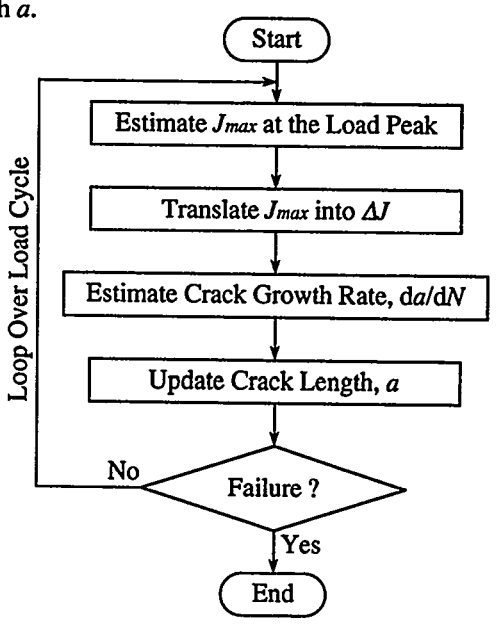

Figure 8 Flow Chart of the Evaluation Procedure

Prediction of Failure Life

The evaluation procedure was applied to predict the crack growth behavior and the failure life for some pipe fracture tests subjected to constant cyclic bending. Figure 9 shows the comparison of the experimental and predicted relation between Δa and N for base metal. In this Figure, ΔJ was calculated using Equation (6), and the failure was identified using Equation (7). To eliminate the initial notch effect on the number of cycles, failure lives were counted from crack initiation. It is found that the predicted behavior is in good agreement with the test result. The unconservative result for the test C-2 seems to be caused by the deviation from the reference crack growth law. Figure 10 shows the comparison of the experimental and predicted failure lives for base metal. Favorable prediction results are obtained by using the proposed method. The predictions with the proposed Equation (6) improved the accuracy compared with the predictions made by the conventional Equation (5).

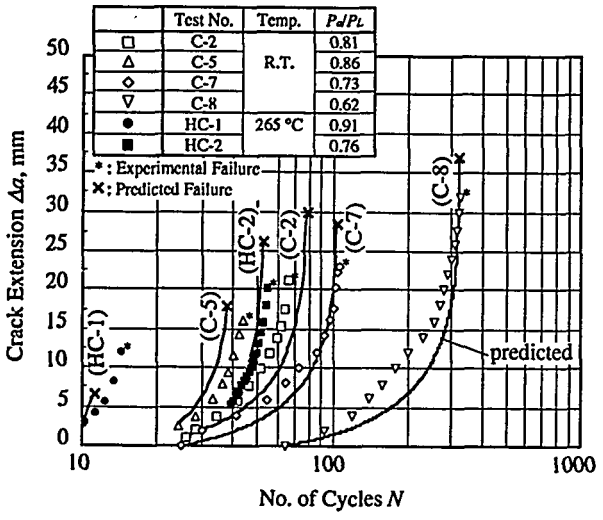

Figure 9 Comparison between Experimental and Predicted Crack Growth Behavior

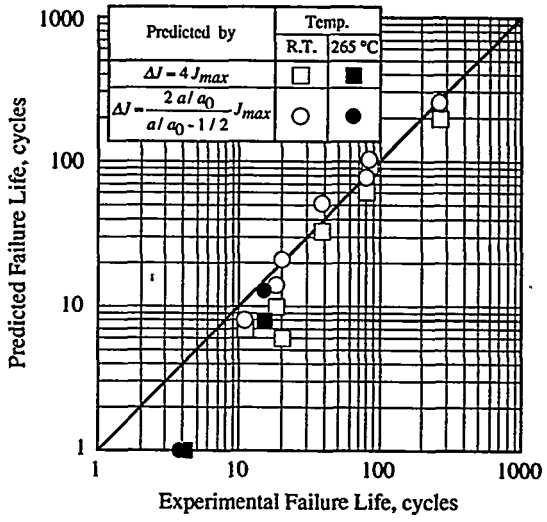

Figure 10 Comparison of Experimental and Predicted Failure Life (Number of Cycles from Crack Initiation)

CONCLUSIONS

In this study, tensile property tests, cracked pipe fracture tests, and failure life analysis were conducted for Japanese representative carbon steel STS410 to examine the effect of dynamic and/or cyclic loading on pipe fracture. Conclusions are summarized as follows:

1) Tensile properties increase with increasing strain rate except for the ultimate strength at high temperature. The flow stress was constant or slightly increasing with increasing strain rate for all cases.

2) The maximum load was slightly increasing with displacement rate for monotonic loading tests. The number of cycles to failure could be related to normalized load amplitude based on the net-section collapse load for constant cyclic loading tests.

3) The new evaluation method to predict the crack growth behavior and the failure life for circumferentially through-wall cracked pipe subjected to constant cyclic bending was developed. The crack growth behavior and the failure life were successfully predicted.

REFERENCES

[1] Kanno, S., et al., "Low Cycle Fatigue Crack Growth and Ductile Fracture Under Dynamic/Cyclic Loadings for Japanese Carbon Steel Piping Part I : Experimental Study," ASME PVP, **266**, (1983), 171.

[2] Miura, N., et al., "Low Cycle Fatigue Crack Growth and Ductile Fracture Under Dynamic/Cyclic Loadings for Japanese Carbon Steel Piping Part II : Analytical Study," ASME PVP, **266**, (1983), 175.

[3] Fujioka, T., et al., "A Fracture Strength Evaluation Method for Carbon Steel Pipes Subjected to Dynamic/Cyclic Loadings -Evaluation of Dynamic/Cyclic Pipe Fracture Tests at Elevated Temperature-," ASME PVP, **304**, (1995), 191.

[4] Kanninen, M. F., et al., "Instability Predictions for Circumferentially Cracked Type-304 Stainless Under Dynamic Loading," EPRI NP-2347, (1982).

[5] Wilkowski, G., et al., "Analysis of Experiments on Stainless Steel Flux Welds," NUREG/CR-4878, (1987).

[6] Kumar, V., et al., "Further Developments in Elastic-Plastic Analysis," EPRI NP-5596, (1988).

[7] Goodall, I. W., et al., "The Development of High Temperature Design Methods Based on Reference Stress and Bounding Theorems," *Transaction of the ASME, Journal of Engineering Materials and Technology*, **101**, (1979), 349.
[8] Dowling, N. E. et al., "Fatigue Crack Growth During Gross Plasticity and the J-Integral," ASTM STP 590, (1976), 82.
[9] Dowling, N. E., "Geometry Effects and the J-Integral Approach to Elastic-Plastic Fatigue Crack Growth," ASTM STP 601, (1976), 19.
[10] Kobayashi, H., et al., "Construction of a Fatigue Crack Growth Data Base for Nuclear Component Ferritic Steels in Japan and Its Statistical Analysis," *Transaction of the JSME* (in Japanese), **55**, 514, (1989), 1225.

SESSION 3: COMPLEMENTARY REQUIREMENTS

Abstract for:

Specialist Meeting on Leak Before Break in Reactor Piping and Vessels, Lyon, France, October 9-11, 1995.

Sponsored by EDF, Framatome, CEA, Nuclear Electric, Siemens, OECD, CE DGXI, IAEA, USNRC.

Leak Detection Capability in CANDU Reactors.

by

N. Azer, D.H. Barber, P.J. Boucher, P.J. Ellis, J.K. Mistry, V.P. Singh and R. Zaidi

In a CANDU reactor each pressure tube is surrounded by a calandria tube and the annular space between these tubes contains carbon dioxide. The CO_2 provides thermal insulation to reduce heat loss from the pressure tube to the moderator surrounding the calandria tube. The channel annuli are connected together by tubing and piping to form a closed loop recirculating Annulus Gas System (AGS). Though primarily designed to provide a thermal barrier and chemistry control of the AGS, the AGS has been developed into a leak detection system. If a leak were to occur through the pressure tube, it would be detected by moisture sensors in the AGS. The AGS is designed and operated to provide the operator sufficient time to take appropriate action to prevent unstable fracture of a leaking pressure tube. This Leak-Before-Break (LBB) capability is used as defence in depth in CANDU reactors.

Unstable fracture of a pressure tube is avoided if the LBB considerations can assure that:

1) the crack length is less than the critical crack length(CCL)

2) the leak is detected

3) appropriate operator action is taken to shutdown, cooldown and depressurise the Heat Transport sytem to ensure that the crack length does not exceed CCL.

This paper addresses the moisture leak detection capability of Ontario Hydro CANDU reactors which has been demonstrated by performing tests on the reactor. The tests confirmed the response of the AGS to the presence of moisture injected to simulate a pressure tube leak and also confirmed the dew point response assumed in LBB assessments.

The tests were performed on Bruce A Unit 4 by injecting known and controlled rates of heavy water vapour. To avoid condensation during test conditions, the amount of moisture which could be injected was small (2-3.5 g/hr). The test response demonstrated that the AGS is capable of detecting and annunciating small leaks. Thus confidence is provided that it would alarm for a growing pressure tube leak where the leak rate is expected to increase to kg/hr rapidly. The measured dew point response was close to that predicted by analysis.

LEAK DETECTION CAPABILITY IN CANDU REACTORS

N. Azer†, D.H. Barber‡, P.J. Boucher#, P.J. Ellis†, J.K. Mistry†, V.P. Singh‡ and R. Zaidi†
†Reactor Engineering Services Department, OH/AECL, Sheridan Park, Mississauga, ON L5K 1B2 CANADA
‡Ontario Hydro Technologies, 800 Kipling Avenue, Toronto, ON M8Z 5S4 CANADA
#Bruce A Generating Station, P.O. Box 3000, Tiverton, ON N0G 2TO CANADA

1. INTRODUCTION

Leak-Before-Break (LBB) is used as defence in depth to avoid unstable rupture of a CANDU[®1] reactor pressure tube (PT). The LBB concept requires timely detection and confirmation of a leak, appropriate operator intervention to shutdown, cooldown and depressurise the reactor before the crack length exceeds the critical crack length (CCL).

In CANDU reactors, pressure tube leak detection capability is provided by the Annulus Gas System (AGS). The AGS contains dry CO_2 recirculating in the annular space between the calandria tubes and pressure tubes. The system has the important design function of insulating the hot pressure tubes (PTs) from the relatively cool Moderator. The fuel channel annuli (up to 480) are connected in a series/parallel configuration to form a closed loop recirculating system consisting of compressors, flow meters, and pressure gauges. An AGS string is defined as a set (from 4 to 12) fuel channel annuli connected in series. The strings are equipped with flow rotameters at the inlet ends. Hygrometers (dew point meters) and beetles (liquid detection devices) are provided to detect the presence of moisture and liquid respectively in the AGS.

Because of deuterium ingress from the Heat Transport System (HTS) and formation of D_2O by reaction with oxygen in the annuli, the humidity in the AGS increases with time. When the dew point temperature of the humid CO_2 reaches a predetermined value, the whole inventory of AGS gas is purged by a once through flow of CO_2 from a dry source. The purge frequency at the Bruce A reactors is typically once every 3 to 5 days.

In the early stages of a pressure tube leak, the moisture from the leakage, carried by the recirculating CO_2 gas stream, is most likely first detected by dew point meters. For a growing crack, the leakage into the annulus increases and the presence of liquid water in the AGS would be detected by beetles (electrodes which conduct in the presence of water). At most Ontario Hydro reactors the dew point and its rate of change is monitored continuously and compared to a computerised dew point 'rate of rise' algorithm. The system is designed to provide alarms and annunciations in the control room when the setpoint (defined rate of rise) is exceeded.

The response time and sensitivity of the AGS to abnormal amounts of moisture is an important parameter in LBB analyses. This response is determined analytically by a computer model which simulates the transport of moisture in the AGS.

At Bruce the AGS utilises a dew point rate of rise algorithm which provides alarms and action limits (to shut down the reactor). This algorithm is based on dew point computer model predictions. Moisture injection tests were undertaken at Unit 4 reactor to confirm the AGS leak detection capability and computer model predictions.

---

[1] CANDU (CANada Deuterium Uranium) is a registered trademark of Atomic Energy of Canada Ltd.

This paper presents the results of tests to determine the Bruce A Unit 4 AGS response to simulated moisture leaks and confirm the performance of the dew point rate of rise algorithm.

2. TEST PROGRAMME

The test programme was divided into two phases. In the first phase moisture was injected into the AGS while the reactor was cold. Three cold tests (tests 1, 2 and 3) were used to commission the test equipment and its installation. These results are not presented here. The second phase of testing consisted of three hot tests (tests 4, 5 and 6), which were performed with the reactor at zero power hot conditions. These are considered the tests representative of the reactor operational conditions and are discussed in this paper.

The objective of the tests were to:

i) measure the response of the AGS to small simulated leaks over the conditions which envelope AGS operating modes.

ii) verify the performance of the dew point rate of rise computer algorithm.

2.1 Description of Test Programme

Figure 1 is a schematic of Bruce A Units 3,4 AGS. It shows the D_2O moisture injection point located just downstream of the individual inlet string rotameters. The test matrix is shown in Table 1.

Table 1 Test Matrix

Test No.	Simulated Leak Rate (g/h)	AGS Operating Mode			Injection Location	
		1 Compressor	2 Compressors	PURGE	12 Ch. string	4 Ch. string
4	3.6		X		X	
5	1.9-2.1	X		X	X	
6	3.4		X			X

The first hot test consisted of injecting D_2O moisture into the inlet end of a 12 channel string while two compressors were operating (test 4). The AGS normally operates with 2 compressors and the longest string at Bruce A units 3, 4 and Bruce B consists of 12 fuel channels in series.

The reactor should not be operated if the AGS flow does not meet a minimum flow requirement. A moisture injection test was performed to determine the system response with AGS flow just above the low flow operating limit (achieved by using one compressor). This case is a bounding case and should produce the slowest dew point response. As purging is also an AGS operating mode, injection during purging was also a feature of this test (test 5).

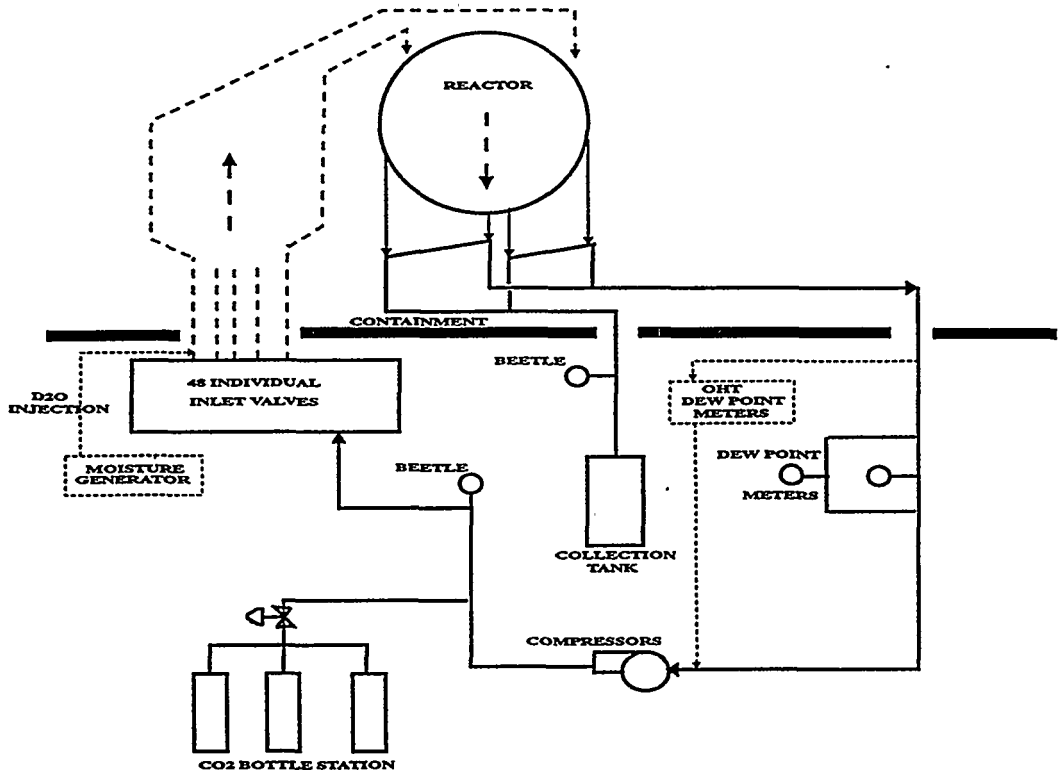

Figure 1 Bruce Units 3,4 AGS Flow Sheet showing Test Injection Location

To envelope the operating cases, moisture was also introduced into the inlet end of the shortest string (four channels in series) while 2 compressors were in operation (test 6). This was expected to produce the fastest dew point response.

Moisture was injected at a constant maximum rate such that the CO_2 gas stream did not saturate (i.e. there was no condensation anywhere in the AGS). If condensation should occur, not all the moisture could be accounted for at the dew point meters. The maximum amount of moisture which can be injected and not cause condensation depends on the total CO_2 flow rate and the coldest temperature in the AGS. The coldest part in this case was the inlet piping (~20°C) leading to the reactor face. The injection rates used in the tests ranged from 1.95 g/hr to 3.6 g/hr of D_2O. In a crack growing by delayed hydride process (DHC), the leak rate from the pressure tube into the AGS increases rapidly from g/hr to kg/hr. Hence these tests are representative of small non-growing through-wall cracks and are therefore considered conservative with respect to a crack growing by DHC.

3. TEST EQUIPMENT AND INSTRUMENTATION

3.1 D_2O Injection Equipment

A moisture generator which produced a metered, unsaturated gas stream of known moisture concentration was used to inject D_2O vapour into the AGS. The D_2O injection rate was measured during the test and later confirmed by measuring the weight increase of a desiccant over a given time interval.

3.2 Dew Point Sampling Equipment

A calibrated dew point sampling facility developed by Ontario Hydro Technologies (OHT) was connected to the AGS as close to the station dew point probes as possible (Fig. 1). It consisted of the following dew point meters in series:

- "Panametrics" probe similar to the station "Panametrics MIT56 & MIT57" which detect moisture by its effect on the electrical impedance of aluminium oxide.

- "MCM" hygrometer which is a silicon-based sensor and detects the changes in capacitance when moisture is adsorbed onto the silicon. These meters are considered to provide an accurate measure of changes in dew point.

- "EG&G" and "GED2" chilled mirror optical hygrometers. Chilled mirror hygrometers work on the principle of maintaining a constant frost layer while monitoring its temperature and are considered to provide the most accurate indication of dew point when conditions are not changing rapidly.

The hygrometers were calibrated prior to the tests with D_2O in CO_2. Each of the hygrometers was connected to a data logging system which recorded the data every 11 seconds.

3.3 Station Instrumentation

The station Panametrics probes were calibrated for D_2O in CO_2 prior to the tests. During the tests, control room records of the AGS dew point records, total AGS flow, pressure, dew point rate of rise, rate of rise setpoints and control room alarms were obtained.

4. TEST PROCEDURE

The procedure for each of the tests was essentially the same. Prior to each test the AGS was purged to -35°C dew point and then operated in the recirculation mode until system flow, temperature and pressure stabilised. Moisture was injected at a constant rate until the system dew point reached about -10°C after which a purge was initiated to dry the system for the next test.

5. TEST RESULTS

5.1 TEST 4 Dew Point Results

This test was conducted with two compressors operating and with moisture injection into the inlet end of the longest string. The AGS flow was 3.2 L/s and the rate of moisture injection was 3.59 g/hr.

The record of dew point increases of the six hygrometers (OHT probes (3.2) and two station probes (3.3)) and the model predictions are shown in Fig. 2.

It took the injected moisture about 75 minutes (Fig. 2) to travel through the 12 channel annuli and to appear at the hygrometers. All the hygrometers showed a step increase in the dew point at the same time. The delay in moisture detection by the dew point meters depends on the string length, AGS gas flow rate, mean pressure, temperature and the vapour mixing phenomenon ("plug flow" or "mixed flow"). The step increase in dew point occurs when the injected moisture exits the 12 channel string and reaches the hygrometers. After the first step change, the rise in dew point is more gradual. The "knee" in the dew point (at ~ 1.5 hours) is the time for the moisture which exits

from the longest string to reach to the inlet side of the AGS. At the inlet this moisture then distributes to all of the strings (of different lengths) in proportion to flow through the strings. This is the beginning of the "second pass" of moisture and all the channels now have moisture from the initial injection travelling through them.

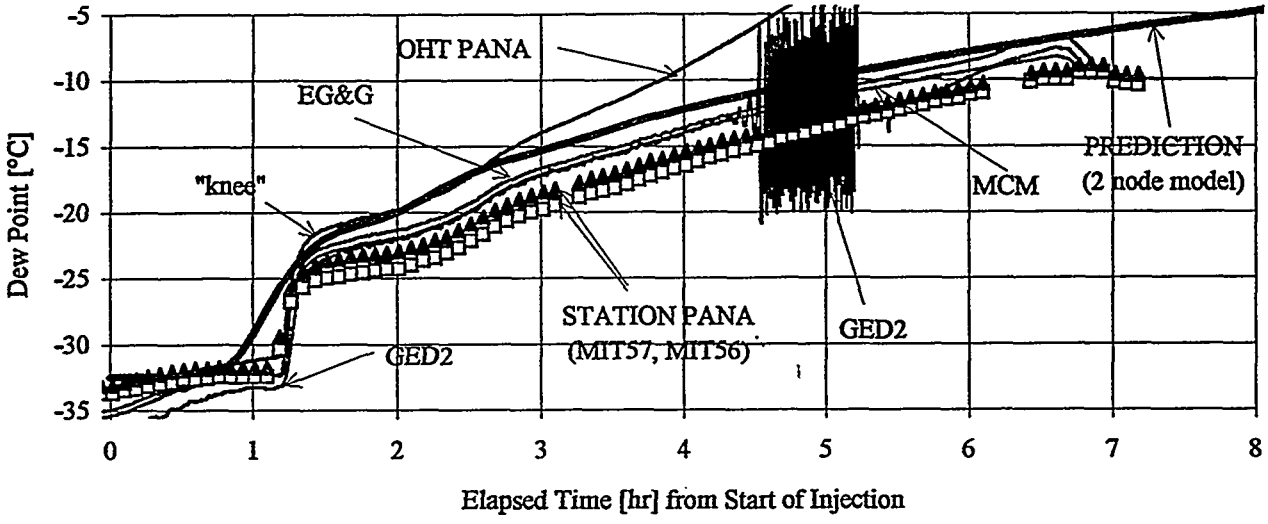

Figure 2 Test 4 Measured Dew Point vs. Predictions

The detection subsequent to injection depends on the transit time of the moisture through the varying length strings. Moisture from the shortest four channel string will be detected first followed by the seven, eight, nine, ten, eleven and twelve channel strings during the "second pass". The different times at which the moisture appears at the hygrometers determines the shape of the subsequent dew point curve. The dew point changes are not as pronounced in the subsequent passes since larger amounts of moisture would be necessary to obtain the same change in dew point at higher dew point levels.

The model predictions indicate earlier and more gradual emergence of moisture at the dew point meters compared to the measurements. The moisture came out about half an hour later than predicted. This difference is due to the number of nodes used in the simulations as discussed in section 6.

5.2 Test 4 Dew Point Rate of Rise Results

At Bruce Nuclear Generating Station, a dew point 'rate of rise' computer algorithm is used to continuously calculate the rate of dew point rise, the high (HI) and very high (VHI) dew point rate of rise alarm setpoints and to annunciate HI & VHI rate of rise alarms. The station computers retain dew point values for six minute periods. The algorithm computes the rate of rise and alarm setpoints over the six minute intervals. If the measured rate of rise exceeds the HI or VHI rate of rise setpoints, it is annunciated in the control room. Figure 3 shows a plot of the dew point rate of rise calculated over six minute intervals. This way of data display clearly shows the step increase in the rate of rise when the moisture exiting the 12 channels is detected at the hygrometers. Control room (C/R) records show a peak of about ~55°C/hr which occurs at 1.5 hrs into the injection, whereas the predicted rate of rise peak occurs about 15 minutes earlier and is lower than in the test. Since the alarms are based on rate of rise, the lower predicted peak is conservative from the alarm and operator actions point of view.

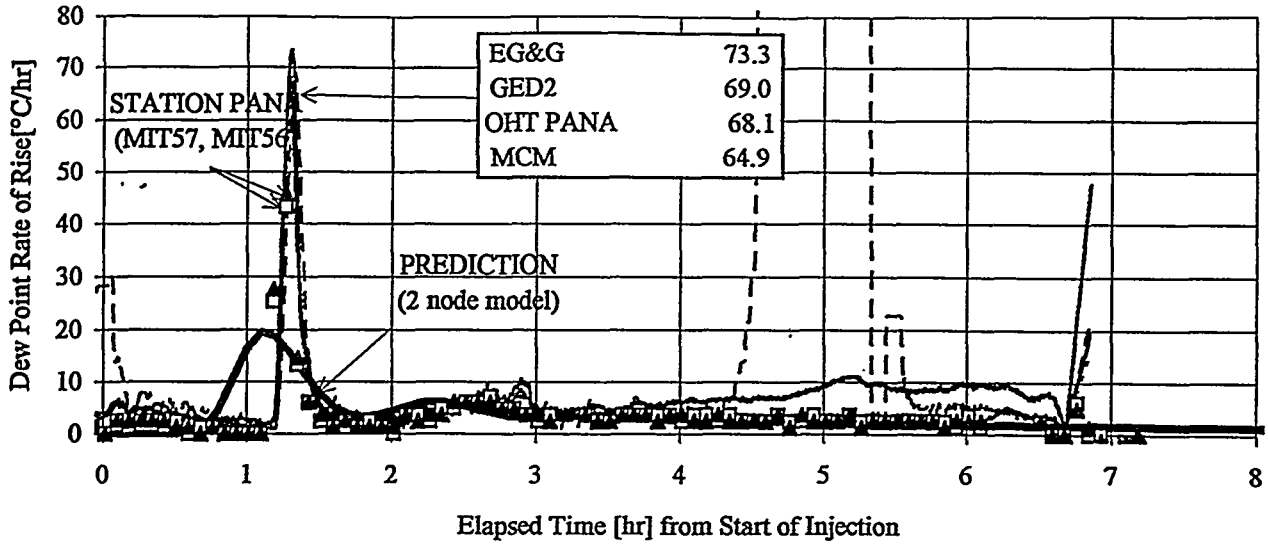

Figure 3 Test 4 Rate of Rise Comparisons of Test Data with Predictions

5.3 Test 5 Dew Point Results

Test 5 was conducted with one compressor operating and injection into the same string as test 4 (i.e. a 12 channel string). The total AGS flow rate (2.1 L/s) was just above the very low flow alarm limit. The moisture injection rate was 2.1 g/hr.

Because of the lower flow, the moisture took longer to appear at the dew point meters. The first moisture front was detected just after 2 hours from the start of injection (Fig. 4). Moisture was predicted by modelling to emerge ~ 50 minutes earlier than the test results. A second front appeared at the 4 hour mark indicating a residence (circulation) time of 2 hours during this test. Injection was continued during the purge mode to compare the measured values to the model's prediction behaviour during purging.

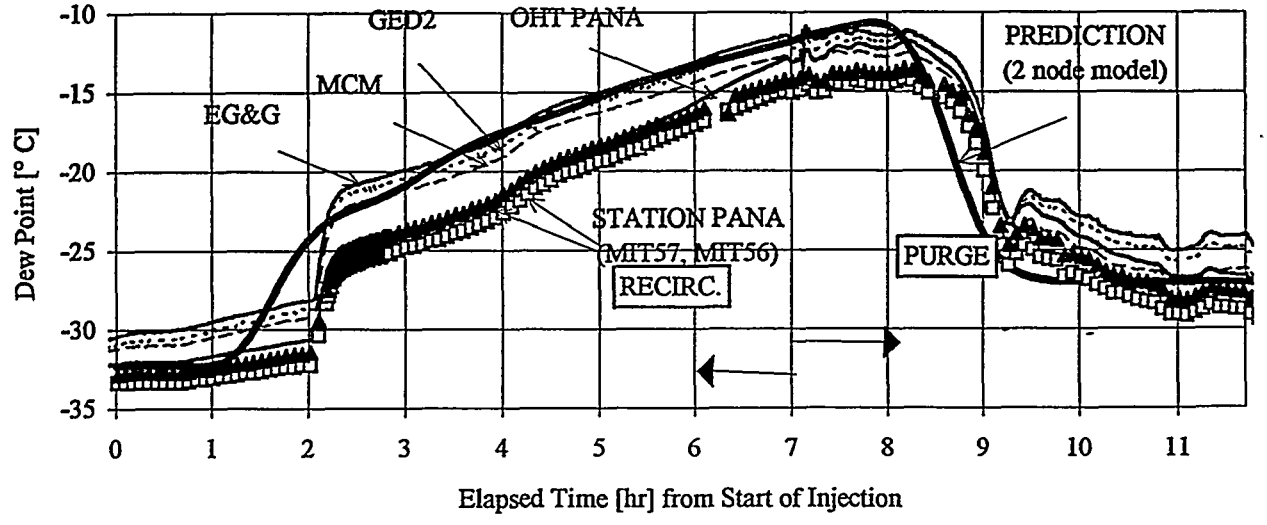

Figure 4 Test 5 Measured Dew Point vs. Predictions

5.4 Test 5 Dew Point Rate of Rise Results

Figure 5 shows the results and predictions plotted as dew point rate of rise. All the OHT and station hygrometers agree well with both the magnitude and timing of the rate of rise peak. The results were also in good agreement with rate of rise from the C/R record of 38°C/hr.

The rate of rise for this test was lower than for test 4 mainly because of the lower AGS flow rate. The lower flow rate allowed more mixing and dilution in the channels compared to the 2 compressor higher flow.

The predicted peak occurs about 30 minutes sooner than the measurement and is much lower.

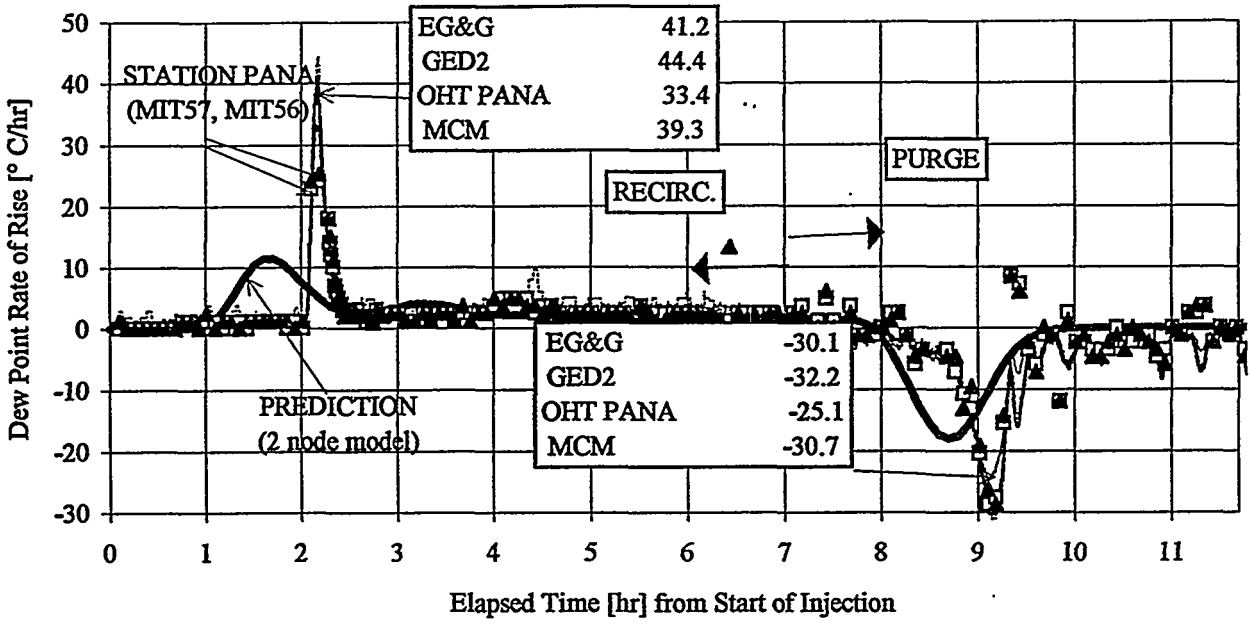

Figure 5 Test 5 Rate of Rise - Measured Values vs Predictions

5.5 Test 6 Dew Point Results

This was a two compressor test with injection into one of the shortest strings (4 channel string). The injection rate was 3.4 g/hr and the AGS flow was 3.1 L/s. Because of the short string, the moisture came out much sooner (Fig. 6) than the previous tests. The difference in moisture detection time after injection between the prediction and the test results is about 15 minutes.

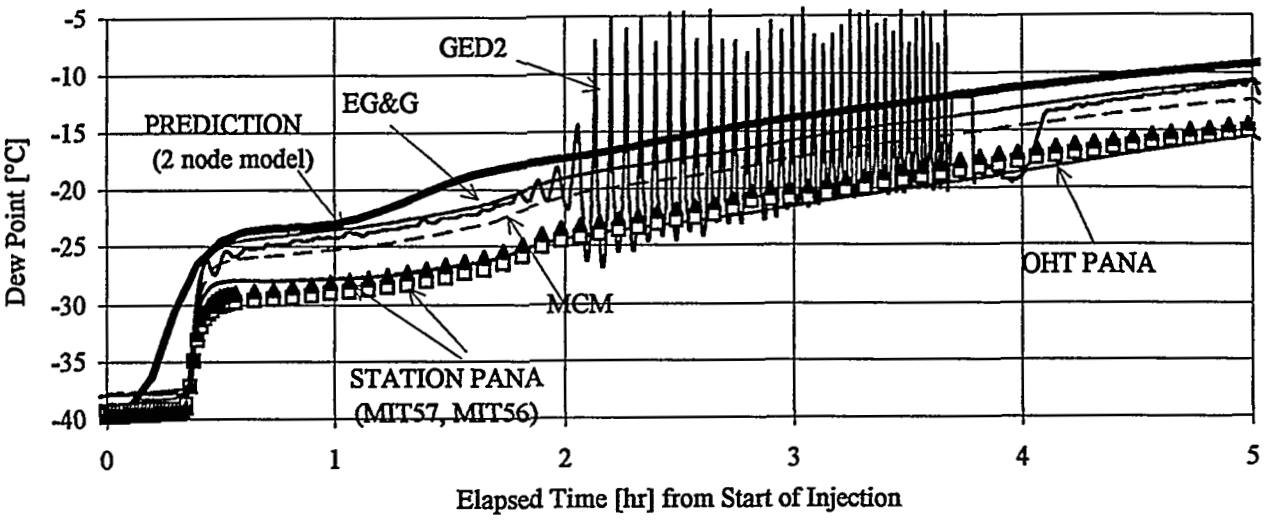

Figure 6 Test 6 Measured Dew Point vs Predictions

5.6 Test 6 Dew Point Rate of Rise Results

The rate of rise at the initial moisture detection was much higher for this test (Fig. 7) since the shorter string length limits the mixing of the moisture as it travels through the channels (i.e. more "plug flow" behaviour).

In this test the VHI alarm (operator action alarm) was annunciated. The 'rate of rise' algorithm is based on a leak occurring at the inlet end of the first channel of a 12 channel string. This is again a conservative situation because it shows detection of a leak which is located furthest away from the dew point meters. The fact that the VHI alarm came in for the 4 channel string demonstrates the sensitivity of the algorithm (designed for leak at the upstream end of 12 channel string). It shows that the AGS is capable of annunciating leaks smaller than ~3.5 g/hr in a 4 channel string or within four channels of the exit of longer strings.

The predicted peak is lower and occurs 7 minutes sooner compared to the test.

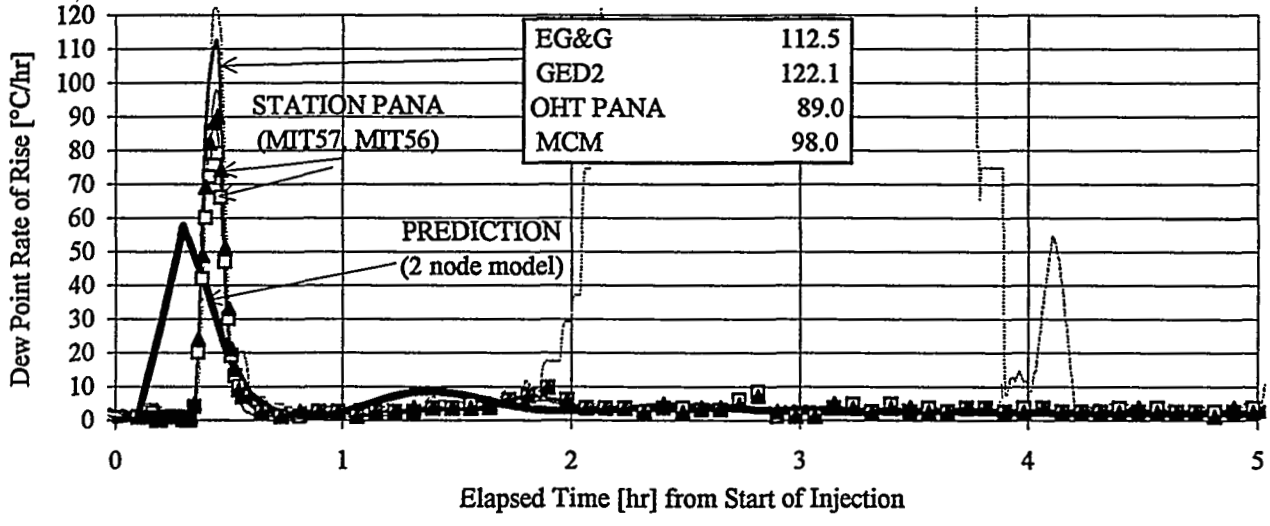

Figure 7 Test 6 Rate of Rise Measurements Compared with Predictions

6. Prediction Method

A computer model was used for predicting the dew point response in the AGS. This model simulates the transport of moisture from the leaking channel through the string of annuli containing the leaking channel. The channel annuli are divided into small volumes (nodes) and humidity balance equations are written for them. The resulting set of linear simultaneous differential equations are solved to generate humidity and dew point variation with time. The moisture concentration at the hygrometers depends on the degree of mixing along the flow path. The time at which moisture emerges from the leaking string, the dew point reached and the step change in humidity depend on the number of nodes used in the simulation. The less the number of nodes in the analysis, the more the mixing, the smaller the delay in moisture exiting the string and the smaller the step change in dew point over a given time interval. A larger number of nodes produces more of a "plug flow" moisture front.

6.1 SENSITIVITY OF PREDICTIONS

The parameter which introduces the most amount of uncertainty in the predictions is the number of nodes used in the model. The current 'rate of rise' algorithm is based on a two node model which simulates more mixing, shortens the delay and produces a lower rate of rise. The moisture mixing phenomenon during its transport in the AGS is not known exactly.

Although a 10 node model provides better agreement with test results (Fig. 8), the 2 node model rate of rise prediction is conservative with respect to setting the alarm setpoints. The 2 node model predicts a lower peak due to more mixing. However, the 10 node model predicts a higher peak and steeper slope and is in closer agreement with test data.

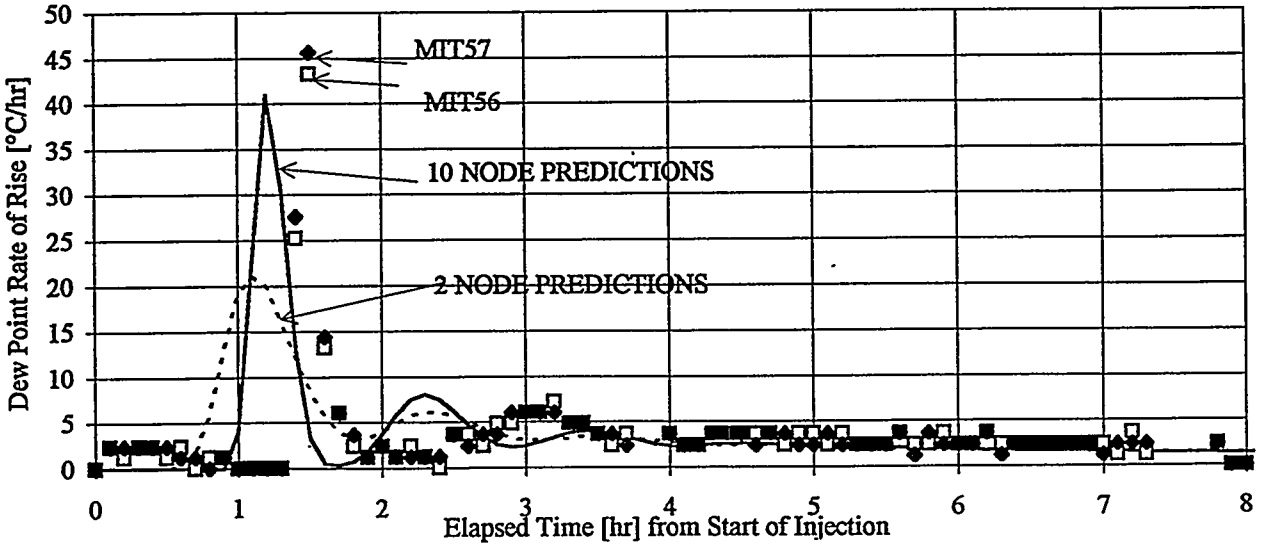

Figure 8 Test 4 Rate of Rise Predictions with 2 and 10 nodes

7. IMPLICATIONS OF TESTS ON LEAK-BEFORE-BREAK ASSESSMENTS

The purpose of these tests was to verify the dew point response assumed in the LBB analysis. From dew point predictions and results of separate fuel channel pressurisation/holdup tests (not reported here) the time at which the dew point VHI rate alarmed was deduced to be 3.5 hours. Using this as the dew point response time and following the station operating procedures, it was demonstrated that LBB was assured for a postulated PT leak event.

The current testing shows that the measured rate of rise is higher than that predicted with the dew point model, which is conservative from the operational safety point of view. Test 5, which is similar to the conditions used for the current Bruce A LBB assessment, shows peak rate of rise at ~ 2 hours. Hence the modelling assumption of 3.5 hours for the VHI rate alarm is conservative.

8. CONCLUSIONS

8.1 All hygrometers detected a rapid rate of increase of moisture at about the same time.

8.2 The tests show that the AGS is capable of detecting and alarming the very small leaks (2-3.5 g/hr) used in the current tests thus providing confidence that for a postulated PT leak with a growing crack (where the leak rate would be much higher) the AGS would detect the leak and alarm the operator.

8.3 The dew point rate of rise algorithm, which is based on the longest string, operates as designed and is sensitive to small leak rates. This was demonstrated by the occurrence of a VHI alarm for the shortest string injection test.

8.4 The measured rate of rise is higher than predicted, which is conservative for alarms, action limits and therefore LBB assessments.

8.5 Testing demonstrates that the VHI alarm time assumed in the LBB assessments is conservative. The difference in predicted and measured HI & VHI rate times do not have any impact on demonstrating LBB.

8.6 Predictions using different numbers of nodes shows that moisture is transported in the AGS in more of a "plug flow" manner rather than in a "mixed flow" regime.

8.7 The dew point model predicts AGS response adequately for use in LBB assessments. Although better agreement between tests and predictions can be obtained with a larger number of nodes, the rate of rise algorithm based on 2 the node model is conservative and provides timely alarms for LBB analyses.

ASPECTS OF LEAK DETECTION

T C CHIVERS, Nuclear Electric plc; Berkeley Technology Centre, Berkeley, Glos; UK.

ABSTRACT. A requirement of a Leak before Break safety case is that the leakage from the through wall crack be detected prior to any growth leading to unacceptable failure. This paper sets out to review some recent developments in this field. It does not set out to be a comprehensive guide to all of the methods available. The discussion concentrates on acoustic emission and how the techniques can be qualified and deployed on operational plant.

1 INTRODUCTION

An essential part of a Leak before Break (LbB) safety case is that a leaking through wall crack will develop, and be detected, prior to the defect reaching critical length and vessel failure.

The magnitude of the leak will depend upon a number of factors including the geometry of the pressurised system, the upstream operating conditions, and the contained fluid. The time for detection is less simply defined as it will be influenced by a number of extrinsic variables (eg leakage of toxic fluids, acceptable temperature rises etc) as well as intrinsic ones (eg fatigue cycles, creep life etc.) Thus there can be no simple panacea to the selection of leak detection equipment, nor to the definition of detection time. Each case needs to be considered on its own individual merits, with solutions tailored to specific needs. Although for specific plant categories generalisations will be possible. Further, it is not adequate simply to determine that leakage is occurring. If expensive plant outages are to be avoided then the source needs to be located. For example, leakage from a valve gland is unlikely to threaten structural integrity, whereas a leak of the same magnitude from a cracked pipeline could be a significant threat.

It is also considered that the definition of a leakage threshold for an acceptable LbB case is inappropriate. Limits should be set simply by confidence in the overall procedure and the strategy for its deployment. This requires that a structural analysis of the plant is undertaken to assess relevant stress levels. Knowledge of defects, or postulated defects will be needed. From this likely leak sources and sizes can be defined for use in leak rate calculations, and the selection of leak detection equipment.

On the basis of the above, this paper will discuss detection systems that have some capability to detect, locate and quantify leakage. It will not attempt to be a wide ranging review of instrumentation, but will concentrate on recent developments and experience within the authors company. The discussion will concentrate on the use of Acoustic Emission (AE) for detection purposes. It will also discuss "Global" and "Local" systems. the former description will relate to systems covering a large section of plant, whereas local is used to describe a system targeted at, say, a specific weld.

2 ACOUSTIC EMISSION

Fluid escaping from a through wall defect will generate two sources of acoustic noise. One is airborne, and is common in most peoples experience as some level of noise (whistling) is usually audible. Structure AE is also generated in the form of surface waves, and this is only detectable using instrumentation. For both emissions there is a wide frequency spectrum, and to limit confusion when interrogating signals it is usual to look at a narrow band of frequencies. For example the microphones used in leak detection normally respond around the 40 KHz level; whereas the transducers used in structure borne AE respond at around the 200 KHz level. The signal level generated will attenuate with distance from the source, and will also need to be discriminated from background noise levels from different origins.

Whilst the physics of acoustics is well developed its deployment on leak detection is not well understood and correlations between leak rates and signal levels are empirical. Whilst several attempts have been made to rationalise the understanding in terms of general relationships, a fully predictive capability does not currently exist. This is particularly the case for air borne emissions.

2.1 GLOBAL LEAK DETECTION

Here global is used to indicate that a single system is used to obtain information on an entire, or a large section of, plant.

2.1.1 Structure Borne AE

With this system a series of transducers are deployed at known intervals. When leakage arises the various signals generated by the transducers can be interrogated to give information on location and magnitude of the leak. The location capability arises because of the signal attenuation with distance, and it is this facet that also dictates the number of sensors that need to be deployed. It is not intended that this paper includes a full description of the technology and the interrogation techniques. For a reasonably comprehensive description the interested reader is referred to Reference 1. The leak rate assessment needs to come from either the users own data base, or if a commercial system is in use then that should be supported by the appropriate information.

The transducers may be mounted directly on to the surface of the pressurised system. However, temperature limitations may decree that wave guides be used. Wave guides are simply cylindrical wires welded onto, or screwed into, the structure which have a cone - cylinder transition at the end on which to mount the sensor. These wave guides will further attenuate the signal, and this needs to be taken into consideration in designing the system.

Signal analysis needs to be computerised, and commercial systems exist that can handle over thirty measuring points. Complications exist in that the pressurised fluid, and other sources, may well generate extraneous noise (background). This is particularly true in pipelines, and this background noise will itself be a variable; depending, for example, on the power level in a reactor. Thus the user needs to understand the behaviour of background noise not only to ensure the correct setting of alarm levels, but also to determine the actual signal associated with the leak. The background levels can only be determined from plant specific measurements. It may mean that alarm levels, and hence detection capabilities, will vary with plant operation. For some operating regimes it may not be possible to rely on such a system. Never-the-less, systems can be designed with confidence and with high reliability. Attenuation data is available for pipeline materials and also for waveguides. This enables the signal information to be interrogated to determine the source of the signal and the strength at source. This source strength then needs to be translated into a leakage rate, and this is more problematical. Various correlations exist, usually of the form (eg Reference 2):

$$RMS(db) = M.\log(P.Q_m) + b$$

Here P is the fluid pressure and Q_m the mass flow rate and the product is dimensional. Thus whilst the form of such correlations may be general the constants, M and b, will be fluid specific and may depend on other factors, such as geometry of the flow path. Recent experiments have looked at flow through a wide range of cracks, and using a number of different gases. In this instance good correlation was obtained using the log of the product of pressure ratio and flow area, figure 1. Again the controlling parameter is dimensional, and care must be taken in the general use of this data.

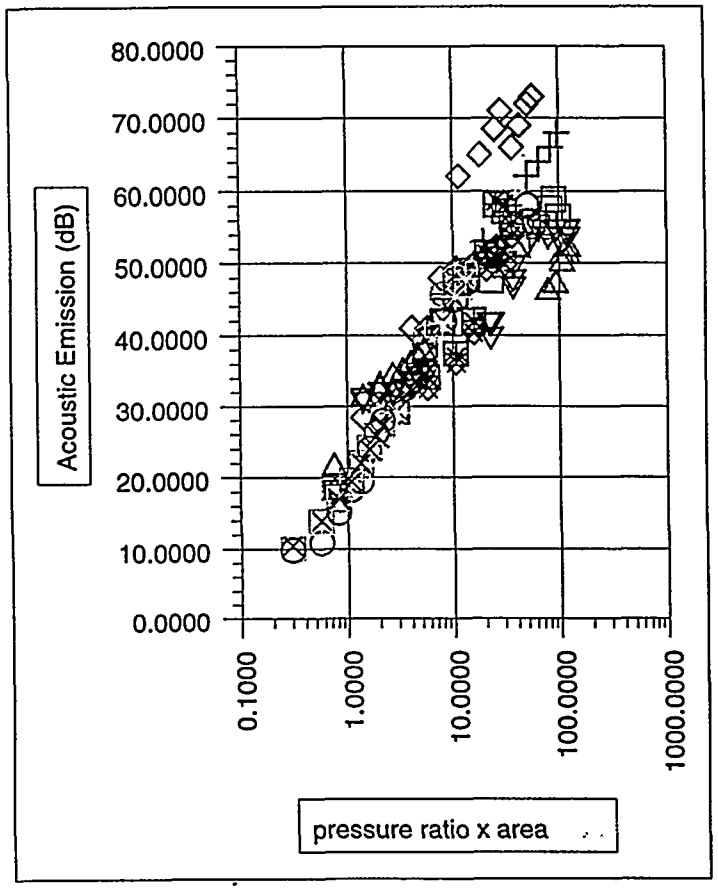

FIGURE 1. Summary of structure borne AE data for six "crack types and four gases and steam.

2.1.2 Installed Air Borne AE Systems

The basic technology in terms of data logging, analysis and interrogation can be as for the structure borne system, but now the transducer is a microphone with a narrow band frequency response. As before background levels have to be determined before alarm levels can be set, and detectable leakage rates determined.

Air borne AE detection systems are, however, more susceptible to spurious signals than those for

structure borne AE. Thus an alarm indication needs to be investigated prior to taking any action if expensive outages are to be avoided. For example, valves that have failed to close completely, have generated spurious signals, as also have leaking airlines, vacuum cleaners etc. There is also the possibility that one leak may mask others, although this possibility should be avoided by adequate deployment of microphones. Indeed one of the major advantages of air borne systems is that they can be deployed or extended whilst plant is on load. Plant experience has shown that detection levels are at about the 10 grams/sec level, subject to the various caveats discussed above.

In addition to the other caveats discussed the role of lagging needs to be considered. The available evidence on leaks arising on steam plant (eg. Reference 3), suggests that in general they arise at geometric discontinuities, such as pipe - elbow intersections. Such features will also coincide with discontinuities in lagging. Should leakage occur at such a feature, then lagging is not expected to inhibit detection using air borne AE, although detection times may be extended. If critical welds are in long straight pipe runs, then lagging junctions and welds may not coincide. Operators then need to be assured that leakage can result in sufficient degradation of the insulation to limit attenuation to tolerable levels. Limited evidence, for a specific insulation design, suggests detection levels are increased from some 10 grams/sec to some 40 grams/sec, with transmission through the outer steel cladding. These limits will be very dependant upon specific design details, and a data base will need to be established.

The quoted detection levels correspond to distances of some 7 metres between source and microphone. Signal attenuation will result in lower detection levels as distances increase, as also will high levels of background noise. Usually microphones tuned to 40 KHz are used, but in some plant areas noise at this frequency is high. Microphones tuned to 200 KHz are being investigated for such areas. Whilst the signal levels will be lower and the attenuation rate higher at this frequency, the background noise levels will be lower.

It should be noted that airborne acoustic noise does not necessarily increase with increasing leakage from a defect. This means that general empirical correlations, such as depicted in Figure 1, are unlikely to emerge, and this will make accurate estimates of flow rates difficult.

2.1.3 Manual Systems

Hand held AE microphones can be used to augment manual surveys of plant areas. When used by a knowledgeable operator they can have similar sensitivities to installed microphones. General background levels need to be known, and action levels decided; this needs to be based on experience. Another use is in investigating alarm levels triggered by an installed system. Here the hand held device can be used to home in on the source of a signal and appropriate action decided.

3 LOCAL DETECTION SYSTEMS

Where calculated leak rates are relatively low, and/or timescales for detection short, or for other specific reasons, global detection systems may not be adequate. Under these circumstances local detection systems may offer an alternative. For the systems to be described here mechanical shrouds are constructed around the feature of interest, Figure 2. Any resultant leakage is then into this contained area, which can be lagged on the outside. Two systems have been used. In the first system, thermocouples are used and thus the system is restricted to plant operating at temperatures different from ambient. The leaking fluid is piped away from the contained area to a volume at ambient temperature containing a thermocouple. This system requires the shroud to have a high degree of leak tightness. For steam leaks from pressurised systems at 550°C flowrates of less than 1 gram/sec can be detected in less than five minutes. Leak rates can be estimated from an analysis of the rate of change of temperature with time data, or temperature rise.

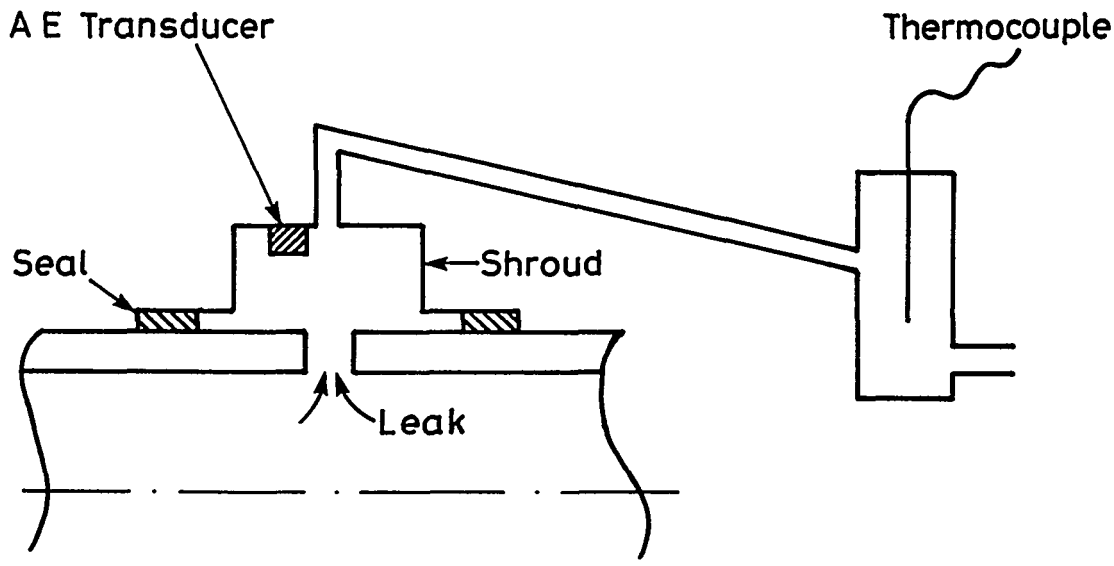

FIGURE 2. Diagramatic representation of a shroud containment around a potential leak site. For use with either Airborne AE or Thermocouples.

The second system relies on air borne AE as a microphone is installed in the cavity, or, if temperatures inhibit this, a air-tube wave guide is used to duct signals to a cooler area. Again detection levels of less than 1 gram/sec can be detected, but this will be influenced by background noise levels. Flow rates can be assessed from signal levels. In this instance it is not necessary for the shroud to be tightly sealed.

For either method of detection it is easy to engineer in suitable alarm signals that are unambiguous.

4. CLOSURE

This paper has reviewed certain aspects of leak detection equipment, concentrating on Acoustic Emission systems. Based on both laboratory experiments and deployment on operating plant, it has shown that where necessary, sensitive monitoring equipment can be deployed to detect relatively small leak rates. It has also shown that global systems can be used effectively to detect, locate, and to some extent, quantify leakage.

5. ACKNOWLEDGEMENT

This paper is published with permission of Nuclear Electric plc.

6. REFERENCES

1) Jax, von P, and Leuker, W, Neue Leck Detektions-und Ortungsverfahren fur Rohrleitungen und Behalter. VGB Kraftwerkstechnik 72(1992) Heft 6.

2) Dumousseau, P, and Roget, J. Application de l'Emission Acoustique a la Caracterisation des Fuites et au Controle d'Entancheite. EdF Centim-Informations No 72,1982.

3) Harrow, J, McLean, R I, and Addie, T, Operating Experience on Steam Generating Plant Pipework. I.Mech.E C376/031 1989.

SESSION 4: LBB ASSESSMENTS AND MARGINS

MARGINS IN HIGH TEMPERATURE LEAK-BEFORE-BREAK ASSESSMENTS

P J Budden* and D G Hooton**
*Nuclear Electric plc **AEA Technology

SUMMARY

Developments in the defect assessment procedure R6 to include high-temperature mechanisms in Leak-before-Break arguments are described. In particular, the effect of creep on the time available to detect a leak and on the crack opening area, and hence leak rate, is discussed. The competing influence of these two effects is emphasised by an example. The application to Leak-before-Break of the time-dependent failure assessment diagram approach for high temperature defect assessment is then outlined. The approach is shown to be of use in assessing the erosion of margins by creep.

INTRODUCTION

Leak-before-Break (LbB) arguments are used to demonstrate that a defect in a pressurised component results in a detectable leak prior to disruptive failure. Appendix 9 of the Nuclear Electric defect assessment procedure R6 (Ref.1) contains advice on performing LbB assessments. The appendix is being revised, and further details are given in Reference 2. The effect of creep on LbB arguments is included in the revised appendix, following principles outlined in Reference 3, using the methods of the high temperature assessment procedure R5 (Ref.4). This paper specifically addresses these high-temperature aspects of LbB and describes their treatment within R6.

For components operating in the creep range, rupture due to continuum damage mechanisms and crack growth need to be considered both before and following defect breakthrough. Creep may both open a through-wall crack and extend it along the wall in general; these effects tend to increase the leak rate and hence enhance the possibility of detection. However the margin between crack length and the critical crack length under fault conditions reduces as the crack grows along the wall. Similarly creep rupture under operating loads may occur prior to the crack attaining the critical length. This degradation of margins is of particular relevance where plant is only intermittently monitored. A particular example of a pressurised pipe under global bending is used in this paper to illustrate these competing effects of creep on crack opening area and crack length.

The calculations of creep crack growth required to both follow crack shape development through the pressure vessel wall and subsequent growth of the fully-penetrating defect involve explicit integration of crack growth rate equations expressed in terms of C*. Recently, however, a simplified approach to assessments of rupture and limited amounts of crack growth under creep and creep-fatigue loading conditions has been developed (Refs.5-7) based on the R6 failure assessment diagram (FAD). The failure assessment curve and the coordinates (L_r, K_r) on the R6 FAD are then functions of time and material creep properties. The approach removes the necessity to perform detailed crack growth calculations. The use of this time-dependent failure assessment diagram approach for LbB arguments is introduced in this paper.

HIGH TEMPERATURE EFFECTS IN LbB

Two levels of LbB argument can be made in general: (1) a full LbB case where flaw shape development is modelled as the crack grows through the wall until breakthrough; (2) a simplified 'detectable leakage' argument where an initial through-wall flaw is assumed to be present. R6 contains both these levels.

A high-temperature leak-before-break case can be made if it is possible to demonstrate that each of the following hold: (i) the defect length at breakthrough, l_b, is less than the limiting through-wall defect length, l_c; (ii) creep rupture of the section has not occurred prior to break-through; (iii) the through-wall defect leaks fluid at a rate which is detectable before the crack grows to the limiting length and before creep rupture of the section occurs.

These principles can be expressed by the following four inequalities:

$$l_b < l_c \tag{1}$$

$$t(l_b) < t_{CD}(l_b) \tag{2}$$

$$\Delta t_d < t(l_c) - t(l_b) \tag{3}$$

$$\Delta t_d < t_{CD}(l_c) - t(l_b) \tag{4}$$

where $t(l)$ is the time for the crack to attain a through-wall length l, $t_{CD}(l)$ is the creep rupture time assuming a constant through-wall crack length l, and Δt_d is the time to detect the leak. Δt_d depends on both the leak rate and the capabilities of the detection system. Creep affects Δt_d by increasing the crack opening area and hence leak rate in general; this is discussed later in the paper. For a postulated fully-penetrating flaw, $t(l_b)=0$, the

start of high-temperature operation. In the case of a full LbB argument, $t(l_b)$ follows from calculating the creep crack growth at both the surface and deepest points of the initial surface flaw. At a certain crack depth, ligament instability occurs and the defect snaps through; l_b is then the re-characterised defect length following instability. It should be noted that a LbB case cannot be made if the surface point is unstable first.

Inequalities (1) and (3) are the same as appear in low-temperature LbB. They ensure that failure by fast fracture does not occur either prior to breakthrough or before the leak can be detected, respectively. The time $t(l_c)$ is however affected by creep crack growth as described below, and the fracture toughness used to evaluate l_c should reflect material which has experienced creep damage. Inequalities (2) and (4) stipulate that creep rupture has not occurred prior to breakthrough and that sufficient time is available to detect the leak before creep rupture occurs, respectively. If $t(l_c)<t_{CD}(l_c)$, then the remaining life of the component is limited by unstable crack growth prior to creep rupture. Conversely, if $t_{CD}(l_c)<t(l_c)$ then creep rupture limits life.

The estimates of rupture times in eqns.(2) and (4) depend on the crack length via the reference stress, σ_{ref}. It is however conservative to assume a constant through-wall crack length, l; that is

$$t_{CD}=t_r(\sigma_{ref}(l)) \tag{5}$$

as this ignores the prior history of crack growth and hence underestimates the time to creep rupture. Here, $\sigma_{ref}(l)$ is the limit load reference stress due to the primary loadings, P, and t_r is the material uniaxial rupture curve. Then $\sigma_{ref}(l)$ is given by

$$\sigma_{ref}(l)=\frac{P\sigma_y}{P_L(l,\sigma_y)} \tag{6}$$

where P_L is the corresponding rigid-plastic limit load for a defect of length l in a material of yield stress σ_y. It is conservative to use lower bound rupture data as these decrease the times to creep rupture and hence reduce margins.

If a high-temperature LbB argument cannot be made due to failure of inequality (4) alone, or if insufficient margins exist, then it is possible to refine the estimate of rupture time and replace inequality (4) by:

$$\Delta t_d < t_{CD}(l_r)-t(l_b) \tag{7}$$

Here l_r and $t_{CD}(l_r)$ are the crack length and corresponding time at

rupture and are obtained by solving $t_{CD}(l)=t(l)$ for $l=l_r$ where $t(l)$ is the time to reach crack length l (see Fig.1). Note from inequalities (2) and (4) that l_r then satisfies $l_b<l_r<l_c$.

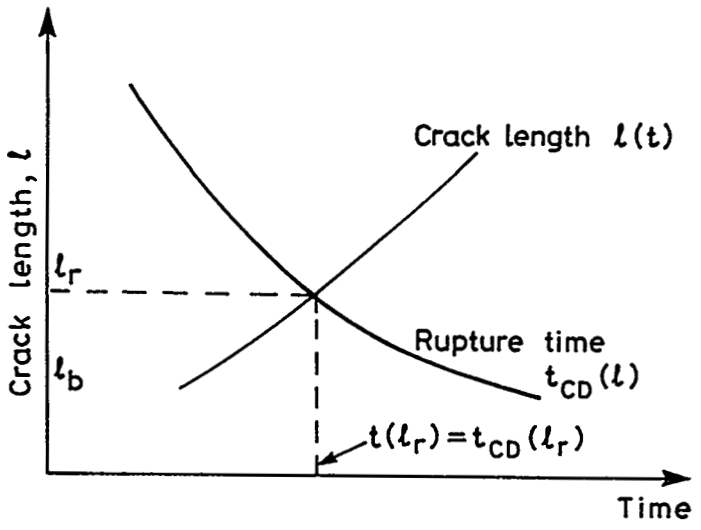

Figure 1. Schematic of calculation of l_r and $t_{CD}(l_r)$

Creep crack growth calculation

In general, creep crack growth rates, $\dot{a}$, obtained from specimen tests are correlated with C* by an equation of the form

$$\dot{a}(C^*)=DC^{*q} \qquad (8)$$

(Ref.4) where D and q depend on material. For assessments, estimates of C* at the surface and deepest points of an assumed surface flaw can be derived from reference stress methods (Ref.4) using creep data for the defective section. Integration of eqn.(8) then enables growth of the defect to be calculated as it grows through and along the wall. Following breakthrough, or for a postulated initial through-wall crack, eqn.(8) determines the variation of through-wall crack length, l, by integration at both crack tips.

CREEP EFFECTS ON MARGINS

Margins in high-temperature LbB can be defined in respect of crack size or the time to detect the leak. Margins are not specified within the R6 procedure but are left to the user to argue on a case-by-case basis. A margin on time in particular may be defined by comparing the detection time for the leak with the available time, the lower of $t_{CD}-t(l_b)$ and $t(l_c)-t(l_b)$, where t_{CD} is the rupture time.

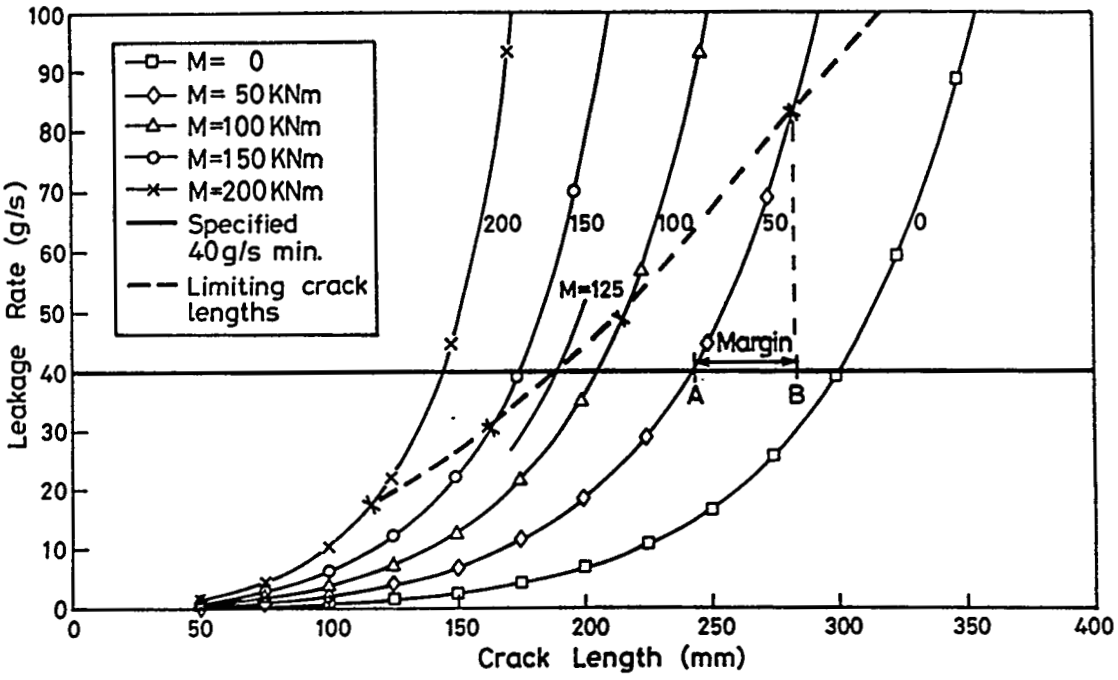

Figure 2. Leak rate against crack length for various bending moments, M at operating pressure. Creep neglected. The limiting crack size at fault pressure is also indicated.

To illustrate these points, consider the example of a plain pipe of mean radius R_m=142.36mm, wall thickness t=37.24mm (R_m/t=3.82) under internal pressure P and subject to a global bending moment M. A fully-penetrating part-circumferential crack of length l at the mid-wall is located at the position of maximum bending stress around the pipe circumference. The operating and fault pressures are 9.7MPa and 13.9MPa, respectively. It is assumed that a steam leakage rate of 40gs^{-1} can be quickly and reliably detected. Calculated flow rates depend on the crack length, crack opening area (COA), fluid properties and the characteristics of the flow path. Figure 2 shows calculated leakage rates as a function of crack length at operating pressure for various bending moments, for particular assumptions on the flow. The effects of creep on the COA have been ignored at this stage, but are considered later. The details of the calculations are not covered here. The limiting crack size at each bending moment, based on initiation of crack extension at fault conditions, is also shown in Figure 2. From the figure, it can be seen that bending moments less than about 125kNm correspond to limiting crack lengths in excess of the crack size corresponding to a detectable leak. The calculated margin on crack size at detection then reduces to zero as the bending moment rises to 125kNm. At a moment of 50kNm, for example, the margin on crack size is simply given by AB in Fig.2, assuming immediate leak detection.

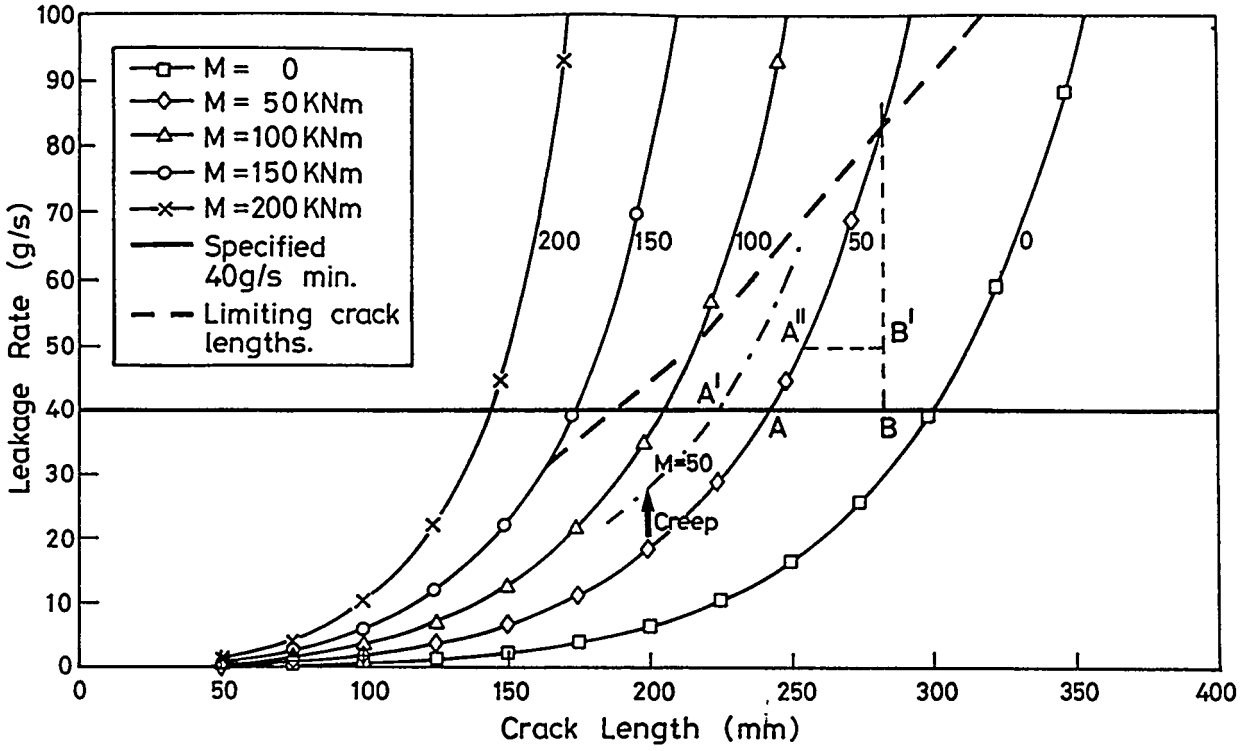

Figure 3. Leak rate against crack length for various bending moments, M. Schematic of the effect of creep.

The effect of creep can be explained from Figs.2 and 3. At a fixed crack length and loading, the effective COA increases and hence the leak rate tends to increase. This tends to move each leak-rate curve in Fig.2 upwards, so that, at the detectable leakage rate, point A moves to A′, say, in Fig.3. The margin on crack size has increased to A′B. Let the COA be denoted A and the creep and elastic components of A by A_c and A_e respectively. Then the rate of change of A_c can be readily estimated (Ref.1) from

$$\dot{A}_c = A_e \frac{\dot{\epsilon}_c(\sigma_{ref}, \epsilon_c)}{\sigma_{ref}/E} \qquad (9)$$

where E is Young's modulus, and $\dot{\epsilon}_c(\sigma_{ref}, \epsilon_c)$ is the creep strain rate at reference stress σ_{ref} and accumulated creep strain ϵ_c. For a steady-state creep law $\dot{\epsilon}_c = B\sigma^n$, where B and n are constants, eqn.(9) can be re-written using the reference stress formulation of C* as

$$\dot{A}_c = \frac{A_e}{t_{red}} \qquad (10)$$

where the redistribution time $t_{red}=K^2/EC^*$ with K the stress intensity factor. (At time t_{red}, $\epsilon_c=\sigma_{ref}/E$ at stress σ_{ref}.) Then from eqn.(10) it follows, for small amounts of crack growth, that

$$A = A_e \left(1 + \frac{t}{t_{red}}\right) \qquad (11)$$

Hence, for $t<<t_{red}$, $A=A_e$ and, for $t>>t_{red}$, $A=A_e t/t_{red}=A_c$ as expected.

Creep crack growth under constant load causes point A to move to A'', say, on Fig.3 in a certain time. This also increases the flow rate, and hence increases the likelihood of detection, but acts to reduce the crack size margin relative to the critical length, to A''B' say. The time available for detection is then given, from inequality (3), by $\Delta t_d=t(l_c)-t(l_b)$. It is necessary also to monitor creep rupture damage accumulation so that inequalities (2) or (4) are not violated. For small amounts of crack growth, where C* varies little, it follows from eqn.(8) that the increase in crack length, Δl, is approximately $2DC^{*q}t$ in time t.

The net effect of the increases in COA and crack size on margins is not evident, a priori; this is determined by the flow calculations. For this reason, it is suggested that best-estimate creep crack growth and deformation data should be used in an initial LbB assessment; other combinations of data may be used as part of a sensitivity study. It is however conservative to ignore the increase in COA as the predicted leak rate is then minimised and subsequent margins on detection time reduced.

THE TIME-DEPENDENT FAILURE ASSESSMENT DIAGRAM AND LbB

Recently, the R6 FAD approach has been extended to address high temperature defect assessment (Refs.5-7). The method uses time-dependent FADs to demonstrate whether or not a specified amount of crack growth is exceeded, or creep rupture of the section occurs, within a given time period. In contrast to the methods referred to above, the amount of crack growth is limited by the consideration that crack growth must be small relative to the initial crack size and the section width. However for LbB applications, the method provides a simple procedure to demonstrate whether or not significant creep-fatigue crack growth of the crack size for detectable leakage, or creep rupture of the section containing the crack, is likely over the time required for leakage detection under normal loading conditions. It is of course necessary to demonstrate that there is sufficient margin between the leakage crack size and the critical crack size under maximum overload conditions.

For time-dependent assessments, the FAD is defined in terms of isochronous stress-strain data, $\epsilon=\epsilon(\sigma;t)$, using the R6 Option 2 curve:

$$f(L_r) = [E\epsilon_{ref}/\sigma_{ref} + \frac{1}{2}L_r^2/(E\epsilon_{ref}/\sigma_{ref})]^{-1/2} \quad (12)$$

where $\epsilon_{ref}=\epsilon(\sigma_{ref};t)$. The cut-off $L_r=L_r^{max}$ is defined as the ratio of the rupture stress to the 0.2% proof stress, $\sigma_{0.2}$, both determined from the isochronous stress-strain curve at the assessment time.

The assessment point (L_r,K_r) is defined by $L_r=\sigma_{ref}/\sigma_{0.2}$ and $K_r=K/K_{mat}$, where, for constant creep loading, K_{mat} is the material creep toughness, K_{mat}^c. K_{mat}^c may be derived either from data presented in the form of eqn.(8) or directly from experimental displacement measurements (Ref.7). K_{mat}^c is a reducing function of time and is also a function of tolerable crack extension, Δl. If additional to creep crack growth, fatigue crack growth occurs, then K_{mat}^c is reduced to a modified toughness given by

$$K_{mat}^{c-f}=K_{mat}^c[\Delta l_c/\Delta l]^{1/2q} \quad (13)$$

where $\Delta l=\Delta l_c+\Delta l_f$. If the assessment point (L_r,K_r) lies within the FAD, then significant crack growth and creep rupture, within the assessment time, are avoided. Thus there is no erosion of the margin between the leakage crack size and the critical crack size, and LbB is demonstrated.

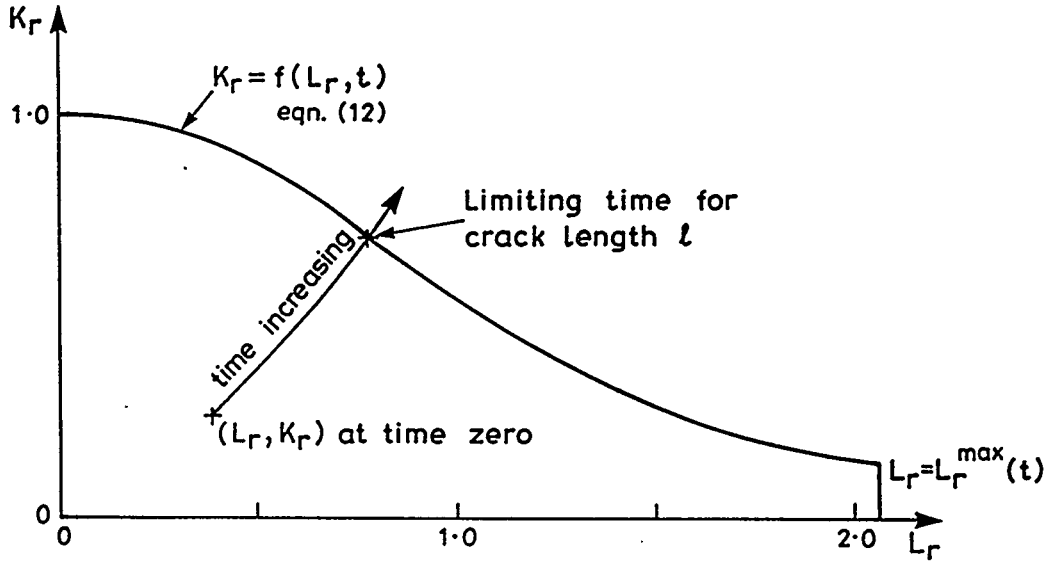

Figure 4. Schematic of calculation of limiting time for insignificant creep

The method also enables a simple approach to be adopted when considering margins in terms of time. The limiting time for tolerable crack growth or non-rupture, for a given crack size and

normal loading condition, may be determined from the intersection of the time locus of the assessment point (L_r,K_r) with the FAD at equal times (Fig.4). In practice, it is found that the dependence on time of the FAD is not large and FADs at longer times provide conservative FADs at shorter times. Thus to simplify assessments, only the FAD at the longest time needs to be used to determine the limiting time for insignificant crack growth as a function of crack length. Then only movement of the assessment point due to reduction in both $\sigma_{0.2}$ and K_{mat} with time needs to be considered.

From the relationship between crack length and limiting time, a time t_m may be determined corresponding to the length l_m which gives the required margin between the leakage crack length (now l_m) and the critical crack length, l_c, under maximum overload conditions. Thus within the time period t_m there will be no significant reduction in the margin between l_m and l_c, and no weakening of an LbB argument based on a simplified 'detectable leakage' procedure.

Consider leakage of an isothermal or polytropic gas. The mass flow rate, Q, may be estimated (Ref.1) by

$$Q=C_D(P\rho)^{1/2}A \qquad (14)$$

where C_D is a discharge coefficient, P and ρ are the pressure and density of the fluid, and A is given by eqn.(11), where A_e under membrane loading, σ_m, is given by

$$A_e=\frac{\pi l^2}{4E}C_{mm}\sigma_m \qquad (15)$$

with C_{mm} a dimensionless elastic compliance factor. Now if detection is dependent on a specified mass, then the time at leakage detection under normal loading conditions, t_d, can be evaluated as a function of crack length from eqns.(14-15). In particular, the value of t_d, corresponding to length l_m, may be determined. The margin between the time for the initiation of significant crack growth, which would erode the margin between the leakage and critical crack size, and the time for leakage detection is then simply t_m-t_d. If this margin is insufficient for a robust LbB argument, then margins may be demonstrated using the more detailed procedures based on crack growth.

CONCLUSIONS

Developments in the defect assessment procedure R6 to include high-temperature mechanisms in Leak-before-Break arguments have been described. The effect of creep on the time available to detect a leak and on the crack opening area, and hence leak rate, has been discussed. The competing influence of creep on these two effects has been emphasised.

The application to Leak-before-Break of the time-dependent failure assessment diagram approach to high-temperature crack growth has been described and shown to be of use in assessing the erosion of margins by creep.

ACKNOWLEDGEMENT

The authors thank Mr P J Bouchard and Mr C J Gardner for supplying the data for Figures 2 and 3. This paper is published by permission of Nuclear Electric plc and AEA Technology.

REFERENCES

1. I Milne, R A Ainsworth, A R Dowling and A T Stewart, Assessment of the Integrity of Structures Containing Defects, Nuclear Electric Procedure R6 Revision 3, 1986.

2. P J Bouchard, Practical Applications of the R6 LbB Procedure, this Seminar.

3. R A Ainsworth and T C Chivers, A High Temperature Leak before Break Approach for Pipework, Proc. Int. Conf. Pipework Engng. and Operation, I. Mech. E. (London), Paper C459/036/93, MEP, 1993.

4. R A Ainsworth (editor), R5 Assessment Procedure for the High Temperature Response of Structures, Nuclear Electric Procedure R5 Issue 2, 1995.

5. R A Ainsworth, The Use of a Failure Assessment Diagram for Initiation and Propagation of Defects at High Temperatures, Fatigue Fract. Engng. Mater. Struct., 16, 1091-1108, 1993.

6. R A Ainsworth, D G Hooton and D Green, Further Developments of an R6 Approach for the Assessment of Creep Crack Incubation, ASME PVP Vol 315, 1995.

7. D G Hooton, D Green and R A Ainsworth, An R6 Type Approach for the Assessment of Creep Crack Growth Initiation in 316L Stainless Steel Test Specimens, ASME PVP Vol 287, 129-136, 1994.

UNCERTAINTY ANALYSIS FOR PROBABILISTIC PIPE FRACTURE EVALUATIONS IN LBB APPLICATIONS

S. Rahman (University of Iowa)
N. Ghadiali and G. Wilkowski (Battelle)

ABSTRACT

During the NRC's Short Cracks in Piping and Piping Welds Program at Battelle, a probabilistic methodology was developed to conduct fracture evaluations of circumferentially cracked pipes for application to leak-rate detection. Later, in the IPIRG-2 program, several parameters that may affect leak-before-break and other pipe flaw evaluations were identified. This paper presents new results from several uncertainty analyses to evaluate the effects of normal operating stresses, normal plus safe-shutdown earthquake stresses, off-centered cracks, restraint of pressure-induced bending, and dynamic and cyclic loading rates on the conditional failure probability of pipes. Numerical examples are presented showing the effects of the above parameters for several nuclear piping systems in BWR and PWR. For each parameter, the sensitivity to conditional probability of failure and hence, its importance on probabilistic leak-before-break evaluations were determined.

INTRODUCTION

During the NRC's Short Cracks in Piping and Piping Welds Program (Ref. 1) at Battelle, a probabilistic methodology was developed to conduct fracture evaluations of circumferentially cracked pipes for application to leak-rate detection (Ref. 2). The methodology involved accurate deterministic models for the estimation of leak rates, area of crack-opening, and maximum load-carrying capacity of pipes and standard methods of structural reliability theory for the evaluation of conditional failure probability of pipes. However, during the International Piping Integrity Research Group (IPIRG-2) Program (Ref. 3), several parameters that may affect leak-before-break and other pipe flaw evaluations have been identified. To make a more rational assessment of the importance of these parameters, several uncertainty analyses were conducted to determine their significance on the probabilistic leak-before-break (LBB) and pipe fracture evaluations.

This paper presents new results from a probabilistic study that accounts for the effects of the following parameters on the conditional failure probability of pipes. They involved: (1) magnitude of normal operating stresses, (2) increased normal plus safe-shutdown earthquake (N+SSE) stresses addressing proposed changes to the ASME Section III design stresses, (3) off-centered leaking cracks, (5) restraint of pressure-induced bending, and (6) dynamic and cyclic load effects on toughness. Numerical examples are presented showing the effects of the above parameters for several nuclear piping systems in Boiling Water Reactors (BWR) and Pressurized Water Reactors (PWR). Pipe sizes, ranging in nominal diameters from 457.2 mm (18 inches) to 812.8 mm (32 inches), and two pipe materials, including wrought stainless steel and carbon steel, and their respective welds, were considered for determining the conditional probability of failure. For each parameter, the sensitivity to conditional probability of failure and hence, its importance for LBB evaluations was determined.

THE PROBABILISTIC LBB ANALYSIS

The application of the LBB methodology requires (1) knowledge of the pipe loads during various operating conditions of power plants, (2) details of geometry and material properties of the pipe, (3) knowledge of the anticipated cracking mechanisms and the resulting crack morphology variables for leak-rate analyses, and (4) methods for thermal-hydraulic and fracture mechanics analyses of a flawed pipe. Some of these items are subject to inherent statistical variability. Therefore, a rational treatment of these uncertainties and an assessment of their impact on system performance should be based on theories of probability and structural reliability.

During the NRC's Short Cracks in Piping and Piping Welds Program, a probabilistic LBB methodology was developed (Ref. 2) based on the general guidelines proposed in Reference 4. The steps of the probabilistic evaluation are very similar to the steps of the deterministic LBB methodology. There are two important steps to an LBB analysis. They are described below.

Probabilistic Characteristics of a Leakage Size Flaw

Consider a circumferential through-wall-cracked (TWC) pipe shown in Figure 1 with mean radius, R_m, wall thickness, t, and crack length, 2a. The pipe is subjected to combined bending and tension stresses under normal operating conditions. The crack length, 2a, is defined as the LBB detectable flaw size for a given leak rate. Following iterative calculations between thermal-hydraulic and fracture-mechanics analyses, 2a can be easily calculated when the leak rate, pipe geometry, material properties, and normal operating loads are specified.

Due to statistical variability of the crack morphology parameters, the flaw size will also be a random variable. Hence, to conduct a probabilistic analysis, the probability distribution of this crack size needs to be specified as well. In this study, a Monte Carlo method was used to determine the probabilistic characteristics of a leakage size flaw. A three-phase approach was adopted. It involved: (1) generation of independent samples of random crack-morphology parameters according to their probability distribution, (2) iterative thermal-hydraulic and fracture-mechanics analyses to determine LBB detectable flaw sizes corresponding to each sample set of crack-morphology parameters and to simulate such samples of flaw size by performing repeated deterministic analyses, and (3) standard statistical analyses of replicated samples of LBB detectable flaw size.

Structural Reliability Analysis

Let M_{max} denote the maximum moment-carrying capacity of the pipe (see Figure 1) with the constant applied tension P (due to constant internal pressure, p). M_{max} can be obtained from the solution of two nonlinear equations based on J-tearing theory (Ref. 2). In a generic implicit form, the solution of M_{max} can be represented by

$$M_{max} = f(\sigma_y, \sigma_u, F, n, J_{Ic}, C, m, 2a) \tag{1}$$

where σ_y is yield stress, σ_u is ultimate stress, F and n are the parameters of a Ramberg-Osgood model for the stress-strain curve, J_{Ic}, C, and m are parameters of a power-law model for J-R curve, and f is a function of various input variables (only the random arguments are shown in the functional dependence of M_{max}). The fracture stability of the leakage size flaw in a pipe can be evaluated by comparing the maximum load-carrying capacity of the pipe (see Equation 1) with the applied load from N+SSE stresses. Mathematically, the failure criterion can be represented by

$$M_{max} < M_{N+SSE} \tag{2}$$

where M_{N+SSE} is the applied bending moment due to normal plus safe-shutdown earthquake stresses. M_{N+SSE} can be estimated from the knowledge of actual N+SSE stresses in nuclear power plants or from the ASME service levels B, C, or D stress limits defined in Reference 5. This failure condition can be conveniently expressed in the traditional form: $g(\mathbf{X}) < 0$, where the performance function,

$$g(\mathbf{X}) = M_{max} - M_{N+SSE} = f(\sigma_y, \sigma_u, F, n, J_{Ic}, C, m, 2a) - M_{N+SSE} \tag{3}$$

in which $\mathbf{X} = \{\sigma_y, \sigma_u, F, n, J_{Ic}, C, m, 2a, M_{N+SSE}\}$ is an augmented vector of input random parameters characterizing uncertainty in all load and system parameters. Note that the performance function, $g(\mathbf{X})$, itself is random, because it depends on the input vector, $\mathbf{X}$, which is random. The reliability, P_S, is the complement of the conditional probability of failure, P_F (CPOF), i.e., $P_S = 1 - P_F$. P_F is defined as the probability that the failure event represented by $g(\mathbf{X}) < 0$, i.e.,

$$P_F \overset{def}{=} Pr[g(\mathbf{X}) < 0] \overset{def}{=} \int_{g(x)<0} f_{\mathbf{X}}(x)\, dx \tag{4}$$

where $f_{\mathbf{X}}(x)$ is the joint probability density function of the random vector, $\mathbf{X}$, which is assumed to be known. When $\mathbf{X}$ follows a normal or lognormal distribution, $f_{\mathbf{X}}(x)$ can be obtained from the marginal density function for each component of $\mathbf{X}$ and their correlation characteristics. The distribution parameters along with the correlation properties of $\mathbf{X}$ were determined from standard statistical analyses of experimental data. See Reference 2 for further details on the procurement of data and their statistical characterization.

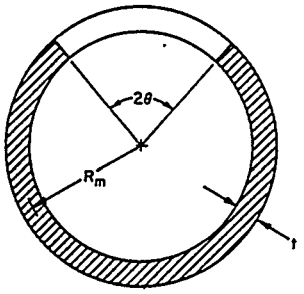

(a) pipe cross-section

(b) pipe under combined bending and tension load

Figure 1 Schematic representation of a pipe with a circumferential through-wall crack

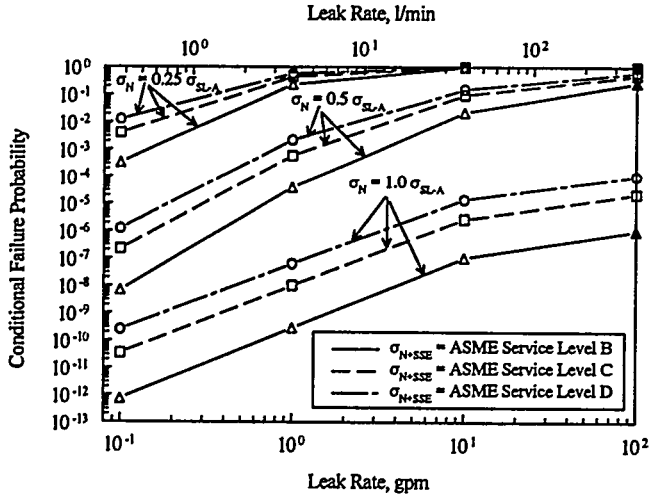

Figure 2 CPOF of BWR-1 for various pipe stresses

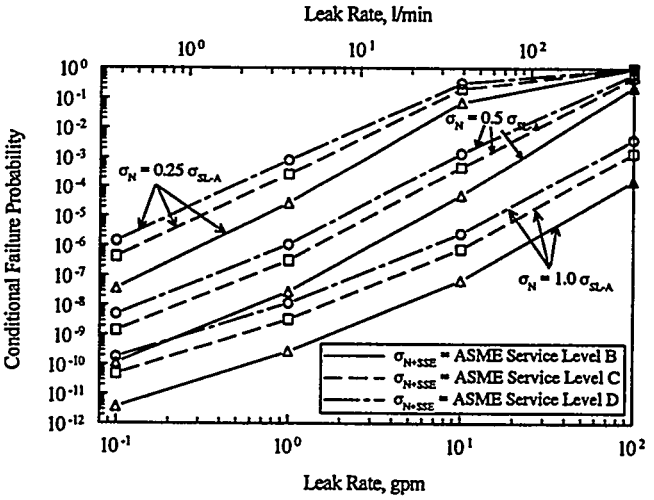

Figure 3 CPOF of BWR-2 for various pipe stresses

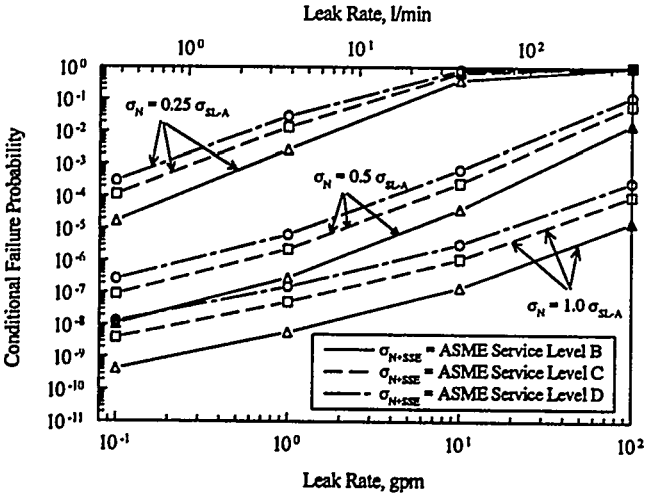

Figure 4 CPOF of PWR-1 for various pipe stresses

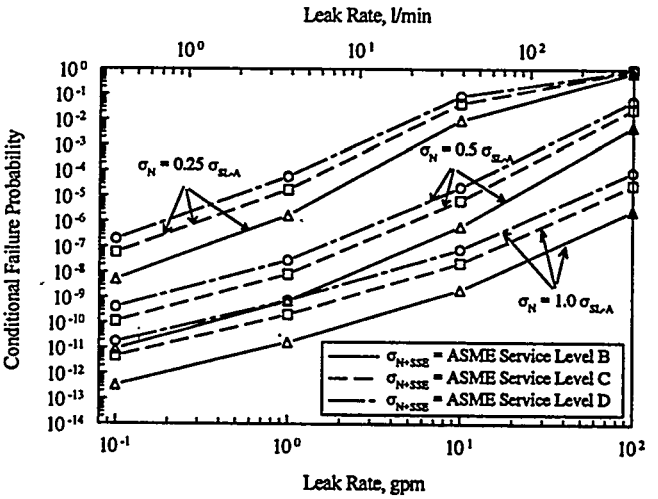

Figure 5 CPOF of PWR-2 for various pipe stresses

In general, the multi-dimensional integral in Equation 4 cannot be determined analytically. As an alternative, numerical integration can be performed; however, it becomes impractical and the computational effort becomes prohibitive when the dimension of X becomes greater than two and, in this case, one may have a maximum of nine dimensions according to Equation 3.

Several approximate methods exist for performing the multi-dimensional probability integration in Equation 4. Among them, First- and Second-Order Reliability Methods (FORM/SORM), Importance Sampling, Directional Simulation, Monte Carlo Simulation, and others can be applied to estimate P_F in Equation 4. For details of these methods, see Reference 2 and other references cited therein. In this study, SORM (Ref. 6) was used to compute the probability failure. In Reference 2, the probability estimates by SORM were validated against the results of Monte Carlo and Importance Sampling analyses. It was also found in that reference that SORM can calculate the failure probability of pipes with much less computational effort than that required by the Monte Carlo method. See Reference 2 for further details on the accuracy and computational efficiency of SORM.

Note that P_F is defined here as a conditional probability of failure. The principal conditions are that (1) the pipe is leaking with an LBB detectable flaw size and (2) an earthquake occurs with N+SSE stresses, resulting in an applied bending moment equal to M_{N+SSE}, also during leakage.

The Computer Codes PSQUIRT and PROLBB

PSQUIRT is a computer code that was developed during the Short Cracks in Piping and Piping Welds Program to estimate the probability density function of an LBB detectable flaw size. It is based on direct Monte Carlo simulation. PSQUIRT, which stands for Probabilistic Seepage Quantification of Upsets in Reactor Tubes, is a combination of three independent programs for conducting pre-processing of input, thermal-hydraulic and fracture-mechanics analyses, and post-processing of output. For further details, see References 2 and 7.

PROLBB, which is an acronym for PRObabilistic Leak-Before-Break, was also developed during the Short Cracks in Piping and Piping Welds Program to evaluate failure probability of flawed nuclear piping subjected to combined stresses due to tension and bending. The deterministic part of PROLBB is based on the LBB.ENG2 method (Ref. 2). The fracture-mechanics equations for this method, used to calculate the J-integral and its applications for computing maximum loads, were defined in Reference 2. The probabilistic part of PROLBB is based on (1) First-Order Reliability Method, (2) Second-Order Reliability Method, (3) Importance Sampling, and (4) Monte Carlo Simulation. Further details of PROLBB code can be obtained from Reference 2.

PIPING SYSTEMS FOR PROBABILISTIC LBB EVALUATIONS

The probabilistic model developed in Reference 2 was applied to various nuclear piping systems in BWR and PWR for calculating the conditional probability of failure. Pipe sizes were selected with large, intermediate, and small diameters typically used. Two pipes of each size were considered with austenitic and ferritic materials. The BWR piping systems included side riser, main steam, recirculation branch, feedwater, bypass, and reactor water clean-up lines. The PWR piping systems included main coolant, surge, feed-water, spray, and steam generator blowdown lines. Several cracking mechanisms, such as intergranular stress corro-sion cracking, corrosion fatigue, and thermal fatigue, were also considered. Crack location was defined in both a deterministic sense (either base metal or weld metal) and a probabilistic sense (random location). Table 1 shows the through-wall-cracked BWR and PWR piping systems which were originally considered in Reference 2. Some of these pipes were used for probabilistic pipe fracture evaluations in the present study.

PROBABILISTIC SENSITIVITY ANALYSES

A two-step procedure developed in Reference 2 was used for conducting the sensitivity analyses. First, for a given pipe with known material properties, loads, leak rate, and crack-morphology parameters, the mean and standard deviation of a leakage size flaw were calculated. In Reference 2, it was found that the flaw size with these distribution parameters would follow lognormal probability fairly well. Second, with the calculated flaw size and known material properties, the conditional probability of failure was calculated. The computer codes, PSQUIRT and PROLBB and their respective derivatives, developed for various required modifications, were used to calculate the flaw size and conditional failure probability, respectively.

The results of sensitivity analyses for each of the parameters considered in this study are given in the next few subsections. In determining the conditional probability of failure, individual sets of calculations were developed for a crack located either in the base metal or in the weld metal. A weighted average of these probabilities, based on the actual likelihood of cracks found in service, was developed to determine the conditional probability of failure for a randomly located crack (Ref. 2). Due to space limitations, only the results of conditional failure probability calculations with random crack locations are presented in this paper (except Figure 15).

Table 1 BWR and PWR piping systems for probabilistic fracture evaluations

Cases	Piping System	Nominal Diameter, mm (inches)	Thickness, mm (inches)	Base Metal	Weld[a] Metal	Assumed[b] Cracking Mechanism
		(a) Through-wall-cracked BWR Piping Systems				
BWR-1	Side Riser	711.2 (28)	35.8 (1.41)	TP304	SS Flux	IGSCC
BWR-2	Main Steam	711.2 (28)	35.8 (1.41)	A516 Gr70	CS Flux	Corrosion Fatigue
BWR-3	Recirculation Branch Line	457.2 (18)	23.9 (0.94)	TP304	SS Flux	IGSCC
BWR-4	Feedwater	457.2 (18)	39.4 (1.55)	A106B	CS Flux	Corrosion Fatigue
BWR-5	Bypass Line	101.6 (4)	8.51 (0.34)	TP304	SS Flux	IGSCC
BWR-6	Reactor Water Clean-up	101.6 (4)	8.51 (0.34)	A106B	CS Flux	Corrosion Fatigue
		(b) Through-wall-cracked PWR Piping Systems				
PWR-1	Main Coolant	812.8 (32)	76.2 (3.00)	CF8M	SS Flux	Thermal Fatigue
PWR-2	Main Coolant	812.8 (32)	76.2 (3.00)	A516 Gr70	CS Flux	Corrosion Fatigue
PWR-3	Surge Line	355.6 (14)	35.8 (1.41)	CF8M	SS Flux	Thermal Fatigue
PWR-4	Feedwater	355.6 (14)	35.8 (1.41)	A106B	CS Flux	Corrosion Fatigue
PWR-5	Spray Line	101.6 (4)	13.5 (0.53)	TP304	SS Flux	IGSCC
PWR-6	Steam Generator Blowdown Line	101.6 (4)	13.5 (0.53)	A106B	CS Flux	Corrosion Fatigue

(a) SS = stainless steel; CS = carbon steel; Flux = submerged arc weld (SAW) or shielded metal arc weld (SMAW)
(b) IGSCC = intergranular stress-corrosion cracking

Normal Operating Stresses

For piping systems to be evaluated, the normal operating stresses (σ_N) are needed to determine the crack size for a given leak rate. However, the actual normal operating stresses and their probabilities of occurring for all plants in the U.S. are difficult to quantify. To simplify this effort, it was assumed that the limits of ASME Section III Code stress level can be applied, even though actual stresses might be lower. Hence, several stress values equal to 25, 50, and 100 percent of the ASME Service Level A stress limit ($\sigma_{SL\text{-}A}$) were used. For Class 1 piping, the Service Level A limit is $1.5S_m$, where S_m is the material design stress intensity from ASME Section III, Appendix I (Ref. 5). The stresses were assumed to be deterministic.

Table 2 shows the calculated mean values of the leakage size flaws for pipes BWR-1, BWR-2, PWR-1, and PWR-2 using the PSQUIRT code. They were developed for various combinations of normal operating stresses and detectable leak rates. The results from Table 2 suggests that for a given leak rate the crack size increases very rapidly with the reduction of normal operating stresses. This can have a significant effect on the failure probability of pipes and is discussed in the next section.

Normal Plus Safe-Shutdown Earthquake Stresses

One of the most difficult aspects of this analysis was the selection of normal plus safe-shutdown earthquake stresses (σ_{N+SSE}) for application to a large numbers of piping systems and plant locations in the U.S. It was beyond the scope of this effort to analyze all plants and piping systems. Instead, the ASME Section III stress limits from the Service Levels B, C, and D were used in this study. According to the ASME Section III code, the Service Levels B, C, and D are defined as the lower values of $1.8S_m$ and $1.5S_y$, $2.25S_m$ and $1.8S_y$, and $3S_m$ and $2S_y$, respectively. The stresses under N+SSE condition were also assumed to be deterministic.

Figures 2 through 5 show the plots of the conditional failure probability of pipes BWR-1, BWR-2, PWR-1, and PWR-2 as a function of leak rate for various combinations of normal operating and N+SSE stresses. The results indicate that the failure probability increases when either the normal operating stress decreases or the N+SSE stress increases. However, the increment of conditional probability of failure is much higher due to the

Table 2 Mean crack length for various leak rates and normal operating stresses for a symmetrically centered crack with unrestrained pressure-induced bending

Leak Rate l/min (gpm)	Mean Crack Length, m			
	BWR-1	BWR-2	PWR-1	PWR-2
		(a) $\sigma_N/\sigma_{SL\text{-}A}$ = 0.25		
0.379 (0.1)	0.2232	0.1362	0.2306	0.1339
3.79 (1)	0.4408	0.2645	0.4078	0.2581
37.9 (10)	0.6843	0.4685	0.6479	0.4753
379 (100)	0.7651	0.7359	0.8849	0.7142
		(b) $\sigma_N/\sigma_{SL\text{-}A}$ = 0.50		
0.379 (0.1)	0.0740	0.0562	0.0518	0.0454
3.79 (1)	0.1790	0.1305	0.1158	0.1020
37.9 (10)	0.3210	0.2715	0.2520	0.2304
379 (100)	0.4520	0.5333	0.4729	0.4553
		(c) $\sigma_N/\sigma_{SL\text{-}A}$ = 1.0		
0.379 (0.1)	0.0195	0.0276	0.0188	0.0219
3.79 (1)	0.0459	0.0647	0.0436	0.0516
37.9 (10)	0.1010	0.1462	0.0988	0.1177
379 (100)	0.1300	0.3090	0.2225	0.2640

reduction of normal operating stresses. Hence, any uncertainty in the normal operating stresses will have relatively larger effects on the failure probability than that in the N+SSE stresses.

Off-Center Cracks

In conducting both leak-rate and flaw stability analyses, a postulated through-wall-crack size (leakage flaw) is often calculated based on its symmetric placement with respect to the bending plane of the pipe. This is usually justified with the reasoning that the tensile stress due to bending is largest at the center of this symmetric crack. However, fabrication imperfections will occur randomly around the pipe circumference. Additionally, during the normal operating condition of a plant, the stress component due to pressure is more significant than that due to bending. As such, the postulated leakage flaw may be off-centered and can thus be located anywhere around the pipe circumference.

In the past, the authors performed an analytical study to investigate the crack-opening characteristics of a pipe with an off-centered crack (Refs. 8 and 9). Methods were developed by both finite element and estimation analyses to predict the crack-opening area for an off-centered crack. The results from that study showed that the crack-opening area for a pipe with an off-centered crack can be determined by normal analysis procedures for a symmetrically centered crack by resolving the applied moment to the effective moment at the center of the off-centered crack and assuming an elliptical profile for the crack-opening shape. This was an important finding since for leak-rate calculations, accuracy in the prediction of crack-opening area is more significant than that of the entire crack-opening shape.

In this study, some pipe specific calculations were performed to determine the effects of off-center cracks on the leakage size flaw under normal operating conditions. Due to uncertainty, the angle of off-center, measured from a vertical axis of symmetry (of a pipe cross-section), was assumed to be a random variable with equal probability (uniform distribution) of occurrence in the range $[0,\pi/2]$. Due to off-center cracks, the crack-opening-area modules of the PSQUIRT code were appropriately modified according to the results obtained in Reference 8. To evaluate their effects on pipe fracture probability, it was, however, assumed that the crack was symmetrically centered during N+SSE condition. This was mainly due to the lack of current methods available to perform fracture-mechanics evaluations (e.g., calculating J-integral and the resulting load-carrying capacity) of flawed pipes with off-center cracks. Hence, the results of failure probability, which involved leak-rate analysis of off-center cracks, but flaw-stability analysis of symmetric cracks, should be interpreted carefully.

Table 3 shows the calculated mean values of leakage size flaw for BWR-1 and BWR-2 pipes for various leak rates and normal operating stresses when the crack is off-centered. The comparisons of these mean flaw sizes with those calculated for symmetric cracks from Table 2 indicate that an off-centered crack can become much longer than asymmetrically centered crack for a given leak rate detection. Correspondingly, the results of conditional failure probability calculations, shown in Figures 6 and 7 for BWR-1 and BWR-2 pipes, respectively, suggest that an off-centered crack can lead to a higher probability of failure for a given leak rate. This was demonstrated for both the austenitic (BWR-1) and ferritic (BWR-2) pipes.

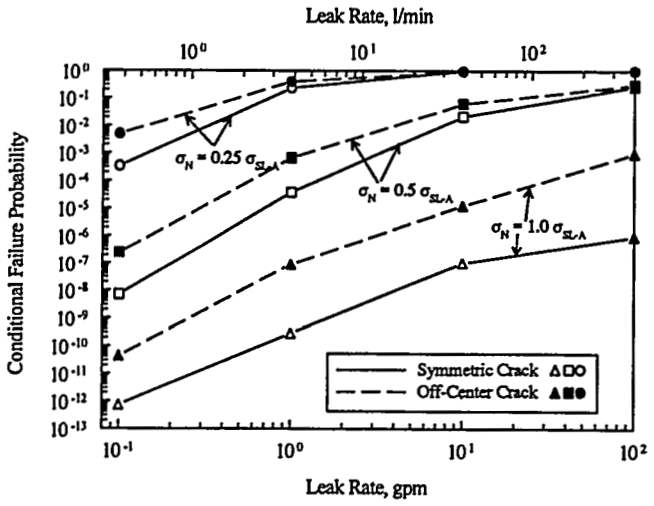

Figure 6 CPOF of BWR-1 for various crack orientations

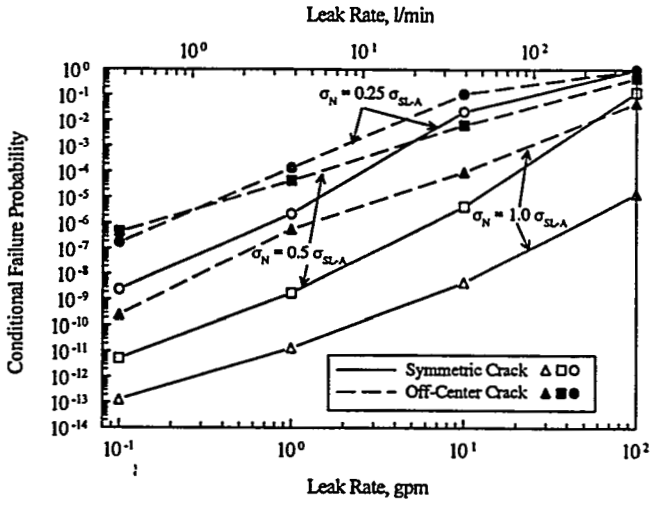

Figure 7 CPOF of BWR-2 for various crack orientations

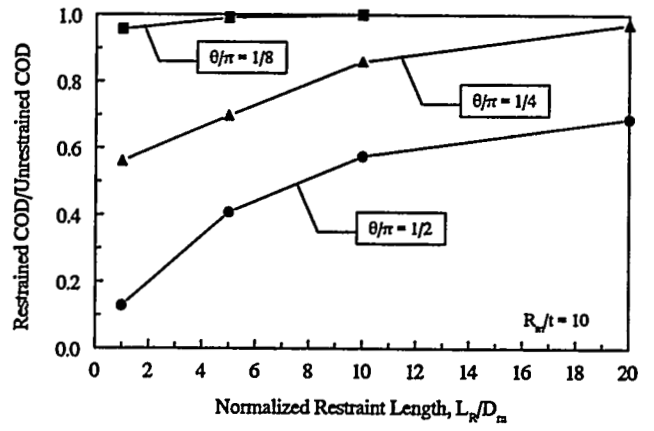

Figire 8 Normalized restrained COD versus restraint length

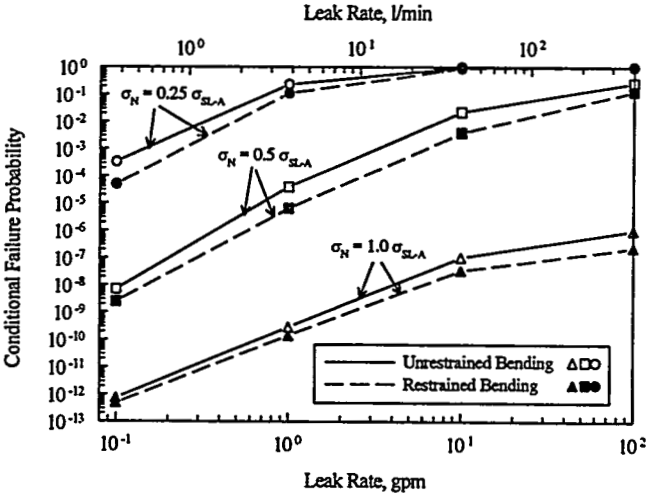

Figure 9 CPOF of BWR-1 for various restraint conditions

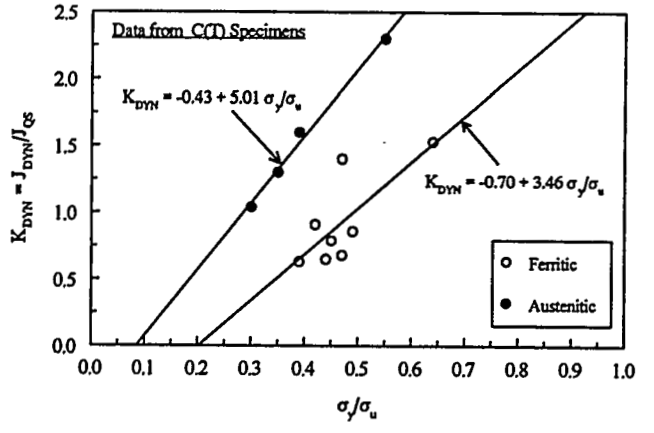

Figure 10 Fracture toughness correction due to dynamic load

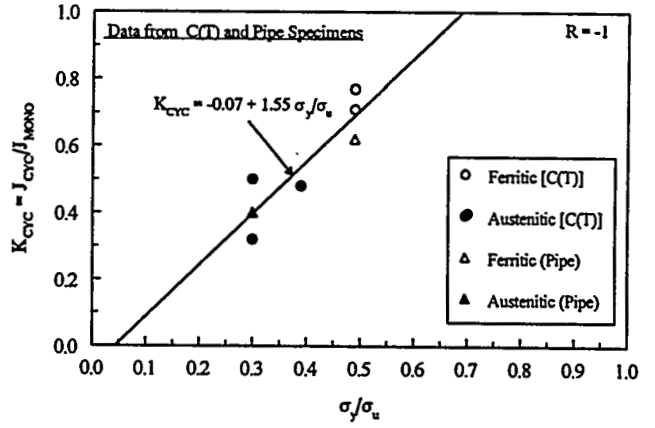

Figure 11 Fracture toughness correction due to cyclic load

Table 3 Mean Crack Length for various leak rates and normal operating stresses for an off-center cracks or restrained pressure-induced bending

Leak Rate l/min (gpm)	Mean Crack Length, m		
	Off-Center Cracks		Restrained Pressure-Induced Bending
	BWR-1	BWR-2	BWR-1
	(a) $\sigma_N/\sigma_{SL\text{-}A} = 0.25$		
0.379 (0.1)	0.2573	0.1525	0.2248
3.79 (1)	0.4865	0.2852	0.4577
37.9 (10)	0.7063	0.4879	0.7261
379 (100)	0.7924	0.7499	0.8267
	(b) $\sigma_N/\sigma_{SL\text{-}A} = 0.50$		
0.379 (0.1)	0.0911	0.0824	0.0745
3.79 (1)	0.2088	0.1730	0.1799
37.9 (10)	0.3530	0.3278	0.3244
379 (100)	0.4570	0.5771	0.4707
	(c) $\sigma_N/\sigma_{SL\text{-}A} = 1.0$		
0.379 (0.1)	0.0265	0.0433	0.0195
3.79 (1)	0.0620	0.0969	0.0461
37.9 (10)	0.1288	0.2024	0.1037
379 (100)	0.1858	0.4353	0.1300

Restraint of Pressure-Induced Bending

Current structural analyses for TWC pipes subjected to axial tension loads (generally pressure induced) or combined bending and tension loads assume that the pipe is free to rotate. The restraint of the rotation increases the failure stresses (Refs. 1, 2, 3, and 10), but can decrease the crack-opening at a given load. If the pipe system restrains the bending, for example from cracks being close to a nozzle or restraint from the rest of the piping system, then the leak rate will be less than the leak rate calculated by using analyses that assume that the pipe is free to rotate. This will cause the leakage crack size to be larger than that calculated by the current analysis methods for the same leak rate. However, for a pipe which restrains bending from pressure loads, its load-carrying capacity will also increase. It is interesting to see how this would counter the effects of crack-opening reduction. Some scoping calculations were performed to assess the magnitude of the trends.

In References 8 and 9, a numerical procedure, based on a linear-elastic finite element method, was developed by the authors to quantify the effects of restraint of induced bending due to pressure on the crack-opening displacement (COD) of pipes. From that study, Figure 8 shows the plots of a correction factor, defined as the ratio of restrained center COD to unrestrained center COD, as a function of normalized restraint length, defined as the ratio of restraint length (i.e., distance of the cracked plane from the restrained plane, L_R) to the mean pipe diameter (D_m), for a pipe with $R_m/t = 10$ with three different crack sizes, $\theta/\pi = 1/8$, 1/4, and 1/2. Using Figure 8, one should be able to determine the appropriate reduction of crack-opening area knowing the normalized restraint length and crack size. For an arbitrary crack size, the correction factor was determined by a linear interpolation of the curves shown in Figure 8. To determine the effects of pressure-induced bending, it was assumed that the crack was located very close to the restrained section. Hence, the normalized restraint length was chosen to be one. As before, the crack-opening-area modules of PSQUIRT were modified by applying the correction factor from Figure 8 on the crack-opening component due to the tension load (pressure-induced). For calculating the maximum load, the PROLBB code was modified to drop the pressure-induced bending component in evaluating the J-integral. See Reference 2 for explicit details of the J-integral equations.

Table 3 also shows the calculated mean values of leakage size flaw for BWR-1 pipe for various leak rates and normal operating stresses when the induced bending due to pressure load is restrained. In general, the length of flaw sizes increased due to restraint of induced bending when compared with the results of Table 2. But, no large differences were found between the flaw sizes obtained from the unrestrained and restrained conditions. This was mainly because the calculated COD due to the pressure was relatively small compared with that due to bending. Hence, the reduction of total COD due to pressure-induced bending from Figure 8 was not significantly large. The subsequent results of the probabilistic analysis, presented in Figures 9 and 10, however, showed that there was a marginal decrease of the conditional failure probability due to the increase of failure loads at restrained condition. Hence, for this particular pipe (BWR-1), the restraint of pressure-induced bending did not seriously affect the conditional probability of failure. Currently, work is in progress to examine the trends for

another small diameter pipe (BWR-6) and will be published in future. In this case the leaking crack length will be a much larger θ/π value, and the failure probabilities may be affected more.

Dynamic and Cyclic Loading Rates

For an LBB analysis, it is usually required to determine the fracture stability of a leakage size flaw under N+SSE stresses. This requires characterization of material properties from laboratory tests that can be used to calculate the load-carrying capacity of a cracked pipe. Typically, the strength (stress-strain curve) and fracture toughness (J-R curve) properties that are used for LBB analysis are obtained under quasi-static and monotonic loading condition. However, due to the dynamic and cyclic nature of the seismic ground motion, questions arise about the adequacy of quasi-static properties and their use for the prediction of failure probability as compared with that using more realistic dynamic and cyclic material properties of a pipe.

During the IPIRG-2 Program (Ref. 3), two correction factors, K_{DYN}, defined as the ratio of J-integral at crack initiation from dynamic load to that from quasi-static load, and K_{CYC}, defined as the ratio of J-integral at crack initiation from cyclic load to that from quasi-static load, were developed. From an experimental study on both compact-tension [C(T)] and pipe specimens, it was found that these correction factors are strongly correlated with the yield-to-ultimate strength ratio (σ_y/σ_u) of the pipe material. For example, Figures 10 and 11 show the plots of K_{DYN} and K_{CYC}, respectively, as a function of quasi-static yield-to-ultimate strength ratio, σ_y/σ_u, for both austenitic and ferritic materials obtained from both C(T) and pipe specimens. Although, the trend curves of K_{DYN} were different for austenitic and ferritic materials (Figure 10), no such difference was found for K_{CYC} (Figure 11). Hence, it was assumed that a single curve can be used for determining K_{CYC} regardless of the material type. This will be verified in the IPIRG-2 Program when further data become available.

From a linear regression analysis of the test data, several equations were developed for K_{DYN} and K_{CYC} in this study and are shown in Figures 10 and 11. Although the data and resulting equations were developed for J-integral at crack initiation, it was assumed that the similar correction factor could be applied for the whole quasi-static and monotonic J-R curves. With this assumption and using these multipliers (correction factors) to account for the dynamic and cyclic load effects on the fracture toughness properties, a number of probabilistic analyses were performed to calculate the conditional probability of failure for a stainless steel pipe (BWR-1) and two carbon steel pipes (BWR-2 and BWR-4). The conditional failure probability calculated using both quasi-static and dynamic and cyclic properties are shown in Figures 12, 13, and 14, respectively. The results suggest that the conditional failure probability will increase when the dynamic and cyclic loading effects are included. The magnitude of their resultant effect will, however, depend on the values of K_{DYN} and K_{CYC} which in turn are strongly dependent on the quasi-static yield-to-ultimate strength ratio. For the specific pipes, BWR-1, BWR-2, and BWR-4, analyzed in this study, the mean values of quasi-static σ_y/σ_u from Reference 2 were 0.35, 0.53, and 0.44 with the corresponding values of total correction factor, $K_{TOT} = K_{DYN} \times K_{CYC}$ being 0.63, 0.83, and 0.5, respectively. Since the value of K_{TOT} for the BWR-2 pipe was close to 1, the increase of failure probability for that pipe by accounting for dynamic and cyclic loads was not significant. In contrast, the above effects can be significant for BWR-1 and BWR-4 pipes for which cases K_{TOT} was significantly lower than 1.

If the BWR-2 pipe were made of A106B instead of A516 Gr70 material (see Table 1), then the value of K_{TOT} would be 0.5. In that case, the conditional failure probability accounting for dynamic and cyclic load effects, shown in Figure 15, would be much higher. (Note, the failure probabilities in Figure 15 were obtained for cracks in base metal only since weld metal tests are no progress at this time.) In summary, the dynamic and cyclic loading rate can affect the prediction of the conditional failure probability for both austenitic and ferritic pipes depending on the quasi-static yield-to-ultimate strength ratio of the material.

RELATIVE SENSITIVITY MEASURES

For determining the relative importance of the parameters considered in this study, a probability ratio, defined as the ratio of the conditional failure probability considering each parameter to the conditional failure probability of a baseline condition, was calculated. The baseline condition for this sensitivity analysis involved: (1) three different normal operating stresses as percentages of ASME service limits, e.g., $\sigma_N/\sigma_{SL\text{-}A} = 0.25$, 0.5, and 1 (2) ASME Service Level B stress limit as the N+SSE stress, (3) asymmetrically centered crack, (4) unrestrained pressure-induced bending, and (5) quasi-static and monotonic strength and fracture toughness properties. Most results for this baseline condition were originally developed in a previous study by the authors (Ref. 2).

Figures 16 and 17 show bar plots of the ratio of conditional failure probability for various parameters accounting for N+SSE stresses (ASME service levels C and D stress limits), dynamic and cyclic loading rates, restraint of pressure-induced bending (PIB), and off-centered cracks. Two pipes from Table 1, one a stainless steel pipe (BWR-1) and the other a carbon steel pipe (BWR-2), were analyzed to calculate the probability ratio when the leak rate was 3.79 l/min (1 gpm) and the crack was randomly located in either the base or weld metal of the pipe. The results are shown in Figures 16 and 17 for BWR-1 and BWR-2 pipes, respectively. One general trend from the results of both figures is that the N+SSE stress (particularly, the ASME Service Level D stress), dynamic and cyclic loading rate, and an off-centered crack can increase the conditional failure probability significantly when compared with the failure probability calculated under the baseline condition. The

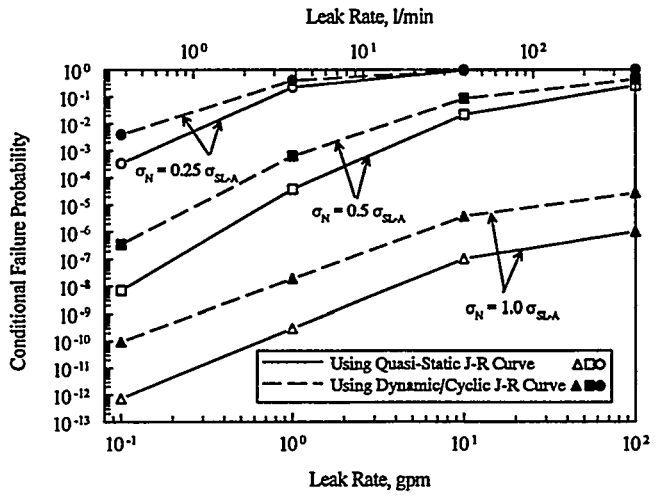

Figure 12 CPOF of BWR-1 for dynamic and cyclic loads

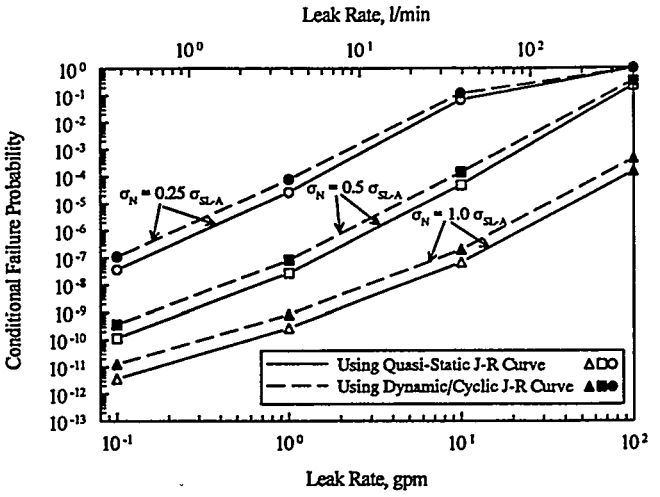

Figure 13 CPOF of BWR-2 for dynamic and cyclic loads

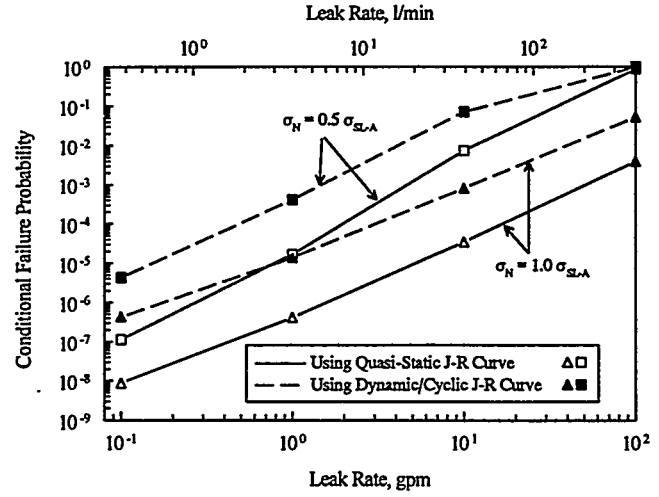

Figure 14 CPOF of BWR-4 for dynamic and cyclic loads

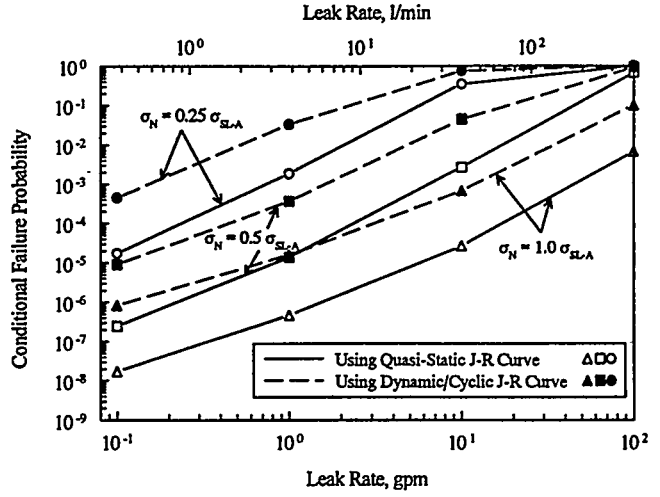

Figure 15 CPOF of BWR-2 using A106B material propertie

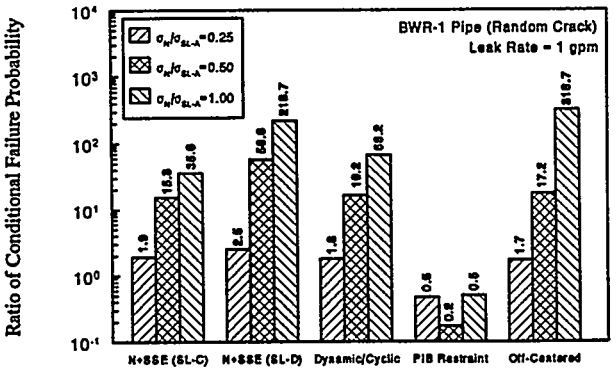

Figure 16 Ratio of CPOF for BWR-1 pipe (stainless steel)

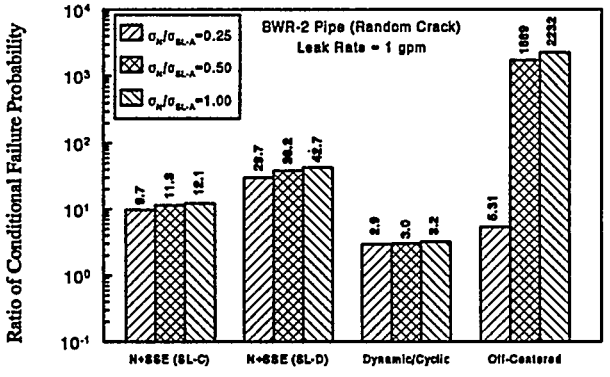

Figure 17 Ratio of CPOF for BWR-2 pipe (carbon steel)

effect due to restraint of pressure-induced bending was marginal. More specifics on the relative significance of these parameters depend on the piping material and the intensity of the normal operating stress.

Table 4 shows the relative ranking of these parameters for various conditions. The parameter which attributed to a largest probability ratio was given a ranking value of 1 and so on. Note that the ranking values were obtained for a stainless steel pipe (BWR-1) and a carbon steel pipe (BWR-2). Further studies are needed to examine these ranking values and determine if they would agree with the results from other piping systems.

Table 4 Relative ranking of the parameters based on the probability ratio of CPOF

Parameter	Ranking Value		
	$\sigma_N/\sigma_{SL\text{-}A} = 0.25$	$\sigma_N/\sigma_{SL\text{-}A} = 0.50$	$\sigma_N/\sigma_{SL\text{-}A} = 1.0$
	(a) Stainless Steel Pipe (BWR-1)		
N+SSE Stress (Service Level C)	2	4	4
N+SSE Stress (Service Level D)	1	1	2
Dynamic and Cyclic Load	3	3	3
Restraint of Pressure-Induced Bending	5	5	5
Off-Centered Crack	4	2	1
	(b) Carbon Steel Pipe (BWR-2)		
N+SSE Stress (Service Level C)	2	3	3
N+SSE Stress (Service Level D)	1	2	2
Dynamic and Cyclic Load	4	4	4
Off-Centered Crack	3	1	1

SUMMARY AND CONCLUSIONS

This paper presents new results from a probabilistic study to evaluate the effects of normal operating stresses, increased N+SSE stresses addressing proposed changes to the ASME Section III design stresses, off-centered leaking cracks, restraint of pressure-induced bending, and dynamic and cyclic loading rate on the conditional failure probability of pipes. Numerical examples are provided showing the effects of the above parameters for several nuclear piping systems in BWR and PWR environments. The key results were:

- The leakage size flaw strongly depends on the magnitude of normal operating stresses in a pipe for any given leak rate. Any uncertainty in the normal operating stresses can lead to large variations in the predicted conditional probability of failure. For a fixed normal operating stress, any increase in the N+SSE stress from ASME service level B to ASME service levels C or D will also increase the conditional failure probability regardless of the leak-rate detection.

- When a crack is off-centered or the pressure-induced bending is restrained, the length of a leakage size flaw will, in general, be increased for a given leak rate. A relative comparison of their separate effects indicate that an off-center crack is likely to increase the crack length much more significantly than the case when a pipe restrains pressure-induced bending. In consequence, for the off-center cracks, the conditional failure probability increased significantly. However, due to a slight increase in the failure load, the estimated conditional failure probability for a restrained condition was slightly lower than that for an unrestrained condition. Additional calculations to assess the affect of the restraint of pressure-induced bending are in the process of being conducted for small diameter pipe.

- The conditional failure probability will increase when the dynamic and cyclic loading effects are included via reduced fracture toughness. The magnitude of their resultant effect will, however, depend on the values of reduction factors (K_{DYN} and K_{CYC}), which in turn are strongly dependent on the quasi-static yield-to-ultimate strength ratio. Based on the results of some specific pipes, the dynamic and cyclic loading rate can affect the prediction of the conditional failure probability for both austenitic and ferritic pipes.

- The calculations of a probability ratio, defined as the ratio of the conditional failure probability considering each parameter to the conditional failure probability of a baseline condition, indicate that for a given normal operating stress level, the N+SSE stress, dynamic and cyclic loading rate, and an off-centered crack can significantly increase the conditional failure, while the effects of pressure-induced bending were marginal.

ACKNOWLEDGEMENTS

This research was sponsored by the IPIRG-2 program, which is an international group program consisting of 22 international organizations from 15 countries that was coordinated by the USNRC's Office of Research, Electrical, Materials, and Mechanical Engineering Branch under Contract No. NRC-04-91-063 to Battelle. The authors would like to thank Mr. Michael Mayfield of USNRC for his encouragement and support of this effort. The support and guidance by the IPIRG-2 Technical Advisory Group are sincerely appreciated.

REFERENCES

1. Wilkowski, G. M., and others, "Short Cracks in Piping and Piping Welds," Semiannual reports by Battelle, NUREG/CR-4599, Vols. 1 to 4, Nos. 1 and 2, U.S. Nuclear Regulatory Commission, Washington, D.C., May 1991 to January 1995.

2. Rahman, S., Ghadiali, N., Paul, D., and Wilkowski, G., "Probabilistic Pipe Fracture Evaluations for Leak-Rate-Detection Applications," NUREG/CR-6004, U.S. Nuclear Regulatory Commission, Washington, D.C., April 1995.

3. Hopper, A., Mayfield, M., Olson, R., Scott, P., and Wilkowski, G., "Overview of the IPIRG-2 Program - Seismic Loaded Cracked Pipe System Experiments," *13th International Conference on Structural Mechanics in Reactor Technology*, Division F, Paper F12-1, August 1995.

4. "Report to the U.S. Nuclear Regulatory Commission Piping Review Committee," Prepared by the Pipe Break Task Group, NUREG/CR-1061, Vol. 3, U.S. Nuclear Regulatory Commission, Washington, D.C., November 1984.

5. 1989 Addenda ASME Boiler & Pressure Vessel Code - Section III, Article NB-3652.

6. Madsen, H. O., Krenk, S., and Lind, N. C., Methods of Structural Safety, Prentice-Hall, Inc., Englewood Cliffs, New Jersey, 1986.

7. Rahman, S., Ghadiali, N., Wilkowski, and Paul, D., "A Computer Model for Probabilistic Leak-Rate Analysis of Nuclear Piping and Piping Welds," Proceedings of *ASME/JSME 1995 Pressure Vessel and Piping Conference*, Honolulu, Hawaii, June 1995.

8. Rahman, S., Brust, F., Ghadiali, N., Choi, Y., Krishnaswamy, P., Moberg, F., Brickstad, B., Wilkowski, G., "Refinement and Evaluation of Crack-Opening-Area Analyses for Circumferential Through-Wall Cracks in Pipes," NUREG/CR-6300, U.S. Nuclear Regulatory Commission, Washington, D.C., April 1995.

9. Rahman, S., Ghadiali, N., Wilkowski, G., and Bonora, N., "Effects of Off-Centered Crack and Restraint of Induced Bending on the Crack-Opening-Area Analysis of Pipes," Proceedings of *ASME/JSME 1995 Pressure Vessel and Piping Conference*, Honolulu, Hawaii, June 1995.

10. Wilkowski, G. M. and others, "Degraded Piping Program - Phase II," Final and Semiannual Reports, NUREG/CR-4082, Vols. 1 to 8, U.S. Nuclear Regulatory Commission, Washington, D.C., 1985-1989.

THE CONCEPTS OF LEAK BEFORE BREAK AND ABSOLUTE RELIABILITY OF NPP EQUIPMENT AND PIPING

By: A.F.Getman, O.V.Komarov (VNIIAES), Yu.G.Dragunov, L.M.Sokov (OKB Gidropress), A.V.Sudakov (CKTI), V.M.Markochev, V.Yu.Goltsev (MIFI), E.I.Mamaeva (CNIITMASH), V.G.Vassilyev (Rosenergoatom), N.I.Karpunin (Research Centre of GAN, Russia)

1. Introduction. Review of some approaches to assurance of safe operation of NPP equipment and piping

The first generation nuclear power reactors were designed assuming a high reliability of plant equipment and piping (E&P). The assumption was based on relatively stringent requirements to the quality of design and manufacturing.

Later on, the requirements to the quality of nuclear-grade E&P design and manufacturing became even more stringent. However, in the frame of the NPP safety concept appeared a notion of maximum design basis accident (MDBA) that is based on the assumption of a possible instantaneous double-ended (i.e. across the whole pipeline section) break of the main reactor coolant pipeline (RCP). (OPB 82 /1/). The MDBA concept merited from the fact that it provided designers with a definite and clear basis for designing NPP safety systems. A shortfall of the MDBA concept is that it creates psychological prerequisites for relaxing the quality requirements to plant E&P. It could adversely affect (and it did!) the state of the third safety barrier, i.e. primary circuit E&P of the reactor. For instance, main reactor coolant pipelines (RCP) of a number of NPPs have been designed in such a way that makes some of their components inaccessible for in-service inspections.

As applied fracture mechanics came into being, the "leak before break" (LBB) concept was formulated /2/. This concept is based on the requirement that a correlation between the crack resistance capability and loads on a pressure vessel should be sufficient enough to allow for existence of a stable through-wall defect without instantaneous breakage of the structure. That means an instantaneous full break of a structure should be preceded by a leakage that signals termination of further operation.

The success of fracture mechanics enabled to put the LBB concept into practice. This concept is also reflected in regulatory documents of a number of countries (for instance /3, 4, etc./).

Merits of the LBB concept are obvious. Its implementation allows to significantly enhance the operational safety of NPPs. However, the concept is not absolutely flawless.

First and foremost, the LBB concept has a negative psychological impact on designers, manufacturers and operators that does not contribute to maximal concentration of efforts on achieving high quality of plant E&P. Apart from that, our review has shown that the LBB concept in the form it exists now in foreign countries (e.g. /3, 4, etc.) cannot fully preclude the likelihood of instantaneous full breakage of pressure vessels without an initial leak.

In fact, according to the LBB concept as stated in /3, 4, etc./, it is necessary to prove the possibility of stable through-wall cracks of a certain length $\leq 2C'_{cr}$ (if $2a'=S$) (See Figure 1). In doing so, critical cracks with the size of $2a'' < S$ and $C''_{cr} > C'$ are not considered. However, operating practices and our review have demonstrated that cracks of the second kind can exist with an ultimate, and relatively high, probability. For instance, according to /5/, at a French NPP a circumferential crack, about 0.9S deep, was discovered on a primary coolant pipeline (See Figure 2). That means the nuclear power plant was really close to an instantaneous double-ended large-bore pipe break not preceded by any initial leakage.

The above mentioned deficiencies can be overcome by developing a new concept of assuring safe operation of plant E&P, that can be called the Concept of E&P Absolute Reliability (the AR concept). The absolute reliability of a pipeline or component is understood as the level of reliability when the probability of instantaneous double-ended break is near zero, or is less than 10^{-6}.

There is no contradiction between the LBB and AR concepts. Moreover, studies and activities required for practical application of the LBB concept should be a part of the work on the AR concept implementation.

The possibility to apply the AR concept was for the first time demonstrated on the basis of results obtained by VNIIAES jointly with the Russian lead organizations under the programs of E&P reliability studies for RBMK and VVER type reactors, as well as the LBB applicability studies for VVER-440 reactors.

Described below are basic methodological principles, methods and approaches that have been developed in the framework of reliability and applicability studies of the LBB concept and provide the basis for implementation of the AR concept.

2. Methodological Basis for the AR Concept

Implementation of the AR concept is aimed at achieving a high level of E&P reliability on the criterion of resistance against an instantaneous double-ended break or an instantaneous leak of unacceptable rate.

Activities and studies are organized following a systematic approach and systems methodology as applied to the reliability of plant E&P that are described in a number of publications /6, 8, etc./.One of the basic notions of the systems methodology is the "Metal-NPP" system, a schematic of which is shown in Figure 3 /6/.

The methods and techniques of the AR concept have been developed as applicable to nuclear power plants already designed and in operation. This fact determines the scope of possible activities under the existing reliability assurance system (See figure 4) /9/. Tables 1 and 2 illustrate differences in the scope of work for operating and newly designed NPPs.

The key phases of studies aimed at determining applicability of the LBB and AR concepts for the operating NPPs are as follows:

1. Proving reference reliability.
2. Proving possible states with a stable leak.
3. Evaluation of probable and low probable (~ 10^{-4} - 10^{-6}) events that may result in full break.
4. Development and justification of engineering actions to assure an acceptable reliability level.

The scope of activities related to the proof of reference reliability includes the following:

1. Check of the design and architect-engineering quality.
   - 1.1. Selection of geometry.
   - 1.2. Selection of material.
   - 1.3. Lifetime and strength justification.
2. Check of the manufacturing and installation quality.
   - 2.1. Metallurgy processes of categories 1 and 2.
   - 2.2. Welding.

2.3. Evaluation of the following:

- chemical composition
- mechanical properties
- micro- and macrostructure
- geometry

3. Review of the plant operations quality.

3.1. Operating modes.

3.2. Maintenance.

3.3. Inspection.

4. Studies of the actual status of metal and piping.

4.1. Degradation and ageing.

4.2. Regimes and stresses.

4.3. Residual lifetime.

4.4. Defects.

4.5. Corrosion.

An assessment of the actual E&P status and a prediction of the residual lifetime can be performed under the framework of the overall in-service inspection system, a block diagram of which is given in Figure 5 /10, 11/.

The proof of a possibility of stable through-wall defects (leaks) and the analysis of critical sizes of defects, their kinetics and E&P crack resistance capability as a whole are carried out in line with regulatory methods approved by the GOSATOMNADZOR of the Russian Federation ("Methods of estimating acceptable defects in operation". NIKIET, VNIIAES, 1989; "Methods of piping analyses under the LBB concept", OKB Gidropress, NIKIET, 1993).

The publications /12, 13/ can give an idea of the approaches used in this case.

Probable and low probable events are analyzed in accordance with the probabilistic method of estimating the strength and residual lifetime of the E&P with crack-type defects, taking into account statistic nature of defects, strength characteristics and loads /14, 15/.

Engineering measures aimed at improving reliability should be developed under the framework of the system for E&P reliability assurance during plant operation (See Figure 4). In doing so, the most effective measures are related to

either better quality of non-destructive testing or introduction of a special regime of hydraulic tests by excessive pressure (See figure 6).

3. Examples of Achieving Absolute Reliability

Figure 7 presents the results of quantitative reliability assessment of the main reactor coolant pipeline (RCP) under the normal operation modes of a VVER-440 reactor, depending on the quality of non-destructive testing (NDT) and hydraulic tests.

As can be seen from Figure 7, an advanced NDT methodology enables to achieve the RCP reliability that is markedly higher than $(1-10^{-6})$ 1/reactor per year.

Following an excessive pressure hydraulic test, the probability of RCP break equals zero for more than two years.

Thus, the Absolute Reliability Concept can be practically applied to the operating nuclear power plants. The AR concept is a logical evolution of the existing NPP safety concepts (See Figure 8).

Conclusions:

1. Implementation of the LBB concept allows to enhance the nuclear power plant safety. The LBB concept should be further developed to overcome a number of deficiencies.

2. Evolution of the LBB concept and studies in the area of plant equipment and piping reliability make it possible to formulate the concept of absolute reliability of plant E&P.

3. The possibility of practical implementation of the AR concept at the operating nuclear power plants has been demonstrated.

Schematic of Two Types of Cracks of Critical Size

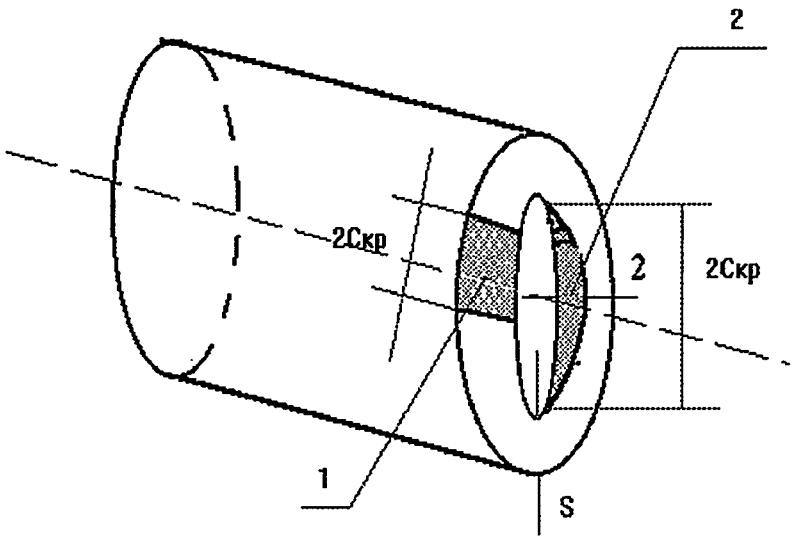

1- through-wall crack with a size of
$2a' = S$; $2C'_{kp.}$
2- non-through-wall crack with a size of
$2a'' < S$; $2C''_{kp.} > 2C'$.
Fig.1

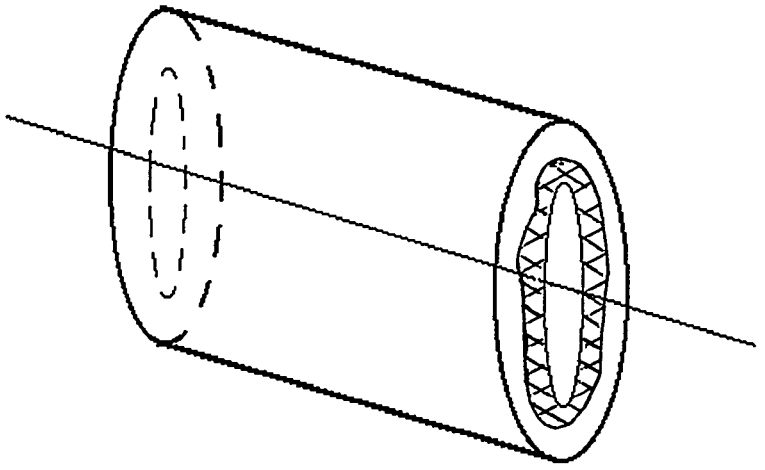

Fig. 2. Schematic of a circumferential crack with the depth of up to 0.9 of the wall thickness

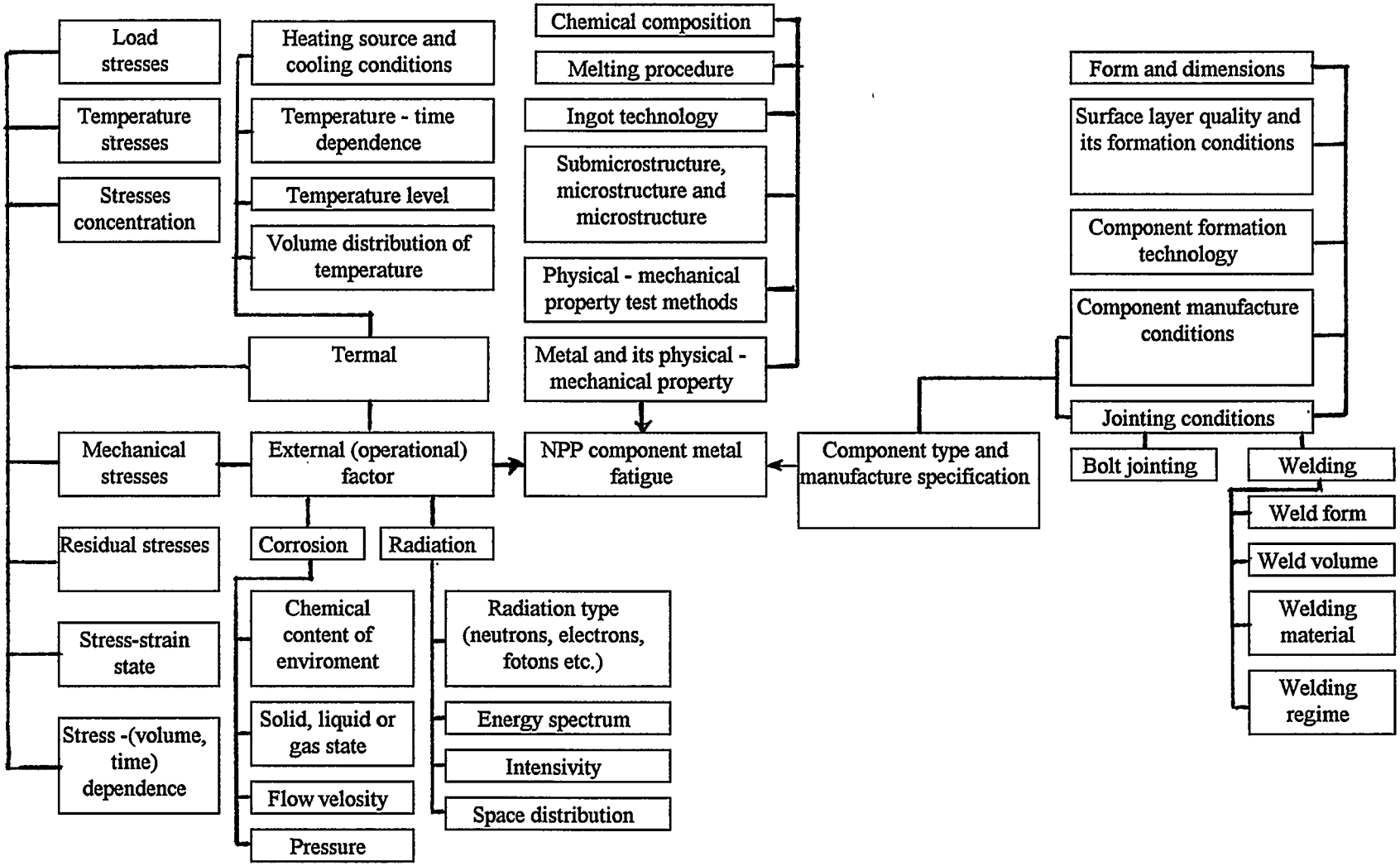

Fig. 3 Main factors influanced to strength of NPP reactor component metal

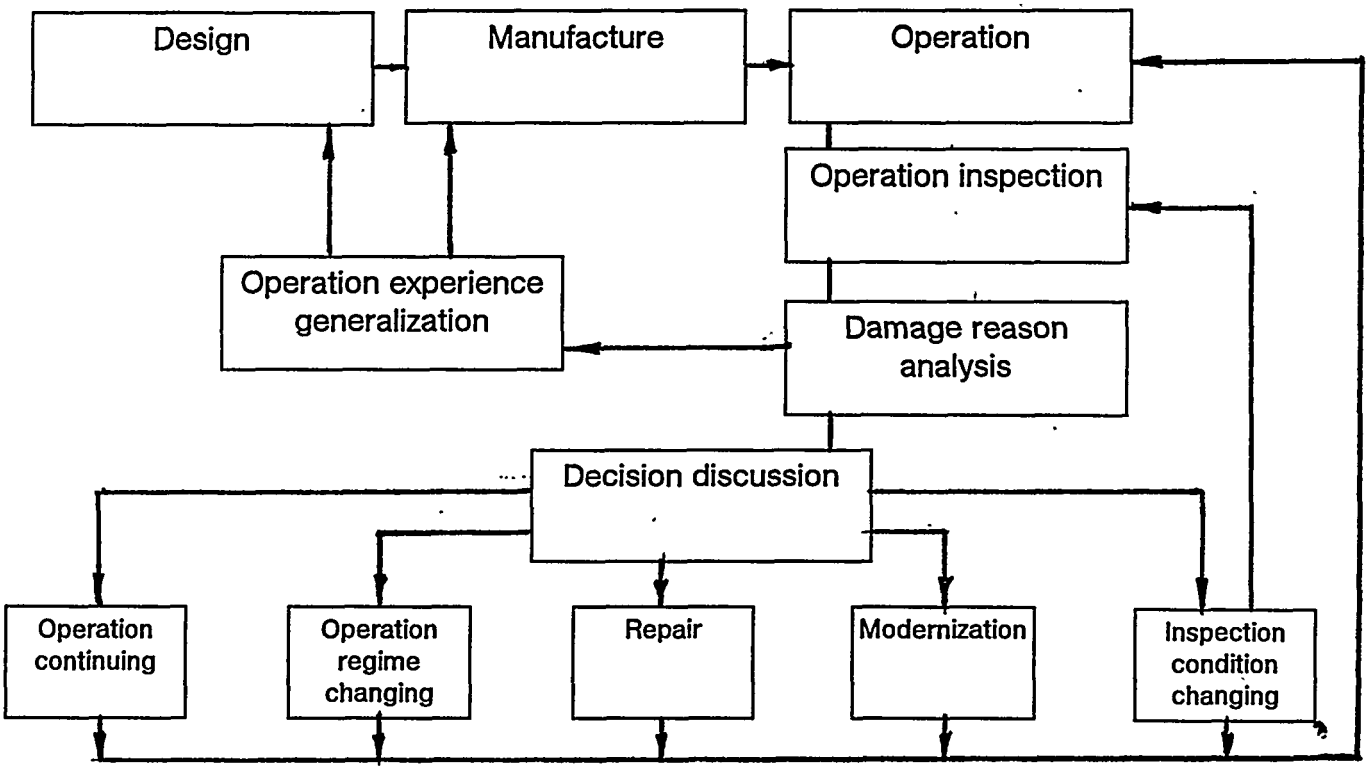

Fig. 4. Scheme of reliability insurance system while operation

Fig. 5. The schematic of NPP equipment metal operational control system

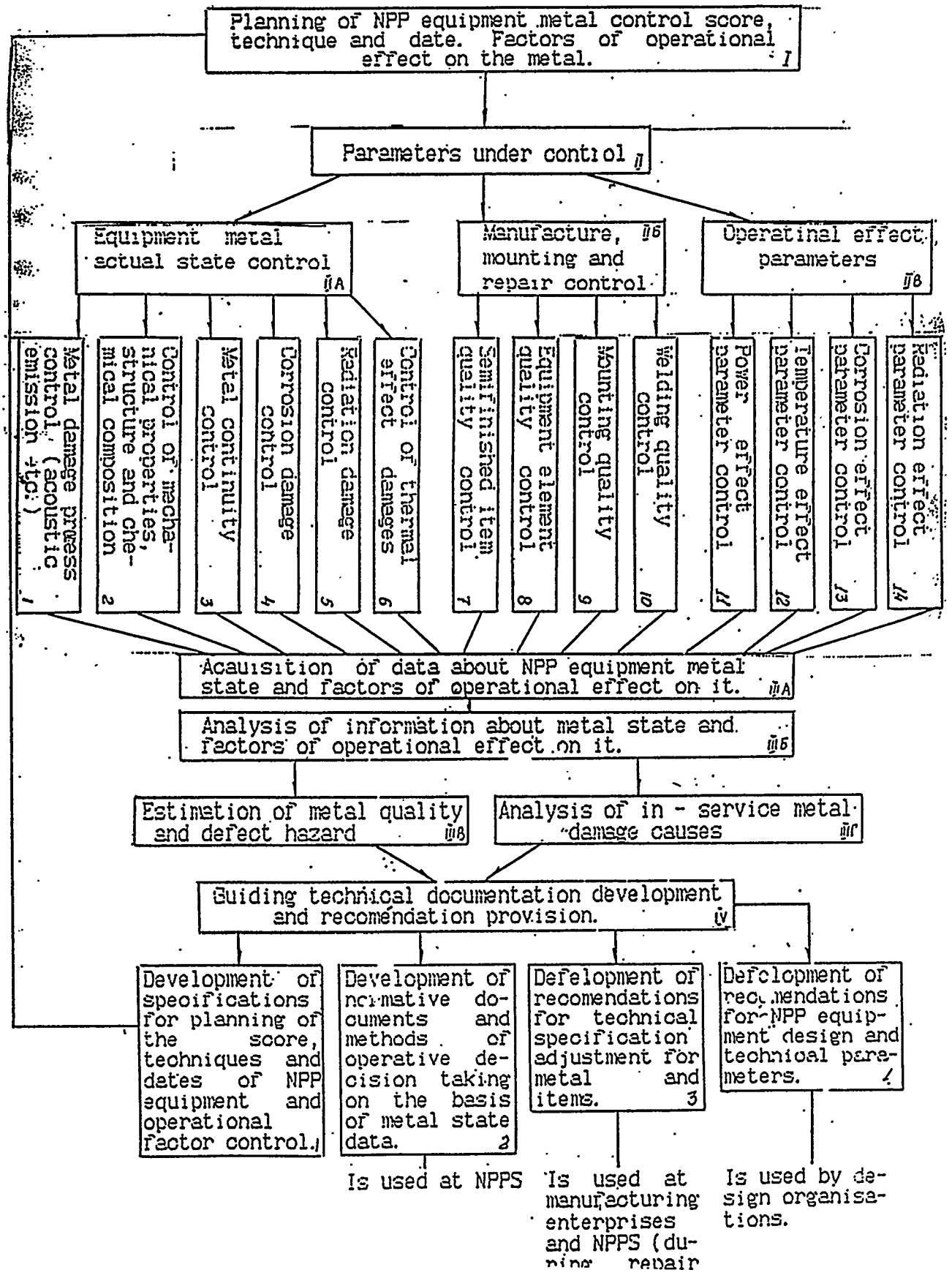

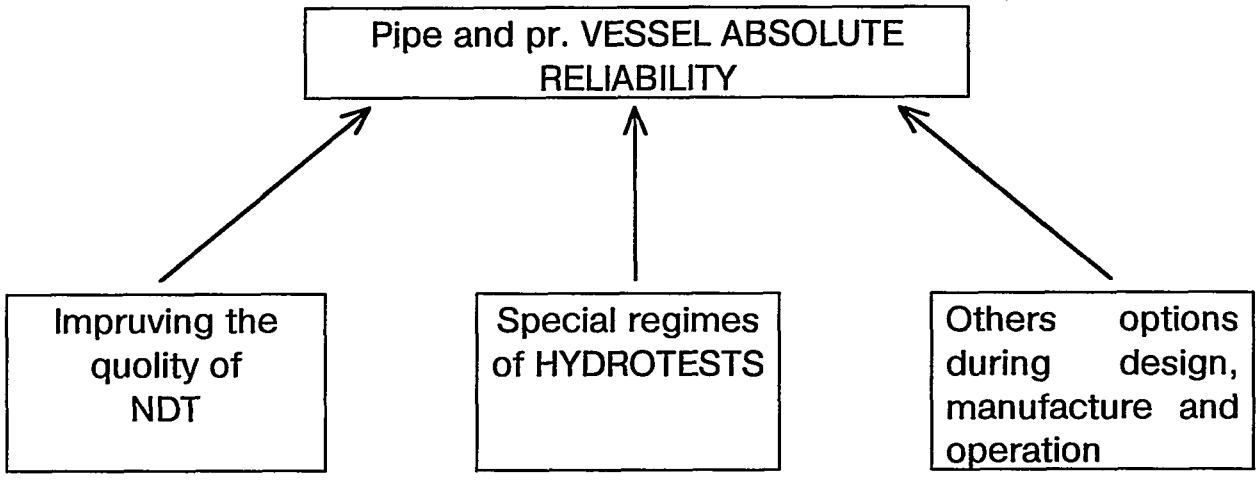
Pipe and pr. VESSEL ABSOLUTE RELIABILITY
Impruving the quolity of NDT
Special regimes of HYDROTESTS
Others options during design, manufacture and operation

Pic. 6.

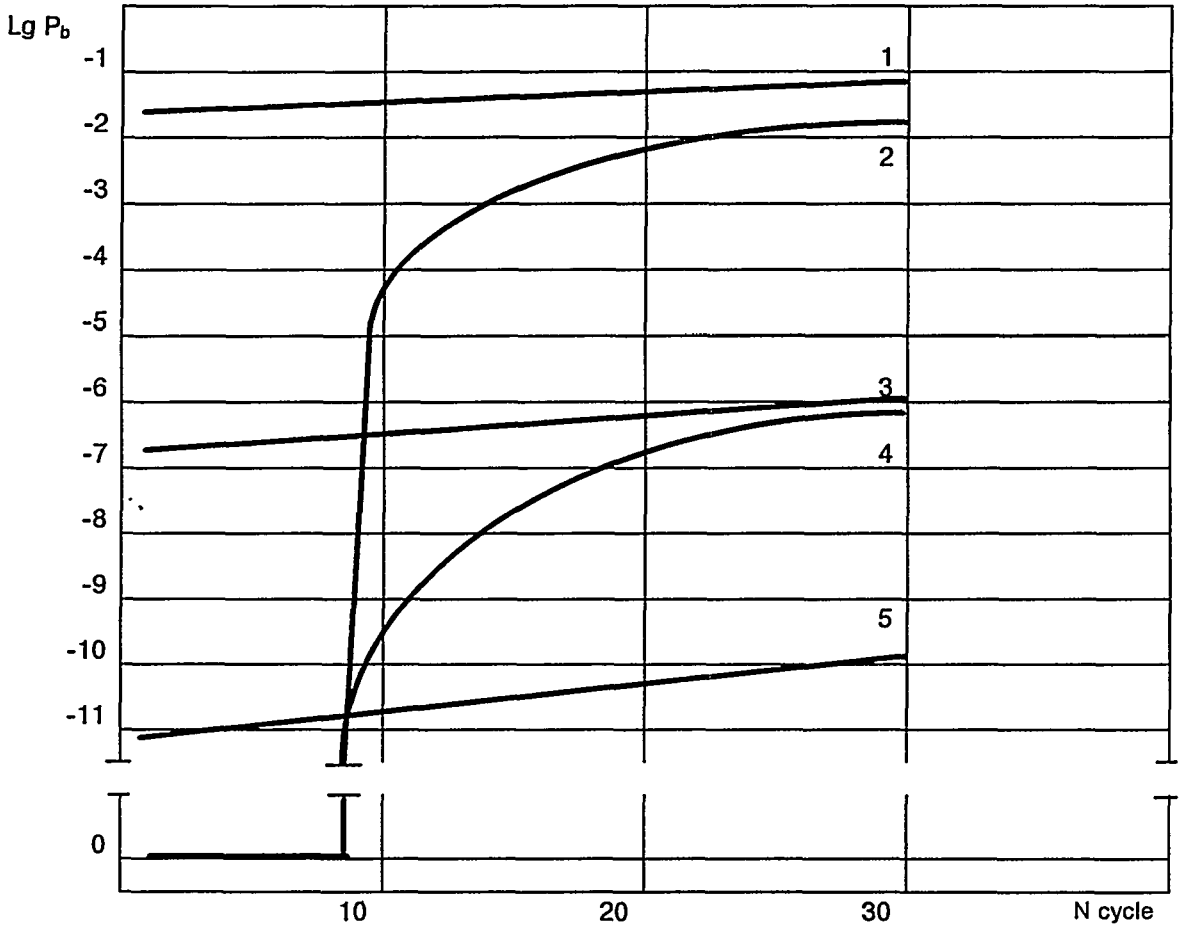

Fig. 7. Probability of pipe break depending on the number of loading cycles

1 - FD and HT not performed
2 - FD not performed, HT was performed
3 - FD was performed, HT not performed
4 - FD and HT not performed.
5 - FD performed with improved technique
HT not performed.
(FD - flaw detection ; HT- hydro-testing)

THE SCHEME OF SAFE RELIABILITY OF NPP EQUIPMENT DEVELOPMENT

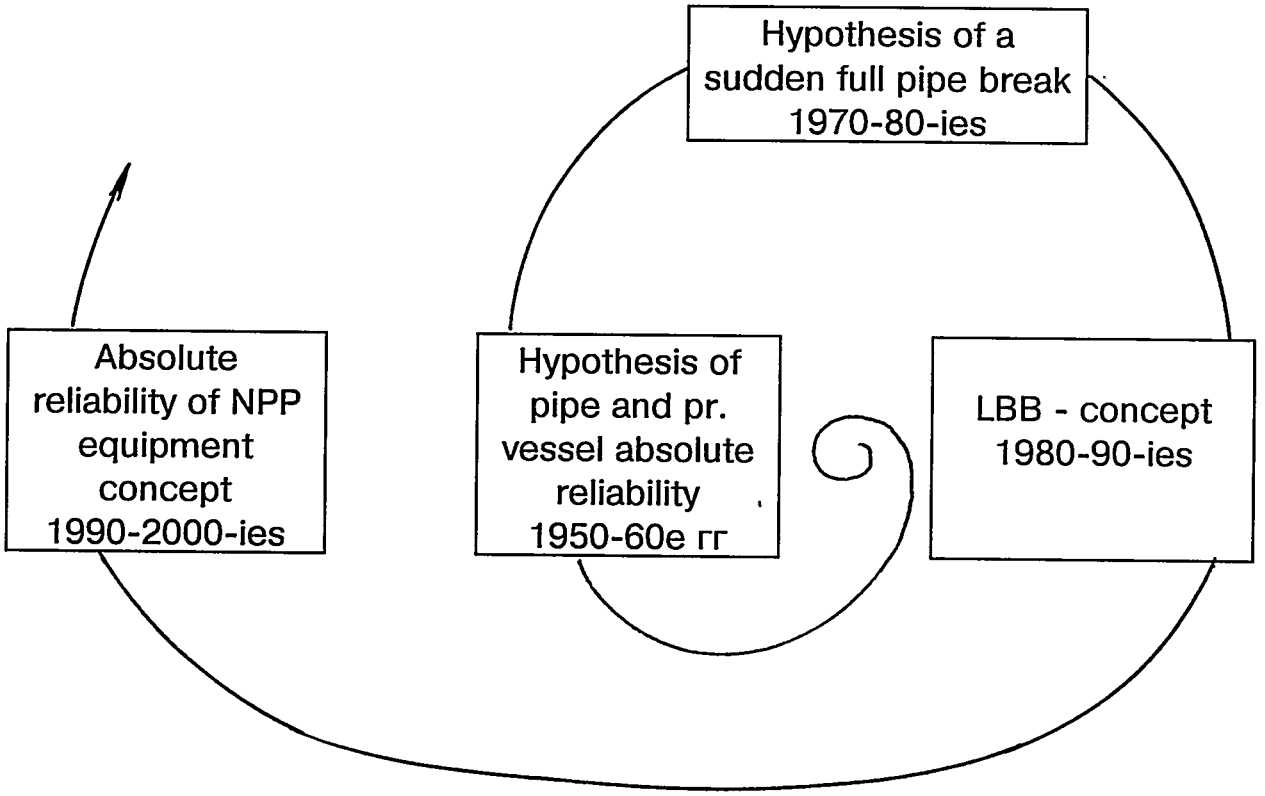

Pic. 8.

Table 1.

IMPLEMENTATION OF LBB SAFETY CONCEPT AT THE DESIGN STAGE

1.	Selection of structural material
2.	Selection of configuration
3.	Selection of operation regime
4.	Selection of manufacturing and mounting process
5.	Selection of in-service maintenance technology

Table 2.

IMPLEMENTATION OF LBB CONCEPT AT THE OPERATION STAGE

1.	Restriction (if necessary) of operation regimes
2.	Backfitting (if necessary) or special technology of preventive-maintenance work
3.	Special technology of flaw detection
4.	Special technology of hydraulic tests
5.	Special technology of leak monitoring

ЛИТЕРАТУРА

1. Общие положения обеспечения безопасности АЭС (ОПБ-82). 1982г. Металлургиздат.

2. Brock D. Fracture mechanic. Brussel. 1975г.

3. US NRC Standart Review Plan, 3.63 Leak Before Break Evaluation Procedures, Wachington DC, 1986.

4. Guidance for The application of the leak before break concept, JAEA, November, 1994.

5. Гетман А.Ф. Обеспечение прочности и надежности оборудования АЭС на основе системного подхода. В кн: Обеспечение надежности АЭС. М., Энергоатомиздат, 1989 г.

6. Гетман А.Ф. Некоторые вопросы исследования конструкционной прочности элементов оборудования АЭС с использованием системного подхода. Сообщение 1. Систематизация объекта исследования. Ж: Проблемы прочности, 1981, N1,111-115.

7. Гетман А.Ф. Некоторые вопросы исследования конструкционной прочности элементов оборудования АЭС. Сообщение 2. Ж: Проблемы прочности, 1981, N1, 71-75.

8. Гетман А.Ф. Некоторые вопросы исследования конструкционной прочности элементов оборудования АЭС. Сообщение 3. Ж: Проблемы прочности, 1981, N1, 75-76.

9. Гетман А.Ф. Системный метод обеспечения прочности оборудования АЭС. В кн: Надежность и долговечность элементов конструкций и оборудования. Выпуск 10. 1986г.

10. Абрамович М.Д., Гетман А.Ф. О комплексной системе эксплуатационного контроля металла оборудования АЭС. В кн: Атомные электростанции. М., Энергоиздат. Вып. 4, 1981 г.

11. Getman A.F. Primary Circuit Metal State With Regard to NPP Lifetime Extension. Journal of Pressure Vessel Technologu 1993, Vol. 115/85.

12. Getman A., Judin L., Babkin B. In-Service Determination of Acceptable Defect Sizes in VVER-1000 Reactor Vessel Metal. Jnt. J. Pres. Ves and Piping. 48 (1991), 253-261.

13. Ривкин Е.Ю., Гетман А.Ф. Методика оценки допустимых дефектов в эксплуатации. В кн: Новости МХО Интератомэнерго. 1989г.

14. Гетман А.Ф., Бабкин Л.Б., Зубов В.Ю., Методика и некоторые результаты по оценке вероятности разрушения трубопроводов Ду-500 АЭС с ВВЭР-440. В кн: Надежность трубопроводов и сосудов высокого давления АЭС. Обнинск. 1989г.

POSTERS

Approach of Czech regulatory body to LBB.

Petr Tendera
State Office for Nuclear Safety (SONS), Prague

At present there are two NPPs equipped with PWR units in Czech Republic . The Dukovany NPP is about ten years in operation (four units 440 MW - WWER model 213) and Temelin NPP is under construction (two units 1000 MW - WWER model 320). Both NPPs were built to Soviet design and according to Soviet regulations and standards but most of equipment for primary circuits was supplied by home manufactureres.

The objective of the Czech LBB programme is to prove the LBB status of the primary piping systems of these NPPs and the LBB concept is a part of strategy to meet western style safety standards. The reason for the Czech LBB project is a lack of some standard safety facilities, too.

For both Dukovany and Temelin NPPs a full LBB analysis should be carried out. The application of LBB to the piping system should be also a cost effective means to avoid installations of pipe whip restraints and jet shields.

The Czech regulatory body issued non-mandatory requirement „ Leak Before Break" which is in compliance with national legal documents and which is based on the US NRC Regulatory Procedures and US standards (ASME CODE, ANSI). The requirement has been published in the document „Safety of Nuclear Facilities" No 1/1991 as „Requirements on the Content and Format of Safety Reports and their Supplements" and consist of two parts

- procedure for obtaining proof of evidence „Leak Before Break"
- leak detection systems for the pressurized reactor primary circuit .

At present some changes concerning both parts of the above document will be introduced. The reasons for this modifications will be presented.

LBB Research Status in China

Wei J.

Nuclear Safety Centre - People's Republic of China

NOT RECEIVED

THE LBB METHODOLOGY APPLICATION RESULTS PERFORMED ON THE SAFETY RELATED PIPING OF NPP V-1 IN JASLOVSKÉ BOHUNICE

KUPČA Ľudovít PhD, BEŇO Peter MSc, Nuclear Power Plants Research Institute
Okružná 5, Trnava, Slovak republic

SUMMARY

The main results of LBB application on the following safety related piping both WWER.440 type units of the NPP V-1 in Jaslovské Bohunice:

- primary circuit
- surge line

as the first step of this project and as the second step the integrity assessment of safety related piping for:

- feed water
- and main steam piping,

which is close related to the LBB methodology applications are summarised in presented paper.

This project under management of NPPRI (VÚJE) Trnava was realized through close cooperation of more than one hundred research specialists from NRI Řež, ŠKODA Works, RI Sigma Modřany, Welding Institute Bratislava, Energy Institute Bratislava and also the engineers and technicians from NPP V-1 Jaslovské Bohunice.

The results of experiments and calculations are divided due to the LBB methodology approach following way:

- stress analysis
- mechanical properties of base metal and weld metal
- corrosion stability analysis
- fatigue damage evaluations
- heavy components stability
- water hammer analysis
- leak rate measurements
- full scale model experiments on the critical parts of piping.

Summary of achieved results were prepared in so called "LBB Handbook". This great effort was finally used for:

- upgrading of the limits of operation for both NPP V-1 units
- recommendations for operation under nonstandard situations
- important data of "basic engineering NPP V-1" reconstruction project.

INTRODUCTION

The start of the realization of this project follows from the Regulatory Act #5, former Czechoslovak Atomic Energy Commission according to the activities relating to the safety improvements of the NPP V-1. This effort continue till this time throughout all WWER-440 units which are under operation, or construction in former Czechoslovak Federal republic NPP V-2 in Jaslovské Bohunice, Mochovce and Dukovany and another units this type operated in Hungary, Bulgaria, Ukraine and Russia, too.

THE FIELD OF APPLICATION

LBB methodology application was performed on the following safety related piping both WWER.440 type units of the NPP V-1 in Jaslovské Bohunice:

- primary circuit (PC)
- surge line (SL),

as the first step of this project, the integrity assessment was performed on the following piping systems:

- main steam piping (MSP)
- feed water piping (FWP),

as next step after finishing previous one.

THE LIST OF RESEARCH PROGRAM TASKS

Following activities were performed under this program:

- the stress and strain calculations for both piping systems including the seismic influences
- the stress, deformation and fatigue calculations in the critical parts of both piping
- the mechanical properties' evaluation realized on the samples cut from NPP Kola primary piping material after 15 years of operation
- the corrosion and erosion analysis on the samples after 15 years of operation
- the material properties analysis:
    a) mechanical testing (static tension, Charpy, fracture toughness, low cycle fatigue)
    b) the microstructural analysis (microimpurities, grain size, microhardness, inclusion identification, ...)
    c) fractography of fracture surfaces on the samples after the mechanical tests using the scanning electron microscopy

RESULTS OF LBB METHODOLOGY APPLICATION

In the LBB methodology application were performed following methods (Fig.1):

- stress analysis of the primary piping and surge line
- analysis of the piping material mechanical properties
- corrosion stability of the primary circuit material analysis
- fatigue damage analysis
- stability of the main heavy components supports
- water hammer analysis
- primary coolant leak measurements
- model experiments (1:1) with through wall cracks in weld joints on following parts:
    a) rectangular elbow on primary piping with circumferencial and longitudinal weld
    b) reactor pressure vessel safend with dissimillar weld
    c) T-joint between primary piping and surge line
    d) feed water elbow.

LBB flow chart

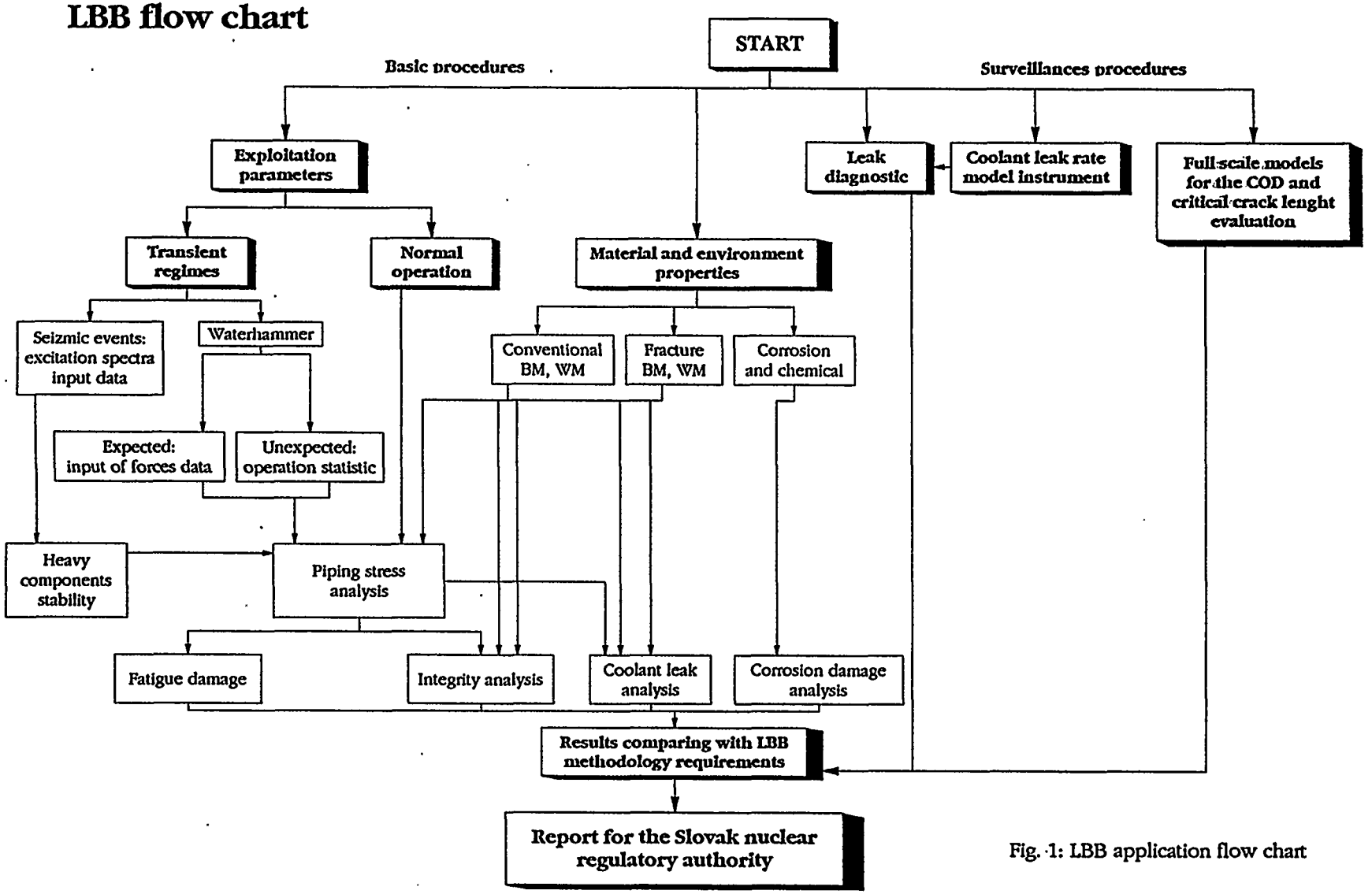

Fig. 1: LBB application flow chart

From the experiments, calculations and model experiments aplied on the primary circuit and surge line pipings of the NPP V-1 follows [1,2,3]:

- all parts of the primary circuit and surge line piping except the upper part of the surge line (Fig.2, 3) fullfilled the LBB method criteria
- the antiseismic eqiupments for the primary and surge line pipings, including the main components like RPV, pressurizer, steamgenerators, main circulating pumps and main insulating valves are resistent to the 8° of MSK-64
- the probability of the integrity loss for the safety significant pipings is extremely low ($< 10^{-6}$)
- from the material properties analysis performed on the archive material of the NPP V-1, and NPP Kola after 100000 hours of operation follows, that there are not present any significant changes of the material properties.

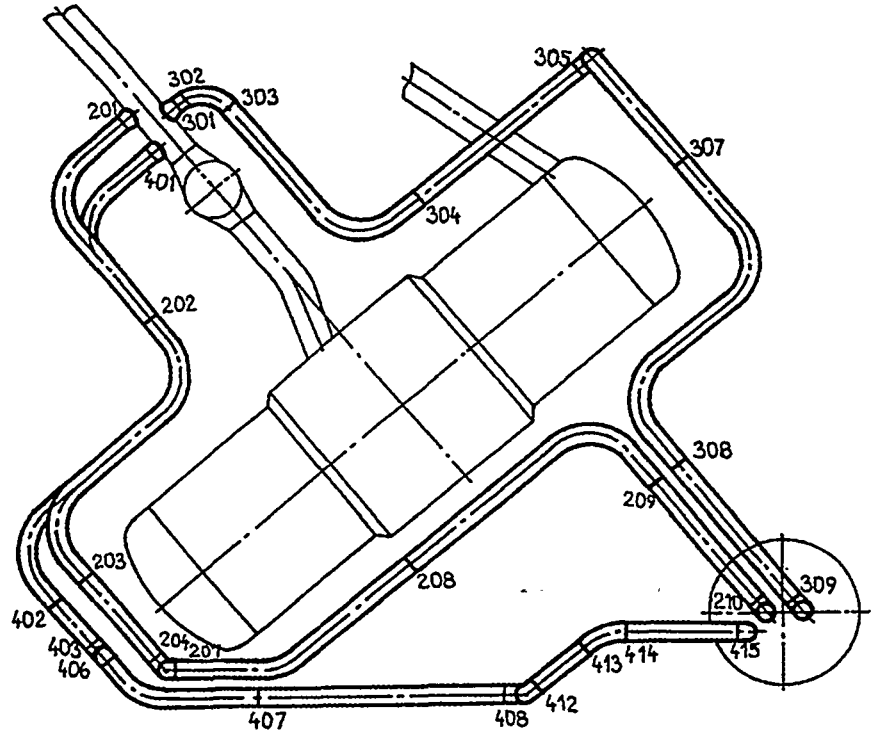

Fig.2: Surge line piping scheme

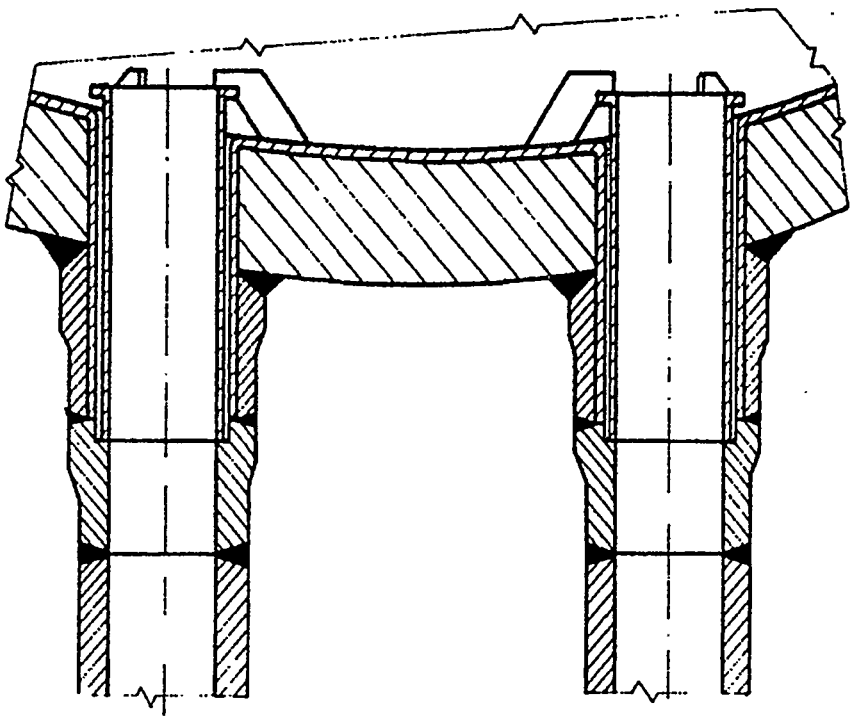

Fig.3: Dissimilar weld of pressurizer safend

From the experiments, calculations and model experiments applied on the main steam and feed water piping of the NPP V-1 follows:

- all values of mechanical properties, for both pipings satisfy the standard requirements
- the mechanical properties of the weld joints for both piping (static tension tests and Charpy) are higher than base material
- the fracture toughness values comparing base and weld material are higher too
- as assumed there were observed the differences of the mechanical properties values based on the samples orientation (texture - effect)
- the stress calculations involved the following parameters:
    a) internal pressure
    b) the weight of coolant and thermal insulations
    c) thermal dilatations
    d) the seismic event
- the results of calculations mentioned above were used for the final integrity assessment

- the detail ultrasonic measurements of the wall thickness did not revealed the significant changes due to the operation conditions
- the chemical composition of both base materials is in good agreement with the standard requirements:
    a) for MSP steel St20 by GOST 1050-60
    b) for FWP steel 12022.1 according ČSN standard 412022
- the composition of weld metals follows the E-4483 electrodes type
- the microstructural properties of analyzed samples cut from piping materials after 15 years of operation NPP V-1 give us following results:
    a) macrostructure of both materials are standard and uniform
    b) the visual control of internal and external surfaces did not revealed anomalous corrosion and erosion influences
    c) macrohardness (Brinell) and microhardness measurements (Vickers) revealed the some differences comparing the values measured in the middle of the wall, and values near both surfaces
    d) microstructure of both materials are typical ferrite - pearlite with the forging texture and uniform impurities distribution
    e) in MSP material we observed the grain size differences between the external surface zone and rest of wall thickness
    f) corrosion influence of the long operation time (more than 100000 hours) on the external surface of both piping is uniform
    g) we observed the pitting corrosion processes on the internal surface of MSP material, but maximal measured penetration was deep to the 100μm only
    h) microimpurities analysis satisfied the standard requirements.

RECOMMENDATIONS

For the NPP V-1 operation we recommended:

- to perform the analysis of the primary piping material after 150000 operation hours only
- the bariers against the primary coolant bleeding are unnecessary
- to prepare new instructions for the leak detection systems signalisation
- to perform the periodical controls of the leak detection systems liability
- in the case of the significant flaws detection perform the material expertize
- in the case of earthquake, or waterhammer accident perform the detail analysis
- in the case of exceeding the standard chemical regimes operation lasting more than one week to perform the corrosion influence analysis
- in the case of long time overheating the seismic atenuators (GERB) to perform the analysis of such event on the safety significant pipings
- to perform the cutting off the upper part of the surge line
- stress analysis of the MSP and FWP including the seismic event of 8°MSK for all 6 loops at both V-1 Units, after antiseizmic backfitting
- analysis of the piping material mechanical properties
- detail corrosion and erosion analysis of the exposed material.

REFERENCES

[1] Kupča, Březina, Beňo: The NNP V-1 primary piping material properties analysis, Report VÚJE, october 1992

[2] Březina et all: Material structures analysis of 08CH18N12T steel, Report VÚJE, november 1992

[3] Kupča et all: The LBB methodology application for safety significant pipings of NPP V-1, Report VÚJE, january 1993

Specialist meeting on LEAK BEFORE BREAK in Reactor Piping and Vessels
LBB95
Lyon, France, 9 - 11 October 1995

German Experimental Programs and Results

Bartholomé, G., Bazant, E., Wellein, R., Siemens KWU
and Stadtmüller, W., Sturm, D., MPA Stuttgart
Germany

1 Introduction

Reactor pressure vessels and piping of the primary circuit form part of the safety research related components in nuclear power plant. The integrity of these components in the presence of defects of limited size has to be guaranteed under both operational and accident loading conditions.

In the period from 1973 to today, on the one hand, within the framework of reactor safety research, the Federal Minister for Education, Science, Research and Technology, Bonn, sponsored a series of research projects which, as seen in **Fig. 1**, are logically linked to each other /1 - 7/. On the other hand the utilities, manufacturers and vendors of nuclear power plants performed series of tests with pipes and components to solve their specific problems. Having regard to the results of the supporting projects the experimental verification of Leak-before-Break behavior was to be demonstrated, the postulation of fracture preclusion for piping (straight pipe, bends and branches) confirmed and thereby the safety margin against massive failure also quantified. **Fig 2** gives a general overview of the types of defects and loadings also the most important objectives.

As the following results reveal, they can be called upon for the safety assessment of ferritic and austenitic piping, in the primary and secondary circuits of nuclear power plant. Moreover, because of the great spread of the test parameters, they are also important for the design and assessment of piping in other technical plant.

On the strength of the test results it appears to be justified to rule out catastrophic fractures (2F-fractures) even on pipes of dimensions corresponding to those of a main coolant pipe of a pressurized water reactor plant on the basis of a mechanical deterministic safety analysis in correspondence with the Basis Safety Concept (Principle of Fracture Preclusion) /8/

2 General

2.1 Material and test pieces

For reasons of transferability of the results to actual components, mostly the Basis Safety material 20 MnMoNi 5 5 employed for piping and pressure vessels in LWR nuclear power plant was used. To cover specific problems also other ferritic materials on the basis of MnNi, MnMoV or austenitic steels as e.g. X 10CrNiTi 18 9 were used. In the quality employed, these materials have a notch impact energy upper shelf value between 100 J and 200 J and thus lie above the minimum value of 100 J required in the RSK Guidelines /9/.

For the investigation of the effect of conditions which overstep the limiting values, especially with respect to a lower notch impact energy upper shelf value, special casts were used as further materials for the manufacture of the test pieces. For the simulation of the end-of-life (EOL) condition an upper shelf energy value of ≅ 50 J could be arrived.

The test pieces were straight pipes. They were closed by heads at each end. The dimensions of the test pieces lie in the range of those applicable to primary circuit components of pressurized water reactors. In preliminary tests other dimensions and materials were employed additionally so that the range shown in Fig. 3 could be investigated.

2.2 Test conditions

As regard pressure and temperature the test conditions were orientated towards the operating conditions of a pressurized resp. boiling water reactor: internal pressure between 9 MPa and 17 MPa at temperatures from ambient temperature to 300 °C. Both water and air were chosen as pressurizing media. The failure of pipes with longitudinal resp. circumferential defects, was effected by raising the internal pressure, or when using an additional external bending moment, the bending moment was increased until failure occurred. In case of an alternating external bending moment was used, the amplitude of which was chosen to correspond to the object of the test, a constant internal pressure of up to 15 MPa was superimposed on the pipe.

2.3 Introduction of defects

The longitudinal and circumferential defects were introduced mechanically using a milling device or by spark erosion. A number of the defects in the pipes were additionally fatigued.

3 Summary of experimental results

3.1 Strength and Leak-before-Break (LBB) behavior

3.1.1 Pipes with longitudinal defects under internal pressure loading

The Leak-before-Break curve which divides the leakage from the massive fracture is, assuming equal pipe dimensions, for corresponding stress values, essentially dependent on the toughness of the pipe material.

Fig. 3 illustrates that not only pipes of ferritic steels but also ones of austenitic steels may accommodated in this form of representation. In order to take account of the different material strengths, in this representation the circumferential stress at fracture σ_n was normalized with respect to the mean flow stress σ_f. The path of the Leak-before-Break curve appears to be independent of whether crack initiation occurs quasi-statically or dynamically.

If a pipe exhibits longitudinal through-wall defects which are shorter than the critical slit lengths derived from the Leak-before-Break curve then in the event of failure a leak or a limited fracture always develops. /10 - 15/

3.1.2 Pipes with circumferential defects under internal pressure and external bending moment loading

For the performance of the bending tests a 4 point bending rig was used. By changing the pressurizing medium (air instead of liquid) in the actuating cylinder of the rig the stiffness of the system could be varied over a wide range. In these pipe bend tests the stiffness of the bending rig exerted more influence on the fracture development than the compressibility of the pressurizing medium in the test pipe. If the stiffness of the bending rig is very large (hard system) then it is possible that after crack initiation, because of the rapidly changing deflection behavior of the test pipe, the bending moment can no longer be maintained. In this case an arrest of the initiated crack in the test pipe has to be reckoned with, i.e. this system favors the development of leakages.

On the contrary for a test rig having less stiffness, in the extreme case for having an infinitely soft system (e.g. creation of moments by dead weight loading) theoretically the bending moment on the test pipe is always present and indeed is independent of the magnitude of its deflection. A crack once initiated under these idealized conditions can more likely lead to a massive fracture, i.e. this system favors the development of a massive fracture.

If pipes with part-circumferential notches or defects are loaded by an external bending moment in addition to internal pressure then failure curves for different notch depth/wall thickness a/t ratios result. From this it holds that the deeper the notch for a given notch length or notch circumferential angle the smaller becomes the tolerable additional bending moment for a constant internal pressure.

As already established for pipes with longitudinal defects, a strong dependence of the failure curve on the toughness of the pipe material was also found for the pipes with circumferential defects, **Fig. 4.** Assuming a low toughness material

condition (KV ≅ 50 J) and normal operational internal pressure loading superimposed by a 5 MNm bending moment, then for the dimensions of the main coolant piping a safety margin of about x4 with respect to the critical slit length results if the maximum permissible defect sizes from the acceptance test, the repeated non-destructive testing and the leakage monitoring system (LMS) are taken as a basis. For toughness of KV > 100 J this safety margin rises to x8. **Fig. 5** illustrates again that not only pipes of ferritic steels but also ones of austenitic steels may accommodated in this form of representation. In order to take account of the different material strengths, in this representation the nominal bending stress at fracture was normalized with respect to the ultimate tensile strength. /16, 17/

3.1.2.1 Fracture opening behavior

The time-dependent development of fracture opening area for longitudinal and circumferential defects was investigated. From this the time required for the formation of a fracture opening of 0.1 F is between 2.5 and 5.4 ms for longitudinal defects and between 29 and 36 ms for circumferential ones.

3.1.3 Pipes with circumferential defects under internal pressure and cyclic external bending moment loading

The investigations served to provide further experimental confirmation of the fracture preclusion postulate for piping with (partial-) circumferential defects, especially under internal pressure loading and simultaneous loading by a cyclic external bending moment. The tests were conducted with the aim of providing data on the crack initiation, cyclic crack growth, the deformation and cyclic strain behavior and also the Leak-before-Break behavior.

For these tests a modified version of the bending rig was employed.

In **Fig. 6** are plotted both the number of cycles to crack formation (N_A) determined of smooth test bars as a function of the total strain amplitude in the form of a scatter band /18/ and also the number of cycles to through-cracking (N_B) determined in pipe bending fatigue tests as curves dependent on the particular defect size.

The number of cycles to through-cracking determined on pipes with circumferential defects lie, depending on defect depth and length, at a greater or lesser distance below the scatterband determined on smooth test bars, in which the test bars from the investigated pipe materials fit well.

The number of cycles to through-wall cracking of the pipes with circumferential defects having a starting defect depth of 10% of the wall thickness (defect depth/wall thickness = 0.1) and a circumferential angle of 42 degrees, lie about a half decade below the scatter band for smooth test bars.

For pipes with deeper starting defects (defect depth/wall thickness = 0.5, defect circumferential angle of 42 degrees) the cycles to through-wall cracking lie up to 2.5 decades lower than the scatter band for the onset of cracking in smooth test bars.

For deeper defects (defect depth/wall thickness = 0.5) with circumferential angle of ≅ 120 degrees only a small difference in the tolerable load cycles was found compared with shorter defects (≅ 40 degrees)

Pipes tested in the region of their natural frequency (4 Hz) lead to the same results as those having comparable defect dimensions when tested at a lower frequency (0.008 Hz).

No effect of pipe geometry (internal diameter of 10 mm to 706 mm) on the number of cycles to through-cracking could be found over the range investigated.

It can be concluded from the investigations that pipes of ferritic materials with crack-like circumferential defects can bear additional high external bending moments in the presence of simultaneously acting internal pressure even if the dimensions of the defects lie considerably above the defect size permitted in the non-destructive acceptance testing.

Furthermore it can be established that pipes with such circumferential defects can still tolerate a considerable number of bending cycles before through cracking of the ligament below the defect occurs. A prerequisite though in this regard is that the defect lengths are shorter than their associated through-wall critical lengths.

3.2 Analytical and numerical analyses

The Leak-before-Break (LBB) concept is an essential part of the Break Preclusion Concept /8,19,20,21/.

3.2.1 LBB Concept

The critical crack size for ductile material is determined using fracture mechanics. The growth of stable cracks is only conceivable due to cyclic loading (corrosion has to be precluded). The cyclic crack growth beyond design can lead to two situations, **Fig. 7**:

First situation: Crack growth smaller than critical through-wall crack length (Leak-before-Break).

Second situation: Crack growth up to a crack length which is greater than the critical through-wall crack length (Break-before-Leak).

If LBB behaviour can be shown, break preclusion is proven with the necessary redundancies; if not, break preclusion can only be obtained by applying equivalent safety measures (e.g. Inservice Inspection, Load Monitoring, Fatigue Monitoring, Continuous Inspection).

3.2.2 Methods applied

LBB is demonstrated by means of fracture mechanics methodology, applying adequate criteria, **Fig. 8**. Siemens performed numerous analyses to preclude breaks based on simplified elasto-plastic fracture mechanics (Flow Stress Concept = FSC, Plastic Limit Load = PLL) for circumferential cracks, **Fig. 9**. The acceptability and applicability of these concepts was discussed with and accepted by the authorities in Germany /20 - 22/. Analogous approaches are used for longitudinal cracks /23/. These approaches are also compared to the more sophisticated approach using J-Integral /27/.

3.2.3 Experimental verification of the methods used for LBB

3.2.3.1 Simplified methods (FSC, PLL, BMI, RUIZ)

The calculation concepts used by Siemens (charpy energy KV > 45 J, material properties of base material BM instead of weld material WM) are validated by numerous tests. As an example typical results for the conservatism of the simplified elasto-plastic fracture mechanics approaches are shown for circumferential through-wall cracks using FSC and PLL /22, 24, 26/,**Fig. 10 and 11.** The comparison of the theoretical prediction to the experimental results for longitudinal through-wall cracks /23/ using BMI and RUIZ shows the conservatism of the used approaches, **Fig. 12 and 13.**

3.2.3.2 J-Integral

The application of the J-Integral approach /27/ for circumferential cracks to the tests available at this time (Battelle, MPA, Siemens/Interatom) shows that, using J_i as the relevant material property, all tests can be predicted conservatively, see **Fig. 14.** The amount of conservatism using FSC and PLL for the same tests also can be seen.

4 Application of the Break Preclusion Concept

4.1 Break Preclusion Concept

In Germany the Break Preclusion Concept, often called Leak-before-Break, being applied since 1979 is based on the Basis Safety Concept /19, 25/. The Break Preclusion Concept for the main coolant line according to German practice is detailed in a logic chart (**Fig. 15**) for the different steps , Inservice Redundancies, Leak-before-Break (LBB), Break Preclusion (BP) and the Break Postulates, derived from the BP.

The two main prerequisites for the general procedure of BP /8/ are Basis Safety and Independent Redundancies.

The safety of the primary piping against break was proven by research programs performed at MPA, Siemens/KWU and Siemens/Interatom. These programs (Fig. 1) included tests on representative pipings under relevant loading conditions.

4.2 Application of the Break Preclusion Concept to the main coolant piping

Siemens performed various analyses to preclude breaks based on simplified elasto-plastic fracture mechanics FSC /20/, PLL /22/. The results of the analysis of a typical PWR main coolant line to the Konvoi plant /20/ are given in **Fig. 16.** With these safety margins, resulting from Basis Safety (piping technology, operational loads and stresses, crack growth and crack stability) and from independent redundancies (field experience - no breaks and leaks occurred, leak detection requirements, transient monitoring and inservice inspection) the German Reactor Safety Commission (RSK) agreed on the application of preclusion of breaks. Restrictions were discussed in the RSK and dealt essentially with corrosion and vibrations. These restrictions, if applicable, can be solved by recommendations for representative ISI-testing of relevant locations. In general the amount of ISI was reduced when following the requirements to succeed in Break Preclusion.

4.3 Break postulates

Applying the above criteria the RSK modified the RSK-Guidelines, the main content of which is given in **Fig. 17:** Postulated leaks and breaks for primary system and corresponding effects.

5 Summary

Extensive experimental and theoretical investigations on the fracture behaviour of pipes gave important results in the following areas:

- Experimental determination of the Leak-before-Break behavior under quasi-static and cyclic loading.
- Experimental determination of effect of toughness on the strength, Leak-before-Break and cyclic crack growth behavior.
- Experimental determination of the fatigue behavior of pipes under quasi-static internal pressure and cyclic external bending moment loading.
- Ascertaining the legitimacy of the transferability of data obtained from small specimens to components.
- Contribution to proving the performance capability of analytical and numerical calculational method
- Proof of the conservatism of the analytical fracture mechanics methods used in Germany for the evaluation of LBB of nuclear piping in respect to
  - circumferential through-wall cracks, using flow stress criterion (FSC) and plastic limit load (PLL) and
  - longitudinal through-wall cracks using (BMI) and (RUIZ) formulae
  together with the adapted flow-stresses.
- Proof of the conservatism of the more sophisticated fracture mechanics method (J-Integral with J_i)

6 Acknowledgment

Sponsorship of most of the projects was provided by the Federal Minister for Education, Science, Research and Technology (BMBF), Bonn, but also by the Technische Vereinigung der Großkraftwerksbetreiber e.V. (VGB) - Kraftwerks technik GmbH, Essen. The Gesellschaft für Anlagen- und Reaktorsicherheit (GRS) mbH, Cologne, were responsible for the administration of the research work. Thanks are due at this juncture to all participants for their support of the research projects

7 References

/1/ HDR-Sicherheitsprogramm, Förderkennzeichen RS 1500 123, Kernforschungszentrum Karlsruhe, 1974 - 1994.

/2/ Sturm, D. und P. Julisch: 'Schnellzerreißversuche mit Rohrproben, 12 MN-Schnellzerreißmaschine (Phase III), Förderkennzeichen 1500 749, Forschungsbericht MPA-Auftrags-Nr. 8540 00 000, Staatliche Materialprüfungsanstalt (MPA) Universität Stuttgart, Dezember 1989.

/3/ Sturm, D. und W. Stoppler: Forschungsvorhaben 'Phänomenologische Behälterberstversuche' - Versuche zum Traglast- und Bruchverhalten von Rohren mit Längsfehlern -. Förderkennzeichen 1500 279, Phase I, Forschungsbericht MPA Stuttgart, Juli 1985.

/4/ Sturm, D und W. Stoppler: Forschungsvorhaben 'Phänomenologische Behälterberstversuche' - Versuche zum Traglast- und Bruchverhalten von Rohren mit Umfangsfehlern -. Förderkennzeichen 1500 279, Phase II, Forschungsbericht MPA Stuttgart, Dezember 1987.

/5/ Sturm, D. und W. Stoppler: Forschungsvorhaben 'Phänomenologische Behälterberstversuche' Versuche zum Traglast- und Bruchverhalten von Rohren mit Längs- und Umfangsfehlern -. Förderkennzeichen 1500 279, Phase II, Forschungsbericht MPA Stuttgart, November 1989.

/6/ Sturm, D. und W. Stoppler: Forschungsvorhaben 'Rißwachstum und Bruchverhalten von rohrförmigen Komponenten mit Umfangsfehlern bei Innendruckbelastung und überlagertem wechselnden äußeren Biegemoment'. Förderkennzeichen 1500 752, Forschungsbericht MPA Stuttgart, April 1993.

/7/ Herter, K.-H. und W. Stoppler: Forschungsvorhaben 'Festigkeits- und Bruchverhalten von Abzweigen und Rohrbogen bei Innendruckbelastung und überlagertem äußerem Biegemoment'. Förderkennzeichen 1500 801, Forschungsbericht MPA Stuttgart, März 1993.

/8/ Kussmaul, K.: German Concept Rules out Possibility of Catastrophic Failure. Nuclear Engineering International, No. 12, 1984, 41 - 46..

/9/ RSK-Leitlinien für Druckwasserreaktoren. 2. Ausgabe 24. Januar 1979.3. Ausgabe 14. Oktober 1981. Druck und Versand: GRS Köln.

/10/ Kußmaul, K., D. Sturm, P. Julisch, W. Stoppler and K. Hippelein: Crack Arrest Behaviour in Pressure Vessels. Transactions of 7th SMiRT Conference, vol. G-H, paper G/F 4/10, August 22-26., 1983, Chicago, USA.

/11/ Kußmaul, K., D. Sturm, W. Stoppler and D. Müller-Ecker: Experimental Investigation on the Crack Opening Behaviour of Cylindrical Vessels under Light Water Reactor Service Conditions. The Reliability and Safety of Pressure Components. The American Society of Mechanical Engineers, New York, N. Y., 1982, PVP-Vol. 62 pp. 97/134.

/12/ Sturm, D., W. Stoppler und K. Hippelein: Phänomenologische Behälterberstversuche - Bruchauslösung, Bruchöffnungsverhalten. Gemeinsames Seminar der MPA Stuttgart und RWTÜV 15.06.1982 in Essen, RWTÜV Schriftenreihe Heft 20.

/13/ Stoppler, W., D. Sturm, P. Scott und G. Wilkowski: Versagensanalyse von längsfehlerbehafteten Rohren und Behältern. 18. MPA-Seminar am 8. und 9.10.1992.

/14/ P. Scott, G. Wilkowski, D. Sturm and W. Stoppler: Development of a Database of Pipe Fracture Experiments. 18. MPA-Seminar am 8. und 9.10.1992, Stuttgart.

/15/ D. Sturm und W. Stoppler: Festigkeitsverhalten von Rohren mit Kerben unter Innendruck und äußerem Biegemoment - Vergleich zwischen Versuch und Rechnung-. 15. MPA-Seminar am 5. und 6.10.1989, Stuttgart.

/16/ Wilkowski, G. M. et al.: Degraded Piping Programm - Phase II. Summary of Technical Results and their Significance to Leak-before-Break and In-Service Flaw Acceptance Criteria. March 1984 - January 1989. NUREG/CR-4082, BMI-2120, Vol. 8, March 1989.

/17/ Takumi K., T. Marno et. al.: Proving Test on the Integrity of Carbon Steel Piping in LWR's. Nupec, 1989

/18/ Luft, G.: Zeitfestigkeitsverhalten von Stählen. Techn.-wiss. Bericht MPA Stuttgart, 1968.

/19/ Kußmaul, K.: Developments in nuclear pressure vessel and circuit technology in the Federal Republic of Germany. SMIRT-6, Post Conference Seminar No. 8, Session 1, Paper No. 1, Paris, Aug. 24, 1981

/20/ Bartholomé, G., R. Steinbuch, R. Wellein: Preclusion of Double-ended Circumferential Rupture of the Main Coolant Line. Nuclear Engineering and Design, 72 (1), 1982, p.97-105

/21/ Bartholomé, G., W. Kastner, E. Keim, R. Wellein: Ruling-out of Fractures in Pressure Boundary Piping. Part 2 "Application on Coolant Pipe of the Primary System" IAEA - Vienna 1983 "Reliability of Reactor Pressure Components" IAEA-SM-269/-7, p. 237-254

/22/ Roos, E., K.-H. Herter, P. Julisch, G. Bartholomé, G. Senski: Assessment of Large Scale Pipe Tests by Fracture Mechanics Approximation Procedures with Regard to Leak-before-Break. Nuclear Engineering and Design 112 (1989), p. 183-195

/23/ Bartholomé, G., R. Wellein: Bruchmechanische Auswertung von Bauteilversuchen (Rohrleitungen) mit Längsdurchrissen zur Absicherung des Leck-vor-Bruchverhaltens.(Fracture mechanics Evaluation of Components Tests (Pipings) with Longitudinal Through-Wall Cracks for Verification of LBB-Behaviour) DVM-Arbeitskreis "Bruchvorgänge", 26. Vortragsveranstaltung, 22./23.03.1994, Magdeburg, p. 407 - 421

/24/ Bartholomé, G., R. Wellein: Evaluation of Components Tests with Analytical Fracture Mechanics Methods (Circumferential Cracks). ECF 10, Berlin, 23.09.1994, p. 1317 - 1326

/25/ Bartholomé, G.: Break Preclusion Concept in Germany. SISSI 94 "Saclay International Seminar on Structural Integrity".April 28-19, 1994, INSTN, Saclay, France. Principles of fracture mechanics application in Nuclear Power Plants, p. 309 - 331

/26/ Bartholomé, G., E. Keim, W. Kastner, W. Knoblach and R. Wellein: Application of LBB in German NPP. LBB 95: Leak Before Break in Reactor Piping and Vessels, Lyon, 9/11 October 1995 (to be published)

/27/ Riccardella, P.: Computer Program pc-Crack. Version 2.1, 1991. Structural Integrity Associates Inc. San José, Ca, USA

1. RESEARCH PROGRAMME TO PROVE A FRACTURE SAFETY DEVICE PROTECTION SYSTEM FOR REACTOR COMPONENTS
(RS 104, KWU) 1973 - 1976

2. INVESTIGATIONS ON INITIATION, PROPAGATION AND ARREST OF AXIAL CRACKS IN PIPES
(150 320, KWU) 1978 - 1982

3. PHENOMENOLOGICAL VESSEL BURST EXPERIMENTS (BV PHASE I + II) - PRIMARY PIPING OF PWR
(150 279, MPA) 1977 - 1987

4. FRACTURE RESISTANT DESIGN OF STEAM PIPES FOR THE THTR MATERIAL X 20 CrMoV 12 1
(BBC, RWTÜV) 1983 - 1984

5. PROOF OF INTEGRITY OF COMPONENTS - PRIMARY PIPING OF BWR
(VGB, KWU, MPA) 1985 - 1987

6. LOAD BEARING CAPACITY OF PIPES UNDER INTERNAL PRESSURE AND EXTERNAL BENDING MOMENT - FERRITIC AND AUSTENITIC MATERIALS
(UTILITIES, MPA) 1983 - 1988

7. HDR SAFETY PROGRAMME (PHASE I, PHASE II, PHASE III)
- BLOW DOWN; EARTHQUAKE AND IMPULSE LOAD ON PIPING SYSTEMS
- FAILURE BEHAVIOUR OF PIPING SYSTEMS
- THERMAL STRIATION
- FAILURE BEHAVIOUR UNDER CYCLIC LOADING
- TRANSIENT LOADING OF PREDAMAGED PIPING SYSTEMS (BLOW DOWN, EARTHQUAKE)
- LEAK RATE TEST OF DIFFERENT PIPING COMPONENTS
(150 123, PHDR KfK, MPA, INDUSTRIES) 1976 - 1994

8. ANALYSIS OF LEAK BEFORE BREAK BEHAVIOUR OF SNR 300 COMPONENTS
(INDUSTRY; RWTÜV) 1983 - 1984

9. ASSESSMENT OF CIRCUMFERENTIAL CRACKS IN HIGHLY LOADED WELDMENTS OF PIPING
(KWU) 1980 - 1982

10. INTERNAL PRESSURE TESTS WITH PIPE BENDS OF FERRITIC STEELS UNDER IN-PLANE BENDING AT TEMPERATURES IN THE CREEP REGIME
(150 726, 150 727, INTERATOM; MPA) 1986 - 1991

11. INELASTIC ANALYSIS OF PIPE BENDS, ANALYTICAL AND EXPERIMENTAL INVESTIGATIONS
(150 705, MPA, SDK) 1985 - 1989

12. LIMIT LOAD ANALYSIS OF FLAWED STREAM GENERATOR TUBES
(RS 624, GRS) 1983 - 1984

13. FLUID-STRUCTURE INTERACTION
(RS 478, GRS) 1983 - 1986

14. ANALYTICAL ACTIVITIES - RUPTURE PHENOMENA WITH VESSEL AND PIPES
(RS 477, GRS) 1980 - 1985

15. CENTRAL INVESTIGATION AND EVALUATION OF MANUFACTURE AND OPERATIONAL DEFECTS OF THE PRESSURIZED COMPONENTS IN NUCLEAR POWER PLANTS
(SR 10/1, MPA) 1983 - 1986

16. DEVELOPMENT OF FRACTURE MECHANICS METHODS FOR THE INTEGRITY DEMONSTRATION OF THE COOLANT BOUNDARY OF SNR-2
(INTERATOM, 29.926.06) 1984 - 1989

17. SNR-2 COMPONENT ASSESSMENT BY FRACTURE MECHANICS ANALYSES (INTERATOM, 22.926.17) 1984 - 1989

18. SNR-2 COMPONENT AND FRACTURE TESTS
(INTERATOM, 22.926/02) 1985 - 1989

19. STRAIN ESTIMATION METHODS FOR LOW CYCLE DYNAMIC LOADS
(INTERATOM, 22.927/02) 1985 - 1988

20. CREEP - FATIGUE EXPERIMENTS ON PIPE GEOMETRIES AND CALCULATIONS
(INTERATOM, V922/10) 1985 - 1989

21. ANALYSIS AND FURTHER DEVELOPMENT OF FRACTURE MECHANICS FAILURE CONCEPTS
(150 488, 150 489, 150 490, FhIWM, BAM, IEHK) 1986 - 1989

22. FRACTURE MECHANICS CHARACTERIZATION OF PIPE MATERIAL AT ELEVATED AND HIGH TEMPERATURES
(INDUSTRY; FhIWM) 1984 - 1987

23. THERMOMECHANICAL MEASURING PROCEDURE FOR FAST DUCTILE FRACTURE
(BMFT 03 S 289, FhIWM) 1982 - 1984

24. INTERNAL PRESSURE TEST ON PIPE BENDS MADE OF CREEP RESISTANT STEEL WITH ADDITIONAL BENDING MOMENTS APPLIED AT TEMPERATURES IN THE CREEP RANGE
(150 727, MPA) 1986 - 1994

25. HIGH RATE TENSILE TESTS WITH PIPE SPECIMENS
(150 749, MPA) 1987 - 1988

26. CRACK GROWTH AND FAILURE BEHAVIOUR OF CYLINDRICAL COMPONENTS WITH CIRCUMFERENTIAL FLAWS, LOADED BY INTERNAL PRESSURE AND CYCLIC OUTER BENDING MOMENT - BV PHASE III
(150 752, MPA) 1987 - 1991

27. TESTS ON THE MAIN COOLING PIPE TO FIND OUT ITS FAILURE DUE TO CREEP FRACTURE UNDER HIGH SYSTEM PRESSURE
(150 771, MPA) 1987

28. STRENGTH AND FRACTURE BEHAVIOUR OF ELBOWS AND T-BRANCHES UNDER INTERNAL PRESSURE AND SUPERIMPOSED OUTER BENDING MOMENT LOADING - BV PHASE IV.
(150 801, UTILITIES; MPA) 1988 - 1991

29. ANALYTICAL ACTIVITIES. COUPLED FLUID AND STRUCTURE DYNAMICS
(RS 478, GRS) 1983 - 1990

30. EXTENSION OF DUCTILE FRACTURE MECHANIC ANALYSES FOR EVALUATION OF THICK-WALLED PIPING LEAKAGE
(RS 697, GRS) 1986 - 1992

31. ANALYTICAL DESCRIPTION OF RUPTURE PHENOMENA IN PRESSURE VESSELS AND PIPES UNDER CYCLIC ELASTIC-PLASTIC LOADING
(RS 788, GRS) 1988 - 1992

32. NUMERICAL SIMULATION AND ASSESSMENT OF INELASTIC MATERIAL BEHAVIOUR USING COMPONENT TESTS IN THE TEMPERATURE RANGE BELOW 400 °C
(150 955, MPA) 1993 - 1996

33. EXPERIMENTAL AND ANALYTICAL INVESTIGATIONS ON AUSTENITIC PIPES
(UTILITIES, MPA) 1993 - 1995

34. CONTRIBUTION TO ENSURE THE FRACTURE MECHANICS INTEGRITY OF PIPING MADE OF HIGH TOUGH MATERIAL
(150 964, MPA) 1993 - 1996

Fig. 1: Piping research in the Federal Republic of Germany - experimental and analytical programs

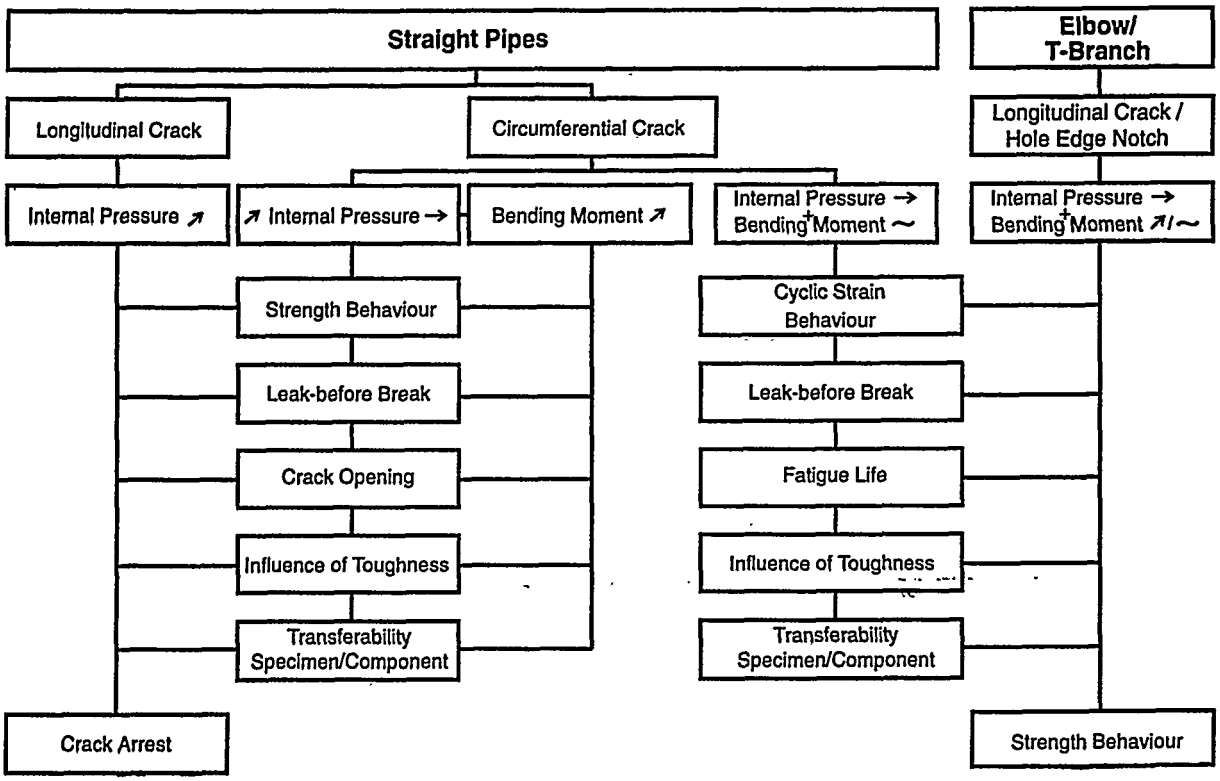

Fig. 2: Objectives of the research programmes

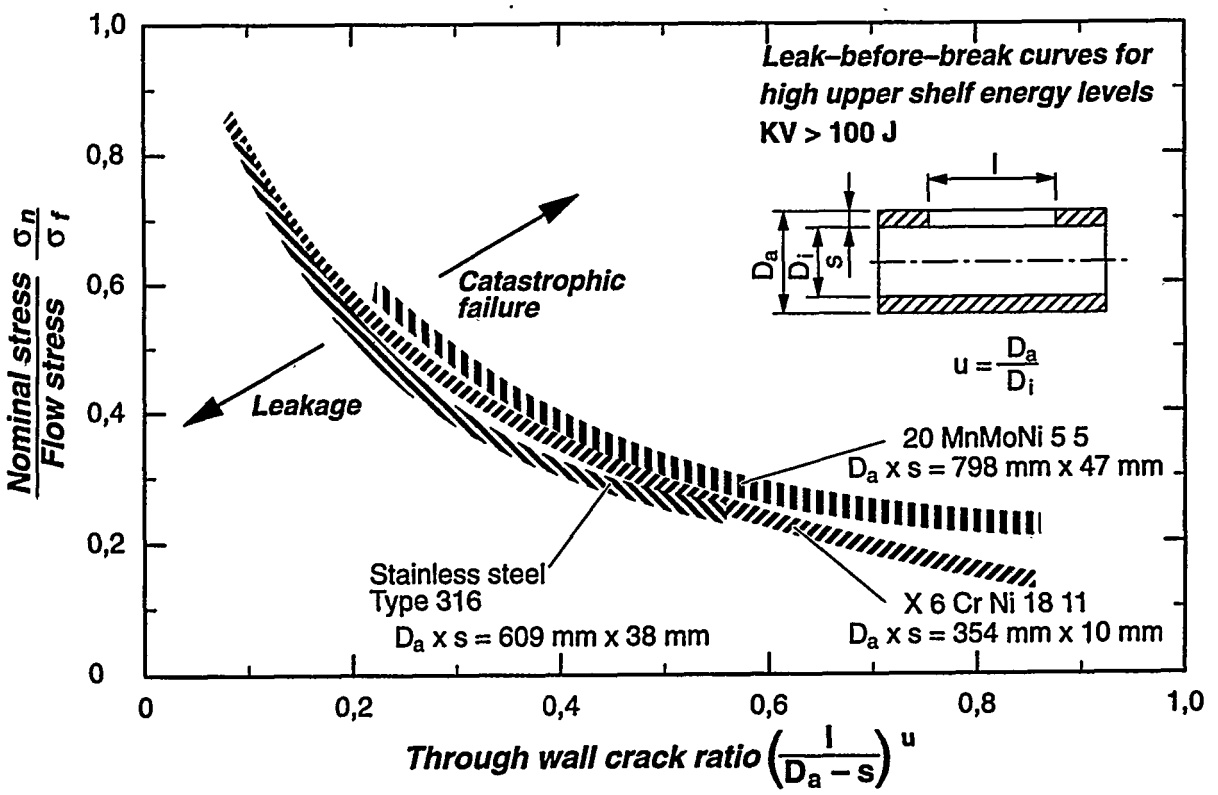

Fig. 3: Leak-before-Break curves for pipes of ferritic and austenitic materials (longitudinal cracks)

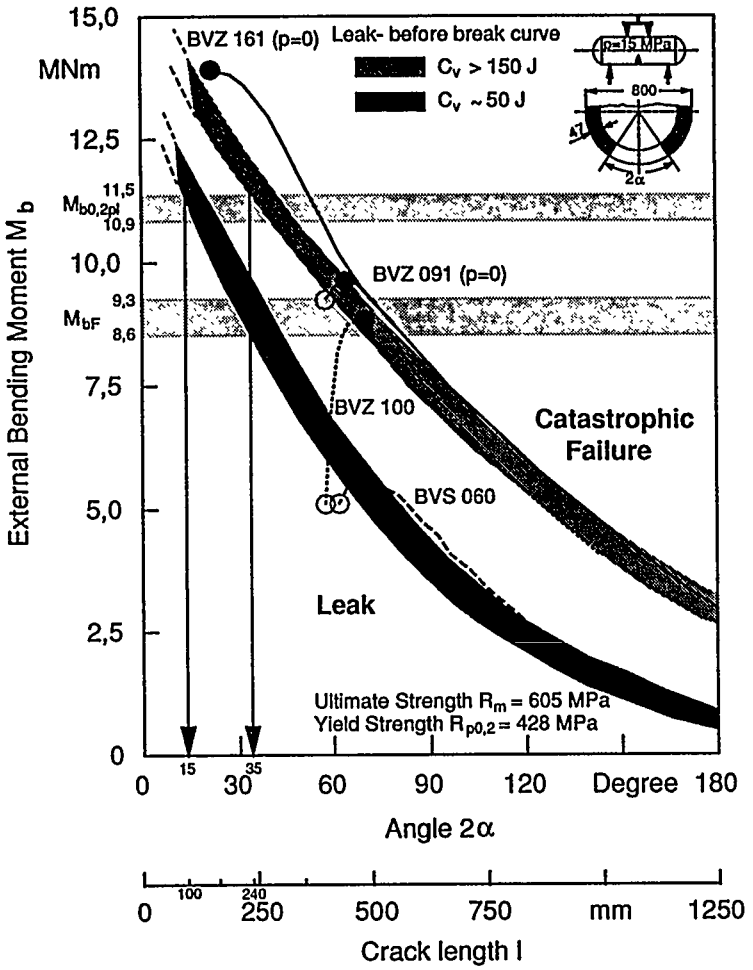

Fig. 4: Leak-before-Break curves for pipes with circumferential defects and different upper shelf notch impact energies

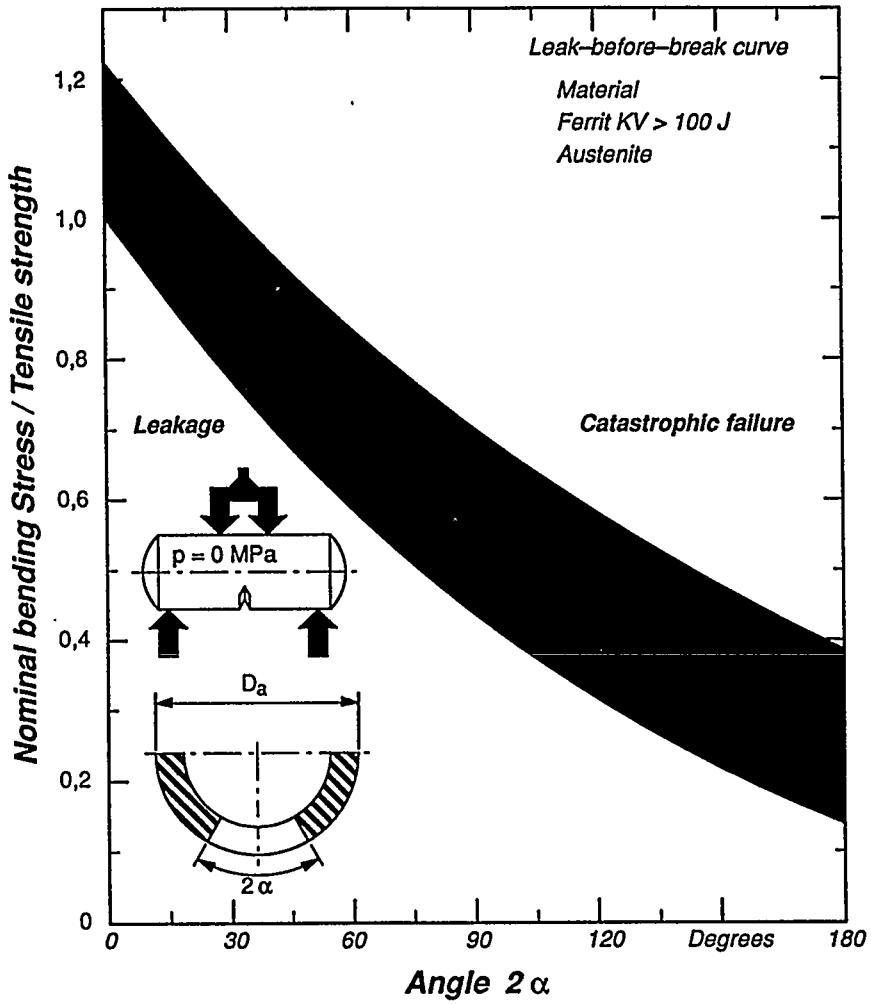

Fig. 5: Leak-before-Break curve for pipes of ferritic and austenitic materials (circumferential defects)

Test	Defect			Test conditions				Equivalent Strain Range	Load cycles	Remarks
	Depth	Length	Position	Temperature	Internal Pressure	Bending Moment				
	mm	mm	Spark Eroded	°C	MPa	MNm Max.	MNm Min.	$\frac{mm}{m}$	N_B	
BVZ 210 ◆	4.7 a/t = 0.1	292 (40 Deg.)	outer + inner surface	20	0	+9.5	–9.5	4.00	2200 2316	Outer Notch: Through Crack Inner Notch: Defect Depth = 35 mm
BVZ 220 ◆			outer surface		15			4.80	1000	Through Crack
BVZ 230 ◆							–0.5	1.80	7998	Test Discontinued Defect Depth: 9.8 mm
BVZ 231 ■	9,8 a/t = 0.2	294 (40 Deg.)				–11.5	–0.25	2.80	724	Test Discontinued Defect depth: 12.8 mm
BVZ 240 ●	23,6	292				+9.5	–9.5	4.80	30	Through crack
BVZ 250 ●	a/t = 0.5	(40 Deg.)		20		+6.5	–6.5	3.16	238	
BVZ 300 ●									320	
BVZ 260 ●						+11.9	–11.9	5.71	4	
BVS 200 ○				80		+6.0	–6.0	2.92	69	
BVS 240 ○									60	
BVS 210 △		140							663	
BVS 220 △		(20 Deg.)				+9.0	–9.0	4.60	41	
BVZ 270 ▲				20		+9.5	–9.5	4.80	274	
BVZ 280 ▲						+12.1	–12.1	5.96	13	
BVZ 290 ▼		838				+6.0	–6.0	3.25	84	
BVS 230 ▽		(120 Deg.)		80		+3.0	–3.0	1.45	606	

BVZ Material : 20 MnMoNi 5 5 BVS Material : MnMoNiV – Special Melt

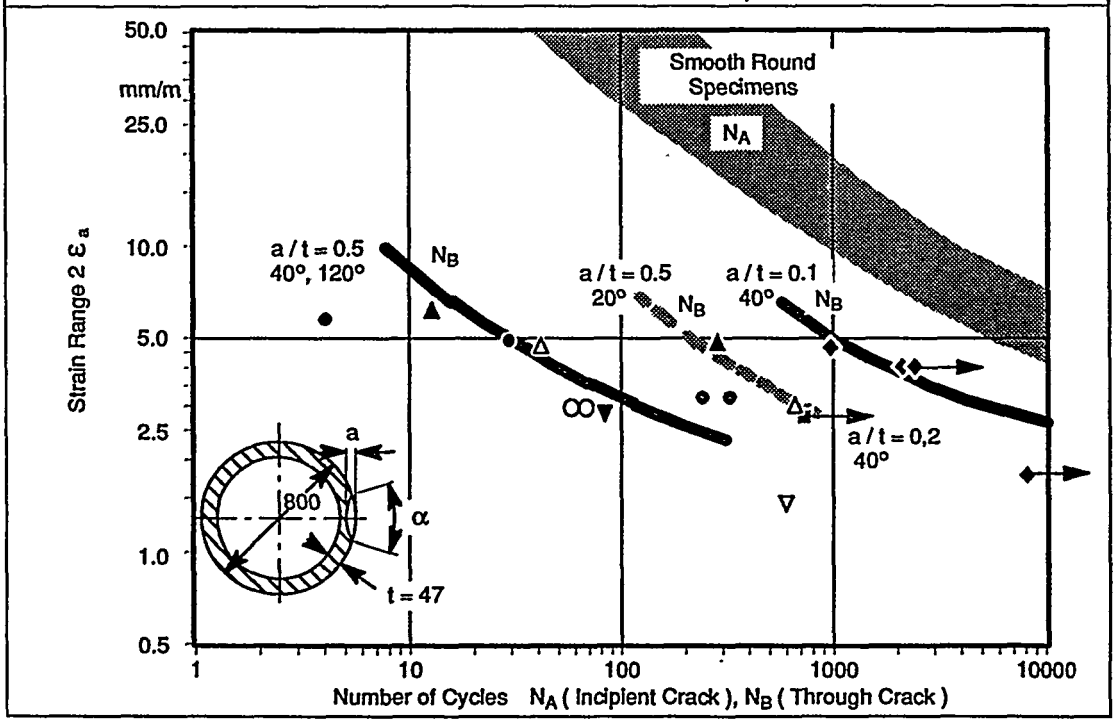

Fig. 6: Tabular and graphical representation of the number of cycles to through cracking as a function of the total strain amplitude (circumferential defects)

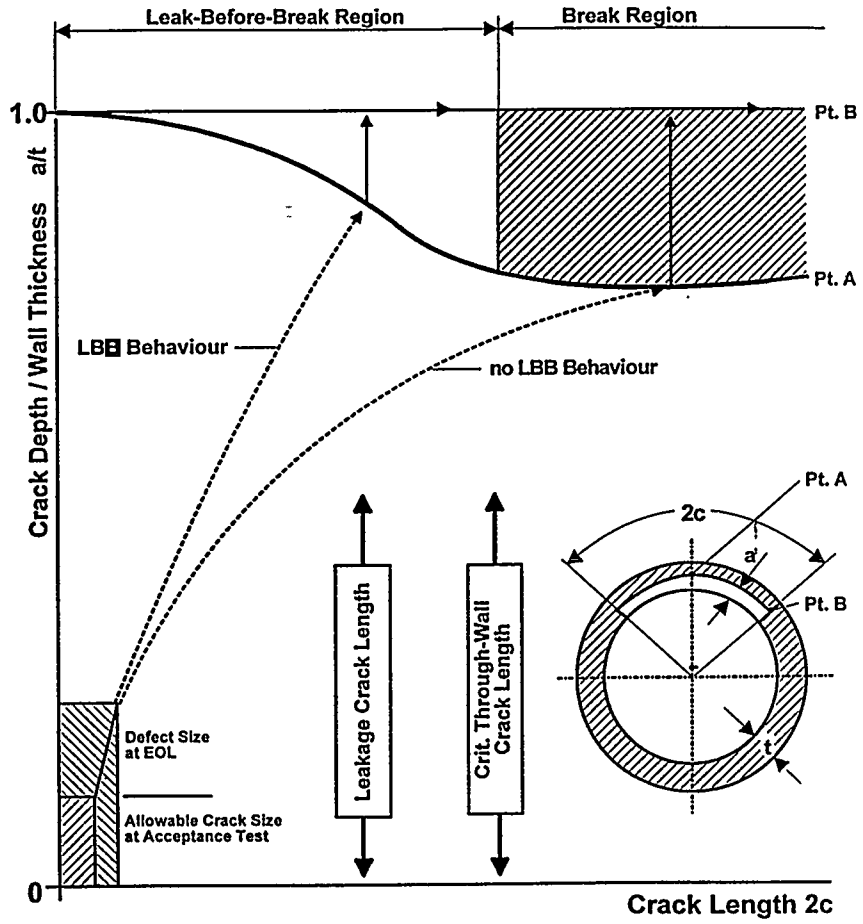

Fig. 7: Procedure of Leak-before-Break (schematic) for circumferential cracks

Description	Methodology	Loads	Results	Criteria
Definition of reference defects	Based on allowable defects + performance of inspection technologies		a_0 $2c_0$	allowable defects
Fatigue crack growth (F. C. G.)	Integration of crack growth law until end of life (EOL)	Normal and upset trans. for 1 specif. load collective	$a_f = a_0 + \Delta a$ $c_f = c_0 + \Delta c$	Small F. C. G. in 1 specif. load collective
Stability of EOL surface crack	qualified methods: Flow stress concept and / or Plastic limit load	all transients + SSE	a_c $2c_c$	Stability of ligament
T. W. C. stability analysis	Same as previous	all transients + SSE	$2c_c$ critical crack length	Stability of ligament
LBB Fatigue crack growth	Integration of crack growth law until break-through of ligament	Normal & upset transients for unlimited specif. load collectives	$2c_f$' leakage crack length	LBB is demonstrated, if $2c_f' \approx 2c_c$ for unlimited specified load collectives if $2c_f' > 2c_c$ equivalent safety measures
Opening area and Leak rate of T. W. C.	qualified methods	normal operation	A $\dot{m}$ $(2c_c)$	Detectability of leak rate

Fig. 8: Break Preclusion: Fracture Mechanics Methodology

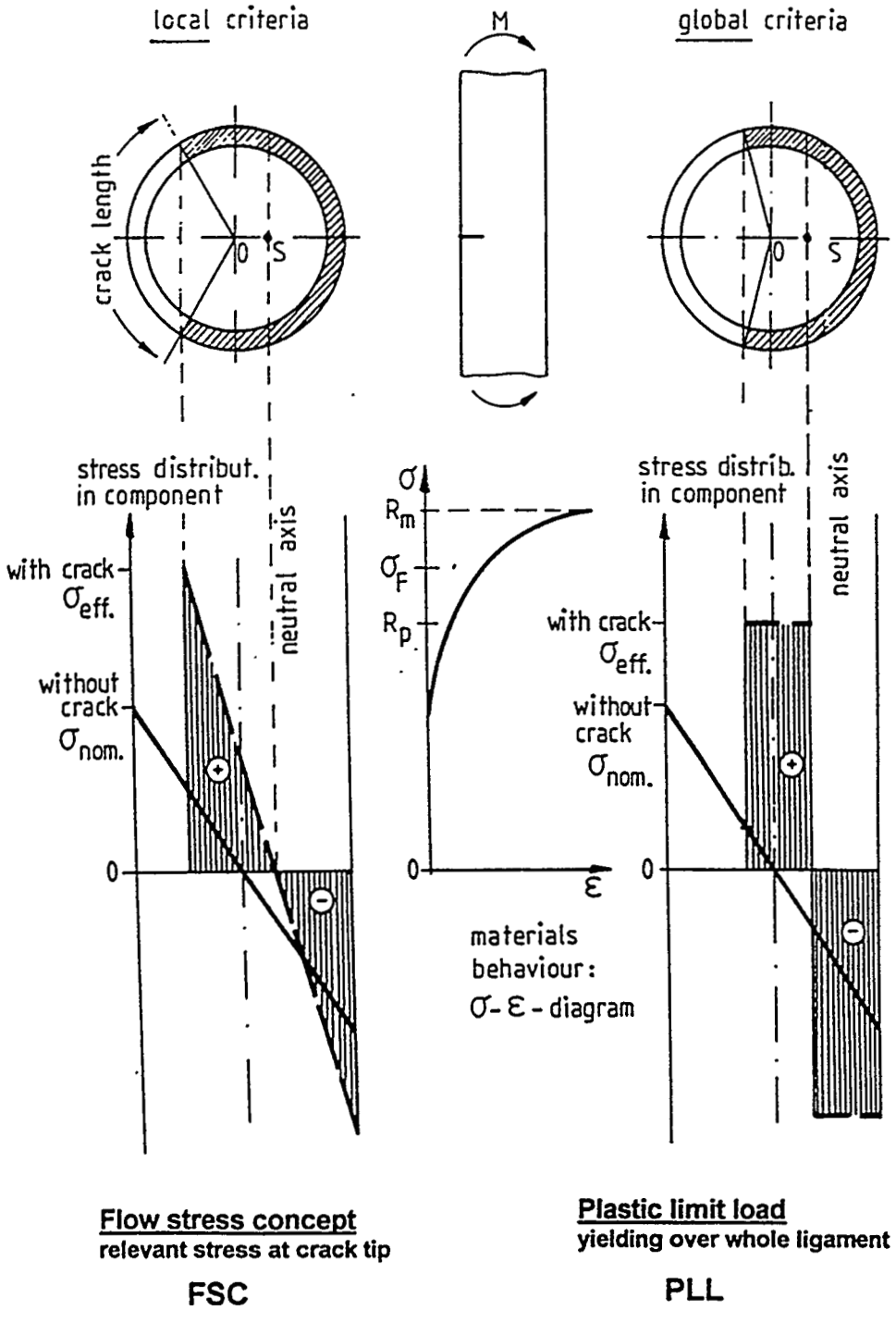

Fig. 9: Models for ductile failure (only bending moment) for circumferential cracks

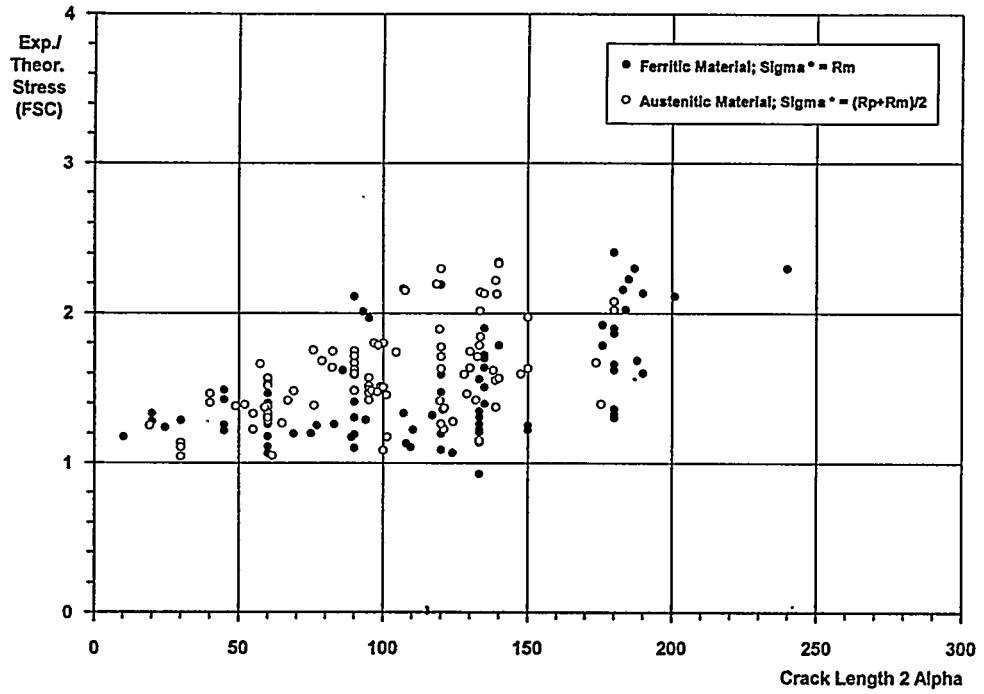

Fig. 10: Circumferential through-wall cracks: Flow Stress Concept (FSC) using experiments with KV>45 J and (WM=BM)

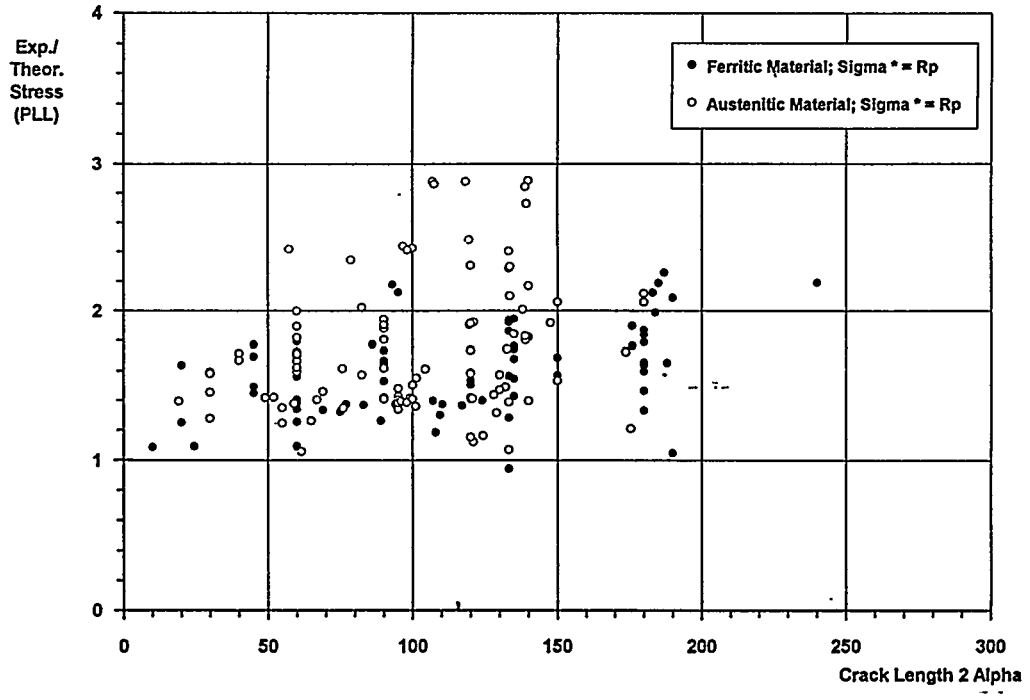

Fig. 11: Circumferential through-wall cracks: Plastic Limit Load (PLL) using experiments with KV> 45J and (WM=BM)

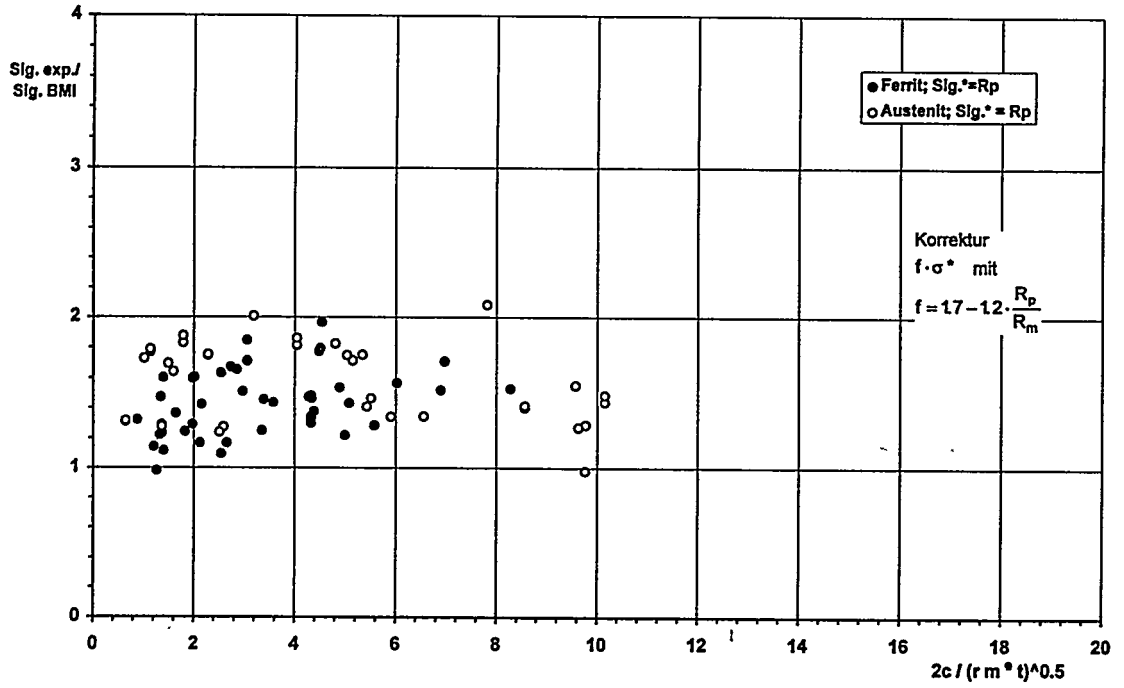

Fig. 12: Longitudinal cracks: All through-wall cracks calculated (KV> 45J) with BMI add. correction

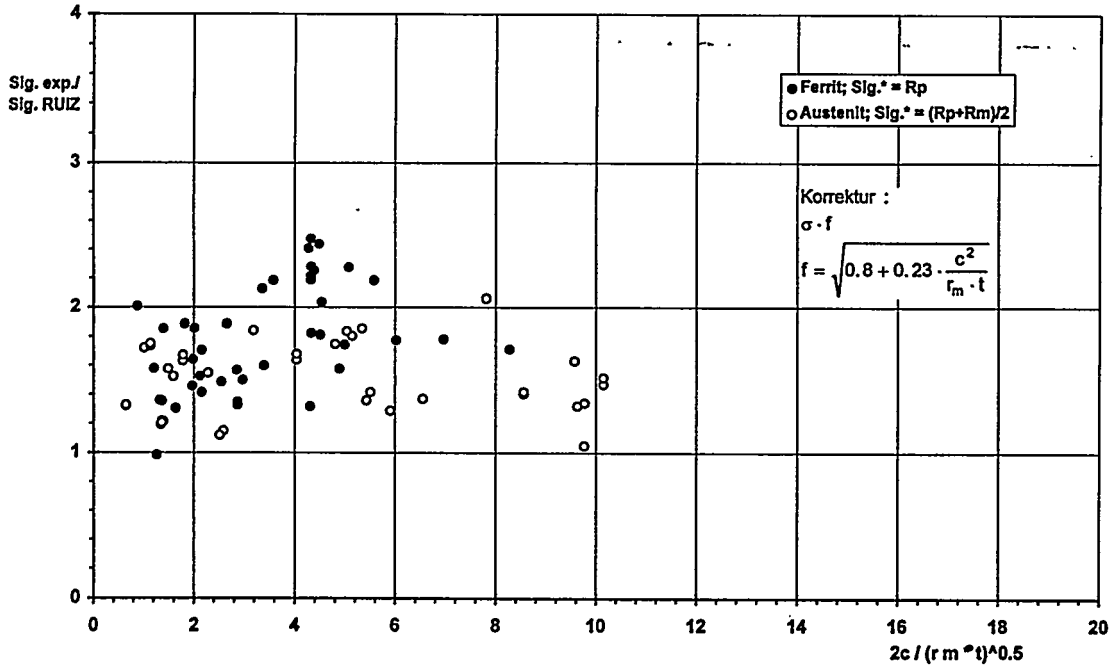

Fig. 13: Longitudinal cracks: All through-wall cracks calculated (KV> 45J) with RUIZ add. correction

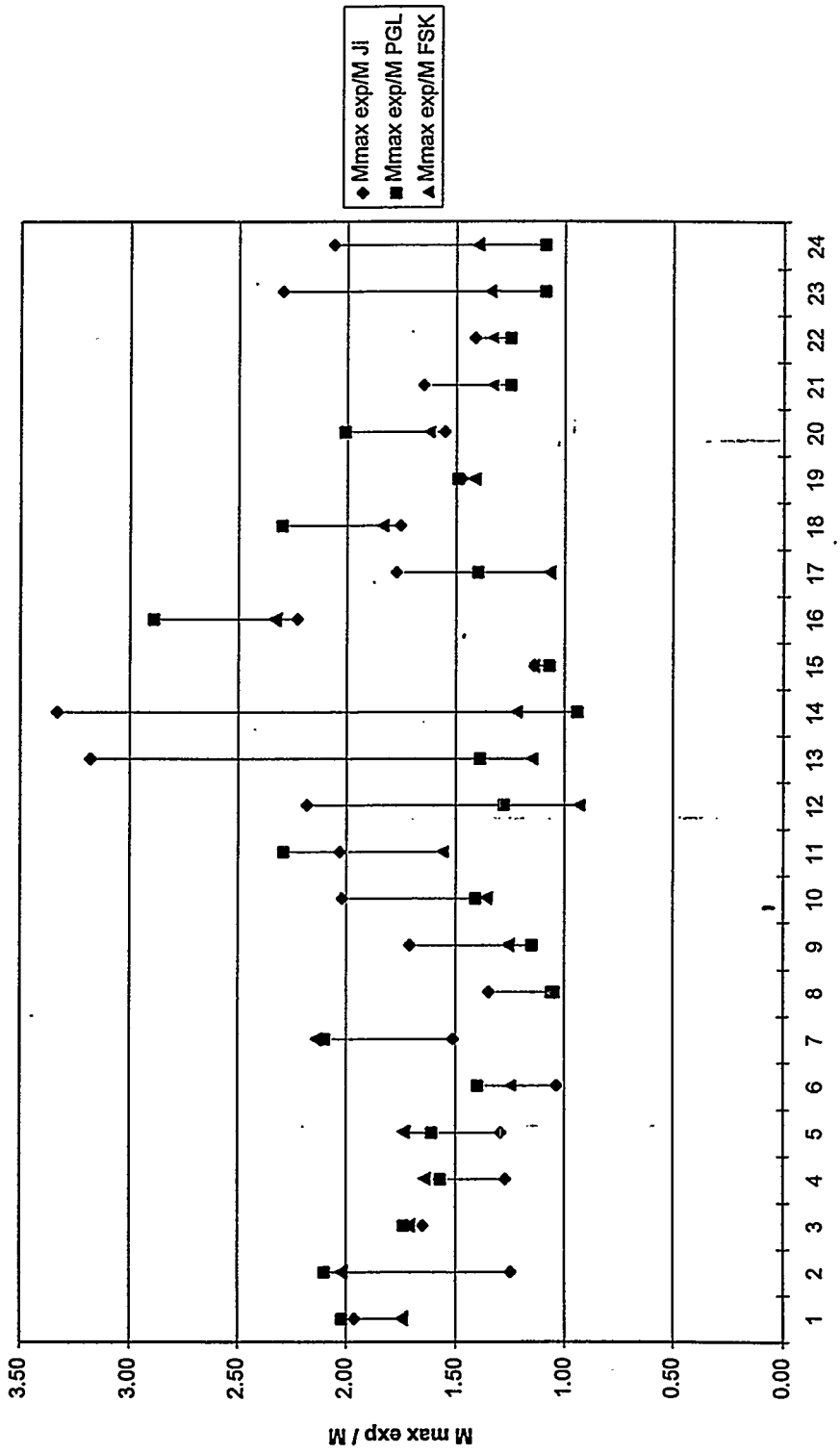

Fig. 14: Comparison of theoretical predictions J_i, FSC, PLL, with BMI-, MPA- and Siemens/Interatom-tests for base material (circumferential cracks)

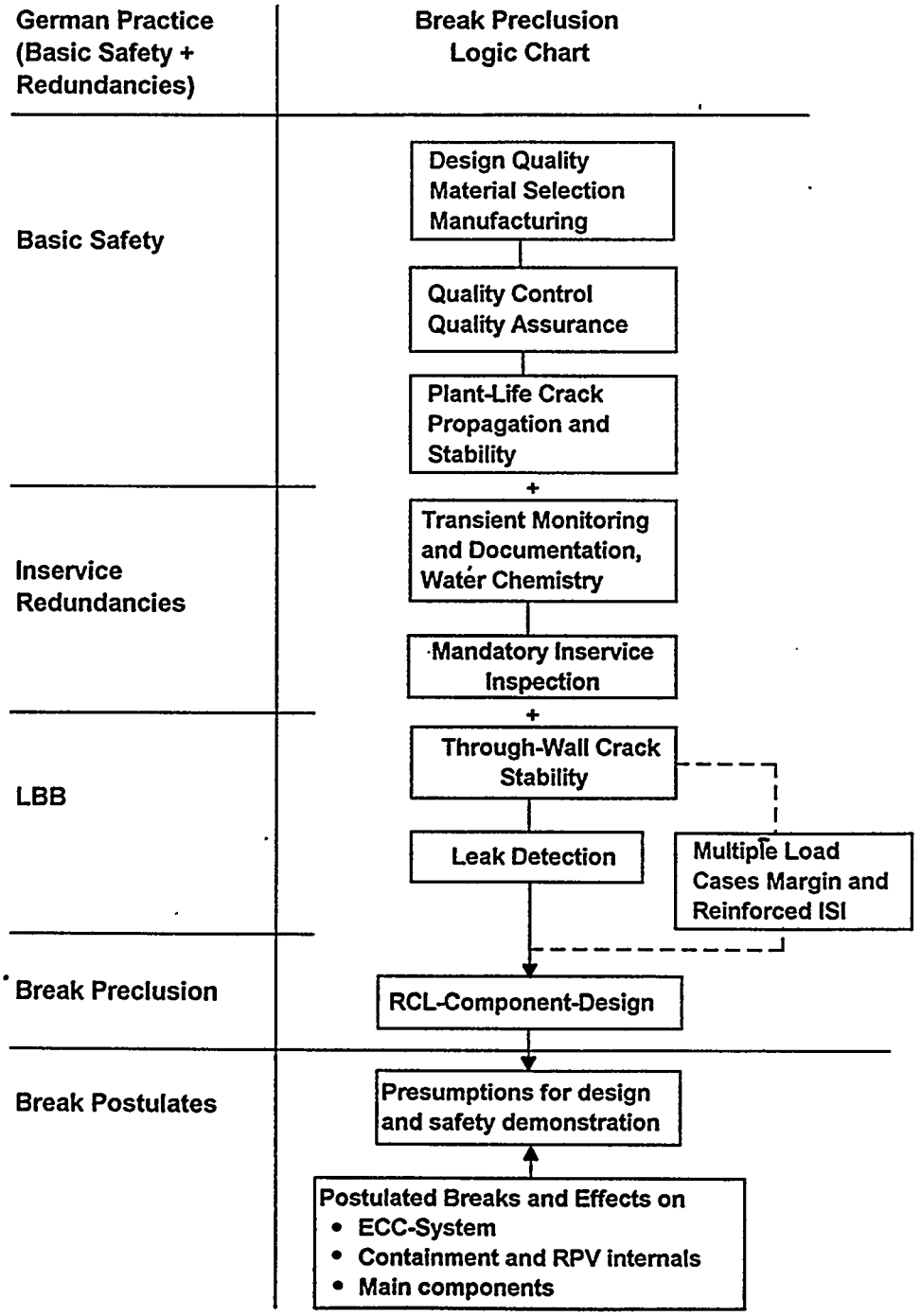

Fig. 15: Break Preclusion Concept according to German practice

Demonstrated by Means of:		Rule	Indication Depth a mm	Indication Length 2c mm	Safety Margin S_c $S_c = \frac{2c_c}{2c}$	Leak Cross Section A mm²	Safety Margin S_A $S_A = \frac{A_c}{A}$
Surface Crack Examination	$2c_0$	KTA 3201	0	0	-	-	-
			1.5	6	-	-	-
UT Examination: Acceptance		KTA 3201	6	10	50	-	-
			4.2	30	17	-	-
UT Examination: In-Service Inspection		KTA 3201.4	3	20	25	-	-
	$2c_f'$			156	3.2		
Leakage Monitoring System:							
• Condensate, Moisture	$2c_0'$	min.	52	70	7	3	70
• Condensate, Moisture		max.	52	130	3.8	10	22
Crit. Through-Wall Crack Length $2c_c$, Cross-Section A_c	$2c_c$		52	500	1	220	1

Fig. 16: Typical analysis of main coolant line of Konvoi (D_i x t = 760 x 52 mm) circumferential crack (Flow Stress Concept, ferritic) and safety margin

Primary System (RSK Guidelines Chapter 21.1, version 3/1984)

	Leak and break postulates	effects
Reactor coolant lines	• 0.1 A, 15 ms, linear	• pressure waves (RPV internals)
	• 0.1 A, steady-state blowdown	• jet force (pipings, components, building) • reaction force (pipings, components, building)
	• < 2A	• LOCA analysis • containment • pressure differences (building) • qualification of I & C
Circumf. nozzle weld	• p·A·S, S = 2	• stability of the components (e. g. RPV, SG, RCP, PRZ)
RPV leak	• 20 cm²	• RPV supporting • RPV internals • LOCA analysis
Austenitic connection lines with DN > 200 (surgeline, ECCS up to the 1st isolation)	• 0.1 A	• jet force (pipings, components, building) • reaction force (pipings, components, building)

(RPV = Reactor Pressure Vessel; SG = Steam Generator; RCP = Reactor Coolant Pump; PRZ = Pressurizer)

Fig. 17: Postulated leaks and breaks for piping systems

"TACIS 91: Application of Leak-Before-Break Concept in VVER 440-230"

Bartholomé G., Siemens KWU, Germany; Faidy C., EdF; Franco C., Framatome, France; A. Getman, VNIIAES, Russia

Specialists Seminar

Leak-Before-Break in Reactor Piping and Vessels

LBB 95

Lyon - 9/11 October 1995

Contents

1 Introduction

In the frame of the TACIS 91-project the applicability of the leak-before-break (LBB) concept of the primary piping in the first generation of VVER-plants in Russia is investigated. The procedures for LBB behaviour used in France and Germany are applied.

With regard to the lack of a containment and the given restrictions of emergency core cooling systems capacities to small diameter pipe breaks, especially the integrity of the primary system is of major concern.

The requirements to be fulfilled acc. to terms of reference (TOR) and the redundancies to be realized (e. g. an adjusted leak detection system) are described in detail.

2 Main Safety Features

Major topics of interest during a safety evaluation of pipework in operating nuclear power stations are external events (e. g. earthquakes) and internal events (e. g. pipe ruptures). Accordingly, the material and structural mechanics aspects of the integrity of such systems will be reviewed. This includes the LBB analysis of the pipings. Emphasis will be on experimental validation of national and international engineering practice for evaluating and optimizing existing installations.

The design criteria of the WWER-plants (design features, regulations, rules, industrial standards) are compared to western standard design. The safety analysis (accident analysis, selection of design basis accidents, operational transients, probabilistic safety and risk analysis, event sequences, etc.) and the lifetime analysis (weak point analysis, evaluation of actual plant conditions, plant life management, preventive maintenance, definition of upgrading measures, monitoring systems, cost-benefit analyses, etc.) are performed.

The main design features [1, 2] are shown in fig. 1. This features are compared with the standardized PWR 1300 "KWU Konvoi" in fig. 2.

In this paper examples are given for the accident spectrum in respect to primary leaks. A comparison of these items is given in fig. 3.

3 TACIS Program 91/1.2/LBB

3.1 Aims of Program [3]

National and international programs for VVER upgrading are going on at this time. As an example of such an attempt the European program TACIS (Technical Assistance for the Community of Independent States) has started the program "Primary Circuit Integrity: Application of Leak Before Break Concept" (TACIS 91/1.2 LBB) within TACIS 91 Nuclear Safety Project, fig. 4 .

The aim of this program is to prove the application of LBB concept to the VVER-440/230 Primary Piping.

The aims of the analysis of a LBB behaviour in the frame of the LBB concept should be:

- to study whether a crack likely to be encountered will not reach a critical length and depth during the plant's anticipated lifetime;

- the critical length has to be based on the maximum accident load (MAL, SSE)

- to study whether a hypothetical through-wall crack will leak at a sufficient rate to ensure its detection before it can grow to a critical size at which failure could occur.

Therefore, the application of the LBB concept to a piping system requires:

- the demonstration that water hammer, corrosion, creep, fatigue, erosion and environmental conditions are remote causes of pipe ruptures;

- to perform a deterministic fracture mechanics evaluation of LBB behaviour and a leak rate evaluation;

- the verification that leak detection systems are sufficiently reliable, redundant, diverse and sensitive, and that margin exsist to detect the through wall flow used ind deterministic fracture mechanics evaluation.

The objective of this TACIS project is to study whether the LBB concept may be applied to the primary circuit of the following VVER-440/230 type units.

- Novovoronezh 3 and 4;

- Kola 1 and 2;

taking into account the units' peculiarities.

3.2 Structure of Program

3.2.1 Main Stage

The first and main stage of this project is the study through analysis and calculations, whether the primary circuit of each plant meets the LBB concept requirements, fig. 5, 6.

3.2.2 Other Stages

The two other stages are, on the one hand, the determinations of requirements for In Service Inspections (ISI) of primary circuit piping and welds to meet the LBB concept, and on the other hand, the determination of requirements for the necessary Leak Detection Systems (LDS).

It is not the aim of this project to include the drawing up of detailed requirements for ISI and LDS. Only the specification of general guidelines, using the results (critical crack, reference flaw, critical leak rate etc.) of the first stage is required.

3.2.3 Future program

The ISI and LDS detailed requirements determination, as well as the finalisation of non destructive testing methods (e. g. US testing) and leak detection system could be the purpose of another TACIS program.

4 LBB Procedures used in TACIS 91/1.2

The procedures of the LBB concept are based on German and French procedures in respect to LBB behaviour, also taking into account international approaches (US, IAEA etc.).

4.1 LBB Concepts in France and Germany

The LBB concept will be based on the methodology used in Germany since 1974 (Basic Safety and LBB behaviour) and the French methodology since 1987 (based on NUREG 1061).

For the piping a LBB behaviour (crack growth through the wall even in multiple specified load collectives producing a leak which can be detected and this leaking crack length having an ample safety margin against the ciritical through wall crack length) has to be shown.

The fracture mechanics approach used for the analysis of LBB behaviour will include

a) accustomed, conservative methods (limit load and flow stress concept) based on available plant specific data (tensile and charpy values). These methods will be used also for screening and sensitivity analysis of the pipings (Siemens)

b) more sophisticated elasto-plastic fracture mechanics methods (J-R-curve approach etc. according to NUREG 1061) based on available plant specific data. This method will be used to establish more realistic margins for the piping. However, if J-R-curves are not available for the plant specific pipings generic and mainly not plant speicific data (J-R-curves etc.) or data drawn from the chemical composition specification will be used (Framatome, EdF).

This procedure (a and b) will be adopted by the partners also for the European Pressurized Water reactor (EPR).

Both methods (a, b) are verified by tests (Germany, France, USA, IPIRG).
Method a) is the basis for the "Break Preclusion" (LBB concept), as proven for all German PWR and BWR main coolant lines.

4.2 Procedure in Germany

4.2.1 Postulated Leaks and Breaks

The demands for postulated leaks and breaks in the FRG are given in [4].

4.2.2 German LBB Concept

Breaks can be precluded if the conditions given below are fulfilled. This generally is called LBB concept.

4.2.2.1 Break Preclusion Concept [4]

The Basic Safety Concept (fig. 7) (the fulfillment of which leads to the Break Preclusion Concept) consists of two main prerequisites

- "Basic Safety"
  and
- "Independent Redundancies"

"Basic Safety" is based on:

"Quality Through Production Principle", e. g.:

- Selection of Materials
- Mechanical Design
- Calculation
- Manufacture and Inspection
- Quality assurance

"Independent Redundancies" are based on:

"Multiple Parties Testing Principle",
"Worst Case Principle",
"Continuous In-Service Monitoring and Documentation Principle" and
"Validation principle", e. g.:

- Hydrostatic Pressure Test
- Inservice Inspection
- Leakage Detection
- LBB Behaviour

4.2.2.2 LBB Behaviour (fig. 8) [1, 4]

The LBB behaviour is an essential part of the break preclusion concept.
The critical crack size for ductile material is determined using fracture mechanics. The growth of stable cracks is only conceivable due to cyclic loading (corrosion has to be precluded). The cyclic crack growth beyond design can lead to two situations:

First situation:	crack growth smaller than critical through wall crack length (LBB) or
Second situation:	crack growth up to a crack length which is greater than the critical throughwall crack length (Break-before-Leak).

If LBB behaviour can be shown, break preclusion is proven with the above stated redundancies; if not, break preclusion is given by applying equivalent safety measures (e. g. ISI, Load Monitoring, Fatigue Monitoring, Continuous Inspection)

4.2.2.3 Fracture Mechanics (fig. 8) [5, 6]

Fracture mechanics methodology and criteria demonstrate LBB behaviour. Siemens performed numerous analyses to preclude breaks based on simplified elasto-plastic fracture mechanics (Flow Stress Concept = FSC, Plastic Limit Load = PLL). The acceptability and applicability of these consepts was discussed with and accepted by the authorities in Germany.

Procedure for fracture mechanics analysis:
- defects to be considered
- fatigue crack growth (FCG)-analysis
- demonstration of LBB fatigue crack growth beyond design ($2c_f'$)

  a) If the crack grows through the wall by fatigue or the ligament breaks without instability in the circumferential or axial direction:
  ($2c_f' < 2c_c$), than "LBB" behaviour

  b) If the crack becomes critical before it grows through the wall:
  ($2c_f' > 2c_c$), than "Break-before-Leak" behaviour.

- analysis of surface crack for end of life (EOL)
- through wall crack (TWC) stability analysis under maximum loads ($2c_c$)
- completeness of loads used for fatigue crack growth and crack stability
- leak rate of stable TWC (leak detection)
- Leak detection system (LDS) [6, 7]

The independent redundancy "LDS" is verified by conventional LDS (temperature, moisture, etc.) and/or acoustic leak monitoring systems ALMS.

Typical locations of sensors for VVER 440/230 (fig. 9) are defined according to the fracture mechanics analysis.

4.2.2.4 Safety Research

- Interpretation of Experimental Results for Austenitic and Ferritic Piping

  All available literature on components testing concerning circumferential and axial through-wall cracks was evaluated by Siemens. The essential data on the geometry of the components and the cracks, on the material properties at test temperature, and on the parameters of loading (i. e. internal pressure, bending moment) were collected in tables. Now the data of about approximately 500 experiments are available.

  The conservatism of the Siemens procedures is checked using these tests. The theoretical value of the failure stress is calculated for the crack length at the begin of the tests and the maximum load using

  - for circumferential through-wall cracks:
    - FSC with material parameter flow stress
      $SF = (RP_{0,2} + R_m)/2$ for austenitic material and
      $SF = (R_m)$ for ferritic material
    - PLL with $SF = Rp_{0,2}$, where $Rp_{0,2}$ and R_m are the the yield and ultimate strength, repectively and

- for axial through-wall cracks:
  - RVIZ-formula with SF = $Rp_{0,2}$ for ferrtic material and SF = $(Rp_{0,2} + R_m)/2$ for austenitic material
  - BMI-formula with SF = $f \cdot Rp_{0,2}$ and $f = 1.7 - 1.2\, Rp_{0,2}/R_m$

- Circumferential Through-Wall-Crack (TWC) (fig. 10)

  The experimental value of the failure stress (sum of the stresses due to measured internal pressure and maximum bending moment at failure) is compared to the theoretical prediction. If the ratio is larger than 1 the procedures FSC and PLL give conservative results.

  The influence of parameters is investigated concerning material properties (toughness, tensile values), dimensions of the components (diameter, wall thickness), loading parameters (Internal pressure, bending moment) and crack lengths. Only the tests with toughness > 45 J (according to [5]) are used for these evaluations and only the material properties of the corresponding base metal are chosen for the prediction, even in the case where the crack was in the weld material.

- Leakage Area and Leak-Rate

  The verification of leakage area and leak rate evaluation by tests is reported in [6, 7].

4.3 French LBB Concept

French rules and regulations relating to pressure components on the one hand, application of the RCCM construction code on the other, involve a certain number of requirements in the design, fabrication and in-service inspection of pressure pipes in pressurized water reactors; the purpose of these requirements is to guarantee circuit integrity not only during normal operation, but also in the case of incidents or accidents.

Furthermore, French regulatory practice is based on the defense "in-depth" principle implying, for the general design of the installation, the study of limited number of postulated piping breaks (longitudinal and circumferential); such breaks may be localized either through conventional approach, or on the basis of mechanistic considerations. Obviously, this method bears heavily not only on the functional design of circuits, but also on the type of supports and their design.

For nuclear units in the design phase, the vendor (FRAMATOME) and the utility (EDF) examine the possibility of applying the LBB concept criterion to a certain number of circuits, particularly the primary circuit and various parts of the secondary circuit. Of course, the purpose of such a course of action is to ascertain, in a first stage, whether any simplification can be obtained in certain equipment such as supports or pipe whip restraints, or even if they may all together be suppressed. In the longer term, it might be possible to rethink the entire layout philosophy of an installation and to arrive at major simplifications.

For the time being, the utility (EDF) has not completed its reflection on the pros and cons of the LBB concept approach and consequently French safety authorities have not been officially notified of any request for assessment of the acceptability of such an approach concerning existing French PWR.

In order to reach an agreement, since 1980, Framatome, the French Utility (EdF) and the Atomic Energy Commission (CEA) have launched fracture mechanic research programs on the validation of the LBB approach applied to austenitic and ferritic pipings. Framatome, CEA and EdF participate to the

IPIRG program (International Piping Integrity Research Group), initiated by NRC. The French safety authorities support this research activity.

On the French Utility's request, Framatome has studied the applicability of the LBB concept concerning the primary loop of reactor N4 (1500 MW, 1987 - 1988) [8, 9].

Numerical methods used for analysis of LBB behaviour approach have been developed and validated from international benchmarks and comparisons with experimental results. For example, fig. 11 visualizes comparisons between J-approach and experimental results on TWC pipes subjected to pressure and bending load. Results are drawn from Degraded Piping Program III [10].

An important numerical program which involved various detailed finite element analysis has been performed to investigate the significance of mismatch effects on structural resistance of weld [11].

Leak rate predictions including two phase flow models have been compared to Siemens investigations on Kozloduj. As indicated on fig. 12, a very good agreement is observed between Siemens and Framatome Codes. An important work has been done in order to predict properly crack areas especially for elbow components [12].

Recently, for the Belgium Compagny Tractebel Framatome has analyzed the primary circuit integrity of two 900 MWe reactors, using strictly the NRC LBB methodology.

4.4 Approach to be Applied in Russia

Due to the experience of Siemens, Framatome and EdF with the analysis of LBB behaviour for VVER-440/230 plants (Greifswald, Bohunice, Kozloduj, IAEA) we could take into account the know how of these analyses.

As the emergency core cooling (ECCS) capacity of VVER 440/230 is based on the break of diameter 32, the consequences of LBB concept have a higher impact than in European countries, where LBB concept only is e.g. for jet and reaction forces. Therefore the LBB concept has to be intensified.

The western rules (US-NRC, France, Germany) clearly exclude the containment design, the ECCS performances and the qualification of the mechanical and electrical equipment from the benefits of the LBB analysis.

The general LBB concept requirements are acc. to Terms of Reference (TOR). The LBB behaviour will be analyzed acc. to the German and French procedures.

5 Status of project

5.1 Completed Work

The work has been completed on

- collection, processing, presentation of initial data
- experimental work
- calculation of earthquake stresses

- proving the absence of corrosion and erosion damage, water hammer, fatigue
- The analysis of results of factory / shop and evaluation of defect detectability has been completed.

5.2 Examples of Performed Work: "Listing of required data"

The national and international approaches need plant specific data.

In order to be able to solve the problem TACIS 91/1.2 (LBB concept) according to terms of reference (TOR) the following required data are listed below.

These data have to be provided for the NPP of Novovoronesh 3 and 4 and Kola 1 and 2.

The input data are necessary for all welds of the main coolant piping and of the surge line, including the bimetallic welds.

- The data have to be provided in tables for each weld, including the base material to the left and the right side. Each weld is characterized by three columns.

Example: Weld Nr. 1

Nr.	Title		CAT	REM	1	CAT	REM		CAT	REM
		left base			weld			right base		
3.1	Grade of mat	XYZ	1	+	YZX	2	+	ZXY	3	+

REM 3.1: Base material (Left) is ...
Weld material is ...
Base material (right) is ...

- Each data has to be categorized (CAT) by
  1. as build
  2. as specified
  3. from other plants
  4. generic

- The tables are split up according to subchapters
  1. Assembly drawings
  2. Detail drawings
  3. Material, manufacture, welding
  4. Defects
  5. Stresses
  6. Leak detection
  7. Failure Probability

- Comments should be given by indexing under "Remarks" (REM)

5.3 Results of the Analysis of LBB Concept

The preliminary results of the calculation of the LBB behaviour by deterministic and probabilistic approach have been obtained. The results show in respect to the implementation of the LBB concept for the NPPs following consequences:

5.3.1 K1, K2-NPP

Results allow to implement LBB concept.

5.3.2 NV3, NV4-NPP

Results allow that LBB concept could be implemented, taking into account the results of the work. Realization in 2 steps:

Step 1 Integrity for Normal Operating Condition (NOC)
It is shown, that a leaking crack can be detected before it reaches the critical size calculated from NOC loads.

Step 2 LBB concept for NOC + SSE (max. acc. load)
Taking into account (NOC + SSE) loads is essential for implementing LBB concept with regard to TOR-Criteria and LBB behaviour acc. to German and NUREG Codes. If the necessary improvements (Analysis of seismicity and seismic stresses and/or implementation of additional optimized seismic supports, etc.) are realized, LBB concept can be implemented.

6 Comparison to other WWER-440/230 plants

The results fit well into the results of Greifswald, Bohunice and Kozloduj. These results are plotted normalized versus the yield strength in fig. 13.

The main coolant and surge lines of different VVER-440/230 have been analysed in respect to LBB behaviour [1, 3, 6, 7]. The conservatism of the analyses can be seen from fig. 13 and 14 showing that all analyses are below the experimental results.

Nomograms (fig. 15) have been developed to calculate critical crack length, leakage area, leakrate and ALMS (acoustic leakage monitoring systems) signal to evaluate and to optimize the effectiveness of the measures of the LBB concept.

7 Recommendations up to now

The main recommendations in respect to LBB concept are:

- Analysis of material, defects and loading

- Proof of LBB behaviour

  - additional nondestructive testing of welds (ISI)
  - installation of an effective leak detection system (LDS)
  - evaluation of dissimilar welds
    (nondestructive testing, toughness properties)
  - LBB behaviour analysis (subcritical crack growth, leakage crack length, critical through wall crack length, leakage area, leakage rate, safety factors) with additional supports.

    Similar recommendations have been derived for the Bulgarian Kozloduj NPP (details see fig. 16, 17, 18).

    The final recommendations will be given in the Final Summary Report.

8 Further work

1. The (first alternative) straight forward way:
   installation of (additional) supports.
   This requires multi-variant calculations of stresses in the pipes with the purpose of optimizing the number and location of supports, procurement of supports, (analysis of building to take over the loads) and their installation.

2. The (second) alternative way is to clarify the level of site seismicity, to take into account the damping effect and (elastic-) plastic stresses when doing the stress calculations. Maybe in this way we will justify the acceptable level of stresses and the installation of supports will not be needed.

3. The (third) alternative way is to increase the strength of piping by improving the quality of flaw detection (and repair) and raising pipe reliability at SSE to the acceptable level.

   The last option is the most economical solution and allows to improve reliability not only for SSE regimes but for all operational regimes. There are doubts on this solution which would be based on probabilistic approaches.

9 Summary

In the frame of the TACIS 91-project TACIS Programm 91/1.2/LBB the LBB concept of the primary piping in the first generation of VVER-plants in Russia is investigated. The procedures used in France and Germany are applied in this project.

- The main safety features and the comparison of design features are given.
- With regard to the lack of a containment and the given restrictions of emergency core cooling systems capacities to small diameter pipe breaks, especially the integrity of the primary system is of major concern.
- The TACIS program is described (aims of program, structure of program, main stages, other stages, future stages).
- The procedures of the LBB concept are explained (TACIS LBB concept, German and French LBB concept, LBB behaviour, fracture mechanics, safety research).
- The status of the project up to now is demonstrated with some results of LBB behaviour .
- The results are compared to other VVER-440/230 NPPS.
- The recommendations from other plants are reported.
- The requirements to be fulfilled and the redundancies to be realized (f. i. an adjusted leak detection system) are described in detail.
- The further work to be done is drafted.

10 Literature

[1] G. Bartholomé, M. Erve
"Evaluation of Operating Plants with Respect to Structural Integrity of Components and Systems"
First International Conference "Problems of Material Science in Manufacture and Service of NPP Equipment" St. Petersburg 17 - 21 June 1991,
Paper 3, p. 3.1 - 3.28

[2] G. Bartholomé, M. Erve, M. Miksch
"Examples for Managing Ageing of Primary Circuit Components of NPP" NS International 4th Annual Scientific & Technical Conference of the Nuclear Society (Nuclear Energy and Human Safety)
Nizhny Novgorod, Russia, 28.06. - 02.07.1993
Paper 21, p. 21.01. - 21.46

[3] G. Bartholomé, C. Faidy, C. Franco
"Safety analysis of VVER-440/230
Primary Piping in Respect to Leak - Before - Break"

International Topical Meeting on VVER Safety, Prague, September 21-23, 1995

[4] G. Bartholomé, G. Schulz
"Basic Safety and Break Preclusion"
2nd Sowjet-German Seminar, 16-22 October 1989, Moscow,
Paper 3, p. 3.1 - 3.24

[5] G. Bartholomé, R. Wellein, G. Senski
"LBB-analysis: Verification of Fracture Mechanics Approaches by Components Testing"
12th SMIRT, 1993, Stuttgart, GF 08/2
p. 393 - 398

[6] G. Bartholomé, W. Kastner
"Requirements on an Acoustic Leak Monitoring System to NPPs with Respect to Mechanical and Thermodynamic Analysis"
European Working Group on Acoustic Emission,
19th EWGAW Meeting, Erlangen, FRG, 3./05.10.1990,
Paper 9, p. 9.1 - 9.17

[7] G. Bartholomé, W. Kastner, E. Keim
"Calculation of Leakage Area and Leakage Rate for the Design of Leakage Detection System"
11th SMIRT, Vol. G2, Paper G22/2, p. 159 - 164
Tokyo, Japan, 18. - 23. August 1991

[8] C. Faidy, P. Jamed, S. Bhandari
"Development in Leak Before Break approach in France Proceed"
Proceed Leak-Before-Break Seminar, Tokyo (1987) (NUREG/CP-0092)

[9] S. Bhandari, Ph. Taupin
"Application of Leak-Before-Break Methodology to demonstrate Leak Before Break behaviour in French PWR's"
Proceed Int. Symposium on PV Technology, Seoul (1989)

[10] B. J. Darlaston, S. Bhandari, Ch. Franco
"Predictions of Failure for Several of the International Pipe Tests Using the R6 Method"
7eme ICPVT 1992, Pressure Vessel Technology vol. 1
Design, Analysis, Materials 327 - 345

[11] Ph. Gilles and Ch. Franco
"A new J-estimation scheme for cracks in mis-matching welds - the ARAMIS method". Mis-Matching of Welds, ESIS 17 (Edited by K.-H. Schwalbe and M. Kocak) 1994, Mechanical Engineering Publications, London, p. 661 - 683

[12] Franco, Ch., Gilles, Ph., Pignol, M.
"Crack opening area estimates in pressurized through wall cracked elbows under bending", to be submitted to LBB 95, Conference 9./11. Oct. 1995

SIEMENS

Main Design Features in Comparison

VVER 440 - V 230	VVER 440 - V 213
Pressurized Water Reactor	
6 SG (6 Loops)	
negative steam bubble coefficient	
RPV with high neutron fluence	
Confinement with Pressure Relief to atmosphere	Confinement with Depressurization System
Safety Systems 2 x 100 %	Safety Systems 3 x 100 %

574

VER - Plants

Figure 1

SIEMENS

Safety Issue		WWER 440 / W 230	WWER 440 / W 213	DWR 1300 "KWU Konvoi"
Containment				
Safety Systems				
Remote Shut Down Station				
Accident Spectrum	Primary Leaks (emergency cooling)			
	Secondary Leaks			
	Steam Generator Tube Leaks			
	Earthquake			
	Aircraft Crash			
	Emergency Power			
	Fire Protection			
	Internal Submergence			

Figure 2

Comparison of Design Features WWER - KWU Konvoi

VVER04.XLS/02.08 1995
S514/B&/KI-10-1

Safety Issue		*WWER 440 / W 230*	*WWER 440 / W 213*	*DWR 1300 "KWU Konvoi"*
Accident Spectrum	Primary Leaks (emergency cooling)	Break of primary connecting piping uo to ND 100 (flow restrictor ND 32 in primary loop)	Break of primary piping (ND 500)	Break of primary piping (ND 750)
External event	Earthquake	not analyzed	not analyzed	mitigated

Figure 3 Comparison of Design Features WWER - KWU Konvoi
(Selected examples of Accident spectrum)

COMMISSION
OF THE EUROPEAN
COMMUNITIES

Electricité de France • Framatome S.A. • Siemens AG

TACIS–91 NUCLEAR SAFETY
Proposal for offer of services for
Technical Assistance to Rosenergoatom reference

Primary Circuit Integrity: Application of Leak Before Break Concept (1.2)

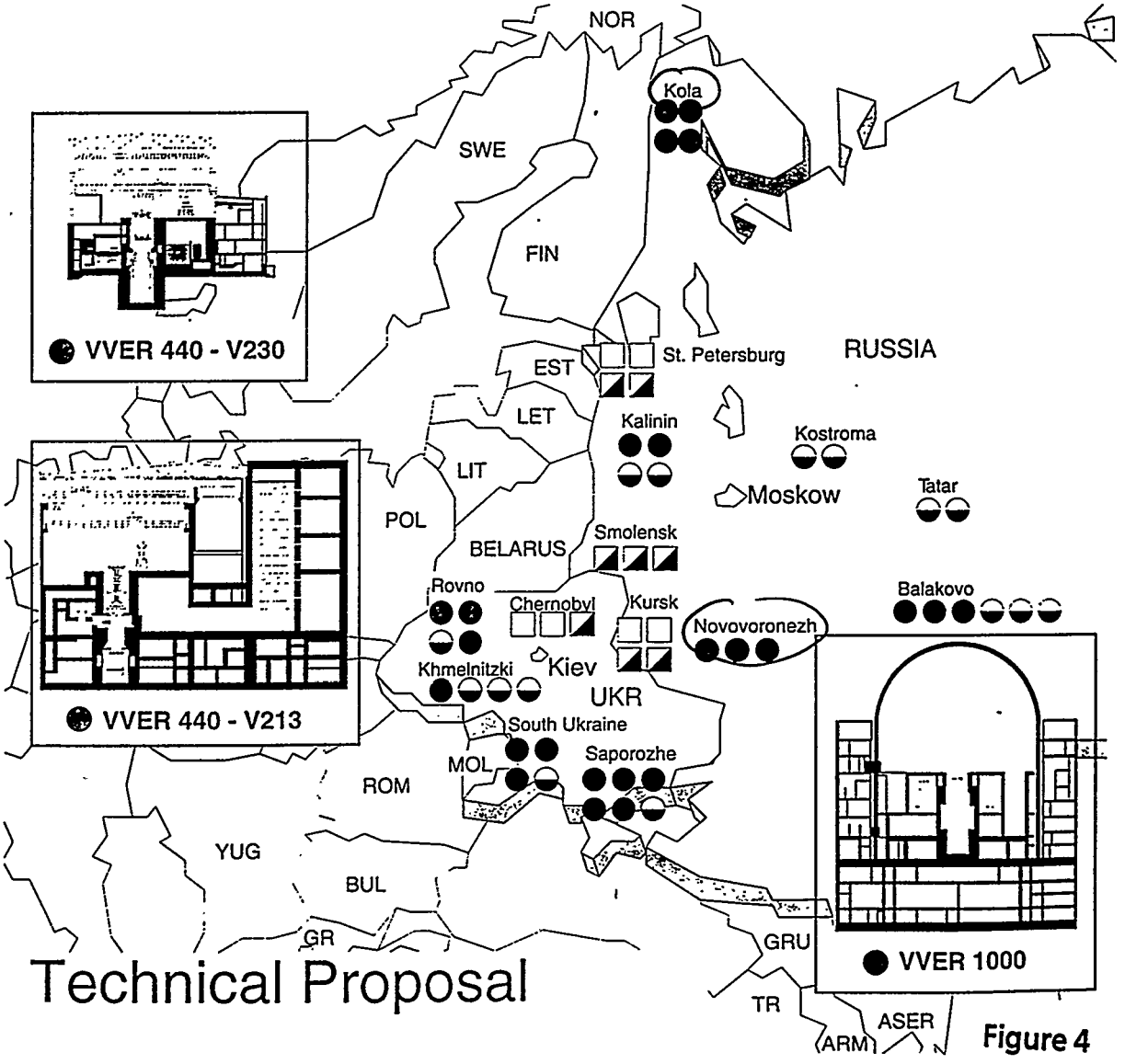

Figure 4

1. Technical Proposal

TACIS '91: LBB

(as used 23. / 24. 11. 93)

Task number	Task title	Phase (1)
1	Listing of required data	1
2	Management of project execution	N/A
3	Subcontracts to Russian counterpart	1 + 2 + 3
4	Evaluation of Kozloduy data and results	3
5	Identification of existing data, translation in English and supply to Consultant	1
6	Verification on site of the conformity of the installation to the design generic documents, identification of the differences, updating of the documentation	2
7	Evaluation of data (5 - 6)	1 + 2
8	Interface document between "R" and "C"	1 + 2 + 3
9	Calculation of new thermal expansion loadings and stresses to taken into account	2
10	Calculation of loads and stresses during an earthquake	2
11	Stress report updating	2
12	Provision of the results of existing fatigue analysis	1
13	Justification of the absence of water hammer	3
14	Justification of the absence of stress corrosion cracking, erosion, corrosion	3
15	Justification that there is no excessive fatigue	3
16	Review and approval of "R" analysis and calculations	3
17	Available data relative to materials (base metal and welds): yield and ultimate stress, toughness, chemical composition	1

Figure 5

Task number	Task title	Phase (1)
18	Data relative to materials: bimetallic welds	2
19	Determination, on the basis of (17) + (18) of the properties of materials, taking into account thermal aging: stress strain curve, tearing resistance, fatigue crack growth law..	3
20	Data relative to non destructive tests performed during manufacture, site erection and in-service: criteria, control methods, results	1
21	Determination of the "reference defect" for fatigue crack growth analysis	3
22	Research on defect detectability	4
23	Design operating transients to be taken into account for the fatigue crack growth analysis	1
24	LBB analysis: a) Identification of critical areas; b) Fatigue crack growth analysis (parametric study); c) Critical crack size, and stability; d) Leak rate calculation	 3 3 3 3
25	LBB final summary report - English	3
26	LBB final summary report - Russian	3
27	Probabilistic LBB analysis a) Feasibility study b) Estimation of the probability of leak or fracture initiation	3
28	Project QA programme	All
29	Recommendations for ISI and LDS	5
30	Obtention of agreement (methodology - results) of the Russian Regulatory Body	3 + 4 + 5

Notes:
(1) See TOR, chapter 5.
(2) With the support of Consultant.
(3) Task number are not sequential
(4) Wniiaes + CSFR

R = CIS
C = Consulta

Figure 6

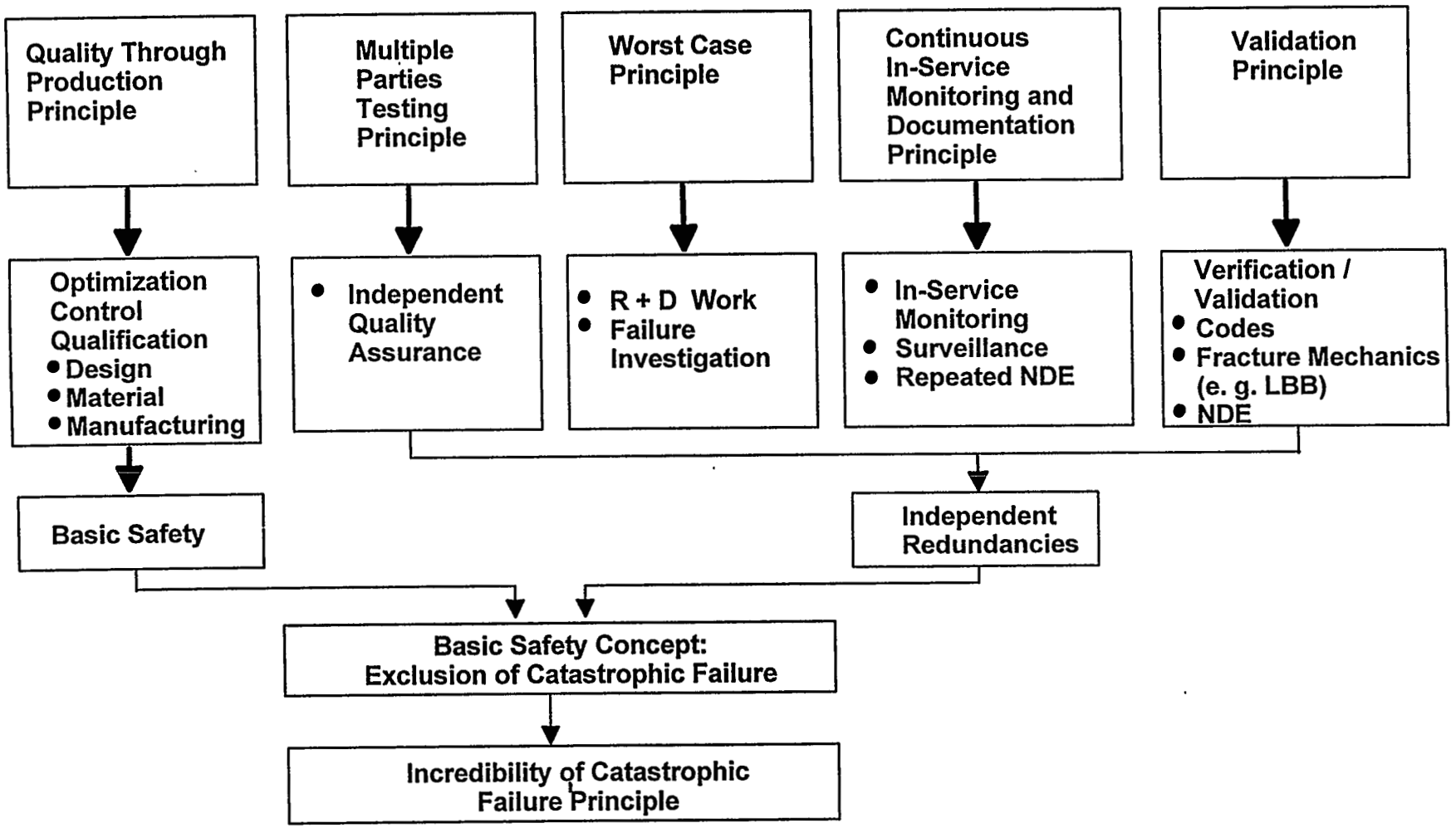

Figure 7

Summary of the Basic Safety Concept

BASAC001.DRW
NT13/d.\Kv\B4\designer

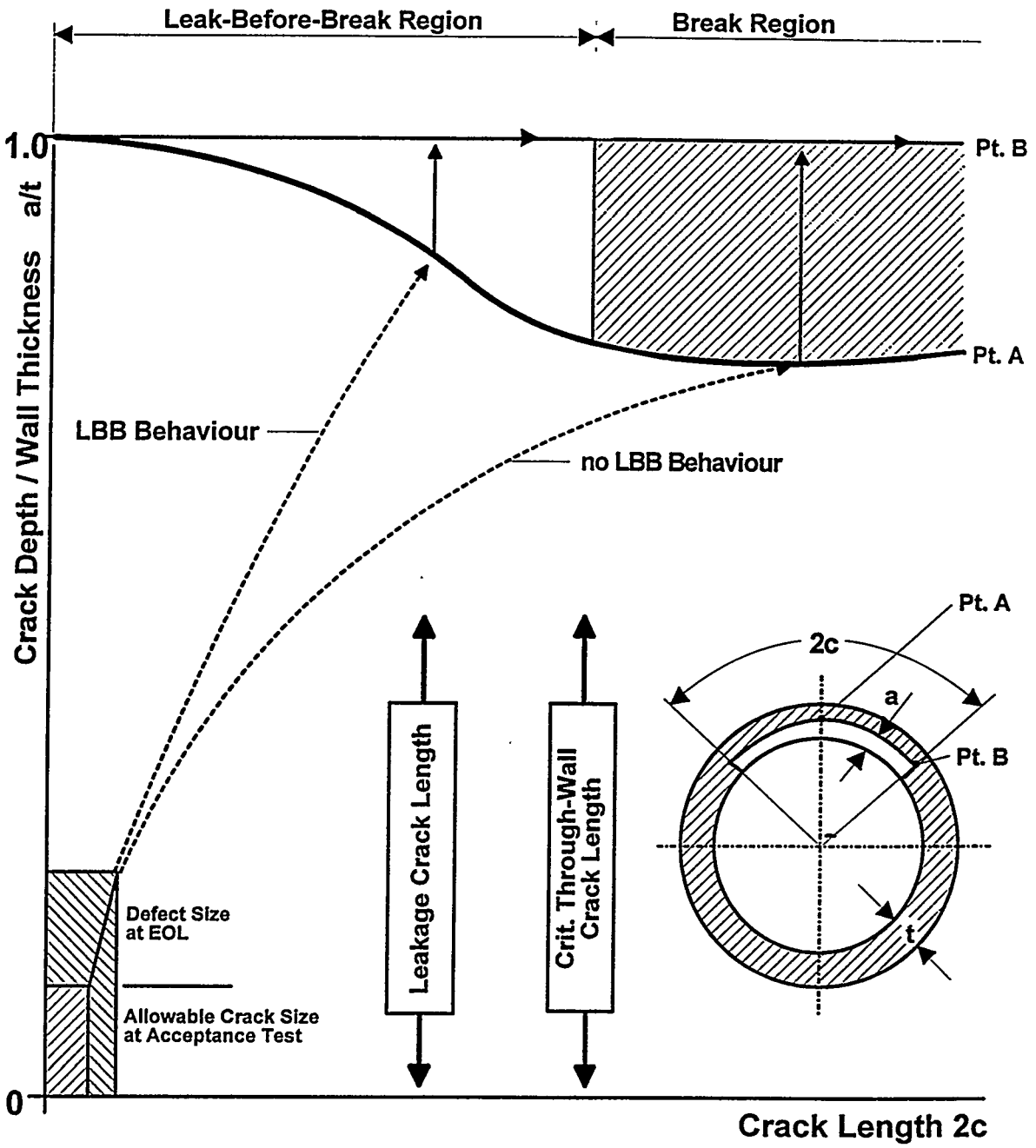

Procedure of Leak - Before - Break (schematic)

BASCHEME.DRW
S514/Wn/KI-09-5

Figure 8

Integrated Concept to Verify the Integrity of Primary Piping and Components

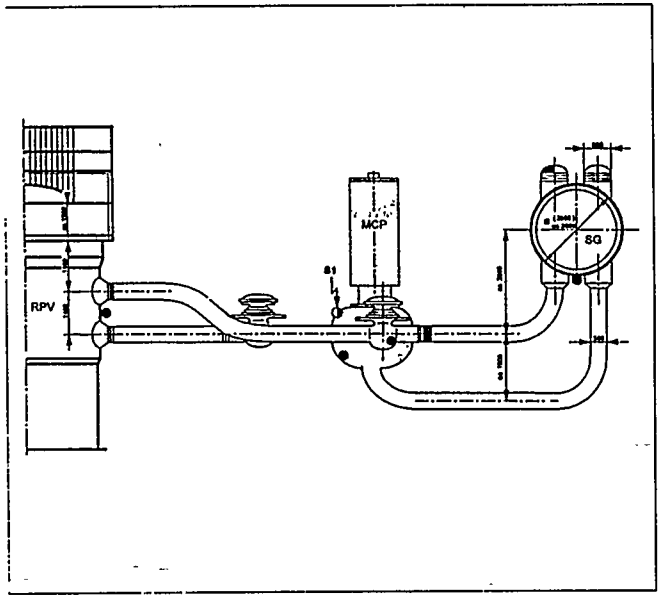

Location of Sensors ALMS

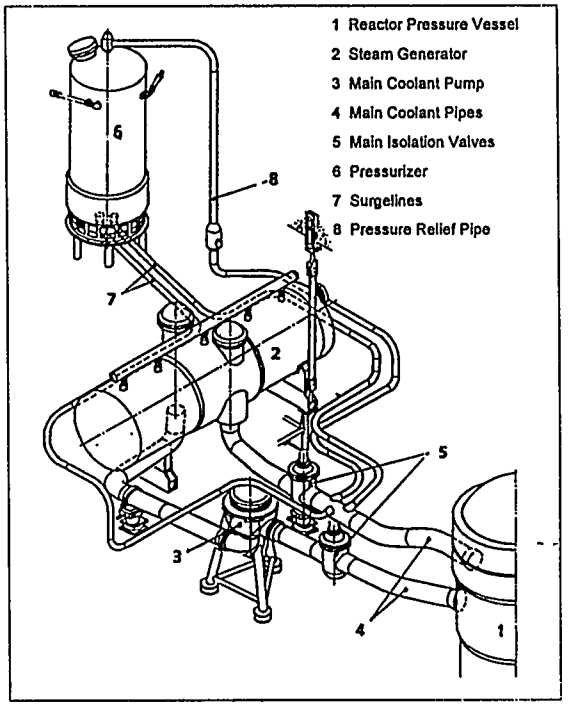

Primary Components of WWER 440/230

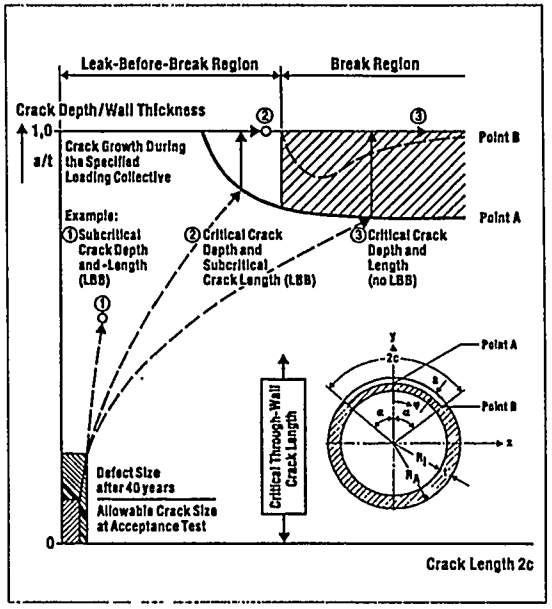

Leak-before-Break Analysis (LBB)

Example: LBB-Analysis and Qualification of ALMS at Greifswald and Kozloduy

LBBVVER.DS4
d:\Ki-Wn-designer

Figure 9

SIEMENS

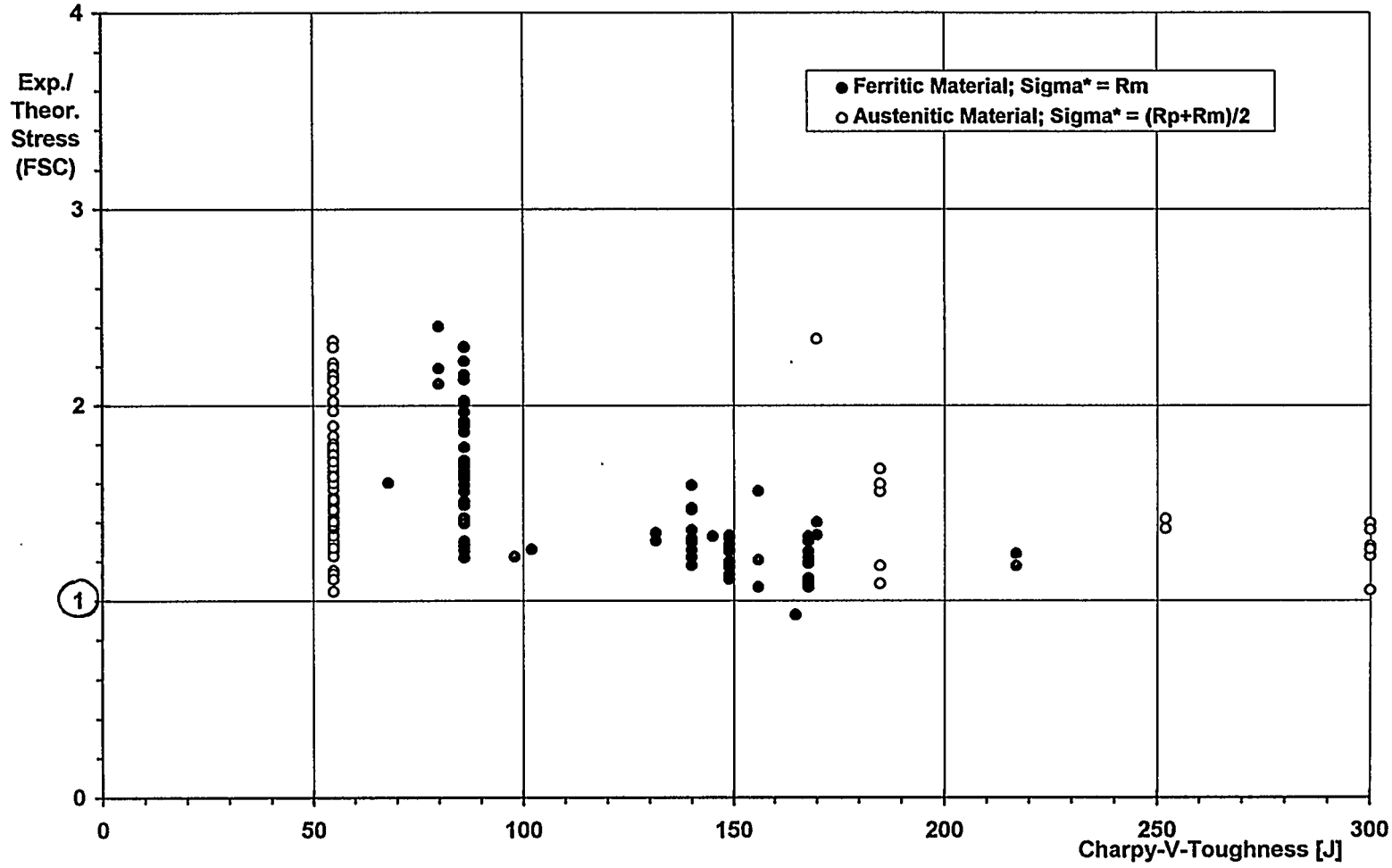

Figure 10

Circumferential Through-Wall Cracks: Flow Stress Concept (FSC)
Using Experiments with Av > 45 J and WM = BM

RRDR-E21.XLS/19.01.1996
NT13/Wn/Ki-09-1

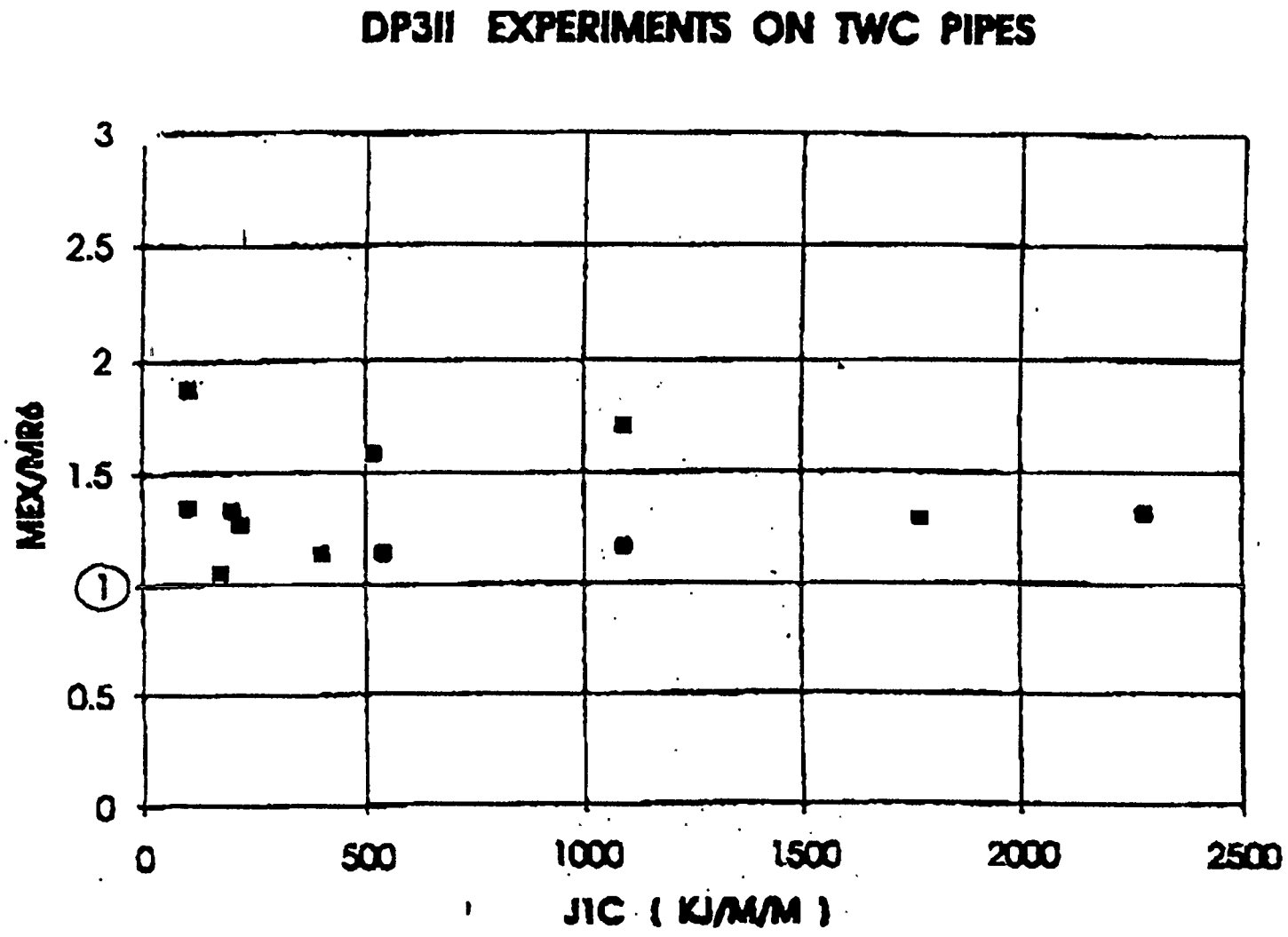

Ratio of experimental to theoretical calculated maximum moment versus toughness property (J_{IC}) (DP3 II Experiments on TWC Pipes)

Figure 11

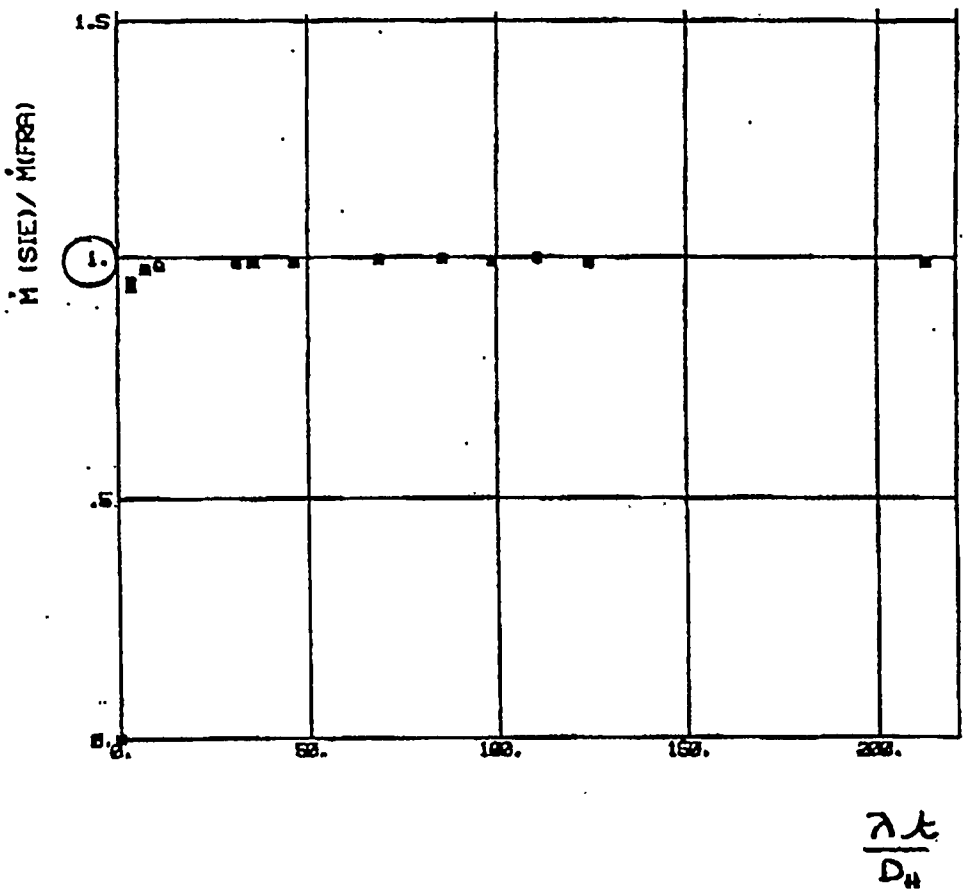

Comparison of flowrates : Code FLORA (Siemens) versus Code ASTEQ (Framatome)
(Based on Siemens / EdF analysis of Kozloduy)
(λ=friction coefficient, t=thickness, D_H=Hydraulic diameter)

Figure 12

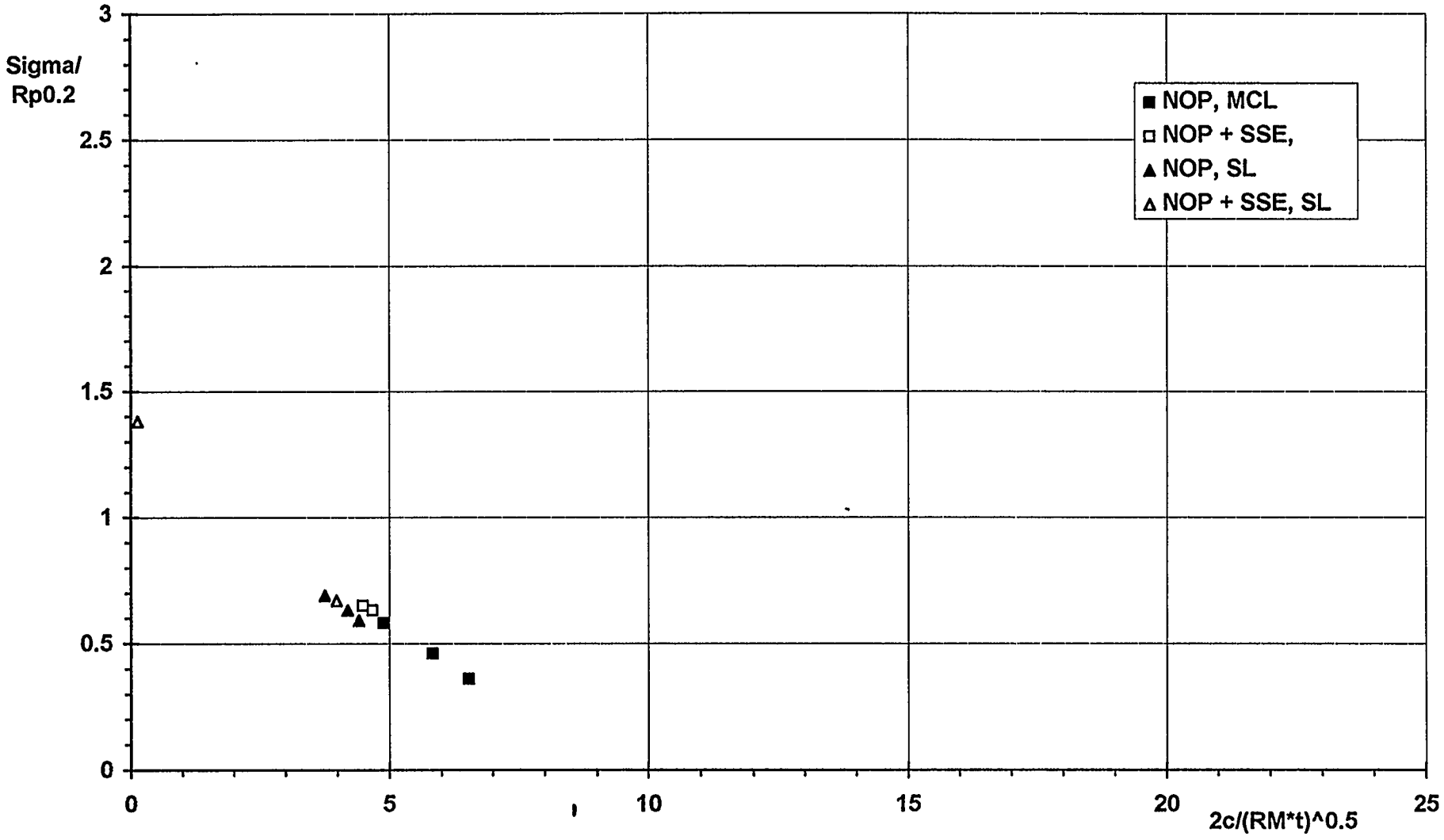

586

Figure 13

Circumferential cracks: ratio stress / yield strength for TWC versus normalized crack length

RR-01-E.XLS/02.08.1995
NT13/Bé/Ki-10-5

SIEMENS

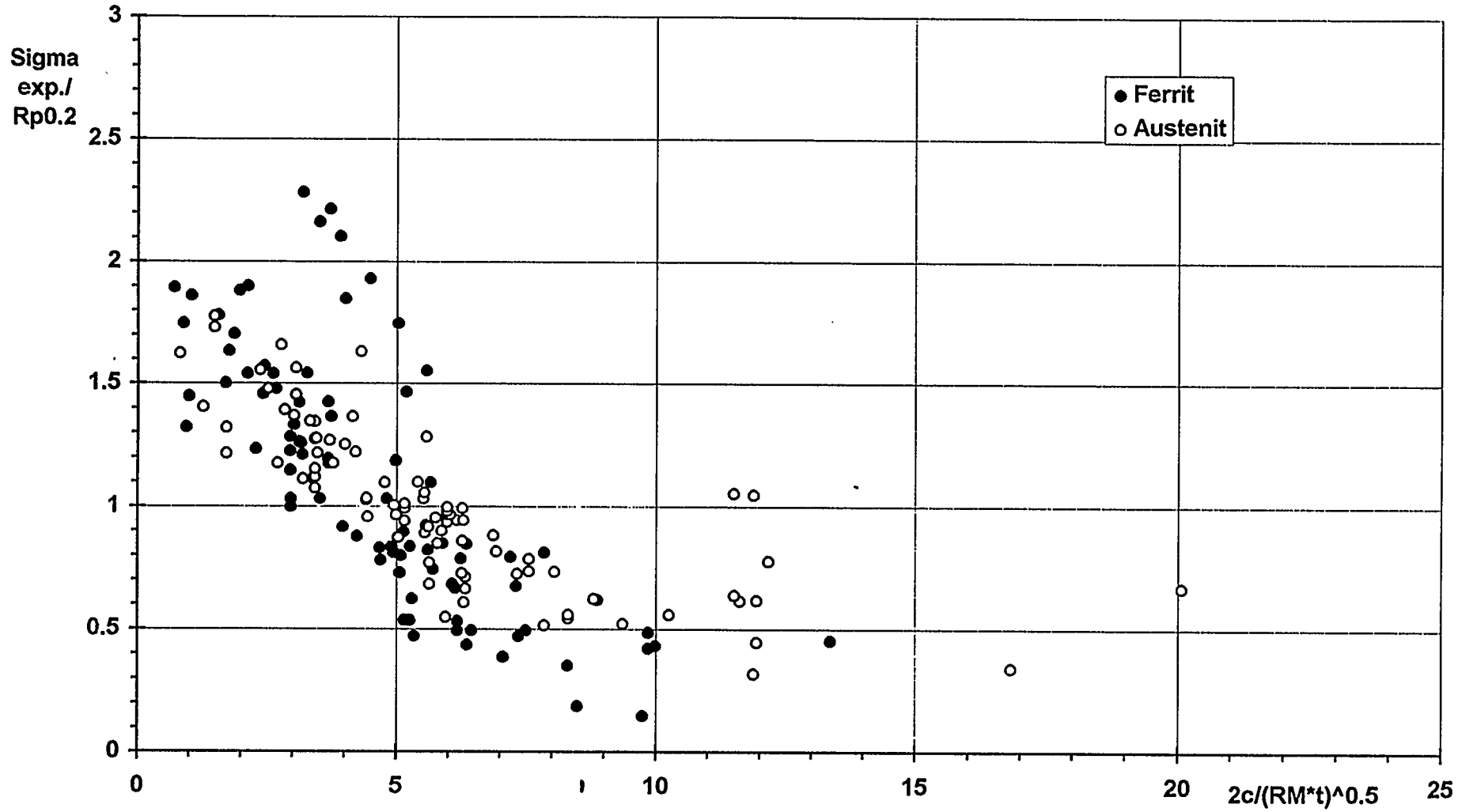

Figure 14

Circumferential crack: ratio of exp. stress to yield strength for TWC versus normal crack length (real $R_{p0.2}$, Base weld, A_v > 45 J)

RR-02-E.XLS/02.08.1995
NT13/Bé/Kl-10-5

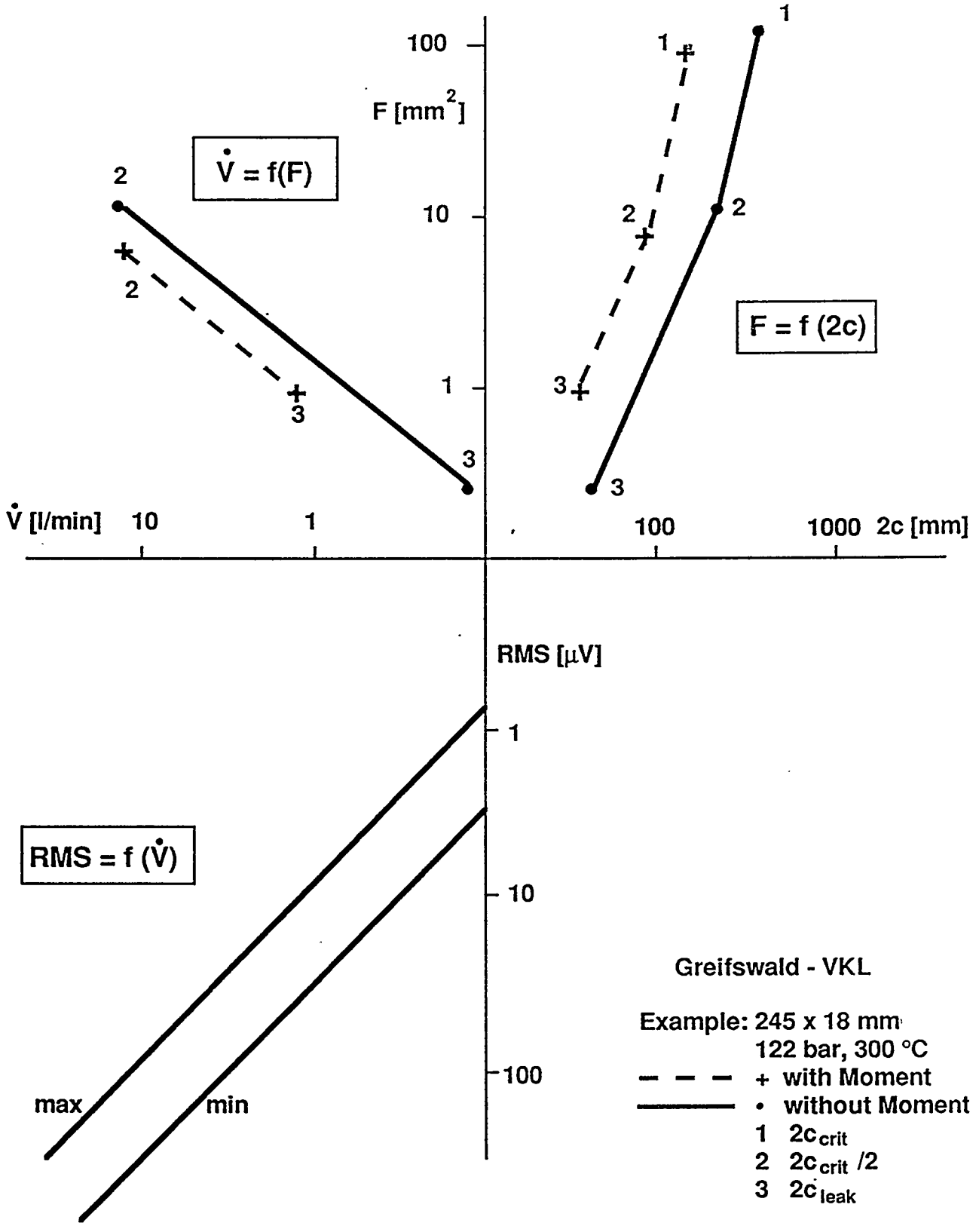

2.11.10e
9.90/E121

Nomogram 3:
Crack Length (2c), Leakage Area (F_{leak})
Leak Rate ($\dot{V}$), RMS-Signal (RMS)

Figure 15

The LBB-analysis in the frame of the WANO 6-Months Programme demonstrated various "weak spots" and problem areas (also taking into account the experience gained with the analysis for NPP Greifswald and Bohunice). It is proposed to gather the necessary informations as soon as possible, in order to have them available at a later stage of the WANO Programme.

The following activities are proposed :

- As a concequence of the very high stresses in the SL for the additional loading case SSE, the dynamic stress analysis should be repeated with optimized supports (especially for the SL). The aim is to reduce the relevant circumferential and axial stresses in the maximum loaded welds to a level where LBB-behaviour can be shown. If there are any necessary modifications of the hardware the static stress analysis should be updated as well.

CONCLUSIONS AND RECOMMENDATIONS (Kozloduj, 1)

Figure 16

- A volumetric non-destructive examination of all welds in the main pipe-werk (e.g. by ultrasonic testing) should be carried out to get informations on real dimensions of defects, i.e. defect depth and defect length. In addition the inner surface of the welds should be examined for defects by means of special ultrasonic testing techniques or by surface crack examination techniques (if accessible).

- According to the dissimilar welds at RPV and PR further informations about material properties (strength and impact energy values as well as crack growth parameters for the various material conditions), defect dimensions (by volumetric NDE) and stresses (due to different expansion of the various materials) are necessary.

CONCLUSIONS AND RECOMMENDATIONS (Kozloduj, 2)

Figure 17

SIEMENS

- A critical review of the operating history is necessary to get better information about the loading conditions in the past and about those expected in the future, especially :

  = temperature measurements concerning thermal stratification of SL

  = inservice measurements concerning vibrations of MCL and SL

  = evaluation of corrosion damage e.g. by a review of the water chemistry

  = evaluation of the occurrence of additional dynamic loads besides SSE, e.g. water-hammer

- Assesment of other leak detection systems besides ALMS, e.g. monitoring systems handling with humidity, radiation, sump level etc.

A re-evaluation of the LBB-analysis should be done in due time.

CONCLUSIONS AND RECOMMENDATIONS (Kozloduj, 3)

Figure 18

THE ANALYSIS OF CRACKS IN HIGH-PRESSURE PIPING AND THEIR EFFECTS ON STRENGTH AND LIFETIME OF CONSTRUCTION COMPONENTS AT THE IGNALINA NUCLEAR PLANT

A.Aleev*,K.Petkevicius, V.Senkus**, A.Ziliukas**, G.Dundulis***, R.Levinskas*****

*Lithuanian Nuclear Power Inspectorate Tel.: +370-2-614427 Fax: +370-2-614487
**Kaunas University of Technology K.Donelaicio st. 73, LT-3006 Kaunas Tel.: +370-7-220411 Fax: +370-7-202640
***Lithuanian Energy Institute: Breslaujos st. 3, LT-3035 Kaunas Tel.: +370-7-757771 Fax: +370-7-751271

ABSTRACT

A number of cracks and damages of other sorts have been identified in the high-pressure parts at the Ignalina Nuclear Plant. They are caused by inadequate production-and repair technologies, as well as by thermal, chemical and mechanical processes of their performance. Several techniques are available as predictions of cracks and other defects of pressurized vessels. The choice of an experimental technique should be based on the level of its agreement with the actual processes.

1. INTRODUCTION

We present the results of our study based on the experimental technique and computer prediction of Safety Assessment in Components with Cracks (SACC), which has been elaborated by Swedish experts and applied primarily to nuclear equipment in Sweden. The SACC computer program predicts both safety and lifetime of construction components with different damages, such as cracks of different locations in pipes, plates and triple joints. It evaluates the probability of a collapse of a structure component, as well as propagation rates of cracks induced either by fatigue or by corrosion. The following types of cracks were considered, Fig. 1:

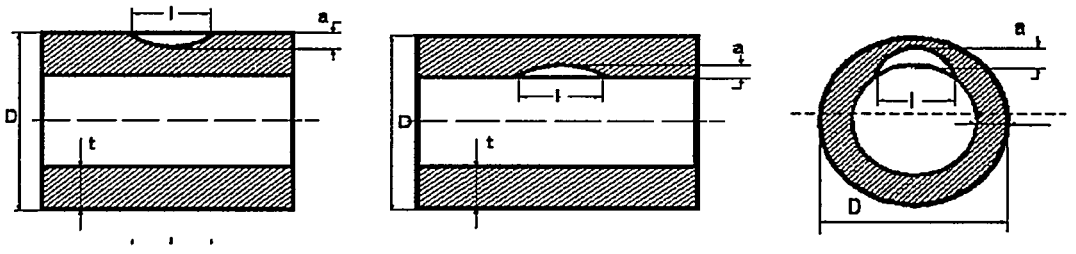

a) b) c)

Fig. 1 A schematic representation of application of SACC: a)- axial crack open at the external surface of a pipe (AI); b)- axial crack open at the internal surface of a pipe (AV); c)- circumferentiall crack open at the internal surface of a pipe (ZV)

The program applies to the above types of cracks for arbitrary stresses. Both linear and non-linear fracture cases can be simulated.

The R6 method was applied to evaluate the safety assessment of construction with cracks. The program includes first options of the method
/1/:

$$f(L_R) = (1 - 0.14L_R^2)[0.3 + 0.7\exp(-0.65L_R^6)] \quad (1)$$

$$K_R = K_I / K_{IC} \le f(L_R) \qquad \text{- by brittle failure}$$

$$L_R = P / P_{cell} \le L_R^{max} = 0.5\left(1+\frac{\sigma_u}{\sigma_y}\right) \qquad \text{- by plastic collapse}$$

Here K_I - is stress intensity factor, MPa$\sqrt{m}$; K_{IC} - critical stress intensity factor, MPa$\sqrt{m}$; P - active load, MPa; P_{coll} - collapse load, MPa.

We separate primary and secondary stresses in the construction components. Primary stresses are induced by loads that lead to plastic deformation over the whole cross section. For internal cracks and for internal or external circumferentially cracks, bending stress must be known along with primary and secondary stresses. Specific properties of the material. such as collapse elasticity and creep limit may be presented for several points in the thickness of the wall. This allows behaviour evaluations for a collapse induced by the temperature gradient or by the increase of brittleness due to radiation. A variation of the physical properties evaluates two boundary states for the hazard of a collapse. For a high creep limit the program simulates an analysis of a linear collapse, and for a high utmost elasticity the program simulates the behaviour at a limiting load. It can predict admissible and critical crack sizes or admissible and critical loads.

The propagation rate of a corrosion-induced crack is found from / 2 /:

$$\frac{dc}{dt} = \left(\frac{K_I}{K_0}\right)^{\alpha} 10^{-11} \qquad (2)$$

with c - size of the crack, m; t - time, h; K_0 and α - material constants for stress corrosion cracking.

The same stresses as in pt. 1. must be evaluated. Here we face the absence of any values for K_0 and α. The data source / 2 / gives the values for austenitic steels in the cooling water of the reactor. For more exact prediction of a collapse, pt.1 of the program must be run for the final size of the crack. The program covers cracks up to 80 % deep in the pipe wall.

Propagation rates of fatigues-induced cracks were found from the Paris equation / 2 /:

$$\frac{dc}{dN} = \left(\frac{\Delta K_I}{\Delta K_0}\right)^{n} 10^{-6} \qquad (3)$$

here ΔK_I - stress intensity range, MPa$\sqrt{m}$; ΔK_0 - material constant for fatigue crack growth, MPa$\sqrt{m}$.

In this approach we employ sum stress states, instead of separate primary and secondary stresses, and present them as data blocks for cyclic loads: 20 such load blocks can be covered with the number of cycles indicated for each. The sequence of summing-up such blocks has no influence on the result. The size of a crack for each number of loading cycles should be compared to the admissible size by pt.1 of the program. Cracks below 80 % of the wall thickness must be included. The results of any strength-and lifetime prediction of damaged structure components are affected by numerous factors, such as geometry, technology of production and repair, physical properties, performance and emergency loads, size and distribution of cracks. Most of the factors can only be evaluated with high error rates which are inevitably reflected in the resulting prediction. To avoid this, a sensitivity analysis may be performed. It also detects the most effective factors and their admissible variation ranges. As the result, closer predictions may be achieved for individual case.

2. MECHANICAL PROPERTIES OF METALS AND THEIR STRESS STATES

Our strength-and lifetime analysis of pressurized vessels covered ∅ 325x15 pipes of group distributors of 08X18H10T stainless steel. They are used for the most important components of nuclear reactor, the results of their defectoscopy are treated with utmost seriousness / 3 /.

The 08X18H10T steel of the pipes of group distributors bears numerous damages of production and repair, such as voids and cracks of inter-crystalline corrosion induced by super-heating in repair. See Table 1 for the physical properties of the steel

Table 1

Param.	Temperature, °C											
	20	50	100	150	200	250	300	350	400	450	500	550
σ_u, MPa	510	471	461	441	421	421	412	412	402	382	353	333
σ_y, MPa	216	206	206	196	187	187	177	177	167	157	147	147
E_0, %	35	32	30	28	27	26	26	25	25	25	25	25
A,%	56	55	55	54	54	53	52	51	50	48	47	45

σ_u - ultimate strength, MPa; σ_y - yield strength, MPa; E_0 - relative elongation, %; A - relative transverse contraction, %.

Utmost admissible temperature for the 08X18H10T steel is 600 C, its thermal resistance is high enough at 550 to 600 C, it is corrosion-proof in water at temperatures up to 360 C and in steam-water mixtures at temperatures up to 650 C. Its corrosion rate at 260 to 315 C is 0.0003 to 0.0018 mm/year.

The pipes operate at internal pressures up to 8.4 MPa, the stresses they induce are primary stresses. The pipes are welded, residual stresses of welding for austenitic steels are secondary stresses, they are determined by / 2 /;

$$\sigma_{rs} = 1.65\sigma_{y\,min} \tag{4}$$

Lifetimes of the pipes were determined for residual stresses of welding, there being no data on residual stresses of rolling, bending and other technologies. The influence of the global bending stress was included because of its high probability.

3. A STRENGTH ANALYSIS OF A PIPE WITH AN INITIAL CRACK

3.1. Estimation of danger failure

Our analysis covered ∅ 325x15 pipes of steel with cracks. Their strength was determined for variable creep limits, utmost resistance, critical stress factors, crack sizes and external loads. Working temperatures and internal stresses were assumed. Admissible and critical crack sizes were determined for variable physical properties. A proportional longitudinal and transverse increase of the crack on a pre-given ratio was assumed. Admissible and critical depths of the cracks are presented in Fig. 2. They suggest an insignificant influence of the length-to-depth ratio on the utmost size of a crack for stresses below 120 MPa$\sqrt{m}$. For circumferentially cracks, important effects of global bending stress and of creep limits of the steels were included. The latter also determines local bending stress in the wall. Axial external cracks are closed up by the internal pressure and are not dangerous. For axial internal cracks the critical stress and the limit creep values are most important.

3.2. Effects of Cracks on Lifetimes of Pipes in Aggressive Media

Propagation rates of cracks in aggressive media may be enhanced by corrosion. The processes are still more active in the presence of stresses. The influence of corrosion is extremely evident in cracks in contact with the circulating heat carrier, the steam-water mixture, that is when they are open the internal surface. Propagation rates of such cracks are closely related to electrochemical metal-fluid reactions and to near-cracks stresses in the metal surface.

Our analysis refers to the lifetime of a pipe as a function of residual stress, see pt.2, for variable factors of the surrounding conditions and of the electrochemical behaviour, which are not known for the metal studied. The other effects were those of the crack size and of global bending stress for circumferentially cracks. Important influences of

residual stresses were observed over the whole range studied. For better lifetime approximations of construction components with cracks in aggressive media, ways must be sought of evaluating the intensity of residual stresses.

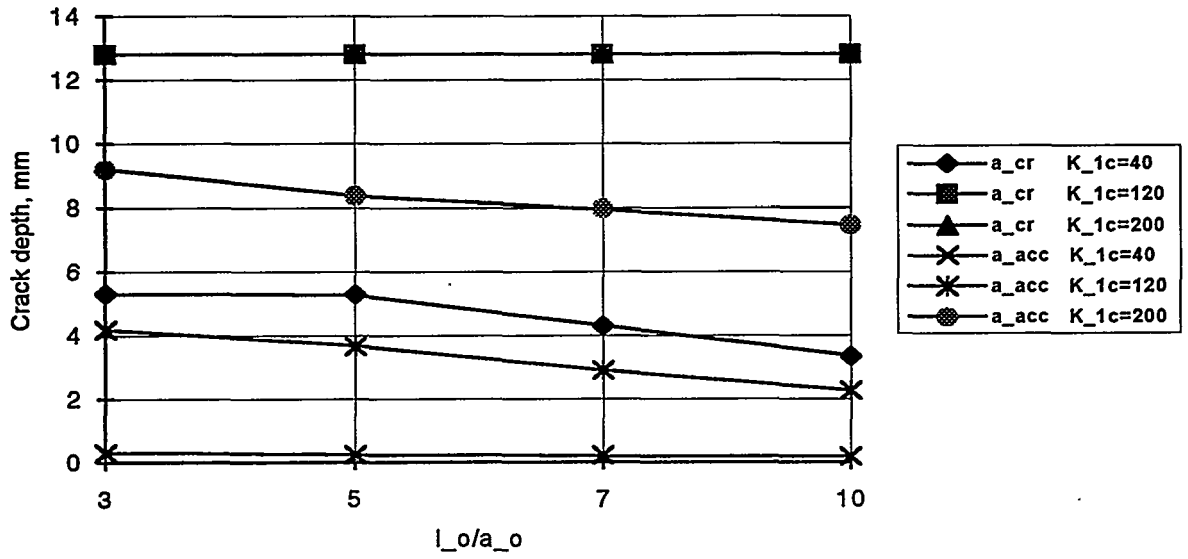

Fig. 2 Critical and acceptable crack depth of a pipe Ø325x15 as a function of rate l/a (σ_{prim}=91 MPa , σ_y=200 MPa,)

A very high influence of global bending stress on the lifetime of a pipe was stated for circumferentially cracks, Fig. 3.Such stresses must be included in any analysis of components with circumferentially cracks. For residual stresses up to 200 MPa, the lifetimes are very different for axial and for circumferentially cracks.

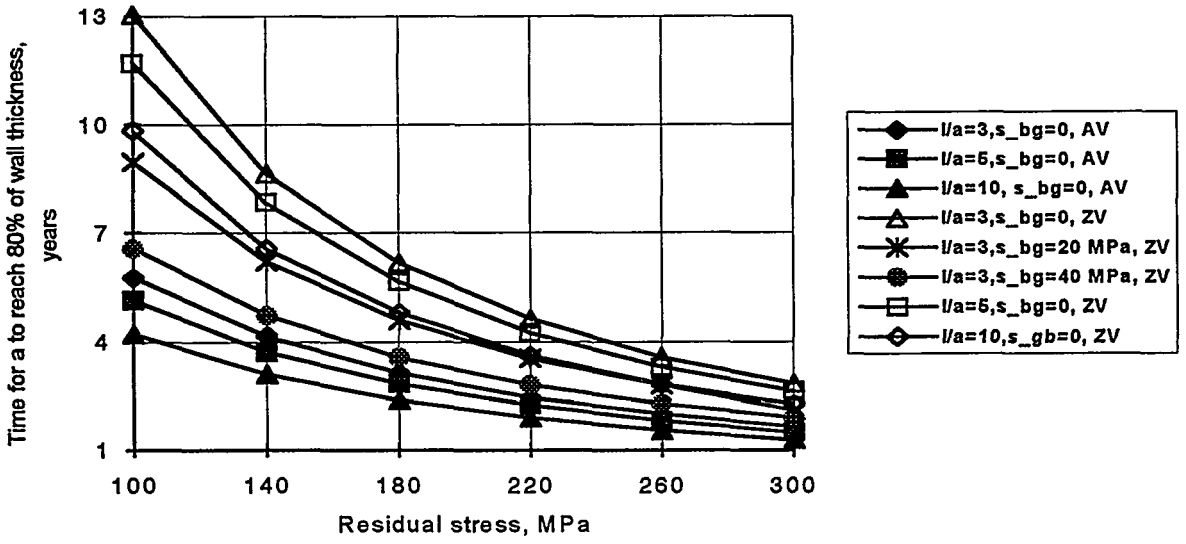

Fig. 3 Lifetime of a pipe Ø325x15 as a function of residual stress (σ_{prim}=91 MPa (AV), and 45.5 MPa (ZV), σ_y=200 MPa, K_0=6.02 MPa$\sqrt{m}$, α=2.161)

Our analysis of the initial depth of a crack suggested its influence on the lifetime only for small depths and low residual stresses, Fig. 4. At higher residual stresses, lower influences of initial crack sizes on the lifetime were predicted.

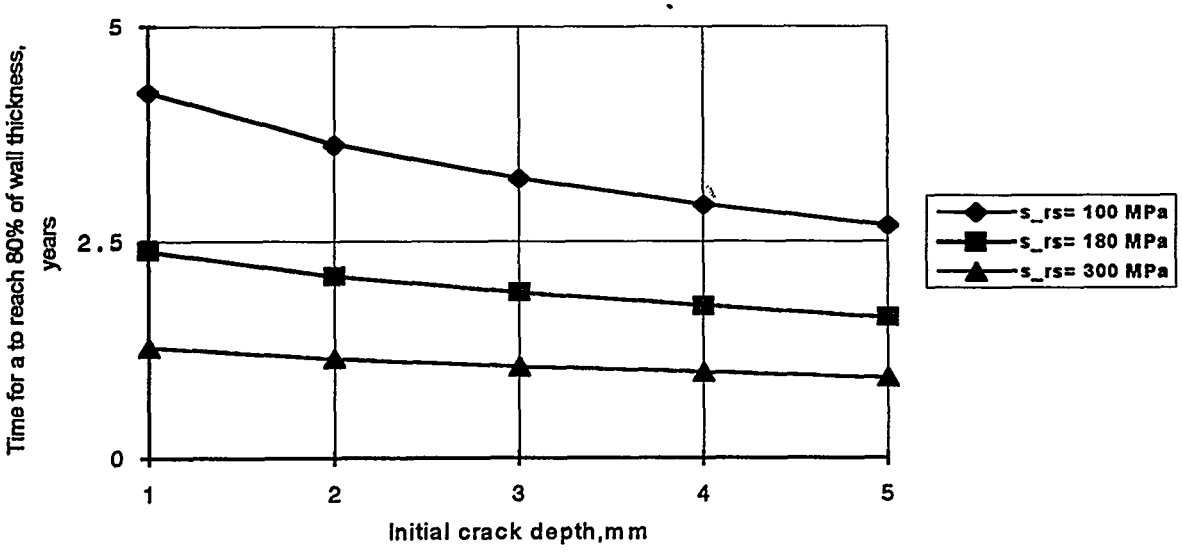

Fig. 4 Lifetime of a pipe Ø325x15 as a function crack depth ($\sigma_{gl.b}$=0, σ_{prim}=91 MPa, σ_y=200 MPa, K_0=6.02 MPa$\sqrt{m}$, α=2.161)

Important influences of factors for corrosive surroundings and for physical properties were found, Fig. 5. Lifetime predictions of structure components with cracks in aggressive media should include exact values of the above factors.

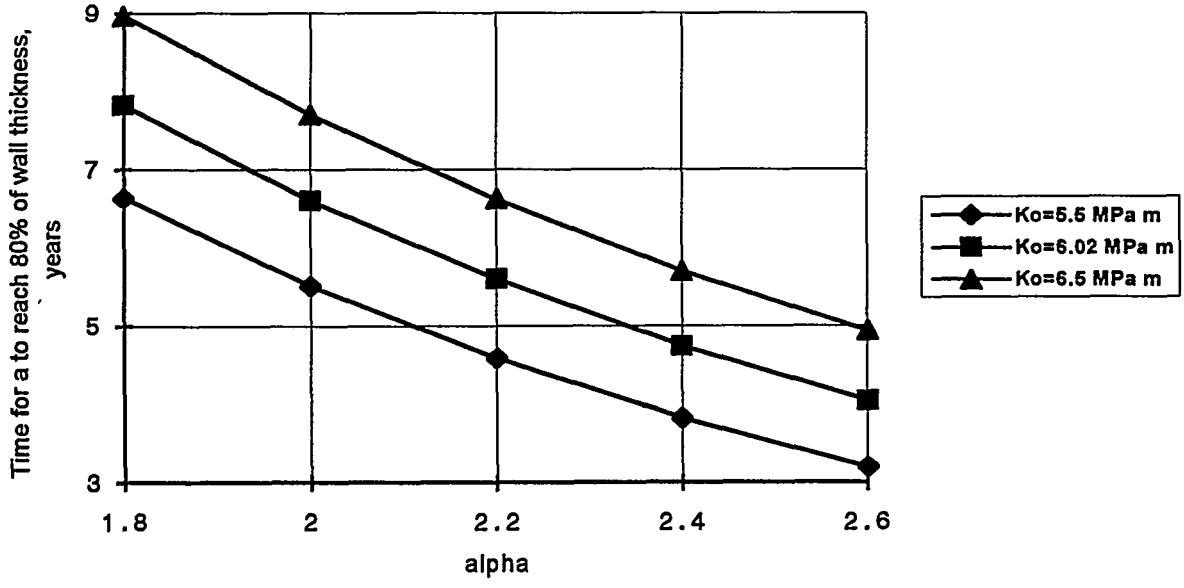

Fig. 5 Lifetime of a pipe Ø325x15 in aggressive media for variable surrounding conditions and physical properties (σ_{bg}=0, $\sigma_{prim\sqrt{}}$=91 MPa, σ_y=180 MPa)

Lifetime predictions of structure components with cracks and with a probability of corrosion must include data on residual stress, bending's stress for circumferentially cracks, and factors for the surrounding conditions and or physical properties.

3.3. Propagation of Fatigue-Induced Cracks

The piping was designed to operate under static loads whenever possible. Variations of internal pressure and of temperature occur at launching, stopping and emergency situations. Therefore the number of loading cycles of important amplitudes of the stress is by no means large.

Another source of loads is due to changes in the conditions of joining and in the mass exchange, it may lead to oscillations of the pipes. This is extremely important for long pipes.

We included in our study the case of an circumferentially crack and assumed the following initial conditions:

- global bending stress ± 2.5, ± 5, ±7.5 MPa;
- initial crack length 1, 4 and 8 mm;
- initial length-to-depth ratio 2, 3 and 4.

To evaluate the influence of physical properties of a pipe on its lifetime, several values of ΔK_0 were computed. The value of ΔK_0 was chosen from the data source / 2 / for austenitic steel SS 2333 in the reactor water environment for 8 ppm oxygen at 288 C. The values were $\Delta K_0=31.2(1-R)^{0.5}$ and n=3.45.

The tests suggest some influence of the length-to-depth ratio only for small initial depths (a_0= 1 mm), and no important influence for larger values of a_0. Important influences of factor ΔK_0 of global bending stress σ_{bg} and initial crack length a_0 were noted. The effects of these factors on the lifetime of a damaged pipe are presented in Fig. 6, Fig. 7 and Fig. 8.

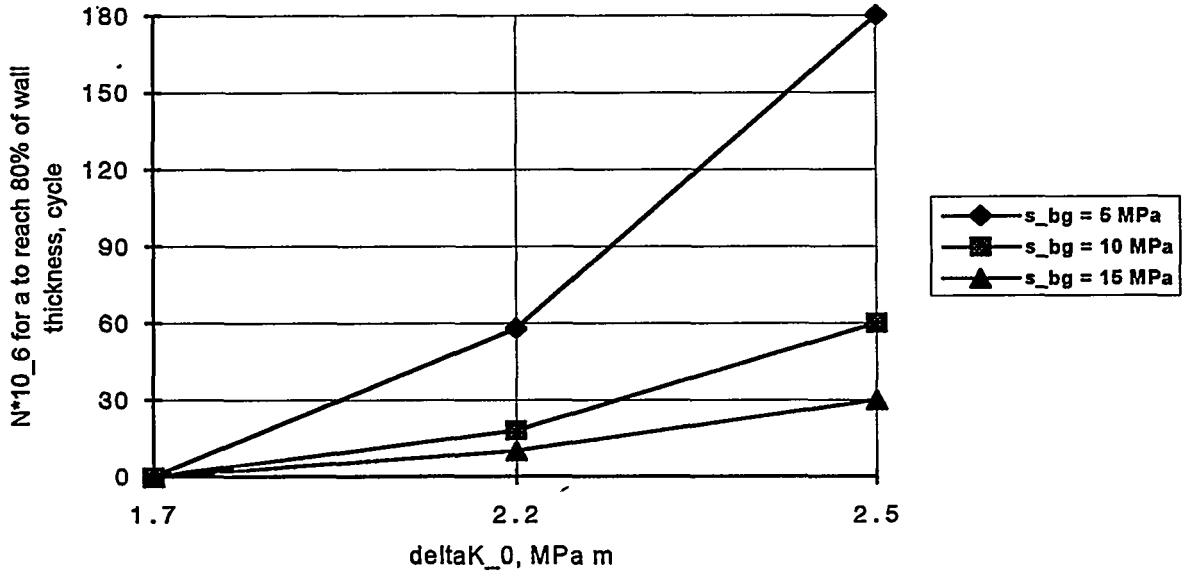

Fig. 6 Durability of high pressure pipe Ø325x15 mm as a function material constant for fatigue crack growth (σ_{prim}=91 MPa , σ_y=200 MPa, R=0.5)

4. CONCLUSIONS

The influences of cracks on lifetimes of Ø 325x15 steel pipes were studied by the Safety Assessment of Components with Cracks technique elaborated in Sweden by Svensk Anlaggningsprovning.

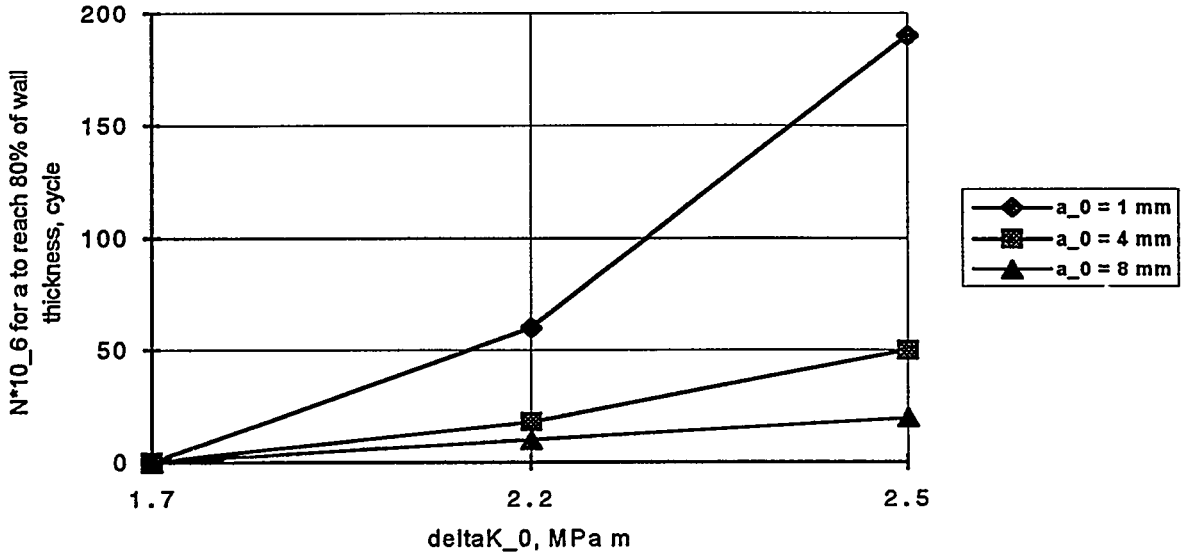

Fig. 7 Durability of high pressure pipe Ø325x15 mm as a function material constant for fatigue crack growth (σ_{prim}=91 MPa , σ_y=200 MPa, R=0.5)

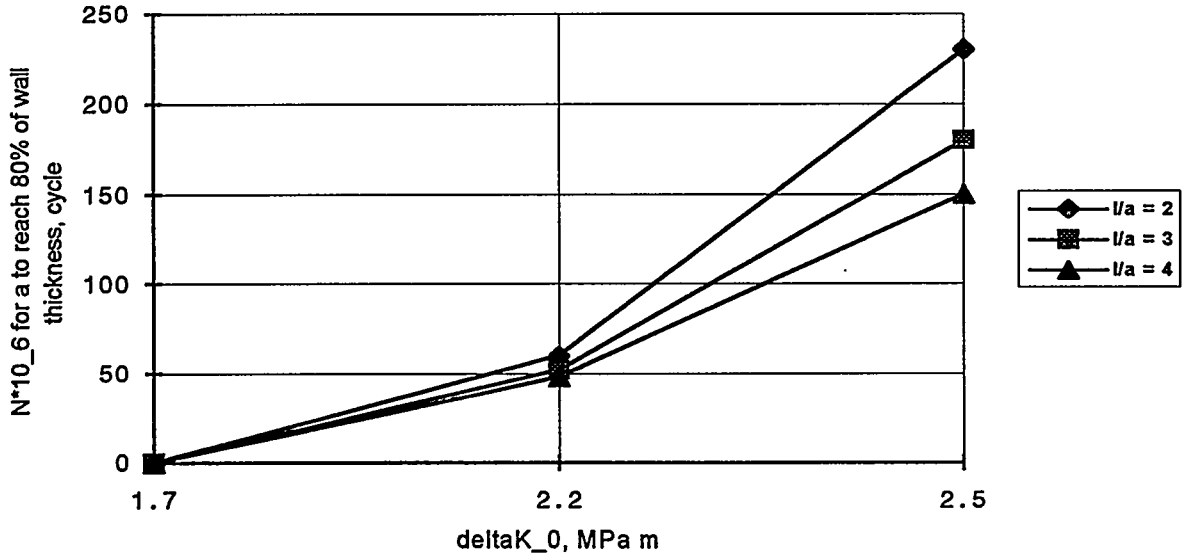

Fig. 8 Durability of high pressure pipe Ø325x15 mm as a function material constant for fatigue crack growth (σ_{prim}=91 MPa , σ_y=200 MPa, R=0.5)

The predictions assumed conservative evaluations of residual stresses related to the creep limit of the metal. More favorable predictions of strength and lifetime could be achieved with more exact values residual stress.

Our study of strength and lifetime of Ø 325x15 steel pipes under the effects of cracks leads to the following conclusions:

1. For an axial crack open at the external or the internal surface of a pipe, both the admissible and the critical sizes of the cracks are closely dependent on the critical stress factor of the steel. Any evaluation of safety must include experimental values of critical stress or of fracture toughness.

2. For circumferentially cracks open at the internal surface, the critical crack sizes are closely related to

global bending stresses in the pipe walls. Their values must be known in any prediction of the effects of a crack.

3. Crack shapes described as their length-to-depth ratios are less important in the range (1/d = 3 to 5) studied. A sensitivity analysis may be performed with just one of the dimensions to check up the reliability of a result.

Lifetime evaluations of damaged structure components subject to corrosion must include the values of factors for the physical behaviour of the metal in corrosion and for the corrosive surroundings.

Propagation rates fatigue-induced cracks depend on their behaviour in fatigue and on the type of loading. Any lifetime evaluation of a damaged pipe must include data on its cyclic load, as well as on frequency and amplitude of its oscillation.

5. REFERENCES

1. The International Journal of Pressure Vessels and Piping. Editor R.W. Nichols, Galliard Ltd., vol. 32, 1988.
2. A Procedure For Safety Assessment of Components With Cracks - Handbook. Mats Bergman, Bjorn Brickstad, Lars Dahlberg, Fred Nilsson and Iradj Sattari-Far. SA/FoU-Report 91/01
3. K. Almenas, A. Kaliatka, and E. Uspuras, Ignalina RBMK-1500, A Source Book, Ignalina Safety Analysis Group, Lithuanian Energy Institute, ISBN 9986-475-02-3, Kaunas, 1994.

ADVANCED LBB METHODOLOGY AND CONSIDERATIONS

R. Olson, S. Rahman, P. Scott, R. Mohan, T. Kilinski
D. Rudland, P. Krishnaswamy, A. Hopper, and G. Wilkowski
BATTELLE, Columbus, Ohio USA

ABSTRACT

LBB applications have existed in many industries and more recently have been applied in the nuclear industry under limited circumstances. Research over the past 10 years has evolved the technology so that more advanced consideration of LBB can now be given. Some of the advanced considerations for nuclear plants subjected to seismic loading evaluations are summarized in this paper.

INTRODUCTION

The application of LBB in the nuclear industry is founded on four basic principles:

(1) Identification of the locations where loads are high in the piping system

(2) Postulation of credible-sized flaws at the high-stress locations, based on leak rate or NDE detectability

(3) Evaluation of the critical flaw size that would result in unstable crack growth, i.e., a double-ended pipe break

(4) An assessment of the margin between the postulated flaw and the critical flaw.

Since the concept of LBB was first advanced for eliminating the dynamic effects of postulated pipe ruptures from the design basis in nuclear power plant piping, knowledge of material property behavior has grown considerably, improvements have been made in leak-rate evaluation, and the state of the art in fracture mechanics has advanced considerably. These enhanced capabilities allow plant owners/designers to take advantage of additional margins that were not previously known or they allow them to avoid unconservative conditions in LBB.

MATERIAL BEHAVIOR CONSIDERATIONS

Material behavior considerations in LBB applications have been dominated by quasi-static specimen testing at plant operating temperatures. More recently, research has suggested that high-rate, i.e., dynamic results typical of a seismic event, and cyclic effects may play a significant role in determining the ultimate behavior of a crack in a pipe. Furthermore, there is evidence, based on the results of pipe and specimen fracture testing, that these two effects interact.

Figure 1 shows a functional relationship between the ratio of cyclic to monotonic J and the yield-to- ultimate strength ratio (J in this case is J after some small amount of crack extension). The data suggest that the cyclic J is a fraction of the monotonic J and that the cyclic effect is material independent. The data also suggest that as the ratio of yield to ultimate strength increases, cyclic effects begin to disappear. In this figure, fully reversed cyclic loading (R = -1) data were used. Evaluation of trends with different R-ratios is in progress. Additionally, analytic work has shown that the R-ratio tends to be more negative in cracked pipe than uncracked pipe (Ref. 1).

The effect of loading rate on J is shown in Figure 2. In this case, there are different curves for ferritic and austenitic steels. For the case of austenitic steel, the data suggest that toughness is generally greater under dynamic loading, while for ferritic pipe materials, there is a reduction in toughness under dynamic conditions for the lower yield-to-ultimate strength ratios and an increase in toughness for the higher yield-to-ultimate strength ratios. In either case, the effect of dynamics becomes more pronounced as the yield-to-ultimate strength ratio increases.

In many practical LBB evaluation cases, i.e., under seismic loading, cyclic and dynamic effects are combined. In some cases the effects are additive and other cases the effects compete. The data indicate that using quasi-static toughness data, as has been traditionally done, may not be adequate for all cases.

LEAK-RATE EVALUATION CONSIDERATIONS

The application of LBB methodology frequently requires the calculation of leak rates from through-wall cracks. Traditionally, idealized crack geometry conditions are assumed when leak rates are calculated. There are, however, other factors which have been recently identified as having a role in determining the leak rate that could impact a decision to implement LBB in a plant.

Residual Stresses

Pipe-to-pipe, pipe-to-elbow, pipe-to-valve, and pipe-to-reducer welds in nuclear power plants all represent potential sites for initiation of cracking. Frequently, such welds are not stress relieved, so there are residual stresses that will modify the crack opening (Ref. 2).

The data in Figures 3 and 4 indicate that the effect of residual stress is more pronounced when the applied stress is low and that thinner-wall small-diameter pipe is more affected by residual stresses

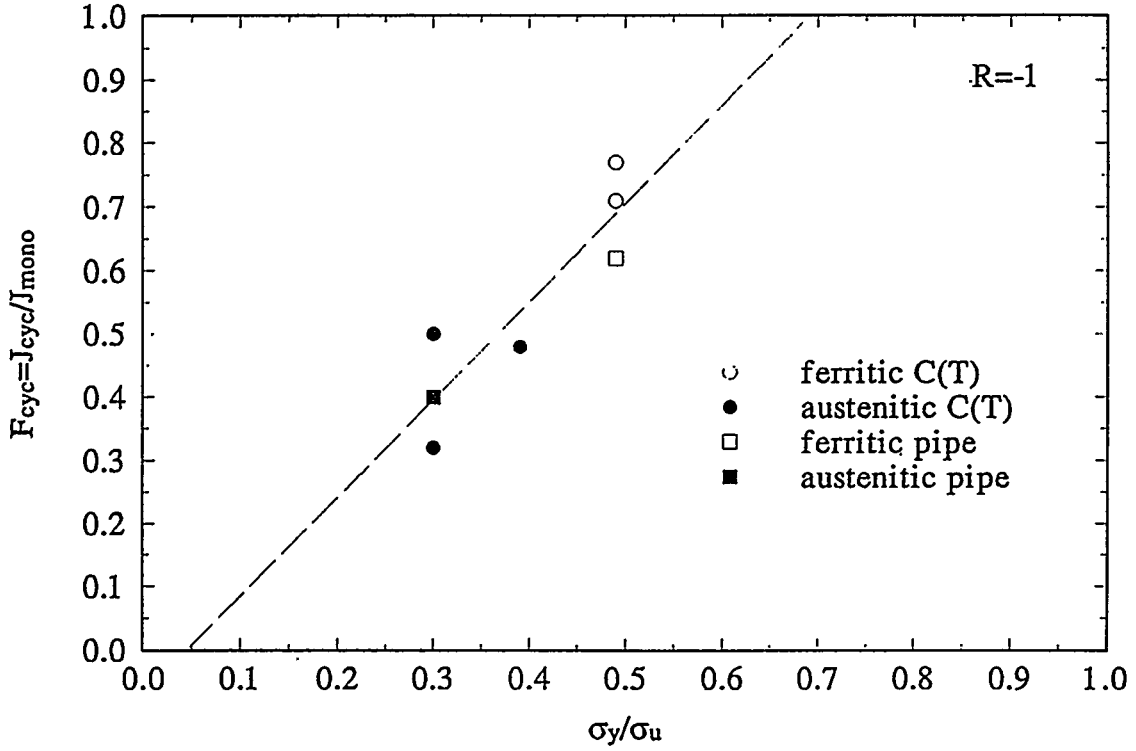

Figure 1 The effect of cyclic loading on fracture toughness

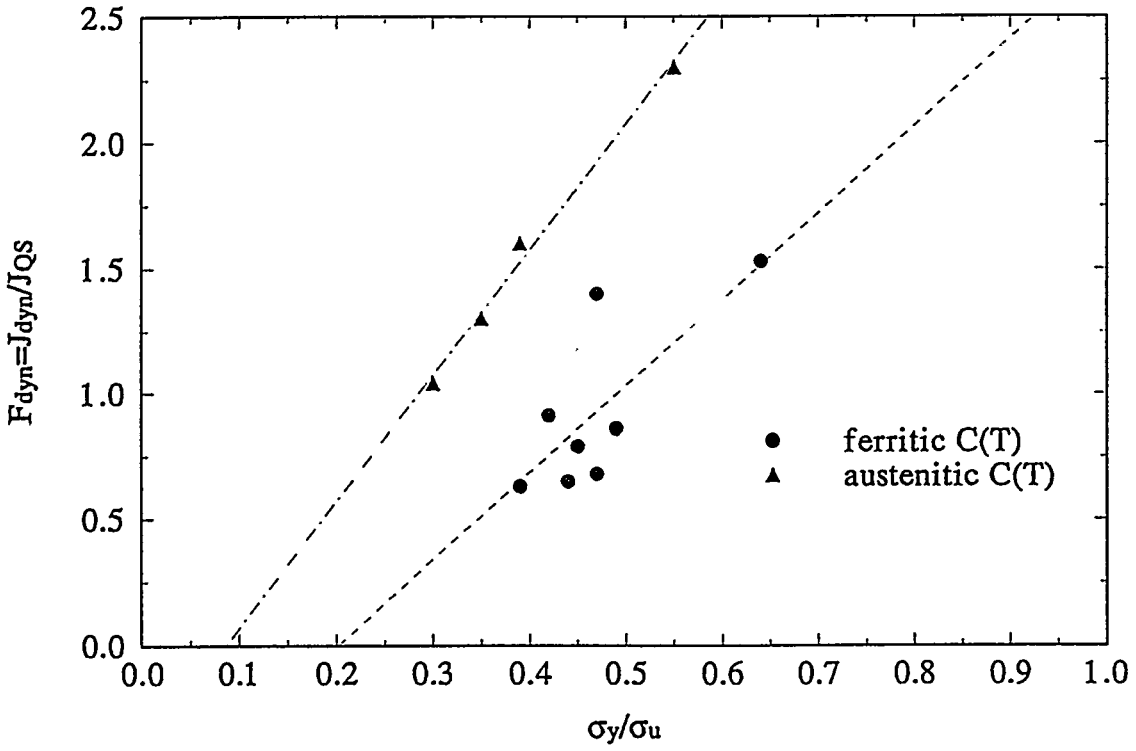

Figure 2 The effect of dynamic loading rate on fracture toughness

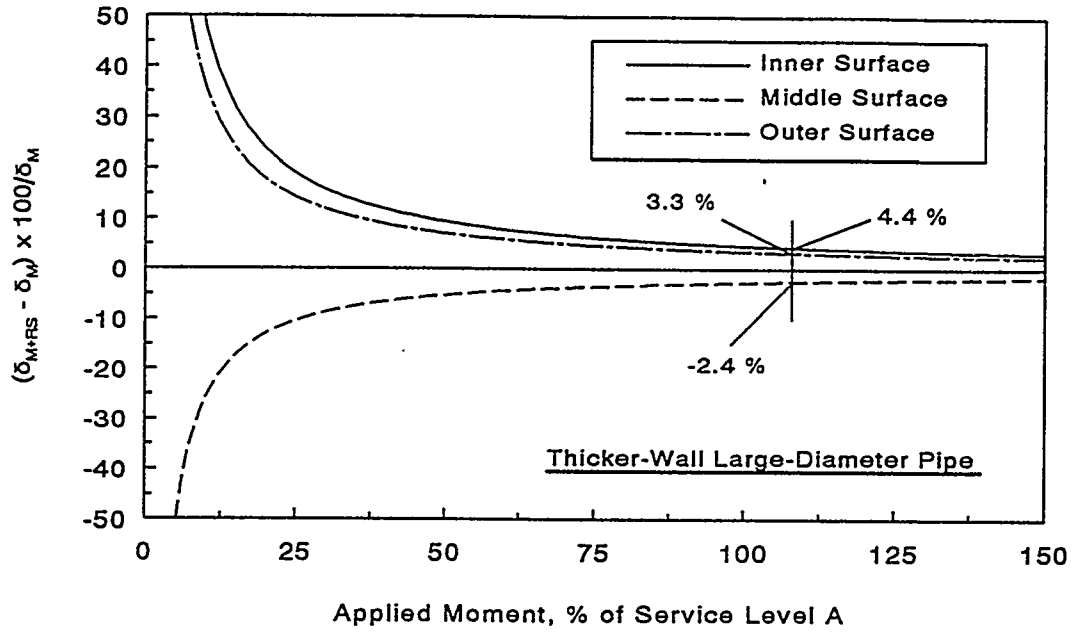

Figure 3 The effect of residual stresses on COD for thicker-wall large-diameter pipe

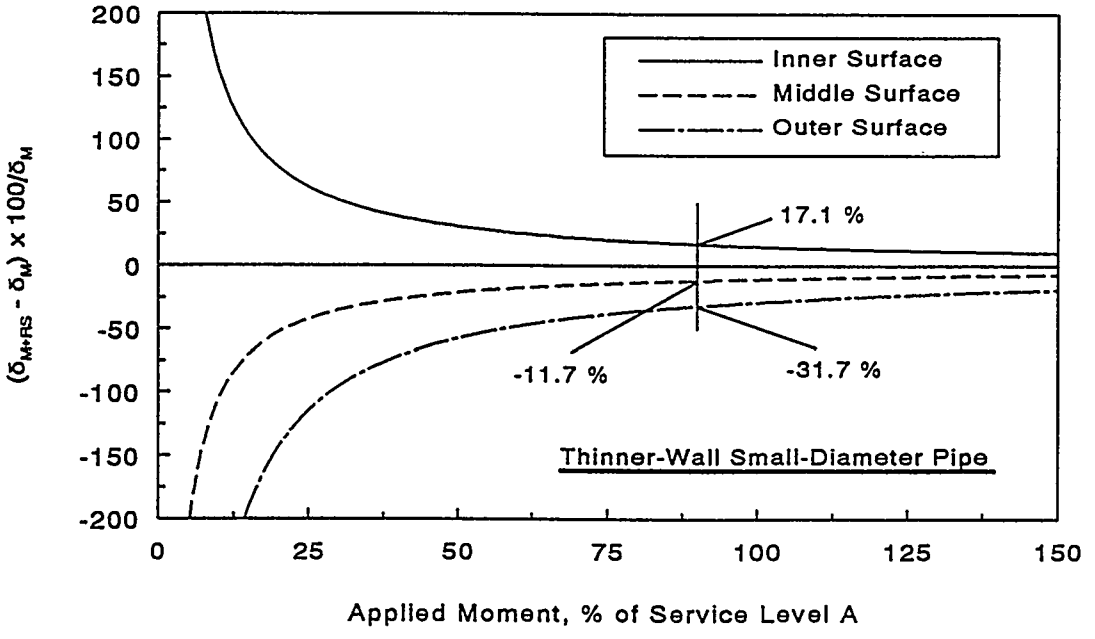

Figure 4 The effect of residual stresses on COD for thinner-wall small-diameter pipe

than thicker-wall large-diameter pipe. The large-diameter pipe always exhibits more COD at the surface when residual stresses are present. The small-diameter pipe, on the other hand, has a larger inner surface COD, but smaller outer surface COD. Consequently, the crack-opening area and the subsequent leak-rate calculations can be affected by the existence of the residual stresses. In fact when $(\delta_{M+RS}-\delta_M)x100/\delta_M$ reaches a value of -100, the COD is zero, i.e., the crack is closed. Furthermore, even if the crack is not completely closed at the center, it will be closed at some point along the length.

From a design perspective, the fact that the residual stresses may close a crack is good, because it means that a larger moment is required to get a given leak rate. However, from a leak detection perspective, closing of the crack by residual stresses implies that there may be a bigger crack than the leak rate would suggest.

Crack Morphology

The key crack morphology variables typically considered in leak-rate analyses are surface roughness, number of turns in the leakage path, and entrance loss coefficients. Examination of service cracks, however, shows that cracks frequently do not grow radially through the thickness, so the leak path may be considerably longer than expected. Current leak-rate calculations also do not explicitly account for the effects of crack-opening area on the crack-morphology parameters. Lastly, most leak-rate calculations are deterministic and ignore the probabilistic distribution of crack morphology variables. Including the effects of crack-path length and COD dependence, and treating the leak-rate analysis in a probabilistic fashion, as illustrated by the data in Figure 5, will give a more realistic calculation of leak rate (Ref. 3).

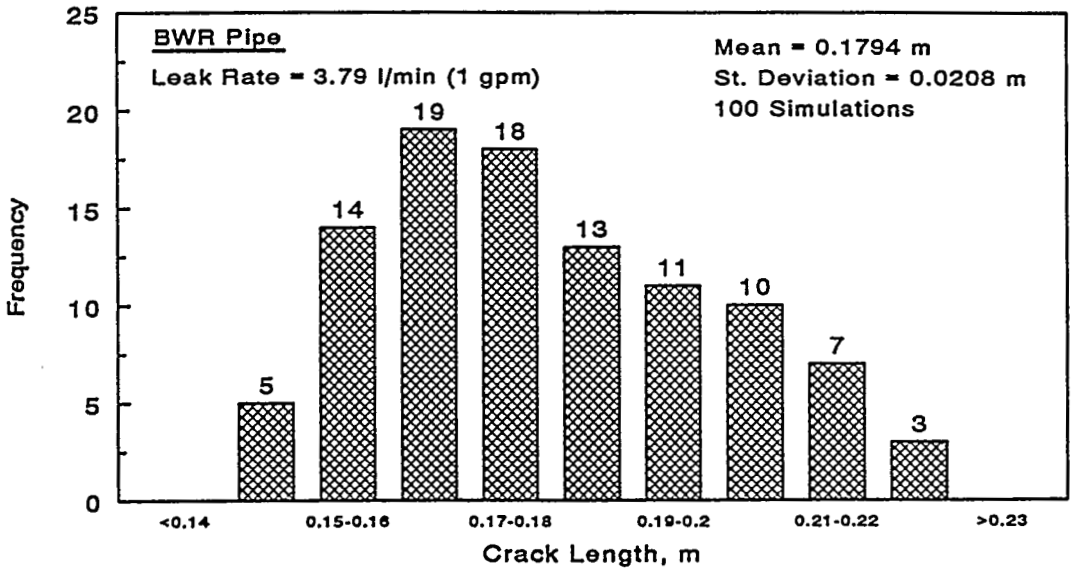

Figure 5 Probabilistic histogram of leakage flaw sizes in a pipe for 3.79 liter/min (1 gpm) leak rate at 50 percent of ASME Service Level A stress limit

FRACTURE MECHANICS CONSIDERATIONS

The ductile tearing moment-carrying capacity of flawed pipe has been a subject of study for many years. In spite of the tremendous advances in fracture mechanics over the past several years, the state of the art is still moving forward at a rapid rate. New experimental data and new analytical developments are changing the perspective of how to perform LBB analyses so that the margin between the detectable flaw and critical flaw can be known with more certainty.

Displacement-Controlled Versus Load-Controlled Stress Classifications

The role of stresses classified as load-controlled (primary) or displacement-controlled (secondary) in pipe fracture has been a subject of debate for many years. In some treatments, only load-controlled stresses are assumed to be able to propagate flaws, while in others, both classifications are considered. There also is considerable debate as to just how to classify stresses arising from inertial loads or seismic anchor motion. In most typical LBB evaluations, linear stress analyses are utilized, so in setting limits based on elastically calculated stresses, consideration must be given to what stresses should be included in the calculation and what effect the stresses have on crack propagation.

Results from the IPIRG-1 program, Figure 6, showed that if the flaw is large and nominal stresses were below yield except at the crack, thermal expansion, seismic anchor motion, and inertial stresses all acted as primary stresses (Ref. 4). For smaller cracks, nominal stresses will be above yield so some nonlinear correction on elastically calculated secondary stresses will be required.

There currently are no data to provide a complete methodology for high stress conditions. Analyses, such as shown in Figures 7 and 8 suggest that if primary stresses are below yield and secondary stresses are displacement controlled, the effect on allowable crack size is not large. In the case of high primary stresses and/or inertial stresses above yield, considerable data and developments will be required to produce the necessary models needed to continue to effectively use elastic analyses.

Combined Torsion and Bending Stresses

Crack growth out of the plane of the circumference has been observed in a large number of circumferential through-wall carbon steel pipe experiments. In these experiments, angled crack growth is of little practical concern because the maximum loads for angled crack growth are greater than those for straight cracks. In real piping systems, however, pipes are subjected to both bending, tension, and torsional stresses and these combined stresses may be more detrimental than expected because of the propensity of cracks to grow out of plane.

A convenient vehicle for handling combined torsion and bending is to use a straight pipe analysis and to consider the crack to be loaded with an effective moment:

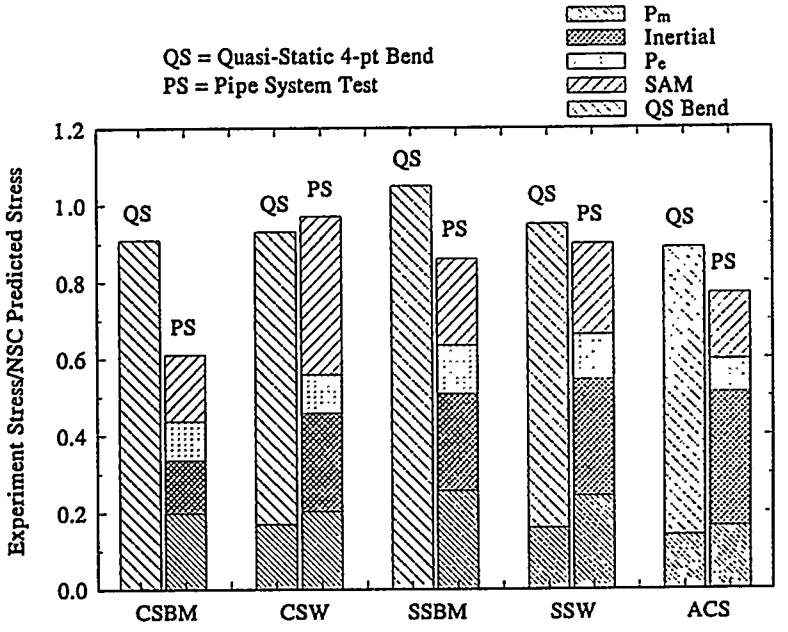

Figure 6 Illustration of the importance of including both displacement- and load-controlled stresses as primary stresses if the crack size is large

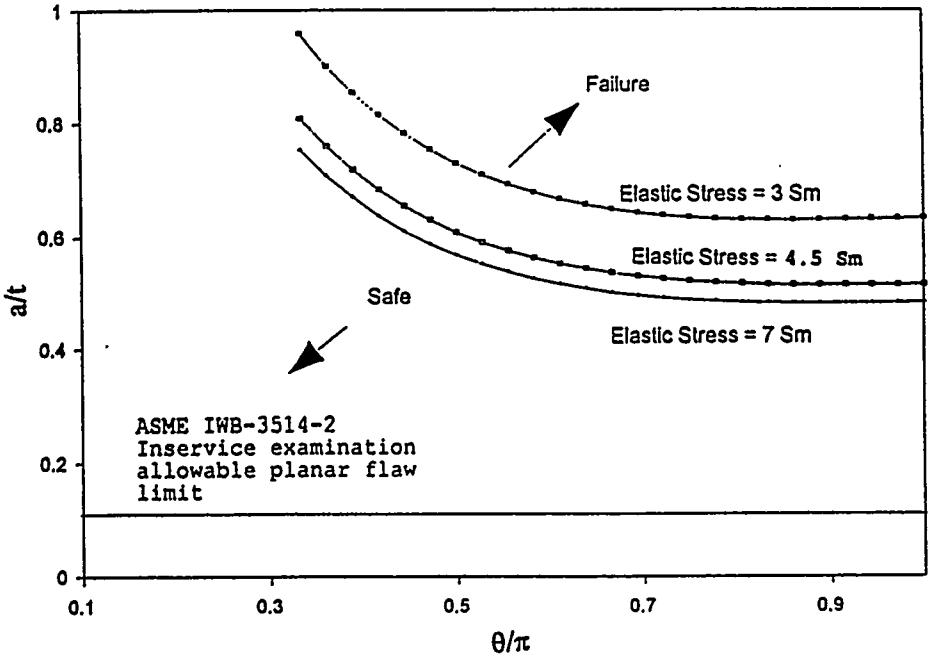

Figure 7 The effect of various stress limits for TP304 stainless steel when high stresses are displacement controlled

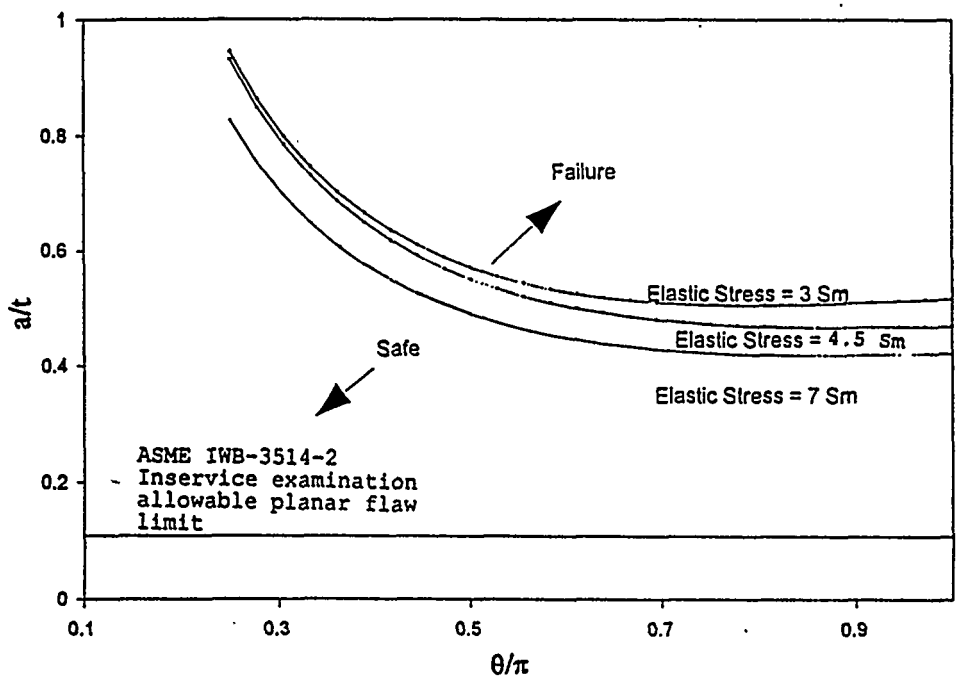

Figure 8 The effect of various stress limits for A106 Gr B carbon steel when high stresses are displacement controlled

$$M_{eff} = \sqrt{M_B^2 + (c_e T)^2} \tag{1}$$

where M_B=bending moment, T=torsional moment, and c_e=effective moment factor.

Based on extensive finite element calculations with both straight and angled cracks, and various combinations of tension, torsion, and bending, an effective moment based on a value $c_e = \sqrt{3}/2$ yields the best fit for crack-driving force, crack-opening area and crack-opening displacement for combined load cases when used in pure bending analyses (Ref. 5).

This result, illustrated by the plot in Figure 9, allows the use of simple engineering estimation schemes for determining fracture parameters when torsion is present. The limitation to this, however, is that the supporting analyses for this conclusion are limited to very small amounts of angular crack growth. Nevertheless, the effective moment concept can be used for combined loading involving torsion and is valid for all leak-rate calculations of concern to LBB analyses.

Margins Gained by Nonlinear Time-History Analyses

Prediction of the behavior of flawed piping sections is very much dependent upon the specific geometry, material properties, and globally applied loads of the piping system, i.e., to know the crack-driving force, the piping system response must be precisely estimated.

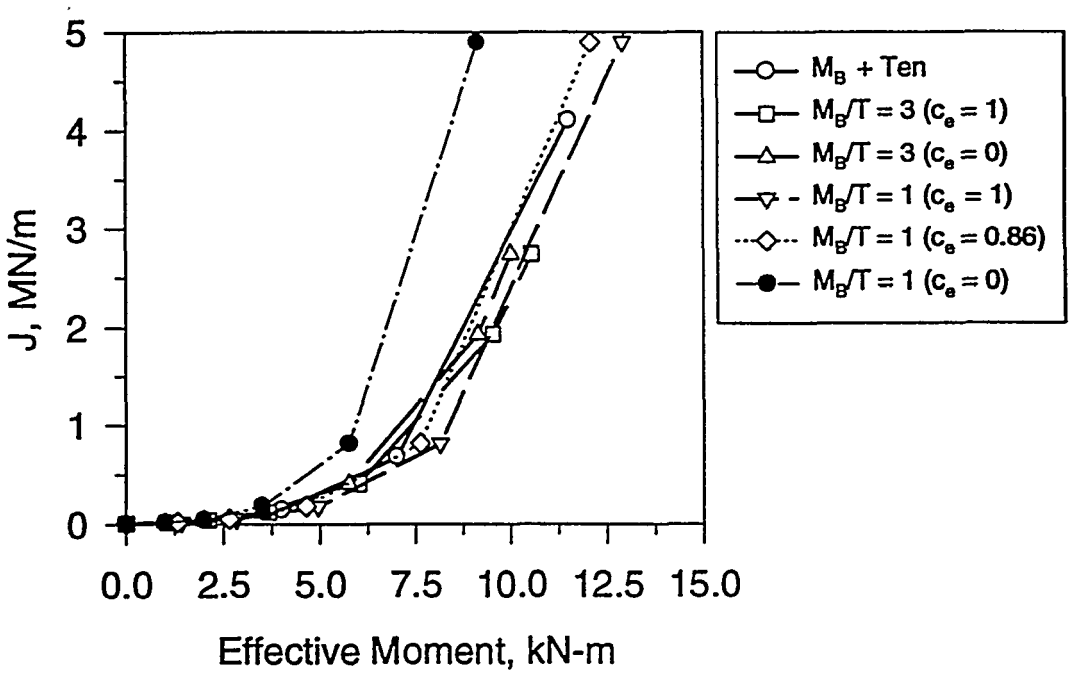

Figure 9 Illustration of the suitability of using an effective moment for combined bending, tension and torsion loading (M_B+Ten is the standard against which other solutions are to be compared)

The method that Battelle has pursued (Refs. 6 and 7) for dynamic analysis of flawed piping uses nonlinear springs to represent the moment-rotation response of the crack, Figure 10. Energy dissipation, due to cyclic loading of the nonlinear crack prior to initiation, is an inherent part of the analysis described above. Loading past maximum moment, transition of a surface crack to a through-wall crack, reinitiation of a crack that has already extended, crack opening as a function of time for blow-down or thrust-load calculations, and direct assessment of the propensity for a DEGB are also possible.

Figure 11 compares the crack-section moments from an LBB-style linear analysis and a nonlinear spring (cracked-pipe) element analysis. Whereas the LBB analysis indicates a failure at an SSE loading, the nonlinear analysis indicates that the flaw will survive a 3 SSE seismic load. A margin of 5.35 on moment is indicated by the nonlinear analysis in this case (Ref. 1).

The Effect of Low Cycle Fatigue During a Seismic Event

In a cracked-pipe system subjected to seismic loading, for a sufficiently shallow crack, fatigue crack growth will govern until the crack reaches some critical size and the mode of crack propagation switches to ductile tearing. In order to make an accurate prediction of cracked-pipe behavior for LBB, the low-cycle fatigue mechanism should be included.

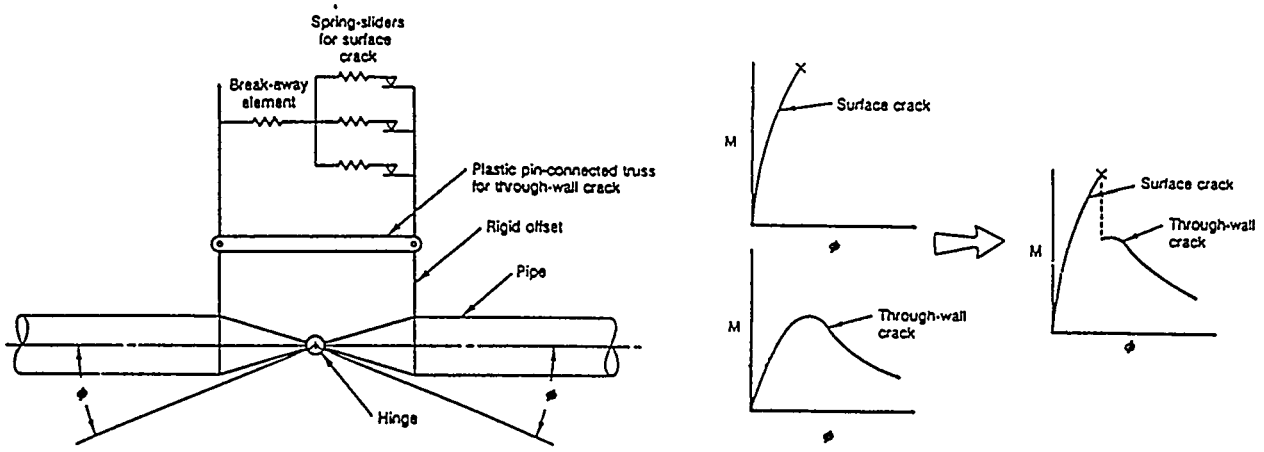

Figure 10 Battelle nonlinear-spring (cracked-pipe) element model

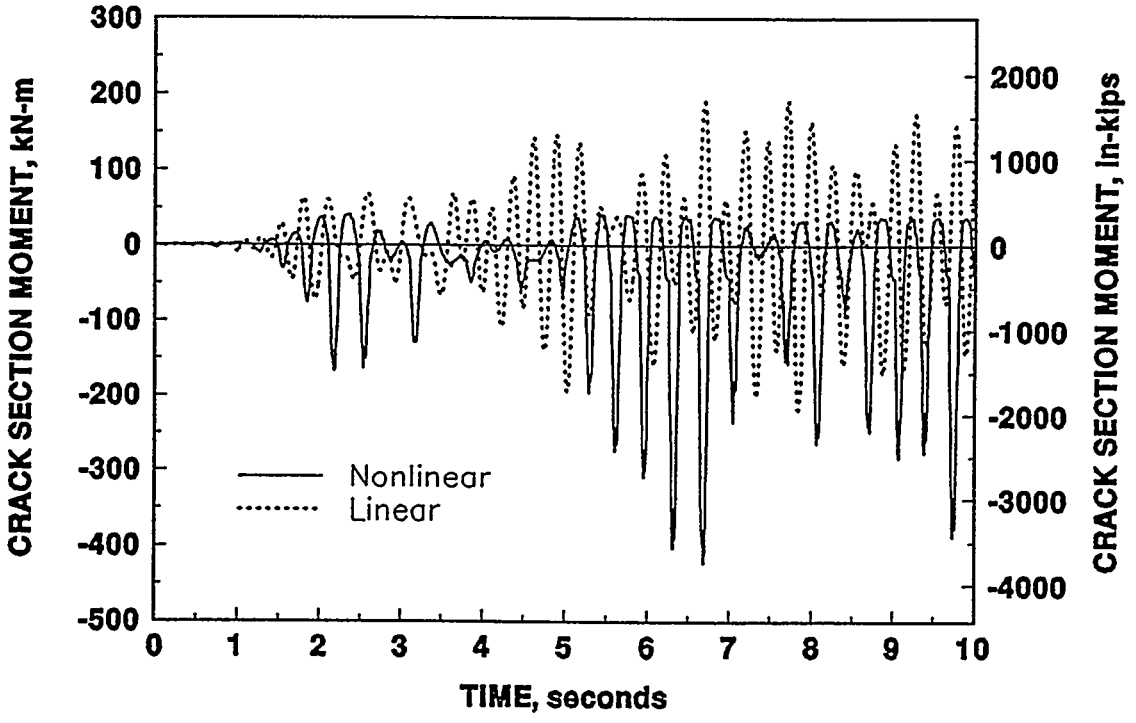

Figure 11 Comparison of linear and nonlinear crack-opening moments for 3 SSE seismic loading of a 75-percent deep 360-degree surface crack with a 518-mm (20.4 inch) long leaking through-wall crack for the U.S. DOE New Production Reactor

For high and low cycle fatigue, the kinetic equation for the crack growth process is characterized by the well-known Paris equation for high cycle fatigue crack growth,

$$\frac{da}{dN} = C(\Delta K)^m \tag{2}$$

where a=crack length, N=number of fatigue cycles, C and m parameters of the Paris equation.

Provided that ΔK is less than the critical value which would cause ductile tearing in a pipe, the growth of the crack due to fatigue cycling can be obtained by integration on a cycle-by-cycle basis.

The driving force for ductile tearing is the J that is applied to the crack, while the driving force for fatigue crack propagation is ΔK. Fortunately, in the linear elastic regime, J is related to K by the following expression for a plane stress condition

$$\Delta K = \sqrt{\Delta J\, E} \tag{4}$$

where E=elastic modulus of the pipe material.

In the case of cracks undergoing reversed loading (crack closure), the cyclic ΔJ using the Dowling approach can be related to the maximum deformation theory J applied in a loading cycle by .

$$\Delta J = \beta J \tag{5}$$

where β is a multiplier that determines the Dowling operational ΔJ during the load cycle (Ref. 8).

Applying this fatigue evaluation technique to the nonlinear cyclic loading shown in Figure 11, the total crack length is predicted to increase by 48 mm (1.89 inch) as shown in Figure 12. The crack extension is not significant enough to make the leak-rate area unacceptably large.

SUMMARY

The LBB concept for nuclear power plant piping is predicated on a good understanding of fracture mechanics, stress analysis, and leak-rate analysis. With carefully executed experiments and timely analytical developments as the basis, the LBB concept has matured to the point of being an accepted design philosophy. This paper has briefly summarized some newly discovered analysis techniques and data that will, eventually, impact implementation of LBB. All of these ideas are quite new and thus require further evaluation and validation. In most cases, the data and ideas offered in this paper are refinements of existing technology/data that will help to more accurately quantify margins in LBB design for seismic applications.

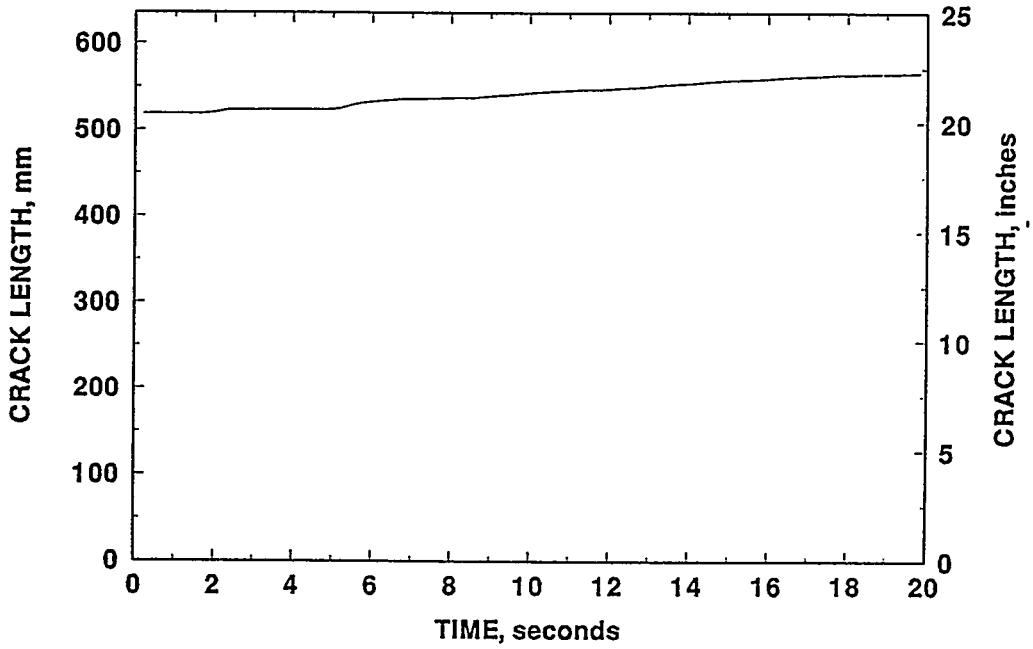

Figure 12 Predicted low-cycle fatigue crack growth for the U.S DOE New Production Reactor for 3 SSE seismic loading of a 75-percent deep 360-degree surface crack with a 518-mm (20.4 inch) long leaking through-wall crack

REFERENCES

(1) Olson, R., *et al*; "Margins for Dynamic FEM Analysis of Cracked Pipe Under Seismic Loading for the DOE New Production Reactor"; PVP Vol 280; June 1994, pp 119-134.

(2) Rahman, S., *et al*; "Refinement and Evaluation of Crack-Opening-Area Analyses for Circumferential Through-Wall Cracks in Pipes"; NUREG/CR-6300; April 1995.

(3) Rahman, S., *et al*; "Probabilistic Pipe Fracture Evaluations for Leak-Rate-Detection Applications"; NUREG/CR-6004; April 1995.

(4) Scott, P., *et al*; "The IPIRG-1 Pipe System Fracture Tests - Experimental Results"; PVP-Vol 280; June 1994; pp. 135-152.

(5) Mohan, R. , *et al*; "Effects of Toughness Anisotropy and Combined Tension, Torsion, and Bending Loads on Fracture Behavior of Ferritic Nuclear Pipe"; NUREG/CR-6299, April 1995.

(6) Olson, R.J., *et al*; "Application of a Nonlinear-Spring Element to Analysis of Circumferentially Cracked Pipe Under Dynamic Loading"; PVP-Vol 233; March 1992, pp. 279-291.

(7) Olson, R.J., *et al*; "Validation of Analysis Methods for Assessing Flawed Piping Subjected to Dynamic Loading"; NUREG/CR-6234; February 1994.

(8) Wilkowski, G., *et al*; "Low-Cycle Fatigue Crack Growth Considerations in Pipe Fracture Analyses"; PVP-Vol. 280; June 1994; pp. 281-297.

ON THE APPROXIMATION OF CRACK SHAPES FOUND DURING INSERVICE INSPECTION

S. R. Bhate, D. S. Chawla, H. S. Kushwaha and S. C. Mahajan
Reactor Engineering Division,
Bhabha Atomic Research Centre,Bombay 400085, India

ABSTRACT

This paper addresses the characterization of axial internal flaw found during inservice inspection of a pipe. J-integral distribution for various flaw shapes is obtained using line spring finite element method. The peak J-value and its distribution across the crack is found to be characteristic feature of each shape. The triangular shape yields peak J-value away from the centre, the point of maximum depth. The elliptic approximation results in large overestimate of J-value for unsymmetric flaws. Triangular approximation is recommended for such flaws so that further service can be obtained from the component.

INTRODUCTION.

ASME Boiler and Pressure Vessel Code[1] requires regular inservice inspection of nuclear power plant components. Any flaws detected during inspection need to be characterized by shape and dimensions according to paragraph IWA-3300 of the Section XI, Division 1[1]. For structural integrity analysis an elliptic flaw model of the size given by rectangle bounding the flaw geometry is common. The calculations in the code for obtaining maximum crack loading intensity take shape of the flaw into account by a shape factor Q which varies with ellipse aspect ratio.

The above simplified procedure yields conservative estimates of stress intensity factor for simple crack shapes. Though code calculations are based on elliptic crack shape, the code permits use of other procedures for calculating maximum stress intensity factor. For flaws having complex geometry and stress distribution, the maximum stress intensity factor may not occur at the point of maximum crack depth. For such flaws, the effect of shape on the stress intensity factor becomes important. The elliptic approximation may promote conservatism and force the component out

of service, while more regorous procedure may accept the component till next inspection. The present work addresses the influence of crack shape on the stress intensity factor and its distribution.

The influence of crack shape in case of plates under tension has been reported by Shiratori and Miyoshi[2]. The case of internal axial surface crack in pressurized pipe is treated here. The crack loading in terms of J-integral value is determined for various crack shapes using elasto-plastic material behaviour and finite element method. The results for circular, rectangular and triangular crack shapes are compared to those for elliptical shape of identical size. Non-elliptical approximation of crack shape is seen to be more appropriate for unsymmetric flaws.

FINITE ELEMENT MODELING

The finite element analysis of a straight pipe with internal axial surface flaw is carried out using "ABAQUS" code For the symmetric crack shapes, the symmetry about two planes is utilized to keep the size of the model small. Eight noded thick shell elements (SFR8) are used for the surface of the pipe and crack is modelled using line spring elements. Near the crack end, smaller elements are employed to account rapidly changing geometry(Fig. 1). Shell discretization used fine mesh near crack while coarse mesh was used in the regions away from the crack. Multipoint constraints facility allowed interfacing different mesh regions. Fig. 2 shows the crack shapes considered in the analysis. The loading consists of internal pressure only. The pipe length of approximately 14 times the crack length is modelled to make the influence of pipe length on the results negligible. The properties of the material [3] are given as:

Modulus of Elasticity: 18318 kg/(sq.mm)
Yield Strength : 18.58 kg/(sq.mm)
Ultimate Strength : 40.84 kg/(sq.mm)
Hardening approximation : isotropic

NUMERICAL RESULTS

The validation of the finite element model using three dimensional finite element results is already reported in reference[4]. Two crack depths were studied here. The peak J- integral values obtained for symmetric crackshapes and their variation with applied pressure is shown in figures 4a and 4b for shallow (a/t=0.25) and deep crack (a/t=0.75) respectively. For all crack shapes, the peak J-integral values increase

rapidly once the average hoop stress (based on uncracked pipe thickness) approaches the yield strength. However, due to considerably high fracture toughness, the crack extension is not likely unless pressure increases further. From the comparison of results for different shapes, the triangular crack appears to produce least crack driving force while rectangular crack results envelope other results. The differences in the values are negligible during elastic deformation but become significant after yield zone developes.

The J-integral distribution for elliptical, rectangular and triangular symmetric cracks is shown in figures 5 through 10. The distribution is flatter for rectangular cracks in comparison with that for elliptical cracks. The rectangular crack may experience extension wide across the crackfront due to flatter distribution of J-integral. On the other hand, the J-integral values for triangular crack (Figs. 9,10) show an interesting feature, more prominently for deep crack (Fig. 10). The J-integral increases with pressure but peak value does not ocuur at centre where depth is maximum. After yield zone developes, the peak J-value occurs at approximately x/c = 0.5 and the peak point starts moving towards the centre with increasing pressure. The J-value at centre is approximately 20 % less than the peak value for normalized pressure 1.176. This indicates that the initial crack extension will not occur at centre, but away from centre. For a given crack extension normal to the front, the area uncovered by crack will be more for locations away from the centre. Moreover, the normal to the crack front is not uniquely defined at centre of crack. Hence crack extension process may choose locations such that the crack shape becomes smoother after the growth. These features are absent in the J-distribution for rectangular or elliptical cracks(Figs. 5-8) This implies that the shape will have strong influence on crack growth and final shape.

In order to demonstrate the effect of irregular crack shape which may be found during inservice inspection, an arbitrary shape shown in Fig. 11 is considered. The distributions of J-integral for the correct geometry, elliptic approximation following the ASME code and unsymmetric triangular shape approximation are presented in Fig. 12. It can be seen that the triangular approximation underestimates the crack driving force by a negligible amount at lower pressure and follows the shape of the distribution closely throughout the crack length. The elliptic approximation yields large overestimate of the J-integral, the difference being highest at shallow end of the crack. At slightly higher pressure, the agreement between J-values for triangular approximation and those for real geometry is quite close with no overestimate. The elliptic approximation, however, gives large overestimate (approximately 30%) of crack driving force at higher pressure. Thus the use of elliptic approximation, though simple due to availability of results in the code, may result in the rejection of the component with useful service life. The reason for this behaviour is the asymmetry

of the triangular shape. The effect of eccentricity on the J-integral distribution is shown in Fig. 13. The dip in the J-value at centre is a characteristic of symmetric shape only. As the eccentricity increases, no such reduction is observed and the point of maximum J-value slowly shifts towards the point of maximum depth. The peak J-value is only slightly affected by the eccentricity.

CONCLUSIONS

For an axial internal surface crack in a pipe subjected to internal pressure, the crack driving force (J-integral) distribution appears to be strongly influenced by carck shape. The peak J-value and its distribution at higher pressures is the characteristic feature of each crack shape. The peak J-value for triangular crack does not occur at centre, the point of maximum depth, but slightly away from the centre. The elliptic approximation results in large overestimate of stress intensity for unsymmetric cracks. ASME code results become overly conservative for these cases. For such cracks, triangular approximation yields more accurate estimate of stress intensity and may allow further service of the component while elliptic approximation may reject the component.

References:

1. ASME Boiler and Pressure Vessel Code, Section XI, Division 1, Rules for Inservice Inspection of Nuclear Power Plant Components.
2. Shiratori M. and Miyoshi T., " Evaluation of J-integral for Surface Cracks", Second ASTM Symposium on Elasto-Plastic Fracture, Philadelphia, Oct. 1981, ASTM STP-803, pp. I-424-460.
3. S. Kanno, K. Hasegawa, T. Shimitzu, T. saitoh and N. Gotoh, "Analysis of leak before break behaviour in failure assessment diagram for carbon steel pipes", Nuclear Engg. Design, Vol. 138, 1992, pp. 251-258.
4. D. S. Chawla, S. R. Bhate, H. S. Kushwaha and S. C. Mahajan, "The Shape Influence on the Behaviour of Surface Cracks", Structural Mechanics in Reactor Technology, 13 th Conference, Brazil, 1995.

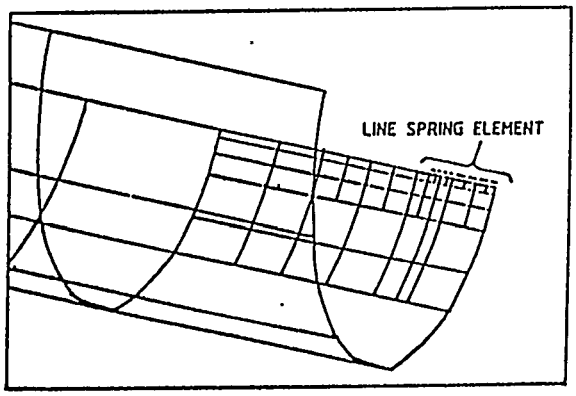

Fig. 1 Finite element mesh near surface crack.

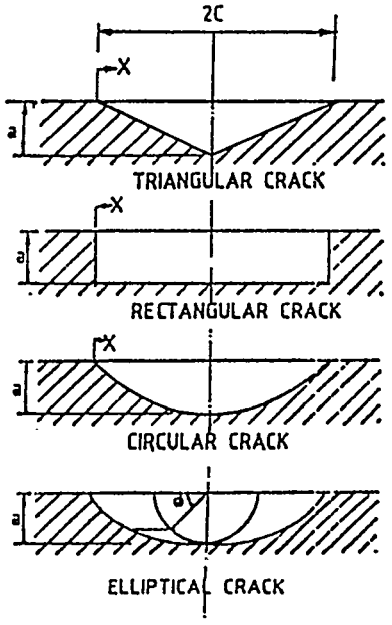

Fig.2: Different shapes of surface. crack.

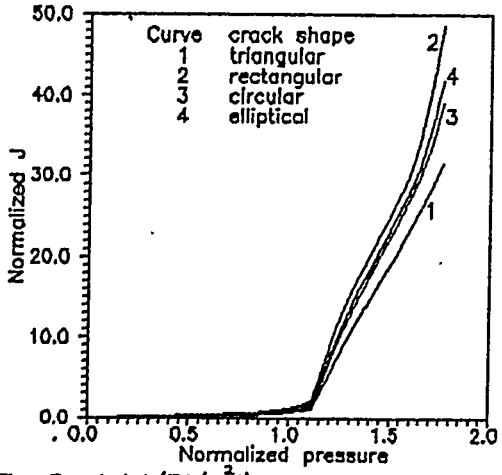

Fig. 3 J-Int.($EJ/\sigma_y^2 t$) at centre of crack vs pressure($pR/\sigma_y t$) for different shapes of shallow crack (a/t=0.25, 2c/a=6).

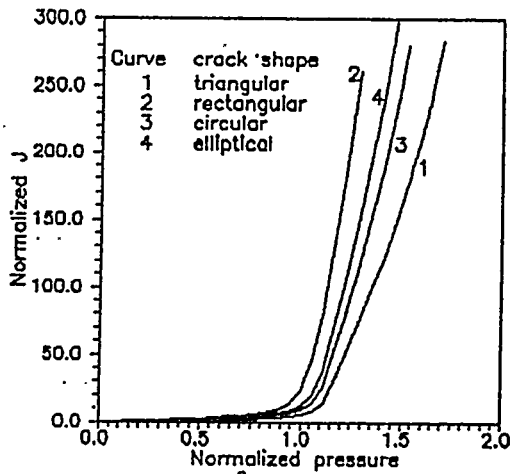

Fig. 4 J-Int.($EJ/\sigma_y^2 t$) at centre of crack vs pressure($pR/\sigma_y t$) for different shapes of deep crack (a/t=0.75, 2c/a=6).

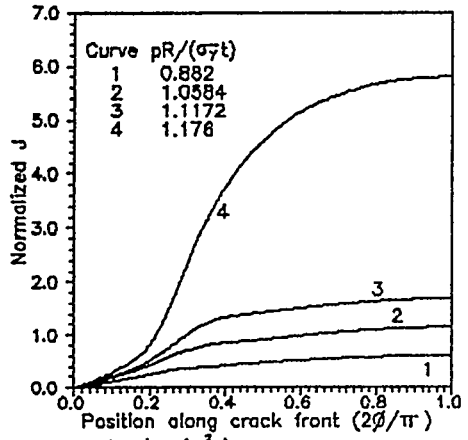

Fig. 5 J-int.($EJ/\bar{\sigma}_y^2 t$) along the crack front for shallow elliptical surface crack (a/t=0.25, 2c/a=6).

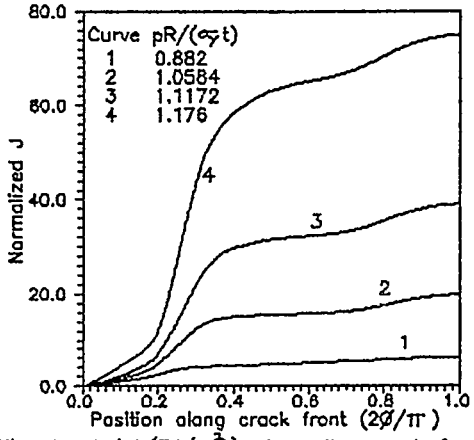

Fig. 6 J-int.($EJ/\bar{\sigma}_y^2 t$) along the crack front for deep elliptical surface crack (a/t=0.75, 2c/a=6).

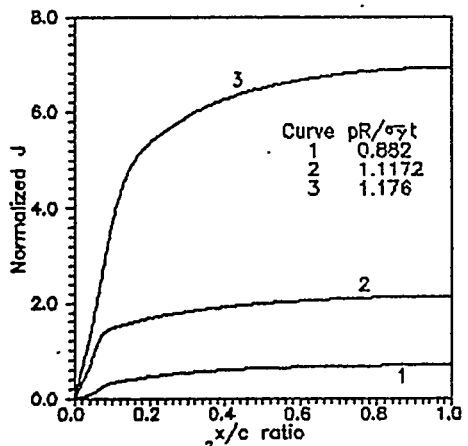

Fig. 7 J-Int.($EJ/\bar{\sigma}_y^2 t$) along the crack front for shallow rectangular surface crack (a/t=0.25, 2c/a=6)

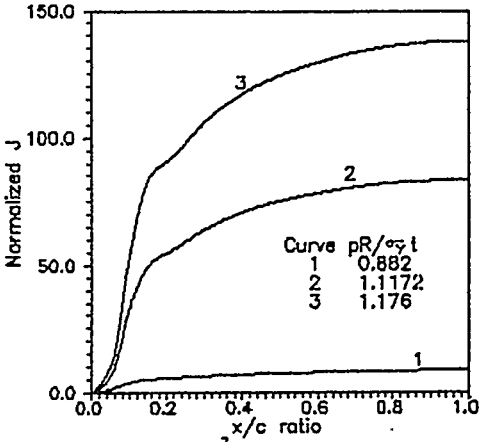

Fig. 8 J-Int.($EJ/\bar{\sigma}_y^2 t$) along the crack front for deep rectangular surface crack (a/t=0.75, 2c/a=6).

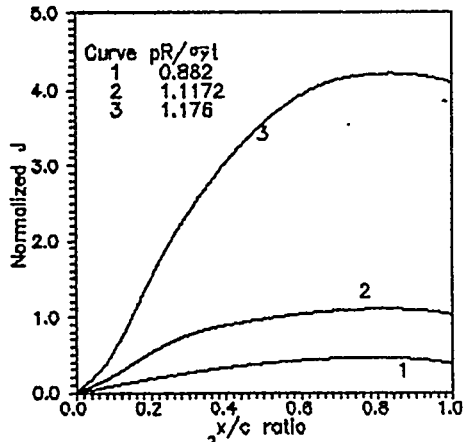

Fig. 9 J-int.($EJ/\bar{\sigma}_y^2 t$) along the crack front for shallow triangular surface crack (a/t=0.25, 2c/a=6).

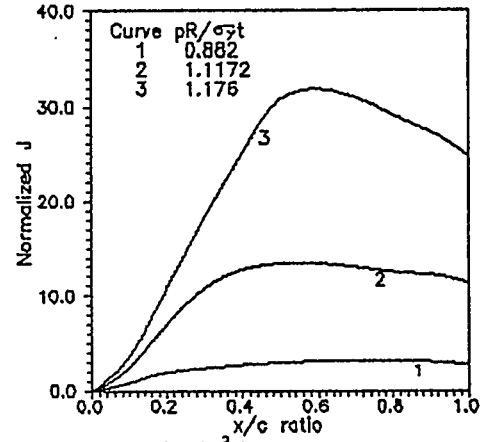

Fig. 10 J-int.($EJ/\bar{\sigma}_y^2 t$) along the crack front for deep triangular surface crack (a/t=0.75, 2c/a=6)

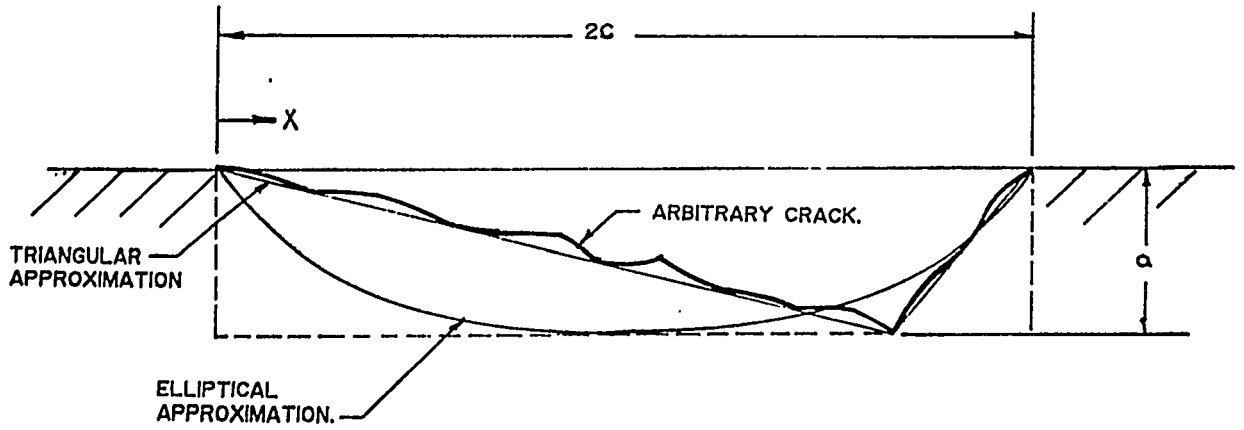

Fig.11: Approximation of arbitrary crack shape by elliptical and triangular shapes.

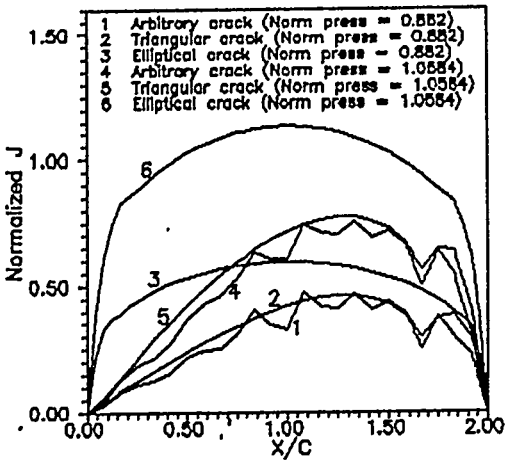

Fig. 12 Comparison of J-int. distribution for arbitrary crack with approximated shapes (a/t=0.25, 2c/a=6).

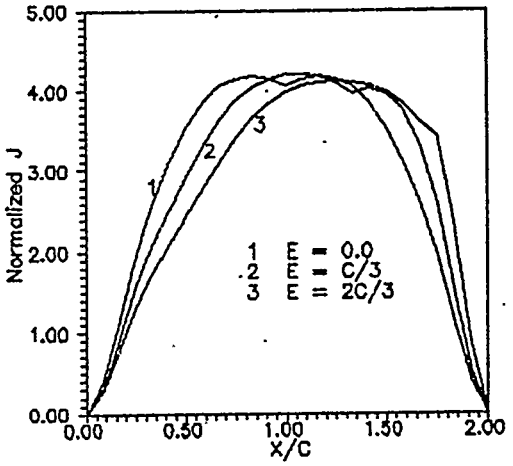

Fig. 13 Effect of triangular crack eccentricity on distribution of J-integral (a/t=0.25, 2c/a=6, Norm.press.=1.176).

Fracture Analysis of Axially Cracked Pressure Tube of Pressurized Heavy Water Reactor

Suresh Krishnan, Vivek Bhasin, H.S. Kushwaha, S.C. Mahajan, A. Kakodkar
Reactor Design & Development Group, Bhabha Atomic Research Centre, Bombay, India

Abstarct

Three Dimensional (3D) finite element elastic plastic fracture analysis was done for through wall axially cracked thin pressure tubes of 220 MWe Indian Pressurised Heavy Water Reactor. The analysis was done for Zr-2 and Zr-2.5Nb pressure tubes operating at 300°C and subjected to 9.5 Mpa internal pressure. Critical crack length was determined based on tearing instability concept. The analysis included the effect of crack face pressure due to the leaking fluid from tube. This effect was found to be significant for pressure tubes. The available formulae for calculating J (for axially cracked tubes) do not take into account the effect of crack face pressure. 3D finite element analysis also gives insight into variation of J across the thickness of pressure tube. It was observed that J is highest at the mid-surface of tube. The results have been presented in the form of across the thickness average J value and a peak factor on J. Peak factor on J is ratio of J at mid surface to average J value. Crack opening area for different cracked lengths was calulated from finite element results.

The fracture assessment of pressure tubes was also done using Central Electricity Generating Board R-6 method. Ductile tearing was considered.

Fracture Analysis of Axially Cracked Pressure Tube of Pressurized Heavy Water Reactor

Suresh Krishnan, Vivek Bhasin, H.S. Kushwaha, S.C Mahajan, A. Kakodkar
Reactor Design & Development Group, Bhabha Atomic Research Centre, Bombay, India

1.0 Introduction

The pressure tube of Pressurised Heavy Water Reactor (PHWR) is a thin walled tube and is one of its key component. Demonstration of Leak Before Break (LBB) and assesment of fracture safety of pressure tube is important from the overall stand point of structural safety. One of the important elements in the assesment of safety is the margin between an existing axial through wall flaw and the critical crack length. The size of such a through wall crack can be assessed by monitoring the leak rate. If the size of the crack is less than critical crack length sudden rupture of the pressure tube and hence sudden loss of coolant accident is avoided.

3-Dimensional (3D) Finite Element (FE) Elastic Plastic Fracture (EPF) analysis was done for through wall axially cracked pressure tubes of Indian PHWR's. The crack opening area for different crack lengths and critical crack length was evaluated based on FE results. The analysis was done for normal operating pressure and temperature. During operation in reactor environment the mechanical properties (strength, ductility and fracture toughness) are considerably affected due to neutron irradiation and hydriding, [1, 2]. Although, the present analysis does not consider the change in mechanical properties but it is still valid for fresh tubes or those which have undergone only a few full power years of operation.

The parameter used to characterise the crack driving force in the present analysis is the J-Integral. Many closed form solutions of J-Integral for through wall axially cracked pipes are available in literature. For an elastic perfectly plastic material Folias, [3] or Zahoor formula, [4] is applicable. In these formulae effect of the pressure exerted on the crack faces by the leaking fluid has not been considered. In case of pressure tubes this crack face pressure increases the values of J-Integral and crack opening area significantly and also reduces the collapse load. The closed form formulae are based on thin shell theory and yield average J-Integral values across the wall thickness, whereas, 3D FE analysis gives insight into the variation of J across the thickness of the tube. It was found that J values are maximum at the mid layer of the tube. In this work, the results have been presented in terms of average J values. A peak factor on J which is defined as the ratio of maximum J to average J across the thickness is also evaluated.

The fracture assesment of pressure tubes was also done using Central Electricity Generating Board (CEGB) R -6 method, [5]. Ductile tearing was considered.

2.0 Structural Details and Material of Pressure Tubes

The pressure tubes house the reactor fuel. The heavy water coolant at about 290°C and 9.5 MPa pressure (maximum) flows through the pressure tubes. There are 306 pressure tubes in a 220 MWe Indian

PHWR. Each pressure tube is surrounded by a calandria tube. The annular gap between the two is maintained by garter springs, fig.1. In older PHWRs the pressure tubes are made of Zr-2 and air circulates through the annular space. In newer PHWRs, the pressure tube material is Zr-2.5Nb and air is replaced by CO_2 gas in the annular gap. The annular gas is being monitored.

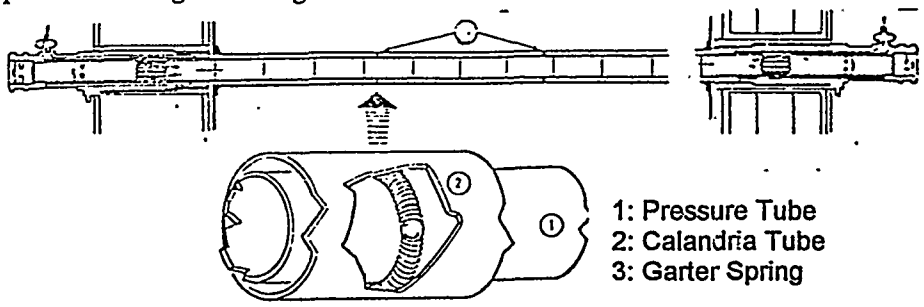

Fig. No.1 Pressure Tube - Calandria Tube Assembly

The Zr-2 pressure tube is about 4.0 mm thick having an inner diameter of 82.6 mm and is about 5.4 m long. Zr - 2.5Nb pressure tube is 3.32 mm thick with an inner diameter of 82.6 mm and are 5.4 m long. The mechanical properties of both the pressure tube materials are given in Table 1, [6]. The stress-strain and J-Resistance data was taken from reference [6] .

Table 1 : Mechanical Properties of Zr - 2 and Zr - 2.5Nb at 300°C

Material	Youngs Modulus (GPa)	Poisson's ratio	Yield stress (MPa)	Ultimate Strength (MPa)	J_{IC} (N/mm)
Zr - 2	78.8	0.43	396.25	408.25	84
Zr - 2.5Nb	78.8	0.43	563.67	594.67	289

3.0 Finite Element Model

The pressure tube was modelled using 3D 20 noded brick elements with reduced integration scheme. Collapsed quarter point singular elements were employed around the crack tip to model the singular stress field. Fig.2., shows the quarter symmetric FE model. Near the crack tip the mesh is extremely refined. A coarser mesh was employed in other regions as the stresses are likely to be within elastic limits. Only a small length of the pressure tube was modelled.

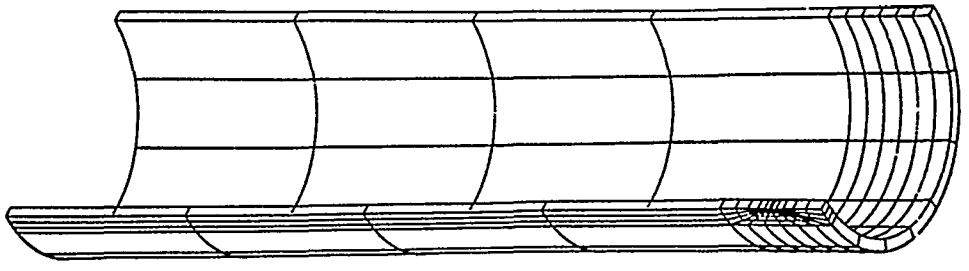

Fig. No.2 Quarter Symmetric Mesh of Pressure Tube

Internal pressure loads were applied to the inside surface of the model. An equivalent end pressure load was applied to simulate the axial stress induced by the pressure acting on the closed ends of the tube. The leaking fluid will exert force onto the crack faces. The effect is considered by assuming crack face pressure equal to internal pressure.

4.0 Elastic - Plastic Fracture Analysis

The elastic plastic fracture analysis was done using the finite element computer code 'ABAQUS' , [7]. For the present study, J-Integral values were obtained from 5 sets of concentric contour paths. For each contour, the J values were obtained at three different locations across the thickness of the tube viz., inner surface, middle surface and outer surface. The average value of J across the thickness is computed by the Simpson's average formula. In order to get insight into the variation of J across the thickness, a peak factor on J was evaluated as the ratio of J value at the middle surface (Jmid) to the average J value across the thickness (Javg). It was found that J value is highest at the middle surface of the pressure tube.

$$\text{Peak Factor} = \text{Jmid} / \text{Javg} \qquad (1)$$

From the FE results, the crack opening area was also evaluated. The initiation of cracking takes place when J_{app} for applied load is greater than J_{IC}. The critical crack length was evaluated for the condition that $J_{app} > J_{IC}$ and applied tearing modulus being greater than the material tearing modulus ($T_{app} > T_{mat}$). T_{mat} was evaluated using the material J - Resistance curve and T_{app} using J v/s crack length curve. The J-T curves for the applied load and the material are plotted and the critical J value is determined. Going back to the J v/s crack length curve, the crack length corresponding to the critical value of J is the critical crack length.

4.1 Zr - 2 Pressure Tube Analysis and Results

In order to validate the 3D solid mesh the through wall axially cracked Zr-2 pressure tube under internal pressure was analysed but without applying crackface pressure. The closed form solutions for this problem are available in the literature e.g. Folias' formula [3] or Zahoor's formula, [4], for elastic perfectly plastic material. The yield and ultimate tensile strength of Zr-2 at 300° C is nearly same and hence it is similar to elastic perfectly plastic material. The comparison between FE and closed form formulae is shown in fig.3. Here the average values of J from 5 different contours are plotted against the half crack length. The values compare with each other very well. The J_{avg} values of 5 different contours contour path, lie within 1 % difference. The path independence of the J values serves as a further check on the quality of the FE mesh.

After validation of FE mesh the problem was reanalysed by accounting for the pressure on the crack faces also. The crack driving force curve is shown in fig.4 , along with the case when crack face pressure was neglected. It is seen that inclusion of crack face pressure in the analysis increase the applied J values significantly. For a half crack length of 35 mm, the increase in J value can be as high as 42%.

The computation of the critical crack length from the tearing instablity concept is illustrated in figs.5 & 6. It was found that at about 25 mm half crack length (50 mm full crack length), the initiation of cracking may take place. The critical half crack length is 44 mm (critical full crack length is 88 mm).

4.2 Zr-2.5 Nb Pressure Tube Analysis and Results

Through wall axially cracked Zr-2.5 Nb pressure tubes were analysed in same way as Zr-2 pressure tubes.The computation of the critical crack length for these tubes is illustrated in figs.7 & 8. It was found that at a half crack length of 32 mm (full crack length of 64 mm), initiation of cracking may occur and a half crack length of 45 mm (full crack length of 90 mm) is the critical length.

4.3 Peak factors and Crack Opening Area of Zr - 2 and Zr - 2.5 Nb pressure tubes

The knowledge of crack opening area is important for leak before break studies. Using crack opening area data, leak rates can be determined. In actual case if a through the thickness crack exists then the data from measured leak rates can be used to assess the crack lengths and margins against critical crack length. The crack opening area was calculated based on FE results. Table 2 shows full crack opening area of Zr-2 and Zr-2.5Nb pressure tubes for different crack lengths. Some closed form formulae for calculating crack opening area are available, like the one given by Tada, [8]. The crack opening area given by FE analysis (with crack face pressure) is higher than that given by Tada's formula, [8]. For 40 mm half crack length, it is higher by about 2.3 times, because Tada's formula does'nt take into account crack face pressure.

Table 2 : Full Crack Opening Areas

Half Crack Length (a) mm	Crack Opening Area (sq.mm) Zr - 2.5 Nb	Zr - 2
10	2.22	2.26
15	5.19	4.25
25	24.14	20.53
30	53.43	47.69
35	114.36	110.06
40	242.77	271.46

Table 3 : Average J acoss the thickness and Peak Factor Effect of Crack Face Pressure considered

Half Crack Length (a) mm	Zr - 2 Avg.J N/mm	Zr - 2 Peak Factor N/mm	Zr - 2.5 Nb Avg.J N/mm	Zr - 2.5 Nb Peak Factor N/mm
10	8.69	1.08	13.10	1.05
15	21.03	1.19	31.37	1.12
20	43.28	1.25	65.18	1.18
25	82.52	1.31	121.03	1.24
30	152.33	1.32	213.03	1.28
35	282.52	1.30	368.63	1.28
40	567.35	1.28	645.11	1.28

The calculation of critical crack length was based on J-values averaged across the thickness.

Actually, J varies across the thickness with highest value at the middle surface of pressure tube. The peak factors on J for each crack length were calculated using equation (1) and the results are shown in Table 3. The peak factors of Zr-2 and Zr-2.5Nb pressure tubes increase as crack length increases and then saturates to a constant value. It is seen that peak factor can be as high as 1.3 i.e. J at midsurface of pressure tube can be 1.3 times the average J value. There exists a possibility that crack may "tunnel" through along the axis in mid surface and little growth at outer or inner surface. For a given crack length and crack opening area the leak rate measurements may indicate little or no crack growth but crack may continue to grow unobserved.

5.0 Fracture Assessment of Pressure Tubes using R-6 Method

The fracture assessment of through wall axially cracked tubes was also done using CEGB R-6 method, [5]. The Failure Assessment Diagram (FAD) was determined using Option 2, based on data in reference, [6]. Ductile tearing was considered. The FAD of Zr-2 and Zr-2.5Nb is similar to Option 1 because at 300° C both these materials are approximately elastic perfectly plastic. In order to evaluate Plastic Collapse Parameter (Lr) and Linear Elastic Fracture Parameter (K'r) the collapse load and stress intensity factors for each crack length (considering crack face pressure) were determined using FE analysis.

FAD for Zr-2 pressure tubes is shown in fig.9. For half crack length less than 25 mm, the points (Lr,K'r) lie within the FAD. For half crack length equal to 25 mm the point (Lr,K'r) lies just outside the FAD i.e. crack initiation may occur at this stage. For higher half crack lengths the points (Lr, K'r) lie outside FAD but after a small crack growth the locus of points (Lr,K'r) falls back within the FAD due to increase in fracture resistance of the material. However, for 40 mm half crack length the locus of points (Lr, K'r) approaches the FAD but after about 3 to 4 mm crack growth the locus starts deviating away from FAD, fig.9. This indicates the onset of fracture instability. Hence, it is concluded that at 50 mm full crack length the crack initiation may occur and 86 to 88 mm full crack length is the critical crack size.

FAD for Zr-2.5Nb pressure tubes is shown in fig.10. Similar to Zr-2 tubes, it can be concluded that at 64 mm full crack length, initiation of cracking may occur and a full crack length of 90 mm is critical.

6.0 Conclusions

3D elastic plastic finite element techniques have been employed for the fracture analysis of a through wall axially cracked thin walled pressure tubes of Indian PHWRs made of Zr-2 and Zr-2.5Nb. The study is applicable for tubes in as received condition subjected to an internal pressure of 9.5 MPa at 300°C. Fracture assesment was also done using CEGB R-6 method.

In case of Zr-2 pressure tubes initiation of cracking takes place at a crack length of 50 mm, 88 mm is the critical crack length. In case of Zr-2.5Nb pressure tubes initiation of cracking is found to occur at a crack length of 64 mm, while the critical crack length is 90 mm. Similar results were obtained from R-6 analysis also

The inclusion of the pressure exerted by the leaking fluid onto the crack faces in the analysis increases the J values significantly. The ratio of J with crack face pressure to J without crack face pressure can be as high as 1.4 to 1.5, for higher crack lengths. The closed form formulae for calculating J, do not take into account the effect of crack face pressure.The inclusion of the crack face pressure in the analysis gives a lower value of the critical crack length.

The detailed 3D analysis also gives insight into variation of J along the tube thickness. In the present work a peak factor on J was computed to get an idea of maximum J value with respect to the average

J value. The maximum value of J always occurs at middle surface of pressure tube. The peak factors for both Zr-2 and Zr-2.5Nb pressure tubes increase as crack length increases and then saturates to a constant value. The peak factor can be as high as 1.3. There exists a possibility that crack may "tunnel" through without indicating any increase in leak rates. However, crack tunnelling may be insignificant in thin tubes.

7.0 Acknowledegements

The authors wish to thank Mr. J.K Behl, Mr. S. Chatterjee and Mr. S. Ananthraman of Radio Metallurgy Division, BARC, Bombay, for providing the material properties of Zr-2 and Zr-2.5Nb.

8.0 References

[1] Simpson,L.A. & Chow,C.K., "Effect of Metallurgical variables and Temperature on the Fracture toughness of Zirconium Alloy Pressure Tubes", ASTM STP-939, pp 579-596, 1987.

[2] Leger,M., "The Mechanism and Criterion for Fracture by Hydride Blister Initiated Cracking", IAEA Consultants meeting on the Effect of Hydride Blisters on the Integrity of PHWR Pressure Tubes, July 25 to 29, 1994.

[3] Hahn, G.T., Sarrate, M. and Rosenfield, A.R., "Criteria for Crack Extension in Cylindrical Pressure Vessels", International Journal of Fracture Mechanics, Vol.5, pp 187-210, 1969.

[4] Zahoor, A, "Ductile Fracture Handbook", EPRI NP 6301-D, 1989.

[5] Milne,I., Ainsworth,R.A., Dowling,A.R. & Stewart,A.T., "Assessment of the Integrity of Structures Containing Defects", Int. J. of Pressure Vessel and Piping, Vol.32, pp 3-104, 1988.

[6] Anantharaman,S., Chatterjee,S. & Behl,J.K., "Material Properties of Zr-2 and Zr-2.5Nb", BARC Internal Communication.

[7] "ABAQUS" Ver.5.3, Hibbit, Karlsson and Sorensen Inc., Pawtucket, RI, USA.

[8] Tada, H., "The Effects of Shell on a Circumferential and Longitudinal Through Crack in a Pipe", NUREG-CR-3464, pp 71-81, 1983.

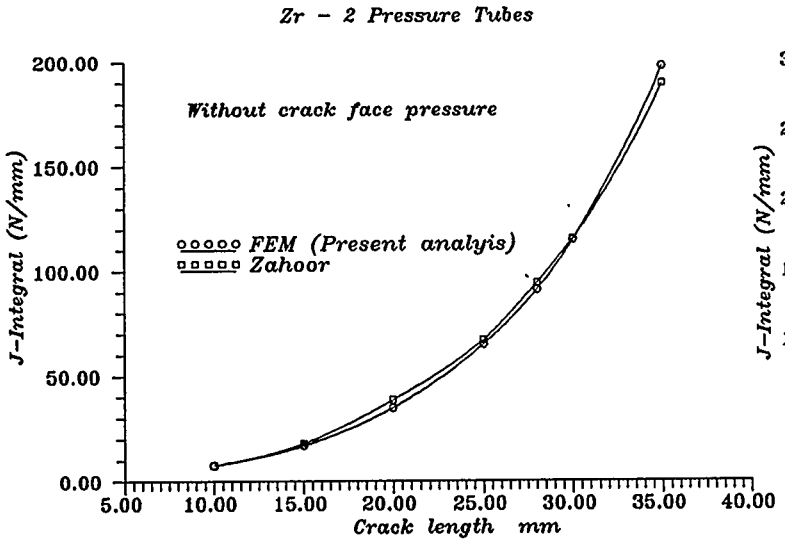

Fig.No.3 Plot of Applied J-integral V/s. Crack Half Length. Crack Driving Force Curve

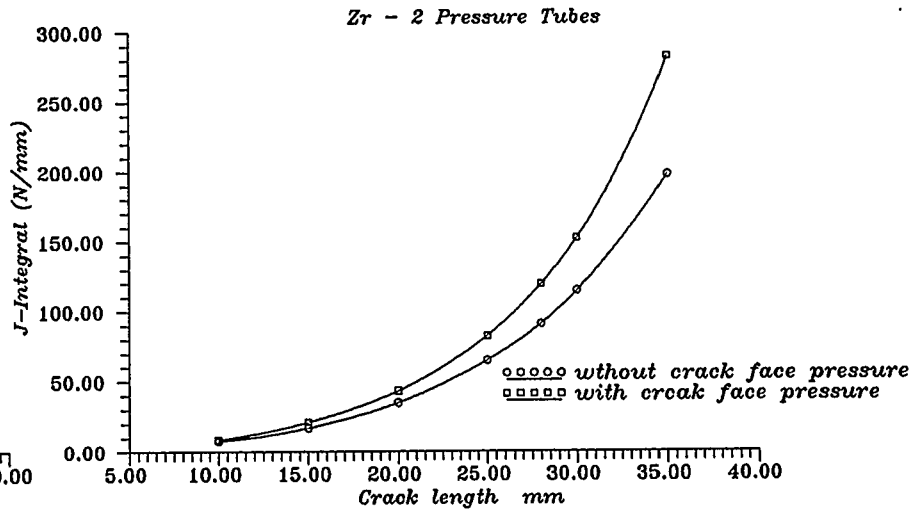

Fig.No.4 Plot of Applied J-integral V/s. Crack Half Length. Crack Driving Force Curve

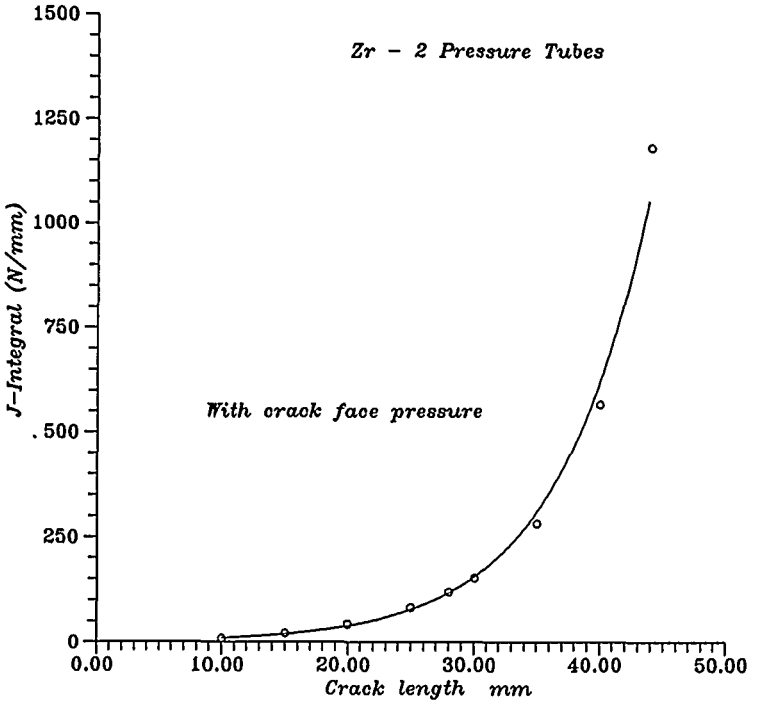

Fig.No.5 Plot of Applied J-integral V/s. Crack Half Length. Crack Driving Force Curve

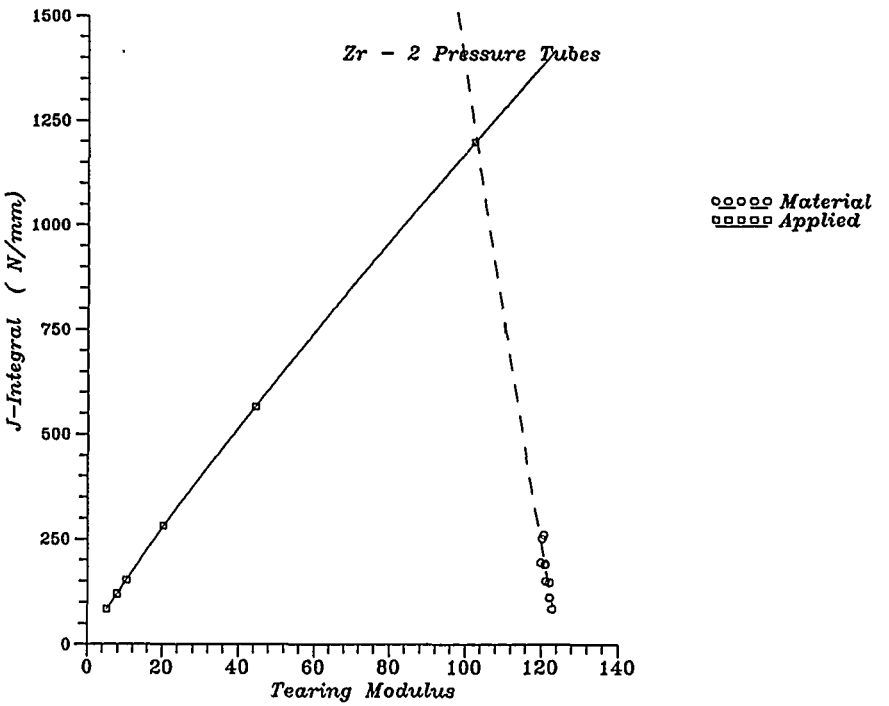

Fig.No.6 Plot of J-integral V/s. Tearing Modulus Elastic-Plastic Fracture Mechanics

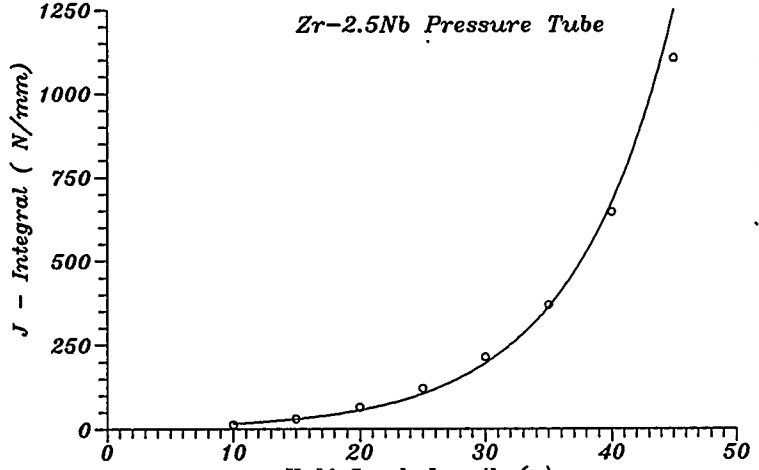

Fig.No.7 Plot of J – Integral V/s Half Crack Length

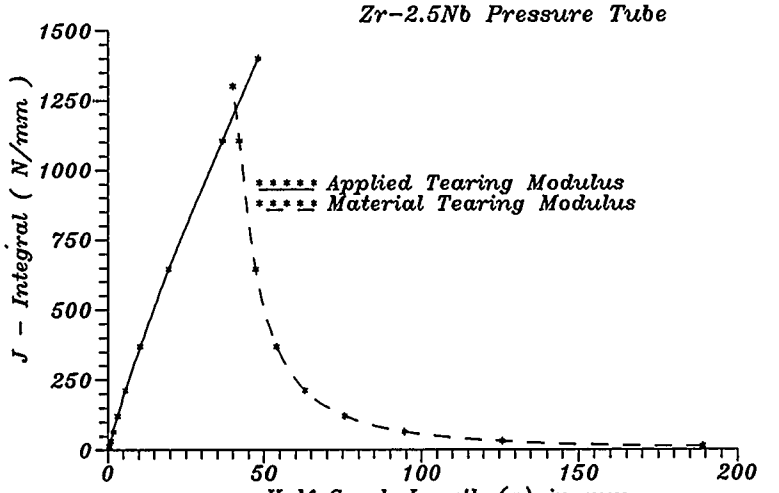

Fig.No.8 Plot of J – Integral V/s. Tearing Modulus

a= Half Crack Length in mm.
Δa= Half Crack Growth in mm.

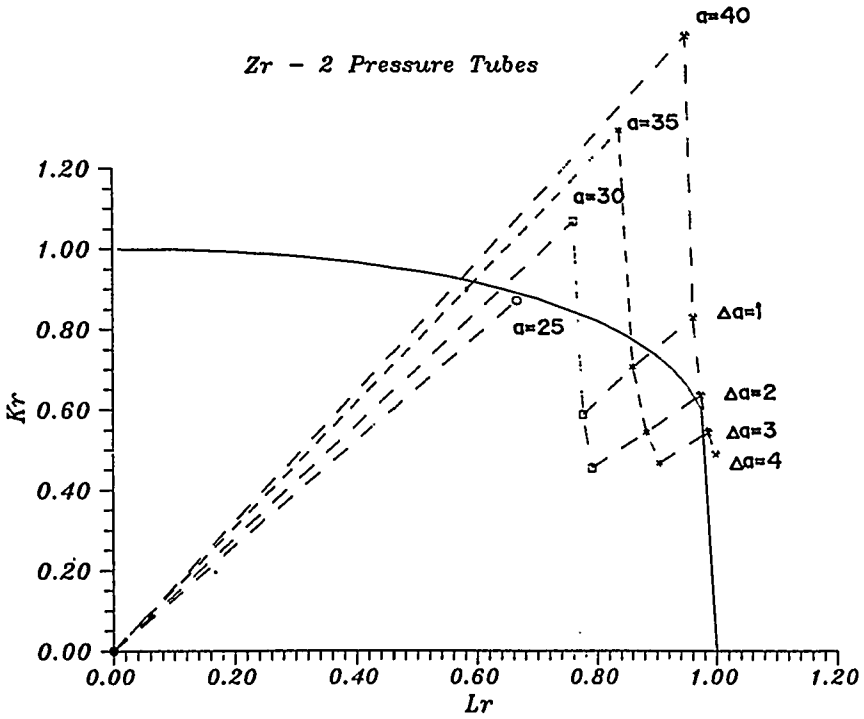

Fig.no 9 Failure Assesment Diagram

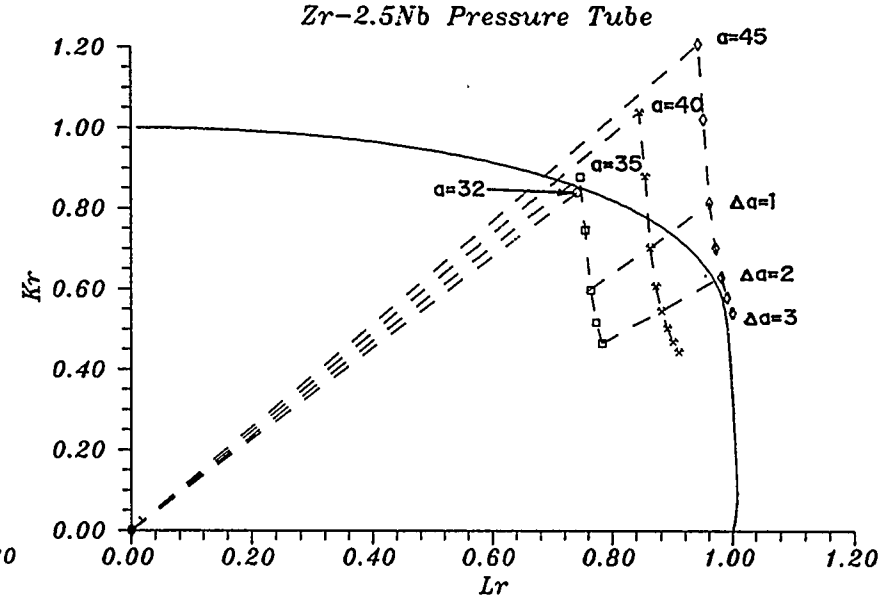

Fig.No.10 Failure Assesment Diagram

A COMPUTING SYSTEM FOR LBB CONSIDERATIONS

Kari Ikonen*, Jaakko Miettinen*, Heikki Raiko* and Rauli Keskinen**
*VTT Energy, Finland
**Finnish Centre for Radiation and Nuclear Safety, Finland

ABSTRACT

A computing system has been developed at VTT Energy for making efficient leak-before-break (LBB) evaluations of piping components. The system consists of fracture mechanics and leak rate analysis modules which are linked via an interactive user interface *LBBCAL*. The system enables quick tentative analysis of standard geometric and loading situations by means of fracture mechanics estimation schemes such as the R6, FAD, EPRI J, Battelle, plastic limit load and moments methods. Complex situations are handled with a separate in-house made finite-element code *EPFM3D* which uses 20-noded isoparametric solid elements, automatic mesh generators and advanced colour graphics. Analytical formulas and numerical procedures are available for leak area evaluation. A novel contribution for leak rate analysis is the *CRAFLO* code which is based on a nonequilibrium two-phase flow model with phase slip. Its predictions are essentially comparable with those of the well known *SQUIRT2* code; additionally it provides outputs for temperature, pressure and velocity distributions in the crack depth direction. An illustrative application to a circumferentially cracked elbow indicates expectedly that a small margin relative to the saturation temperature of the coolant reduces the leak rate and is likely to influence the LBB implementation to intermediate diameter (300 mm) primary circuit piping of BWR plants.

A COMPUTING SYSTEM FOR LBB CONSIDERATIONS

Kari Ikonen*, Jaakko Miettinen*, Heikki Raiko* and Rauli Keskinen**
*VTT Energy, Finland
**Finnish Centre for Radiation and Nuclear Safety (STUK), Finland

ABSTRACT

A computing system has been developed at VTT Energy for making efficient leak-before-break (LBB) evaluations of piping components. The system consists of fracture mechanics and leak rate analysis modules which are linked via an interactive user interface *LBBCAL*. The system enables quick tentative analysis of standard geometric and loading situations by means of fracture mechanics estimation schemes such as the R6, FAD, EPRI J, Battelle, plastic limit load and moments methods. Complex situations are handled with a separate in-house made finite-element code *EPFM3D* which uses 20-noded isoparametric solid elements, automatic mesh generators and advanced colour graphics. Analytical formulas and numerical procedures are available for leak area evaluation. A novel contribution for leak rate analysis is the *CRAFLO* code which is based on a nonequilibrium two-phase flow model with phase slip. Its predictions are essentially comparable with those of the well known *SQUIRT2* code; additionally it provides outputs for temperature, pressure and velocity distributions in the crack depth direction. An illustrative application to a circumferentially cracked elbow indicates expectedly that a small margin relative to the saturation temperature of the coolant reduces the leak rate and is likely to influence the LBB implementation to intermediate diameter (300 mm) primary circuit piping of BWR plants.

1 INTRODUCTION

The LBB evaluation of real nuclear piping systems typically presents a remarkable computational task where cracks have to be postulated in several locations and analysed under various loading conditions. Iterative procedures, involving repetitive fracture mechanics and/or leak rate calculations are necessary in determining the leakage and critical crack sizes. To overcome these difficulties, an efficient integrated computing system *LBBCAL*, supplemented with a powerful finite element code *EPFM3D* , was developed at VTT Energy by order of the Finnish nuclear regulatory body STUK. This paper describes of the main features of the system with emphasis on a leak rate evaluation code *CRAFLO* which is currently being validated. An illustrative application is made to a BWR plant primary circuit piping with a postulated circumferential through wall crack.

2 INTEGRATED LBB ANALYSIS ENVIRONMENT

The LBB evaluation system developed at VTT Energy consists of structural, fracture mechanics and leak rate analysis modules which make up an integrated computational environment as shown in Figure 1. The first step of analysis is determining the global forces and moments unless they are known from existing stress analysis. For static or quasi-static loading situations, including complex thermal stratification phenomena, a code *PIPING* was developed. Another code, named *PIPEBREAK* , was originally devoted to pipe whip analysis but is equally suited to other dynamic situa-

tions. The main features of the *PIPING* code are:

- the code is based on beam element theory being supplemented by the theory of curved pipe bending elements,
- thermal loads in axial and lateral directions can be handled,
- restraints with gaps, pre-tensioning and friction can be taken into account and
- deformations, stress and strain components, von Mises stress and principal stresses needed in determining ASME-stress intensities can automatically be visualised with colour graphics.

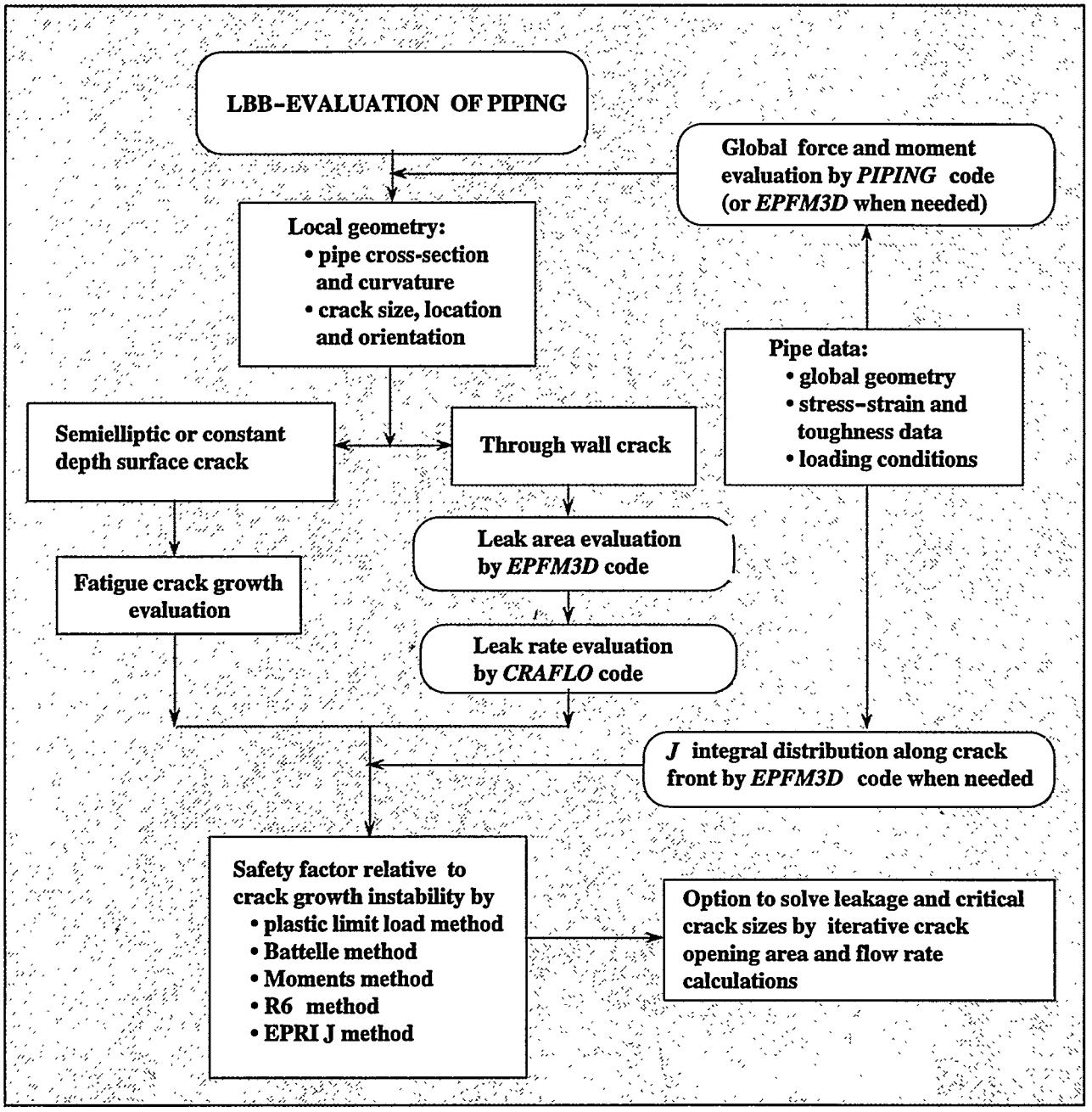

Figure 1. The integrated LBB analysis environment developed at VTT Energy.

An interactive interface *LBBCAL* is a key part of the system and constitutes a link between the CRAFLO leak rate code and subroutines making use of well known fracture mechanics estimation schemes. The estimation scheme library mainly serves crack stability and leak area analysis of straight and curved pipes and offers the following options:

- plastic limit load method for circumferential cracks,
- Battelle's method
- EPRI J method,
- Moments method,
- R6 and FAD methods

For crack opening area evaluation the *LBBCAL* system provides several closed-form formulas based on plasticity-corrected linear-elastic fracture mechanics.

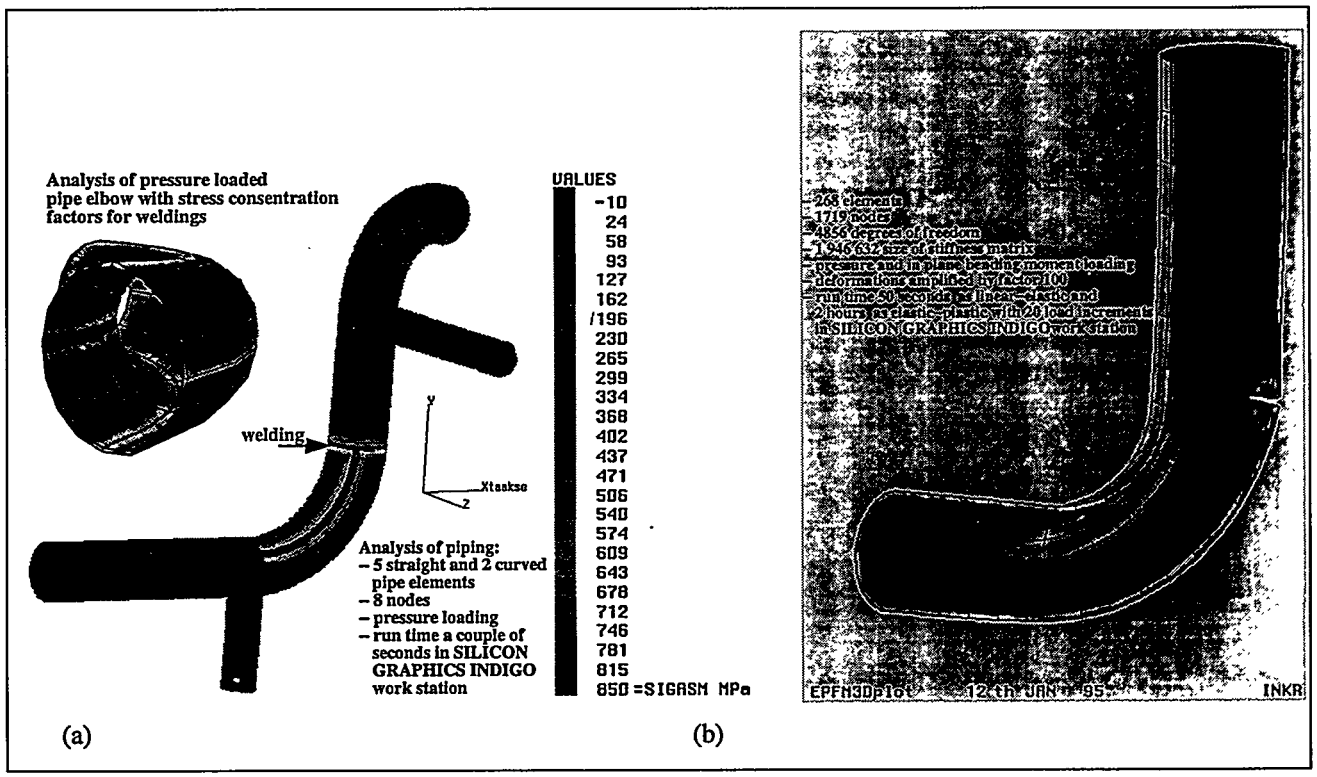

Figure 2. Stresses at an elbow as calculated by the PIPING code (a); a detailed finite element analysis by the EPFM3D including a through wall crack (b).

3 THE FINITE ELEMENT CODE *EPFM3D*

The finite element code *EPFM3D* was developed for the analysis of three-dimensional pressure vessel and piping components for which analytical methods and solutions do not exist in literature. Stress analysis of complex mechanical and thermal transient loading situations makes up an important application area but the code is also ideally suited to advanced elastic-plastic fracture mechanics analysis of cracked components. *EPFM3D* offers colour graphics visualisation of about 25 quantities involving deformations, applied loads and restraints, material types, distributions of stress and strain components, von Mises stresses, main stresses etc. Separate plottings from zoomed crack area show the applied stress and *J* integral distributions. The other features include:

- 20-noded isoparametric solid elements,
- mesh generators for different pipe and crack geometry combinations composed of straight and curved pipes, axial and circumferential cracks, through wall cracks and semi-elliptic part-through cracks in inner or outer surface, cracks at intrados and extrados of elbows,
- automatic generation of pressure, axial force, shearing force, twisting moment and bending moment loads,
- von Mises type isotropic strain hardening with Ramberg-Osgood or piecewise linear stress-strain dependence,
- option to model piping systems with cladding,
- automatic leak area calculation with pressurised crack faces,
- solving the system of equations by the Cholesky decomposition method (skyline technique) and iteratively in case of very large systems,
- updating the tangential stiffness matrix along with plastic deformations
- coupled displacements (master and slave degrees of freedom)
- calculation of J integral and crack tip opening displacement (*CTOD*) along crack front,
- operations for shallow cracks (for cleavage fracture, based on maximum principle stress area method) and
- J integral calculation for mechanical and thermal loads by the domain integral method.

An essential feature of the *EPFM3D* code is automation of finite element method based calculations for efficient LBB related analysis of complicated structures. Special attention has been given to reliable operation of the code. Numerous verification examples, for which analytic solutions are known, have been carried out involving mechanical and thermal loadings as well as calculation of stress intensity factors and J integrals. The code uses several internal controls to quarantee the reliability of the model and the calculation process.

4 THE LEAK RATE EVALUATION CODE *CRAFLO*

4.1 Physical and numerical modelling

A computer code *CRAFLO*, standing for *CRA*ck *FLO*w, has been developed for the analysis of leakage issuing from a through wall crack. The solution in *CRAFLO* can be characterised as a nonequilibrium model taking into account velocity slip between steam and liquid. A detailed pressure, quality, temperature, velocity and heat transfer coefficient calculation model predicting local conditions along the flowpath is coupled to the global flow rate model.

The mass conservation equation defines that the total mass flow rate is constant along the crack length. The mass conservation equation in a crack with a variable flow area may be expressed as

$$\frac{dG}{dz} + \frac{G}{A}\frac{dA}{dz} = 0 , \tag{1}$$

where G means mass flow density, A local flow area and z the coordinate in the flow direction. The energy conservation equation may be expressed by assuming that the enthalpy difference between the inlet and exit planes of the crack is transformed into kinetic energy

$$G_e = \rho_{m,e}\sqrt{2(h_{m,o} - h_{m,e})} . \tag{2}$$

In Equation (2), ρ means actual mixture density in the exit plane (subscript e) and h enthalpies in the inlet (subscript o) and exit planes. The mixture density in the equation is calculated by using the nonequilibrium quality. The actual

quality taking into account the nonequilibrium effect is used for the actual density and it may be expressed with a relaxation model based on the Henry nonequilibrium model [1]:

$$X_{ac} = N\ X_{eq}\ (1 - e^{-B(L/D_i - 12)})$$
$$N = 20X_{eq} \text{ for } X_{eq} < 0.05,\ N = 1 \text{ for } X_{eq} > 0.05\ . \tag{3}$$

Here L is the flowpath length, D equivalent diameter of the crack, $B = 0.0523$ a constant for nonequilibrium. The momentum conservation equation may be written as

$$-\frac{dp}{dz} = \frac{1}{A}\frac{d}{dz}\left(\frac{G^2 A}{\rho_m}\right) + \frac{X}{2}\frac{G^2}{\rho_m}, \tag{4}$$

where p denotes pressure and X is the total friction coefficient. The phase separation predicted by difference slip model may be taken into account for two-phase mixture. The friction coefficient can be considered as a generalised coefficient. It includes the pressure loss due to entrance, the wall friction and the bends along the flowpath. The governing expressions of these contributions are clarified in Table I.

TABLE I. Friction loss terms for different pressure loss forms.

Pressure loss form	Mass flux G	Density ρ_m	Friction X
Entrance pressure loss	G_o	ρ_{mo}	$1/C_D^2\ /L$
Wall friction	$0.5(G_o + G_e)$	$\rho_{m,ave}$	$(C_1 \log(\frac{D_i}{R}) + C_2)^{-2}/D_i$
Velocity heads due to bends	$0.5(G_o + G_e)$	$\rho_{m,ave}$	e

In case of the entrance pressure loss C_D means the friction discharge coefficient and L is the crack depth. The discharge coefficient varies from 1.0 for small cracks to 0.5 for large cracks. In case of pressure loss due to wall friction R means the surface roughness. In the friction coefficient, based on Schlichting [2] C_1 and C_2 are equal to 2.00 and 1.14 for $(D/R) > 100$ and 3.39 and −0.866 for $(D/R) < 100$. The average mixture quality used for the average mixture density is calculated in the average pressure along the crack and it is defined as $p_{ave} = 0.5(p_0 - \Delta p_{entrance} + p_1)$. In case of the pressure loss due to bends in the flowpath e is the density of velocity heads per unit flow length ($X = 1$ for a single velocity head with 90° bending). A nonlinear function has been defined for the reduction of this pressure loss as a function of increasing gap width. The phase and area change acceleration pressure losses are calculated from the first term on the right hand side in the momentum Equation (4).

For calculation of the flow rate an iterative procedure is needed, where as a function of stagnant conditions the flow is maximised with a three step numerical procedure.

Step I: Find numerically the maximum critical flow rate based on the energy equation. This value is typically much higher than the final flow rate and will be used as a start point for the next step.

Step II: Find numerically such exit plane pressure and corresponding exit quality values that also the momentum balance equation becomes satisfied.

Step III: Calculate detailed through wall distributions inside the crack.

Diamond, rectangular and elliptic shapes may be used to characterize the crack inlet and exit plane geometries. The

crack depth, length, interior gap and exterior gap define the dimension of the crack. As thermal hydraulic boundary conditions the fluid pressure, fluid temperature and fluid quality or subcooled enthalpy inside the pipe and pressure outside the pipe are given. The output for the integral calculations includes several interesting parameters. Among them is the total friction loss which sums up the partial pressure drops arising from the entrance loss, the acceleration loss, the wall friction pressure loss, the area change loss and the effect of velocity heads.

The detailed distributions are calculated for a fine mesh point grid, consisting of typically 100 points for the pressure, liquid temperature, liquid quality, coolant density, coolant enthalpy, liquid and steam velocity and heat transfer coefficient. The detailed distributions may be used for studying the effect of nonequilibrium and phase separation models on the local distributions. Optionally the detailed distribution model can be used for the momentum balance solution. For structural calculations the local coolant temperatures and heat transfer coefficients are essential.

4.2 Validation against the SQUIRT2 code and experimental results in literature

The code validation is in progress. The well established *SQUIRT2* code [5] was used as the first benchmark. Some results are presented in Figure 3 for an elliptic crack with COD's of 0.1, 0.5 and 2.0 mm and internal pressures of 6.0 and 8.0 Mpa. The liquid subcooling assumed values of 2, 30 and 60 K. The comparison shows that good agreement can be achieved at COD's falling below 1 mm and a small deviation occurs at higher COD's. The comparison is sensitive to the modelling of velocity heads, approaches used for the nonequilibium model and the definition of the average mixture density. The nonequilibrium model will be studied further by comparing results against critical flow data in two-phase flow facilities. As a second case comparison results are presented for measured leakages from a through wall crack in a circumferential girth weld [3]. The pipe had a diameter of 168 mm, wall thickness of 8.28 mm, crack length of 33.3 mm and COD between 0.106 and 0.181 mm. The density of velocity heads was defined as 6 heads/mm. The surface roughness was assumed to be 0.004 mm. Figure 4 shows a comparison of the calculated and measured mass flows. A slight underprediction is observed in the calculated mass flow.

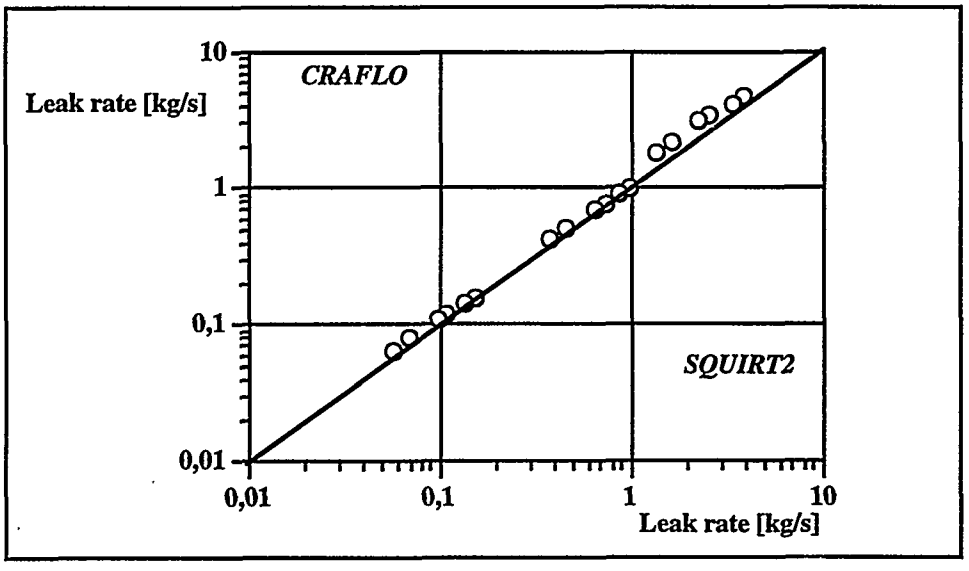

Figure 3. Comparison of leak rates predicted by SQUIRT2 and CRAFLO.

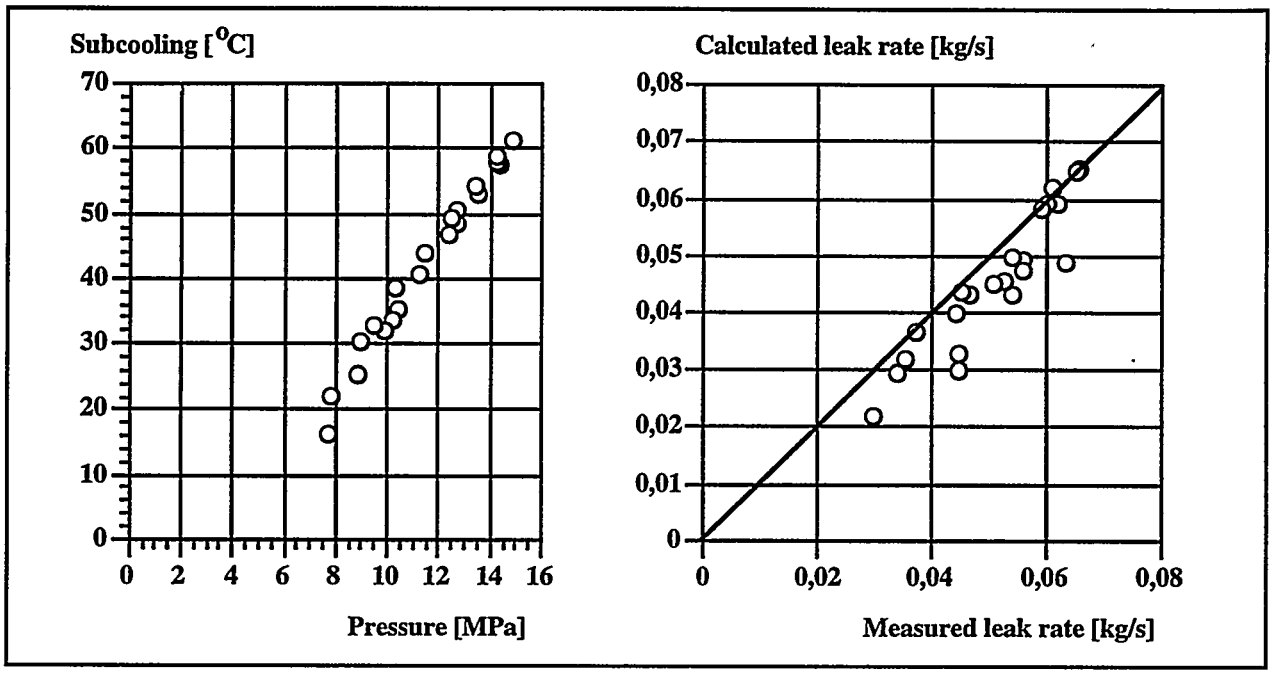

Figure 4. Experimental parameter range and leak rates predicted by CRAFLO for a through wall crack in a circumferential girth weld [3].

A third benchmark was taken from reported leakages of a pipe with an intergranular stress corrosion crack [4]. The wall thickness and the crack surface roughness were 17.3 mm and 0.00178 mm, respectively. The COD varied

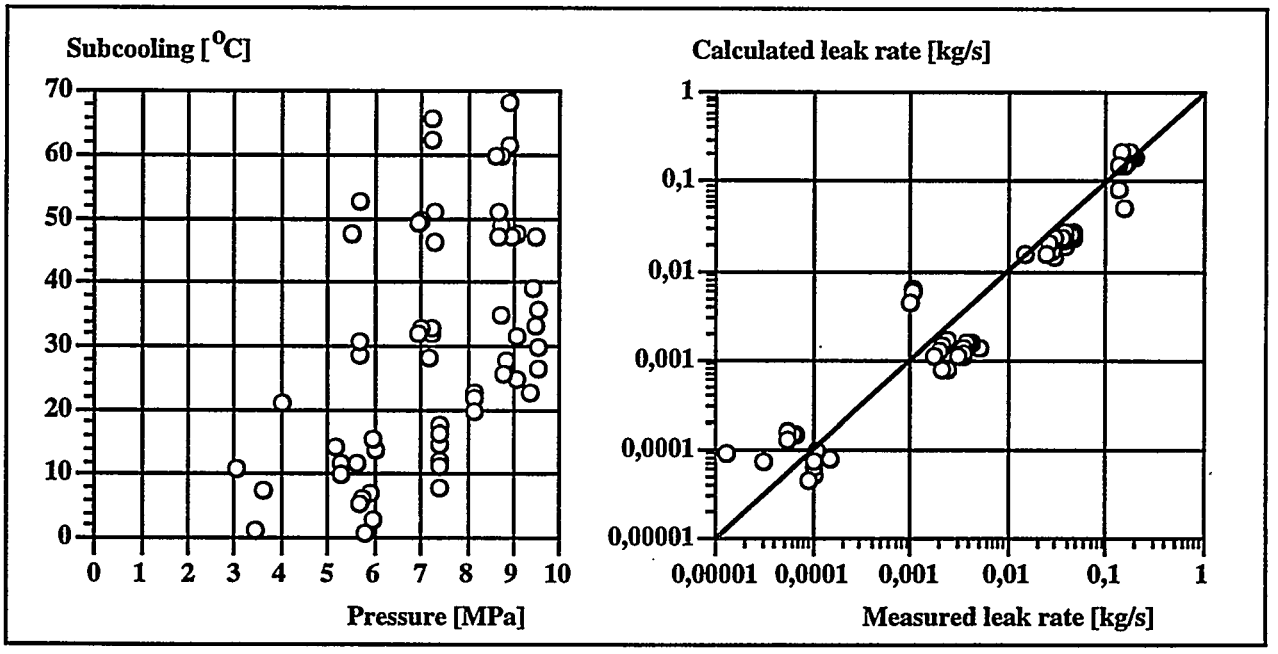

Figure 5. Experimental parameter range and leak rates predicted by CRAFLO for an intergranular stress corrosion crack [4].

between 0.02 and 0.228 mm and the crack length range was from 0.74 to 27.9 mm. No data was available regarding the density of velocity heads so it was assumed to be zero. In Figure 5, presented are the thermal hydraulic parameter range and the predictions of *CRAFLO* plotted against the measured mass flow rates. The comparison shows remarkable deviations from a few experimental observations and their origin clearly deserves further investigation. Some experimental points appear to present disagreement in the data when compared to other data points.

The validation runs presented above were undertaken during the basic testing of the program. The work will be continued using other data, also including critical flow data from thermal hydraulic experiments. After finishing the first validation phase the reasons for the deviations will be analyzed and the necessary model improvements will be made. At present, the phase separation and nonequilibrium models seem to call for improvements. In some cases the deviations may be also explained by uncertainties in the wall friction model, in the entrance coefficient and in the density of velocity heads.

5 APPLICATION TO A CIRCUMFERENTIALLY CRACKED BWR PIPING

The LBB evaluation system was applied to a postulated circumferential through wall crack in a BWR plant primary circuit piping. The exact location, as shown by Figure 2b, is the extrados side of a welded connection between an elbow and a straight pipe. The pipe has an outer diameter of D_O = 323.9 mm, wall thickness of t = 18.0 mm, radius of curvature of R = 650.0 mm and is subjected during normal operation to an internal pressure of Δp = 7.0 MPa and a maximum in-plane bending moment of M = 26810 Nm. The pipe is fabricated from AISI 304 type austenitic stainless steel which presents at the operating temperature of +286 ^{o}C a Young's modulus E = 180 GPa, Poisson's ratio ν = 0.3, yield stress σ_y = 120 MPa, ultimate stress σ_u = 380 MPa and elongation 40 %.

The LBB evaluation procedures followed the US practice according to which there should exist a safety margin of 2 between critical crack size and leakage crack size, corresponding to a leakage of 10 gallons per minute during normal operation, and the leakage size crack should remain stable if 1.4 times the normal plus safe-shutdown earthquake loading is applied. However, no distinction was made to the loading conditions since no earthquake loadings have been specified for the particular piping system.

The *EPFM3D* code was employed in the finite element analysis. Straight pipe sections of length 1 m were added to the ends of the elbow to enable realistic modelling of the stiffness. One end of the model was fixed and the other subjected to the given bending moment. For elastic-plastic calculations a Ramberg-Osgood fitting was made through the two known points, resulting in the parameters n = 4.6 and σ_0 = 88.4 MPa (α = 1 in Ramberg-Osgood fitting). The flow stress was set to $\sigma_f = 0.5(\sigma_y + \sigma_u)$ = 250 MPa. Straight crack fronts, perpendicular to the pipe surfaces were assumed and the crack growth phase was not considered. The circumferential crack length was varied in the range 2θ = 60^{o} to 160^{o} using 20^{o} increments. Several further runs were needed to find out adequate element mesh densities in different directions and adequate size of load increment to reach sufficient accuracy. The crack is not merely loaded in the crack opening mode (I), also the shearing and twisting modes (II and III) are present. The K_J values include the effect of these three modes though the mode I is dominant.

The leak rate calculations were carried out using both the *CRAFLO* and the *SQUIRT2* codes. An estimate of 0.04 mm was used for the surface roughness, corresponding to typical fatigue cracks. The analyses were very sensitive to the selected density of velocity heads and its reduction as a function of increasing gap size.

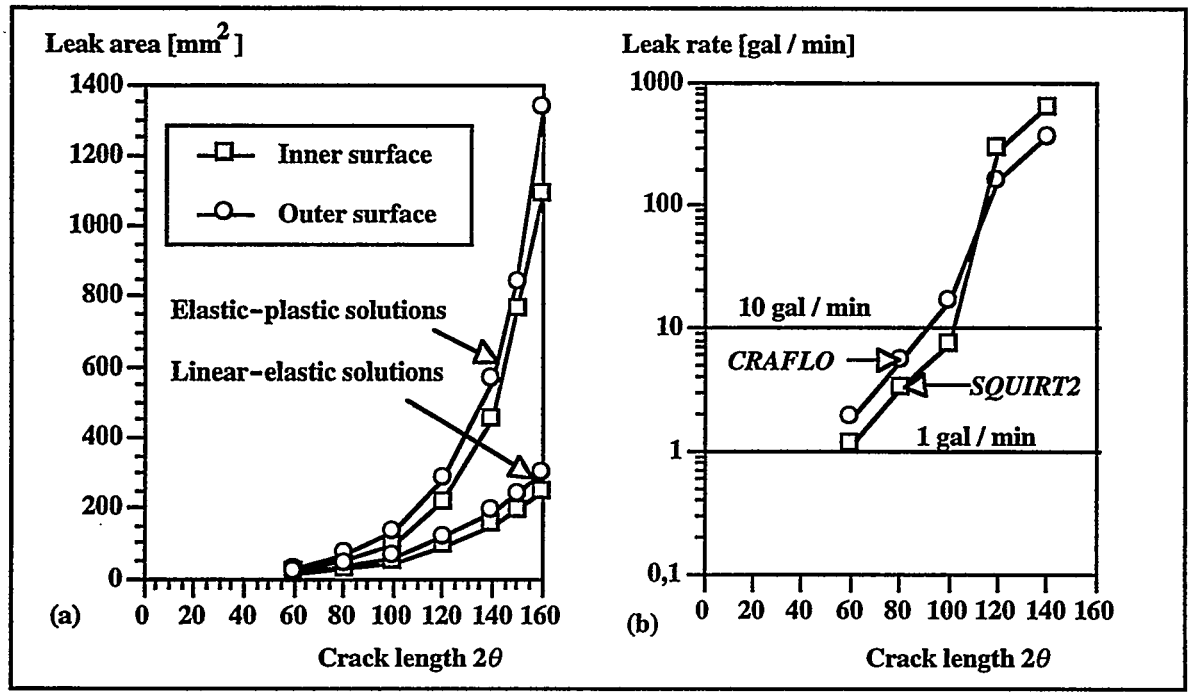

Figure 6. Linear-elastic and elastic-plastic leak area predictions of EPFM3D for various crack lengths (a); leak rate predictions of CRAFLO and SQUIRT2 corresponding to elastic-plastic leak areas at various crack lengths (b).

The computed leak areas and leak rates are plotted against the circumferential crack length (subtended angle in degrees) in Figures 6a and 6b, respectively. Figure 6a shows remarkable growth of leak area with increasing plasticity at crack lengths exceeding $2\theta = 60^{\circ}$. Plasticity-corrected estimation scheme solutions would settle well above the purely linear-elastic one but would still lead to a serious underprediction. Figure 6b in turn shows that the leakage size crack corresponds to a subtended angle of ca. 100°.

The high-toughness material enabled a simple safety margin evaluation by means of the limit load method. The well known governing equations are

$$\beta = \frac{\pi}{2}\left(1 - \frac{\theta}{\pi} - \frac{\sigma_m}{\sigma_f}\right)$$
$$\pi\,\sigma_b = 2k\,\sigma_f\,(2\sin\beta - \sin\theta)\,. \qquad (5)$$

The safety margin in terms of loading turned out to be 2.95. This result was verified by a finite element analysis where the pressure and bending moment were increased monotonically while their ratio remained constant. For evaluation of the safety margin in terms of crack size, the limit load analysis routine contained in the LBBCAL system first predicted a value $2\theta = 185^{\circ}$ for the critical crack length. Hence, the safety margin may be taken as the ratio 185° / 100° to yield the value of 1.85. Finite element analysis resulted in a value of 1.7.

From the above results it may be concluded that the safety margin in terms of loading exceeds well the required value of 1.4. However, the safety margin in terms of crack size falls 7.5 - 15 % below the required value of 2, irrespective

of the application of normal loading conditions to the crack stability analysis. This suggests that the LBB concept would not be formally applicable. Among the likely reasons may be mentioned that the liquid main coolant has in BWR conditions a small margin relative to the saturation temperature which tends to reduce the leak rate. At the same time the fairly small pipe size category reduces the leak area. A possible remedy for the situation would be providing justification of smaller postulated leakage size crack e.g. based on improved leak detection systems.

6 CONCLUSION

The LBB evaluation of real nuclear piping systems typically involves repetitive fracture mechanics and leak rate calculations for several cracks postulated in the most stressed locations. VTT Energy's solution to this challenging task is an integrated, highly automated LBB evaluation environment which was developed in the course of a project supervised by the Finnish nuclear regulatory body STUK. It includes both simple estimation schemes, linked by an interactive user interface *LBBCAL*, and sophisticated finite element procedures provided by an in-house developed code *EPFM3D*. The first experiences verify that this type of diversity guarantees the most powerful system. A novel contribution to the system is the leak rate code *CRAFLO* which is based on a nonequilibrium two-phase flow model with phase slip. Ongoing benchmarking against the well established *SQUIRT2* code and experimental results in literature indicate reasonable accuracy. The computing system has been applied to a postulated circumferential through wall crack in an elbow of a BWR plant primary circuit piping. This illustrative case shows expectedly that a small margin relative to the saturation temperature reduces the leakage and may influence the LBB implementation to intermediate diameter (300 mm) primary circuit piping of BWR plants. A high degree of plasticity in turn strongly increases the leakage owing to a larger leak area. In case of complex piping components such as elbows, advanced finite element calculations are necessary since plasticity-corrected linear-elastic approach models this effect inadequately.

ACKNOWLEDGEMENTS

This work was supported by the Finnish Centre for Radiation and Nuclear Safety.

REFERENCES

[1] Henry, R.E. (1970), The Two-Phase Critical Discharge of Initially Saturated or Subcooled Liquid, Nuclear Science and Engineering, Vol 41, pp. 336-342.

[2] Schlichting, H. (1968), Boundary Layer Theory, McGraw-Hill.

[3] Paul, D.D., Ahmad, J.J., Scott, P.M., Flanigan, L.F., Wilkowski, G.M., Evaluation and Refinement of Leak Estimation Models, NUREG/CR-5128, BMI-2164.

[4] Collier, R.P., Stulen, F.B., Mayfield, M.E., Pape, D.B., Scott,P.M. (1984). Two-Phase Flow Through Intergranular Stress Corrosion Cracks and Resulting Acoustic Emission, EPRI Report No. NP-3540-LD.

[5] SQUIRT User's Manual, Version 2.2, D. D. Paul, N. Ghadiali, S. Rahman, P. Krishnaswamy, G. Wilkowski, Battelle, Columbus, OH, USA.

[6] Ikonen, K., Raiko, H., Leak-Before-Break Evaluation Procedures for Piping Components, Report STUK-YTO-TR 90, Finnish Centre for Radiation and Nuclear Safety, Helsinki, 1995, 58 p.

OVERVIEW OF LARGE SCALE EXPERIMENTS PERFORMED WITHIN THE LBB PROJECT IN THE CZECH REPUBLIC

Petr Kadečka, Dana Lauerová
Nucler Research Institute, 250 68 Řež, Czech Republic

INTRODUCTION

During several recent years NRI Řež has been performing the LBB analyses of safety significant primary circuit pipings of NPPs in Czech and Slovak Republics. The analyses covered the NPPs with reactors WWER 440 Type 230 and 213 and WWER 1000 Type 320.

Within the relevant LBB projects undertaken with the aim to prove the fulfilling of the requirements of LBB, a series of large scale experiments were performed. The goal of these experiments was to verify the properties of the components selected, and to prove the quality and/or conservatism of assessments used in the LBB-analyses.

In this poster, a brief overview of experiments performed in Czech Republic under guidance of NRI Řež is presented.

BACKGROUND OF EXPERIMENTS

The fundamental idea underlying the LBB approach is based on the assumption that significant coolant leakage from the cracked component will be detected prior to excessive pipe cracking. The minimum detectable leakage for PWR WWER was established as 3.8 l/min; with margin of 10 this represents 38 l/min. In accord with regulations of State Office of Nuclear Safety in Czech Republic and Office of Nuclear Supervision in Slovak Republic, the cracked component must stay stable during the experiment when loaded by maximum superimposed loading (i.e. normal operating plus SSE loading).

Experimental tests were divided into two stages. The goal of the first stage is to verify that no excessive component cracking, such as unstable crack growth or plastic collapse, will occur under maximum superimposed loading. During the second stage of experiment the component is loaded by only external forces without internal pressure, until a sufficiently large increase in crack length is reached, and the maximum sustainable load is established.

For the experiments were chosen components for which there were doubts about conservatism in their evaluations or this evaluation was difficult to perform.

The following actions are necessary for both experimental set up and carrying out of the experiments:

- calculation of the crack length corresponding to minimum detectable leakage (38 l/min) as well as calculation of the loading parameters representing the maximum superimposed loading.
- ensuring either the original piece of the component, if this is available (archive component) , or manufacturing a new model with as most similar properties as possible.
- manufacturing of the required throughwall crack and its sealing.
- arrangement of the whole experimental facility so that experiment can be performed in the required way and the loading of the model simulate the loading of primary piping.
- measuring and recording various quantities according to the requirements of both experiment stages.

During the experiment, the following quantities were measured:

- loads
- displacements in different places of the model
- temperatures
- CMOD-values
- various quantities concerning the crack behaviour and crack growth

EXPERIMENTS PERFORMED ON COMPONENTS OF PRIMARY PIPINGS OF WWER 440 TYPE 230 NPPS

Three components of primary pipings of WWER 440 Type 230 NPPs were experimentally tested: elbow to steam generator, pressurizer safe-end and RPV safe-end.

In the first experiment the weld joining the elbow with the primary piping was tested. The elbow was manufactured from austenitic steel 08CH18N10T and was composed from two parts welded together by an axial weld. Material of the primary piping was also austenitic steel 08CH18N10T and therefore the tested weld was a homogeneous one. Material filling the weld was the weld metal SV04CH19N11M3.

In Fig. 1, a drawing of the experimental model is seen. Since the model of the original elbow containing axial weld was not available, a similar but not exactly the same model of elbow from the same material had to be used.The pipe welded up to elbow was the original archive pipe. In the weld joining the experimental elbow model with the pipe an artificial throughwall crack was manufactured. The crack was sharpened manually using a thin saw. This way of crack manufacturing was used also in the case of the other experiments. The outer surface length of the circumferential crack was 215.6 mm.

The experimental arrangement is seen in Fig. 2.

In the second experiment the heterogeneous weld of pressurizer safe-end was experimentally tested. The original component of safe-end was not available and therefore the test was performed on a little different model manufactured by welding up two pipes. For this model , the base material, weld metal and production technology were the same as for the original component.

Material of one pipe constituting the experimental model was feritic steel 22K and material of second pipe was austenitic steel 08CH18N10T. Heterogeneous weld contained two transition layers. Materials of the two layers were: steel SV10CH16N25AM6 (first layer) and SV04CH19N11M3 (second layer). The material filling the weld was the weld metal SV04CH19N11M3.

The experimental facility (Fig. 3) was composed of the base frame containing a flange. Experimental model was welded up to the flange on one side and on the other side it was joined by a weld to an arm on the end of which the force was applied. In the tested weld a circumferential throughwall crack was manufactured. The outer surface crack length was 170.5mm.

In the third experiment the heterogeneous weld joining the reactor pressure vessel with the safe-end was tested. Experimental model is seen in Fig. 4. The central massive part of the model, representing the reactor pressure vessel, was manufactured from ferritic material 15CH2MFA; the two safe-ends and two pipes were manufactured from austenitic material 08CH18N10T.

The model contains two heterogeneous welds located symmetrically in the model. One of the welds was manufactured by manual arc welding and the second by an automatic welding under flux. Both types of welds are found in primary pipings of the first and second units of NPP Jaslovské Bohunice (Slovak Republic).

Each of the tested heterogeneous welds contained a sharpened throughwall crack of length 478 mm. The crack was located in such a way that the crack tip crosses succesively weld metal, two transient austenitic layers, heat affected zone and ferritic material.

Results of all experiments showed that no crack initiation occurred within the first stage experiment and that the component behaviour under the loading prescribed was stable.

Summarizing the results of the second stages of experiments, it was stated that plastic collapse occurred in the case of elbow model, and in the case of other components, significant stable crack growths were observed so that unstable crack growing (after large amount of stable growing) may be assumed to be the failure mode of each of the component.

EXPERIMENTS PERFORMED ON COMPONENTS OF PRIMARY PIPINGS OF WWER 440 TYPE 213 NPPS

Two components of primary pipings of WWER 440 Type 230 NPPs were experimentally tested: heterogeneous weld of ECCS nozzle and pressurizer surge lines T-joint.

The tested model of ECCS nozzle (including heterogeneous weld as well as pipe welded up to the nozzle) was in accord with the real component with respect to both geometry and materials. Experiment was performed with using the same facility as experiment performed on the safe-end of RPV, described above. The model was very similar (with the only exception of geometrical dimensions) to the model of pressurizer safe-end. The throughwall crack was located in the region of fusion line of heterogeneous weld and its length on outer surface was 300 mm.

This experiment was of a special significance since the same materials and welding technology were used for manufacturing of heteregeneous weld of RPV safe-end of WWER 440/213 and thus also the behaviour of this weld may be expected to be simulated by the experiment.

The T-joint model represents a real component forming a part of WWER 440/213 primary lines. The T-joint was manufactured by welding up two austenitic steel pipes. The arrangement of the experiment is seen in Fig. 5. The facility consists of firm base, the experimental model and the loading unit containing a hydraulic piston. The bending force is applied to the top of the T-joint branch and the resulting bending moment opens the crack.

The experimental model of the T-joint is shown in Fig. 6. The smaller pipe of the model was stiffened by welding up another pipe of greater diameter in order to exclude an additional critical location outside the weld. The crack shape followed the boundary of the weld. The outer surface crack length was 338 mm. The location of the crack in the region of fusion line of the weld was selected according to material tests indicating it as the most limiting location.

In the second stage of experiment the crack propagated into the weld material. After completion of the experiment it was found that crack extension on the inner surface was about 3 times smaller than on the outer surface. The right crack tip behaviour was similar to the left one. The final crack extension on the outer surface was on the one side 40 mm and on the other side 40.5 mm.

EXPERIMENTS PERFORMED ON COMPONENTS OF PRIMARY PIPINGS OF WWER 1000 TYPE 320 NPPS

Two components of primary pipings of WWER 1000 Type 320 NPPs were experimentally tested: ECCS nozzle with adjacent part of WWER 1000/320 piping and pressurizer surge lines T-joint.

Two types of heterogeneous welds occur in ECCS piping system.

The first type weld joints the RPV nozzle made from material 15CH2NMFA with straight part of the piping made from ferritic-perlitic material 10GN2MFA. The weld is filled by austenitic material using electrode EA 400/10 T.

The second type of weld joints two pipes. One of them is made from ferritic-perlitic material 10GN2MFA and the second one is made from austenitic material 08CH18N10T. The weld is also filled with austenitic material using electrode EA 400/10 T.

In Fig. 6, one half of the experimental model containing both welds is seen. The middle part of the model was manufactured from steel 15CH2MFA and represents the nozzle and the stiffness of the RPV. The second part of the model is a pipe made from steel No. 16220.4 which is Czech equivalent of steel 10GN2MFA. The last part of the

model is represented by a straight pipe made from austenitic steel No. 17248.4 having similar properties as the original material 08CH18N10T. The methodology of welding process is the same as in the plant. Each of the heterogeneous welds contains artificial through-wall crack of length of 169 mm, located in the region of HAZ.

Results of this experiment showed meeting of the LBB criteria for this component.

For the experiment on T-joint a prototype of T-piece, machined in Modrany Steelworks, was used. Experimental model contained a through-wall crack, located in the weld of the model. The crack length was 512 mm, measured on the outer surface. During machining the crack, pieces of materials were removed from the model for producing the test specimes.

Experiment was performed as follows. The model was heated up to 320 °C and then bending moment has been increased until such level of loading was reached that small increase in bending force caused relatively large increase in displacements.

During the experiment crack growth (on both ends of the crack) was observed. Increase in crack length was, at each end of the crack, approximately 50 mm.

Results of this experiment were of great importance for verification of our computational methods, since in this case the uncertainty in input material data has been substantially lowered.

CONCLUSION

When evaluating globally the experiments it may be stated that two main goals of experiments were fulfilled:

1. Experiments directly verified meeting of the LBB criteria for the tested components.
2. Comparing of the experimental results with the results of procedures used in the LBB analyses proved conservatism of these procedures.

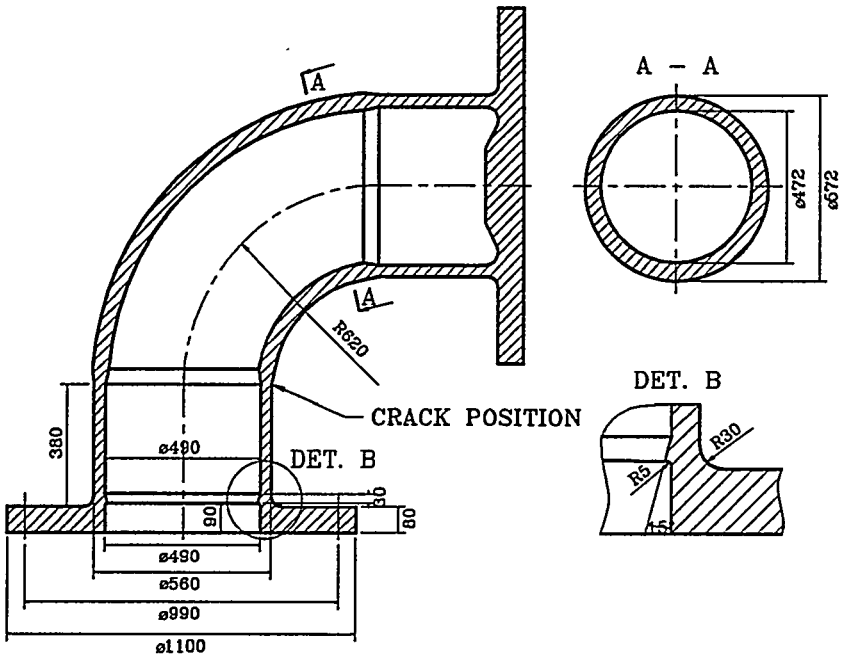
A – A
ø472
ø572
A
A
R620
CRACK POSITION
DET. B
DET. B
R30
R5
45°
380
ø490
30
80
90
ø490
ø560
ø990
ø1100

Fig. 1

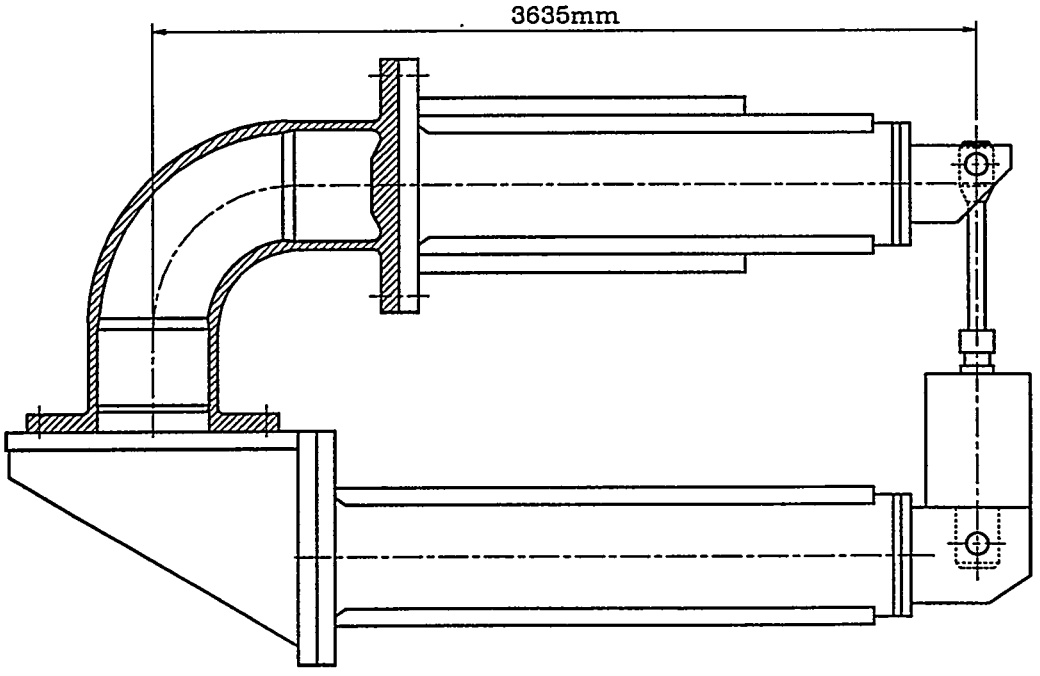
3635mm

Fig. 2

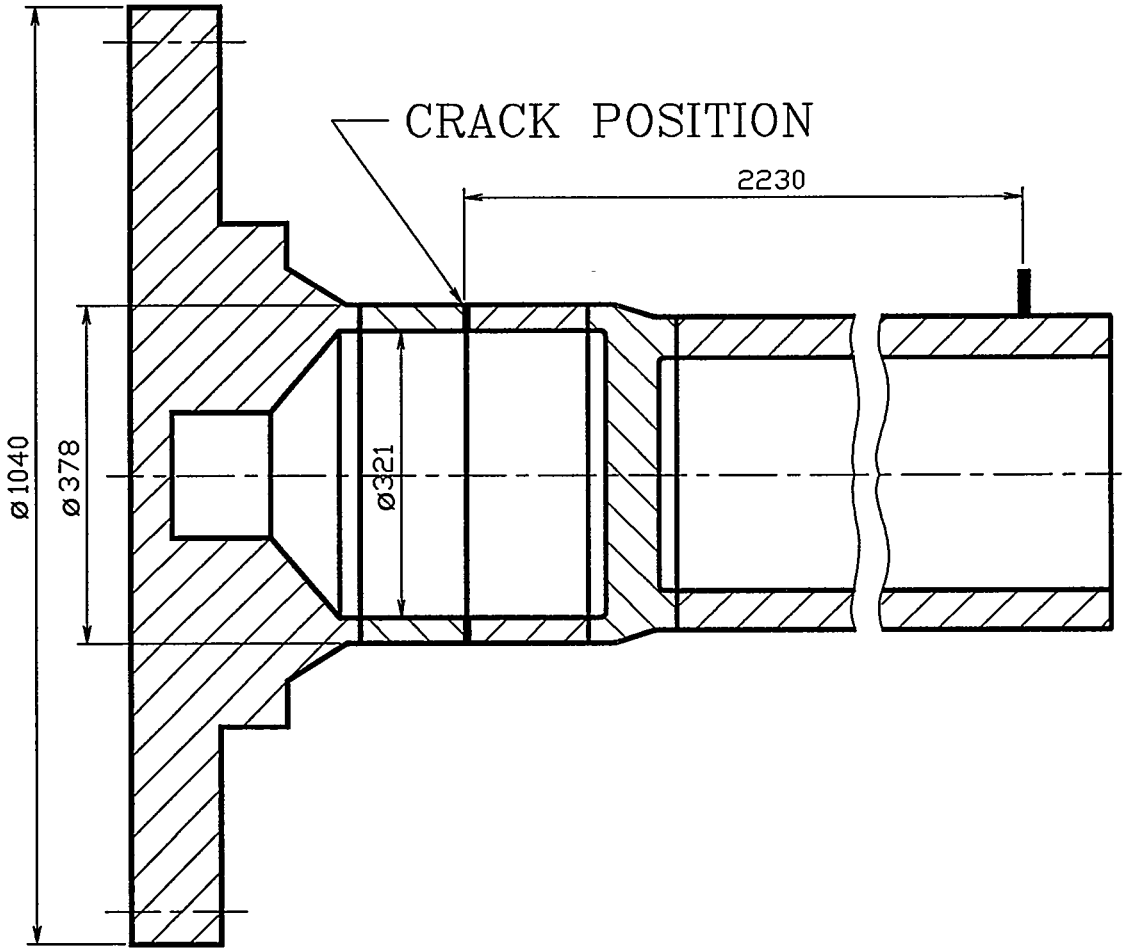

Fig. 3

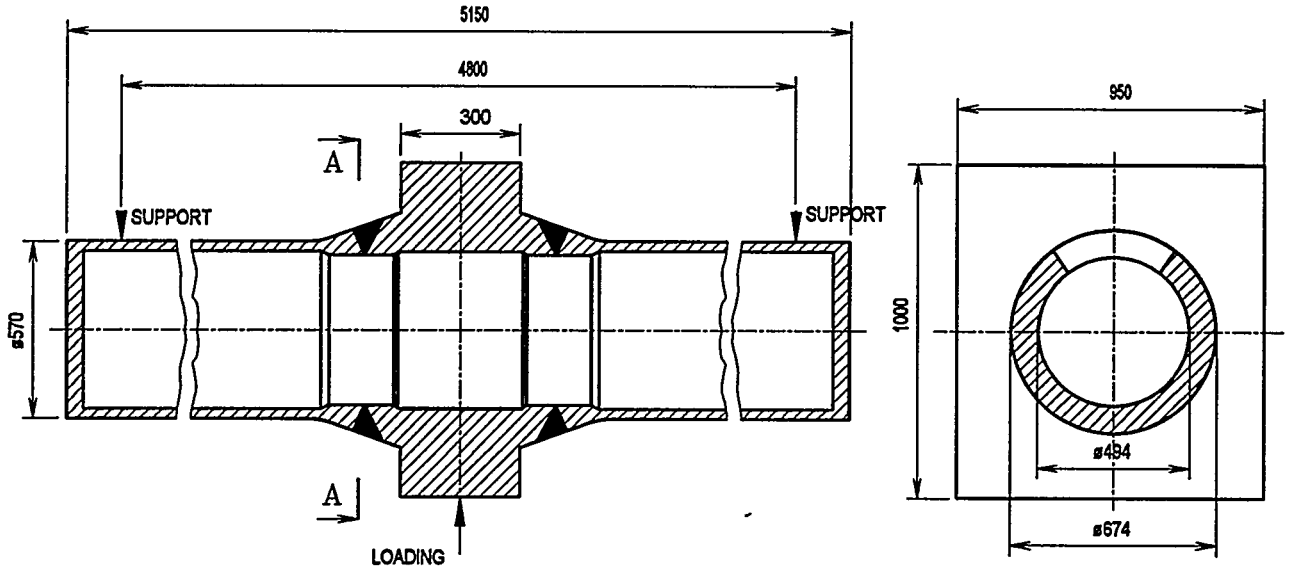
5150
4800
300
A
SUPPORT
SUPPORT
ø570
A
LOADING
950
1000
ø494
ø674

Fig. 4

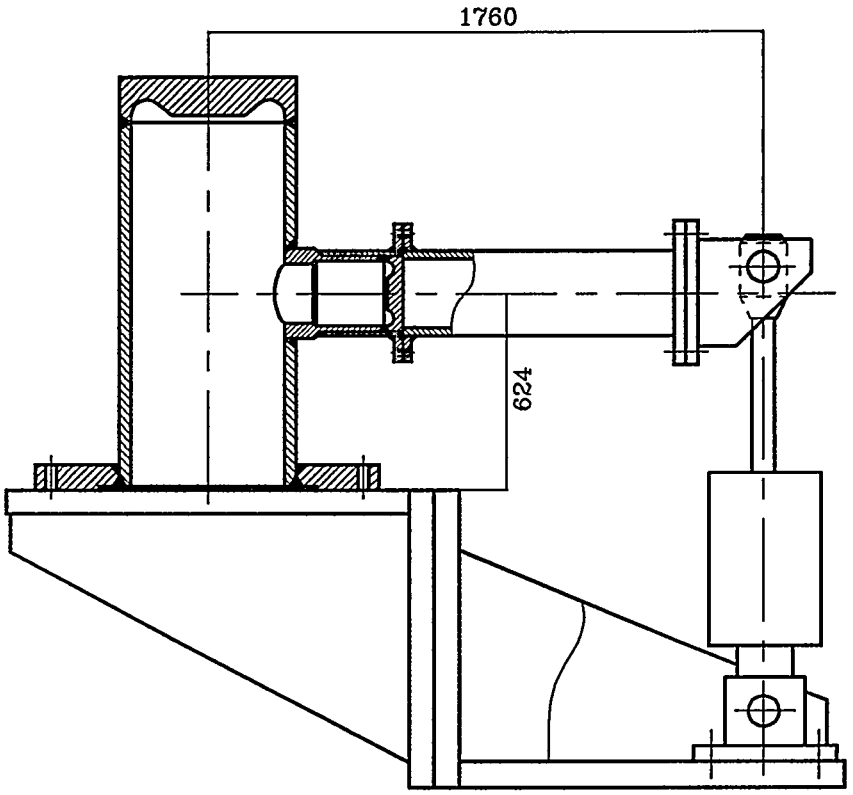
1760
624

Fig. 5

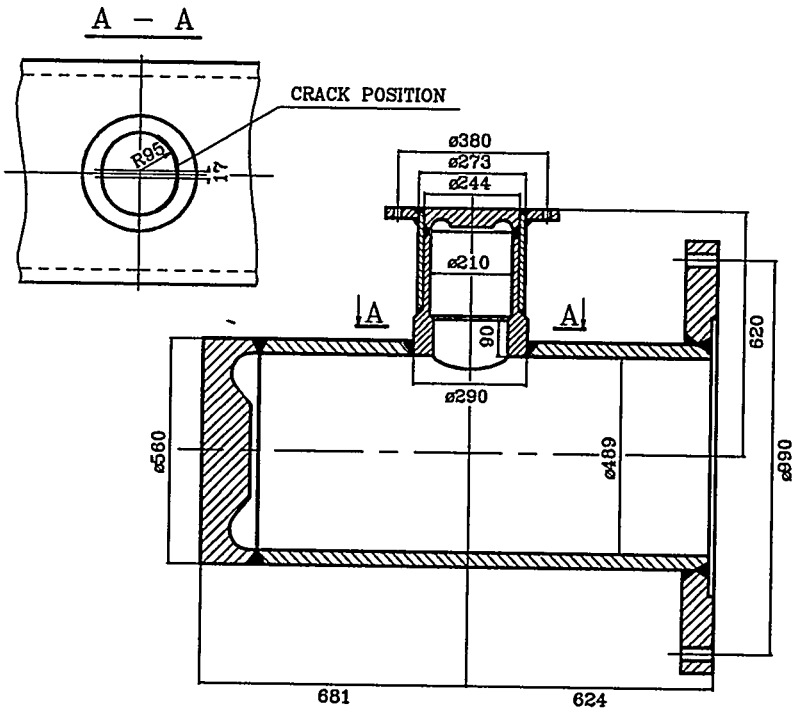
A – A
CRACK POSITION
R95
17
ø380
ø273
ø244
ø210
A
A
90
ø290
620
ø560
ø489
ø690
681
624

Fig. 6

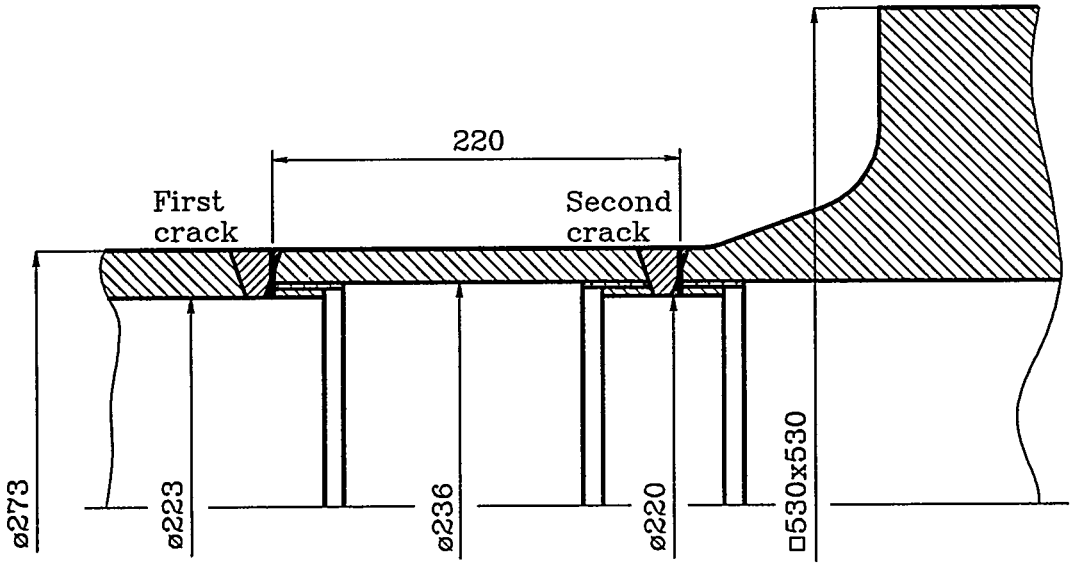

Fig. 7

THE CRITERIA OF FRACTURE IN THE CASE OF THE LEAK OF PRESSURE VESSELS

Dr. Habil., Prof. **Antanas Žiliukas**
Kaunas University of Technology, K. Donelaičio str. 73, LT-3006 Kaunas
Tel.: +370-7-220411 Fax.: +370-7-202640 E-mail: ANTANAS.ZILIUKAS@CR.KTU.LT

ABSTRACT

In order to forecast the break of the high pressure vessels and the network of pipes in a nuclear reactor, according to the concept of leak before break of pressure vessels, it is necessary to analyse the conditions of project, production, and mounting quality as well as of exploitation. It is also necessary to evaluate the process of break by the help of the fracture criteria. In the Ignalina Nuclear Power Plant of, in Lithuania, the most important objects of investigation are: the highest pressure pipes, made of Japanese steel 19MN5 and having an anticorrosive austenite coat inside; the pipes of distribution, which are made of 08X1810T steel. The steel of the network of pipes has a quality of plasticity; therefore the only criteria of fragile is impossible to apply to. The process of break would be best described by the universal criteria of elastic - plastic fracture. For this purpose the author offers the criterion of the double parameter.

NOMENCLATURE

The basic accepted symbols are those:

ε - deformation;
K_1 - stress intensity factor;
δ - opening of the crack;
σ - stress;
l - crack's length;
N - loading cycles;
R - asymmetrical factor.

INTRODUCTION

At the top of the crack the deformation $\varepsilon_{1\sigma}$ is calculated according to the formula:

$$\varepsilon_{1\Sigma}^{S} = \varepsilon_{1}^{S} + \varepsilon_{nom}^{S} \qquad (1)$$

here using

$$\varepsilon_1 \cdot \frac{\alpha(1-\nu^2)}{\sigma_{0.2} E h} K_1^2,$$

(ν - the coefficient of Puason, E- the modulus of elasticity, $\sigma_{0.2}$ - the yeld point , α - the coefficient, K_I - stress intensity factor); S - the parameter of interpolation (S = 2); ε_{nom} - the nominal deformation.

In addition, it is known, that the opening of the crack δ is calculated:

$$\delta = \frac{\alpha(1-\nu^2)K_I^2}{\sigma_{0.2}E}; \tag{2}$$

Using the (1) and (2) formulas it is possible to write the criterion:

$$K_I^2 K_{IC}^{-2} + \varepsilon_{nom}^2 \varepsilon_C^{-2} = 1 \tag{3}$$

or, if evaluated, that $\varepsilon_C = \varepsilon_{0.2} = \sigma_{0.2}E^{-2}$ and $\varepsilon_{nom} = \sigma/E$ (σ- stresses), the criterion would be:

$$K_I^4 K_{IC}^{-4} + \sigma_{nom}^2 \sigma_{0.2}^{-2} = 1 \tag{4}$$

(σ_{nom}- the nominal stress).

Having accepted the increase of the stress intensity factor, which is proportional to the increase of the break zone, we could write:

$$\frac{dK}{K} = D\frac{da}{a} \quad , \tag{5}$$

here $D = \sigma_i/3\sigma_o$ (σ - the intensity of stress, σ_o- the octahedral stress).

On the surface of the bodies D=1/2 integrating the (5) equation we get:

$$K^2 = Ca \quad , \tag{6}$$

here C- constant.

Then we can write, that

$$a/a_C = (K_I/K_{IC})^2; \tag{7}$$

here a_C- the critical length of the break zone.

If we put the (7) value into the (4) formula, we will get:

$$\left(\frac{a}{a_c}\right)^2 + \left(\frac{\sigma_{nom}}{\sigma_{0.2}}\right)^2 = 1 \tag{8}$$

Evaluating, that the increase of the break zone is proportional to the deformation and to the opening of the crack, we get the fracture criterion in the case of a static load:

$$(\frac{\delta}{\delta_c})^2 + (\frac{\sigma_{nom}}{\sigma_{0.2}})^2 = 1, \quad (9)$$

and in the case of cyclic load:

$$(\frac{\delta_{var}}{\delta_{var,c}})^2 + (\frac{\sigma_{var}}{\sigma_{var,o}})^2 = 1, \quad (10)$$

here $\sigma_{var,o}$ - the limit of steadiness for the cycle of pulsating tension.

Considering that the speed of crack development in pulsing cycle is calculated by formula:

$$dl/dN = C_{-1} \exp \lambda(R+1)\Delta K^{m_{-1}}, \quad (11)$$

here C_{-1}, m_{-1} - constant of material to symmetrical cycle.

When R=0,

$$\lambda = \ln V_0 / C_{-1}\Delta K^{m_{-1}}, \quad (12)$$

here λ - constant, V_0 - speed of crack development in pulsing cycle.

So the speed of crack development is calculated

$$dl/dN = C_{-1} \exp \ln \frac{V_0}{C_{-1}\Delta K^{m_{-1}}}(R+1)\Delta K^{m_{-1}}. \quad (13)$$

Now we will obtain the number of admitted loading cycles

$$N_{adm} = \int_{l_0}^{l_{adm}} \frac{l_{adm}^{1-m_0/2} - l_0^{1-m_0/2}}{C_o(\Delta\sigma\sqrt{M})^{m_0/2}(R+1)(1-m_0)}, \quad (14)$$

here M - the factor of model and geometry; C_0, m_0 - constant of materials to pulsing cycle.

RESULTS

The criteria of double parameter (9) and (10) were tested experimentally and can be applied while describing the process of break in the case of the leak of pressure vessels.

For pipes from steel 08X1810T ($\delta_{var,c}$ = 0.015 mm, $\sigma_{var,c}$ = 240 MPa) with surface crack orientated circumferentially on the inside of a cylinder, experimental and theoretical subordinates are given in Figure 1 (complete line - experimental, dotted line - theoretical).

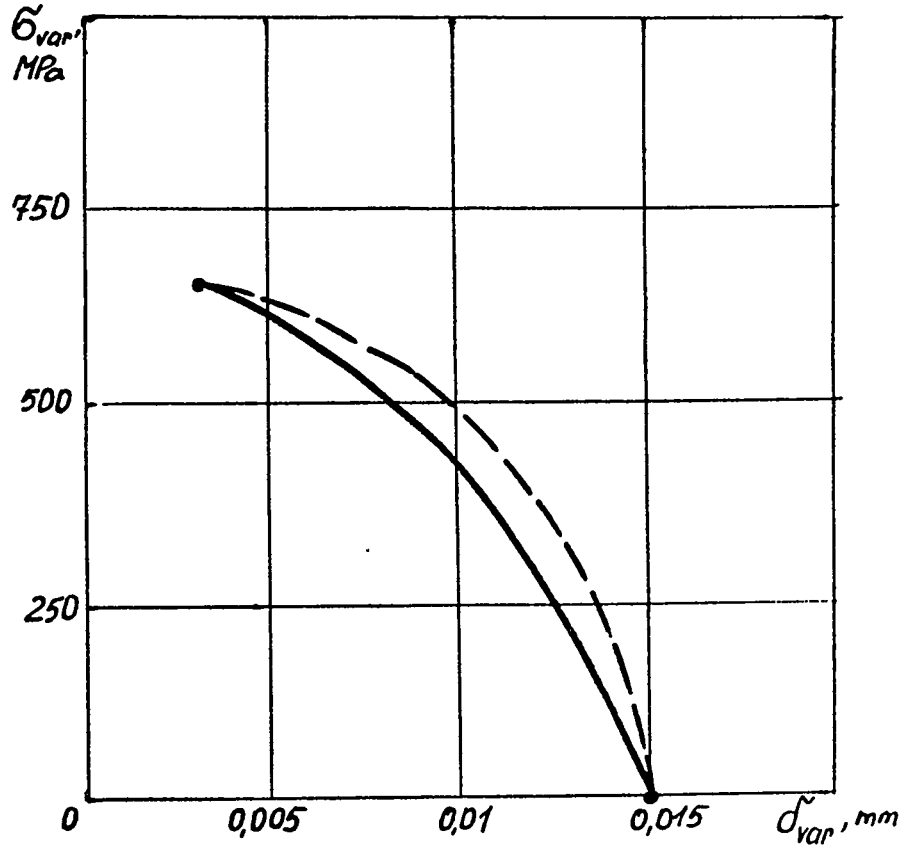

Figure 1

If we know the initial crack length, this formula allows to calculate the numbers of admitted loading cycles till the failure of construction or its model in all cases of cyclic loading.

Using this formula, the results of the loading cycles' calculations of the pipes produced from steel 08X1810T where $m_0 = 2.71$, $C_0 = 6.7*10^{-12}$ m/cycl, are given in Table 1.

Table 1

Amplitude of nominal stress $\Delta\sigma$, MPa	Initiator crack's length l_0, mm	Admitted crack's length l_{adm}, mm	Amplitude of stress intensity factor ΔK, MPa*M$^{1/2}$	Speed of crack development v_0, m/cycl	Asymetrical factor R	Admitted cycles of loading N_{adm}
160	0.8	10	31.75	$7.8*10^{-8}$	0.1	$1.07*10^5$
140	0.9	12	30.4	$6.99*10^{-8}$	0.2	$1.3*10^5$
120	1.0	14	28.2	$5.7*10^{-8}$	0.3	$1.75*10^5$
100	1.1	16	25.1	$4.16*10^{-8}$	0.4	$2.6*10^5$

CONCLUSIONS

The crack resistance criteria are classified and the range of their application is shown. The problem of the relation of the crack opening and its apex strain is theoretically solved by rising the pre-failure zones representing the area of the highest strain intensity. A multi-parametric strain criterion of failure, incorporating crack opening, the strain at its apex and nominal strains, is obtained.

REFERENCES

1. A.Žiliukas, Fracture members of constructions. Vilnius, Science, 1989, 102 p.

Fracture Mechanism Analysis of Cracked Elbow for LBB Evaluation in Main Circuit Piping of RMBK-1000 Reactor

Kyselyov V., Smirnov Y., Arjaev A.

RDIPE - RUSSIA

NOT RECEIVED

A SIMPLIFIED LBB EVALUATION PROCEDURE FOR AUSTENITIC AND FERRITIC STEEL PIPING

R.M. Gamble, Sartrex Corporation
K.R. Wichman, U. S. Nuclear Regulatory Commission

INTRODUCTION

The NRC previously has approved application of LBB analysis as a means to demonstrate that the probability of pipe rupture was extremely low so that dynamic loads associated with postulated pipe break could be excluded from the design basis (1). The purpose of this work was to: (1) define simplified procedures that can be used by the NRC to compute allowable lengths for circumferential throughwall cracks and assess margin against pipe fracture, and (2) verify the accuracy of the simplified procedures by comparison with available experimental data for piping having circumferential throughwall flaws. The development of the procedures was performed using techniques similar to those employed to develop ASME Code flaw evaluation procedures (2,3).

The procedures described in this report are applicable to pipe and pipe fittings with: (1) wrought austenitic steel (Ni-Cr-Fe alloy) having a specified minimum yield strength less than 45 ksi, and gas metal-arc, submerged arc and shielded metal-arc austenitic welds, and (2) seamless or welded wrought carbon steel having a minimum yield strength not greater than 40 ksi, and associated weld materials. The procedures can be used for cast austenitic steel when adequate information is available to place the cast material toughness into one of the categories identified later in this report for austenitic wrought and weld materials.

DEFINITION OF THE EVALUATION PROCEDURE

Summary of the NRC LBB Criteria

Two steps are required to perform a LBB evaluation. First, a leak rate analysis is performed to determine the throughwall crack length that will ensure reliable leakage detection with margin (a factor of 10 on leak rate) at normal operating loads. This crack length is designated as the leakage size flaw. Second, flaw evaluations are performed to determine the allowable circumferential throughwall flaw lengths for various combinations of normal plus postulated SSE loads.

Determination of the allowable flaw length, margins against pipe fracture, and compliance with the LBB criteria are based on the method used to combine the various normal and postulated SSE load components. When either the absolute or algebraic sum method is used to combine the load components, the allowable crack length is determined using loads equal to (normal plus SSE) and must be at least twice the length of the leakage size crack. A second condition also must be satisfied when using the algebraic sum method. In this case the allowable crack length is determined using loads equal to (1.4) • (normal plus SSE) and must be equal to or greater than the length of the leakage size flaw.

Allowable Circumferential Throughwall Flaw Length Determination

Compute the non dimensional quantities

$$\zeta \cdot C \cdot (S_a + S_b) \quad (1)$$

and

$$\zeta \cdot C \cdot S_a \quad (2)$$

where

ζ = stress multiplication factor (ksi^{-1}) defined in Table 1 or 2 for austenitic steels and in Table 3 or 4 for ferritic steels,
C = the margin (non dimensional) associated with the load combination method,
S_a = the combined applied axial stress (ksi) = $F_{combined}/2\pi Rt$,
$F_{combined}$ = combined axial force (kips) including pressure, deadweight and thermal expansion at normal operation, and seismic components,
S_b = the combined applied bending stress (ksi) = $M_{combined}/\pi R^2 t$,
$M_{combined}$ = combined bending moment (in-kips) including deadweight and expansion at normal operation, and seismic components,
R = the mean radius of the pipe cross section (inches), and
t = the pipe wall thickness (inches).

The allowable flaw length at any specified location in a pipe system is determined by entering Figure 1 with the quantities computed from Eqs. 1 and 2 for the location specific values of S_a and S_b, the value of C associated with the method used to combine loads, and the appropriate material and location specific value of ζ from Table 1, 2, 3, or 4. Tables 1 and 3 can be used for austenitic and ferritic steel piping, respectively, when heat specific yield and ultimate stresses are not available, while Tables 2 and 4 can be used for austenitic and ferritic piping, respectively, when heat specific yield and ultimate stresses are available.

Margin Assessment

The following two paragraphs summarize the procedures that can be used to determine if the required margins on load and flaw size are met for either the absolute or algebraic sum load combination method.

For the absolute sum load combination method compute the quantities in Eqs. 1 and 2 using C = 1.0, the location specific values of S_a and S_b, and the appropriate material and location specific value of ζ from Table 1, 2, 3, or 4. The allowable flaw length is obtained by entering Figure 1 with the coordinate values computed from Eqs. 1 and 2. If the allowable throughwall flaw length from Figure 1 is at least twice the length of the leakage size flaw then the load and leakage flaw size margins are met and the LBB criteria are satisfied.

For the algebraic sum load combination method two conditions are used to determine if the margins on load and leakage flaw size are satisfied. First, compute the quantities in Eqs. 1 and 2 using C = 1.4, the location specific values of S_a and S_b, and the appropriate material and location specific value of ζ from Table 1, 2, 3, or 4. The allowable flaw length is obtained by entering Figure 1 with the coordinate values obtained from Eqs. 1 and 2. If the allowable flaw length from Figure 1 is at least as large as the leakage size flaw, then the margin on load is met. Second, the process is repeated except C = 1.0 is used to compute the coordinate values from Eqs. 1 and 2. If the allowable flaw length from Figure 1 is at least twice the length of the leakage size flaw, then the margin on flaw size is met. If both the load and flaw size margins are met the LBB criteria are satisfied.

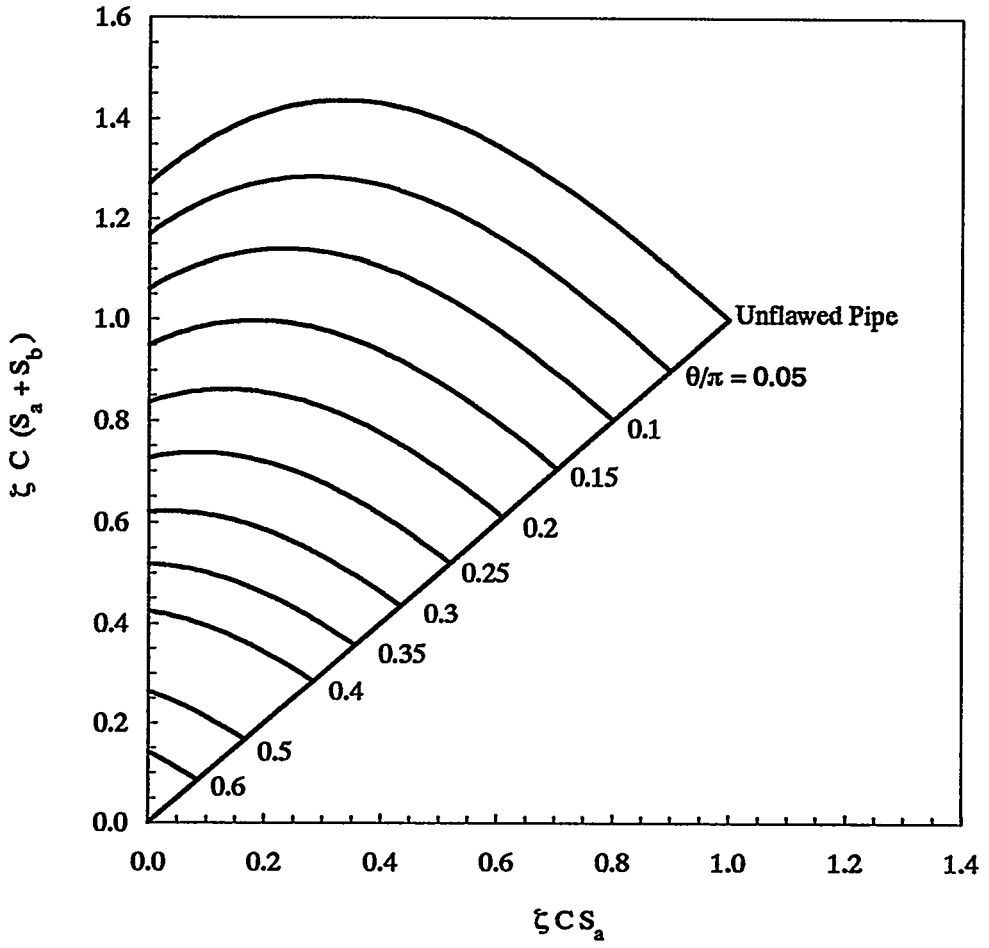

Figure 1. Allowable Circumferential Throughwall Flaw Length as a Fraction of Circumference

Table 1. ζ Factors For Austenitic Steel Pipe Materials Without Heat Specific Yield and Ultimate Stresses.

Material	ζ (ksi $^{-1}$)
Wrought Base Metal and Gas Tungsten Arc Welds (GTAW)	0.0227
Shielded Metal Arc Welds (SMAW) [a]	0.0261[1 + 0.130(NS-4)]
Submerged Arc Welds (SAW) [a]	0.0295[1 + 0.010(NS-4)]

a. NS = nominal pipe size (inches). if NS is less then 4, set NS = 4.

Table 2. ζ Factors For Austenitic Steel Pipe Materials With Heat Specific Yield and Ultimate Stresses.

Material	ζ (ksi $^{-1}$)
Wrought Base Metal and GTAW [a]	$1/\sigma_f$
Shielded Metal Arc Welds [a,b]	$(1.15/\sigma_f)[1 + 0.130(NS-4)]$
Submerged Arc Welds [a,b]	$(1.30/\sigma_f)[1 + 0.010(NS-4)]$

a. Flow Stress (ksi), $\sigma_f = 0.5\ (\sigma_y + \sigma_u)$, where σ_y and σ_u are the 0.2 % offset yield and ultimate strengths, respectively, for the pipe base metal at the temperature of interest. If $\sigma_f > 65$ ksi, set $\sigma_f = 65$ ksi.

b. NS = nominal pipe size (inches). if NS < 4, set NS = 4.

Table 3. ζ Factors For Ferritic Steel Pipe Materials With Heat Specific Yield and Ultimate Stresses.

Material Category	ζ [c] (ksi^{-1})
1 [a]	$0.0200\ [1 + 0.021 \bullet A \bullet (NS -4)]$
2 [b]	$0.0225\ [1 + 0.018 \bullet A \bullet (NS-4)]$

a. Material Category 1: Seamless or welded wrought carbon steel pipe and pipe fittings that have a specified minimum yield strength at room temperature equal to or less than 40 ksi and welds made with E7015, E7016, or E7018 electrodes in either the as welded or post weld heat treated conditions.

b. Material Category 2: Except as identified in Category 1, all ferritic shielded metal arc and submerged arc welds in either the as welded or post weld heat treated condition.

c. $A = [0.125(R/t) - 0.25]^{0.25}$, for $5 \le R/t \le 10$, or
$A = [0.4(R/t) - 3]^{0.25}$, for $10 \le R/t \le 20$,
NS = Nominal pipe size (inches). If NS < 4, set NS = 4.

Table 4. ζ Factors For Ferritic Steel Piping Materials With Heat Specific Yield and Ultimate Stresses.

Material Category	ζ [c,d] (ksi^{-1})
1 [a]	$(5.474/\sigma_f)(B)[1 + 0.021 \cdot A \cdot (NS-4)]/\sigma_y^{0.46}$ [e]
2 [b]	$(6.158/\sigma_f)[1 + 0.018 \cdot A \cdot (NS-4)]/\sigma_y^{0.46}$

a. See footnote a, Table 3.
b. See footnote b, Table 3.
c. See footnote c, Table 3
d. $\sigma_f = 0.5\ (\sigma_y + \sigma_u)$, where σ_y and σ_u are the 0.2 % offset yield and ultimate strengths, respectively (ksi), for the pipe base metal at the temperature of interest.
e. $B = 1 + 0.28 \cdot \text{Tanh}[(\sigma_f - 56)/5]$.

BASIS FOR THE EVALUATION PROCEDURE

The development of the evaluation procedure generally follows that used for the development of the flaw evaluation procedures in Section XI of the ASME Code (2, 3). These procedures were based on limit load analysis modified, where applicable, by factors to account for conditions where pipe failure would occur by ductile crack extension.

Analytical Development

First, the predicted bending stress at limit load, σ_b, for a circumferential throughwall flaw is (2, 3, 4)

$$\sigma_b = 2(\sigma_f/\pi)\ [2 \sin \beta - \sin \theta] \qquad (3)$$

where

$\beta =$ $0.5\ [1 - (\theta/\pi) - (\sigma_m/\sigma_f)]\pi$
$\theta =$ the half throughwall crack angle,
$\sigma_m =$ the axial stress at limit load, and
$\sigma_f =$ the material flow stress, typically defined as $0.5\ (\sigma_y + \sigma_u)$,
$\sigma_y =$ the material yield stress, and
$\sigma_u =$ the material ultimate stress.

In general, demonstration of piping integrity requires margin to exist between the predicted failure load and the applied loads. Following the ASME Code procedure the margin is applied to the sum of the applied bending and primary membrane stresses, and the relationship between the predicted limit load, applied loads, and margin is

$$C \cdot (S_a + S_b)/\sigma_f = (\sigma_b + \sigma_m)/\sigma_f. \qquad (4)$$

Because the load carrying capacity associated with failure by ductile tearing typically is less than that corresponding to limit load, a factor (Z) is applied to Eq. 4 to account for ductile tearing. These factors are material dependent and have been derived for austenitic and ferritic piping materials (2, 3, 5, 6). Applying the Z factor to Eq. 4 gives

$$Z \cdot C \cdot (S_a + S_b)/\sigma_f = (\sigma_b + \sigma_m)/\sigma_f. \qquad (5)$$

In the NRC LBB criteria, the applied axial stress S_a is required to include the margin and load modification terms; consequently, the following condition also must be applied

$$Z \bullet C \bullet S_a/\sigma_f = \sigma_m/\sigma_f. \quad (6)$$

The flow stress, σ_f, has been used on both sides of Eqs. 5 and 6 to produce normalized, non-dimensional quantities. Defining $\zeta = Z/\sigma_f$, Eqs. 5 and 6 can be written as

$$C \bullet \zeta \bullet (S_a + S_b) = (\sigma_b + \sigma_m)/\sigma_f \quad (7)$$

and

$$C \bullet \zeta \bullet S_a = \sigma_m/\sigma_f, \text{ respectively.} \quad (8)$$

The evaluation procedure is now defined by Eqs. 7 and 8 and can be applied using the concept in Figure 1 in the following manner. Eq. 3 is used to determine σ_b/σ_f as a function of σ_m/σ_f for any specified value of normalized circumferential flaw length, θ/π. These results are used to plot $(\sigma_m + \sigma_b)/\sigma_f$ as a function of σ_m/σ_f and construct the curves shown in Figure 1. The location specific normalized applied stress quantities, $C \bullet \zeta \bullet (S_a + S_b)$ and $C \bullet \zeta \bullet S_a$, now become the axes for Figure 1 as indicated by the left sides of Eqs. 7 and 8.

ζ Factor Definition

The basis used to define the ζ factors for the LBB evaluation procedure were the forms of the Z factors previously used to develop part-throughwall flaw evaluation procedures for the ASME Code (2, 3, 5, 6). The general forms of the ζ factors used for austenitic steel pipe are

$$\zeta = 1/\sigma_f, \quad \text{for base metal,} \quad (9)$$

$$\zeta = (1.15/\sigma_f)[1 + 0.130(NS-4)], \quad \text{for SMAW, and} \quad (10)$$

$$\zeta = (1.30/\sigma_f)[1 + 0.010(NS-4)] \quad \text{for SAW.} \quad (11)$$

For the development of the LBB criteria, the fixed value of flow stress was determined from data correlations; the associated values of ζ are presented in Table 1. The LBB criteria development also allowed flow stress to be defined on a heat specific basis; the associated values of ζ were determined from data correlations described in the following section, and are presented in Table 2.

The flaw evaluation procedure specified in the ASME Code for ferritic piping defines two material categories (see footnotes a and b in Table 3). The ζ factor relationships for ferritic piping material categories are

$$\zeta = (2.281/\sigma_f)(\sigma_f/S_m)[1 + 0.021(NS-4)A]/\sigma_y^{0.46}, \quad \text{for Category 1, and} \quad (12)$$

$$\zeta = (2.566/\sigma_f)(\sigma_f/S_m)[1 + 0.018(NS-4)A]/\sigma_y^{0.46} \quad \text{for Category 2.} \quad (13)$$

For the development of the LBB criteria, the fixed value of flow stress was determined from data correlations described in the following section; the associated values of ζ for Category 1 and 2 materials are presented in Table 3. Eqs. 12 and 13 also were evaluated for applications where heat specific yield and ultimate stresses are available. For this instance the value of the term (σ_f/S_m) was always taken as 2.4, while the values of flow and yield stresses were taken as the heat specific values; the associated values of ζ were determined from data correlations described in the following section, and are presented in Table 4.

VERIFICATION OF THE EVALUATION PROCEDURE

The results from previously conducted experimental programs (7 - 11), and unpublished data provided by JAERI to NRC, were used to bench mark the evaluation procedure. The experimental data were for pipes with circumferential throughwall flaws, test temperatures ranging from 70 to 575°F, and diameters ranging from 2.5 to 36 inches.

The experimental results were used to define the maximum bending load carrying capacity of the pipe. The experimental axial and bending stresses were computed using the relationships specified for S_a and S_b in Eqs. 1 and 2. The force, F, due to internal pressure, p, was computed using the relationship $F = \pi p R_i^2$, where R_i is the pipe inner radius. These stresses were compared to the stresses predicted by using Eqs. 7 and 8 with C = 1 and the appropriate ζ factor. The results were used to determine the ratio of the experimental to predicted maximum loads.

Austenitic Steel

The ratios of experimental to predicted maximum bending plus axial load as a function of pipe diameter first were determined using the values of $\zeta = Z/\sigma_f$ defined by the ASME Code for wrought base metal and GTAW, SMAW, and SAW. The Code uses a constant value of σ_f = 51 ksi for all materials. The results showed the ratios of the experimental to predicted loads are distributed as follows: 84% ≥ 1.0, 91% ≥ 0.9, 97% ≥ 0.8, 100% ≥ 0.75, and 100% ≤ 1.7. However, it was concluded from these results that an assumed flow stress of 51 ksi produced results that were not conservative enough, primarily because there were some ratios below 0.8. Consequently, the data were reanalyzed using various assumed flow stresses until all ratios were 0.9 or greater. The flow stress meeting this condition was 44 ksi, and the ratios were distributed as follows: 93% ≥ 1.0, 100% ≥ 0.9, and 100% ≤ 2.0. The ζ factors listed in Table 1 were obtained by substituting a flow stress equal to 44 ksi into Eqs. 9, 10, and 11.

To enable heat specific properties to be included in the evaluation, the flow stress was computed as $\sigma_f = 0.5(\sigma_y + \sigma_u)$ and was used to predict the maximum bending stress from each of the pipe experiments. When welds were evaluated σ_f was computed using the yield and ultimate stresses reported for the base metal, while the Z factors are the same as those defined by the Code. When the data were evaluated with these assumptions, it was observed that the loads predicted from the limit load analysis tended to be larger than the experimental loads when σ_f was greater than 65 ksi. Consequently, σ_f was set equal to 65 ksi when the values from the heat specific data were greater than 65 ksi. The results showed the ratios of the experimental to predicted load sums were distributed as follows: 76% ≥ 1.0, 100% ≥ 0.9, and 100%≤ 1.4. These results also showed that using the heat specific flow stress (including an upper flow stress limit of 65 ksi) significantly reduces the scatter in the predictions. The ζ factors listed in Table 2 were determined from Eqs. 9, 10, and 11 based on using the actual material flow stress with an upper limit of 65 ksi, and the Z factors used in the ASME Code.

Ferritic Steel

The ratio of experimental to predicted maximum bending plus axial load as a function of pipe diameter were computed for Category 1 and 2 ferritic steels, where the values of $\zeta = Z/\sigma_f$ from Eqs. 12 and 13, respectively, were determined for the Code default values, σ_f = 43.4 ksi, σ_y = 27.1ksi, and (σ_f/S_m) = 2.4. The calculated ratios were all above 1.2, which indicates the Code default tensile properties can produce very conservative results. To reduce the conservatism associated with the Code default values a second evaluation was performed to determine the flow stress that would result in the ratio of experimental to predicted load being 0.9 or greater for all experiments. The flow stress that allowed this criterion to be met was 60 ksi. The ratios for the Category 1 materials are distributed as follows: 97% ≥ 1.0, 100% ≥ 0.9, and 100%≤ 1.9. The margins for the two experiments with Category 2 materials are roughly about the same as the margins for comparable size diameter piping having Category 1 materials. The ζ factors contained in Table 3 were obtained by substituting σ_f = 60 ksi, σ_y = 27.1ksi, and (σ_f/S_m) = 2.4 into Eqs. 12 and 13; these factors can be used when no heat specific yield and ultimate stress are available.

To enable heat specific tensile properties to be used in the evaluation, the data for Category 1 and 2 materials were evaluated using heat specific values of yield and ultimate stresses in Eqs. 12 and 13, respectively. The ratios of experimental to predicted loads were distributed as follows: 82% ≥ 1.0, 97% ≥ 0.9, 100% ≥ 0.8, and 100% ≤ 2.0. The margins for the two experiments with Category 2 materials are roughly about the same as the margins for comparable size diameter piping having Category 1 materials. The data for Category 1 materials were initially evaluated without the quantity B indicated in Table 4. This evaluation indicated a trend where pipe material with flow stress greater than approximately 56 ksi often had predicted loads greater than the experimental values, while pipes with flow stress less than approximately 56 ksi had predicted loads less than the experimental values. To improve the accuracy of the prediction method the B term was developed and incorporated into the ζ factor for Category 1 ferritic materials.

REFERENCES

1. Nuclear Regulatory Commission, 10 CFR, Part 50, General Design Criterion 4, "Modification of Requirements for Protection Against Dynamic Effects of Postulated Pipe Rupture", Federal Register, Vol. 52, No. 207, October 27, 1987.

2. Section XI Task Group for Piping Flaw Evaluation, "Evaluation of Flaws in Austenitic Steel Piping," EPRI Report NP-4690-SR, Electric Power Research Institute, Palo Alto, CA, July 1986.

3. Novetech Corporation, "Evaluation of Flaws in Ferritic Piping," EPRI Report NP-6045, Electric Power Research Institute, Palo Alto, CA, October 1988.

4. M.F. Kanninen, et. al., "Toward an Elastic Plastic Fracture Mechanics Predictive Capability for Reactor Piping," Nuclear Engineering and Design, 48, 117-134, 1978.

5. A. Zahoor and R. Gamble, "Proposed Evaluation Procedure for Austenitic Stainless Steel Flux Welds," Presented to the ASME Section XI Task Group on Piping Flaw Evaluation, Palm Springs, CA, February 11, 1985.

6. A. Zahoor, "Revised Criteria for Evaluation of Flaws in Carbon Steel Piping", Presented to the ASME Section XI Task Group on Piping Flaw Evaluation, Long Beach, CA, January 1987.

7. M.F. Kanninen, et. al., "Instability Predictions for Circumferentially Cracked Type-304 Stainless Under Dynamic Loading," Electric Power Research Institute Report NP-2347 (Vol. 1: Summary; Vol 2: Appendices), April 1982.

8. M.G. Vassilaros, R.A. Hays, J.P. Gudas, And J.A. Joyce, " J-Integral Tearing Instability Analyses for 8-Inch Diameter A106 Steel Pipe, NUREG/CR-3740, U.S. NRC, Washington, DC, April 1984.

9. C. Maricchiolo, and P.P. Milella, "Fracture Behavior of Carbon Steel Pipes Containing Circumferential Cracks at Room Temperature and 300°C", Nuclear Engineering and Design III (1989) 35-46.

10. G.M. Wilkowski, et. al., "Degraded Piping Program - Phase II, " NUREG/CR-4082, Vol. 8, U.S. NRC, Washington, DC, March 1989.

11. C. Maricchiolo, P.P. Milella, and A. Pini, "Fracture Behavior of Stainless Steel Pipes Containing Circumferential Cracks at Room Temperature and 280°C", Int. J. Pres. Ves. & Piping 43 (1990).

APPLICATION OF THE CRACKED PIPE ELEMENT TO CREEP CRACK GROWTH PREDICTION

J. BROCHARD - T. CHARRAS
C.E.A. - C.E.-SACLAY DRN/DMT, GIF SUR YVETTE FRANCE
M. GHOUDI
C.E.A. - C.E.-SACLAY, INSTN, GIF SUR YVETTE FRANCE

Several years ago, a cracked pipe element was implemented is CASTEM2000 computer code for ductile fracture assessment of piping systems with postulated circumferential through-wall cracks under static or dynamic loading. We undertake a development to extend the capabilities of the element to the determination of fracture parameters under creep conditions (C^*, $\dot{\Phi}c$ and $\dot{\Delta}c$).

In a first step, a time independant strain rate law ($\dot{\varepsilon} = A\sigma^n$) is considered, so that the ductile fracture formulae proposed by Zahoor can be used. Under combined tension and bending the C^* expression is :

$$C^* = A\,R\,(\pi-\theta)\,(\theta/\pi)\,h_1\,(\frac{P}{P_o'})$$

$$\text{with } P_o' = 0.5\left[-\lambda R P_o^2 / Mo + \left\{\left(\lambda R P_o^2 / Mo\right)^2 + 4P_0^2\right\}^{0,5}\right]$$

$\lambda = M/PR$
$Po = 2\,Rt\,[\pi-\theta-2\sin^{-1}(0,5\sin\theta)]$
$Mo = 4\,R^2\,t\,[\cos(\theta/2) - 0,5\sin\theta]$

Cinematic parameters $\dot{\phi}_c$ and $\dot{\Delta}_c$ are deduced from C^* and loads values at each step of the calculation.

Under secondary creep conditions, this element is now available to carry out a complete simulation by performing successive resolutions increasing the defect size with the material rule : $\Delta a = B\,(C^*)^m$.

The main advantage of this element is that by modelling the complete piping system using classic pipe elements and this special element at the crack location, the secondarity of the loads such as thermal loads can correctly be evaluated. An application has been conducted on a FBR-type piping system, for which the crack growth predictions considering the thermal stresses as primary or secondary stresses are significantly different.

THE CORROSION AND CORROSION MECHANICAL PROPERTIES EVALUATION FOR THE LBB CONCEPT IN VVERs

Martin Ruščák, Petr Chvátal, Dalibor Kárník
Nuclear Research Institute, 250 68 Řež, Czech Republic

1. Introduction

One of the conditions for the "Leak Before Break" concept to be valid is the verification that the influence of corrosion environment on the material of the component can be neglected. Both the general corrosion and/or the initiation and growth of corrosion-mechanical cracks must not cause the degradation. The primary piping in the VVER nuclear power plant is made from austenitic steels (VVER 440) and low alloy steels protected with the austenitic cladding (VVER 1000). Austenitic steels are not generally sensitive to the stress corrosion cracking, nevertheless the degradation must be evaluated in terms of threshold value, crack growth rate and degradation extent (mass loss, cracks density). These measurements must prove that there is not the ability to the initiation of critical defect between two inspections.
In the reference [1], the results from the base metal and heterogeneous weldments from the NPP VVER 440 were showed. It was proved, that the crack growth rates are below 10m/s, if low oxygen level is kept in the primary environment. No intergranular cracking was observed in low and high oxygen water after any type of testing, with constant or periodic loading.
In the framework of the LBB assessment of the VVER 1000 MW, also the corrosion and corrosion mechanical properties were evaluated.
The corrosion and corrosion mechanical testing was oriented predominantly to three types of tests:

* stress corrosion cracking tests
* corrosion fatigue tests
* evaluation of the resistance against corrosion damage.

In this paper, the methods used for these tests will be described and the materials will be compared from point of view of response on static and periodic mechanical stress on the low alloyed steel 10GN2MFA and weld metal exposed in the primary circuit environment. The slow strain rate tests and static loading of both C-rings and CT specimens were performed in order to assess the stress corrosion cracking characteristics, the cyclic loading of CT specimens was done to evaluate the kinetics of the crack growth under periodical loading. Several results are showed to illustrate the used approaches. The obtained data were evaluated also from the point of view of comparison of the influence of different structure on the stress corrosion cracking appearance. The results obtained for the base metal and weld metal of the piping are presented here.

2. Experimental

2.1. Test material

Here presented experiments were performed with two types of materials:

- low alloyed steel 10GN2MFA
- weld metal E PT-30, the root of the weld Sv08GS

The chemical composition of the tested materials is shown in Tab.1, the base mechanical properties in Tab.2. The metallographic analysis was done [2]:
The base metal, 10GN2MFA, can be characterised as the mixture of bainite and proeutectoid ferrite. The prior austenitic grain size was 35μm. The inclusions MnS and complex sulfides were found in the structure.
The filler weld consists of the mixed ferritic-bainitic microstructures within the columnar or equiaxial (bottom of beads) primary austenitic grain boardered by a proeutectoid ferrite.

Tab.1: Chemical composition of tested steels, wt. %

MATERIAL	C	Mn	Si	P	S	Cu	Ni	Cr	Mo	V
10GN2MFA	0.10	0.80	0.26	0.010	0.008	0.07	1.92	0.17	0.50	0.04
WELD METAL	0.043	0.81	0.21	0.017	0.008	0.07	1.48		0.64	

Tab.2.: Basic mechanical properties of tested steels

MATERIAL	T = 20 °C				T = 350 °C			
	$R_{p0.2}$ (MPa)	R_m (MPa)	A_5 (%)	Z (%)	$R_{p0.2}$ (MPa)	R_m (MPa)	A_5 (%)	Z (%)
10GN2MFA	452	573	24	64	401	540	20	
WELD METAL	468	618	22.8	72.1	425	559	22.4	65.1

2.2. The testing conditions

All tests were performed in the solution of 0.6% boric acid with the addition of 6ppm KOH. Which is typical environment for the VVER 1000 MW primary circuit. Two environments were used: one with low oxygen content (less than 20ppb), second saturated with oxygen. The high oxygen content was reached by bubbling air through the test medium in the reservoir throughout the test. Bubbling of hydrogen was used to reach low oxygen content. The reason of using this environment was to get remarkable stress corrosion cracking in the tested material. In all the tests, the pressure was kept approximately 2 MPa above the equilibrium pressure-temperate curve to keep the pressurised condition. The tests have been performed at temperature 320°C.

2.3. The slow strain rate tests

Stress corrosion cracking properties were tested by slow strain rate test. The SSRTs were carried out with the tensile specimens. The testing facility consisting of autoclave with refreshing water loop and loading machine were employed. The environment was refreshed with the rate of 2ml/min. The tensile specimens were loaded at a deformation rates of $10^{-6}s^{-1}$. Two types of specimens were used for the test: parallel cylindrical specimens and tapered specimens. From the first one, the mechanical properties as yield strength, tensile strength, total elongation and area reduction have been evaluated. After the test, all the specimens were examined in optical and SEM microscopes to evaluate the fracture mechanism and the changes on the specimen surface. From the fracture surface, the number and depth of facets were evaluated. The cracks were examined on the specimens surface as well.
The diameter of parallel specimens was 6m, gauge length 30mm. The cylindrical specimens [3] with 3° surface angle were used to test the initiation conditions for the corrosion cracks in the base metal. The minimal diameter was 6mm. They were loaded with the extension rate corresponding to that used for the parallel specimens until the tensile strength level was reached in the thinnest part of the specimen. After that, the test was terminated and the surface of the specimens was searched for the cracks. The thickness diameter with found crack was used for the calculation of the initiation stress.
Two orientations of specimens made from the base metal were tested:

- circumferential, marked "C"
- longitudinal, marked "L".

The specimens made from the weld metal were cut in the circumferential direction, as the model weldments were circumferential.

2.4. The constant loading of CT specimens

The pre-fatigued 0.5T CT specimens were wedge loaded end exposed in the static autoclave. The desired stress intensity factor was reached on the conventional loading machine, then the wedge was inserted inside the notch. The crack increment was evaluated periodically form the outside surface, he total increment was measured after the final

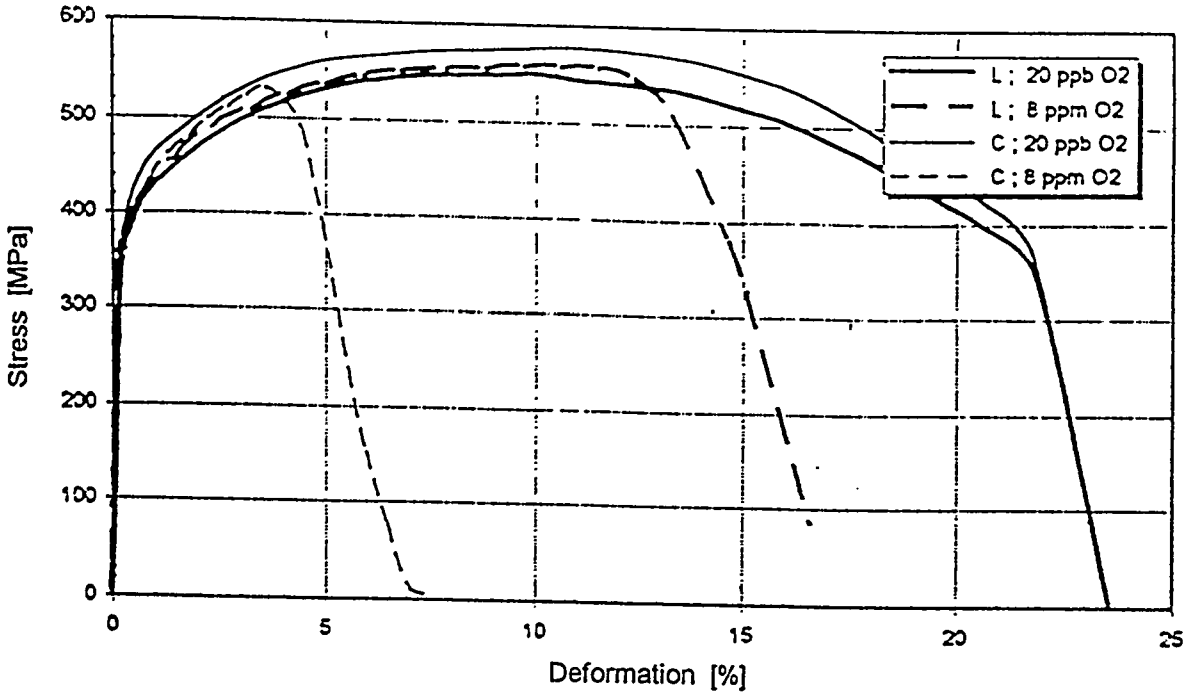

Fig.1 The stress - strain curves for the base metal tested at $10^{-6}s^{-1}$ SSRT. Directions of specimens: L-longitudinal, C-circumferential

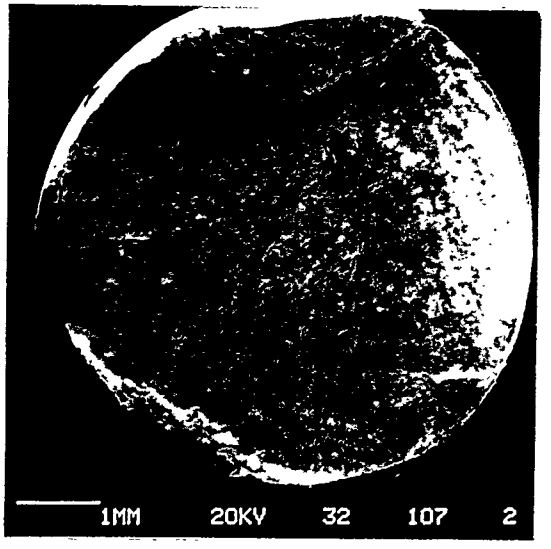

Fig.2a The fractograph of the fracture surface of the specimen with orientation C, base metal, high oxygen content environment

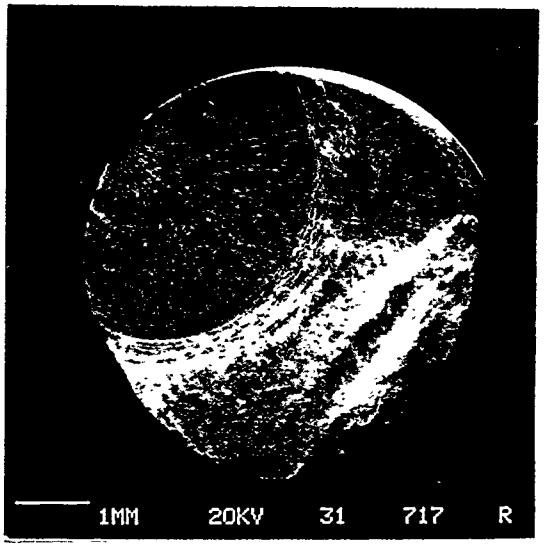

Fig.2b The fractograph of the fracture surface of the specimen with orientation L, base metal, high oxygen content environment

exposition in he environment. These experiments were carried out only in the low oxygen environment. The goal of the tests was to measure the conditions for the initiation of the rack growth as well as the crack growth rate under static long term load. The duration of the tests was 4500 hours. The cracks were considered to be stopped if no increment was found during last 1000 hours of exposure.

2.5. The cyclic loading of CT specimens

The aim of these experiments was to assess the possibility of the crack growth under the periodic loading. The kinetics of growth was measured as well as the fracture mechanisms were evaluated. The tests were carried out with 0.5T CT specimens in the 7 litres autoclave connected with the INSTRON loading machine. The pre-fatigued specimens were used. The specimens were loaded with the saw-type cycle, the asymmetry of the cycle was 0.2 the frequency 0.085Hz. The crack length was monitored during the test using the compliance method. The calibration curve was used for the compliance measurement. The tests were stopped at the ΔK values above 30-40 $MPam^{1/2}$. Again, the fracture surface was examined to find the typical fracture mechanism in this paper two tests are addressed. The first one was performed with the base metal 10GN2MFA, the second one with the crack growing from the base metal to the austenitic cladding. The thicker cladding was used in this case on the base metal.

3. Results

3.1. The slow strain rate tests

In Fig.1, there are the stress-deformation diagrams for the base metal tested in two orientations, circumferential and longitudinal. There is no difference in the response on the loading if tested in the environment with low oxygen content. The values, if compared with he basic properties in Tab.2 are not changed in the respect of the yield strength, tensile strength or total elongation. The fracture surface showed the 100% ductile fracture and no stress corrosion cracks were observed on the fracture surface or on the rest of the surface of the specimens. Much difference was observed between both orientations if tested in the environment with high oxygen level. As the tensile and yield properties are not changed substantially, the total elongation was nearly three times higher for the longitudinal orientation comparing with the circumferential one. Moreover, both values, 16% respectively 7% are much lower comparing with the air-test data (20%). The difference can be seen also on the fractographs, Fig. 2a,b. Both possess the same type of fracture feature: one transgranular crack growing from the initiation centre complemented with he ductile tearing region. However, the crack facet in the C orientation is deeper comparing with the L. From the tapered specimens, the initiation stress and strain was estimated. For the L orientation it was 297 MPa respectively 0.15%, for the circumferential orientation 554MPa and 2.2%. The calculated mean crack growth rate, which was obtained as the depth of the facet divided by the time between initiation of the rack and the final rupture was $1.4x10^{-8}$m/s for the orientation L, $2.1x10^{-7}$m/s for orientation C respectively. The difference more than one range means, that once the crack is initiated in the C orientation of specimen, it grows fast, however the initiation happens later than for the orientation L.
The comparison of the SSRT results from the weld metal is in Fig.3. The decrease of total elongation was observed in both environments comparing with the air data. However, the decrease in the environment with high oxygen content is bigger and corresponds with the data observed for the base metal, orientation C. The fractographic analysis showed similar picture as in the case of base metal. The fracture surface of the specimen tested in low oxygen solution was fully ductile without any trace of stress corrosion cracking. The typical fracture surface from the high oxygen solution is showed in Fig.4a and in the detail in Fig.4b. Several transgranular facets were observed, their depth was up to 1.5mm. As can be seen in Fig.4b, remarkable lines are visible on the surface of transgranular facets. Their distances are not equal and they seem to decrease as the crack increased. This was typical also for other specimens from both base metal and weld metal. No interaction between the weld structure features and the crack growth were observed.

3.2. The static loading of the CT specimens

The static loading of the CT specimens was performed on the initial stress intensity factor values between 20 and 30 MPa. In the base metal, no crack increment was observed during the test time (4500 hours). The crack growth rate on the level of 10^{-11}m/s was observed in the case of the specimen made from the weld metal. These results are consistent with he SSRT results, however, the decrease of load due to stress relaxation during the exposure could take this test not conservative. Unlike the SSRT fracture surfaces, no step-like marking was found on these specimens.

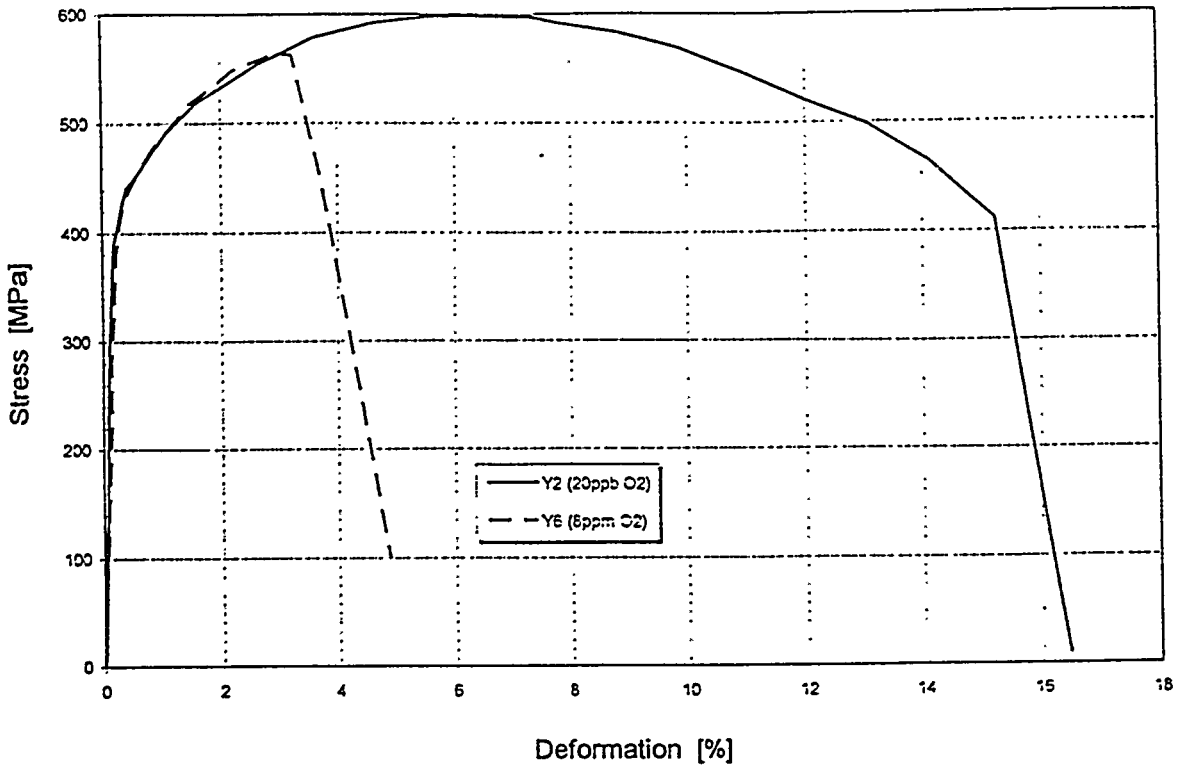

Fig.3 The stress - strain curves for the weld metal tested at $10^{-6}s^{-1}$ SSRT. Weld metal.

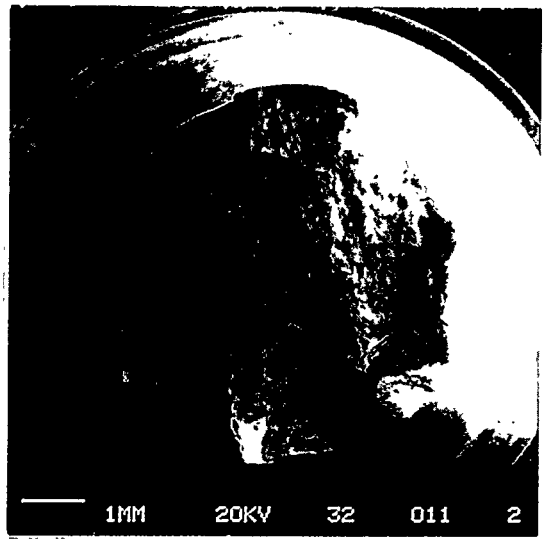

Fig.4a The fractograph of the fracture surface of the specimen with orientation C, high oxygen content environment, weld metal.

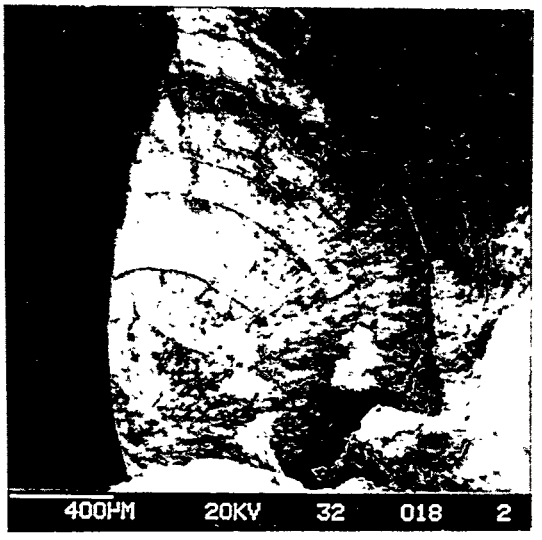

Fig.4b The detail of Fig.4a

3.2. The cyclic loading of the CT specimens

The main aim of the cyclic tests was to prove that even if there is in the material the crack, its kinetics is too slow to reach the critical value. For the low alloy materials the ASME XI flaw curve can be used as the reference curve.
As the material of the primary piping consists of base metal, weld metal and heat affected zone, all three materials were tested.
The comparison with this curve is shown in Fig.5 for the base metal of the primary piping, 10GN2MFA. If tested in the environment with low oxygen content, all results are below the ASME XI curve, approximately between one half of range to one range of the crack growth rate. The tests performed in the high oxygen content environment led to the slightly higher crack growth rates, however still all data points are below the reference curve and many of them are consistent with the low oxygen data. Only one point, at 33MPam$^{1/2}$ lies slightly above the ASME curve.
The fractographic analysis did not show the appearance of the intergranular fracture. The crack growth was transgranular, the secondary cracks, perpendicular to the plane of the main crack were found across all corrosion fatigue region, however their size increases as crack length and the stress intensity factor amplitude increased. In Fig.6 there is an example of the transgranular facets with visible structure of striations. The average distance between them is 1.2 μm. If compared with the crack growth rate from Fig.5 which is for this crack length between 6x10^{-4}mm/cycle and 1x10^{-3}mm/cycle, the local estimation is on the higher side of this interval.
In Fig.7, the results for the weld metal are shown. Similarly as for the base metal, all low oxygen data are well below the ASME XI curve. To compare the results for both materials, the correlation of measured crack growth rates was performed with the result shown in Fig.8. They are very near to the line with slope 1. From this, no substantial difference is between both materials. The results obtained if the material is tested in the environment with high oxygen contents were above the ASME line if the stress intensity factor was below 19MPam$^{1/2}$. Nevertheless the difference is low. From the fracture surface no intergranular cracking was observed and the fracture surface corresponding with the crack advance was similar to that obtained from the environment with low oxygen content.

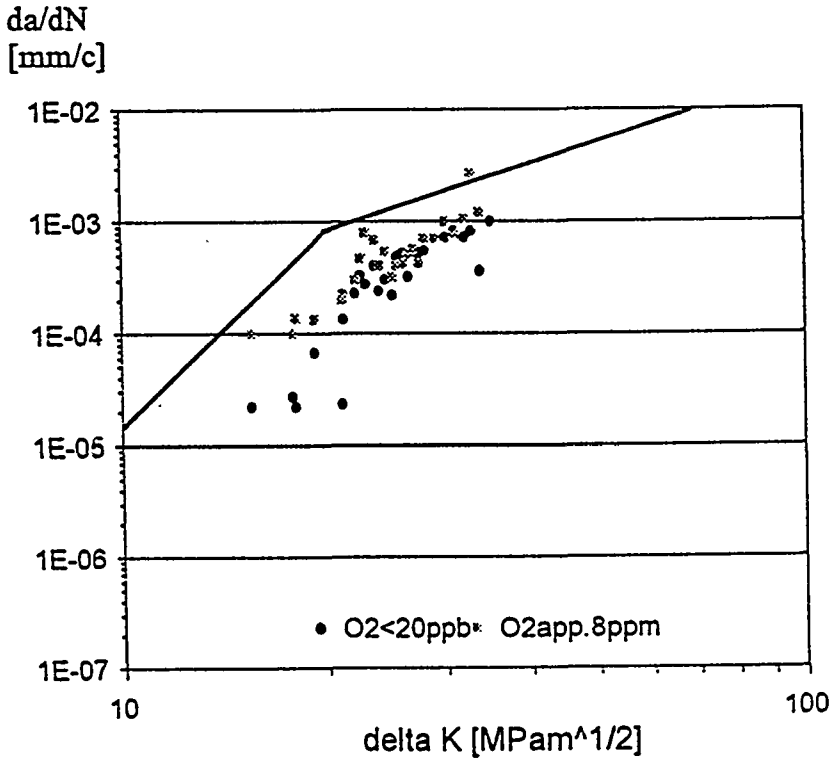

Fig.5 The crack growth rate vs ΔK values for the base metal

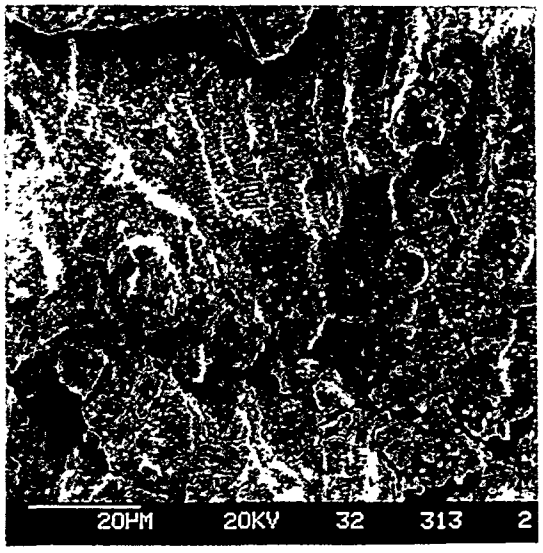

Fig.6 The detail of the trasgranular facet from the fracture surface of CT specimen base metal, cyclically loaded in the primary environment

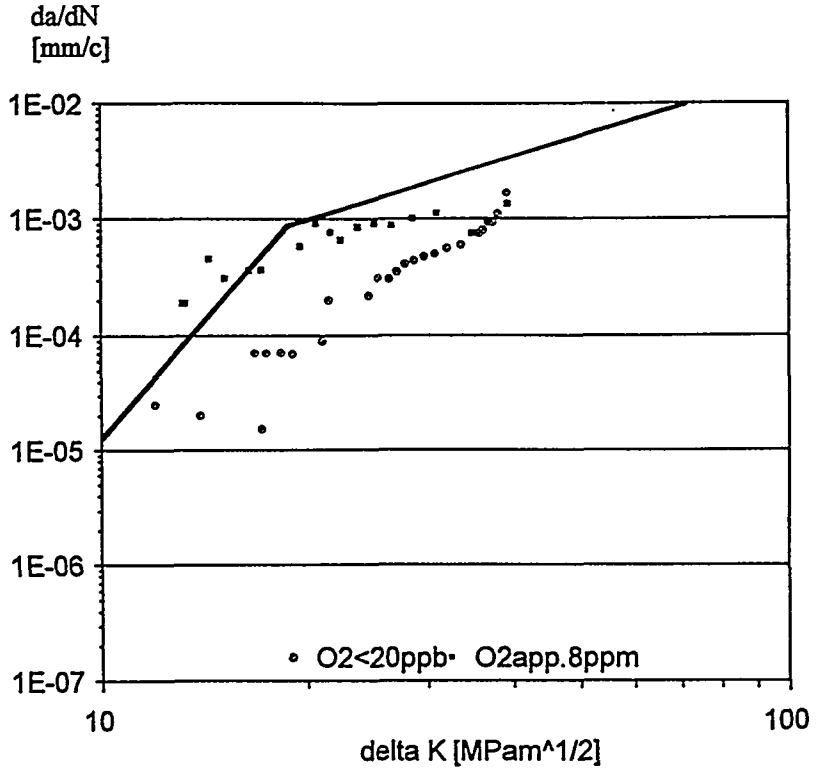

Fig.7 The crack growth rate vs ΔK values for the weld metal

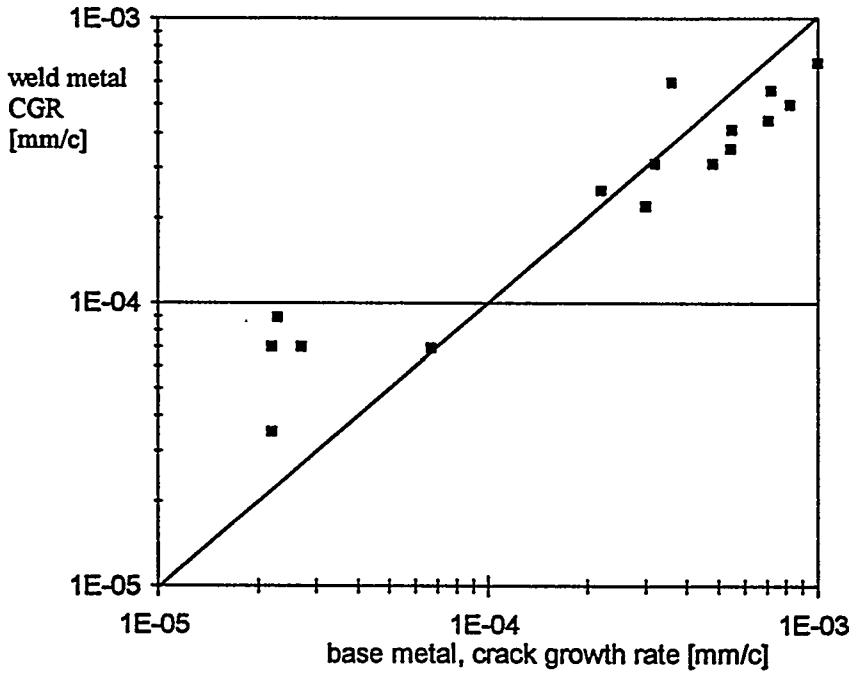

Fig.8 Comparison of equivalent data for crack growth rates in base metal and weld metal cyclically loaded in primary environment

4. Conclusion

The corrosion-mechanical properties of the primary piping materials of the NPP VVER 1000MW were tested in the framework of the leak before break project. The results showed that the material of the base metal and weld metal is not sensitive to the stress corrosion cracking. No substantial difference between tensile properties were observed between these materials tested in the air and inthe water environment at operation parameters. The typical fracture process for the material tested in high oxygen content was transgranular cleavage with remarkable crack arrest lines. The cyclic loading led to the increase of crack length in the CT specimens, the crack growth rates were below the ASME XI lines.

References

[1] Ruščák, M., Otruba J, Kaplan J.: Report Nuclear Research Institute, No. 9542 M, 1991 (in Czech)
[2] Keilová, E., Kočík J.: Report Nuclear Research Iinstitute No. DIM/302/25, 1995 (in Czech)
[3] Yu et al.: Fatigue Fract. Engn. Mater. Struct., 12,6,1989,p.481

THE PRIMARY CIRCIUT MATERIALS PROPERTIES RESULTS ANALYSIS PERFORMED ON ARCHIVE MATERIAL USED IN NPP V-1 AND KOLA NPP UNITS 1 AND 2

KUPČA Ľudovít PhDr, BEŇO Peter, Nuclear Power Plants Research Institute Inc.
Okružná 5, 918 64 Trnava, SLOVAK REPUBLIC

SUMMARY

The primary circuit piping material properties analysis was close related to the LBB methodology applications on the both units of the NPP V-1.

The asessment was performed on the following piping materials:

a) primary piping archive material used in NPP V-1

b) primary piping material cut from NPP Kola Units 1 and 2 after 100000 hours of operation

c) final correlations between the Russian and our experimental results.

Main research program tasks were:

1) analysis of the piping material mechanical properties (static tension, charpy, fracture toughness, fatigue)

2) corrosion stability of the primary circuit material analysis (igscc)

3) microstructural properties analysis which involved:

a) visual inspection of exposed internal surface

b) chemical composition analysis

c) hardness measurements

d) stainless steel macro and microstructural properties evaluations

e) delta-ferrite contents measurements

f) thermal fatigue and operational influences evaluation

g) substructure of both material evaluations using the TEM

h) fractography of samples after mechanical tests.

FRACTURE PROPERTIES EVALUATION OF STAINLESS STEEL PIPING FOR LBB APPLICATIONS

Y.J.Kim, C.S.Seok, Y.S.Chang
Sung Kyun Kwan University, Suwon, Korea

ABSTRACT

The objective of this paper is to evaluate the material properties of SA312 TP316 and SA312 TP304 stainless steels and their associated welds manufactured for shutdown cooling line and safety injection line of nuclear generating stations. A total of 82 tensile tests and 58 fracture toughness tests on specimens taken from actual pipes were performed and the effect of various parameters such as the pipe size, the specimen orientation, the test temperature and the welding procedure on the material properties are discussed. Test results show that the effect of the test temperature on the fracture toughness was significant while the effects of the pipe size and the specimen orientation on the fracture toughness were negligible. The material properties of the GTAW weld metal was in general higher than those of the base metal.

1. INTRODUCTION

Recently nuclear piping systems can be designed in accordance with the leak-before-break (LBB) design concept which is based on elastic-plastic fracture mechanics. In LBB analysis[1,2], both the J-integral and tearing modules (J/T) method and the limit load method (net section collapse) are recommended for the stability analysis of the cracked piping. It is generally regarded that the J/T method is appropriate for the analysis of carbon and stainless steel pipings while the limit load method is appropriate for the analysis of stainless steel pipings.

The J/T stability analysis method can be stated as follows.

$$T_{LOAD} < T_{MATERIAL} \tag{1}$$

The stress-strain (σ-ε) curve of piping material is needed to compute the left hand side of Eq.(1) while the J-resistance (J-R) curve is needed to compute the right hand side of Eq.(1).

A comprehensive material test program was prepared to generate material properties as required for the LBB application to the newly-built nuclear generating stations in Korea. In a previous paper[3], authors evaluated the material properties of SA106 Gr.C carbon steel and its accociated welds manufactured for main steam line. The objective of this paper is to evaluate the material properties of SA312 TP316 and SA312 TP304 stainless steels and their associated welds manufactured for shutdown cooling line and safety injection line. Tensile and fracture toughness tests on specimens taken from actual pipes were performed. In this paper, the effects of various factors such as the pipe size, the specimen orientation, the test temperature and the welding procedure on the material properties are discussed.

2. MATERIAL TEST PROGRAM

2.1 Test Material

Test materials were SA312 TP316 and SA312 TP304 stainless steels and their associated welds. The test specimens for SA312 TP316 steel were machained from the 12", 14" and 16" pipes, and the test specimens for SA312 TP304 steel were machined from the 14" pipe.

The weld coupons were prepared at shop and field for simulating the different fabricating conditions of pipe spools for installation. In order to ensure good fracture toughness, full gas tungsten arc welding (GTAW) procedure with post weld heat treatment (PWHT) was adopted.

2.2 Test Specimen

Based on the NUREG-1061 Vol.3[1] and SRP 3.6.3[2], at least two stress-strain curves and two J-resistance curves should be developed for each of the minimum of three heats of materials having the same material specifications and thermal and fabrication histories as the in-service piping material. If the data are being developed from an archival heat of material, a minimum of three stress-strain curves and three J-resistance curves from that one heat of material is sufficient. Table 1 summarizes the test material, pipe diameter, thickness, required number of specimens and test temperature. For SA312 TP316 steels, 1/2"ϕ round bar specimens were used for tensile tests and 1T-CT specimens were used for fracture toughness tests. However for relatively thin SA312 TP304 steels, the largest specimens that could be machined were used.

2.3 Test Method

Tensile tests were performed in accordance with ASTM E8(Standard Test Methods for Tension Testing of Metallic Material) and E21(Standard Test Methods for Elevated Temperature Tension Tests of Metallic Materials). Upper temperature tests were performed after maintaining the required temperature for two hours.

Fracture toughness tests were performed in accordance with ASTM E813(Standard Test Method for J_{IC}, A Measure of Fracture Toughness) and E1152(Standard Test Method for Determining J-R Curves). An

unloading compliance technique with high temperature COD gage was utilized to determine the J-R curves.

Table 1. LBB Test Program Summary

Material		Size	σ - ε Test		J -R Test		Temp.(℃)	
			Upper	Lower	Upper	Lower	Upper	Lower
Base Metal	SA312 TP316	12"S/160	12	1	4	1	49	20
		14"S/160	12		4		296	
		16"S/160	12		4		327	
	SA312 TP304	14"S/STD	12	1	12	1	49	
Shop Fab. Weld Metal	SA312 TP316	12"S/160	3	1	3	1	49	20
		14"S/160	3	1	3	1	296	
		16"S/160	3	1	3	1	327	
	SA312 TP304	14"S/STD	3	1	3	1	49	
Field Fab. Weld Metal	SA312 TP316	12"S/160	3	1	3	1	49	20
		14"S/160	3	1	3	1	296	
		16"S/160	3	1	3	1	327	
	SA312 TP304	14"S/STD	3	1	3	1	49	

3. TEST RESULTS

In this section, test results are grouped and summarized to show the effect of various factors which have an influence on the material properties.

3.1 Test Results

For tensile tests, the nominal stress-strain curves were obtained from the load-displacement curves, and the yield strength and the tensile strength values were determined. Subsequently the true stress-strain curves were generated and, by curve-fitting to the Ramberg-Osgood equation, α, n material constants were obtained.

For fracture toughness tests, the J-R curves were obtained from the load versus load line displacement curves. Accordingly the C_1, C_2 and J_{IC} values were then obtained by a power law curve fitting method. The ASTM validity requirements such as data spacing, regression line, crack shape and amount of crack extension were satisfied. However the ASTM requirements for J_{max} and ω were not satisfied. This may be due to the high toughness values of the tested materials.

3.2 Effect of Pipe Size

Fig.1 shows the effect of the pipe size on the room temperature stress-strain curves of SA312 TP316 steel(for shop weld and field weld specimens) in the L orientation. Although the stress-strain curves of the 12" and 16" pipes were higher than those of the 14" pipe for the shop weld specimens, the stress-strain curve of the 12" pipe was higher than those of the 14" and the 16" pipes for the field weld specimens. Therefore it is not possible to clarify the effect of the pipe size on the tensile properties.

Fig.2 shows the room temperature fracture toughness test result of SA312 TP316 steel in the L-C orientation. The J-resistance curve of the 14" pipe was higher than that of the 16" pipe. However, no definite trend was observed for the J-resistance curve of the 12" pipe.

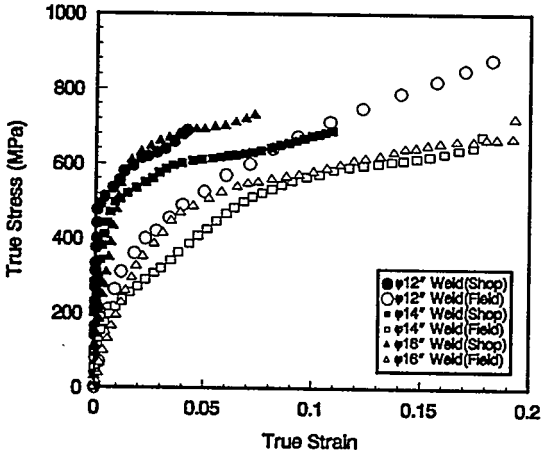

Fig.1 Effect of pipe size on σ - ε curves(SA312 TP316)

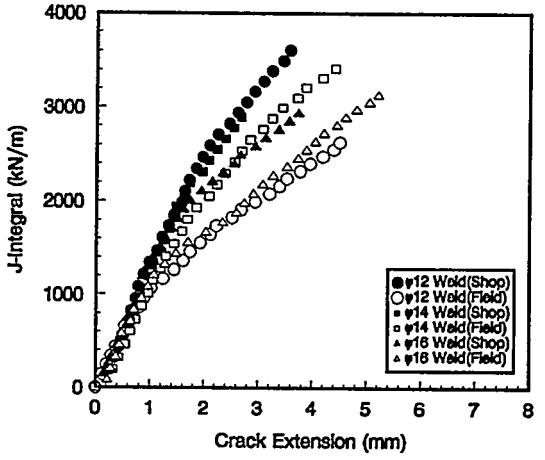

Fig.2 Effect of pipe size on J-R curves(SA312 TP316)

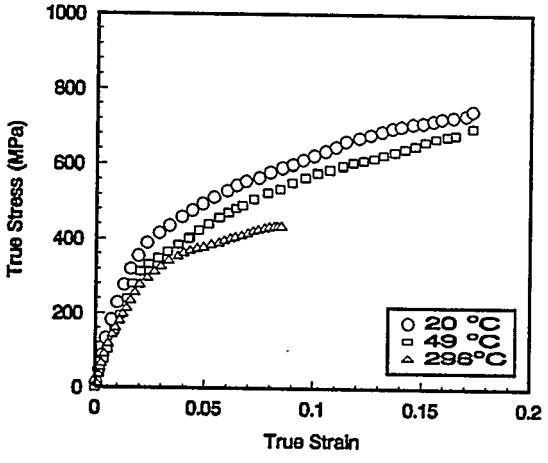

Fig.3 Effect of test temperature on σ - ε curves(SA312 TP316)

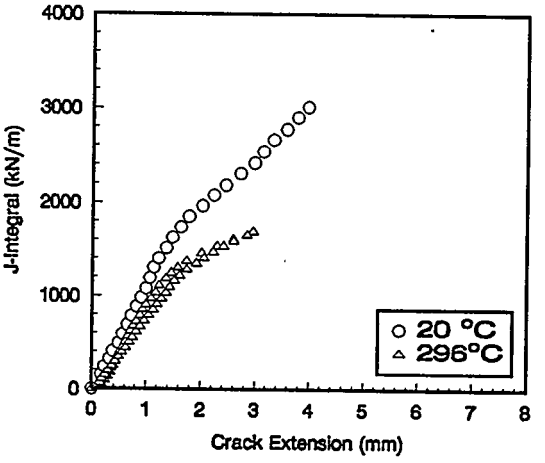

Fig.4 Effect of test temperature on J-R curves(SA312 TP316)

3.3 Effect of Specimen Orientation

The median S_y and S_u values of the 14" pipe of SA312 TP316 steel in the L orientation are 179 MPa and 462 MPa respectively, while those in the C orientation are 165 MPa and 448 MPa respectively. The median S_y and S_u values of the 14" pipe of SA312 TP304 steel in the L orientation are 324 MPa and 552 MPa respectively, while those in the C orientation are 310 MPa and 538 MPa respectively. Therefore it can be stated that the effect of specimen orientation on the tensile properties is negligible.

3.4 Effect of Test Temperature

Fig.3 shows the effect of test temperature on the stress-strain curves of SA312 TP316 steel, and Fig.4 shows the effect of test temperature on the J-resistance curves of the 14" pipe of SA312 TP316 steel. Both the stress-strain curves and the J-resistance curves are lowered with an increase in the test temperature, similar with carbon steel data[3]. This trend, however, was not observed for SA312 TP304 steel.

3.5 Effect of Welding

The effect of welding on the stress-strain curves of the 14" pipe of SA312 TP316 steel is shown in Fig.5. The stress-strain curves of the weld metal are higher than that of the base metal, and the stress-strain curves of the weld metal produced by shop fabrication is higher than that produced by field fabrication. It was not, however, possible to obtain full stress-strain curves for the weld metal specimens due to necking of the region outside of the gage length.

Fig.6 shows the effect of welding on the J-resistance curves of the 16" pipe of SA312 TP316 steel. Against the tensile test results, the J-resistance curve of the field weld was higher than that of the base metal while the J-resistance curve of the shop weld was slightly lower than that of the base metal.

4. DISCUSSION

4.1 Comparison Between SA312 TP304 and SA312 TP316 Steels

The room temperature stress-strain curves of two test materials are compared in Fig.7. As shown in the figure, the tensile properties of SA312 TP304 steel were higher than those of SA312 TP316 steel. The room temperature J-resistance curves of two test materials are shown in Fig.8. As shown in the figure, the fracture properties of two stainless steels are almost identical.

The 0.3T-CT specimens were used for SA312 TP304 steel. Therefore, if 1T-CT specimens were also used for SA312 TP304 steel, the J-resistance curves would be lowered. Also the effects of the specimen orientation and the test temperature were not significant due to the small size of specimens.

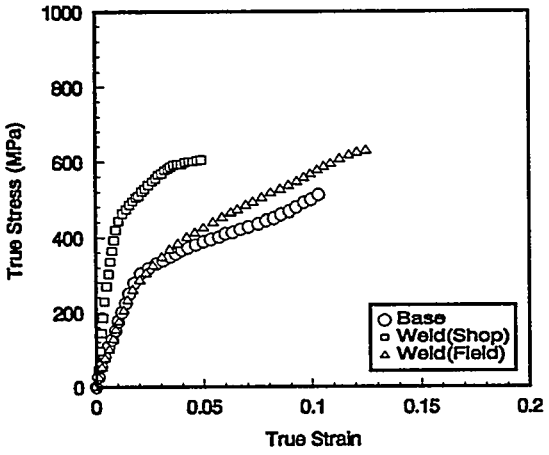

Fig.5 Effect of welding on σ - ε curves(SA312 TP316)

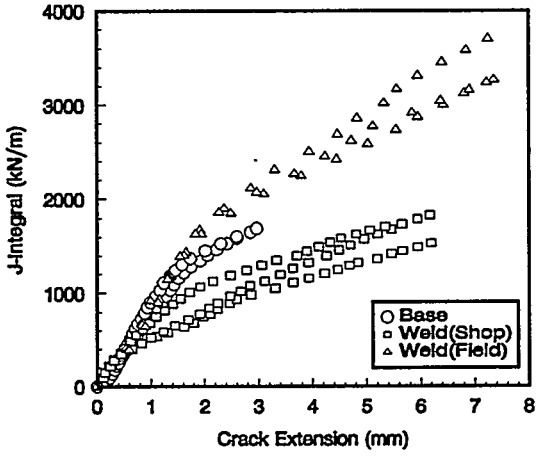

Fig.6 Effect of welding on J-R curves(SA312 TP316)

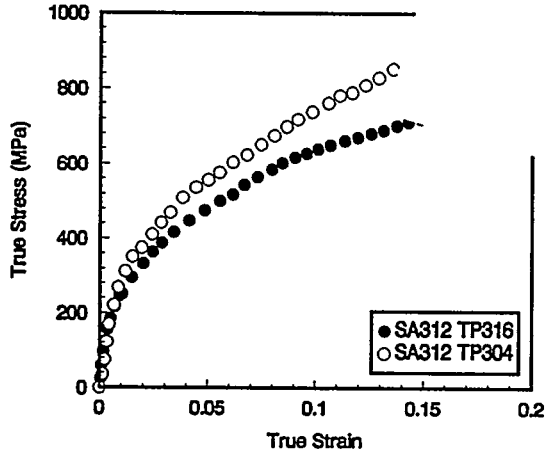

Fig.7 Comparison of σ - ε curves between SA312 TP304 and SA312 TP316

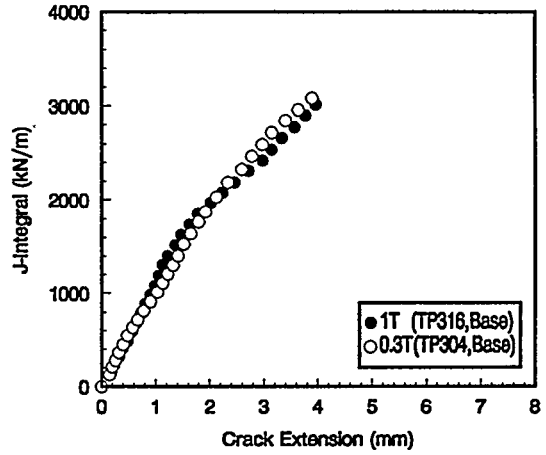

Fig.8 Comparison of J-R curves between SA312 TP304 and SA312 TP316

4.2 Correlation Between Tensile And Fracture Toughness Data

An attempt to correlate between tensile and fracture toughness data was made. After performing the tensile test, the specimen diameter at fracture(d_f) was measured and the critical strain at fracture(ε_c) was defined as following :

$$\varepsilon_c = 2\ln\left(\frac{d_o}{d_f}\right) \qquad (2)$$

The non-dimensional parameters such as S_u' and C_1' can be defined as following :

$$S_u' = \frac{S_u}{E} \tag{3}$$

$$C_1' = \frac{C_1}{Ek} \tag{4}$$

where E is Young's modulus and k is 1 mm.

Fig.9 shows the correlation between the parameter $S_u' \times \sqrt{\varepsilon_c}$ and the parameter C_1', and the following empirical equation is obtained.

$$C_1' = 1.687 \times (S_u' \times \sqrt{\varepsilon_c})^{1.06} \tag{5}$$

From Eqs. (3), (4) and (5), the C_1 value can be obtained as following :

$$C_1 = 1.687Ek \times (S_u' \times \sqrt{\varepsilon_c})^{1.06} \tag{6}$$

The C_2 parameter is independent of tensile property in the range of 0.55 ~ 0.75, as shown in Fig.10. Therefore the C_2 value can be regarded as

$$C_2 = 0.61 \tag{7}$$

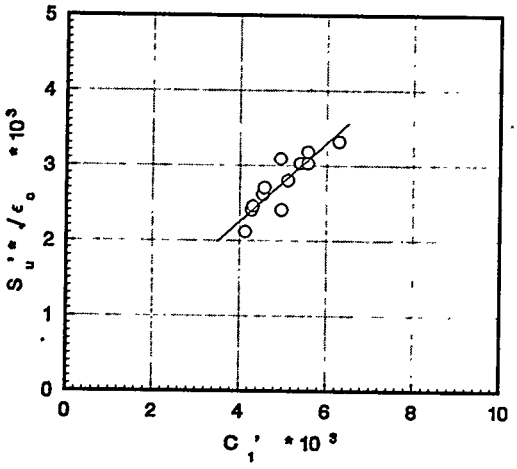

Fig.9 Correlation between C_1 and tensile properties

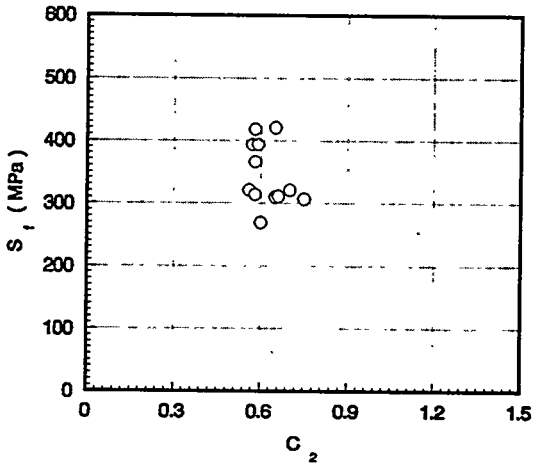

Fig.10 Correlation between C_2 and tensile properties

5.CONCLUSION

Following conclusions were made from the LBB material test program on SA312 TP316 and SA312 TP304 stainless steels.

1) Effects of the pipe size and the specimen orientation on the tensile property and the fracture property were not significant.

were not significant.

2) Both the tensile property and the fracture property were lowered with an increase in the test temperature.
3) The tensile property of SA312 TP304 steel was higher than that of SA312 TP316 steel, while the fracture properties of both steel were similar.
4) Due to high toughness of the material, the ASTM E813 validity requirement was not satisfied.

REFERENCE

[1] USNRC, Evaluation of Potential for Pipe Breaks, NUREG-1061 Vol.3 (1984)

[2] USNRC, Leak Before Break Evaluation Procedure, NUREG800, Standard Review Plan 3.6.3, (1987).

[3] Y.J.Kim, et al., Fracture Properties Evaluation of Carbon Steel Piping for Main Steam Line, Int.J. of Nuclear Engineering and Design(in press).

EFFECTS OF TOUGHNESS ANISOTROPY AND COMBINED TENSION, TORSION, AND BENDING LOADS ON FRACTURE BEHAVIOR OF FERRITIC NUCLEAR PIPE

R. Mohan, C. Marshall, N. Ghadiali and G. Wilkowski
Battelle; 505 King Avenue; Columbus, OH-43201; U. S. A.

This paper summarizes work on angled through-wall-crack initiation and combined loading effects on ferritic nuclear pipe performed as part of the Nuclear Regulatory Commission's research program entitled "Short Cracks in Piping and Piping Welds". The reader is referred to Reference 1 for details of the experiments and analyses conducted as part of this program. The major impetus for this work stemmed from the observation that initially circumferentially oriented cracks in carbon steel pipes exhibited a high tendency to grow at a different angle when the cracked pipes were subjected to bending or bending plus pressure loads. This failure mode was little understood, and the effect of angled crack growth from an initially circumferential crack raised questions about how cracks in a piping system subjected to combined loading with torsional stresses would behave.

There were three major efforts undertaken in this study. The first involved a literature review to assess the causes of toughness anisotropy in ferritic pipes and to develop strength and toughness data as a function of angle from the circumferential plane. The second effort was an attempt to develop a screening criterion based on toughness anisotropy and to compare this screening criterion with experimental pipe fracture data. The third and more significant effort involved finite element analyses to examine why cracks grow at an angle and what is the effect of combined loads with torsional stresses on a circumferentially cracked pipe. These three efforts are summarized below.

1. LITERATURE REVIEW OF TOUGHNESS ANISOTROPY AND DATA DEVELOPMENT

The literature review of toughness anisotropy showed that there were three contributors to toughness anisotropy (Refs. 2-5). By far, the largest contributor was the size and shape of elongated nonmetallic inclusions, predominantly manganese sulfides. Smaller contributions were thought to come from crystallographic texture and microstructural banding. Crystallographic texture arises when the individual grains (crystals) are not randomly oriented but have a preferred orientation dictated by the thermo-mechanical processing, while microstructural banding is the result of alternating bands of ferrite and pearlite aligned in the principal working direction. An Anisotropy Index was developed which was the ratio of the maximum toughness (usually in the L-C orientation, i.e., the circumferential through-wall crack growth direction), to the minimum toughness (usually in the C-L orientation, i.e., the axial through-wall crack growth direction). Anisotropy Index values of approximately three are common for ferritic pipes, although for plates heavily rolled to increase the strength, the Anisotropy Index was found to be greater than six. Cross-rolling of plates can bring this ratio to one (isotropic toughness) which is possible with seam-welded pipes, but not with seamless pipes.

Also, in this effort, tensile and C(T) data were developed at various angles for one particular A333 Grade 6 pipe used in the Degraded Piping Program Experiment 4111-1. This was a seamless pipe (Pipe DP2-F11) and had nonmetallic inclusions with large aspect ratios oriented at an angle of approximately 66 degrees to the circumferential plane. The results of the tensile tests, shown in Figure 1, indicate that the effect of inclusion orientation is insignificant. The C(T) specimens were side grooved in order to force the cracks to grow at a

predetermined angle. As was expected, cracks growing along the inclusion direction yielded the lowest fracture toughness values, while those growing normal to the inclusions yielded the highest values. This can be evidenced in the orientation dependence of J_i values (Figure 2). The Anisotropy Index based on the initiation toughness values was 3.1 for this pipe steel. Additionally, Charpy tests at a temperature corresponding to the upper shelf on five other steels revealed strong orientation effect (see Figure 3). Metallographic examinations of the five pipes revealed that nonmetallic inclusions with large aspect ratios were aligned either at 66 degrees to the circumferential plane (in one pipe) or more commonly along the pipe axis. The Anisotropy Index for each pipe was then determined from the Charpy values and ranged from 1.7 to 3.4. However, from 0 to 45 degrees, the slope of the Charpy energy versus angle data was very similar for each of the five steels. Beyond 45 degrees the data from one steel had a slope change.

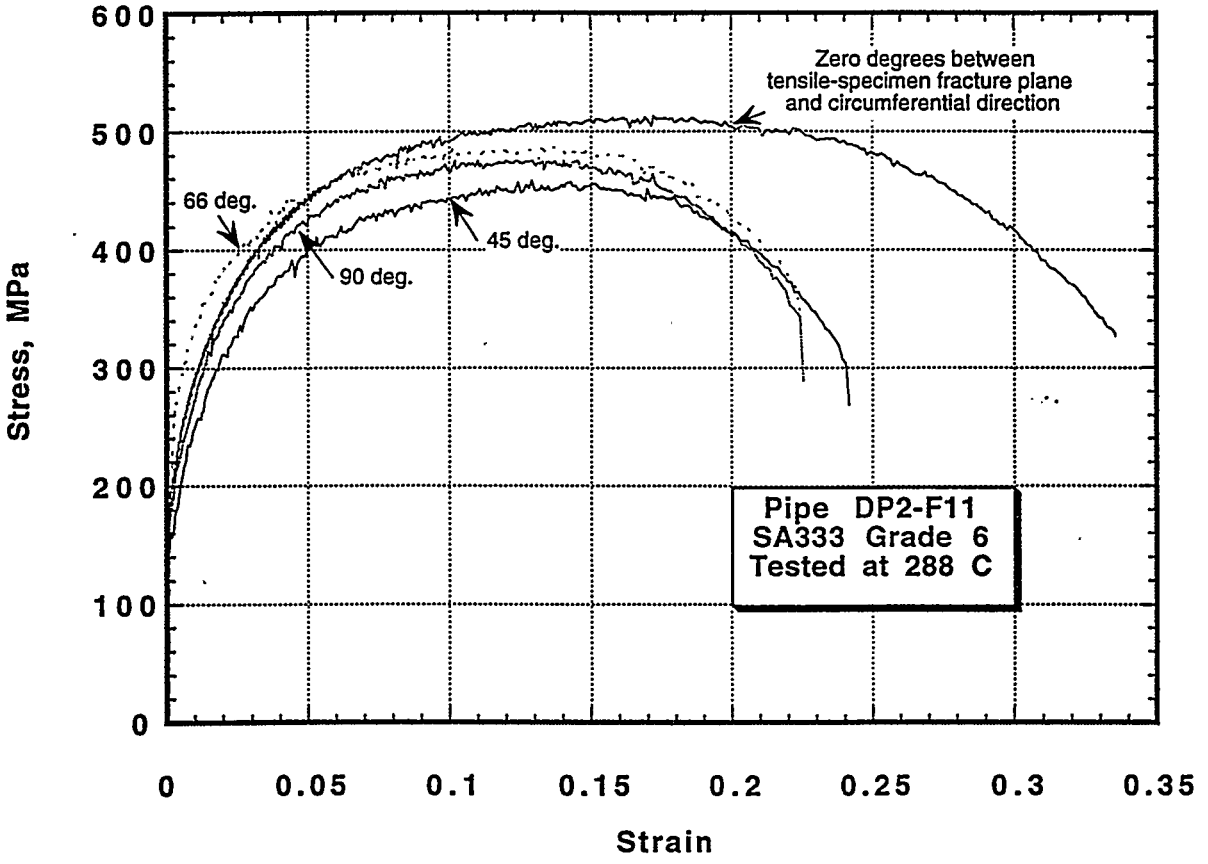

Figure 1. Engineering stress-strain curves for several different tensile specimens orientations in Pipe DP2-F11.

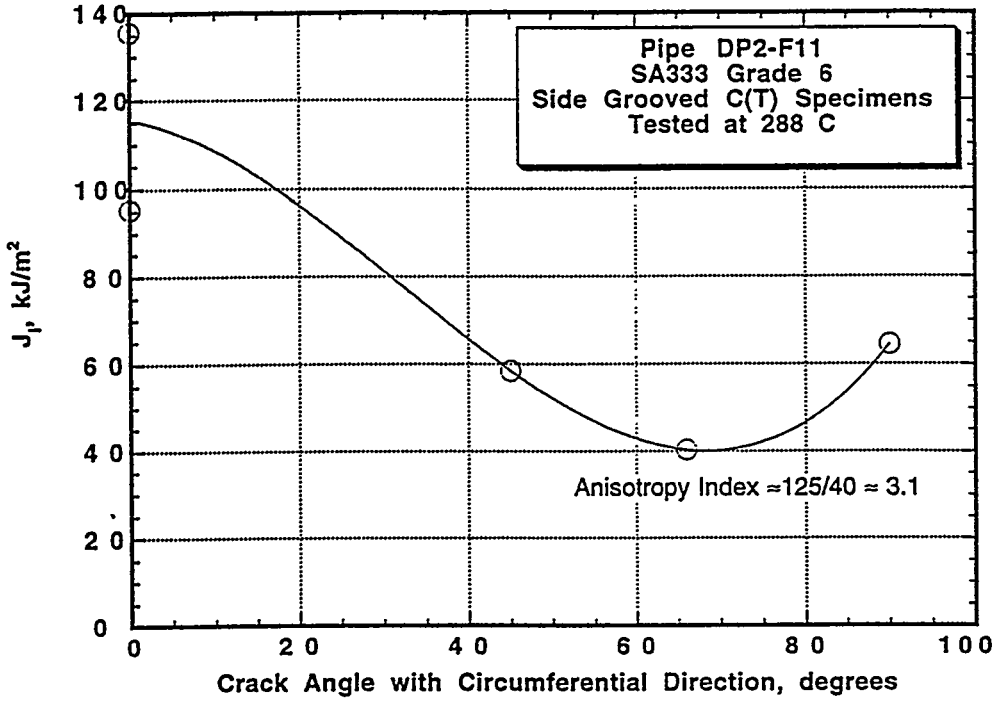

Figure 2. Orientation dependence of J_i values in Pipe DP2-F11 material.

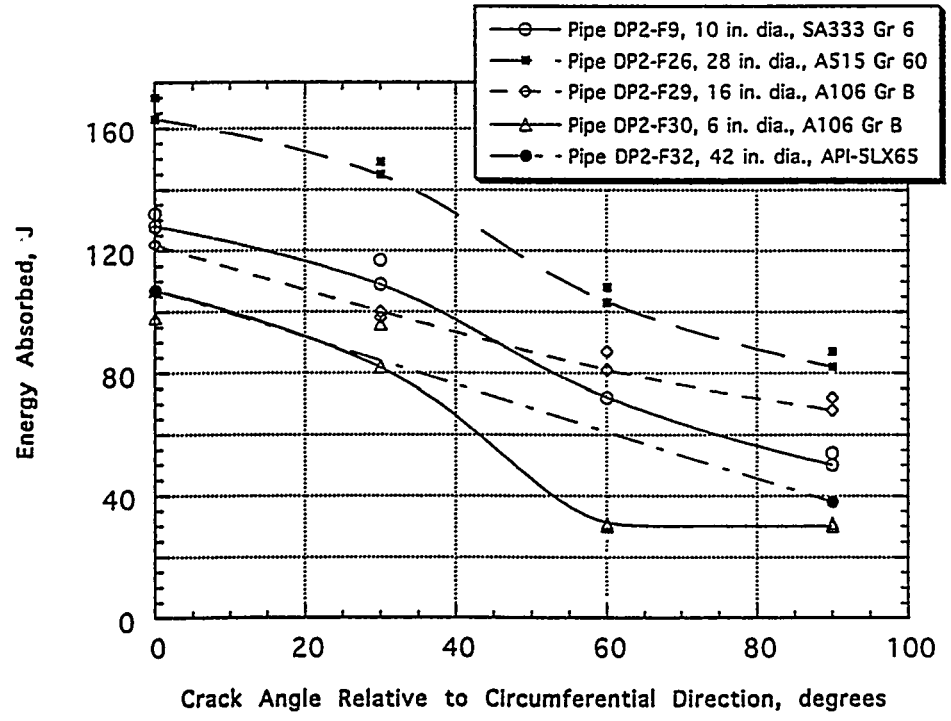

Figure 3. Energy absorbed by Charpy V-notch specimens as a function of orientation (Note: All fractures were 100% ductile).

2. SCREENING CRITERIA BASED ON TOUGHNESS DATA

The angles of crack initiation from numerous past carbon steel pipe tests from the Degraded Piping, IPIRG-1, and the Short Cracks in Piping and Piping Welds programs (Refs 6-8) were documented. The angle of crack initiation versus Anisotropy Index, shown in Figure 4, indicate a high degree of scatter. A slightly better trend was evidenced in the variation of crack initiation angle versus the pipe diameter-to-thickness ratio (Figure 5). However, it seems clear from these two figures that a simple screening criterion based on either the Anisotropy index or the diameter-to-thickness ratio is of little value. Indeed there were many cases of pipe experiments using pipe from the same heat of pipe where the crack initiation angle varied from 20 to 65 degrees.

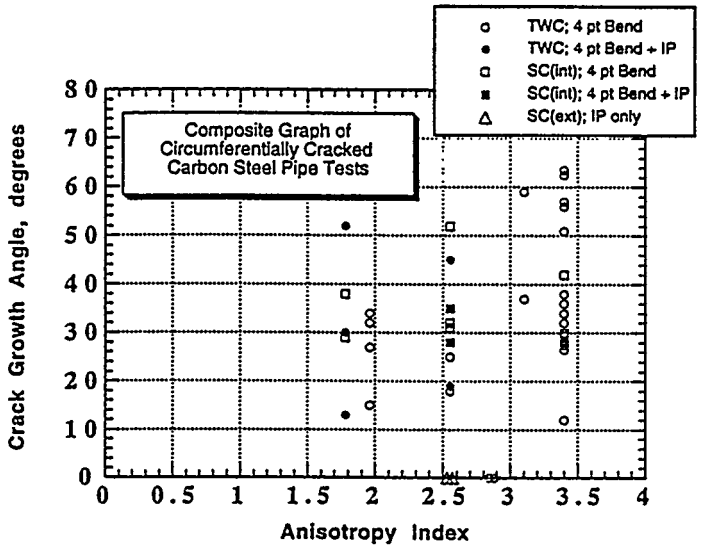

Figure 4. Crack initiation angle versus Anisotropy Index for circumferentially cracked carbon steel pipes tested at Battelle (TWC = through-wall crack, SC = surface crack, IP = internal pressure).

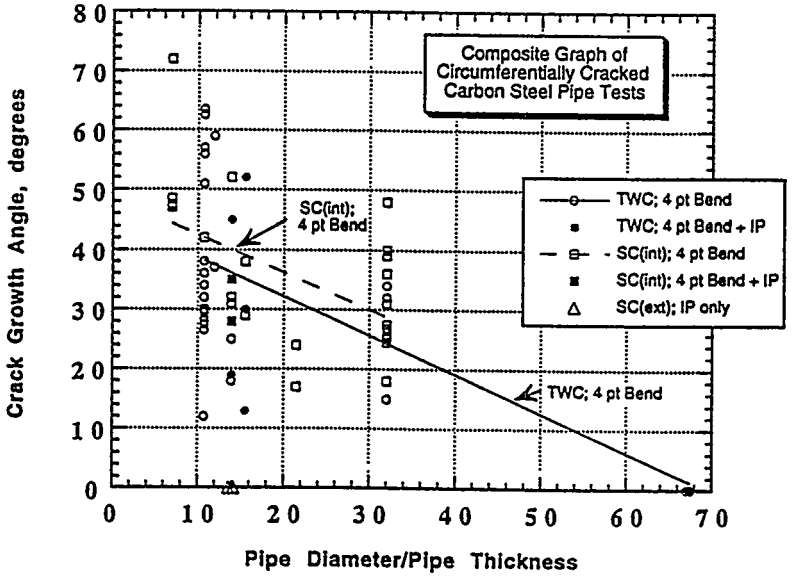

Figure 5. Crack initiation angle versus pipe diameter/thickness for carbon steel pipe tests (TWC = through-wall crack, SC = surface crack, IP = internal pressure).

3. FINITE ELEMENT ANALYSES

The main objectives of this effort were to examine if angled crack initiation could be explained analytically, and to investigate combined tension, bending, and torsion loading on circumferential through-wall-cracked pipes. To accomplish these objectives, Experiment 4111-1 on a 4-inch nominal diameter Schedule 80 A333 Grade 6 pipe from the Degraded Piping Program was analyzed. This pipe had a 37-percent long circumferential through-wall crack. These pipe and crack dimensions were used in numerous other finite element analyses. The finite element analyses were conducted for straight circumferential cracks as well as circumferential cracks with a short length of angled tip. The angular crack tip length was chosen to correspond to mean particle spacing of the sulfide inclusions. Crack tip angles (Ω) of 0, 25, 45, and 65 were analyzed. Even under pure bending conditions, the angled crack tip invokes combined mode loading, i.e., Mode I (opening), Mode II (sliding shear) and Mode III (out-of-plane tearing). A review of combined-mode, elastic-plastic fracture parameters showed that although the analysis procedure is pushing the state-of-the-art, what was done was reasonable. Detailed descriptions of the finite element analyses and boundary conditions are given in detail in Reference 1, since under the various loading conditions, one cannot assume quarter symmetry, especially for the case of the angled crack tip or combined loading involving torsion. The analyses were done using the ABAQUS® computer code.

3.1 Angled Crack Initiation Phenomenon

The results of the elastic-plastic analyses of straight and angled cracks, subjected to bending, indicated that the normalized angular crack-driving force, $J_\Omega/J_{\Omega=0}$ [ratio of the $J_{applied}$ value for an angled crack (J_Ω) and the corresponding value for straight crack ($J_{\Omega=0}$)] had a constant value once plasticity occurred (Figure 6). While this trend of normalized angular crack-driving force is important, it does not provide a direct explanation for the onset of angled crack growth. Thus, a normalized angular crack growth parameter, A, was developed, where

$$A = \frac{\text{normalized angular fracture resistance}}{\text{normalized angular crack driving force}} = \frac{J_{i\Omega}/J_{i\Omega=0}}{J_\Omega/J_{\Omega=0}} \qquad (1)$$

and $J_{i\Omega}$ is the initiation toughness at an angle Ω, and $J_{i\Omega=0}$ is the initiation toughness in the L-C orientation (circumferential crack growth direction). It is important to mention that this parameter is not a material parameter, but rather a combination of the directional sensitivity of both the fracture toughness and the crack-driving-force. This parameter was found to be useful in gaining an understanding of the angular crack initiation phenomenon. When this parameter has a value of unity or higher for a given crack-tip angle, then the tendency for the crack to grow along the circumferential plane is higher than the tendency for it to propagate along that angle. Similarly, if the parameter is less than one at other than $\Omega=0$, then the crack should grow at that angle. The variation of this parameter with the crack tip angle from the circumferential plane for the analysis of Experiment 4111-1 shows that the crack would be more likely to grow at an angle, and the parameter A was essentially the same from 25 to 65 degrees (Figure 7). Hence, the crack could grow in any direction from 25 to 65 degrees. This observation agrees well with the experimental observation that the crack propagated at 37 and 59 degrees from the two crack tips in Experiment 4111-1.

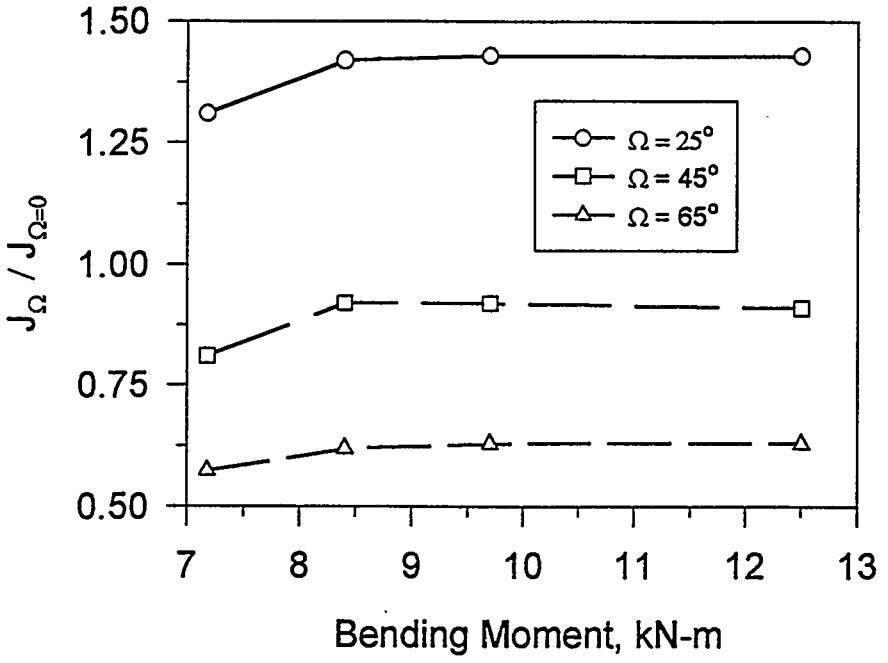

Figure 6. Normalized angular driving force, $J_\Omega / J_{\Omega=0}$, as a function of bending moment. This figure illustrates the saturation attained by these values).

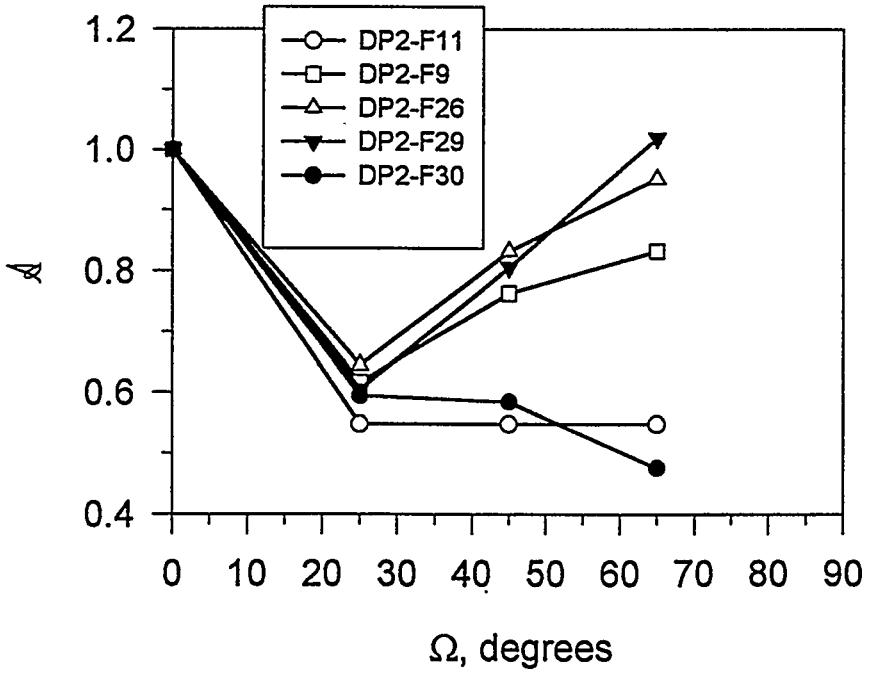

Figure 7. Variation of normalized angular crack growth parameter, A, with crack-tip angle, Ω, from the circumferential plane.

Since the analyses reported pertain only to this pipe, strictly speaking the results obtained for the driving force for straight and angled cracks cannot be used to examine the experimental data obtained for the other pipes. This limitation is because the $J_{applied}$ term used in $J_\Omega / J_{\Omega=0}$ may be sensitive to crack length, pipe diameter-to-thickness ratios, and stress-strain characteristics of the material. However, the normalized angular fracture resistance values from the Charpy tests on the other pipe materials evaluated were used with the results from the finite element analyses to see if pipes similar in geometry to Experiment 4111-1, and made of these other ferritic steels, would exhibit angular crack growth. It was found that the range of angles over which the crack may propagate varied considerably from pipe to pipe, even though the slopes of the Charpy energy versus Ω graphs were only slightly different (see Figure 7). Hence, it is believed that local variability in toughness anisotropy may significantly affect the direction of crack growth. The sensitivity of the $J_\Omega / J_{\Omega=0}$ term to crack length, pipe diameter-to-thickness ratio, and stress-strain properties is not known. The development of the proposed A parameter appears promising in explaining angled crack initiation in ferritic pipes, but it is not generally validated for other crack lengths and pipe sizes.

3.2 Combined Loading Effects

The other main objective of this work was to assess the fracture behavior of pipes subjected to torsional stresses (τ_t) in addition to bending stresses (σ_B) and tension stresses from internal pressure. Prior to starting this analysis, a survey of piping stress analyses results from various companies was undertaken. This survey showed that bending moment-to-torque (M_B/T) ratios of 3.0 were common and occasionally this ratio was as low as 1.0. Analyses of straight as well as angled circumferential cracks were then conducted using both of these ratios. Four different approaches to handle combined torsion and bending were developed. These can be cast in the form of a single equation defining the effective moment, M_{eff}, as given below:

$$M_{eff} = \sqrt{M_B^2 + (c_e T)^2} \qquad (2)$$

where,

$c_e = 1 \rightarrow$ Effective moment from resultant of bending moment (M_B) plus torque

$c_e = \frac{\sqrt{3}}{2} \rightarrow$ Effective moment calculated from $\sigma_{eff} = \sqrt{\sigma_B^2 + 3\tau_T^2}$

$c_e = \frac{1}{2} \rightarrow$ Effective moment calculated from $\sigma_{eff} = \sqrt{\sigma_B^2 + \tau_T^2}$

$c_e = 0 \rightarrow$ Effective moment calculated ignoring torque

In Equation 2, c_e defines the effective moment parameter. The upper and lower bounds for calculating the effective moment are defined by $c_e = 1$ and $c_e = 0$. The other two approaches lie in between these two extremes as indicated by Equation 2.

The variation of crack-driving force with the effective moment for the case of straight crack subjected to a bending moment-to-torsion ratios of 1 and 3, shown in Figure 8, indicate that the finite element solutions obtained for the crack-driving force under bending conditions may be used in evaluating the corresponding

quantity for cracked pipes subjected to combined bending and torsion, provided the effective moment is calculated using Approach (3). Similar conclusion was apparent for other fracture parameters, such as crack-opening displacements and crack-opening areas. The finite element results demonstrated the validity of this approach for an angled circumferential through-wall crack with a crack-tip angle of 45 degrees as well. This significant conclusion enables the use of simple engineering estimation schemes of through-wall-cracked pipes under bending to be used to determine fracture parameters when combined loading with torsion occurs. The limitation to this approach, however, is that the analyses conducted to date were restricted to very small amounts of angular crack growth. For large crack growth at an angle, there may be some deviations from the results obtained to date. For instance, the ratio of the J-R curves at different orientations do not seem to be constant with crack growth, and the ratio of the $J_{applied}$ values with crack-tip angle for a growing crack is unknown. Also we did not conduct crack growth analyses for the straight growing crack to examine the validity of the effective moment concept, but anticipate that this approach would work. Nevertheless, the conclusion of using this effective bending stress for combined loads involving torsion is valid for all leak-rate calculations of concern to LBB analyses and for determining loads up to crack initiation. Finally it should be noted that these results are for circumferential through-wall-cracked pipe, and surface-cracked pipe may behave quite differently under combined loads.

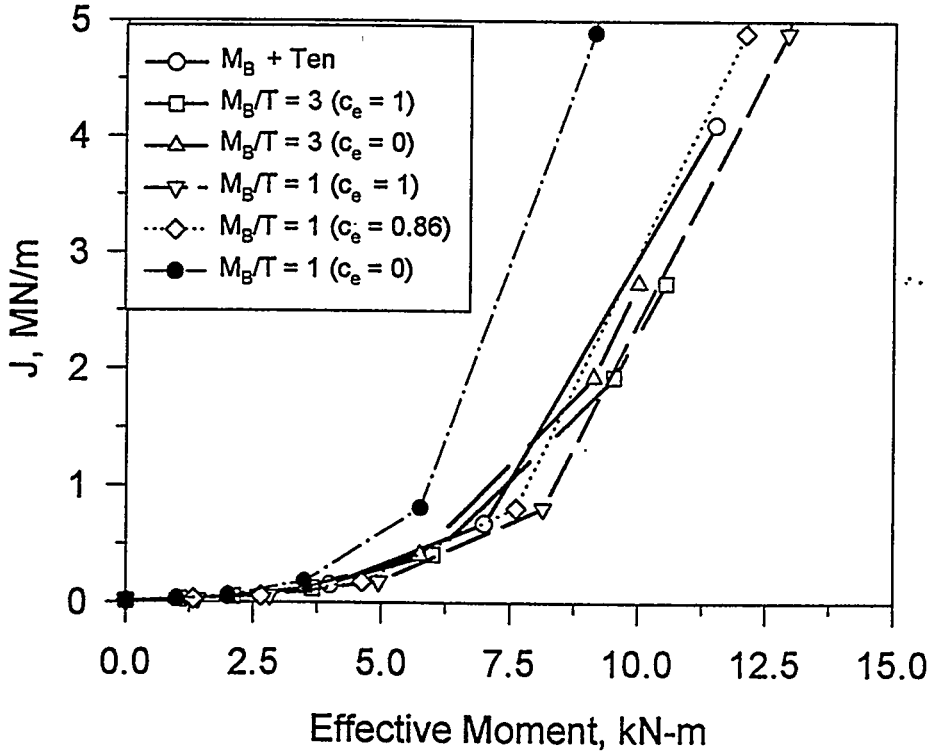

Figure 8. Effect of combined loading on the variation of J at mid-thickness versus effective moment for various pure and combined loading cases.

4. CONCLUSIONS

It was seen that in order to gain an insight into the angled crack initiation phenomenon observed in circumferential TWC ferritic pipes, simple screening criteria based on Anisotropy Index or diameter-to-thickness ratio are not very valuable. However, based on detailed finite element analyses of a circumferential TWC pipe, an angular crack initiation parameter is developed which offers promise in explaining this phenomenon. Additional work is needed to validate this parameter for several other pipe and flaw geometries. It should be emphasized that this parameter has meaning only for crack initiation.

In addition, a simple engineering approach was developed to evaluate fracture parameters for cracked pipes subjected to combined bending and torsion. This approach is valid only for non-growing cracks but is still useful for LBB analyses.

5. REFERENCES

(1) R. Mohan, G. Wilkowski and others, "Effects of Toughness Anisotropy and Combined Tension, Torsion, and Bending Loads on Fracture Behavior of Ferritic Nuclear Pipe," NUREG/CR-6266, April 1995.

(2) G. Wilkowski and others, "Short Cracks in Piping and Piping Welds," NUREG/CR-4599, BMI-2173, Vol. 1, No.2, December 1991.

(3) J. M. Hodge, R. H. Frazier, and F. W. Boulger, "The Effect of Sulphur on the Notch Toughness of Heat-Treated Steels," *Transactions of Metallurgical Society of AIME*, Vol. 215, pp. 745-753, October 1959.

(4) Y. I. Matrosov, and I. E. Polyakov, "Improving Toughness and Ductility and Reducing Property Anisotropy in Low Alloy Steels," BISI Translation 14384, *Stal'* (2), pp. 162-167, 1976.

(5) D. M. Fegredo, B. Faucher, and M. T. Shehata, "Influence of Inclusion Content, Texture and Microstructure on the Toughness Anisotropy of Low Carbon Steels," *Strength of Metals and Alloys*, Vol. 2, Pergamon Press Ltd. Oxford, pp. 1127-1132, 1985.

(6) G. Wilkowski and others, "Degraded Piping Program - Phase II," Summary of Technical Results and Their Significance to Leak-Before-Break and In-Service Flaw Acceptance Criteria, March 1984-January 1989, Battelle Columbus Division, NUREG/CR-4082, Vol. 8, March 1989.

(7) R. A. Schmidt, G. Wilkowski, and M. Mayfield, "The International Piping Integrity Research Group (IPIRG) Program-- An Overview," SMiRT-11 Proceedings, Paper G23/1, August 1991.

(8) P. Scott, G. Kramer, P. Vieth, R. Francini, and G. Wilkowski, "The Effect of Dynamic and Cyclic Loading During Ductile Tearing on Circumferentially Cracked Pipe-- Experimental Results,: ASME PVP, Vol. 280, pp. 207-220, June 1994.

MATERIAL PROPERTY EVALUATIONS OF BIMETALLIC WELDS, STAINLESS STEEL SAW FUSION LINES, AND MATERIALS AFFECTED BY DYNAMIC STRAIN AGING

D. Rudland, P. Scott, C. Marschall, and G. Wilkowski
Engineering Mechanics Group, Battelle Memorial Institute, Columbus OH 43201

ABSTRACT

In many cases, current pipe fracture analyses can reasonably predict the behavior of flawed piping. However, there are several material applications where there are uncertainties in the fracture behavior. This paper summarizes the work on three such cases: stainless steel submerged-arc weld fusion lines, carbon-to-stainless steel bimetallic welds and ferritic steels affected by dynamic strain aging (DSA) at LWR temperatures. These investigations were performed during the U.S. Nuclear Regulatory Commissions research program entitled "Short Cracks in Piping and Piping Welds".

First, the fracture behavior of bimetallic welds, which are found in both PWRs and BWRs are discussed. The incentive for this study was to determine if current fracture analyses can be used to predict the response of pipe with flaws in bimetallic welds. The weld in this study joined sections of the A516 Grade 70 carbon steel cold-leg piping system to a F316 stainless steel safe end that was to be welded to stainless steel pump housings. The crack was located along the carbon steel base metal to Inconel 182 weld metal fusion line. Material properties derived from tensile and C(T) specimens were used to predict large pipe response. The major conclusion from this work is that the fracture behavior of this bimetallic weld could be evaluated with reasonable accuracy using properties of the carbon steel pipe and conventional J-estimation scheme analyses. However, these results may not be generally true for all bimetallic welds.

Second, the toughness of austenitic steel submerged-arc weld (SAW) fusion lines is discussed. It was noticed that during large-scale pipe tests with flaws in the center of the SAW, the crack tended to grow into the fusion line. The fracture toughness of the base metal, the SAW, and the fusion line were determined and compared. The major conclusion reached is that even though the SAW fusion line had a higher initiation toughness than the SAW weld metal, the fusion-line J-R curve reached a steady-state value while the SAW J-R curve continued to rise.

Finally, several carbon steel fracture experiments containing circumferential flaws that experienced periods of unstable crack jumps during steady ductile tearing are discussed. These instabilities are believed to be due to dynamic strain aging (DSA). This paper will discuss DSA, a simple screening criteria developed to predict this phenomena, and the ability of the current J-based methodologies to assess the effect of these crack instabilities. The effect of loading rate on the strength and toughness of several different carbon steel pipes at LWR temperatures is also discussed.

INTRODUCTION

As part of the Short Cracks in Piping and Piping Welds Research Program[1] conducted at Battelle-Columbus for the U.S. Nuclear Regulatory Commission (USNRC) a number of research activities/tasks were conducted. The two main tasks involved developing experimental data and developing/refining fracture prediction methodologies

for through-wall-cracked[2] and surface-cracked[3] pipe. In addition to these two tasks, a number of complimentary tasks were undertaken to address specific issues related to the further understanding of pipe fracture of nuclear grade piping materials. The impetus of this paper is to summarize the findings from three of these complimentary tasks, i.e., the bimetallic weld task[4], the stainless steel submerged-arc weld (SAW) fusion-line toughness task[5], and the dynamic strain aging task[6]. Further details of the efforts involved with and the results from each of these tasks can be found in the three NUREG reports from these tasks[4,5,6].

Bimetallic Weld Evaluations

In both BWRs and PWRs, there are many locations where carbon steel pipes or components are joined to austenitic pipes or components with a bimetallic weld. The objective of the research associated with Task 3 of the Short Cracks Program was to assess the accuracy of current pipe fracture analyses for the case of a crack along a carbon steel to austenitic weld fusion line.

The bimetallic welds evaluated were obtained as part of the Degraded Piping Program[7] from a canceled Combustion Engineering nuclear power plant. The welds joined sections of the carbon steel cold-leg piping system to stainless steel safe ends that were to be welded to stainless steel pump housings. The carbon steel pipe material was A516 Grade 70. The safe ends were fabricated from SA182 F316 stainless steel (forged TP316 stainless steel). The welds were fabricated by first buttering the beveled end of the carbon steel pipe with an ENiCrFe-3 (Inconel 182) electrode. The welds joining the buttered pipes and the stainless steel safe ends were then completed using a shielded-metal-arc weld (SMAW) process, using Inconel 182 weld rod, see Figure 1. Several such welds in the nominal 914-mm (36-inch) diameter by 76-mm (3.0-inch) thick pipe were available for testing.

To achieve the program objective, material property data and data from a large diameter pipe fracture experiment were developed to assess current analytical methods. The material property data developed included longitudinal tensile data from specimens machined from the various parts of the pipe weldment as well as data from compact (tension), C(T), tests with cracks located along the carbon steel to Inconel 182 weld fusion line to determine the fracture toughness of the fusion line. The large diameter pipe experiment evaluated a circumferential through-wall crack along the bimetallic weld fusion line subjected to bending at 288 C (550 F). The various analysis methods were then compared with the pipe experimental data.

The major conclusion reached as a result of this research was that the fracture behavior of the bimetallic fusion line tested in this program could be predicted with reasonable accuracy using the strength and toughness properties of the carbon steel pipe material in conjunction with conventional elastic-plastic fracture mechanics analysis. This is believed to be due to: (1) the fusion-line toughness, evaluated in C(T) specimen tests, being slightly higher than the toughness of the carbon steel base metal, (2) the Inconel weld metal being higher strength than the carbon steel base metal allowing the crack to grow more in the carbon steel than in the Inconel 182 weld metal, and (3) the higher strength Inconel 182 weld metal may be shielding some of the plastic strains between the crack section and the lower strength stainless steel safe end on the other side of the weld. Consequently, the carbon steel base metal strength properties were more appropriate to use in the simple pipe fracture analyses, see Figure 2.

One point that should be emphasized is that the data presented in this paper, and the conclusions drawn from these data, are applicable only to this one class of bimetallic welds, i.e., a low strength carbon steel pipe welded to a stainless steel safe end using an Inconel weld procedure. The fracture behavior of other classes of bimetallic welds, made up of different material systems, may not be the same. For instance, for bimetallic welds associated with low alloy ferritic steel nozzle forgings, the strength and toughness properties of the various materials may be such that the crack will tend to grow in the weldment. In addition, if the bimetallic weld was made with stainless steel buttering rather than Inconel, then the crack may grow into a softer, carbon-depleted, region near the heat-affected-zone of the carbon steel material. Figure 3 compares C(T) specimen fracture toughness data from this program with C(T) data developed at NRI-Rez in the Czech Republic for a weld fabricated using a stainless steel

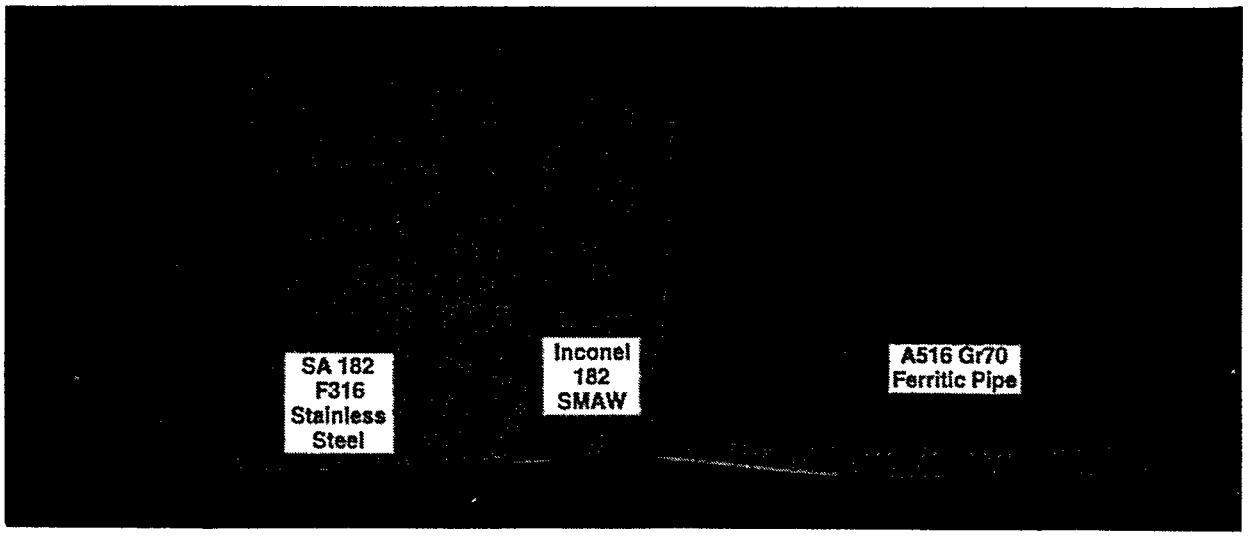

Figure 1. Cross section of bimetal weld evaluated showing various materials that make up the weldment

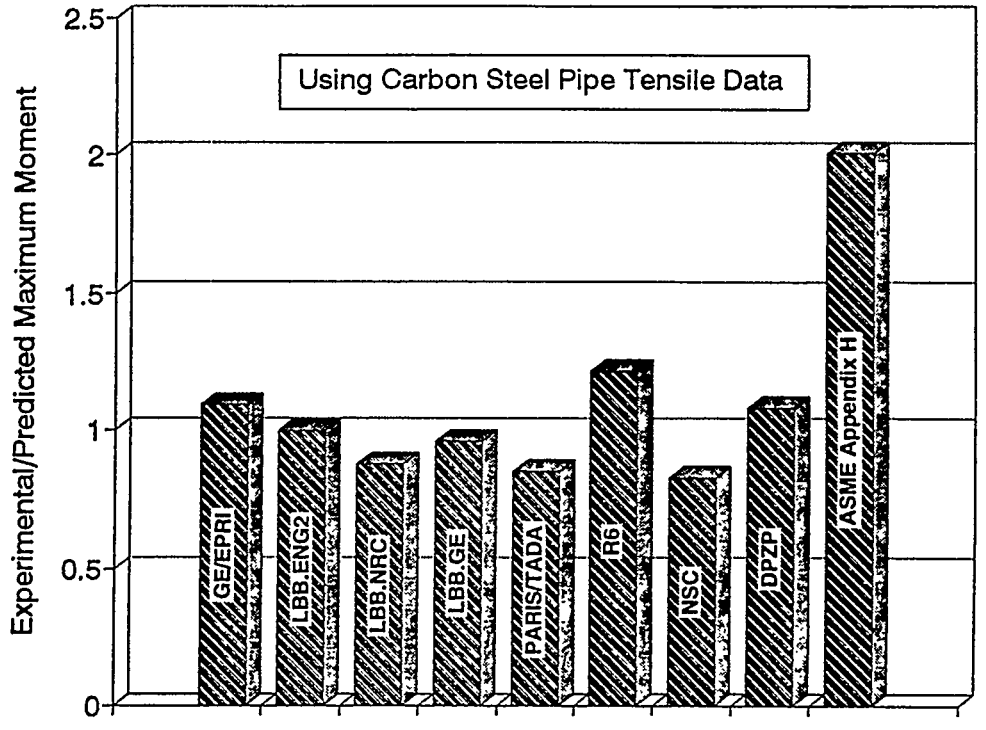

Figure 2. Comparison of maximum experimental moment with maximum predicted moments for bimetal weld pipe experiment using the fusion-line C(T) specimen J_D-R curve with the carbon steel pipe stress-strain curve and nine different analysis methods

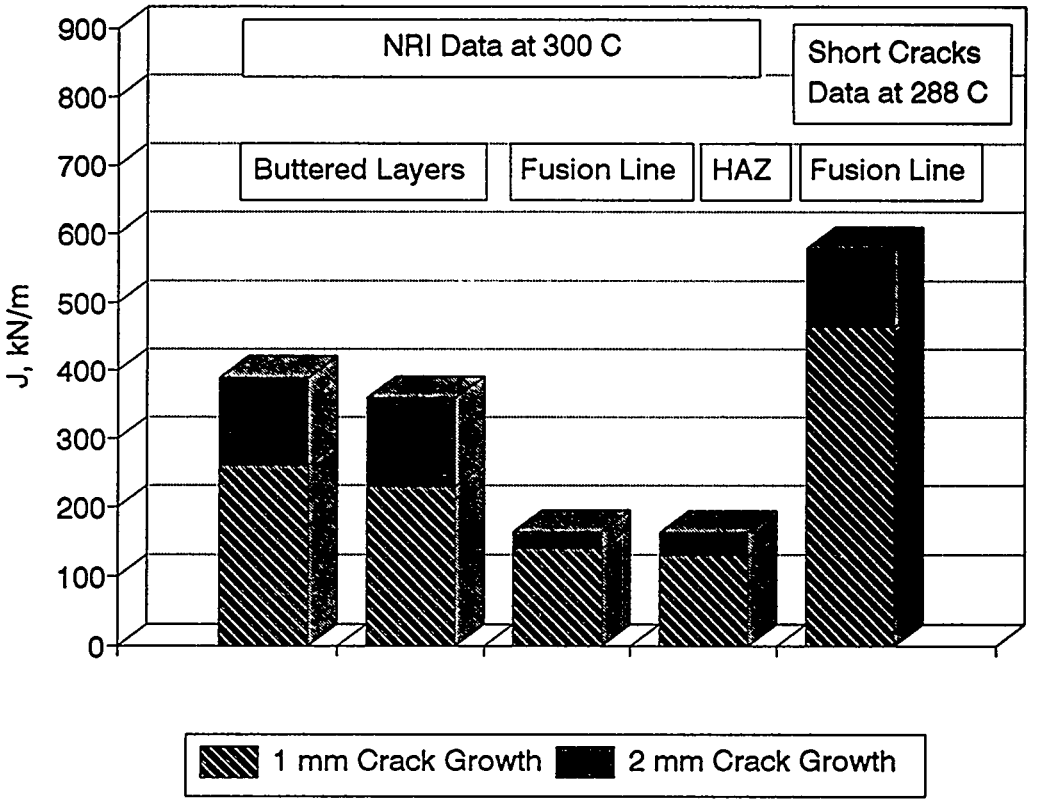

Figure 3. J-values at 1 mm (0.04 inch) and 2 mm (0.08 inch) of crack extension for bimetallic welds evaluated by NRI-Rez and during Short Cracks program

buttering procedure. As can be seen, the fracture toughness of the Inconel weld fusion line is significantly higher than for the weld fusion line made using the stainless steel weld metal. If evaluating such a weld, the fracture moments may be less than would be predicted using the carbon steel pipe properties in conjunction with conventional elastic-plastic fracture mechanics analysis methods.

Stainless Steel Fusion-Line Toughness Evaluations

The objective of this effort was to evaluate the fracture toughness of the fusion line of stainless steel submerged-arc welds in stainless steel pipe. The incentive was to explain why the cracks grew into the fusion line in many of the stainless steel pipe tests which were conducted with cracks initially in the center of the weld. The concern is that the fusion line may have a much lower toughness than the submerged-arc weld metal. Since the submerged-arc weld metal toughness is considered the lowest toughness for pipe flaw evaluation in the ASME Section XI austenitic pipe flaw evaluation criteria, and would typically be used in LBB evaluations, the implication of this work could be significant.

To conduct this evaluation, Charpy V-notch and compact tension [C(T)] specimens were fabricated from two different welds. One weld was a standard single-Vee weld from a girth-welded pipe, and the other was a slant-Vee weld from a plate weld that had one of the fusion lines perpendicular to the plate surface, see Figure 4. The standard single-Vee weld C(T) specimens had the notch machined along the fusion line, i.e., they had a slant notch. The slant-Vee weld C(T) specimens had standard (flat) notches machined along the fusion line, which was perpendicular to the plate face. The C(T) specimens were tested at 288 C (550 F) at quasi-static monotonic

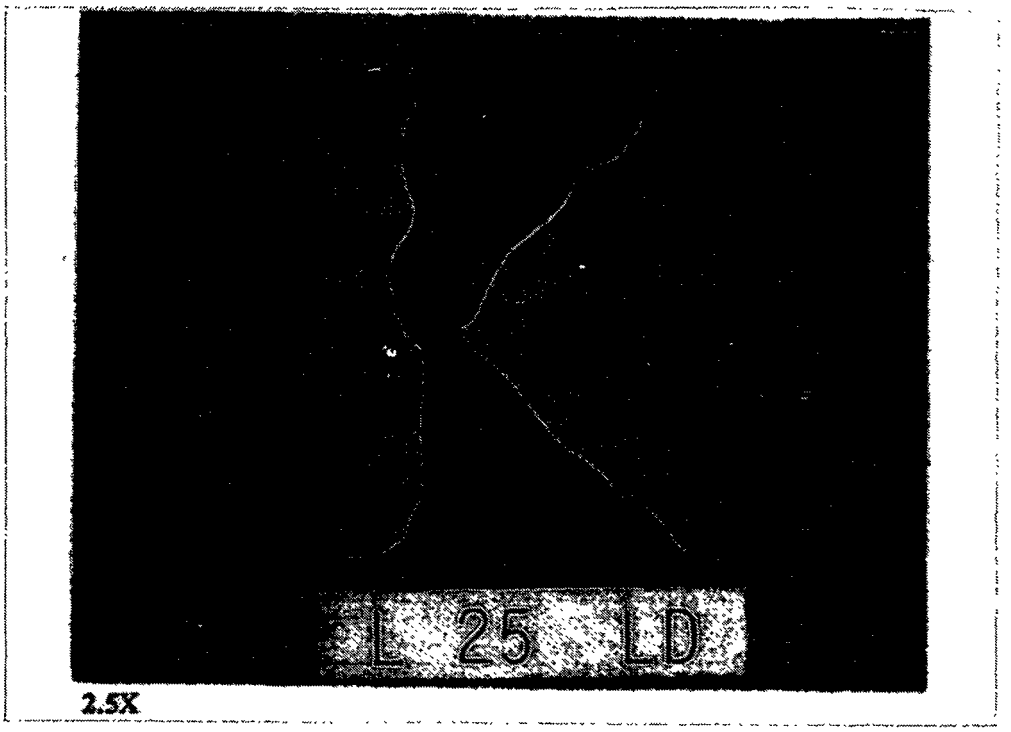

Figure 4. Example of K-weld preparation with out-of-plane bulging of the fusion line at the root passes

loading rates. Charpy specimens were tested at room temperature and 288 C (550 F). Data for cracks in the center of the weld and in the base metal were available from previous work[8] for comparison with results in this program.

The results showed that:

(1) The value of toughness determined at the fusion line using a sharp crack specimen is highly sensitive to the crack tip location relative to the fusion line. This result was expected.

(2) The J_{1mm} values calculated from the Charpy energy data using the ASME Section XI Appendix H correlation were less than the C(T) specimen J_{Ic} values. Hence, the ASME Charpy energy correlation can be used, but it may be very conservative, e.g., by a factor of 9 in one case.

(3) From the data developed in this paper, the initiation toughness of the stainless steel base metal is much higher than determined from either the SAW or the fusion line. The fusion-line initiation toughness J_{Ic} was greater than that at the SAW centerline.

(4) The crack growth resistance at the fusion line appeared to reach a steady-state value, while the SAW J-R curve had an increasing J_D-R curve, see Figure 5. This result may explain why in the pipe experiments, the cracks eventually turned and grew along the fusion line. Also, this result implies that the weld metal J-R curve should be used up to the fusion-line steady-state J value for stainless steel welds. A large C(T) specimen test with the initial crack in the fusion line would help to confirm this conclusion.

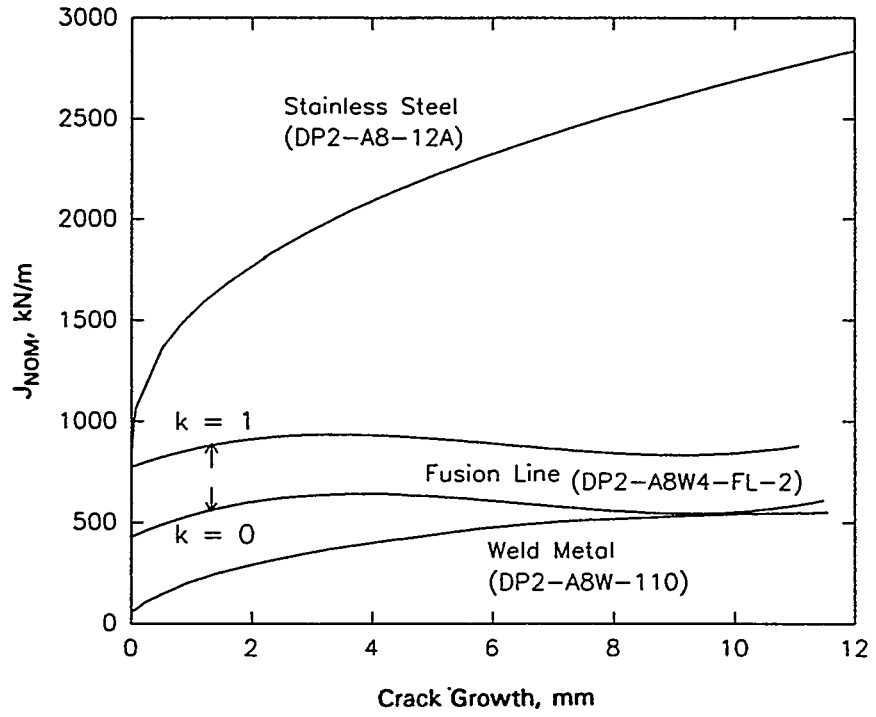

Figure 5. Comparison of J_{nom} resistance curves for base metal, weld, and fusion line

(5) If the crack tip is slightly off the fusion line in the base metal, the initiation toughness may be high, but the crack can quickly grow into the lower toughness fusion line and produce a decreasing J-R curve. Such a decreasing toughness curve has not been observed when testing homogeneous specimens.

(6) The most important conclusion is that the fusion-line J-R curve results can have an impact on the ASME Section XI austenitic pipe flaw evaluation criteria and LBB analyses for wrought and probably cast stainless steels. In the past, the weld metal toughness has been the limiting toughness; whereas the fusion-line and heat-affected-zone toughnesses have been given little attention.

A final relative comparison involved comparing results from this program with those from experiments from the Degraded Piping Program. The implication from the comparison of the weld metal and fusion-line crack-tip-opening angle data from single-edge notched tension, SEN(T), specimens was that the fusion-line toughness was a factor of 3 less than that of the weld even at small amounts of crack growth, see Figure 6. The lower toughness of the fusion line at small amounts of crack growth was not observed in the work performed in this effort. A contributing factor may be the direction of crack growth in the SEN(T) versus C(T) specimens. In the C(T) tests performed in this effort, the crack is growing as a through-wall crack parallel to the weld; whereas, for the past SEN(T) specimens, the crack was growing as a surface crack. Conducting tests in the through-thickness or radial direction with SEN(T) or bend-bar specimens might help to clarify this discrepancy.

Dynamic Strain Aging Evaluations

The incentive for this particular task in the Short Cracks Program was the NRC's concern over the occurrence of unstable crack jumps, see Figure 7, in ferritic nuclear pipe tests at LWR temperatures, and their potential effect on Leak-Before-Break (LBB) and in-service flaw evaluation criteria. Such instabilities had been observed previously in the NRC's Degraded Piping Program[7] and the International Piping Integrity Research Group (IPIRG) program[8]. The overall objective of this task was to predict the occurrence of and evaluate the effects of

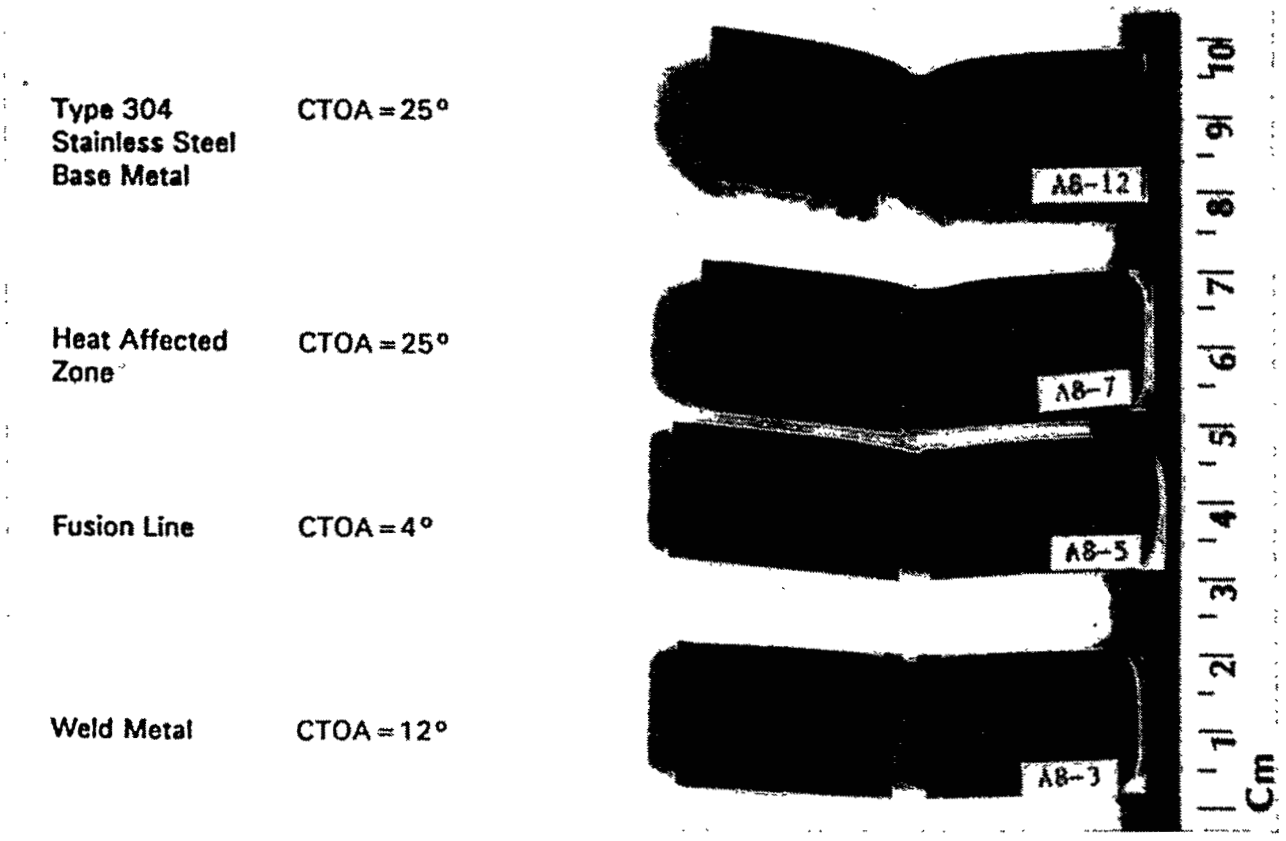

Figure 6. Crack propagation in base metal, HAZ remote from fusion line, and weld metal in single-edge notch tension specimens at 288 C (550 F)

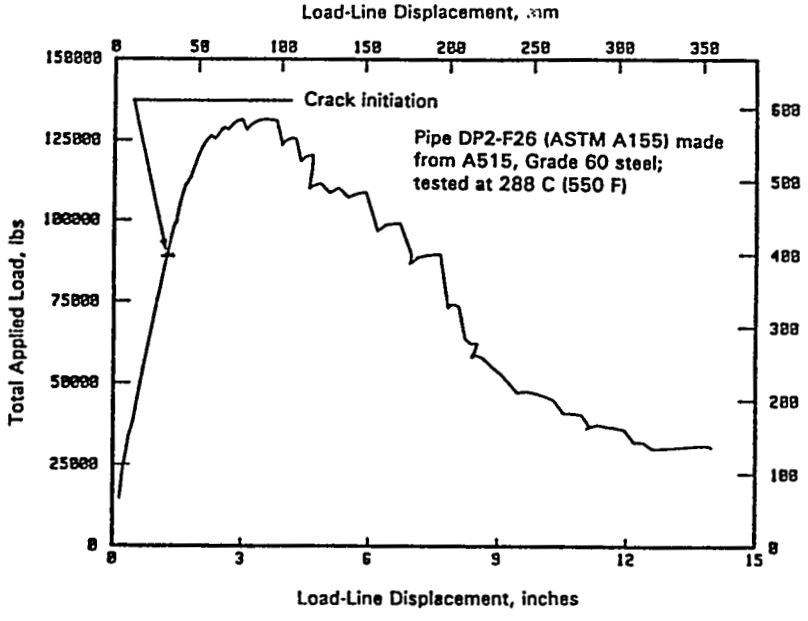

Figure 7. Load-displacement record from a full-scale pipe test from the Degraded Piping program (Experiment No. 4111-2) to illustrate crack instabilities at 288 C (550 F)

these ductile crack instabilities. These instabilities are believed to be due to dynamic strain aging (DSA), on flawed nuclear carbon-steel piping. DSA is a phenomenon observed in many carbon steels at light-water reactor operating temperatures. It involves interactions between highly mobile nitrogen and carbon atoms dissolved in the steel and moving dislocations associated with plastic strain. At certain combinations of strain rate and temperature, these interactions can lower the crack-growth resistance and can cause a stably growing crack to become temporarily unstable, i.e., to jump. Specific objectives of this study were to: (1) establish a simple screening criterion to predict which ferritic steels may be susceptible to crack jumps, and (2) evaluate the ability of current J-based analysis methodologies to assess the effect of crack instabilities on the fracture behavior of ferritic steel pipe.

Regarding the establishment of a screening criterion, laboratory tests were conducted on specimens machined from four carbon steel pipes. The carbon steel pipe materials evaluated included ASTM A333 Grade 6, A515 Grade 60, A106 Grade B, and a submerged-arc girth weld in an ASTM A106 Grade B pipe. Earlier work within the NRC's Degraded Piping Program[7] had indicated that these materials represented a range of susceptibilities to DSA and to crack instabilities. An A516 Grade 70 steel was also found susceptible to DSA in the Degraded Piping Program[7], but was not included in this study. The tests in this study included tensile and Brinell hardness tests conducted over a range of temperatures to evaluate the susceptibility of each material to DSA, and companion fracture toughness tests using compact specimens over a range of temperatures to see whether a material's propensity for crack instabilities could be correlated with its susceptibility to DSA. Additionally, experiments were conducted to ascertain the reproducibility of crack jumps in replicate tests on a single material. Finally, crack jump behavior in compact specimens was compared with that in full-scale pipe fracture experiments for a number of different pipes from both the Short Cracks and Degraded Piping Programs.

The laboratory tests revealed that steels susceptible to DSA exhibit a peak in both the ultimate tensile strength (UTS) and Brinell hardness number (BHN) at temperatures near the operating temperatures of light-water reactors, see Figure 8. The peak occurred at a higher temperature in the Brinell tests than in the quasi-static tensile tests. This is because the strain rate in the Brinell hardness test is approximately two orders of magnitude greater than in the tensile test and DSA is a rate-sensitive phenomenon. The ratio of maximum-to-minimum values in the strength or hardness curves provides a useful, though not completely reliable, measure of a steel's propensity for crack jumps. Hardness tests, because they are simpler and less costly to perform than tensile tests, and because they could be used to assess piping in situ or as a mill quality control test, are preferred over tensile tests for estimating susceptibility to crack jumps of both existing and future piping. Examination of both the laboratory specimen fracture data and the full-scale pipe test data indicated that the DSA-induced crack jumps are random in nature. As such, the prediction of the occurrence of DSA-induced crack jumps and their effect on toughness in pipe tests from simpler laboratory tests will require the accumulation of more extensive data than are now available. In the interim, steels that test positive for crack jumps in the laboratory screening tests should be used with caution since some very large crack jumps have occurred in pipe experiments using these steels.

Additionally, a review of data developed from the IPIRG-1 and IPIRG-2 programs[8] showed that changing the strain rate from quasi-static loading to rates comparable to seismic loading at 288 C (550 F) can have a significant effect on tensile strength and fracture toughness of ferritic steels. Some ferritic steel-base metals had a loss of both strength and toughness at seismic rates, see Figure 9, while one ferritic weld showed a significant increase in toughness at seismic rates. The different behaviors at 288 C (550 F) were shown to be due to DSA sensitivity over different temperature ranges for these base and weld metals. It may be possible to relate this drop in apparent resistance to the Brinell hardness number. Figure 10 shows a plot of the carbon steel C(T) data taken during the Short Cracks, IPIRG-1 and IPIRG-2 programs. This figure shows the relative change in fracture resistance due to an increased loading rate as a function of the change in the Brinell hardness number with increasing temperature. Clearly, as the Brinell harness ratio becomes greater than unity, the fracture resistance at seismic loading rates decreases rapidly. Note, this conclusion is based on the limited data shown in Figure 10. More toughness data needs to be generated before a clear trend can be identified.

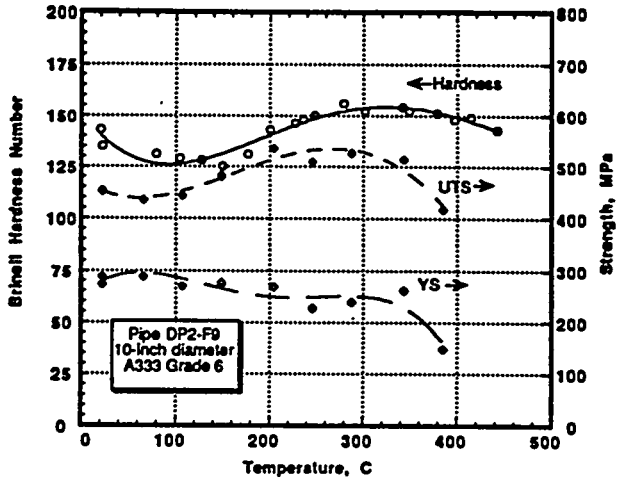

Figure 8. Yield strength, ultimate tensile strength, and Brinell hardness as functions of test temperature for an A333Gr6 carbon steel

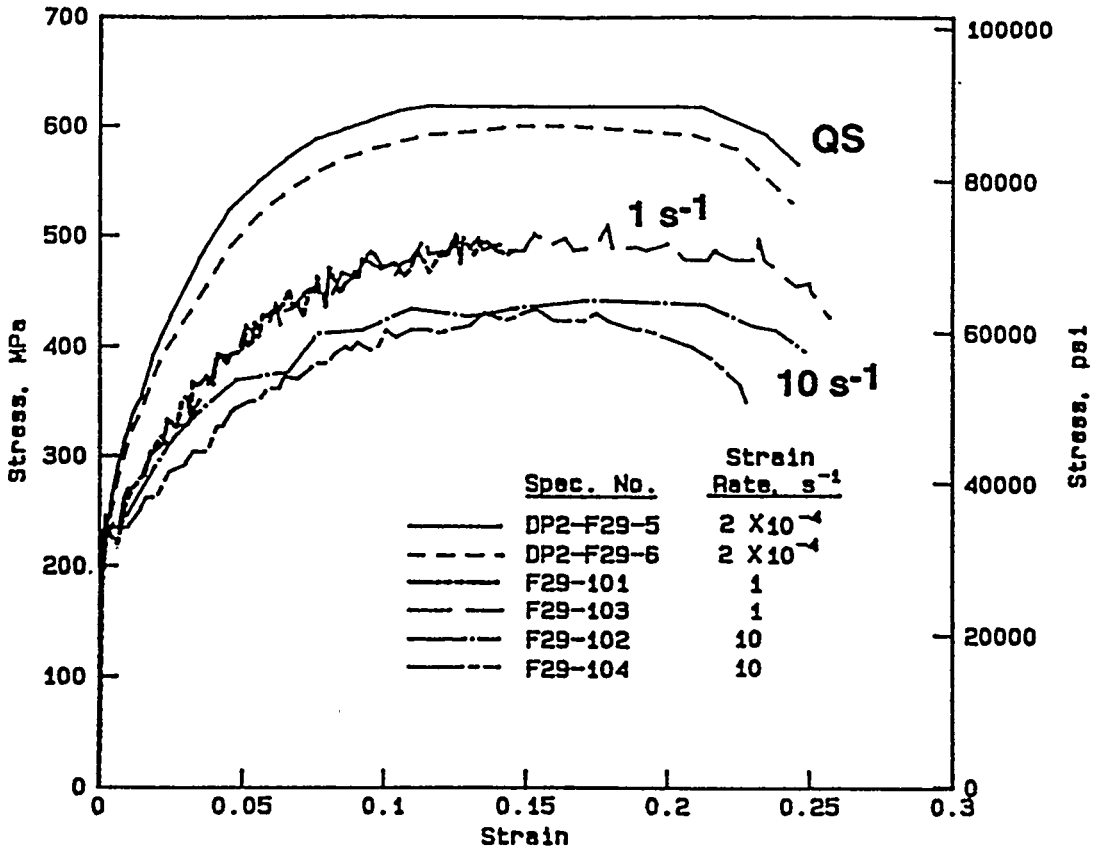

Figure 9a. Engineering stress-strain curves at 288 C (550 F) for Pipe DP2-F29 (A106 Grade B carbon steel) tested at several different strain rates

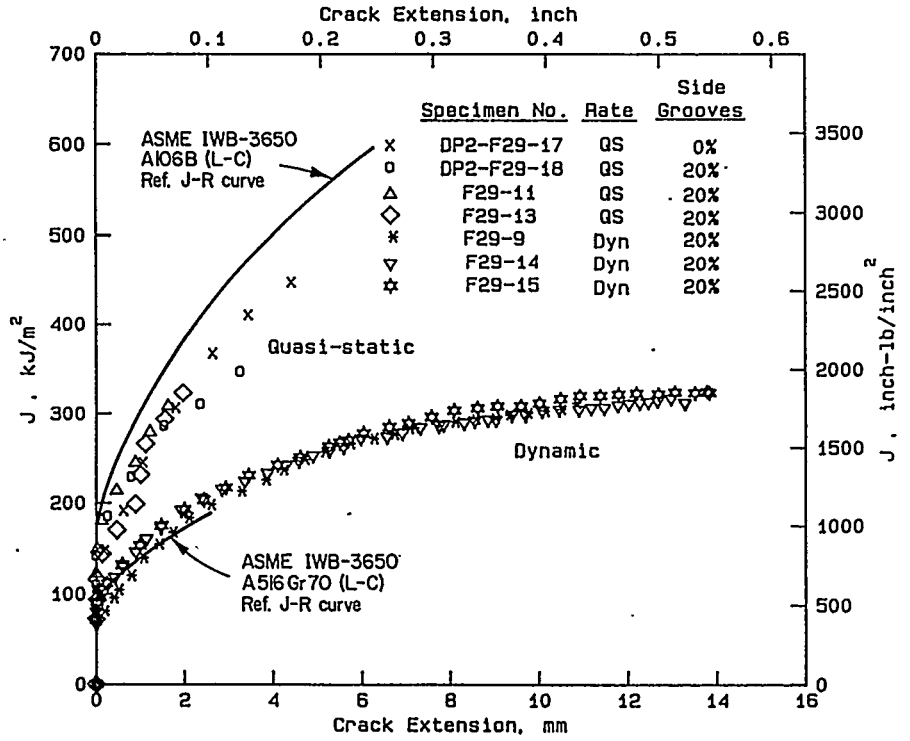

Figure 9b. **J-resistance curves for compact specimens from Pipe DP2-F29 (A106 Grade B carbon steel) tested at 288 C (550 F)**

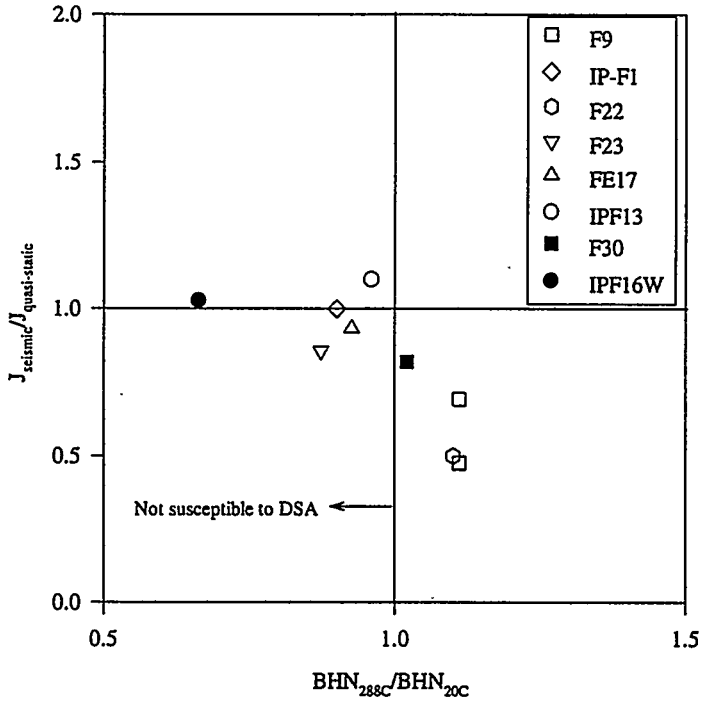

Figure 10. **Relative change in fracture resistance at seismic loading rates versus relative change in Brinell hardness number at PWR temperatures**

The analysis efforts were directed at studying the crack tip fields in a C(T) specimen before, during, and after a crack jump event caused by DSA. Finite element (FE) analysis of one C(T) specimen was conducted using the experimental load-line displacement and crack growth data as input values. The loads as well as the values of J were then computed during the analysis. The predicted loads were in excellent agreement with the experimentally measured values for the plane strain analysis. The J-integral values along far-field paths calculated using domain-integral method agreed well with the corresponding values calculated using standard ASTM procedures, but only up to crack growth of 5.5 percent of the original uncracked ligament. For crack growth amounts beyond this point, significant deviation between the values calculated using the two methods was observed. This was consistent with results from past FEM analyses by other researchers. Also, the values of J decreased just prior to the crack jump. These discrepancies are attributed to the decrease in the elastic strain energy which overrides the contribution from the plastic dissipation. The crack opening profile from the FE results showed that the crack blunts upon the unstable jump and subsequently resharpens.

A comparison between the FE results, experimental data and fractographic examinations suggests that even though the crack jumps are apparently random, stress triaxiality ahead of a stable crack is a necessary condition for crack jumps to occur in a material susceptible to DSA. However, further work is needed to substantiate this observation.

REFERENCES

1. "Short Cracks in Piping and Piping Welds," Seventh Program Report, NUREG/CR-4599, Vol. 4, No. 1, April 1995.

2. "Assessment of Short Through-Wall-Circumferential Cracks in Pipes," NUREG/CR-6235, April 1995.

3. "Fracture Behavior of Short Circumferentially Surface-Cracked Pipe," NUREG/CR-6298, submitted for publication August 1995.

4. "Fracture Evaluations of Fusion-Line Cracks in Nuclear Pipe Bimetallic Welds," NUREG/CR-6297, April 1995.

5. "Stainless Steel Submerged Toughness Arc Weld," NUREG/CR-6251, April 1995.

6. "Effect of Dynamic Strain Aging on the Strength and Toughness of Nuclear Ferritic Piping at LWR Temperatures," NUREG/CR-6226, October 1994.

7. "Degraded Piping Program - Phase II, Semiannual Report, NUREG/CR-4082, Vol. 8, March 1989.

8. "Loading Rate Effects on Strength and Fracture Toughness of Pipe Steels Used in Task 1 of the IPIRG Program," Topical Report, NUREG/CR-6098, October 1993.

LEAK DETECTION/VERIFICATION

Vl. Krhounek, J. Žďárek, L. Pečínka
Nuclear Research Institute Řež, Czech Republic

The Leak Before Break (LBB) concept is one of the most important methods ensuring an extremely low probability of guillotine-break of pipes. The LBB statute guarantees that for a loss of coolant less than the nominal, there is a probability of large LOCA 10^{-6}/reactor year.

Within the framework of the LBB project the loss of coolant experiments were performed in the State Machinery Research Institute Běchovice (SVÚSS). The aim of these experiments was to postulate the leak rates of the coolant. In the water loop it was possible to perform experiments under coolant pressure up to 19.7 MPa and temperatures up to 350°C. The circulation pump ensured a mass flow rate in the pipe up to 50 m^3h^{-1}. The functional scheme of the experimental set up is seen in Fig. 1. The experiments with leak rate 10 litres per minute were performed.

The experimental specimens were prepared from pipes with diameters in the range from 89 mm to 219 mm and 6 m in length. The through-wall cracks were introduced in the pipe by fatigue cycling. The test specimen was located in the experimental part of the water loop. A hydraulic loading device was placed underneath the through-wall crack and various crack openings were imposed. The leak of coolant in the form of steam water mixture was passed through a condenser chamber where the steam phase of leak was condensed. The quantity of water was measured.

During the experiment the following measurements were performed:

1. Pressure and temperature of the coolant in the experimental part of the water loop
2. Quantity of the lost coolant
3. Displacement of a specimen
4. Acoustic emission

After each experiment the specimen was fractured and the shape of the crack and the surface roughness were determined. The crack opening was calculated from the known geometrical data of the crack. The leak rate of the coolant was determined by means of the LEAKH code and results were compared with measured data.

The following results were obtained:

1. Small cracks were plugged with particles being available within the coolant. In large-crack experiments the influence of plugging was much smaller, probably in dependence on the maximum dimension of particles in the coolant. The size of particles found in the coolant within the experimental loop ranged up to 20μm. It is believed that the plugging will have no effect in the cracks for which the leak rates above 35 litres per minute are assumed according to safety assessments.
2. Taking into account the fact that the crack shape is very complicated the re-calculation of a crack opening is necessary. The calculations were performed by the PICEP code and new computations will be carried out using a finite element method.
3. The leak rate safety margin of 10 is sufficient for cracks in which the leak rate is more than 5 litres per minute.

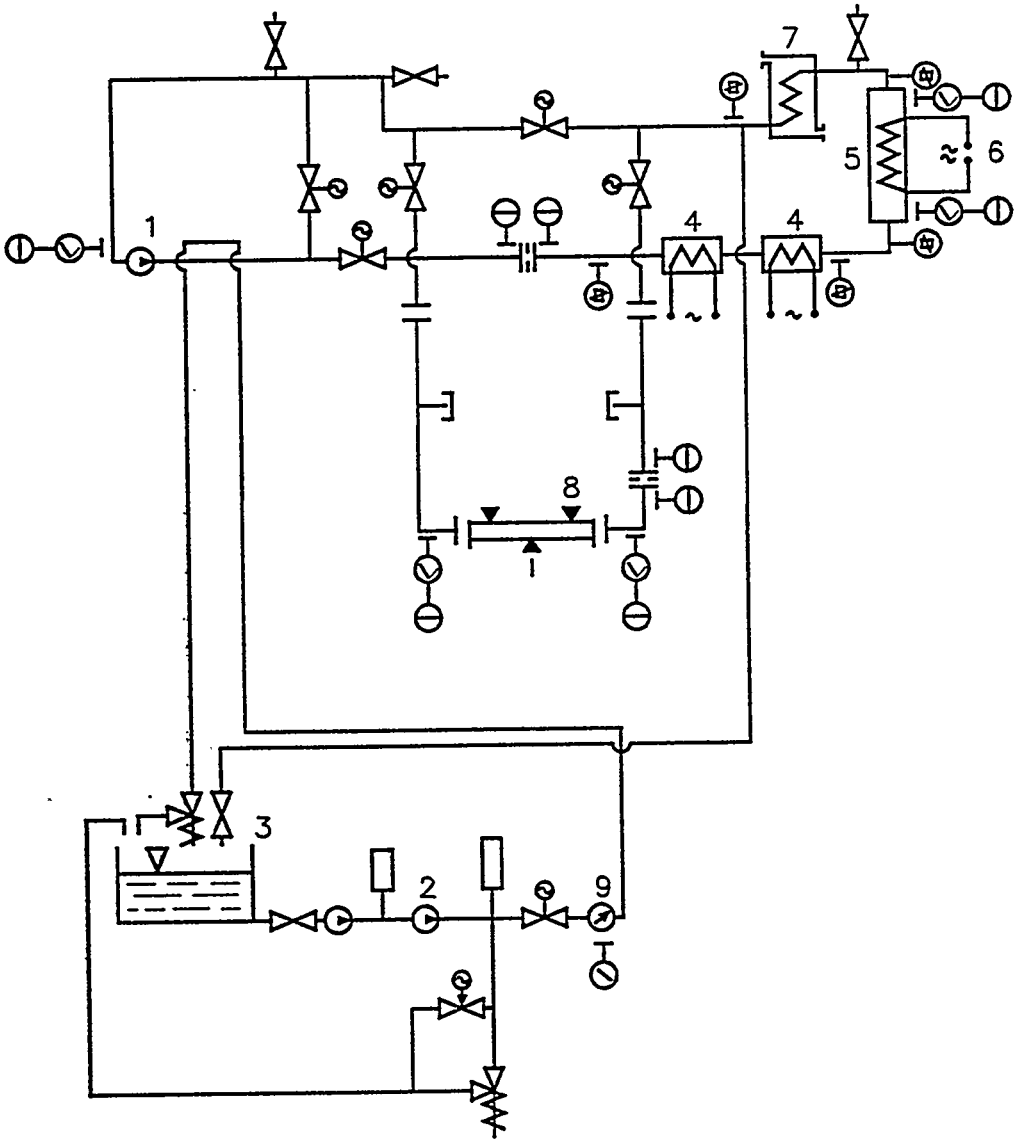

1 – circulating pump
2 – plunger pump
3 – water supply tank
4 – heat exchanger
5 – heat exchanger (main)
6 – constant power supply
7 – air condenser
8 – tube with TWC
9 – turbine flowmeter

– thermocouple

– pressure sensor

– turbine flowmeter

– resistent thermometer

Fig. 1

THE "LEAK-BEFORE-BREAK" APPLICABILITY IN DECISION SUPPORT SYSTEM "STRENGTH"

Torop V. M. [*], Orynyak I. V. [*] and Kutovoy O. L. [**]
[*] Institute for Problems of Strength, 252014 Kiev, Ukraine
[**] Institute of Structure Integrity, Aquilon-Ukraine Corporation, Kiev, Ukraine

INTRODUCTION

Serviceability of NPP's pressure vessels and pipelines, as well as their service conditions are characterized by a big quantity of parameters which can vary in time. Today the trend in collecting information at NPPs implies, in addition to standard data transmitters, the use of automated strain measuring and diagnostic systems operating in the "on-line" regime. Furthermore, periodic non-destructive inspections of NPP pressure vessel and pipeline metal and welded joints are performed. The accumulated data arrays have to be processed in the context of the concepts of safety which either exclude failure of NPP critical equipment and pipelines, or substantiate local character of consequences of such failure. For this reason, the solution of the problem of safe operation of NPP pressure vessels and pipelines, which requires the knowledge of many different disciplines and solving the problems in real time, came to be basically possible with the utilization of computer systems of artificial intelligence. The knowledge accumulated in various fields of activities of men can be formalized to the level of specific problems solution algorithms, whereas high-speed processors allow the solutions to be obtained in real time considering varying factors and operating on vast data arrays.

A software complex (SC) "STRENGTH" has been developed at the Institute for Problems of Strength of the National Academy of Sciences of Ukraine which is oriented to solve the above problems in the regime of the decision support system.

We shall demonstrate how the concept of "leak-before-break" safety has been realized in the computer decision support system "STRENGTH".

METHODOLOGICAL BACKGROUND OF THE "LEAK-BEFORE-BREAK" SAFETY CONCEPT

The postulate of the "leak-before-break" safety concept which we use says: "Surface and part-through defects, which can be detected in NPP pipelines or pressure vessels by non-destructive inspection, should not be critical (i. e. should not cause a supercritical crack growth) under normal service conditions and / or when the latter are upset, and when their fatigue or corrosion-fatigue extension leads to the formation and stable growth of a through crack with a 100 % possibility to detect the outflow of a coolant through it".

Since pipelines and pressure vessels of most NPPs were designed without considering the concept "leak-before-break", the first stage of solving the problem involves the analysis of the operating pipelines and pressure vessels in terms of the above postulate. For the pipelines and pressure vessels which do not meet the requirements of the "leak-before-break" concept postulate, we locate dangerous sections and define critical size of surface, part-through and through defects capable of initiating brittle, mixed-mode or ductile fracture. Since multioptional computations of current loading parameters for different types of defects, and of varying properties of the metal and welded joints are required, the software complex "STRENGTH" has to be used. Owing to the fact that service regimes for NPP

pipelines and pressure vessels are rigidly regimented, SC "STRENGTH" can be used with the files of stress-strain state computed earlier for normal service conditions and for the upset ones. In order to reduce the amount of computations for obtaining current values of the stress intensity factors, the SC "STRENGTH" employs the weight function method [1-4], whereas for the computation of ductile fracture limit load it employs the fracture models for a pipe with an axial surface crack [5, 6], with an axial through crack [7], with a crack in the connection zone [8], for a pipe with a surface defect [9].

The P_{LL} value describes the limit load level. To define current loading conditions in terms of ductile failure criteria it is helpful to use the notion of reference stresses introduced by Ainsworth [10].

$$\sigma_r = \sigma_u \frac{P}{P_{LL}} = \sigma_u S_r \tag{1}$$

where σ_u is the ultimate strength of the material. σ_r can be also defined using another procedure which does not require a formal usage of the ultimate strength and yields identical σ_r values. It is described elsewhere [9]. There σ_r is the imaginary thought-for ultimate strength at which a body with a specified system of external loads is in the ultimate state.

Thus, NPP pipelines and pressure vessels are separated into those which fit the aforementioned postulate of the "leak-before-break" concept and those which do not. For each group recommendations are elaborated for keeping track of their serviceability.

In the second stage of the use of the "leak-before-break" concept, specific defects detected by the NDT instrumentation in NPP pipelines and pressure vessels are analyzed. The analysis is based on the two-criteria approach devised by the authors [11, 12] and on the classification of defects by the degree of their danger developed on its basis.

The degree of the defect danger is characterized by the mode of possible failure (brittle, mixed-mode or ductile) and by a real safety factor, whose magnitude depends on the defect dimensions (considering its orientation and location), geometrical parameters of the object, mechanical properties and characteristics of the material or welded joint and loading conditions (external loading factors). Therefore, a correct classification of defects by the degree of their danger should take into account at least four groups of factors which characterize the defect, the object, the properties and loads [13]. Other factors, such as the influence of the environment, loading rate, service temperature, fluence, etc. are considered by dependences, e. g. by the dependence of mechanical properties and fracture toughness characteristics of materials upon the above parameters or by the dependence of current (computed) loading parameters, e. g. stresses or stress intensity factors, upon the load application rate, etc.

An important place in the classification of defects and in the construction of computation schemes belongs to the problems of schematization. The basis of schematization is the principle of a conservative estimate which results in that the lack of knowledge leads to an increase of a safety factor. In accordance with this principle, the minimum values of mechanical properties and fracture toughness characteristics of metals and their welded joints are used in the computations; in the case of brittle fracture three-dimensional defects are substituted by crack-like ones. Schematization of defects involves not only bringing them to canonical types for which the solutions are available, but also implies that the propagation of schematized defects represents most closely the growth of real defects. For example, the use of stable modes of fatigue crack growth [14] for the prediction of real crack behaviour is an illustration of the above statement.

Schematization of structural elements involves the rules of strength of materials discipline, wherein structural elements are interpreted as beams, cylinders, frames, etc. Specific rules are used to interprete load signals from pipelines and pressure vessels coming on-line from strain-measuring systems.

A two-criteria fracture assessment diagram presented schematically in Fig. 1 and proposed earlier in [11-13] is an illustration of a possible classification of defects by the degree of their danger which takes into account the four groups of factors mentioned above.

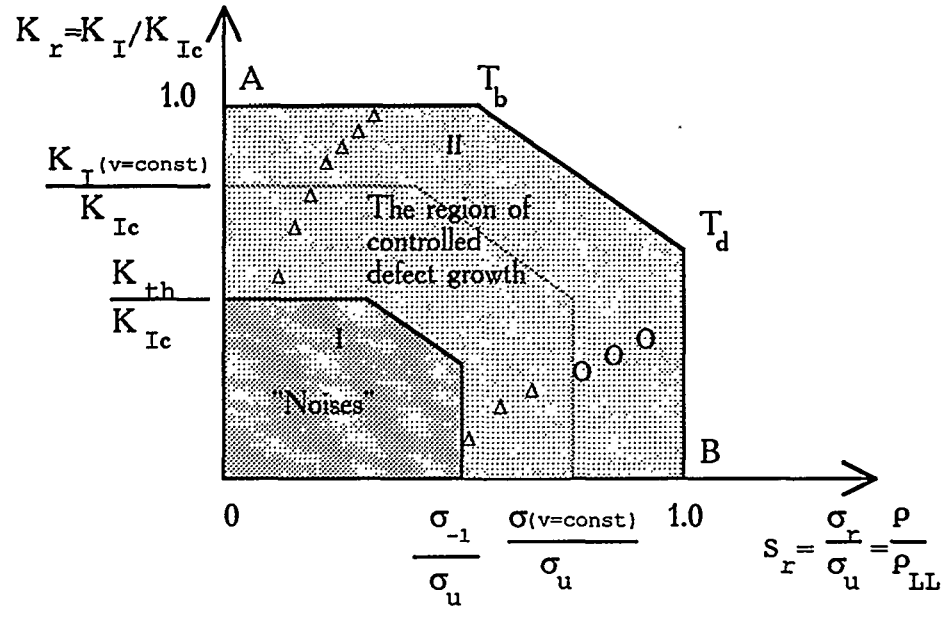

Fig 1 The use of a fracture assessment diagram to classify defects by the degree of their danger.
Δ = surface or part-through defect; O = through-the-thickness defect

Here K_{th} is the threshold value of the current (calculated) fracture mechanics parameter, σ_{-1} is the material fatigue limit. These parameters are related to the beginning of subcritical growth of a crack-like defect. K_I ($v = const$) is a characteristic value of the stress intensity factor for a specified propagation rate v of a crack-like defect, σ_r ($v = const$) is the value of the reference stress at a specified rate $v = const$ of the defect growth in a cycle, K_{Ic} is the critical value of the material static fracture toughness, P_{LL} is the limit load of ductile fracture, T_b is the critical temperature of the brittle-to-mixed mode fracture transition, T_d is the critical temperature of the mixed-to-ductile fracture transition.

The ordinate axis K_r (K_I / K_{Ic}) of the fracture assessment diagram (Fig. 1) involves the criteria of the linear elastic fracture mechanics, while the abscissa axis S_r (P / P_{LL}) involves those of the ultimate plastic state.

Thus, three characteristic regions can be distinguished on the fracture assessment diagram (Fig. 1) for which it is possible to arrange three characteristic classes of defects. We shall designate region I as "noise" since it is bounded by the limit curve $K_{th}/K_{Ic} = f(\sigma_{-1}/\sigma_u)$. This means that the defects located within region I will not grow under the given conditions.

Region II is the region of controlled (subcritical) growth of defects. In this region one can construct limit curves which characterize the growth of crack-like defects at the rate $v = const$. The limit curve (A-T_b-T_d-B) corresponds to the transition from the region of the controlled growth of defects to the region of their supercritical growth. In this case if part-through or surface defects in region II extend to become through ones, whose stable growth can be

detected by the coolant outflow facilities until they intersect the limit curve (A-T_b-T_d-B), they are classified as "leak-defects". Otherwise the defects are referred to "break-defects".

REALIZATION OF THE "LEAK-BEFORE-BREAK" CONCEPT IN THE DECISION SUPPORT SYSTEM "STRENGTH"

Decision support system (DSS) [15, 16] has been developed for strength accompaniment of safe operation of pressure vessels, pipelines, storage tanks and other structural elements during their life cycle (beginning with engineering design and ending with taking a decision to remove them from service), including the cases when defects of different origin are detected. Its structure and functions are presented in a block diagram of Fig. 2.

Basic principles of the DSS "STRENGTH" functioning afford structural strength assessment and life prediction for a defect-free or defected structural element taking into account the diversity of service conditions. Strength accompaniment of the diagnostics object has been oriented to multilevel representation of the life cycle of the defect growth from its nucleation to the assessment of consequences of possible failure caused by the growth of this defect.

The software complex offers the following possibilities:

- solving the problems on the assessment of structural strength, predicting residual service life, defect nucleation and growth kinetics, scheduling the inspection and maintenance intervals;
- giving recommendations to the users as to the choice of materials, the limiting allowable defect sizes, the parameters of hydraulic testing and hydrostatic prestressing, the choice of rational service regimes, scheduling of the inspection intervals, the time and methods of load-carrying capacity recovery for a structural element with defects.

The software complex is intended for use by the organizations engaged in designing, assembling and operation.

The SC "STRENGTH" is designed to be used in a stand-alone regime and / or as a part of the automated expert diagnostics system. The SC structure incorporates three blocks:

1. The "Information model of the diagnostics object" data-base management system (DBMS) intended for the data-base updating:
   - The "Objects" data-base which stores information on geometrical dimensions and attitude of structural elements;
   - The "Defects" data-base containing information on the detected defects (their geometry, orientation and location site);
   - The "Loads" data-base which stores information on external loading factors;
   - The "Properties" data-base containing information on mechanical properties and fracture toughness characteristics of materials and their welded joints under real service conditions, environment, temperature, loading rates.
   -

The "information model of the diagnostics object" DBMS has been organized in such a way as to afford the simplicity of the data input and on-line access to all the information and the possibility of its presentation in the most convenient and clear form.

2. The "Computation modules" consisting of the software packages:
   - computation of the stress-strain state, stability and strength assessment in terms of allowable stresses (according to the National standard documents ASME code, R6, etc.);
   - calculation of the stress intensity factors by the weight function method;

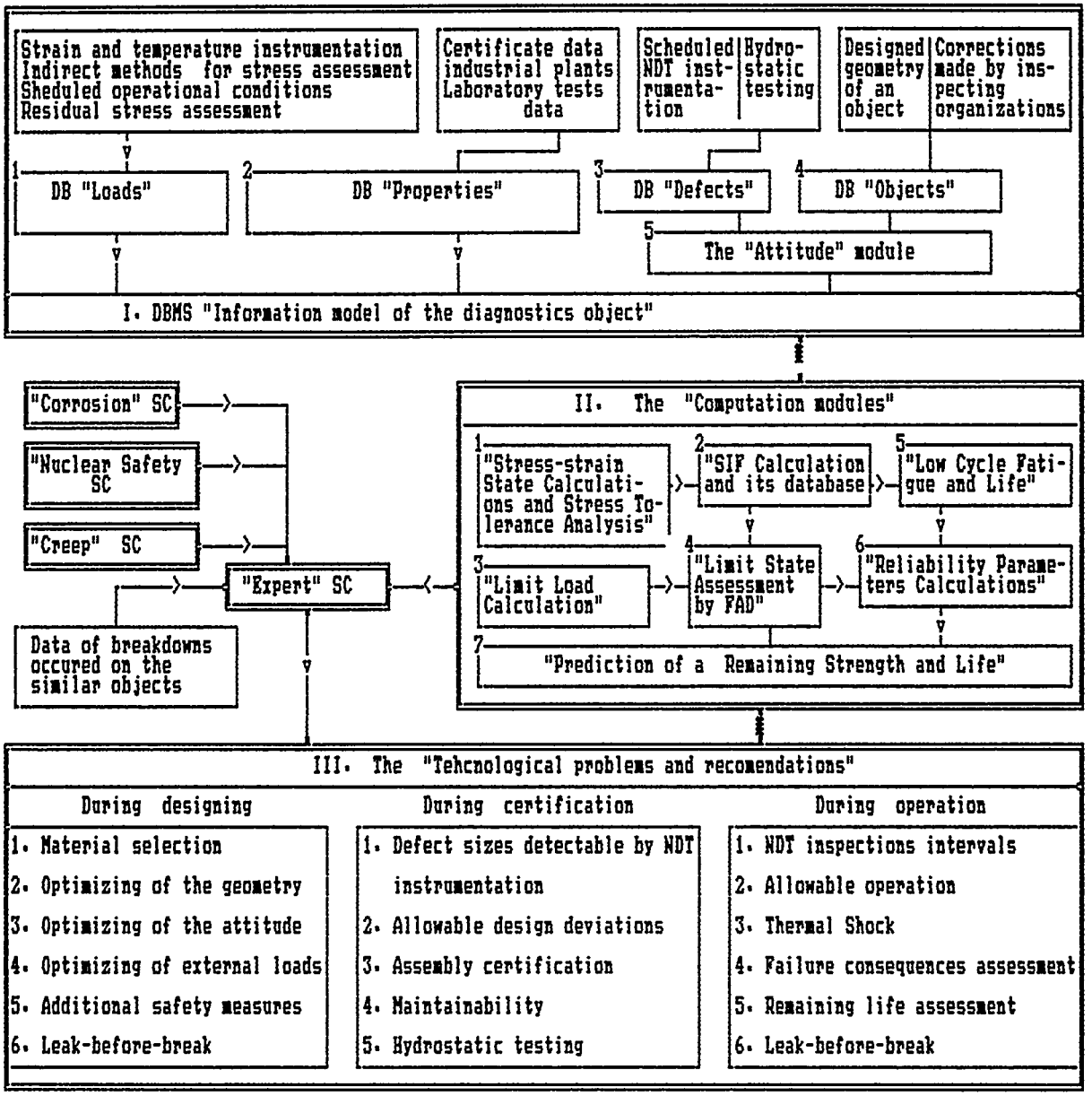

Fig. 2 Operational scheme of the Decision Support System "Strength".

- calculation of the ductile fracture limit load;
- two-criteria failure diagram;
- evaluation of strength under low-cycle loading and calculation of lifetime to crack nucleation;
- evaluation of lifetime for structural elements with crack-like defects;
- reliability and probabilistic aspect of failure.

The main requirement imposed on the computation modules is reliability and high-speed solution of problems.

The third block is "Technological problems and recommendations".

The owners of equipment and engineering and technical staff, who operate this equipment, need a system for the support of decisions on strength important for safe operation, timely repair or replacement of the equipment. For this reason, even the names of such technological problems as "Prestressing", "Prestressing terms", "NDT inspection intervals", "Maintainability", "Thermal shock" are self-explanatory. The solution of the problem "leak-before-break" described above also refers to technological problems. Algorithms of their solutions are based on the aforementioned blocks (the DBMS "Information model of the diagnostics object" and "Computation modules") not only because of multioptional cumbersome computations, but also because initial information on serviceability and technological features of the processes occurring in NPP pipelines and pressure vessels considered should be arranged according to certain laws.

REFERENCES

1. Orynyak I. V. Constructing the weight function for flat solids with cracks. Problemy Prochnosti. No. 8 (1990) 10-14 (in Russian)
2. Orynyak I. V., Borodii M. V. and Torop V. M. Approximate construction of a weight function for quarter-elliptical, semi-elliptical and elliptical cracks subjected to normal stresses. Eng. Fract. Mech. vol. 49, No 1 (1994) 143-151
3. Orynyak I. V. and Borodii M. V. Point weight function method application for semi-elliptical mode I cracks. Intern. J. Fract. vol. 70 (1995) 117-124
4. Orynyak I. V. and Borodii M. V. The combined weight function method application for a hole emanated crack . Eng. Fract. Mech. vol. 48, No 6 (1994) 891-894
5. Krasowsky A. Ya., Orynyak I. V. and Torop V. M. Brittle fracture of the internally pressurized cylinders with axial cracks. Strength of Mater. No 2 (1990) 16-20
6. Orynyak I. V. and Borodii M. V. A ductile fracture model for a pipe with an axial surface crack. Eng. Fract. Mech. vol. 49, No 2 (1994) 287-294
7. Orynyak I. V. and Torop V. M. The ultimate ductile state models for a pipe with an axial through crack. Intern. J. Fract. (in press)
8. Orynyak I. V. and Torop V. M. Ductile failure of a thin-walled nozzle with an axial crack. Problemy mashinostroeniya i nadeznosti mashyn (in press) (in Russian)
9. Orynyak I. V., Torop V. M. and Borodii M. V. Ductile failure of pipe with a part-through slot. Intern. J. Pres. Ves. and Piping 63 (1995)
10. Ainsworth R. A. The assessment of defects in structures of strain hardening material. Eng. Fract. Mech. 19 (1984) 633-642
11. Torop V. M. and Orynyak I. V. The evaluation of the structural strength of pipes and pressure vessels with axial cracks // Intern. J. Pres. Ves. and Piping. vol. 53 (1993) 159-180
12. Krasowsky A. Ya., Orynyak I. V. and Torop V. M. The assessment of the limit state and the transition temperatures in hollow cylinders with axial cracks. Intern. J. Fract. vol. 61 (1993) R55-R59

13. A. Ya. Krasowsky, I. V. Orynyak, S. V. Romanov and V. M. Torop. Assessment of strength and life of pipes and pressure vessels by an expert system. "Materials science problems by production and operation of NPP facilities" - St. Petersburg, Russia, vol. 1 (1992) 255-262
14. Jolles M., Tortoriello V. Effects of constraint variation on the fatigue growth of surface flaws. Fracture mechanics: Fifteenth symposium ASTM (STP 833), Ph. (1984) 300-311
15. V. M. Torop, A. Ya. Krasowsky, S. V. Romanov, I. V. Orynyak. Methodological background for strength accompaniment of craced structures safe operation. Institute for Problems of Strength, National Academy of Sciences of Ukraine. Preprint. Kiev, (1993).
16. Torop V. M., Orynyak I. V., Panchenko V. P. Software complex "Strength" of the diagnostic system. Intern. J. Pres. Ves. and Piping. (1995) (to be published).

APPLICATION OF LBB TO HIGH ENERGY PIPING SYSTEMS IN OPERATING PWR

S. A. Swamy, D. C. Bhowmick, Westinghouse
Nuclear Technology Division, Pittsburgh, PA, U.S.A.

Abstract

The amendment to General Design Criterion 4 allows exclusion [1], from the design basis, of dynamic effects associated with high energy pipe rupture by application of leak-before-break (LBB) technology. This new approach has resulted in substantial financial savings to utilities when applied to the Pressurized Water Reactor (PWR) primary loop piping and auxiliary piping systems made of stainless steel material. To date majority of applications pertain to piping systems in operating plants. Various steps of evaluation associated with the LBB application to an operating plant are described in this paper.

1.0 INTRODUCTION

General Design Criterion 4 (GDC-4), "Environmental and dynamic effects design bases," requires the consideration of the dynamic effects of postulated loss-of-coolant accidents, including missiles, pipe whipping, and discharging fluids. In October 1987, the NRC revised GDC-4 (via the broad scope final rule, 52FR41288) to allow the use of Leak-Before-Break (LBB) concepts to exclude the dynamic effects of postulated pipe ruptures from the design basis of certain plant structures. The LBB technology has been used since 1978 to justify elimination of postulating pipe breaks in high energy piping systems in pressurized water reactors (PWR). Use of LBB technology saved substantial backfit costs to many operating plants. Application of this technology to plants under construction also results in significant cost savings due to substantial reduction of whip restraints, jet shields, and associated analysis and documentation. Added cost savings result due to reduced man-rem exposure during inservice inspection and maintenance. Improved inspection reliability is achieved due to less clutter and better accessibility of inspection area. The dynamic effects resulting from pipe rupture which can be virtually excluded from the piping design basis include the following:

- Missile generation
- Pipe whipping
- Pipe break reaction force
- Jet impingement forces
- Decompression waves within the ruptured pipe
- Dynamic or nonstatic pressurization in cavities, subcompartments and compartments

The general guidelines for LBB demonstration are contained in References 1, 2 and 3. Specific requirements, criteria and associated steps of evaluation to demonstrate LBB for the Reactor Coolant System (RCS) in an operating PWR plant are summarized in this paper.

2.0 REQUIREMENTS AND CONDITIONS FOR APPLYING LBB TO OPERATING PWR PLANTS

1. The plant leak detection system must be capable of detecting 1 gpm leakage as specified in Regulatory Guide 1.45.

2. LBB should be applied to the entire piping system anchor to anchor.

3. Only high energy piping in nuclear power units is covered by the LBB acceptance criteria (P >275 psig, or T >200°F).

4. The probability of rupture of the candidate pipe should be "extremely low" (of the order of 10^{-6}).

5. The analysis must address

   - Erosion Corrosion
   - Water Hammer
   - Stress Corrosion Cracking
   - Low Cycle Fatigue
   - High Cycle Fatigue
   - Creep

6. LBB evaluation should use design basis loads and should be based on the as-built configuration.

7. There are various analytical requirements such as

   Availability of:

   - Valid Leak Rate Calculations
   - Valid Fracture Mechanics Calculations
   - Valid Approach to Address Long Terms Effects Such as Thermal Aging
   - Valid approach to incorporate the effects of thermal stratification
   - Material property data and valid correlations for strength and toughness properties of welds and base metals.

8. Assure that the material is not susceptible to cleavage-type fracture over the full range of system operating temperatures.

3.0 LBB EVALUATION STEPS

1. Calculate the applied loads. Identify the location at which the highest stress occurs.

2. Identify the materials and the associated material properties.

3. Postulate a surface flaw at the governing location. Determine fatigue crack growth. Show that a through-wall crack will not result.

4. Postulate a through-wall flaw at the governing location. The size of the flaw should be large enough so that the leakage is assured of detection with margin using the installed leak detection equipment when the pipe is subjected to normal operating loads. A margin of 10 is demonstrated between the calculated leak rate and the leak detection capability.

5. Using faulted loads, demonstrate that there is a margin of at least 2 between the leakage size flaw and the critical size flaw.

6. Review the operating history to ascertain that erosion-corrosion operating experience has indicated no particular susceptibility to failure from the effects of corrosion, water hammer or low and high cycle fatigue.

7. For the base and weld metals actually in the plant provide the material properties including toughness and tensile test data. Justify that the properties used in the evaluation are representative of the plant specific material. Evaluate long term effects such as thermal aging where applicable.

8. Demonstrate margin on applied load. The leakage size flaw should be shown to be stable for a load equal to $\sqrt{2}$ times the faulted load. Per Reference [3], this factor on load can be reduced to one if all the faulted loading components are combined based on individual absolute values.

4.0 THERMAL AGING ISSUE

In a nuclear power plant of Westinghouse design the primary piping may be forged or cast stainless steel and varies from plant to plant. The large primary loop fittings are always cast. Both forged and cast product forms exhibit exceptionally high toughness in the as-built condition; however the cast material is susceptible to thermal aging. Essentially, the fracture toughness may be significantly reduced with time at operating temperatures for the cast material. The toughness degradation in cast austenitic stainless steel has been attributed mainly to the successive precipitation of chromium in the ferrite phase due to the large miscibility gap in the Fe-Cr binary system. During aging at temperature, the ferrite phase gradually develops a cleavage transition behavior somewhat like that of ferritic stainless steel.

The thermal aging toughness degradation has only within the last decade been recognized as occurring in cast stainless steels at the operating temperatures of nuclear reactors. Useful material test data and acceptance criteria became available only recently.

The detrimental effect of thermal aging on the cast stainless steel material is shown in Figure 1 for a typical cast stainless steel material. As can be seen the initial toughness of this material measured in terms of J_{IC} drops by over 50% in 12,000 hours at typical PWR plant operating temperature. Detailed review of materials data for many heats of the cast stainless steel material indicates that the end of life fracture toughness could be reduced by over a factor of five which raises concerns about the integrity of the piping system.

The thermal aging issue has been technically addressed and the procedure currently used by the authors to address thermal aging has been approved by the U.S. NRC.

5.0 EFFECT OF THERMAL STRATIFICATION

The effect of thermal stratification phenomenon must be evaluated where applicable. For example, the pressurizer surge line in a PWR is known to be subjected to thermal stratification. Thermal stratification in the pressurizer surge line is the direct result of the difference in densities between the pressurizer water and the generally cooler RCS hot leg water. the lighter pressurizer water tends to float on the cooler heavier hot leg water (see Figure 2). The potential for stratification is increased as the difference in temperature between the pressurizer and the primary loop hot leg increases and as the insurge or outsurge flow rates decrease.

At power, when the difference in temperature between the pressurizer and the primary coolant loop hot leg is relatively small, the extent and effects of stratification have been observed to be small. However, during certain modes of plant heatup and cooldown, this difference in system temperature could be as large as 320°F, in which case the effects of stratification are significant.

The effects of stratification must be incorporated in the LBB evaluation by considering all the modes of plant operation since the stratification effects vary from mode to mode. This results in multiple LBB calculations due to variations of loads (both with respect to time and location).

6.0 DISCUSSION AND CONCLUSION

The modified GDC-4 provides the regulatory basis for eliminating postulation of breaks in high energy piping systems in a nuclear power plant. The approach, criteria and the steps of evaluation have been summarized in this paper. Phenomena such as thermal aging of austenitic stainless steels and thermal stratification have significant impacts on the integrity of the piping systems. Thermal aging reduces the toughness of the material thereby reducing the ability to withstand high magnitude of loads in the presence of flaws. Thermal stratification causes high magnitude of loads. Clearly, the thermal aging and thermal stratification effects must be evaluated and incorporated as part of the piping integrity demonstration using the LBB technology.

7.0 REFERENCES

1. Federal Register Notice, "Modification of General Design Criterion 4 Requirements for Protection Against Dynamic Effects of Postulated Pipe Rupture," Volume 52, No. 207 (41288-41295), U. S. Nuclear Regulatory Commission, October 27, 1987.

2. NUREG-1061, Volume 3, "Report of the U. S. Nuclear Regulatory Commission Piping Review Committee, Evaluation of Potential Pipe Breaks," U. S. Nuclear Regulatory Commission, November 1984.

3. Standard Review Plan 3.6.3, "Leak-Before-Break Evaluation Procedure," U. S. Nuclear Regulatory Commission, as published in the Federal Register, Volume 52, No. 167 (32626-32633) August 28, 1987.

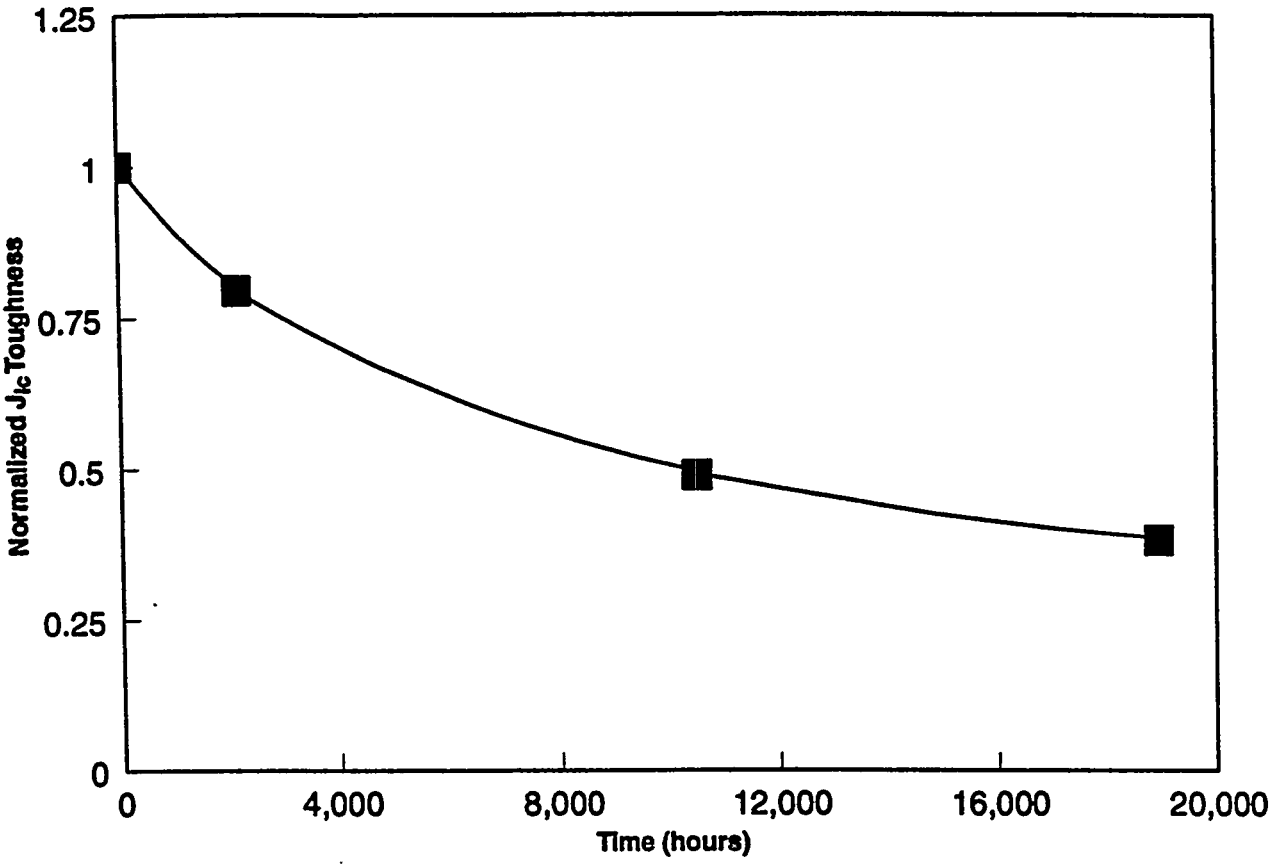

Figure 1. Typical Responses of J_{IC} to Thermal Aging

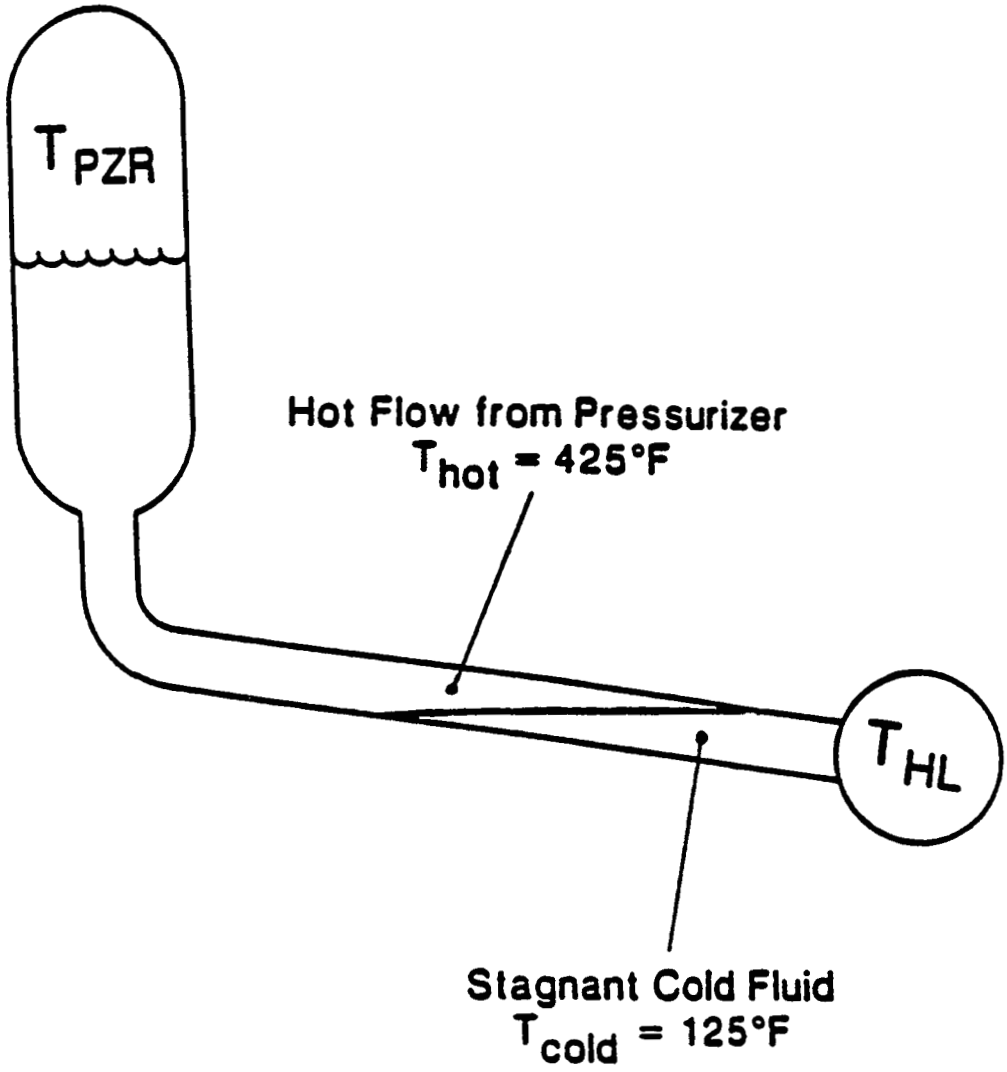

Figure 2. Thermal Stratification in Pressurizer Surge Line

A PROBABILISTIC METHOD FOR LEAK-BEFORE-BREAK ANALYSIS OF CANDU REACTOR PRESSURE TUBES[1]

M.P. Puls†, B.J.S. Wilkins†, G.L. Rigby†, J.K. Mistry# and P.J. Sedran#
†Materials and Mechanics Branch, AECL, Whiteshell Laboratories, PINAWA MB R0E 1L0 CANADA; #Reactor Engineering Services Department, AECL, Sheridan Park, MISSISSAUGA ON L5K 1B2 CANADA

1. INTRODUCTION

In the core of current CANDU®[2]reactors, cold-worked Zr-2.5Nb pressure tubes (PT's) are used to contain the fuel bundles and the Primary Heat Transport System (PHTS) fluid. At operating conditions, the PT's are subject to pressures ranging from 11 to 9 MPa and to temperatures ranging from ~250°C at the inlet to ~310°C at the outlet. Over their 30 year design life, the tubes would be subjected to a total fluence of 3 x 10^{26}n·m^{-2}, degrading their fracture toughness properties. In addition, the PT's gradually pick up deuterium as a result of a slow corrosion process, and if the hydrogen (H) plus deuterium (D) concentration were to exceed the H/D solvus, the tubes would be susceptible to a crack initiation and growth process called delayed hydride cracking (DHC). If undetected, crack growth by DHC may lead to PT rupture. Each PT is surrounded by a calandria tube which is used to separate the moderator from the PT. The annular space between the PT and the calandria tube is filled with recirculating gas. Coolant will enter the gas annulus should there be a penetration of the PT wall. The annulus gas system (AGS) is equipped with sensitive dew-point monitors to detect the presence moisture in the AGS and with 'beetle' sensors to detect liquid which may condense in the AGS. Operating procedures for responding to indications from the AGS instrumentation of a PT leak, outlined further on, are in place in all CANDU reactor stations. Once a leak has been confirmed, the procedures require a systematic shutdown/cooldown of the reactor, to minimize the risk of PT rupture. Therefore, the early detection of moisture after through-wall cracking of the PT, is essential for assuring PT rupture is avoided, which is the definition of Leak-Before-Break (LBB) [1]. LBB in PT's requires that in the event of through-wall cracking, the crack length at all times from the start of leakage to when the reactor has been shutdown to a cold and depressurized state, will be less than the critical crack length (CCL) for unstable propagation. For a given incident of through-wall cracking, an LBB analysis consists of calculating CCL as a function of PHTS pressure and temperature, and crack length, L(T,t) at discrete times, from the start of leakage at t = 0 to when the reactor is cold and depressurized. L(T,t) for double-ended crack growth is given by:

$$L(T,t) = LP + 2\int_0^t DHCV(T)\,dt \qquad (1)$$

where LP is the initial crack length at first breakthrough and DHCV(T) is the axial velocity of the crack tip, which depends strongly upon PHTS temperature. The considerable variability in the parameters of LBB analysis has led to the development of probabilistic methods of LBB analysis [2]. The BLOOM code is the latest of a series of computer programs written for the probabilistic LBB analysis of CANDU reactor PT's.

---

[1]Partially funded by the CANDU Owners Group (COG) under WPIR 2-31-6634

[2]CANDU (CANada Deuterium Uranium) is a registered trademark of Atomic Energy of Canada Ltd.

2. SEQUENCE OF EVENTS FOLLOWING LEAKAGE INTO THE AGS

The AGS is instrumented with hygrometers for the continuous monitoring of dew point temperature which, under normal PHTS operation, rises slowly as deuterium diffuses from the PHTS into the AGS. Hardware and software have been implemented for the sounding of alarms should abnormally high dew-point (or rate-of-rise) levels be detected. If a crack (length LP) were to penetrate the PT wall, PHTS vapour would leak into the AGS and the dew-point rate-of-rise would be much higher than normal. Depending on the crack location and the AGS configuration, there is a characteristic time required to produce a dew-point alarm after the crack has penetrated the tube wall. In the AGS, the fuel channel annuli are connected in series to form individual AGS strings. The PHTS vapour will condense and partially fill the fuel channel annuli in the AGS string prior to leaking into the beetle well, located at each end of the AGS strings, activating the beetle alarm. The leak rate into a collection tank located downstream of the beetle well can be measured. The amount of leakage required for a beetle alarm to sound depends on the location of the leaking PT in the AGS string and on the number of annuli comprising the AGS string. The rate at which PHTS fluid would leak into the AGS is an important parameter since it would influence the timing to a beetle alarm and the rate of collection in the beetle well. Either type of alarm can occur first. Dew-point and beetle alarms are treated independently since they are different methods of leak detection and, in general, lead to different actions.

Although procedures for responding to AGS indications are station-specific, common features are as follows. With the first indication of excessive moisture in the AGS, the operator must start activities to confirm the indication. A cold finger sample is to be taken and analyzed for percent isotopic D_2O and ^3H (tritium). If the analysis shows that the leak is from the PHTS, the reactor must be shut down to Zero Power Hot (ZPH) to commence leak rate monitoring. The reactor must be cooled down and depressurized given any of the following conditions: (1) a collection rate from the PHTS of D_2O exceeding 2 kg/h, (2) reaching a time limit after a confirmed beetle alarm or, (3) identification of the AGS string containing the leaking PT. It is possible for the beetle alarm to occur before dew-point rate-of-rise alarm indication is received. If the beetle alarm is confirmed, the reactor will be shut down to ZPH and then depressurized and cooled after a prescribed time limit. The cooldown from ZPH to the cold, depressurized state at which the crack stops growing, must follow a specific pressure/temperature path, designed to maximize, within practical limits, CCL during the cooldown. The cold

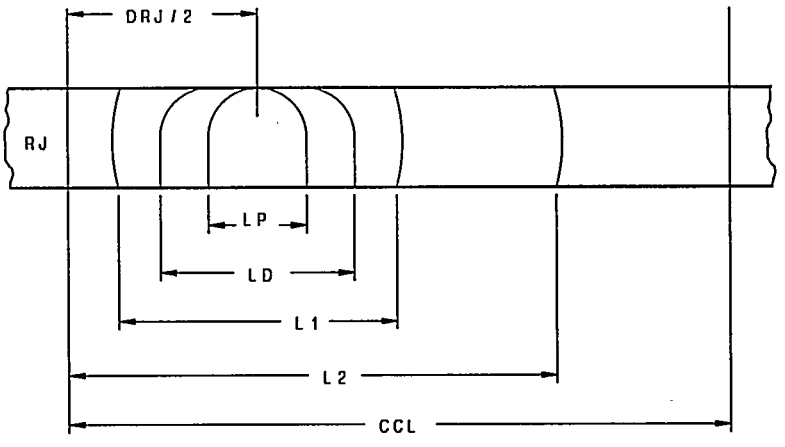

Figure 1 Cross-section of PT wall showing LBB scenario for a shutdown sequence.

depressurized state means negligible PHTS pressure (~0.2 MPa) and a temperature in the range from 50 to 40°C, depending on reactor.

A generic scenario for crack growth during the sequence of events is shown in Figure 1. It is assumed that a crack initiated at the PT inner surface has grown by DHC [3,4] in the radial-axial plane and has penetrated the tube wall (at length LP), leaking coolant, and will grow in the inboard and outboard directions. LD is the crack length at the first alarm. If crack initiation is close to a Rolled Joint (RJ), the outboard crack tip will stop at the RJ (because of compressive stresses). The inboard tip will continue to move toward the reactor core with a velocity DHCV, until either the crack becomes unstable, or the reactor is put into the cold, depressurized state and the crack stops growing. Note that between LP and DRJ, when DRJ $\leq$ LD, and between LP and LD, when DRJ $\geq$ LD, the crack grows at both ends and dL/dt = 2·DHCV; but between DRJ and LD, when DRJ $\leq$ LD, the inboard crack has stopped at the RJ and growth is single ended, so that dL/dt = DHCV.

Unstable fracture, which constitutes Break-Before-Leak (BBL), is possible before any or either of the alarms is activated and before the outboard crack tip reaches the RJ.

3. METHODOLOGY OF PROBABILISTIC LBB ANALYSIS

Since some of the main parameters of the LBB analysis, ie, CCL, DHCV and LP are distributed quantities with considerable variability, the difference between the crack length, L(T,t), at any given time from the start of the sequence of events and the CCL, which will determine whether LBB will be achieved, will vary substantially from case to case. However, in a deterministic LBB analysis, lower-bound values of CCL are compared with values of crack length, based on upper-bound values of LP and DHCV [1]. The deterministic analysis represents only one of a number of possible scenarios which can result from the occurrence of through-wall cracking of a PT. In addition, the overall probability of BBL associated with the deterministic case cannot be determined while the results of the deterministic analysis may be too conservative.

In contrast, in the probabilistic analysis, CCL, DHCV and LP are each assigned a range of possible values and specific values are selected from within this range over a number of distinct simulations (realizations) of the growth of the crack during the sequence of events. The probabilistic LBB method will predict the probability of PT rupture for the entire set of possible realizations.

The mathematics involved in a probabilistic LBB analysis have been described in [2]. Earlier codes, such as MARATHON [2], calculated the cumulative distribution function of the time to LBB, resulting in the storage of large arrays that precluded the use of a personal computer (PC). BLOOM departs from this practice. It simplifies the computation by counting cumulative ruptures at times after the start of leakage, specified by the user. This has allowed for PC-based calculations.

3.1 General Description of BLOOM

Basically, BLOOM produces a number of realizations, which are numerical simulations of crack length and CCL obtained during the sequence of events described, at discrete times after the start of leakage. BLOOM contains algorithms to account for: (1) the variation of DHCV with PHTS temperature as the PHTS is cooled, (2) the variation of CCL with PHTS temperature and pressure as the PHTS is cooled and depressurized, (3) the variation of leak rate with crack length and PHTS pressure, and (4) the variation for the time and water quantity required to set off the dew-point and beetle alarms, respectively.

All of the parameters are assumed to be normally distributed (and some vary with the coolant condition), except for DHCV which is assumed to be lognormally distributed. BLOOM was designed for Ontario Hydro's Bruce,

Darlington and Pickering reactors, but can be used to analyze any existing CANDU reactor that has characteristics similar to the foregoing ones. The users are required to specify: (1) mean and standard deviation values for LP, for DHCV at predetermined temperatures, and for CCL at predetermined temperatures and pressures in the shutdown/cooldown, and (2) AGS characteristics. For modelling the cooldown (Figure 2), from ZPH, seven times ($TM1 \le TM2 \le TM3 \le TM4 \le TM5 \le TM6 \le TM7$) at which the above CCL parameters are calculated, may be input by the user. Between certain specified times, e.g., between TM2 and TM3, coolant pressure is kept constant. Pressure changes occur abruptly at specified times, if desired.

DHCV follows an Arrhenius relationship with temperature [3,4]. In BLOOM this Arrhenius relationship is expressed as:

$$\mathrm{Log_{10}DHCV} = \mathrm{Log_{10}}\alpha + (\gamma \cdot \mathrm{Log_e}10)/T. \qquad (2)$$

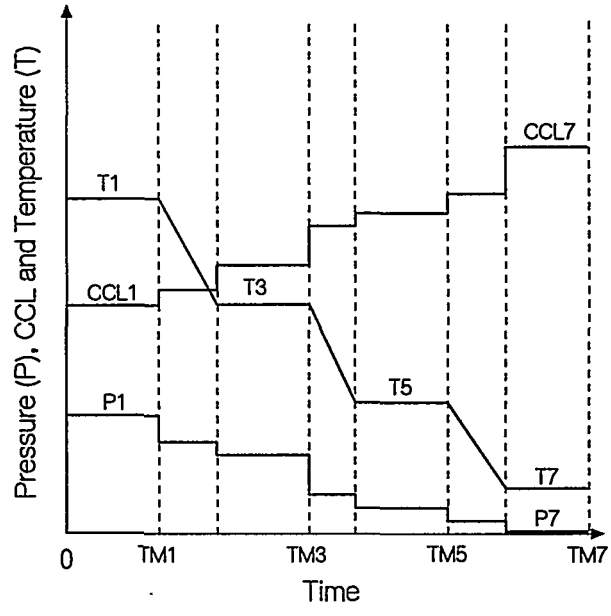

Figure 2 A possible cooldown sequence from ZPH showing how CCL could vary with time as PHTS pressure and temperature are changed.

Required input are the mean and standard deviation of $\mathrm{Log_{10}DHCV}$. T is the temperature that corresponds to the mean of $\mathrm{Log_{10}DHCV}$. Given values for $\mathrm{Log_{10}DHCV}$, $\gamma \cdot \mathrm{Log_e}10$ and T, a corresponding value for α is calculated. For a given realization, DHCV is found as a function of temperature only.

The leak rate dQ/dt is modelled as a function of L (the crack length) and the PHTS pressure, P:

$$dQ/dt = K \cdot L^m \cdot P^{1.5} \qquad (3)$$

where K and m are constants, treated as distributed variables. This equation is a lower-bound curve derived from experimental data and takes account of the possible difference between the maximum axial extent of the crack in

the wall of the tube (L) and the length of the crack at the outer surface. The AGS characteristics are defined by the two distributions: (1) the time to dew-point alarm (TMDP) and (2) the quantity of water (QF) needed to activate the beetle alarm. The distribution of TMDP is defined by a set of paired variables: a value of time to dew-point alarm (TF) and the percentage of PT's in the core to which TF would apply. The same scheme is used for defining the distribution of QF.

Monte Carlo (MC) selection is made from the distribution of LP and DHCV to estimate the crack length. This process is repeated at each specified time in the shutdown sequence to create independent realizations of crack length and the appropriate CCL. The appropriate CCL also is selected by the MC process. The derivation of the mean and standard deviation values to describe the distribution of CCL was deliberately omitted from BLOOM and must be carried out separately by the user. Forcing the user to evaluate the CCL distribution separately emphasises the need to carefully examine the fracture toughness data to assess their range of validity and applicability to the probabilistic analysis. In addition, improvements in the data base for fracture toughness (CCL) can be taken into account without having to alter the BLOOM code. The probability of PT rupture at any time is the quotient: (number of PT ruptures predicted)/(cumulative number of realizations plus one).

3.2 Estimation of Crack Size at and After an Alarm

BLOOM estimates separately the crack size (LD) at the dew-point alarm and at the beetle alarm. Assuming both alarms are available, the one associated with the smaller value of LD must occur first.

If the beetle alarm were to occur first, the crack length can be estimated using Equation 3. Integration of Equation 3 provides an expression which can be solved for LD in terms of QF, LP and DRJ. Different integration limits apply, depending on whether $LP \leq DRJ \leq LD$ or $LD \leq DRJ$. If the dew-point alarm occurs first, a somewhat more complicated procedure is needed to determine the crack length at the beetle alarm, depending on whether or not a ZPH shutdown is instigated.

If the dew-point alarm comes first, the estimation of the crack size at the dew-point alarm is determined from the time, TMDP, to activate this alarm. As an example, if $LP \leq LD \leq DRJ$, the crack length, LD, at the dew-point alarm is found from $TMDP = (LD-LP)/(2 \cdot DHCV)$.

Once an alarm has been activated, leak confirmation activities would start. A shutdown to ZPH would precede a cooldown to the cold, depressurized state. While the reactor is in (or approaching) the ZPH state, various hold times are specified after which the reactor shutdown/cooldown is begun. The calculations of crack lengths at these hold times involve the solution of straightforward algebraic expressions, but their solution are made complex because the correct crack length is obtained by choosing the crack length that satisfies the appropriate inequality between the lengths shown in Figure 1. These inequality relations differ depending on the possible location of the crack in relation to the RJ.

3.3 Counting, Probability and Generation of Random Variables

For each realization, the crack lengths predicted at dew-point and beetle alarm and at the discrete times, TM1 to TM7 (beginning with L1 - the crack length corresponding to time, TM1) are taken in sequence and compared with the estimate of CCL under the PHTS conditions at the corresponding time. There are eight possibilities: $CCL \leq L1$ through to $CCL \leq L7$, and $L7 \leq CCL$. If $CCL \leq L1$, the realization is counted as a PT rupture at time $\leq TM1$, and at times $\leq TM2$ through TM7. It does not matter that later pressure reductions may increase the CCL; the tube has already ruptured. If $CCL \geq L1$, no count is made and CCL is then compared with L2, etc. Similarly, if $LD \geq CCL$, the tube is counted as having ruptured at times $\leq t = 0$ and at times $\leq TM1$ to TM7.

At time TM1, if N1 is the number of realizations for which PT rupture has occurred (including those that ruptured at t = 0) and N is the total number of realizations, then the cumulative probability (CPROB) of PT rupture at TM1 is N1/(N + 1). Similarly, if the number of realizations for which rupture has occurred at time TM2 (including those that ruptured at time ≤ TM1) is N2, then the CPROB of tube rupture at TM2 is N2/(N + 1). Thus (N2 - N1)/(N + 1) is the probability (PROB) of tube rupture occurring between times TM1 and TM2. In the above manner the CPROB (PT rupture) can be found at a dew-point alarm, at a beetle-alarm time (and at various hold times) and at times TM1 through TM7 (i.e., throughout a shutdown/cooldown procedure). Also PROB (PT rupture) can be found for the interval between any two of the above times.

To ensure that the selection process is as random as practical, care was taken to choose a pseudo-random number generator with a sufficiently high periodicity. The number generator used in BLOOM is based on Marsaglia's method [5], which, in theory, should have a periodicity of 4×10^9. Tests were carried out to show that the periodicity of the generator is at least 1×10^9. Using this random number generator, a pseudo-random number, P ($0 < P < 1$) is generated for the MC process. From $X = F^{-1}(P)$, where $F^{-1}(P)$ is the value of the inverse, standard, cumulative probability function for the chosen probability, P, a random selection of a variable, A, is obtained, according to $A = \mu_A + X\sigma_A$, where μ_A and σ_A are the given mean and standard deviations, respectively, of A. If the random number generator were sufficiently random, for a large number of realizations, the distributed variables should have μ_A and σ_A values close to the given ones. Specific tests showed this to be the case.

4. TYPICAL OUTPUT OF A PROBABILISTIC ANALYSIS

An example of typical input conditions for a probabilistic analysis are summarized in Table 1. The results of this probabilistic analysis for a run having N= 9345 realizations are summarized in Table 2.

Table 1. Input Conditions for a Typical BLOOM Run.

(a) Water quantities needed to activate the beetle alarm, WT, and time intervals needed to activate the dew-point alarm, TMDP, plus corresponding percentages (%) of total tubes requiring these given amounts.

WT (kg)	10	20	30	40	50	60	70	80	90	100	110	120
TMDP (h)	0.07	0.17	0.31	0.47	0.64	0.83	1.0	1.19	1.4	1.6	1.79	2.0
%	10	10	10	10	9.17	9.17	9.17	8.33	7.5	6.67	5.83	4.16

(b) μ_K (σ_K) = 3.6 (0.01); μ_m (σ_m) = 2.5 (0.001); P = 10.5 and 7.5 MPa at first leakage and at the end of the ZPH shutdown, respectively; μ_{DRJ} (σ_{DRJ}) = 25 (0.01) mm; μ_{LP} (σ_{LP}) = 16 (1) mm.

(c) Time, temperature (T), mean and standard deviation of the critical crack length (μ_{CCL} and σ_{CCL}) at temporal points 0, TM1 to TM7 (*linear reduction in temperature between adjoining temperatures)

Time Step	0	TM1	TM2	TM3	TM4	TM5	TM6	TM7
Time (h)	0	0.001	0.691	0.971	1.321	1.741	1.771	240
T (°C)	253(T0)	258(T1)	*	175(T3)	*	100(T5)	*	50(T7)
μ_{CCL} (mm)	52.5	69.8	60.3	60.3	81.7	69	77.0	60.5
σ_{CCL} (mm)	12	16	12	12	18	12	16	12

Table 2. Results of Probability and Cumulative Probability for the Input Conditions of Table 1.

(a) BBL possibilities before shutdown/cooldown (shutdown time clock is at 0 h for all possibilities):

Event Labels	Probability	Possible Outcome of Events Prior to Reaching Conditions for a Shutdown/cooldown
i	0	Break before any alarm
ii	0	Beetle alarm; break during ZPH shutdown
iii	0	Beetle alarm; break during ZPH shutdown at times < specified hold time
iv	3×10^{-4}	Dew-point alarm; break during ZPH shutdown; no beetle alarm
v	0	Dew-point alarm; break during ZPH shutdown after beetle alarm
vi	2×10^{-4}	Dew-point alarm followed by beetle alarm during the ZPH shutdown; break before time < specified hold time (after beetle alarm)
vii	2×10^{-4}	Dew-point alarm followed by ZPH shutdown; break during ZPH hold with no beetle alarm
viii	40×10^{-4}	Dew-point alarm followed by a ZPH shutdown, then beetle alarm; break at time < specified hold time (after beetle alarm)
ix	47×10^{-4}	Total (cumulative probability) of probabilities i to viii which do not reach the start of shutdown/cooldown

(b) During the shutdown/cooldown (the cumulative probabilities include all BBL possibilities summed in ix):

Time Step	Time (h)	Cumulative Probability	Possible Outcome of Events
TM1	0.001	81×10^{-4}	BBL, plus running total of LBB
TM2 to TM6	0.691 to 1.771	103×10^{-4}	BBL, plus running total of LBB
TM7	240	153×10^{-4}	BBL, plus running total of LBB

Table 2(a) shows that in 47 out of 10^4 realizations, the PT ruptures before the cold depressurized state is reached. The difference between the cumulative probability of BBL given in line ix of Table 2(a) and time TM1 in Table 2(b) is because the latter includes ruptures caused by the abrupt change in pressure at time TM1. From TM2 to TM6 the cumulative probability remains unchanged at 103×10^{-4}, which is achieved upon reaching time TM2. At the final time considered (TM7, 240 hours after the start of leakage) the table shows that 153 PT's have ruptured out of 10^4 total occurrences of leakage. BLOOM also has the capability to simulate the unavailability of the AGS. This, however, has not been included in the above example.

5. CONCLUSIONS

For CANDU reactors, the probabilistic LBB code, BLOOM, can be used to predict the cumulative probability of PT rupture, resulting from the axial growth by DHC of through-wall cracks in the PT's, at specific times after the start of leakage. In BLOOM, the major phenomena are modelled that affect crack length and CCL during the reactor sequence of events following the first indications of leakage. BLOOM can be used to develop unit-specific estimates of the actual probability of PT rupture in operating CANDU reactors and supplement the existing deterministic LBB analysis.

REFERENCES

1. G.D. Moan, C.E. Coleman, E.G. Price, D.K. Rodgers and S. Sagat, Int. J. Pres. Ves. & Piping, Vol. 43. pp. 1-21, 1990.

2. J.R. Walker, Int. J. Pres. Ves. & Piping, Vol. 43. pp. 229-239, 1990.

3. San-Q. Shi and M.P. Puls, "Advances in The Theory of Delayed Hydride Cracking in Zirconium Alloys," Atomic Energy of Canada Limited, Report RC-1295, COG-I-94-449 (1994), to be published in "Proceedings of the 5th International Conference on Hydrogen Effects on Material Behavior", Jackson Lake Lodge, Wyoming, U.S.A., 1994, September.

4. S. Sagat, C.E. Coleman, M. Griffiths and B.J.S. Wilkins, "Zirconium in the Nuclear Industry: Tenth Inernational Symposium, ASTM STP 1245, A.M. Garde and E.R. Bradley, Eds., ASTM, Philadelphia, U.S.A., pp. 35-61, 1994.

5. G. Marsaglia, "Expressing a Random Variable in Terms of Uniform Random Variables," The Annuls of Mathematical Statistics, Vol. 32, 1961.

LBB 95 - LYON - 9-11 October 1995

STUDIES OF THE STEAM GENERATOR DEGRADED TUBES BEHAVIOUR ON BRUTUS TEST LOOP

C. CHEDEAU*, B. RASSINEUX*, B. FLESCH**,
M. Cl. GRANDJEAN***, D. PAGES****, P. PITNER*****

The steam generator tube bundle in PWR power plant sets ELECTRICITE DE FRANCE stakes of safety and operability : simple or multiple corrosion cracks are developing on different tube points (span, roll transition zone, U-bend, ...). The operating policy uses the Leak Before Risk of Break among others : every in-depth defect, which products a leakage between the primary and secondary systems, is detectable before the crack reaches a critical size and opens the tube suddenly.

COMPROMIS software, realised in the Steam Generators Maintenance Probabilistic Study, allows to value the failure probability according to the operating time. The behaviour of cracked tubes has to be modelled with mechanical and thermohydraulic phenomena : opening areas, leak rates and bursting pressures must be determined for different crack configurations and operating conditions.
For this purpose, simplified modellings of opening area and leak rate are made respectively from elastic-plastic finite element calculations and thermohydraulic experimental studies. They need a validation by experimental results.

Consequently, BRUTUS loop was built at EDF Research Center Les Renardières. This test device is specifically designed for the study of leak rate and mechanical behaviour of cracked tubes under operating and upset conditions.

As we can not test contaminated components, tubes are cracked with different means in longitudinal and circumferential directions :
- machining in order to validate simplified laws and to quantify the influence of different parameters (strain hardening on the roll transition zone, tubesheet effect, complex geometry of longitudinal cracks, ligament between two circumferential cracks),
- stress corrosion and intergranular corrosion in order to obtain primary and secondary realist failures,
- fatigue to simulate the circumferential crack propagation by vibrations.

Actual tests results are discussed, as their interpreting by simplified formula. We show the uncertainties and the difficulties to extend these models to in-service behaviour.

* EDF/DER/MTC - Centre des Renardières - 77250 MORET SUR LOING - FRANCE
** EDF/EPN/DMAINT - 13 Espl. Ch. de Gaulle - 92060 PARIS LA DEFENSE - FRANCE
*** EDF/DE/SEPTEN - 12,14 avenue Dutrievoz - 69628 VILLEURBANNE - FRANCE
**** EDF/DER/TTA - 6 quai Watier - 78401 CHATOU - FRANCE
***** EDF/DER/REME - 25 allée Privée - Carrefour Pleyel - 93206 SAINT DENIS - FRANCE

STUDIES OF THE STEAM GENERATOR DEGRADED TUBES BEHAVIOUR ON BRUTUS TEST LOOP

C. CHEDEAU, B. RASSINEUX (EDF/DER), B. FLESCH (EDF/EPN),
M. Cl. GRANDJEAN (EDF/DE), D. PAGES, P. PITNER (EDF/DER)

INTRODUCTION

The steam generator (SG) tube bundle forms a substantial proportion of the second fission product barrier in PWR power plant and sets ELECTRICITE DE FRANCE (EDF) stakes of safety and operability. SG tubes are made of Inconel 600 which is sensitive to primary and secondary water stress corrosion cracking. Also, simple or multiple corrosion cracks are developing on different tube points (span, roll transition zone, U-bend, ...).
The operating policy relies on the Leak Before Risk of Break among others : every in-depth defect, which products a leakage between the primary and secondary systems, is detectable before the crack reaches a critical size and opens the tube suddenly.
Some studies are developed at EDF Research Centers [1] : global tests of crack leak rates, numerical calculations of crack opening area, thermohydraulic studies leading to research into the parameters governing leaks, development of a mechanical probabilistic design code by means of analytical models.
This paper describes precisely the first two studies and briefly the last two.

THE PROBABILISTIC FRACTURE MECHANICS CODE FOR TUBE MAINTENANCE

EDF has developed the COMPROMIS [2] software realised in the Steam Generators Maintenance Probabilistic Study. This code optimizes the tube bundle maintenance of steam generators ; it is used for the non-destructive examinations optimisation, the tube closing criterions establishment, the forecast and the optimisation of steam generators replacement.
The model, based on probabilistic fracture mechanics, makes it possible to quantify the influence of in-service inspections and maintenance work on the risk of an SG tube rupture, taking all significant parameters into account as random variables : initial defect size distribution, reliability of non-destructive detection and sizing, initiation and propagation, critical sizes, leak before risk of break, ...

THE BRUTUS LOOP AND TEST PROCEDURES

BRUTUS test loop was built at EDF Research Center Les Renardières in 1991. It is specially designed for the study of leak rate and mechanical behavior of throughwall cracked tubes under operating and upset conditions.
The test facility allows :
- the reproduction of different pressure deviations between primary and secondary systems under operating (10 MPa) and upset conditions (17,2 MPa) ;
- the reproduction of the primary temperature (303 °C) ;
- the measurement and the shimming of leak rates up to 30 m^3/h ;
- the determination of bursting pressures up to 50 MPa while keeping a representative flow rate through the crack in order to evaluate the possible margins.

BRUTUS loop [3] includes a high pressure system which simulates the primary circuit and a medium pressure system (the secondary circuit). The first one supplies the test section on temperature, pressure and flow rate conditions, the second one absorbes the continuous leak.

The test conditions are generally : internal temperature from 270°C to 303°C, external temperature of 265°C, internal pressure from 10 to 22,2 MPa, external pressure of 5 MPa.

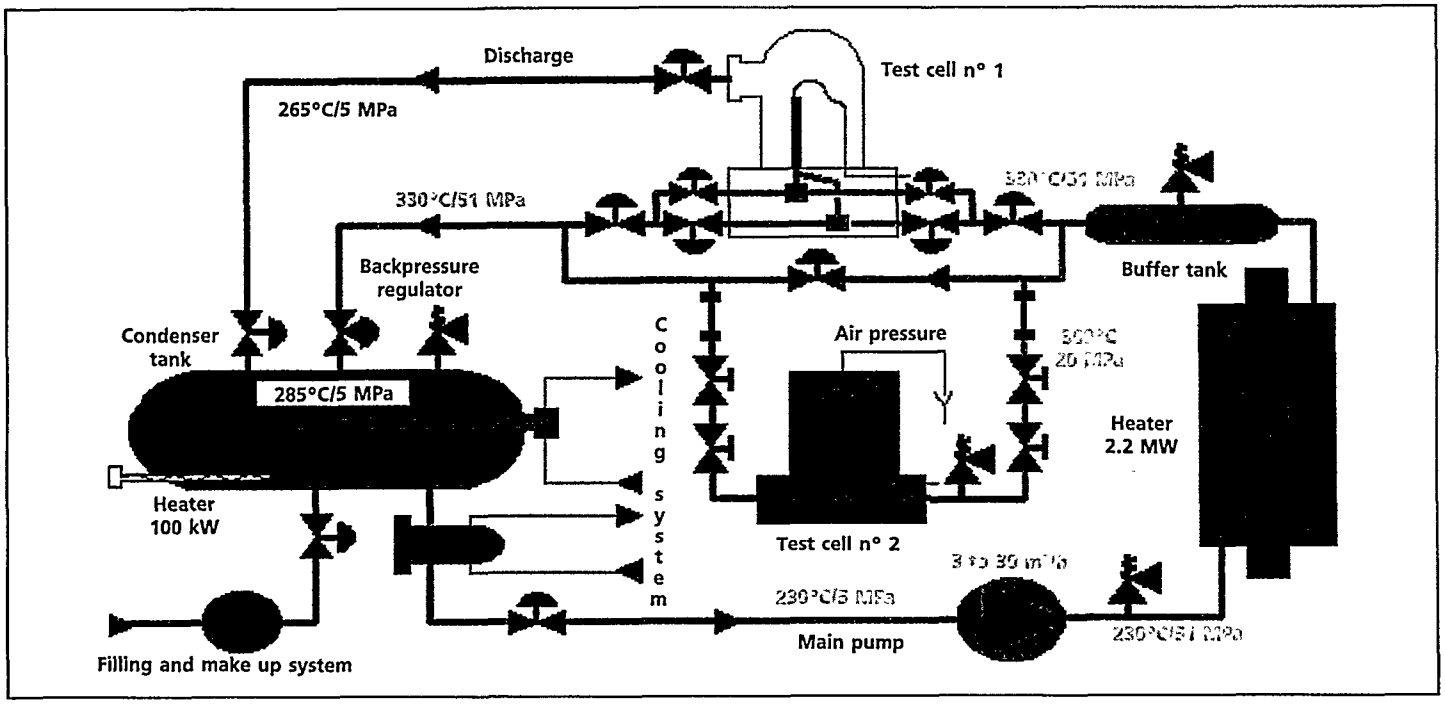

Figure 1 - The BRUTUS test loop.

The cracks measurement is as follows : during the tests, the flow rate is measured between 0,1 and 80 liters/hour by weighing and to 30 000 liters/hour by turbine flowmeters.
The defects geometries are analyzed using image processing techniques. These techniques provide access to zones, lengths and widths, either internal or external, as well as to wetted perimeters or hydraulic diameters (only for longitudinal cracks). These dimensions are measured after the operating and accident conditions.

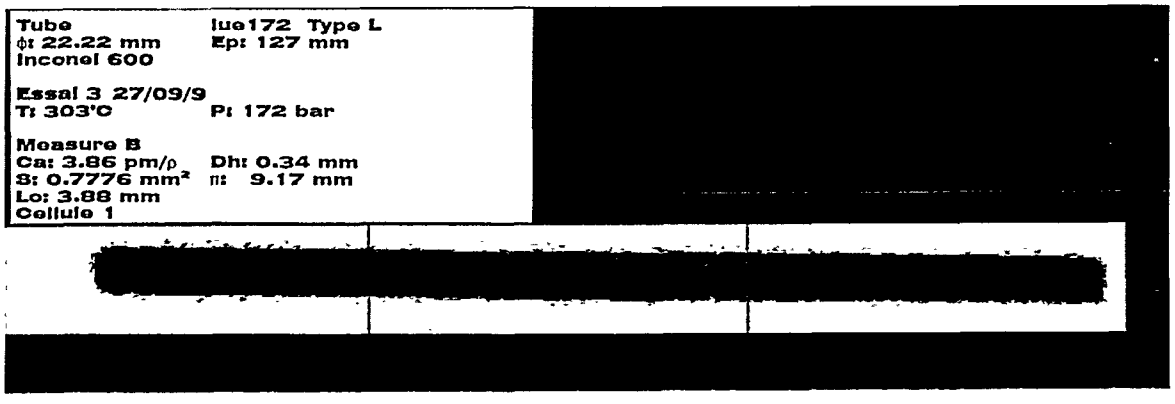

Figure 2 - Measurement of the opening area using image processing technique.

DEFECTS TESTED ON BRUTUS LOOP

Tests are particularly conducted on BRUTUS loop on tubing with external diameter of 22,22 mm and wall thickness of 1,27 mm. Longitudinal cracks lengths change between 2 and 15 mm.
At the present time, EDF is not able to test contaminated components. So tubes are cracked with different means in longitudinal and circumferential directions :

- machining in order to validate simplified laws and to quantify the influence of different parameters :
  - the tube is expanded on the tubesheet and corrosion cracks are positioned on the roll transition zone ;
  - principally this corrosion cracking appears on the inner surface and go across the wall thickness, also the internal length is taller than the external one ;
  - circumferential cracks expand usually on the same circumference and the resistance of the ligament between two defects is important against the tube integrity,
- stress corrosion [3] and intergranular corrosion in order to obtain primary and secondary realist failures,
- fatigue to simulate the circumferential crack propagation by vibrations.

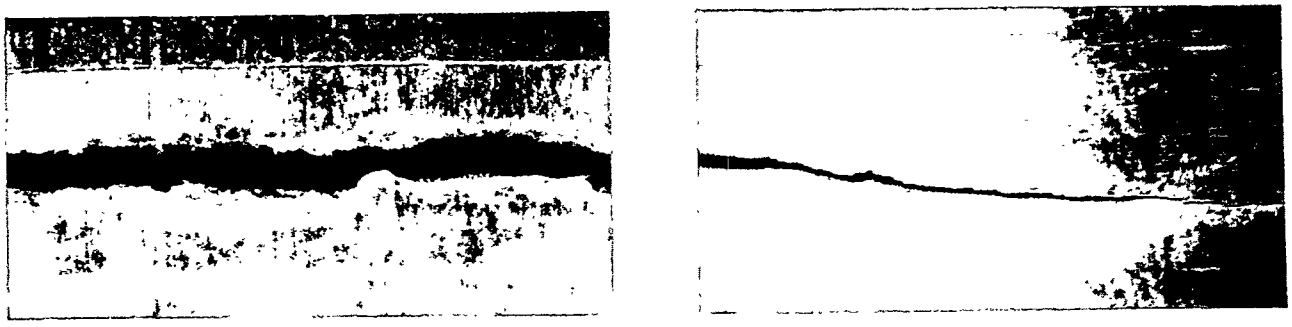

Figure 3 - Cracks geometries obtained by corrosion and fatigue experiments.

OPENING AREA SIMPLIFIED CALCULATIONS

The opening area simplified computation depends on the crack direction, longitudinal or circumferential. It takes into account material properties (Young's modulus, yield strength, rupture stress), cracked tube sizes (middle diameter, wall thickness, crack length) and loadings (internal and external pressures). The following models calculate an elastic area and then apply a plastic correction.

For longitudinal cracks we use Tada and Paris model [4] associated with a Dugdale type plastic correction [5] or a EDF/SEPTEN analytical model. The last model of the opening area A can be written in the following form :

$$A = \frac{a^2 \cdot N \cdot \sigma_\theta(\Delta P)}{E \cdot (b_0 + b_1\beta + b_2\beta^2 + b_3\beta^3)} \quad \text{and} \quad \beta = \frac{M \cdot \sigma_\theta(\Delta P)}{\sigma_Y}$$

with : $\sigma_\theta(\Delta P)$ the circumferential stress proportionnal to the primary to secondary differential pressure,
a the crack length,
N the amplification factor,
E the Young's modulus,
M the bulding factor,
σ_Y the yield strength.

For circumferential cracks we use Zahoor model [6] associated with an Irwin type plastic correction [7] or Framatome model associated with a Dugdale expression of the plastic zone radius at the defect end. These expressions take one's stand on the linear plastic fracture mechanics applied to plates and are used for joint loadings (pressure, bending and traction). They calculate the stress intensity factor and then deduce the opening area. Some correction factors are introduced to represent the radius effects (hull parameter, bulging factor).

By comparison with tests and Finite Elements results, we advise EDF/SEPTEN model for longitudinal cracks and Framatome model for circumferentiel cracks.

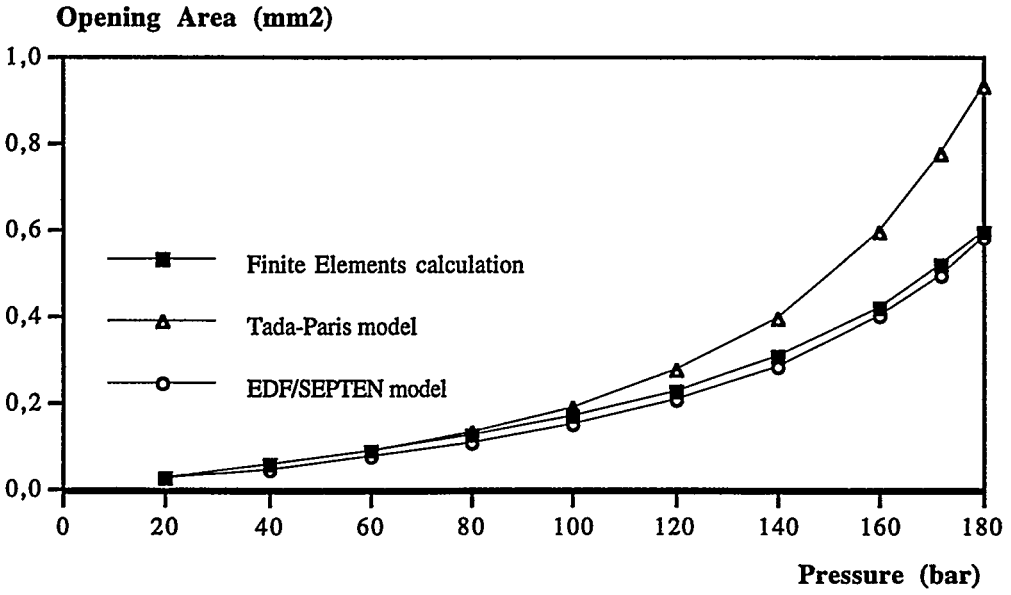

Figure 4 - Longitudinal crack opening area : comparison between different models.

FINITE ELEMENTS CALCULATIONS

3D elastic-plastic finite element calculations have been carried out in order to interpret the BRUTUS tests and to validate the numerical models. Tubes with longitudinal or circumferential cracks are meshed with I-DEAS or GIBI code. The numerical analysis is performed using *Code_Aster* developed at the Research and Development Division of EDF. Tubes are modelled with 20-nodes quadratic elements and mesh contains between 5000 and 10000 nodes. The effect of pressure on the surface of the defect is taken into consideration, as the traction due to the hydrostatic end force.

Different calculations are made :
- for longitudinal cracks, we compute areas, opening displacements of defects under load, as well as residual areas corresponding to situations when ΔP is equal to 10 and 17,2 MPa ; these values are compared with tests results. Also we determine the influence of the embelling on the tubesheet and the strain hardening on the transition zone.
- for circumferential cracks, we determine principally the resistance of the ligament between two defects : the rupture criterion depends more on the ultimate tensile strength than on the Inconel 600 toughness.

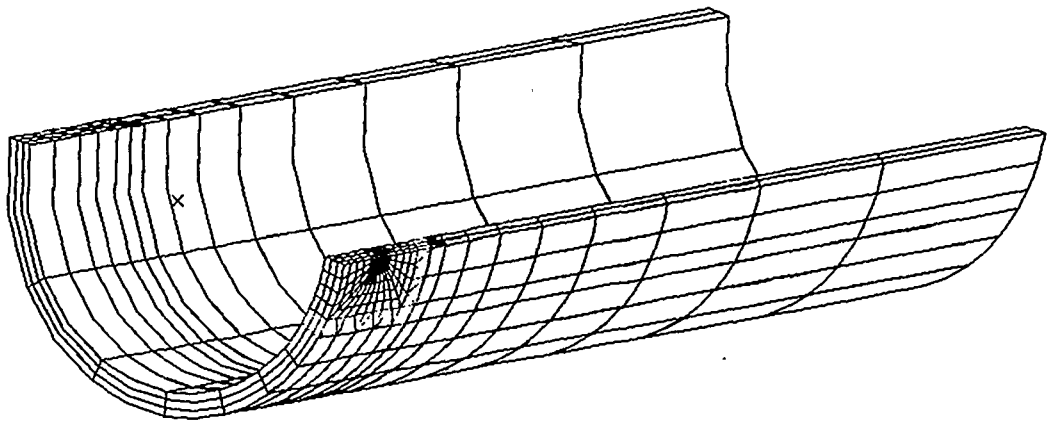

Figure 6 - Meshing of a longitudinal crack.

LEAK RATE SIMPLIFIED COMPUTATIONS

The internal coolant is under-saturated inside the tube from more than 20°C ; during the flow through the crack, it expands and can vaporized.
The critical flowrate model in steady-state operating conditions is based on the Lackmé pattern [8] which is adjusted to steam generator tubes. It implies different assumptions : monodimensionnal, permanent and adiabatic flow, the same speed on the liquid and the steam phases. It allows the mass flowrate calculation by the Bernouilli formula :

$$Q_m = A \cdot \sqrt{\frac{2 \cdot \rho \cdot (P_p - k \cdot P_{sat}(T_e))}{1+\xi}}$$

with A the flowing opening area,
P_p the internal pressure,
ξ the global pressure drop coefficient, which is calibrated by experiments,
Psat(Te) the saturated steam pressure at the internal temperature,
ρ the density of primary coolant
k an correction factor depending on ξ.

Simplified computations estimate test leak rates with good agreement ; the main difficulty is the determination of global pressure drop coefficient value .

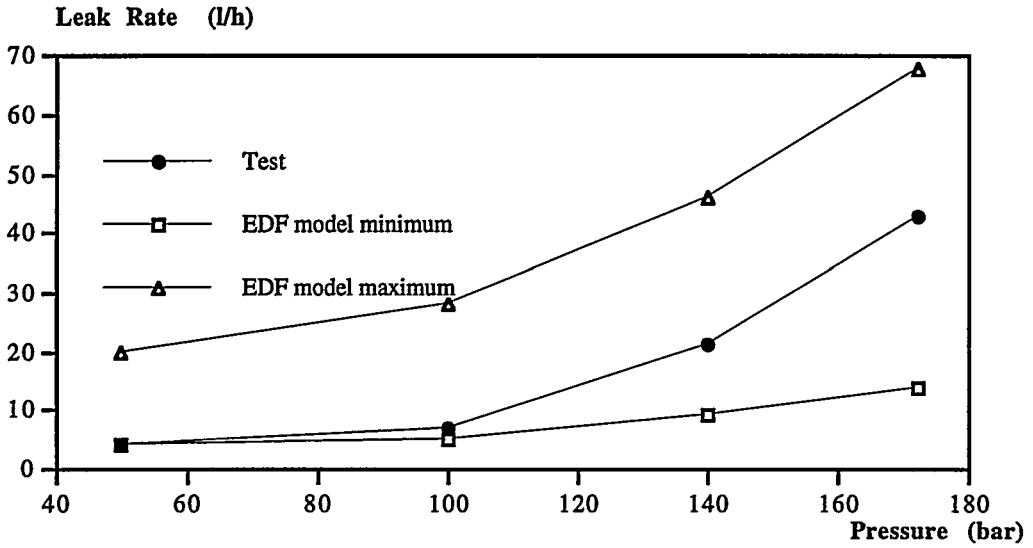

Figure 5 - Longitudinal crack leak rate : comparison between test and simplified model.

CONCLUSION

This paper has presented some studies made at EDF on steam generator tubes : we dispose of BRUTUS loop which is specifically designed for the study of opening area and leak rate of cracked tubes. Tests interpretations and finite element computations allow the development and the validation of simplified models.

They will be introduced in the COMPROMIS software realised in the Steam Generators Maintenance Probabilistic Study.

REFERENCES

[1] Recent developments in the field of leak before risk of break for steam generator tubes.
B. Flesch, R. Gâté, B. Cochet.
11th International Conference on Structural Mechanics in Reactor Technology, 18-23/08/91.

[2] Application of probabilistic fracture mechanics to optimize the maintenance of PWR steam generator tubes.
P. Pitner, T. Riffard, B. Granger, B. Flesch.
Nuclear Engineering and Design 142 (1993) 89-100.

[3] Mechanical and thermohydraulic testing on steam generator tubing cracked by in laboratory stress corrosion.
R. Gâté, B. Rassineux, A. Gelpi, M. Le Calvar.
10th European Corrosion Congress BARCELONE, 5-8/07/93.

[4] Application of fracture proof desing methods using tearning instability theory to nuclear piping postulating circumferential through wall cracks.
P.C. Paris, H. Tada.
NUREG/CR-3436, September 1983.

[5] Yielding of steel sheets containing slits.
D. S. Dugdale.
Journal of Mechanics and Solids, vol. 8, pp. 100-104, 1960.

[6] Fracture analysis for pipes containing full circumference internal part - throughwall flow.
M.D. Rajab, A. Zahoor.
International Journal of Presure Vessel and Piping, vol. 41, pp. 11-23, 1990.

[7] Fracture strengths relative to onset and arrest of crack propagation.
G.R. Irwin, J.A. Kies, A.L. Smith.
ASTM, vol. 58, pp. 640-660.

[8] Incompleteness of the flashing of supersaturated liquid and sonic ejection of the produced phases.
C. Lackmé.
International Journal Multiphase Flow, 31-141, 1979.

APPENDIX A
LIST OF ATTENDEES

1	. HAVEL Radim	IAEA	AUSTRIA
2	. GERARD Robert	TRACTEBEL	BELGIUM
3	. MALEKIAN Christian	TRACTEBEL	BELGIUM
4	. MOLITOR Francis	Serv. Sécurité Tech. Inst. Nuc	BELGIUM
5	. ROUSSEL Guy	A.V.N.	BELGIUM
6	. VAN ZEVEREN François	LABORELEC	BELGIUM
7	. WEYN André	AIB VINCOTTE	BELGIUM
			Compter 6
8	. GUENKOV HRISTOFOR	KOZLODUY NPP	BULGARY
9	. OUROUTCHEV Vladimir	KOZLODUY NPP	BULGARY
			Compter 2
10	. CASSIS Hani	ONTARIO HYDRO	CANADA
11	. JARMAN Brian	AECL	CANADA
12	. MISTRY Jagu	ONTARIO HYDRO	CANADA
13	. PEREIRA Ken	ATOMIC ENERGY CONTROL BOARD	CANADA
14	. PULS Manfred	AECL	CANADA
			Compter 5
15	. KADECKA Petr	NUCLEAR RESEARCH INSTITUTE REZ	CZECH REPUBLIC
16	. ONDROUCH Jan	NUCLEAR RESEARCH INSTITUTE REZ	CZECH REPUBLIC
17	. PECINKA Ladislav	NUCLEAR RESEARCH INSTITUTE REZ	CZECH REPUBLIC
18	. SAMOHYL Pavel	NUCLEAR RESEARCH INSTITUTE REZ	CZECH REPUBLIC
			Compter 4
19	. KESKINEN Rauli	STUK	FINLAND
20	. AMIEL Paul	E.D.F.	FRANCE
21	. ARDILLON Emanuel	E.D.F.	FRANCE
22	. BENOIT Manuela	FRAMATOME	FRANCE
23	. BEZDIKIAN Georges	E.D.F.	FRANCE
24	. BHANDARI Surender	FRAMATOME	FRANCE
25	. BLAY Nadine	C.E.A.	FRANCE
26	. BONNY Nadine	C.E.A. CENTRALE PHENIX	FRANCE
27	. BROCHARD Jacqueline	C.E.A.	FRANCE
28	. CAMPAN Jean-Louis	C.E.A.	FRANCE
29	. CARLUEC Bernard	FRAMATOME	FRANCE
30	. CAUQUELIN Claude	NPI	FRANCE
31	. CHAPULIOT Stéphane	C.E.A.	FRANCE
32	. CHARRAS Thierry	C.E.A.	FRANCE
33	. CHEDEAU Catherine	E.D.F.	FRANCE
34	. CHURIER-BOSSENNEC Henriet	E.D.F.	FRANCE
35	. COLACICCO Myriam	E.D.F.	FRANCE
36	. DAYVE Cyril	E.D.F.	FRANCE
37	. DE KEROULAS François	E.D.F.	FRANCE

38	. DEBEC-MATHET Eric	C.E.A.	FRANCE
39	. DEBOOS Réjane	E.D.F.	FRANCE
40	. DRUBAY Bernard	C.E.A.	FRANCE
41	. FAIDY Claude	E.D.F.	FRANCE
42	. FAYOLLE Patrice	E.D.F.	FRANCE
43	. FRANCO Christian	FRAMATOME	FRANCE
44	. GANTENBEIN Françoise	C.E.A.	FRANCE
45	. GILLES Philippe	FRAMATOME	FRANCE
46	. GOETSCH Denis	C.E.A.	FRANCE
47	. GRANDJEAN Marie-Claire	E.D.F.	FRANCE
48	. GUEDON Daniel	FRAMATOME	FRANCE
49	. GUILLAUME Maurice	FRAMATOME	FRANCE
50	. HEDIN François	E.D.F.	FRANCE
51	. HERVET Pascal	FRAMATOME	FRANCE
52	. HOROWITZ Hélène	C.E.A.	FRANCE
53	. HOUSSIN Bernard	FRAMATOME	FRANCE
54	. IGNACCOLO Salvatore	E.D.F.	FRANCE
55	. JOURNET Jacques	E.D.F.	FRANCE
56	. LAURET Philippe	FRAMATOME	FRANCE
57	. LE DELLIOU Patrick	E.D.F.	FRANCE
58	. MARQUES M.	C.E.A.	FRANCE
59	. MARTY Patrick	E.D.F.	FRANCE
60	. MEISTER Eric	E.D.F.	FRANCE
61	. MEZIERE Yves	E.D.F.	FRANCE
62	. MIANNAY Dominique	C.E.A.	FRANCE
63	. MICHEL Bruno	C.E.A.	FRANCE
64	. MILLER Alex	OECD-NEA	FRANCE
65	. MOCHE Laurent	DSIN/BCCN	FRANCE
66	. MOREL Gilles	FRAMATOME	FRANCE
67	. MOULIN Didier	C.E.A.	FRANCE
68	. NEDELEC Michel	C.E.A.	FRANCE
69	. NOE Hervé	E.D.F.	FRANCE
70	. PAGES Danielle	E.D.F.	FRANCE
71	. PAPIN Marie-Hélène	SOCOTEC INDUSTRIE	FRANCE
72	. PAYAN Francis	E.D.F.	FRANCE
73	. PELLISSIER-TANON André	FRAMATOME	FRANCE
74	. PICHON Christian	E.D.F.	FRANCE
75	. PITNER Patrice	E.D.F.	FRANCE
76	. PLOYART Robert	C.E.A.	FRANCE
77	. POETTE Christian	C.E.A.	FRANCE
78	. PORCHET Armelle	FRAMATOME	FRANCE
79	. PREVOST Alain	E.D.F.	FRANCE
80	. RADAT Marie-Pierre	E.D.F.	FRANCE
81	. RASSINEUX Bruno	E.D.F.	FRANCE
82	. RIEG Claude-Yves	E.D.F.	FRANCE
83	. ROUSSELLE Jacky	E.D.F.	FRANCE
84	. SALLES Bernard	E.D.F.	FRANCE
85	. SEMETE Patrick	E.D.F.	FRANCE
86	. TANCELIN Denise	C.E.A.	FRANCE
87	. TERNON Françoise	E.D.F.	FRANCE
88	. TURBAT André	FRAMATOME	FRANCE
89	. VALETA Marie-Pierre	C.E.A.	FRANCE
90	. VENDROUX Maurice	E.D.F.	FRANCE

91	. VOUILLOUX Francis	FRAMATOME	FRANCE
92	. WADIER Yves	E.D.F.	FRANCE
			Compter 73
93	. BARTHOLOME Gunther	SIEMENS/KWU	GERMANY
94	. BEUKELMANN Dieter	TÜV Bayern Sachsen	GERMANY
95	. BIENIUSSA Klaus	GRS	GERMANY
96	. BOROSKE Ernst	TUV HANNOVER/S.-A.	GERMANY
97	. ENGELLAND Hans-Carsten	TÜV Südwest e.V.	GERMANY
98	. GREBNER Hans	GRS	GERMANY
99	. KRÖNING Jürgen	TÜV Nord	GERMANY
100	. KUSSMAUL Karl	MPA Stuttgart	GERMANY
101	. OTREMBA Frank	HEW	GERMANY
102	. SCHULZ Helmut	GRS	GERMANY
103	. STADTMULLER Werner	MPA Stuttgart	GERMANY
104	. STURM Dietmar	MPA Stuttgart	GERMANY
105	. WELLEIN Robert	SIEMENS/KWU	GERMANY
			Compter 13
106	. ANDREANI Marco	ENEL	ITALY
107	. PINO Giovanni	ANPA	ITALY
108	. ZANABONI Piero	ANSALDO	ITALY
			Compter 3
109	. HOJO Kiminobu	MITSUBISHI HEAVY INDUSTRIES	JAPAN
110	. ISOZAKI Toshikuni	JAERI	JAPAN
111	. KASHIMA Koichi	CRIEPI	JAPAN
112	. KITSUKAWA Keisuke	TOSHIBA Co.	JAPAN
113	. MURAYAMA Kouichi	HITACHI Ltd.	JAPAN
114	. OGATA Yoshiki	MITSUBISHI HEAVY INDUSTRIES	JAPAN
115	. YOKOTA Hiroshi	MHI	JAPAN
			Compter 7
116	. KIM Yong-Beum	KINS	KOREA
117	. LEE Jeong-Bae	KINS	KOREA
			Compter 2
118	. ALEJEV Aleksandr	VATESI	LITHUANIA
119	. LEVINSKAS Rimantas	LEI	LITHUANIA
120	. ZHILIUKAS Antanas	KAUNAS UNIV OF TECHNOLOGY	LITHUANIA
			Compter 3
121	. CRUTZEN Serge	JOINT RESEARCH CENTER OF EC	NETHERLANDS
122	. KEVENAAR Jos	ECN	NETHERLANDS
			Compter 2

123	. CALNITSCI Victor	ATOMENERGOPROEKT	RUSSIA
124	. KISELYOV Vitaly	ECS MAE RDIPE	RUSSIA
125	. SMIRNOV Leonid	ATOMENERGOPROEKT	RUSSIA
			Compter 3
126	. BENO Peter	VUJE	SLOVAK REPUBLIC
127	. CEPCEK Stefan	NUCLEAR REGULATORY AUTHORITY	SLOVAK REPUBLIC
128	. KUPCA Ludovit	VUJE	SLOVAK REPUBLIC
			Compter 3
129	. KIRK R.A.	COUNCIL FOR NUCLEAR SAFETY	SOUTH AFRICA
130	. AXELSSON Roger	OKG AB	SWEDEN
131	. BRICKSTAD Bjorn	SAQ Inspection Ltd	SWEDEN
132	. FREDLUND Lars	VATTENFALL	SWEDEN
133	. HEDNER Gert	SKI	SWEDEN
134	. LETZTER Adam	SAQ Inspection Ltd	SWEDEN
135	. WILDHEIM Jorgen	VATTENFALL	SWEDEN
			Compter 6
136	. AUST Olivier	NOK NPP BEZNAU	SWITZERLAND
137	. PRANTL Gustav	HSK	SWITZERLAND
138	. WANNER Robert	KKL Leibstadt	SWITZERLAND
			Compter 3
139	. HO Hann Long	TAIWAN POWER CO.	TAIWAN R.O.C.
140	. KANG Lung Chyuan	INER	TAIWAN R.O.C.
141	. LIN Li-Fu	INER	TAIWAN R.O.C.
			Compter 3
142	. BOUCHARD P. John	NUCLEAR ELECTRIC plc	UNITED KINGDOM
143	. BUDDEN Peter John	NUCLEAR ELECTRIC plc	UNITED KINGDOM
144	. CHIVERS Terry	NUCLEAR ELECTRIC PLC	UNITED KINGDOM
145	. DUNN John	SCOTTISH NUCLEAR	UNITED KINGDOM
146	. HARROP L. Paul	NII	UNITED KINGDOM
147	. HOWSON John	ROLLS ROYCE & ASSOCIATES	UNITED KINGDOM
148	. HURRELL Paul	ROLLS ROYCE & ASSOCIATES	UNITED KINGDOM
149	. PEAT Noel K.	ROLLS ROYCE & ASSOCIATES	UNITED KINGDOM
150	. SHARPLES John	AEA Technology	UNITED KINGDOM
151	. STEWART George	BNFL	UNITED KINGDOM
			Compter 10
152	. BHOWMICK Dulal	WESTINGHOUSE	U.S.A.
153	. GAMBLE Ron	SARTREX CORPORATION	U.S.A.
154	. HOPPER Allen	BATTELLE	U.S.A.
155	. KILINSKI Thomas	BATTELLE	U.S.A.

156	. MAYFIELD Michael	USNRC	U.S.A.
157	. OLSON Rick	BATTELLE	U.S.A.
158	. RAHMAN Sharif	THE UNIVERSITY OF IOWA	U.S.A.
159	. RUDLAND David	BATTELLE	U.S.A.
160	. SCOTT Paul	BATTELLE	U.S.A.
161	. SWAMY Seth	WESTINGHOUSE	U.S.A.
162	. WICHMAN Keith	USNRC	U.S.A.
163	. WILKOWSKI Gery	BATTELLE	U.S.A.

Compter 12

APPENDIX B
BANQUET KEYNOTE ADDRESS

LBB 95 Banquet Keynote Address

Ladies, Gentlemen, Dear Colleagues:

I would like to thank all of you for your participation and your interest in the leak-before-break (LBB) seminar, LBB 95. The high quality of the presentations and the posters, as well as the presence of world-wide specialists are transforming this event into a success. I wish to express my gratitude to the organizers: EDF, the CEA, Framatome, and the sponsors, especially to the European Working Group on Codes and Standards. The active participation of the OECD, Nuclear Electric, the USNRC, and the IAEA attest to the international interest in the seminar. I would also like to thank the French Nuclear Energy Society, SFEN, as well as the SEPTEN division of EDF, and the two organizers, namely Phillipe Gilles and Claude Faidy for their contribution in the organization of the seminar.

For over a decade, large progress in research has been achieved in this field and the LBB concept is applied in the USA, Germany, and other countries. These results are of great interest to Framatome, who applies the LBB approach to fast breeder reactors, uses the concept in safety analyses, and performs LBB studies for foreign utilities (Belgium, Switzerland, the C.I.S.) Together with EDF and CEA, Framatome has taken an active part in the International Piping Integrity Research Group (IPIRG) Program and established, in parallel, a large experimental and analytical research program. The objective of the LBB 95 seminar is to summarize these results and to compare experiences and codifications developed in different countries. We expect this seminar will contribute to the ongoing discussion of LBB procedures between the European safety authorities, utilities, and vendors.

In France, we are convinced that the LBB approach marks a step forward for safety and equipment integrity analyses:

- The LBB concept was not used in the design of the various series of standardized French PWR plants because the decisions on the design of the N4 series, of which Civaux 1 and 2 are still under construction, were taken in 1983. At this time, there was little awareness and few demonstrations of the potential of this concept in the French PWR community.

- However, in existing plants, we have used this approach for equipment integrity and Defense-in-Depth analyses.

- For the European pressurized water reactor, Siemens, Framatome, and the French and German utilities are working to bring together the break preclusion and the leak-before-break concepts, by coupling features of the German Basic Safety Concept and those of the French Defense-in-Depth concept.

Before ending, I would like to give recognition to the sustained efforts of Phillipe Gilles and Claude Faidy to increase acceptance of the LBB concept within the French PWR community in light of its success in other countries.

The most interesting feature of this seminar, most desired by Phillipe Gilles and Claude Faidy, is that we have been able to assemble specialists and project managers from safety authorities, utilities, and vendors. We hope this will lead to a better validation of the LBB approach and improvements in its codification.

J. Branchu
Head of Primary Nuclear Components Division
Framatome

NRC FORM 335 (2-89) NRCM 1102, 3201, 3202

U.S. NUCLEAR REGULATORY COMMISSION

BIBLIOGRAPHIC DATA SHEET

(See instructions on the reverse)

1. REPORT NUMBER (Assigned by NRC. Add Vol., Supp., Rev., and Addendum Numbers, if any.)

NUREG/CP-0155

2. TITLE AND SUBTITLE

Proceedings of the Seminar on
Leak Before Break in Reactor Piping and Vessels

3. DATE REPORT PUBLISHED

MONTH	YEAR
April	1997

4. FIN OR GRANT NUMBER

D2060

5. AUTHOR(S)

Edited by C. Faidy, EDF, and Ph. Gilles, Framatome

6. TYPE OF REPORT

Conference Proceedings

7. PERIOD COVERED *(Inclusive Dates)*

October 9-11, 1995

8. PERFORMING ORGANIZATION — NAME AND ADDRESS *(If NRC, provide Division, Office or Region, U.S. Nuclear Regulatory Commission, and mailing address; if contractor, provide name and mailing address.)*

EDF - Septen
12 Av. Dutrivoz
69628 Villeurbanne
France

Battelle
505 King Avenue
Columbus, OH 43201

9. SPONSORING ORGANIZATION — NAME AND ADDRESS *(If NRC, type "Same as above"; if contractor, provide NRC Division, Office or Region, U.S. Nuclear Regulatory Commission, and mailing address.)*

EDF (Electricite' de France)
12 Av. Dutrivoz
69628 Villeurbanne
France

Framatome
Tour Fiat - Cedex 16
92084 Paris La De'fense
France

Div. of Engineering Technology
Office of Nuclear Research
U.S. Nuclear Regulatory Commission
Washington, DC 20555-0001

10. SUPPLEMENTARY NOTES

Other sponsoring organizations per the title page and M. Mayfield, NRC Project Manager

11. ABSTRACT *(200 words or less)*

The sixth in a series of international Leak-Before-Break (LBB) Seminars was held at Hotel Sofitel in Lyon, France on October 9 through 11, 1995. The seminar updated international policies and supporting research on LBB. Attendees included representatives from regulatory agencies, electric utility representatives, fabricators of nuclear power plants, research organizations, and academic institutions.

The objective of the seminar was to present the current state of the art in LBB methodology development, validation, and application in an international forum. With particular emphasis on industrial applications and regulatory policies, the seminar provided an opportunity to compare approaches, experiences, and codifications developed by different countries.

The seminar was organized into four topic areas: Status of LBB Applications, Technical Issues in LBB, Methodology, Complementary Requirements (Leak Detection and Inspection), and LBB Assessment and Margins.
In addition to the formal sessions where papers were presented by participants from France, Germany, Japan, Korea, Belgium, the United Kingdom, the Czech Republic, Finland, Russia, Sweden, Canada, the Netherlands, and the United States, informal LBB poster sessions were available outside the presentation hall.

As a result of this seminar, better estimates of the limits to the LBB approach should follow, as well as an improvement in codifying methodologies.

12. KEY WORDS/DESCRIPTORS *(List words or phrases that will assist researchers in locating the report.)*

Leak-before-break, policy, fracture, leak rate, toughness, crack

13. AVAILABILITY STATEMENT

Unlimited

14. SECURITY CLASSIFICATION

(This Page)

Unclassified

(This Report)

Unclassified

15. NUMBER OF PAGES

16. PRICE